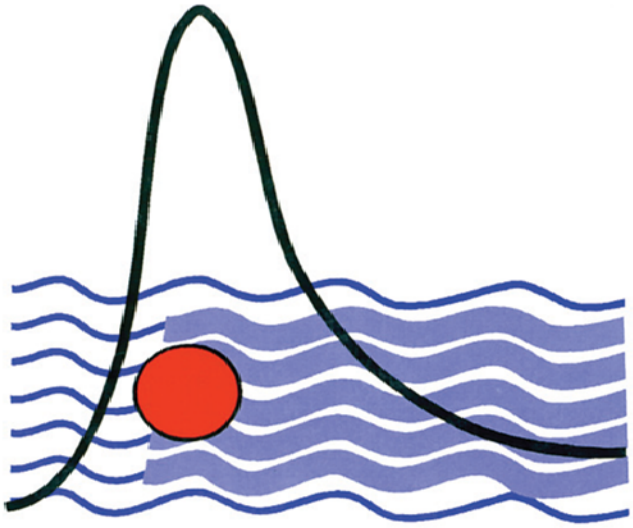

Werner Käss

Tracing Technique in Geohydrology

TRACING TECHNIQUE IN GEOHYDROLOGY

Taylor & Francis
Taylor & Francis Group
http://taylorandfrancis.com

Tracing Technique in Geohydrology

by
Werner Käss
Umkirch, Lkr. Breisgau-Hochschwarzwald, Germany

with contributions by
H. Behrens, Th. Himmelsbach, H. Hötzl, D. Hunkeler, Ch. Leibundgut, H. Moser, P. Rossi, H. D. Schulz, I. Stober & A. Werner

CRC Press
Taylor & Francis Group
Boca Raton London New York

CRC Press is an imprint of the
Taylor & Francis Group, an informa business

CRC Press
6000 Broken Sound Parkway, NW
Suite 300, Boca Raton, FL 33487
270 Madison Avenue
New York, NY 10016
2 Park Square, Milton Park
Abingdon, Oxon OX14 4RN, UK

The publication of this work was made possible by the financial support of Inter Nationes, Bonn.

An edited and updated translation of: Werner Käss, *Geohydrologische Markierungstechnik,* Lehrbuch der Hydrogeologie, Band 9. © 1992, Gebrüder Borntraeger Verlagsbuchhandlung, Berlin / Stuttgart. ISBN 3-443-01013-X Reprinted 2009 by CRC Press

Authorization to photocopy items for internal or personal use, or the internal or personal use of specific clients, is granted by A.A. Balkema, Rotterdam, provided that the base fee of US$ 1.50 per copy, plus US$ 0.10 per page is paid directly to Copyright Clearance Center, 222 Rosewood Drive, Danvers, MA 01923, USA. For those organizations that have been granted a photocopy license by CCC, a separate system of payment has been arranged. The fee code for users of the Transactional Reporting Service is: 90 5410 444 9/98 US$ 1.50 + US$ 0.10.

Published by
A.A. Balkema, P.O. Box 1675, 3000 BR Rotterdam, Netherlands
Fax: +31.10.413.5947; E-mail: balkema@balkema.nl; Internet site: http://www.balkema.nl

A.A. Balkema Publishers, Old Post Road, Brookfield, VT 05036-9704, USA
Fax: 802.276.3837; E-mail: info@ashgate.com

ISBN 90 5410 444 9

© 1998 Gebrüder Borntraeger Verlagsbuchhandlung, Berlin / Stuttgart
© English translation, 1998 A.A. Balkema, Rotterdam

Motto

'If we look at the measures and methods applied when investigating the connections between underground waters, we see that the tests are indeed based upon injecting a foreign substance at one site and trying to detect this foreign substance at another site. If this foreign substance, which neither naturally occurs in the water nor in the earth, that was injected in one site can be detected in another site, there can be no doubt that a connection between the injection site and the sampling site exists.'

'Wenn man darüber Ausschau hält, welche Mittel und Methoden zur Anwendung gelangen, um den Zusammenhang unterirdischer Gewässer festzustellen, so sehen wir, daß die Versuche durchwegs darauf beruhen, auf der einen Seite eine Stelle mit einem fremden Stoff zu beschicken und auf der anderen Seite bei der Entnahme zu versuchen, diesen sonst fremden Stoff nachzuweisen. Wenn nun der, ansonsten weder in der Flüssigkeit noch im umgebenden Boden vorkommende, an der einen Stelle eingebrachte Stoff an der anderen Stelle nachgewiesen werden kann, so wird darüber wohl kein Zweifel bestehen, daß zwischen der Beschickungs- und Entnahmestelle ein Zusammenhang besteht.'

GEORG KYRLE, 1928

Taylor & Francis
Taylor & Francis Group
http://taylorandfrancis.com

Contents

Editor's Preface XIII
Author's Preface XV

1 INTRODUCTION 1
W. Käss
1.1 Exordium 1
1.2 Nomenclature and definitions 11
1.2.1 Artificial tracers 11
1.2.2 'Naturally occuring' tracers 14
1.3 Application areas 14

2 TRACERS 17
2.1 Dyes 18
W. Käss
2.1.1 Fluorescent compounds 19
2.1.2 Non-fluorescing dyes 55
2.1.3 Analysis 56
2.1.4 Physiology of the fluorescent dyes 105
2.2 Salts 122
W. Käss
2.2.1 Sodium chloride 123
2.2.2 Lithium 131
2.2.3 Potassium chloride 138
2.2.4 Borax 143
2.2.5 Other salts 146
2.3 Surfactants, aromas, and other chemicals 151
W. Käss
2.3.1 Surfactants (wetting agents) 151
2.3.2 Aromas 160
2.3.3 Other chemicals 164
2.4 Radioactive and activable isotopes 167
H. Behrens
2.4.1 Introduction and basic principles of radioactivity 167

2.4.2 Radioactive decay 169
2.4.3 The measurement of radioactive radiation 172
2.4.4 Activable isotope tracers 178
2.4.5 Selected radionuclides and activable isotopes used as hydrological tracers 180
2.4.6 Hydrological applications of radiotracers 184
2.5 Club moss spores 187
W.Käss
2.5.1 Natural spores 190
2.5.2 Simply dyed spores 193
2.5.3 Fluorescent spores 197
2.5.4 Conducting spore drift tracing tests 201
2.6 Fluorescent microspheres 214
W.Käss
2.7 Bacteria 223
W.Käss
2.7.1 Introduction 223
2.7.2 Requirements for bacteria as tracers 224
2.7.3 Bacteria types used in water tracing 224
2.7.4 Application areas 236
2.8 Phages 244
P.Rossi & W.Käss
2.8.1 Introduction 244
2.8.2 What is a bacteriophage? 245
2.8.3 The idea of bacteriophages 246
2.8.4 Preparation of a phage suspension 248
2.8.5 Environmental influences on the survival of phages 249
2.8.6 Sample collection, transport, and storage. Counting phages in water samples 251
2.8.7 Range of application of bacteriophages as tracers 257
2.8.8 Natural distribution of phages 268
2.8.9 Types of phage species 269
2.8.10 Evaluation of phages as tracers 270
2.9 Geobombs 271
W.Käss
2.10 Other drift particles 272
W.Käss
2.11 Environmental isotopes 279
H.Moser
2.11.1 Introduction 279
2.11.2 Detection, occurence, and behaviour of environmental isotopes presently applied in hydrological investigations of the water cycle 281
2.11.3 Special evaluation methods for environmental isotope measurements 293
2.12 Environmental chemicals 303
W.Käss

2.12.1 Creeping release 303
2.12.2 Cases of accidents with groundwater damage 307
2.13 Environmental organisms 310
W.Käss
2.14 Physical environmental effects 311
W.Käss

3 PREPARATION AND REALISATION OF TRACING TESTS 315
W.Käss
3.1 Preliminary surveys and preparations 315
3.2 Test preparation 316
3.2.1 Legal questions 316
3.2.2 Choosing the injection site 317
3.2.3 Choosing the observation sites 317
3.2.4 Choosing the tracer 318
3.2.5 Deciding on the necessary tracer quantity 323
3.2.6 Test plan 328
3.3 Tracing procedure 328
3.3.1 Time of injection 328
3.3.2 Tracer injection 329
3.3.3 Sampling 333
3.4 Sample analysis 336
3.5 Documentation of tracing tests 337
3.6 Presentation of the results 339

4 EVALUATION AND INTERPRETATION OF TRACING TESTS 341
H.D.Schulz
4.1 Physical fundamentals of solute transport underground 342
4.1.1 Solute transport and dispersion 342
4.1.2 The dispersion coefficient 347
4.1.3 Spatial distribution of the tracer cloud 349
4.1.4 Temporal distribution of tracer clouds 352
4.1.5 Computer models for solute transport simulation 355
4.2 Solute transport and geochemical reactions 356
4.2.1 Distribution coefficient and retardation factor 356
4.2.2 Decay reactions 357
4.2.3 Cation exchange reactions, selectivities 359
4.2.4 Dissolution and precipitation reactions 361
4.2.5 Computer models for simulation of reactive solute transport 362
4.3 Evaluation of breakthrough curves 366
4.3.1 Determination of the effective flow velocity 366
4.3.2 Determination of the dispersivities 369
4.3.3 Recognition and rating of geochemical reactions 371
4.3.4 Case evaluations from tracing tests 372
4.4 TRACI – An example for mathematical tracing-interpretation-model 377
A.Werner
4.4.1 Analytical solutions 377

4.4.2 Conducting a tracing test for an evaluation with analytical solutions 379
4.4.3 Determination of the parameters 379
4.5 Radiohydrometrical single-well-methods 382
H.Moser
4.5.1 Introduction 382
4.5.2 Tracer dilution logging and tracer flowmeter 382
4.5.3 Application areas 384

5 PRACTICAL EXAMPLES OF APPLICATIONS AND INTERPRETATIONS 387
5.1 Unsaturated zone 387
5.1.1 Hazardous waste site – Eckenweiherhof/Mühlacker 387
H.Hötzl
5.1.2 Horizontal lysimeter – Egelsee 396
W.Käss
5.2 Karst groundwater 398
H.Hötzl
5.2.1 Recommandations for conducting tracing tests 398
5.2.2 Drainage systems of alpine karsts 402
5.2.3 Defining the boundaries of catchment areas in the Swabian Alb 411
5.2.4 Water management aspects – Danube percolation 417
5.3 Fissured aquifers 426
5.3.1 General remarks 426
W.Käss
5.3.2 Deep-seated rock creeps and rock slides 428
H.Hötzl
5.3.3 Tracer experiments in a highly permeably fault zone 437
Th.Himmelsbach
5.4 Porous groundwater 458
W.Käss
5.4.1 Hydraulic – Merdingen 458
5.4.2 Solute transport – Savinja Valley 463
5.4.3 Water protection area Merdingen 465
5.5 Investigations on river bank infiltration 467
5.5.1 Drinking water protection 467
H.Moser
5.5.2 Pollution propagation – Böckinger Wiesen, Heilbronn/ Southwest Germany 470
H.Hötzl
5.5.3 Quantification in fissured rocks 478
W.Käss
5.6 Deep waters 479
W.Käss
5.6.1 Deep water circulation – Saulgau 480
5.6.2 Oil field waters – Steimbke 482

5.7 Glaciers 486
Ch.Leibundgut
5.7.1 Models in hydroglaciology 486
5.7.2 Tracer applications in hydroglaciology 487
5.7.3 Requirements of artificial tracers used in hydroglaciology 488
5.7.4 Conducting tracing tests 489
5.7.5 Case example: Findelen-Glacier 490
5.8 Surface water 493
Ch.Leibundgut
5.8.1 Particularities of applying tracers in surface water 494
5.8.2 Lakes 496
5.8.3 Flowing water 502
5.9 Engineering 510
W.Käss
5.9.1 Leakage tests 510
5.9.2 Deep well techniques 513
5.9.3 Hydraulic tests 514
I.Stober
5.9.4 Partitioning tracing 517
D.Hunkeler

References 523

Conversion Tables 569

Index of Localities 571

Subject Index 575

Color Plates 585

Taylor & Francis
Taylor & Francis Group
http://taylorandfrancis.com

Editor's Preface

Within the last decades hydrogeology has developed, especially in Germany, into an independent discipline, studying the rules governing the occurence, balance, and properties of groundwater in close cooperation with the related disciplines of soil science, hydrology, hydromechanics, and hydrochemistry. This field is increasingly challenged by the public interest in the problems concerned with management, use, but also the protection of groundwater against contamination. This interest should be considered as a challenge to promote the respective research, but also to publish the results in an adequate way. This specific task is addressed by the Textbook of Hydrogeology, which was started by Prof. Wolfgang RICHTER and the publishing company Gebrüder Borntraeger. It aims to publish the rapidly growing knowledge on groundwater in separate volumes written by specific experts on the respective topics. After the tragic death of Professor RICHTER in a road accident in 1977, I was asked by the publishing company Gebrüder Borntraeger to take over the editorship. I shall pursue this task in his spirit and his intention.

The volumes 'Allgemeine Hydrogeologie – Grundwasserhaushalt' (General Hydrogeology – Groundwater Regime), 'Die Beschaffenheit des Grundwassers' (The Properties of Groundwater), 'Geohydraulik' (Geohydraulics), 'Talsperren' (Dams), 'Das Wasser in der Litho- und Asthenosphäre – Wechselwirkungen und Geschichte' (The Water in the Litho- and Asthenosphere – Interactions and History), 'Mineral- und Thermalwasser – Einführung in die Balneogeologie' (Mineral- and Thermal Water – An Introduction into Balneogeology), 'Isotopenmethoden in der Hydrologie' (Isotope Methods in Hydrology), and 'Geohydrologische Markierungstechnik' (Geohydrologic Tracer Methods) have been published and are obtainable separately. Further volumes are being prepared: 'Grundwassererschließung' (Groundwater Development), 'Hydrogeologie des Karstes' (Karst Hydrogeology), 'Geophysikalische Methoden in der Grundwasserexploration' (Geophysical Methods in Groundwater Exploration), and 'Grundwassermodelle – Strömung und Stofftransport' (Groundwater Models – Flow and Substance Transport).

The volume 'Geohydrologische Markierungstechnik', presented here in the translated version 'Tracing Techniques in Geohydrology', was published in 1992. It was well accepted by the science community as well as by users in water-consuming industries, consulting bureaus, and public services. It was evident, that an English version would find interest. The publishing company A.A. Balkema, Rotterdam/

Brookfield, supported this project by organizing the translation and by publishing the English version in this volume as licence from Gebrüder Borntraeger Publ. The volume describes in a comprehensive manner the techniques which enable us to study the subterranean flow paths of water, its flow velocity and residence times in the subsurface. These methods have been receiving interest in recent years, as they provide models for investigating the transport and distribution behaviour of contaminants. These fields of interest also include the interactions between subterranean water and surface water. Therefore, in this volume, the use of tracer techniques in surface water is also described. Due to the complexicity of the problems treated, it is understandable that the authors of this volume belong to such varied disciplines as chemistry, geochemistry, geology, hydrology, and physics. Thanks to the longtime cooperation of the authors, but also to the never ending engagement of Prof. Dr. habil. Werner KÄSS, the present revised volume has been put together.

The contributions on the use of tracers in fissured rocks and surface water could not be finished in time for the German version, due to the serious illness of the respective author, Professor Dr. T.CH. LEIBUNDGUT, Freiburg i.Br. Therefore only a short review of these topics could be included in the 1992 German version of this volume. However, after his recovery, Professor LEIBUNDGUT wrote the sections Glacier water and Surface water.

In the English version the following new sections have been added: 4.4 TRACI, a model for tracing tests (A. WERNER/Karlsruhe); 5.3.3 Test experiments in a highly permeable fault zone (TH. HIMMELSBACH/Bochum); 5.7 Glacier Water (CH.LEIBUNDGUT); 5.8 Surface water (CH.LEIBUNDGUT), and 5.9.4 Partitioning tracing (D.HUNKELER/Zürich). The Section 2.8 Phages was revised by P.ROSSI (Neuchâtel).

Kiel, August 1997
GEORG MATTHESS

Author's Preface

It is certainly no accident that this book was written in a country in which the first scientifically applied tracing tests were conducted. As early as 1869 a tracing test was initiated by the geognost Prof. A. KNOP at the percolation sites of the Upper Danube between Immendingen and Tuttlingen. That test was unsuccessful, but 8 years later more tests followed, which were successful.

In densely populated Southwest Germany with its industrial centres, the high demand for water and the exploitation of new groundwater sources present a constant conflict of interests with regards to expanding settlements, new highways, and industrial areas as well as with the disposal of waste and sewage. The geology of Southwest Germany is manifold and the Geological Survey Baden-Württemberg plans, organizes, determines, and evaluates between 50 and 100 tracing tests yearly with 20,000 up to 25,000 separate determinations.

I want to thank the Geological Survey Baden-Württemberg that I was allowed to make my experience on hydrogeological tracing techniques which I gathered over decades, accessible to the public. My thanks also go to the co-authors who contributed to this book.

Compared to the German edition from 1992, essential extensions have been added and recent literature regarded.

I would like to express my thanks and great praise to Mrs. Dipl.-Hydrol. KAREN SCHNEIDER who has brilliantly coped with the partly very difficult specialized translating work.

Last, but not least, I want to thank my dear wife HANNA whose unremitting effort in procuring the needed literature, in preparing and looking through the German manuscript as well as the English one was essential for the achievement of both books.

Umkirch, August 1997
WERNER KÄSS

Taylor & Francis
Taylor & Francis Group
http://taylorandfrancis.com

CHAPTER 1

Introduction

W. Käss

1.1 EXORDIUM

Hydrological tracing techniques (German: Markierungstechnik, French: traçage) use tracers (German: Markierungsmittel, French: traceur) to follow flowing water. Surface waterways such as rivers, lakes, and ocean currents can be followed, as well as underground waterways. In this field, the most important applications are in groundwater. Thus, this subject is now covered in the series 'Textbooks of Hydrogeology' ('Lehrbuch der Hydrogeologie'). Tracing techniques in surface water are covered here as well.

Tracing techniques address a plenitude of scientific disciplines: geology, hydrology, chemistry, physics, water management, civil engineering, biology, limnology, etc. Therefore, the relevant scientific literature covers many fields and is found in the publications of many different disciplines. A trademark journal for tracing techniques is the journal 'Styrian Contributions in Hydrogeology' ('Steirische Beiträge zur Hydrogeologie'), titled 'Contributions in Hydrogeology' ('Beiträge zur Hydrogeologie') after 1994, published in Graz, Austria by the Hydrogeological Research Union (Vereinigung für hydrogeologische Forschungen). Other noteworthy publications, in which branches of tracing techniques are handled, are: MOSER & RAUERT (1980) 'Isotope Methods in Hydrology', Vol. 8 of this textbook series that covers tracing with isotopes, ZÖTL (1974) 'Karsthydrogeology' and BÖGLI (1980) 'Karsthydrology and Physical Speleology.' Several journals contains summaries of tracing techniques. However, the main focus of these summaries lies in different areas. In 1959, MAURIN and ZÖTL published an extensive representation of the possibilities for tracing in karst regions then. Each of the proceedings published from the International Symposium on Underground Water Tracing (SUWT) conferences from 1966 until 1986 contain references to the advances made in tracing techniques in the introductory chapters. A more detailed report on tracing techniques, which covered mostly groundwater, was written by DAVIS, CAMPBELL, BENTLEY and FLYNN and was published in 1985 by the American Water Well Association. The 'Leitfaden für den Gebrauch künstlicher Tracer in der Hydrogeologie' by PARRIAUX, LISZKAY, MÜLLER and DELLA VALLE (1988) covers only the common tracer properties. In conclusion, the numerous publications, books as well as proceedings, by the Interna-

tional Atomic Energy Agency (IAEA) dealing with isotopes in hydrology needs to be mentioned (comp. Sections 2.11 and 4.4).

Originally, tracing experiments were used to find underground waterways.

In antiquity, the God Mercury used his staff 'Virgula divina seu mercurialis (trepidano)' to open the gates to the underworld.

The library of Ninive has documents about a goddess with a magical rod. During the Middle Ages, the so-called science of the Rhabdomants (dowsers) developed around magical rods. In one BC, the Roman masterbuilder VITRUV taught a method for discovering underground waterways by laying facedown on the ground at sunrise in places where fog occurs.

PLINIUS continued the ideas of VITRUV and taught that underground waterways could be surmised at sites where small insects appear at the surface (TIMEUS 1926).

Underground connections between surface waters have been long supposed in many regions. In ancient Greece the traveling writer STRABO conjectured that the water that seeped underground near San Cozian (Slovenian Karst) fed the Timavo spring located 130 stadia away (PFEIFFER 1963).

PFEIFFER (1963) collected and published a series of further ancient and medieval documents that reported percolating rivers, their underground passage, and their supposed resurgence points. According to STRABO (Geographia, Book VI), there are even two writers, OVID (Book XV) and HERODOT, who wrote about the percolating river Lykos (= Lykus) near Kolossä in the Middle East and its probable resurgence point in the Menderes Valley.

The first certain record of a tracing experiment that was actually carried out is over 1900 years old. The Jewish-Roman writer FLAVIUS JOSEPHUS wrote in circa 90 AD that the tetrarch PHILIPPUS from Trachonitis established the spring source of the Jordan around 10 AD by having fed chaff into Phialo, a circular pond. The chaff reemerged out of the cave spring Panium, which had been considered the source of the Jordan river (Fig. 1). The Phiale Lake is called Berekhat Ram now and lies near

7. Now this lake of Gennesareth is so called from the country adjoining to it. Its breadth is forty furlongs, and its length one hundred and forty; its waters are sweet, and very agreeable for drinking, for they are finer than the thick waters of other fens; the lake is also pure, and on every side ends directly at the shores, and at the sand; it is also of a temperate nature when you draw it up, and of a more gentle nature than river or fountain water, and yet always cooler than one could expect in so diffuse a place as this is. Now when this water is kept in the open air, it is as cold as that snow which the country people are accustomed to make by night in summer. There are several kinds of fish in it, different both to the taste and the sight from those elsewhere. It is divided into two parts by the river Jordan. Now Panium is thought to be the fountain of Jordan, but in reality it is carried thither after an occult manner from the place called Phiala: this place lies as you go up to Trachonitis, and is a hundred and twenty furlongs from Cesarea, and is not far out of the road on the right hand; and indeed it hath its name of Phiala [vial or bowl] very justly, from the roundness of its circumference, as being round like a wheel; its water continues always up to its edges, without either sinking or running over. And as this origin of Jordan was formerly not known, it was discovered so to be when Philip was tetrarch of Trachonitis; for he had chaff thrown into Phiala, and it was found at Panium, where the ancients thought the fountain-head of the river was, whither it had been therefore carried [by the waters]. As for Panium itself, its natural beauty had been improved by the royal liberality of Agrippa, and adorned at his expenses. Now Jordan's visible stream arises from this cavern, and divides the marshes and fens of the lake Semechonitis; when it hath run another hundred and twenty furlongs, it first passes by the city Julias, and then passes through the middle of the lake Gennesareth; after which it runs a long way over a desert, and then makes its exit into the lake Asphaltitis.

Figure 1. Abstract of page 736 from 'Wars of the Jews' by FLAVIUS JOSEPHUS, Book III, Chapter 10, Section 7. Translated by WHISTON(1957).

Banyas, the ancient Caesarea Philippi. Israeli geographers however call the Berekhat Ram a crater lake (Maar) and since chaff is not a very good tracer, the positive result of PHILIPPUS's experiment is doubted (MAZOR 1976, ZÖTL 1989). RÖGNER however interprets the Berekhat Ram as a karst cave-in, which happened in the underlying Cretaceous chalk and carried through to the surface (1979).

The well-known percolation of the Upper Danube in Germany was described back in 1719 by the Prelate F.W. BREUNINGER, who wrote that the river noticeably lost water at the 'Kalch-Steinen' (= lime stones). He correctly surmised that the water that percolated between Immendingen and Möhringen reemerged at the Aach spring.

In the 17th century, just as PHILIPPUS had done in 10 AD, the Parson M.J. MAYER conducted tracing experiments in the Swabian Alb, Southwestern Germany: Besides chaff and sawdust that were introduced into the doline, only a few days after a thunderstorm, the Blautopf Karst spring carried muddy water.

Thus, for quite a while now, people have wondered how they could follow underground waterways with positive proof. Chaff and sawdust were used as a first resource as well as thunderstorms in distant catchment areas of karst springs, as already mentioned. In the summer of 1924, such a thunderstorm was recorded in the Swabian Alb on the NW-border of the Blautopf catchment. After 24-30 hours, the Blautopf spring, 14 km away, carried muddy water (SIHLER 1929). These more or less suitable means have been used for quite a long time. For example, young eels with notched tails were introduced into the Reka percolation site near San Cozian, and they were then observed in the Timavo spring. Even flotation devices such as wooden balls, cork pieces and so on were used up to the 1950s in karst channels, although it had to be assumed that siphons would retain them.

The first groundwater tracing experiment, known to the author, which was scientifically carried out and semi-quantitatively recorded, was carried out in the northern Swiss Jurassic platform. In the summer of 1872, almost one fifth of the population of Lausen in the Ergolz Valley, developed typhoid. The hygienist HÄGLER, from Basel, discovered that the first cases of typhoid had occurred unbeknownst in the early summer of the same year in an out of the way farm south of Lausen. The creek that flowed by the farm also carried away the sewage from the farm and percolated a short distance further downstream in a sink hole from the year 1862. The underground is composed of a thick layer of oolitic limestone (Hauptrogenstein), which borders to the west on a fault against Liassic marl. Back then, Lausen's public water supply came from the oolitic (Hauptrogenstein) talus slope on the south flank of the Ergolz valley (Fig. 2). The mining director GLENK supplied the salt for the tracing test on 7 September 1872: 2045 Maas (ca. 3070 l) with a salt content of 18 hundredweights and 18 pounds (ca. 9 kg) from the nearby Saltworks Schweizerhalle. After one day the water supply showed a strong reaction to chloride with silver nitrate. Noticeable was also that only those villagers whose water came from the village water supply developed typhoid. In those homes, which had their own dug wells, no one developed typhoid. After the salt tracer test, a mixture of 50 hundredweights of flour was also poured into the sink hole. However, starch could not be detected in the water supply (HÄGLER 1873).

The best known river percolation in Middle Europe is the Upper Danube in southwestern Germany. The Danube is hardly on its way from its two spring sources, according to the saying:

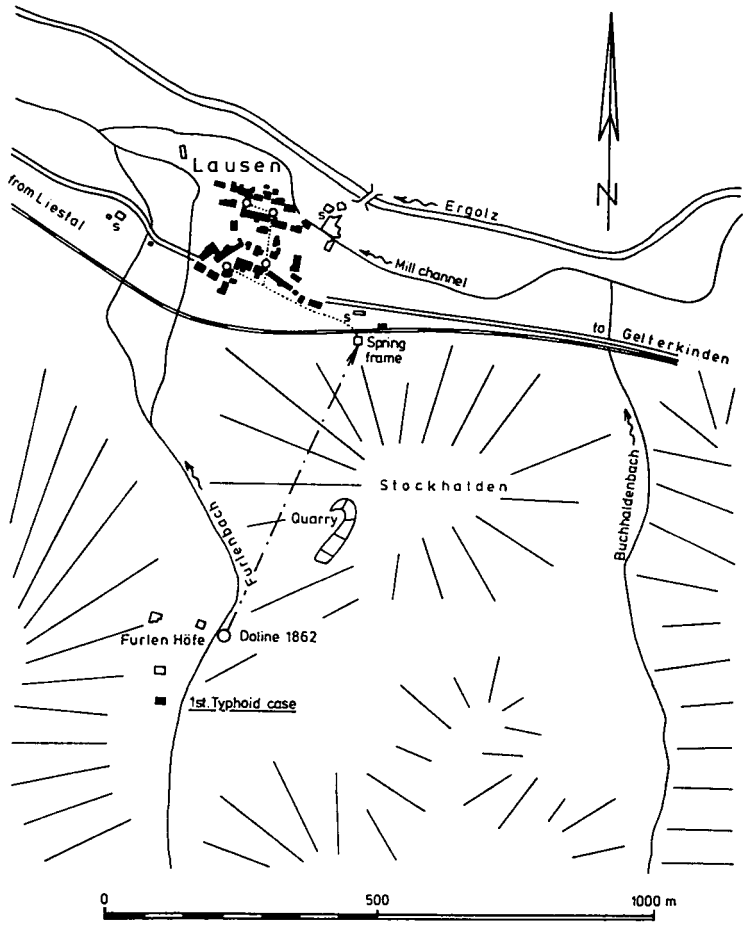

Figure 2. Site of the 1872 salt tracing test at the time of the Typhoid epidemic in Lausen (Canton Baselland) after HÄGLER (1873). Dotted/dashed line: path of the infiltrating water from the doline from the year 1862 to the spring frame Lausen. Dotted line: water supply pipelines from the spring frame to the village wells (circles). Filled-in building symbols: Typhoid cases. Not filled-in building symbols: no typhoid cases in homes with own dug wells (S).

'Brigach and Breg start the Danube on its way'
('Brigach und Breg bringen die Donau zuweg')

when after approx. 30 km the river loses its water in minimal precipitation times to the karstified ground. When industrialization began in the last century, water power was the main energy source. The already quoted BREUNINGER verified that the water losses at the swallow holes had already been observed at the beginning of the 18th century and that they had tried to divert the Danube around them. However, the water losses increased instead and the disputes over the Danube's water intensified. The main infiltration points as well as the assumed resurgence point lay in grand-duchy Baden, whereas the industrial area near Tuttlingen that was affected the most by the

water losses was in the kingdom Württemberg. Both sides started fighting: Baden did not want to change the natural infiltration due to the assumed resurgence in the Aach and possible problems there, in the Kingdom of Württemberg, the water dependent industries needed the water. In the summer months the sanitary situation in Tuttlingen was unbearable. Therefore, they tried to plug up the Danube's swallow holes in the main infiltration site, 'Brühl,' between Immendingen and Möhringen with twigs and loam. Not only did that not work, but it was forbidden under penalty of a heavy fine by the Baden County court in Engen. Since the fight could not be left unsettled, the jurisdiction decided to try to obtain legal proof about whether the infiltrating Danube water reemerged in the Aach spring, the largest spring in Germany. An Aach riparian, the spinning-mill owner TEN BRINK in Volkertshausen, most likely had connections to a dye factory. In 1869 he inserted 14 kg of aniline red (probably parafuchsine = pararosaniline, C.I. 42,500, CAS: 569-61-9) in the Danube percolation. The test failed however, due to the sorption properties of aniline red (KNOP 1875). Therefore, the grand-duchy Baden's Ministry of Commerce commissioned the geognostic Prof. A. KNOP, from Karlsruhe, with the demonstration. In his tracing experiment in September 1877 he wanted to cover all his bases and used three tracers: 12 hundredweights of shale oil from Glasgow, 200 hundredweights of salt from the saltworks Dürrheim, and 10 kg sodium fluorescein. The latter was again donated by TEN BRINK. This time all three tracers reappeared in the Aach spring after two days: Glasgow shale oil recognized by the heavy creosote taste, salt proven by an increase in chloride content from 8.6 to 27.4 mg/l, and sodium fluorescein shown by a 'splendid green illuminating' water (KNOP 1878).

Tracing the Danube infiltration can be thought of as the start of the tracing techniques:

The salt tracing test on 24 September 1877 was the first tracing test to be carried out quantitatively. KNOP determined the salt content of the Aach spring hourly and used the concentration curve to calculate a return of 9330 kg salt. Repeat calculations by Gg. WAGNER (1961) and by the author confirmed that, taking contamination and the wet content of the salt into account, almost the entire amount of the introduced salt came out again.

On 9 October 1877 uranine was first used as a tracer and with visible, glowing results.

From then on sodium fluorescein began its victory march that has continued until today. This unique tracer was especially recognized and used in the large European karst regions. In France, the names DIENERT, MARTEL and MARBOUTIN deserve to be mentioned. Fluorescopes were developed there to at least quasi-quantitatively determine the dye content. Scientists also worked on methods to concentrate uranine. The main areas under investigation then were mostly in the Middle France cretaceous karst. Belgian scientists were also working on karst tracing techniques.

It has almost been forgotten that from 16 June to 15 December 1903, four conferences were held by the Belgian Society for Geology, Palaeontology and Hydrology about tracing with uranine in karst regions (VAN DEN BROECK 1904).

At the same time, tracing experiments with bacteria were also carried out to investigate the possible infection paths in ground water. E. PFUHL, a military doctor in Strassburg, carried out drift tracing experiments in the pore water aquifer of the Upper Rhine Valley using *Serratia marcescens* bacteria and uranine (PFUHL 1896, 1897,

1899). In Turin, ABBA also used *S.marcescens* as a tracer. In contrast to PFUHL, he took the unsaturated zone into consideration, i.e. he introduced the *S.marcescens* bouillon at the surface, where in 1.5-2.5 m depth the infiltration gallery for Turin's water supply was located (ABBA et al. 1899).

However, in the area near Krain, which gave the karst its name, systematic experiments of the underground waterways were also being conducted. As mentioned above, the travelling writer STRABO had written in antiquity about the underground passageway of the Reka to the Timavo springs. Worries about Trieste's drinking water, which tapped the karst spring Aurisina on the Adriatic coast, motivated as early as 1891 the first targeted investigations as to the course and length of stay of the underground Reka River (F. MÜLLER 1891). Further investigations in that area were carried out by BOEGAN, BERTARELLI and TIMEUS until into the late 1920s. These researchers used uranine as a tracer just as F. MÜLLER did, they also tried to carry out combined tracing tests and sometimes had pioneering ideas. They deliberated about what other tracers would be suitable for experiments in the Triestine Karst.

The novel tracers used as early as the first decade of this century were lithium chloride, strontium chloride and radioactive pitchblende. Fuchsine was also used with success, whereas flotation devices did not prove to be viable tracers (BOEGAN 1906, TIMEUS 1910, BERTARELLI & BOEGAN 1926). BERTARELLI and BOEGAN wrote, rather as an aside, that they had also used club moss spores.

The Swiss hydrologist SCHARDT conducted very many tracer tests in the Swiss Jurassic. As an example, he investigated the catchment of the Orb spring in the Canton Waadt. In the 1920s, he instructed a doctoral candidate of his to conduct experiments in the area between the Danube and the Aach spring (SCHAUFELBERGER 1929). To examine the spring water samples for uranine, the fluorescope from SCHARDT was used. Such instruments made at least a quasi-quantitative uranine concentration determination possible. Besides that, the enrichment method using ether-alcohol extraction in acidic water samples was used and developed further. Between the two world wars, other tracers besides uranine and salts were used such as phenol, ammonium sulfate, and bichromate.

After WW2, tracing techniques developed rapidly. In 1950/1951, E.KNOP was the first to report using radioactive tracers, here iodine-131. In the first cases using radioactive isotopes, much higher activities were used, which would not be allowed nowadays. The somewhat more time-consuming, but completely harmless application of activated isotopes as tracers was reported in 1962 in Athens (DIMITROULAS et al. 1963, 1964)

Meanwhile, A. MAYR rediscovered the spore drifting method in 1952 (MAYR 1953), which was further implemented and used in hydrogeological investigations in the Austrian upper alpine karst region by V. MAURIN and J. ZÖTL. Soon the Institute for Mineralogy and Technical Geology at the Technical College and the Association for Hydrogeological Research in Graz became the main centres for karst water tracing research. In 1959 a chemist, DECHANT, was able to dye the club moss spores with different colours. As a result, several sites in hard to reach alpine regions could be injected. Plankton nets were used to collect samples at the presumed reemergence sites. Thus, a high recovery rate and therefore a high level of certainty was assured. Drifting spores were soon used in many other karstified areas.

At the same time, great advances were being made in measurement technology. At the end of the fifties, the photo-electronic multipliers in the optical instruments replaced the low resolution photoelectric cells and hard to handle photographic plates. Water analysis methods became better and more exact. As a result, the swift analysis of a large number of water samples could be carried out: a prerequisite for a comprehensive quantitative evaluation of tracing tests. Rational flame photometry made groundwater tracing with alkaline salts possible. The first use of potassium salt and the subsequent flame photometric analysis of potassium was in 1964 and 1965 (KÄSS 1966a, 1967b). Using potassium salts for tracing tests has the advantage that much less needs to be used in comparison to rock salt, because groundwater normally has fewer potassium ions than sodium ions.

Even more revolutionary was the possibility of carrying out exact fluorescence measurements using the new optical-electronics. At the end of the fifties/beginning of the sixties, the author investigated the physico-chemical and chemical properties of uranine and completed as early as 1960 routine quantitative uranine analyses for tracing tests at the Geological Survey of Baden-Württemberg (KÄSS 1964).

The manifold geological structure of the province Baden-Württemberg put high demands on the tracing techniques used. This led to new methods and techniques, especially related to the time-consuming collection of the water samples, which were necessary for a thorough comprehension of the concentration curves. Thus, ways were sought to introduce more than one tracer into a system at a time. The second fluorescent dye, eosin, was used by the author on 14 August 1962 in the Ulmer Alb in SW-Germany together with uranine, sodium chloride and lithium chloride.

During the German Geological Society's spring conference in Essen in 1964, while talking to V. MAURIN, the author proposed a conference on ground water tracing to be held among the experts in the subject. This suggestion was taken up by J. ZÖTL and V. MAURIN and in the spring of 1966 a conference was held in Graz on 'Fachtagung über die Anwendung von Markierungsstoffen zur Verfolgung unterirdischer Wässer.' What was at first planned as a symposium for a few experts grew to an international conference with 125 participants. During the conference, tracing tests in the karst regions nearby were carried out by several participants. The results were, as far as possible, displayed and discussed during the conference.

A review of the groundwater tracing conferences held up to now is presented, starting with the conference held in 1903, see below.

Discussion sur la Vitesse de Propagation des Eaux souterraines et de la Fluorescéine dans les Canaux et Fissures des Terrains calcaires/Brussels/Belgium (16&30 June, 14&28 July, 20 October and 15 December 1903)

Proceedings: Ernest VAN DEN BROECK 'L'étude des eaux courants souterraines/Eaux alimentaires en régions calcaires par l'emploi des metières colorantes (Fluorescéine)'. Bull.de la société belge de Géologie de Paléontologie et d'Hydrologie; XVII: pp 239-635, I-IV (43 lectures and numerous discussion remarks), Brussels 1904.

1. Fachtagung über die Anwendung von Markierungsstoffen zur Verfolgung unterirdischer Wässer/Graz/Austria (28 March-1 April 1966), Participants: 125 from 13 countries.

Proceedings:

I. Lectures: Steir. Beitr. Hydrogeol. 1966/67: pp 11-328 (31 papers with discussion remarks) Graz 1967.

II. Accompanying Tracing Tests: 'Vergleichende Markierungsversuche im Mittelsteirischen Karst 1966'. Steir. Beitr. Hydrogeol. 1966/67: pp 331-404, Graz.
- Lurbach cave system near Semriach (17 km north of Graz), Lurbach percolation with Iodine-131, Tritium, Manganese-EDTA-complex for activation analysis, brown *Lycopodium*-spores; Katzenbach green *Lycopodium*-spores, Ammoniumbromide for activation analysis; ice pit-sinkhole with blue *Lycopodium*-spores.
- Feliferhof sinkhole-Bründl spring in the Buchkogel region (8 km southwest of Graz) with surfactants, tritium, chromide-51 as EDTA-complex, sodium chloride, potassium chloride, sulforhodamine G extra, violet *Lycopodium* spores.

Excursions:
- 28 March 1966: Test area Lur cave system,
- 29 March 1966: Test area Buchkogel region aquifer 'Schachenwald', Water works Graz-Feldkirchen.

Short report: PINNEKER, E.W. & G.B. PALSCHIN (1966): Geology and Geophysic: pp 137-139, Nowosibirsk (russ.)

2. Internationale Fachtagung zur Untersuchung unterirdischer Wasserwege mittels künstlicher und natürlicher Markierungsmittel/Freiburg/Br., Germany (10-14 October 1970); 162 Participants from 9 countries.

I. Proceedings: Geol.Jb. C2: 382 p., Hannover (27 papers and 2 Excursion reports).

II. Accompanying tracing tests (from the second conference onward, the traces were carried out before the actual conference and the results presented at the conference as printed papers):
- Danube percolation/Aach spring (70 km east of Freiburg) with uranine, sulforhodamine G extra, sodium chloride, potassium chloride, brown and green *Lycopodium* spores, lanthane and ammonium bromide for activation analysis, limonene, and isobornylacetate as aromas, a 'hard' and a 'soft' surfactant, chromium-51, *Serratia marcescens*.
- Pleistocene of the Riegeler passage (18 km north of Freiburg) with uranine, *Serratia marcescens*, tritium, iodine-131, 'hard'surfactants, eosin, potassium chloride.

Test reports:
BATSCHE, H. et al. (1970): Kombinierte Karstwasseruntersuchungen im Gebiet der Donauversickerung (Baden-Württemberg) in den Jahren 1967-1969). Steir. Beitr. Hydrogeol. 1970: pp 4-165, Graz.
KÄSS, W. (1972): Grundwassermarkierungsversuche im Pleistozän der Freiburger Bucht. Geol.Jb. C2: pp 119-151, Hannover.

Excursions:
- 11 October 1970: Danube percolation site near Immendingen and Fridingen-Aach spring,
- 13 October 1970: Test area in Pleistocene of the Breisgauer Basin near Riegel-Breisach.

3rd International Symposium of Underground Water Tracing (SUWT)/Bled/Slovenia (27 September-1 October 1976), 109 Participants from 11 countries.

I. Proceedings: Papers 3rd Intern.Symp.Underground Water Tracing (3.SUWT) I: pp 1-213, II: pp 215-396, Ljubljana 1976 (31 lectures).

II. Accompanying tracing tests:
- expanded karst-catchment area of the Ljubljanica (southwest of Laibach) with uranine, rhodamine FB, green, brown, red, and blue spores, tinopal CBS-X, hardsurfactants, LiCl, indium, eosin, amidorhodamine G extra, chromium-51, and KCl.

– Pore-groundwater trace in Savinja valley west of Celje with uranine, eosin, KCl, and *S.marcescens.*

Test report: Markierung unterirdischer Wässer – Untersuchungen in Slowenien 1972-1975. Steir. Beitr. Hydrogeol. 1976: pp 7-257, Graz 1976 and Underground Water Tracing – Investigations in Slowenia 1972-1975. 312 p., Ljubljana 1976.

Excursions:
– 30 September 1976. Ljubljanica-springs-Bistra-Idria-Vipava-Postojna,
– 1 October 1976: Planina-Lake Cerknica-Rak percolation.

4. SUWT – Internationale Fachtagung über die Anwendung von Tracermethoden in der Hydrologie/Bern, Switzerland (28 September-3 October 1981), 160 Participants from 16 countries.

I. Proceedings: Tracermethoden in der Hydrologie; Beitr.Geol. Schweiz-Hydrologie 28(I): pp 1-236, (II): pp 237-552, Bern 1982 (46 lectures).
II. Accompanying tracing tests:
– Neuenburg Jurassic with uranine, rhodamine B, eosin, sulforhodamine G extra, tinopal, NaCl-brine, KCl, *S.marcescens*, blue and red spores,
– Pleistocene plain in Langeten valley, Canton Bern, with uranine, eosin, tinopal, NaCl-brine, indium, borax,
– High alpine karst in Hinter Muota valley, Canton Schwyz, with uranine, eosin, rhodamine B, amidorhodamine B extra, tinopal, NaCl-brine, LiCl, hard surfactants, red, blue, green, and orange fluorescing *Lycopodium*-spores, *S.marcescens*.

Tests reports:
– Karsthydrologische Untersuchungen mit natürlichen und künstlichen Tracern im Neuenburger Jura (Schweiz). Steir. Beitr. Hydrogeol. 1980: pp 5-10, Graz 1980.
– Tracerhydrologische Untersuchungen im Langetental (Schweiz). Steir. Beitr. Hydrogeol. 1981: pp 5-123, Graz 1981.
– Hydrologische Untersuchungen im Karst des hinteren Muotatals (Schweiz). Steir. Beitr. Hydrogeol. 1981: pp 125-264, Graz 1981.

Excursions:
– 29 September 1981: Neuenburg-Val de Travers-Les Verrières,
– 30 September 1981: Langetental,
– 2/3 October 1981: Muota valley, Hölloch cave.

5th SUWT – International Symposium on Underground Water Tracing/Athens, Greece (22-27 Sept. 1986), 104 Participants from 15 countries.

I. Proceedings 5th Int.Symp. Underground Water Tracing. IGME – Institut of Geology and Mineral Exploration, Athens, Greece (Eds.): 476 p., Athens 1988 (45 lectures).
II. Accompanying tracing tests:
– middle to eastern peloponnesusian Karst with uranine, pyranine, rhodamine B, naphthionate, eosin, tinopal, NaCl, LiCl, KCl, chromium-51-EDTA-complex, indium-EDTA-complex, blue and red spores, orange fluorescing and blue fluorescing spores, G-, f_2- and H_5-coliphages.
– fissure groundwater investigations in the Swiss Molasse with uranine, eosin and geophysics.

Test reports:
– Karst Hydrogeology of the Central and Eastern Peloponnesus (Greece). Steir. Beitr. Hydrogeol. 1985/86, 301 p., Graz 1986.
– Proceedings 5th Int.Symp.Underground Water Tracing. Test area of the Int. Working Group. Fissured Aquifer in the Swiss Molasse: pp 389-421.

Excursions:
– 24 September 1986: Marathon-Dam,
– 26/27 September 1986: Test area in Middle and Eastern Peloponnesus.

6th SWT – International Symposium on Water Tracing/Karlsruhe (21-26 Sept. 1992), 196 Participants from 28 countries.

I. Proceedings: HÖTZL, H. & A. WERNER (eds) (1992): Tracer Hydrology. 464 p., Rotterdam/Brookfield (A.A. Balkema) (78 papers).
II. Accompanying tracing tests:
– Lake Bled, Slovenia,
– Porous aquifers of the Emme (Canton Bern, Switzerland) and of the Upper Rhine (Merdingen, Baden-Württemberg, Germany),
– Fissured aquifer in the granite (Southern Black Forest, Germany),
– Lurbach Karst System (Styria, Austria).

Test report:
Transport Phenomena in Different Aquifers (Investigations 1987-1992). Steir. Beitr. Hydrogeol. 43, 283 p., Graz (1992).

Excursions:
– 23 Sept.: Kraichgau,
– 25/26 Sept.: Southern Black Forest-Grimsel/Switzerland.

7th SWT International Symposium on Water Tracing/Portorosz (Slovenia) (26-31 May 1997), 146 Participants from 17 countries.
I. Proceedings: KRANJC, A. (ed.) (1997a): Tracer Hydrology 97. 450 p., Rotterdam/Brookfield (A.A. Balkema) (63 papers).
II. Accompanying tracing tests: Karst hydrogeological investigations in South-Western Slovenia (1997): Acta Carsologica, XXVI/1, 388 p., Ljubljana.
III. Field Guide of Karst in Slovenia: A. KRANJC (ed.) (1997b): Acta Carsologica, XXVI/1, 98 p. (Supplementum), Ljubljana.

The Association of Ground Water Scientists and Engineers held a conference in Houston/Texas on 30 October/1 November 1989 about tracing techniques, which were tailored to fit North American needs.

Ever since the first international conference in 1966 in Graz, Austria, further developments in tracing techniques have been rapid. The author showed that two fluorescence dyes, e.g. uranine and eosin, could be used together in a tracing test at once. However, the necessary instruments to measure the true concentration of two different components, which also interfered with each other, were not available then. Therefore, mathematical and graphical calculations were necessary to determine the correct concentrations. Later, H. BEHRENS introduced the double-scanning method to separate xanthic dyes in the registration diagrams. In Erlangen, FRG, later in Würzburg, FRG, W.A. SCHNITZER tried to develop further tracing methods. He conceived ideas for using surfactants, aromas, and sound waves, but although his methods were ingenious, they only served to complement reliable tracers.

In the fifties, the single bore hole method was developed in Vienna, Austria and Munich, FRG (MOSER et al. 1957, MAYRHOFER 1967) to determine the groundwater flow direction and speed in a single bore hole. These were starting points for devel-

oping tracing techniques for the up to then neglected, yet just as important as karst aquifers, pore water aquifers.

Further developments in the tracing techniques occurred through the usage of bacteriophages (1968) and due to the improved colouring of spores with fluorescence dyes (1978).

During the discussion about the test results from the first international conference in 1966 in Graz, Austria, the experts decided that only using tracers to investigate groundwater flow, was not enough to fully understand the groundwater flow problems in an investigation field. Therefore, for the second international conference, a research program was set up for the test area Danube percolation/Aach spring, which not only used tracers, but also long term observations with naturally occurring isotopes and the chemical properties of the groundwater. These marginal considerations and conditions were continually developed in the following conferences and their accompanying tracer tests. As a result, research programs without a comprehensive acquisition of the isotope, hydraulic, hydrometeorological, chemical and bacterial relationships present in the groundwater system are unthinkable. Additionally, according to the geological-hydrological conditions, geophysical, e.g. VLF and virological investigations can be carried out.

In past years, halogen hydrocarbons have also been used as tracers (e.g. THOMPSON et al. 1974). However, although these can be identified with a high sensitivity, their usage will remain restricted due to the complicated analysis and environmental considerations.

1.2 NOMENCLATURE AND DEFINITIONS

Tracing tests can be carried out in two ways. Either:

– Tracers are introduced into the water system that is under investigation, or

– Naturally occurring constituents or other properties are determined, which produces the same result.

The first case uses *artificial tracers*, the second case *'natural' tracers*.

1.2.1 *Artificial tracers*

This method is by far the older of the two. A substance is introduced into the water system that can be recognized and identified at another site. Such substances need to fulfil the following requirements:

– Absent in the natural waters or present only in low concentrations,

– Good quantitative analysis with a high sensitivity,

– Harmless for man, animals, and plants,

– Good water solubility or dispersion properties,

– A good resistance to chemical, biological or physical attacks; i.e. stable with regards to oxidating, reducing, acidic, or basic reactions, nonbiodegradable as well as resistant to light and temperature,

– No interactions with the flow medium; i.e. free from sorption and ion-exchange properties,

– Economical with regards to its buying, using and analysis.

There is no *one* ideal tracer. For example, uranine has for the most part, all of the above mentioned characteristics. However, it cannot be used quantitatively in surface waters due to its sensitivity to light. Furthermore it has sorption properties in acidic media. Other substances have other advantages and disadvantages.

When using artificial tracers, it is important to obtain a concentration-time-curve from the sample sites, also simply called a concentration curve (Fig. 3). The concentration is plotted on the ordinate and the time on the abscissa. The three times, $t_1 - t_3$, are very important in evaluating a tracing test. How this is carried out is handled in Chapter 4 'Evaluation of Tracing Tests.'

Due to the different concepts that are connected with the passage times, here are a few clarifying definitions:

t_0: The time of injection. With injections that cover a period of time, t_0 is the injection begin.

t_1: The first detection of the tracer. The first proof of the tracer is dependant upon the analytical sensitivity and is therefore not identical with the first appearance of the tracer. Since the rise in concentration happens quite rapidly at first, t_1 can usually be extrapolated. The first detection of the tracer is very important, especially from a hygienist's viewpoint. The time t_1 is the time needed by the tracer particle that took the shortest path.

The actual velocity can be calculated using the length of the flow path. Due to possible confusion with the actual velocity at the concentration maximum, this velocity is not called the maximum velocity, but rather the 'fastest' velocity (v_{a1})

t_2: Time at the concentration maximum (c_{max}). In general, this time is easily recognized; however, sometimes it must be interpolated. It is independent of the analytical method and its sensitivity. The resulting dominating velocity is also sometimes called the intensive or most frequent velocity, although these terms are not as useful. In the field more than one concentration maximum can occur, due to changing hydraulic conditions or when the underground flow paths separate (Fig. 4). The concentration curve's apsis is at t_2.

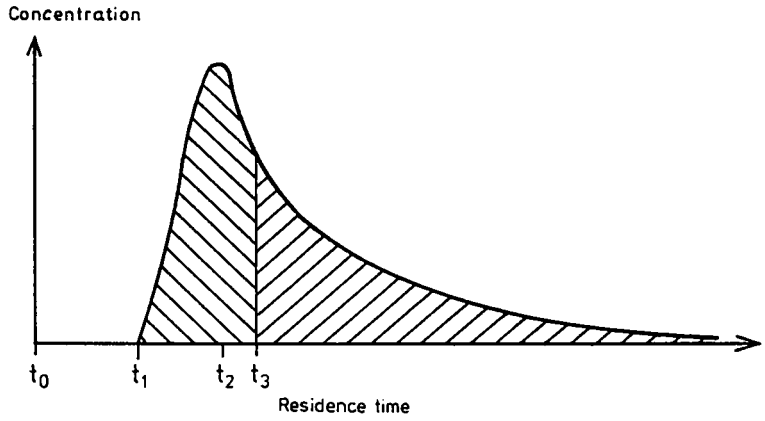

Figure 3. Ideal concentration curve from a tracing test. t_0: injection time; t_1: first arrival time; t_2: time at highest concentration; t_3: half-life time. In cases with equal flow, the area under the curve to the left and right of t_3 must be equal.

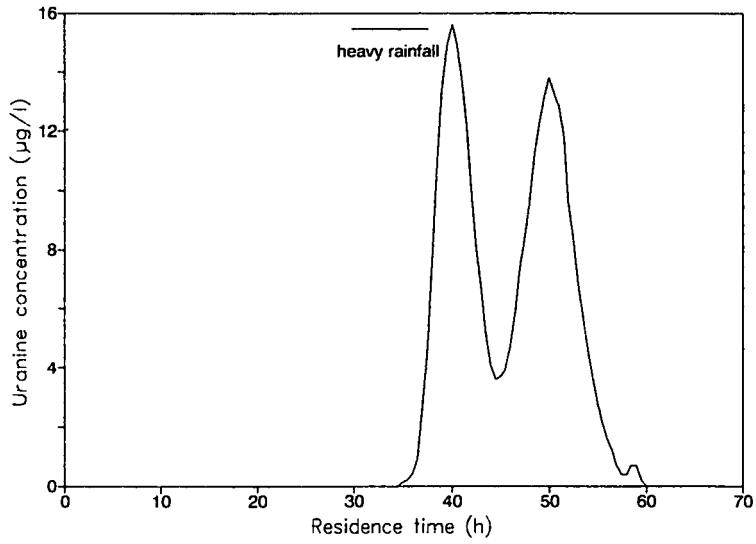

Figure 4. Concentration curve with more than one maximum at the tracing test Danube percolation/Aach spring (SW-Germany) from December 1978. Excessive precipitation fell during the tracing test, which triggered the second maximum.

t_3: Half-life time, which is determined from the concentration curve. Normally, it is reached when the concentration falls between two-thirds and half the maximum concentration. The half-life time is defined as the time where the half the tracer has reappeared at the sampling sites. Possible changes in the flow volume need to be considered in the calculations. Other calculated terms are the average velocity, v_a, and its corresponding concentration, (c_m), also called 'concentration centre' or 'half load'.

t_4: Last detection time. As with the first detection, this term is critically dependent upon the analytical sensitivity. In many cases the tracer can also reappear in the aquifer and observation sites after a heavy rainfall.

Beyond the half-life time, which assumes an even water flow over the entire tracing test, sometimes the *centre* of the concentration curve is calculated. This is determined by integrating over concentration and time for each point of the concentration curve. The centre time is after t_3 and is only calculated for cases with two or three dimensions or for sorption. Due to the analytical uncertainties towards the end of the curve, its accuracy is low, however it has a larger impact than initially.

The following table provides a review of the above terms:

Point of time	Concentration	Flow velocity
t_0 input	–	–
t_1 first detection time	Detection limit (c_E)	Fastest flow velocity (v_{a1})
t_2 highest concentration	Maximal conc. (c_{max})	Dominating f.v. ($v_{a\,dom}$)
t_3 half-life time	Half load (c_m)	(Median) flow velocity (v_a)
t_4 last detection time	Detection limit (c_E)	–

1.2.2 *'Naturally occurring' tracers*

The phrase 'naturally occurring' is not completely correct. Unintended tracers, which were introduced by mankind, also fall into this group. Such cases can happen during accidents, e.g. as when 6500 hl Absinthe and Brandy leaked during a fire near Pontarlier and reemerged in a spring 10 km away. Groundwater pollution due to halogen-hydrocarbons or waste sites and thermal wastes also fall into this category, as well as unintended changes in the microbiologoical stock of a water body.

However, the most important group of naturally occurring tracers are the natural chemical constituents of the water, as well as its isotope content. Important results can be determined from the naturally occurring contents as well as from those changed by civilisation.

1.3 APPLICATION AREAS

Hydrological tracing techniques are used in almost all water bodies. The best overview for its applications are the following questions:

Where to?
It needs to be established, where the groundwater flows to, which has been marked at one single spot. To do this, all possible reemergence points need to be analysed for the tracer. One single tracer is sufficient.

Examples: Possible consequences from a discharge, building permits.

From where?
The point in question here, is to establish from where *one* certain water body gets its water. To do so, several sites must be simultaneously injected with different tracers or the same tracer must be used several times, with the tests spaced adequately apart. The first method is the preferable to the second, because it takes place within the same certain hydrometeorological state and is less time and expenditure consuming. To round up the hydrogeological picture, however, not only the possible reemergence points need to be observed, but rather the neighbouring points also.

Examples: Planning water protection zones, establishing the catchment area of a spring.

Whether?
The question here is a possible hydrological connection between two points. It needs to be established whether water from point A flows, or can flow, to point B. It is sufficient to use one tracer at one injection point and one observance point.

Examples: Legal proof whether a percolating pollutant from property A impairs property B, bank filtration determination.

How?
A comprehensive scrutiny is often necessary to clarify hydrological questions, which often occur with water prospecting measures. The results from tracing tests can contribute to establishing the water flow, not only according to direction and speed, but

also in determining further hydraulic parameters such as dispersion, porosity, hydraulic conductivity etc. Often further inquiries regarding the chemical, isotope, and petrographical nature are necessary.

Examples: Water prospecting in pore or joint groundwater, scientific investigations of an aquifer.

How much?

Quantitative determinations as to the flow of surface or groundwater demand the highest stability for the tracers during the tests. In many cases, artificial and natural tracers allow an exact determination of the flow volumes. Most likely the most important application is in the discharge measurement of surface waters through deliberate marking with a tracer, followed by an analysation of the resulting concentration curve at a site, where an even distribution of the tracer over the entire cross-section of the water body is attained. Other methods allow the determination of the bank filtration percentage of the nearby wells with the aid of tracer injection in the receiving stream or with the help of naturally occurring constituents, which must have different concentrations in the receiving stream and groundwater. If the water from a spring or source comes from different catchments, isotope or chemical investigations can ascertain the percentage of the different waters.

Examples: Determination of the flow volume of a spring or a river discharge, establishing how quickly glacial melt water reaches the glacier outlet, quantitative dam leakage measurements.

Which means and methods used in each case need to be of course decided in each individual case. In general, larger projects need extensive preliminary investigations, such as:

- Chemical water analyses,
- Precipitation, evaporation, and discharge measurements,
- Isotope analyses,
- Data collection as to land usage,
- Geological, hydrogeological and soil mapping,
- Geophysical investigations.

Taylor & Francis
Taylor & Francis Group
http://taylorandfrancis.com

CHAPTER 2

Tracers

The artificial and naturally occurring tracers, which are available for tracing in water bodies can be classified into the following groups:

- Artificial tracers (2.1-2.10);
- Water soluble tracers (2.1-2.4),
  dyes (2.1),
  salts (2.2),
  surfactants, aromas, and other chemicals (2.3),
  active and activation analytical isotopes (2.4);
- Particulate tracers (2.5-2.10),
  club moss (*Lycopodium*) spores (2.5),
  fluorescent microspheres (2.6),
  bacteria (2.7),
  bacteriophages (2.8),
  geobombs (2.9),
  other particulate tracers (2.10);
- Naturally occurring water constituents (2.11-2.14),
  environmental isotopes (2.11),
  environmental chemicals (2.12),
  environmental organisms (2.13),
  physical environmental influences (2.14).

These tracers are of course not all used to the same degree. The fluorescent tracers, as the most often used in tracing techniques, are written about the most, whereas, e.g. geobombs, can be described in few words.

Detection limits

Detection limits for the water soluble tracers are reached when the measured values for the tracer no longer significantly differ from the background levels. Background levels are measured either physically or chemically. An example of a physical method is the opto-electronic measurement of fluorescent materials. Here, the intensity of the fluorescence excitation of the dye-free samples and the increase need to be large enough to register a signal. An example for a chemical analysis method is the determination for chloride during salt tracer tests using sodium chloride as a tracer. Since there are no water bodies that are completely free of chloride ions, an increase

in chloride needs to be significantly over the background chloride level, to be a positive proof for the tracer.

When particulate tracers are used, the appearance of one single piece can be proof enough for a hydrological connection. Many drifting materials do not occur naturally, such as dyed club moss spores or microspheres.

Single finds of bacteria or bacteriophages cannot always be used as positive proof, since they can occur just as well in nature. *Serratia marcescens* for example, are not normally found in water, yet these bacteria are found in routine bacteriological drinking water analyses, in approximately every thousandth sample. Bacteriophages occur similarly in water samples, yet they are even rarer in water bodies than bacteria. Furthermore, bacteriophage analyses in groundwater often require considerable time-consuming efforts with enrichment methods using several litres of sample water to be able to use statistical methods.

If the results of the normal investigations do not produce a satisfactory breakthrough curve, sometimes an enrichment measure must also be carried out. Such measures are available for a few tracing methods, such as fluorescent tracers, salts, and isotopes. However, it must be remembered that such enrichment methods are labourious and time-consuming and only for use in special cases.

2.1 DYES

W.Käss

Dyes, which are still visible or measurable when very diluted, are suitable as tracers, as long as they have water soluble properties.

In 1864, the Triestine, P. KANDLER, presented the first stimulus for dyeing water; he suggested dyeing the Reka sinkhole with the completely water-insoluble dye indigo. To illustrate his needs, Guido TIMEUS from the year 1911 is cited:

'...The first investigations about the connection between the upper and lower Timavo springs were made at the end of the 16th century by the Father IMPERATI, who lived in the castle Duino, by using floating articles and exotic seeds. After this test, others took place, also using floating articles, starch, or seeds, yet never dyes. A manuscript in the possession of the diplomatic archives in Trieste describes, that in 1864, the Triestine historian Peter KANDLER first proposed dyeing the water as a hydrological investigation. He wrote: I have proposed and demanded, that the underground waterways be investigated by dyeing all the surface waterways and lakes of Trebiciano, San Cozian, San Maria di Cacitti and Wippach blue. These dye experiments could be of use to Istria and could explain the whole subterranean drainage system of the karst in Istria, Croatia, Dalmatia, Herzogewina and contiguous Greece, i.e. of all the areas that show the same phenomena. Thus, already in the year 1864, the great Triestine pointed hydrology towards the using dye to trace water.'

In the year 1869, A. KNOP tried in vain to dye the percolating water of the upper Danube with aniline red (most likely pararosaniline). After the discovery of fluorescein, it was soon realized that dyes with fluorescent properties were better for tracing water than those without. This is due not only to their better recognizability, but also, in general, to the lesser sorption properties of fluorescent dyes.

2.1.1 *Fluorescent compounds*

As the most important tracer group, the fluorescent tracers deserve to be handled first.

The fluorescent properties of certain compounds can be used to reach a high analytical selectivity. In contrast to colorimetry, where light absorption can only be measured and analytically exploited at one single wavelength, namely the absorption maximum, the fluorimetrical analysis utilizes two wavelengths, specifically the excitation and emission wavelength. Since fluorimetry measures fluorescent compounds at two wavelengths specific for each compound, it is far superior to colorimetry. Its detection limits are also on an order of four lower.

Fluorescence is a branch of luminescence. Every cold energy transition, with or without a visible emission of light, is called luminescence. Depending on whether the transition is caused by a chemical reaction, crystal fracture, heat, enzymase activity, electrons or electromagnetic waves, the process is called chemi-, tribo-, thermo-, bio-, cathodo- or photoluminescence. The excitation spectrum ranges from visible light over ultraviolet light and x-rays through to gamma rays. The most common fluorescence materials in tracing techniques use wavelengths between 300 and 600 nm.

In photoluminescence, photons that have the necessary corresponding energy can excite certain atoms, ions, or molecules upon collision. These can then emit the absorbed energy as light, which is called fluorescence; a delayed emission of 10^{-6} to several seconds is called phosphorescence. Figure 5 clearly shows how fluorescence and phosphorescence can occur by absorbing light = absorbing energy. During the energy absorption, electrons are excited from their ground electronic state S_0 to a higher energy level S_1. Electrons stay at this higher level only a short time. They can

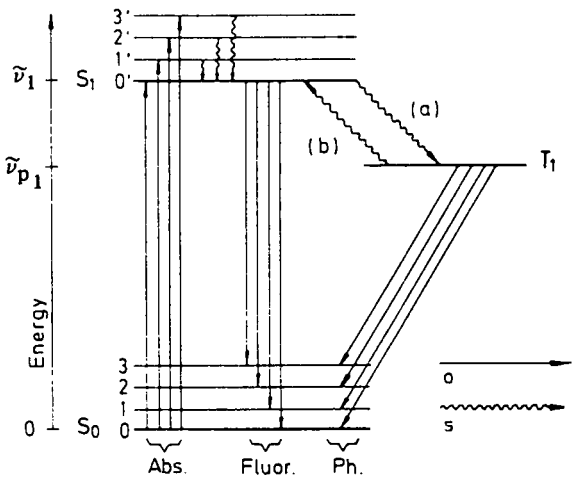

Figure 5. Term schematics of innermolecular energy transitions (after KLING 1974, RHYS WILLIAMS 1980): S_0 (0,1,2,3) = ground electronic state, S_1 (0'1'2'3') = higher energy electronic level; singlet, T_1 = triplett, Abs. = absorption-, fluor. = fluorescence-, Ph. = phosphorescence transition, o = optical, s = non optical transition.

however, especially in fluids, lose energy in collisions, before they drop back down to the lower energy level by emitting light. Therefore, fluorescence always has a longer wave length than the light absorbed (STOKES rule). The excitation spectrum corresponds to a large extent to the absorption spectrum; it is generally the mirror image of the fluorescence spectra (Fig. 6).

The radiation free transition from the singlet (S_1) into the triplet level (T_1) is partially possible. However, a transition from the triplet (T_1) to the base (S_0) level is 'forbidden,' which is why T_1 has a relatively long lifespan. This radiation energy, which is delayed and in comparison to the fluorescence, lower in energy and therefore in the long wave range, is phosphorescence.

The fluorescence of many substances is used in the modern quantitative analysis. Accuracies and extremely low detection limits can be achieved with modern measuring instruments that are not possible with any other methods. Since the start of the sixties, fluorimetrical analysis has been used not only in tracing techniques to investigate fluorescent substances. Nowadays, numerous organic and inorganic substances and groups are preferentially determined fluorimetrically. At times, fluorimetrics is coupled with other investigation methods, e.g. with high pressure liquid chromatography (HPLC). Elaborate analysis method guides already exist for the analysis of polycyclical aromatic hydrocarbons, for many pesticides, as well as for several elements, e.g. uranium or selenium. Fluorimetry is also used to determine enzymatic activity and porphyrins.

A large number of fluorescent substances, all with separate and differing chemical

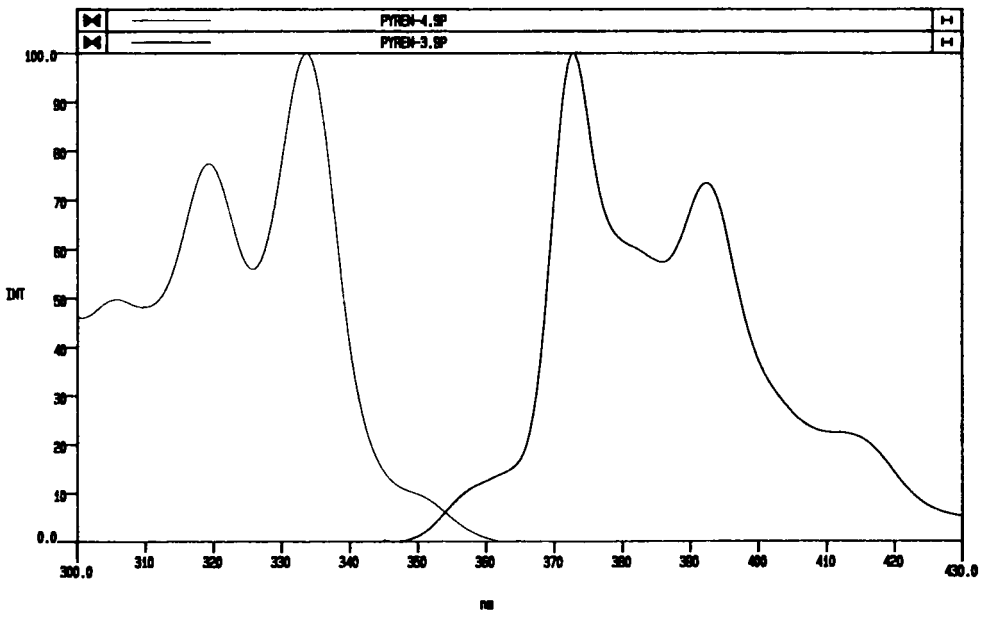

Figure 6. Absorption spectrum (left) and fluorescence spectrum (right) of a saturated aqueous pyrene solution. The mirror image effect of both spectra would be even more prominent if the x-axis were in vibration values rather than in wavelengths.

and fluorimetrical properties, are used in tracing techniques. They are all organic substances and can be classified into three groups:

1. Xanthene dyes (green to red fluoresce). *Uranine, eosin, rhodamine,* erythrosine;
2. Other fluorescent dyes (blue to green fluoresce). *Pyranine, sodium naphthionate,* amidoflavine, lissamine;
3. Optical brighteners (blue fluoresce).

The most commonly used dyes in tracing techniques are in italic print.

In the following sections, the chemical, physical, and optical properties of the separate dyes are described. To represent the chemical constituent formulas, a benzene ring with double lines for smeared double bonds was chosen instead of the benzene hexagon with an enclosed ring. When necessary, besides the common names and the chemical names according to the IUPAC (International Union for Pure and Applied Chemistry), synonyms are also given. C.I. means the Colour Index (1971). When available, the C.I. 'Constitution-Numbers' and the C.I. 'Generic Names' are also given. This large standard work helps identify commercial dyes when in doubt due to the numerous trade names available. QUINLAN and SMART recommended back in 1976, that publications about dye tracer tests always use the C.I.-Numbers and -Names for the dyes used. Furthermore, the number for the 'Chemical Abstract Service' (CAS) is also given here.

At the end of the separate descriptions about the most important properties several tables and graphs provide further information.

2.1.1.1 *Uranine*

C.I. 45 350, Acid yellow 73 CAS: 518-47-8

Chemical name: 3-Hydroxy-6-oxo-9-(2'-carboxyphenyl)-xanthene, disodium

Synonyms: Spiro[isobenzofuran-1(3H),9'-[9H]xanthene]-3-one,3',6'-dihydroxy-, disodium
Fluoreszein Natrium
Sodiumfluorescein
Resorcinphthaleinsodium
Basacidgelb 226
Sicomet
Hydroxy-o-carboxy-phenyl-Fluoran-Natrium

Chemical formula: $C_{20}H_{10}Na_2O_5$

Molecular weight: 376.28

Structural formula: Figure 7.

Ligands		2	4	5	7	Me^+
Fluorescein		H	H	H	H	H^+
Uranine		H	H	H	H	Na^+
Eosin yellowish		Br	Br	Br	Br	Na^+
Eosin bluish		Br	NO_2	NO_2	Br	Na^+
Erythrosine		I	I	I	I	Na^+
Rose bengale		I	I	I	I	Na^+
(Tetrachloro-	3'	4'	5'	6'		
tetraiodofluorescein)	Cl	Cl	Cl	Cl		

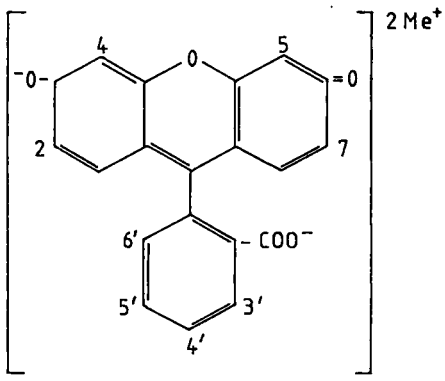

Figure 7. Structural formula of the fluorescein derivatives.

Extinction maxima: 491 nm (main absorption)
322 nm (secondary maximum)
Fluorescence maximum: 512 nm
Specific decadic extinction at 491 nm: 0.2001 (l cm^{-1} mg^{-1})
Molar decadic extinction at 491 nm: 84,000 (l cm^{-1} mol^{-1})
Water solubility (20°C): >600 g/l, insoluble in benzene, petrol (gasoline), ethyl acetate; hard soluble in propanols, 1-butanol, acetone; 10 g/l in ethanol at room temperature
Diffusion constant: $1.9 \cdot 10^{-5}$ ($cm^2 s^{-1}$) (KOZLOV & SARZHEVSKII 1975)
Beilstein: *19*: 222
MERCK-Index: *9*: 4042
Manufacturers and distributors:
MERCK (Uranin AP, powdered, concentrated, Nr.8462)
FLUKA (Fluoreszein-Natrium, pract. Nr.46970)
SIMON & WERNER (Sicomet-Uranin, coarse-crystallized)
L.B. HOLLIDAY (Fluorescein LTS)
EGA-Chemie
TAKEDA-CHEMICAL Co Ltd. Tokyo

In 1871, A.v. BAEYER, the Nobel prize winner for chemistry in 1905, discovered fluorescein by melting resorcinol and phthalic anhydride together in the molecular ratio 2:1, using zinc chloride as a catalyst (BAEYER 1871a, b).

Fluorescein ($C_{20}H_{12}O_5$), Molecular weight: 332.31 CAS: 2321-07-5
Chemical name: Hydroxy-6-oxo-9-(2'-carboxyphenyl)-xanthene
Synonyms: Spiro[isobenzofuran-1(3H),9'-[9H]xanthene-]-3-one,3',6'-dihydroxy,
Phenyl-2-oxyfluoron-2-Carbonacid,
Resorcinphthaleine

Fluorescein forms red crystals, which are soluble in water at 20°C only to 0.05 g/l. The aqueous solution fluoresces only very faintly. Fluorescein is well soluble in alcohol and ether, on which one of the enrichment methods is based. Adding alkaline

salt increases the fluorescence and the solubility of fluorescein greatly. The fluorescence is due to the anion of the alkaline salt in fluorescein.

Often, especially in the Anglo-American literature, 'fluorescein' is falsely used for the salt, sodium fluorescein, i.e. uranine, as noted by QUINLAN in 1989.

Fluorescein salts used in water tracing

Of all known substances, the fluorescein-anion has the strongest fluorescence. It has been used as a tracer for over a hundred years and its properties as a tracer are unsurpassed. This well soluble in water alkali-salt is used in tracing tests. For a long time now, the sodium salt of fluorescein, sold and known as uranine, has prevailed for use in tracing tests. Its name is most likely based on the similar colour of the fluorescing uranyl salts. The earliest mention of 'uranine' in a scientific paper concerned the compatibility of uranine solutions for fish (RUPP 1885). The name was most likely introduced by BASF, since J. FRISCHAUF carried out tests in 1888 near Graz, Austria with uranine, which he bought at a 'Kilogram price of 20 Mk from the Badischen Aniline and Soda Factory in Ludwigshafen' (FRISCHAUF 1890).

The very first application of alkali-fluorescein was in the Danube sinkholes between Immendingen and Möhringen by the Geognost Prof. A. KNOP, Karlsruhe/ Germany. Proof as to the whereabouts of the percolated Danube water had been called for in the legal battle between Baden and Württemberg. In 1869, aniline red was used first, but the test failed, most likely due to its sorption properties (KNOP 1875). On the afternoon of 9 October 1877, KNOP injected 10 kg fluorescein in sodium hydroxide solution in the Danube sinkholes (KNOP 1878). The water in the Aach spring, 12 km away, displayed a 'brilliant green luminance' 2-4 days after the injection. Thus, the first use of alkali fluorescein was a success.

Today, tracing technology without uranine is unthinkable. It is the most frequently used tracer!

Characteristics of uranine

A comprehensive description of the physico-chemical and chemical properties of uranine with respect to its suitability as a hydrological tracer was given by KÄSS in 1964 and 1965.

During crystallization, uranine forms dark-red longish crystals, which do not fluoresce. Concentrated uranine solutions are also dark-red and do not fluoresce. Not until strongly diluted with water does the solution dissociate into sodium cations and uranine anions; the latter fluoresce (Fig. 8).

In 1958 ZANKER and PETER carried out thorough investigations about the prototropical forms. They established the equilibrium constants for the prototropical forms:

$$P_k \frac{\text{cation}}{\text{neutral molecule}} = 1.95$$

$$P_k \frac{\text{neutral molecule}}{\text{univalent anion}} = 5.05$$

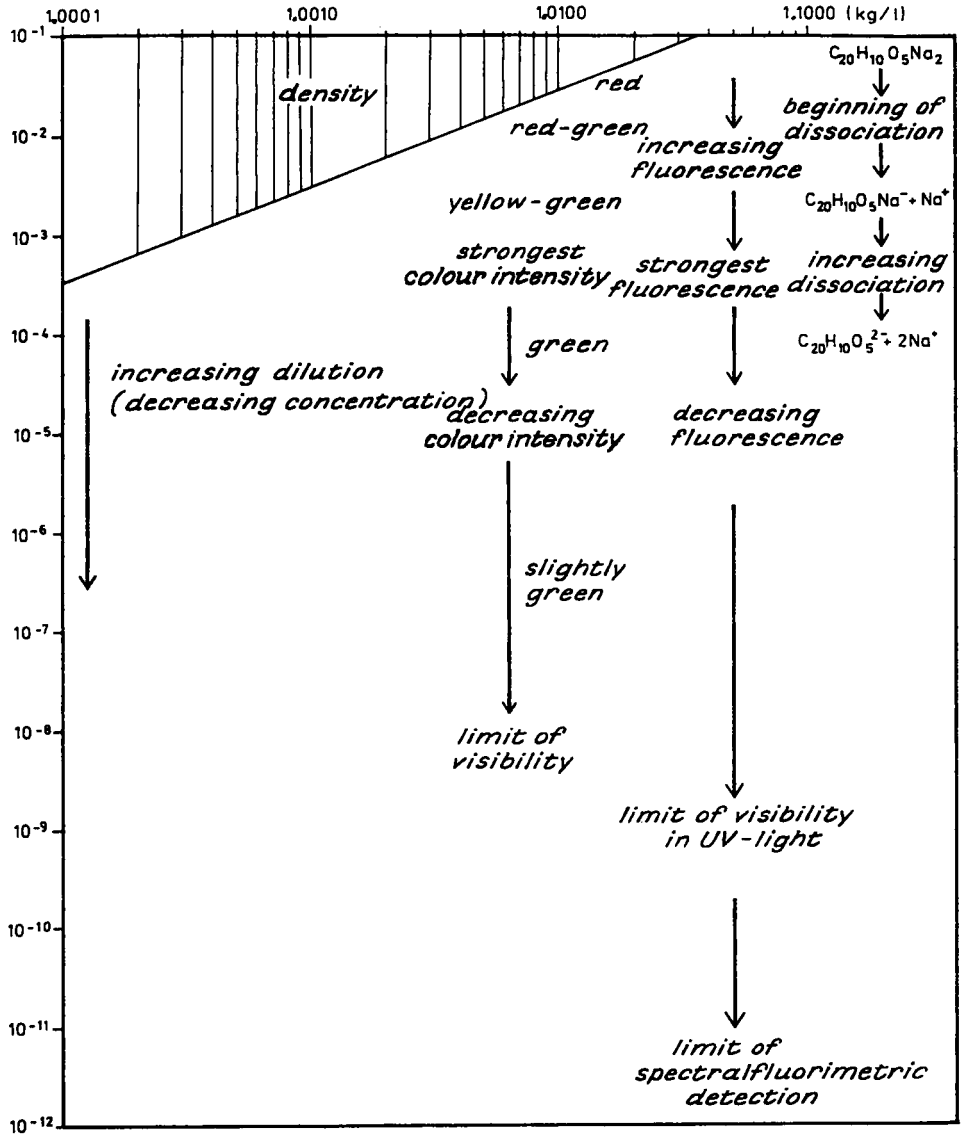

Figure 8. Characteristics of aqueous uranine solutions in various dilutions.

$$P_k \frac{\text{univalent anion}}{\text{divalent anion}} = 7.00$$

These investigations proved the existence of the univalent anion. The states of the separate form are displayed in Figure 9.

During dilution, the transition from the red molecule to the green anion can be seen conspicuously (Plate 1). In diluted solutions, the degree of dissociation is only dependant upon the pH-value.

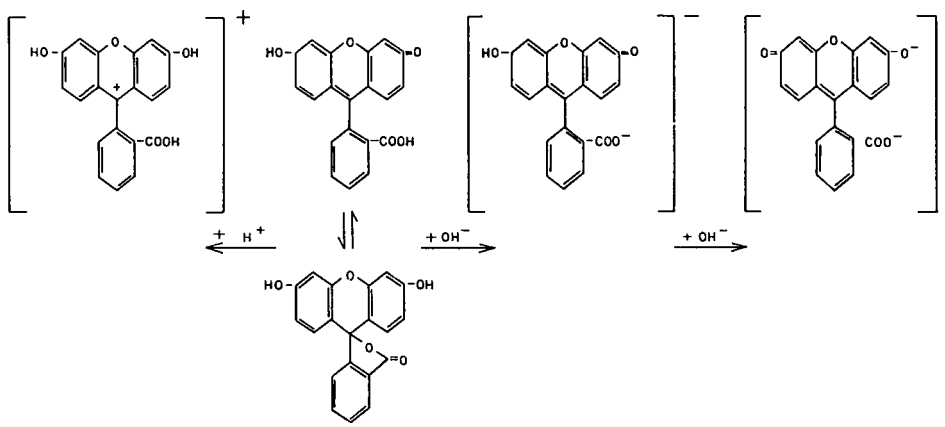

Figure 9. The prototropical states of fluorescein (after FÖRSTER 1951). From left to right: The univalent cation; the two forms of the neutral molecule, on top the quinonoid, below the lactone form; the univalent anion; the divalent anion.

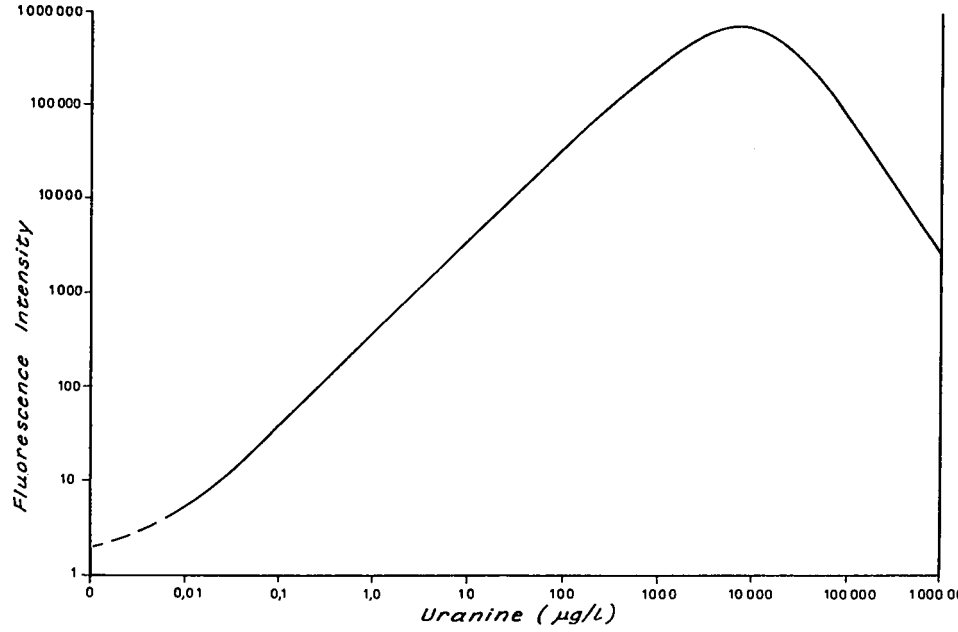

Figure 10. Course of the intensity of a uranine-calibration curve. At very high concentrations, the fluorescence decreases again.

The quantum yield and therefore the intensity of the fluorescence is exceptionally high. Uranine is the most intensive fluorescing substance known. Modern spectrofluorimeters have a detection limit for uranine of 0.002 µg/l = $2 \cdot 10^{-12}$. The calibration curves are linear over five concentration ranges (Fig. 10). At very high concentrations over 10,000 µg/l, the intensity of the fluorescence decreases in consequence

of its individual light absorption and due to retrograde dissociation. High fluorescence intensities are assigned to two dye concentrations. More intensively dyed samples can be measured better through extinction determination (see Section 2.1.3.3, Quantitative determination).

The intensity of uranine's fluorescence depends strongly upon the prevailing hydrogen ion concentration. The maximal fluorescence is reached at pH-values over 8.5. At the neutrality point (pH 7), the fluorescence intensity is only 80% of the maximal value. In solutions with pH-values, which are too low, the intensity falls (Fig. 11). The more acidic the medium, the more blue-green uranine-cations are present, which are only faintly fluorescent. The uranine-cation has strong sorption properties and is lipophil, i.e. solvents can extract the cation out of the sorbents. The conversion of the uranine-anion into the cation is reversible; after the pH rises, the fluorescence is restored to its original intensity. According to KRÜGER (1876), fluorescein is also a good indicator for acid-base titrations.

In pH-neutral solutions, the fluorescence maximum for uranine is at 512 nm. However, it must be noted that there can be a 1-2 nm deviation from the stated maximum, depending on the instruments and the spectral sensitivity distribution of the multiplier. Of course, the same holds for all the other stated wavelengths. The position of the fluorescence maximum is also dependant upon the concentration; at uranine concentrations higher than 200 µg/l, the maximum is displaced towards longer wavelengths due to individual absorption. It can be seen in Figure 12, that the fluorescence falls more steeply to the shorter wavelengths than to the longer wavelengths. Below 470 nm and above 620 nm there is virtually no uranine fluorescence. The corresponding excitation at 322 nm is theoretically at 1050 nm.

The spectral course of the uranine extinction coincides to a large extent with the fluorescence excitation, the main and secondary maxima correspond exactly with those of the excitation curve. Figure 12 shows the molar decadic extinction, which is the calculated decadic extinction for 1 cm thickness of a 1-molar solution. The spe-

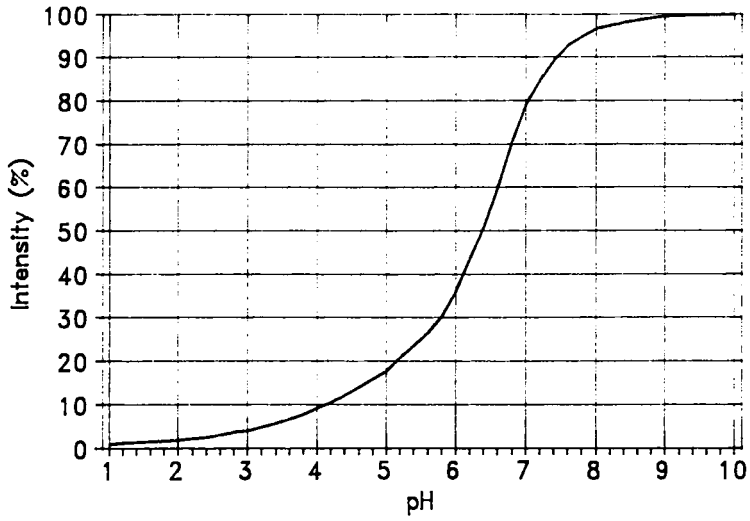

Figure 11. Dependence of the intensity of uranine's fluorescence upon the pH-value.

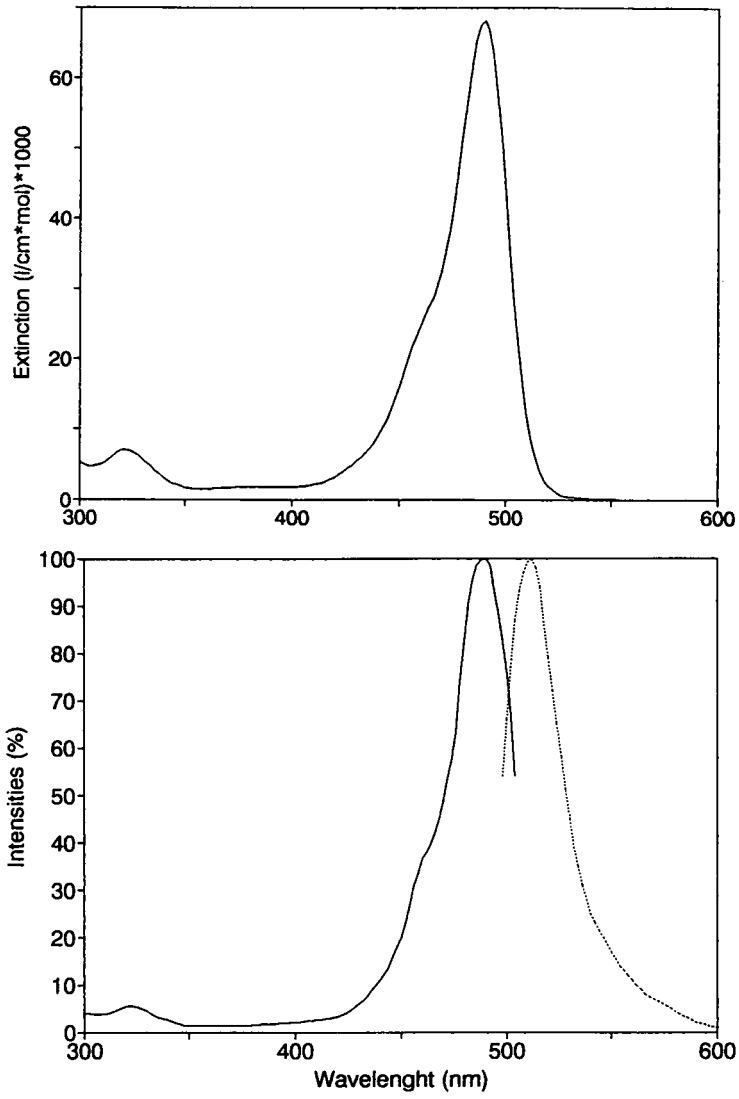

Figure 12. Top: Uranine extinction course (10 mg/l). Besides the maximum at 490 nm, there are secondary maxima at 322 and at 465 nm; bottom: Spectral course of the excitation and fluorescence intensities (in %). The excitation curve (left) is practically identical with the extinction curve.

cific decadic extinction, on the other hand, is the extinction of a solution with a concentration of 1 mg per liter for a 1 cm thickness.

In the following sections, uranine's characteristics as a tracer will be summarily covered with the other fluorescence dyes. Here, only the characteristics specific for uranine will be qualitatively handled.

Uranine belongs to the group of dyes with poor fastness characteristics, since it reacts sensitively to certain environmental influences. The reversible influence of the pH-value was handled above. Other effects are irreversible.

Strong oxidizing agents destroy uranine, especially the chemical agents used as disinfectants in water purification (Fig. 13). Chlorine dioxide breaks down uranine faster than chlorine, yet the latter does it more completely. Ozone can also destroy

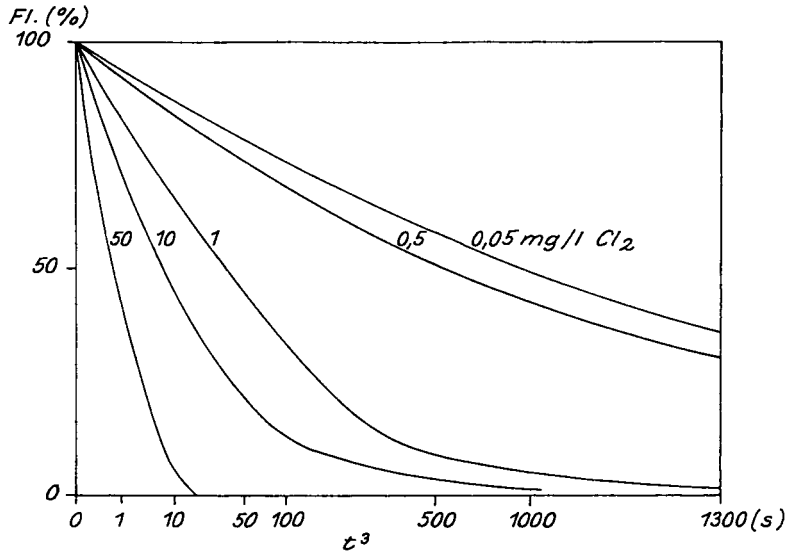

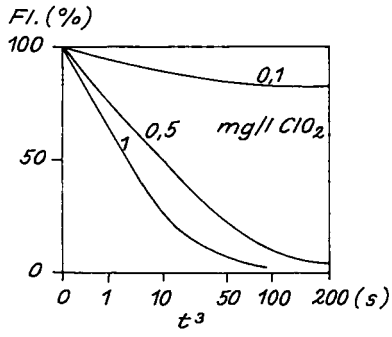

Figure 13. Temporal course of the fluorescence decrease in uranine solutions (10 µg/l). Top: due to chlorine, bottom: due to chlorine dioxide.

uranine, as an experiment near Oberndorf proved (SCHULZ 1961). There, a high concentration of uranine of 125 µg/l, which was introduced into the ozone system of the Dieselbach springs, was destroyed in a very short time, so that only colourless water arrived at the water supply system. These observations prove that during tracer tests in systems where oxidizing agents are used, water samples must be taken at sites ahead of the purification system. On the other hand, the water supply system needs not to be disconnected, since the dye will be destroyed. At higher dye concentrations, a short term increase in the chlorination can be carried out. Furthermore, during dye tracer tests in groundwater replenishing plants, the sterilization of the replenishing water with strong oxidizing agents should be temporarily stopped.

Other oxidizing agents such as permanganate or chromate are not strong enough to destroy uranine. Store tests with 100 mg/l $Cr_2O_7^{2-}$ in uranine solutions with 6.5 µg/l which stood over four weeks showed no decrease in fluorescence.

Reducing agents also have no influence upon uranine. The DIN-Bureau of Standards (DIN-Norm) from 1988 recommends adding 25 g/m^3 uranine to district heating

water, which also contains the strong reducing agent hydracine. Uranine is added to show leakage points, the hydracine is added to combat corrosion.

Light destroys dissolved uranine. Figure 14 shows how a 1 µg/l uranine solution in brown and colourless glass bottles decomposes when subjected to daylight. It is obvious from the graph that brown glass delays the decomposition of uranine. In colourless glass bottles, the light from cloudy days is sufficient to destroy uranine within a week.

Every now and again, it is assumed that adsorption of uranine occurs on clayey, marly or silty rock layers (PRINZ 1923, KEIL 1959). The author's tests led to the conclusion that clay minerals do not adsorb uranine. Shaking tests using 10 µg/l uranine solutions with 200 g kaolinite, 200 g red marls (mainly illite), and 5 g tech. bentonite (main constituent montmorillonite) respectively, showed no cases of uranine decrease (KÄSS 1964). According to manifold experience, uranine is capable of traveling great distances in gravelly-sandy subsoil. Wells that have a percentage of bank filtrate water that comes from rivers with a high pollution load, can have a traceable uranine content which came from sewage (see Section 2.12). To that extent, uranine can be assumed to be a quasi-ideal tracer. When it is purported that other tracers, such as bromide or iodine travel faster than uranine and it is then concluded that uranine is held back or adsorbed, it must be retorted thus: Bromide and iodine anions have a strong negative charge that is repulsed from the surface of the grains, since they themselves are also negatively charged. Therefore, bromide and iodine ions are preferentially propelled into the voids. In contrast to this, the uranine ion is only faintly negatively charged. Uranine ions can spread out and move throughout the pore space and therefore follow the groundwater flow rather exactly.

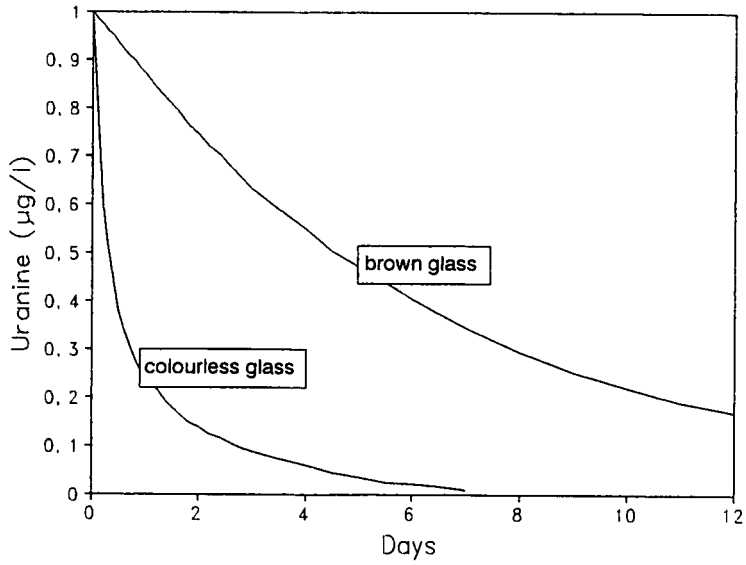

Figure 14. Decomposition due to light of two 10 µg/l uranine solutions in a brown (upper curve) and a colourless (lower curve) 250-ml-glass bottle. The bottles were kept on an eastern window sill in November during a weather spell with little sunlight (after KÄSS 1964).

Merely with groundwaters, which are acidic, do tracing tests with uranine fail.Particularly from the northern German plains with their marshy and boggy subsoil are several failed tests with uranine known. In such areas, uranine takes on the cationic, non-fluorescing and sorbing form and therefore cannot be observed. To investigate uranine's behaviour in acidic subsoil, a flow passage test was carried out in a plexiglass column filled with turf. The liquid phase was moor water with a pH-value of 5.1. The added 100 mg uranine was also dissolved in moor water. After the passage, the uranine sample was exposed to an ammonia atmosphere until they reacted alkaline. Uranine was not found in any of the samples.

Uranine will always be the first choice for groundwater tracer investigations. Due to its low detection limit, the modest interaction with the aquifer, and its favourable price, uranine has more advantages on its side than all the other tracers used in water investigations. Especially in cases with long distances and a wide range of possible reemergence sites, uranine is the best choice and when needed the injected amount can be increased. The largest recorded amount injected was 160 kg in a karst water tracing test in Dalmatian, in the Popovo-Polje north of Dubrovnik (MILANOVIC 1976).

Other than as a tracer, uranine is used for other purposes. According to Announcement 3 of the Dye Committee of the German Research Council (Deutsche Forschungsgemeinschaft, (DFG 1971)), uranine can be used as a dye in cosmetics. Uranine is called 'C-external Yellow 16' ('C-extern Gelb 16') there. Numerous bathing additives and cleaning supplies often have considerable amounts of uranine, which wind up in the sewage flow. Uranine is also used to find leaks in water supply systems. As mentioned above, the German Bureau of Standards DIN 1988, part 4 (1989) recommends adding 25 g uranine + 25 g pyranine to every cubic metre of district heating water. Uranine has also been used for checking and following discharge channels and sewage effluents. Consequently, due to uranine's low detection limit, interferences during dye traces can occur, if the background water is contaminated. Therefore, in 1983 the Groundwater Chemistry Section of the German Association for Water Management and Cultural Technology (DVWK, Scientific Committee 3.5, groundwater chemistry) published the following in various scientific periodicals (DVWK 1983):

'Limit the use of uranine!
Uranine has been used successfully for over one hundred years in investigating the direction and speed of groundwater flow. Modern investigation methods using fluorescence allow the detection of very low amounts of uranine. Thus, now only very small amounts of uranine are needed in tracing tests and therefore drinking water supplies and surface waters need not be impaired.

Due to the intensive dyeing ability of uranine, it is also used in checking leaks in piping, following sewage channels, and for other control measures in flow systems. Withal, uranine passes over into groundwater systems. This causes serious falsification of groundwater tracing tests.

To avoid such disturbances, uranine should only be used in groundwater tracing tests and even then only in amounts absolutely necessary.

For all other purposes, potassium permanganate solution is sufficient as a dye. If a tracing test is to be carried out in a water body with a high organic load, the food dye

Methyl Violet can be used. Both dyes are hygienic and toxicologically harmless and furthermore reasonably priced. Such a limit on uranine's use would decisively promote groundwater research.'

Aqueous solutions of potassium permanganate are a brilliant violet. The visible detection limit in a beaker is approx. 0.9 mg/l. Potassium permanganate is indeed quite reasonably priced, however, in the presence of organic substances, the permanganate ion is rendered colourless by reduction. In such cases, the somewhat more expensive methyl violet B, Colour-Index 42 535 can be used. It has an even more intensive colouring, a visible detection limit of ca. 0.05 mg/l, and is not reduced by organic substances. Furthermore, it is also an allowed food colouring additive for certain foods, according to German federal law (BGBL I, 1981).

Uranine is also used in ship rescues due to its brilliant visibility from afar. In ophthalmology, uranine has been used to make cornea injuries visible, as well as in angio-fluoroscopy.

Lately, observations about a rare microbiological degradation of uranine in sample bottles has been reported (see Section 2.1.4.1).

2.1.1.2 *Eosin*

C.I. 45 380, Acid red 87 CAS: 17372-87-1

Chemical name: 3-Hydroxy-6-oxo-2,4,5,7-tetrabromine-9(-2'-carboxyphenyl)-xanthene-disodium

Synonyms: Spiro[isobenzofuran-1(3H),9'-[9H]xanthen]-3-one,2',4',5',7'-tetrabromo-3',6'-dihydroxy-disodium
2,4,5,7-Tetrabromfluoresceinsodium
Eosin yellow
Eosin G, A, YS, Y, J, 3G, 3Y, BS, FA, GF, YB, OJ, DA, GS
Basacid red 316

Chemical formula: $C_{20}H_6Br_4Na_2O_5$

Molecular weight: 691.88

Structural formula: Figure 7

Extinction maxima: 516 nm (main maximum)
480 nm, 340 nm, 300 nm (secondary maxima)

Fluorescence maximum: 538 nm

Specific decadic extinction at 516 nm: 0.1034 ($l\ cm^{-1}\ mg^{-1}$)

Molar decadic extinction at 516 nm: 67,000 ($l\ cm^{-1}\ mol^{-1}$)

Beilstein: *19*, 230

Water solubility: Good

Eosin was first prepared in 1871 by CARO; it is formed by brominating fluorescein. Other than being used as a tracer in waterways, eosin is used in manufacturing red ink and red stamp pads, as 'theatre blood,' to dye wool, cotton, and silk, and for denaturing road salt in Austria. Besides possibly causing problems with the availability, the last use listed can also be a disturbance during tracing tests. As a colouring in lipsticks, only the free acid form, 2,4,5,7-Tetrabrom fluorescein = C-Red 30 ($C_{20}H_8Br_4O_5$), is allowed (DFG 1971). Since eosin-coloured lipsticks have been in use, there have been no health problems connected with eosin reported. According to the cosmetic ordinance, appendix 3, part A, section a (red dyes No. 18) from 16th

December 1977 (BGBL I 1977b), eosin is permitted for use in eye, mouth, and lip cosmetics and for personal hygiene.

In cellular diagnostics, eosin blue, C.I. 45 400 Acid red 91, is also used besides eosin yellow. In contrast to eosin yellow, which has two bromide atoms, the eosin blue molecule has two NO_2-radicals ($C_{20}H_6Br_2N_2Na_2O_9$, Molecular weight 624.06). Eosin blue has almost the same optical fluorescent characteristics as eosin yellow, however, the production costs are almost twice as much.

Dibrom fluorescein (C.I. 45 370 Acid orange 11, $C_{20}H_8Br_2Na_2O_5$) and spriteosin, the sodium salt of tetrabrom fluoresceinethylester, are soluble in alcohol.

At the end of the last century, TRILLAT (1899a,b) carried out adsorption tests with several dyes, including eosin. However, neither he nor others used eosin as a hydrological tracer, until KÄSS used eosin in 1962 along with three other tracers in the Ulmer Alb karst (see Section 1.1). Due to eosin's low sorption properties, it is often used as a second tracer along with uranine in Southwest Germany with success, even though both tracers interfere with each other during analysis (KÄSS 1991). Therefore, practical methods to analyse for both tracers in one water sample were developed (see Section 2.1.3.3). Using these techniques, several injection sites using more than one tracer can be planned during extensive tracing tests with long distances and observation time spans. Such a trace was carried out in May 1988 in the outer catchment area of the Blautopf spring, Germany with the dye tracers eosin (20 kg), uranine (10 kg) and sodium naphthionate (40 kg). During this triple trace, eosin and uranine visibly reemerged in the Blautopf spring that was 19,020 m, respectively 16,960 m away (VILLINGER & UFRECHT 1989). The working commission on tracing in hydrology (ATH) carried out, in preparation for the third, fourth, and fifth symposiums, combined karst water tracing tests with eosin:

1973 in Savinja Valley near Celje (pore groundwater) with 2 kg/64 m (BAUER et al. 1976),
1975 in Krain (dalmatian karst) with 25.5 kg/7100 m (BAUER et al. 1976),
1979 in Neuchâtel Jura (malm karst) with 12 kg – no results (BAUER et al. 1980),
1979 in Hinter Muota Valley (high alpine karst) with 10 kg/5800 m distance and 937 m difference in level (BEHRENS et al. 1981),
1979 near Langenthal (pore groundwater of the Swiss subalpine region) with 20 kg/3500 m (BAUER et al. 1981),
1984 in central Peloponnesus (subalpine karst) with 25 kg/6000 and 7000 m (MORFIS & ZOJER 1986),
1988 in Lur cave system (southern alpine karst) with 5 kg/3100 m (ATH 1992).

As mentioned above, eosin has only slightly more sorption properties compared to uranine. On the other hand, the fluorescence of eosin is not as pH dependant as uranine is. Eosin cannot be used in surface waters however, due to its strong sensitivity to light.

2.1.1.3 *Rhodamine B*
C.I. 45 170, Basic violet 10 CAS: 81-88-9
Chemical name: 3,6-bis-diethylamino-9-(2'carbophenyl)-xanthylium-chloride
Synonyms: Xanthylium, 9-(2-carboxyphenyl)-3,6-bis(diethylamino)-chloride

Tetraethyldiamino-o-carboxy-phenyl-xanthenyl-chloride
Diethyl-m-amino-phenolphthaleinhydrochloride
Hydrochloride of the N.N.N'.N'-Tetraethylrhodamine
Basonyl-S-Rot 542, Basonylred 540
Brillantrosa B
Brilliantpink B
Rhodamine FB, O, BH, BA, BN, S, BS, BX, BXL, BXP,
Safraniline, Fettrot A, Rosaceine

Chemical formula: $C_{28}H_{31}ClN_2O_3$
Molecular weight: 479.02
Structural formula: Figure 15
Extinction maxima: 554 nm (main absorption)
520, 355, 300 nm (secondary maxima)
Fluorescence maximum: 576 nm
Specific decadic extinction at 554 nm: 0.227 (l cm^{-1} mg^{-1})
Molar decadic extinction at 554 nm: 108,000 (l cm^{-1} mol^{-1})
Water solubility: Good

Rhodamine B was the first produced rhodamine; it was discovered independently in 1887 by CERESOLE and in 1888 by HOMOLKA & BOEDEKER.

Other than rhodamine B, there is a series of similar compounds, which belong to the same family, the so-called aminoxanthenes. Their name comes from their strong red coloured solutions. Many of them fluoresce in the orange-red-range. The structural formula of those rhodamines used in water tracing can be seen in Figure 15. All rhodamines have two amino radicals in the 3,6-positions, furthermore sulfo- and carboxyl-acid radicals in the 9(2',4')-positions.

Rhodamine B crystallizes as metallic dark green needles. The chemical is used in histology to colour cells and was used earlier in lipsticks. This rhodamine is reported to have cancerous and genetical mutation properties. The LD 50-value for rats i.v. is 89.5 mg/kg (ROTH & DAUNDERER 1990).

Rhodamine B has a low sensitivity to light and its fluorescence is not very pH dependant, which make it suitable for tracing tests. However, it has strong sorption properties: a solution of 100 µg/l is retained to 99.3% by a nitrocellulose membrane filter.

The rhodamine dyes are not recommended for lengthy tracing tests. In the test field Merdingen (Southwest Germany), a tracing test was carried out on 6 April 1982 with 100 g rhodamine B to test its suitability as a pore water tracer. After 33 days, the cross section 10 m downstream showed a maximum rhodamine B concentration of 205 µg/l. After four months, at a distance of 25 m downstream the maximum concentration was 33 µg/l. After 8½ months, the 75 m downstream observation profile reached a maximum concentration of 1.6 µg/l. In contrast to the results from the uranine test that was carried out in the same area, these concentrations are on an order of 500 too low.

Meanwhile, at the injection site and the nearest sampling sites, rhodamine B was retained by sorption in the aquifer. Even after nine years, the water still showed a strong pink colour. A closer look at the spectral characteristics of the sample water showed that only a small percentage of the original rhodamine B spectrum was still

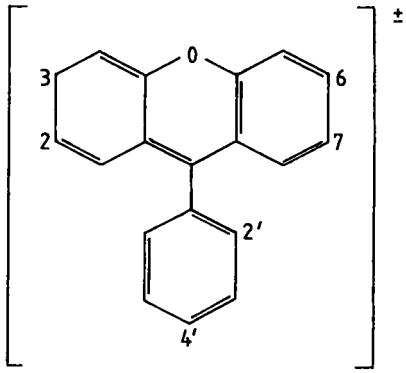

Figure 15. Structural formulas for the rhodamines used in water tracing tests:

	2	3	6	7	2'	4'	±
Rhodamine B	–	$N(C_2H_5)_2$	$N(C_2H_5)_2^+$	–	COOH	–	Cl^-
Sulforhodamine B	–	$N(C_2H_5)_2$	$N(C_2H_5)_2^+$	–	SO_3^-	SO_3^-	Na^+
Amidorhodamine G	CH_3	NHC_2H_5	$NHC_2H_5^+$	CH_3	SO_3^-	SO_3^-	Na^+
Rhodamine WT	–	$N(C_2H_5)_2$	$N(C_2H_5)_2^+$	–	COO^-	COO^-	Na^+
Rhodamine 6G	CH_3	NHC_2H_5	$NHC_2H_5^+$	CH_3	$COOC_2H_5$	–	Cl^-
Rhodamine 3G	CH_3	NH_2	$N(CH_3)_2^+$	–	$COOC_2H_5$	–	Cl^-

The notation of the positive charge at position '6' is only meant as a guidance. It could also be set at '9' and for rhodamine 3G at best at '3.'

effective or present (Fig. 16). Due to deaminoalkylation, a secondary maximum in the shorter wavelength side appeared in the excitation spectrum at 554 nm. Later, this second maximum was displaced even more towards the shorter wavelengths, and now exceeds the rhodamine B excitation maximum greatly. After nine years, the secondary maximum has approached uranine's maximum to a large extent; the last measurement there of the excitation maximum was at 496 nm, of the fluorescence maximum at 519 nm. Evidently, the fluorescence of the component that causes the second maximum is substantially stronger than rhodamine B's, since the sample water is pink and not green. Furthermore, the secondary maximum component is most likely not subject to much sorption, since only it appears in several neighbouring and downstream sample sites.

Deaminoalkylation appears to affect several, if not all rhodamines. In a sulforhodamine B tracing test in the pore water aquifer of Wilerwald (Kt.Bern, Switzerland) carried out by MÄGDEFESSEL (1990), deaminoalkylation was detected within nine months. The fluorescence peak at 585 nm of the deaminoalkylation product was displaced 43 nm towards the shorter wavelength side.

Thus, if multiple tests with different dyes including rhodamines, are to be carried out in a test area, the appearance of secondary peaks needs to be expected, which could lead to confusion.

Due to its high sorption properties, rhodamine B is not suitable for use in pore-groundwater aquifers. In fracture aquifers, considerable sorption loss must also be expected, although several successful tracing tests in fracture aquifers have been re-

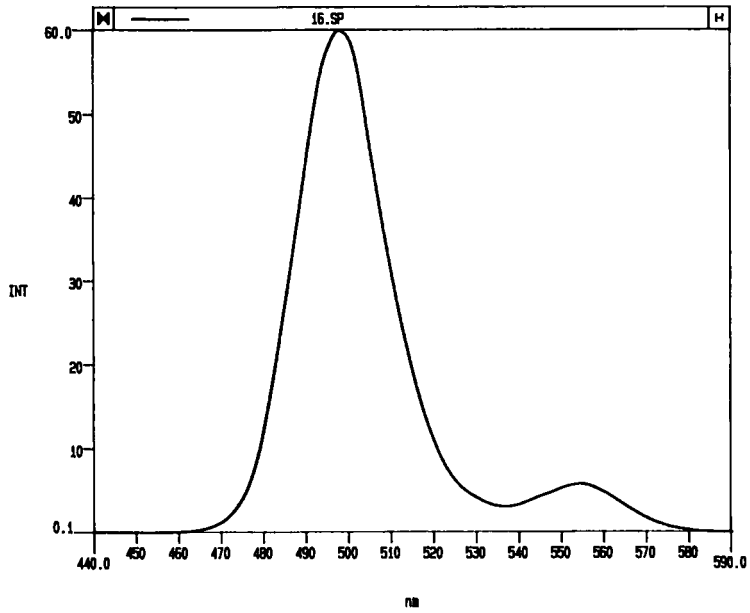

Figure 16. Deaminoalkylated rhodamine B after a residence time of nine years in a pore-groundwater aquifer. Synchronscan with $\Delta\lambda$ 20 nm. Originally, rhodamine B fluoresces at 554 nm only. In time, the deaminoalkylation increases: the deaminoalkylation product is displaced towards the shorter wavelengths (here at 498 nm) and finally exceeds the fluorescence of the excitation substance. X-axis: excitation wave length.

ported (HÖTZL et al. 1982, in quarries and ACKERMANN et al. 1982, in ore lodes in crystalline). Rhodamine B can be used best in karst aquifers. The surface contacts are minimized there; when quantitatively evaluating such a trace, adsorption losses must be considered. Examples for successful karst water traces with rhodamine B were carried out by the ATH:

1975 in Krain with 26.4 kg/12,300 m and 152 m grade (BAUER et al. 1976),
1979 in Neuchâtel Jura with 10 kg/6550 m (BAUER et al. 1980),
1979 in the Hinter Muota Valley with 10 kg/3050 m (BAUER et al. 1981),
1984 in the central Peloponnesus with 25 kg/42,000 m (MORFIS & ZOJER 1986),
1988 in the Lur cave system with 5 kg/3100 m (ATH 1992).

Rhodamine B can only be used as a tracer in surface waters when little or no organic or inorganic suspended solids are present. RODIER and MARICHAL (1961) used rhodamine B to determine the mixing in the lower Rhône after a supposed pollutant influx at the nuclear power plant Marcoule. A noteworthy unwanted river trace occurred after a fire in the chemical plant SANDOZ/Basel in Switzerland in the night from 31 October/1 November 1986, as along with the fire fighting water, besides pesticides also large amounts of rhodamine B poured into the Rhine river. The pollutants could be followed fluorimetrically all the way to Mannheim in Germany. Therefore, specific warnings could be issued to the river bank water works (SCHMITZ

1989). Rhodamine B has also been successfully used in glacial traces (MOERI & LEIBUNDGUT 1986, RAMSPACHER 1981).

2.1.1.4 *Sulforhodamine B*
C.I. 45 100, Acid red 52 CAS: 3520-42-1
Chemical name: 3,6-Bis-diethylamino-9-(2',4'-disulfophenyl)-xanthylium-sodium
Synonyms: Xanthylium, 3,6-bis(diethylamino)-9-(2,4-disulfophenyl)-sodium
Tetraethylamino-3,6,-phenyl-9-xanthyliumdisulfonat-sodium
Duasyn-Säurerhodamin B 01 (HOECHST)
Pontacyl Brilliant Pink B (DUPONT)
Orcoacid sulforhodamine B (ORGANIC CHEMICAL Corp.)
Amidorhodamine B
Xylenrot B
Chemical formula: $C_{27}H_{29}N_2NaO_7S_2$
Molecular weight: 580.65
Structural formula: Figure 15
Extinction maxima: 564 nm (main absorption)
525, 342 nm (secondary maxima)
Fluorescence maximum: 583 nm
Specific decadic extinction at 564 nm: 0.155 ($l\ cm^{-1}\ mg^{-1}$)
Molar decadic extinction at 564 nm: 89,900 ($l\ cm^{-1}\ mol^{-1}$)
Water solubility: ca. 10 g/l (20°C)

In 1906, sulforhodamine B was prepared for the first time by EMMERICH. This dye is well-suited for dyeing wool and polyamide and is produced under several different trade names by several different companies. To avoid confusion, it is suggested that only the name ' sulforhodamine B' be used in hydrological tracing techniques.

Back in 1963, FEUERSTEIN and SELLECK mentioned the suitability of this chemical for tracing techniques. In 1964 LALLEMAND and PALOC published test results from the catchment area of the karst spring Clamouse (Dept. Hérault/France) using 'Pontacyl Brilliant Pink B' (1964a). KILPATRICK (1967) used sulforhodamine B successfully in discharge measurements in an ice-covered channel. Sulforhodamine has also been used successfully in tracing tests in pore-groundwater aquifers. KÄSS and STRAYLE (1990) investigated the operation of a UVB (UVB = Unterdruck-Verdampfer-Brunnen = Vacuum evaporation well) during a chlorinated hydrocarbon pollution accident with uranine. BRANNATH repeated the test in 1991 under different conditions. Then, an injection of only 200 g sulforhodamine B in the turbulent air of the UVB caused a strong foaming, which temporarily shut down the system. The sulforhodamine B molecule has bipolar characteristics, due to its spatially separated positive and negative charges and is therefore a wetting agent.

In 1990 in the test area Wilerwald (canton Bern/Switzerland), MÄGDEFESSEL carried out investigations in a pore-groundwater aquifer and found a retardation factor, R_f, of 2.0 compared to uranine. Tracing tests using sulforhodamine B and uranine in pore-groundwater aquifers were carried out in the Merdingen test area near Freiburg in Breisgau/Germany. The injection amounts of 20 g sulforhodamine B and 10 g uranine were sufficient to prove a flow distance of 100 m during the test. Figure 17

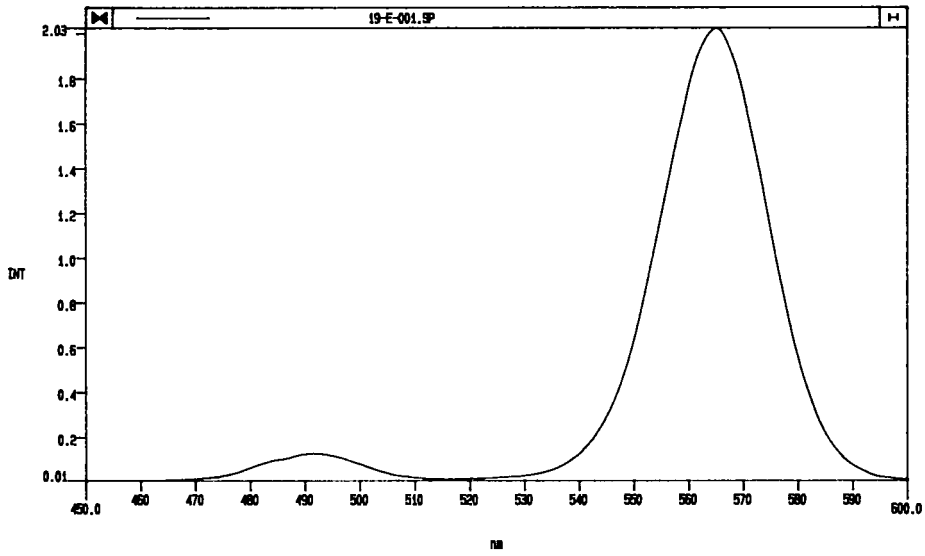

Figure 17. Synchronscan of a groundwater sample from a combined tracing test using uranine and sulforhodamine B in the Merdinger test area pore-groundwater aquifer from 1989. The graph shows the uranine peak (left) and the sulforhodamine B peak (right) in a sampling site 12.5 m downstream from the injection site after 150 days. Monochromator distance between excitation and fluorescence: 20 nm; shown are the excitation wavelengths. The uranine and sulforhodamine B intensities can be easily determined from the graph: uranine concentration: 0.3 µg/l, sulforhodamine B concentration: 4.2 µg/l.

shows a synchronscan of a sampling site 12.5 m away from the injection site, which clearly shows that sulforhodamine B and uranine can easily be separated.

These investigations in Wilerwald and in Merdingen, as well as laboratory tests indicate that sulforhodamine B is very suitable as a hydrological tracer. It has low sorption properties; it is not sensitive to light nor pH. The most important advantage however is that it is easily detected when used along with uranine. Sulforhodamine B has the longest excitation and fluorescence of all the rhodamines used in hydrological tracing techniques. The wavelength difference between excitation and fluorescence is 21 nm for uranine, for sulforhodamine B it is 18 nm. Thus, especially when using a synchronscan, both substances can be used at one time and each easily detected. Nevertheless, sulforhodamine B has been rarely used, perhaps partly since scientists are unacquainted with its advantages and partly due to hardships with its delivery. Figure 18 displays the fact that sulforhodamine B, compared to uranine, has only low sorption properties. A retardation factor, R_f, of 1.4 was determined.

2.1.1.5 *Amidorhodamine G*
C.I. 45 220, Acid red 50 CAS: 5873-16-5
Chemical name: 3,6-Bis-ethylamino-2,7-dimethyl-9-2',4'-disulfophenyl-sodium
Synonyms: Xanthylium, 9-(2,4-disulfophenyl)-3,6-bis(ethylamino)-2,7-dimethyl-sodium
Sulforhodamin G (extra) (HOECHST)

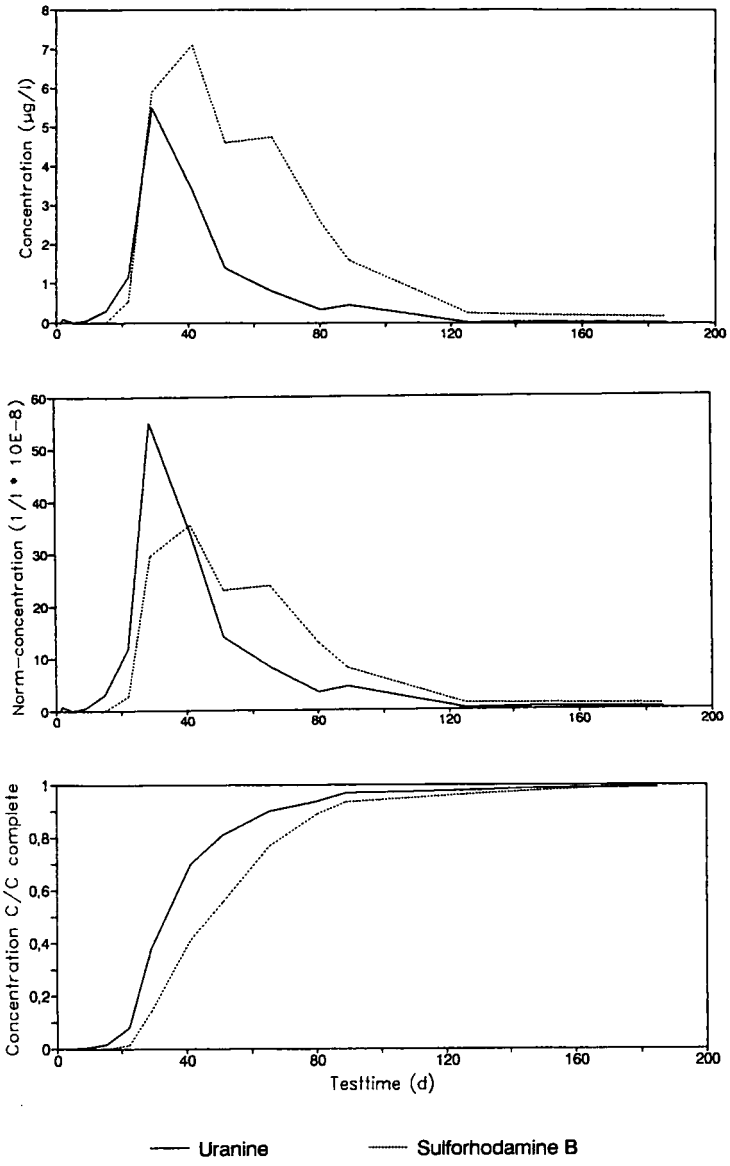

Figure 18. Top: Breakthrough curves for uranine and sulforhodamine B in pore-groundwater aquifer of the Merdinger test area. Injected amount: 10 g uranine + 20 g sulforhodamine B: Distance from injection site to sampling site: 50 m.
Middle: Normalized breakthrough curves for upper graph. The intensities (y-axis) were based upon the same injection amount. This type of graph shows how many parts per 1-l-sample water.
Bottom: Summation curve for top graph. Here, the data for both dyes is shown as the culmative amount over time. Derivable are the average residence time t_m (uranine: 33 days, sulforhodamine B: 47 days) and the average flow speed v_m (uranine: 1.75, sulforhodamine B: $1.23 \cdot 10^{-5}$ m/s) and the retardation factor $v_m$uranine/v_m sulforhodamine B: 1.4.

Orcoacid sulforhodamine g (ORGANIC CHEMICAL Corp.)
Amidorhodamin BG
Diethylamino-3,6-dimethyl-3,7-phenyl-9-xanthylium-disulfonate-2,7-sodium
Chemical formula: $C_{25}H_{25}N_2NaO_7S_2$
Molecular weight: 552.59
Structural formula: Figure 15
Extinction maxima: 531.5 nm (main maximun)
495, 346 nm (secondary maxima)
Fluorescence maximum: 552 nm
Specific decadic extinction at 531.5 nm: 0.0602 (l cm^{-1} mg^{-1})
Molar decadic extinction at 531.5 nm: 33 270 (l cm^{-1} mol^{-1})
Water solubility: Good

Amidorhodamine G is often used in tracing tests in Europe, because it is reasonably priced and, in contrast to eosin, easily spectrally differentiated from uranine. Its sensitivity to light and pH-values is low. To avoid confusion with other rhodamine dyes, it is suggested that only the name 'Amidorhodamine G' be used.

Sometimes commercial products are offered with an 'Extra' in their name and there are additives in the product, such as other fluorescent dyes, e.g. auramine. In such cases, a sample of the dye should be ordered and tested for purity by comparing with chemically pure substances or with samples with a known content before being used in a trace.

The ATH-Group has successfully used amidorhodamine G in combined tracing tests:

1966 in the Buchkogel karst region west of Graz/Austria with 0.07 kg/800 m (BATSCHE et al. 1967),
1969 in the Danube River seepage area – Aach spring (SW-Germany) with 8 kg/11,400 m (BATSCHE et al. 1970),
1975 in Krain with 26 kg/12,800 m (BAUER et al. 1976),
1979 in the Neuchâtel Jura with 10 kg/8750 m (BAUER et al. 1976),
1980 in the high alpine karst of the Muota Valley with 15 kg/6500 m (BEHRENS et al. 1981),
1988 in the Lur cave system with 3 kg/3100 m (ATH 1992).

Further successful traces with amidorhodamine G were carried out in the karst of the Salzburger Alps (BRANDECKER & MAURIN 1982), in the high alpine karst of the Krottenkopf region (CRAMER 1967, APEL & WROBEL 1975), and in the southwest German Muschelkalk (Middle Triassic) karst (JUNGBAUER 1983). MARTI et al. (1979) carried out drifting tests in the northern Swiss Quaternary with bacteria and phages and also used fluorescent dyes, among others also amidorhodamine G. Successful traces in glacial waters were carried out by ASCHWANDEN and LEIBUNDGUT (1982), amidorhodamine G is also well suited as a tracer in lakes (LEIBUNDGUT & HIRSIG 1977).

Due to the manifold uses for amidorhodamine G, the European Union has exempted 'Orcoacid Sulphorhodamine G' from customs duties (EWG 1989).

2.1.1.6 *Rhodamine WT*
C.I. Acid red 388 CAS: 37299-86-8
Chemical name: 3,6-Bis-diethylamino-9-(2',4'-dicarboxyphenyl)-xanthylium-sodium
Synonyms: Xanthylium,9-(2,4-dicarboxyphenyl)-3,6-bis(diethylamino)-sodium
Dicarboxy-2,4 phenyl-9-diethylamino-G-xanthen-yliden-3-diethyl-ammonium-3-sodium
Chemical formula: $C_{29}H_{29}N_2NaO_5$
Molecular weight: 480.55
Structural formula: Figure 15
Extinction maxima: 555,5 nm (main maximum)
515, 380, 355, 310, 290 nm (secondary maxima)
Excitation maximum: 554 nm
Fluorescence maximum: 580 nm
Specific decadic extinction at 555.5 nm: 0.142 (l cm^{-1} mg^{-1})
Molar decadic extinction at 555.5 nm: 80,450 (l cm^{-1} mol^{-1})
Water solubility: Good

Rhodamine WT is a fluorescent dye, which was developed especially for water tracing by DUPONT (WT = Water Tracing, US Patent Office No. 3 367 946, 6 Feb.1968). The dye is sold as a 20% solution. The above specifics are based on the dry substance. Rhodamine WT can contain up to several per mille uranine.

SABATINI and AUSTIN (1991) discovered that Rhodamine WT is made up of two isomers with different sorptive properties (Fig. 19). This is due to the different positions of the carboxyl groups in the phenol ring. The isomer 1 with the lower sorptiv-

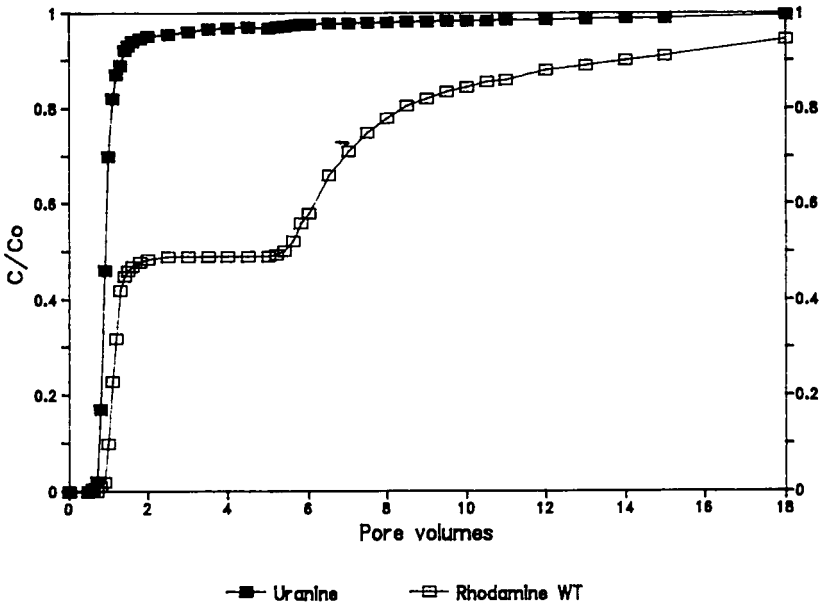

Figure 19. Breakthrough curves for uranine and rhodamine WT from a column test through a 300 m long column filled with 'Rosenmound Outwash' sand (FAY et al. 1995).

ity has the configuration displayed in Figure 15. Both carboxyl groups are in the 2',4'-position. Isomer 2 with the stronger sorpitive properties has the carboxyl groups in the 3',4'-positions (BEN SHIAU et al. 1992).

The dye has good properties for hydrological tracing purposes. Especially worth mentioning is its stability regarding light as well as the low dependency of its fluorescence upon pH-values. Rhodamine WT is chiefly used in the USA, for groundwater as well as for surface water traces. In Europe, this dye was seldom used for a long while, due to supply and delivery problems and customs.

Rhodamine WT has proven itself:

- In many karst water traces (AULENBACH et al. 1978, MOHRING & ALEXANDER 1988, MULL et al. 1988, QUINLAN 1989),
- In tropical karsts (SMART & SMITH 1976),
- In periglacial karst (SMART 1988),
- For glacial traces (COLLINS 1982),
- For sewer discharge traces (AULENBACH et al. 1978),
- In the unsaturated zone (ALEXANDER et al. 1988).

Remarkable was the tracing test with 1000 l = 200 kg Rhodamine WT on 11 September 1990 used to colour the Rhine river near Basel by Ch.LEIBUNDGUT (Plate 2). Through this test, the residence time and the longitudinal dispersion in the Rhine from the river site km-172 through to the German-Dutch border (river site km-853) was to be modelled.

2.1.1.7 *Rhodamine 6G*

C.I. 45 160, Basic red 1, Pigment red 81 CAS: 989-38-8

Chemical name: 3,6-Bis-ethylamino-2,7-dimethyl-9-(2'-ethoxycarbonylphenyl)-xanthylium-chloride

Synonyms: Xanthylium,9-[2-(ethoxycarbonyl)phenyl]-3,6-bis(ethylamino)-2,7-dimethyl-chloride
Diethylamino-o-carboxy-phenyl-xanthenylchloridethylester
Rhodamine 6 GDN
Basonylrot 482

Chemical formula: $C_{28}H_{31}ClN_2O_3$ (as Rhodamin B)

Molecular weight: 497.02

Structural formula: Figure 15

Extinction maxima: 526 nm (main maximum)
495, 345, 285 nm (secondary maxima)

Fluorescence maximum: 552 nm

Specific decadic extinction at 526 nm: 0.168 ($l\ cm^{-1}\ mg^{-1}$)

Molar decadic extinction at 526 nm: 80,280 ($l\ cm^{-1}\ mol^{-1}$)

Water solubility: 20 g/l; in ethanol 120 g/l, in mixture with tannin 350 g/l (Rh.6G: tannin = 1:1).

Rhodamine 6G is mainly used in colour printing, due to its good solubility in alcohol. It is also used in microscopy to colour tissue.

There have been only a few tracing tests published using rhodamine 6G. One reason is due to the strong sorption properties of the dye. In a combined trace in the tropical karst in New Guinea, JAMES and MARTIN (1980) reported that, at a distance

of 1100 m, 30% of the injected uranine reappeared, yet only 0.2% of the rhodamine 6G reappeared.

A further reason for the rare use of this dye in traces is its high cost. Moreover, rhodamine 6G is according to ROTH & DAUNDERER (1990) toxic and possibly carcinogenic.

According to ARBELOA et al. (1982), at concentrations higher than 1 mg/l, similar to rhodamine B, double molecules are present (dimerisation). The absorption maximum at 526 nm is diminished in favour of another at 497 nm. Thus, if higher concentrations are to be measured by extinction determination, extra calibration curves are necessary. At 40 g/l, the extinction at both absorption wavelengths is the same.

2.1.1.8 *Other xanthene dyes*

Rhodamine 3G

C.I. 45 210, Basic red 3 CAS: 3262-60-6

Chemical name: 3-amino-6-dimethylamino-2-methyl-9-(2'-ethoxycarbonylphenyl)-xanthylium-chloride

Synonyms: Xanthylium, 3-amino-6-(dimethylamino)-9-[2-(ethoxycarbonyl)phenyl]-2-methyl-chloride
Amino-methyl-dimethylamino-o-carboxy-phenyl-xanthenyl-chloride-ethylester

Chemical formula: $C_{25}H_{25}ClN_2O_3$

Molecular weight: 436.65

Structural formula: Figure 15

Fluorescence: Redbrown

Water solubility: Good

This dye is, as rhodamine B and 6G, in dilute solutions cationic and thus has strong sorption properties. It is used only seldomly and moreover, the production costs are quite high. Some producers have cut it from their production lists.

Erythrosine

C.I. 45 430, Acid red 51 CAS: 568-63-8

Chemical name: 3-hydroxy-6-oxo-2,4,5,7-tetraido-9-(2'-carboxyphenyl)-xanthene-disodium

Synonyms: Spiro[isobenzfuran-1(3H),-[9H]xanthen]-3-one,2,4,5,7-tetraiodo 3',6'-disodium
Tetraiodofluorescein
Erythrosine B,C,FD
Food red 14
EWG-Nr.122

Chemical formula: $C_{20}H_6I_4Na_2O_5$

Molecular weight: 879.87

Structural formula: Figure 7

Extinction maximum: 525 nm

Fluorescence maximum: 547 nm

Specific decadic extinction at 525 nm: 0.083 ($l\ cm^{-1}\ mg^{-1}$)

Molar decadic extinction at 525 nm: 73,010 ($l\ cm^{-1}\ mol^{-1}$)

In Germany, erythrosine is an approved food additive for use in certain food groups according to the BGBL I from 1981. Therefore, it has been suggested at times, that erythrosine be used instead of uranine for hydrological tracing tests. Due to its low fluorescence yield of 1/160, compared to uranine, tracing tests with this dye have been rather unsuccessful.

Bengal rose
C.I. 45 440, Acid red 94 CAS: 632-69-9
Chemical name: 3-hydroxy-6-oxo-2,4,5,7-tetraiodo-9-(2'-carboxy-3',4',5',6'-tetrachloro-phenyl)-xanthene-disodium
Synonyms: Xanthylium, 9-(2-carboxy-3,4,5,6-tetrachloro-phenyl)-3,6-dioxy-2,4,5,7-tetraiodo-disodium
2,4,5,7-tetraiodo-3',4',5',6'-tetrachloro-fluorescein-disodium
Rose bengale
Bengal rose B
Chemical formula: $C_{20}H_2Cl_4I_4Na_2O_5$
Molecular weight: 1017.64
Structural formula: Figure 7
Extinction maximum: 540 nm, Excitation maximum: 518 nm
Fluorescence maximum: 535 nm
Specific decadic extinction at 540 nm: 0.071 ($l\ cm^{-1}\ mg^{-1}$)
Molar decadic extinction at 540 nm: 72,710 ($l\ cm^{-1}\ mol^{-1}$)
Absorption- and maxima excitation do not coincide

Bengal rose has similar properties as erythrosine. Practical applications with it as a hydrological tracer are not known.

Dimethylfluorescein, diethylfluorescein, sulfofluorescein
According to DEMUTH (1988), 4,5-dimethyl fluorescein, 2,7-diethylfluorescein and sulfofluorescein should be well-suited as hydrological tracers, since they fluoresce with a high quantum yield in UV and have low sorption properties. However, practical applications with these dyes are impaired due to the high background levels. The sensitivity to light of the first two products is even larger than eosin's, so that use in surface waters is even more impaired (BEHRENS & DEMUTH 1990). However, these products can be used in photolytical light measurements in rivers and lakes.

2.1.1.9 *Pyranine*
C.I. 59 040, Solvent green 7 CAS: 63358-69-6
Chemical name: 1-hydroxy-pyren-3,6,8-trisulfon-trisodium
Synonyms: 1,3,6-pyrentrisulfon,8-hydroxy-trisodium
3-oxypyren-5,8,10-trisulfon-trisodium
D & C Green 8
Pyranin 120%
Chemical formula: $C_{16}H_7Na_3O_{10}S_3$
Molecular weight: 524.39
Structural formula: Figure 20a, top left

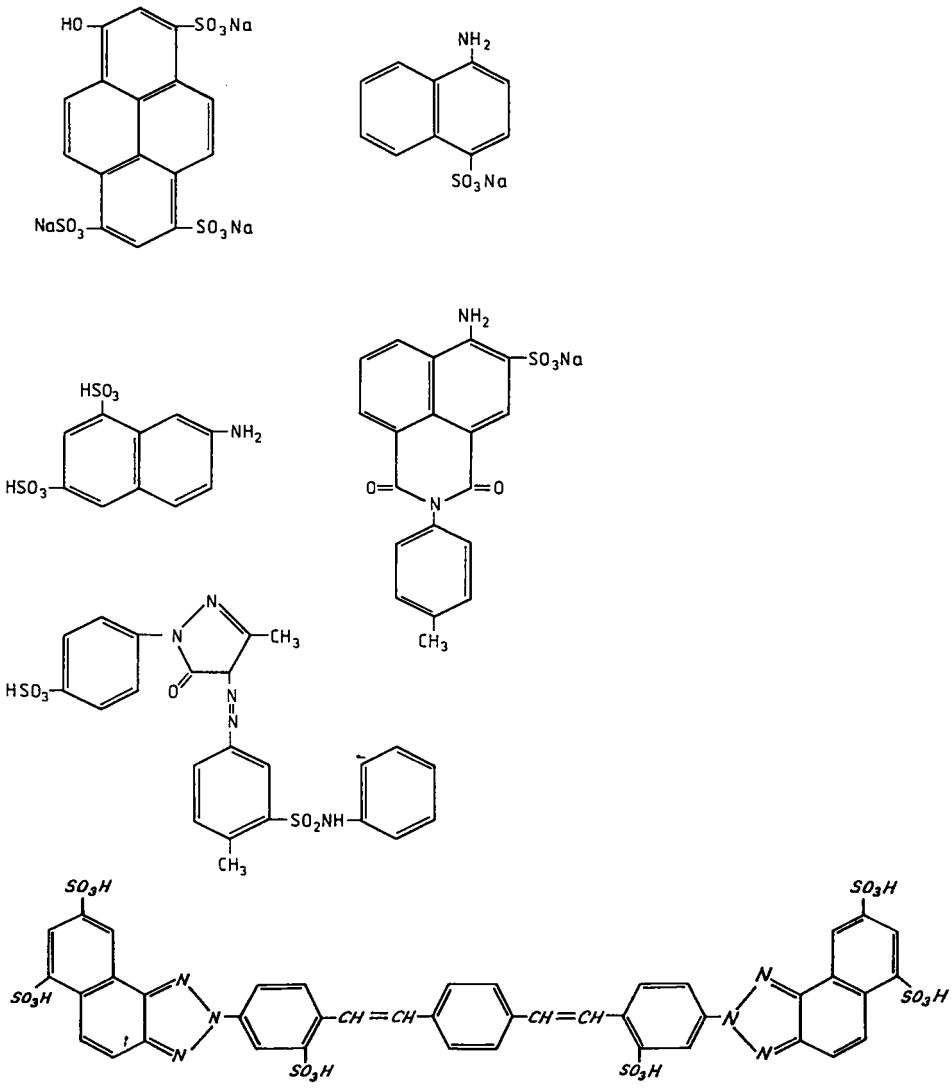

Figure 20. Structural formula. a) Left top: Pyranine, right top: Na-Naphthionate, Middle left: Amino G acid, Middle right: Lissamine, Bottom: Lanaperl fast yellow; b) Direct yellow 96 (free acid).

Extinction maxima:	main maximum:	455 nm (>pH 7.7),
		405 nm (<pH 7.7)
	secondary maxima:	455 nm (pH 6 – pH 7.7),
		380 nm (<pH 8), 365, 297 (>pH 8)
		290 nm (<pH 8), 280 nm

Fluorescence maximum: 512 nm (>pH 2.5); 445 nm (<pH 2.5)
Specific decadic extinction at 455 nm: 0.0412 (l cm^{-1} mg^{-1})
Molar decadic extinction at 455 nm: 21,600 (l cm^{-1} mol^{-1})
Water solubility: 178 g/l (20°C).

Pyranine was developed in the Bayer-Laboratories (TIETZE & BAYER, 1939). ATKINSON et al. (1973) first reported using this dye as a hydrological tracer in the Carboniferous karst in the Mendip Hills, southwest of Bristol/United Kingdom.

This fluorescent dye is, not only with regards to its fluorescence, but also to its excitation and absorptions spectra, markedly pH-dependent (Fig. 21). These relationships are described in detail by BEHRENS (1988a,b) and BENISCHKE & SCHMERLAIB (1988).

According to ZHUJUN & SEITZ (1984), the 8-hydroxy radical is the cause for this behaviour: At pH 7.3 equilibrium prevails, above that the anion $C_{16}H_6O_{10}S_3^{4-}$ $+3Na^+$ $+H_3O^+$ (absorption wavelength 455 nm) prevails, under that the anion $C_{16}H_7O_{10}S_3^{3-}$ $+3Na^+$ $+H_2O$ prevails (absorption wavelength 405 nm). No cation develops at the pH-change due to the low sorption properties of pyranine even at low pH-values.

This was verified by flow tests in 1.25 m long plexiglass columns, with a cross-section of 10 cm^2. The columns were filled with sphagnum from Lower Saxony and with moor water with a pH of 4.3; they were also rinsed with the same water out of MARIOTT bottles. The two columns were wetted with 20 ml of a 100 mg dye solution; one with uranine, the other with pyranine. The discharge was collected in 100-ml graduated flasks and brought to a pH of 9 in an ammonia atmosphere. After 2.5 l of solution passed through the columns, not a trace of uranine had been washed out, but 70 mg = 70% of the pyranine, whereby in the last sample 0.11 mg/100 ml pyranine was determined.

Pyranine is thus well-suited for traces in acidic underground, whereas uranine is not. In those cases where both dyes are used together, problems will arise during analysis. Although both dyes fluoresce at different wavelengths, in neutral and alkaline pH-ranges, both dyes have their fluorescence maximum at the same wavelength, 512 nm.

Apart from tracing tests, pyranine is also used in cosmetics, in markers and to colour district heating water (DIN 1988).

The application of pyranine in a trace in 1973 by ATKINSON et al. in the karst in southwest England was already mentioned. Other successful traces reported are:

- SMART & SMITH (1976) in tropical karst on Jamaica over 5000 m,
- JUNGBAUER (1983) in north Württemberger Muschelkalk karst over 1730 and 2180 m,

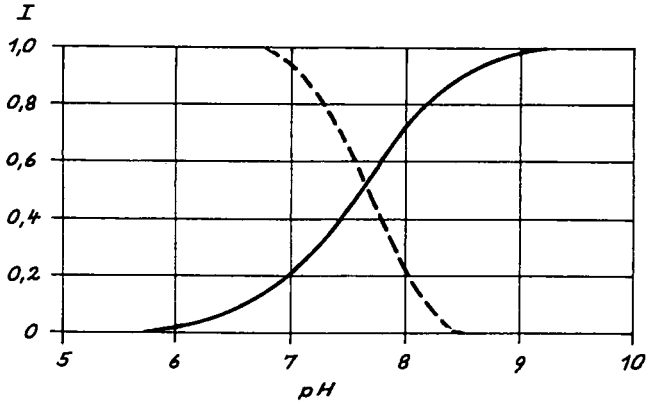

Figure 21. pH-Dependency of the fluorescence intensity of pyranine. Solid line: excitation at 455, fluorescence at 512 nm, dotted line: excitation at 405, fluorescence at 445 nm.

– ATH-Group in Carboniferous karst of the Central Peloponnesus over 9800 and 11,400 m (MORFIS & ZOJER 1986),

– ATH-Group in the southern alpine karst of the Lur cave system over 3100 m (ATH 1992).

2.1.1.10 *Sodium-naphthionate*
CAS: 130-13-2
Chemical name: 1-Aminonaphthalin-4-sulfon acid, sodium salt
Synonyms: Naphthion acidic, sodium salt
1-naphthylamin-4-sulfon acidic, sodium salt
Chemical formula: $C_{10}H_8NNaO_3S$
Molecular weight: 245.23
Structural formula: Figure 20a, top right
Extinction maxima: 320 nm (main maximum)
237 nm, 218 nm (secondary maxima)
Fluorescence maximum: 420 nm
Specific decadic extinction at 320 nm: 0.0322 ($l\ cm^{-1}\ mg^{-1}$)
Molar decadic extinction at 320 nm: 7870 ($l\ cm^{-1}\ mol^{-1}$)
Water solubility: 240 g/l (21°C).

Sodium-naphthionate is a gray-pink powder, which can contain several percent water. The fluorescence intensity is only approx. 1/14 of uranine's. Although it has low sorption properties, since the fluorescence background is markedly higher than uranine, almost twenty times the amount needs to be used in tracing tests. The fluorescence intensity is between pH 4 and 9 virtually constant, towards lower pH-values it sinks quickly, towards higher pH-values it sinks more slowly. Between the excitation and fluorescence maximum is a wavelength difference of 100 nm.

A great advantage of traces using sodium-naphthionate is that it is not visible at the sampling sites in the concentrations used. Under 1000 mg/l, sodium-naphthionate is virtually not organoleptically sensible, only the injection solutions attract attention due to their iridescent blue-violet colour. This tracer is well suited to be used along with uranine, eosin, and the rhodamines without interference (WERNLI 1986, LEIBUNDGUT & WERNLI 1988).

Sodium-naphthionate is actually only an intermediate product in the dye syntheses, but it has proven itself in successful traces:

– Karst of the eastern Peloponnesus over 25,000 m (MORFIS & ZOJER 1986),

– Alpine karst of the Säntis-Altmann-Stocks over 1200 and 6800 m (LEIBUNDGUT & ATTINGER 1988),

– South alpine karst in the Lur cave system over 3100 m (ATH 1992),

– In the fracture groundwater of the Oberharz over 8 m (LEIBUNDGUT & WERNLI 1988),

– In the pore-groundwater of the Swiss Mittelland over 50 m and 1500 m (LEIBUNDGUT & WERNLI 1988),

– In glacial water traces (MATHEZ 1986).

Amino G Acid
CAS: 86-65-7

Chemical name: 2-aminonapthaline-6,8-disulfon acid
Synonym: 7-amino-1,3-naphthalindisulfon acid
Chemical formula: $C_{10}H_9NO_6S_2$
Molecular weight: 303.32
Structural formula: Figure 20a, middle left
Extinction maxima: 359 (Main maximum)
308 nm, 247 nm, 218 nm (secondary maxima)
Fluorescence maximum: 450 nm
Specific decadic extinction at 359 nm: 0.028 (l cm^{-1} mg^{-1})
Molar decadic extinction at 359 nm: 8500 (l cm^{-1} mol^{-1})
Water solubilty: Moderate.

Amino G Acid is chemical related to sodium-naphthionate, visibly, as well as in its fluorimetrical characteristics. Under a pH of 5, its fluorescence decreases strongly. Sorption properties have not been recorded in laboratory tests. The commercial product contains approx. 25% water. This dye is often mentioned in literature summaries, e.g. SMART & LAIDLAW (1977), however, field tests have not been described in scientific literature.

2.1.1.11 *Lanaperl fast yellow*
C.I. 18 835 Acid yellow 25 CAS: 6359-85-9
Chemical name: 4-(4'-methyl-3'-sulfanilido-1-azo)-3-methyl-1-(4"-sulfophenyl)-pyrazol-5-on-sodium
Synonyms: Benzolsulfonsaures, 4-[4,5-dihydro-3-methyl-4-[[4-methyl-3-[(phenylamino)sulfonyl]phenyl]azo]-5-oxo-1H-pyrazol-1-yl]-Natriumsalz
Lanaperl-Echtgelb 10 GFF (HOECHST)
Säuregelb 25
Supramingelb R
Jaune sulfacide
Chemical formula: $C_{25}H_2ON_5NaO_6S_2$
Molecular weight: 549.55
Structural formula: Figure 20a, bottom
Extinction maxima: 449 nm (main maximum)
478 nm, 265 nm (secondary maxima)
Fluorescence maximum: 508 nm
Specific decadic extinction at 445 nm: 0.0021 (l cm^{-1} mg^{-1})
Molar decadic extinction at 445 nm: 1210 nm (l cm^{-1} mol^{-1})
Water solubility: Good

Lanaperl fast yellow, an orange-red powder, has a constant fluorescent intensity over a wide pH range, yet marked sorption properties.

In hydrology, lanaperl fast yellow has been only used rarely. FOURNEAUX and ROCHAT (1982) carried out a combined trace using this dye along with three others (amidoflavine, rhodamine B, and amidorhodamine G) in the southern French Jura karst. 500 g of each dye was injected in a well and out of the four injected dyes, all but amidoflavine were detected in the sampling well, which was 250 m away. Lanaperl fast yellow is related to amidoflavine.

In the jurassic karst of Causse de Gramat (Dpt. Lot./France) a hydrological connection of a length of more than 12 km was proved with 10 kg lanaperl fast yellow (DZIKOWSKI et al. 1993). The yield amounted to 73% in this trial.

Amidoflavine
C.I. Acid yellow 215:1
Synonyms: Amido-Flavin FF-PW (HOECHST)
Amido-Flavin FFP
Säuregelb 215:1
Chemical formula: (unknown)
Extinction maxima: 440 nm (main maximum)
345, 282 nm (secondary maxima)
Fluorescence maximum: 518 nm
Specific decadic extinction at 440 nm: 0.01 (l cm^{-1} mg^{-1})
Water solubility: 80 g/l (20°C)

Amidoflavine is a lemon-yellow powder. Chemically, it is a naphthalimide. Its fluorescence intensity is less than 1% of uranine's.

As mentioned above, this dye was injected by FOURNEAUX and ROCHAT along with lanaperl fast yellow, rhodamine B, and amidorhodamine G in the French Jura karst. However, it could not be detected, most likely due to a too low injection amount.

2.1.1.12 *Lissamine*
C.I. 56 205, Acid yellow 7 CAS: 2391-30-2
Chemical name: 1-amino-N-(4-methylphenyl)-4,5-napthalimide-2-sulfon acid, sodium salt
Synonyms: 1H-benz[de]isochinolin-5-sulfon acid,6-amino-2,3-dihydro-2-(4-methylphenyl)-1,3-dioxo, sodium salt
Brillantsulfoflavin FF (HOECHST)
Brilliant Sulfoflavine (ALDRICH CHEMICAL Co.Ltd.)
Orcoacid sulfo flavine FF (ORG.CHEM.Corp.)
Lissamin FF
Lissamin Flavin FF
Lissamin yellow FF (ICI Corp.)
Säuregelb 7
Brilliant acid yellow 8 G (ALLIED CHEMICAL Corp.)
Chemical formula: $C_{19}H_{13}N_2NaO_5S$
Molecular weight: 404.38
Structural formula: Figure 20a, middle right
Extinction maximum: 422 nm, excitation maximum: 432 nm
Fluorescence maximum: 508 nm
Specific decadic extinction at 422 nm: 0.0202 (l cm-1 mg^{-1})
Molar decadic extinction at 422 nm: 8160 (l cm^{-1} mol^{-1})
Water solubility: 22 g/l

Lissamine is an orange powder; chemically, it is an aminoketone. In scientific lit-

erature, only a few tracing tests using Lissamine have been described. SMART and SMITH used it in a river in Jamaica over a flow distance of 1.25 and 6 km, whereby on two traces, the reemerged yields were over 100%. These high reemergence rates are most likely due to the high background levels in tropical rivers. Further traces with lissamine were successful in the melt water of the Columbia glacier in Canada. The melt water seeps directly beneath the glacier into the karstified underground and reemerges 3 km away in the karst springs. SMART (1988) determined yields between 5.1 and 53%.

Direct yellow 96
Direct yellow 96 is similar in colour to lissamine and is a chemical suitable for water tracing.
Chemical name: 4',4"-bis-(5,7-disulfo-1,3-naphthotriazolyl)-distyryl-benzene-2',2"-disulfon acid, hexasodium salt
Synonyms: Direktgelb 96
Solophenyl Flavin 7GFF (CIBA-GEIGY)
Diphenyl Brilliant Flavin 7GFF
Pyrazol Brilliant Flavin 7GF (SANDOZ)
Chemical formula: $C_{42}H_{22}N_6Na_6O_{18}S_6$
Molecular weight: 1229.02
Structural formula: Figure 20b
Water solubility: Very good

This dye is an orange coloured stilbene derivative. It is stable, has low sorption properties and is physiologically harmless.

According to a data sheet from CIBA-GEIGY, Diphenyl Brilliant Flavin 7GFF has the following properties:

BOD_5:	0.48 mg/mg
Chemical Oxygen Demand:	1.07 mg/mg
LD_{50} (Rat, oral):	23.1 g/kg
LC_{50} (Fish test, 96 hours):	>1000 mg/l

In the concentrations used in water tracing tests, it is not visible at the reemergence sites. The production costs are moderate. Unfortunately, the fluorescence is pH-dependant. QUINLAN used it in the Kentucky (USA) karst over distances up to 16 km (1976). The injection solution had a concentration of 125 g/l.

At the sampling sites, the dye is adsorbed on cotton swabs, which are hung in the water. The swabs are collected and kept wet in plastic bags and either qualitatively analysed under a quartz lamp or semi-quantitatively in a filter fluorimeter. The detection limit is 1 µg/l (MULL et al. 1988). When using different filters, optical brighteners can be detected besides direct yellow 96.

A dye related to direct yellow 96 is sold by DUPONT under the name 'Pontamine Brilliant Flavine 66' (C.I. Direct Yellow 131). How suitable it is a water tracer has not yet been reviewed (QUINLAN 1976).

2.1.1.13 *Optical brighteners*
Optical brighteners are chemicals used to brighten textiles and paper, laundry soap

can also contain considerable amounts. In Germany, some 700 t of optical brighteners annually flow essentially unclarified through the sewer systems into the receiving streams (KANOWSKI 1985). Other names in English are brightening agents or colourless dyes; in German: optische Aufheller, Weißtöner, Fluoreszenz-Bleichmittel, in French: produits de blanchiment optique, avivrages optiques.

The members of this group absorb UV-light and radiate violet to blue light. They are often derivatives of the stilbenes, benzidines, cumarines, thiazols, triazines and other ring systems with such functional groups as the amino- and sulfo-groups.

In 1906, SACHS and HILPERT described the blue-violet fluorescence of an ether solution of amino stilbene ($C_{14}H_{13}N$). Later, KAUFFMANN (1917) listed several substances, whose solutions also fluoresce blue, among them p-distyrylbenzene (p-C_6H_5-CH=CH-C_6H_4-CH=CH-C_6H_5-p) and p-dimethylamino stilbene.

Optical brighteners are now so numerous that one can hardly tell them apart, not only with respect to their chemical composition, but also with trade names: there are fifty different kinds of BASF-Blankophor. Often, the same chemical compound is sold by different companies under different names. Here a selection of typical product groups from several companies:

- BAYER: Blankophor,
- CIBA-GEIGY: Tinopal, Uvitex,
- HICKSON & WELCH: Photine,
- SANDOZ: Leukophor,
- HOECHST: Hostalux,
- AMERICAN CYANAMID: Calcofluor.

These products are sold either as a powder or as a viscous fluid. Since a large amount of the substance is often needed to be successful as a tracer, most of the powdery optical brighteners need to be dissolved in a large quantity of water before they can be injected into the underground. Especially in tracing tests in karst water with high calcium concentrations, precipitation is to be expected. Thus, liquid optical brighteners are preferable in water tracing tests. Analysing the water samples for optical brighteners is occasionally difficult. The background levels at these wavelengths are quite high, even with very clean water samples, in comparison to the analysis for green or orange fluorescing dyes. Furthermore, suspended solids influence the spectral fluorimetrical properties greatly, due to dispersion. The detection limit for optical brighteners is at the best hardly under 0.1 µg/l. The excitation maxima for the optical brighteners suitable for hydrological tracing tests lie between 340 and 360 nm, the fluorescence maxima between 430 and 465 nm. Substances which have only a, e.g. 60 nm, wavelength difference between excitation and fluorescence maximum have a RAMAN-Peak at 390/450 under the synchronscan. Therefore, during the intensity measurements at specific wavelengths as well as under the synchronscan, provisions have to be made to make sure that the RAMAN dispersion does not interfere with the measurements.

Another measurement method is to hang cotton or other textile swabs in the water sampling sites ('cotton detectors'). After they are collected, they are kept wet and analysed for the fluorescence under the fluorimeter.

The first hydrological application with optical brighteners in a tracing test was by CRABTREE (1970, 1971). He used them in karst water investigations with leucophor BS and cotton as adsorbents. SMART (1976a,b) published a review of the application

possibilities, properties regarding adsorption, pH-, light and temperature influences, as well as about the toxicity of several products.

MULL et al. (1988) point out in detail, that the background levels need to be adequately investigated, before optical brighteners are used in tracing tests.

As a representative for the numerous optical brighteners used in water tracing tests, the product tinopal CBS-X, which is preferably used in Europe, is described.

Tinopal CBS-X
C.I. Fluorescent brightener 351 CAS: 27344-41-8
Chemical name: 4,4'-bis-(2-sulfostyryl)-1,1'-biphenyl-disodium
Synonyms: Dibenzenesulfonic acid, 2,2'-([1,1'-biphenyl]-4,4'-diyldi-2,1-ethenediyl)-bis-disodium
Disodium 4,4'-bis(2-sulfostyryl)biphenyl
Stilbene 3
Chemical formula: $C_{28}H_{20}Na_2O_6S_2$
Molecular weight: 562.57
Structural formula: Figure 22a, top
Extinction maxima: 346 nm (main maximum)
223 nm (secondary maximum)
Fluorescence maximum: 435 nm
Specific decadic extinction at 347 nm: 0.126 (l cm^{-1} mg^{-1})
Molar decadic extinction at 347 nm: 59,600 (l cm^{-1} mol^{-1})
Water solubility in dist. water at 10°C: 0.4-0.5 g/l, at 25°C: 25 g/l, in water with 7 meq/l hardening agents at 10°C: 3-5 mg/l.

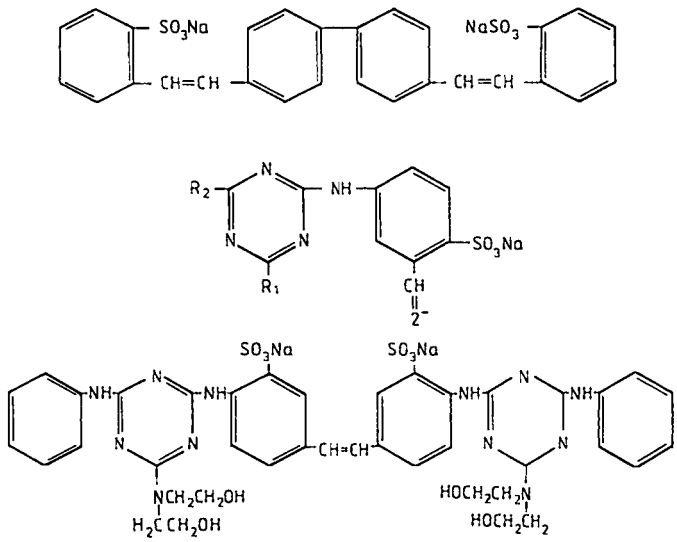

Figure 22. Structural formula of some optical brighteners. a) Top: Fluorescence brightener C.I. 351 (tinopal CBS-X); Middle: Fluorescence brightener C.I. 15 (photine CU) (after SMART & LAIDLAW 1977); Bottom: Fluorescence brightener C.I. 28 Nr. 40 622 (after ALDRICH 1988).

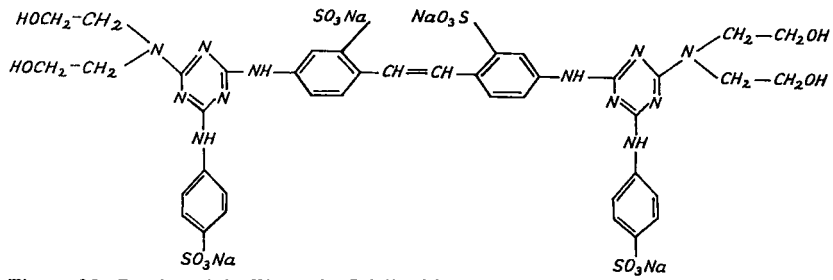

Figure 22. Continued. b) Tinopal ABP liquid.

Tinopal CBS-X is a light yellow, granular powder, which can only be dissolved in a large quantity of water. Using a chelating agent helps keep it in solution.

In Europe, numerous tracing tests have been conducted using tinopal-CBS-X. A selected few are listed here:

– Swabian Jura. Since 1978, several tracing tests in the Upper Jurassic karst have been carried out over distances up to 8.1 km.

– Muschelkalk karst of the southwestern German cuesta lands over 1.8 km (JUNGBAUER 1983, TENHAEFF & KÄSS 1987). Uranine, tinopal CBS-X and fluorescing microspheres were injected into the Frauenbach sinkhole on the Dinkelberg mountain northeast of Lörrach/Germany (SCHABER 1993). In springs near the Hasel tunnel exit, approx. 1.5 km away, 24% of the injected uranine reappeared and only 4% of the tinopal. From the average residence time, a retardation factor of 1.4 was calculated (Fig. 23).

– Northern Calcareous Alps. Tracing tests have been carried out in the Leoganger Steinberge (VÖLKL 1981), Tennengebirge (BRANDECKER & MAURIN 1982), Zahmer Kaiser (VÖLKL 1988) and Dachstein massif (BAUER 1989).

– Dinaric karst: Tracing tests carried out by the ATH-Group in 1974 over a distance of 11.8 km with a 151 m grade (BAUER et al. 1976).

– Eastern Peloponnesus: Cretaceous karst over 4.8 km (MORFIS & ZOJER 1986).

– Fissure water in an ore lode in the Southern Black Forest over a distance 220 m (ACKERMANN et al. 1982).

– Pore-groundwater in the gravelly alpine foreland of the Iller Valley over a distance of up to 380 m (GLMZ 1980).

– Pore-groundwater in the gravelly-sandy Upper Rhine Valley Quaternary aquifer. In the Merdinger test field here, tinopal appeared in the 25 m-observation wells only after a delay and without a typical breakthrough curve. However, only 50 g of tinopal was injected.

In reviewing the investigation reports of the case studies, the constant and conspicuously low recovery of tinopal attracts attention, which rarely reaches even 50% of the uranine recovery yield. At the same time, a delay in the time-concentration curve is also apparent (Fig. 23). Similar results were reported by BAUER in 1976.

The more close-grained the pore-groundwater aquifer is, the less suitable tinopal CBS-X is for tracing tests. The trace in the Frauenbach sinkhole (Fig. 23) was carried out in the Muschelkalk karst of the Dinkelberg mountain. It is, as an old land surface, deeply weathered basin karst and tectonically stressed. The Muschelkalk is interca-

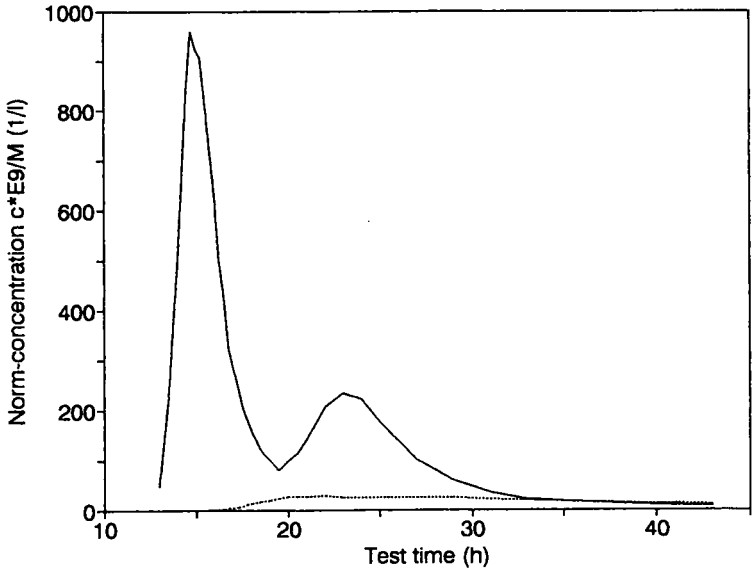

Figure 23. Standardized breakthrough curves for uranine (top curve) and tinopal (bottom curve) in the Lower Brunnmühle spring in the tracing test carried out in the Frauenbach sinkhole near Hasel/Cty.Lörrach (SW-Germany) on 4.Nov.1987. Aquifer: Muschelkalk karst; injection amount: 50 g uranine (3:00 pm) + 500 g tinopal CBS-X (5:00 pm); distance: 1484 m, grade: 48 m, discharge: 7.5 l/s. In the neighbouring Upper Brunnmühle spring with approx. the same discharge, almost identical breakthrough curves were determined. The standardized uranine concentrations are at first considerably higher than those of tinopal; at the end of the breakthrough curve, uranine's standardized concentration sinks below that of tinopal.

lated with marl – all factors that promote sorption. In wide karstified cavities in lime formations with low clay percentages however, tinopal can be successfully used in traces, even over long distances.

To test how tinopal CBS-X reacts in acidic medium, a flow test was carried out with moorwater in a column filled with sphagnum. The test conditions were identical with those described in the flow test with pyranine (Section 2.1.1.9). Tinopal was completely held back in the column. Thus, tinopal and probably all optical brighteners are not suitable for traces in acidic groundwaters.

Tinopal ABP Liquid
Producer: CIBA-GEIGY
Chemical name: 4,4-bis-[3-diethylamino-5-(4-sulfanilino)-s-triazinyl-amino]-stilbene-2,2'-disulfon-tetrasodium
Synonym: Bis-diethylamino-bis-4-sulfo-anilino-CC-DAS
Chemical formula: $C_{40}H_{40}O_{16}N_{12}Na_4S_4$
Molecular weight: 1146
Structural formula: Figure 22b.
Extinction maximum: 350 nm
Fluorescence maximum: 435 nm

In Switzerland, where the connections to the producers are wellfounded, numerous tracing tests with liquid tinopal ABP have been carried out. Liquid tracers are harder to transport, have however the advantage that they are easier to inject.

– ATH-Group: In the Neuchâtel Jurassic, 100 l of tinopal ABP was injected in the active doline Petit Cachot. In the Areuse spring, the detection was negative; in the Noiraigue-spring, 6.8 km away, tinopal was not detected with complete certainty (BAUER et al. 1980).

In the combined trace in the pore-groundwater aquifer in the test area Langeten Valley, 100 l of tinopal ABP and 20 kg of eosin were injected in the same site. In the nearest observation site, 1175 m away, eosin was detected in a concentration of over 13 µg/l, whereas tinopal was under the detection limit of 0.1 µg/l (BAUER et al. 1981).

– ASCHWANDEN and LEIBUNDGUT (1982) traced the meltwater of the Gorner glacier with 100 l of tinopal ABP. In the glacial outlet, approx. 7 km away, tinopal was detected with a maximal concentration of 15 µg/l and at a meltwater flow of approx. 16 m^3/s.

The fluorescence intensity increases when the aqueous solution is illuminated, especially in a spectrofluorimeter. Therefore with tinopal ABP liquid a semi-quantitative result can be obtained only.

Leucophor, leukophor

The first traces carried out using leucophor BS (C.I. Fluorescent brightener 49) were done in the carboniferous karst of the Mendip Hills in County Somerset/England (CRABTREE 1970, 1971, GLOVER 1972). The observation sites were sampled in the first tests with cotton detectors. Further successful traces were carried out by GASCOYNE (1974) in Venezuela with leucophor BS and leucophor C (C.I. Fluorescent brightener 232). GASCOYNE ascertained however that, leucophor C is adsorbed on organic material considerably stronger than leucophor BS. Both chemical compounds are no longer available. They have been replaced by the producers by other compounds.

Lately, a liquid leucophor product, namely L.PBS has been used. MULLEN and THORN (1988) reported a trace in eastern Ireland, where a combined trace was carried out near a dumpsite. The underground consists of carboniferous karst. Uranine was detected in 5 springs in 500-800 m distance; NaCl and leucophor PBS only in the main spring 600 m away.

Leucophor PBS has also been tested in the pore-groundwater aquifer of the Merdinger test area. In the test where 500 ml was used, it could be detected at a distance of 50 m. Due to the high background level caused by humic acid, it could not be detected at 100 m above the detection limit of 1 µg/l. Astonishingly, the maximal leucophor concentration was only slightly delayed in comparison to the simultaneously injected uranine. Leucophor's sensitivity to light in fluorimetrical measurement will however limit its use to the usual quantitative determination.

Photine CU

Photine CU (C.I. Fluorescent brightener 15) is a 20% solution in ethanolamine with urea and photine UC is the pure substance (Fig. 22a). Another photine product is P.CSP, a powdery substance with approx. 40% NaCl. Both substances, photine CU

and CSP were used by SMART and SMITH (1976) on Jamaica; the first one in a tropical river, the latter one in karst. In both cases the breakthrough curves showed a marked loss of photine due to adsorption onto organic material. Also, problems arose during analysis: During the determination of photine CSP, the background fluctuated between 12 and 50 µg/l-photine-equivalents. During the trace in the karst however, it was possible to follow the underground waterway over a distance of 12 km, by using an injection amount of 2.2 kg photine.

SMART (1988) described a trace in the karst in South Wales, where over a distance of 1.6 km, 35% of the uranine injected and 31% of the simultaneously injected photine CU was recovered.

Fluorescence-brightener 28
C.I. Fluorescent brightener 28, No.40 622
Chemical name: 4,4'-bis-(3.anilino-5-diethanolamino-s-triazinyl)-stilbene-2,2'-disulfonic acid, disodium salt
Synonyms: Calcofluor White ST,
Tinopal LPW, Tinopal 4BM
Phorwite BBH (MOBAY CHEM. Corp.,Pa.)
Chemical formula: $C_{40}H_{42}N_{12}Na_2O_{10}S_2$
Molecular weight: 960.96
Structural formula: Figure 22a
Extinction maxima: 349 nm (main maximum)
240 nm (secondary maximum)
Fluorescence maximum: 430 nm
Specific decadic extinction at 349 nm: 0.053 ($l\ cm^{-1}\ mg^{-1}$)
Molar decadic extinction at 349 nm: 5088 ($l\ cm^{-1}\ mol^{-1}$)
Water solubility: Good

According to SMART (1976a), this tracer is often used by Quinlan in karst traces in Kentucky. They succeeded in tracing underground waterways over a distance of 16 km.

In contrast to most of the other optical brighteners, fluorescence brightener 28 is stable in light.

Hostalux
BAUER, PERLEGA and VÖLKL (1980) tested the optical brightener hostalux PN liquid in the Lur cave system as to its suitability as a karst water tracer. In comparison to the simultaneously injected uranine (3 kg), hostalux (28 kg) reappeared in the 3.1 km away Hammerbach spring with a delay and a 80% lower yield. The hostalux investigation was carried out with the Double-Scanning-Method; in laboratory tests, a detection limit of 1 µg/l was determined. According to the report, hostalux reacts similarly to tinopal in karst water traces. The losses at the injection site were probably the result of adsorption, due to the high concentration of tinopal.

2.1.2 *Non-fluorescing dyes*

P.KANDLER is reported (TIMEUS 1911) to have been the first, to consider tracing per-

colating water with dyes. In 1864, he suggested dying the Reka percolation near San Cozian with indigo, yet never carried out his idea.

A few years later in 1869, KNOP carried out a dye tracing test with aniline red in the Danube percolation, but it was unsuccessful (KNOP 1875). KNOP presumed that it was due to the sorption properties of the dye used, although the injected amount of 14 kg should have been enough to visibly colour the Aach spring.

The sorption properties of dyes was used by HÖTZL et al. (1982) to investigate fractures in quarry walls. They injected solutions of methyl blue, astra diamond green, and rhodamine B into small bore holes in the working walls. The fissures were measured before and after the blasting operations. Thus, not only the spatial distribution of the fissures could be determined, but also the form and size of the rock fragments.

The recommendations published for using non-fluorescing dyes in water tracing tests are numerous. They cover aniline violet (C.I. 42 535, basic violet = methyl violet), congo red, malachite green, auramine and fuchsine (TRILLAT 1899a,b, GÄRTNER 1915, BENDEL 1948, SCHIECK 1958). However, it is not always obvious as to which fuchsine is meant, as there are three different fuchsine types: (basic) fuchsine = magenta = rosaniline ($C_{20}H_{19}N_3 \cdot HCl$, molecular weight 337.86, C.I. 42 510), neutral- or new fuchsine = fuchsine N ($C_{22}H_{23}N_3 \cdot HCl$, molecular weight 365.91, C.I. 42 520) and acid fuchsine = fuchsine S = rubine S ($C_{20}H_{17}O_9N_3S_3Na_2$, molecular weight 585.55, C.I. 42 685). The last form has, according to tests by TRILLAT (1899a), low sorption properties.

Only a few traces which used non-fluorescing dyes have been successful:

– KYRLE (1928) injected in February 1927 in the Lur cave system 500 g fuchsine twice. In preliminary tests, he had determined a detection limit of 20 µg/l in test tubes. However, during the trace, Kyrle observed that after a flow distance of 50 m, the dye was no longer visible.

– DREW (1968) investigated the Mendip Hills karst with congo red and malachite green. The dyes were sorbed onto cotton swabs, which were hung in the sampling sites.

Non-fluorescing dyes are suitable for tracing tests in aquifers which have a relatively small surface and only over short distances. These dyes, due to their poor detection limits, are only useful as backup tracers.

Nevertheless, the operational possibilities for using these dyes are not totally exhausted. Modern spectral photometers can measure extinctions with thicknesses up to 1 m in cuvettes using multiple light paths. Non-fluorescing dyes can only be used as tracers in surface water with extremely good quality. The advantage of this dye group in surface waters lies in the fact that they normally have a good light and pH stability.

Non-fluorescing dyes should be used in tracing tests where tracing with fluorescent dyes would cause disturbances (see Section 2.1.1.1).

FLURY and FLÜHLER (1994, 1995) successfully applied Brilliant Blue FCF ($C_{37}H_{39}N_2Na_2O_9S_3$, molecular weight 792.85, C.I. 42090, CAS 3844-45-9) for the determination of the infiltration into the unsaturated zone along transsections.

2.1.3 *Analysis*

In practice, fluorescent substances occur for the most part as traces. Therefore, their

determination is often accompanied by problems which can only be solved if the analyst has sufficient knowledge of the substances' properties as well as the technical specifics of the laboratory apparatus. Thus, the physico-chemical properties of the fluorescent substances are handled here first.

2.1.3.1 *Physico-chemistry of fluorescent substances*

Publications concerning the properties and reactions of the fluorescent substances that are used in water tracing can be found in different disciplines. In 1964 and 1965, KÄSS described the most important properties of uranine. Other tracers were handled by other authors, e.g. SMART (1976a,b) described optical brighteners. BAUER (1976) investigated tinopal for its suitability as a karst tracer, as WERNLI (1986) and LEIBUNDGUT and WERNLI (1988) did for sodium-naphthionate. BENISCHKE and SCHMERLAIB described the tracer pyranine (1988) in detail. SMART & LAIDLAW'S publication (1977), is worth mentioning, which covered not only the physico-chemical properties of eight fluorescent dyes with regards as a tracer, but also with regards to their toxic properties. These eight dyes are: uranine, rhodamine B, sulforhodamine B, rhodamine WT, pyranine, amino G acid, lissamine FF and photine CU. Many of the following explanations are based on these articles.

pH-dependency of the fluorescence

The fluorescence intensity in the aqueous solution of a fluorescent dye is dependant upon the pH-value. Uranine's pH-dependency was already described in Section 2.1.1.1 of this book. Figure 24 (bottom) displays the pH-dependency of most of the fluorescent dyes used in water tracing. The figure clearly shows that at the neutral point, pH 7, uranine reaches only 80% and pyranine only approx. 20% of their maximal fluorescence intensity. Eosin's fluorescence is much less pH-dependant. All of the rhodamines, including sodium-naphthionate and amino G acid have a constant maximal fluorescence between pH 5 and pH 8. Among the presented fluorescent dyes, amidorhodamine G has the least pH-dependency. Sulforhodamine B is not dis-

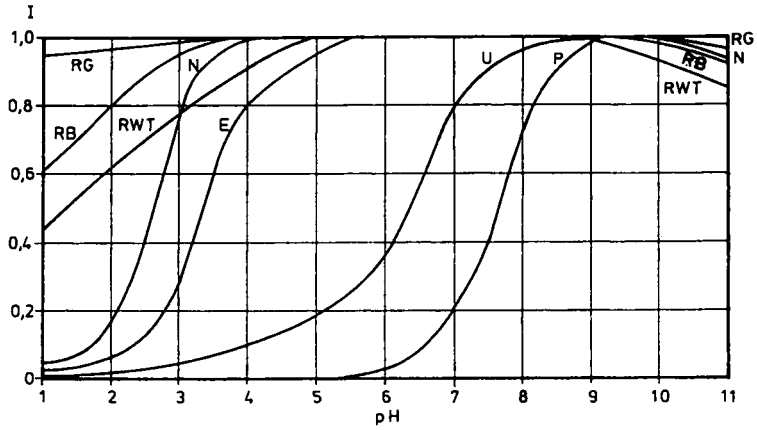

Figure 24. pH-dependency of the fluorescence of some chosen fluorescent dyes. a) U = uranine, E = eosin, RB = rhodamine B, RG = amidorhodamine G, RWT = rhodamine WT, P = pyranine, N = sodium-naphthionate.

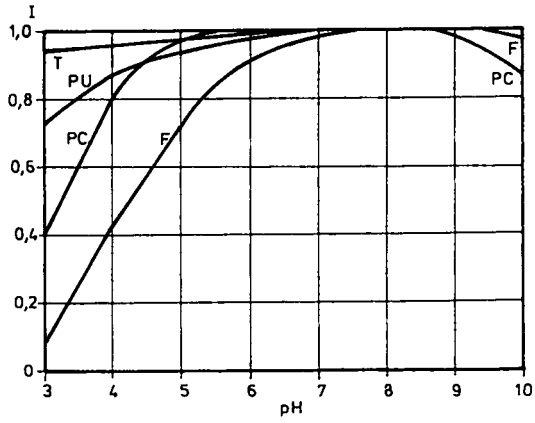

Figure 24. Continued. b) T = tinopal CBS-X, PU = photine CU, PC = photine CSP, F = fluolite BW (partially according to SMART 1976a).

played, since it practically maintains its maximal fluorescence at pH-values between 3 and 11.

In the lower part of Figure 24, the pH-curves for 4 different optical brighteners are shown. Their fluorescence maximum lies between pH-values of 7.5-8.5. In both alkali and acid pH ranges, their fluorescence intensities drop off, due to their different molecular structures.

During the quantitative determination of fluorescent dyes, the pH-value of the water being investigated needs to be considered. It is not sufficient to just know the pH-value of the water sample. After sampling, all groundwater samples gradually start to lose their dissolved free carbon dioxide. Thus, the pH-value starts to rise. Karst waters have an in-situ pH-value of approx. 7.3. Even in well-sealed sample bottles, the pH-value rises to approx. 7.9 after two weeks at room temperature and in unsealed bottles, the pH-value rises even higher to 8.3. Samples from other calcareous groundwater aquifers also show a weakened pH rise.

When measuring the fluorescence signal, it is necessary to make sure that a certain pH-value in the sample is observed. During in-situ-measurements, except during flood events, no noticeable pH-change occurs during a limited observation period. However, usually during dye traces, the water samples are taken and stored in the laboratory for analysis as a series after enough samples have been collected. The sample taken last will have the lowest pH-value. The true fluorescent dye content can be determined using pH-fluorescence calibration curves or tables. This is especially necessary with the strong pH-dependant dyes uranine and pyranine. It is simpler to bring the sample solutions up to a certain pH-value. To do this, BEHRENS (1988a,b) uses an alkali buffer; he adds 0.5% of a solution made of equal parts of tetrasodium ethylene diamine-tetracetic acid (NaEDTA) and water to the samples, which raises pH-value to >10 in the sample. Adding the complexing agent EDTA also prohibits the precipitation of $CaCO_3$. The following method is also well-proven: the opened sample bottles are placed in a closed container with a bowl of ammonia solution (Fig. 25). pH-values of 10 and over can be reached overnight. Clouding due to precipitated carbonate or hydroxide (BEHRENS 1988b) has never been observed, since the pH-value increase occurs slowly. Any precipitation occurs on the bottle wall.

However, it is not always advisable to cause a strong alkali reaction. Some fluorescent dyes, such as most of the rhodamines and some optical brighteners, have a decrease in their fluorescence intensity at high pH-levels. The level of alkalinity that will be reached in the samples during the exposure to the ammonia vapours depends on the geometry of the bottles as well as the ammonia concentration and length of time allowed. Preliminary tests need to be carried out, in case a certain pH-value is wanted.

The pH-value is not just a determining factor for the fluorescence intensity of a fluorescent dye, it also determines the excitation wavelengths. The most striking examples are uranine and pyranine (Fig. 26). This dependency can be used to determine two, in some cases three fluorescent dyes in the same sample (Section 2.1.3.3). For example, uranine's fluorescence above pH 5 is best excited at 491 nm, below pH 5 at 438 nm.

Excitation conditions for pyranine are very differentiated. The excitation at 455 nm for the fluorescence at 512 nm goes to practically zero below pH 5. Below pH 7 however, the fluorescence at 445 nm is intensified at 405 nm. If the excitation

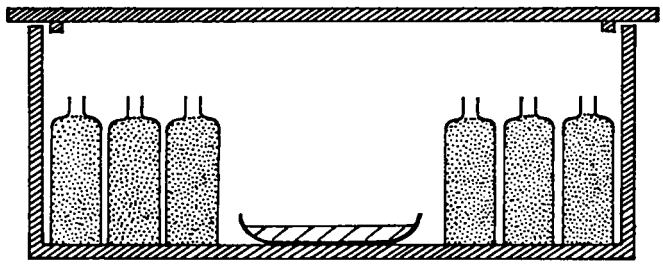

Figure 25. Closed container with sample bottles next to a bowl filled with ammonia solution (hydrochloric acid) in order to raise (lower) the pH-value without changing the volume.

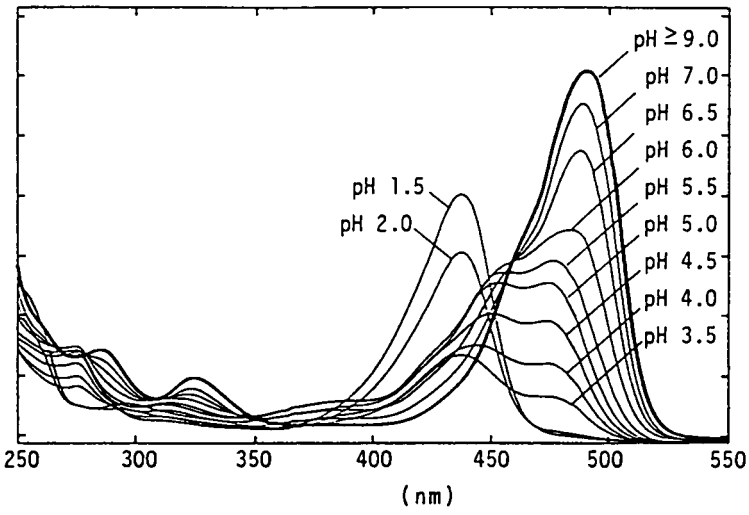

Figure 26. a) Absorption spectra of uranine.

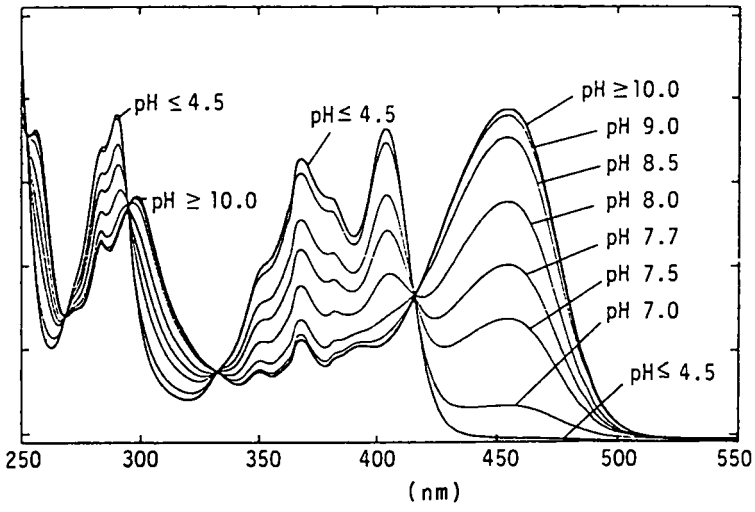

Figure 26. Continued. b) Pyranine solutions (bottom) depending on pH-value (from BEHRENS 1988a).

(and absorption) spectra are graphed for different pH-values, the spectral curves meet at four points, namely at 265, 292, 330, and 413 nm. These are the isosbestic points, where the fluorescence excitation and absorption are pH-independent, although not optimal. The occurrence of isosbestic points indicates that the investigated substance occurs in two different forms. If there are no isosbestic points, as in uranine's case, more than two different forms of the substance occur.

The suppression of the fluorescence at certain acidities can be used when analysing mixtures. For example, at pH 4.6, uranine's fluorescence can be suppressed so low, that eosin traces could be measured next to it, whose fluorescence is only slightly lowered. BEHRENS (1988b) recommends adding 0.5% of a buffer, made up of acetic acid (5.5 molar) and potassium acetate (4.5 molar) to the sample.

As shown in Figure 25, an acidic reaction in the sample can be caused without a volume change, if the samples are exposed to hydrochloric fumes. In a laboratory test, a pH-value of 2 was measured after three days.

Sorptivity of fluorescence dyes

All substances that are transported with water undergo interactions with the solid state. These interactions are as low as 'not measurable' to 'extremely strong.' If the substance is held onto the solid phase without a chemical reaction, it is called sorption. If this bond is so loose that the substance can become detached, it is called desorption.

If reversible chemical reactions take place, it is called ion exchange. There are however, irreversible chemical processes where the dissolved substance is incorporated into the crystal lattice of the solid phase; an example is the bonding of boron in clays. This is a case of absorption.

It is not always possible to separate sorption and ion exchange from one another. Both processes are however dependent upon the concentration in the liquid phase, upon the charge, type of charge and polarity of the dissolved substance, upon the length of time, and upon the material of the solid phase.

The reversible processes sorption/desorption and ion exchange play an important

role in the behaviour of tracers. In general, cationic dyes are more susceptible to sorption and ion exchange than anionic or electro-neutral dyes, since the solid material on the surface is negatively charged. Thus, the cationic rhodamine B, 6G and 3G (Fig. 15) are not suitable for tracing tests in pore groundwater aquifers, due to the intensive surface contact. Organic rests such as peat have stronger adsorptive effects upon the dissolved substances than clastic rocks.

Yet even the anionic fluorescent dyes have gradual differences with regards to their interactions with the solid state surface.

If a water constituent has a different transport behaviour, due to sorption or ion exchange, than the water molecule, it will be held back (Fig. 18). Retention can be so strong that the constituent cannot be recovered. A tracer's sorptivity is an important criterion in deciding whether and how to use a tracer and in evaluating the tracing test.

Many experts have carried out experiments regarding the sorptivity of dyes. One of the first tests was carried out by KNOP (1878) before his significant test with fluorescein in 1877. Since the trace using aniline red to dye the Upper Danube sinkholes had been unsuccessful, he carried out preliminary sorption experiments with fluorescein before using it in a tracing test. He filtered fluorescein solutions through thick layers of arable humic soil and ascertained that 'the optical effects are not appreciably changed.'

Further sorption experiments were carried out by TRILLAT (1899a,b) with fluorescein, eosin, malachite green, methylene blue, fuchsine, acid fuchsine, Paris-violet, safranines, auramine and congo red. He filtered solutions with a concentration of 1 mg/l through 30 cm thick layers of different soils and rock types. Except fluorescein, all of the dyes were more or less strongly retained. Peaty soils also retained fluorescein. In all cases however, acid fuchsine could be made visible again by adding acetic acid.

FEUERSTEIN and SELLECK (1963) carried out adsorption experiments with fluorescent dyes on sediments from the San Francisco Bay (48% clay + 42% silt), composed of illite, montmorillonite, quartz, and chlorite with 500 mg/l sediment and different dye concentrations.

It was ascertained for rhodamine B, that the amount of dye sorbed is only dependent upon the sediment concentration, not upon the rhodamine B concentration. Furthermore, the sorption is also dependent upon the salinity of the water. The time needed for equilibrium to set in was not reported, but most likely an hour is sufficient. Uranine and Pontacyl Pink B were not adsorbed.

Further sorption experiments were published in 1969 by SCOTT et al. using rhodamine WT and Pontacyl Pink B. Sludge from the Rio Puerco near Bernardino (N.Mex.) was used as the adsorbent. At the time of the sampling it amounted to 17.3 weight-% of the river water. After decanting the sand fraction, the following grain size composition (pipette method) was found:

mm	Wt.-%
<0.0625	99.9
<0.016	99.5
<0.004	85.6
<0.002	72.5

According to the x-rays, the suspended sediments were composed of montmorillonite, kaolinite and illite.

Several dilutions of the initial suspension were diluted with Rio Grande river water and shaken with different concentrations of dye solutions for one minute, centrifuged and with the Turner-Fluorimeter 111 measured. Shaking and centrifuging were repeated at different intervals up to 176 hours. It was ascertained that a shaking time of one minute was sufficient for sorption equilibrium to set in. The authors found out that:

– The percentage of the dye adsorption was not dependent upon the dye concentration, but rather upon the sediment concentration,

– The adsorption does not increase along with the sediment concentration, but rather increases slowly (Fig. 27),

– Pontacyl Pink B is more strongly sorbed than rhodamine WT.

SMART and LAIDLAW (1977) and LAIDLAW and SMART (1982) carried out shaking tests with several dye solutions of 100 mg/l. The sediment concentrations were between 2 and 50 g/l. The following list is a summary of the results according to increasing sorption.

Solid substance

Kaolinite	Humic soil	Sandstone (2 mm)	Limestone (2 mm)	Peat
Amino G acid	Sulforh.B	Lissamine FF	Uranine	Lissamine FF
Pyranine	Lissamine FF	Rhodamine WT	Lissamine FF	Amidorh.G
Photine CU	Pyranin	Sulforh.B	Sulforh.B	Sulforh.B
Uranine	Amino G acid	Uranine	Rhodamine WT	Uranine
Lissamine FF	Rhodamine WT	Amidorh.G	Amidorh.G	Rh.WT
Rhodamine WT	Uranine	Rhodamine B	Rhodamine B	Rhodamine B
Sulforh.B	Photine CU			
Rhodamine B	Rhodamine B			

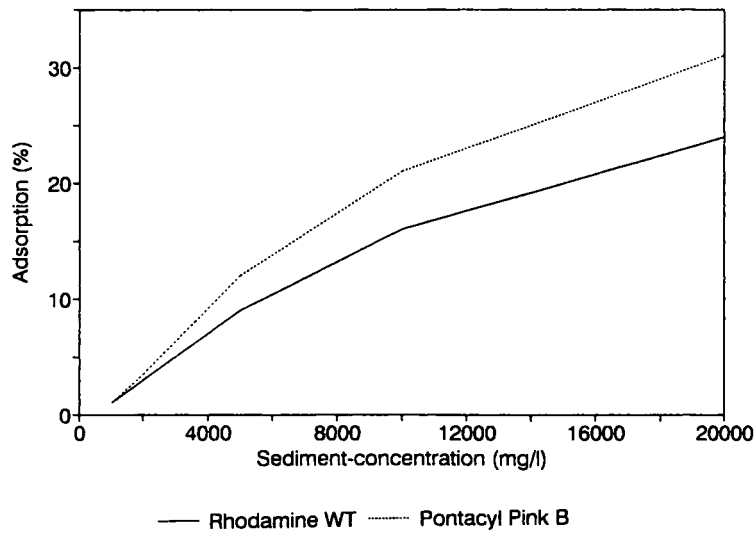

Figure 27. Adsorption of rhodamine WT and Pontacyl Pink B (sulforhodamine B) in shaking tests with river sludge (after SCOTT et al. 1969).

SMART (1976a) published sorption results from 25 hour shaking test for optical brighteners. However, the grain size of the inorganic solid phase was not reported:

Adsorption for a photine CSP-solution (10,000 µg/l)

Solid phase content (g/l)	10	2	0,4
Inorganic material (kaolinite, limestone, quartzite)	17	7	0
Bentonite	42	–	3
Organic material (humic soil, heather roots)	37	17	4

Other shaking tests with concentrated solutions conducted by SMART with photine CSP resulted in lower adsorption:

Adsorption (%) of different optical brighteners (100 µg/l)

	Photine CSP	Photine CU	Fluolite BW
Kaolinite (6 g/l)	12	18	18
Humic soil (2 g/l)	66	77	81

There have been many experiments to determine the sorption properties of fluorescent dyes with regards to their possibility as a tracer. In 1974, LEIBUNDGUT used the term 'adsorption coefficient' for the percentage of sorbed matter after passage through the soil or rock layers. He found that the dye in more concentrated solutions was less adsorbed than from less concentrated solutions. The author compared uranine with amidorhodamine G after passage through sand and humic fine soil. On the average, amidorhodamine G was 7½ times more sorptive than uranine.

According to LEIBUNDGUT & LÜTHI (1976), the sieve coefficient is determined from the ratio of the recovered to injected tracer amount. This coefficient was developed primarily to characterize the sieving or straining properties of soil profiles. Under the same test conditions, it can also be used to identify different tracers according to their sorpitivity. In the laboratory tests, LEIBUNDGUT and LÜTHI used uranine and amidorhodamine G. On the average, a ratio of the sieve coefficients Sk(uranine): Sk(amidorhodamine G) = 0.57:0.12 was determined in 5 different columns. Remarkable in the test results was that in the undisturbed high humic soil profile, uranine was held back more strongly than amidorhodamine G.

In flow tests, LEIBUNDGUT (1981) determined parameters, which characterize the tracer as well as the flow medium. He used the same volume – approx. 10 l – for the test solutions as for the column contents. The tracer solutions in the tests were relatively highly concentrated; between 90 and 12,500 µg/l.

Two parameters were determined:

1. Saturation factor F_s. Weight unit of the tracer (µg) per volume unit of the column contents (dm^3), which is retained in the column in equilibrium after several passages through the column.

2. Adsorption factor F_{ad}. Weight unit of the tracer (µg) per volume unit of the column contents (dm^3), which remains in the column after several rinses with pure water after the equilibrium state from the saturation factor set in.

In the cited publication from LEIBUNDGUT, F_s– and F_{ad}-factors for uranine and three optical brighteners were reported, which were determined in the substrates sand

and braunerde. Uranine was not adsorbed by the sand and only slightly by the braunerde. In contrast, the optical brighteners reacted very differently; liquid tinopal ABP came off the best with relatively little adsorption.

In 1985 DERVEY extended the experiments from LEIBUNDGUT (1981) with the tracers amidorhodamine G, eosin, and rhodamine B and the substrates two-mica granite, Malm limestone, molasse sandstone (all crushed), and peat dust. However, he reported the LEIBUNDGUT saturation and adsorption factors in percentages. His findings confirmed the nearly ideal transport behaviour of uranine, closely followed by eosin. In terms of sorptivity, amidorhodamine G lies between eosin and rhodamine B. Furthermore, DERVEY recognized that uranine has a marked affinity for organic matter (peat dust), in contrast to its behaviour in mineral matter.

It must be noted with regards to the experiments from LEIBUNDGUT and DERVEY, that:

– Some of the tracer solutions used were highly concentrated, and such concentrations are not observed at the observations sites during actual tracing tests,

– Since different initial concentrations and rinsing amounts were used, the tracers can only be conditionally compared with one another.

The retention of a tracer during the passage through saturated or unsaturated rocks, can be defined most easily by the following:

$$C = C_0 e^{-1k_1k_2}$$

where C is the final concentration, C_0 is the start concentration, l is the length of the one-dimensional passage, k_1 is the sorption constant of the tracer, and k_2 is the sorption constant of the solid phase.

Experiments to determine the constants k_1 and k_2 would be certainly very expensive and time-consuming. They have also not been carried out according to the publications available.

To characterize the sorptivity, KÄSS recommended in 1967 the filtration of tracer solutions of a specific concentration and amount (KÄSS 1967a). The tracer loss is given in %:

Uranine:	0
Eosin:	1
Sulforhodamine B:	97.5
Rhodamine B:	99.3.

Such half-quantitative data allow at least a descriptive comparison among the fluorescent dyes (Fig. 28). Data gained this way are not readily transferred to flowing groundwater, yet can serve when used judiciously as supporting help in deciding which tracer to use in a test. However, other test conditions are necessary with regards to the behaviour in inorganic substrates.

KLOTZ (1982d) investigated the sorptivity of three gravely sands from Upper Bavaria against eleven different tracers, including four fluorescent dyes. He determined the retardation factor in column tests:

$$R_D = \frac{v_a}{v_t}$$

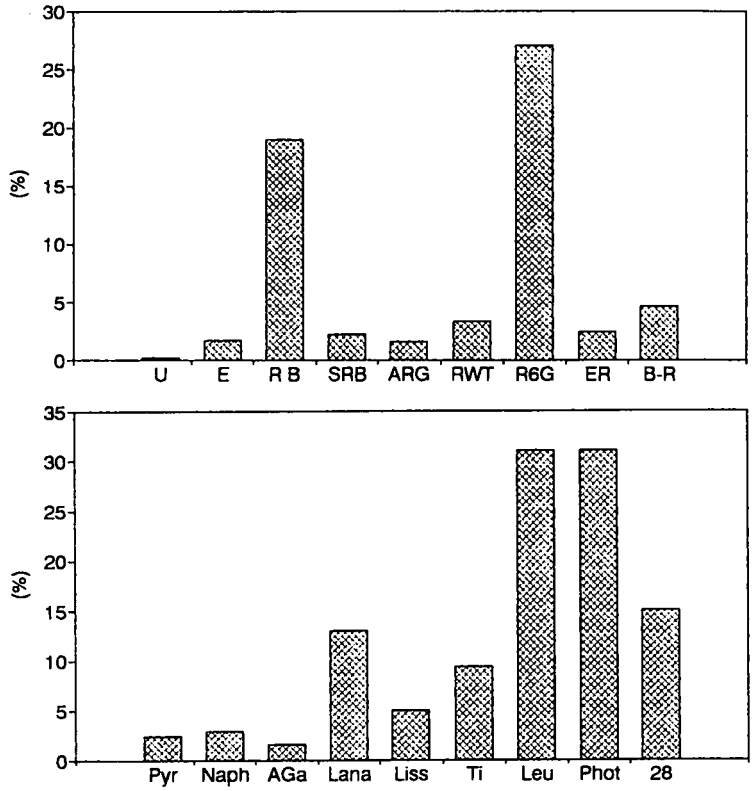

Figure 28. Sorption loss of fluorescent dyes (%) during passage of 100 ml solutions with concentrations of 10 mg/l (= 1 mg) through 50 mm cellulose nitrate membrane filters with 0.2 mm pore size. Top = xanthene dyes; U = uranine, E = eosin, RB = rhodamine B, SRB = sulforhodamine B, ARG = amidorhodamine G, RWT = rhodamine WT, R6G = rhodamine 6G, ER = erythrosine, B-R =rose bengale; bottom: other dyes and optical brighteners: Pyr = pyranine, Naph = sodium-naphthionate, AGa = amino G-acid, Lana = lanaperl fast yellow, Liss = lissamine FF, Ti = tinopal CBS-X, Leu = leukophor PBS, Phot = photine CU, 28 = fluorescence brightener 28.

where v_a = mean flow velocity of an 'ideal' tracer, v_t = mean flow velocity of the trace used.

And the distribution coefficients in shaking test

$$K_d = \frac{C_2}{C_1}$$

where C_2 = sorbed substance/solid substance, C_1 = substance concentration of the solution.

The test averages from the three gravelly sands resulted in the following values:

	Uranine	Eosin	Pyranine	Rhodamine B
Retardation factor R_D	1.13	1.45	1.11	>7
Distribution coefficient K_d	0.074	0.413	0.172	4.41

After converting according to the equation from MAYER & TOMPKINS (1947),

$$R_D = 1 + \frac{\gamma}{n} \cdot K_d$$

where γ = density of dry solid phases, n = total porosity, the determined values and the calculated retardation factors were not in agreement. Therefore, KLOTZ had to introduce a correction factor.

In practice, in order to determine the retardation factor R_D, it is necessary to use a quasi ideal substance for $R_D = 1.0$ as a comparison. Usually uranine is used. Other substances that also have very little interaction with the aquifer are pyranine, heavy and tritiated water. However, these substances have other disadvantages; and they are not – including tritium – ideal tracers.

The determination of retardation factors in field tests has just started. In the pore groundwater aquifer of the Merdingen Test Field, the following values were determined (as compared to uranine):

R_D eosin:	1.3
R_D sulforhodamine B:	1.4
R_D tinopal CSB-X:	38

Photolysis

Uranine's sensitivity to light has long been known, but it was KÄSS (1964) who first showed that uranine's decay due to light is similar to the exponential decay of radioactive matter (Fig. 14).

In the sixties, when uranine and eosin were first being used together in tracing tests, it was discovered that eosin decays in light almost twice as fast as uranine. Numerous publications are concerned with the photochemical decay of fluorescent dyes. What derivatives form is unknown and a regeneration has not been reported. According to the literature, dye solutions with a high concentration are subject to lower decay rates than those with a lower concentration. Various observations have also verified the fact that the rhodamines have very little to no measurable light sensitivity. It was possible to dye the Rhine river over several hundred kilometres using the rhodamines due to their insensitivity to light.

MOSER and SAGL (1967) recognized that the reduction in fluorescence proceeds according to the exponential decay of the form

$$F = F_0 e^{-1I_t}$$

where l is the specific photolytical coefficient, I is the light intensity and t is the duration of exposure.

In groundwater tracing tests, the tracers' sensitivity to light is of no great importance. The highly concentrated tracer solutions used during the injection can withstand the sunlight for a short period. However, in choosing the sampling sites and the further handling of the samples, care should be taken to avoid sunlight (Fig. 31). Furthermore, extremely sensitive optical brighteners decay measurably during measurement in a fluorescence spectraphotometer (Fig. 29).

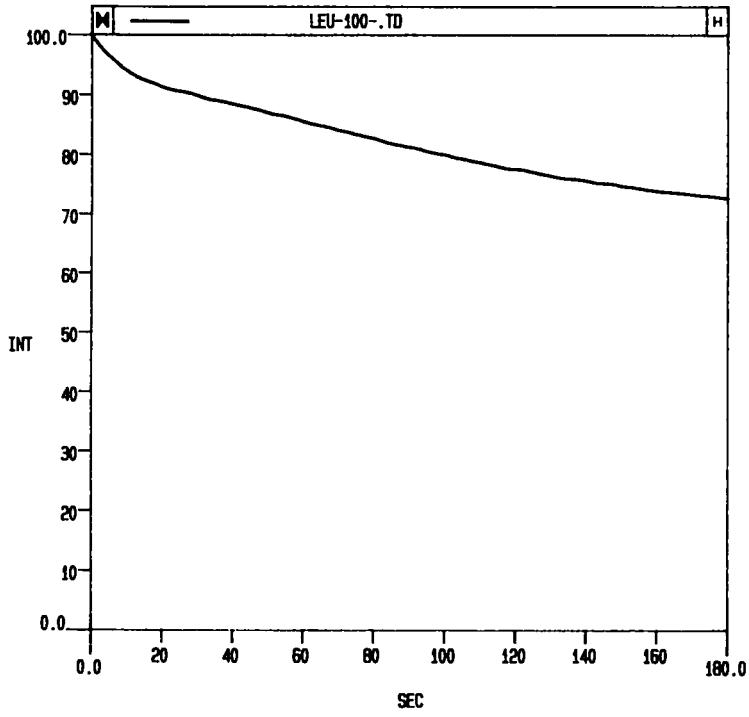

Figure 29. Photolytical decay of an optical brightener (Leukophor PBS) during measurement in the spectrofluorimeter. During the 180 seconds needed for the measurement, the concentration dropped from 100 to 73 µg/l.

The sensitivity to light of fluorescent dyes can also be useful as an actinometer. BEHRENS and DEMUTH (1990) and DEMUTH (1988) investigated the intensity of the incoming radiation in two Middle Franconian rivers, Regnitz and Altmühl, and the attenuation of light with depth in Vierwaldstätter Lake with UV-sensitive xanthenes.

In 1982, BEHRENS and TEICHMANN completed extensive investigations as to the sensitivity to light of a large number of aqueous solutions of fluorescent dyes. They used a sample carrousel filled with the solutions in an area that was exposed to a xenon-high pressure lamp to assure uniform illumination. Table 1 and Figure 30 show the results of these experiments, with the half-life times converted to photochemical decay coefficients.

The strongest photolytical decay occurs at the wavelengths of the excitation maxima. Therefore, the synchronscan should be used with short instead of long wavelengths for light sensitive substances. However, this is not possible when using all of the commercial fluorescence spectraphotometers. BEHRENS and TEICHMANN (1989a) investigated in detail the connection between the light sensitivity and pH-value for uranine, eosin and pyranine. They found, analogous to the extinction coefficients, that at the excitation maximum, a relationship exists for uranine and eosin; i.e. their tautomer forms in acid pH-ranges are less sensitive to light than in neutral and alkali ranges. Moreover, uranine's fluorescing tautomer form at pH-values <5 shows only very little sensitivity to light. In contrast, pyranine shows in neutral to alkali ranges a low, yet changing and at acidic pH-values a strong sensitivity to light.

The photolytical coefficient is dependant on the temperature; with increasing temperature the sensitivity to light also increases (BEHRENS & DEMUTH 1990).

Turbidity effects

During absorption measurements, as well as during fluorimetrical detection, the determination of fluorescent dyes can be disturbed. In the first case, the intensity decreases and in the second, it increases. Turbid water samples occur mainly in new groundwater survey sites, after heavy rains in karst (KNORR 1935), and in all surface

Table 1. Photolytical coefficient l for eosin = 1000. Data source: BEHRENS & TEICHMANN (1982), if not otherwise noted; see also Figure 30.

Fluorescent dye	L	Source
Uranine	550	
Eosin	1000	
Rhodamine B	7.7	
Sulforhodamine B	7.3	
Amidorhodamine G	8.0	
Rhodamine WT	4.6	
Rhodamine 6G	16	
2,7-Dichlorfluorescein	270	BEHRENS & DEMUTH (1990)
4,5-Dimethylfluorescein	42900	BEHRENS & DEMUTH (1990)
2,7-Diethylfluorescein	1330	BEHRENS & DEMUTH (1990)
Sulfofluorescein	320	BEHRENS & DEMUTH (1990)
Pyranine	130	
Na-Naphthionate	150	WERNLI (1986)
Amino G acid	80	SMART & LAIDLAW (1977)
Lissamine	5	
Tinopal CBS-X	350	
Leukophor PBS	3890	KÄSS (unpubl.)
Photine CU	2330	SMART & LAIDLAW (1977)
Fluorescent brightener 28	4750	KÄSS (unpubl.)

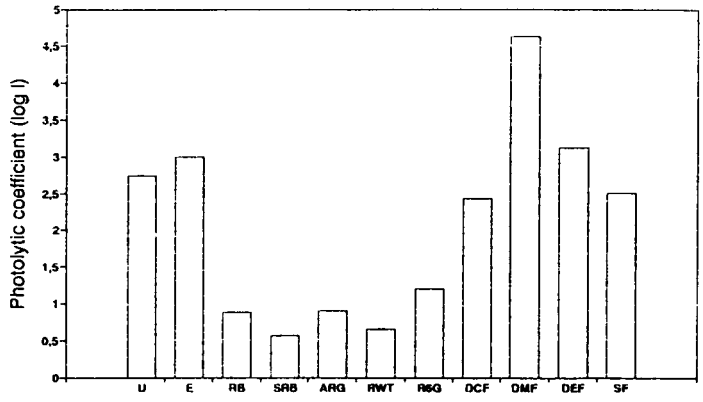

Figure 30. Photolysis of fluorescent dyes in logarithmic representation of the photolytical coefficients from Table 1. a) U = uranine, E = eosin, RB = rhodamine B, SRB = sulforhodamine B, ARG = amidorhodamine G, RWT = rhodamine WT, R6G = rhodamine 6G, DCF = 2,7-dichlorfluorescein, DMF = 4,5-dimethylfluorescein, DEF = diethylfluorescein, SF = sulfofluorescein.

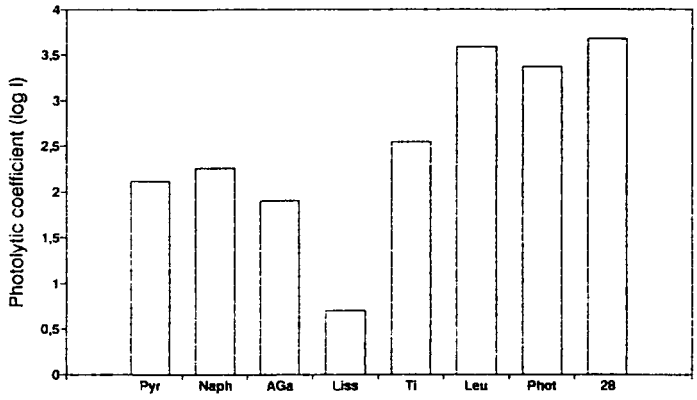

Figure 30. Continued. b) Pyr = pyranine, Naph = Na-naphthionate, AGa = amino G-acid, Liss = lissamine, Ti = tinopal CBS-X, Leu = leukophor PBS, Phot = photine CU, 28 = fluorescent optical brightener 28.

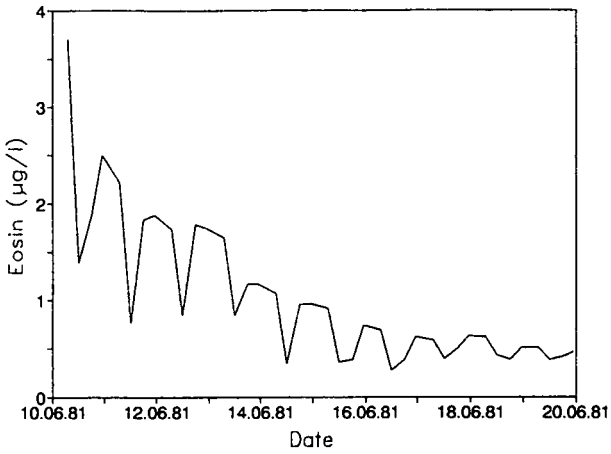

Figure 31. Eosin contents in the Zwiefaltener Ach (Swabian Alb/SW-Germany) after a flow distance of 1¾ km in midsummer. The dates on the x-axis show the zero-hour of each day. The extensive decay of the midday samples due to light is clearly visible (from document M 237/10 of the Geological Survey in Baden-Württemberg).

waters. The turbidity may be of organic or inorganic origin. In reduced waters with high dissolved iron contents, colloidal ferric hydroxide will separate after the sample has been taken. Furthermore, humic acids also cause turbidity.

During the fluorimetrical determination, turbidity causes a signal, which breaks through the best optics to the receiver, thus causing a false positive result. This is due to refraction, bending and scattering in the optical system, above all due to dust particles and irregularities and impurities of the cuvette walls. The more the samples are turbid or contain colloids, the more the light is scattered. The following paragraphs explain measures for determining and eliminating the turbidity disturbances.

Low to mid turbidity, up to a value of approx. 200 formazine units, can be determined by a scattered light turbidity indicator. Every spectral-fluorimeter can also be used as a scattered light indicator, if the input and output beam are both set to 600 nm. It is then calibrated with formazine solutions and turbidity glass standard. By measuring the scattered light, an increase in the measured signal in the sample series can be differentiated from the actual positive fluorescent value.

Another way to correctly recognize a positive fluorescent signal is to record the synchronscan spectrum. To do this, it is necessary to record the spectrum of a sample with a low signal. Modern instruments allow for a superimposition of both spectra and a differentiation of the two. Although time consuming, such manipulations allow a faultless detection of possible positive values.

Scattered light, which leaves perpendicular to the incoming radiation, is polarized perpendicular to the radiation plane. This scattered light can be partially suppressed by interposing a polarization filter. The polarization direction of the filter has to be directed to the radiation plane.

The following results were obtained by using a polarization filter to examine a sample containing uranine, which was clouded by colloidal ferric oxide (uranine equivalents in µg/l):

	W/o filter	With pol.-filter
Whole signal	0.370	0.135
Scattered light signal	0.150	0.035
Part of uranine (%)	0.220	0.100
Part of uranine (%)	59	75

This example shows that the use of a polarisation filter suppresses the scattered light by a factor of only 1.25 and that a two-thirds decrease in intensity must be taken into account. Since the scattering of light increases with the wave number to the fourth power, at shorter wavelengths the fluorescence yield is greater. However, polarisation filters in the UV-range are increasingly impermeable towards shorter wavelengths.

In 1962, KLATTE recommended centrifuging cloudy samples. To remove even the finest turbidity, KLATTE used an ultracentrifuge with 12,000 rpm, which produces a 17,000-fold gravitational acceleration. According to KLATTE, after centrifuging for two hours, all particles over 0.04 mm are sedimented. In practical use, this method is most likely rarely used since it is time consuming and has a high expenditure.

Filtering through paper filters removes suspended solids over 25 µm. Smaller particles can be removed with membrane filters. Using this method, clear samples can be obtained (KÄSS 1964). Filtration is carried out with either excess or subpressure. The latter is easily obtained using a filter outfitted with a 50-mm-glass-frit, which is attached to a water jet pump. With the appropriate arrangement, the filtrate can be filtered directly into the cuvettes, thus avoiding possible contamination during decanting. Membrane filters are available down to a size of 0.01 µm. However, such narrow filter pores are easily clogged and cause long filtration times. Usually a filter size of 0.2 mm is a good compromise between filtration time and filter effect. It must be noted, that the membrane filters are impregnated with hardeners, which, espe-

cially in shortwave ranges, fluoresce and absorb. For precision work, the membrane filters must be watered before being used.

Through the addition of solid calcium oxide, humic acid colloids can be precipitated. The accompanying electrolyte increase and alkalinity also promote the precipitation of ferric hydroxide and other suspended solids. Adding complexing agents – also as a solid – dissolves the ferric hydroxide and lime suspensions. However, they are not able to eliminate the clay suspensions or organic colloids.

During the filtration of sample solutions, it must be noted that paper filters as well as membrane filters made of cellulose nitrate or acetate adsorb dyes. Preliminary tests must be carried out to establish how much sample solution as filtrate must be rejected to assure that the sorption capacity of the filter has been reached.

Natural background fluorescence

Detailed observations concerning naturally occurring fluorescence were made by DIENERT (1909a,b). He found three types of fluorescence: Green, greenblue and blue.

The green fluorescence was found in deep water, the greenblue in moor water and in streams polluted with sewage, and the blue in rain water.

The fluorescing properties of a moor water from the Hinterzarten Moor (Southern Black Forest/SW-Germany) were described by KÄSS (1965). The dark-brown sample had a pH-value of 5.4 and an oxidizability with permanganate of 120 and with bichromate of 381 mg/l O_2. The fluorescent spectrum covered a relatively wide range with a maximum at 528 nm and a half-width value of 98 nm. Using a uranine setting resulted in a fluorescence signal of 2.1 µg/l uranine equivalents.

A moor water sample from the Bad Aiblinger Moor (Upper Bavaria) with an oxidizability with permanganate of 56 mg/l O_2 resulted in a uranine interference of 0.3 mg/l. The fluorescent properties of this moor water sample were investigated further and showed that the fluorescence spectrum was strongly dependent upon the excitation wavelengths:

Excitation (nm)	Fluorescence-maximum (nm)	Relative fluorescence-intensity	Half-width value (nm)
250	440	0.03	90
275	445	0.07	90
300	447	0.24	90
350	455	0.82	95
400	480	1	105
492	528	0.28	95

According to these results, the main interferences due to humic acid are at excitations between 350 and 450 nm.

In 1976, SMART and SMITH reported on the high background between 12 and 50 mg/l of the optical brightener photine CSP in river sources on Jamaica. Furthermore, SMART and LAIDLAW (1977) reported in detail about the different fluorescence backgrounds. Their compilation about surface water fluorescence reported fluorescence wavelength maxima between 400 and 670 nm.

Communal sewage can contain high amounts of optical brighteners from laundry detergents. Thus, receiving streams that are polluted with sewage have high back-

grounds for optical brighteners. Due to their high sorption properties, optical brighteners are rarely found in artificially recharged groundwater.

Water that comes in contact with natural mineral oil and mineral oil products can also exhibit fluorescence. GANDENBERGER and OEHLER described in 1963 the 'uncharacteristic fluorescence' of the dissolved mineral oil. A groundwater sample taken from soil strongly contaminated with mineral oil products, showed a strong light-blue fluorescence under a quartz lamp. Its fluorimetrical measurement resulted in a near constant excitation between 310 and 330 nm and a pronounced fluorescence maximum at 362 nm. This groundwater sample, which was saturated with hydrocarbons had a fluorescence signal of 9 µg/l uranine equivalents. As a result, before tracing tests can be carried out near areas contaminated with mineral oil, extensive preliminary tests must be completed in order to register the fluorescence background.

KÄSS (1965) described green fluorescing water from water outlets from tufaceous limestones. The acid-resistant green fluorescence was most likely caused by lime-secreting algae.

Via the fish hatchery spillways, sizable amounts of green fluorescing Trypaflavine can enter the receiving streams. Trypaflavine is used to combat fungal disease in the fishes' gills. Its fluorescence maximum is at 510 nm.

Temperature dependency of fluorescence

Numerous publications deal with the dependency of the fluorescence intensity upon the temperature of the sample being investigated. Fluorescence intensity decreases with increasing temperature, although the rate depends on the dye. The half-width value of the fluorescence spectrum increases also with increasing temperature; i.e. lower temperatures produce better developed fluorescence peaks.

WILSON (1968) and DUNN and VAUPEL (1965) observed during measurement of the fluorescence of rhodamine B, that after running for a long time, the cuvette slot in a Turner Filter Fluorimeter 111 has a temperature of 103.5°F = 39.7°C. Compared to the room temperature, that made for a decrease of almost 40% in the fluorescence. Modern spectral fluorimeters now have built-in forced air ventilation as well as pulsing xenon lamps that give off less warmth than continuously burning bulbs.

Table 2. Coefficients, *n*, for the temperature dependency of fluorescent dyes used in water tracing.

Tracer	*n*	Source
Uranine	0.004	MOSER & SAGL (1967)
	0.0036	SMART & SMITH (1976), SMART & LAIDLAW (1977)
	0.0041	STAMPFLI (1983)
Eosin	–0.00036	STAMPFLI (1983)
Rhodamine B	0.017	DUNN & VAUPEL (1965)
	0.028	MOSER & SAGL (1967)
	0.026	WILSON (1968)
	0.027	SMART & LAIDLAW (1977)
Sulforhodamine B	0.028	MOSER & SAGL (1967), WILSON (1968)
	0.029	SMART & LAIDLAW (1977)
Amidorhodamine G	0.0035	BEHRENS (1971)

Table 2. Continued.

Tracer	*n*	Source
Rhodamin WT	0.026	WILSON (1968), Jahresbericht Institut f.Radiohydrometrie München 1968
	0.027	SMART & SMITH (1976), SMART & LAIDLAW (1977), ALEXANDER et al. (1988)
Pyranine	0.0019	SMART & SMITH (1976)
Amino G acid	0.0019	SMART & LAIDLAW (1977)
Lissamine FF	0.004	MOSER & SAGL (1967)
	0.0020	SMART & SMITH (1976), SMART & LAIDLAW (1977)
Tinopal	–0.0365	STAMPFLI (1983)
Photine CU	0.012	SMART (1976a), SMART & SMITH (1976), SMART & LAIDLAW (1977)
Photine CSP	0.013	SMART (1976a)
	0.020	SMART & SMITH (1976)
Fluolite BW	0.011	SMART (1976a)

HERZBERG (1954) set up the laws governing the inverse variation of the fluorescence intensity with the temperature:

$$F = F_0 e^{-n(t-t_0)}$$

where F, F_0 = fluorescence intensity at temperature t or t_0, t = temperature during measurement (°C), t_0 = reference temperature (°C), n = temperature coefficient.

Fluorescence quenching

According to FÖRSTER (1951), fluorescence quenching occurs with all fluorescing materials. In solutions, the quenching is activated by solution partners, whereby the quenching can also be only partially effective, depending on the concentration of the partner. Neither the fluorescing material nor the quenching partner undergoes a chemical change. The absorption spectra stay complete and the fluorescence spectra retain their form. Fluorescence quenching of the xanthene dyes occurs mainly due to iodine ions and heavy metals. The half-life concentration is the concentration of the quenching partner, which decreases the fluorescence by half:

Uranine (10 µg/l), half-life concentration for Cd^{2+} (as sulfate): 650 mg/l.
Half-life concentrations with potassium iodide (mol/l) for:

Uranine:	0.125
Rhodamine B:	0.19
Amidorhodamine G:	0.067
Rhodamine WT:	0.19

Concentrations of the fluorescing dyes lie under 10 µg/l (ANDRÉ & MOLINARI 1976).

Quinine (1 g/l) in nH_2SO_4, half-life concentration for $CuSO_4$: 0.275 (mol/l), for $CoSO_4$: 0.021 (mol/l) (FÖRSTER 1951).

Chromate ions with a concentration of 100 mg/l Cr-VI do not disturb uranine's fluorescence.

SMART and LAIDLAW (1977) published a table about the stability of eight fluorescent dyes compared to sodium chloride:

Dye	Fluorescence (initial concentration) (%)	
	0.1 mol/l	0.5 mol/l
Uranine	100	100
Rhodamine B	100	98
Sulforhodamine B	100	96
Rhodamine WT	97	92
Pyranine	100	100
Amino G acid	100	100
Lissamine FF	100	100
Photine CU	100	100

According to the same publication, the chloride influence upon the fluorescence intensity of rhodamine WT is a function of time, whereby potassium chloride suppresses the fluorescence more strongly than sodium chloride does.

Own investigations resulted in a constant fluorescence for uranine close to the saturation concentration for sodium chloride.

Nitrate ions quench the fluorescence of the fluorescein cation (excitation: 438, fluorescence: 512 nm) at pH-value of 2. According to MIGUEL & BRAUN (1974), this can be used for the fluorimetrical analysis of nitrate.

In practical use, the fluorescence quenching has scarcely any effects. Such concentrations of the fluorescence quenchers occur at most during hazardous waste accidents.

Another effect according to FÖRSTER (1951) is the 'sensitized fluorescence' in mixes of two fluorescent dyes, if the excitation maximum is near the fluorescence maximum of the other dye. Part of the shorter wavelength fluorescing partner is absorbed for the excitation of the other. Such occurrences happen e.g. at high concentrations of uranine + eosin or eosin + amidorhodamine G (KÄSS 1964, LEIBUNDGUT 1974, BEHRENS 1971). Such cases of quenching happen only in cases with longer light paths in large cuvettes and at concentrations over 10 µg/l. In smaller cuvettes with an area of 10 × 10 mm, sensitized fluorescence is not expected.

Oxidizing agents

Many water supply facilities use strong oxidizing agents such as chlorine, chlorine dioxide, or ozone to sterilize the water supply. These agents can also destroy the fluorescence dyes. In 1964, KÄSS investigated the decay of uranine due to chlorine and chlorine dioxide. The following half-life times were found for the fluorescence decay of a uranine concentration:

Cl_2, ClO_2 (mg/l)	Half-life (seconds)	
	Cl_2	ClO_2
50	<5	–
10	6	–

Cl_2, ClO_2 (mg/l)	Half-life (seconds)	
	Cl_2	ClO_2
1.0	36	9
0.5	500	11
0.1	–	>120
0.05	960	–

At concentrations over 0.1 mg/l, chlorine dioxide affects uranine faster than free chlorine. At lower concentrations, chlorine's influence is stronger (compare Fig. 13).

Furthermore, KÄSS (1964) reported, that during a tracing test in Muschelkalk karst near Oberndorf/Neckar, a well visible uranine concentration of 125 µg/l was destroyed by the ozone treatment of the water. Milder oxidizing agents such as hydrogen peroxide or chromate do not bother uranine's fluorescence.

According to HAIDER (1991), by the addition of sodium thiosulfate, the uranine elimination due to chlorine can be made reversible.

HAIDER also reported, that rhodamine B is more sensitive to chlorine than uranine. The authors SMART and LAIDLAW (1977) cited DEANER, that in sewage water treatment plants, rhodamine B is destroyed faster by chlorine additions than rhodamine WT. In two hours with a dye concentration of 10 µg/l, rhodamine B decreased by 60% and rhodamine WT by only 10%; the rest chlorine concentration was in both cases 40 mg/l.

Non-Xanthene fluorescent dyes are also influenced by chlorine. Different amounts of chlorine were added to a 10 µg/l pyranine solution and the following changes were recorded:

Cl_2 (mg/l)	50% fluorescence after (s)	10% fluorescence after (s)
5	26	446
4	36	(only slow decrease)
1	886	(only slow decrease)
0.5	1320	(left overnight: 0% fluorescence)

If 1.5 mg/l of chlorine are added to solutions of Na-Naphthionate or amino G acid, an obvious decrease in fluorescence can be seen under the UV-lamp. If the chlorine addition is increased, the fluorescence ceases completely.

In some circumstances, this decaying of the dyes is an advantage. For example, during tracing tests in catchment areas of a water supply facility, if oxidation destroys the visibility of the dyes, the water supply need not be interrupted.

2.1.3.2 *Qualitative investigations*

Fluorescent dyes can be easily observed due to their specific optical properties. At the start of hydrological dyeing techniques, only simple and subjective dye observations could be made. In the first dye tracing test carried out, KNOP (1878) described the reemergence of the dye in the Aach spring as a 'gorgeous green luminescence for over 36 hours' and estimated its dilution at 'a 40 millionth'! This inexact statement can have different meanings:

A dilution of 40:1,000,000 or 1:40,000,000. The first possibility would be a so-

dium fluorescein concentration of 40 mg/l, which would be improbably high, thus the second example with 25 µg/l can be regarded as right.

Even long after the introduction of uranine as a hydrological tracer, water tracing tests were evaluated with purely qualitative and organoleptical dye observations. At times, there have even been extensive hydrogeological investigations that were only qualitatively evaluated, although quantitative dye detection methods were already routine (ZANDER 1973).

Due to its enormous dyeing properties, the most frequently used dye, uranine, can be seen with the naked eye even at very high dilutions. KÄSS listed in 1964 the visibility limits of 0.25 l uranine solutions in erlenmeyer flasks (uranine contents in µg/l):

	Recognizable as a single sample	Recognizable compared to pure water
Subdued daylight, white background	40	30
Subdued daylight, black background	20	10
Under a quartz lamp, black background	10	5

Using a quartz lamp, the UV-insensitivity of the human eye acts as a band-elimination filter, so that the visibility detection limits are lower, as compared to daylight (compare Fig. 8).

In open waterways, where springs crop out, or lakes, where the surfaces are larger, the detection limit can drop to 1 µg/l uranine, under favourable conditions. Furthermore, oblique sunlight, dark backgrounds, and clear water as well as deep water favor the detection of fluorescent dyes.

In a darkened room, 5 µg/l of uranine is well visible if a sharply focused flashlight is beamed horizontally onto a beaker. Such an arrangement is actually a primitive fluorescope.

The oldest fluorescopic observations of natural fluorescence in surface and groundwaters were made by TRILLAT in 1899. His fluorescope was made of two 1.2 m long and 2 cm wide glass tubes, which were closed with black plugs at the bottom. One tube was filled with the sample water, the second with a reference water sample, both at the same level. With lighting from the side, and an axial observation against a dark background, TRILLAT was able to recognize fluorescein concentrations of 0.5 µg/l (1899a,b). In 1906, MARTEL used a TRILLAT fluorescope, which had been improved by MARBOUTIN (1901a,b), and was able to supposedly detect a uranine concentration of 0.05 mg/m^3. MARBOUTIN attached 12 TRILLAT tubes next to each other and filled them with hourly samples. Thus, he was able to compare a large number of samples with one another and could exactly determine the first appearance of the dye. In the Upper Cretaceous south of the city Verneuil/Dpt.Eure, the underground waterways are very dispersed. In the tracing tests here, MARBOUTIN was able to draw so-called isochronochromes, i.e. lines of equal arrival time for the first appearance of the dye (Fig. 140). MARTEL recommended using ammonia to make the water samples alkaline for a better fluorescein detection and to filter cloudy samples. In 1909, DIENERT constructed a fluorescope, that was built according to Figure 32 (DIENERT 1909b). The light source was either sunlight or an electric arc. Due to the

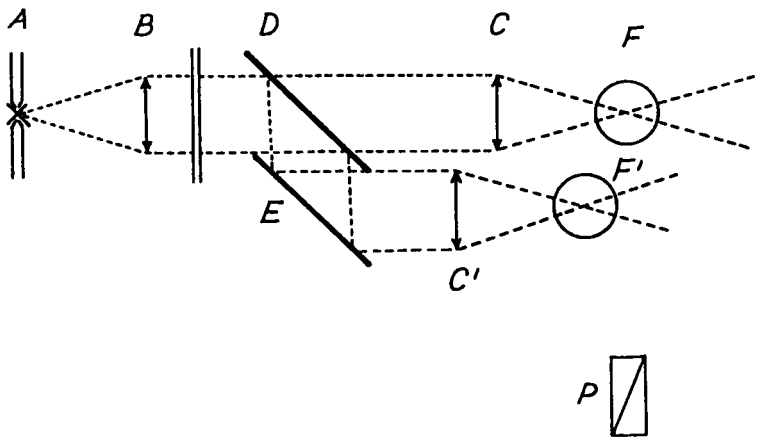

Figure 32. Fluorescope according to DIENERT (1907b). A = electric arc; B, C and C' = collecting lenses; D = half-opaque mirror; E = mirror; F = sample; F' = reference sample; P = polarizer to suppress the Tyndall-effect of turbidity.

irregular burning of the electric arc and to be able to better compare the samples with samples of a known concentration of fluorescing substance, DIENERT used a light divider and two 45 ml cuvettes. The samples were observed from the side through a polarizing prism, to suppress scattered light. DIENERT investigated mainly natural fluorescence.

A TIMEUS (1911) fluorescope consists of a wooden box that is blackened inside and out. It has three openings, whereby the two side openings are fitted with 1.30 m long and 3 cm wide glass tubes with a wall thickness of 1 mm. They are closed with black plugs and covered with black paper so that only 4-5 mm wide slits are left down the length of the tubes. The slits are turned to each other. A row of 10 carbon filament lamps each 16 candles strong is stacked in the middle between both tubes. If one tube was filled with a reference uranine solution and the other with the sample, dilutions of 1:20 billions could be recognized. The measurement had to be done in a darkroom. Later, (1926) TIMEUS wrote that for faultless recognition of uranine traces, one needed a minimum of experience and that the examiner should neither drink alcohol nor smoke!

According to SPRING (1905), $1 \cdot 10^{-18}$ g potassium fluorescein can be detected in 1 ml water, if the light from an electric arc with 110 V and 12 A is concentrated upon the sample solution with the help of a concave mirror with a 12 cm diameter.

In his numerous dye tracing tests in the Swiss Jura, SCHARDT used looking glasses similar to the fluorescope from TRILLAT. They were test tubes with a length of 20 cm and a diameter of 1 cm that were covered with black paper (Fig. 33 left). Along their length, there was a slit in the paper of approx. 1 mm width, which allowed sunlight to shine through. Looking through the top, uranine concentrations of 0.1 mg/m^3 could be recognized (SCHAUFELBERGER 1929). The 'Stuttgart fluorescope', which allowed a uranine recognition of 1 mg/m^3 (Fig. 33 right) has been described by EGGER (1929).

During tracing tests in the Slovenian karst the fluorescope developed by Prof. N.CADEZ-NOVAK (Ms.) is frequently used. This instrument was presented at the first symposium in Graz/Austria in 1966, yet never published as an article. Since it is a useful instrument for field work, especially due to its simplicity, it will be described in detail here (Fig. 34). Sunlight or a point light source is needed. The light is directed upwards with a revolvable mirror, so that the test tube bottoms act as collecting lenses. The focal points can be viewed from the side. One test tube is filled with the sample water, the other with either pure water or a reference fluorescing solution. This way, a semi-quantitative determination can be carried out. The detection limit for uranine lies at ca. 0.1 mg/m^3. The instrument is made of black japanned sheet metal. Under glaring light conditions, it helps to work with a black cloth covering one's head and the viewer.

During the meetings of the Belgium Society for Geology, Paleontology and Hydrology in 1903 in Brussels, MARBOUTIN (1904) voiced his opinion that the idea

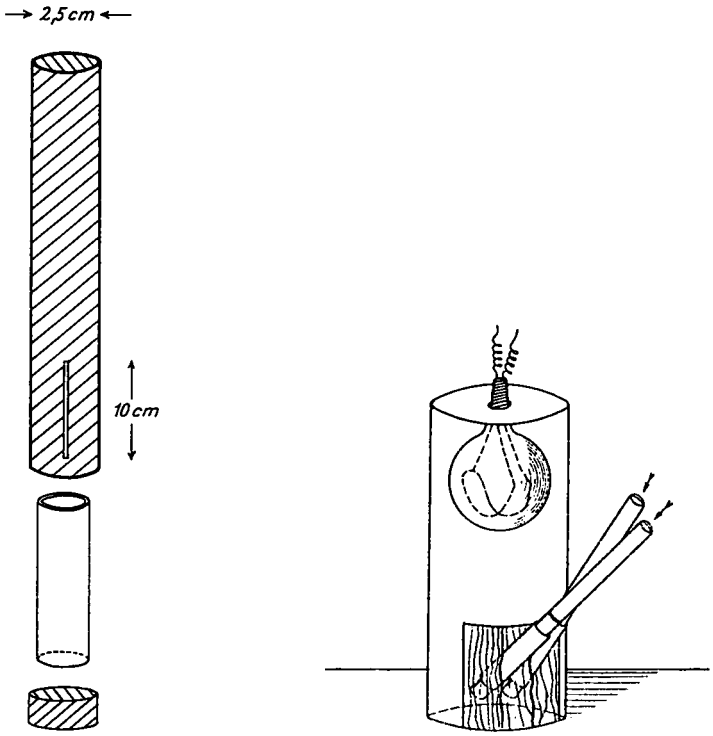

Figure 33. Left) Fluorescope according to SCHARDT (1913). Bottom part: Glass tube, ca. 15 cm high, filled with sample water. Top part made of cardboard, in- and outside covered with black paper, in bottom part a 10 × 0.2 cm slit. For viewing, the top part is placed over the bottom part and looked at through the top in sunlight or strong artificial light. It is held together by a black plug at the bottom. Right) 'Stuttgart Fluorescope' by EGGER (1929). A black cardboard cylinder is fitted at the top with a 1200 Watt light bulb. Part of the bottom of the cylinder is cut away and covered with a black curtain through which the reference and sample SCHARDT tubes are introduced.

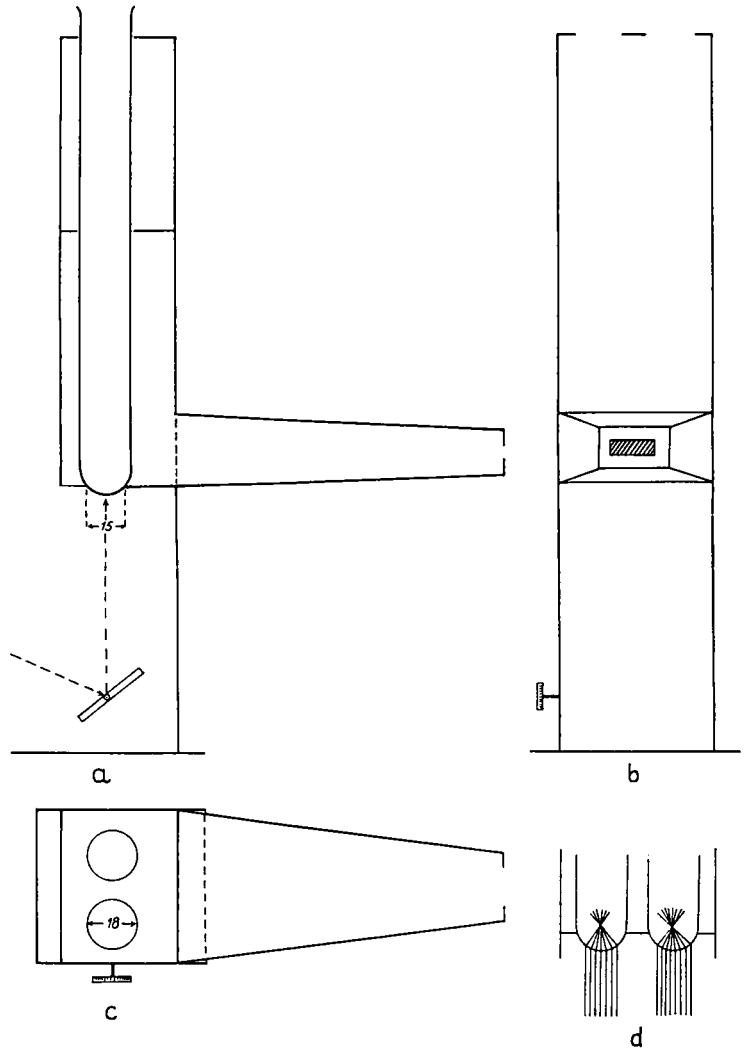

Figure 34. Fluorescope by Prof. CADEZ-NOVAK (Ms.). a) Cross-section. Sunlight or light from a point source is directed upwards vertically by a revolving mirror. It is focussed upon the curved test tube bottoms, b) Front view. Top: opening for two test tubes for the sample and reference solution; middle: viewer; bottom left: handle for the revolving mirror, c) Top view with two opening for two test tubes, d) Ray path. In the test tubes, the ray focal points intensify the fluorescence and make it visible.

fluorescope and not fluoroscope should be used. He substantiated this with the fact that fluorescence is being investigated. The participants voted unanimously to use fluorescope, which was also supported by TRILLAT. Since it is technically and factually better, this book also uses 'fluorescope' instead of 'fluoroscope.'

2.1.3.3 *Quantitative determination*

In 1910 SCHARDT pointed out that a quantitative determination of fluorescein was

important. Using the mountain stream Cairasca on the south side of the Simplon an example, SCHARDT showed, that at different discharges, different stream percentages emerged in the Simplon tunnel. He carried out the (semi-)quantitative determination with titrated reference solutions in his fluorescope.

Quite a while went by after SCHARDT's suggestion before a quantitative determination of fluorescent dyes was possible with photodetectors and electronics. In 1964 and 1967 KÄSS published a paper about using a spectrofluorimeter for measuring dye content with examples (KÄSS 1964, 1967a). In following years, many authors researched the conditions needed for the quantitative determination of fluorescent dyes in tracing tests and the optical properties of the tracers.

Table 3 lists the most important fluorescence optical properties important for the quantitative determination of fluorescent dyes in hydrology. The listed values were determined with a Perkin-Elmer Spectrofluorimeter LS 50. Depending on the model and type, spectral sensitivity of the PEV, as well as the purity of the reference substance, possible deviations in the given data are to be expected.

Spectrophotometry

Determining the extinction at the absorption maximum of a light absorbing substance in solution is simply determining the concentration. This is a routine method in an analytical laboratory.

Table 3. The most important fluorescence analytical data of some given fluorescent dyes in water tracing tests: Exc. = excitation, Fl. = fluorescence, Fl.Int. = fluorescence intensity.

Tracer	Exc. (nm)	Fl. (nm)	$\Delta\lambda$ (nm)	Fl.Int. (Uranine=100)	Testsubstance Producer, article No.
Uranine[1]	491	512	21	100	MERCK 3992
Uranine[2]	438	512	74	20	MERCK 3992
Eosin	516	538	22	18	MERCK 1343
Rhodamine B	554	576	22	60	MERCK 7599
Sulforhodamine B	564	583	19	30	ALDRICH 23,016-2
Amidorhodamine G	530	551	21	14	ALDRICH 23,056-1
Rhodamine WT	554	580	26	25[4]	DUPONT
Rhodamine 6G	526	552	26	20	MERCK 7600
Erythrosine	525	547	22	0.65	MERCK 1355
Rose bengale	518	535	17	0.3	FLUKA 11950
Dichlorfluorescein	502	518	16	77	ALDRICH 20,148-0
Pyranine 108%[1]	455	512	57	18	BAYER 957024530300
Pyranine 108%[2]	405	445	40	6	
Na-naphthionate	320	430	110	8	FLUKA 70862
Amino G-acid	359	450	91	1.0	HOLLIDAY Bt 42
Lanaperl fast yellow	469	508	39	6.2	HOECHST EA AL 005
Lissamine	432	508	76	1.6	HOECHST EA AA 005
Tinopal CBS-X	346	435	79	60	CIBA-GEIGY
Leucophor PBS[3]	348	430	82	1.1	SANDOZ
Photine CU[3]	345	435	90	3.6	HICKSON & WELCH 23/187
Optical brightener 28	349	430	81	2	ALDRICH 29,418-7

[1] At pH 9.5, [2] At pH <2, [3] Liquid, [4] Referred to solid matter.

For tracing techniques, spectrophotometry is used if concentrations above ca. 500 µg/l are to be measured, since the calibration curves used in the fluorimetrical measurements are not linear due to self-absorption (Fig. 10). However, there are upper and lower limits to the concentrations in spectrophotometry also. At high concentrations, linear deviations can appear due to dimerisation. Such a case is described by ARBELOA et al. (1982) for rhodamine 6G. Dimerisation can also be expected for many other substances.

Spectrophotometry is a simple method to check the purity of fluorescent and non-fluorescing dyes. For convenience, a 10,000 mg/l concentrated solution is made up by dissolving 20.0 µg in 2 l. This concentration is suitable for measuring the extinction in 1-cm-cuvettes for almost all substances (Table 4). At extinctions under 0.1/cm larger cuvettes are needed.

Strictly speaking, the extinctions listed in Table 4 are only valid for the concentration 10,000 µg/l and for neutral aqueous solutions (pH = 7.0). At higher dilutions, the specific decadic extinction increases, as shown for uranine:

Concentration (µg/l)	Dilution	Extinction/cm
10,000	10^{-5}	1.812
1,000	10^{-6}	0.2001
100	10^{-7}	0.0215.

Table 4. Extinctions of fluorescent and non-fluorescing dyes used in water tracing (10,000 µg/l and pH 7). The last column lists the multiplication factor, for the extinction for each cm layer, needed to obtain the concentration. For fluids, the reference concentration is also 10,000 µg/l.

Dye	Absorption maximum (nm)	Extinction/cm	µg/l per Extinction 1/cm
Uranine	491	1.812	5520
Eosin	516	1.01	9900
Rhodamine B	554	2.21	4525
Sulforhodamine B	564	1.50	6667
Amidorhodamine G	530	0.69	14,490
Rhodamine WT	554	1.38	7245
Rhodamine 6G	526	1.65	6600
Erythrosine	525	0.82	12,190
Rose bengale	540	0.70	14,285
Pyranine 120%	455	0.40	25,000
Na-naphthionate	320	0.32	31,250
Amino G acid	359	0.27	37,040
Lanaperl fast yellow	440	0.061	164,000
Lissamine	422	0.20	50,000
Tinopal CBS-X	346	0.500	20,000
Leucophor PBS, liquid	348	0.112	89,300
Photine CU, liquid	345	0.111	90,090
Fluorescence bright. 28	349	0.53	18,870
Fuchsine, new	543	1.30	7690
Malachite green	616	0.444	22,500
Methyl Violet	585	0.398	25,120
Chromate (CrO_4^{2-})	372	0.040	250,000
Potassium permanganate	524	0.162	61,730

Furthermore, the hydrogen ion concentration also influences the value of the extinction, especially for substances whose fluorescence is pH-dependent. Figure 26 showed such a pH-dependency for uranine and pyranine. Substances, which do not have more than two mesomer forms due to pH-influence, display one or more isosbestic points; it is at these wavelengths that the substance has a pH-independent absorption. However, the extinction here is much lower than at the extinction maximum. Pyranine has for example four isosbestic points between 250 and 450 nm (Fig. 26 bottom).

Fluorescence spectrometry

Fluorimetrical analyses are superior to many other analytical methods, since they, compared to spectrophotometry, use two specific wavelengths and are therefore much more selective. Thus, the detection limits are lower in comparison to colorimetrical methods on an order of 3-4 magnitudes.

Filter fluorimeter

Instruments that are built as in Figure 35, have a primary filter between the light source and the sample, which matches the specific band of the dye sample's excitation spectra, thus allowing only those wavelengths through to the sample. A secondary or band-elimination filter is placed between the sample and the photo-detector, so that scattered light that could also excite to fluorescence does not reach the photodetector. The filter pairs have to be exchangeable, to allow optimal conditions for each specific dye under investigation. Filter fluorimeters are generally very sturdy and well-suited for use out in the field. The most widely used filter fluorimeter is made by the company G.K.Turner Associates. This instrument has an automatic range selector and a recorder can be connected if wanted. Filter fluorimeters with recorders can be installed in hard to reach sampling sites out in the field. However, filter fluorimeters have neither the selectivity nor the sensitivity of the spectrofluorimeter, discussed below.

The Turner Field Fluorimeter 111 uses ca. 400 W of electric power and runs on

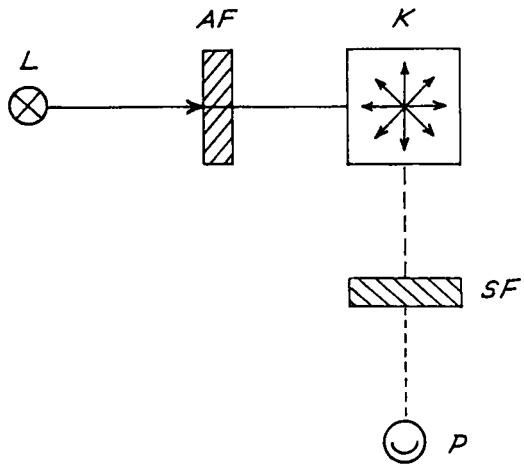

Figure 35. Light path in a filter fluorimeter. L = light source; AF = excitation filter; K = sample cuvette; SF = secondary filter; P = photodetector.

110 V. Therefore, usage in the field is only possible with energy-wasting converters or transformators or portable generators. BEHRENS et al. (1986) reported over their field experiences with the filter fluorimeter from Turner.

The filter fluorimeter Turner 111 can also be used for fluorimetrical intensity measurements of cotton swabs that adsorbed optical brighteners (SMART 1976a,b).

An instrument sold under the name Variosens can have up to 6000 m of cable (FRÜNGEL & KOCH 1978). Specially constructed models also permit measurements in the same depth underwater. With appropriate filter sets, uranine, rhodamine or chlorophyll or turbidity can also be measured out in the field. The pulsing xenon lamps, optics, filter and preamplifier are stored in pressurized casing. It needs a power source with 20-30 V direct current and the power input is only one Watt. The Variosens can be towed behind a boot for surface water profiles and the intensities are recorded. This way, HIRSIG et al. (1982) could trace a sewage plume with uranine in Lake Murten (Ct.Bern, Switzerland). Another Variosens model has two receiver systems that can record the intensities for two different emission wavelengths.

An important development in filter fluorimetry opened with the photo-conductor fluorimeters. With these instruments, in-situ measurements are possible e.g. in boreholes, in groundwater monitoring wells, or in artificial aquifers setups. Photo-conductor lengths of up to 500 m are possible (BARCZEWSKI 1990, SCHMID & BARCZEWSKI 1995). Photo-conductor fluorimeters can operate several probes at once and record the intensities at preset intervals. This measurement method is especially useful e.g. when discharge or dilution measurements at several sites on large river cross sections need to be taken simultaneously.

The fibre optic fluorimeter for water tracers was developed in a field-tested four channel system which operates with good accuracy and high sensitivity (Halogen lightsource: 0.02 mg/l uranine). It can be adapted to different tracers by changing the optical filters and, if required, the light source. With one device, four measuring points can be monitored simultaneously with low operational requirements because it is equipped with an automatic amplification selection, an overload protection circuit for the photomultipliers and an integrated data recording system.

The experimental setup of a fibre optic fluorimeter (FOF) for detecting water tracer is shown schematically in Figure 36. The fluorescent dye is stimulated in-situ by a light source which is connected to an optical fibre. As a light source, a halogen lamp, a flash lamp, a light emitting diode (LED), or an argon-laser for example can be selected, according to the excitation wavelength of the tracer dye and the application conditions. Part of the fluorescent light, which is emitted isotroply by the dye in the measuring volume (ca. 1 cm^3), is collected by a second optical fibre. Then the light is guided to an optical filter, which removes the part of the scattered and reflected excitation light. A photomultiplier creates an electrical signal, which is amplified and connected to a data processing system.

Spectrofluorimeter

Spectrofluorimeters are instruments with one or two monochromators, although instruments with just one are no longer being produced. They were generally hybrid instruments built along the unit-process system. Depending on the optical path, other than the monochromator, they needed either a filter for excitation or a band-elimination filter. Excitation and fluorescence spectra could be recorded (Fig. 37).

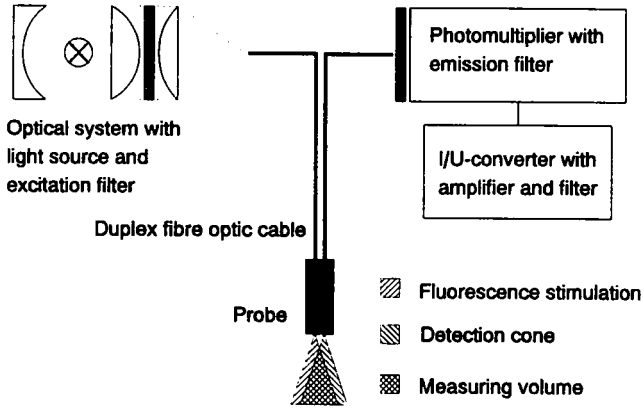

Figure 36. Basic structure for the photo-conductor fluorimeter after BARCZEWSKI (1990).

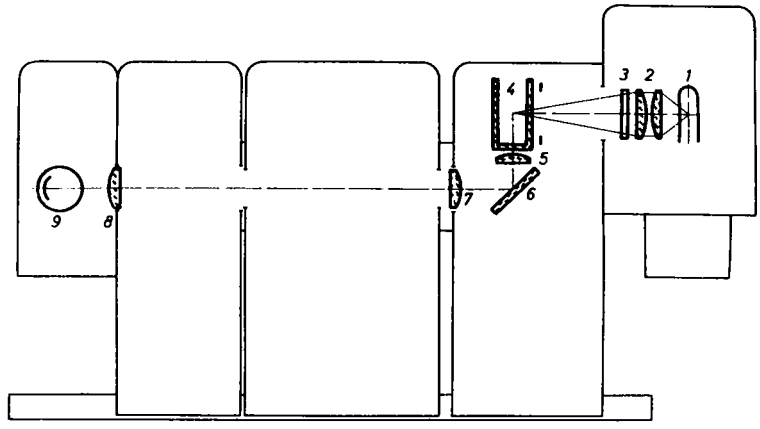

Figure 37. Optical path in a spectrofluorimeter with a monochromator (company sketch ZEISS, Oberkochen). 1 = light source, 2 and 5 = collecting lenses, 3 = excitation filter, 4 = sample cuvette, 6 = deflecting mirror, 7 = monochromator entrance opening, 8 = – exit opening, 9 = photo detector. Light source and photo detector are exchangeable.

Usually, the sample is excited at intensive green line of mercury with the monochromatic filters, which however, was only optimal for a few cases.

Spectrofluorimeters with two monochromators are standard in modern compact instruments. With these instruments, both the excitation and emission wavelengths can be selected to allow for optimal work. Most suppliers offer the possibility of running both monochromators simultaneously with stepping motors programmed with specific wavelengths. Such programs are indispensable for investigations in hydrological tracing techniques. Figure 38 shows the principle setup of a spectrofluorimeter with two monochromators.

Modern spectrofluorimeters operate with computers. This has the advantage, that specific determination programs can be stored and can be faultlessly and reproducibly called up at any time. Furthermore, the computer programs permit interactive

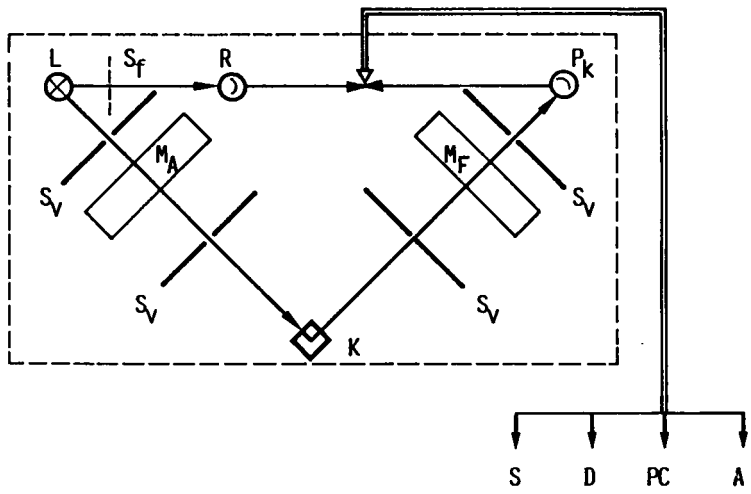

Figure 38. Principle setup of a modern spectrofluorimeter (from KÄSS 1990b). L = light source, Sf = unchangeable slit, S_v = changeable slit, M_A = excitation monochromator, M_F = fluorescence monochromator, K = sample cuvette, P_k = photomultiplier, R = reference ray receiver, S = analog exit to recorder, D = digital exit to printer, PC = data processing and storage, A = exit to digital or analog display.

work, so that the measurement values, value pairs, spectra, or time series can be stored, printed, or plotted while measuring.

A 150-W xenon lamp is usually used as the light source. It operates on a pulse and thus the lamp lasts longer and the ozone burden in the laboratory air is reduced. Also, pulsating excitation with the respective circuitries decreases the influence due to scattered light. For measuring phosphorescence, pulsating light sources are needed at any rate.

To spare the lamp, it should be turned off during long measurement pauses. Some models turn off automatically, if for example a break of longer than 10 minutes occurs between signals. The instrument's sensitivity stays in effect until reactivation, i.e. the concentration calibration remains.

The fluorescence measurement with laser excitation is not yet past the trial stage (BARCZEWSKI 1990). Tuneable lasers needed for hydrological spectrofluorimetry, are still too bulky and expensive for routine laboratory analysis.

The entrance and exit slits for both monochromators are quasi-continuously adjustable in half-width values of 5 to 25 nm or in increments of 0.1 nm, according to the instrument type, thereby allowing for an optimal energy flow. The sum of the entrance and exit slit width needs to be in any case smaller than $\Delta\lambda$ (Table 3). Furthermore, both slits need to be of equal size.

The monochromators are used to separate the light ray into the different spectra. Up into the sixties, glass or quartz prisms were used. Later, grating monochromators were used. Compared to prism monochromators, these transmit light better if they are outfitted with a holographic grid. By rotating the prism or the grid, changes in the spectral setting are achieved. The selected spectrum is displayed either in wavelengths λ in nanometers (nm) or as the wave number ν in vibrations per cm, with

$$\nu = \frac{10 \cdot 10^6}{\lambda}$$

Wavelengths are normally used with air and wave numbers for vacuum. Wave numbers are inversely proportional in air and vacuum to their speed of light. Given a wavelength λ of 500 nm, the wave number in vacuum is 20,000/cm and in air 20,005.6 per cm.

The selection of either wavelength or wave number on the monochromator is obtained by turning the prism or grating. Due to the spectral dependency of the dispersion, in the prism, the angle of rotation is not proportional to the wavelength. In a diffraction grating, the rotation angle = wavelength change; grating monochromators have a linear wavelength scale.

After microelectronics was introduced, this advantage of the grating monochromators became less important. Display readings in wave numbers are physically more meaningful. Since the RAMAN-lines always have, independent of the position of the spectrum, the same wave number distance to the exciting line, the distances in a wave number scale are always the same.

Grating monochromators with concave holographic gratings yield an increase in intensity, since the separated light beam is not necessarily limited to a small slit. An additional increase in intensity is achieved by using so called 'blazed' gratings. However, these gratings have an intensity maximum only for a distinct wavelength or wave number. To optimize the advantages of these monochromators for spectrofluorimeters, a blazed wavelength, which is located below the wavelength of the fluorescence monochromator, is used for the excitation monochromator: At 400 and 500 nm for instance.

All modern spectrofluorimeters are equipped with a programmable spectral sequence, where the beginning and end of the spectrum as well as speed of the spectral change (nm/min) can be selected. These commands can be carried out jointly or separately for the excitation as well as for the fluorescence monochromators. If both monochromators are moved simultaneously, the recording speed for both must be the same and the wavelength steps or wave number difference must remain constant. The latter method is called synchroscan. It is especially important for the identification of traces of fluorescence substances and for the detection and determination of two flourescent dyes in one solution.

The beam emanating from the excitation monochromator enters the sample cuvette where the sample is excited to fluorescence. The fluorescence light – with longer wave lengths than the exciting light – radiates in all directions the same. Normally, the fluorescing light path is perpendicular to the excitation light path, since the set up is perpendicularly aligned. Many fluorimeter models are set up for a fluorimetrical determination with high pressure liquid chromatography with flow-through micro cuvettes. These instruments have parallel entrance and exit slits (Fig. 39 left). A disadvantage to this alignment is that there is a low fluorescence yield. Since there is usually enough sample water in hydrological investigations, the cuvette set up according to the middle or right side of Figure 39 should be chosen.

These alignments allow detection limits of almost an order of magnitude lower. To lower the scattered light during hydrological fluorescence measurements, it is better to use larger cuvettes than the normal 1 × 1 cm size. A mirror coating of the

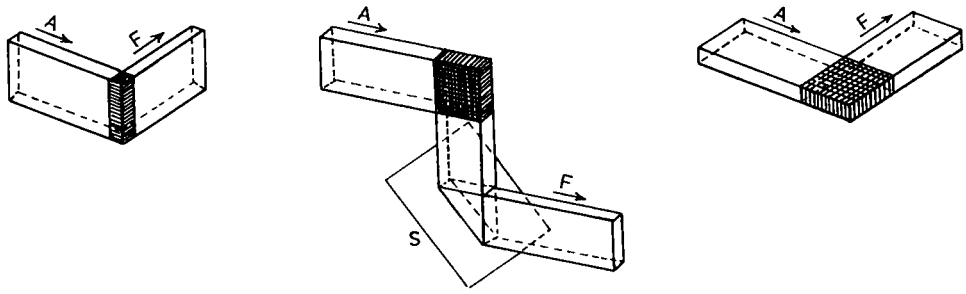

Figure 39. Possible cuvette alignments in fluorescence instruments. A = exciting path, F = fluorescence path, hatched = measuring volume. Left: perdendicular slits in most instruments. Fluorescence is recorded from only a narrow column. A relatively low volume is measured. Suitable for flow-through cuvettes in HPLC-investigations. Middle: Slits are parallel; fluorescence radiation is taken off the cuvette bottom and through the deflecting mirror (S). A comparatively larger volume is measured (system ZEISS-Oberkochen). Right: Slits are perpendicular to each other. A larger volume than as in the alignment on the left-hand side (system HITACHI).

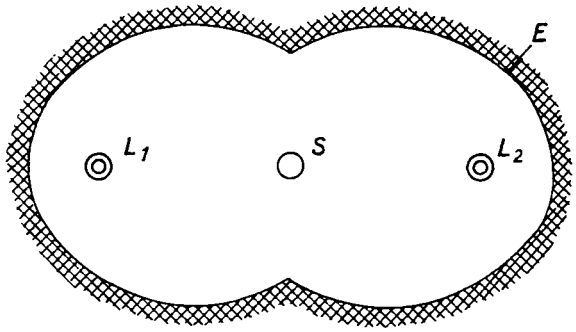

Figure 40. RAMAN-cuvette after KORTÜM (1955). The cuvette wall (E) is formed as two ellipses and mirror coated. The common focus point, S, excites the RAMAN-radiation or the fluorescence of both emitters in both other focus points, L_1 and L_2. The cuvettes can be filled with a liquid that screens the exciting radiation. The sample solution is in the tube S.

cuvette back wall that the exciting light would hit and which would reflect the fluorescent light, would indeed increase the intensity, but it would also simultaneously increase the scattered light unproportionally, so that it is better to use a varnish such as a non-fluorescing black iron lacquer.

The RAMAN-cuvettes, shown in cross-section in Figure 40, would also yield a high fluorescence efficiency (KORTÜM 1955). They are made of two overlapping elliptically formed and mirror coated walls, which have a common focal point where the RAMAN-lines, resp. the fluorescence is very strongly excited in both other focal points. Apparently, the RAMAN-cuvette has never been built into an instrument for fluorescence measurement.

In grating monochromators, an overlapping of spectra with higher orders can occur, i.e. shortwave peaks appear in the longwave spectral range. Many spectro-

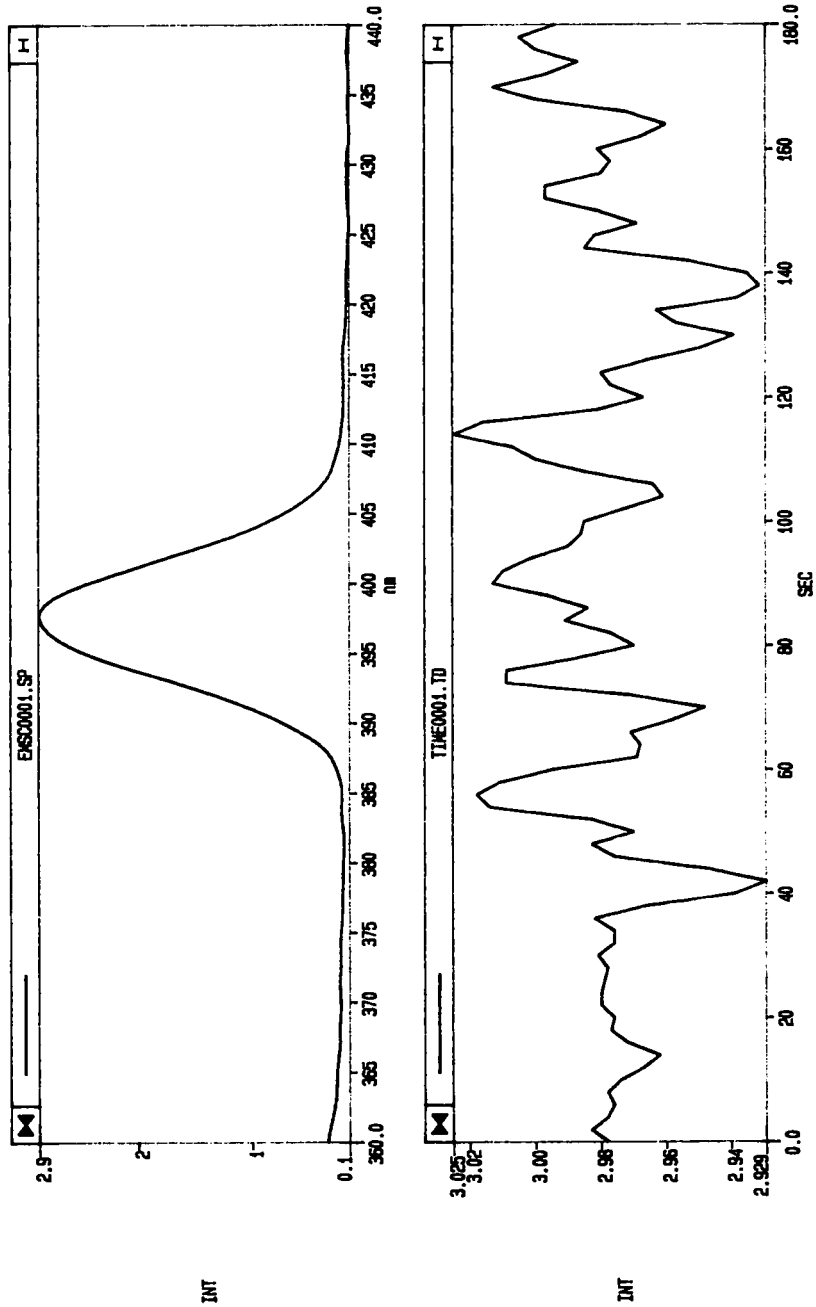

Figure 41. Signal to noise ratio measurement in a PERKIN-ELMER spectrofluorimeter LS 50. Top: RAMAN-scattering in the emission spectrogram at 397 nm with excitation at 350 nm. Bottom: Noise in the RAMAN-Linie at 397 nm over 3 minutes. The signal to noise ratio is 2.9-0.1/3.025-2.929 = 29.2.

fluorimeters are equipped with band-elimination filters, that can be automatically tilted in and out. However, sometimes 'ghost peaks' appear anyway. Using suitable filters, e.g. Schott-filter FG 10, 1.0, or 2.0 mm thick, in the fluorescence path can help screen out the wavelengths under 400 nm. In a pinch, slide covers also help.

Only photomultipliers with an especially low dark current should be used, in general the photomultiplier supplied with the spectrofluorimeter are adequate for hydrological fluorimetry. It is not necessary to install red light sensitive multipliers.

Other than the photo detector for fluorescent light, all spectrofluorimeters are outfitted with a second one as a reference light receiver. It receives the weakened light from the light source directly and the built-in electronics uses the reference light to compensate for fluctuations in the intensity and possible light source drifting.

The quality of a spectrofluorimetrical set up is defined by the RAMAN-scattering. The signal to noise ratio (S/N-ratio) of the RAMAN-line in bidistilled water is determined under the following conditions:

Excitation:	350 nm
Fluorescence:	397 nm ($\Delta\lambda = 47$ nm)
Slit widths:	5 nm
Response:	2 sec (0 to 98% display)
Recording time:	180 sec.

Good set ups should have a S/N-ratio of 25 at least. For microcells, e.g. HPLC determinations, a ratio of 20 can be designated as good. Figure 41 shows a measurement example for the signal to noise ratio.

The RAMAN-effect is caused by O-H-vibrations in the water molecule. The vibration frequency is $1.05 \cdot 10^{14}$/s, which corresponds to a wave number of 3500/cm. The energy used to excite the O-H-vibrations is impressed upon the scattered light, i.e. the wave number of the scattered light is decreased by the amount 3500/cm or a multiple of it. Most of the time, only the single multiple appears in a RAMAN-spectrum, since the multiple RAMAN-lines are too weak to be recorded. Although the wave numbers for the RAMAN-scattering are constant, the wavelength distance increases towards the longwave spectral range. In the shortwave spectral range, the RAMAN-scattering can be taken for a fluorescent peak. In Figure 42, the spectral position of the first degree RAMAN-lines and the wavelength differences in dependency upon the excitation wavelengths are plotted.

Calibrating fluorimeters is not as easy as calibrating photometers. To calibrate the latter, only a cuvette with pure solvent is needed and either the transmission set to 100% or the extinction set to zero; transmission = 0% is present with a darkened optical path. Fluorimeters need standards for calibration. This calibration standard has the same dimensions of the sample cuvette and consists of either uranyl glass or plexiglass. Unfortunately according to information from the glassworks, uranyl glass is no longer produced due to environmental protection reasons. Uranyl glass contains small quantities of uranium oxide, which is dissolved in the glass stem and fluoresces green. The uranyl glass standards are extremely durable and are excellent for calibrating fluorimeters. The uranyl glass that was formerly available had a fluorescence with an intensity of 100 µg/l uranine equivalents or more. For calibration, a reduction of the amplification was required or an attenuator or a blind had to be used. Plexiglass standards are used with different fluorescent dyes and are therefore applicable

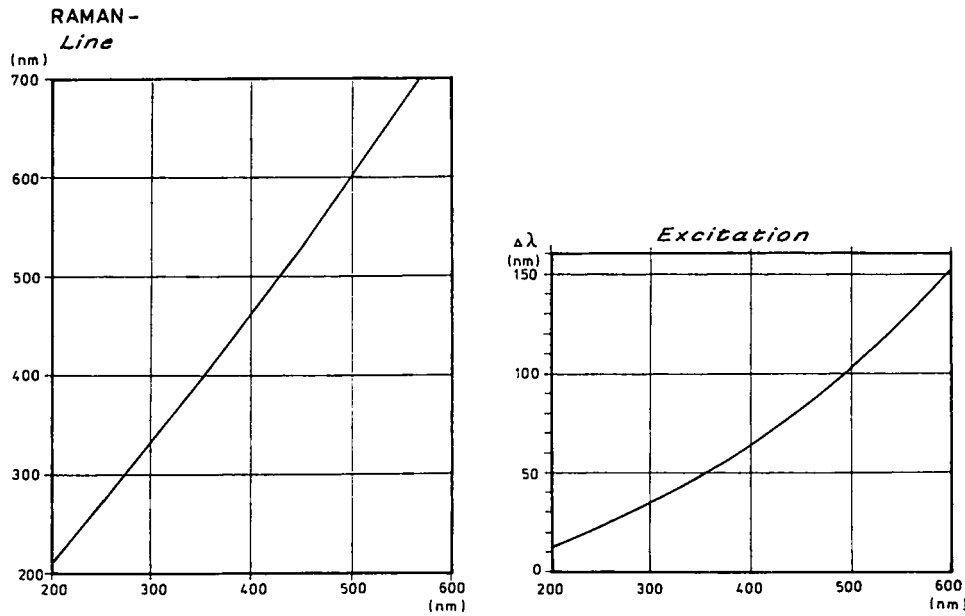

Figure 42. RAMAN-scattering in dependency upon the excitation wavelengths. Left: Wavelengths of the RAMAN-line, right: wavelength difference.

for different spectral regions. However, plexiglass standards are, as opposed to uranyl glass, not indefinitely tenable. After constructing a calibration line by utilizing a series of solutions with defined contents of the substance to be calibrated, the concentration of the calibrations standards can be assigned. All further measurements do not require the time-consuming production of the comparison solutions, which are also not very tenable.

By utilizing the spectrofluorimeters, calibrated in the described manner, series of measurements with fixed wavelengths pairs or spectrograms can be measured. Figure 43 shows three spectra of the same uranine solution that were recorded under different conditions. As the solid curves show, the wavelengths of the excitation and the fluorescence are 21 nm apart for the uranine used. During synchroscans, both monochromators are moved synchronously over the spectrum with a constant distance of the wavelength of 21 nm. The recorded synchron-spectrum is shown for the fluorescence wavelength in Figure 43 as a dotted line. Compared to the excitation and fluorescence spectra, the synchron-spectrum yields a higher discrimination. Moreover, the synchron-spectrum is almost symmetrical, similar to a normal distribution. The synchron-spectrum is nothing more than the product of excitation and fluorescence intensity. As will be discussed later, the sychroscan is indispensable for the identification of solutions with xanthene dyes. Synchronscans are used in hydrological spectrofluorimetry almost exclusively.

2.1.3.4 *Dye separation*

Sampling is one of the largest cost factors in tracing tests. In order to determine hydraulic and hydrological parameters, evaluable breakthrough curves with the neces-

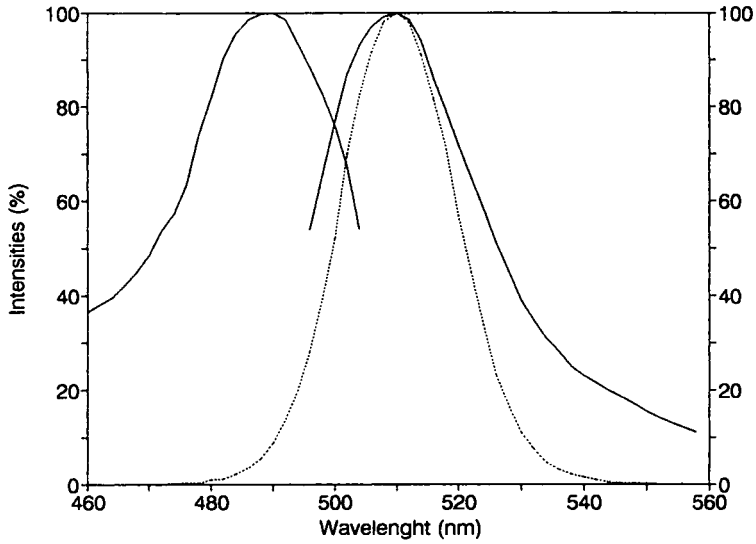

Figure 43. Fluorimetrical uranine spectra as different presentations. Solid curves: left side excitation and right side fluorescence spectrum for uranine (enlarged section out of Figure 12). Dotted curve: synchronscan with a wavelength difference of 21 nm plotted as fluorescence.

sary data for determining the first arrival time (t_1) and the time at the centre (t_3) are essential. Therefore, when planning tracing tests, it is necessary to allot for sufficient sampling. Often, the simultaneous use of more than one tracer in different injection sites during a tracing test brings about better results and more answers to the questions being asked. If the different tracers can be analysed and detected simultaneously in the sample, the costs can be lowered.

TRILLAT (1899a,b) recognized that, excepting fluorescein, nine other dyes had more or less strong sorption properties and were thus not suitable for dye tracing tests. Only acid fuchsine could be made visible after a passage through soil by adding acetic acid. Based on his observations, he recommended carrying out combined tracing tests using fluorescein and acid fuchsine. Obviously, his suggestion was not followed.

When two fluorescent dyes are used in a tracing test simultaneously and are present in the same sample, there can be disturbances. If the fluorescence maxima are close together, ca. less than 50 nm, the two dyes interfere with each other, i.e. a certain part of the fluorescence of the one dye is superimposed upon the fluorescence of the other dye.

Along with uranine, eosin is used as a second fluorescent dye, since it has low sorption properties and is also low in price. Figure 44 shows the synchroscan spectra of uranine and eosin, both separately and together. Two facts are obvious in the graph:

1. The fluorescence is additive; at the fluorescence maximum of the one dye an increase in the fluorescence signal happens due to the presence of the other dye and vice versa.

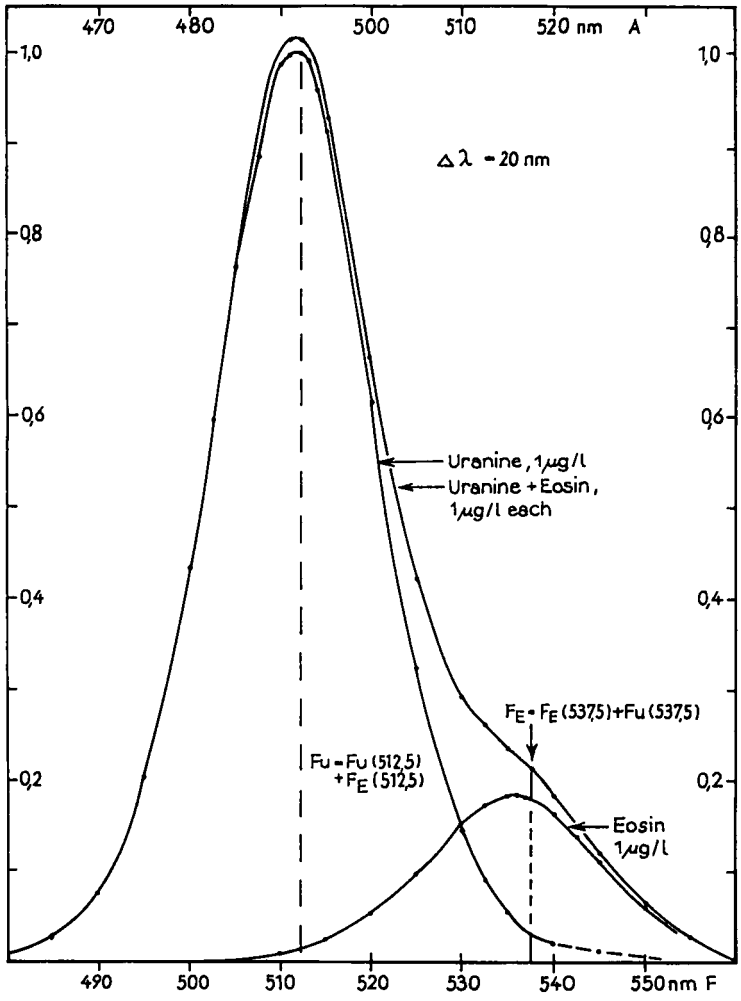

Figure 44. Synchroscan spectra for 1 µg/l uranine (left) and 1 µg/l eosin (right) as well as a solution with 1 µg/l each of uranine + eosin (encasing curve). Distance between excitation and fluorescence $\Delta\lambda$ = 20 nm; bottom abscissa fluorescence, top abscissa excitation wavelengths. The fluorescence intensities of both dyes are additive (from KÄSS 1982d).

2. Although the dyes have the same concentration, the peaks have different heights.

There are different methods for separating the fluorescent dye mixes.

Synchroscan

The easiest way to recognize two or more fluorescent dyes in one solution is to run a synchronized wavelength change of the excitation and fluorescence monochromators through the spectrum of interest with a constant wavelength distance $\Delta\lambda$. This wavelength distance is determined by the spectral position of the excitation and fluorescence maxima. For most of the xanthene dyes it is between 20 and 25 nm. The

synchroscan spectrum is much more focussed than the separate excitation and fluorescence spectra. Figure 43 displays uranine's spectral half-width values of 36 nm, 31 nm, and only 21 nm for the excitation, fluorescence, and synchroscan respectively. The synchroscan spectrum is the product of the course of the intensity of excitation and fluorescence:

$$I_{S(\mathrm{mm})} = I_{A(\mathrm{mm})} \cdot I_{F(\mathrm{mm})-A(\mathrm{mm})}$$

The height of the peaks' maxima does not change, since both intensities = 1. The low differences in $\Delta\lambda$-values for the separate xanthene dyes are of no practical importance if an average, ca. 22 nm, is used. Due to the flat peaks in the excitation and fluorescence spectrum, the intensity losses at differences in $\Delta\lambda$-values of 2-3 nm can be neglected.

During the Second Expert Conference in 1970 in Freiburg/Br., BEHRENS presented the synchroscanning method (discussion contribution to BAUER 1972a). Further descriptions of the synchroscanning method were published by BEHRENS in 1971 and 1973.

The synchroscan method is now also used in analysing for other substances (VO DINH 1981). Especially the content of the poly-cyclical aromatic hydrocarbons, which is required by the drinking water act, can be quantitatively determined with this method (INMAN & WINEFORDNER 1982).

Figure 45 shows a synchroscan of a turbid pore-groundwater sample from the Merdingen test field. The record proves that even samples with a high background can deliver evaluable spectra. In this example, the maxima of both fluorescent dyes are 72 nm apart, so that an evaluation was possible, even with larger intensity differences. An interpretation is more difficult if the peaks are closer together. BEHRENS

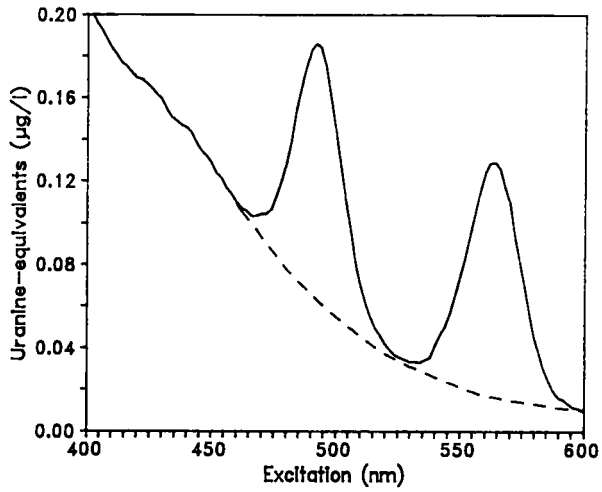

Figure 45. Synchroscan of a turbid groundwater sample with uranine and sulforhodamine B traces recorded with a HITACHI-F 4000 spectrofluorimeter. The intensities and concentrations can be easily determined due to the separate peaks: Uranine: 0.125, sulforhodamine B: 0.11 × 3.3 = 0.36 µg/l. Distance from excitation and fluorescence monochromator: 20 nm, recording speed: 240 nm/min, slit widths: 5 nm.

(1973) and BEHRENS , ZUPAN and ZUPAN (1976) published several impressive examples that show that at high concentration differences and low wavelength distances, complications can arise during evaluation. Furthermore, the synchroscan method cannot be used if the dyes to be separated have wavelength differences of the maxima that are far apart. An example of this is a sample containing pyranine $\Delta\lambda$ = 57 nm) and a xanthene dye $\Delta\lambda$ = rd. 22 nm). Other methods must be used to separate such mixes.

Computative dye separation

The fluorescence intensities of two fluorescent dyes, whose spectra are mutually superimposed, are additive, i.e. the encasing curve of both spectra is the sum of the separate intensities (Fig. 44). Since the respective percentages from the additional intensities of the pure solutions can be determined, the true concentrations can be graphically or arithmetically calculated.

Figure 46 shows a nomogram for graphically determining concentrations of solutions containing a mix of uranine and eosin. A nomogram is made by completing the following steps: setting up intensity scales F_U and F_E for pure uranine and eosin solutions, entering the four intensities for the pure solutions, connecting the related in-

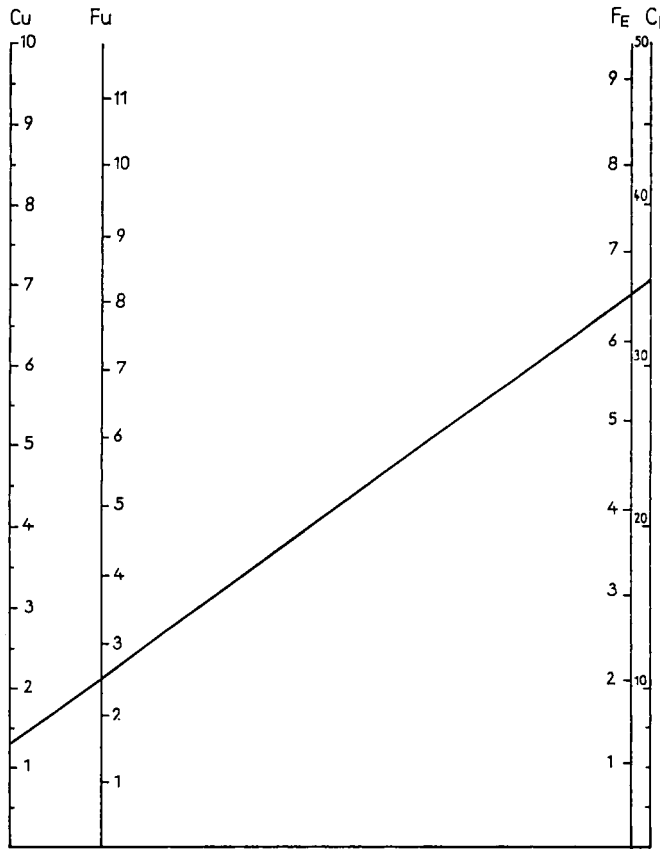

Figure 46. Nomogram for the graphical determination of true concentrations of mixes containing two substances (from KÄSS 1982d). Displayed are the scale values, recorded for the uranine setting (F_U = 2.5) and for the eosin setting (F_E = 6.5) on the instrument. The true concentrations for uranine (C_U = 1.3) and for eosin (C_E = 35) can be read off the concentration scale.

tensity points, the intersection points of the extended connecting lines with the abscissa result in the zero value for the corresponding concentration scale, and the upwards extended connecting line results in the corresponding concentrations on the concentration scale. The nomograms can be made with logarithmic scales for large concentration ranges.

Instead of using a nomogram, the true concentrations can also be arithmetically determined. KÄSS (1967a) published instructions for such calculations for mixes of uranine and eosin using the extinctions on the absorption maxima. In the example from Figure 44, a calibration to a uranine concentration in mg/l with $\Delta\lambda = 20$ nm was carried out. The uranine fluorescence intensity F_U at the fluorescence maximum 512.5 nm was 1.0; at the eosin setting there is still a trace fluorescence from uranine with an intensity of 0.0213. Conversely, eosin has with an optimal setting in comparison to uranine, only an intensity of 0.18, at settings for uranine there is still a percentage of 0.115. In 1982 KÄSS published a calculation method for the true concentrations of a mix containing uranine + eosin (KÄSS 1982d):
With a uranine setting, the fluorescence intensity F_U shows up as:

$$F_U = C_U k_U + C_E k_E z_{EU} \tag{2.1}$$

with a setting of the fluorescence intensity F_E so:

$$F_E = C_E k_E + C_U k_U z_{UE} \tag{2.2}$$

with: C_U = the uranine concentration to be calculated, C_E = the eosin concentration to be calculated, k_U = a constant for converting the fluorescence intensity in pure uranine solutions to a concentration C_U; here 1.0, k_E = a constant for converting the fluorescence intensity in pure eosin solutions to the concentration C_E; here = 0.18, z_{EU} = the intensity ratio for pure uranine solutions with the settings eosin to uranine, here 0.0213, z_{UE} = the intensity ratio for pure eosin solutions at the settings uranine to eosin, here 0.115.

Equations (2.1) and (2.2) are two equations with two unknowns.

Solving for:

$$C_U = 1.00246\, F_U - 0.1153\, F_E \text{ and}$$
$$C_E = 5.569\, F_E - 0.1186\, F_U$$

The general equations for two component systems are:

$$C_A = \frac{F_A - (F_B z_{BA})}{k_A (1 - z_{AB} z_{BA})}$$

$$C_B = \frac{F_B - (F_A z_{AB})}{k_B (1 - z_{AB} z_{BA})}$$

The calculations for C_A are simplified if the instrument is calibrated to the component A, generally uranine. Then $k_A = 1$.

The computations can be completed on programmable calculators, yet it is more convenient to use spreadsheet data programs such as LOTUS, QUATTROPRO, etc. for mass tests.

With these computations, dye mixes, e.g. uranine and pyranine, can also be calculated, even if both dyes fluoresce at the same wavelength. Necessary for this are, that:

1. Only the netto intensities are used in the equations; i.e. the background was accounted for and removed,

2. Constant pH-conditions during the measurements, which will guarantee an optimal fluorescence intensity.

A special advantage of the method is that it can also be used for fluorescence signals, which were recorded with a filter fluorimeter.

The arithmetic elimination can also be used for mixes with three components. When using three superimposed fluorescence spectra, the following conditions prevail for the substances 1, 2 and 3:

$$F_1 = k_1C_1 + k_2C_2z_{21} + k_3C_3z_{31}$$
$$F_2 = k_2C_2 + k_1C_1z_{12} + k_3C_3z_{32}$$
$$F_3 = k_3C_3 + k_1C_1z_{13} + k_2C_2z_{23}$$

To simplify the calculations, it can be assumed that the instrument is calibrated to substance 1, then $k_1 = 1$. Using matrix algebra, the equations are solved as (GEISTER-FRANTZ 1981):

$$\begin{Bmatrix} C_1 \\ C_2 \\ C_3 \end{Bmatrix} = \begin{bmatrix} l \cdot k_2 z_{12} \cdot k_3 z_{13} \\ z_{21} \cdot k_2 \cdot k_2 z_{23} \\ z_{31} \cdot k_2 z_{23} \cdot k_3 \end{bmatrix}^{-1} \begin{Bmatrix} F_1 \\ F_2 \\ F_3 \end{Bmatrix}.$$

This matrix can also be solved with a computation program on a personal computer. The requirements are: constant pH-conditions during the measurements, an instrument with a good stability, and a precise determination of the constants k and z.

Dye separation with pH-adjustment

The first experiments using pH-value adjustment for dye separation were published by BAUER (1972a). He investigated two dye systems (uranine/amidorhodamine G and uranine/sulforhodamine B) in a spectrophotometer with one monochromator at pH 8 and at pH 2. By using suitable band-elimination filters in the fluorescence pathway, it was possible to separate the fluorescent dyes, if they were present in different concentrations in the ratio range of 10:1 to 1:10.

Eosin's fluorescence can be suppressed by acidifing to a pH-value <2. Uranine fluoresces in acid solutions, if it is excited at 438 nm (BEHRENS 1982). Even if the fluorescent intensity is only about 1/5 of the intensity in neutral to alkaline uranine solutions, this way small amounts of uranine can be detected and measured with large amounts of eosin present. The samples must be free of nitrate when using this uranine analysis method in strongly acidic solutions, since uranine's fluorescence is partially quenched when nitrate ions are present. This phenomenon is the basis of a nitrate determination method from MIGUEL & BRAUN (1974). In constrast, uranine's fluorescence decreases with a pH-adjustment to 4.6 so low, that eosin's fluorescence remains to a large extent (Fig. 47). The necessary buffer for this pH-adjustment is described by BEHRENS (1988b) thus: 5.5 M acetic acid + 4.5 moles of potassium

acetate are added to the sample in the ratio 0.6:100. The small change in volume can be neglected.

To achieve pH-values of over 10, where uranine, eosin, and pyranine reach their highest fluorescence intensities, BEHRENS recommends adding 0.6% of a 10% tetra sodium-ethylene-diamine-tetra-acetate solution. The same high pH-values without increasing the volume can be had by letting the open sample bottles stand in an ammonia atmosphere (see Fig. 25). Carbonates and hydroxides precipatate only at slow rates and as large crystals on the bottom of the bottle. BEHRENS (1988b) and BEHRENS and TEICHMANN (1989b) published detailed instructions for their method of separating two- and three-component mixes of uranine, eosin and pyranine. However, it must be noted that such procedures are not only time-consuming, there are often losses in intensity also.

Dye separation with thin layer chromatography

In 1975, ROCHAT et al. described a thin layer chromatographic method for separating the three rhodamines: rhodamine B, WT, and G. They used activated silicon gel plates and the solvent mixture n-butanol-ethanol-ammonia solution in a ratio of 10:4:2. In this setup, rhodamine B travelled farther than amidorhodamine G. Rhodamine WT showed two spots, one that stopped before and one that stopped after the amidorhodamine G spot. A quasi-quantitative concentration determination was possible by comparing the fluorescence intensity with standard solutions under an UV-lamp.

Using paper chromatography, it is possible to separate mixes of uranine, eosin and amidorhodamine G, if the concentrate is eluated with the solvent mixture water +

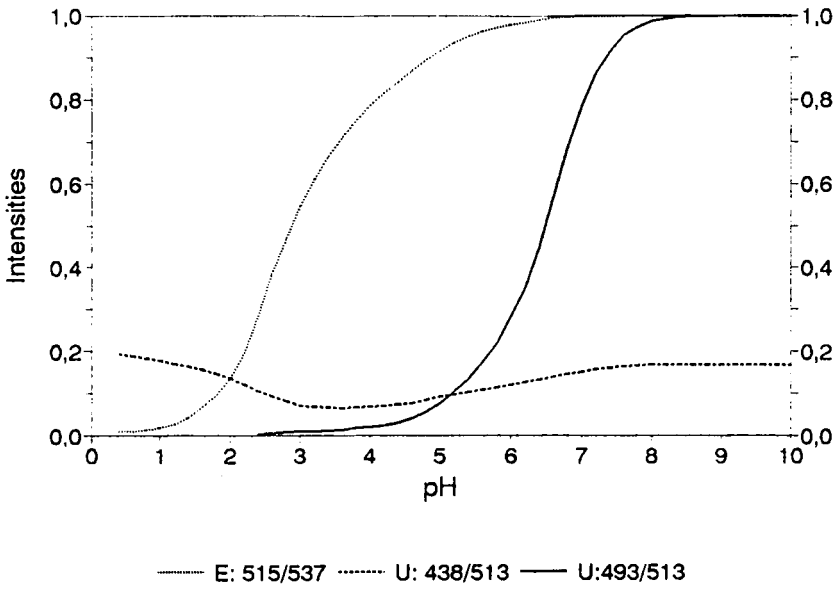

Figure 47. pH-dependency of the fluorescence intensities of uranine at 513 nm under excitation conditions at 493 nm (thick line) and at 438 nm (dotted line). As a comparison, the eosin intensities, fluorescence 537 nm, excitation 515 nm (broken line) are shown (from BEHRENS 1982).

ethanol + amyl alcohol. Amidorhodamine G can be recognized better, if the fluorescence of the eosin spot is suppressed during the UV-check with diluted sulphuric acid (BEHRENS, ZUPAN & ZUPAN 1976).

With thin layer chromatography, isopropyl alcohol-eluates from activated charcoal samples can be examined for uranine and eosin, if a mixture of propanol-1 /acetic acid ethylester/25% ammonia solution (6:2:2) is used as the solvent (BEHRENS et al. 1981).

The possibilities for quantitatively determining fluorescent dyes in direct samples as well as in activated carbon eluates have been well investigated by the Karlsruher Research Group. In laboratory tests it was possible to quantitatively determine the five dyes uranine, amidorhodamine G, tinopal CBS-X, eosin, and rhodamine B in the direction of the solvent (BUB et al. 1979). These laboratory techniques were put into practice in the field during the combined tracing test in the Neuchâtel Jura. The spectrofluorimetrical analysis of the direct samples of both Areuse Springs resulted in good evaluable breakthrough curves for uranine and amidorhodamine G; however, in the thin layer chromatograms, rhodamine B was also quantifiable in trace amounts (BUB & HÖTZL 1980).

Thin layer chromatography is indeed time-consuming and painstaking work, but it can be a valuable supplement to spectrofluorimetrical direct determinations and of activated carbon samples. The detection limits are not quite as low as those from spectrofluorimetry. However, thin layer chromatography has superior dye separation abilities as compared to spectrofluorimetry, if the solvent mixture propanol-1/acetic acid ethylester/ammonia solution (25%)/water in the ratio of 6:1:2:1 is used (ACKERMANN et al. 1982).

Dye separation with High Pressure Liquid Chromatography (HPLC)

The first tests to directly determine the fluorescent dyes, which are used in hydrological tracing tests, were carried out by BUB et al. (1979). Due to disturbances, only concentrations over 10 µg/l could be separated and only through a very time-consuming process.

LUTZ et al. (1986) had more success with HPLC-investigations of activated carbon eluates with methanol-ammonia(25%)-mixtures in a ratio of 95:5. Activated carbon eluates using dimethyl formamide were not produced because of the slow filtration due to viscosity and because of the toxicity and high production costs. To enrich the volatile components of the eluates, they were reduced. They used 0.005 mol tributyl-ammonium-hydroxide (pH = 7.5), methanol and acetone in a ratio of 85:10:5 as the liquid phase. Uranine produced a perfect signal, which was not disturbed by any other peaks, with a retardation time of 85 seconds. Unfortunately, a reference to an absolute tracer concentration was not given. In another publication, (LUTZ & PARRIAUX 1988) they demonstrated that direct samples could also be investigated via HPLC. For the carbon extraction, they found that a mixture of ammonia solution (10%) in alcohol was a good solvent. Inevitably, ammonium carbonate forms in the eluate, which can disturb the chromatographic investigation. Better extractions can be achieved with pyridine in percentages of 5-100% in water, methyl- or ethylalcohol or in acetone. In chromatography, silica gel filled columns with nonpolar aliphatic C-18-surface covers are used. A complete separation of fluorescing humic acid can be achieved with a selection of solvent mixtures.

A method was developed at the University of Amsterdam by which in a single passage 126 dyes could be determined (WEGENER et al. 1987). Columns filled with 3 mm particles and C-18-covers were used. The mobile phases were water and 0.005 m tetrabutylammonium in methanol in a ratio of 75:25 at the start of the passage and 0:100 after 25 minutes. The passage was finished after 40 minutes with an instrument temperature of 30°C. The detection was achieved through absorption at wavelengths 500 and 425 nm. All the fluorescent dyes used in hydrological tracing tests could be identified except Rhodamine WT. This method was developed especially for analysing cosmetics. The sensitivity limit is 2-15 ng. This method could be an advantageous supplement for the spectrofluormetrical determination of water contents after appropriate modifications.

Dye separation using liquid-liquid-extraction
Rhodamine B and rhodamine WT have carboxyl-groups, on the contrary, amidorhodamine G and sulforhodamine B have sulphonic acid groups. In strong sulphuric acid solutions with pH-values under 5, the carboxyl-rhodamines can be transferred into the chloroform phase. In contrast, the sulforhodamines stay in the aqueous phase (ROCHAT et al. 1975). Uranine no longer fluoresces at this pH-value, so that a uranine separation is not necessary.

Dye separation through photolysis
Eosin's strong sensitivity to light can be used to separate eosin in mixtures (BEHRENS 1982). A Schott-filter OG515, 3 mm thick, suppresses the wavelengths below 505 nm that negatively influence uranine. If the solution is also acidified to pH = 5.5, uranine's light sensitivity is further reduced.

Dye separation with fluorescence quenching
Fluorescence quenching due to iodide ions have varying effects upon the different fluorescent dyes. According to ANDRÉ & MOLINARI (1976), a 1 mol potassium iodide solution decreases the fluorescence of amidorhodamine G by a factor of 37; with rhodamine WT, the factor is 3.5, with rhodamine B it is 4.1. The publication has examples for the detection and the quantitative determination of rhodamine B and rhodamine WT together with amidorhodamine G.

Dye separation with fluorescence decay times
According to SEIDLITZ & BEHRENS (1991), the registration of the fluorescence decay time can be used to detect eosin traces next to fluorescing humic acid. The investigations are still in the initial stages; further developments are in process.

2.1.3.5 *Enrichment methods*
It is an advantage in hydrological tracing tests, that enough water is generally available. However, the tracers are sometimes so diluted that the detection limits are reached or surpassed. Numerous procedures for tracer enrichment have been described. Many of these methods not only concentrate the tracer, they also serve as a separation method. Several procedures can be used to accumulate the tracer during tracing tests in remote and hard to get sampling sites as average samples. Each method has special application areas and analysis specifics. In each separate case, it

must be decided which method is the best choice. In some cases, a combination of methods may be best.

Enrichment with activated carbon

In 1904, MAYRHOFER (OHLMÜLLER 1904) presented instructions for concentrating uranine in single samples. He shook 5 l of sample water with 5 g crushed animal charcoal; after filtering and drying, the charcoal was washed with 15 ml 'weak ammonia' alcohol. The alcohol eluate was then further reduced. Uranine could be detected in dilutions of 1:4 billion in the converging light bundle.

In 1967, WHITE presumed that the suggestion to use activated carbon in the sampling sites for the uranine observation was an idea from J.R. DUNN (1957). HAAS described this method in 1959. According to his report, TURNER (1958) carried out karst water tracing tests in Central Pennsylvania and ZOTTER (1963, 1965) in West Virginia. The investigation of the activated coconut carbon, which had been filled in plastic tubes, was carried out with the naked eye using alcoholic potash lye eluates in white porcelain bowls.

The activated carbon method was taken up by the French researchers LALLEMAND and PALOC and used in karst as well as in pore groundwater (1964b, 1967). They hung their activated carbon, which they called fluocapteurs (= fluotransducers), in either perforated brass cylinders or in nylon sacks. Out in the field, they hung their fluotransducers in the sampling sites simultaneously and took them out of the sites one after the other. They found that the eluates from the samples that had hung for an hour in the sampling sites showed four times the amount of uranine than the direct samples in the fluorimeter. They listed the advantages of using the activated carbon method in a table.

Due to his extensive experience with activated carbon sampling in alpine karst, BAUER (1967b, 1972b) was able to publish detailed information about the preparation, use of, and investigation of activated carbon.

BAUER recommended an activated carbon grain size of 1,5 mm (MERCK-No. 2514), which should be repeatedly shaken in tap water before use to remove the carbon dust. Before filling in gauze sacks, the carbon grains must be reactivated by heating for several hours at 110°C. Then the grains can be filled in the nylon sacks such as pictured in Figure 48. Possible confusion can be avoided by using double numbering. The sacks should be lightly kneaded underwater when they are put in place to remove air bubbles so that all of the grains are uniformly wetted. The author carried out basic research as to the connection between uranine adsorption and length of time suspended in the water: Increasing the time suspended from two to eight hours rendered approx. three times the yield. Furthermore, the relative enrichment is the higher, the lower the uranine concentration is. BAUER also established that even suspending the activated carbon sacks for two hours caused an enrichment in the eluates of fifty times that in the direct samples. Besides suspending the sacks in the water, the possibility of investigating the single samples is pointed out. An impressive comparison between single measurements and activated carbon samples with varying lengths of time suspended in the water was given for the results of the uranine tracing test in the Lur cave system in 1966 (BATSCHE et al. 1967).

BAUER gave the following instructions for the eluation of the activated carbon samples: For every 2 g of dry carbon, 10 ml of a mixture of 96% alcohol and 15%

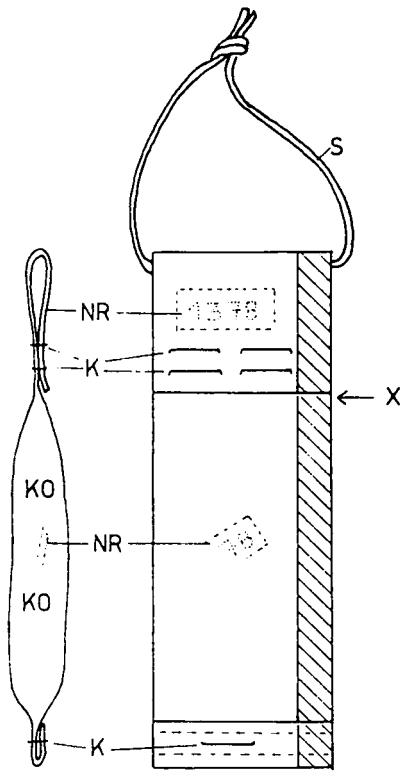

Fig. 48. Activated carbon sack (from BAUER 1967a). 8 cm wide strips of nylon gauze No.30-GG/370 with 11½ threads/cm and a mesh size of 0.67 mm are sewn together with nylon band (hatched) into long tubes and cut into 14 cm long pieces. Then the bottom is closed with staples (K) to a sack and filled with ca.20 g activated carbon (KO) with a grain size of 1.5 mm. Two 1 × 2 cm, permanently numbered plastic tags (NR) are inserted, one in the sack and one in the flap. Then the top is folded over and also closed with staples (K). The loop (S) is used to hang the sack in the flowing water. To remove the activated carbon, the sack is cut open at the X.

potash lye (1:1) is added as a layer to a nonfluorescing 70-75 mm high and 20-25 mm wide glass test tube with a flat bottom. After shaking repeatedly and allowing to settle, the clear liquid can be measured in a spectrofluorimeter without needing to be decanted, if the test tube is held at an angle in the light path. Decanting into a fluorescence cuvette is not recommended because the eluate will etch the cuvette glass. By so recording the fluorescence spectra, it was possible to establish the reemergence of uranine in the Aach spring during the mass tracing test from 1969 near the Danube percolation. The uranine had been injected in the periphery of the Aach drainage area (BATSCHE et al. 1970). At first, the fluorescence spectra showed a maximum due to humic acid at 530 nm. During the uranine passage, the maximum was displaced to 523 nm, so that a qualitative breakthrough was proved, which was not possible with direct measurements.

A method for determining uranine, called the 'Ultra micro method' by the authors, was published in 1967 by POLLAK et al. The authors used the following setup: out in the field, a 5-l-plastic bottle with the bottom cut out is placed upside down in a frame. A hole is drilled in the screw top, which is now at the bottom, and an activated carbon paper filter is placed there between two perforated plastic disks. These filters are specially made for this purpose at the University of Ljubljana out of cellulose and activated carbon powder in a 1:1 ratio. The paper was produced with a grammatur of 90 g/m². Normally, 5 l of sample water was filtered through the activated carbon filter. The extraction of the filter was completed with 5-10 ml of a

mixture of 15% potassium hydroxide solution and alcohol (1:1). The eluate was then examined for uranine fluorescence semi-quantitatively in a CADEZ-NOVAK fluorescope (Fig. 34) with standards. The detection limit was around 0.01 µg/l. An example of the results obtained with this method, along with the investigation methods from BAUER and the results of the direct determinations for the trace in the Lur cave system from 1966 was published in BATSCHE et al. (1967).

For qualitative observations, POLLAK et al. (1967) constructed 10 × 15 cm filter plates to hold the activated carbon filter paper. The filter plates are hung in remote springs for long periods of time. Later the filter paper is extracted and analysed in the manner described above.

According to MATHEY (1971), the optimal flow velocity is 0.5 m/s when using 9 cm long and 1 cm wide tubes made of brass wire netting. These tubes are filled with 4 g activated carbon MERCK 2514 or Norit PKST 1-3 mm.

There are other recommendations for the composition of the solvent used in extracting the activated carbon besides the aforementioned (MULL et al. 1988), which recommend using isopropanol or 1-propanol instead of ethylalcohol. These solutions should be suitable for all the fluorescent dyes and very stable.

PERLEGA (1976) enhanced the activated carbon method by introducing the solvent dimethylformamide, which extracts practically all the fluorescent dyes adsorbed on the activated carbon within two hours. The extraction of 0.5 g dried activated carbon (MERCK 2514) is carried out with 7 ml of a solution that contains 80% N-N-dimethylformamide (MERCK Uvasol 2937) and 20% water. Uranine's fluorescence is quenched in the eluate. Thus, all the other fluorescent dyes can be measured in the eluate. After adding one drop of ammonia (25%), uranine fluoresces again. In the solvent dimethylformamide, almost all the fluorescence maxima are displaced towards longer wavelengths (VÖLKL 1988, PERLEGA 1976, BAUER & PERLEGA 1980):

	Fluorescence maximum		Detection limit
	in water	in dimethylformamide	in eluate (µg/l)
Uranine	515	530	rd. 0.1*
Eosin	538	550	rd. 0.1
Rhodamine B	578	578	rd. 0.05
Amidorhodamine G	553	555-560	rd. 0.05
Tinopal CBS-X	405	407	100-10
Tinopal liquid	428	432	100

* after adding ammonia.

The eluate can be further worked upon when several orange fluorescing fluorescent dyes are present. Rhodamine B can be removed through filtration in filter tubes with strongly acidic cation exchanger (e.g. Bayer Lewatit S 1080 G1). Conversely, rhodamine B passes through a filtration with strongly basic exchangers (e.g. Bayer Lewatit 600), whereas uranine, eosin and amidorhodamine G are held back. Eosin and amidorhodamine G can be separated by filtering with silica gel: eosin passes quantitatively through and amidorhodamine G is held back (BEHRENS , ZUPAN & ZUPAN 1976). Rhodamine B can also be separated from amidorhodamine G by

shaking the dimethylformamide extract with chloroform: Rhodamine B passes into the chloroform phase, amidorhodamine G stays in the extract (ROCHAT et al. 1975).

WITTWEN et al. (1971) investigated several activated carbon products as to their suitability for adsorbing sulforhodamine B and amidorhodamine G. Out of eight investigated products, six had the required properties. The authors carried out the eluations with several solvents, whereby at higher concentrations, diethylenglycol gave the highest yields compared to ethylenglycol and ethanol-methanol-mixtures. At lower rhodamine concentrations, there was no single best extraction solvent recognizable. The enrichment factors were between 100 and 1000.

The adsorption of rhodamine WT onto activated carbon was investigated by SMART & BROWN (1975). Out of twenty different solvent variations including methanol, H_2SO_4, HNO_3 and detergent, the best elution solvent they found was 5-10% NH_4OH in ethanol. Furthermore, they established that the desorption proceeded all the better, the higher the elution temperature is.

Uranine can also be concentrated out of large volume single samples with activated carbon. For this, 3-4 l of sample water are shaken with 3 g of fine-powdered activated carbon for 15 minutes. After the carbon settles and decanting most of the supernatant, the carbon is collected on a small filter paper. The uranine is removed with 10 ml ammonia alcohol (MERCK 1986).

Enriching onto wool and cotton

In 1926 TIMEUS pointed out that wool fibres adsorb uranine and take on an orange-red colour. He figured out that 1/100 mg uranine could be thus detected.

To investigate optical brighteners and direct yellow 96, cotton wool is best used (QUINLAN 1976). In contrast to activated carbon, cotton swabs can be hung to swim freely in the sample water, whereby it must be avoided that they contact a solid surface (stream bed, the wall of a water tapping). QUINLAN presents a technique for suspending the cotton wool detectors on a self-orienting support above the stream beds. The cotton wool detectors must be kept from contact with all material that contain optical brighteners (paper, textiles). They should only be transported to and from the sampling sites in plastic bags. SMART (1976b) established that after only 15 minutes of exposure, equilibrium sets in between the liquid and solid phases. The investigation was carried out with a Turner-fluorimeter using wet cotton wool. Dirty cotton wool means losses in intensity and so the cotton wool detectors must be washed in water with detergents and then rinsed before measuring. With the appropriate filter combinations, direct yellow 96 and rhodamine WT can be detected along with the optical brighteners (MULL et al. 1988).

Enrichment through liquid-solid-extraction

Uranine has sorption properties in acidic pH-ranges. An enrichment method, already published in 1913 by DIENERT is based on this. He added 1 ml sulphuric acid to 1 l sample water and filtered the mixture through acid-washed sand. DIENERT obtained the sand from alluvions of the Seine. The uranine is released out of the sand with a little ammonia and is now more concentrated in the solution.

For modern liquid-solid-extractions, a stationary phase is silica gel with a grain size of 40 µm and occupied by octadecylsilane (C_{18}). Such exchangers are sold as finished products in plastic tubes by various companies under their own brand names

(e.g. MERCK: Adsorbex, BAKER: Bakerbond). The tubes need to be washed first with methanol and then wetted with the sample water. The adsorbed tracer is then extracted with methanol.

Enrichment through liquid-liquid-extraction (extraction with diethylether)
Under acidic conditions, uranine changes into the fluorescein-cation, which not only has sorption properties, but is also lipophilic. In 1902 OHLMÜLLER published instructions for extracting with diethylether in strongly diluted uranine solutions: 300-400 ml sample water is mixed with acetic acid and reduced to approx. 50 ml in a plastic bowl. Then hydrochloric acid and ether are added. The decanted ether phase is then shaken with alkaline distilled water. The concentrated uranine is then in the aqueous phase (LUKAS 1959a).

When the clarifying pond at Kahnsstein near Salzgitter-Bad in 1893 was dyed with uranine, the dye visibly reemerged in only three springs. In four further springs as well as in the river Innerste near Ringelheim, OHLMÜLLER was able to irreproachably detect uranine using this method.

OHLMÜLLER'S method has been modified and improved by various authors, whereas acetic acid was left out (DOSCH, QUITZOW) or substituted by sulphuric acid (LOMBARD) or by nitric acid (KLATTE). The following detection limits, relative to the initial concentration of uranine (mg/l) in the sample water are notable:

QUITZOW (1915):	0.1
LOMBARD (1921):	1.0
EGGER (1929):	0.1
RICHTER (1944):	0.2
DOSCH (1956):	0.1
KLATTE (1962):	0.01

LOMBARD recognized that when organic material was present, that the ether layer could not be faultlessly clarified. In such cases, adding one drop of alcohol resulted in a clear solution. KLATTE investigated solutions that had been ultracentrifuged and thus free of turbidity.

RODIER and MARICHAL (1961) used rhodamine B to investigate the flow velocity of the river Rhône near the nuclear research centre Marcoule. They also determined the flow path of the dye introduced into the Rhône until it was distributed uniformly in the river cross section. The corresponding trace analysis for rhodamine B was prepared by MARICHAL & BENOÎT (1961): 2 l of river water, if it is turbid, is centrifuged for 10 minutes at 3000 rpm and poured into a separating funnel. Then 5 ml of 2 M hydrochloric acid and 75 ml of isoamylalcohol are added. After shaking heftily for three minutes, the solution is left to settle completely. The supernatant alcohol phase is decanted and 0.5 g anhydrous sodium sulfate added to clarify the opalescent turbidity. The authors determined the rhodamine by measuring the extinction at 551 nm. Since isoamylalcohol is to some extent water soluble, either reference samples must also be measured or a calibration and correlation of the remaining isoamylalcohol volume must be considered. For quantitative determinations, a detection limit of 1.0 µg/l is given and for qualitative determinations 0.001 µg/l.

Enrichment through volume reduction

SHOTTON and HABEEB (1955) boiled a 1000 µg/l uranine solution for 80 hours, without a loss in uranine. According to FABIOL & POUZANCRE (1981), an 8% loss only occurs when uranine solutions with distilled water are kept eleven days at 200°C.

Therefore, solutions that contain uranine concentrations near or under the detection limit, can be boiled down without a loss of uranine. In 1944, RICHTER noticed that the visibility limit for uranine solutions could be lowered from 33 to 10 µg/l by reducing the volume. According to KÄSS (1976a), groundwater can be reduced to 1/20 of its original volume in a drying oven. In the reduced sample there are crusts of lime and silica which can be removed by filtering through a fine-mesh paper filter or a membrane filter. The filtrate, which now has a pH-value of over 8, can be poured directly into the measuring cuvette. There is no advantage to a further volume reduction, since fluorescing humates and non-filterable colloids would disturb the measurements. The detection limit can be lowered with such a volume reduction by circa one order of magnitude (Fig. 49).

2.1.4 *Physiology of the fluorescent dyes*

In this chapter, the behaviour of the fluorescent dyes in living organisms is de-

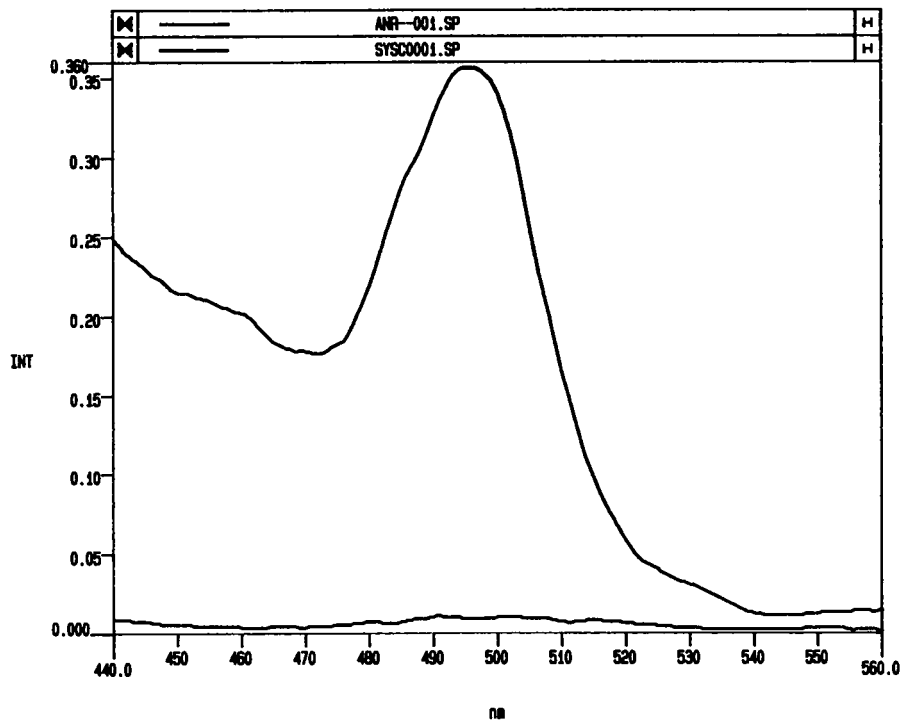

Figure 49. 2 Synchroscan spectra of a groundwater sample with a low uranine concentration of approx. 0.003 µg/l. Bottom curve: Direct measurement; top curve: after a 20-fold reduction.

scribed. Often asked questions are handled here and these very questions show how little is definitely known about the decay of the fluorescent dyes and their impact upon the living organisms.

2.1.4.1 *Fluorescent dye decay in natural water*

In 1982, ZUPAN reported on the decay of fluorescent tracers in polluted surface water. She carried out storage tests of up to 150 days on six river water samples from the Ljubljana River as well as on samples from the Savinja with different degrees and types of pollution. She found, especially in rivers strongly polluted by organic-chemical industries, that sometimes there was a strong decrease in the fluorescence. The decrease was most evident with sewage water containing phenols, which decreased the fluorescent dyes investigated (uranine, eosin, amidorhodamine G and rhodamine) by one-third to one-tenth of the initial concentration. The initial concentrations were between 0.1 and 10 µg/l. In the samples containing phenols, they immediately caused the fluorescence to drop by 55 to 12% in all four dyes and at all concentrations. Since the fluorescence decreased by 92 to 58% in the pure water blanks, it can be assumed that the observations reported do not describe microbiological decay, but rather fluorescence quenching.

ZUPAN (1989) carried out further storage tests, adding phenol, ammonium-nitrogen and formaldehyde to samples of uranine and eosin. The fluorescence intensity remained unchanged for 90 days after adding 0.25 mg/l phenol. If 1 mg/l ammoniacal nitrogen is added to spring water samples, the fluorescence intensity of uranine as well as eosin falls after 90 days to ca. ¼ of the initial value. Different combinations of phenol, formaldehyde and ammonia additives lower the fluorescence intensities, but not as far. During these tests it was also noted that the samples which received no additives also had a decrease in intensity of up to 75% of the initial value.

Figure 49 in 'Markierung unterirdischer Wässer – Untersuchungen in Slowenien 1972-1975' (Steirische Beiträge zur Hydrogeologie, year 1976) shows the uranine passage in the springs near Bistra. The curves shown are from two laboratories and are from different times. It was assumed that the general decrease in uranine, which reached 80% in some cases, was caused by decay, which is more pronounced, the more polluted the sample water is. Since then, it must be noted that the investigations were carried out by different analysts with different instruments in different sample bottles. Furthermore, a close examination of the curves show that some samples had higher concentrations in the repeat measurements. Also, losses in accuracy during the concentration determination due to the simultaneous presence of rhodamine FB must be assumed. Therefore, there are several uncertainty factors, which lead to the conclusion that microbiological decay is not the only possibility here.

Further suppositions concerning uranine decay are discussed in 'Karst Hydrology of the Central and Eastern Peloponnesus (Greece)' (Steirische Beiträge zur Hydrogeologie, Jahrgang 1985/86) on page 244. Inside five months, the uranine in samples from the Dara spring supposedly decreased by 15%, in the Ladon spring by 30%. As in the example from Slovenia, two different laboratories with different instruments were used to determine the uranine in these springs on the Peloponnesus. Furthermore, other than uranine, pyranine was also present, which adds to the measurement

uncertainty due to the fluorescence wavelength similarity. Microbiological decay is not the only possibility causing the uranine reduction.

There are numerous examples for uranine's stability underground. If injections are carried out in the unsaturated zone or in less permeable rocks, uranine can remain almost unchanged for years. BAUER (1969) reported continuing traces of uranine emerging from Schneealpe tunnel in Lower Austria, which came from a tracing test that had been carried out two years earlier. In 1987, the public works of the city of Lörrach pumped a strongly coloured green groundwater sample out of an inlet pipe in the Wiesental valley. The sample had a uranine content of approx. 40,000 µg/l; the uranine was from a tracing test from 9 November 1970! A further example of uranine's stability underground can be found in the Swabian Alb in Southwestern Germany. Uranine was injected in a groundwater monitoring well of the Lake Constance Water Works in 1967 and in 1987 there was still 878 µg/l uranine in a groundwater sample.

Yet, surface and groundwater samples can also retain their dye content for years if stored at room temperature. Several storage tests carried out over years have proved that even organically polluted samples sometimes only suffer low uranine losses:

	Uranine (µg/l)		Decrease
	1975	1980	(%)
Pore groundwater, Test area OMW Karlsruhe with 13.7 mg/l petrol hydro-carbons and 0.25 mg/l volatile phenols	12.5	1.6	86
River water, Neckar near the Deißlinger Keck springs, heavily polluted with organics	30	21	30
Spring water, Izvir pod skalo (No.1.43) Slovenian, lightly polluted with organics	8.5	3.1	66
Calibration solution, slightly ammoniacal in dist. water	144	134	7.6

More extensive tests are needed for definite proof of microbiological impact on samples. The easiest tests to carry out are storage tests, where the samples suspected of possible microbiological decay are injected with different dye amounts.

Gross discrepancies between the observations recorded at several sampling sites in Southwestern Germany and the concentrations measured in the laboratories resulted in thorough investigations into possible causes of uranine's decay. Since there were repeated witnesses to the intensive green colour of the water being sampled, a uranine reduction after sampling must have occurred in the time before the samples were measured. The first such case occurred during a uranine tracing test in the quarry Äckerbühl near Aalen-Waldhausen (East-Alb, Southwestern Germany) on 28 June 1982. Of thirteen observed sampling sites, four showed no traces of uranine throughout the sampling period of several months. A small part of the dye moved southeast to the catchment area of the Danube; at five sampling sites there, weak dye traces were recorded. The main part of the dye flowed west towards three strong springs in the upper course of the Weißen Kocher (approx. 4 km) and showed classic breakthrough curves with approx. 20 µg/l uranine each (Fig. 50). In the following dry months, the uranine concentrations in these three springs dropped down to values under 0.1 µg/l. On 5 October heavy rains set in and 34 mm of precipitation were re-

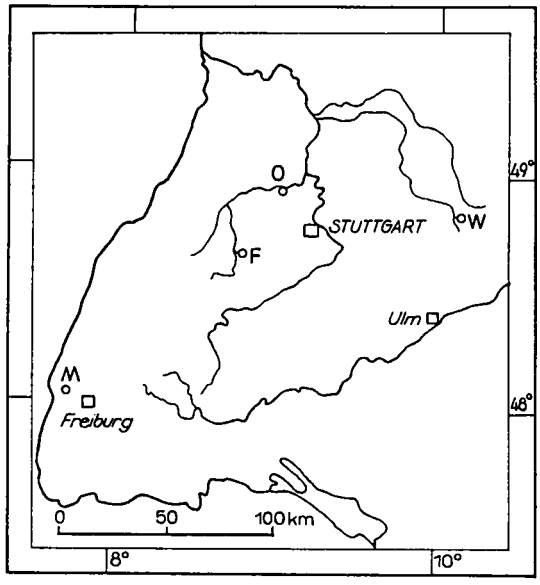

Figure 50. Location of the uranine reducing groundwaters in Southwestern Germany. W = Spring region of the Weißen Kocher; O = Oberriexinger Mühlbrunnen; F = Fuchtbach spring; M = Merdingen test field.

corded on 6 October at the weather station Heidenheim. As of 9 October, the three springs flowed with such a strong green colour, that the spring that fed into Unterkochen's water supply had to be turned off. Therefore, after 9 October no more samples were taken there. The samples from the other two springs (Weißer-Kocher-spring and Waschhalden spring) were not spectro-fluorimetrically analysed for uranine until the end of October 1982 in the laboratory. The analysis resulted in uranine concentrations only between 0.07 and 0.21 µg/l. A check with the sampler takers verified the definite green uranine colouring of the spring between the 9th and 11th of October, with an estimated uranine concentration of at least 20 µg/l. At that time, the harvested fields on the Härtsfeld were covered with manure and therefore the three springs were contaminated with the solid wastes. Upon opening the sample bottles weeks later in the laboratory, a definite manure odour was perceivable. The reduction in the uranine concentration was presumed to have been caused by either the contamination with organic substances or due to microbiological decay.

On 13 March 1985, a uranine tracing test was carried out in the catchment area of the Fuchtbach spring, 1 km northeast of Wildberg-Gültlingen/Lkr. Calw in Germany. The trace's breakthrough curves were nearly textbook perfect, for the tapped spring as well as for the nearby untapped spring. To more closely define the protection area of the Fuchtbach spring, another uranine trace was carried out on 5 May 1986. Before the tracing test began, the samples from the Fuchtbach spring had a rest concentration of uranine from 13 March 1985. Eight hours after the dye injection, the Fuchtbach spring was coloured green; the green colouring continued for two days. Surprisingly, when the supposedly dye-containing samples were measured later in the laboratory, they had less uranine than the measured background from before the test began; only two samples showed a somewhat lower reduction of the uranine concentration (Fig. 51).

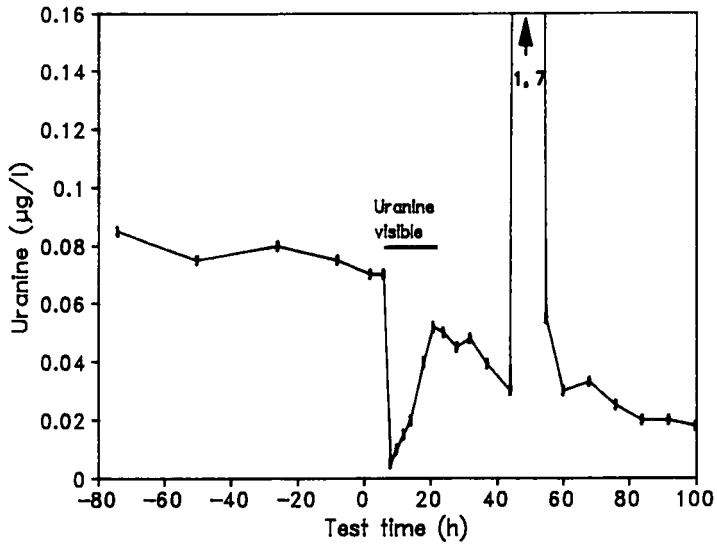

Figure 51: Dye breakthrough curves for the test in the Fuchtbach spring from 5 May 1986. The background of 0.09-0.07 µg/l uranine came from an earlier tracing test. Approximately eight hours after the dye injection, the dye reappeared and the uranine concentration began to sink to what was then measured in the laboratory later. The decay does not happen everywhere: In the sample from the 50-hour test series, there is little or no decay.

On 7 January 1987 the tracing test from 5 May 1986 was repeated. The results were almost identical: Immediately after sampling, the presence of uranine in the visibly green samples was verified by checking the samples under an UV-lamp. However, when the samples were analysed a month later, only traces of uranine were present as in the test from 5 May 1986.

Two articles describe the investigations carried out concerning the conditions under which uranine decay happens (SAYER 1988, 1990). The author carried out three additional tracing tests in the Fuchtbach spring under the same conditions as earlier but with uranine, eosin and pyranine. Of the three injected dyes, a reduction occurred only with uranine. Furthermore, she carried out storage tests with Fuchtbach spring water. She came to the conclusion that no decay occurred in those Fuchtbach spring samples which had been injected or doped with rhodamine B and rhodamine 6G. During the storage tests, the different uranine concentrations displayed only between 1 and 1000 µg/l of the expected decay, which usually set in after 18 days. SAYER also showed, that there was no decay in the Fuchtbach spring samples which had been injected with uranine, if they had been heated in the autoclave (Plate 3). The uranine decay can be suppressed by adding the following:

$HgCl_2$, hypochloride, formaldehyde, phenol, manganese, copper-, zinc- and cobalt-ions: each 10 mg/l,

Glucose: 1 mg/l,

Penicillin: 13 units/l,

Streptomycin: 270 units/l.

Other than the Weißer Kocher and Fuchtbach spring regions, two further groundwater aquifers with definite microbiological decaying properties for uranine were

discovered through irregularities in the breakthrough curves: Mühlbrunnen and the Merdingen test field.

A listing of the results from the Mühlbrunnen tracing test from 12 March 1974 in the Roll Quarry near Markgröningen/Lkr.Ludwigsburg (Fig. 50) exemplifies what the microbiological decay of uranine can look like in a tracing test (KÖHLE 1980).

Sampling Day	Time	Uranine (µg/l)	Visibility at sampling	Sampling Day	Time	Uranine (µg/l)	Visibility at sampling
13.3	20	0.45	–	15.3	9	105	++
	22	0.47	–		12	1.3	++
14.3	2	0.45	–		15	53	++
	5	0.9	–		18	42	++
	8	8	–		21	40	++
	10	57	+	16.3	7	19	+
	11	110	++		12	16	+
	12	210	+++		18	12	+
	12:35	250	+++	17.3	7	10	+
	13:35	330	+++		18	9	+
	14	2.4	+++	18.3	7	16	+
	16	3.9	+++		17	12.5	+
	18	620	+++	19.3	7	0.13	+
	20	580	+++		17	30	+
	22	490	+++	20.3	7	0.13	+
15.3	6	170	++		17	6	+

Similar results were obtained from the uranine tracing test from 30 April 1990 in the Merdingen test field. Storage tests with uranine doping from 1991 in Mühlbrunnen and also in some of the monitoring wells in the Merdingen test field verified that microbiological uranine decay activity is present.

The spring region of the Weißer Kocher is in the Oxford limestones of the Upper (Weißer) Jura. Numerous uranine tracing tests have been carried out in the catchment area of these karst water discharges (WEIDENBACH 1960, GROSCHOPF 1972). Excepting after heavy rains and snow melts, these waters carry little germs and can be used as drinking water.

Few uranine tracing tests had been carried out in the region near the Fuchtbach spring until the test with the visible uranine decay. The Fuchtbach spring water is karst water from the Lower Muschelkalk. The spring has a very low bacteria content with an average colony count of under 10/ml.

The Mühlbrunnen spring taps the Hauptmuschelkalk (Middle Triassic). Several tracing tests with uranine and eosin were carried out in its catchment area by KÖHLE (1980) in 1973 and 1974. The area is mainly used for agriculture. Nothing is known about the microbiological content of the Mühlbrunnen.

Uranine tracing tests have also been carried out in the Merdingen test field since 1979 (KÄSS 1990b). The pore groundwater is potable.

A summary of the criteria for the microbiological decay of the uranine follows (see also Table 5).

– A definite microbiological decay of the uranine has only been proven at four sites in Southwest Germany. Surveys of numerous workers who conduct tracing tests

Table 5. Criteria concerning microbiological uranine decay.

Uranine decay does *not* occur	Uranine decay *can* occur
In groundwater heavily polluted with organics	In organically unpolluted groundwater
In regions with no previous uranine tracing tests	In regions with previous uranine tracing tests
Within 10 days	Within 11-60 days
With very low and very high uranine contents	With uranine contents between 0.5 and 5000 µg/l
In heated samples, or with chemical or antibiotic additives	With untreated samples

at home and abroad resulted in no indications of other occurrences following the displayed decay patterns.

– Microbiological uranine decay occurs only at those sites where uranine has already been introduced into the system.

– The groundwater does not need to be heavily polluted with organics for the uranine decay to occur. A test with uranine in an empty manure pit from an agricultural property on 17 March 1964 in Heilbronn-Horkheim resulted in a well-documented passage of the percolating uranine-coloured pit-water up to distances over 400 m in two months in the pore-groundwater. There is no uranine decay in sewage plants (KANOWSKI 1985) or sewage farms.

– There are indications that the uranine decaying microorganisms only attack the uranine if all other nutrient sources have been exhausted. During storage tests where the uranine test solutions have been diluted with distilled water, the decay sets in more quickly (SAYER 1988).

– Very high and very low uranine contents are not subject to decay.

– The decay starts very suddenly, but at the earliest after setting for ten days; until then the uranine concentration stays constant or it decreases only minimally. The decay proceeds further for 2-3 days until it reaches a minimum concentration, which does not decay further (Fig. 52). The minimal concentration is normally under 1 µg/l and lower than 1% of the initial concentration (Fig. 53 top).

– There is no definite relationship between the initial concentration of the uranine and the time needed for decay to half that concentration (half-concentration time) or to the final concentration (minimal concentration) (Fig. 53).

Since then, it has not been possible to identify the uranine decaying microorganisms nor to produce a pure culture of it. Furthermore, there was no indication of a specific population of microorganisms in the uranine decaying groundwater. There were also no peculiarities regarding the enzymatic activity of these groundwaters found (OBST & HOLZAPFEL-PSCHORN 1988). LUKAS (1959c) supposed that nitrifying bacteria could be responsible for the uranine decay.

Meanwhile, the possibility of a tracing test being ruined due to this is not very large. These uranine decaying microorganisms occur only rarely and only in places where tracing tests with uranine have already been carried out. If there is a suspicion that uranine was destroyed in a tracing test, there will still be always uranine rests detectable. In such cases, the test can be carried out again, either with another tracer or even with uranine a second time. Then, the samples should be quantitatively de-

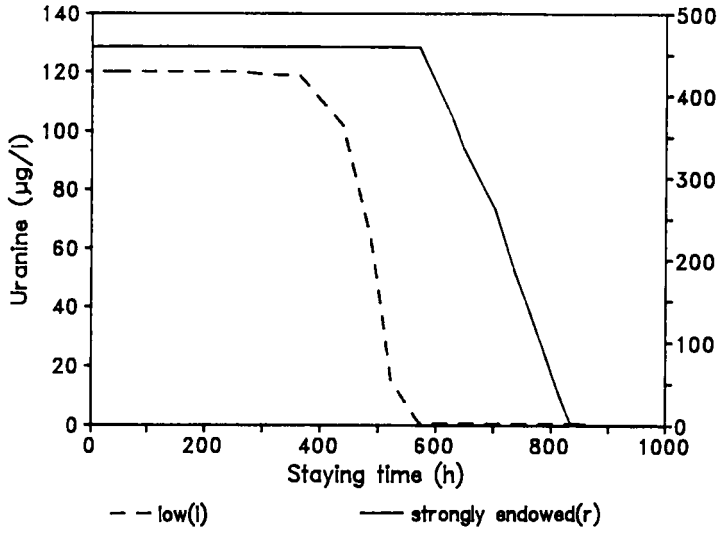

Figure 52. Concentration-time-course of two typical storage tests with groundwaters that contain uranine decaying microorganisms. Karst water samples from the Oberriexinger Mühlbrunnen taken on 11 November 1991 were injected with 120 and 460 µg/l uranine. The decay process in the diluted solution started after 430 hours (18 days) and reached a final concentration of 0.4 µg/l (= 0.33%); in the concentrated solution it began after 610 hours (25 days) and went to a final concentration of 1.6 µg/l (= 0.35%).

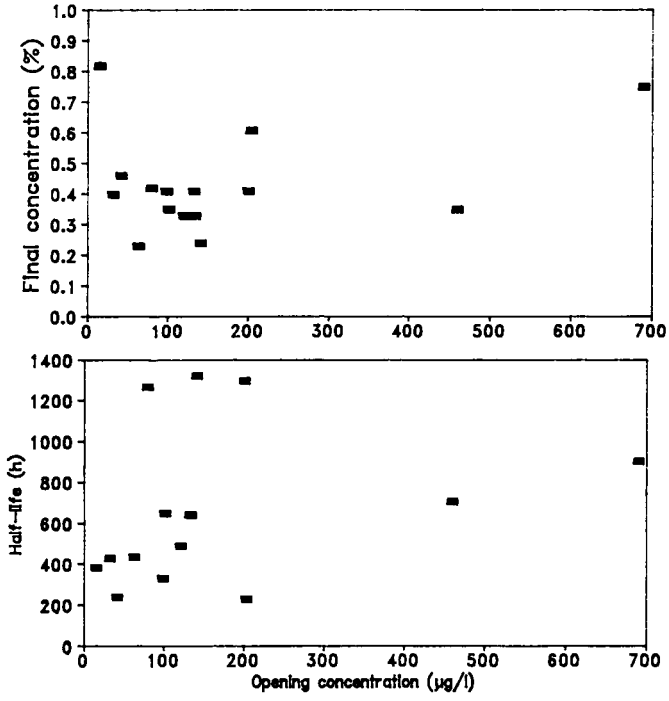

Figure 53. Results from several storage tests with uranine decaying groundwater. Top: Relationship between initial and final concentration (%); bottom: Relationship between initial concentration and half-concentration time.

termined as soon as possible after being taken or a decay-prohibiting addition such as glucose must be added directly after the sample is taken.

2.1.4.2 *Toxicology*

There have been numerous articles published which are concerned with the toxicology of the fluorescent tracers used in hydrology. In general, those planning and carrying out a tracing test are required to prove that the tracers used are not toxic. Since there are no guidelines from the water management agencies, inquiries as to the fluorescent tracers' toxicity have to be made to the producer or the health department. However, one can only expect carefully worded replies from these sources – since neither source wants to assume responsibility. None of the tracers used in water tracing are listed in the cancerous substances list – Appendix II of the Dangerous Substance Act of the Federal Republic of Germany (BGBL 1986b). Nor are there any in the catalogue of substances hazardous to water quality (UBA 1988) or in the handbook of dangerous goods (HOMMEL 1987).

Summary

SMART and LAIDLAW (1977) carried out a thorough literature study reviewing the toxicity of eight fluorescent dyes: uranine, rhodamine B, sulforhodamine B, rhodamine WT, pyranine, amino G acid, lissamine and photine CU. The studies were later expanded to include eosin, amidorhodamine G, direct yellow 96 as well as the optical brighteners tinopal CBS-X and calcophor white ST (SMART, P.L. 1982, 1984). SMART (1976a) published a summary on toxicological investigations of optical brighteners. Special toxicological literature about rhodamine B was put together by MOLINARI & ROCHAT (1978), about pyranine by BENISCHKE & SCHMERLAIB (1988).

Effects upon the human organism

In the Federal Republic of Germany, the following dyes, among others, are certified for use as a colouring in certain foods:

Erythrosine (C.I. 45 430) (for colouring cherries),
Methyl violet (C.I. 42 535),
Brilliant black (C.I. 28 440),
Patent blue V (C.I. 42 041),
Victorian blue R (C.I. 44 040),
Victorian blue B (C.I. 44 645),
Sudan blue II (C.I. 61 554).

Neither uranine, eosin, nor the rhodamines are mentioned in this ordinance (BGBL 1981).

The following dyes are listed, among others, in the 'Cosmetics-Act' (BGBL 1977b), Appendix 3 (Dyes for use in cosmetics), Part A, Section a (red dyes), No.18 for use as a cosmetic in the eye, mouth, and lip area and in personal hygiene:

Eosin (C.I. 45 380) with following purity conditions: Fluorescein under 1%, Monobromfluorescein under 2%,
Erythrosine (C.I. 45 430),
Acid red 98 = Phloxin (C.I. 45 505),
Sudan red = Fettrot G (C.I. 12 150).

Uranine and fluorescein are not listed in the Cosmetics-Act.

In contrast, fluorescein and eosin are listed as cosmetic dyes in the lists from the 'Dye Commission of the German Research Association' (DFG 1971, 1977, 1984). Only the free acid is allowed for use as a lipstick. Since 1912 there have been no damage reports in the production of eosin. Uranine (Fluorescein) is often used to produce striking colours in bathing and cleaning products. Sometimes pyranine is also added to these products (see Section 2.12).

Uranine is used in two medical areas: in ophthalmology and angiography.

In ophthalmology, fluorescein is used to colour the vessels and to investigate disorders of the choroiden, optical nerve and the retina. In doing so, 10 ml of a 5% or 5 ml of a 10% fluorescein solution are quickly injected intravenously. According to STEIN & PARKER (1971), reactions were observed in approx. 0.6% of the cases. Of the 55 screened cases, 37 were cases with allergic symptoms with rashes, in a few cases also facial edema. The remaining 16 cases (= 29%) were not of an allergic nature: cases of shock or similar conditions with breathing or heart problems (dyspnoe, respiratory arrest, cardiac arrest). One patient died several hours after the fluorescein injection of myocardial infarction. The other patients with positive reactions recovered quickly. STEIN and PARKER suspect that most of the patients with a positive reaction had an allergic history. Furthermore, they suspected a hypersensitization due to the overall presence of fluorescein.

Contrary to these findings are the reports in the publication from the International Symposium 'Fluorescein Angiography 1969', which contained only reports about the use of fluorescein by ophthalmologists (AMALRIC 1971). None of the 124 articles reported negative effects of colouring the damages in the cornea, retina, or choroiden.

BRAUNER and NIEBAUER (1955) reported on the clinical treatment of peripheral circulation problems, where to determine the flow velocity 10 ml of a 10% sodium fluorescein solution is injected in either the Vena cubitalis or in the Arteria femoralis inside five seconds. To determine the arrival of the fluorescein cloud, every three seconds drops of blood are taken from the bottom of the big toe and index finger and put on Whatman paper strips. Under the UV-lamp, the fluorescing and non-fluorescing blood drops can be distinguished from one another. The authors reject the method of setting histamine hives to determine the flow times, since deciding whether or not the hives glow in UV-light is too subjective. In healthy young patients the circulation requires ca. 25 seconds, in patients with circulatory problems twice that time has been measured. Of the 88 examined persons, there was only one with a rash that stayed for three hours. All other test persons had no reactions. Fluorescein goes through the body quickly and is passed through with the urine.

PÄSSLER (1952) set novocain-histamine-hives in the thighs near the injuinal region or on the backs of the feet. The circulation time from injecting the 3 ml intravenous shot of 20% fluorescein solution in the arm vein until the hives glow under ultra violet light in a darkened room is stopclocked. If fluorescein is injected in the arm vein, after 12.4-13.5 seconds, the dye can be observed in the retina (GILLANO et al. 1965). If there is a stenosis of the carotid arteries, it takes much longer. Other than a temporary dyeing of the skin and urine, there were also nausea and the need to cough as side effects.

To test renal (kidney) function, a patient can be given 1 g uranine per os (orally).

Elimination starts after 10-20 minutes; after 35-40 hours, the whole dose of this harmless substance has been eliminated (GRÜTZNER 1939).

In ascertaining whether the heart has stopped beating, ICARD (1907) recommended injecting a solution of 2 g uranine in a vein: If alive, the skin and mucous membranes will turn yellow and the eyes green.

According to WILSON (1968), the workers involved with the production of rhodamine B, who over the years often had their hands and arms in contact with the dye showed no symptoms of disorders.

For optical brighteners (stilbene triazine brighteners), a daily dose of 0.1 mg for 60 days is according to SMART (1976a) not harmful.

Indications as to the tolerance of certain substances in humans can be obtained by carrying out repeated insult patch tests or clamp tests according to SHELANSKI & SHELANSKI (1953). SNYDER et al. (1963) investigated five optical brighteners using this method. There were no tissue alteration or injury found in any of the cases. CIBA-GEIGY-Data sheets list negative results for direct yellow 96 and tinopal CBS-X. These data sheets also have details about the test conditions which are cited here: 'In a collective of 50 persons, 5% aqueous solutions were dermally applied using an occlusive bandage and 10 days later an allergy test was carried out.' 1000 mg Na-Naphthionate was taken by an adult per os at one time, and there was no effect!

The Environmental Agency at the Ministry for Environment, Nature Conservation, and Reactor Safety of the Federal Republic of Germany ordered basic toxicological investigations to be carried out for the most common fluorescent dyes. These investigations were conducted using the *salmonella*-microsomas test and with the cytogenetical analysis in the permanent cell line V 79 of the Chinese hamster. The test results indicated that the following substances can be used in groundwater tracing with no qualms as to their toxicity to humans: uranine, eosin, sulforhodamine B, amidorhodamine G, pyranine tinopal CBS-X, tinopal ABP liquid, and sodiumnaphthionate. With this, it is assumed that the injected substance amount is minimized for the investigation program. The dyes not listed here are being tested further (UBA 1997).

Impact upon other warm-blooded animals

To determine the toxicity of a substance to humans, tests are carried out on other warm-blooded animals, usually rats, mice, or rabbits. The data and symptoms obtained through such tests cannot be directly transferred to humans, yet they provide starting points for the magnitude of the tolerance levels (DRUCKREY 1955). It is not possible to list all the data available from laboratory animal tests found in the literature here. However, the most important LD_{50} are listed in Table 6. Other than the LD_{50} tests with one (acute) oral dose or injection, there are also tests on warm-blooded laboratory animals through feed additives for 90 days (chronic effects) or applying to the skin or inhaling. None of these tests provide further information concerning the toxicological properties of the substances listed in Table 6. Therefore, they are not handled here any further.

Nonetheless, it is evident from Table 6, that rhodamine B has the lowest LD_{50} concentration of all the substances listed. This fact has also been verified by other tests. UMEDA (1956) from the Cancer-Institute in Tokyo carried out tests with subcutaneous injections of xanthene dyes on rats and mice. He used the dyes uranine,

Table 6. Warm-blooded toxicity of fluorescent and other dyes used in hydrological tracing tests (LD_{50}-values).

Substance	LD_{50} (mg/kg)	Test animal	Source
Uranine	6721	Rat, oral	MERCK 1990/91
	4740	Mouse, oral	S
	300	Mouse, i.v.	S
	1000	Wm-bl.,i.v.	McDONALD et al. (1974)
Eosin	> 1000	Rat, oral	S
	550	Mouse, i.v.	LUTTY (1978)
Rhodamine B	89.5	Rat, i.v.	WEBB et al. (1961)
	120	Rat, i.p.	ROCHAT et al. (1978)
	95	Mouse, i.p.	ROCHAT et al. (1978)
	890	Mouse, oral	ROCHAT et al. (1978)
	(less than Rh.WT)	Mouse, i.v.	S
Sulforhodamine B	> 10000	Rat, oral	S
	(larger than Rh.B)	Mouse, i.v.	S
Amidorhodamine G	> 10000	Rat, oral	S
	(larger than Rh.B)	Mouse, i.v.	S
Rhodamine WT	> 25000	Rat, oral	S
	430	Mouse, i.v.	LUTTY (1978)
Erythrosine	700	Mouse, i.v.	LUTTY (1978)
Pyranine	ca.16000	Rat, oral	PROCTER & GAMBLE (1970)
	> 5000	Rat, oral	BAYER- safety sheet (1983)
	10000	Mouse, oral	PROCTER & GAMBLE (1965)
	1050	Mouse, i.v.	LUTTY (1978)
Amido flavine FF-PW	8524	Rat, oral	HOECHST- data sheet
Lissamine	8560	Rat, oral	S
	110	Mouse, i.v.	LUTTY (1978)
Direct yellow 96	23100	Rat, oral	QUINLAN (1976)
	> 5000	Mouse, i.v.	S
Tinopal CBS-X	7800	Mouse, oral	CIBA-GEIGY-data sheet
	6000	Rat,oral (CMC)	CIBA-GEIGY-data sheet
	5600	Rat,oral (corn oil)	CIBA-GEIGY-data sheet
Opt.brightener	7000	Mouse, oral	AKAMATSU & MATUSO (1973)
(Triazin-Stilbene)	> 10,000	Rat, oral	GLOXHUBER et al. (1962)
Opt.brightener	14500	Rat, oral	S
(C.I. 28)	> 10000	Mouse, oral	S
Methyl violet	105	Mouse, oral	MERCK (1990/91)

Wm-bl. = warm blooded animals, i.v. = intravenous, i.p. = intraperitoneal injection, S = SMART (1982, 1984), CMC = carboxylmethylcellulose.

eosin yellow, rhodamine B, rhodamine 6G, rhodamine 3G, erythrosine and real acid violet (C.I. 45 190). Until their death, the laboratory animals were injected with an aqueous solution of the dyes in concentrations between 0.02 and 5% and always in the same spot. The injections were given three times a week to twice a month. One laboratory animal that received 104 injections over a period of 661 days with a total of 5350 mg uranine (= 36,700 mg/kg), did not develop a tumour. Four of the eight animals in the test developed tumours, two fibromas and two sarcomas. In the tests using rhodamine B, 12 of the 41 animals developed fibrosarcomas by the end of the test; moreover, most of the animals had atrophic livers and kidneys.

Most of the laboratory animals were albinos, which could have made them more susceptible to the photolytical dye decay (GRÜTZNER 1939). In the tests with rhodamine 3G and erythrosine, none of the animals developed tumours; nor did they in the tests using fluorescein, which was firstdissolved in olive oil and then injected. The tests from UMEDA not only subjected the animals to an unusually high circulatory stress by always injecting the dye in the same spot on the animal, they most likely also reduced their resistance. UMEDA conceded that similar tests with harmless solutions of glucose, glycogen, fructose, galactose and lactose could also produce sarcomas. Furthermore, he cited co-workers who reported neither tumours nor liver damage after having fed rats rice with 0.1-0.2% rhodamine B for over 200 days, which is over 2 g per animal.

In the literature review of cancer studies about fluorescent dyes and optical brighteners, SMART (1984) found only definite indications for rhodamine B. All other substances were not cancerous. WEBB and HANSEN (1961) established that 1% rhodamine B in the rat feed inhibited growth and produced a 2% liver enlargement. In contrast, 2% erythrosine produces no organ damage at all, since it is eliminated completely. In warm-blooded animals, rhodamine B is dealkylated, mainly to 3',6'-Diaminofluoran, which is much less toxic than rhodamine B (WEBB et al. 1961). According to WILLHEIM & IVY (1952), rhodamine B is 'neither cancerous nor poisonous' for rats.

GLOXHUBER et al. (1962) carried out animal tests with 12 different optical brighteners from the dye factory BAYER AG (Blankophores). The test animals were rats, guinea pigs, rabbits, and cats. The LD_{50} values were between 3000 and over 10,000 mg/kg for rats, for guinea pigs between 250 and over 2500 mg/kg and for rabbits and cats around 1000 mg/kg. The authors found out that in living organisms, Blankophores showed no inhibiting effects upon the blood clotting, even in high doses. Photosensitizing did not occur with the mice after subcutaneous injections of two Blankophore preparations with a dosis of 250 mg/kg in sunlight.

Five optical brighteners, two triazine stilbenes among them, were investigated by SNYDER et al. (1963) as to their damage potential. The test animals were mice, rats, guinea pigs, and albino rabbits and an oral toxicity (LD_{50}) between 2.8 and 21.5 g/kg was found. Even with longer skin contact, the animals did not develop any tumours.

Four tinopal products, including CBS-X, which is widely used in water tracing tests, were tested by KEPLINGER et al. (1974) as to their toxicity. As in the tests results from SNYDER et al., these dyes were toxic only at exceptionally high doses. The authors concluded from their results that the use of optical brighteners, even over the course of years, is not dangerous.

Impact upon fish

For water organisms, the damage potential of a substance is determined by the 'Lethal Concentration' (LC_{50}), i.e. the statistically determined concentration of the substance, which would produce a fifty percent chance of survival. The length of the test must also be given in the test results. However, it is not uniformly reported in all publications; it ranges between 12 and 96 hours.

Table 7 lists the literature LC_{50} values for most of the dyes used in hydrological tracing tests. It is noticeable that the trout, which is usually the most sensitive of all fish to pollution, does not always have the lowest LC_{50} value.

Table 7. Fish toxicities from hydrological fluorescent dyes (LC_{50}-values).

Dye	LC_{50} (mg/l)	Test fish	Source
Uranine	1372 (96 hrs.)	Rainbow trout	MARKING (1969)
	2269 (96 hrs.)	Catfish	MARKING (1969)
	> 752 (24 hrs.)	Killi fish (Guppy)	BENOÎT-GUYOD (1979)
Eosin	> 138 (24 hrs.)	Killi fish	BENOÎT-GUYOD (1979)
Rhodamine B	217 (96 hrs.)	Rainbow trout	MARKING (1969)
	526 (96 hrs.)	Catfish	MARKING (1969)
	86 (24 hrs.)	Killi fish	BENOÎT-GUYOD (1979)
Sulforhodamine B	100-500 (48 hrs.)	Trout	HOECHST-data sheet
	60-120 (24 hrs.)	Killi fish	BENOÎT-GUYOD (1979)
Amidorhodamine G	> 88 (24 hrs.)	Killi fish	BENOÎT-GUYOD (1979)
Rhodamine WT	> 1360 (24 hrs.)	Killi fish	BENOÎT-GUYOD (1979)
Rhodamine 6G	0.5 (24 hrs.)	Killi fish	BENOÎT-GUYOD (1979)
Pyranine	> 500 (96 hrs.)	Fish test	BAYER- data sheet
Amido flavine FF-PW	> 500 (96 hrs.)	Guppy	HOECHST- data sheet
Direct yellow 96	> 1000 (96 hrs.)	Fish test	CIBA-GEIGY- data sheet
Optical brighteners			
(3-Triazin-Stilbene)	108-1780 (96 hrs.)	Trout	KEPLINGER et al. (1974)
	86-1060 (96 hrs.)	Catfish	KEPLINGER et al. (1974)
(Tinopal CBS-X)	130 (96 hrs.)	Trout	KEPLINGER et al. (1974)
	126 (96 hrs.)	Catfish	KEPLINGER et al. (1974)
(Triazin-Stilbene)	2000 (96 hrs.)	Goldfish	AKAMATSU & MATUSO (1973)

Tests with fish investigating uranine's tolerance have been conducted since shortly after uranine was first used in a tracing test. In the Chemical Laboratory of the Technical University of Karlsruhe, tenches were kept over eight days in water containing uranine. The concentration was raised in stages from 0.05 to 4 mg/l (RUPP 1885). The fish showed no signs of being influenced by the strongly coloured green water; their movements were lively and they ate their food of ant eggs.

Similar tests were carried out by QUEDNAU (1930) with crucian carp, dwarf stickleback, tench, and eels up to a uranine concentration of 1.2 mg/l. After the dye was injected, he observed accelerated breathing, which went back to normal after some time. Other than that, there were no other reactions or tissue alterations recognizable.

BANDT (1957) conducted tests with roach and trout using very high concentrations. He came to the conclusion that 100 mg/l uranine or eosin was not poisonous to fish. A good tolerance of 50 mg/l uranine, in spite of a partial dye secretion on the backs of the fish was reported by EGGER (1929). Small killi-fish tolerate 30-150 mg/l eosin over three weeks and could still reproduce. Rainbow trout also showed no peculiarities after two days in a solution of 100 mg/l eosin (GEISLER 1953).

On the occasion of a dye tracing test in the Odenwald, this author was able to observe the behaviour of trout in a stream containing uranine (KÄSS 1976a). The Eierbrunnen, Höllbach Valley, Waldbrunn-Waldkatzenbach, was investigated to discover if it carried surface water. To do this, an uranine tracing test was conducted by dyeing the stream Höllbach near the Mill Oberhöllgrund with uranine. At the level of the Eierbrunnen, the Höllbach, which flowed nearby, was coloured green for almost ten hours. The uranine concentration in the Höllbach was measured every half hour. The highest value measured was 4.5 mg/l, but the actual maximal concentration most

definitely exceeded 5 mg/l for a short time. A group of brook trout showed no reaction when the dye cloud arrived. This is even more astonishing since trouts react very sensitively to foreign substances. Obviously, trout tolerate such a concentration without any problems.

An unknown, but glaringly green uranine solution did not damage six longnose daces; they still felt fine after five days in a 12-l-test-tank, which also contained 0.63 µg of Pronoxfish (SOWARDS 1958).

Demonstrating on the killi-fish, BENOÎT-GUYOD et al. (1979) were able to show, that the length of time the fish spend in the water containing the dye is the deciding factor for the tolerance level. At a rhodamine B concentration of 240 mg/l, the fish lived for less than one day, at 50 mg/l twelve days and at 24 mg/l sixteen days. However, these results are in gross contradiction to those from RODIER & MARICHAL (1961), where fish survived two months in a rhodamine B solution of 100 mg/l.

PARKER (1973) investigated smolt from silver salmon and Donaldson trouts as to their behaviour towards rhodamine WT. He kept the fish in a dye concentration of 10 mg/l at 22°C for over 17.5 hours; compared to the control fish, there was no discernible change. The dye concentration was raised to 375 mg/l over a further 3.2 hours. Then the fish were put in fresh water and observed for one month; there were no negative effects observed.

MARKING (1969) investigated the synergistic effects between uranine and rhodamine B on the one hand and Antimycin A on the other. With rainbow trout, the LC_{50} value stayed at approx. 0.05 µg/l Antimycin A for uranine additions between 0 and 100 mg/l practically the same. With rhodamine B additions of 100 mg/l, the LC_{50} value was lowered however to 0.026 µg/l!

A remarkable observation was made by ABIDI (1982) concerning the decay process of the rhodamines with diethylamino groups in surface waters. In laboratory tests, he added between 1 and 20 µg/l of rhodamine B and rhodamine WT as well as between 10 and 100 µg/l nitrite to river water samples. After a reaction time of 24 hours at 20°C, between 0.13 and 7 µg/l of the suspected cancerous substance diethylnitrosamine was found in the solutions. At dye concentrations of 1 µg/l, diethylnitrosamine was only detected in concentrations under 0.4 µg/l, if over 100 µg/l nitrite was present. On the other hand, the author showed that light causes photolysis of diethylnitrosamines.

Impact upon other water organisms

PANCIERA (1967) observed the development of oysters in solutions containing rhodamine B. At concentrations up to 1 mg/l, the egg development of *Crassostrea virginica* is normal; at concentrations of 10 mg/l, 27% of the eggs develop abnormally, whereas the remaining 73% develop into healthy oysters. In solutions with 100 mg/l rhodamine B, the eggs do not develop within two days; larva also die within this time span. PARKER (1973) tested the eggs and larva of the Pacific oyster (*Crassostrea gigas*) with rhodamine WT solutions with concentrations of 1 and 10 mg/l over 48 hours at 24°C. The result was that the eggs and the larva developed as if they had been in dye-free water.

Fish food organisms, such as water-louse, daphnia (water flea), mud snail, and dragon-fly larva, were exposed by QUEDNAU (1930) to uranine concentrations up to 1.2 mg/l. The daphnia were in a state of alarm for the first 2-3 minutes, but not later.

All of the tests came to the end conclusion that the specified maximal concentrations are well tolerated by all of the tested organisms.

In France, the standardized daphnia test using the water flea *Daphnia magna* (STRAUSS) is described by ROCHAT et al. (1978) with rhodamine B. This test determines the concentration, at which after 24 hours of contact, 50% of the daphnia no longer move. For rhodamine B, 22 mg/l was found, as compared to 1 mg/l for potassium bichromate. Further daphnia tests were set up by a group, where ROCHAT was a member (BENOÎT-GUYOD et al. 1979). These researchers determined the following concentrations: rhodamine G: 72 mg/l, rhodamine 6G: 1 mg/l. For the other rhodamines, sulforhodamine B, amidorhodamine G and rhodamine WT, there are only approximate values listed; they are between those for uranine and eosin or lower than eosin.

Impact upon plants

Eosin treated sprouts show an abnormal geotropical behaviour. Fluorescein and eosin accelerate the diastase activity to starch decay. Eosin solutions of 1:400,000 = 2500 µg/l still show an influence (GRÜTZNER 1939).

SMART (1984) reported on two studies, where algae growth was investigated: the fluorescent brightener 28 did not influence the growth of the algae, whereas rhodamine B in a concentration of 10 mg/l did. A surprising result from another study was that in contrast to the previous observations, rhodamine B has less impact upon algae than eosin or uranine.

Beans and corn which are grown on nutrient solutions containing tinopal CBS-X, concentrate the optical brightener in the root surface without invading the rest of the plant (CIBA-GEIGY data sheet).

Unfortunately, in the literature, concentration data about the endowments used in the plant experiments are rare. Therefore, a quantitative comparison is only possible in some cases.

Impact upon microorganisms

Amoebae of the genus *Balantidium coli* do not suffer any damages when exposed to very high uranine concentrations of 1000 mg/l in the dark (GRÜTZNER 1939). If light enters, they lose their flagellates and can make only rolling movements and die. With eosin, the photodynamic effect upon the amoebae is approx. five times as strong. GRÜTZNER supposes the formation of phthalic acid, oxalic acid and hydrobromic acid because of the photolytic deacy of the eosin.

NESTMANN et al. (1980) carried out mutagenity tests according to AMES (AMES et al. 1975). Using five stocks of *Salmonella typhimurium*, the authors did not find a positive reaction, even with concentrations of uranine up to 100 mg/l. Rhodamine B however, was definitely positive, which leads to the conclusion that it is cancerous.

JENSEN and KRISTENSEN (1989) investigated the impact that rhodamine WT has upon the colony number of *Escherichia coli*. There was no impact upon the *E.coli* with a colony number between 13 and 135 · 10^6/ml discernible with a contact time between 2 minutes and 16 hours. The tested rhodamine WT concentrations were between 0.1 and 100 mg/l.

SMART (1984) published a summary of the interactions of bacteria in aerobic activated sludge with dye concentrations of 100 mg/l. Only rhodamine B acted bacteri-

cidal upon the microflora of the activated sludge, whereas nine other dyes had no impact. The optical brightener 28 was microbiologically decayed in the activated sludge. The other dyes remained untouched. The colony growth of *Salmonella typhimurium* on plates was inhibited by the addition of 10 mg uranine per plate, with rhodamine WT not until 21 mg per plate.

Very high concentrations of pyranine were investigated as to their bacterial toxic impact. Even a concentration of 10,000 mg/l had no damaging impact upon *E.coli* nor upon *Pseudomonas fluorescens* (Data sheet BAYER). In the fermentation test, the impact of amido flavine upon sewage bacteria was tested. According to the BAYER-data sheet, the concentration for an expected impact is over 5000 mg/l.

Appraisal of the toxicological investigations

There are no indications of toxicity connected with uranine, the dye most widely used in hydrological tracing tests, nor of mutations nor teratomas. When swallowed by warm-blooded organisms, uranine is introduced into the system, it is however soon eliminated through the kidneys. In the warm-blooded organism, sometimes harmless metabolites, among them monoglucosides are formed. Under strong exposure with a high fluorescein concentration of 1/500 molar, photodynamic hemolysis can occur after 35 minutes, at 1/2000 molar, after 120 minutes (GRÜTZNER 1939). These are however such high concentrations, which are not even used in angiofluorescopy. Without exposure to light, GRÜTZNER could discern no hemolysis. Uranine's photolytical decay products are not toxic (BENOÎT-GUYOD 1978). Uranine is not only used in the field of medicine, it is also certified for use as a dye in many cosmetics and cleaning agents. The complete harmlessness of hydrological tracing tests with uranine has been verified by notable institutions (Dye commission of the German Research Assoc.: SCHMÄHL 1981, German Federal Health Dept. Berlin: AURAND 1979, Hygiene-Institute of the Ruhr Region, Gelsenkirchen: JUNG 1977).

Eosin is also certified as a cosmetic dye by the German Federal law. The photodynamic impact is somewhat stronger than with uranine, but it is even stronger with erythrosine (GRÜTZNER 1939). According to LUTTY (1978), besides uranine, eosin can also be used in optical angiography. Pyranine, lissamine and rhodamine WT could also be used for this according to LUTTY. Eosin is partially eliminated by the kidneys and partially resorbed by the liver (WEBB & HANSEN 1961).

Rhodamine B appears to be the most toxic of all fluorescing tracers. This is evident according to the LD_{50}- and LC_{50}- data listed in Tables 6 and 7. Rhodamine B is mainly resorbed in the intensines by warm-blooded animals. In laboratory animal tests with extremely high amounts, liver and kidney damage have been determined (WEBB et al. 1961). The rhodamine B metabolites, diaminofluorane and monoethylated Rh.B, are quite non-toxic however (WEBB & HANSEN 1961, WEBB et al. 1961). Sometimes the accompanying impurities are more toxic than the dye.

The optical brighteners do not interact with warm-blooded organisms. SMART and LAIDLAW (1977) calculated that an adult could daily ingest several grams of the substance for a long period of time without any ill-effects.

Summarizing, fluorescent substances can be used in tracing tests in surface and groundwaters without restrictions. At most, the temporary high dye concentrations at the time of the injection could possibly harm the microflora and -fauna. Meanwhile,

the SANDOZ accident on the Upper Rhine from 1986 showed that the microorganisms can quickly repopulate.

Nonetheless, the psychological adversities, that can occur due to a visible reemergence of dyes from springs and tappings should be avoided. The United States Geological Survey therefore recommends that during tracing tests, the highest concentration at the observation sites be under 10 µg/l (WILSON 1968).

2.2 SALTS

W. Käss

Hydrological tracing tests with salts can deliver good results. Here, the term, salts, describes mainly the inorganic compounds, which dissociate in aqueous solutions into cations and anions. When using salts in a tracing test, it is important to remember that surface and groundwaters naturally have a more or less high background of salts. Especially sewage water, landfill drainage water, and polluted rivers have high backgrounds of salts and can cause problems in using salts as a tracer.

During the underground passage, the cations are subjected to a loss due to adsorption or ion exchange, with the loss being naturally larger in pore-groundwater than in karst water. A groundwater aquifer, which is rich in organic material, such as turf or humic layers, has an especially high adsorption capacity. The ion exchange capacity for cations is primarily dependent upon the ionic potential (charge/ionic radius): the smaller the ionic potential, the larger the exchange (KÄSS 1990a). Lithium, with an ionic potential of 1.28, has a relatively low, cesium however with an ionic potential of 0.61, has a high exchange. Cations can also suffer further losses due to complexation, such as with humic acid. On the other hand, cations can also be protected against ion exchange by forming complexes. However, this is only applicable in activation analytical tracing methods. In Section 2.4, the metal-anion-complexes are described more closely. Ion complexation would be too expensive for straight salt tracing tests. When ion exchange with cations occurs, other cations must be set free to balance the charges. As will be shown later, these are normally the hardeners $Ca^{2+} + Mg^{2+}$.

Anions undergo ion exchange to a lesser extent or in unrecognizable amounts. Under close examination, anions, due to their negative charges, are faster than the water molecule during transport in the aquifer exclusive chromatography (Fig. 54). Also, anions are subject to a marked sorption in aquifers with organic layers. During the underground passage, some anions are subject to change caused by redox- or biological reactions. An example of the first case is nitrate, for the second iodide. An increase in pH-value causes an increase in the sorption capacity of the groundwater aquifer for anions (MATTSON 1929).

In spite of the sorption properties of the cations, they are mainly used in salt tracing tests. This is definitely due to the problems encountered in analysing for anions as well as due to the greater choice in cations.

Salts, which are undissociated or only weakly dissociated, do not readily adsorb or experience ion exchange. One example is borax, which hydrolyses to the weakly dissociated boric acid (see Section 2.2.4).

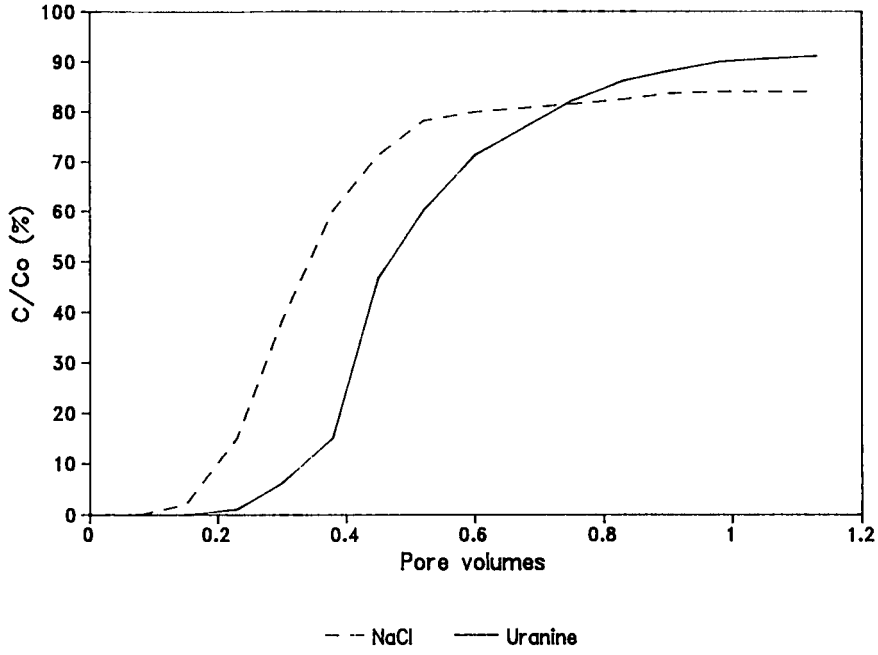

Figure 54. Breakthrough curves for a simultaneous injection of a mixture of uranine (——) and sodium chloride (---) in a column test. Evidently the salt is quicker than the uranine. The salt concentration was determined by measuring the electr. conductance (private communication MÜHLHAUSEN 1990).

In any case, when carrying out salt tracing tests, it is necessary to judge which interactions with the aquifer or with organic material are to be expected. The backgrounds and ranges must be determined before each test to correctly choose the amount of salt needed for a successful trace. LUKAS (1959b) wrote that too large an amount of salt would not hurt, the breakthrough curves would only get clearer. However, an excess amount of salt is damaging for two reasons: First, high salt concentrations can be harmful for the biology and microbiology of the water system (see also Section 2.2.1), second, with a high electrolyte concentration, there is the danger that the clay minerals will coagulate and therefore lower the permeability of the aquifer (SCHIECK 1958).

The increase in the electrical conductivity caused by the electrolyte can be used to determine the salt concentration. However, this method can only be used with large amounts of salt, generally only in tracing tests with rock salt.

2.2.1 *Sodium chloride (NaCl)*

Synonyms: Rock salt, cooking salt, livestock salt, table salt, 'salt', boiling salt, road salt, mine salt, industry salt, raw salt, waste salt.
Molecular weight: 58.44 g/mol
Water solubility L (D'ANS & LAX 1970):

Temperature(C)	L (g/l)
0	356
5	356.5
10	357
15	357.5
20	358.5
25	360
30	361.5

The first and most widely used salt tracing tests were and are still carried out with sodium chloride. In water, sodium chloride splits into the positively charged sodium ion (Na^+) and into the negatively charged chloride ion (Cl^-). Both ions occur naturally in water and in well detectable concentrations (concentration ranges in Southwest Germany):

	Na^+ (mg/l)	Cl^-(mg/l)
Quaternary (crystalline)	5-15	6-30
Quaternary (calcareous)	5-20	6-30
Tertiary	5-40	1-6
Upper Jurassic	2-10	6-15
Lower Triassic (Bunter)	2-15	5-12
Crystalline basement	1-10	5-12
Glacial water (Aletsch 25 July 1991)	1.3	

The concentrations in deep water and sewage water can range much higher. Wherever rock salt is used in the winter to keep the roads clear, the chloride content can also be much higher (SCHLOZ 1980).

In German, tracing tests using sodium chloride have been called 'Chlorung' (MAURIN & ZÖTL 1959), which is as unfitting as 'Chlorierung' which has also been used (KYRLE 1928). In English, both translate to chlorination and relate to the treatment of water through the addition of chlorine to purify drinking water. Tracing tests with other dissociating inorganic compounds could also be called 'salting.' However, it is generally used to designate a water tracing test with NaCl (LUKAS 1959b).

So far known, the first salt tracing test was carried out in 1872 near Lausen (southeastern Liestal/Canton Baselland, Switzerland) in the folded Jura Mountains (Fig. 2). The test was conducted to clarify whether a typhoid epidemic had been caused by a sewage carrying stream in a neighbouring valley which influenced the central water supply for the village. They poured 18 Zentner (= 900 kg) of table salt in a reopened doline from 1862 near the Furlerbad. The ca. 2 m deep hole was filled with water which immediately flushed away the salt. The source of Lausen's water supply came from behind a low ridge of Middle Jurassic (Bajocian 3 = Hauptrogenstein/Dogger). Only one day after the salt injection, the water supply well had a 'definite' and in the end a 'very strong chlorine reaction' (HÄGLER 1873). A quantitative determination was not carried out.

In 1877, a few years after HÄGLER carried out his tracing test, KNOP carried out his fundamental tracing test at the Upper Danube percolation sites between Immendingen and Möhringen (Baden-Württemberg), using shale oil, uranine, and rock salt.

After an unsuccessful tracing test with 14 kg of aniline red in 1869, KNOP injected the three named tracers to obtain legally binding proof of a hydrological connection between the percolating Danube and the Aach spring (KNOP 1875, 1878). After injecting 10,000 kg waste salt from the Saltworks Dürrheim into the Danube sinkholes at Hattinger Weg on 24 September 1877 between 11:45 and 12:45 hours (1 in Fig. 75), KNOP had hourly samples taken from the Aach spring and quantitatively measured for chloride by precipitating as AgCl out of an 0.5-l-sample in the Mineralogical Laboratory of the Technical University of Karlsruhe. Figure 55 shows the resulting

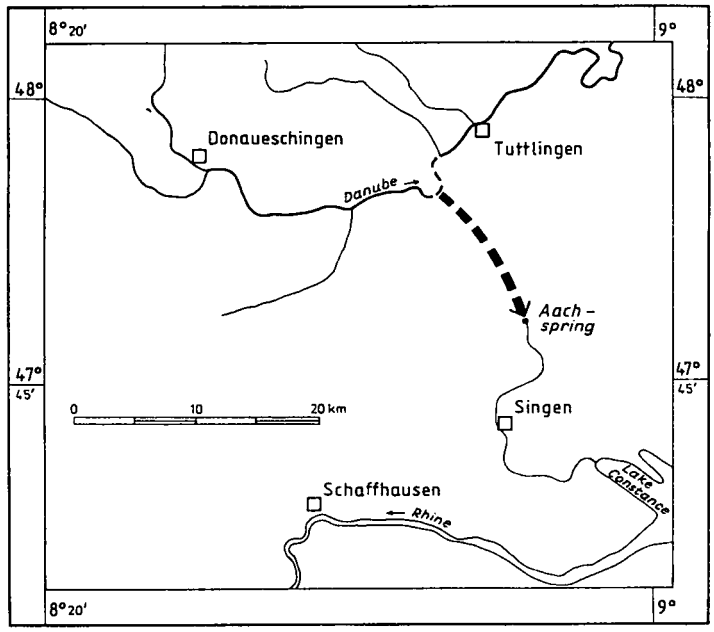

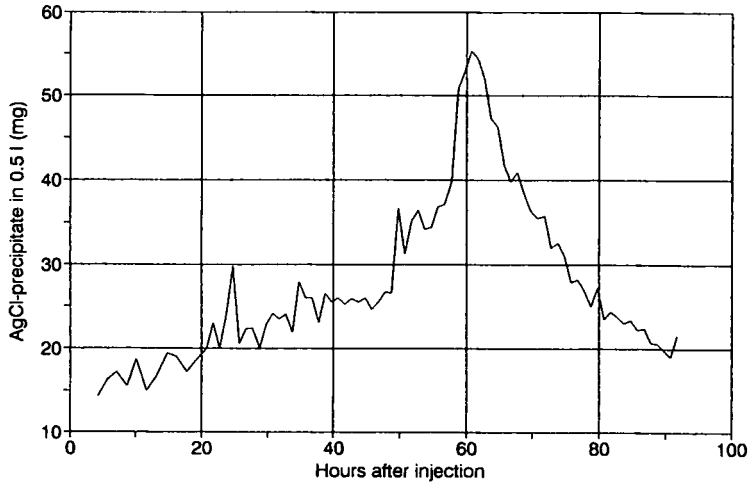

Figure 55. Top: Map of KNOP's tracing test from 1877 on the Upper Danube (Southwest Germany). Bottom: First quantitatively evaluated salt tracing test from 24 September 1877 by A.KNOP. Breakthrough curve from the Aach spring.

breakthrough curve. Calculations made to verify the results using an Aach spring discharge of 3500 l/s resulted in an almost 100% recovery of the injected salt in the Aach spring.

Before it was technically possible to determine the uranine concentrations with sufficient accuracy in a large enough set of samples in dye tracing tests, sodium chloride was used to quantitatively determine the tracing tests. Salt traces were carried out in considerable extent until the middle of the sixties. SCHULZ (1957) published a review of numerous salt traces in Southwest Germany with chloride breakthrough curves. SCHULZ noted in his review that 'salt traces are better than dye traces for quantitative measurements, and that dye traces understandably should not be carried out in springs that are used.'

The quantitative determination of the chloride ion was completed by serial titrating, often on the spot with silver nitrate and potassium bichromate as indicators.

Above all, it was the hygienists, who conducted the salt traces in catchment areas of endangered water tappings. KISSKALT and KNORR (1930) carried out numerous salt traces to determine the borders of such water catchment areas. They carried out basic investigations concerning the Gollinger springs in the Alpine Foreland that had been tapped by the city of Munich, Germany. Further important salt traces were carried out after the Pforzheim typhoid epidemic in 1919 in the region of the contaminated springs (DAUR & RÖHRER 1921). In 1935, HORNUNG reported thoroughly about the course of a typhoid epidemic at a scenic tourist attraction in the Middle Black Forest and about the definite proof of the spring water contamination due to sewage water percolation by carrying out a salt tracing test.

If large amounts of salt are needed for a trace, the cost factor plays a large role in choosing the tracer and how it will be bought, delivered, dissolved, and injected. In a combined tracing test in preparation of the 'Second Symposium for Tracing Underground Water' on 26 August 1969, 50 tons of road salt from the potassium saltworks in Buggingen/Cty.Freiburg were used. It was dissolved in a large, specially made wooden tub, in which a fire engine C-tube syringe was hung. The tub was filled using shovel loaders with a constant water flow. The salt solution spilled over a wooden gutter into an old sinkhole that was used as a storm-overflow in the southern part of Tuttlingen (29 in Fig. 75). Dissolving and injecting the salt took eight hours (KÄSS 1970b). The road salt used in the Tuttlingen salt trace had the following composition:

	(Wt.-%)
Sodium chloride	89.00
Potassium chloride	1.46
Moisture (105°C)	4.08
Impurities (anhydrite, clay)	5.46
Total	100.00

The potassium contents in the road salt trace needed to be considered during the evaluation of the simultaneous potassium chloride salt trace near Immendingen (see Section 2.2.2).

The large amount of sodium chloride needed to raise the background levels of chloride and sodium high enough for a positive trace, results in a large amount of

injection solution, which has a higher density than the water being investigated. The densities, D, of aqueous sodium chloride solutions, L, at 15°C are, according to D'ANS & LAX (1970):

L(g/l)	D(kg/l)
10	1.0071
100	1.0744
200	1.1525
357.5 (saturated)	1.2024

Due to the difference in density, it is possible for the injected tracer solution to sink to a much lower depth and need a long time to mix with the rest of the water. This is especially true in karsts. EISSELE (1963) reported on such a case in the fissure aquifer of the Bunter (Lower Triassic) of the Middle Black Forest, where the salt tracer had a long delay before reappearing.

Samples taken during a sodium chloride tracing test should be analysed for both sodium and chloride, not just chloride. Since sodium as a cation is subjected to ion exchange, the ratio of the Na^+ Cl^- equivalents in the breakthrough curve provides an indication of the ionic exchange capacity of the flow path. In karst regions, even with long flow paths, there is little danger of sodium undergoing ion exchange (Fig. 56). On the other hand, during salt traces in pore-groundwater, there can be considerable sodium losses. During a salt tracing test in the Neckar valley plain between Rottenburg and Tübingen, on 20 October 1965, 6000 kg of mine salt was injected in the pore-groundwater aquifer. In an observation well 180 m away from the injection site, more than 50% of the sodium was retained as compared to the chloride (Fig. 57). After a flow path of 320 m, the sodium loss was approx. 65%; at 500 m, the sodium ion exchange had occurred to such a large extent that the sodium ion could no longer

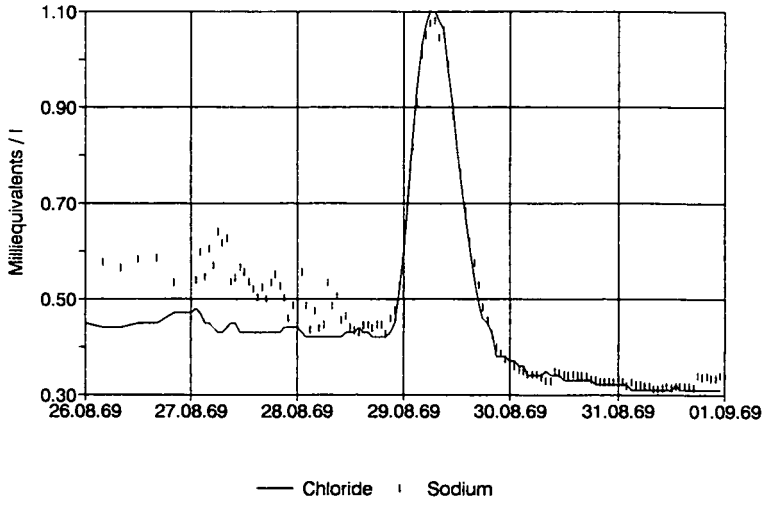

Figure 56. Salt breakthrough curve from the salt tracing test in the southern part of Tuttlingen on 26 August 1969 in the Aach spring. Sodium- and chloride equivalents coincide.

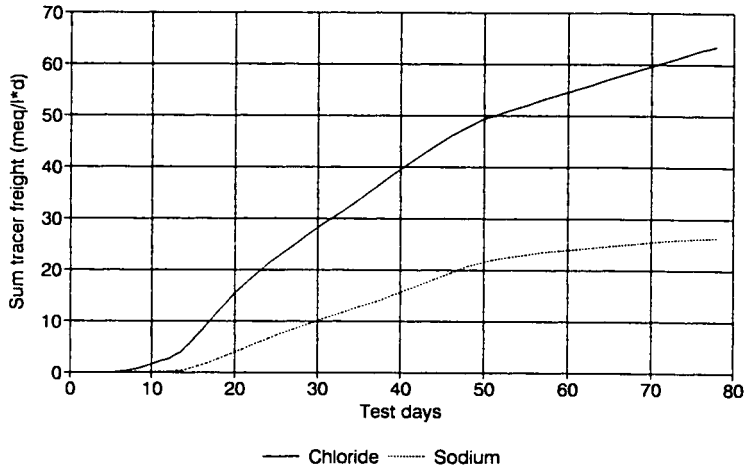

Figure 57. Chloride- and sodium flow rates from the salt tracing test on 20 October 1965 in the Neckar valley plain between Rottenburg and Tübingen in an observation well 180 m downstream from the salt injection site. The decrease in sodium, as compared to chloride, is due to ion exchange.

be significantly detected over the background level. The simultaneously injected potassium salt was not detected anywhere (KÄSS 1967b).

When sodium and other alkali ions are exchanged, the hardeners calcium and magnesium are set free, causing a hardening of the water. Quantitative investigations concerning ion exchange during tracing tests with sodium and potassium salts are described in BUCHTELA & JOB (1970), in JOB (1972), and in KÄSS (1972 and 1976b). An example of a well documented ion exchange occurrence is presented in Section 2.2.3 (Fig. 66).

The oldest and most proven analysis conducted during salt traces with sodium chloride is the analysis of the chloride ion. To obtain a significant level of chloride over the background level, a comparably large amount of salt must be injected. This results in a marked rise in the ion content, which corresponds to an increase in the electrolytic conductivity. During a salt trace in the Lur cave system near Graz/Austria in 1952, 800 kg of salt, denaturated with crystal violet, was injected in the Lurbach percolation. The injection was on May 10, 1952 at 16:20 hours at the entrance to the Lur cave (MAURIN & ZÖTL 1959). The only positive reemergence site was at the Hammerbach spring (Fig. 58 top). Besides the chloride determination, the conductivity was not measured, but rather the el.resistance of the spring water with an ohmmeter. The reciprocal behaviour of both values, chloride content and el.resistance can be clearly seen in the curves. Furthermore, it is also obvious that the chloride determination is a more effective value than the resistance measurement (Fig. 58 bottom).

Nevertheless, the determination of the el.conductivity is comparatively easy and exact. There is no alternative for the use of salts in flow volume determination in small and middle channels with the aid of computer controlled instruments.

A further application with salts is in geoelectric investigations. If salt is injected in a groundwater borehole, the voltage decrease can be measured spatially using probes

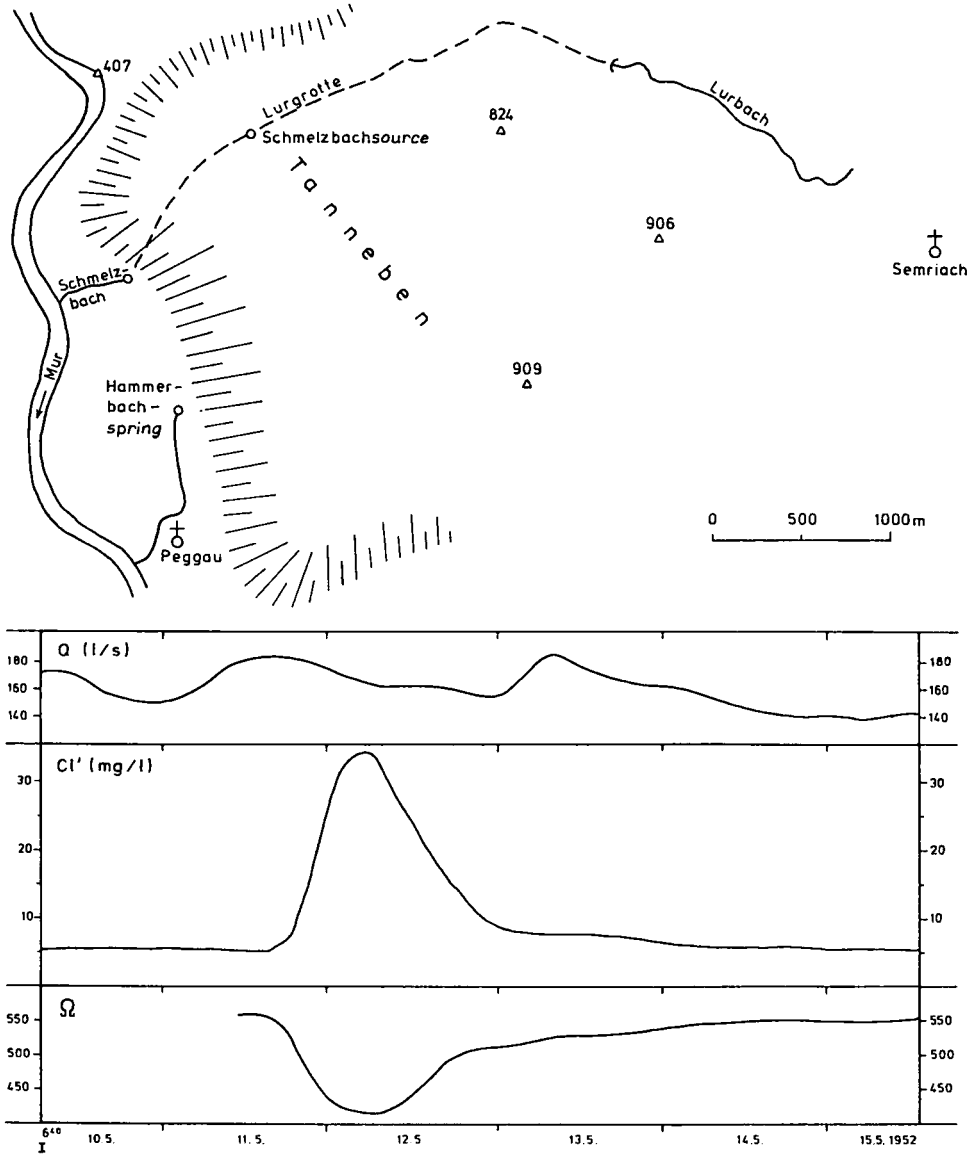

Figure 58. Top: Map of the salt tracing test from 1952 in the Lur cave system. Salt injection site at the entrance of the Lurbach into the Lurgrotte. Heights Δ in metres over the Adria, o = springs; bottom: discharge, chloride content and el. resistance in the Hammerbach spring during the salt tracing test in 1952, I = injection time (after MAURIN & ZÖTL 1959).

with the help of an auxiliary voltage between the borehole and an earthing set far away.

Where salt is present in the groundwater, the el.conductivity is higher, in relation to the salt concentration compared to the period before the salt injection. With repeated measurements, the spatial and temporal distribution of the salt with the

groundwater flow can be followed. The prerequisites for applying this method are: shallow groundwater table, an appropriate amount of salt relative to the background level, no disturbances due to train tracks, fences, etc. An advantage of this method is that no other groundwater observation well is needed for measurements. KRULC published several examples of geoelectrical groundwater traces in 1967.

Remarks on conducting salt tracing tests

When using sodium chloride in a salt tracing test, the purity of the salt is not important. In evaluating the test however, the degree of the purity, i.e. the actual amount of sodium chloride must be known. The background level of the chloride and how it varies in the sampling sites must also be known, to correctly judge the amount of salt to be injected. When organizing the salt tracing test, the availability of large enough containers for dissolving the salt, stirring utensils, and sufficient water to dissolve the salt tracer and for flushing the salt must be assured. If it is plausible that the salt tracer solution will sink instead of mixing with the groundwater, it must be sufficiently diluted so that it flows with the groundwater instead. To avoid such a case, the chloride concentration of the injection solution should not be greater than 3 g/l = 0.5% NaCl (DAVIS et al. 1980). Using warm water to dissolve the salt can also help against the sinking.

In Austria, road salt is denatured with eosin and this must be considered in combined tracing tests using road salt and eosin. However, disturbances must also be expected in tracing tests with eosin in catchments where road salt is heavily used in the winter.

Salt tracing tests in surface waters are not advisable, since especially trouts are very sensitive to electrolytes.

The type of sample containers is uncritical. Plastic or glass bottles are both suitable even for long waiting periods. If the chloride ion is to be titrated, the sample bottles should have a minimum volume of 250 ml.

NaCl analysis

The gravimetrical chloride determination method used by A.KNOP in 1877 is very exact, but also painstaking and time-consuming. Only at very high chloride contents, over ca. 150 mg/l Cl^-, is the gravimetrical determination method better than the titrimetrical.

The titrimetrical chloride determination according to MOHR has been used for a long time (1855). For the titration, a few drops of a potassium bichromate solution as an indicator are added to 100 ml of the sample and tritrated with a reference silver nitrate solution until the colour changes from yellow to brown (DEV, D1,2 and DIN 38 405, Part 1). Since it is easy to over-tritrate with this method, another chloride determination method is also often used: the titration with mercury-II-nitrate in nitric acid solution with diphenylcarbazone as an indicator. Although this method is more accurate than that from MOHR, it should be avoided out of environmental considerations due to the mercury.

The sodium determination is completed best with flame emission at 589.3 nm. Atomic absorption is not as exact, as with all alkali metals.

Ion sensitive electrodes are available for Na^+ as well as for Cl^- determination. An example of registering the sodium ion using a sodium sensitive electrode in a salt

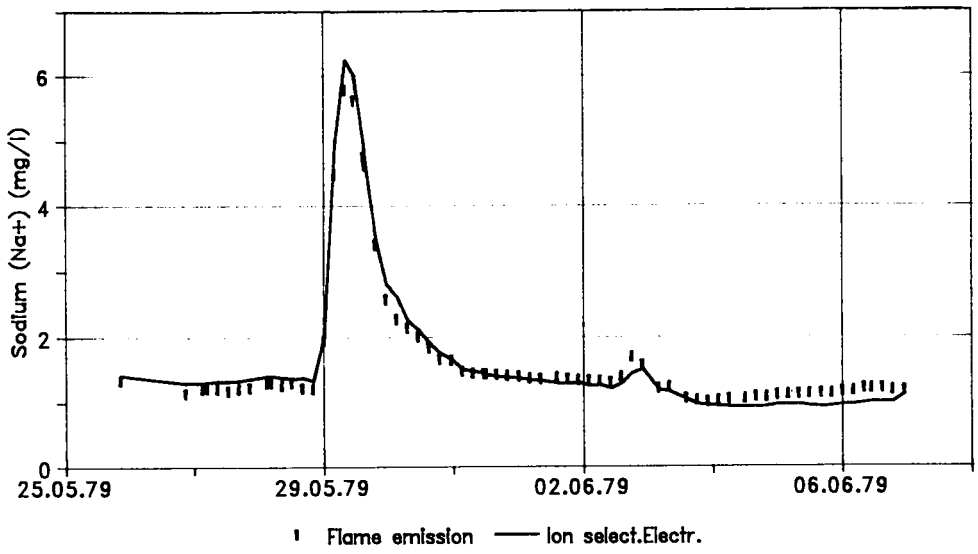

Figure 59. Breakthrough curves in the Areuse spring-East (Val de Travers/Swiss Jura) for Na^+ in a salt tracing test at the exit of the Lac des Tailleurs on 26 May 1979 using 9000 litres of brine = 2750 kg NaCl = 1082 kg Na^+. Solid line: Na^+-passage recorded with the ion sensitive Na-electrode. Row of vertical slashes: passage ascertained with single samples determined with flame emission. The curves show the good agreement of both determination methods; until 1 June 1979, the ion sensitive Na-values were slightly over the flame-photometric values, afterwards slightly under.

tracing test in Val de Travers was described by MÜLLER and KÄSS in 1980. The results were in good accordance with those from the flame photometrical sodium determination (Fig. 59).

A corresponding ion sensitive chloride determination is not known. When using the ion sensitive electrodes, it must be taken into consideration that only the ionic activities are measured, not the total content of sodium or chloride. In case of a continuous registration, from time to time a repeat calibration is necessary.

Simpler, but with a much greater background level, is the measurement and registration of the el.conductivity. There are numerous measuring and registering instruments available nowadays, which are suitable for continuous use. The measurement values can be recorded in either conductivity units (µS/cm) or directly in NaCl-content values and recorded either on paper or digitally.

Toxicology of sodium chloride

For warm-blooded animals (rats), a 50% lethal dosis (oral) of 3000 mg per kg body weight is given. Fish and fish fry tolerate 10,000 mg/l NaCl (SCHÄPERCLAUS 1954).

2.2.2 *Lithium*

The lithium ion is the cation that is the least subjected to ion exchange due to its small ionic radius. Lithium salt traces can therefore be conducted in pore-groundwater aquifers as long as the flow path is under approx. 200 m.

The first indication that a trace using lithium would be possible was reported by FRANKLAND and KAILBACH (TIMEUS 1926). The first successful trace was carried out by VORTMANN and TIMEUS near the percolation of the Notranjska Reka near San Cozian in the Slovenian karst in 1907 (TIMEUS 1928).

Prof.G. VORTMANN from the Viennese Polytechnic suggested using lithium. He had read about G. TIMEUS's decision to investigate the connection between the Reka and the possible reemergence points near the Timavo springs and other springs in scientific literature. On 23 December 1907, 50 kg of lithium chloride in linen sacks were hung in the Reka inflow near the San Cozian mill to dissolve. In the Timavo spring, the first Li-traces were recorded after eight days on 31 December 1907. On the nineteenth day of the trace (11 January 1908), the 'Li-reaction was very strong' and from 14 January 1908 until the end of the observation on 2 February 1908, the Li findings were negative. Six samples were taken daily (TIMEUS 1912). Lithium was also supposedly detected in the water tapping S.Giovanni di Guardiella on the east side of the city Trieste and it was verified by VORTMANN through repeat analyses on samples which had been held in reserve (TIMEUS 1928). Further lithium tracing tests in the catchment area of the Timavo, which were carried out by TIMEUS, some using other tracers also, resulted in a clear picture of the large underground hydrological system between San Cozian and the Timavo springs near Duino (TIMEUS 1910b).

At approximately the same time as the tracing tests carried out by VORTMANN and TIMEUS (VORTMANN & TIMEUS 1910a), TRESH (1907) reported that 'frequently lithium salts in place of common salt' could be used to trace water. TRESH stated a detection limit of 1:1,000,000 (= 126 µg/l Li) for lithium sulfate, made however no further statements.

Astonishingly, these pioneering results from TIMEUS were forgotten. Not until the improved analytical possibilities in the fifties, was lithium used in traces again, and only rarely at first. Most likely the author carried out the first qualitatively evaluated tracing test in 1959 (SCHULZ 1961). With other tracers, a comparative tracing test was carried out in the Middle Triassic (Muschelkalk) karst on the upper Neckar near Oberndorf. Over a distance of 3.5 km, as the crow flies, the karst groundwater was traced through a doline with 1.5 kg lithium chloride. Nearly the entire amount of lithium was recovered in the Dieselbach springs (Figs 60 and 61).

Further comparative tracing tests were conducted in the well-known test region 'Lur cave system' of the South Styrian karst in 1988. There it was shown that lithium can be also a useful tracer in karst (compare Section 4.3.4 and BEHRENS et al. 1981).

Lithium can also be used as a tracer in pore-groundwater with short flow paths. In the test area near Merdingen in the Upper Rhine valley, after 10 kg of lithium chloride was injected, the lithium ion could still be detected in traces over a distance of 100 m. The passage at a sampling site at 50 m is displayed in Figure 62 (compare also Section 5.5.3). In this test, with a flow path of 50 m, a retardation factor as compared to uranine of 1.7 was determined.

Remarks on conducting lithium tracing tests.

As a tracer, usually lithium chloride is used, which is the least expensive of all the lithium salts. The price per kilogram is approx. (1990) DM 20. Other lithium salts, e.g. lithium bromide, are much more expensive. For use as a tracer, a technical purity grade is sufficient, which is 99% pure.

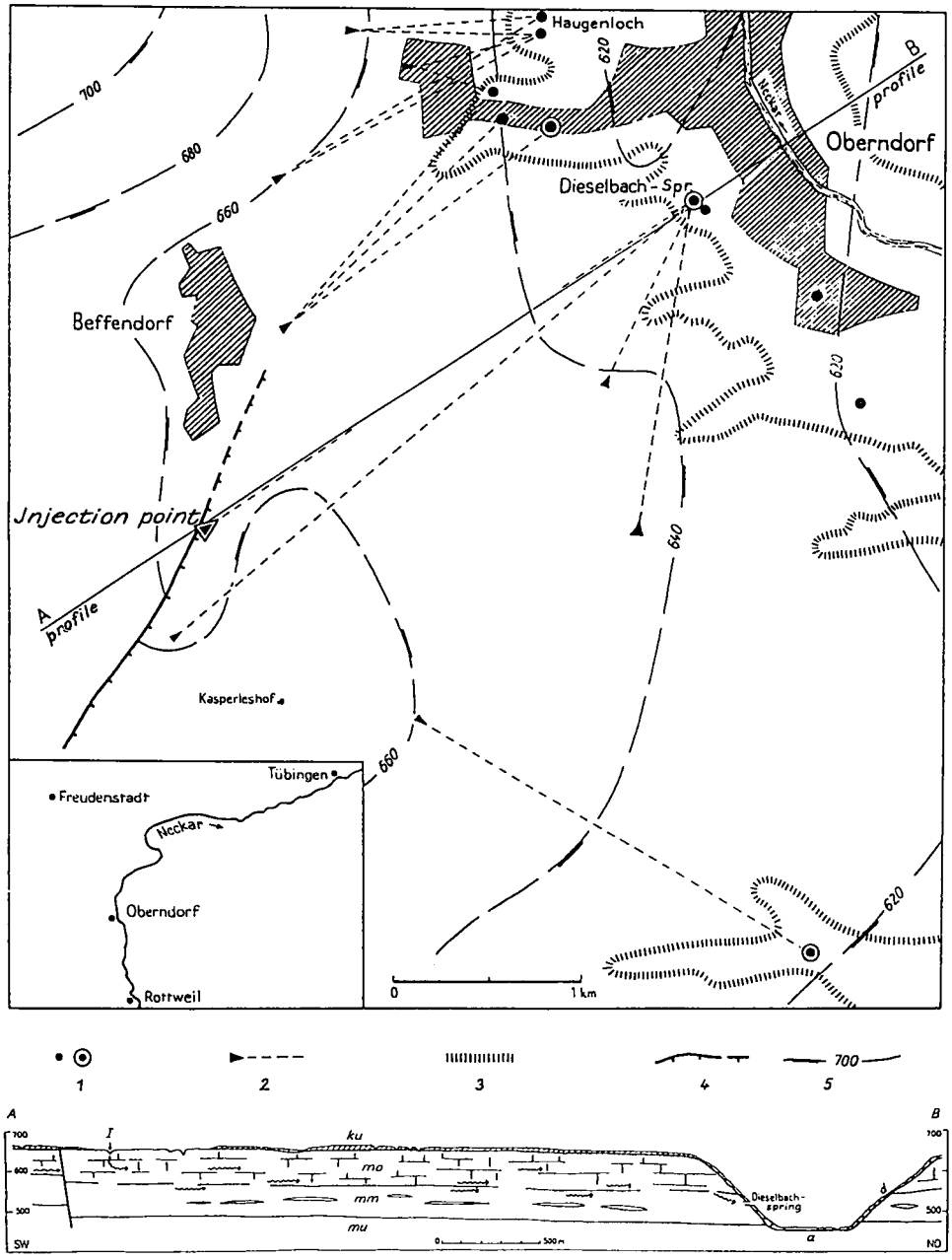

Figure 60. Map and geological profile of the combined tracing test on 1 and 2 June 1959 near Oberndorf/Neckar (from SCHULZ 1961). Top: 1 = springs, 2 = seepages and underground waterways, 3 = rim of plateaus, 4 = fault, 5 = surface of stratum mo a.s.l. Bottom: I = injection point, ku = Lower Keuper, mo = Upper Muschelkalk (limestone, dolomite), mm = Middle Muschelkalk (marl, anhydrite), mn = Lower Muschelkalk (limestone), a = Aluvion of the Neckar valley, d = talus slope.

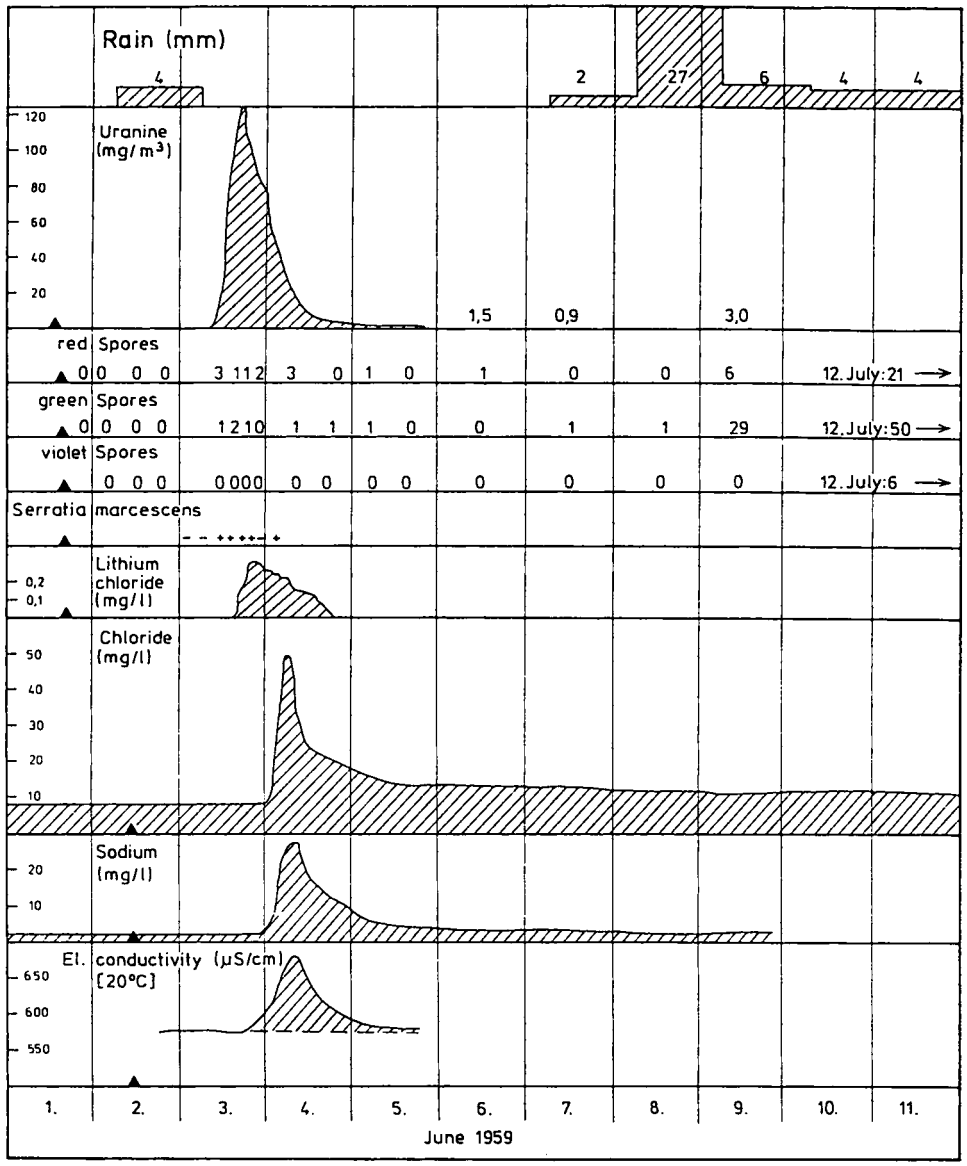

Figure 61. Breakthrough curves of lithium and other tracers in the test on 1 and 2 June 1959 near Oberndorf/Neckar (from KÄSS 1990b).

Because of its exothermal reaction, lithium chloride is easily dissoluble in water. At 20°C the solubility of lithium is 832 g, at 60°C 984 g per litre water (ULLMANN 1978, 1988). If a large amount of lithium chloride is to be injected, it should not be dissolved in plastic containers, since plastic can warp at high temperatures. To avoid lumps when dissolving the lithium chloride, it should be added slowly to the solvent under constant stirring.

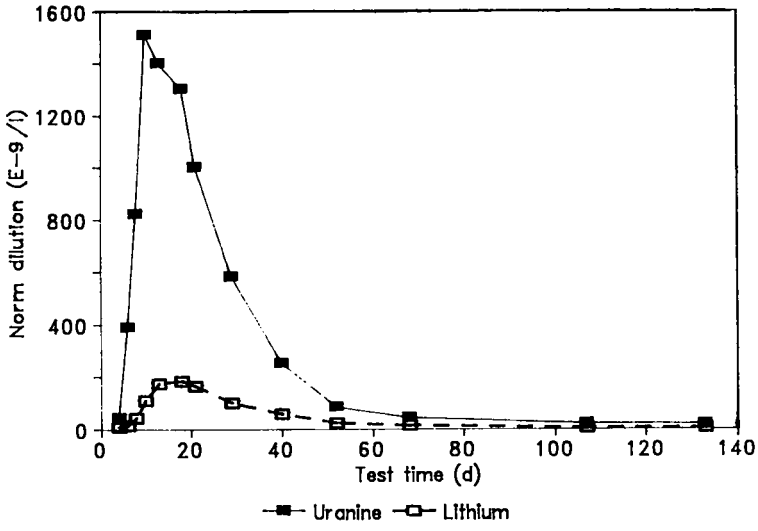

Figure 62. Results of the Li – and as a comparison the uranine passage – in the multiple tracing test in the pore-groundwater of the test area Merdingen/Lkr.Breisgau-Hochschwarzwald from 20 August 1986 in a sampling site 50 m away from the injection site. 10 kg of lithium chloride and 10 g of uranine were injected. Standardized breakthrough curves for a dilution to 10^{-8}/l. The slight time delay and the concentration decrease in lithium as compared to uranine is clearly seen.

Sample containers for the lithium determination should be made of clear glass. There is no data published concerning the adsorption of lithium ions onto plastic containers. Since lithium is usually injected together with uranine, brown bottles are necessary to avoid the decrease in uranine due to photodecay. In these cases, the lithium should be determined within one week, since there have been cases reported that brown bottles give off lithium, thus increasing the sample contents. Most brown bottles contain lithium (HOFMANN & HOFMANN 1948). The increase is the higher, the longer the samples are kept in the bottles and the darker the brown colour of the bottles. The increase can be up to several µg/l Li^+ which is particularly noticeable in determining the background before the actual lithium cloud passes.

Lithium analysis

The first lithium salt tracing tests conducted by VORTMANN and TIMEUS were only qualitatively investigated (1910a). They used a large spectroscope with two prisms according to STARKE as well as a Bunsen burner. The flame colour was excited by the sample solution on a platinum loop. This resulted in a detection limit of '1 mg LiCl in 40 l water'; which is 4 µg/l Li. By evaporating volumes of water larger than 40 litres and the uptake of the evaporation residue with alcohol, the thousandth part of the detection limit stated above can be reached. Freely, such low detection limits are unnecessary, since the Li-background levels in karst waters are around 1 µg/l. Yet it is astonishing that VORTMANN and TIMEUS could detect Na, K, Ca, and Sr in the waters of the Julia region, however not Li.

Today, either flame-photometry or ICP (Inductive Capacitivity Plasma Emission) is used. Atomic absorption spectrometry (AAS) is not very suitable for Li determination nor for the other alkalis. Lithium generates a strong line at 670.8 nm and weaker ones at 610.3, 460.3, and 323.3 nm. At concentrations over 9 mg/l inherent absorption appears at 670.8 nm, that is determined either by using a cooler flame, e.g. propane/air, or with other wavelengths. In any case, when using flame-photometry for lithium determinations, a red sensitive photoelectron multiplier is needed. A detection limit of 0.1 µg/l is easily achieved.

Since calcium is present at a much higher background level than lithium in all natural waters, the extensive calcium bands disturb the lithium lines at 670.8 nm. To remove the calcium ions from the sample water, ammonium oxalate ($(NH_4)_2C_2O_4 \cdot H_2O$) in powder form is added (Fig. 63).

However, the lithium emission is then increased due to the oxalate ions by approx. 25%. The maximal increase which leads to an additional excitement of the lithium line at 670.8 nm, is reached with an ammonium oxalate addition of 1000 mg/l. With additions with higher oxalate percentages, the lithium emission no longer rises. Therefore, the standard solutions must contain at least this amount of ammonium oxalate.

On the average, karst waters contain 6 meq/l calcium ions or a calcium hardness of approx. 17°d. To precipitate 1 meq/l Ca^{2+}, 71 mg/l ammonium oxalate is needed, for karst waters therefore at least 426 mg/l. To be sure that all of the calcium has

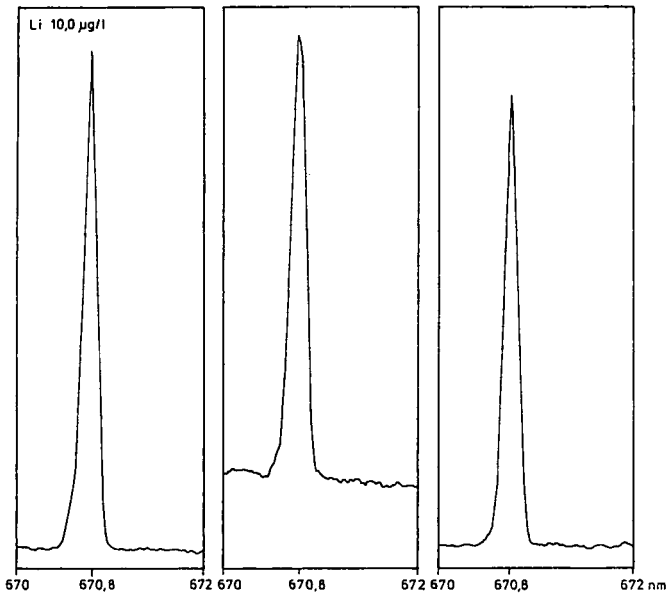

Figure 63. Flame-spectrogram between 670 and 672 nm with the main lithium line at 670.8 nm. 1 = 10 µg/l lithium in dist. water, 2 = karst spring Schlatt which taps the Hauptrogenstein/Dogger (Bajocium 3) near Bad Krozingen (SW-Germany) from 20 July 1987 with 91.2 mg/l calcium, 3 = as 2, however after the Ca-precipitation with ammonium oxalate. 91.2 mg/l Ca simulate a lithium content of 1.4 µg/l. The lithium content in the sample was 9.0 µg/l.

been precipitated, at least 1500 mg/l should be added, with sample bottles with a volume of less than 1 l, the corresponding lower aliquote amount. An excess of ammonium oxalate is not harmful, as long as it is not too high. The low hydrate water percentage in ammonium oxalate can be neglected compared to the solvent volume. When using the same kind of sample bottles with approximately the same volume, the oxalate amount needs to be weighed only once exactly; the amount for the remaining samples can be estimated once the correct amount is known. After the sample is shaken, it should be allowed to settle overnight, before it is analysed. For the Li-determination with the ICP-technique, the oxalate addition is not necessary because of the high flame temperature.

Since only a few millilitres of sample solution are needed for the lithium determination, almost the whole sample can be used for the determination of the other tracers in combined tracing tests. Lithium is not known to disturb any of the other analysis methods in the normally occurring concentrations. Since the ammonium oxalate addition raises the pH-value of the sample solution to over eight within a few days, this is even an advantage for the strong pH-dependent fluorescence yield for uranine and pyranine determinations.

The natural lithium contents of selected water bodies

To estimate the needed amount of lithium salt, knowledge of the natural background level of lithium in the body of water to be traced is important. Basement rock aquifers and karst waters have extremely low lithium contents, pore-groundwater aquifers have middle, and mineral, landfill seepage and sewage water have high lithium contents. The following list of selected values can help:

	Li (µg/l)
Fissure aquifers	
Public water supply Hammereisenbach/Southern Black Forest (Gneiss)	1.1
Karst aquifers	
Urach Waterfall/Swabian Alb (Malm)	0.4
Hammerbach Peggau/Styria (Devon)	0.3
Hubelj-spring/Slovenia (Jura)	0.04
Pore-groundwater aquifer	
Merdingen/Upper Rhine valley (calc-alpine gravel)	8
Umkirch near Freiburg/Br. (gravel from basement rock)	0.4
Böckingen near Heilbronn (Quaternary cuesta landscape)	17
Deep aquifers	
Rottenacker/Donau/SW-Germany, Br.I (Malm, 200 m)	8
Saulgau/SW-Germany, thermalwater well 1 (Malm, 618-623 m)	15
Mineral- and thermal aquifers	
Bad Pyrmont, Eichenkellerquelle (Bunter, Ca-Mg-HCO_3-SO_4-acidulous spring)	26
Bad Teinach/Black Forest, Hirschquelle (Bunter, Na-Ca-HCO_3-acidulous spring)	1400
Baden-Baden, Friedrichsstollen (Upper Carboniferous-arkose and –conglomerates, F-Rn-Na-Cl-thermals)	9020
Badenweiler/Black Forest (Quartz riff, thermal)	570
River water	
Neckar near Heilbronn (1989)	17-85
Glacier water (Aletsch, 25 July 1991)	1.4
Ocean water	170

Toxicology of lithium
In the 'Nauheimer conclusions' from 1911 of the German Bathing Localities, the classification qualification for mineral waters was set at contents over 1 mg/kg. They assumed that the lithium ions had medicinal effect upon uric salts (gout, kidney stones) (HOFMANN & HOFMANN 1948). Later, lithium was removed from the list of classified substances for medicinal waters. The toxic effect upon warm-blooded animals is very small. The lethal dosis LD_{50} for rats, oral, is 526 mg/kg LiCl (MERCK-Katalog 1990/91). 20 mg Li per day and kg weight is said to kill dogs in 14-20 weeks (PASCAL 1966). For fish, a lithium chloride content of 2-3.5 g/l is lethal (LIEBMANN 1960). On the other hand, lithium carbonate is used successfully to combat manic-depressive disorders with a long-term daily dosis of 0.5 g (ULLMANN 1978, 1988).

The German Environmental Agency recommends setting the injected amount at such a level so that the lithium concentration only amounts to 0.5 mg/l at reemergence sites that serve as a public water supply, but a short-time tenfold excess is tolerable (UBA 1997).

Remarks on evaluating lithium tracing tests
A prerequisite for evaluating a lithium tracing test is to have ascertained the natural background level of lithium and its range in the area to be investigated. As with all salt tracers, only concentrations above the background can used in the evaluation. Although the lithium ion shows little tendency to ionic exchange, some adsorption loss during the underground passage is to be expected and needs to be considered in the evaluation of the results.

Examples of salt tracing tests with lithium chloride
Karst: Oberndorf/Neckar (SCHULZ 1961 and Figs 60 and 61), Lur cave system (BEHRENS et al. 1992).
Pore-groundwater: Section 4.3.4

2.2.3 *Potassium chloride (KCl)*

Synonyms: Potash-fertilizer, Potassium salt
The fertilizer industry produces potash-fertilizer in different grades:
with 60% K_2O = 95% KCl, 50% K_2O = 79% KCl, 40% K_2O = 63% KCl.
Molecular weight: 74.553 g/mol
Solubility (10°C): 313 g/l (D'ANS & LAX 1970)

There are many advantages in using potassium chloride instead of sodium chloride in a tracing test. They are: lower background levels of potassium, therefore lower injection amounts and thus lower costs for the transport and less work during the injection. A disadvantage is the greater tendency towards ion exchange.

Natural background levels for potassium in selected groundwaters are listed in the following:

	K^+(mg/l)
Crystalline basement rock	0.2-1
Bunter (Lower Triassic)	0.5-2

	K^+(mg/l)
Malm-karst aquifers (Upper Jurassic)	0.2-1
Alpine karst aquifers	0.05-0.1
Quaternary, crystalline gravel	0.5-5
Quaternary, calc-alpine gravel	5-8
Glacier water (Aletsch, 25 July 1991)	1.6

Several tracing tests with potassium chloride have been carried out in karst areas. The first such tracing test known to the author was carried out on the eastern Swabian Alb in 1964 (KÄSS 1966a). During the test, 300 kg potash-fertilizer with 60% K_2O-content was injected in a doline. The only possible reemergence site was the Brenz spring, 4.1 km away. The difference in altitude was 148 m or 3.6% slope. Figure 64 displays the potassium breakthrough curve. At the same time, rock salt was also injected 2.5 km away from the Brenz spring and thus a price comparison could be carried out.

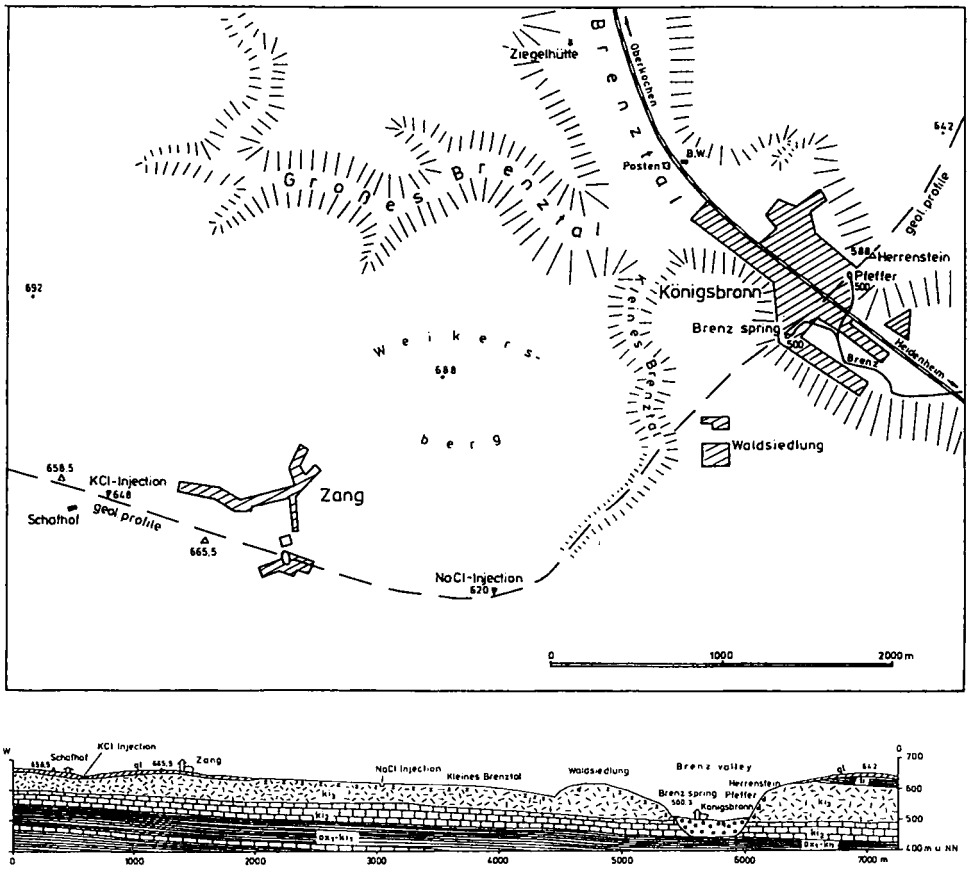

Figure 64. a) Map and geological cross section of the combined potassium and sodium chloride tracing tests on 11 November 1964 in the eastern Swabian Alb.

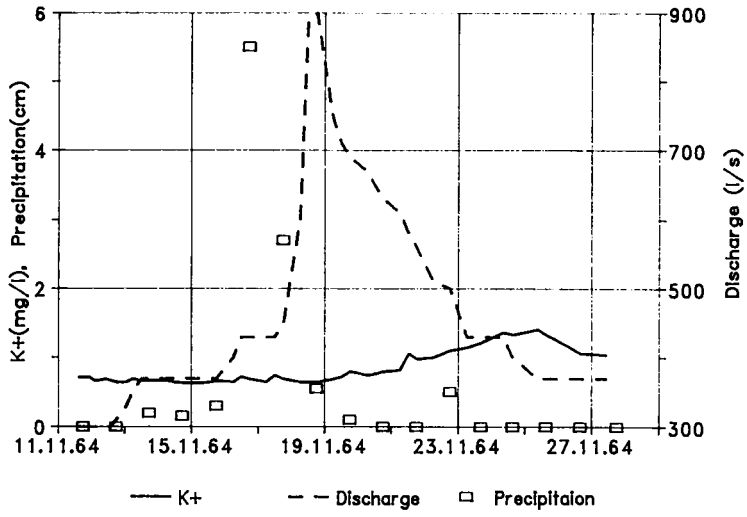

Figure 64. Continued. b) Potassium breakthrough curve and discharge of the Brenztopf spring (Malm-karst); precipitation levels from Heidenheim.

Costs for the rock salt trace were around four times as high as for the potassium chloride trace. Approximately 92% of the injected potassium amount reemerged in the Brenz spring.

During the 'First Symposium on Tracing Underground Water' in 1966 in Graz/Austria, tracing tests were also carried out as demonstrations.

In the Buchkogel karst region southwest of Graz/Austria, potassium chloride was also used as a tracer among other tracers, and reermerged after an underground flow path of 800 m with a 73.5% recovery rate (BATSCHE et al. 1967).

In the combined tracing test from 1969 in the percolation area of the Upper Danube, the tracers potassium chloride (Fig. 75: 18) and sodium chloride (Fig. 75: 29) were injected on the same day in different sites. The sodium chloride was obtained from the Potassium Saltworks Buggingen as 'road salt' and contained besides 89% NaCl also 1.46% potassium chloride (comp. Section 2.2.1). Taking into account the injection amounts of 1000 kg potash fertilizer (60% K_2O) and 50,000 kg road salt and assuming a negligible ion exchange in the Malm karst, a correction of the determined potassium contents in the only possible reemergence site, the Aach spring, was possible (Fig. 65).

Potassium was also successfully used with nitrate in a groundwater tracing test where it was necessary to keep the thermal springs in Bad Gastein free from colour (JOB & ZÖTL 1969). In that test, 500 kg of potassium salt was used and reemerged over a distance of 500-550 m and detected in several thermal springs.

An especially instructive tracing test, which clearly showed the ion exchange process, was conducted in 1969 east of Bad Gastein (Province of Salzburg/Austria) with 10 kg of potassium chloride. The underground is boulders on gneiss, which is interspersed with raw humus and covered with moss. This test using potassium chloride and other tracers was a preliminary test to decide which tracer was the most suitable for tracing karstwater influxes in certain Gasteiner springs (JOB et al. 1969). The other tracers tested were nitrate, uranine, sulforhodamine G extra, and indium-

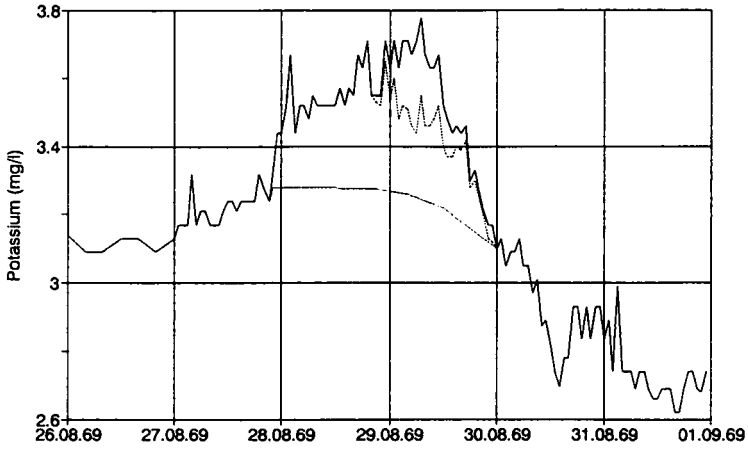

Figure 65. Potassium breakthrough curve in the combined KCl-NaCl-tracing tests on 26 August 1969 near Immendingen (KCl) and near Tuttlingen (NaCl) in the Danube. Top curve: analysed K-content in the Aach spring, middle curve: corrected breakthrough curve due to the potassium from the NaCl-injection. Dotted curve: supposed course of the background potassium level.

complex. The dyes uranine and sulforhodamine G extra were more or less strongly sorbed in the test path, whereas the cations clearly underwent ion exchange.

The injection site has an altitude of 1770 m.a.s.l. and is the percolating drain of a marshland. Obviously, the traced water reacts acidic. Below the injection site, the percolating water rises again to the surface several times. These sites were used as observation sites in the preliminary test.

Figure 66 shows the course of the exchanged cations and chloride after a flow path of 160 m as the crow flies. Notable is that, besides the alkaline earths, sodium can also be exchanged for the potassium (BUCHTELA & JOB 1970). However, a small part of the recovered sodium must be attributed to the Na-EDTA, which was used as the complexing agent for the indium and also injected as a tracer. After a flow distance of 220 m, the ion exchange had progressed further. At the observation sites 305 m and 350 m, the potassium was totally exchanged.

Similar observations about ion exchange with potassium salts were made in pore-groundwater in tracing tests in the Neckar valley, in the Rhine valley, and in the Savinja valley near Celje/Slovenia. In the first case, the potassium from 6000 kg KCl (60% K_2O) was completely exchanged over a flow distance of 180 m (KÄSS 1967b). In the second case, 100 kg of potash fertilizer (60% K_2O) was used. Over a distance of only 10 m there was indeed an increase in chloride and a hardening of the water detected, but there was no trace of the potassium (KÄSS 1972). In the third case, in the Savinja valley, after only 2.5 m the potassium, as compared to the chloride equivalents, had diminished 50%, after 25 m 90% (Fig. 212).

Remarks on conducting salt tracing tests with potassium chloride

Such groundwater tracing tests are only recommended in open-grained aquifers. In fine-grained pore-groundwater aquifers as well as in underground that is rich in organic substances, a potassium ion exchange must be considered even over short dis-

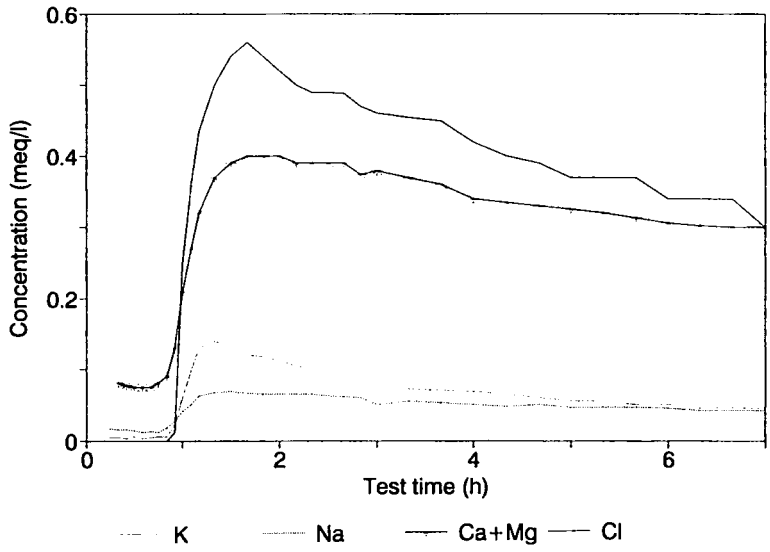

Figure 66. Breakthrough curves from the potassium chloride test east of Bad Gastein in the observation site I after a flow path of 160 m (after BUCHTELA & JOB 1970).

tances. In some tests in karst groundwater, potassium has proved to be a suitable second or third tracer. However, since even in karst channels ion exchange is to be expected, there should be a security factor added to the injection amount.

Compared to sodium chloride, potassium chloride has a much stronger temperature dependency of its water solubility. As a result, during injections with concentrated KCl solutions in narrow probes, they can become clogged with crystals formed during cooling (KÄSS 1972).

Sample containers for the potassium determination can be made of glass or plastic, both are equally suitable. To avoid possible sorption losses onto the bottle walls or the reverse, a gain in potassium from certain glass types, the samples should be analysed within one week of being taken.

KCl analysis

Potassium is, as all alkalines, analysed better with the flame emission method instead of with AAS at 766.5 nm. The use of ion sensitive electrodes is possible, however it has not been written about.

Determination of chloride also is advisable, although a significant increase over the chloride's natural background level cannot always be expected.

The physiology of potassium

Potassium is, as all alkaline metals, everywhere and necessary for life. However, too high a potassium concentration can cause metabolism disorders. In tracing tests, such high levels are not normally expected in the sampling sites.

LIEBMANN (1960) listed a lethal concentration for fish of 0.7-5.2 g/l, and for the rest of the water organisms 0.4-5 g/l. For people, an oral dose of 2430 mg per kg weight is lethal.

2.2.4 *Borax ($Na_2B_4O_7 \cdot 10H_2O$)*

Synonym: di-sodiumtetraborate-dekahydrate
Molecular weight: 381.37 g/mol
Water solubility (10°C): 16.2 g/l
(20°C): 25.2 g/l.
To dissolve 1 kg of borax at least 62 l of 10°C water are needed.
Density of a saturated borax solution (10°C): 1.0198.

Borax is obtainable in technical purity grades from 96-99.5% in 50-kg-paper sacks from Turkey or France.

Boric acid salts hydrolyse in water to almost undissociated boric acid. At first, it was assumed that the undissociated form was metaboric acid. Therefore, it was decided that the medicinal and mineral water analyses would list the boron contents as m-boric acid (HBO_2) (Begriffsbestimmungen 1987). Although newer investigations have revealed that undissociated boric acid is not m-boric acid, but rather predominantly o-boric acid (H_3BO_3) (SENFTEN 1972), the analyses are still written with the meta-form.

Due to the predominance of the undissociated form of the boric compounds in water, the tendency towards ion exchange and adsorption is very slight. Only clay minerals can adsorb small amounts of boron (HARDER 1960/61). This property is used to distinguish between marine and fresh water clay stone series, since oceans contain much more boric acid than fresh water lakes.

The use of borax as a tracer is based on these considerations. In 1948/1949, several tracing tests using borax were conducted in three oil field flood waters in Kansas and Oklahoma, some successful, some not (CARPENTER et al. 1952). The most successful was carried out in Burkett Oil field, Greenwood County/Kansas, where 110 kg borax were injected over 34 hours in an injection well. Only one of the four production wells within 200 m showed a reaction. After 15 hours, the boric contents rose from 1 mg/l to over 100 mg/l. A dilution of the injection water of 1:5 to 1:6 could be calculated.

During preparations for the 'Fourth International Symposium on Tracer Techniques in Hydrology 1981' in Bern/Switzerland in 1979, a tracing test with borax was conducted in Langetental (KÄSS 1981a). 10 kg uranine and 100 kg borax were injected in a groundwater monitoring well in Pleistocene pore-groundwater. The only two observations sites with an increased boric acid content were 610 and 1010 m downstream of the groundwater flow (Fig. 67 top). The breakthrough curves for m-boric acid and uranine for both sampling sites are shown in Figure 67 middle and bottom. The curves show, that boric acid, as compared to uranine, had a slight delay in the passage. Furthermore, the curves show that the sampling site 209 had a boric acid background level of approx. 200 µg/l as compared to only around 100 in the sampling site 278. This is due to the nearness of the river Langeten to the sampling site 278, where with certainty river water containing very little boric acid seeps underground. In contrast, the sampling site 209 is in the middle of a fertilized meadow, which can deliver boric acid. The shown curves allow a comparison between uranine and boric acid regarding their behaviour during the underground passage. If the dilu-

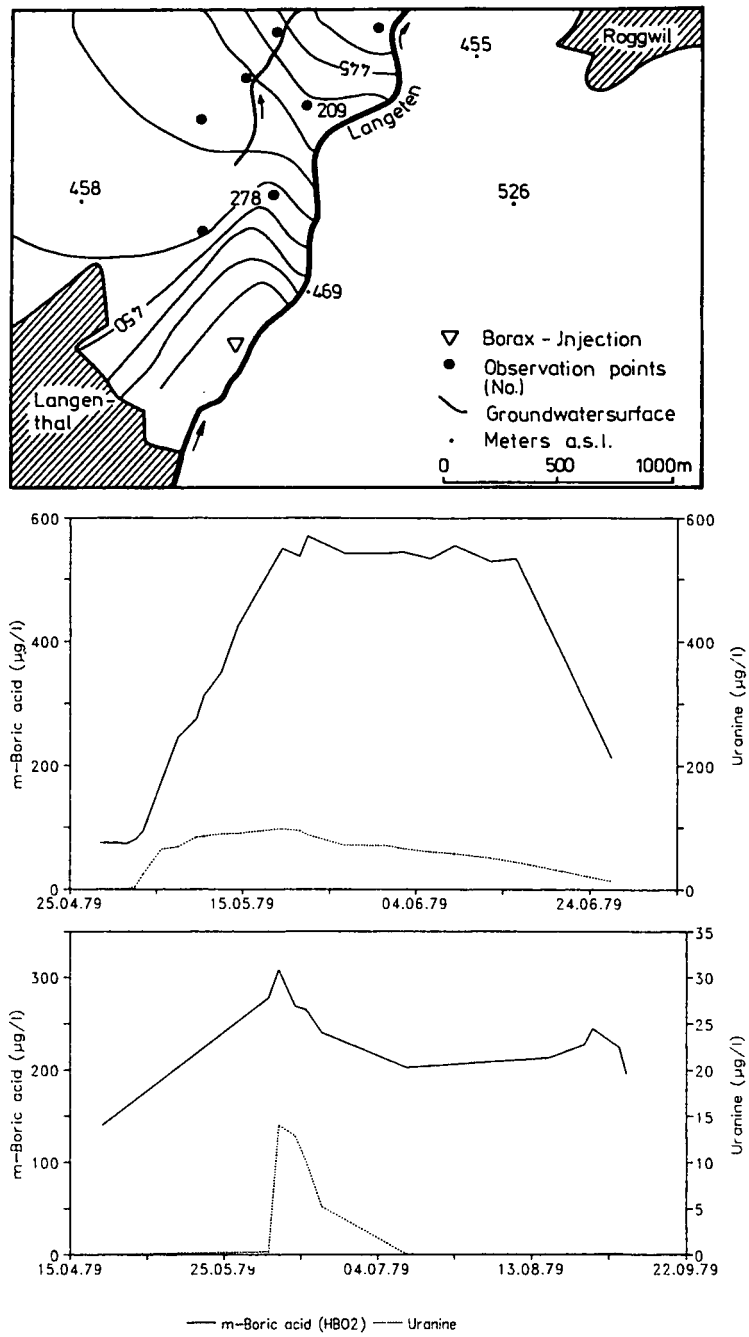

Figure 67. Top: Map of the first tracing test with borax near Langenthal (Canton Bern/Switzerland) on 28 April 1978. Groundwater contours from 26 April 1978 (after KÖVESDI 1980). Middle: breakthrough curves from the sampling site 278 for metaboric acid and uranine; flow path distance 610 m. Bottom: breakthrough curves from the sampling site 209 for metaboric acid and uranine; flow path distance 1010 m.

tions of the injected amounts are calculated per litre at the maximal concentration increase, the following values are obtained (10^{-8}/l):

Site	m-boric acid	uranine	m-boric acid/uranine
278	0.85	1	0.85
209	0.115	0.15	0.77

Notable is the low interaction of boric acid with the underground material over a flow path distance of over 1000 m.

Further tests with borax in the Pleistocene of the Upper Rhine valley have shown the suitability of this tracer in fine-sandy underground.

Remarks on conducting borax tracing tests

The natural background level of boric acid in the area under investigation must be known to determine the injection amount. It must also be considered that the underground will also retain part of the borax. Since borax is overall, the injection amount should not be skimped on. Problems can arise if large amounts of borax are to be dissolved, due to the low water solubility. Trying to speed up the process by warming the water is not recommended, since the cooling caused by mixing with the cooler groundwater will result in recrystallisation. Large containers with stirring utensils work the best, whereby one should stay well under the saturation concentration. CARPENTER et al. (1952) found a considerable increase in the solubility by adding 30% boric acid to the borax.

The choice of sample containers is open: plastic or glass are both equally allowed. Even borosilicate glass does not influence the boron content of the sample according to observations up to now.

Boron analysis

The determination of boron with the colorimetrical method according to the German standardized methods (DEV, D17 = DIN 38 405, Part 17) is so sensitive, that in each case the natural background levels can be ascertained. In this somewhat complicated procedure, the reagent Azomethin H is used to convert the borax into a yellow dye whose colour corresponds to the boric acid concentration. The dye needs two hours to form.

Much quicker and just as sensitive as the colorimetrical method is ICP (Inductive Capacitivity Plasma Emission).

According to EISENBRAND (1966) and RADLEY (1946), a fluorimetrical boric acid determination is also possible after coupling with benzoin and sulfosalicylic acid in sulfuric acid solution.

The natural m-boric acid content in selected ground- and surface waters

	HBO_2(µg/l)
Quaternary gravel	20-150
Malm-karst water	50-100
Keuper sandstone in SW-Germany	50-100

	HBO_2(µg/l)
Bunter in SW-Germany	10-50
Crystalline basement rock	20-100
Gypsum Keuper, Vaihingen-Horrheim	2,100
Middl.Muschelkalk, Bad Wimpfen, Brine well 9	35,000
Malm mass. Limestone, Saulgau, Thermal well 3	210
Upper Karbon-arkose, Baden-Baden, Murquelle	260
Tertiary, Meletta-layers Upper Rhine valley	
Oil-field water wells Leopoldshafen Lh 3+6+11+12	120,600
Thermalwater, Wiesbadener Kochbrunnen	3,690
Rhine near Basel (22.2.1981)	190
Rhine near Emmerich (16.10.1976)	710
Neckar near Stuttgart (20.8.1976)	1,360
Main near Kelsterbach (21.1.1981)	340

Groundwater aquifers which have not been subjected to saline deposits or to anthropogenic impacts have m-boric acid contents under 150 µg/l. Deep lying aquifers, saliniferous waters, and numerous formation waters often have much higher boric acid contents. Also groundwater aquifers with catchment areas with agricultural crops that are heavily fertilized, can have increased boric acid contents, since mineral fertilizers have boron compounds with between 0.1 and 0.65% B added. Modern laundry detergents contain a large percentage of oxygen donating perborates. In household wastewater systems, these boron compounds hydrolyse to boric acid. Therefore, sewage water, landfill seepage water, and polluted surface water contain above average concentrations of boric acid (compare Section 2.12).

Physiology of boron compounds

Boron is an essential trace element. A boron deficiency causes dry rot in sugar beets. Above all, citrus plants are sensitive to too much boron.

According to LIEBMANN (1960), 3-7 g/l borax is deadly for fish; for other water organisms, the lethal borax concentration is between 0.54 and 9.9 g/l. For an oral dose with rats, a LD_{50}-value of 4.5-5 g/kg weight is given for borax. The lethal dose of boron for people, relative to age, weight and kidney function is between 0.5 and 5 g (MOESCHLIN 1964).

According to these values, tracing tests with borax cause no harm to any life forms.

2.2.5 *Other salts*

Strontium

Details about the first tracing tests with strontium salts are found in TIMEUS 1926 and 1928. Accordingly, 50 kg of strontium chloride and 10 kg of lithium chloride were injected on 20 May 1910 in the gravelly riverbed of the Vipava near Vertoce near Bilje (south of Nova Gorica/Slovenia). The tracers arrived in the reemergence sites, which were mostly south of the injection site, after 2-5 days. TIMEUS wrote that the strontium was determined spectroscopically; however, more details were not given. All of the reemergence sites were either in lakes (Lago Doberdo, Lago Pietrarossa,

Lago Sablici) or in rivers (Isonzo, Timavo). At these enormous dilutions, the strontium determination must have been conducted very exactly, in order to prove a concentration increase due to the tracing test.

Newer tracing tests in the pore-groundwater of the Upper Rhine valley in calc-alpine gravels show that when injecting 2 kg of $SrCl_4 \cdot 6H_2O$, after a flow path of 100 m, just enough of an increase in concentration is present to be ascertainable. A retardation factor of 10 was determined, as compared to uranine (KÄSS 1990a).

Selected background levels of strontium	(µg/l)
Calc-alpine gravel, Upper Rhine valley, Merdingen test field,	321
Basement rock gravel, Upper Rhine valley, Umkirch	48
Malm-karstwater, Uracher Waterfall	42
Malm-karstwater, Gütersteiner Waterfall	31
Lower Triassic (Muschelkalk) in North Württemberg (JUNGBAUER 1983)	up to 1200
Lower Triassic (Muschelkalk) in North- and Northeast Hessen (pers. communication B.TOUSSAINT)	up to 14,000
Upper Muschelkalk (Lower Triassic), Heilbronn-Böckingen, Well 3041	3290
Basement rock, Granite, Hammereisenbacher Dorfbrunnen	8
Neckar near Heilbronn-Böckingen	618
Elbe near Sandau	616
Glacial water (Aletsch)	5

Extremely high strontium contents in groundwater are reported in Champaign County, Ohio. The Upper Silurian underground there contains celestine; the resulting unconsolidated glaciated rocks contain up to 30 mg/l Sr (FEULNER & HUBBLE 1960).

Water samples are analysed for strontium by either flame emission or by AAS at 460.7 nm. Emission determination will be more exact according to local reports, if the reference solutions have about the same composition as the sample water. When using ICP, reproducible results can also be obtained.

The analysis of the samples should be conducted within 48 hours of taking the samples, to avoid Sr precipitation.

Neither the European nor the American drinking water laws state maximum levels for strontium. ODUM (1951) reports that, strontium is not any more toxic for people than calcium. The German Environmental Agency allows the use of strontium salts in tracing tests if the injection amount is properly minimized regarding the test goal (UBA 1997).

Strontium ions are lethal for trout at a concentration of 10,000 mg/l and a contact time of one day (HOMMEL 1987).

Cesium

TIMEUS used cesium chloride as a second tracer at the entrance of the Notranjska Reka in the limy underground near Vremski Britof (Slovenia). On the average, the river loses one-third of its water there. Along with the cesium chloride, uranine was injected and although the uranine was detected at the entrance of the cave San Cozian, cesium could not be detected. TIMEUS (1926, 1928) did not report as to when this test occurred; most likely before the First World War. Details as to the amount of cesium chloride used and such are also missing. Only the geographical data is listed:

sea level of the injection site: 350 m, sea level of the sampling site: 252 m, horizontal distance: 7 km, flow time for uranine: 12¾ hours. TIMEUS attributes not being able to detect the cesium to the large dilution or to the sinking of the cesium chloride to a greater depth. The true reason as to why the cesium could not be detected lies in its sorptivity and in the dilution.

The high sorptivity of cesium ions has been verified in field tests in a pore-groundwater aquifer in the Upper Rhine valley (KÄSS 1990a).

Ammonium

In 1907 TRESH suggested favouring the use of ammonium chloride instead of uranine as a groundwater tracer. TRESH'S main argument for favouring ammonium was its invisibility, although uranine was a better buy and more effective. However, it was not until 1942 that ammonium salts were used again in the Warsteiner Massenkalk as a groundwater tracer (RICHTER 1944). To investigate where the water disappeared to in the sinkhole Wäsche, 72 kg of ammonium sulfate were injected on 26 November 1942. In the Range spring, 2.8 km away, the ammonium was qualitatively detected using NESSLERS reagent between 03:00 hours on 28 Nov. and 04:00 hours on 29 Nov. The sulfate was also detected using ion sensitive electrodes, with good results. A chloride sensitive electrode was also used.

In spite of the good detectability of the ammonium, ammonium salts are not often used as tracers. It seems that such large amounts must be used and that it involves more work, than compared to other tracers. A further reason for not using ammonium salts are their sensitivity to sorption and oxidation.

Ammonium is also strongly toxic to fish in alkaline ranges. Especially in strong sunshine, the pH-value increases in surface waters to at least 8, at times even over 10. At concentrations over 0.3 mg/l, the behaviour of trout and plankton is disturbed. The lethal amount is between 1.25 and 5 mg/l (HOMMEL 1987).

Dichromate ($Cr_2O_7^{2-}$)

For discharge measurements in channels, besides sodium chloride, potassium or sodium dichromate is also used. In 1963, GUIZERIX et al. still recommended using sodium dichromate ($Na_2Cr_2O_7$) for discharge measurements in rivers up to a water flow of 50 m^3/s. He recommended a minimum concentration for clean water of 0.2 mg/l and for swiftly flowing rivers 0.5-1.5 mg/l. GUIZERIX calculated the necessary injection amount to be 2 kg per m^3/s discharge.

Only 77 g/l of potassium dichromate ($K_2Cr_2O_7$) is soluble in 10°C, sodium dichromate-dihydrate ($Na_2Cr_2O_7 \cdot 2H_2O$), however, has almost the content of chromate as potassium dichromate, yet it is much more water soluble (1700 g/l at 10°C). Both salts make intensive yellow solutions with absorption maxima at 372.5 nm. One extinction unit/cm corresponds to a chromium content of 11.25 mg/l = 23.36 mg/l Cr_2O^{2-}. With diphenylcarbazide, an exact colorimetrical chromate determination can be carried out.

The advantages of tracing with dichromate are the easy and exact photometrical detectablitity and that chromate is not present in natural waters. There are also major disadvantages: Dichromate can be reduced by organic substances to trivalent chromium; therefore the water samples should be reoxidated. The most decisive reason against using chromates as tracers are their toxic properties. According to HOMMEL

(1987), for trout (at pH 7-8) 0.2-0.35 mg/l of Cr-VI are tolerable, for mini crustaceous 0.12 mg/l. Most decrees pertaining to drinking, mineral, and surface waters permit a maximum level of 0.05 mg/l total chromium. The 'dangerous working materials' decree (BGBL I 1980) set the chromates in the list of cancerous work-substances as 'hazardous' to 'strongly hazardous', if it is in a breathable form (dust).

Nitrate (NO_3^-)
In those cases where uranine cannot be used as a tracer due to acidic underground conditions, it is possible to substitute nitrate. This was shown by JOB, MUTSCHLECHNER and ZÖTL (1969) in comparison tests in 1968 in a landslide area northeast of Bad Gastein/Austria, where over a flow distance of 350 m, uranine was retained strongly, yet not the nitrate. These preliminary tests were conducted as part of the investigation of the catchment area of the Bad Gasteiner Thermal springs. It was possible there to detect nitrate over a distance of 320 m with an injection of 20 kg of sodium nitrate (JOB & ZÖTL 1969).

Nitrite (NO_2^-)
Occasionally, nitrite is recommended for discharge measurements in channels (SPENCER & TUDHOPE 1956). The analysis of the water samples using sulfanilic acid and -naphthylamine is comparably easy and exact, yet with large sample series very painstaking. Furthermore, nitrite is unstable towards oxygen and therefore the measured values are too low in long tests.

Thiosulfate ($S_2O_3^{2-}$)
In several publications between 1900 and 1914, VAN ITERSON praised the use of sodium thiosulfate for measuring surface run-off (cited in SPENCER & TUDHOPE 1956). The titrimetric thiosulfate determination is exact, yet, thiosulfates are unstable when dissolved in oxygen-rich waters.

Manganese Salts (Mn^{2+})
Manganese-II-sulfate has been repeatedly recommended and used in discharge measurements (SPENCER & TUDHOPE 1956). The analysis is carried out by oxidizing with persulfate to permanganate and then titrating with Fe-II solution.

Nickel Salts (Ni^{2+})
SCHMITT et al. (1969) and DIETZEL (1979) found, that for discharge measurements, nickel ions in the form of nickelnitrate ($Ni(NO_3)_2 \cdot 6H_2O$) were more suitable than manganese salts. The nickel analysis was conducted by the authors in 100-ml-samples with 2,3-butanedione dioxime in ammonia solution in the presence of bromine. At a content of 1 mg/l $Ni(NO_3)_2 \cdot 6H_2O$, an extinction of 0.183/cm is observed during colorimetry at 525 nm.

Zinc Salts (Zn^{2+})
In the karst water tracing test in the cockpit karst southeast of Guilin (Province Guangxi/South China), CHAI WUTIAN et al. (1988) used zinc chloride. With an injection amount of 45 kg $ZnCl_2$, a detection at a distance of 1.4 km was still possible. The zinc background level is listed at 1-27 µg/l; zinc can be determined by polaro-

graphy, colorimetry, or with AAS. Since zinc, as the third most frequent heavy metal after iron and manganese, is present in all water bodies, the above authors do not expect reactions underground. In fact, they underscore that zinc salts are inexpensive in comparison to other tracers.

However, zinc salts are poisonous for fish (SCHÄPERCLAUS 1954). Carps die inside of one day when exposed to a zinc concentration of 1 mg/l; eels are more sensitive, they die after being exposed for only a half a day to a zinc content of 0.65 mg/l, whereas daphnia can survive 1.36 mg/l Zn^{2+} for five days (HOMMEL 1987).

Molybdate ($Mo_4O_{24}^{6-}$)

Next to zinc salt, CHAI WUTIAN et al. used molybdate as a groundwater tracer in the cockpit karst near Guilin/South China. Due to the very low background level of molybdate in natural waters of only 0,1 µg/l, it is quite suitable as a tracer, especially since there are no interactions known with the underground.

In the cockpit karst, two tests were carried out with 30 and 45 kg of ammonium heptamolybdate. The polarographic detection with a detection limit of 0.1 µg/l, was successful over 830 m and 2000 m.

Thiocyanate (SCN^-)

To determine in which probes flood water reemerged, DOLAK (1969) carried out a tracing test with, among others, potassium thiocyanate. With an injection amount of 4 kg KSCN, the detection over a distance of between 190 and 540 m in several probes was possible.

Bromide (Br^-)

Some publications do not make it definitely clear as to whether the bromide used as the tracer was determined through chemical methods or using activation analysis at the sampling site.

Bromide as a tracer for water has been recommended by various groups (DAVIS et al. 1985). The advantages are: It is present only in traces in groundwater, it does not tend towards sorption and is stable towards microbiological activities. Disadvantages are: High costs as a tracer and a painstaking analysis.

In column tests it was ascertained that bromide travels slower than chloride (WOOD & EHRLICH 1978). Compared to chloride, bromide is present in groundwater aquifers only in subordinate amounts. The ratio chloride:bromide is according to DAVIS et al. (1980) 300:1, according to SCHÖLLER (1983) between 419:1 and 877:1. The second author found bromide concentrations between 70 and 200 µg/l in groundwater wells near Bisamberg (Lower Austria). Water in the Söse valley dam in the Südharz (Lower Saxony/Germany) contains 13.1, a spring in the catchment area of this dam has 19.6 µg/l Br^- (HEUMANN & SEEWALD 1985).

Bromide can be determined in many ways. The simplest method is with ion sensitive electrodes; however, the detection limit is very high, namely 50 µg/l. Somewhat more sensitive is ion chromatography, very sensitive is the method of isotope dilution analysis (HEUMANN & SEEWALD 1985).

In salt tracing tests using bromide, it is best to use sodium bromide (NaBr) because of its comparatively low cost and because of its good water solubility (850 g/l

at 10°C). Almost as cost effective and water soluble are potassium bromide and ammonium bromide.

According to UBA (1997), tracing tests with bromine salts should not be conducted if water treatment facilities using oxidizing agents could be afflicted. This way, the formation of cancerous compounds such as bromates or bromide hydrocarbons can be prevented.

Iodide (I^-)

Iodide is present in even smaller concentrations than bromide in groundwater. In the water from the Söse valley dam/Germany, a concentration of 1.25 µg/l was found, in a spring north of the dam only 0.39 µg/l (HEUMANN & SEEWALD 1985). DAVIS et al. reported in 1980 of successful tracing tests in ground- and oil field waters.

However, iodide can be chemically and microbiologically converted. BEHRENS (1967) added sulfite to the samples being investigated to prevent oxidation to iodate (IO_3^-). He also described the incorporation of iodide in organisms (BEHRENS 1988a). Therefore it follows that iodide is only suitable as a tracer for short flow distances, for short residence times, and also only in undergrounds with low organic pollution. In field tests, iodide ions had an approximately five times slower effective velocity than yeast cells (WOOD & EHRLICH 1978).

The determination for iodide can be carried out with ion chromatography, with ion sensitive electrodes or using mass spectroscopic dilution analysis.

2.3 SURFACTANTS, AROMAS AND OTHER CHEMICALS

W.Käss

This chapter covers all those substances that do not fit in the other categories. They are mainly organic substances and are used in different ways, as their hydrological behaviour and determination methods are also different. In general, these tracers are used as a second or third backup tracer with a proven one.

2.3.1 *Surfactants (wetting agents)*

Surfactants or wetting agents (German: Tenside or schäumende Netzmittel; French: agents tensioactifs) are organic chemicals, which can be used in qualitative or quantitative water tracing tests. Of the different types of surfactants, i.e. anionic, cationic and non-ionic, only the anionic types are used in tracing tests. In particular, these are the alkylarenesulfonates and alkylbenzenesulfonates (ABS), which are produced industrially for laundry and cleaning supplies. In Germany, approximately 70,000 t are produced annually (KANOWSKI 1985). According to the German Detergent Decree from 1 Oct.1964 (BGBL 1961) only biologically degradable, the so-called 'soft' surfactants are allowed on the market, those that are more than 80% biodegradable. However, the so-called 'hard' agents, which are not as biodegradable, are more suited as tracers than the 'soft' ones. If the hard surfactants are to be used in a tracing test, an official exception ruling is needed. A handle for using hard surfactants in tracing tests is provided in Paragraph 1, Section 3 of the named law; accordingly, these substances can be used for investigatory purposes.

The anionic surfactants are well soluble in water. They work by lowering the surface tension; thus they are also called surface- or boundary-layer-active agents. They are concentrated at the air/water boundary layer, where the foam forms. The formation of the foam is supported by mixing (shaking, turbulence).

This strong tendency of the surfactants to foam induced W.A. SCHNITZER to try them as a tracer. In the summer of 1964, he was the first to inject a surfactant in the karst of the Franconian Alb (SCHNITZER 1965a). In three test paths with different lengths between 300 and 2500 metres, 0.75 to 3 kg of soft surfactants were used. The only observations made at the reemergence sites were if foam appeared. In sites where the foam forms only slightly and there is doubt as to whether the surfactant has reappeared, SCHNITZER recommends shaking the sample in test tubes or better yet in 0.5- or 1-l-flasks. Shaking in flasks has the advantage of the foam being concentrated in the neck of the flask.

A bit later (SCHNITZER 1965b) it was emphasized, that the surfactant method can deliver quantitative results if the height of the foam is determined. In the combined tracing tests in the Buchkogel region as a part of the First Tracing Symposium in 1966, a breakthrough curve with 'relative foam heights' was shown (BATSCHE et al. 1967).

Conducting tracing tests with surfactants

The different types of the anionic surfactants are not equally suitable as tracers. Due to their higher stability, the hard surfactants are preferable to the soft ones. The surfactants used in many of the tracing tests that are described in German literature, were made available without charge by the largest German manufacturing company of surfactants, the Hüls AG in Marl/Germany.

Table 8, which lists the most important surfactant tracing tests, can be helpful in deciding the amount of surfactants to be used. Furthermore, the detection limits and the background must be considered also. In the surfactant tracing tests in Slovenia in 1974, the supposed, measured on the path length, minimum amount of 50 kg of hard surfactants was injected. Unfortunately, the background at the reemergence sites was so high – the catchment area takes in the sewage water from numerous villages – that it was impossible to obtain a definite passage/breakthrough curve.

Over short and quick flow distances, the soft, biodegradable surfactants can be used, since the breakdown does not begin immediately. An injection permit will be also more likely granted for soft surfactants than for hard ones. Commercially produced soft surfactants such as Marlon AFR from the Hüls AG company can be used. This product is a viscous liquid that can easily be diluted with water and has approx. 30% anion-active substances.

Hard surfactants are preferable on long flow paths, although a certain amount of decay must be expected here too. Marlon TP 350 is made out of 50% tetrapropylene benzene sulfonate. The commercial product is a viscous liquid with flocs of tetrapropylene benzene sulfonate. A tracing injection is only possible here after diluting in a 1:1 ratio and considerable stirring. The highly concentrated Marlon 375 with 75% tetrapropylene benzene sulfonate is no longer produced. It could be cut and sliced and was delivered in paper sacks. To be injected as a solution, it had to be intensively stirred with water for a long time (Fig. 68).

Surfactant tracer solutions should be injected with as little turbulence as possible. It is best to use a hose underwater and if this is not possible, then quite a lot of foam can

Table 8. Groundwater tracing tests with surfactants. Except the last one, all tests were carried out in karstic waters; the last one was applied in the porous groundwater of the Upper Rhine valley. s.s. = soft surfactants; h.s. = hard surfactants.

Year and site	Distance (m)	Amount (kg) and species	Result and author
Pegnitz percoloation, northern Franconian Alb (1964)	300-350	0.75 s.s.	Strong foam after 90 min. (SCHNITZER 1965a)
Unteremmendorf, southern Franconian Alb (1964)	1,500	3 kg s.s.	Mid-strong foam after 4 hrs.(SCHNITZER 1965a)
E. Enkering, southern Franconian Alb (1964)	2,500	3 kg s.s.	Foam after 2½ hrs. (SCHNITZER 1965a)
Morschreuth, northern Franconian Alb (1965)	3,100	60 kg s.s.	Foam in Wiesent river after 6-8 hrs. (SCHNITZER 1967c)
Stücht, northern Franconian Alb (1965)	1,200	40 kg s.s.	Positive after 22-26 hrs. (SCHNITZER 1967c)
Gößmannsberg, northern Franconian Alb (1965)	2,700	60 kg s.s.	Foam for some days (SCHNITZER 1967c)
Pfahldorf, southern Franconian Alb (1966)	3,000	20 kg s.s.	Foam after 1 day (SCHNITZER & WAGNER 1967)
Buchkogel near Graz (1966)	800	10 kg s.s.	Maximum after 2½ days (BATSCHE et al. 1967)
Danube-Aach-area (1969)	11,800	200 kg h.s. and 62 kg s.s.	Visible foam after 6 days (BATSCHE et al. 1970)
Planina depression, Slovenia (1974)	10,000-11,500	50 kg h.s.	No detection (BAUER et al. 1976)
Riegel passage, SW-Germany (1970)	10	30 kg h.s.	Maximum after 22 days (KÄSS 1972)

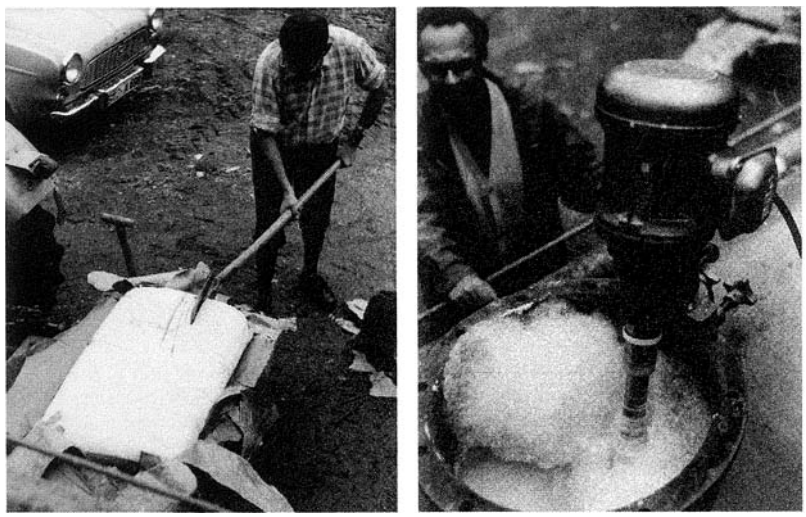

Figure 68. Preparation of the 200 kg of hard surfactants (Marlon TP 375) for injecting near Liptingen/Cty.Tuttlingen. Removal from the package (left) and stirring with electro-stirrers in 1700 l barrel (right). Photos: W. KÄSS, 25 Aug. 1969.

form at the injection site. A large amount of rinse water is then needed to rinse the mountain of foam underground. The foam is best displaced at the injection site with a spray nozzle. If stream or river sections are to be traced with surfactants, a great deal of foam must be expected. During the preliminary tracing tests for the Fourth Tracing Symposium in 1982 in Bern/Switzerland, 200 kg of 50% hard surfactants (Marlon TP 350) were injected in the dry stream bed of the Muota. As the evening outlet runoff water from the upstream electric works flowed down the bed, metre high mounds of foam developed. Had it not turned dark, they would have caused quite a sensation (BEHRENS et al. 1981).

If the samples are to be investigated by determining the foam heights, adding 1% foam stabilisers, e.g. Marlopon AT 50, is recommended. However, with the colorimetric determination, this addition should be left out, since stable foam mounds can be a disturbance during injection, at the sampling sites, and during analysis.

Surfactants are used only rarely and then only as a backup tracer. The sample bottles chosen should not be too small. Brown sample bottles with a volume of at least 250 ml will provide the required sample volume for a fluorimetrical as well as a colorimetrical determination and a repeat analysis. It is important that the sample bottles are rinsed after being washed with detergents. Furthermore, the bottles should be shaken and rinsed with sample water before the sample is taken.

Whether hard or soft surfactants are used as the tracer, the samples should be stored and transported cool and in the dark. Completing the analysis as soon as possible prevents severe losses due to decay. Figure 69 shows the decay behaviour of soft surfactant solutions in water with different degrees of pollution. It shows that the soft surfactants have different decay rates, even down to a complete decay, for different degrees of pollution. Other publications have described a decay of only 60% in sewage treatment plants, by which the foaming properties of the soft surfactants decreased 90% (KANOWSKI 1985).

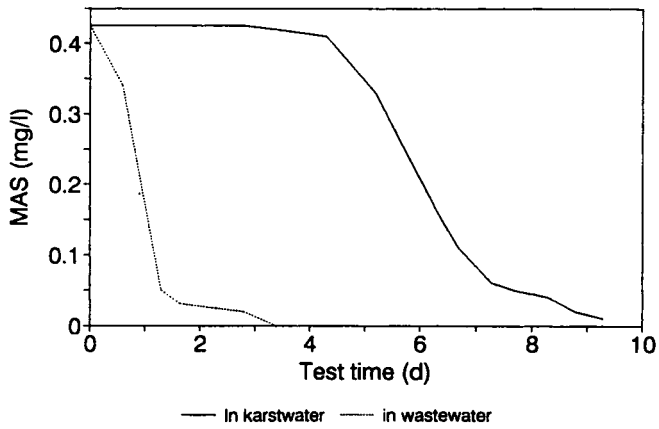

Figure 69. Soft surfactants (Marlon AFR) decay in strongly polluted sewage water from a biological sludge sewage plant and in water with little pollution (Aach spring water). Hard surfactants showed no decay over the same period in Aach water (after GEISLER in: BATSCHE et al. 1970).

Analysing for surfactants

During the first tracing tests, the surfactants were not only determined by observing the foam at the reemergence sites, but also by determining the foam height in shaken 500-ml or 1000-ml-Erlenmeyer flasks (SCHNITZER 1965a). If the flasks are filled to the necks with sample water and then well shaken for one minute, foaming occurs at the air/water boundary layer due to the activity of the surfactants. The resulting foam height in the flask neck is used as 'relative foam height' for the half-quantitative surfactant determination. In 500-ml-flasks, SCHNITZER (1967b,d) reached a detection limit of 1:2 million. In 'special' flasks, which are not described anywhere – most likely 1-l-flasks with very narrow necks – dilutions up to 1:5 million are supposedly still recognizable.

Admittedly, the foam height of the same surfactant concentration is not the same in water with different hardness levels. The Hüls AG company quoted the following dependencies in centimetres for shaking tests in a mixing cylinder with sieve plate:

Water hardness	°d	ppm	meq/l	Foam height (cm)*
Deionized water	0	0	0	28
	5	90	1.8	22.5
	10	180	3.6	11
	15	270	5.4	9.5
	20	355	7.1	7
	30	535	10.7	6
	40	715	14.3	5.5

*Today, foam volumes are recorded in millilitres.

Figure 70 shows the breakthrough curves for surfactants and for chloride from the combined tests in the Buchkogel region southwest of Graz/Austria, which were con-

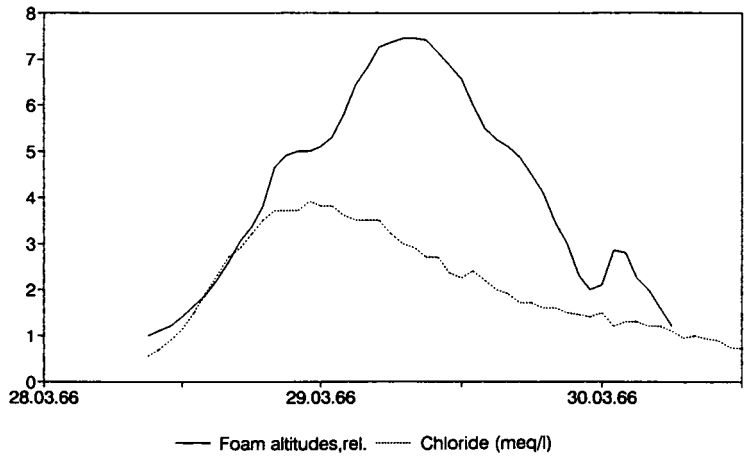

Figure 70. Breakthrough curves in the Bründl spring from the combined tracing test in 1966 in the Buchkogel region southwest of Graz/Austria for the surfactant Marlon AFR and chloride (after BATSCHE et al. 1967). Detection limit for the surfactant (begin and end of the breakthrough curve): 1:2 million; the maximum corresponds to a dilution of approx. 1:600,000. Distance injection site – Bründlspring: 800 m.

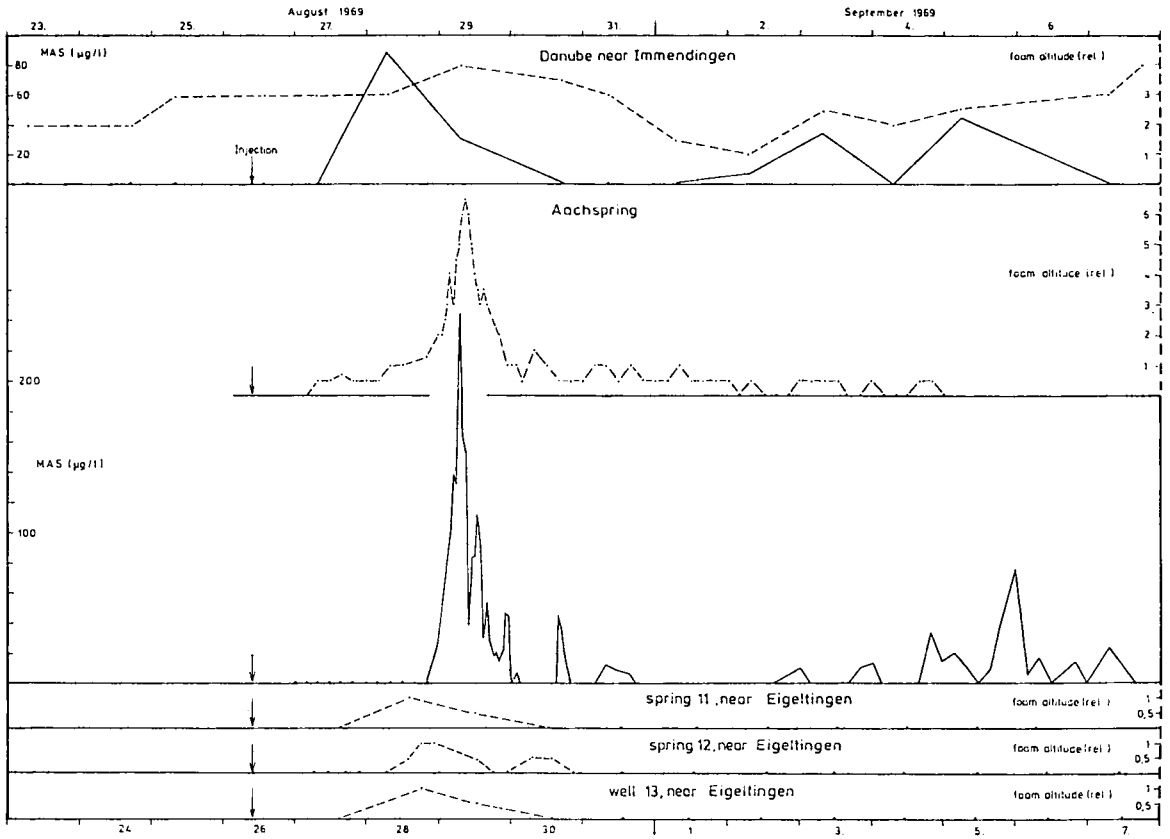

Figure 71. Comparative determination of surfactants with the shaking method and the colorimetrical method in the Danube-Aach-Test. Injection of hard and soft surfactants east of Liptingen (Injection sites 24,25 in Fig. 75). Dotted line: Foam height determination by SCHNITZER, solid line: methylene blue active substances, determined by GEISLER at the Danube percolation sites and in the main reemergence site, the Aach spring. In the three Eigeltinger observation sites, the MBAS was under the detection limit of 2 µg/l.

ducted during the First Tracing Symposium in 1966 (BATSCHE et al. 1967). Ten kg of soft surfactants (Marlon AFR) were injected in the Feliferhofschwinde sinkhole west of the Buchkogel on 26 March 1966 between 16:30 and 16:40 hours and 300 kg of table salt between 16:45 and 17:05 hours as well as 100 kg of potash fertilizer with 60% K_2O between 17:05 and 18:00 hours. The ordinate depicts the relative foam height for the surfactants, which W.A. SCHNITZER had determined later in the laboratory of the Geological Institute of the University of Erlangen. Both curves agree very well. However, the chloride maximum appears much earlier than the surfactant maximum: the surfactant after 62 hours with chloride the maximal concentration appears after 54 hours. Surfactants were also used in the preliminary tests for the Second Tracing Symposium in Malm Karst with other tracers (BATSCHE et al. 1970). The tests were conducted on 26 August 1969 in a total of nine injected sites in the Danube-Aach-region. In the brick factory pit east of Liptingen/Cty. Tuttlingen, 200 kg of a hard surfactant, Marlon TP 375, and 200 l of a soft surfactant, Marlon AFR with a 30% surfactant content, were injected (Fig. 75: E). The samples were analysed with two methods, the shaking method and the more exact colorimetrical method (Fig. 71). The second method allows, with the help of the coupling of the anionic surfactants onto methylene blue, a quantitative determination of the so-called methylene blue active substances (MBAS). This method was first developed by LONGWELL and MANIECE (1955) and, after a manifold of modifications, included in the German Standard Methods (DEV, H23). A summary of the method used by R. GEISLER in the Danube-Aach-Test surfactant determination follows.

Summary of the surfactant determination in water
100 ml sample water in a 250-ml-shaker-funnel
+ 10 ml disodium phosphate solution (12.52 g/l, pH 10.0)
+ 5 ml methylene blue solution, neutral (0.35 g/l)
+ 15 ml chloroform (purified),
shake for two minutes, allow to settle.

Pour the chloroform phase into another 250-ml-shaker funnel, which already contains:

100 ml dist. water + 5 ml methylene blue solution, acidic (0.35 g methylene blue + 6.5 ml conc. sulfuric acid per litre).

Add to the first shaker funnel:

10 ml chloroform (purified),

shake for one minute, let it settle, drain the chloroform phase into the second shaker funnel, repeat the shaking of the first shaker funnel with 10 ml of chloroform for one minute, after allowing to settle, drain the chloroform phase into the second shaker funnel.

Shake the second shaker funnel, which now contains a total of 35 ml chloroform, for two minutes and again allow to settle. Drain the chloroform phase over chloroform soaked cotton wool into a 50-ml-flask and fill with chloroform up to 50 ml and swirl lightly.

Colorimetry is carried out at 650 nm against a distilled water blank that was prepared in the same manner. Reference solutions are made by diluting tetrapropylene benzene sulfonate-reference solution, e.g. 5% MERCK 8202. 1 µg/l anionic-active surfactants have an extinction of approx. 0.9 per cm. A detection limit of 1 mg/l can

be reached with samples from very clean waters when using a layer thicker than 1 cm.

Attention: All glassware can be cleaned only with chloroform and alcoholic hydrochloric acid (10% HCl + 2% alcohol)! All reagents must stand for 48 hours. Samples, which are not analysed within one day must be prepared with 2-3 ml 0.001% corrosive sublimate solution per litre of sample water (FISCHER 1962).

Note: This method measures hard and soft anionic surfactants, but not cationic and non-ionic surfactants. Results are given in 'Methylene blue active substances (MBAS).'

Comparing both methods in Figure 71, an approximate agreement for the main reemergence site, the Aach spring, can be seen. In the Danube near Immendingen, where the greater percentage of the Aach spring water seeps underground into the percolation sites there, there are considerable differences between the foam heights and the MBAS results. Apparently, the foam height method also records other substances than just the surfactants. Similar results have been recorded at the three springs near Eigeltingen, where surfactants were detected with the foam height method, but the colorimetric method did not deliver positive values. Due to the almost simultaneous appearance of the positive foam height results near Eigeltingen with the main surfactant reappearance in the Aach spring, a connection to the Liptinger injection site can be assumed with all probability.

Of late, the HPLC-determination method for surfactants with fluorimetrical detection is being used more and more. Excepting the detection limit of 1 µg/l, this method has no disturbances, since matter specific components are determined (HUBER 1989).

Application areas

The main application area has been in karst groundwater tracing tests. Most tests were conducted by W.A. SCHNITZER. The farthest distance successfully traced with surfactants was 11.9 km and was between Liptingen and the Aach spring (compare previous section). Of the 262 kg of hard and soft surfactants injected in the Aach spring, nearly 80% was recovered, with the spring discharge taken into consideration. If it is remembered that soft surfactants undergo a partial decay underway, there was an almost complete quantitative recovery in the Aach spring. The breakthrough maximum of 235 µg/l in the Aach spring was 69 hours after the injection. The centre of the breakthrough curve was reached 83 hours after the injection; the resulting flow velocity (along the crow-fly distance) was 144 m/h. (BATSCHE et al. 1970).

The only test in a pore-groundwater aquifer, which has been described, was conducted in the Pleistocene of the Upper Rhine valley (KÄSS 1972). This tracing test was carried out during the Second Tracing Symposium. In a depth of 21-23 m under the surface, 30 kg of hard surfactants were injected in September 1970. Due to the narrowness of the injection hose and the viscosity of the injection solution, the injection took 26 hours. In the same depth 10 m downstream, an observation borehole was set up and 6 m to the right and left of it further boreholes in the same depth also. Figure 72 shows the breakthrough curve from the downstream borehole. Surfactants were not detected in either of the side boreholes. From the mean flow time of 30

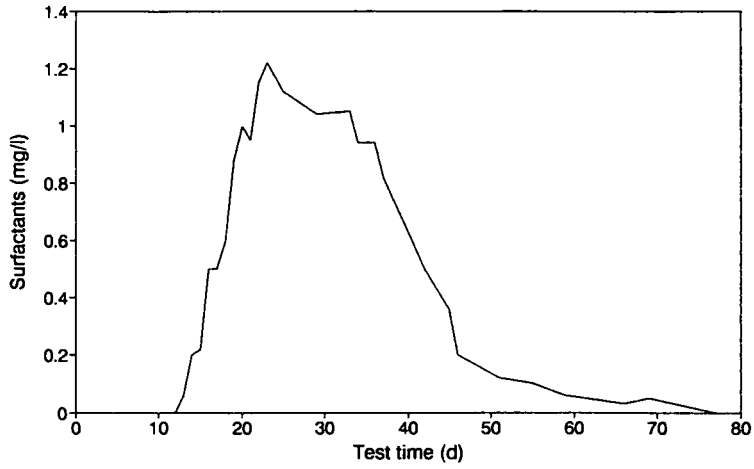

Figure 72. Breakthrough curve for hard surfactants in pore-groundwater at a distance of 10 m in natural groundwater flow.

days and a groundwater table gradient of 0.6 ‰, a permeability coefficient of $6.0 \cdot 10^{-4}$ (m/s) can be calculated for a hydraulic effective pore space of 0.25.

In tracing tests in oil field waters, surfactants have been successfully used in Pennsylvania over a distance of approx. 160 m in sandstone oil fields (STURM & JOHNSON 1950).

With river bank filtration in polluted receiving streams, anionic detergents can breach nearby groundwater tappings and act as 'natural tracers' (see Section 2.12).

Ecotoxicology of the linear alkyl benzene sulfonates

Since only the anionic surfactants are used in tracing tests, only the linear alkyl benzene sulfonates (LAS) are considered here. According to all observations, anionic surfactants are non-toxic for warm-blooded animals. They are used in considerable amounts in cleaning and laundry supplies. The drinking water decree for Germany (TVO) recommends a limit value for 'surfactants' of 0.2 mg/l, requires however as a reference substance dodecylbenzenesulfonicmethylester (BGBL 1986a).

For the water flea (*Daphnia magna*), a LC_{50} value between 4 and 20 mg/l was determined for four different products, for ide (*Leuciscus idus*) between 1.0 and 6 mg/l (FISCHER & GODE 1977). LIEBMANN reported the following results in 1960 (in mg/l):

Lethal	For fish	For other aquatic animals
Alkyl sulfonate	4- 5	5-10
Alkyl arylsulfonate	3- 4	2-10
Non-ionic surfactants	5-10	5-10.

Further detailled investigations about the influence of linear alkyl benzene sulfonates upon algae and other water organisms can be found in KIMERLE (1989). Long chained LAS are somewhat more toxic than short, decay however faster.

Plants such as grass, beans, radishes, and potatoes do not suffer growth damage even at a load of up to 0.1 mg per gram fresh weight. Newspapers have reported that flowers watered by lock keepers with lockage river water grow exceedingly well!

Appraisal

Surfactants can be used as a helpful accessory tracer in many cases. If hard surfactants are used and determined with colorimetric or HPLC-analysis, good quantitative results can be achieved. Due to the anionic form of these substances, interaction with the underground due to adsorption is not to be expected. The production of foam at the injection and recovery sites needs to be kept to a minimum.

The analysis is complicated, if traces of the substances are to be detected. Therefore, the application possibilities are limited with respect to the analytical aspects, although the production costs are comparatively low for surfactants.

2.3.2 *Aromas*

Along with surfactants, W.A. SCHNITZER also introduced aromas into hydrological tracing techniques (SCHNITZER & WAGNER 1967). The authors reviewed a large number of organic chemicals with respect to their toxicity, intensity, stability, and cost and selected three substances for testing. The properties of the three substances are listed together in Table 9. The requirements which aromas need to fulfil as tracers, were listed by SCHNITZER and WAGNER in 1968.

The following can be said regarding the three suggested aromas:

Limonene (CAS: 138-86-3) is the main ingredient in turpentine and in citrus oils. Special care is required in handling limonene, since the considerable vapour pressure leads to a high risk of ignition (BGBL 1986b). Moreover, limonene vapours irritate the eyes and can produce dizziness (HOMMEL 1987). Furthermore, according to the

Table 9. Aromas for water tracing (after SCHNITZER & WAGNER 1967).

Species	Limonene	Isopentyl salicylate	Isobornylacetate
Synonyms	Dipenten, (±)-limonene, p-mentha-1,8-dien, 4-isopropenyl-1-methyl-cyclohexen, carven	Isoamyl salicylate	2-exo-bornylacetate, isoborneolcamphor-acetate
Chem.formula	$H_3CC_6H_8CCH_3CH_2$	$C_{12}H_{16}O_3$	$C_{10}H_{17}OCOCH_3$
Appearance	Liquid, colourless, easily movable	Liquid, colourless	Liquid, colourless
Density	0.848	1.065	0.98
Boiling point	178°C	275°C	225°C
Properties	Inflammable, vapour explosive	Inflammable	Inflammable
Stability in air contact	Easily oxidizable, sensitive to light	Very good	Very good
Toxicity	Poor toxic, vapour irritable for eyes and skin	See text	Poor toxic, vapour irritate eyes, narcotic
Solubility	Poor in water, soluble in alcohol	Nearly insoluble in water, good in alcohol	Poor in water, good in alcohol, ether, benzene, trichlormethane
Ability to emulsify	Good	Good	Very good
Odour	*Like turpentine, diluted: like lemon*	*Like orchid blossoms*	*Like pine needles*
Olfactiometric value	$5 \cdot 10 \cdot 10^{-6}$	$100 \cdot 10^{-6}$	$50 \cdot 10^{-6}$

dangerous substances decree appendix, Section VI No. 967, limonene is a skin irritant; if it comes in contact with the skin, it should be immediately washed off with plenty of water (BGBL 1986b). The LC_{50} value is 33 mg/l for ide (JUHNKE & LÜDEMANN 1978). With proper care taken in handling limonene, no health risks are to be expected. In the catalogue of substances harmful to water, limonene is listed as 'weakly dangerous to water' (LTwS 1980). Limonene smells strikingly like lemon oil. Due to limonene's oxygen sensitivity, its odour can change to pine needles after a time being, which can cause it to be mistaken for isobornylacetate. This was also observed during the Danube-Aach-Tracing tests in 1969.

Isopentylsalicylate (CAS: 87-20-7). This ester of salicylic acid and pentyl alcohol can be split into its components in the body. SCHNITZER and WAGNER (1967) found nothing published concerning the pharmacology of the ester. Salicylic acid methylester however, is contained in some medications, which are for topical application only. Salicylic acid is practically non-toxic; it is bactericidal, a fungicide and antipyretic. Isopentylsalicylate has a very intensive odour and smells like orchid blossoms.

Isobornylacetate (CAS: 124-76-5). It is a synthetic product and does not occur naturally. Related esters are used as medications, e.g. as a sedative. A toxic effect is not to be expected. It smells strongly like pine needles.

Since all three suggested aromas are liquids and not very soluble in water, they must be emulsified before they can be injected. To do this, the liquid aroma is intensively stirred with approx. 1/10 of its volume with soft surfactants. With amounts over 10 l, a strong electro-stirrer is a great advantage. Isobornylacetate is readily emulsified, the other two less so.

In the northern and southern Franconian Alb, SCHNITZER and WAGNER conducted several karst water tracing tests using aromas in 1967. Most of them were accompanied by other tracers as a comparison. At the well-known underground Pegnitz flow under the Wasserberg near the city of Pegnitz, the first tests using all three aromas, one after the other, were conducted in 1966 (Fig. 73).

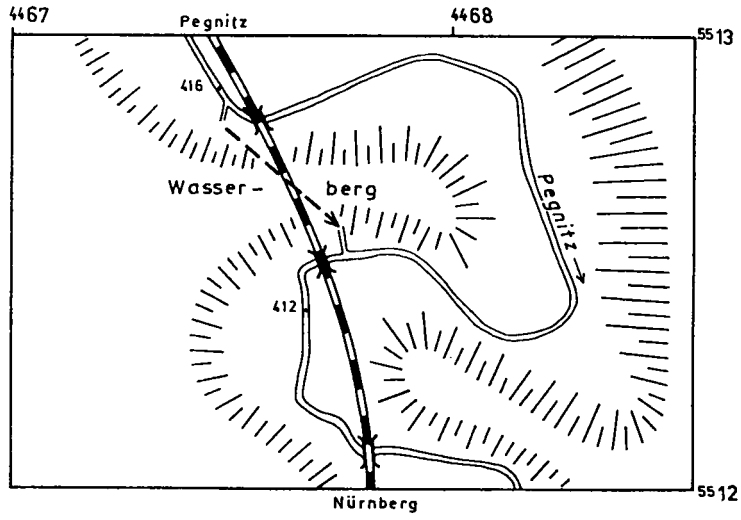

Figure 73. a) Map of the Wasserberg near Pegnitz/northern Franconian Alb, South Germany.

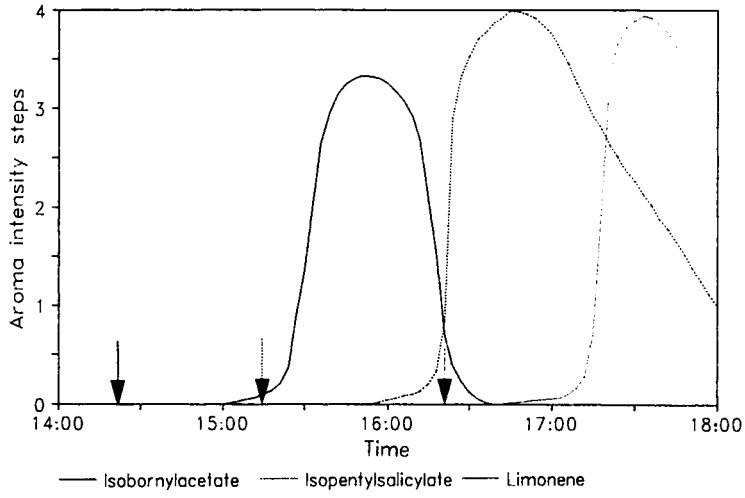

Figure 73. b) Breakthrough curves for the triple test using aromas near Pegnitz/northern Franconian Alb, South Germany (after SCHNITZER & WAGNER 1967).

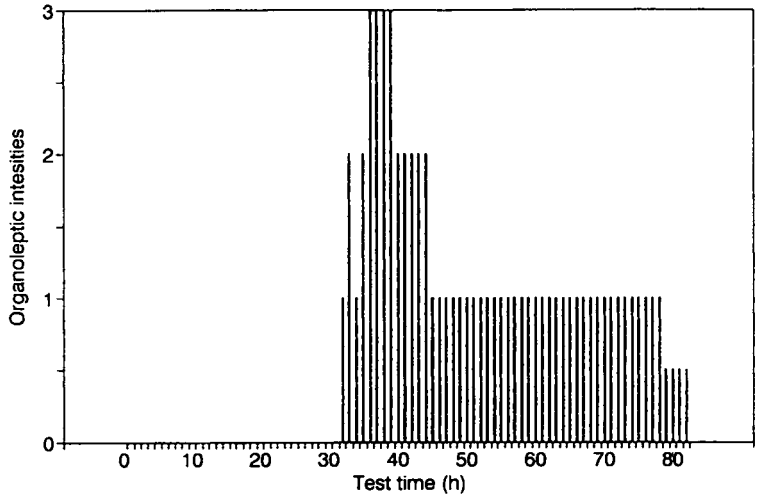

Figure 74. Breakthrough curve for limonene in the Aach spring after the injection in the Danube sinkhole near Immendingen on 26 Aug.1969. Flow distance: 13,380 m. Intensity according to the organoleptic sense test; 1 = weak, 2 = mid-strong, 3 = strong pine needle smell. After 79 hours there was only a very weak taste noticeable.

The authors stressed that quantitative results cannot be achieved with these tracers, since the sense and sensitivity of smell are subjective. For example in mineral oil accidents, it was found that smokers were less sensitive to organoleptical influences than nonsmokers. The same holds true for people with colds. Nevertheless, the authors' publication shows several breakthrough curves with 3-4 organoleptic intensity levels, such as 'very weak – weak – definite – (strong)' (Fig. 74).

In the meanwhile, it has been shown that aromas can be quantitatively determined at

the observation sites using gas chromatography. With pentane extracts, these tracers could be definitely detected at the starting level of organoleptic sensitivity.

Most substances that have an intensive odour also have a noticeable taste. In the Danube-Aach-Tracing-Test in 1969, aromas were injected at two sites: 1. In the Danube sinkhole near Immendingen (No.19 in Fig. 75) 150 l of limonene (together with 1000 kg of KCl with 60% K_2O), 2. east of Liptingen (No.25 in Fig. 75) 70 kg of isobornylacetate (together with 262 kg of hard and soft surfactants). In the night from 27th to the 28th of August, i.e. approx. 1½ days after the injection, a strong foreign odour

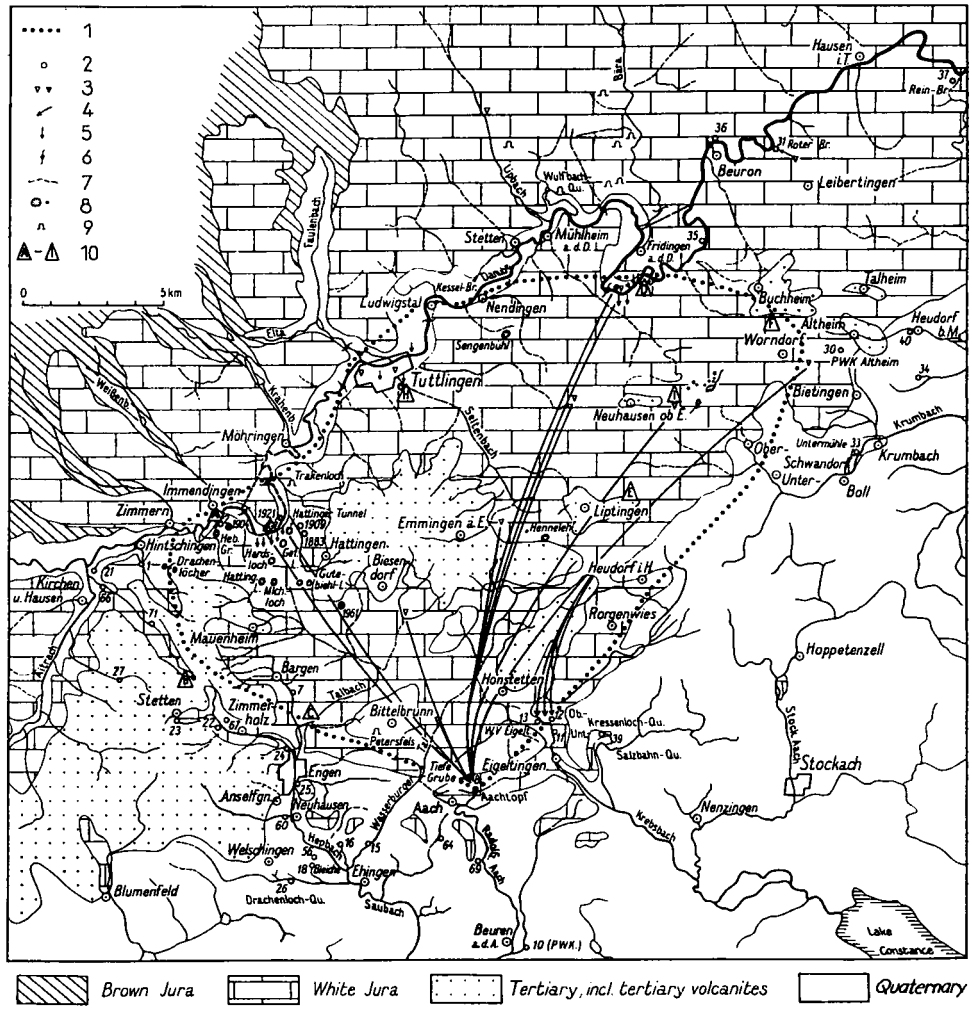

Fig. 75. Tracing test in the area of the percolation sites of the Upper Danube – Aach spring (Southwest Germany). The numbers at the injection sites (triangles) correspond to the chronology of the tracing tests, 1 = supposed karstic hydrographical recharge area of the Aach spring, 2 = springs, wells, 3 = tracing tests No. 1-35, 4 = subterranean waterways with tracing tests, 5 = percolation points, sink holes, 6 = discharge registration, 7 = dry valleys, 8 = dolines, partly with year, 9 = caves, 10 = injection points of the preparation work for the 2nd Symposium Water Tracing 1970.

was noticed in the Aach spring and was noticeable even up to a radius of 50 m around the spring. The water was tasted immediately and a pine needle taste was identified in the Aach spring in the hourly samples. However, the organoleptical effect was not from the isobornylacetate, but rather, as the analogy with the simultaneously appearing potassium shows, from the lemon oil smell of the limonene. Since limonene is oxygen sensitive, it was most likely transformed during the underground passage. The taste intensities in the Aach spring, the main reemergence site, were divided into three levels 'weak – middle – strong.' The strongest intensities correlated to the beginning of the potassium increase. The pine needle taste could be identified throughout the whole appearance of the potassium (Fig. 65). If the substance had been isobornylacetate, it could not have appeared before the 69th hour of the test, in accordance with the surfactant passage. Therefore, the tasteable and smellable substance in the Aach spring must have come from limonene.

Approx. three weeks later, W.A. SCHNITZER undertook the laboratory analysis of the aromas by distilling 20 ml out of 100 ml sample water. The intensity of the odours from the distillate ranged from 'very low' to 'very acrid'. However, there is hardly any correlation with the breakthrough curves from the accompanying tracers (Fig. 71).

An interesting test was conducted by A. KNOP with shale oil in 1870 at the Danube's main percolation site at Brühl between Immendingen and Möhringen (KNOP 1878). Along with road salt and uranine, the strong smelling shale oil from the shale oil deposit Dalkeith between Glasgow and Edinburgh was injected to see if the percolating Danube water flow to the Aach spring. On 22 September 1877, KNOP injected 600 kg of the 'Glasgow shale oil' in the Danube sinkhole near the 'Hattinger Weglöchern' (No.1 in Fig. 75). Indeed, 62 hours later, the Aach water had a 'foreign, creosote-like taste'. Oil streaks were not observed.

For a while, the company H.Nördlinger sold a product for checking pits, 'Pit-check Saprol,' that smelled strongly like illuminating gas and tar (OHLMÜLLER & SPITTA 1921).

2.3.3 *Other chemicals*

Phenols

Phenols are organic compounds with one or more hydroxyl radicals on the benzene ring.

In 1926 TIMEUS recommended using creosote and phenols in tracing tests in karsts. However, whether Timeus actually used these compounds is not known, nor how he would have identified them.

In 1937, HETTCHE (1941) from the Munich Hygiene Institute was the first to conduct a tracing test with phenol (Acid. Carbolicum liquefactum) in a groundwater tracing test in the moraine area Mangfall (Upper Bavaria, Germany). 10 kg of phenol and 3 kg of uranine were injected by HETTCHE into the infiltrating sewage water of the city H. (? Holzkirchen). The 21 observation sites, which were situated in a half circle around the injection site with a radius of several km, were certainly too far away to provide positive proof.

Another test conducted by the Hygiene Institute of the University of Munich in the Munich Gravel Plain in 1940 was able to prove that phenol can be successfully used as

a groundwater tracer (KISSKALT 1941). On 9 April 1940, 3 kg of a phenol solution was injected in a well with a water level 12.4 m deep. On 5 May 1940, 26 days later, the phenol reappeared for the first time in an observation well north-northeast of the injection site. WEBER (1941) analysed the daily samples and published the breakthrough curve from the data. On 31 May 1940, after 52 days, the maximum was reached with 207 mg/l phenol; on 30 June 1940, a phenol content of 0.2 mg/l was still ascertainable in the observation well.

The phenol contents were analysed qualitatively as well as quantitatively. The qualitative analysis was completed by adding 2 ml of a 1% Caporite solution to 100 ml of sample in a sealable bottle (Caporite is calcium hypochlorite, $Ca(OCl)_2$, and used for medicinal purposes). After warming to 50°C, fixing salt $Na_2S_2O_3$ to bind the excess chlorine is added (HETTCHE 1941). The chlorophenols produced by this reaction have an extremely intensive taste and smell and are therefore dreaded in water supply plants. Due to their distinctive phenolic taste and odour, chlorophenols are still clearly recognizable in a dilution of 0.002 mg/l.

For the quantitative determination, WEBER used the colorimetrical method after GIBBS (1927). In this method, a pH 9.24 saturated solution of 2,6-dibromchinon-4-chlorimide is added to the sample. In the presence of phenols, the sample will then turn blue. The pH 9.24 buffer solution is made by dissolving 19.12 g sodium tetraborate-monohydrate in 1 l water. Gibbs' reaction should produce a detection limit of 0.04 mg/l. The more sensitive coupling reaction with p-nitraniline is more troublesome, yet it can reach a detection limit of 1 mg/l in clean water.

DOLAK (1966, 1969) described the possibility of tracing oil field waters with phenol (see also Section 5.6.2).

In 1957, GROSCHOPF reported on an unplanned trace, which resulted in considerable damage. According to the report, a sudden foul smell and taste occurred on 29 September 1954 in the water supply system of the city of Ulm (South Germany). Painstaking research revealed, that the source of the pollution was coal tar used in road construction on the karstic Alb flat upland area in the catchment area of one of Ulm's water tappings. Heavy rainfall washed out the soluble contents of the coal tar oil into the water supply and due to the chlorination in the system, the chlorophenols were produced and disrupted the water supply.

Carbohydrates

According to DANIELS and MAYER (1957), the Wintershall AG company regularly uses dextrose to trace re-injection water in oil fields. The tracer used is Hydrol, which is a 40% by-product from the 'Maizena' production. The quantitative determination with potassium hexacyanoferrate-III and iodometrical titration supposedly reaches a detection limit of 10 µg/l.

DOLAK (1969) reports that Lower Austrian oil fields have been successfully traced over distances between 105 and 520 m with 5 kg of 'glucose.'

m-Trifluormethyl Benzoic Acid (m-TFMB), CAS 454-92-2

Synonyms: 3-Carboxybenzotrifluoride,
α,α,α-trifluor-m-tolyl acid

Chem. formula: $HCOOC_6H_4CF_3$, $C_8H_5O_2F_3$

MALCOLM et al. (1980) emphasized the high sensitivity of this and related substances in the HPLC-analysis. The NAGRA (National Assocation for storing radioactive wastes) uses m-TFMB for the determination of the revolution speed of the drilling mud. This substance is well soluble in alkaline water and acts anionic. Thus, it is not adsorbed by clay minerals. In drilling muds that are only weakly polluted, a detection limit of 0.1 µg/l can be reached with UV-detection after HPLC-columns. This low detection limit was only possible because in the described case, deionate + groundwater was used as the drilling mud (NAGRA 1985). Analysis is complicated and time-consuming; in 1985, 1 kg of m-TFMB cost 500 Swiss Francs.

Perfluor chemicals

This group contains sulfur and carbon compounds that are totally fluorinated, i.e. other than S- or C-atoms, they have only fluorine in the molecule. The sulfur-fluorine compound SF_6 is a gas; the carbon-fluorine compounds mentioned here are liquid at normal temperatures. Due to their extremely low detection limit, they are used as a tracer in surface waters, preferably in lakes and oceans. Analysis is completed exclusively with gas chromatography with electron capture detectors (ECD). In all publications, the high stability of the perfluor compounds is stressed. This is however a reason to exercise caution in using these substances considering the decay in the ozone layer caused by the fluor compounds.

Sulfurhexafluoride (SF_6) (CAS: 2551-62-4)

Sulfurhexafluoride is a gas. It sublimates at –64°C. SF_6 is non-toxic and dissolves in 25°C water only to 32 mg/l. This substance has been used several times in Californian lakes and drinking water reservoirs to determine the water balance. In further tests in Rockland Lake in New York/USA, the gas exchange coefficient in dependency of the wind speed was measured (WANNINKHOF et al. 1985). Injection in surface water is completed with an atomizer under the water surface or by producing large quantities of SF_6-saturated water. The gas chromatographical analysis of gas and water samples is described in WATSON et al. (1987). The detection limit in water is at 10^{-16} mol/l SF_6. In evaluating the tests, it must be remembered that there is a worldwide increasing tendency in the background levels in the oceans as well as in the air. In the North Atlantic in June 1984, $3 \cdot 10^{-16}$ mol/l was measured at the water surface. At the same time, the air contained approx. $1.5{:}10^{12}$ volume parts SF_6. In 1992, the content in the air was already globally $2.8 \cdot 10^{-12}$. Assuming an annual increase of 8.3%, in the year 2030, there will be $20 \cdot 10^{-12}$ SF_6 in the air worldwide (MAISS & LEVIN 1994).

In her dissertation, ROBERTS (1986) described the infiltration through the unsaturated zone, whereby along with SF_6, also bromodifluoromethane and chlorfluoroethane were used as tracers.

Perfluor hydrocarbon compounds

In the literature, the compounds listed in Table 10 are mentioned as possible tracers in lakes and oceans.

PF3 is a skin irritant according to ALDRICH (1996/97). Only perfluorodecalin appears to have reached a certain importance in water tracing. To inject perfluorodecalin, an emulsion must be made using ultrasound and surfactants. It has been calculated that

Table 10. Perfluor hydrocarbon compounds used as tracers.

Species	Perfluorodecalin	Perfluoromethyl-cyclohexane	Perfluoro-3,4-di-methylcyclohexane
CAS RN	306-94-5	355-02-2	335-27-3
Abbreviation	PFD, PP5	PF2	PF3
Synonyms	octadecafluoro-decahydro-naphthalene	tetradecafluoro-methylcyclo-hexane	hexadecafluoro-1,3-dimethyl-cyclohexane
Chem. formula	$C_{10}F_{18}$	$C_6F_{11}CF_3$	$C_6F_{10}(CF_3)_2$
Mol mass	462 g/mol	350 g/mol	400 g/mol
Melting-point	–10°C	–	–55°C
Boiling-point	142°C	76°C	101-102°C
Density	1.908	1.787	1.828

a $C_{10}F_{18}$-drop with a diameter of 1 µm needs 3 hours to totally dissolve (WATSON et al. 1987). Using a drip attached to a buoy that is towed by a ship, the 20% $C_{10}F_{18}$-emulsion can be injected in the ocean. For 1 l emulsion, over 1½ hours are needed. In February 1985 in Lyme Bay/English Channel, a $C_{10}F_{18}$-test was started to investigate the drifting and gas exchange. The tracer was injected in the manner described above in approx. 5 m depth. Around two weeks later, the ship 'Hermes' collected samples northeast of Cape Start Point. These samples only recorded the border areas of the $C_{10}F_{18}$-distribution with a maximum of $15 \cdot 10^{-15}$ mol/l.

Benzoic acid

In Dixie valley (Nevada/USA), 100 kg of benzoic acid, which had been dissolved with benzenesulfonic acid in 36 m^3 hot brine, was used as a tracer in thermal water. It was necessary to prevent oxygen in the air from coming in contact with the injection solution (ADAMS et al. 1989).

2.4 RADIOACTIVE AND ACTIVABLE ISOTOPES

H.Behrens

2.4.1 *Introduction and basic principles of radioactivity*

The group of radioactive and activable isotopes includes all those tracers intentionally injected into the system that are detected (concentration measurements in the water sample) by measuring the radioactive radiation. Radioactive tracers are those substances that are already radioactive when injected into the hydrological system. In fact, only the small amount of the radioactivity, which is actually transmitted into the sampling site or the sample itself is measured. With activable isotopes, non-radioactive substances are used, which can be transformed with a good yield into radioactive tracers through appropriate nuclear reactions, preferably by irradiation with neutrons. The activation occurs after the sample has been taken and thus only the small amount of injected tracer that is actually in the sample is activated. The tracer is detected by measuring the radioactivity produced in the sample.

Radioactivity is the energy released during the decay process of unstable nuclides (atomic types) as is emitted as radioactive radiation. The known chemical elements are made of stable and radioactive nuclides (in terms of a specific element, they are referred to as isotopes). Some elements, specifically technetium, promethium, and all elements with an atomic number >84, only exist as radioactive isotopes. During radioactive decay of a nuclide, another nuclide develops, which can be either stable or also radioactive (radioactive mother/daughter pairs). Every radioactive decay ends finally with a stable endproduct.

There are radionuclides, which are so long-lived, that they have not yet completely decayed since the earth was created (uranium, thorium, potassium-40, and others). Radionuclides with a shorter lifespan occur in natural decay series (e.g. in the uranium decay series). Some radionuclides, including some of the most important ones, are only accessible through nuclear processes. Other than the 270 stable nuclides there are also ca. 1000 radionuclides known today. These nuclides and their properties are listed in nuclide lists (e.g. LEDERER & SHIRLEY 1978) or in well-organized nuclide charts (e.g. SEELMANN-EGGEBERT et. al. 1984). As an example, the makeup of the element indium and the neighbouring elements from different isotopes is displayed from a section out of the nuclide table in Figure 76.

The amount or concentration of radioactive substances is usually given in activities. In general, well detectable activities of radioactive substances correspond to extremely small quantities of the substance. Due to this high sensitivity in detecting the radioactive substances and since they were easily available after World War Two, they have been used as very interesting hydrological tracers. The discussion as to their applicability and even their practical use itself, has added important impulses to advances in tracer hydrology. Since then, their importance as a tracer group has decreased because of increasing concerns about using radioactive substances in the environment as well as further developments in other competing tracers.

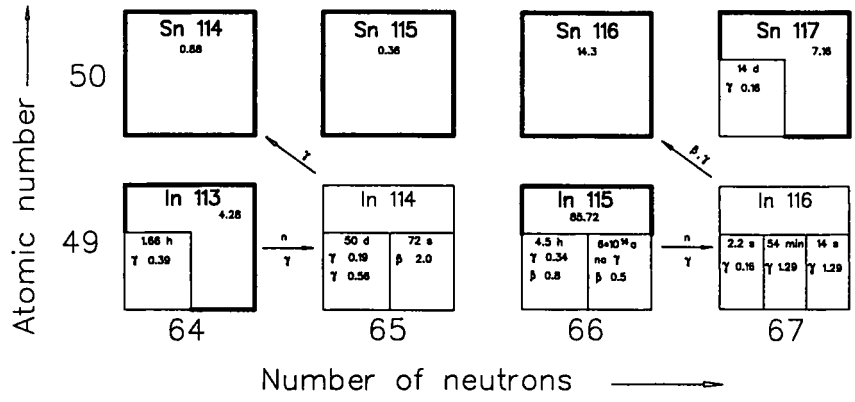

Figure 76. Section out of the nuclide table in the area of the elements with the atomic numbers 49 (indium) to 50 (tin). Boxes with thick frames show the stable, the other boxes show the radioactive nuclides. Half-life times and energies of the emitted radiation listed in the boxes. Examples: ^{114}In ($T_{½}$ = 50d) and ^{116}In ($T_{½}$ = 54 min) decay to ^{114}Sn and ^{116}Sn, respectively under transmission of 0.56 and 0.72 resp. 1.27 MeV γ-radiation (after SEELMANN-EGGEBERT et al. 1984).

The likewise very efficient activable isotopes, whose use does not radioactively stress or burden the environment, have not been utilised as much due to their relatively high analytical expenditure.

2.4.2 *Radioactive decay*

There are specific probabilities for the atoms of the different radioactive nuclide types to decay spontaneously inside a specific timespan. Although the point in time of the decay for each individual radioactive atom is not known, it is possible to statistically exactly describe the decay for a sufficient quantity of atoms through the decay law (see Section 2.11.3.1).

2.4.2.1 *Law of radioactive decay*

The radioactive decay law states that the number of the decaying atoms in the time unit (decay rate) is proportional (decay constant λ) to the actual number of atoms in the radionuclide:

$$-dN/dt = \lambda N \tag{2.1}$$

where N = number of atoms, t = time, λ = decay constant.

After time t, there are still N of the initial N_0 atoms present:

$$N = N_0\, e^{-\lambda t} \tag{2.2}$$

The time, after which half the initially present atoms have decayed, is called the half-life time ($T_{1/2}$). The following relationships are given:

$$N/N_0 = 0.5 = e^{-\lambda . T_{½}} \tag{2.3}$$

therefore:

$$\lambda = 0.693/T_{½} \tag{2.4}$$

and

$$N = N_0\, e^{(-0.693\, t)/T_{½}} \tag{2.5}$$

Radioactive decay is a first order reaction. If the logarithm of the amount of a radionuclide still present at time t (which corresponds to the measurable radioactivity at this time) is plotted against time, the curve is linear (Fig. 77).

2.4.2.2 *Activity units and amounts of radionuclides*

In quantitatively determining the amount or concentrations of radionuclides, the fact that the decay rate is proportional to the amount of the respective radionuclide is used (Eq. 2.1). However, the results are usually not expressed as the amount of the chemical substance, as in moles, but rather the results of the radioactive measurements are given. The concentration in radiological units corresponds to the decay rate per sample volume.

Earlier, radioactivity was given in Curie (Ci), which was the decay rate for 1 g of

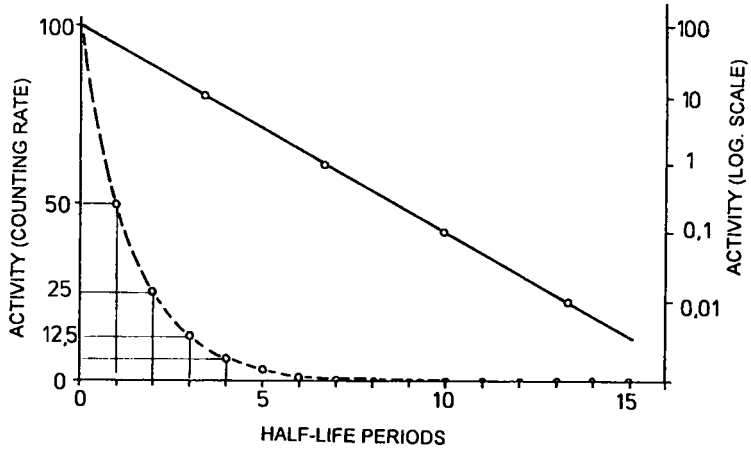

Figure 77. Decrease of activity of a radionuclide with the decay time; linear (---) and semi-logarithmic(——) graphs.

radium of about $3.7 \cdot 10^{10}$/s (subunits: mCi, μCi, nCi, pCi). Today, bequerel (Bq) is the official activity unit (1 Bq = 1 decay/s).

The relationship between activity, half-life time, and substance amount of a radionuclide can be derived from the Equation (2.1) and (2.4):

$$-dN/dt = (0.693/T_{½})\, N \tag{2.6}$$

N is the number of atoms, which have the activity dN/dt, in Bq, with $T_{½}$ in seconds. The number, N, can be expressed as a mass (M):

$$M = N\,(A/6.023 \cdot 10^{23}) \tag{2.7}$$

where A = atomic mass, $6.023 \cdot 10^{23}$ = AVOGADRO'S constant, the number of atoms in a gram atomic weight

As an example, the mass M of 100 Bq of bromine-82, whose activity which can be measured very well and accurately with customary radiation measuring units, is calculated here ($T_{½}$ for Bromine-82: 36 h = 129,600 s):

$$M_{Br\text{-}82} = (100 \cdot 82 \cdot 129\,600) / (0.693 \cdot 6.023 \cdot 10^{23}) = 2.55 \cdot 10^{-15}\ g$$

It is obvious that practicable activities from so-called 'carrier-free' radionuclides (no addition of stable isotopes of the same element) are identical with very small substance amounts. The relationship between activity and amount of substance is defined as the 'specific' activity. If for example, stable bromine (which consists of the stable isotopes bromine-79 and bromine-81) is added to the carrier-free bromine-82, the specific activity of the total radioactive bromine is reduced, but the activity itself stays the same.

2.4.2.3 *Decay types and properties of radioactive radiation*

Radionuclides can release their decay energy in different ways. The decay energy can be released as kinetic energy in small emitted particles, which usually carry an electrical charge (α- and ß-radiation) or the energy can be emitted as pure radiation

(x-ray and γ-radiation). Frequently, both radiation types (corpuscular and electromagnetic radiation) occur simultaneously during decay.

Both radiation types can interact with matter. This occurs mainly with the electron shells of the respective atoms. The removal of electrons that occurs results in ionization, which is why radioactive radiation is also called 'ionizing' radiation. Due to this absorption process, the radiation vanishes. The interaction with matter is a necessary process for detecting radioactive radiation, e.g. in radiation instruments, but also with simple methods such as the blackening of photographic film.

The energy from radioactive radiation is usually given in electron volts (eV). An eV is the energy, which a charged particle with one electrical unit charge gains when accelerated by an electric potential of 1 Volt. The units keV (= 1000 eV) and MeV (= 1000 keV) are also used.

α-(alpha-)radiation

The particle radiation called α-radiation is emitted by only a smaller portion of the known radionuclides, mainly those in the region of the heavy elements from atomic number 84 on. The α-particles consist of two protons and two neutrons and thus correspond to the atomic nucleus of Helium-4. α-particles possess high energies of several MeV with specific discrete energy values for the individual nuclides. Due to their size, they react very strongly with material. They are completely absorbed by a few cm thick layer of air or a piece of paper, i.e. α-rays have a high ionization density.

Due to this property, α-activity is difficult to determine and thus α-radiation does not play much of a role in water tracing.

ß-(beta-)radiation

ß-radiation is also particle radiation. The ß-particles are either electrons (negatively charged) or positively charged particles with the same mass (positrons). Depending on the nuclide, the kinetic energy can be up to several MeV. The energy spectrum does not display discrete energy levels, but is rather a continuum from 0 MeV to a maximal ß-energy specific for each nuclide. The range of ß-radiation in air is on the order of several metres, in water the range is only a few millimetres for ß-radiation of ca. 1 MeV. Positrons react with electrons after they have released their kinetic energy. In this process, the mass of the two particles is completely transformed into radiation, resulting in emission of two γ-quanta of 0.511 MeV each ('annihilation radiation, cf. γ-radiation), which can be used for detection of positrons. The detection of ß-radiation is done preferably with laboratory instrumentation, ß-emitting radionuclides are only used in special applications as artificial hydrological tracers.

γ-(gamma-)radiation (incl. x-rays)

Essentially, there is no difference between x-rays and γ-radiation. Both are pure electromagnetic radiation, just as e.g. light or radio waves, and they consist of individual photons (quanta). X-rays originate by excitation of the electron shell and the energy ranges from 0.1 keV to 100 keV, whereas the energy released from the atomic nucleus by the γ-radiation is in the range of 10 keV to 10 MeV.

Photons can penetrate material unchanged, until they finally undergo interaction. The higher the photon energy, the lower the probability for such an interaction. The

larger penetration capability of the higher energy 'hard' radiation is based on this. Besides the mass of the absorber, the atomic number of the absorber also plays an important role in the absorption process.

Some properties of the γ-emitters make them especially suitable as radioactive water tracers. These properties, all mainly concerned with tracer detection, are:

– The high penetration capability of the γ-radiation; thereby, the γ-radiation can be also directly detected in a larger water sample and thus a good detection sensitivity can be achieved,

– The presence of discrete 'mono-energetic' γ-energies ('lines'), which are different and specific for each particular γ-emitting radionuclide; this allows a definite detection of the particular radioisotope even in mixtures with several radiotracers (examples for γ-spectra shown in Figs 81 and 82) and the ability to distinguish them from the background radiation (natural radioactivity, mainly cosmic radiation and radiation from the rocks),

– The availability of robust detectors suitable for field work, e.g. ones that can be placed directly in the water or in a well.

Therefore, the absorption processes of the γ-radiation are dealt with here:

– Photo effect: upon contact with the atom, the γ-quant fully passes its energy to an electron (excitation), which can then pass it on further in other processes,

– Compton effect: only part of the energy from the γ-quant is passed on to the electron, the rest of the energy stays in a new scattered γ-quant, which can leave the interaction site due to the penetration capability of the radiation. If this 'Compton quant' is absorbed in the same body, e.g. in a radiation detector, by a photo effect, the result is the same total-energy absorption as with an immediate photo effect.

– Further interactions, such as 'pair formation' (this is the reverse of the 'annihilation radiation' process mentioned above, see also further literature, such as SCHMEISER 1963, LIESER 1991, FRIEDLANDER et al. 1981, EHMANN & VANCE 1991), do not play an important role in tracer detection.

2.4.3 *The measurement of radioactive radiation*

The measurement of the radioactive radiation presupposes an interaction with the detection instrument, whereby physical signals are produced that serve as proof of detection. In early instruments, the energy from numerous individual decay processes were summarized as electric current (ionization chamber). Today the individual decay events are recorded. Almost always, the released electrical 'pulses' are counted and in some cases further characterized by determining their intensity. Radiation detectors generally consist of radiation sensitive detectors, which are connected to electronic equipment for processing and registration of the detector signals. The following deals shortly with the main features of the mode of action of different radiation detectors.

2.4.3.1 *Radiation detectors*

Counting tubes (Geiger counters)

Counting tubes are chambers filled with special 'counting gases', with an internal electrical field, usually between the electrically conducting counting tube which acts

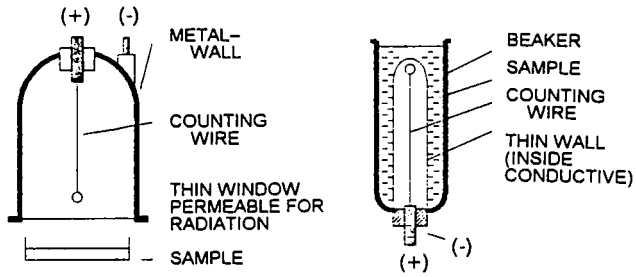

Figure 78. Counting tubes for detecting ß-radiation: End-window ('Bell') type (left) and beaker type for liquids (right).

as the (negative) cathode and the anode, usually a wire. If ions (e.g. ß-particles) enter this field, they are accelerated. When they hit the gas molecules, an ion avalanche is released, which is registered as an electrical pulse. γ-rays can also be registered, if they release electrons due to interaction in the counting gas or counting tubewall. The radioactive sample to be measured is either outside the chamber (Fig. 78 left) or in special cases, it is placed directly in the counter. The least expensive, but also least sensitive detectors can be inserted directly in the water with the dissolved radioactive tracer (Fig. 78 right). For particle radiation, the counting efficiency is high, provided that the particles actually enter the sensitive inner chamber of the counter. For γ-radiation, the efficiency ratio is usually low, since the mass of the counter with which the γ-radiation can cause an interaction is small.

Scintillation detectors

In scintillation detectors, crystals or other suitable transparent materials are used, in which entering radioactive radiation excites the atoms or molecules. Emitting light quanta, they then return to the initial state. These light quanta, which appear as weak flashes (Lat.: scintillare = sparkle) are recorded with photo-detectors, usually with photocathodes and secondary electron multipliers (photomultiplier tubes, PMT) and intensified to electrical pulses.

Such detectors often use NaI-crystals that are doted with Tl, that must be air- and light-proof, e.g. through an aluminium cover. These are optically connected by a window to the photocathode of the PMT. The γ-rays from a sample located outside the counter can easily enter the crystal due to their high penetration capability. Since the mass of the crystal is high, there is a considerable amount of interaction and thus a corresponding counting efficiency (Fig. 79).

It is important that there is a good proportionality between the transposed γ-energy and the height of the produced electrical pulse, so that with a pulse-height-analyser, the energy of the respective γ-radiation can be determined. This allows the identification of the γ-emitters.

Due to statistical scattering of the involved processes, most importantly the pulse amplification of the PMT, the height of the received electrical pulses varies. This limits the discrimination of the different γ-energies.

Suitable plastics can also find use as scintillation detectors. A special type of scintillation detector is used in the liquid scintillation counters.

In this case, a liquid scintillator, a mixture of suitable organic materials, is mixed directly and homogeneously with the emitter to be measured, here water or a sample

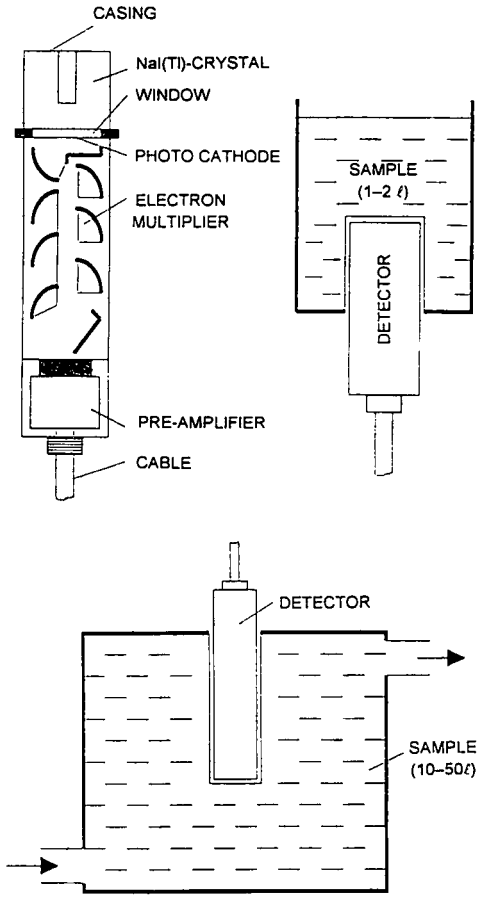

Figure 79. NaI(Tl)-scintillation detectors (left: well type, for insertion of small samples; right: arrangement with ring beaker; below: arrangement with large flow-through container).

so prepared. The 'cocktail' so obtained is then filled into counting vials and the flashes so produced are registered by two PMT's (Fig. 80). Since in this arrangement the radiation to be measured is set free directly in the scintillator, low-energy ß-radiation (e.g. from tritium or carbon-14) can be measured. Only the pulses that occur in both PMT's simultaneously are registered; this way electronic background counts are eliminated (coincidence technique).

Semiconductor detectors

Certain semiconductors are also suitable as radiation detectors. The radiation energy set free in them is converted to an electrical charge and transformed to a current pulse.

Semiconductor detectors have a high energy resolution and thus allow an identification and instrumental individual determination of γ-emitters directly in mixtures of numerous radionuclides. The high discriminating capability of a semiconductor detector as compared to a NaI-scintillation detector is demonstrated in Figure 81. Another example for a γ-ray energy spectrum, which was recorded with semiconductor detectors is shown in Figure 82.

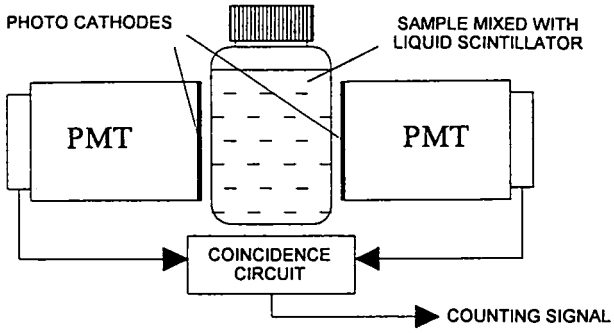

Figure 80. Liquid scintillation counting arrangement.

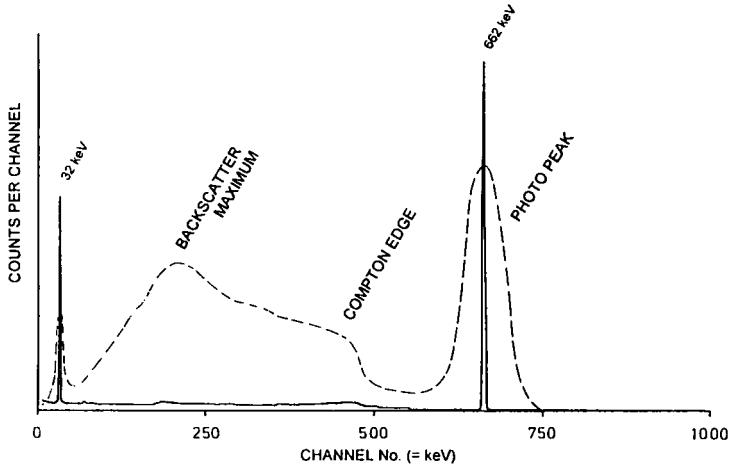

Figure 81. γ-spectra of ^{137}Cs, recorded with a semiconductor detector (——) and a NaI(Tl)-scintillation detector (-----).

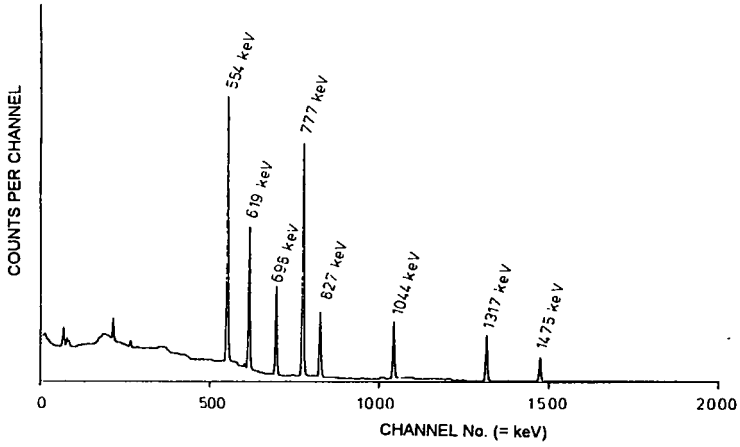

Figure 82. γ-spectrum of ^{82}Br, recorded with a semiconductor detector.

2.4.3.2 *Radiation measurement electronics*

The radiation measurement electronics and peripheral equipment (recorder, printer, and other data output devices) are used to process the pulses produced in the detectors into practical and evaluable values. In this, the pulse counters and timers play an essential role, in converting the count rate into pulses/min or other units. After transforming into analog values, count rates can also be continually recorded (rate metres, e.g. for the direct registration of a tracer breakthrough curve). In so-called multichannel analysers, the pulses are sorted according to their height and thus e.g. γ-spectra produced. More recently, radiation measurement electronics is being coupled with computers, which enable the values to be processed faster and more completely.

2.4.3.3 *Accuracy and sensitivity of radioactivity measurements*

Counting statistics

The task in measuring radioactivity is to determine how many decays per time unit occur in a radioactive sample. Or more generally, how many pulses per time unit are to be measured. Since the individual decays occur independently of one another, repeated measurements of a sample, under constant conditions, would give different results that are statistically scattered around a defined average value. The more pulses measured at single measurement, the lower the relative deviation from the average.

It can be shown, that the standard deviation of the measured values from the average equals the root of the number of measured pulses of the single measurement. If for example, a sample has an average pulse rate of 1000 pulses per minute (ipm), 68.3% of the repeated measurements (each measured for 1 min) will have values in the interval $1000 \pm \sqrt{1000}$, i.e. between 968 and 1032 ipm, the rest of the values will have larger deviations. Each individual measurement has, with a probability of 68.3%, a statistical counting error of $\pm \sqrt{x}$ (1 σ-criterion, x = number of registered pulses). If the measuring time is increased, the number of measured pulses increases also and correspondingly, the relative counting-statistical error decreases. If a higher probability is required, to be sure that the measured value lies in the stated error interval, a corresponding multiple of the standard deviation is needed:

with $x \pm \sqrt{x}$	68.3% of the measured values lie in the error interval (1 σ-criterion)
with $x \pm 2\sqrt{x}$	95.5% of the measured values lie in the error interval (2 σ-criterion)
with $x \pm 3\sqrt{x}$	99.9% of the measured values lie in the error interval (3 σ-criterion)

For example, if a measurement with a 95.5% certainty is to have a counting-statistical inaccuracy of $\leqq$ 2%, $\geqq$ 10,000 pulses must be measured.

With low level radioactive samples, long measuring times can be necessary, to assure the wanted measurement accuracy. Thus when using tracers, the chosen activity must be high enough to ensure realistic measuring times. On the other hand, applying

additional processes, e.g. enrichment of the radiotracer from a large sample volume, will also reduce the measurement time needed.

In the preceding paragraphs about counting statistics, the fact that every measurement setup also registers pulses without a radioactive sample was not considered, to promote better comprehension. This 'blank value' or background is mainly produced by radiation due to cosmic rays and from the rocks. Thus, in practical use the wanted value is the measured total count minus the background count. Since the measurement of the background also follows the laws of statistics, the corresponding error calculations according to the following relationship need to be carried out:

$$FM = \sqrt{(FP)^2 + (FL)^2} \tag{2.8}$$

where FP = sample measurement error (incl. background, gross counts), FL = background measurement error, FM = net error value (sample background).

(in words: The error of a difference is the root of sum of the squares of the separate errors).

For example, the measurement of a sample with a net pulse rate of 1000 ipm in a measurement setup with a background of 500 ipm with a 2 σ-statistic and a measuring time of 10 min (for the sample and background measurements) has a counting statistical error of ± 2.83% (in comparison to ± 2.00%, if the background was not considered).

The error can be reduced, if the background is measured over a longer period; with a background measurement over e.g. 100 min, the error would be ± 2.49%.

During series measurements, the background only has to be measured occasionally. However, then it should be measured over a long period. To yield minimal counting errors, the optimal division of the available measurement time between sample measurements and background measurements can be found through calculations with the above formula.

As a technical measure to reduce the background, radiation measurement setups (detector and sample) are shielded with lead or other materials. With more expenditure, the shield effect can be further improved with a shield counter around the sample counter. In both counters, simultaneously released pulses are removed from the sample gross count by subtraction with the help of an anti-coincidence circuit.

Measuring geometry and self absorption

With a radioactive emitter located outside a detector, only that radiation which is transmitted in the solid angle between the detector and the emitter can be detected. Thus, a specific activity, which is in a small volume close to the detector, has a higher count rate than the same activity, if it was emitted from a larger volume at the detector or farther away from it. Furthermore, a part of the radiation emitted in the direction of the detector is absorbed in the detector casing and in the sample itself, and this all the more, the larger the sample.

The fraction of the radiation emitted from the sample, which registers pulses at the detector, is called the counting efficiency of the measurement geometry. The measurement of a large sample with a low counting efficiency can be more favourable than measuring smaller amounts of the same sample with higher efficiencies, because the lower efficiency is overcompensated by the size of the sample.

Accuracy and precision of radioactivity measurements, absolute and relative measurements

The previous sections showed that the quality of the radioactivity measurements depends on several factors, especially upon the counting statistics, the measurement geometry, and the counting efficiency. At best, the impact of the counting statistics can be kept small by using sufficiently high activities or measuring for a long enough time. The measurement geometry can also be repeated very accurately. In contrast, the exact determination of the counting efficiency using normal methods is limited.

Therefore in practice, exact absolute measurements of the activity of a sample are hardly realizable, whereas relative measurements with a reproducibility of better than ± 1% are quite possible. Hence, in hydrological applications, relative measurements are used. This is done by removing a small precisely known fraction of the used tracer amount and producing standards, which are measured under the same conditions as the samples from the tracing test.

2.4.4 *Activable isotope tracers*

In order for a substance to be detected by activation, the element should preferably be only present in the investigation area in trace amounts or better yet not detectable, to eliminate possible background disturbances. Also, not all nuclides can be equally well activated, which is another criterion in choosing the substance. Finally, activable isotope tracers must also have representative transport properties (Section 2.4.5). Hence, the use of activable isotopes is based on rare elements, although in developing this method more frequently occurring elements were also detected with activated analytical methods (e.g. bromide by BUCHTELA et al. 1964).

The most important method for activation is irradiation with neutrons. Hereby, a neutron is adsorbed by an atomic nucleus of the tracer nuclide. The former is transformed into a heavier isotope of the respective element with its atomic mass plus one. The so formed new nuclides are normally not stable and instantaneously give off energy (γ-radiation) or also nucleons (protons or α-particles).

Examples:

n,γ-process:	^{115}In (stable)	—>	^{116}In ($T_{½}$ = 54 m)
n,*p*-process:	^{32}S (stable)	—>	^{32}P ($T_{½}$ = 14.2 d)
n,α-process:	^{6}Li (stable)	—>	^{3}H ($T_{½}$ = 12.26 a)

With the *n*,*p*-process and the *n*,α-process, elements form with an atomic number that is one, resp. three lower, with respect to the initial nuclide.

The nuclides formed are mostly unstable and decay with specific half-life times, i.e. radioactive material is produced by the described process. Only a small fraction of the target nuclide undergoes this conversion, while the rest remains in the initial form.

The aim of the activation is to produce radioactive transformation products from the tracer element, whose radiation data (half-life time, type of radiation) is suitable for the radioactivity measurement. The higher the radioactivity produced by the atomic reactions from a specific amount of substance, the higher the sensitivity of detection for the corresponding activation tracer.

The activity formed by the neutron irradiation depends on the amount of the irradiated initial nuclide, upon the neutron flux (density), upon the length of irradiation, and upon the half-life time and the so-called activation cross section of the initial nuclide according to the following relationship:

$$A = \sigma \varnothing N_L (G/M) H (1 - e^{-(0.693\, t/T_{1/2})}) \tag{2.9}$$

where σ = activation cross section (cm^2), $\varnothing$ = neutron flux (number/($cm^2 \cdot s$), N_L = AVOGADRO'S constant, G = mass of the irradiated element or compound, M = atomic or molar mass of the irradiated element or compound, H = frequency of the initial nuclide in the irradiated element or compound, t = irradiation time, $T_{1/2}$ = half-life time of the product nuclide.

The highest neutron fluxes are obtainable in atomic (research) reactors. Therefore, irradiation for activation analysis is conducted preferably in atomic research reactors. Depending on the nuclide however, other irradiation methods are also suitable (fast-neutron generators, activation through protons at corresponding generators and so on).

The radionuclide formed by the activation starts to decay immediately after the activation begins. Whereas the transformation rate stays practically constant, the decay rate increases according to the amount of the product nuclide, until finally the decay rate is equal to the transformation rate; the corresponding saturation activity under these irradiation conditions has then been reached. The connection between the half-life time and the temporal course of the activation production is visualized in Figure 83; after the half-life time, half the saturation activity has been produced. In general, irradiation periods of ca. ½ to 2 half-life times are used.

On one hand, the activity of the product nuclide produced in a period of irradiation which practical is the larger, the shorter the half-life time is. On the other hand, the half-life time cannot be too small due to practical handling of the nuclides and a necessary good measurability. It must also be considered that a radiochemical reprocessing of the irradiated sample to remove disturbing radioactive by-products might be necessary between the end of the irradiation and the start of the measurements. Favourable half-life times are on the order of between 0.1 and several hours. In case an automatic, i.e. immediate measurement can be carried out at the end of the irradiation period, product half-life times of a few minutes to fractions thereof can also be important.

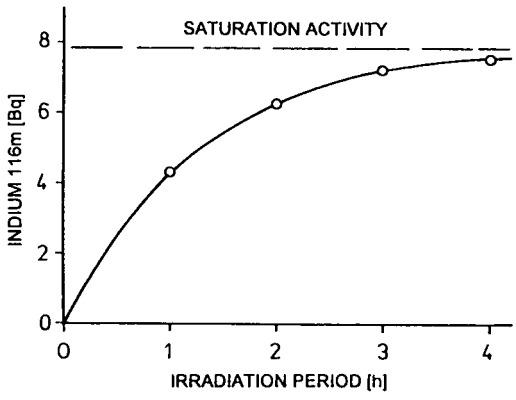

Figure 83. Production of ^{116m}In by irradiation of 10^{-12} g natural (stable) In with thermal neutrons at a flux of $10^{13}/cm^2s$.

As an example for the methodology, the technique developed by BEHRENS et al. (1977) is mentioned, in which before the activation was carried out, the indium was removed from the water sample through coprecipitation, enriched, and purified from disturbing sample components in one treatment step. Thus, a detection limit for indium of 0.0005 ppb (based on 100 ml samples) was achieved.

2.4.5 *Selected radionuclides and activable isotopes used as hydrological tracers*

When searching for suitable isotopes among the known 1000 radioactive and 270 stable nuclides for use as water tracers, two sets of criteria must be considered. On the one hand, those properties important for detection of the tracer and on the other hand, those essential to suitable tracer behaviour. For good detectability, the radiological properties are defining, whereas the chemical structure of the tracer is important for a so-called 'ideal tracer' with respect to transport behaviour. Considering these as-pects, only a relatively small group of radionuclides are ideally suited for use as water tracers.

A review is given in Table 11 and the tracers used in activation analysis are listed in Table 12.

Table 11. Radioactive hydrological tracers.

Nuclide	$T_{½}$	Chem.compound	Emitter	Properties
^{3}H	12.35 a	^{3}HHO (water)	ß	Chemically identical with the marked water
^{51}Cr	27.7 d	EDTA-complex	γ	Low sorption
^{114m}In	50 d	EDTA-complex	γ	Low sorption
^{58}Co	70.8 d	$[Co(CN)_6]^{3-}$-complex	γ	Low sorption
^{60}Co	5.3 a	$[Co(CN)_6]^{3-}$-complex	γ	Low sorption
^{82}Br	36 h	Br^--anion	γ	Very low sorption Chemically very stable
^{131}I	8.05 d	I^--anion	γ	Chemically instable, Sometimes sorption through oxydation
^{24}Na	15.0 h	Na^+-cation	γ	Is sorbed, applicable in canals and sewer treatment plants
^{198}Au	2.7 d	Au^{3+}-cation	γ	Is strongly sorbed, used as a 'reactive' tracer

Table 12. Tracers used in activation analysis.

Tracer element	Chemical compound	Activation product	$T_{½}$
Bromine	Br	^{80}Br	17.6 min
Indium	EDTA-complex	^{116m}In	54 min
Dysprosium	EDTA-complex	^{165}Dy	139 min
Technetium	$^{99}TcO_4^-$-anion	^{99m}Tc	6 h
Europium	EDTA-complex	^{152m}Eu	9.2 h

2.4.5.1 *Radiation properties*

The first important property that must be considered when selecting radionuclides is the steadily decreasing amount of the tracer amount or concentration due to radioactive decay. This is expressed in the half-life time. After four half-life times have passed, less than a tenth of the initial tracer is present. After seven, less than a hundredth and finally after ten half-life times less than a thousandth of the initial amount is present. Due to this, a radionuclide selected as a tracer should have a half-life time on the order of the presumed length of the tracing test. In practical use, this is normally between several days (e.g. ^{82}Br, $T_{½}$ = 36 h) and several months (e.g. ^{114m}In, $T_{½}$ = 49.5 d). It is mentioned here again, that the activity decrease due to decay process regularities can be corrected for exactly. However, along with the decrease in activity, the counting statistical error increases if the measurement period is limited. Conversely, the radioactive decay of the radioactive tracers is also an advantage. After the tracing test is over, any remaining traces of the tracer are removed, so to speak, automatically. Thus, the same tracer can be used in the same area more than once, which is not always the case with conservative tracers due to continuing contamination. The half-life time of the product radionuclides is also a criterion for the detection with the tracers used in activation analysis (see Section 2.4.4).

A further criterion in selecting tracers is the dependence of the detection technique of radiotracers upon the type of radiation emitted. As described in Section 2.4.2.2, γ-radiation, in comparison to the other types of radiation with direct measurement (no sample preparation), can be detected by far the best, which is why they are the radiotracers used the most. An exception is the low energy ß-emitter, tritium, which is a part of the water molecule and has reference tracer properties. Tritium is detected exclusively in the laboratory. Due to its neutral molecule, tritiated water can exhibit different transport behaviour as compared to other tracers, as the example in Figure 84 clearly shows. In this example tritium, which represents the transport of the water in the soil in total, lagged behind bromide, which was faster due to anion exclusion. Due to its low energy radiation, tritium also causes only relatively low radiation exposure,

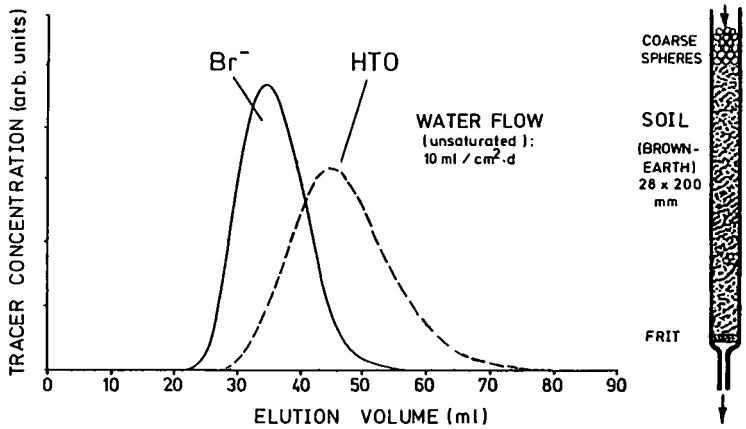

Figure 84. Tracer breakthrough in a simultaneous tracing test with ^{82}Br and tritiated water in a laboratory column with surface soil under unsaturated flow conditions (from BEHRENS 1988a).

which is why it is particularly chosen for use in discharge measurements in larger rivers (FLORKOWSKI et al. 1969) (see Section 2.4.6.1).

In groundwater systems however, tritium should be only used as a tracer as an exception, in order to keep its viability as an environmental tracer (Section 2.11) intact. As a warning example, RANK (1991) discussed a groundwater tracing test from 1964 in the region of the Neusiedler Lake with 100 Ci tritium. Twenty years later, the tritium could still be detected in the groundwater.

The fact that radioactive tracers decay, can cause problems in the supply of the tracer material, especially with short-lived radionuclides. This can be remedied by using so-called nuclide generators (examples in Table 14). Such systems are composed of radioactive mother/daughter pairs, with the longer-lived radioactive mother fixed in a suitable apparatus, e.g. in a sorption column; the shorter-lived, also radioactive daughter can then be eluted, and used as a tracer. This procedure can be repeated several times as soon as the activity of the daughter nuclide in the elution apparatus reaches appropriate levels again (e.g. after three half-life times of the daughter ca. 85%).

2.4.5.2 *Chemical properties of radiotracers*

The physical properties of radioactive and activable tracers, especially their transport behaviour, depend, as with all tracers, on the chemical state of the specific tracer. It is generally known, that anionic substances are more suitable as tracers than cations, because cations are generally subject to a much stronger sorption on minerals due to ion exchange. Hence, the chemically simple halide anions $^{82}Br^-$ and $^{131}I^-$ have been successfully used as radiotracers. However, iodine as a radioactive tracer has registered time and again a negative tracer behaviour (retardation, losses), which was interpreted in earlier articles (KAUFMANN & ORLOB 1956) as a tendency of the I^- to sorption at low chemical concentrations, which is typical for radionuclides. Bromide does not display this phenomenon. However, it was proven in systems such as surface waters or soil water, that the chemically redox-sensitive iodine is oxidized enzymatically through microbial activity and thus sorbed onto organic substances, whereas the chemically unchanged I^- continues to behave as a conservative tracer (BEHRENS 1985). In deeper groundwater systems with low microbial activity, this reaction only occurs to a much lesser extent. By adding additional non-radioactive I^- (carrier), this reaction can be partially suppressed, since the enzymatic activity that causes it has a limited turnover capacity. This example points out that a tracer not only has to be used in the appropriate chemical form, but also that its invariability must be assured.

There are numerous radioactive and through activation analysis determinable nuclides, that would be suitable as tracers according to their radiological data, but are not at all suitable in their simple chemical forms. They are however quite suitable water tracers after forming anionic complexes (LACEY & DE LAGUNA 1956). These complex compounds consist of a central atom, which can be as a free ion a cation, and ordered around the central atom 'Ligands' with a negative charge. Especially well-proven are the so-called chelate complexes, which are formed by complexing agents such as ethylene diamine-tetracetic acid (EDTA). As an example, the structure of the Indium-EDTA-complex is shown in Figure 85. The complexation occurs according to the relationship stated in Equation 2.10. Accordingly, such a solution always has a very

small amount of the uncomplexated tracer nuclide in equilibrium with the other reaction partners. This amount is all the smaller, the larger the complex stability constant, K_S, is.

$$K_s = \frac{[M_n \cdot L_m]}{[M]^m \cdot [L]^n} \tag{2.10}$$

where $[M_nL_m]$ = concentration of the complex, $[M]$ = concentration of the free central atom, $[L]$ = concentration of the free ligands, m = valence of the central atom (M), n = valence of the ligands (L).

Examples for such chelate complexes, which have been used as tracers, are listed in Table 13.

The detectability characteristics of tracers so formed are determined by the central atom. For this, a suitable radionuclide or in the case of an activation analysis tracer, a well activable and sufficiently rare element is chosen.

The quality of the transport properties of the tracer is defined through the anion forming properties of the ligands. In practical use it has been shown that only those complexes with very high complex stability constants (log K_S >20) have sufficient tracer properties. With less stable complexes, it seems that due to sorption along the flow path, free cations are continually lost and then must be replaced from the complex in order to maintain equilibrium. In this way, it can happen that an anionic complex tracer is lost due to cation sorption. The EDTA-complexes with chromium and indium have proven themselves as viable tracers, whereas the corresponding Mn- and La-compounds, which have a lower stability have failed. Properties of chelate com-

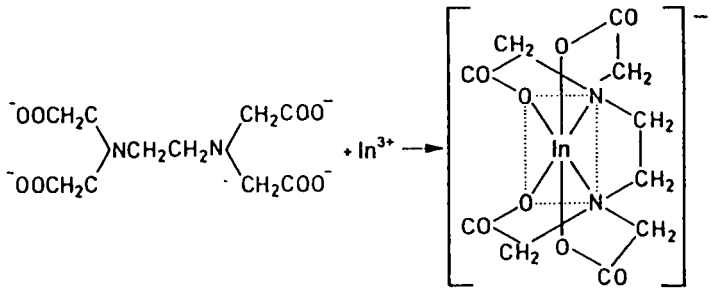

Figure 85. Structure of indium-EDTA-complex (anion).

Table 13. Radioactive and activation analysis used chelate complexes and their complex stability constants (K_s) in neutral aqueous solution. DTPA= ethylene triamine-pentacetic acid.

Complex	log K_s
In-EDTA	24.9
Cr-EDTA	24
Bi-EDTA	22.8
Dy-EDTA	17.6
Mn-EDTA	13.8
La-EDTA	15.4
La-DTPA	19.5

Table 14. Nuclide generators for short-lived radioactive hydrological tracers.

Nuclide	$T_{½}$	Chem.Compound	Properties
^{132}I (from ^{132}Te, $T_{½}$ = 78 h)	2.3 h	I^--anion	(s.Table 11: ^{131}I)
^{99m}Tc (from ^{99}Mo, $T_{½}$ = 66 h)	6 h	TcO_4^--anion	low sorption in aerobic media
^{113m}In (from ^{113}Sn, $T_{½}$ = 115 d)	99.5 min	EDTA-complex	low sorption

plex tracers with indium, dysprosium, samarium, and lanthanum have been comprehensively investigated by DRABAEK (1982).

2.4.6 *Hydrological applications of radiotracers*

Radioactive and activable isotope tracers are used to investigate the same kind of hydrological questions as the other types of tracers. Working with these tracers is only different with respect to the detection methods. The general principles of how the tracers are used in surface and groundwater have been handled in the corresponding chapters of this book.

In some cases however, radioactive tracers have obtained a special status due to technical developments, e.g. in single-well methods (cf. Section 4.5). This is especially true for the determination of the groundwater flow direction, which utilizes the penetration capability of the γ-radiation; in this application, radioactive tracers cannot be substituted by any other tracers.

Advantages of the radioactive tracers are their low chemical stress on the water body and additionally their disappearance due to radioactive decay. A disadvantage of using radioactive tracers is indubitably the possible radiation exposure. Mainly radiation exposure of the occupied personnel is possible during injection, when the total activity is concentrated in a limited volume. However, technical precautions (shields, injection pumps, remote-controlled manipulators, etc.) can reduce the radiation exposure to an acceptable level, or practically eliminate it all together. After the tracer is diluted and distributed in the hydrological system, the specific radioactivity in the water is so low, assuming appropriate measures were carried out, that the radiation exposure from the tracing test is only insignificantly over the natural background radiation.

For working with radioactive materials and injection of radioactive tracers into hydrological systems, the respective regulations of radiation safety and water protection must be observed. Appropriate special training for the personnel is also essential, as well as the availability of suitable technical equipment when working with radioactive materials. In most countries, working with radioactive materials must be licensed by competent authorities.

Hydrological applications of radiotracers are also summarized in the literature. Especially the 'Guidebook' from the IAEA (1983) should be mentioned here. Furthermore, a series of reviews has been published (e.g. SMITH 1964, EVANS 1983). Radiotracers have been handled in detail by GASPAR (1987). Applications for this tracer group were thoroughly covered in the symposium 'Radioisotopes in Hydrology' (IAEA 1963).

2.4.6.1 *Applications in surface water*

Direct measurements are completed either with detectors hanging directly in the water (unknown arbitrary measuring geometries) or with detectors in calibrated flow containers, that have a continuous sample flow (ELLIS 1967). Collective samples can also be taken and the activity then measured in the laboratory with whatever measuring time is wanted. During direct measurements, the possible measuring time is limited to the tracer passage time. Radiotracers from large samples can also be enriched in smaller samples in order to increase the detection sensitivity. If quantitative measurements are to be taken (e.g. discharge measurements), unknown, arbitrary measurement geometries can be calibrated by comparing a spot sample from the tracer passage taken at a specific time with a standard prepared from the inoculation activity. The total tracer passage is related to this measurement (GARDNER & DUNN 1964).

In rivers, radioactive tracers are used to determine flow times, dispersion processes, and for quantitative determination of the discharge with the tracer dilution method. Among others, $^{131}I^-$ (MOSER et al. 1962), $^{82}Br^-$, ^{198}Au and ^{51}Cr-EDTE (PILGRIM 1966), $[^{60}Co(CN)_6]^{3-}$ (GILATH 1983) and ^{22}Na have been used as tracers for these purposes. ^{82}Br was, also with tritium and uranine, used to measure discharges of up to several 1000 m^3 (PLATA BEDMAR et al. 1991). FLORKOWSKI (1991) published a summary of numerous measurements carried out using tritium on high discharges, mostly in hydraulically very unregular channels in tropical countries. Besides their application in discharge measurements, the suitability of radiotracers for these applications has also been discussed (e.g. by PILGRIM 1978). Historically, it is very interesting that radium (prepared out of pitchblende itself) was suggested in 1922 by JOLY as a radioactive tracer for use in discharge measurements. The high accuracy of radioactive measurements was also explicitly stated (then still done with the electroscope). A remarkable procedure was developed for discharge measurements with momentary tracer injection (HULL 1958). The necessary integration of the tracer breakthrough curve according to Equation 2.11 is carried out by accumulating the count pulses during the tracer passage. On the other hand, the calibration of the integral was completed by comparing the count rate of a sample taken at a specific time in the tracer passage with that of a standard. In this way, with the help of the single events of the radiation signal, a quasi-digital integration of tracer breakthrough curves was carried out early (today, analog breakthrough curves are digityzed with computers and integrated).

$$Q = \frac{A}{\int_0^\infty c\,dt} \tag{2.11}$$

where Q = discharge, A = injected quantity of tracer, c = tracer concentration. The integral is the area under the tracer breakthrough curve.

The application of γ-emitters is seen as especially suitable in measurements in standing bodies of water, since tracer clouds can be followed with a scintillation detector hanging from a boat.

Radioactive tracers are also used to determine flux processes in sewage systems and industrial plants (SCHMITT et al. 1969). As compared to dye and chemical tracers, the fact that radioactivity measurements are not disturbed by high contents of pollutants is

advantageous. To conclude, radiotracers have also been used to identify infiltration sites in reservoirs (PLATA BEDMAR 1991).

2.4.6.2 *Applications in groundwater*

The first radioactive groundwater tracing tests were carried out only a few yeas after radioactivity was discovered. VORTMANN and TIMEUS (1910b,c) carried out two tracing tests with pitchblende in the Triestine Karst (TIMEUS 1912, 1926). They hung granulated pitchblende from Joachimsthal in the Reka percolation near San Cozian. The first test was on 15 April 1909 and used 15 kg pitchblende in 13 sacks. The recovery investigation was carried out in the Timavo Springs by measuring the emanation concentration with the ENGLER-SIEVEKING fontactoscope. The activity increased from 0.4 to 4 MACHÉ-units. During the second test on 18 October 1909, flood waters tore the sacks with the 38 kg of pitchblende (containing 6.3 mg Ra) away from their fittings and they were carried into the cave system.

Since aquifers, especially those in finely porous unconsolidated rock, have large surface areas, the tracers injected can be adsorbed and thus changed in their transport behaviour. Therefore, tracers used in groundwater application must meet extremely high requirements as good tracers. Not only are the tracer properties important, the type of rock is also. Clays adsorb stronger than quartz. Since cationic ion exchange predominates in minerals, anions are mainly used as radiotracers. The chemically stable $^{82}Br^-$, which has been successfully applied in numerous groundwater investigations (HOURS 1955, THATCHER & RAMSEY 1977, IVANOVICH & SMITH 1978), is unfortunately limited by its short half-life time. Non-radioactive bromide has been repeatedly used as a neutron activable tracer (SCHMOTZER et al. 1973, JESTER et al. 1977). However, this detection method has probably become invalid in the meantime, since bromide can now be detected with ion chromatography with less work and a detection limit far below the natural background level in surface and groundwaters. Other than tritiated water, which can be justifiably applied in local investigations, especially in small scale measurements of water movement in soils and in the unsaturated zone (RAO 1983), the anionic chelate complexes of radionuclides and of stable elements have been mainly used in groundwater. As an example, indium has been used in karst tracing tests as a neutron activable tracer (measured as ^{116m}In, $T_{½}$ = 54 min) as well as a radiotracer (used as ^{114m}In, $T_{½}$ = 50 d) (BEHRENS et al. 1977, 1992). The $(^{60}Co(CN)_6)^{3-}$-complex has also been successfully applied as a groundwater tracer (HALEVY et al. 1958, STERNAU et al. 1967). The properties and suitability of different radiotracers have been checked in numerous laboratory and field investigations (KNUTSON et al. 1963, JENNINGS & SCHROEDER 1968, BRUSCATO & MCHENRY 1970).

In local investigations, e.g. in circulation tests between two wells, measurements can be directly taken with field equipment, whereas in large scale and long lasting tests, samples are normally taken and measured in a central laboratory (unavoidable with neutron activable tracers). Since radiotracers do not differ from the other tracers with respect to tracing techniques, further applications can be taken from the other sections in this book.

Outlook

Radioactive and activable tracers have shown good performance and usefulness in hydrological applications. However, they are used with reservation due to their

measurement expense and radiation protection aspects. Considering that in the future, the demands required of tracers will be increased and are only met by traditional tracers to a limited extent (BEHRENS 1988a), radioactive and activable tracers will not lose their importance. On the basis of their chemical variability, they still offer wide possibilities for developing further tracers with suited and optimal tracer behaviour.

2.5 CLUB MOSS SPORES

W.Käss

Spores from the club moss (*Lycopodium*) are suitable as flotation devices for tracing wide underground waterways. In the group of successfully used flotation devices, they have the largest diameter (Fig. 86).

Drifting tests with club moss spores have been widely used in karst regions. In tracing with spores, ZÖTL (1957b) suggested using the term 'spore-drift'. When investigating the discharge relationships in alpine karst, tracing without spores is no longer imaginable, in fact they have become indispensable in some cases. Tests with spores in fissure groundwater aquifers or in coarsely crushed gravel aquifers have not yet been carried out to the author's knowledge.

The spores of the Canadian club moss (*Lycopodium clavatum* L.) are used exclu-

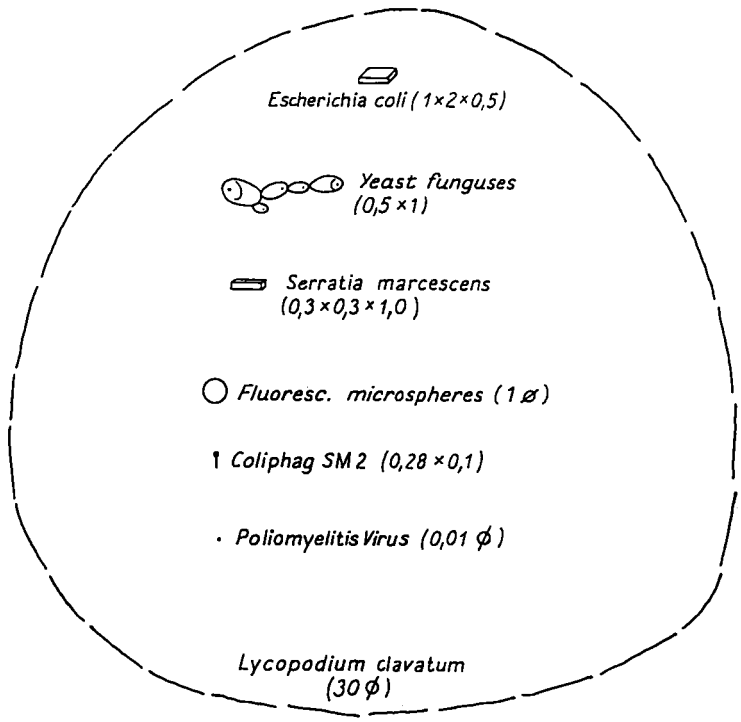

Figure 86. Size comparison of *Lycopodium* spores with other selected flotation devices.

sively in the spore-drift tracing tests. The spores are mechanically harvested in Canada after the incubation period.

The spores of the club moss measure 33 µm in diameter on the average (BAUER 1967b) or, according to data from KIRCHHEIMER (1933), 28 µm. They can range between 26 and 39 µm. Depending on the size and age of the spores, 1 kg contains 100 to 300 (BAUER 1967b), according to MAYR (1954b) circa 500, according to BAUER, ZÖTL and MAYR (1959) 80 billion specimens (BAUER et al. 1959).

The individual spore has a tetraedrical form (Fig. 87). The arched tetraeder surfaces are covered with a meshwork. This mesh structure can be used under the microscope to positively identify the spores during sample checking (Figs 87 and 88).

The spores are covered with wax. This property makes them easily inflammable. At the start of photography, *lycopodium*-powder was blown into a candle flame and used as a flash.

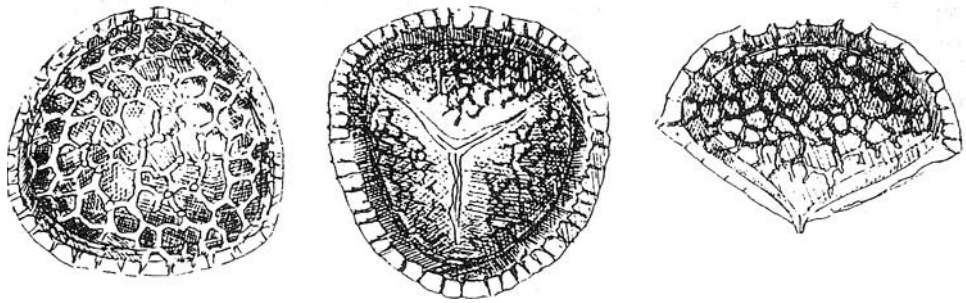

Figure 87. *Lycopodium clavatum* spores from ERDTMANN (1954). Left: distal, middle: proximal, right: lateral view.

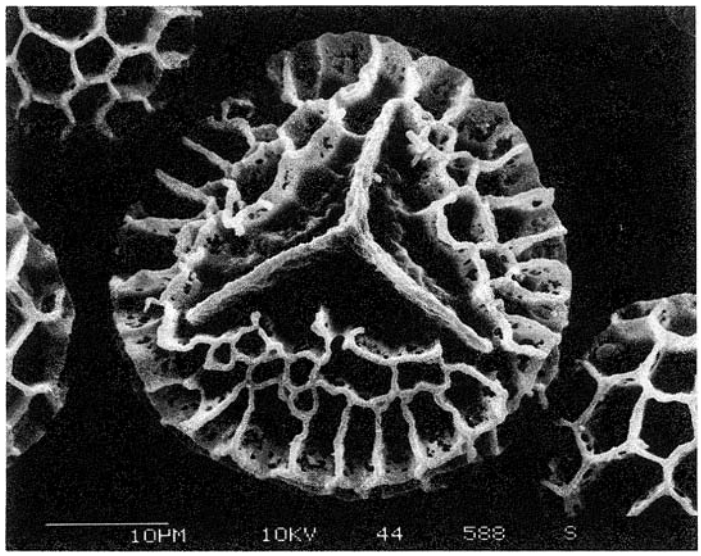

Figure 88. Photo from a scanning electronic microscope of a club moss spore. Photo: CH. SAMTLEBEN/Kiel.

Care should be taken in handling the spores. In closed rooms, explosive aerosols can develop. *Lycopodium* powder, also called witches dust, is officinally used to dry wounds, among other purposes.

The spores are bought as a dusty, light yellow powder with a density of circa 0.42; 1 kg takes up therefore approx. 2.4 l of space (DECHANT & HACKER 1988). Due to the wax covering of the separate spores, they have no wetting capacity with water.

In order to dye the spores, the wax covering must be removed. In the mid-eighties, the price per kilo was about DM 150 (in 1953: 60-70 Austrian schillings).

The outer layer of the spore (Exine) is extremely resistant to chemical and microbiological influences. In 1931, ZETZSCHE and KÄLIN described this substance and named it sporopollenin, most likely it is an oxidated polymer of carotenoids and their ester. Deposited in sediments, it can survive many million years (KIRCHHEIMER 1933). Sporopollenin is most likely the most resistant substance of the entire living world (FAEGRI & IVERSON 1964).

Spore-drift method

The advantage in tracing with club moss spores is no doubt in the accumulation of the samples. Separate samples, i.e. samples taken at a specific time in a container, can only be used in spore investigations if larger samples of water, circa 1 l and more can be taken and if high spore concentrations are expected (BAUER 1967b). Determining the number of spores in smaller samples would not be successful, since the concentration would be much too low. Thus, samples are taken over a period of time, between several hours and several days, by laying out so-called spore nets, through which water continuously flows. This way, it is possible to capture spores from a large volume of water. However, this is also a disadvantage for a quantitative determination, since it is only possible in special cases to determine the water amount, which has flowed through between changing the net each time. In practice, the nets are placed in the channel, so that the water flows freely all around. With nets that are hung so that the inflow has a specific volume, a gradual clogging of the mesh pores must be considered. This causes the net to overflow and thus a decrease in the flow is hardly unavoidable.

Compared to separate samples, as they are usually taken in dye and salt tracing tests, the spore-drift method has a definite advantage. Since the nets are in the water for a long period of time, the tracer can be concentrated in the net. This is especially valuable and not to be underestimated in hard to reach sampling sites, such as high mountainous areas (MAURIN et al. 1959).

The 'spore sample,' which is taken when the nets are changed is not large; it fits in a 50 ml or 100 ml bottle. Each person taking samples can complete a large number of net changes on each round. Thus, problems related to the distance may arise, but not due to transport.

However, the prominent times, such as the 'first appearance' or 'maximal concentration,' that can be very exactly determined with separate samples in quick succession or through registration, can only be determined with net samples imprecisely.

Yet if the nets are changed very carefully and regularly, semi-quantitative results can be achieved and recorded (Fig. 97). The spore-drift method is not to be outdone, when it comes to proving hydrological connections where other tracers have failed. For example, when other tracers have been diluted to under their detection limit. If

appropriate caution has been taken against spore contamination, in some cases a single spore can prove the connection.

Spores can sink in slowly flowing underground channels, since they have a density of approx. 1.1 and are thus a bit heavier than water. If the water flow is stronger later, they can reappear, even if a negative result was registered first. ZÖTL (1957c) observed such cases of single latecomers even in the first tests with dyed spores in the eastern Dachstein region in 1956 (Fig. 90):

Injection	Maisenberg 1,860 m	Miesboden 1,415 m
On	4 August	16 August
With	12 kg blue spores	7 kg red spores
Observation site: 648 m above Mühlreit		
Distance	13 km	6.5 km
Altitude difference	1030 m	590 m
Spore counts:		
8 August	1	0
10 August	4	0
12 August	0	0
20 August	0	6
22 August (after heavy rains)	3	4

Spores can drift over relatively long distances. Due to the accumulation effects of the net sampling, they can be detected in very small quantities, where other tracers would be too diluted to detect. In 1982 in the Peloponnesus for example, acridine dyed spores, which had been injected in the Alea-Ponor were detected in the Lerni spring, 30 km away (BRICELJ et al. 1986b).

Lycopodium spores can be used for hydrological tracing tests without reservations with respect to all water management purposes, since it is a natural product. *Lycopodium clavatum* is used in large quantities in homoeopathy. Dyed spores can also be used without hesitation, for the dye is only a filmy covering on the natural spore. Even when large quantities of spores are injected in the underground, they are invisible at the reemergence sites.

2.5.1 *Natural spores*

Natural spores have been used for a long time in karst water tracing tests. Although club moss spores also grow in Mid-European latitudes, there have been no problems in the tracing tests. On the one hand, the club moss grows preferably on acidic and carbonate-poor soils, i.e. not in karst regions. On the other hand, the fir club moss spore, *Lycopodium selago* L., that is prevalent in Mid-Europe up to an altitude of 1800 m, is much smaller than the exclusively used spores of the Canadian club moss *Lycopodium clavatum* L. and seldom bears fruit. Other club moss species which grow in the Alps are marsh club moss, *L.inundatum* L., and interrupted club moss, *L.annotinum* L., (MAYR 1954a). *Lycopodium clavatum* is occasionally found in Mid-Europe, but the European form has smaller spores than the North American.

Microscopically, the spores of *Lycopodium clavatum* can be easily distinguished from those that are found in the Mid-European calcareous Alps. *L.annonitum* has wide-meshed, *L.complanatum* has close-meshed nets. *L.inundatum* has vermicular convoluted strips and *L.selago* has no pattern at all.

For a long time, A.MAYR was thought of as the first to have used *Lycopodium* spores in investigating underground water (1953a,b, 1954a,b). MAYR investigated the springs in the Dachstein karst and was able to ascertain whether glacier meltwater flowed in the springs by determining whether pollen was present in the springs. Then the idea formed to deliberately add allochthonous pollen to a spring as a karst tracing test. On 5 March 1953, MAYR conducted a drifting test with 100 g of *Lycopodium* spores in the northwestern spur of the Totes Gebirge (Offensee region, Upper Austria) near the Gimbach percolation. In 1950, a salt tracing test proved that the infiltrating water reappeared in a downstream spring group 180 m away. Ten minutes after the injection, the first spores reappeared in the spring group. After 50 minutes, the maximum with 976 spores in a quarter-hour sample occurred (MAYR 1953b).

A short while later, MAYR conducted a spore drift test near a sinkhole in Hinterer Gosau Lake in the Dachstein region, province of Salzburg/Austria, 1156 m, with 8 kg of spores. To improve the mixing of the dusty spores, he added the detergent 'Presto.' The spores reappeared at the Vorder Gosau Lake (northwest flow direction) and on the other side of the Langthalkogel (2086 m) in the Waldbach spring (northeast flow direction) (Fig. 90). MAYR wrongly called this 'spore dyeing' and in 1954a wrote, that it was the 'first time that a karst water passageway was faultlessly traced using plant spores.'

In 1962 however, Josef VORNATSCHER called attention to the fact that G.TIMEUS had published an article in 1926 in the 'Duemila grotte' (BERTARELLI & BOEGAN, p.155) with the title 'Le indagni sull' origine delle aeque sotteranee.'

VORNATSCHER was mistaken in this point. It must be noted that TIMEUS had already suggested tracing with *Lycopodium* in 1910 (TIMEUS 1911). In all of TIMEUS' publications, *Lycopodium* spores are only listed as a tracer, but never used as one. Most likely, the engineers from Innsbruck/Austria were the first to trace with *Lycopodium* spores in the spring of 1940 near 'St. Maria am Heiligen Wasser' near Igels (VORNATSCHER 1962).

The first semi-quantitative results from tracing tests with natural spores were achieved in tests in the southern Styrian karst (MAURIN & ZÖTL 1959). Three kilos of spores were injected on 22 May 1956 in the Feliferhof sinkhole. The first spores reappeared 800 m away in the Bründl spring 14 hours later. This is the same flow time that the nearly simultaneously injected uranine needed (Fig. 89). Two spore nets that were used next to each other and also changed simultaneously resulted in the following spore counts:

Test time (hours)	1. Net	2. Net
10-12	0	0
-14	2	6
-16	8	8
-18	933	840
-20	1278	1120
-22	111	87
-24	67	59
-26	15	17
-28	13	16
-30	12	15
-68	3	5

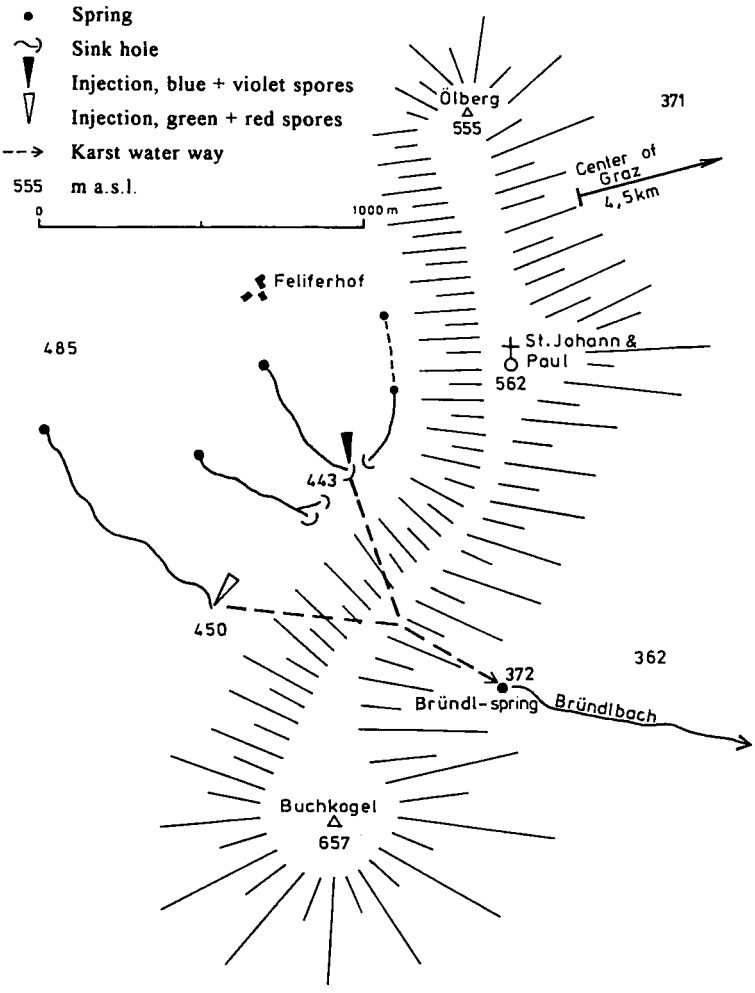

Figure 89. Map of the tracing tests in Buchkogel-Kalkstock south-west of Graz/Austria (after MAURIN & ZÖTL 1959).

Spore counts in both nets agree surprisingly well. Therefore, it can be assumed that if the spore count in a net is missing, a parallel net can be readily used to complete the breakthrough curve.

Differing from the simultaneous first appearance of the dye and spores, the dye maximum did not appear until 32 hours after the injection. One explanation for the advanced maximum of the spores is that the natural spores floated on the surface and were quickly propelled to the exit of the underground channel.

ZÖTL (1957b) prepared the natural spores for tracing tests as follows:

Start with 5 kg of dry spores. Remove 250-500 g and mix with 2 l of water plus a handful of detergent. Then 250-500 g of dry spore powder is repeatedly added to the mixture and kneaded with the hands. Wetting the spores this way requires less time than if the whole five kilos were to be added at once. Only if the mix becomes too thick should more water be added. This procedure does not require warming.

Denatured alcohol can also be used to wet the spores; 600 ml are needed for 1 kg of spores.

Nowadays, natural, undyed spores are no longer used, since their retrieval is hard and their occurrence might be natural or due to previous tracing tests. Taking several preliminary samples at the observation sites can only partially help.

2.5.2 *Simply dyed spores*

The Laibach cave explorer, Franz BAR, supposedly suggested dyeing club moss spores (MAURIN & ZÖTL 1959). In 1962 however, VORNATSCHER called attention to the fact that differently dyed spores must have been used earlier.

He cited KYRLE (1928): 'If a sinkhole is to be repeatedly or several sinkholes (simultaneously) fed with drifting materials, they must be of different types or of a water insoluble *colour*'. However, *Lycopodium* spores are not mentioned in KYRLE'S publication. Further details are unfortunately not available.

The first detailed publications about drift tracing tests with dyed spores were by ZÖTL (1957a,b) and DECHANT (1959) first described the dyeing technique.

ZÖTL (1957a) described five tracing tests that were carried out in July and August 1956 in the eastern Dachstein region using natural and two differently dyed spore types (Fig. 90).

This pioneering test showed that with the corresponding planning, spores can be used in high mountainous regions to determine flow conditions over large areas. It was notable, that in the interior of a karst aquifer, the flow directions are radial, in the border areas the flow is directed outwards. Furthermore, the author stresses the economics of this method. If salts had been used in the five tests instead of spores, instead of the 2.5 to 12 kg of spores, approx. 8 tons of rock salt with 100 pack-animals would have been needed just to raise the chloride contents in the corresponding springs by 5 mg/l. The average flow time from the injection sites to the observation sites was four days.

This first tracing test with dyed spores proved their usefulness in investigating underground karst flows. During the very first use of dyed spores in 1956, other than natural spores, only the spore colours blue and red were used. These three categories were still used by ZÖTL in 1957 in different northern alpine karst regions (ZÖTL 1958). There were difficulties during the first tests due to partial fading of the dyed spores during preparation. However, the dyeing technique was perfected by DECHANT in the following year, 1957, so that four different spore colours could be used. In 1959, MAURIN and ZÖTL reported on the first simultaneous application in 1957 of four different spore colours in preliminary tests in the hydrologically well-known Buchkogel region southwest of Graz/Austria, to investigate the possibilities of applying this new method.

In 1957, four differently dyed spore types were injected in two ponors west of the Buchkogel chain, which is made up of Devonian limestones and dolomites (Fig. 89). One kilo of blue and one kilo of violet spores were injected in the northern ponor at an altitude of 443 m and in the southern ponor 1 kg of green and 1 kg of red spores were injected. The injections were completed in the named order on 23 March 1957 between 15:15 hours and 16:25 hours. MAURIN and ZÖTL (1959) did not report any

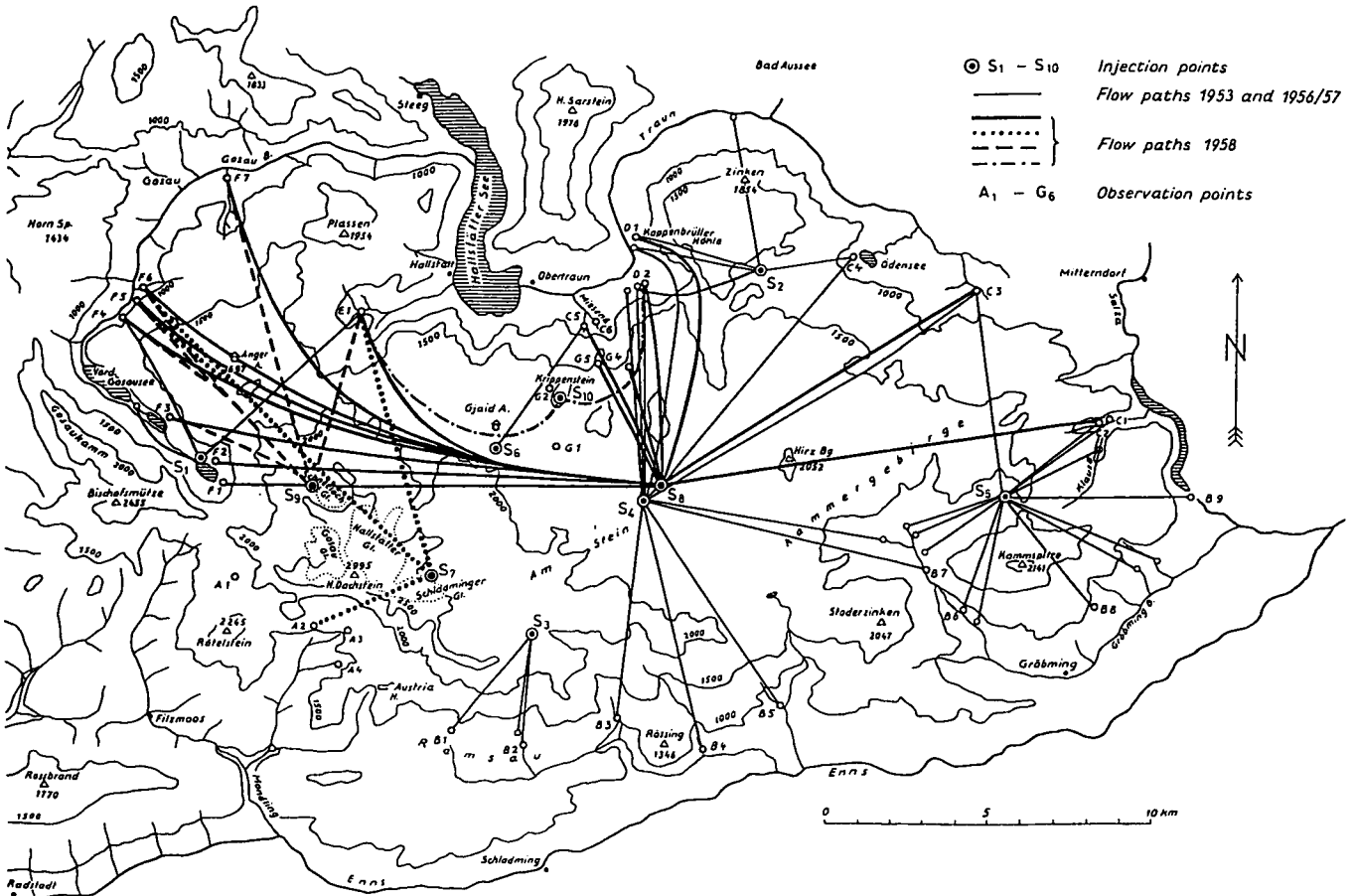

Figure 90. Spore drift tracing test in the Dachstein Massif 1953-1958 from: BAUER et al. (1959), MAYR (1954a), and ZÖTL (1957a,b).

Legend to Figure 90.

S1 – S10 = injection sites;			
S_1:	14 August 1953,	Hinterer Gosausee,	Undyed spores
S_2:	14 July 1956,	Herrenalm,	Undyed spores
S_3:	22 July 1956,	Landfried Tal,	Undyed spores
S_4:	4 August 1956,	Maisenberg,	Blue spores
S_5:	16 August 1956,	Miesboden,	Red spores
S_6:	4 Nov. 1957,	Oberfeld,	Blue spores
S_7:	13 August 1958,	Schladminger glacier,	Red spores
S_8:	13 August 1958,	Wurzkar,	Green spores
S_9:	13 August 1958,	Schneeloch glacier,	Blue spores
S_{10}:	16 August 1958,	Krippenstein,	Violet spores

A1 – G6 = observation sites

detailed particulars about the recovered spores found in the Bründl spring. Thus, the scant report is quoted here:

'The first spores showed up in the sample from the Bründl spring that was taken on 24 March at 04:00 hours. The main passage was found in the sample taken on 24 March, 24:00 hours. The passage times as well as the amounts of the passing spores coincide to a large extent without prejudice as to the different injection sites. It can be assumed from this that both sinking channels, 600 m apart, soon unite to common karst system.'

Since then, numerous tracing tests have been carried out using this method in many karst regions.

Further basic tests, in which the dyed spores have proven themselves, were carried out in 1958 in the Malm karst of Southwest Germany and also in the Dachstein Massif. In EISSELE's publication (1961), he summarized the expertise won from the tracing tests conducted by the Geological Survey of Baden-Württemberg in the Swabian Alb north of Sigmaringen/Germany. It was based mainly upon the tracing techniques detailed in MAURIN & ZÖTL (1959) and provided new aspects in the spore investigation. In the investigation area Dachstein massif, four differently dyed spore types could be applied, thanks to the new and improved dyeing technique (DECHANT 1959). Forty-six observation sites were set up around the massif (BAUER et al. 1959). The results from these tests, with spores reappearing in 18 sites, showed the great advantages of this method (Fig. 90).

Dyeing Lycopodium spores with non-fluorescing dyes

Being able to dye spores with more than one colour was a great advancement in tracing techniques. After the first field test in 1956 in the eastern Dachstein region, the dyeing technique was perfected. The credit for having developed the applicable technique for dyeing the spores with colour goes to M.DECHANT from Graz/Austria.

In 1959, DECHANT listed several prerequisites dyes need to fulfill to be able to be used in spore dyeing:

– Colour fast. The dye must adhere well to the spores, be water-fast and be stable with regards to the constituents naturally occurring in groundwater.

– Dye intensity. The colour of the dye should be as intensive as possible, so that spores dyed with several dyes can be well differentiated under the microscope, even only in daylight.

– Spore conservation. The dyeing process should not destroy the spores, nor should it allow agglomeration. The separate spores must retain their buoyancy.

– Harmlessness. The dyes should be harmless for people and animals.

Spores are naturally covered with a wax layer that is water-repellent. If *Lycopodium* powder is poured on a water surface, a layer of it spreads over the entire surface, so that an object can be inserted without it becoming wet. Before the spores can be dyed, this wax layer must be removed. This can be done with solutions that dissolve fat, e.g. with alcohol, gasoline, or carbon tetrachloride. It is more expedient to use anionic tensides. Household and laboratory detergents are normally 10 to 30%. Household detergents also normally contain perfume, which is however no bother to the spore treatment.

In 1967, DECHANT published detailed instructions for dyeing spores. Accordingly, 1 kg of spores at 40°C are mixed with 2.5 l of water and 40 g detergents until a uniform pulp forms. Then it is heated until it boils. With this, the pulp becomes viscous and more water is gradually added until a total of 4 l of water is reached for the 1 kg of spores. After 1.5 hours, the mixture has become homogeneous. Clumps, which are not wetted, rise to the surface and must be dissipated. The mixture is heated for another hour and continually stirred so that scorching or boiling over is avoided. While stirring, the alcoholic dye solution (200 ml alcohol + 10 g dye) is added to the boiling pulp and then stirred for another ¼ hour at 80-90°C. 50 g Bismarck brown is dissolved in 200 ml denatured alcohol, all the other dyes are dissolved in the ratio of 10 g to 200 ml.

DECHANT recommended mixing the spore pulp by hand, yet since 1958, the Geological Survey in Baden-Württemberg/Germany has used an electric stirrer, 'Ultra Turrax'. Using such a stirrer has several advantages:

– Reduction of possible contamination due to dyed spores under fingernails and in cracks in the skin,

– Ability to stir near the boiling point,

– Easy, quick, and safe homogenization of the spore pulp.

Following dyes can be used for a simple spore dyeing. For easy identification, the COLOUR INDEX (1971) number and CAS RN are listed below.

In dyeing *Lycopodium* spores, basic dyes are mainly used. Acidic dyes are less suitable (DECHANT 1967). Malachite green, fuchsia and crystal violet are triphenylmethanes, safranin is a phenazine dye. Bismarck brown is an acidic azo dye; much more of this dye is needed to faultlessly dye the spores, as compared to the basic dyes.

If a spore drift tracing test using dyed spores is to be conducted in aggressive or 'acrid' sewage water, DECHANT (in DECHANT et al. 1958) recommends coating the spores with a resistant carbamide resin layer. In such cases, for each kilogram of spores, 60 g urea and 180 ml formalin as well as 100 ml caustic potash solution (10%) is added to the still hot spore mixture, while stirring.

The cooled spore mixture is filtered through a Büchner funnel using a round paper filter (240 mm). After suctioning, the same amount of water is added on top of the spores and again suctioned. The spores are then placed on an aluminium dish to dry at 80°C in an oven.

BAUER (1967b) and DECHANT (1967) enumerated the spore colours red, blue, green, violet, and brown that had been used up to then. However, a tracing test using all five

spore dyes simultaneously is not known. In the tracing tests in the Dachstein karst region from 1958 and in the Slovenian karst from 1975, four spore dyes were used.

In 1976, GARDNER and GRAY (1976) established that the spore dyes red, violet, and green can be distinguished most easily from one another.

	C.I.	CAS RN
Violet		
Fuchsin, basic = Pararosanilin = parafuchsine = magenta 0 = basic red	42 500	569-61-9
Cristal violet = Kristallviolett = methyl violet 10 B = basic violet 3 = gentian violet	42 555	548-62-9
Methyl violet 2 B = Methylviolett = methylrosaniline = pyoctanin = pyoctanum coeruloum = basic violet 10	42 535	8004-37-3
Red		
Solvent red 7 B = Sudanrot 7 B = Fettrot, bläulich	26 050	6368-72-5
Solvent red B = Sudanrot B	26 110	3176-79-2
Congo red = Kongorot = cotton red B,C = cosmos red = direct red 28	22 120	573-58-0
Ponceau S = Ponceaurot	27 195	6226-79-5
Orange		
Safranin O,Y,A = Safranin T = cotton red = gossypimine = basic red 2	50 240	477-73-6
Orange G = wool orange 2 G = acidorange 10	16 230	1936-15-8
Brown		
Bismarck brown G,B,Y = vesuvin = basic brown 1	21 000	10114-58-6
Bismarck brown R = basic brown 4	21 010	5421-66-9
Green		
Malachite green (-oxalate) = Malachitgrün = Diamantgrün B = Echtgrün = basic green 4	42 000	2437-29-8
Light green SF yellowish = Lichtgrün SF gelblich = acid green 5	42 095	5141-20-8
Blue		
Nile blue (A) = Nilblausulfat = Nilblau A = basic blue 12	51 180	3625-57-8
Black		
Solvent black B = Sudanschwarz B = Fettschwarz = Ceresschwarz = solvent black 3	26 150	4197-25-5

2.5.3 *Fluorescent spores*

The time needed to examine the spore samples in the laboratory is a disadvantage of the spore drift method. MAYR (1954a) expects the counting of a sample to last 1-2 days; HOFER (1959) 6 per day and BAUER (1967b) assumes 4-8 samples per workday after preparation.

The preparation of *Lycopodium* spores with fluorescing substances eases the examination of the spore samples. Under a fluorescence microscope, the spores are much easier and faster to recognize due to the dark background (KÄSS 1982c). Compared to the time-consuming examination with simply dyed spores in incident light, a time factor of 5-10 can be saved when using fluorescent spores. Furthermore, it is also possible use fluorescent and conventional types simultaneously (KÄSS & REICHERT 1988).

The dye adsorptivity is not equally good for each single spore. Fluorescence intensity and dye tone are slightly different from spore to spore. At this time, no more

than three fluorescent dyes can be used simultaneously and still be assured of a clear identification of the differently dyed spores:

Acridine orange (yellow fluorescence),
Pyronin (red fluorescence),
Tinopal CBS-X, (blue-white fluorescence).

Fluorescent spores, dyed with acridine orange, were first used in December 1978 at the percolation sites of the Upper Danube. The tracing test, which was carried out in a well-known underground channel together with uranine, verified the usefulness of this new tracer and its superiority over the spore drift method with spores dyed with non-fluorescing substances (Fig. 91).

Spore dyeing with fluorescent dyes
Parts of the dyeing method for dyeing *Lycopodium* spores with fluorescent dyes differ greatly from dyeing with non-fluorescent dyes. With tinopal for example, several processing steps are involved. A detailed description of the dyeing process for the three named fluorescent dyes follows.

Dyeing with acridine orange ($C_{17}H_{20}ClN_3 \cdot ½ZnCl_2$)
C.I. 46 005 CAS: 65-61-2
Synonyms: 3,6-Tetramethyldiaminoacridine-hydrochloride,
Basic Orange 14.

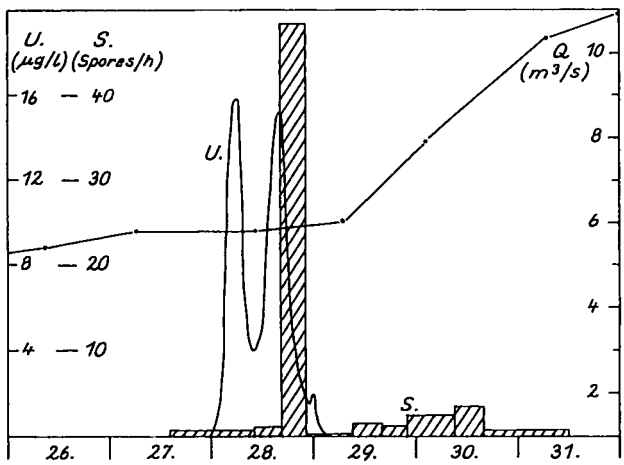

Figure 91. Breakthrough curves from the first use of fluorescent spores along with uranine at the Aach spring. On 26 December 1978 at 13:15 hours, 6 kg of acridine orange dyed spores and at 13:30 hours, 3 kg of uranine were injected in the Danube percolation between Immendingen and Möhringen (river-km 174 + 450). The uranine breakthrough curve (U.) shows two large and one smaller concentration peaks, that are due to underground ramification and to the heavy rains in the night from the 27th to the 28th of December, as well as rainfall on the 28th. The main spore appearance does not occur until shortly after the second uranine peak (s.). Daily average discharge of the Aach spring (Q). Site plan and map see Figure 75:G.

Acridine orange is a zinc containing closed ring quinone dye, which is often used in histology for DNA- and RNA-staining, because of its good tissue adhesion (WITTEKIND 1979).

For one kilogram of spores, the dyeing process is as follows (KÄSS 1981b):

¾ l of an aqueous solution with 0.1% acridine orange and 5% surfactants (e.g. Marlon 375) is added to a 5-l-beaker. Then while slowly stirring and on low heat, gradually add the spores. In case the spore pulp can no longer be stirred, add more dye-detergent-solution. After bringing to a short boil, let the mixture cool overnight.

After settling, the spore pulp is decanted twice with tap water. While stirring, 1 l of a 5% formaline solution is added and the mixture brought to a short boil. After decanting twice with tap water, the intensively coloured orange-yellow spore pulp is suctioned off in a Büchner funnel and put in the oven to dry in aluminium dishes at 80°C.

Instead of a 5% surfactants solution, 7.5% of a cleansing agent can also be used.

The preparation step with formaline can be left out if the dried spores are to be used within one week.

Dyeing with pyronin GY ($C_{17}H_{19}ON_2Cl$)
C.I. 45 005 CAS: 92-32-0
Synonyms: Xanthylium,3,6-bis (diethylamino)chloride,
Pyronin G,
Pyronin Y,
Pyronine bleuâtre.

Pyronin, like acridine orange, is a closed ring quinone dye and also belongs to the group of xanthene dyes. In cell staining, pyronin is used to differentiate between DNA and RNA.

Pyronin is well soluble in water, its fluorescence maximum is at 551 nm and has a fluorescent intensity of 60% of uranine's. However, its use as a tracer in the aqueous phase is not likely due to its relatively high cost.

In preliminary tests, several red-fluorescing dyes were examined as to their suitability as spore dyes (DREYER 1987). According to EISENBRAND (1953), Hostasol Red 5b (HOECHST), nile blue (= basic blue 12, C.I. 51 180), erythrosine (C.I. 45 430), and azlaktone (1-phenyl-4-dimethylaminobenzoloxaolinone) did not adhere to the spore surface. Sulforhodamine B (C.I. 45 100) and amidorhodamine G (C.I. 45 220) had only very slight fluorescence effects. The four dyes, rhodamine 6G (C.I. 45 160), Hostasolrot GG (HOECHST), pyronin B (C.I. 45 010), and pryonin GY (C.I. 45 005) remained. Pyronin GY was chosen, because this dye produces a uniformly strong red fluorescence of the spores. Furthermore, due to its good water solubility, the dyeing process is relatively simple. Following instructions are for 1 kg of spores:

1 l of a 5% detergent solution is added to each of two 5-l-beakers. The solution can be made with Marlon 375 or with a 10% cleansing agent. While stirring, gradually add portions of a ½ kg of spores to each beaker. In case the spore pulp becomes too viscous, more detergent solution can be added. Be sure that the spores are uniformly wetted. When finished, each beaker should contain 1.5 l of the detergent solution.

Let the spore mixture swell overnight. It is then slowly heated to 70°C with continuous stirring on a magnetic stirrer with a hotplate and kept at this temperature for another ¾ hour while still being stirred. The treated beaker is then removed from the hotplate and the second beaker prepared in the same manner. The still warm contents from the first beaker are added to a Büchner funnel with a 240 mm inner diameter with a round filter paper that is placed on a 10-l-filter flask. The spore mixture is suctioned off and then rinsed with approx. 10 l of warm water. The mixture must be suctioned dry for ¼ of an hour. Then the spore pulp is placed in a 5-l-beaker for the dyeing process. To dye 1 kg of spores, 2 g of pyronin GY are dissolved in 4 l water. To ensure that the dye is completely dissolved, it must be stirred for a long time in a 5-l-conical shoulder reagent bottle. The dye solution is then poured evenly in the two 5-l-beakers with the degreased and suctioned dry spore mixtures. While stirring, the mixtures are heated to 70°C and then left to cool overnight. The next day, the mixtures are again slightly heated, filtered through a Büchner funnel and then each rinsed with 10 l of warm water. Then the spore pulp is placed on aluminium dishes to dry in the drying oven at 70°C for 2-3 days.

Dyeing with tinopal CBS-X (Ciba-Geigy)

In the first tracing tests with spores dyed with acridine orange, during examination under the fluorescence microscope, broken pieces of fibre were noticed that were impregnated with optical brighteners. They shined light blue and irradiated their surroundings. Thus, it was natural to try and also dye spores with optical brighteners.

Several preliminary tests with different optical brighteners produced only unsatisfactory results. The optical brighteners could not be made to adhere to the spores, neither in acidic nor in basic medium, nor using metallic salts. Mr.Dir.Dr.RÜHLE from the BASF-plant 'Farben und Fasern' (dyes and fibres) in Besigheim/Württemberg, FRG, suggested using cationic surfactants as a dye coupler; he also provided trial samples. Using these dye couplers, it was possible to dye the *Lycopodium* spores with optical brighteners.

In the tests the dye couplers used were the cationic surfactants from BASF, Dinorame O (= N-Oleyle-propylen-diamine) and Armeen C = Noram C (= N-Kokosalkylamine). In the field, only Armeen C was used. The latter is not soluble in water; therefore, it must be converted into the water-soluble acetate. The dyeing process is somewhat more painstaking than with either acridine orange or pyronin. Detailed instructions for dyeing 1 kg of spores follows:

1. Degreaseing and dewaxing of the spores

The dyeing process is similar as for pyronin: 2 × 0.5 kg spores in 2 5-l-beakers are mixed with 5% detergent solution and heated to 70°C, filtered through large Büchner funnels and rinsed several times with warm water.

2. Applying the dye coupler

To produce the dye coupler solution: 2 parts of Armeen C are mixed with 4 parts of glacial acetic acid, heated and diluted to 100 parts with water. Careful, caustic!

Add the 0.5 kg spore pulp from the Büchner funnel to a 5-l-beaker. Layer with 1 l of the dye coupler solution, stir and heat to 70°C.

Filter the still warm spore pulp through the Büchner funnel (the first filtrate can be used for treating the second 0.5 kg of defatted spore and for further batches). The dye coupler residue in the spore pulp in the Büchner funnel must be completely rinsed out

with warm water. As a check, a few drops of tinopal solution can be added (see Part 3: Dyeing); flocculation indicates dye coupler residue!

3. Dyeing

The spore pulp is removed from the Büchner funnel and put into a 5-l-beaker; then 1 l of a 0.5% tinopal CSB-X solution is added, stirred well and heated to 70°C and, while stirring, kept at this temperature for ¼ hour. The warm spore pulp is then rinsed several times in a Büchner funnel with warm water. The first filtrate can be used several times for the dyeing process! If the spores are not to be used within one week, then the spore pulp in the Büchner funnel is covered with a 1 cm layer of 5% formaline solution and suctioned through.

4. Drying

The spore pulp is removed from the Büchner funnel and put in aluminium dishes and dried at 70°C in the drying oven for 2-3 days.

The fluorescence measurement of the fluorescent spores according to the excitation and fluorescence intensity is carried out in a fluorescence spectrometer with 2 monochromators. To do this, the spore powder is gently pressed into the powder cuvette, which is delivered with all spectral fluorimeters. In the following table it can be seen that the maxima of the aqueous solutions do not coincide with those of the spores. The spores' maxima are all displaced towards the longer wavelengths (values in nm at absorption maximum A and at fluorescence maximum F):

Spectra from fluorescing dyed spores are shown in Section 2.5.4 in 'Examination of fluorescent spores'.

	Aqueous solution		Fluorescent spores	
	A	F	A	F
Acridine orange	491	521	515	547.5
Pyronin GY	524	551.5	580	596
Tinopal CBS-X	360	435	395	447.5

2.5.4 *Conducting spore drift tracing tests*

Application areas

The spore drift method was developed in the calcareous alpine karst and successfully used in the 1950s. The major advantage of the spore drift method is the given opportunity for servicing hard to reach sampling sites. However, numerous spore tracing tests have also been conducted in karsts of the German Uplands (SCHULZ 1961, HÖLTING & MATTHESS 1963). Furthermore, spores have also proven themselves in tropical karsts, where the sampling sites can only be reached with great difficulty (SMART & SMITH 1976). With great success, watercourses in basalt conduits have been followed (HACKER et al. 1983).

It is not known here whether spore drift tracing tests have been successfully carried out in fissure groundwater aquifers, in open or large grained pore-groundwater aquifers or in surface waters.

Injection amounts

Determining the amount of spores to be injected depends mainly on the local condi-

tions. ZÖTL (1957b) recommends 3-5 kg for a flow distance of 5 km, for a distance of 10 km, 10 kg spores. In 1974 however, he noted that an excess of spores is an advantage and therefore 1½ to 2 times the calculated amount should be injected. Further calculation methods are noted in Section 3.2.5.

Several examples from field tests can serve as support in deciding the amount of spores needed:

Test area, year	Spore type and amount	Flow path (km) grade	Evaluation	Author
Buchkogel, 1956	Undyed, 3 kg	0.8 1:11	Good	MAURIN & ZÖTL 1959
Dachstein region, 1956	Blue, 12 kg	up to 13 1:12	Minimum spore amount	ZÖTL 1957b
Tauplitzalm, 1957	Blue, 6 kg	3.8 1:6.1	Good	ZÖTL 1961
Dachstein, 1958	Red, 20 kg	up to 12.5 1:5.7	Very good	ZÖTL 1961
Oberndorf, 1959	Violet, 1.4 kg	3.1 1:22.5	Bad due to pretreatment (spores were not dried)	SCHULZ 1961

Transport and injection of Lycopodium spores

It is advisable to dry the spores in the laboratory after the dyeing process.

The dried spores are then placed in a plastic container or pail, filling only half full, and covered with a well-fitting lid to avoid spillage during transport through rough terrain. At the injection site, the spores can be stirred in the transport container.

In 1976, DECHANT described a 'new preparation method' for spores, namely, not bothering to dry the spores after dyeing and injecting the wet spore pulp straight after the dyeing process, in order to avoid the painstaking and time-consuming wetting of the spores. This would indeed stop spore loss and possible contamination due to spillage or strong winds during the injection. However, he also mentioned the disappointing low yield obtained in 1975 in the Slovenian karst using this method. During the combined tracing tests there on 27 May 1975, 14 different tracers were injected in 12 ponors, some very far apart (BAUER et al. 1976). At Ponor Ribce in the Planina basin, 10 kg of green and 10 kg of brown dyed spores were injected simultaneously. The green spores were dry and wetted shortly before the injection. The brown spores were not dried in the laboratory after dyeing and brought to the test area as a 25-l-suspension and injected after diluting to 50 l. The main recovery sites of the spores were in three spring groups 11.5 to 12 km away from the injection site. The percentage of the brown spores recovered, which were not dried after dyeing, as compared to the green spores, which were, was between 28 and 41%, on the average only 37%!

It must be noted however, that in 1959 during the Oberndorf tracing tests, the same unsatisfactory results using spores that were not dried were obtained (EISSELE 1961, SCHULZ 1961) (Figs 60 and 61). There, 0.4 kg red, 0.8 kg green, and 1.4 kg violet spores were injected simultaneously in a sinkhole and observed in the Dieselbach spring, 3.1 km away. The red and green spores were dried in the lab after dyeing and

mixed with water shortly before the injection. The violet spores were left in the dye solution after the dyeing process was completed and brought to the injection in that condition. The results from the spore counts for the observation period from day 1 to 42 are listed with the injection amounts here:

	Red	Green	Violet spores
Ratio at injection	1:	2:	3.5
Observed single spores	39	89	6
Ratio in sampling	1:	2.3:	0.15

Compared to the dried spores, the reappearance of the spores, which were left in solution, was approx. 25 times lower.

Naturally, the reason for this occurrence was sought. Mainly, it is assumed that the spores that are not dried after dyeing have an increased sinking speed in flow sections that are not turbulent. On the other hand, the spores that are dried after dyeing have most likely regained their floatability.

In laboratory tests, DECHANT and HACKER (1988) ascertained that when wetting the spores in the field according to the following procedure, a lower sinking speed, a lower sorptivity as well as a higher dye intensity of the single spores is obtained:

For 1 kg of dried spores, 3 l of a solution of 10% citric acid + 1% Extran neutral, MERCK, is added (called 'Citran 10/1' by the authors) and stirred. However, it must be noted that lab tests do not always suffice for recommendations if not comparable to field conditions.

It can take quite a long time to wet the spores dyed with non-fluorescing dyes, since they are hydrophobic. In such cases, detergents can be added to help the wetting process. Up to now, the wetting of fluorescent spores causes no problems.

After wetting the spores, they are passed through a 2-mm-sieve, which is placed in a large metal or plastic funnel. The sieve holds back large clumps and provides a way to crush the clumps. At the injection site, a hose that is as wide as possible should be attached to the injection funnel and placed as far down into the karst opening as possible. If the injection site is a sinkhole with a water flow of approx. 1 or more litres per second, there are generally no problems with the injection. With lower flow rates, another source of constantly flowing water should be provided, either through the sieve or next to the hose in the funnel. In this case, take care to provide a uniform spore injection.

Contamination precautions

As a rule, the workers who handle the spores, also during the injection, should wear gloves and protective overalls. Often all that is needed is a small flow of air to blow the spores away. Furthermore, precautions must be taken to avoid spore contamination. Thus, workers involved in the dyeing or the injection of the spores, should not be involved with their examination. The dyeing should also not be carried out in the same rooms that are used to examine the spores (BAUER 1967b).

Spore sampling

For sampling, plankton nets are hung in the presumed reappearance sites. The funnel-shaped nets are made of nylon gauze. The brand 'Nylobit 25 T II-25' from the

Swiss silk gauze factory 'Schweizerische Seidengazefabrik AG.' in Zürich works exceedingly well. This type of gauze has a free sieve area of 9% with a sieve opening of 25 µm. Gauze made of natural silk does not last as long as synthetic gauze. Natural silk becomes brittle with use; moreover, caddis fly larva like to nest in the fabric and are very hard to remove. In spite of being washed out after every use, the natural silk nets were no longer usable after only six weeks.

During the tracing tests in the Lur cave system in 1966, basic investigations concerning the best outfitting for the spore nets were undertaken (BATSCHE et al. 1967). The following noteworthy stipulations were made:

– Nylon nets have a ca. ten times higher spore yield than silk nets,

– Sieve openings of 60, 45, and 35 µm had, compared to a sieve opening of 25 µm, a higher spore yield of only 0.5-5%, 10% and 60%.

– If nylon spore nets with a 25 µm sieve opening are hung in the sampling site for 6, 12, and 24 hours instead of 2 hours, there is only an increase in the spore count from 5000 to ca. 7500, 10,100, and 11,000 spores.

– If the nets are not hung horizontally, but rather vertically according to Figure 92, there is a yield of 50-100% more spores.

Since both synthetic and natural silk nets are hard to sew, only professional silk sewing should be used to make the nets. The net opening is made of a stainless steel ring with a 12-cm-diameter (Fig. 93). The end of the funnel-shaped 20 cm long net narrows to 2.4 cm, with a holder for a replaceable glass funnel.

In BAUER (1967b), detailed experience concerning the placing of the nets in the field is given. In channels, the nets are placed in a wooden frame with the measurements 19 × 19 × 40 cm (Fig. 93). The 6 piece collapsible wooden frame, consisting of 4 wooden rods and 2 square wooden frames is best put together in the field with wing-nuts (MAURIN & ZÖTL 1959). To prevent larger drifting matter from clogging or damaging the net, the front of the frame is best covered with a 2-mm-brass mesh. A mesh size of 1 mm clogs according to BAUER (1967b) very quickly, thus stopping the flow to the net. If possible, channels which carry large amounts of sand or pebbles should be fitted with a sand trap (Fig. 92). The wooden frames should be weighted down with

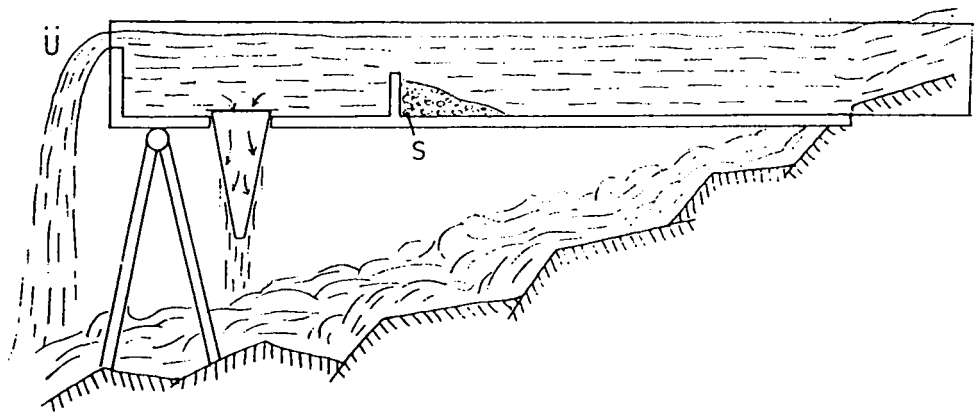

Figure 92. Vertical placement of the spore nets; Ü = overflow weir; S = sand trap (from BAUER 1967b).

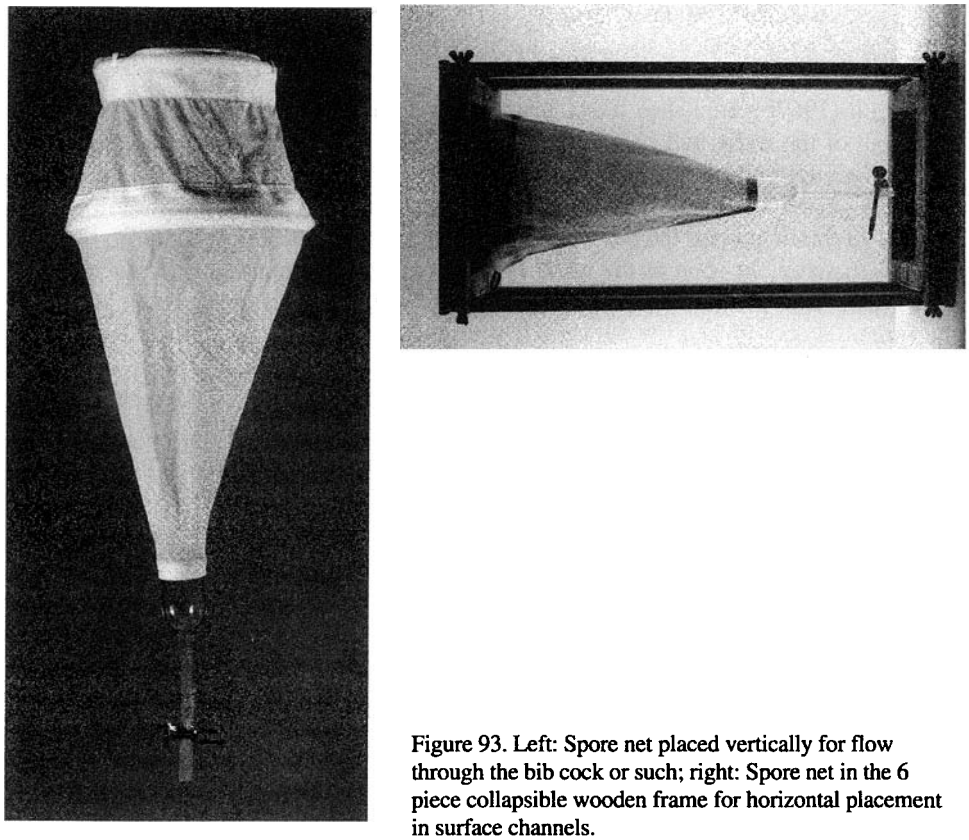

Figure 93. Left: Spore net placed vertically for flow through the bib cock or such; right: Spore net in the 6 piece collapsible wooden frame for horizontal placement in surface channels.

stones or tied down with wires or strong string. This is especially necessary if heavy flow is expected during the drift tracing test. MAURIN and ZÖTL reported in 1959, that the spore nets can be astonishingly resistant. They mentioned that during a drift tracing test in the Dachstein region, heavy rains fell on the evening of the 10th of August in 1956 and as a result, heavy debris overwash occurred in the Enns valley. The spore net hung in the Feisterbach in the Ramsau (B_2 in Fig. 90) was completely covered, only the fastening ropes were visible in the gravel. Although the net and frame were buried 40 cm deep in the gravel, they were undamaged, although taut full with fine sand! Siphon piping with 2-3 cm hoses can also be used. If the nets can be hung without the frame, sampling is easier. If pumping wells are incorporated in the investigation net, vertically hung nets with continually open bib cocks are the only possible sampling method.

A complete listing of all sampling possibilities cannot be given here. It is important that the following points be regarded:

– The spore nets should be installed so that a uniform flow is assured.

– In shallow, open channels, the nets hung in the wooden frames need to be protected from debris with suitable means.

– To avoid being swept away, they need to be weighted down (see Fig. 24 in MAURIN & ZÖTL 1959).

– The nets need to be easily accessible for the sampling teams. On the other hand, they should not be placed too conspicuously to avoid tampering with by other people.

BAUER (1967b) published exact instructions for taking spore samples. The net is taken out of the water and held vertically so that the water can slowly flow out. Since the nets are normally covered with clay particles after being hung in the water for the sampling period, the water only flows out slowly. The water flows out better by drumming with the fingers on the net when it is tautly filled with water, which also removes most of the clay. As soon as the net is empty, it is rinsed from the inside several times with water from a squirt bottle. During the last rinse, the pinch-cock at the bottom of the funnel is opened and the net contents emptied into the sample bottle. The sample bottles should not be made of plastic, but rather out of brown glass, to prevent spore adsorption onto the bottle sides. Bottle sizes between 30 and 250 ml have been recommended in the literature. Previous experience shows however that place-saving 100-ml-rectangle-brown-glass bottles are sufficient to hold the net contents. To prevent spore contamination when reusing the bottles, the tightly closing screw lids should not have inserts.

The nets must be thoroughly washed both inside and out after removing the sample before they can be reinserted in the sampling site. After the last sample has been taken, the nets should be carefully washed and dried to prolong their durability. In case holes develop in the nets through usage, they can be closed with water insoluble glue.

Sample pretreatment

The samples can rarely be examined for *Lycopodium* spores without pretreating. Depending on the purity of the water being sampled, more than just the spores were also sampled. Samples from springs or wells out of deep and covered karst sampling sites are normally very clean and contain in general very little additions, such as calcite crystals or rust particles. Springs that tap deep or covered karsts can often be only sampled at the outlet weir. Such samples are considerably dirtier; besides inorganic particles, they also contain plant matter, such as torn algae filaments, leaves, and in the fall also decay residue from foliage.

The amount of foreign material is considerably larger, if springs which tap shallow karsts or even surface water bodies are sampled.

To remove organic residues to a large extent, MAYR (1954b) and HOFER (1959) followed the advice of BERTSCH (1942) and added caustic potash solution to the samples. In the lab, the samples are poured into test tubes and treated with 3 ml 10% caustic potash solution and then kept for 20 minutes in a water bath at a low boil. MAYR (1954b) also wrote that treating with acetic anhydride-sulfuric acid results in good microscopic detection. During the examination of undyed spores, HOFER added a bit of glycerine to the samples which had been centrifuged and decanted twice, to prevent the sample from drying out in the slide glass while under the microscope. HOFER protected the colour of the dyed spores by adding a pinch of urea and 1 ml of formaldehyde before adding the caustic potash solution. Through this procedure, the spores receive a protective coating of carbamide resin. Glycerine is not added with dyed spores.

DECHANT, MAURIN and ZÖTL (DECHANT et al. 1958) and DECHANT (1959) recommend always coating the spores with a carbamide resin before further treatment, if not already done after the dyeing process. To do this, for 100 ml of a sample from the spore

net, ca. 5 g urea and ca. 5 ml of formalin as well as 5 ml 10% caustic potash solution are added and kept for 10 minutes in a water bath.

BAUER (1967b) removed larger calcite particles in the spore sample by pouring into, diluting, stirring, and decanting in a 250-ml-beaker (high form). Finer calcite particles were dissolved with hydrochloric acid. DECHANT and HACKER (1988) recommend pretreating the 100 ml-spore samples with 15 ml of 'Citran 15/2', i.e. a solution of 15% citric acid with 2% Extran neutral, MERCK. With this, most of the calcite debris can be dissolved.

HÖLTING and MATTHESS (1963) separated the spores from the foreign particles with a gravity solution of potassium iodide-cadmium iodide with a density of 2.0. After the samples were put into suspension, they were centrifuged and the unwanted foreign particles settle to the bottom of the container. The spores still float in the liquid phase and can be decanted onto a filter. Due to health and environmental dangers, this spore treatment method should not be implemented.

During the spore drift tracing tests conducted by the Geological Survey of Baden-Württemberg/FRG at the end of the fifties and the start of the sixties, the samples of the simply dyed spores were filtered in the lab. The filter apparatus, which was set on a filter flask, was sold by the companies that specialize in membrane filtration. It consists of the following separate pieces (from top to bottom):

Filling funnel made of porcelain or glass, 45 mm high, 65 mm inner diameter = 20 cm^2, content: 260 ml,

Upper aluminium stretch frame, 4.5 mm thick with three 56 mm long screws at the joints with washers and butterfly-nuts,

Silicon gasket, 70 mm inner, 90 mm outer diameter, 2.5 mm thick,

Round paper filter, 90 mm diameter, quantitative, wide pore (white ribbon),

Glassfrit poretype 0 with a solid border, 85 mm diameter (porcelain-bolt circles proved not sufficient),

Silicon gasket as above,

Outflow funnel made of porcelain or glass with 65 mm long tilted outflow and 13 mm outer diameter for setting in the filter flask,

Lower aluminium stretch frame with 3 slots to hold the clamp bolt of the upper stretch frame.

EISSELE (1961) came to the conclusion, that the spore sample in the bottle could simply be poured into the filling funnel. The turbid particles settle and the spores stay afloat in the water. Even a 1 mm thick turbidity layer would not disturb the spore examination later on. Furthermore, EISSELE recommended taking the round filter out of the filtering apparatus after filtering and laying it on a square piece of filter paper and covering with a square of plastic wrap of the same size. Samples prepared in this manner could be kept permanently and used for later investigations.

All of these treatment methods are carried out to free the spore sample of sediments and suspended solids before being examined under the microscope. Then, the better the spores are concentrated in the prepared samples, the easier, the faster, and more reliable the spore count.

To reach this goal without harming the spores and without contamination risks, the following method is suggested: Before the sample bottles are emptied, an ultrasound probe is inserted in the sample solution for one minute, to loosen adhering spores from the bottle walls. This also frees the spores from clay particles. Then the

entire sample is passed through a metal sieve with 0.1 mm mesh openings into a 1-l-beaker (high form). Then the sieve is rinsed with a jet of water from the tap. A wash bottle is used to thoroughly rinse the sieve edges. Sieves with a narrow mesh opening of 0.06 mm have the disadvantage that the rinse process takes too long and that larger spores could stay in the sieve. Then the sample is filled with tap water to the 1-l-mark. If there is a large amount of ferrous hydroxide in the sample, ca. 1 g of EDTA-powder can be added. Then the sample is mixed well and left to settle overnight covered with a watch-glass. In case not all of the ferrous hydroxide is dissolved after the first addition of EDTA, repeat. EDTA also dissolves carbonate, which is also desirable. If the samples from a certain sampling site regularly contain large amounts of ferrous hydroxide, the original sample bottles can be pretreated with EDTA-powder. In these cases, ca. 250 mg EDTA-powder is sufficient for each 100 ml of sample volume.

The next step is to prepare the sample for counting under the microscope. For this, a membrane filtration using a filter apparatus according to Figure 94 is prepared. A black-grey cellulose nitrate membrane filter with a diameter of 50 mm, a pore width

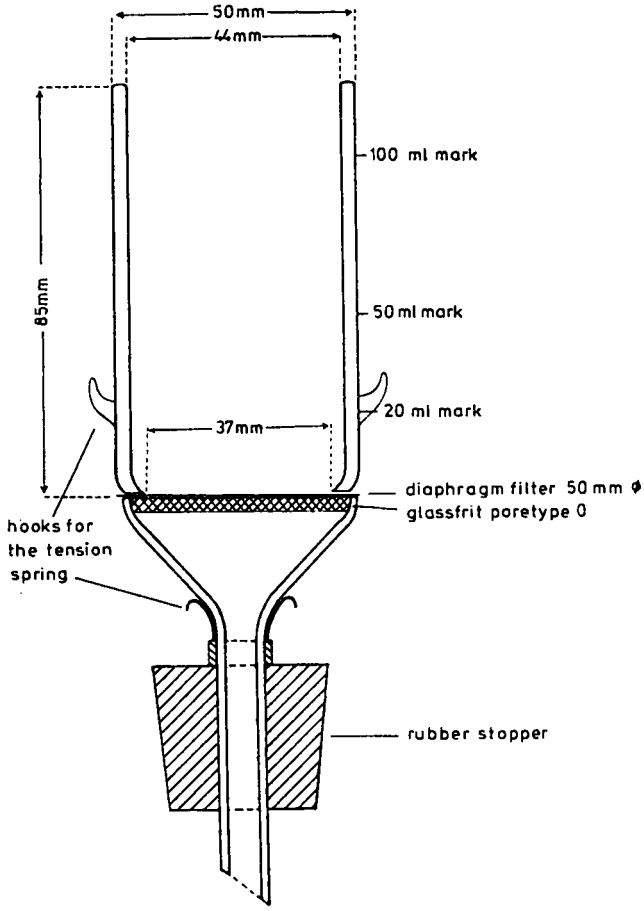

Figure 94. Filter apparatus for preparing the membrane filters for counting the spores under the microscope (cross section).

of 8 µm, and imprinted with a grid is fastened onto the glassfrit of the filter apparatus (e.g. Type SM 130.01 of the SARTORIUS-Membrane filter company in Göttingen/FRG). The membrane filter must be wetted before being inserted, so that they are supple. Dry filters are brittle and swell in water somewhat. Thus if they were to be inserted dry, they might wrinkle when wetted.

Then the suspension is stirred in the beaker; hereby the larger particles, which at any rate are not spores, collect in the middle of the beaker's bottom. After stirring, 1-2 minutes are waited to allow the suspension to settle. After this liquid is decanted into the suction filter, the sample is mostly free of suspended solids. Except for samples with very little residue, filtering is always done in aliquote parts; the filtration amount must be limited so that the imprinted grid is always well visible. For easier measuring of the aliquote parts, the suction filter should have marks at 20, 50, and 100 ml.

If these guidelines are adhered to, the spores will be preferably concentrated in the sample fraction. The separations achieved are:

Wire mesh on the flow side of the spore nets >2 mm
Wet sieving of the sample in lab >0.1 mm
Decanting before filtration of mineral grains ca.>0.05 mm
Plankton nets <0.025 mm
Membrane filter <0.008 mm

The separations are not quantitative. A major part of the clay particles in the sample water adheres to the nets. Furthermore, lime-rich karst water samples tend to precipitate calcareous deposits upon standing, reduced water samples tend to precipitate ferrous hydroxide deposits.

Examining for spores

The instructions from HOFER (1959) and BAUER (1967b) aim to produce slide glasses containing the spore samples. After centrifuging, the spore samples are conveyed to the slide glasses with pipettes or glass rods. To count the samples they are covered with cover glasses and protected from drying out at the edges with a bit of glycerine. The slide glass is fastened under the microscope on the cross table and enlarged 100- to 200 times. This way, the spores can be counted. HOFER used a counting plate with a counting chamber with millimetre grid, such as those used in haematological labs for blood cell counts. Sideways lighting with a microscopic lamp should help in identifying the spores. It is further recommended for ease in differentiating between the blue and violet spores to insert a blue filter in front of the lamp.

GARDNER and GRAY (1976) found that in incident light both orange spores and spores dyed with solvent black 3 appear dark-grey and cannot be differentiated. If however, transmitted light with a condensor and stops are used, both spore types can be identified easily by their orange and grey colouring. The authors did not write however, what was used to dye the spores orange.

After filtering the spore sample suspension through a 65-mm-filter apparatus, a filter with a surface area of 20 cm^2 is obtained. The spores can be easily counted using such a filter under a microscope with two eyepieces. A glass plate with a ruled grid is placed on the prepared filter (see previous section), which allows, even with a high amount of spores, a counting of aliquote areas (EISSELE 1961).

Preparing the spore samples on 50-mm-membrane filters has special advantages, since during the pretreatment almost all of the unwanted matter has been removed and thus the spores are massed together on a circular area with a diameter of 37 mm. The area is thus exactly 10 cm^2 and has 100 squares in the grid. Each square corresponds therefore to one percent of the filtered sample suspension, which makes the aliquote counting of the spores easier, even with high spore concentrations. To assure that no major errors occur when calculating the total spore count after counting the aliquote parts, the principles of statistics must be heeded (HOFER 1959).

To examine the membrane filter area, the microscope must be outfitted with a large mechanical stage with a moving radius of ca. 50 × 75 mm.

The membrane filtration method was first developed for fluorescent spores. However, conventionally dyed, non-fluorescent spores can also be examined under the microscope with incident light. The spores are set off well against the dark membrane background. The spores can also be well identified under a fluorescence microscope. With green excitation, the spores dyed blue appear red and those dyed red also appear red, but a dark red (KÄSS & REICHERT 1988).

When examining the fluorescent spores, the still wet membrane filter is placed on the square glass plate which fits on the cross table, so that the ruled grid is exactly parallel to the glass plate edges. A cover glass is not needed. One starts at the outer edge of the filtercake and examines each square in a zig-zag pattern, until all 100 squares have been examined. With a dense spore covering, only a fraction of the squares needs to be counted.

Modern fluorescence microscopes are outfitted with cross tables with different choices of filter combinations for specific selection of the excitation and fluorescence wavelengths. These filter combinations have three optical filters: 1. Excitation filter, usually a band pass filter (BP) for selecting the exciting radiation. 2. The colour divider (FT) reflects the incoming light up to a certain wavelength, lets however light in longer wavelengths unhindered through. 3. Fluorescence filter: usually a long pass filter (LP), which only lets the excited fluorescence light through (Fig. 95). Choosing the suitable filter combination is based on the excitation and fluorescence spectra of the spores being examined (Fig. 96). For the three types of fluorescent spores used up to now, the following optimal filter combinations have been determined (values in nm):

Dyeing with	Acridine orange	Pyronin GY	Tinopal CBS-X
Excitation filter	BP 450-490	BP 510-560	BP 395-425
Excitation colour	Blue	Yellow	Violet
Colour divider	FT 510	FT 580	FT 425
Fluorescence filter	LP 520	LP 590	LP 450
CARL ZEISS-Filter set	9	14	18

The following graduations for the objectives have proven suitable: 6×, 10×, 16×, 25× and 40× magnification.

The membrane filter is examined with the lowest magnification in a zig-zag-pattern. The field of view through the oculars is 10 times so wide, that the height of a square of the ruled grid on the membrane filter can be sufficiently examined. For viewing, the UV-excitation filter set 18 is used, which allows the identification of the spores with all three fluorescent dyes.

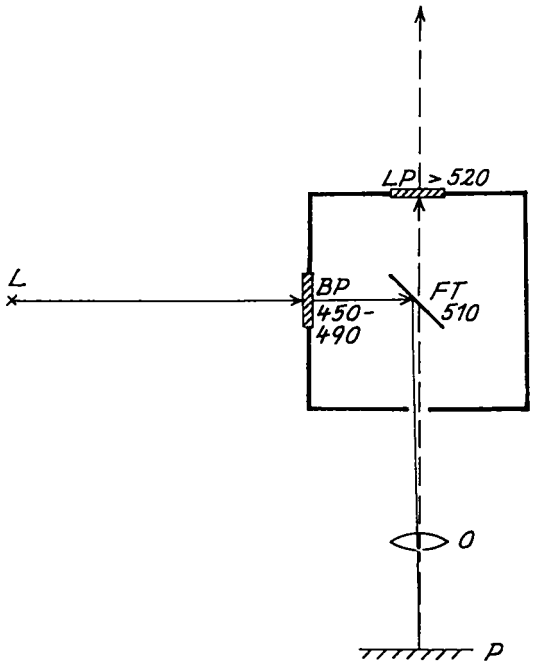

Figure 95. Schematics of the radiation path in the selection unit of an incident light fluorescence microscope with wavelengths for the CARL-ZEISS-Filter set 9 used to examine for spores dyed with acridine orange (in nm). L = light source (mercury-high pressure lamp 50 W), BP = band pass-excitation filter, FT = colour divider, O = objective/condensor, P = prepared filter, LP = long pass-fluorescence filter. Solid arrow = excitation radiation path light source – prepared filter, dotted arrow = fluorescence radiation path prepared filter – ocular.

Spores dyed with acridine orange have an intensive green-yellow colouring under blue excitation. The mesh structures are somewhat out of focus at higher magnifications. Under violet excitation, the spores have only a slight green luminescence (Plate 5).

Under yellow excitation, spores dyed with pyronin shine with an intensive red, whereas the remaining fluorescent spore types are no longer visible. Under blue excitation, these spores shine weaker and under violet excitation, they shine only a very weak red. Under a green filter excitation (510-560 nm), besides the fluorescent spores, non-fluorescent spores dyed red and blue can also be identified.

Spores dyed with tinopal shine with a light blue luminous under violet excitation. It is noticeable that each spore shines with a slightly different intensity. Under blue excitation they only shine with a weak vitreous blue-yellow colour.

When examining the prepared spores with objectives stronger than 6.3×, it should be remembered that due to the strong focussing of the light rays, water can evaporate out of the membrane filter and condense on the objective. Therefore, high objectives should only be used for short times.

Since besides the spores, other particles similar to the spores in form, size and colour can also appear under the microscope, it is advisable to identify the mesh structure on the calottes. Only this way is it possible to avoid false counts. It is advisable to have prepared spore samples ready for comparison.

Disturbing fluorescing particles sometimes occur under the microscope.

Mineral pieces of calcite shine with a blue luminous under violet and blue excitation; they are however easily identified due to their sharp edges as minerals. Chloro-

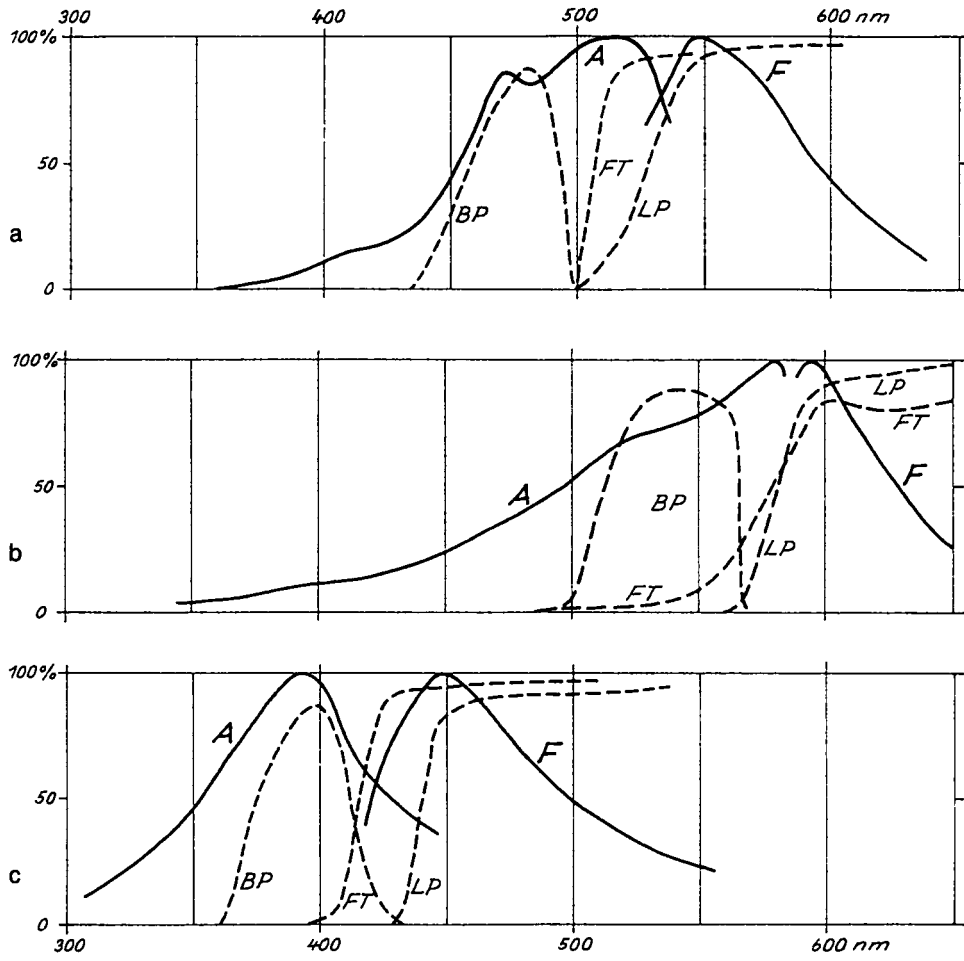

Figure 96. Fluorescence spectra and the corresponding transmittance for their filter sets. Excitation and fluorescence intensities for spores dyed with acridine orange (a), pyronin GY (b) and tinopal (c) are given relative to maximal fluorescence at 100%.

phyll bodies shine with an intensive red. Samples which have been stored a long time before being examined, can sometimes be covered with thin layers of red fluorescing algae. Light blue strings under violet excitation are with certainty foreign textile fibres.

Other foreign fluorescing matter can have originated from the following materials (HAITINGER 1959): porphyrines, glucoside-plant dyes, woody parts of the berberis (green), B-vitamines, flavines, and vitamin A_1 (intensive green), woody parts of the mahonia and acacia (yellow), other woody plant parts (blue to blue-green), chlorophyll and porphyrines (red), vitamin A_2 (yellow-brown).

Presenting and evaluating spore drift tracing test results

In contrast to most other tracers and tracing methods, in spore drift tracing tests the samples are not taken at specific times, but rather accumulated over a more or less

long period of time. The results are customarily presented as column diagrams (Fig. 97 top). The area displayed by such a presentation suggests a spore concentration which is not actually true. Somewhat better would be a presentation with vertical lines at the times when the spore nets were hung in the sampling site (Fig. 97 middle). At any rate, it would be totally inappropriate to present the data the same way as momentary samples, namely as concentration points connected with lines. An examination with units 'spores per hour' would be more suitable, if experience did not speak against it. Namely, the nets become clogged while hanging in the sampling sites so that more spores are collected at the beginning of the period than towards the end (Fig. 97 bottom).

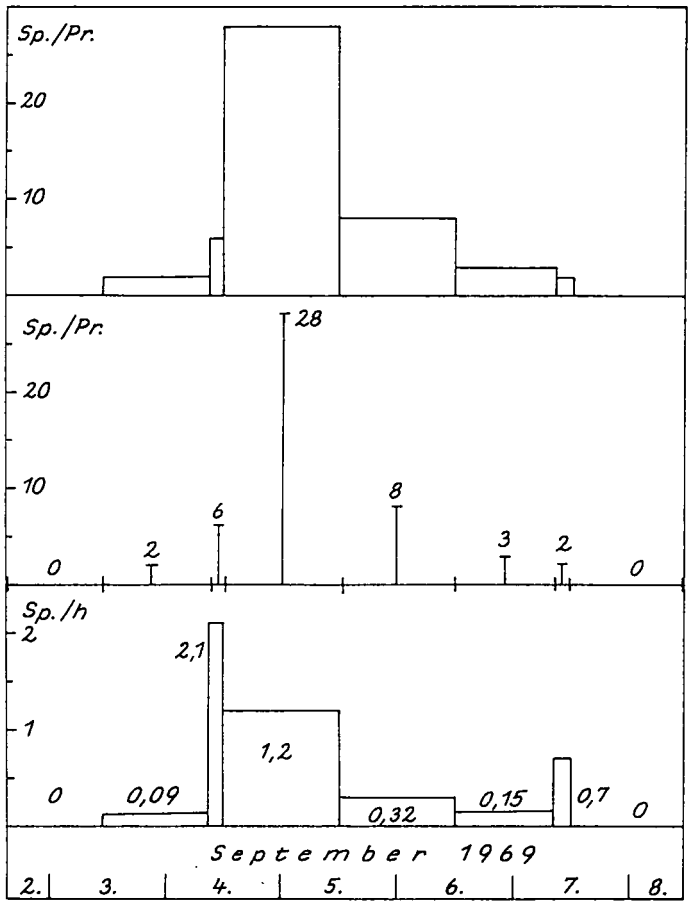

Figure 97. Different presentation methods for a spore passage. As an example the drift tracing test at the Danube percolation site from 26 August 1969 with the observation site Engen-Altdorf from 2 September, 15:00 – 8 September 11:00 hours; Distance:8,036 m (BATSCHE et al. 1970). Top: Column diagram, ordinate corresponds to the spore count per sample; middle: Length of the vertical line corresponds to the spore count per sample in the middle of the observation period; bottom: Column diagram, column area corresponds to the spore count per sample, column height corresponds to the spore count per time.

If the flow area of the nets and the discharge of the sampling site are known, the total spore content at the sampling site can be calculated.

Several different observations speak for the fact that spores travel faster than other tracers. During six tracing tests in the Buchkogel region southwest of Graz/Austria between 1956 and 1966, the spores were always observed first in the sampling sites in combined tracing tests. On the other hand, spores can stay a long time in karst waters before being washed away during maximum flow. For example, after injecting 10 kg of *Lycopodium* spores dyed brown on 26 March 1966 in the Lur Cave system, the main spore passage in the Hammerbach spring, 3.2 km away, was observed after 2¼ days. Later, two-hour samples were taken every 14 days; in the net sample from 10 Dec. 1966 there were still ten spores counted (BATSCHE et al. 1967). After a flood, there were 112 spores counted in a net sample from 28 January 1967, i.e. ten months after the injection. Similar observations were made by HACKER (1988) in Weizer Bergland. Spores injected in a sinkhole there did not reappear until nine months later after heavy rains.

Obviously, the type of dye affixed to the spores also plays a role in their transport behaviour in the karst underground. During the combined tracing tests in the Muota valley, Canton Schwyz/Switzerland, two differently dyed spore types were injected as a comparison in Hölloch, the so-called 'Wasserdom'. On 31 July 1979, 5 kg of green spores and 3.4 kg of spores dyed with acridine orange were injected almost simultaneously. Even during the injection already, the different reactions of the two spore types were noticed. It was much easier to wet the spores dyed with the fluorescent dye acridine orange than the conventionally dyed green spores. The main reappearance site of the spores, 'Schleichender Brunnen', lies only 1.4 km away from the injection site and 190 m lower. The actual underground flow distance covered is assumed to be ca. 3 km. From the injection site, the karst water in the Hölloch cave system first flows north and then turns southwest to the receiving stream Muota. In two observation sites inside of the Hölloch north of the injection site, many many more green spores were observed than the fluorescent spores, namely 16-125 times as many. At the main reappearance site of the spores, 'Schleichender Brunnen', however, double as many fluorescent spores reappeared as green spores. It can be concluded from these observations that the more easily wetted fluorescent spores sink quicker into deep caverns from where they can join the receiving stream more quickly. In contrast, the spores which are not so easily wetted float preferably on the surface of the karst waterways and therefore their flow is delayed by the siphon-like flow (BEHRENS et al. 1981).

Spore drift tracing tests show water ways where bacteria and viruses can easily drift. In planning water protection areas, drift tracing tests can be very helpful.

2.6 FLUORESCENT MICROSPHERES

W.Käss

Fluorescent microspheres are microscopically small plastic particles as spheres, coloured with fluorescent dyes. They have been produced by the company Polysciences, Inc., Northampton UK, and sold under the name of 'Fluoresbrite™ Plain Microspheres' for physiological purposes and by the company 'Molecular Probes Europe BV, Leiden, The Netherlands, under the name of 'FluoSpheres®'. Only the micro-

spheres made of polystyrene have an electrically neutral surface. Other products with carboxylate- or polyacrolein-surfaces with the functional groups CO_2 and aldehyde, are not as suitable for water tracing. In field tests it was ascertained that they have sorptive characteristics.

The first indication that fluorescent microspheres could be used as tracers can be found in SCHRÖTER (1987). He used them in a tracing test in fissure groundwater in a test area in the Canadian Province Ontario.

Drift tracing with fluorescent microspheres

Fluorescent microspheres are synthetically produced spherical drift bodies made of polystyrene. The following is a listing of their characteristics according to the Polysciences data sheets:

Density: D = 1.05
Available form: Aqueous suspensions (= latex) with solid concentrations W = 0.025 = 2.5%. Unit sizes: 1, 2, 5, and 10 ml
Fluorescent dyes: YG (yellow-green), excitation: 458 nm, fluorescence: 450 nm, PC,RED (polychromatic-red), excitation: 591 nm, fluorescence: 657 nm
Diameter: 0.05 – 90 µm
Diameter deviation between 0.35 and 3 µm: maximal 3%
Number of microspheres ∅ 1.0 µm: $4.55 \cdot 10^{10}$
Number of particles per ml =

$$\frac{6W \cdot 10^{12}}{D \cdot \pi \cdot \varnothing^3}$$

Stability at least 2 years at room temperature. Microbial growth can be averted by the incorporation of 0.0005% sodium azide, formaldehyde, or hexamine.

Drift tracing tests with fluorescent microspheres can, providing that the appropriate diameter of the drift body has been chosen, simulate the propagation of pathogenic bacteria. However, this method has important simplifications and advantages in comparison to tests with bacteria. Firstly, the microspheres do not need to be cultured for the injection and secondly, the examination of the samples is simpler and faster. Furthermore, the rate at which the bacteria die off between the time of injection and time of examination does not need to be considered, since the microspheres are stable during the tests. Last, but not least, the approval procedure for injecting synthetic microspheres is most likely easier than for bacteria. All in all, a tracing test with plastic microspheres has a much lower cost than a similar test with bacteria.

A major advantage with tracing with microspheres is complete lack of disturbing influences upon other possible tracers. Only in the case of very high microsphere concentrations could measuring signals with certain fluorescent dyes happen. Also, even if microspheres with a diameter larger than the mesh of the spore nets are used, a cross-disturbance with fluorescent dyed spores is imaginable.

Conducting drift tracing tests with fluorescent microspheres

Drift tracing tests with fluorescent microspheres represent a transition from tracing

tests with dissolved substances such as fluorescent dyes or salts and spore drift tracing tests. The following instructions concerning the organisation, injection, sampling, and examination of the samples during drift tracing tests with fluorescent microspheres originate for the most part from the Geological Survey in Baden-Württemberg/FRG. Since then, there have been very few such tracing tests reported in the scientific literature.

In dealing with fluorescent microspheres, particular attention must be taken to avoid possible contamination, even more so than with spores. Much more of the microscopically small plastic particles is used in such tracing tests than in comparable spore tracing tests and they are easily embedded in cracks in the skin, in pores, in hair, under nails, in clothing, etc., due to their microscopic size.

In deciding upon the injection amount, it must be considered that the samples are taken as single samples and not like spore samples from accumulating nets. Furthermore, experience shows that a considerable amount of the injected microspheres will be retained by the underground. It depends above all, that the detection limit is definitely exceeded. One single particle is not sufficient positive proof. Table 15 lists the injection amounts used in such tracing tests up to now for use in determining the needed injection amounts. The dilutions listed were standardized according to the injection amounts and determined at the peak concentrations of the breakthrough curves. If uranine, as a non-sorptive dye, was injected simultaneously, the percentage of the actual from theoretical maximal breakthrough can be calculated from the ratio of the standardized dilutions $V_{microspheres}/V_{uranine}$. This percentage lies between 0.002 and 17.4% for the five tracing tests listed in Table 15. In a tracing test in Belgian Carboniferous karst, which is described below, the percentage was as high as 26.9%.

Due to the expected wide range in the yield of the fluorescent microspheres, the injection amount should not be skimped on.

The microsphere size chosen, depends on the test goals. Usually, the goal is an evaluation of a drift tracing test for the transport of bacteria and for this, a micro-

Table 15. Comparative dilutions V_K/V_U (%) from combined tracing tests with uranine and fluorescent microspheres made of polystyrene.

Tracing test	Chalk river (Ontario/Canada)	Frauenbach-sinkhole (S.Baden)	Merdingen testfield (Upper Rhine valley/FRG)		Lur cave system (Styria/Austria)
Date	28 Aug.1985	4 Nov.1987	4 Apr.1988	4 Apr.1988	28 June 1988
Distance (m)	12.7	1465	50	100	2250
GW-aquifer	Frac.(gneiss)	Karst	Pore	Pore	Karst
Microspheres (10^9)	5.3	31.5	46	46	53
Diameter (µm)	2.0	1.13	1.0	1.0	0.95
C_{max} (n/l)	274,000	603	90	102	440
Dilution $V_K(10^{-8}/l)$	51	1.91	0.234	0.221	0.83
Uranine (kg)	0.001	0.05	0.02	0.02	2
C_{max} (µm/l)	2.31	55.1	5.03	6.77	83.9
Dilution $V_U(10^{-8}/l)$	213	11	26	22.1	4.19
Ratio V_K/V_U (%)	0.002	17.4	2.7	1.0	0.98
Remarks			5 sites	4 sites	
Author	SCHRÖTER 1987		SCHABER 1993		

sphere diameter of ca. 1 µm is recommended. However, it must be noted that the delivered microsphere size often differs slightly from the ordered size. The microsphere particle count must be then calculated according to the formula given above.

Only microsphere types with neutral surfaces, polystyrene microspheres, are used in tracing tests. The polycarboxylate type is unsuitable for water tracing tests due to its charged surface. In the combined tracing test in the Lur cave system in 1988 (Table 15), polystyrene and orange- and blue-white fluorescent microspheres made of polycarboxylate were injected. Whereas, a good breakthrough was recorded at the sampling sites for the polystyrene microspheres with uncharged surfaces, not a single specimen of the carboxylated microspheres was found. HARVEY et al. (1989) also reported disappointing results with carboxylated microspheres.

Red fluorescent microspheres with the designation PC,RED are hard to tell apart from chlorophyll bodies and could be mistaken for them or vice versa. Thus, they should only be injected in channels that are chlorophyll free.

The microspheres are delivered in small glass or plastic bottles. Disposable gloves must be worn when handling the microspheres and they should not be reused. At the injection, it is expedient to empty the bottles by rinsing out with a wash-bottle. The opened bottle and cover can also be tossed into a pail half full with water and with intensive stirring and several rinses, the microspheres can be nearly quantitatively injected. The rinse water for the pail should contain detergents, to better remove the microspheres from the pail walls. The rinsed out bottles will still contain microspheres, which can serve as comparisons under the microscope later. Caution must be taken to avoid contamination. Those persons present at the injection may neither take samples nor count them under the microscope.

Sampling at the observation sites is conducted as with soluble tracers, i.e. fluorescent dyes or salts. Plastic bottles are not recommended due to possible sorption on the bottle walls. Since fluorescent microspheres are only used as an auxiliary tracer in combined tracing tests, glass sample bottles should be used, which then allows the examination for the other tracers. The place saving brown glass bottles with a minimum content of 250 ml have proven themselves.

Examining for fluorescent microspheres

Examining the samples for fluorescent microspheres is similar to examining for fluorescent dyed spores. However, the samples in this case are single samples, not accumulative. A fluorescence microscope with a large cross table as well as a suction source for membrane filtration are needed, as described and depicted in Section 2.5.3.

The same type of membrane filter as for fluorescent spores is used here: the dark-grey cellulose nitrate filter with lattice imprint. It is expedient to choose a filter cross-section of 10 cm^2, which has exactly 100 squares in the area filtered. To do this, 50 mm filters are needed. The size of the pores must be under that of the microspheres. Filters with pore sizes in the following graduations are available from the company SARTORIUS GmbH in Göttingen/FRG: 0.45, 0.65, 0.8, and 8 µm as type number SM 130-06, –05, –04, and -01, for example. The filters do not need to be sterile. Unnecessarily small pore sizes prolong the flow times and hold back more turbid matter than larger pores.

The sample is well shaken before filtration and then an ultrasound probe is held in the sample for ca. 30 seconds. This produces a uniform distribution of the particles in the sample and loosens any microspheres that might be clinging to the sample bottle wall.

How much sample water needs to be filtered depends on the microspheres concentration and upon the turbidity of the sample. With samples that appear clear, 100 ml is filtered for starts. Rust particles and calcite crystals interfere with the examination under the fluorescence microscope. The first because it blocks the lattice from view, the second because of its bluish fluorescence. Both disturbances can be eliminated by adding EDTA-powder to the sample. Adding the powder right after the sample is taken will prohibit both precipitations. If rust or calcite has already formed, the EDTA is allowed to work overnight. The lowest amount of precipitation occurs if the samples are kept well closed, transported cool, and examined soon. Nothing can be done about clay detritus held in suspension.

Up to 1 l can be filtered through the membrane filter with very clear water. With a higher microsphere concentration, less sample water needs to be filtered. Hence, it is imperative to have enough sample water for repeat examinations.

Using tweezers, the moist membrane filter is placed on a slide glass (50 × 70 mm) so that the lattice is parallel to the sides of the slide glass.

The room where the microscopic work is carried out needs to be dark, since even weak lighting interferes with the work under the microscope. The filter is examined in a zigzag pattern under the fluorescence microscope with the lowest objective. The fluorescence equipment for the microscope used should have at least two filter combinations. The yellow-green fluorescing YG-microspheres are best examined with the same filter set, which is used for examining acridine orange dyed spores. This is the filter set 9 from the CARL-ZEISS-filter sets with excitation at 450-490 nm and the fluorescence filter >510 nm. With this excitation, the YG-microspheres shine with a brilliant yellow-green against the dark background. The appearance of a fluorescent microsphere can be compared to the shining of a bright fixed star in the sky at night (Plate 6). However, not all microspheres shine with the same intensity or in the same shade. When in doubt, a stronger objective must be used to verify the spherical form. Stronger objectives can only be used for a short time with the moist membrane filters however, since the objectives tend to mist up due to the stronger focussing of light.

With UV-excitation, the microspheres shine light-blue, but not as intensive as with blue-excitation. If yellow excitation is used, e.g. with the CARL-ZEISS-filter set No.14, the microspheres remain invisible.

During the examination of the membrane filter under the fluorescence microscope, interfering foreign fluorescences can appear, depending on the origin, contamination possibilities, and age of the sample. Calcite crystals fluoresce with blue excitation light-blue, chlorophyll bodies fluoresce red, and textile fibres shine a garish light-blue. There are also numerous other indefinable inorganic and organic particles in many different fluorescence colours. In water samples that have been kept a long time, biological slime can grow even in the dark and in weakly mineralized waters. These films fluoresce either green-blue or light-red.

It must be stressed here that a minimum of experience is necessary to examine the filters successfully. It takes quite a while before the skill of spotting the fluorescent

microspheres under the fluorescence microscope is developed. A helpful resource for training are comparative slides with cover glasses, which were made up by personnel who are not involved with the microscopic examination.

After enough training under the microscope, 4-6 samples can be counted in an hour, not including the time needed for the sample preparation, which depends largely on the amount of foreign particles in the sample.

After 2-3 hours of microscopic work, fatigue can set in, which can lead to miscounts. Hence, frequent breaks are necessary during a workday.

Application areas

The actual application area for fluorescent microspheres is physiology. They have been used only seldomly in hydrological tracing tests. It is certain, that this section in tracing techniques can be developed further.

In laboratory tests, BEDBUR (1989) used fluorescent microspheres in column tests as a comparison with different bacteria types. He discovered that in quartz sands, a large part of the injected microspheres are retained in the granular skeleton. The retention of the particles, i.e. microspheres and bacteria, is the lowest at a grain diameter of ca. 1 µm. Quantitative determinations with different grain sizes in column tests resulted in retention rates for *E.coli* of ca. 20% lower than for polystyrene microspheres with a diameter of 1 µm.

In fissure groundwater of the Chalk-River-test area (Prov. Ontario/Canada), comparative tests were conducted with fluorescent dyes, cationic, anionic, and undissociated substances and with *E.coli*. It was shown that even with relatively short flow distances in fracture systems in monzonite gneiss, only a very moderate recovery rate could be achieved (SCHRÖTER 1987) (Table 15).

Such drift tracing tests in pore groundwater were carried out at first without much hope of success. On 4 April 1988 in the shallow pore groundwater aquifer of the Merdingen test area in the Upper Rhine valley/FRG, 46 billion fluorescent microspheres with a diameter of 1.0 µm and 20 g of uranine were injected into an inlet pipe. Figure 98 shows the breakthrough curves for both tracers in the row of monitoring wells, 100 m away, with a natural groundwater flow gradient. It is obvious that the microsphere maximum is reached before the uranine maximum; an aspect that is regularly seen in microsphere drift tracing tests. In contrast to substances which are actually dissolved in the medium, drift bodies only flow through the larger pore spaces and thus flow faster through the medium on the average. In the column tests from BEDBUR (1989), ratio of the flow velocities of the microspheres with a diameter of 1.17 µm to those of the conservative substances such as uranine and chloride was 1.45:1.

Further combined pore groundwater tracing tests were carried out in the most eastern lobe of Massachusetts/USA near Cape Cod in glacial sandy aquifer sediments. The sands have an average grain size of 0.5 mm and a hydraulic conductivity of ca. 10^{-3} m/s and are composed of mainly quartz and feldspar with a low percentage of clay. Tracing tests were conducted under two flow conditions: 1. natural gradient groundwater flow over a flow distance of 6.9 m, 2. forced-gradient flow in which radially divergent flow was induced by continuously pumping 1,5 l/s groundwater from a supply well into an injection well with observation wells located 1.7 and 3.2 m away (HARVEY et al. 1989).

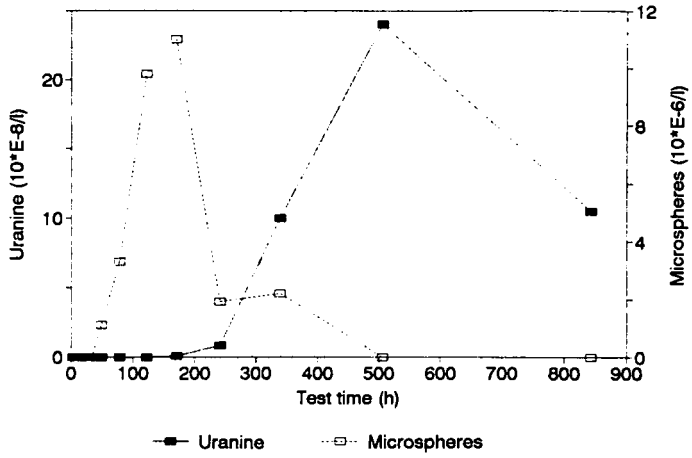

Figure 98. Standardized breakthrough curves from the combined tracing test in the Merdingen test field from 5 April 1988 with 20 g uranine and 46 billion fluorescent polystyrene microspheres with a diameter of 1.0 µm. The breakthrough curves were standardized for uranine to 10^{-8}/l, for microspheres to 10^{-6}/l. The averages from a row of seven monitoring wells, located 100 m away, were used for the values. The microspheres display a higher flow velocity than uranine.

In the natural groundwater flow tracer test (1), chloride and different types of polystryrene microspheres were injected. The plain latex type had a diameter of 0.6 µm and had uncharged surfaces. Another type was made of carboxylated latex in different size groups (0.23, 0.53, 0.91, and 1.35 µm) and another were polyacrolein and had carbonyl surface groups (0.84 µm diameter). The carboxylated microspheres with the different diameters had approx. all the same flow velocity, yet different recovery rates, a factor of 0.8 lower than the recovery rates for chloride and the polystyrene microspheres. The polyacrolein microspheres had an even lower flow velocity, namely around the factor 0.72 lower.

In the forced-gradient groundwater flow tracer test (2), bromide, fluorescent, carboxylated microspheres with diameters of 0.2, 0.7, and 1.2 µm, and groundwater bacteria stained with a DNA-specific fluorochrome were injected. In the first observation well only 1.7 m away, the microspheres arrived after thirty minutes, before the bromide and before the bacteria and were also present much longer. In the second sampling well, 3.2 m away, only isolated microspheres appeared, far below levels required for quantification.

The authors came to the conclusion that polystyrene microspheres with uncharged surfaces have similar transport behaviour as bacteria. As PETERS (1989), they also came to the conclusion that ca. micrometer large particles have the best transport chances in sand. Larger particles can be filtered out and smaller ones contact and sorb onto stationary surfaces, due to BROWNian motion.

Several tracer tests carried out in karsts showed the good applicability of fluorescent microspheres as tracers. In the Lur cave system in the southern calcareous Alps north of Graz/Austria, the use of drift particles had remarkable hydrogeological results. With the simultaneous injection of eight different dissolved tracers and two different types of drift particles, namely phages and microspheres, it was observed that

the dissolved substances and the particles showed different transport behaviour during the floods that followed the injection. The dissolved substances – dyes and salts – reappeared only in the main reemergence site, the Hammerbach spring. Both types of drift particles were also recovered as traces in the overflow of the Lur cave system. It can be concluded from these results that particles can be retained in karst cavities; with rising flood waters they can be then washed out of the system.

Figure 99 displays an example of a combined uranine and particle tracing test in the Carboniferous karst south of Liège/Belgium.

On 15 August 1990 at 10:10 o'clock, 20 ml of a microsphere suspension with 48 billion particles/ml with a diameter of 0.98 µm were injected in a stream sinkhole above Crossée. The injection of 1.008 kg uranine occurred in the same site between 10:25 and 10:40 o'clock. The percolating stream had a flow of ca. 0.5 l/s. During this tracing test, both tracers were recovered, with nearly congruent breakthroughs, at the major reemergence site, a karst spring with a discharge of ca. 200 l/s in Comblain-au-Pont in the Ourthe valley. The recovery rate at the maxima was the highest rate for the microspheres, that has been recorded up to now. Compared to uranine's, it was 26.9% (Fig. 99 and Table 15). Remarkable in this test were the isolated and trace amounts of the microspheres and uranine recovered between the third and fifth day of the test in the well P14, with a pumping rate of 0.56 l/s (Table 16). The preparation and organisation of the tracing test, as well as the sampling and sample transport was gratefully provided by Mr.P. MEUS from the University of Liège.

Fluorescent microspheres have yet to be used in surface waters. Examining samples from such tracing tests would be complicated due to the inevitably high amount of suspended solids in the samples. At most, it would be plausible to conduct a tracing test in extremely clean and clear water bodies.

Evaluation and prospects

Fluorescent microspheres are only suitable as auxiliary tracers. Nevertheless, the few

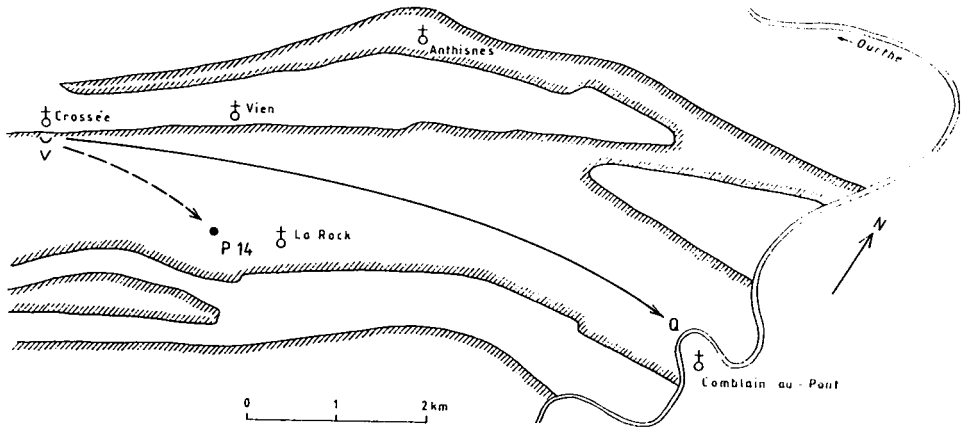

Figure 99. a) Map of the combined tracing test with microspheres and uranine in the Carboniferous karst south of Liège/Belgium. V = percolation/injection site, Q = major reemergence site, P14 = secondary reemergence site (well), shaded line = boundary of the Carboniferous limestone.

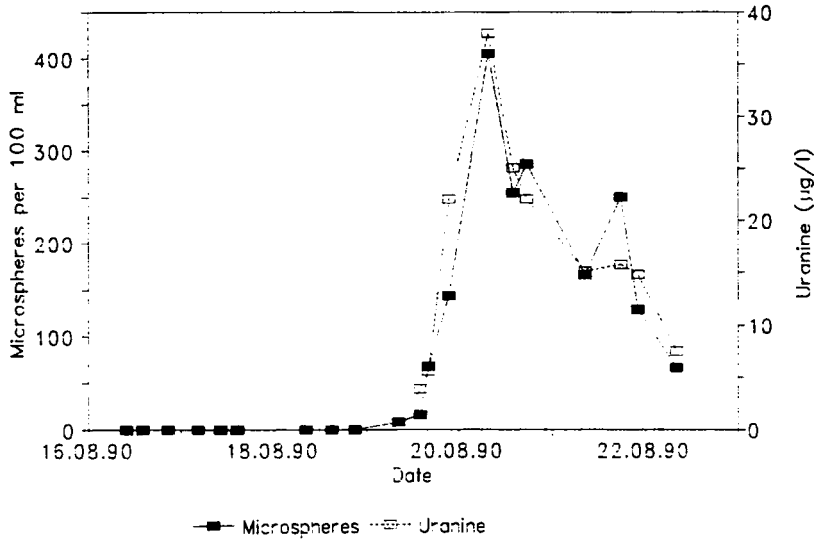

Figure 99. Continued. b) Breakthrough curves for the microspheres and uranine in the karst spring Comblain-au-Pont in the Ourthe valley.

Table 16. Trace recovery of uranine and microspheres in the well with a filter at a depth of 33-58 m P14 near La Rock. The detection limit for uranine after sample reduction to 1/10 was below $1 \cdot 10^{-12}$.

Day and time of sampling 1990		Uranine (µg/l)	Microspheres (per 100 ml)
15.8., 11:25			
to 17.8.	8:00 (22 samples)	0	0
	10:00	0.007	3
	12:00	0.001	4
	14:00	0.002	1
	16:00	0.004	5
	18:00	0.019	18
	20:10	0.004	2
18.8.,	7:51	0.001	3
	16:00	0.005	0
19.8.,	9:45	0.043	0

existing examples show that they are suitable for describing the transport behaviour of bacteria in fracture, pore- and karst groundwater aquifers, allowing for certain restrictions. Several studies have ascertained that the optimal microsphere size for a drift tracing test in pore groundwater is around 1 µm. This is the size of most bacteria; hence, drift tracing tests that are carried out for a hygienic evaluation should use this size of microspheres.

The smallest microspheres obtainable are 50 nm and are the same size as viruses. They can no longer be recorded with a normal microscope. A minimum diameter of 100 nm is necessary; a size that is only reached by few viruses.

Microspheres with diameters much larger than 1 µm have not been described anywhere. It might be plausible to think of using microspheres with a diameter of ca. 30 µm as a substitute for *Lycopodium* spores and then using nets at the sampling sites to recover them.

Microspheres with active surfaces represent another attenuation underground. If the sorptivity of microspheres can be quantified, the dying rate of microorganisms could be simulated. To do this, extensive tests would have to be conducted first.

The problems associated with learning to faultlessly recognize fluorescent microspheres under the fluorescence microscope was mentioned above. The needed experience to do this can be acquired, but must be practised or retrained after some time. A possibility would be to set up or retool an automatic cytometer so that it could be used to count the microspheres.

2.7 BACTERIA

W.Käss

2.7.1 *Introduction*

Bacteria have been used as hydrological tracers since the end of the last century. In 1894, E. PFUHL was the first to suggest and actually use bacteria in a drift tracing test (PFUHL 1896).

As a tracer, bacteria can be a good auxiliary support, especially in deciding the boundaries for water protection areas for drinking water supplies. Since solute tracers undergo molecular dispersion and have no problems with narrow pore spaces, a direct comparison with drift tracers such as bacteria or viruses is not given. The evaluation of dye tracing tests for hygienic significance has been and is the theme of many discussions and papers (DOMBROWSKI 1972).

KESWICK et al. (1982a) wrote, that almost half of all waterborne illnesses reported every year, are a result of contaminated groundwater. In industrialized countries, the broad irrigation of sewage and the deposition of sewage sludge and wastes are taking up more and more space. Furthermore, the increasing expansion of the sewage canals also increases the danger of sewage leakage. A comprehensive knowledge of the transport behaviour and survival of microorganisms underground is thus imperative (GÄRTNER 1902).

To determine the state of the knowledge of the 'Lifespan of bacteria and viruses in groundwater with regard to the determination of water protection areas for development of groundwater resources,' the Dept. of Health of the Federal Republic of Germany commissioned a research group to conduct a literature study in 1980 (MATTHESS 1980, ALTHAUS et al. 1980).

Later, an extended research group was commissioned to carry out investigations in characteristic aquifers in Germany. The investigation results were published in official reports (DVGW 1983, UBA 1985).

To summarize the results, it can be said that isolated microorganisms can survive for longer than fifty days in groundwater. However, the minimum residence time of 50 days as postulated by KNORR (1937) for the determination of the water protection area II can still be kept as a standard. On the one hand, within the fifty days the death

rate for all microorganisms is so high that only isolated germs survive. On the other hand, it must also be considered that during the fifty-day flow time in the aquifer, a significant portion of the microorganisms is retained.

2.7.2 *Requirements for bacteria as tracers*

Microorganisms, which are to be used as tracers, must fulfill the following criteria: They should

- Be easily grown in large cultures,
- Be nonpathogenic to man, animals, or plants,
- Not be present in the water body about to be traced,
- Be readily and quantitatively determinable in water samples,
- Have no own motion,
- Have no sorptive properties,
- Have as long a lifespan as possible,
- Not be able to multiply in the groundwater aquifer,
- Be readily distinguishable when using more than one tracer.

To distinguish injected and natural microorganisms from one another, antibiotic-resistant strains can be used.

2.7.3 *Bacteria types used in water tracing*

The different bacteria used in water tracing are presented here.

2.7.3.1 *Serratia marcescens (BIZIO 1823)*

Synonyms: *Bacillus prodigiosus* FLÜGGE
Micrococcus prodigiosus COHM
Monas prodigiosus EHRENBERG
Polenta porporina

S. marcescens was named by the naturalist BIZIO in honour of the nature lover and inventor of the steamship, Serafino SERRATI, marcescens means putrefactive.

Serratia marcescens was the first and is the bacteria type most often used in water tracing. The blood-red colour of its colonies is typical for this bacteria type. *S. marcescens* can be found in spoiled food and also sometimes on the host; thus the common name 'host fungus'.

The genus *Serratia* has other species besides *marcescens:* the species *rubidaea* (STAPP 1940), *plymuthica* (LEHMANN & NEUMANN 1896), *liquefaciens* (GRIMES & HENNERY 1931) and *odorifera* (GRIMONT, GRIMONT, RICHARD, DAVIS, STEIGERWALT & BRENNER 1978). *S. rubidaea* and *S. plymuthica* form, as *marcescens,* red pigments, *S. liquefaciens* and *S. odorifera* do not (BLACEVIC 1980). The genus *Serratia* belongs to the family of enterobacteriaceae and to the class of the *Klebsielleae.* The species *S. indica* (EISENBERG 1886), often mentioned in hydrological literature, has been included in the species *S. marcescens.*

The first use of the bacteria *S. marcescens* in water tracing was by FRÄNKEL and PIEFKE in 1889 in sand-filter models (see Section 2.7.4.5) (FRÄNKEL & PIEFKE 1890). PFUHL (1896) carried out laboratory tests in 1895, to investigate the vertical distribu-

tion in a metal box filled with Upper Rhine Quaternary material using well water at different flow speeds. He showed, that *S. marcescens*-germs were retained stronger than sodium chloride and fuchsine solutions (PFUHL 1896).

A year later, PFUHL (1897) published the results from his first field tests, which were conducted 100 m downhill of the Strassburg Water Works in 1896. There he had a 2 x 2 m pit dug down into the groundwater carrying gravel layer; this was to be the injection site. The groundwater was laid free 8 m below in a 12 m long ditch and lowered 20 cm for the drift tracing test by pumping 6-8 l/s with hand-pumps. The results from the samples taken every half-hour out of the ditch are remarkable: uranine was visible in the ditch after ½ hour, *Serratia marcescens* was detected after 1 hour and shining *Vibrionaceae* (*Luminous vibrio*) was not detected until after 2 hours. PFUHL concluded from these results, that cholera bacteria could be transported in gravelly groundwater, since they are similar in shape, size, motion, and resistance to the *Vibrionaceae*.

At the same time, Prof. ABBA and coworkers were working in Turin on whether bacterial surface contaminations can break through the unsaturated zone to reach the groundwater (ABBA et al. 1899). To investigate this they flooded 40-50 square-metres of ground over the infiltration gallery and up to a distance of 27.5 m away several times with water from a brook. Before flooding, 20 l *Serratia marcescens*-suspension was poured on the ground. The depth of the aquiferous gravels was not recorded, but judging however by the incomplete records, it must have been ca. 1.5-2.5 m under the surface. Other tests were carried out – with positive results – with besides *S. marcescens* also *Sarcina lutea* (yellow pigment) and chrome-yellow gelatine-soft micrococci. In all seven of the conducted tests, after a few hours or at the latest several days, *S. marcescens*-germs were found in the gallery water. Furthermore, it can also be noted that the tap water in Turin had an overly proportional amount of *S. marcescens*-germs for over two years. Also, even after two months, a 'very strong growth' of *S. marcescens* in soil samples between 0.1 and 2.5 m depth was found during digging at the percolation sites.

It can be seen from a discussion published by PFUHL (1899) regarding the tests from ABBA, that PFUHL and ABBA independently used *S. marcescens* as a tracer in field tests. ABBA used *S. marcescens* in a tracing test to mark simulated flood waters through the unsaturated zone and PFUHL in a pore groundwater tracing test.

Tracing with Serratia marcescens

Tracing tests with bacteria have been and are conducted most frequently with *Serratia marcescens*. The use of *S. marcescens* is comparatively easy. To examine the samples all that is needed is a more or less germ-free laboratory and the identification of the *S. marcescens*-colonies is unproblematic. Furthermore, *S. marcescens* is found only rarely in natural waters (BOLTON 1886).

Only in about every thousandth drinking water sample, which undergoes a bacteriological examination contains a *S. marcescens*-colony. In the Turin tap water, there were germs from *S. marcescens* only every 2-3 years (ABBA et al. 1899). DURAND et al. 1967 reported about the African fish *Auchenoglanis occidentalis* that was infested with *S. marcescens*.

WRIGHT et al. (1976) investigated vegetables and salads from Florida and Califor-

nia/USA and found, after rinsing for five minutes with tap water, *Serratia marcescens* along with twelve other microorganisms in 29% of the macerated samples.

There are only few references regarding the survival rates of *S. marcescens*. BOLTON observed in 1886 a steady decrease in colony counts during storage tests with well water, even in samples heavily contaminated with organics. The decrease in the colony count was much stronger at 35°C than at 20°C. MERKLI also carried out storage tests with pure well water at 15°C with pH 7.8 (MERKLI 1974). He put up 10-l-samples containing ca. 10^6 germs/ml. The average daily death rate from 2-5 tests was for *S. marcescens* 5%, for *E. coli* however, 22.7%. After 32-137 days, 99.9% of the *S. marcescens*-germs had died. During tests in the pore groundwater of the Merdingen Test Field in the Upper Rhine Valley in 1983, two groundwater samples were examined for *S. marcescens* immediately and after 22 days at 5°C. One sample originally had a colony count of 22, the other 132 per millilitre. At the end of the test, no colonies of *S. marcescens*-germs were found. During a drift tracing test in the Merdingen Test Field with $2 \cdot 10^{11}$ *S. marcescens*-germs as injectate, the last positive *S. marcescens* examination was found after exactly three months; the colony count decreased from 300 to 2 per ml from the 17th to the 94th day of the test. After the 108th day of the test, all samples were negative. However, in three sampling sites that were 12.5 m from the injection site in the groundwater flow direction, 1-2 colonies per millilitre were detected after the 108th day of the test (KÄSS et al. 1983).

There are possible indications that *S. marcescens* not only can survive for long periods underground, but might also be able to multiply. TRESH wrote in 1907: 'If *S. marcescens* germs are found underground, they are no longer eradicable'. Especially remarkable are the observations made in the Iller Valley south of Ulm near Erolzheim/FRG. Several tracing tests were conducted there with uranine, eosin, and *S. marcescens*, so that the groundwater flow conditions in the test area were well known. A service pipe, that ended ca. 1 m above the gravelly groundwater body, served as the injection site. The average flow velocity was ca. 20 m/day, the hydraulic conductivity ca. 0.02 m/s. The Hygiene-Institute of the University of Tübingen/FRG injected ca. 10^{13} *S. marcescens* germs and they were flushed with 50 l of water. On the following day, innumerable *S. marcescens*-colonies were detected in the groundwater samples from 3 sampling sites located 10, 30, and 63 m away from the injection site (Fig. 100). After three days, large quantities of *S. marcescens* also appeared in a sampling site 192 m away.

With intermittent decreases, the large quantities of *S. marcescens* appeared over several months in the three sampling sites 13, 14, and 15. In the sampling site closest to the injection site, there were still large quantities of *S. marcescens* even 4 months after the injection. Therefore, a decision was made to pour caustic soda into the injection well as well as all the sampling wells to kill off the *S. marcescens*-germs. As a result, in the next two months, there were only two germs detected in the three sampling sites. These observations suggest that not only can *S. marcescens* survive in the unsaturated zone, it can also multiply. Thus, it can be concluded from this that suspensions with *S. marcescens* used in tracing tests must be always injected *into* the body of water to be traced.

The Bacterium Serratia marcescens

The *S. marcescens*-bacterium is a 0.3-0.5 µm thick and 1.0-1.5 µm long peritrichous

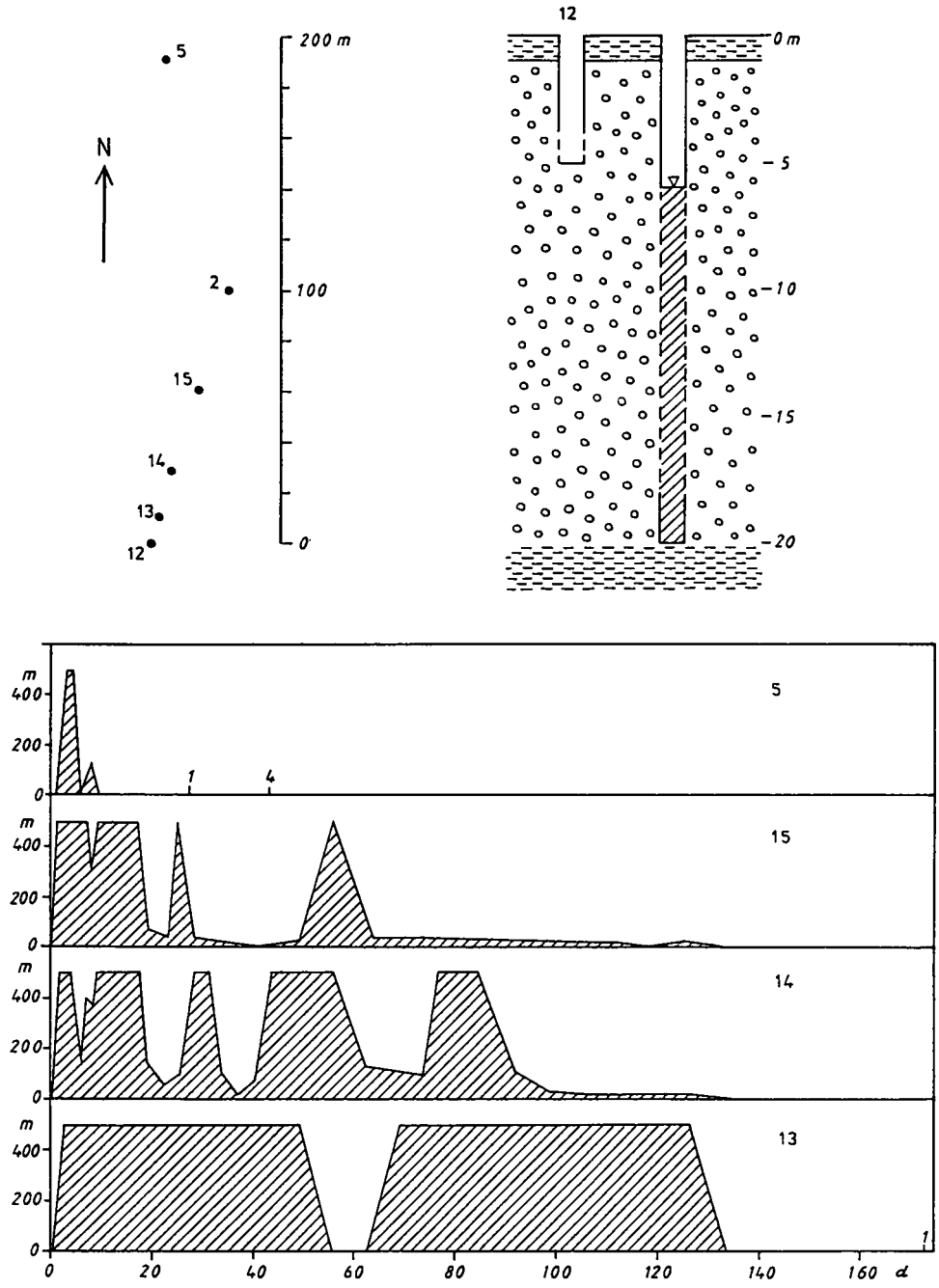

Figure 100. Tracing test on 28 Sept. 1972 in the Iller Valley near Erolzheim with *Serratia marcescens*. Top left: Schematic map of the injection site (12) and the sampling sites; top right: Borehole profile of the injection site 12 and the sampling wells. Bottom: Breakthrough curves in the four sampling wells 13, 14, 15, and 5 in colony counts per ml; m = mega colony counts (after documents from the Geological Survey of Baden-Württemberg).

gram-negative rod. Due to the flagellates, the rod is capable of motion (BERGER & HUMMEL 1964). Most often it occurs as a single form, rarer as a 5-6-membered chain.

The bacterium is fairly undemanding and prefers carbohydrate-rich nutrient medium. *S. marcescens* haemolyses blood agar, can coagulate milk, can produce acid out of glucose, and can reduce nitrate to nitrite.

The most distinguishing feature of *S. marcescens* is the formation of its blood-red pigment. Due to the preference of the bacterium for carbohydrates, *S. marcescens*-cultures sometimes coloured the hosts and polenta red, which lead to the names 'Host fungus' and 'Polenta porporina.'

The red dye is prodigiosine, an organic compound with three pyrene rings ($C_{18}H_{23}ON_3$). It is not soluble in water, however easily soluble in alcohol, acetone, ether, benzene, and glacial acetic acid. The red pigmentation makes *S. marcescens* distinctive. Thus it is a substance that is well suited for water tracing. Special culture media and incubation methods allow for definite recognition and quantification.

Producing injection suspensions

A high microbial count is necessary for tracing tests, since the injection will be quite diluted by the time the samples are taken and only 0.5-1 ml sample is needed for the investigation, when no enrichment methods are used.

It is easiest to buy suspensions. The company E.MERCK/Darmstadt, FRG takes orders for cultures produced in fermenters and sends the centrifuged finished product, ca. 20-28% dry substance and packed in dry ice in 500-g-portions (METZ 1973).

KRUSE (1919) described a method where especially well coloured colonies are transferred onto potatoes and bred at 22°C. When using such cultures, the peptone-meat broth should not be inoculated in too thick a layer.

OHLMÜLLER and SPITTA (1921) recommend breeding on large agar plates at 22°C until a strong red has formed and then washing down with sterile 0.8% salt solution.

LUKAS (1959c) used tilted agar plates, on which 'very red' *S. marcescens*-colonies grew over 48 hours. The cultures were washed out into 10 l normal nutrient bouillon and alternately incubated at 25°C and 37°C, whereby sterile compressed air was pumped in daily. After five days, the fermentation was completed; the end product is a non-coloured injection suspension.

WILLIAMS et al. (1971) conducted basic research concerning the conditions for breeding *S. marcescens* in suspensions. The authors used the *S. marcescens*-strain 'Nima' and the following nutrient solution:

1%	glycerine
0.5%	ammonium citrate
0.05%	magnesium sulfate
1.0%	secondary potassium phosphate
0.5%	NaCl
0.005%	Fe-III-NH_4-citrate
0.1%	'Yeast-Extract' (DIFCO)
0.2%	'N.-Z.Case peptone' (SHEFFIELD CHEMICAL, Norwich N.Y.)

The nutrient solution should be adjusted to pH 7.2. The highest colony count is ob-

tained with an incubation time of 48 hours at 18°C; after this the count decreases. However, the best colour formation is obtained after the 24th hour at 27°C.

OETZEL (1990) transferred cell material from refrigerated plate cultures with an inoculation eye onto several 98x16-mm-culture tubes, which contained 10 ml MÜLLER-HINTON-nutrient bouillon. These were then kept at 30°C for ca. 16 hours. These so incubated cultures were then centrifuged, the supernatant pipetted off and discarded. After addition of 10 ml physiological salt solution, it was resuspended onto the breeder-shaker-apparatus 'Vortex'. Mixing served to remove any remaining nutrient solution; the shaking prohibits the formation of bacteria agglomerates.

In any case, before the bacteria suspension is injected during a tracing test, the colony count must be determined with dilution series.

Injection of S. marcescens-suspensions

High colony counts are necessary, to assure evaluable results during bacteria drift tracing tests. In pore groundwater, a total-colony count of ca. 10^{12} is necessary, to obtain positive results in the downstream observation sites. At least this amount should be also used in karst and fissured groundwater. As an indication for determining the amount needed in fissured and karst water, about 10^{13} colonies take the place of 1 kg uranine.

If the permeability of the unsaturated zone for *S. marcescens* is to be investigated, very high colony counts are necessary. During tests in the Southern German alpine foreland, up to 6×10^{14} cells were used above the groundwater level in the coarse gravelly-sandy aquifer. Only by using such high counts was it possible to obtain positive results in the test.

The injection of the bacteria suspensions in the groundwater or in surface water is generally unproblematic. The determination of the colony count in the injection solution should correspond to the injection time.

During transport to the injection site, the suspension should be kept cool. As always, to avoid possible contamination, which is much higher with bacteria than with say salts, workers who are present at the injection may not carry out the incubation.

Sampling and transport of bacteriological tracing test samples

When samples are taken that are to be examined for bacteria, the general guidelines set up by the hygiene institutes should be followed. Special measures are only necessary when sampling at groundwater monitoring sites. If the groundwater table is not lower than 3 m, the samples can be suctioned into evacuated bottles with a permanently installed PVC-hose (ALEXANDER & SEILER 1983).

Another method for obtaining faultless samples suitable for bacteriological examinations is described in KÄSS et al. (1983): Using a peristaltic pump with a silicon hose with a polyamide filter weighted down with a small stone, the groundwater is suctioned to the surface. Several of the germ-free hoses are kept in sterilizable polyamide sacks and transported to the observation site and then affixed to the peristaltic pump. Sample water so collected only comes into contact with the inside of the hoses (Fig. 101). Each observation site should have its own germ-free hose.

The sampling is completed quicker if a submersible electromagnetic reciprocating pump is used and at the suction socket a ca. 1.5 m long silicon hose fixed with a weighted suction filter (Fig. 102). The pump is not allowed to become wet, only the

Figure 101. Peristaltic pump for sterile collection of water samples from observation sites in shallow aquifers.

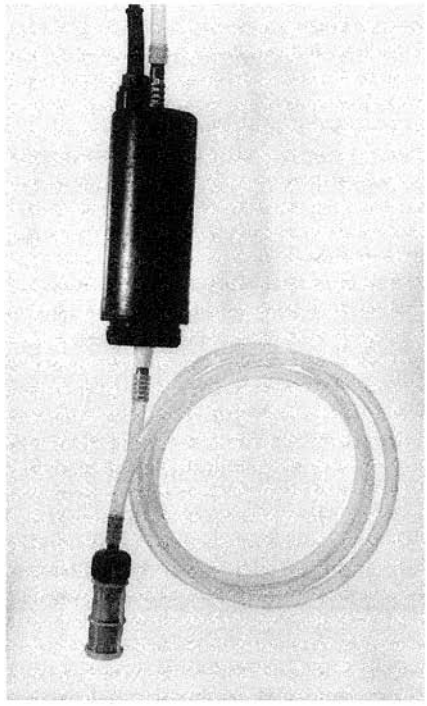

Figure 102. Submersible electromagnetic reciprocating pump with silicon hoses and polyamide filter for collecting sterile samples from deep aquifers, up to 50 m.

suction filter and part of the hose. After taking the sample, the ca. 1 m long silicon hose is fastened to the socket of the suction side of the pump and 70% alcohol is circulated through the hose for about 10 minutes by turning on the pump for a short time. With these measures, sterile samples down to a groundwater depth of 100 m can be taken. After using, the hose-filter-combination is packed separately in PVC-sacks and autoclaved at 130°C and 1.5 bar in preparation for the next series of samples (KÄSS et al. 1983).

The water samples should be filled into germ-free glass bottles and examined as soon as possible. During transport, they should be kept cool.

The size of the sterile bottles needed should be arranged with the examining laboratory; normally a volume of 100 ml is sufficient.

Examining for Serratia marcescens

The aim of the examination should be the colony count per ml in the collected water samples. Some researchers are content with the qualitative examination, as to whether *S. marcescens* is present or not. OHLMÜLLER and SPITTA (1921) base this on the very different colony counts obtained, according to which incubation method is used. Thus, many publications contain only qualitative (DOMBROWSKI 1978) or at the most semi-quantitative data (RICHTER 1944).

However, it is quite advisable to determine the colony count from tracing tests with *S. marcescens*. A prerequisite for a meaningful evaluation is incubating under optimal conditions.

In the literature there are an immense number of methods and formulas for determining the colony count for *S. marcescens*. GÄRTNER (1915) recommended the following nutrient solution:

0.2%	K_2HPO_4
0.2%	$MgSO_4$
0.2%	asparagine
1.5%	glucose
1%	peptone
0.15%	salt
10%	gelatine or 1.5% agar

dissolved in meat broth or 1% meat extract.

The pigmentation is better with gelatine than with agar; adding tyrosine (LEHMANN 1899) supposedly helps *S. marcescens* grow. According to UNKELBACH et al. (1991), traces of iron and zinc are necessary for pigmentation. On the other hand, sample water with heavy microbial growth can inhibit or even suppress the pigmentation of *S. marcescens* (HILGERMANN 1906).

Nowadays, ready made and pre-weighed nutrient media are available, which can simply be dissolved in water to form pourable solutions. The following method has proven itself:

Dissolve in 1 l water:

37 g MERCK Standard-I-Nutrient agar (No. 7881) and 370 mg mannitol,
or 40 g Tryptic Soy Agar (DIFCO, Detroit, Mich./USA) and 400 mg mannitol,
after the material is sufficiently swollen, the solution is homogenized by stirring.

The homogenized solutions are – with a stirring rod – autoclaved at 130°C and 2 bar for 20 minutes or held at 135°C for 10 minutes. After cooling to ca. 50°C the autoclave is opened and 20 ml of the nutrient solution is poured into prepared petri dishes.

Care should be taken to assure that the petri dishes are kept level during the solidifying process, so that the nutrient media are uniformly thick.

Each so prepared and well-cooled agar plate can be filled with at the most 0.5 ml sample water. Thus, it is best to divide 1 ml from each sample onto 2 plates. If high colony counts are expected – more easily recognized with a simultaneous dye tracing – serial dilutions of the sample water 1:10, 1:100, etc. should be made up and incubated. By rotating the plate, the sample water can be uniformly distributed over the nutrient medium. By using a DRIGALSKI-spatula, a uniform distribution can also be achieved, whereby the plates must also be kept horizontal.

Ready made nutrient media are also available with standard nutrient agar. However, these plates do not contain mannitol. Nevertheless, good results can also be obtained.

The incubation temperature should be around 22°C. The following optimal growth conditions for *S. marcescens* can be summarized from the numerous publications:

– Best pigmentation at 27°C,
– Highest colony counts at 18°C,
– Subdued daylight is necessary for prodigiosine to form,
– pH-value should be neutral or weakly alkaline; the data from WILLIAMS et al. (1971) (growth optimum for suspensions at pH 8.0-8.3) and from DAUBNER (1972) (no growth over pH 8.0) contradict each other,
– Culture medium should be carbohydrate rich for *S. marcescens*.

By incubating for 12 hours at 37°C, GÄRTNER (1915) provided the *S. marcescens*-bacteria with a head start compared with the other bacteria and then continued the incubation at room temperature. Depending on the incubation temperature, the blood red *S. marcescens*-colonies (Plate 7) show up after 24 to 48 hours. The colony count can be carried out at the earliest after 48 hours. Afterwards, the colonies are larger – they can reach a diameter of up to 10 mm – but overgrowth is then also a factor.

High amounts of common bacteria colonies can cause problems during counting. Further problems can arise when using culture media that contains gelatine, if the samples contain liquefacient bacteria. Sometimes the incubated plates also contain colonies from *Micrococcus roseus*, which can be mistaken for *S. marcescens*. However, when examined closely *M. roseus* can be identified by the much smaller colonies and the pink colouring.

Enriching *S. marcescens* with the membrane filter method is only feasible if the samples are low on germs.

Toxicology of Serratia marcescens – Is S. marcescens pathogenic?

As early as 1903, BERTARELLI published his observations about the biology and pathogenicity of *Bac. prodigiosus*. Pathogenic impacts were only observed with inoculations in the abdominal cavity and with subcutaneous injections of 0.8-2.5 ml in guinea pigs, mice, and rats. As a result, *S. marcescens* was considered to be a fully harmless bacterium for a long time, which 'has no pathogenic characteristics for

people' (OHLMÜLLER & SPITTA, 1921) and thus usable as a tracer without hesitation. In the clinical dictionary by PSCHYREMBEL (1964), *S. marcescens* is also listed as nonpathogenic. Even the well-known hygienists GÄRTNER, KNORR, and KISSKALT also used *S. marcescens* as a tracer.

Since circa 1960, there have been frequent publications about cases of infection, some deadly, caused by pigmentation forming and colourless strains of *S. marcescens*. According to DODSON (1968), the infections affect the urinary tract, lungs, and sinus cavities and range from inflammation, suppuration, and blood poisoning to lung abscess, peritonitis, endocarditis, and meningitis. WILKOWSKE et al. (1970) reported 176 cases of *S. marcescens*-infections, whereby it was proven with 98 patients that they had become infected in the clinic. More than 90% of the infected patients had had an operation. Wounds, probes, catheters, and dialysis machines were named sources for the infections. All of the infected patients, who suffered from respiratory tract illnesses had received inhalations. Of the isolated *S. marcescens*-strains, 93% had lost their pigmentation capability. The strains were resistant against most antibiotics. Only gentamicin had an antibiotic effect against most of the strains (DAVIS et al. 1970). In the laboratory, WINKLER et al. (1978) was able to grow several *S. marcescens*-mutants, which had a high resistance against a series of antibiotics.

YU (1979) conducted a clinical review with a historical perspective of the vast amount of scientific literature; v. GRAEVENITZ (1980) and DASCHNER (1980) examined the pathological literature about disease symptoms and hospitalism through *Serratia marcescens*.

All of the established causes of the diseases were infects caused by external operations or through inhalation. Obviously, antibiotic resistant strains of *S. marcescens* can breed and multiply in clinics. Even more so, if they have lost their pigmentation forming ability and are thus no longer noticeable. Furthermore, it can be gathered from the literature that only weakened patients are affected by the antibiotic resistant strains of *S. marcescens*: 'These data demonstrate that *S. marcescens* can become pathogenic for man in certain clinical situations, especially in patients with chronic debilitating disease who have been treated with multiple antibiotics' (DODSON 1968).

In spite of these definite facts of its harmlessness, there have been agitated reports in the technical journals as well as in the daily papers about the 'pathogenic organism' *S. marcescens* (IRSCH 1980).

However, there is no case known, in which an infection was caused by ingesting food or liquids. So it was understandable that the parliament member, GORDON, remained unharmed although he tried a test in 1906 and gargled with a suspension of *S. marcescens* in the British House of Commons to prove that germs could be transmitted through the air. He recited Shakespeare verses in front of the empty House of Commons, whereby agar plates were on the seats; after the following incubation of the plates, he could detect pigmented *S. marcescens*-colonies and so demonstrated how contagious the speeches, coughing, and clearing of their throats could be for the parliament members. The test was undertaken because of a flu epidemic that had run wild in London (YU 1979). R. MÜLLER (1950) carried out the same test during his lectures. A similar demonstration for the harmlessness of *S. marcescens* for people in good health was seen in 1976 by the participants of the Third International Sympo-

sium of Underground Water Tracing (SUWT) in Bled, when H. DOMBROWSKI drank ca. 1/3 litre of a rosy *S. marcescens*-suspension in front of them. In his lecture, DOMBROWSKI (1977) stressed the unrestricted applications of *S. marcescens* as a tracer. In a written communication W.H. TRAUB (1975) from the Institute for Clinical Microbiology and Infection Hygiene of the University of Erlangen-Nürnberg/FRG, substantiated that 'practically, *S. marcescens* has gained exclusively in clinical situations importance as an opportunistic-pathogenic germ.' Besides, it is harmless for healthy people. Up to now, there has been not one case of enteritis reported. As always, pigmented strains can be used harmlessly in hydrogeological tracing tests!

2.7.3.2 *Escherichia coli* (ESCHERICH 1885)

This bacteria type is often used instead of *Serratia marcescens* as a tracer. The advantages are that it practically does not occur in natural waters. Only if *E. coli* has been detected in surface or groundwaters, is it indicated that there is impact due to warm-blooded faecal excretions. Thus, institutions that conduct water analyses often routinely analyse for *E. coli*. However, according to the pertinent ordinances, only the coli titer must be determined, i.e. the dilution volume, in which the bacteria with lactose fermentation is detectable. The determination of the colony count should be also determined in tracing tests by counting on ENDO-agar plates.

Now and again, *E. coli* is reportedly used instead of the 'pathogenic' *Serratia marcescens*-bacterium. Since there are also pathogenic strains of *E. coli* (PSCHYREMBEL 1964, LUKAS 1959c), nonpathogenic strains obtained from the German Collection of Microrganisms in Göttingen/FRG (Deutsche Sammlung von Mikroorganismen/Göttingen) are used, e.g. Strain ATCC 11229. Whereby, compared to *S. marcescens*, these have a much more painstaking examination method, which is gladly put up with.

When applying *E. coli*-bacteria, it must be considered that they are very sensitive to copper ions. At a concentration of 0.5 mg/l Cu^{2+}, *E. coli*-bacteria are reduced to at least 90%. Adding ascorbic acid causes an *E. coli*-reduction of over 99% (RAGAP-DEPRE 1982).

2.7.3.3 *Bacillus stearothermophilus*

This bacterium is easily isolated from other microorganisms, since it shows optimal growth at 56°C (SATTAR et al. 1972). However, it occurs in soil and is washed into the groundwater, especially during heavy rains (PYLE et al. 1979, SINTON 1979b).

2.7.3.4 *Pseudomonas violacea*

This bacterium was used in the first well-directed drift tracing tests in the sand filter models of the Berlin Waterworks from FRÄNKEL & PIEFKE (1890). Then it was called *Bacterium violaceum* or *Bacillus violaceus*, later *Chromobacterium violaceum.*

On gelatine plates, *Ps. violacea* initially forms yellowish, then violet roundish colonies; on agar plates it forms blue-violet colonies. The dye janthine forms only after exposure and is water insoluble, yet soluble in alcohol. Alkalis transform the colour to green (OHLMÜLLER & SPITTA 1921). Sometimes the pigmentation does not occur. The incubation at 25°C happens slower than that from *Serratia marcescens*, whereby *Ps. violacea* can be overgrown from other colonies (LUKAS 1959c).

2.7.3.5 *Bacillus acidocaldarius* (DARLAND & BROCK 1971)
This bacterium was isolated by BROCK from acidic reacting hot springs in Hawaii/USA and in mainland USA. It does not occur in groundwater. The best growth conditions are obtained on agar plates with yeast extract and glucose at pH 3 and 65°C. For identification, its capability to split starch can be applied (DARLAND & BROCK 1971).

During several tracing tests in the Southern German alpine foreland, in a sandy-coarse gravelly aquifer with flow paths of 80 and 240 m using $8 \cdot 10^{11}$ and $1 \cdot 10^{14}$ germs from Strain DSM 446/ATCC 27009, no positive results could be obtained, although at the same site the injected dyes reappeared after 8 and 81 hours respectively. The negative results are most likely due to the large pH-buffer capacity of the samples taken from the calcareous aquifer (GLMZ 1980).

Better results can be expected in mineral-poor groundwaters. Buffered waters should be adjusted to pH 3 before being spread with mineral acid, as with the culture media.

2.7.3.6 *Other microorganisms*
Here are further microorganisms listed, which have been suggested as tracers or actually used with more or less good success.

Streptococcus faecalis, together with *E. coli*, both streptomycin-resistant strains, have been used as tracers near leaky septic tanks (HAGEDORN et al. 1978). Coliform bacteria, *Streptococcus aureus*, and *Bacillus pumilis* were used by MARTI et al. (1979) in investigating pore groundwater flow.

Bacillus pyocyaneus is a pigment forming microorganism. It was suggested by WEBER (1941) and OHLMÜLLER & SPITTA (1921).

Further pigment forming microorganisms are *Sarcina lutea* with yellow and a *Micrococcus*-species with chrom-yellow pigment and gelatine liquefying properties (ABBA et al. 1899).

Diverse groundwater bacteria were stained with 4,6-diamidino-2-phenylindole – (DAPI) – by HARVEY et al. and used to investigate pore groundwater (HARVEY et al. 1989).

BENDEL (1948) mentioned that other than *B. pyocyaneus* also *B. subrusus* and *B. aceti* seemed suitable as groundwater tracers.

Endospores from *Bacillus globigii* ATCC 9272 (= *Bac. subtilis*) were used by HENRY (1989), to detect sewage water leaks from houses in groundwater. *B. g.* can be distinguished by its fast growth in 24 hours on soy agar and by its orange colonies. Also, a further selection is gained by heating the water samples with the endospores before incubation for 15 minutes at 80°C. However, there have been indications that *B. g.* has clinical pathogenic properties (SATTAR et al. 1972).

Other authors have used *B. g.* var. *niger*-spores preferrably for tracing sewage dispersion in the sea (PIKE et al. 1969) and in aerobiology to trace air currents (SATTAR et al. 1972).

To trace a sewage plume and its dilution in a stream (Lennefer Bach, NRW, Germany), SCHUBERT and SCHÄFER (1971) used a threefold genetically marked mutation of *Aeromonas hydrophila* and a nonpathogenic mutant from *Salmonella typhimurium*.

As early as 1896, PFUHL (1897) successfully used shining water *Vibrionaceae* (*Lumineus vibrio*) as groundwater tracers. He observed that *L. vibrio* does not lose its brilliance during its stay in the groundwater and that this bacterium could be recommended as a tracer in drift tracing tests, since 'the standard enrichment procedure used with cholera can be applied.'

The *L.vibrio*-bacterium is a monotrichic curved rod. It sometimes occurs naturally in groundwater in hot weather, however. In 1915, GÄRTNER published guidelines to examine for *Vibrionaceae*.

Mycoderma aceti is the scientific name for the film that forms on the surface of standing water bodies; the major component is *Acetobacter xylenium*. According to DIENERT (1912), *M. aceti* has been often used as a groundwater tracer. It practically does not occur in groundwater. DIENERT also published guidelines for growing the injection suspensions as well as for examining the water samples.

A further literature review on the use of bacteria as groundwater tracers was published by KESWICK et al. in 1982b.

2.7.4 *Application areas*

It was especially the hygienists who furthered the use of microorganisms along with uranine and salts as tracers. After the aforementioned basic research by PFUHL and ABBA, GÄRTNER underscored in his 'Hygiene of Water' in 1915 the importance of tracing tests for hygienists. After it became known that cholera and typhoid epidemics could be caused by bad drinking water, water protection zones around water tappings were started to be set up. Here it was above all KNORR (1937), who brought about the use of tracing tests with dyes and *S. marcescens* in water protection zoning questions. Unfortunately, combined bacteria and dye tracing tests are only seldom applied in determining water protection zones.

2.7.4.1 *Fissured groundwater aquifers*

The most important water tappings of the city of Pforzheim in southwestern Germany are in the fissured rocks of the Bunter sandstone. After the typhoid epidemics from 1894 and 1897, there followed another in 1919 with 4000 cases of illness and 131 dead. DAUR and RÖHRER reported in 1921 about the investigation as to the cause of the catastrophe in detail. Accordingly, during thawing weather and snow melt in the middle of February 1919, liquid manure was spread on the eastern edge of the village Waldrennach. The snow melt water mixed with the liquid manure which came from a farm, where there was a case of typhoid, that had been first diagnosed as intestinal flu. After a short flow path on the surface of the easterly sloping meadows, the water trickled away into several swallowholes at the start of the talus. The terrain farther downhill changes to a boulder field, where at the bottom in the Grösselbach Valley, the Pforzheim water tapping Keck's well lies. The assumed major percolation site of the typhoid bacilli lies at ca. 537 m NN, the Keck's well water tapping at 438.9 m, hence ca. 100 m lower. The distance between both sites is only 380 m. A salt tracing test from 15 July 1919, in which 3 centner, i.e. a total of 150 kg salt were injected in 3 neighbouring swallowholes, resulted in a faultless detection of chloride in the Keck's well water tapping: already after 6 hours, the chloride content had risen from 10.7 to 102 mg/l. This was already after the maximum,

since the following samples taken at 9 and 12 hours contained only 56 and 42 mg/l respectively. The mean residence time for this tracing test was most likely ca. 12 hours.

A few weeks later, on the 30th of August, with obviously better weather conditions than during the salt tracing test on the 15th of July, a *S. marcescens*-suspension was injected in the said percolation site downhill of the 'typhoid meadow.' This time, the first appearance in the Keck's well of *S. marcescens* was after 7½ hours and the maximum was attained after 9½ hours with 38 colonies on gelatine plates. The last positive result was observed after 21 hours. With this tracing test, it could be established that under the combined conditions of a case of typhoid, the deposition of liquid manure in the catchment area of a water tapping, and snowmelt runoff, the mean residence time of the water flowing underground was much too short to allow the pathogenic germs to decay.

Connected with this situation, a salt tracing test was carried out on the other side of the Gösselbach Valley on three neighbouring sites in the Bunter sandstone-boulder debris on 26 July 1919. After only two hours, a chloride increase from 8.5 to almost 48 mg/l was detected in the Jages spring, 480-450 m away, which was also the maximum. Another tracing test with *S. marcescens* was carried out on 31 July 1919. Samples were taken every quarter-hour at the Jages spring and the *S. marcescens*-cultures, which were incubated on agar and gelatine plates, resulted in great breakthrough curves. Since there was only one injection site in this tracing test, more specific information concerning the test conditions can be obtained. The distance from the injection site to the Jages spring was 450 m with an altitude difference of 50 m. The first *S. marcescens*-bacteria arrived after 2¼ hours, the maximum was reached after only 2¾ hours and the last bacteria probably arrived after 6½ hours.

The three Pforzheim tests show definite connections between the infiltration sites for bacteria in boulder debris and in fissures in the Bunter sandstone with utilized water tappings. However, there are the following two deficiencies in the setup of the tracing tests: First, the accompanying salt tracing tests were not just injected at the injection site of the *S. marcescens*, but rather also at neighbouring sites. Therefore, the information about the flow paths is restricted. Secondly, both tracers were not injected simultaneously nor under identical hydrometeorological conditions. Thus, a direct comparison between the flow behaviour of salt and *S. marcescens* is unfortunately not possible.

2.7.4.2 *Pore groundwater aquifers*

KNORR (1951) carried out tracing tests in the gravelly pore-groundwater of the Upper Bavarian alpine foreland with uranine and *S. marcescens* in the catchment area of a well. The tracers arrived at the observation well, located 44 m away in 15, resp. 17 hours. In the delivery well, 310 m away, the dye arrived after 75 hours or with an effective flow velocity of 310 m/day. The *S. marcescens*-bacteria never arrived. Unfortunately, KNORR was only interested in the first appearance of the tracer. A hydrological evaluation and an indication as to the survival time of *S. marcescens* are not recorded in his report.

A tracing test in the Upper Rhine valley (Southwest Germany) showed the filtration effects of the gravelly-sandy aquifer with a hydraulic conductivity of $4 \cdot 10^{-3}$ (m/s) (KÄSS 1972). Uranine first appeared after only 29 hours 11.2 m away. From the

breakthrough curve, a mean residence time of 533 hours = 22.2 days can be determined. Four weeks after the uranine injection, 0.5 l of a *S. marcescens*-suspension was injected in the same filter flow path. According to H. DOMBROWSKI, who had produced the *S. marcescens*-suspension, there were $3 \cdot 10^{19}$ *S. marcescens*-colonies in the suspension, which however cannot be correct, since a half litre does not provide enough room for so many colonies! Most likely only ca. 10^{13} colonies were injected. Nevertheless, simple calculations yield, that under the same conditions, the *S. marcescens*-colonies would have appeared at least 10,000 times over the detection limit, if they had survived or not been adsorbed. Sorption and a short survival time prevented a reappearance.

With higher k_f-values, bacteria can of course drift over longer distances. In tracing tests in the Erolzheim Field near the Iller River in Southwest Germany with a hydraulic conductivity of around $2 \cdot 10^{-2}$ (m/s), the *S. marcescens* colonies covered a flow path distances of 42 m in 27 hours.

The longest distance covered by bacteria in pore-groundwater, is according to SINTON (1979a,b) 920 m. The tracing tests that support this were conducted in a sandy aquifer in New Zealand, where in a borehole on the downcurrent edge of a waste dumpsite, *Bac. stearothermophilus* and H_2S-producing *E. coli* were injected. The resulting groundwater-flow velocities were very high, between 200 and 350 m/day.

Extensive tracing tests in the coarse-gravelly aquifers of Northern Switzerland were carried out by MARTI et al. (1979). Besides dyes and phages, the authors also used various types of bacteria. The results from these noteworthy tests are summarized in Table 17. Merely for the test area Uttingenfeld/Aare is a hydraulic conduc-

Table 17. Summarized results of the tracing tests by MARTI et al. (1979) in pore-groundwater aquifers in Northern Switzerland with specifics about the injection amount, and tracers, the flow paths (m), and the maximal effective flow velocity v_{max} (m/Std.). No reappearance: '–'.

Neuenegg			90 m		>90 m	
$3 \cdot 10^{12}$	Coliform bacteria		14 m/h		–	
Fraubrunnen			43 m	52 m	70 m	
$6.4 \cdot 10^{12}$	Coliform bacteria		1.8	7.4	3.5	m/h
$1.04 \cdot 10^{7}$	*Streptococcus faecalis*		2.1	7.4	3.5	m/h
?	Uranine		3	7.4	3.5	m/h
Cortébert					60 m	
$3.2 \cdot 10^{11}$	*Escherichia coli* 119:B14				1.8	m/h
$1.2 \cdot 10^{11}$	*Staphylococcus aureus* ATCC 29 923:3				–	
$8 \cdot 10^{10}$	*Streptococcus faecalis* ATCC 19 433:2				1.9	m/h
$8.4 \cdot 10^{11}$	*Serratia marcescens* ATCC 8 100				–	
5 kg	Uranine				1.9	m/h
Uttingenfeld/Aare		45 m	90 m	90 m	90 m	
				15 m	30 m lateral	
$4.5 \cdot 10^{9}$	*Strept. faecalis*	9	13	10	–	m/h
$7.5 \cdot 10^{8}$	*Bac. pumilis*	–	–	–	–	m/h
$2.25 \cdot 10^{13}$	*Bac. subtilis*	4.5	7	7	1	m/h
$2.23 \cdot 10^{13}$	*S. marcescens*	8	12	12	–	m/h
6 kg	Uranine	45	12	9	3	m/h
$2 \cdot 10^{9}$	Nonpathog. poliovirus	–	–	–		m/h

tivity of $2\text{-}3 \cdot 10^{-2}$ (m/s) given. Notable is the different behaviour of the microorganisms. *Str. faecalis* and *S. marcescens* show similar flow behaviour in the test area Uttingenfeld, at Cortébert however, *S. marcescens*, in contrast to *Str. faecalis*, could not be detected. Furthermore, it is conspicuous that the nonpathogenic viruses injected in the test area Uttingenfeld never reappeared.

Results from further published bacteria drift tracing tests in pore-groundwater are summarized in Table 18. Remarkable are the times for the longest detection of the injected test bacteria, which are partially far over the 50 days used to determine the Water Protection Zone II in Germany.

When the hydrogen sulfide contents in almost all of the medicinal springs in Bad Nenndorf (Niedersachsen, Northern Germany) after 1969 apprehensively decreased, it was presumed that pesticides sprayed in the Health Spa Park, which is in the closer catchment area of the medicinal springs, had damaged the sulfate reducing bacteria. Two injections of together ca. $3 \cdot 10^{11}$ *S. marcescens*-germs in the 3.4 m, resp. 4.7 m deep groundwater each flushed with 100 l resulted in a positive detection over dis-

Table 18. Results from several selected bacteria drift tests from the literature with comparisons to conservative tracers.

Date and place	Amount and type	V_{max} (m/h)	V_a (m/h)	L_{max} (m)	T_{max} (d)	Author(s), k_f-value
Celje/Slovenia						
18.9.1973	*S. marcescens*	0.9	0.28	25	6	KÄSS 1976b
19.9.1973	1 kg uranine	1.5	0.35	900	150	$2 \cdot 10^{-2}$ (m/s)
Dornach near Munich						
1979-1982	10^7-10^{11} *E. coli*	3-7	1.2-1.5	180	>150	ALEXANDER & SEILER 1983
	Uranine, Br-82	3	20-46	180	> 12	$5 \cdot 10^{-2}$ (m/s)
Haltern (Nordrhein-Westfalen, Germany)*						
1981-1982	$3\text{-}6 \cdot 10^{12}$ *E. coli*	0.01	0.004	13.5	257	JUNG & SCHRÖTER 1983
	0.5 kg uranine	0.04	0.03	55	>150	$5 \cdot 10^{-4}$ (m/s)
Segeberger Forst (Schleswig-Holstein, Germany)						
1981-1982	*E. coli*	0.03	0.002	11.5	200	HAVEMEISTER et al. 1983
	Pyranine	0.24	0.07	11.5	172	$2\text{-}5 \cdot 10^{-4}$ (m/s)
Merdingen, Upper Rhine Valley (Germany)						
28.3.1982	$7 \cdot 10^7$ *E. coli*	0.26	0.14	12.5	37	KÄSS et al. 1983
16.8.1982	$8 \cdot 10^{11}$ *E. coli*	1	0.009	37.5	155	$5 \cdot 10^{-3}$ (m/s)
15.8.1982	20 g uranine	2.5	1.2	87	300	
24.6.1983	$2 \cdot 10^{11}$ *S. marc.*	5.5	1.7	50	108	
23.6.1983	20 g uranine	11	0.9	200	320	
28.8.1989	$2.7 \cdot 10^{11}$ *S. marc.*	0.25	0.15	100	131	OETZEL 1990
28.8.1989	52 g uranine	0.4	0.05	100	250	$5 \cdot 10^{-3}$ (m/s)
Cape Cod (Mass./USA)*						
	DAPI-res.bact.	1.1	0.7	3.2	0.25	HARVEY et al. 1989
	Bromide	0.7	0.5	3.2	0.4	$1 \cdot 10^{-3}$ (m/s)

v_{max}: effective flow velocity at first appearance, v_a: mean effective flow velocity, l_{max}: maximum range, t_{max}: last detection. DAPI-res.bact.: Groundwater bacteria, resistant to the DNA-specific fluorochrome 4',6-diamidino-2-phenylindole (Sigma Nr. D 1388). *Tests conducted with a lowered groundwater level.

tances of 25 resp. 65 m in four of the hydrogen sulfide medicinal springs. The shortest flow time over 65 m was only 38 hours. After the observations were stopped after 32 days, two springs still showed positive results (DOMBROWSKI 1978). These tests prove that *S. marcescens* can also survive in a reducing environment over several days.

2.7.4.3 *Karst water*

Published articles concerning bacteria drift tracing tests in karsts are rare. In the combined tracing test in the Buchkogel Region southwest of Graz/Austria (Fig. 89) on 20 May 1958, in spite of the large injection amount of 10 litres of bacteria nutrient broth with *Serratia marcescens*, only a few colonies were detected in the only possible reappearance site, the Bründl spring, 820 m away. In three samples between the 64th and 70th hour after the injection, a total of only 8 colonies were detected. In the comparable tracing tests conducted by SCHULZ (1961) near Oberndorf/Neckar (Germany), only a few colonies could be counted although there was also an abundant injection amount. Nevertheless, over a comparatively short flow distance of 3100 m, the *S. marcescens* cells travelled with a similar velocity as the simultaneously injected uranine (Fig. 61). On the other hand, RICHTER and colleagues (1944) were able to achieve semi-quantitative results in Devonian massive limestone in Warstein (Nordrhein-Westfalen/FRG) by differentiating the *S. marcescens*-colony density in five stages. The investigations were carried out there with 80-l-nutrient broth culture over an underground percolation distance of 1650 m.

Extremely remarkable was the combined tracing test between the Upper Danube and the Aach spring in 1969, in which *S. marcescens* and brown *Lycopodium*-spores, besides other tracers, were used (BATSCHE et al. 1970). Both tracers were injected almost simultaneously in the karstified underground of the main Danube infiltration site downstream of Immendingen. The major part reappeared, as expected in the Aach spring (Fig. 103). In a few secondary reappearances sites with a main focus west of the Aach spring, isolated spores and *S. marcescens* colonies were also found. Both drift tracers reappeared only in one site, namely in a spring north of Engen, and only sparingly. Other than the Aach spring, there were 4 reappearance sites with trace amounts of brown spores and 6 for *Serratia marcescens*. The combination of both tracers proves that the percolating Danube water does not exclusively flow to the Aach spring, as had been generally assumed up to then. Only because the drift tracers can still be detected in extremely small amounts, could this be proven. To achieve the same effect with fluorescent dyes, extremely large amounts would have been needed; salts could not have been used for this purpose.

2.7.4.4 *Unsaturated zone*

Tracing tests in the unsaturated zone with *S. marcescens* were carried out as early as 1899 by ABBA et al. near Turin. To carry out his tests in the pore groundwater in the Upper Bavarian alpine foreland, KNORR (1951) had a 4 m deep lysimeter-like system built. A *S. marcescens*-suspension and 300 g dissolved uranine were poured on the surface. Through natural and artificial sprinkle irrigation of 55.5 mm on the first day and 41.5 mm on second brought the uranine after 72 hours to the 4 m depth, where a receiving apparatus was attached; *S. marcescens* did not reach this depth. In following 29 days, it 'rained' 527 mm on the test area, more than half of the annual pre-

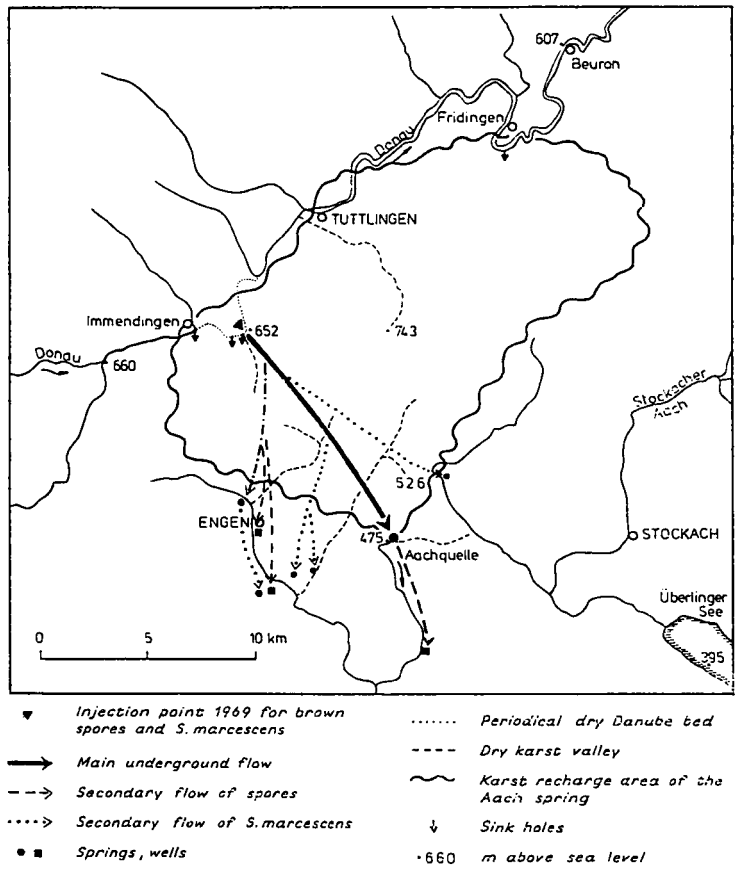

Figure 103. Schematic underground flow path of the *Serratia marcescens*-cells and brown *Lycopodium*-spores in the combined karst water tracing test in 1969 near the Danube percolation site. The main reappearance site is the Aach spring; further secondary reappearance sites are found mainly west of the Aach spring.

cipitation, without *S. marcescens* reaching the 4 m depth. After the infiltration section was opened, it was established that *S. marcescens* had only reached a depth of 1.8 m, i.e. the same distance that the roots from a pine forest would. KNORR deduced from these observations that it would also be hardly possible through natural fertilization for the bacteria to reach the groundwater. Assuming of course, a powerful and unharmed upper confining bed. Later, KNORR published further tests, that he conducted with MUSELMANN (1940) in a 3.4 m deep shaft with a 2.9 m thick infiltration section. After 81 mm of sprinkle irrigation within 11 days, *S. marcescens* had reached a maximum of 2 m depth.

The research group lead by HAGEDORN at Oregon State University in Corvallis, OR/USA (HAGEDORN et al. 1978, RAHE et al. 1979) has carried out extensive research concerning the infiltration of sewage water through the unsaturated zone. They also used sprinkler irrigation in the tests; as the tracer bacteria, they used

Streptococcus faecalis as well as *Escherichia coli*, the latter also partially as antibiotic resistant strains.

HENRY (1989) also investigated sewage percolation by injecting test bacteria. He chose three sites in Ireland with different permeabilities and depths of groundwater table between 2 and 6.5 m. He obtained good results with the easily identified bacteria *E. coli*, streptomycin resistant, and the thermophilic *Bacillus globigii*.

2.7.4.5 *Column tests*

Tests with columns or box shaped containers have the advantage that they can be carried out under controlled conditions. Different parameters such as temperature, flow velocity, grain size, flow path and length, and the composition of the mobile phase can be varied. Also, substances which cannot be used freely in the field without a permit, which is hard to obtain, can be investigated in the laboratory – even if only on a smaller scale.

Unfortunately, there are no standard column sizes. A comparison of the test results can often be only carried out with strong reservations. The diameter of the columns should not be too narrow, so that effects from the walls are suppressed. An inner diameter of 18 cm is sufficient for all commonly occurring filling materials. The length of the columns depends on the permeability of the filling. Well permeable materials need longer columns than less permeable material.

The first column tests with bacteria were carried out by FRÄNKEL and PIEFKE in 1890 in a 75 cm wide and 2.1 m high wooden tub. They simulated the effectivity of the sand filter in the Berlin Water Works for retaining pathogenic organisms. Typhoid and cholera bacteria as well *Bacillus violaceus* were not retained, even with low flow velocities of 10 and 30 cm/hour.

KNORR and MUSELMANN (1940) used 2.5 m high glass tubes with 9 cm diameter, that were filled with a natural soil profile. A positive detection was never obtained of the injected tracers after applying 10^{10} *S. marcescens* cells and staphylococci phages. After opening the columns, it was established that *S. marcescens* had only attained a depth of 1.5 m.

The Geological-Paleontological Institute of the University of Kiel under the management of G. MATTHESS, deals intensively with bacteriological column tests. Besides tests in columns and in pore groundwater, bacteria drift tracing tests in channels have also been carried out. *Escherichia coli, Serratia marcescens, Streptococcus faecalis*, and *Pseudomonas cepacia* have been used to investigate the filtration capacity of different grain sizes and the survival time of bacteria especially with respect to water protection area questions for water supply plants (RIEMER 1983, HAVEMEISTER & RIEMER 1983, SCHRÖTER 1983, PETERS 1989). Similar tests such as those by the group in Kiel have also been carried out by OETZEL (1990) in Tübingen with *S. marcescens*. As a surprising result from both groups, it was found that in the column discharge, the bacteria appear *before* the conservative tracers. It is presumed that this is because the drift tracers only travel through the widest pores, whereas uranine for example travels through the entire pore volume. Additionally, some microorganisms have their own transport methods. Due to its negative charge, the transport velocity of the anion chloride lies between that of the drift tracers and conservative tracers.

2.7.4.6 *Surface water*

To study flow velocity and dilution in the Taff, a heavily polluted river near Cardiff (Wales/Great Britain), besides phages and pigmented yeasts, *Serratia marcescens* was also used (WIMPENNY et al. 1972). The injection of $2.5 \cdot 10^{14}$ organisms, made resistant to penicillin, streptomycin, aureomycin, and actidione, was done from a footbridge at Taff Wells. Downstream, the river flows overs a weir. Before the injection, a large number of blank samples from the Taff were examined for *S. marcescens*, without exception, all were negative. The survival of the *S. marcescens*-organisms was also tested in different media and the 90% reduction rate in viability (T_{90}) in sterile distilled water and in non-sterile tap water in the dark and in the light was between 40 and 48 hours; in 1% sterile saline in light the T_{90} was 82 hours. The sampling site was 9000 m downriver. The *S. marcescens*-organisms were not detected until 55 minutes after the injection; the maximum with 500 colonies was reached after 70 minutes, the end of the detection was after only 85 minutes. The authors decided that *S. marcescens* are a reasonable tracer for rivers, even if heavily polluted. The addition of antibiotics to the nutrient broth during the incubation of the 0.2-ml-samples was not useful. Without the addition, colony counts for *S. marcescens* were 10-15 times higher.

SCHUBERT and SCHÄFER (1971) injected a polluted stream with a threefold genetically marked mutant of *Aeromonas hydrophila*, with a nonpathogenic mutant of *Salmonella typhi murium*; and also the poliomyelitis-vaccination virus Type II. Over a flow distance of 8 km the elimination rate under low river pollution was for *A.hydrophila* 99.8%, for *S.typhimurium* 99.9%; under higher pollution conditions at a dry period, only *A. hydrophila* was used; elimination was only 97.4%.

To study circulation in a small stratified lake in southeastern Norway, BAALSRUD (1961) used *Serratia indica*. The enrichment of *S. indica*-organisms was carried out with membrane filters.

2.7.4.7 *Coastal water*

In the Blackwaters estuary (English North Sea coast), RIPPON (1963) used *S. marcescens* to investigate sewage discharge. An antibiotic-resistant strain was used, to suppress the sea-water microorganisms during incubation. RIPPON found a considerable distribution of the injected organisms after 12 hours over a distance of 8.2 km and after 36 hours over 15.8 km. For sea-water, a survival time of 5 days was determined.

On the south coast of England, ROBSON (1956) and PUTMAN et al. (1956) followed the discharge from a sewer canal into the sea by injecting antibiotic-resistant mutants of *Serratia indica*, that were produced by gamma radiation. The pigmentation of the *S. indica*-colonies was not inhibited. By incubating the colonies in nutrient broth containing streptomycin, penicillin, and aureomycin, antibiotic resistant strains were produced. *S. indica*-organisms were chosen, because their occurrence in sea-water had not been described up to then anywhere. They also succeeded in producing a strain that was not only resistant to the named antibiotics, but also formed dark-red colonies at 20°C after incubating for 24 hours.

To trace the sewage discharge, 10^{15} organisms of *S. indica* and 11 Ci phosphorus-32 were added within 2½ hours to the discharge, that entered the sea at low tide ca. 60 m away from the beach. During the test, the wind came from NW with a wind

force of 2. Surprisingly, it was established that the tracer distribution in the sea depended more on the tides than on the wind. The *S. indica*-organisms as well as the radioactive phosphorus-32 were moved along the coast towards the east over one mile. However, the oil that was also discharged into the sea with the sewage, drifted on top of the water east-southeast.

Similar investigations as on the southern coast of England were conducted in Norway by ORMEROD (1964) in the Oslo fjord and by EIELAND (1966) in Trondheim fjord. Like RIPPON and PUTMAN et al., both authors used strains of *S.indica* resistant to antibiotics to trace sewage effluent.

Further tests were conducted by PIKE et al. (1969) on two non-specified British coastal waters with antibiotic-resistant *Serratia indica*-organisms, with spores from *Bac. subtilis* var. *niger* and with Bromine-82. The sewage plumes were also successfully traced with these tests. Whereas *S. indica* in sunlight showed a high survival loss, the *Bac. subtilis* var. *niger* spores were essentially more enduring. The authors stressed the advantages of a short-term injection as compared to an injection that lasts a long time.

2.8 PHAGES

P.Rossi & W.Käss

2.8.1 *Introduction*

The lack of environmentally innocuous tracers encouraged hydrogeologists to increase the number available by using biological agents. These tracers belong to a separate class since they are not solutes, but form a suspension of microscopic particles (colloidal suspension).

The requirements for a good biological tracer are numerous. The characteristics listed in the table below, eight in all, were taken in extenso from KESWICK et al. (1982a). They would be equally valid for chemical, isotopic or fluorescent tracers if the word 'nonpathogenic' under point one was replaced by 'nontoxic'.

Desirable properties of a microbial tracer

– The tracer should be nonpathogenic (i.e. not capable of causing disease in man, animals or plants).

– The tracer should not be present normally in ground water. It should be readily distinguishable from microorganisms found in water with a stable marker for its identification.

– The tracer should not affect the flow of ground water.

– The tracer should be stable in the environment for a suitable length of time.

– A tracer should move with the flow of ground water and not be filtered, adsorbed or otherwise removed during its underground travel.

– A tracer should be readily assayble in low concentrations by inexpensive methods.

– A tracer should not interact with other microorganisms present in the ground water, since this may cause changes to its properties or to those of the ground-water organisms.

– If it is desirable to use several tracers at once, they should be readily distinguishable.

Of all the possible biological tracers, bacteriophages certainly present the most advantages. Their small size places them in the same scale as pathogenic viruses of eucaryotic organisms. However, contrary to their 'cousins', they are nonpathogenic and nontoxic. By choosing an appropriate phage/host bacterium (BHB) system one can avoid all risks of influencing the aquifer's micro-flora.

2.8.2 *What is a bacteriophage?*

The term bacteriophage, or, more simply, phage, is used to designate bacterial viruses. Like all other viruses, bacteriophages are incapable of multiplying independently. They must insert themselves into the metabolism of their specific host, in this case a bacterium, and divert it in favour of their intracellular multiplication. Thus, bacteriophages exclusively and specifically invade bacterial cells. The word bacteriophage means 'which feeds on bacteria' from the Greek word, φαγειν, to eat.

Bacteriophages have adapted to the whole bacterial kingdom. The possibility of isolating at least one phage for all known bacteria proves the ubiquity of these viruses. A great number remain certainly to be discovered. In 1987, ACKERMANN and DUBOW counted no less than 2700 different tail-bearing phages of all shapes and sizes and over a hundred other shapes. Phages range in size from 20 to 350 nm, though some may have a total length of over 1000 nm (Fig. 104). Phages consist of an external proteic structure, formed by the assembling of many smaller proteic subunits called capsomers. This is generally called the head of the phage and is usually shaped like an icosahedron, a solid with 20 faces, or sometimes a cylindrical rod. The head encapsulates the genetic material, which, in over 90% of the cases, consists of double-stranded DNA. The remaining 10% contain single-stranded RNA or DNA.

Some phages also have a tail. It may be ornamented with various fibres or spikes,

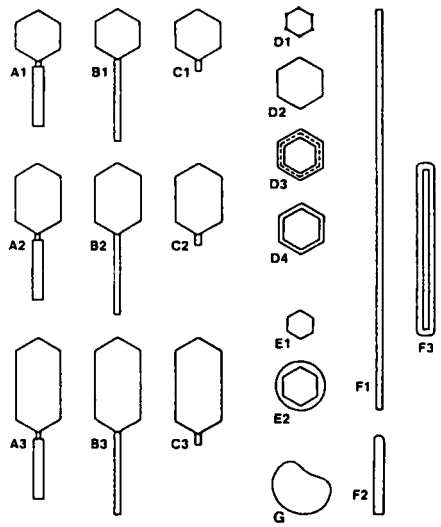

Figure 104. Phage morphotypes presently recognizable, including the new type F3 (ACKERMANN & DUBOW 1987).

may be contractile and more or less supple. More details on this subject may be found in the two excellent volumes by ACKERMANN & DUBOW (1987).

The majority of bacteriophages are specific to one species of bacteria and are therefore called monovalent phages. A limited number of phages, described as polyvalent, are capable of invading several different bacterial hosts. A phage is called virulent when it is capable of attacking its host bacterium. Several physico-chemical factors may lead to loss of virulence. The phage is then inactivated and will remain undetected by classical analytical methods. This will be discussed later on.

When a virus invades a bacterium, its genetic material may physically combine with the bacterial genome. In this latent form, the phage, then called a prophage, is not transcribed but multiplies passively with each bacterial division (OGUSEITAN et al. 1992). This type of phage is called 'temperate'. It will multiply inside its host cell, i.e. be transcribed, only following some particular external stimulation, such as UV-irradiation, of the host cell. This ability to physically insert its DNA fragment into the bacterial genome is not common to all the members of the viral world. All the other phages, which do not share this capacity, are called 'lytic'. Their intracellular multiplication occurs immediately after the infection of the host cell.

Unlike viruses which attack plants or animals, bacteriophages in natural environments have no active mode of motion: They wait passively for their host.

2.8.3 *The idea of bacteriophages*

In 1978, KINNUNEN published a very detailed description of how to use phages as tracers, many aspects of which are taken up here. Other contributions to the understanding of the behaviour of phages as tracers came from HAVELAAR (1986), PRIMROSE et al. (1982), SCHLEGEL (1985), and ROSSI (1994).

The first true tracing experiment with phages was carried out in the former USSR by a friend of d'HERELLE, the discoverer of phages. It seems he was accused of poisoning a well with phages and executed. The next tracing tests only came much later. SCHÜBEL (1936) isolated polyvalent phages from stream water. He injected them, along with uranine, in the catchment basin of the city of Bamberg's pumping station. He found that they travelled in the underground much like uranine. In October 1968, a tracing experiment was carried out in the Kymi River in southern Finland by NIEMELÄ and KINNUNEN (1968), where an *E. coli* bacteriophage belonging to the T-series was used. Since then, many experiments in surface and underground waters have been carried out.

The use of bacteriophages as biological tracers answers the growing need for environmentally harmless investigation tools. In short, this biological tracing method has the following advantages:

– Phages are nonpathogenic, nontoxic, and invisible. So this method can also be used for studying drinking water (springs, reservoirs, etc.).

– Each phage generally attacks only one bacterial species. With a careful selection of the bacteriophage and its bacterial host, any effect on the aquifers microflora can be avoided. Furthermore, there is no background in the aquifers, since the selected phages do not occur there naturally. Neither will a background level be generated nor will one persist over time, due to the short life span of the phages.

– The classical analytical method to examine for phages in water samples, using the

agar overlay in Petri dishes, is fast and cheap. Only a few millilitres of water are necessary for the enumeration of the phages. The detection level of this routine analysis technique is about 1 phage per 2 ml of water. This sensitivity is comparable, and most often superior, to that of the best fluorescent tracers. When VIROSORB filters are used, a detection limit of even 1 can be achieved (ALTHAUS & JUNG 1983, 1985).

– It is also possible to differentiate and count a mixture of phages in a single sample. Theoretically, bacteriophages offer nearly unlimited possibilities for multiple combined tracing tests.

– Ten to twenty litres of phage culture are necessary for one tracing experiment. Such an amount is easily transportable, even to inaccessible injection sites. It will contain 10^{14}-10^{15} phages, which represents in all about 1 gram of protein and a few grams of mineral salts and of various organic substances (amino acids, growth medium components). The influence on the aquifer will be negligible, even if the flow is small.

However, one must not overlook the fact that the preparations for such experiments are time consuming and accessible only to specifically equipped labs with trained personnel. The water samples to be analysed must be properly handled during storage and transport. These difficulties obviously make it desirable to limit the number of samples.

Virologists call plaques 'Pfu' = *P*laque *f*orming *u*nit. The plaque count per unit of volume gives a measure of the phage concentration in the waters analysed. Just as with bacteria, breakthrough curves may then be drawn, from which hydrological parameters may be determined. However, even if one knows exactly the number of phages injected, the quantitative experimental results must be handled with care.

The sample containers, the storage and transport conditions, the duration and conditions of the phage multiplication all have a decisive influence on the plaque count and size. An efficient collaboration and coordination between the commissioner and the microbiologists are essential for the success of the enterprise.

Because of the amount of work involved in a tracing with phages, only a small number of organizations are competent for organizing such experiments. In Central Europe for example, the following institutions conduct research on bacteriophages:

– Microbiology Laboratory of the University of Neuchâtel, CH-2000 Neuchâtel,

– Biology Institute of the University of Ljubljana, SL-1000 Ljubljana,

– Institute for Medical Microbiology of the Canton of St. Gallen, CH-9016 St.Gallen.

Selection of the Bacteriophage/Host Bacterium (BHB) System

The selection of the bacteriophage, and therefore of its bacterial host, is very important and influences all further work. Indeed, the host bacterium must possess certain essential biological characteristics:

– It must be easy to grow in liquid or solid media. This will therefore restrict the choice to the aerobic, heterotrophic, and mesophilic bacteria that grow rapidly on a simple medium.

– It must be totally absent from natural waters (karst, streams, porous environments). This second condition is necessary to avoid an excessive background noise, which might interfere with the results of a tracing test. If the host exists in the waters, phages of this species are sure to be present too.

– The bacterial strain must be nonpathogenic. When producing phages in great quantities, it is difficult, even with chloroform or cyanide, to totally eliminate the remaining bacteria. Some will inevitably be injected into the aquifers. One can therefore seriously question the ethics of performing tracing experiments using phages belonging to the genera *Salmonella, Shigella* or other enteropathogens, chosen mainly for the ease with which they can be cultivated, or for the great resistance of the phages of these bacterial species.

– No cross lysis reactions should exist between the different phages and bacteria chosen, since this would prohibit their use in multi-tracing experiments.

To the necessary qualities of the host bacteria, one must add a few for the phage itself. They mostly concern its physical and natural properties:

– It should have a high multiplication rate when produced in liquid media. It is important to be able to obtain as large a quantity of phages as possible, to reduce the volume of medium that must be prepared and injected. The lowest acceptable concentration is about 10^9 phages/ml.

– When using the agar overlay technique, the lysis plaques must be clear and well-defined. This is a considerable advantage when many samples have to be counted.

2.8.4 *Preparation of a phage suspension*

This preparation is carried out in the laboratory. There are two ways of obtaining very concentrated phage suspensions. One can either use a fermentor, a special vessel for the large-scale cultivation of bacteria, where all the cultivation parameters may be closely controlled. In this case, the volume of the culture is generally fixed. The second way is to simply use a large number of glass flasks placed on a shaker. The physico-chemical parameters are not controlled as closely as in the first case, but the culture volume may be varied as required. In both cases, the physico-chemical parameters of the cultures (pH, O_2, agitation) must be optimized for a maximal yield of bacteriophages.

Like all viruses, bacteriophages use the enzymatic machinery of their host to multiply. Consequently, there is a direct correlation between the physiological state of the host-cell and the concentration of phages in the medium at the end of the culture. So, the physico-chemical parameters of the bacterial culture must be optimized first: agitation, pH, concentrations of salts and organic substrates, and temperature. SARGEANT et al. (1968) recommend a Tryptone-Glucose-Yeast extract broth with 0.25 /l magnesium sulphate as the culture medium. The Casamino acids-glycerol medium of FRASER and JERREL (1953) or the PAB medium of ADAMS (1966) did not produce better results than the Tryptone-Glucose-Yeast extract medium according to KINNUNEN (1978), who increased the glucose concentration to 2 g/l.

KRUSÉ et al. (1973) recommend, both for cultivation and for detection, a Tryptone-Yeast extract broth containing 10 g Tryptone, 8 g NaCl, 1 g Yeast extract and 0.22 g $CaCl_2$ per litre.

The temperature of the fermentor is maintained constant, at the optimum of the host-bacterium. The agitation of the medium ensures that all the constituents are homogeneously distributed and that oxygen diffuses throughout the culture, as host-bacteria are usually aerobes.

If glass flasks are used (ARAGNO & MÜLLER 1982, WIMPENNY et al. 1972, BROWN et al. 1979), they should be placed on a mechanical shaker. The temperature may also be controlled by using an agitated water bath or an incubator.

In optimal conditions, concentrations above 10^{11} bacteriophages per ml may be reached in a fermentor culture. SARGEANT and YEO (1966) even mention a case where 10^{13} phages per ml were obtained. In glass vessels, somewhat lower final concentrations are reached: around 10^{10} phages/ml (ROSSI 1994). It must be noted however, that the maximum concentrations obtainable vary greatly from phage to phage.

At the end of the culture, generally once all the bacterial cells have been lysed, the phage suspension may be stored for several weeks at 4°C, with no significant decrease in the phage concentration.

2.8.5 *Environmental influences on the survival of phages*

Many publications (BITTON 1975, KOYA & CHAUDHURI 1977, BIXBY & O'BRIEN 1979, SEELEY & PRIMROSE 1980, LIPSON & STOTZKY 1983, NASSER et al. 1993) demonstrate the importance of research on phage inactivation and adsorption, if one intends to study their migration and persistence in the underground seriously.

The first process influencing the survival and propagation of phages and viruses in general is inactivation. The phage loses its capacity to infect its host-cell, and therefore its possibility to multiply. This is also called 'loss of virulence'. A virus can lose its virulence for several reasons (BABICH & STOTZKY 1980):

- Following the alteration or destruction of the phage capsid or tail,
- If its specific receptors are destroyed, making it impossible for the phage to recognize its host,
- Due to the chemical or physical alteration of the phage's genetic material,
- Because of its bonding onto adsorbent surfaces, generally a reversible occurrence.

For a homogeneous phage population, the inactivation rate follows an exponential decrease (STAGG et al. 1977) and depends on the physico-chemical parameters of the environment and on the amount and type of colloidal particles or organic macromolecules (humic acids).

Temperature

The influence of temperature on the inactivation of phages and viruses has been closely studied. It is largely recognized that the inactivation of viruses increases with temperature. YATES et al. (1985) state temperature as the main cause for the inactivation of viruses in natural environments.

The inactivation temperature varies between 30° and 60°C (JAWETZ et al. 1970). POLLARD and REAUME (1951) showed that *E. coli* T1 phages are only significantly inactivated above 60°C, while for T7 phages the limit is 50°C. The waters of central and northern Europe generally never reach such temperatures. Our experience showed that a change of temperature from 15°C to 20°C can already have a definite increase on virus inactivation.

Solar radiation

Several recent studies (NOBLE & FUHRMAN 1996, SUTTLE et al. 1992) have shown the strong influence of solar radiation on the survival of bacteriophages in marine

environments. A comparison of their inactivation rates showed that bacteriophages isolated from the Pacific Ocean are more resistant than those isolated from the North Sea (MOEBUS 1992, MOEBUS & NATTKEMPER 1989). The inactivation is believed to be caused by the alteration of the genetic material by UV irradiation (240-280 nm).

However, no inactivation due to solar radiation has ever been reported during underground or river tracing experiments. A river tracing experiment (ROSSI et al. 1996b) showed no correlation between the intensity of the solar radiation and the survival of the bacteriophages injected, contrary to the effect of the solar radiation on the used fluorescent dye, uranine.

Special precautions should nevertheless be observed when taking samples and storing them. Coloured or light-proof bottles should be used and the samples should be stored in the dark.

H^+ and OH^- concentrations

It is generally agreed that slight variations of the pH around neutrality do not influence the virulence of phages. However, a calcium hydroxide solution at pH 10.5 inactivates bacteriophage T2 by 90% in 90 minutes (SPROUL 1972). Very acid environments like gastric juices (pH around 2) also inactivate phages, thus eliminating all risks for human beings (MARTIN & THOMAS 1974). POLLARD and REAUME (1951) showed that above 10.5 and under 3.5 Coliphage T1 was completely inactivated in 24 hours.

Chemicals

Compared to bacteria, viruses are astonishingly resistant to a variety of toxic chemical substances. In 1955, MILLS studied the effect of about 1600 substances on S 13 *Salmonella* phages. 16 inhibited the growth of the *Salmonella*, while the phages retained their virulence. Urea and its derivatives inactivate the various types of phages to different extents (ADAMS 1966). The resistance to surfactants also varies from phage to phage, though they generally tolerate them better than bacteria do (ADAMS 1966, KALTER et al. 1946). The effect of chloroform is also variable.

F2 phages resist best to chlorinated water, better even than MS2 and the other *E. coli* phages. Under comparative conditions, phages may be considered rather resistant to noxious substances. Significant inactivation during tracing experiments can be excluded, except in highly polluted waters.

Strong agitation

Two plausible explanations can be given for the inactivation caused by mechanical agitation. First the capsid may be destroyed due to the mechanical stress caused by the movement of the waters. The second hypothesis, proposed by ADAMS (1959) and taken up by BRICELJ and SISKO (1992), states that the phages are inactivated by the surface tensions at the air/water interface. Shaking the liquid environment brings the phages to the surface. The surface of the liquid in contact with air strongly attracts proteic molecules that possess hydrophobic domains (WAN et al. 1993). At the air/water interface the surface tension is strong enough to cause the capsid to rupture. Some experiments (ROSSI 1994) show that when these interfaces are saturated with organic material, the inactivation of the phages is slowed down considerably. This second assumption seems therefore to be correct.

Colloidal particles

The presence of suspended material, organic or inorganic, also plays a role in the behaviour of viruses. Many studies have shown that phages or viruses are adsorbed very rapidly and in great quantities onto the colloidal particles present in the waters. (CARLSON et al. 1968, BITTON & MITCHELL 1974, HURST et al. 1980, GERBA & BITTON 1984, ARMON & CABELLI 1988, POWELSON et al. 1991). The adsorption mechanisms between the viruses and the particles are governed by the laws of attraction and repulsion. They are due to electrostatic and Van der Waals forces and to hydrophobic attractions (SMITH et al. 1978, BABICH & STOTZKY 1980, LIEW & GERBA 1980, BALES et al. 1991).

Not only does adsorption on these particles not inactivate all bacteriophages (MOORE et al. 1975), but it may procure them some important advantages. The work of SCHAUB and SAGIK (1975) shows that adsorbed phages are protected from rapid inactivation. This way, they can be transported by water over longer distances, both massively and rapidly. GRANT et al. (1993) define three possible types of behaviour, depending on the phage and on the kind of particle with which it interacts. These behaviours range from a feeble interaction, with no influence on the survival of the phage, to a very strong adsorption, resulting in a considerable loss of virulence (f1 for instance). The influence on the behaviour of the phage of the physico-chemical parameters and of the colloidal particles present in the environment may be assayed by simple laboratory experiments (ROSSI 1994).

Adsorption is reversible. The viruses inactivated by adsorption can recover their virulence if the physico-chemical conditions of the environment change. In laboratory experiments they were desorbed by modifying the pH, increasing the concentration of organic matter, or by decreasing the ionic concentration (OSTLE & HOLT 1979). The use of chaotropic agents or surfactants is also an effective way of desorbing them (ARMON & CABELLI 1988).

Biological inactivation

Phage capsids may also be destroyed biologically. First, by proteolytic enzymes released by bacterial cells. Second, when ingested by protozoa. These two mechanisms have recently been shown to exist in marine environments (SUTTLE et al. 1992). However, their influence could not be demonstrated during tracing experiments in underground or surface waters, even very polluted (ROSSI 1994).

Another biological mechanism that may cause bacteriophage inactivation is non-specific adsorption on bacterial cell walls (BITTON & MITCHELL 1974).

2.8.6 *Sample collection, transport, and storage. Counting phages in water samples*

The transport and storage conditions of the samples have a decisive influence on the preservation of phage virulence. To avoid contamination, the samples should be taken exclusively by people who did not participate in the preparation of the phage suspensions or their injection. Brown plastic vessels of at least 100 ml should be used. The samples should be transported and stored cool and in the dark. They must be kept at 4°C and brought as quickly as possible to the laboratory for analysis. If samples must be kept for a long period, they can be frozen (KESWICK et al. 1982b). However, this may not be possible with all types of bacteriophages.

Conflicting evidence exists in the literature concerning the decrease in phage numbers (ALTHAUS et al. 1980):

Phage and medium	Times of inactivation (d)			Reduction	Literature
	up to 5°C	up to 10°C	up to 20°C		
Coliphage			>100	–	BAGDASAR'JAN & ABIJEWA 1970
T4, springwater		112 (8-10°C)		85%	GILCREAS & KELLY 1955
T7, groundwater	>64 (3°C)		>64 (20°C)	99.9%	NIEMI 1976
T7, surfacewater	>64 (3°C)		21-35 (20°C)	99.9%	NIEMI 1976
T4, tap water	35 (4-8°C)		77 (18-25°C)	99.9%	LEFLER & KOTT 1975
T4, dest. water	231 (4-8°C)		77 (18-25°C)	90-99.9%	LEFLER & KOTT 1975

ALTHAUS et al. (1985) showed that proteins (1.5% Beef extract) protect phages from adsorption onto the walls of the glass vessels (Table 19).

However, this is used rarely in practice, since no measurable adsorption of selected phages onto the walls of plastic bottles has been detected (ROSSI 1994).

Detection and enumeration of bacteriophages:

The main problem when studying bacteriophages is their extremely small size. It is generally between a few tens and a few hundreds of nm. There are numerous requirements that any detection and enumeration method must fulfil to be considered scientifically valid. It is stressed that the method must be precise and reproducible. The financial aspect must also be considered: the method will not only be used in the laboratory, but also for the analysis of numerous water samples during tracing experiments. The specifications required of such a method follow, listed in the order of importance:

1. Very low detection limit (<1 phage/ml),
2. High reproducibility,

Table 19. Change in phage-number, each in 0.5 ml of coliphage F2 in tap water (pH 7-8) with different added amounts of beef-extract and different temperatures. Enumeration after ADAMS (1966) with double-agar-layer method upon Tryptone-yeast-extract-agar at 37°C.

	0%			1.5%			5%		
Days	5°C	20°C	37°C	5°C	20°C	37°C	5°C	20°C	37°C
0	232	258	348	230	242	214	294	262	213
4	163	6	0	226	297	49	227	224	80
7	147	0	n.a.	250	198	19	220	174	34
13	64	n.a.	n.a.	227	50	1	234	76	5
22	31	n.a.	n.a.	194	28	0	176	47	0
35	17	n.a.	n.a.	207	7	n.a.	222	29	n.a.

3. The method must be practical, as simple and rapid as possible, and adapted for the serial analysis of a great many samples,

4. Low cost,

5. If possible, usable under non-sterile conditions.

Some of these requirements are contradictory. Points 1 and 2 concern the analytical aspect. They conflict with the requirements 3 to 5 which regard the practical aspects of the method. So, in this case, perfecting the enumeration technique also means accepting a compromise.

Detection and enumeration methods independent of the host-bacterium

These modern methods are the results of the technological developments in biology. We will discuss the three techniques most frequently used today, starting with electron microscopy. This technique, perfected and brought up-to-date, can be used to detect viral populations in concentrations above 10^4 phages/ml (BERGH et al. 1989, BØRSHEIM 1993).

However, it cannot be used for the systematic counting of very diluted populations of phages. Nor is it possible to determine the 'physiological' state of the phages observed. Another disadvantage of this method is the fact that it detects all viruses present in a sample. Thus, the specific phage being examined for may be lost among the sometimes considerable indigenous population of viruses (BRATBAK et al. 1990).

PCR (*P*olymerase *C*hain *R*eaction) (ERLICH 1989) is based on the selective amplification of genetic material. It is extremely sensitive for the detection of bacteriophages and viruses (ATMAR et al. 1993). Unfortunately, the quantification of the phages present in the sample is still too complex for this method to be useful in analysing numerous samples. Using the host-bacterium still remains a more specific way of detecting and counting a population of phages than the use of genetic probes. PCR is nevertheless a powerful detection tool of the presence/absence type. However, the cost of this technique is also quite high because of source material and enzymes.

The last technique in this category we will discuss is used in immunology. The phages are detected on dilution plaques by a reaction with specific antibodies (ELISA technique). With this very sensitive method it is possible to determine the various types of relations between the phage and its host-bacterium (TORTORELLO et al. 1991). However, TARTERA and JOFRE (1987) have shown that this method is not as sensitive as ADAMS' (see below). Furthermore, the dilution plaques can only contain a couple of hundred µl. This is a problem when detecting very low concentrations of bacteriophages during tracing experiments. The reactants and the antibodies must be specific for the phage used: if possible, no cross-reaction should exist. So the cost of such a method is quite high.

Detection and enumeration using the host-bacterium

In the methods described below the host-bacterium is indispensable to detect the bacteriophages. One measures in fact the lysis of bacterial cells. If the conditions are favourable, this will be marked by the liquid or solid culture becoming transparent. The most common method today is the one ADAMS described in 1959, using a double agar layer. This analysis is done on Petri dishes filled with a first layer of solid medium (1% agar). The bacteriophages and bacteria are poured onto this surface with a few millilitres of soft molten agar (0.6% agar) at 45-50°C. In this way, phages

and bacteria are trapped in a medium pliable enough to allow their diffusion, but solid enough to stop any movement of fluids. This allows the formation of lysis zones, also called lysis plaques (Plate 8).

LURIA et al. (1951) showed that the relation between the number of phages counted on Petri dishes and the amount of phage material assayed is perfectly linear. This proves that each plaque stems from the action of one material particle. This does not necessarily mean that every phage particle present is counted as a plaque, but only that a constant fraction of the particles produces plaques. The phages detected by electron microscopy are more numerous than those appearing on a Petri dish through the disappearance of their host bacterium. The correlation between these two counts is between 40 and 100%.

Their appearance is due to a rapid succession of attacks on bacteria and production of phages. Each plaque originates from a single virus that invades a bacterium (LURIA et al. 1951). The plaques contrast with the rest of the surface of the dish, covered by a uniform bacterial carpet in the soft upper agar layer. According to the literature, it is the technique most commonly used by scientists all over the world.

Efforts have been made to improve it by eliminating the first agar layer. GRABOW and COUBROUGH (1986) treat samples by mixing 100 ml of the sample water with soft agar and distributing it into 10 Petri dishes of 14 centimetres in diameter. This rather tedious method is neither more reproducible nor more efficient than the one developed by ADAMS (1966). KOTT (1966) developed a numeration method in liquid cultures. The samples are serially decimal diluted in tubes. A culture that becomes clear after incubation signals that at least one bacteriophage was present in the tube at the beginning. Using the *M*ost *P*robable *N*umber (MPN) technique, it is possible to determine the initial concentration of phages.

This method cannot be used when numerous samples have to be treated. Besides, CORNAX et al. (1990) have shown that the double agar layer technique gives better results than serial dilutions in tubes or microtiter plates (TORTORELLO et al. 1991). The MPN method tends to underestimate the number of bacteriophages present in a sample.

Many authors have used filtration-elution methods to detect and count viral particles in large volumes of water (SEELEY & PRIMROSE 1981, PAYMENT et al. 1988, LOGAN et al. 1980, GERBA & GOYAL 1982). These procedures are very complex. Numerous steps are required, first to wash the filters, then to adsorb and desorb the viruses, sometimes to concentrate them, chemically or physically, and finally to count them on Petri dishes. An example of these very long manipulations can be found in GOYAL & GERBA (1979). Often it is impossible to go through so many steps, due to the large number of samples that have to be analysed. It is also probable that only a small number of viruses are actually retained (PURDY et al. 1984), and that the cumulated losses at each step can reach 10 to 90% of the initial number of viruses. Some authors use a pre-filter to eliminate suspended particles. However, this also eliminates the viruses adsorbed onto the particles (SCHAUB & SORBER 1977).

ARMON and KOTT (1993) have developed a particularly ingenious method to detect phages in samples of 500 ml of water. The detection limit seems to be 1 phage per 500 ml. The originality of this method consists in plunging the bacterial carpet (the bacteria in soft agar on a holder) directly into the container holding the 500 ml of water. The phages attack the bacteria and lysis plaques develop in the same way as in the

double agar layer. A certain amount of time would be necessary to adapt this technique to the analysis of large series of samples. It remains a powerful means of presence/absence detection, without the numerous steps of the filtration-elution techniques.

The last method presented is particularly original and deserves attention. PURDY et al. (1984) detect bacteriophages by placing the host-bacteria directly in the water sample to be analysed. Bivalent ions (Ca^{2+}, Mg^{2+}) are added to increase the efficiency of the method. After a period of latency permitting the definitive adsorption of the phages onto their host-bacterium, the sample is centrifuged. The pellet of cells is then diluted and analysed by the double agar layer technique. This method has a definite advantage over all the others using the host-bacterium: the adsorption of the phages on the bacteria occurs in a liquid environment. The possibilities of contact are far better than those in a gel media, no matter how soft it may be.

Two examples of bacteriophage analysis

Method of ALTHAUS & JUNG (1983) for the detection of phage F2:

– 9-cm-Petri dishes are prepared with Tryptone-Yeast extract solid agar (1.5%),

– The host bacterium *E. coli* K13 is harvested from a 6-hour culture,

– 5 ml Tryptone-Yeast extract soft agar (0.7%) are mixed with 0.5 or 1 ml of the water or filter desorbate to be analysed and poured over the solid agar layer,

– As soon as the soft agar has solidified, the dishes are turned over and incubated 16 hours at 37°C, when the lysis plaques can be counted.

General comments: the more polluted the water or filter desorbate, the sooner one must count the plaques, before they are covered by the growth of contaminants. Lysis plaques may easily be distinguished from air bubbles in that the border between the bacterial carpet and a plaque is light, while between the carpet and a bubble it is dark. Changes in the recommended method will result in differences in the size and number of lysis plaques. The following conditions should be respected:

– The optimum agar volume on a 90-mm-dish is 30 ml. Smaller or greater volumes result in plaques less than 2.5 mm square.

– The amount of host bacterium suspension used should exceed 0.1 ml.

– During the first 7 hours after inoculation, the size of the plaques increases proportionally with the incubation time. Afterwards, no significant size increase occurs.

– The diameter of the plaques is inversely proportional to the agar concentration in the overlay (soft agar). This is due to the greater diffusion rate of the phages in more diluted solutions.

– The diameter of the plaques and their multiplication rate depend on the type of phage: the 23 nm long phage PhiX174 multiplies fast and generates large plaques, the 26 nm long phage F2 multiplies slowly and forms small plaques, the over 100 nm long phage T4 multiplies fast and forms small plaques.

Method of ROSSI (1994)

It is almost impossible to define physico-chemical conditions that would be optimal for the enumeration of all bacteriophages. Each bacteriophage/host-bacterium (BHB) system has its own particularities. Enumeration therefore must inevitably pass an optimization stage. This does not mean, however, that all the phages present will be detected. The aim of this optimization is to make it possible to count the maximum number of phages, regularly and reproducibly.

The main modification to the classical agar overlay method consisted in giving the phages time to establish contact with their host bacterium in a liquid environment. The other modifications were aimed at adapting the analysis to each specific BHB system:

1. Optimal contact interval in liquid medium,
2. Optimal bacterial concentration in the Petri dish,
3. Choice of the solid growth medium,
4. Optimal growth temperature,
5. Mineral requirements: Ca^{2+}, Mg^{2+} and colloidal clay particles.

The contact interval allows the adsorption of the phage onto the bacteria (LURIA et al. 1951) and the beginning of the infection. The infected bacteria is then trapped in the top agar layer of a Petri dish. This procedure, used by PURDY et al. (1984) as a biological detection technique, substantially improves the enumeration technique. The analysis of the samples from a tracing test is then carried out in two stages. The first is a simple presence/absence test. It also gives an estimate of the number of dilutions necessary for the second step, a quantitative analysis.

Presence/absence test

All the manipulations of liquids are done using automatic pipettes with adjustable volumes (Socorex). The polypropylene tips are sterilized before use. 2 ml of the sample and 0.2 ml of bacterial culture are mixed in a sterile glass tube and left for 15 to 30 minutes at room temperature. This long interval allows definitive contact between the phages and bacteria to be established. The entire content of the tube is then simply poured onto a Petri dish containing 20 ml of solid medium (1% agar). 4 ml of molten 0.6% agar medium kept at 50°C are then added. This is then gently mixed, left to cool and incubated at the optimal temperature of the host bacterium.

If the result of this first step is positive (lysis plaques detected), a second analysis of the sample is performed, following the method presented below.

Quantitative analysis

0.4 ml of the suspension containing the phages are added to 3.6 ml of diluted (0.1M) phosphate buffer (DPB) at pH 7 in a glass test tube. Sometimes it is necessary to decimal dilute the sample beforehand in a sterile saline solution (0.9% NaCl) or in DPB. The number of phages in the last tube must be comprised between 20 and 200 per ml. 0.4 ml of an exponentially growing bacterial culture ($5 \cdot 10^7$-$1 \cdot 10^8$ bacteria/ml) are also added to the last tube.

The last tube containing the bacteria is left to sit at room temperature for an interval of time permitting adsorption of the phages on the bacteria (5 to 20 minutes depending on the phage). 1100 µl of the contents of the last test tube are poured onto a Petri dish already containing 20 ml of solid medium (agar 1%). 1 ml of DPB and 4 ml of molten 0.6% agar medium kept in a water bath at about 50°C are then added. This is then mixed by gentle rotation and the dishes are left to cool, before being incubated at the optimal temperature.

For certain phages, *S*ynthetic *F*reshwater (SF), to which 20 mM Tris-HCl pH 7.4, 50 mM Ca^{2+} and 5 mM Mg^{2+} are added, is used for the contact interval and the dilutions (MOORE et al. 1982). A mixture of bivalent cations and colloidal clay may also be used for phage PSF2 (*P.fluorescens*).

All the analyses are normally carried out on three parallel Petri dishes. This number can be doubled or even increased to 10 for certain analyses. The lysis plaques (Pfu) are counted after 18 to 24 hours and again after about 48 hours. Each result is the mathematical average of the plaques counted on the three or more Petri dishes, multiplied by the inverse of the dilution factor. When no dilution is necessary, the host-bacteria are directly added to 4 ml of the sample, tenfold diluted, in a sterile glass tube.

In addition to Pfu count statistics
If several series of samples are to be analysed during one tracing experiment, the following steps must be taken to ensure comparable plaque counts (ELLIS & DELBRUCK 1939): A comparative sample of known titer must be treated along with the samples of each of the series to be analysed. The comparative samples must be kept in the dark at 4°C. When all of the series has been analysed, the comparative sample which gave the highest plaque count is chosen as reference (Pfu_{ref}). The phage counts of the other series are multiplied by a factor K, corresponding to:

$$K = \frac{Pfu_{ref}}{Pfu_{cult}},$$

where Pfu_{cult} is the plaque count of the comparative sample of the series.

2.8.7 *Range of application of bacteriophages as tracers*

There are almost no restrictions to the use of phages as hydrological tracers. If the dilution is high, large amounts – up to 10^{16} – can be injected. They have demonstrated hydrological connections, where no others tracers could be used.

Additional information on phage migration may be found in the publications of ABU-ASHNOUR et al. (1993), BALES et al. (1993), BITTON (1975), BITTON & GERBA (1984) and CORAPCIOGLU & SHIYAN (1993).

Unsaturated zone
Since discovering that viruses can migrate through the soil and reach the groundwater, they have gained importance as markers of vertical flow of infiltration waters. (VAUGHN et al. 1978). In 1977, SCHAUB and SORBER carried out a tracing experiment with coliphage F2 in an irrigation field at Fort Devens near Boston/MA, USA. During 7 days, they injected 10^8 phages into each litre of sewage. The sewage flow varied between 3800 and 5700 m^3/day and was used during the experiment to irrigate 4 fields of 0.324 ha each. Compared to the bacterial counts, the F2 phages were not significantly retained in the soil or in the underlying unsaturated layer some 28 m thick. In the groundwater, bacteriophages were found in a sampling point ca. 180 m downstream from the irrigated field. The enteroviruses deposited along with the sewage on the irrigated fields were retained to a degree intermediate between the bacteria and the bacteriophages. These observations may contradict those of CARLSON et al. (1968) and of many other authors, who reported a high affinity between viruses and clay particles. However, several authors have shown (BIXBY & O'BRIEN 1979, POWELSON et al. 1991) that organic matter considerably prolongs the survival and

migration of viruses in the soil. Furthermore, the interaction of the viruses with the clay particles is also reduced.

BROWN et al. (1979) carried out experiments on leaching of sewage in three soils of varying permeability, using lysimeters and sewage drains. They marked the sewage with coliphage F2 and observed that in most cases it only penetrated a few cm into the underground. Only very rarely did phage F2 reach 1 m under the infiltration point.

In 1978, GERBA and GOYAL used agitation experiments to show that the adsorption of viruses on soil material is very variable. It depends first of all on the type of virus. These experiments also showed that adsorption decreases when the soil pH is lower. Very similar conclusions may be drawn for the behaviour of bacteriophages.

BURGE and ENKIRI (1978) obtained very similar results in agitation experiments with 5 different soils, using coliphage PhiX174 (ATCC-13706 B6). They showed that for soils with a pH below 7, the adsorption of the test phages followed FREUNDLICH isotherms. For the acid soils, a direct correlation between sorption and the content in organic matter was shown to exist. Similar experiments were carried out by MOORE et al. (1981) and LIPSON & STOTZKY (1983). ROSSI (1994) showed that the behaviour of bacteriophages mainly depends on the type of phage. Its physical characteristics, surface charge and hydrophobicity determine the degree of sensitivity to the physico-chemical parameters of its environment, such as pH, salt concentrations, organic matter, temperature, and to the presence of colloidal mineral particles.

Pore groundwater

The first tracing experiment in porous material was described by KINNUNEN in 1974. It was carried out in a 10.6 by 2.7 m water saturated model system with a steady flow. Along with the T7 and F137 phages, NaCl, rhodamine B, and the radioactive isotope ^{82}Br were also injected. Of the $9 \cdot 10^{10}$ F137 phages injected, 0.7% reached the outlet of the model, 10.3 m away, after a mean retention time of 85 hours. $7.5 \cdot 10^{9}$ T7 phages were injected. They were only detected in the first observation tube, 1.85 m away from the injection point. From these observations, it appeared that phage T7 was not suited for tracing in porous environments, due to its sorptive characteristics.

A water tracing test in the Aare valley by MARTI et al. (1979), combining uranine, bacteria, and polioviruses, gave positive counts for the bacteria and dyes 45 and 90 m away from the injection site, but not for the viruses.

Multiple tracing tests in porous groundwater were carried out in the Upper Rhine valley, with T4 coliphages of *E. coli* strain (ATCC 13706), uranine, sulforhodamine B, and cesium chloride. In one test, in an environment with a hydraulic conductivity of about $5 \cdot 10^{-3}$ m/s and a flow velocity of about 2 m/day, the phages had a radius of action between 25 and 50 m. In another multiple tracing test in the same area with PhiX phages, *S. marcescens,* uranine, rubidium bromide, and heavy water, single phages were detected at a distance of 100 m. In the first case, the phages survived for 10 months in the underground, in the second case only six months (OETZEL et al. 1991).

In the framework of a national research project on the survival of bacteria and viruses in groundwater (commissioned by the German Ministry of the Interior) with

the aim of defining protection areas for groundwater pumping plants, the Hygiene Institute of the Ruhr Region carried out tracing experiments with bacteria and bacteriophages in the porous groundwater of the Haltern Sands. ALTHAUS and JUNG (1983, 1985) injected coliphage F2 (ATCC 15766-B1). $1.7 \cdot 10^{11}$ phages were injected into the trial field with a maximum flow distance of 20 m. The phages were calculated to survive a minimum of 572 days, compare sections 2.7 bacteria and 5.4 pore water.

ROSSI et al. (1994) used two bacteriophages, T7 and f1, and the fluorescent dye Na-naphthionate, in a saturated porous environment in the test-field of Wilerwald (Switzerland). The permeabilitiy distribution and the thickness of the aquifer were indirectly determined by Radio-Magnetotellury (RMT 12-240 kHz). The results showed a good correlation between the permeability distribution obtained by RMT and the breakthrough curves and migration speeds of all three tracers. The restitution levels were far superior, by two to three orders of magnitude, in the more permeable zones, as opposed to those observed in the piezometers in less permeable zones. The phage T7 was present in samples taken 162.5 m away the injection borehole, 19 days after the injection.

The speed of the migration of the biological tracers was much greater than that of the naphthionate. In the most extreme case, the T7 bacteriophage migrated about 3.15 times faster than the chemical solution. These results indicate that bacteriophages are able to travel considerable distances along permeable gravel channels.

A second experiment was carried out in the same site by these authors. Two different phages, T7 and a marine phage H40/1, uranine, and iodine were injected into the same piezometer. The results illustrate the remarkable behaviour of the marine bacteriophage. It was recovered in great quantities, 10 to 20 times greater than T7. As in the first test, the phages migrated much faster than the two chemical tracers. After travelling about 64 m through a permeable zone (10^{-3} m/s), the uranine broke through some 240 minutes later than the viral particles, while the iodine was more than 600 minutes behind. The dispersion of the chemical tracers was also much greater (Fig. 105).

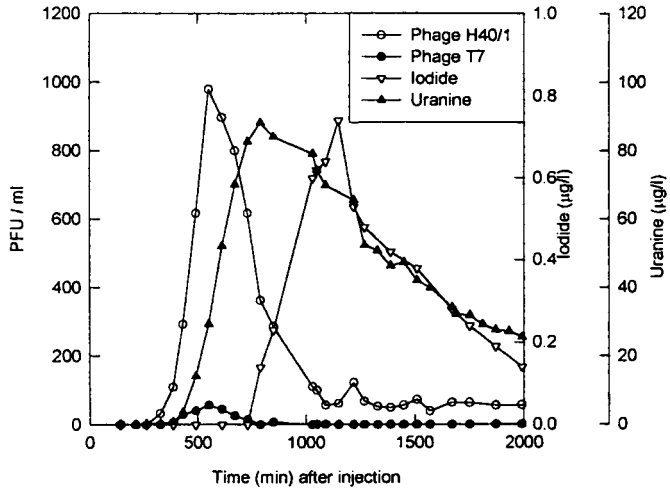

Figure 105. Breakthrough curves of bacteriophages T7 and H40/1, uranine, and iodine for borehole D7, 64.3 m from the injection borehole, on the test-field of Wilerwald, Switzerland (ROSSI 1995, unpublished data).

BALES et al. (1993) suggest that this is due to differences in the mode of migration of these two classes of tracers. Chemical tracers interact with the porous matrix just like in a classical chromatography experiment. The viral particles interact strongly with the negatively charged sites on the clay particles. Adsorption, if it occurs, is generally considered irreversible. Only changes in the environmental conditions, i.e. lowering the ionic strength, an increase in dissolved organic matter, may induce desorption and remobilization of the phages. A direct consequence of this is the sharp drop in the concentration of phages as the distance travelled increases or the permeability decreases. When a tracing experiment is to be carried out in an area of low permeability, the phage used must be chosen very carefully, giving special attention to its physico-chemical characteristics. The amount of phages necessary to obtain a breakthrough curve must also be calculated with care.

Karst groundwater

In 1974, FLETCHER and MYERS used phage T4 as a tracer in a very vulnerable karst aquifer. It was injected in the overlying soil and the phages were recovered in cave water about 1 mile from the injection site (Fig. 106).

In the Neuchâtel Jura, ARAGNO and MÜLLER (1982) carried out two tracing experiments with phages in the catchment basin of the Areuse spring. On the same day, they injected two different phages in different points.

Phage T7 was injected at the site called 'Grand Cachot' in the syncline of the Brévine. This site is 14.4 km away from the Areuse spring. On the day of the injection, there was a very strong hailstorm and 73.6 mm of rainfall were measured in the Brévine. Consequently, the discharge of the Areuse spring rose from 2.5 to over 16 m^3/s. On the day following the injection, T7 phages were detected in both of the main tributaries of the Areuse spring and they reached their maximum concentration of 10-15 phages/ml on the third day. From this data, one obtains a transit velocity of about 400 m per hour. The second injection site, 'Belle Perche', is located 4.5 km away the Areuse spring, near the village of Les Verrières. There, the wild phage of *Pseudomonas fluorescens,* NEU P 1, was injected. Contrary to what happened at the Brévine site, only 31.3 mm of rain were recorded on that day. However, here too, the

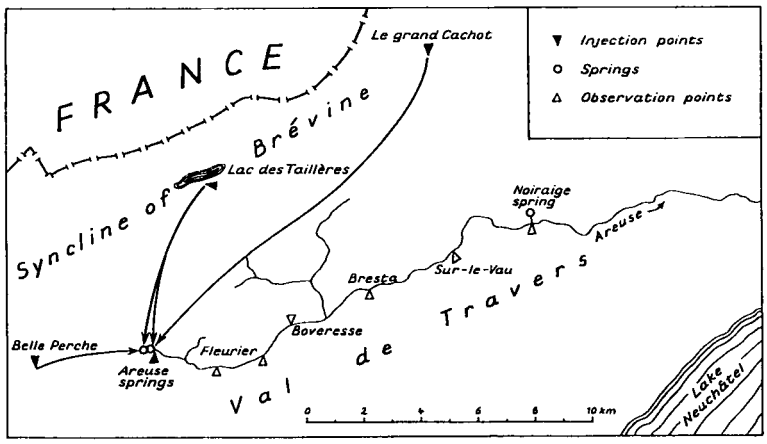

Figure 106. Locations of the tracer experiments in Swiss Jura.

phages reached the two Areuse tributaries rapidly with a transit velocity of 375 m/h. The maximum restitution level was about 60-70 phages/ml (Fig. 106).

Several other tests were carried out after that on the Areuse spring (ROSSI et al. 1996a). Four marine bacteriophages were tested with success, demonstrating excellent qualities as biological tracers for hydrology. Their restitution levels are generally far higher than those of phage T7. The restitution level of the marine phage H40/1 is generally almost equal to that of uranine, the tracer used as reference. Furthermore, marine bacteriophages present many advantages. First of all, they are totally absent in fresh water (no background). Second, the analysis of these samples is done on a solid medium containing high salt concentrations. The growth of the indigenous, non halophilic bacteria is strongly inhibited. This reduces the errors in the phage counts due to the interference of bacterial colonies. As a consequence, these phages can be used for highly contaminated waters (Fig. 107).

In 1984, in preparation for the 5th International Symposium on Underground Water Tracing (SUWT), multiple tracing experiments were carried out in the Peloponnesus karst. Phages were also used here (ALTHAUS et al. 1986). Two research teams took part in this project.

The Gelsenkirchen research team, H. ALTHAUS, W. ENGEL and K.D. JUNG (1986), injected phages into two swallowholes. The phage 'Kanata G' was isolated from sewage from the city of Tripolis. An enrichment culture of Kanata G of $3.9 \cdot 10^{12}$ phages was injected in one of the swallowholes.

Phage G was recovered in three coastal springs on the Gulf of Argos, situated 29 to 31 km from the point of injection, in stronger or weaker waves, following the hydrological conditions. ^{51}Cr was injected along with the phages. The spring which had a 95% ^{51}Cr-yield, however, only showed a slight increase in phages, for the same retention time. Phage F2 was injected into the karst at another swallowhole at a concentration of $5.8 \cdot 10^{16}$. Phage breakthrough could only be clearly demonstrated in a

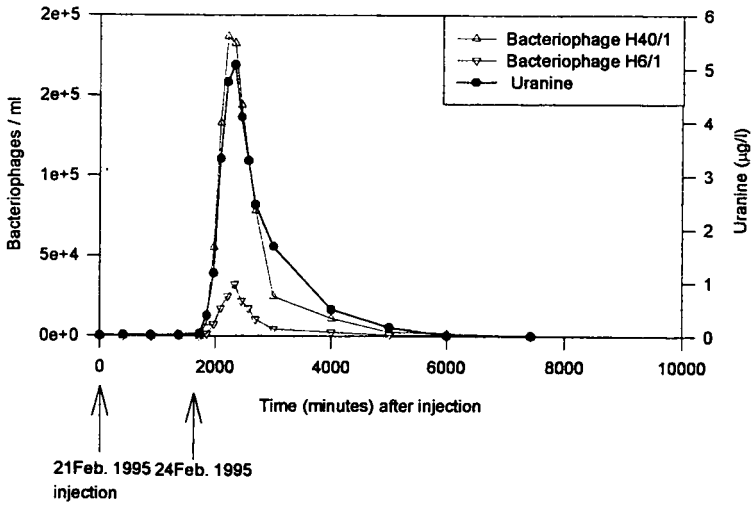

Figure 107. Recovery curves of the marine bacteriophages H40/1 and H6/1 and of uranine in the Areuse spring. Injection in the Taillères'Lake swallowhole.

coastal spring, some 26 km away. However, in that site a phage concentration up to 1200/l with practically no background noise was obtained.

The Ljubljana research team, M. BRICELJ, G. KOSI and D. VRHOVSEK (1986a), used *Salmonella* phage P22H5, specific for *Salmonella typhimurium*, in its experiment. $5.8 \cdot 10^{16}$ phages were introduced into an active swallowhole and reappeared in a coastal spring 39 km away. The highest concentration reached was 5 phages/ml after 222 hours of retention. The yield was only about one millionth the initial amount injected.

In 1988, SKILTON and WHEELER carried out similar experiments with three different phages in eastern England. They injected them in a karstic-fissured aquifer with a considerable pore volume (14-20%), during pumping tests. Bacteriophages of *Serratia marcescens, Enterobacter cloacae*, and *Escherichia coli* K12 were injected. With a flow distance of 122 m, the first phages detected travelled at a uniform speed of 4.9 m/h for all types, with yields varying between 0.12 and 0.49%. For the longest flow distance of 366 m, the maximum speeds ranged between 6.12 and 10 m/h and the yields between 0.1 and 1.9%. The fastest were the *S. marcescens* phages, by a short lead.

Experience shows that when tracing in karstic-fissured environments, two important parameters must be considered. The first is the phage itself: depending on its structure, and, as shown for porous environments, on its physical characteristics, a phage will be more or less adsorbed onto the colloidal particles transported by the water or onto the walls of the aquifer. Phages with a high recovery rate are those that react very little with the aquifer through which they are travelling.

The second important parameter is the flow of the aquifer. This will not only determine the mean transit time, but also the dilution factor and the concentration of colloidal particles in the water. Our experience with many tracing experiments in the fissured environment of the Swiss Jura shows that the breakthrough will be low to negligible when the waters are low. In conditions such as these, more bacteriophages must be injected.

In karstic-fissured environments, bacteriophages migrate at the same speed as chemical tracers (NaCl, uranine, sulforhodamine). This means that transit times are nearly identical. However, the dispersion of the phages is smaller and the time of first detection quicker. This is due to the sensitivity of the detection method: one single phage per ml is enough to detect the biological tracer in a sample, while the lower detection level of uranine, the best fluorescent tracer, is about 0.002 µg/l (about 10^{11} molecules/ml). The fluorescent tracer is certainly present in the first 'phage-positive' samples, but it cannot be detected by the instruments.

Fissured aquifers

A tracing experiment with phages in a fissured aquifer was described by KINNUNEN and JOKINEN in 1972. Phage T7 was released in a polluted well and recovered after a passage of 12 m.

In 1974, MARTIN and THOMAS reported a tracing experiment with phages in the Brithdir Sandstone, in the South-Wales coal-mining district. The fissured-aquifer there was inoculated with the type 2 phage of *Aerobacter aerogenes* 243. The phages were detected up to 680 m away. Between the injection and observation sites rose an

almost 100 m high cinder tip. The breakthrough occurred between the 4th and 9th day of the experiment.

Rivers

The first river tracing with phages was described in 1968 and was carried out in the Kymijoki river in southern Finland (NIEMELÄ & KINNUNEN 1968). T phages were injected below the Keltti power plant (Fig. 108). The sampling sites lay 8 km and 17.2 km downriver, near the main sewage outlet of the town of Kouvola and in the reservoir of the Myllykoski power plant. The unsatisfactory detection of the phage breakthrough caused the authors to further perfect their bacteriophages tracing techniques.

Later, 5 other tracing tests were carried out in this river (KINNUNEN 1978):

Phage	Test day (start)	Flow distance (m)	Number of phages(10^{14})	T_m (h)	V_m (m/h)	Q (m^3/s)
T	18 Oct. 1968	8400	1.15	9	935	262
T	18 Oct. 1968	17200	1.15	20	870	262
T7	15 May 1970	8800	2.01	7.31	1208	374
T7	6 June 1971	8760	4.64	6.90	1270	386
T7	17 Aug.1971	8760	1.2	10.44	839	258
T7	7 Sept.1971	8760	5.0	9.62	912	283
F52	1 Apr. 1975	8760	9.75	4.68	1872	574

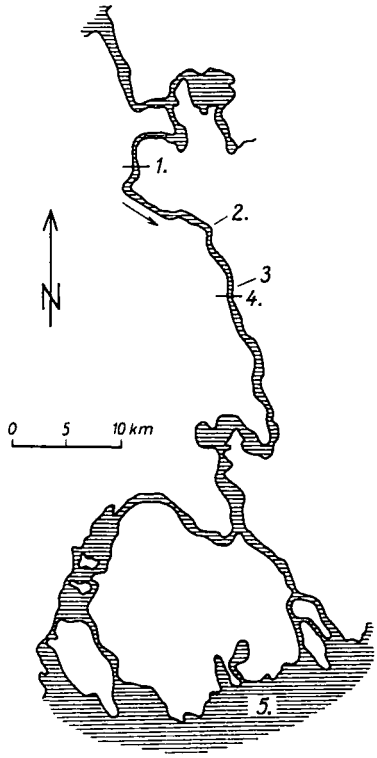

Figure 108. Tracing experiments in the Kymijoki River 1968-1975 (KINNUNEN 1978). 1 = power station Keltti, injection 1965, 2 = observation 1968, injections 1971 and 1975 into the main sewage outlet of the town Kouvola, 3 = observations 1968-1975, 4 = power station Myllykoski, 5 = bay of Finland.

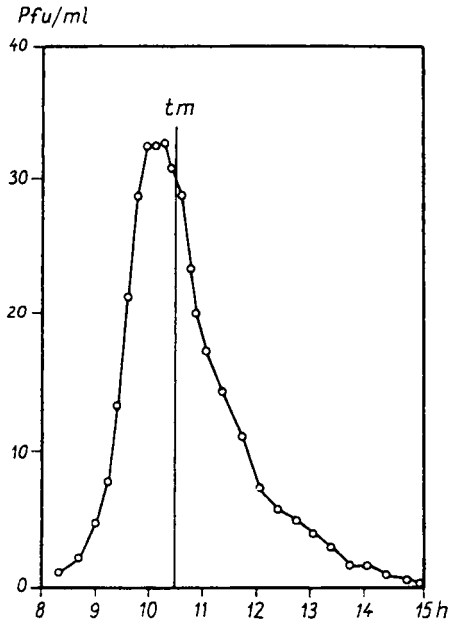

Figure 109. Breakthrough curves for the phage T7-test in the Kymijoki river/South Finland on 17 August 1971. Injection amount $1.2 \cdot 10^{14}$ phages, distance: 8760 m, discharge: 257 m^3/s, medial transition time: 10.44 h (after KINNUNEN 1978).

4 to 5 l of phage suspension were injected. They contained between 0.34 and $1.95 \cdot 10^{11}$ phages per ml, i.e. phage count between 1.2 and $9.75 \cdot 10^{14}$. Figure 109 shows the breakthrough curves from 17 and 18 August 1971.

During these tests, the level of the river was maintained as constant as possible, by controlling it at the dam. It did not vary by more than 5 cm. The relation between the flow velocity and the flow volumes corresponds precisely to CHEZY'S equation: v (m/h) = 13 + 3.29 Q (m^3/s), with a correlation coefficient: 0.9997!

In 1974, KINNUNEN (1978) carried out the first multiple tracing experiment in southern Finland, with the simultaneous injection of 4 different phages (Fig. 110). Phages T7, F46, F52 and F132 were introduced into three tributaries and the upper reaches of the Vantaanjoki River. Between 1 and 3 l of suspension at concentrations of 0.58 to $12 \cdot 10^{10}$ Pfu/ml were injected. The flow distances ranged from 24 to 62 km. During the 3 days of the experiment, from January 19 to 21, 1974, the flow at the sampling point of the Helsinki Pitkiikoski waterworks experiment was low: 3.9 m^3/s, the yearly average is 12.7 m^3/s.

The breakthrough curves of the four phages are superimposed (Fig. 110), but were easily counted separately. At the same time as the phage tracing, the waters downriver from the Pitkiikoski water works were marked with rhodamine. Portions of river 2-3 km long were traced and the travel times of the highest dye concentrations were thus measured. It was calculated that the dye always took longer than the phages to cover the same distance.

ROSSI et al. (1996b) injected a marine bacteriophage into the waters of the Areuse river (Switzerland). The phages were followed over more than 28 km, from the source of the river to its mouth into the lake of Neuchâtel. 22.5 l of culture, amounting to a total of $2.89 \cdot 10^{15}$ bacteriophages and 4.5 kg of uranine were introduced simultane-

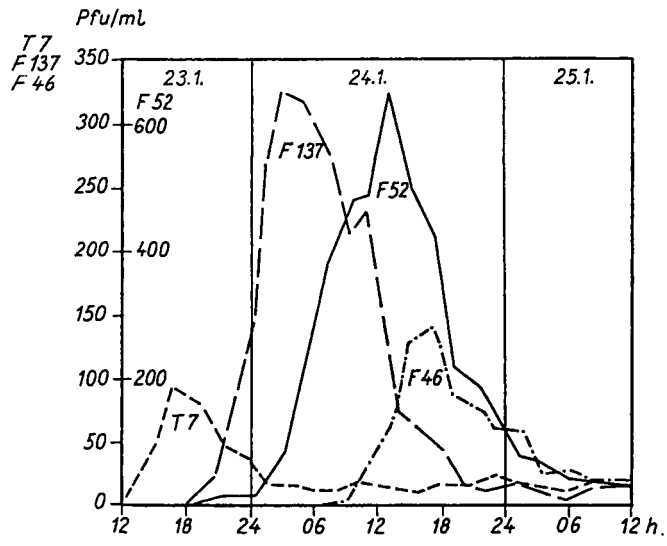

Figure 110. Breakthrough curves for the fourfold phage tracing test in the Vantaan-joki river system 1974 (KINNUNEN 1978).

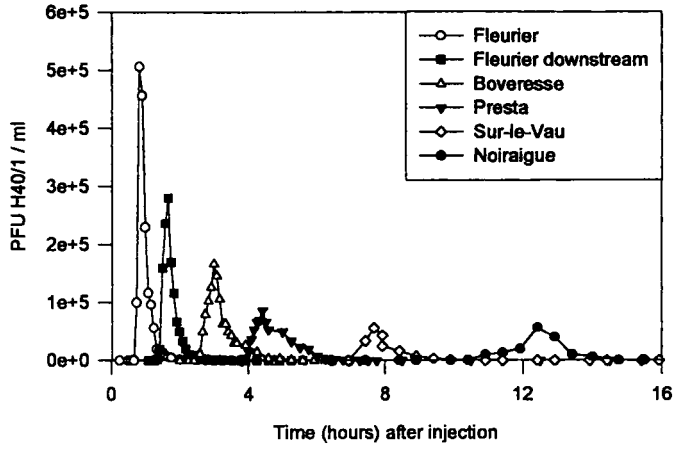

Figure 111. Breakthrough curves of the bacteriophages and uranine along the Areuse river.

ously. The breakthrough curves of both tracers along the first half of the river's course (14.2 km) are presented in Figures 106 and 111.

This test showed that phages migrate just like a dissolved chemical tracers. After some 14 km of migration, 67% of the uranine and 94% of phage H40/1 had been recovered. The spectacular decrease of the uranine concentration is believed to be induced by solar irradiation.

Just as was shown for karstic-fissured and porous environments, the use of marine bacteriophages considerably reduced the problems due to the presence of indigenous bacteria in the samples analysed on the Petri dishes. Furthermore, suspended particles did not interfere with the analysis of bacteriophages on Petri dishes, contrary to what happened with uranine. So phages can be used during high waters, when mineral or organic suspended particles are abundant. This type of biological tracer also

has an important psychological advantage: phages are totally invisible, at whatever the concentration used.

Lake tracings

KINNUNEN (1978) carried out a tracing in the southern part of Lake Saimaa (southern Finland), where two paper mills pollute the lake with their waste waters. In winter, this sewage flows practically unmixed into the hypolimnion and then follows the morphology of the lake floor. North-east of the island of Kätkytsaari, part of these waste waters reunite. At the same time, the hypolimnion current also divides into two branches, one flowing southeast and the other northwest. The flow of sewage coming from the southwest was marked with phages before it united with the one coming from the south. On 12 April 1976, this sewage current, some 2 m thick, was marked 0.5 m above the lake floor with 37.2 l of a suspension of phage F52. The concentration was $5.3 \cdot 10^{10}$/ml, for a total of $2 \cdot 10^{15}$ phages.

The samples taken above the lake floor showed that at least part of the sewage flows northwestwards, in quite the opposite direction from the surface waters. The most distant sampling point was 13.2 km away. 216 hours after injection, it still showed a phage concentration of 5 Pfu/ml and after 336 hours, of 2 Pfu/ml (Fig. 112).

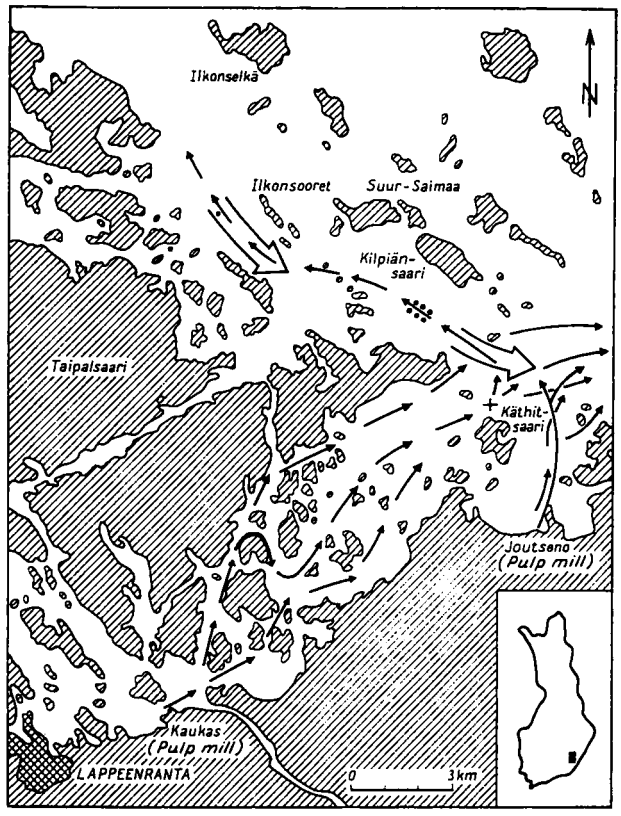

Figure 112. Tracing test in the hypolimnion of the Saimaa lake on 12 April 1976 (after KINNUNEN 1978). Large arrows = flow direction of the surface water; small arrows = flow direction of the hypolimnion; + = injection point in the hypolimnion, • observation sites. South of the island Kilpiänsaari, only 6 dots are shown for 34 observation sites.

KINNUNEN admits that the phage cluster was only partially defined and so only a rough travel velocity of about 1.3 km per day for the higher phage concentrations can be given. The resolution of the spatial and temporal distribution of the phages would surely have been clearer, if the 34 sampling points south of the island of Kilpiänsaari had been distributed over several transverse profiles instead of clumped together.

Sewage

In the preparation section of the Lammi sewage treatment plant, the faecal sewage is treated with quicklime and, then, after an equilibration tank, mixed with the wash water and precipitated with iron sulfate. After the settling tank, the cleaned sewage leaves the preparation plant. To study the retention times of the various water streams in the plant, KINNUNEN (1978) marked the faecal sewage with $2.8 \cdot 10^{12}$ T7 phages and 2 g of red-coloured *Lycopodium* spores. The wash water was marked with $1.2 \cdot 10^{11}$ T52 phages and 2 g of green-coloured spores.

The water leaving the quicklime reactor has a pH of over 11. No T7 phages were found there. Remarkably, the phages were then reactivated during the next stages of the treatment, since at the outlet of the plant 0.023% of the phages injected were recovered. The yield in the wash water was 25%. Both tracing tests gave retention times amounting to only 19 to 56% of the calculated ones. This was proof that the mixing in the plant was unsatisfactory. Only individual *Lycopodium* spores were recovered at the outlet. The experiment was not further pursued.

KINNUNEN (1978) also studied the flow through a settling pond of a waste water treatment plant near Saimaanharju in the Taipalsaari area with a phage tracing. The settling pond was 19,000 m^2 in area and on the average 0.9 m deep, for a total volume of 17,000 m^3 (Fig. 113). During the experiment, the hourly flow through the

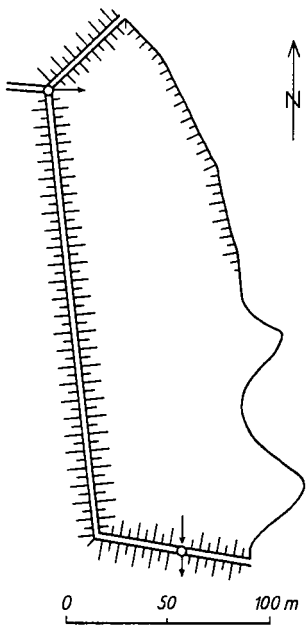

Figure 113. The stabilisation pond of Saimaankarju (KINNUNEN 1978).

pond was 200 m^3; and the calculated retention time 85.5 days. The current basically followed the long axis of the pond. On 23 November 1978, when the pond was covered with ice, the tracing test was initiated at the inlet. 1 l of a suspension of phage F52 at a concentration of $5.5 \cdot 10^{10}$/ml was used.

The highest phage concentration measured at the outlet was 700/ml, for a total yield of about 10%. The mean retention time was 8.8 days, only one-tenth the calculated value. So the efficient volume actually amounted to a mere 1750 m^3.

PYLE et al. (1979) introduced bacteria and phages T4 and PhiX174 into the outflow of a landfill in the Netherlands. The T4 phages and bacteria were still detectable after a distance of 920 m, while the PhiX174 phages only reached 140 m. The speed of travel was very high, about 300 m/day.

2.8.8 *Natural distribution of phages*

Not only is the diversity of phage habitats great, but the number of viral particles found in some samples is often quite impressive. BØRSHEIM'S comprehensive review (1993) of research on the ecology of viruses and bacteriophages since 1979 shows that concentrations of viral particles in sea and fresh water varies from 10^3 to 10^7 per ml (BERGH et al. 1989, BRATBAK et al. 1990). It may even reach $4.6 \cdot 10^8$. This absolute record was measured far out at sea (Gulf Stream).

Obviously an important part of these particles are viruses of eucaryotic cells (algae, protozoa, fish etc.). Counts of phage particles, as opposed to bacteriophages only, are done by electron microscopy. Inactivated phages are therefore also counted with this method.

In seawater, the biomass of viral particles is estimated at 0.27 mg C/l. That of bacteria reaches 2-40 mg C/l. The half-life of the viruses is about 1.3-2 hours (BØRSHEIM 1993). This means that the turnover of viral and bacterial populations is very rapid. Bacteriophages, though they form but a small fraction of the total biomass, certainly play an important role in the regulation of the various bacterial populations and in the exchanges of genetic material (BRATBAK et al. 1990, WOMMACK et al. 1992).

Habitats of bacteriophages (from ACKERMANN & DUBOW, 1987)

Water	Surface water	Lakes, ponds, streams, cisterns, drinking waters, hot springs, irrigation channels, salt ponds, lagoons
	Seawater	Brackish water, deep sea, coastal sediments, tidal ponds
	Sewage	Raw or chlorinated, activated sludge
Soil	Types	Arable, clay, compost, forest, moor, mud and silt, podzol rhizosphere, sand
Air		Droplets, dust particles
Plants	Organs	Buds, leaves, nodules (leguminous plants), rotting fruit, roots, seeds
Animals	Species	Healthy or diseased humans, ass, bee, cattle, chicken, crab, earthworm, squirrels, horse, mouse, pig, rabbit, turkey, water buffalo, various fish, mosquitoes, mussels
Food	Dairy products	Raw and skim milk, butter, cheeses (cheddar, cottage), cheese starter (Bel Paese, Emmental), yoghurt
	Meat, fish	Chicken, beef, salami, steaks, fish fillets, fish sauce
	Other	Lactic acid beverage, oysters, sake starter, wine.

2.8.9 *Types of phage species*

A short review of phages species which have been used as tracers follows. At the end of the list a few vertebrate viruses that have also been used as tracers are described.

F2:
This phage was widely used as a tracer until the middle of the eighties, because it resembles the enteroviruses in size and morphology. It is less sorptive than animal viruses and survives longer than enteroviruses in sewage (WANG & GERBA 1980).
- Tracer in waters for an irrigation field (SCHAUB & SORBER 1977)
- Tracer in sewage infiltration tests (BROWN et al. 1979)
- Pore groundwater tracing (ALTHAUS & JUNG 1983, 1985)
- Karstic water tracing (ALTHAUS et al. 1986)

MS2:
According to the conclusions of YATES et al. (1985), this phage is at least as resistant as an enterovirus and should therefore be an adequate model for animal viruses. Its behaviour during transport is mainly influenced by temperature and less so from pH, ammonium concentration, hardness, nitrate or other transported substances. In this respect, it seems to show better qualities than phage F2.
- Transport in porous media (BALES et al. 1993)
- Complexation experiments in soils (BIXBY & O'BRIEN 1979)

F46:
- Tracing in rivers (KINNUNEN 1978)

F52:
- Tracing tests in rivers (KINNUNEN 1978)
- Tracing tests in a pore groundwater model (KINNUNEN et al. 1974)
- Influence of solar radiation (NIEMI 1976)

F137:
- Tracing tests in rivers (KINNUNEN 1978)
- Observation of the growth of a phage culture (KINNUNEN 1978)
- Tracing in a pore groundwater model (KINNUNEN 1978)

H40/1, H4/4, H6/1:
Marine bacteriophages:
- Numerous water tracing experiments in rivers and in porous and karstic environments (ROSSI 1994)

Phage of Escherichia coli, strain K12:
- Tracing in rivers (WIMPENNY et al. 1972)
- Karst water tracing during a pumping test (SKILTON & WHEELER 1988)

Phage of Serratia marcescens:
- Karst water tracing during a pumping test (SKILTON & WHEELER 1988)

Phage of Enterobacter cloacae:
- Karst water tracing during a pumping test (SKILTON & WHEELER 1988)

P22H5: phage of Salmonella typhimurium, strain LT-2 (TL747):

– Karst water tracing (BRICELJ et al. 1986, BRICELJ 1988)

PhiX174:
– Marking of landfill leachate (PYLE et al. 1979)
– Tracing in pore groundwater (this book)

T2:
– Experiments on the effect of pH (SPROUL 1972)

T4:
– Karst water tracing (FLETCHER & MYERS 1974)
– Marking of landfill leachate (NOONAN and McNABB 1979)
– Tracing in pore groundwater (this book)

T7:
– Tracing in a pore groundwater model (KINNUNEN 1974)
– Effect of solar radiation (NIEMI 1976)
– River tracings (KINNUNEN 1978)
– Karst water tracing (ARAGNO & MÜLLER 1982)

Type 2 phage of Aerobacter aerogenes 243:
– Cleft water tracing (MARTIN & THOMAS 1974)

Wild phage of Aerobacter aerogenes, strain NEU 1022 VM1:
– Karst water tracing (ARAGNO & MÜLLER 1984, FLURY 1984)

Wild phage NEU-P1 of Pseudomonas fluorescens:
– Karst water tracing (ARAGNO & MÜLLER 1982)

Wild phage Kanata G:
– Karst water tracing (ALTHAUS et al. 1986)

Viruses

Nonpathogenic polio viruses (MARTI et al. 1979)

Bovine enteric viruses Type 1 (SCANDURA & SOBSEY 1981):
– Tracing tests in rivers

Polio viruses Type 1 LSc (STRAMER & CLIVER 1981)

Polio viruses Type II (SCHUBERT & SCHÄFER 1971):
– Tracing tests in rivers

2.8.10 *Evaluation of phages as tracers*

ARAGNO and MÜLLER (1982) pointed out the merits of tracing with phages and stressed the simplicity, cost-effectiveness, invisibility, and harmlessness of the phages compared to other tracers. However, it must be remembered that there is a considerable amount of work involved both in the preparation of the tracing tests and in the examination of the samples. Only microbiological laboratories are competent enough to conduct such tracing tests. Furthermore, the samples must sometimes undergo special treatment to be transported or stored. These difficulties naturally limit the number of samples that can be examined.

Difficulties also arise from the fact that phages tend to adsorb onto solid surfaces. Of course, these sorptive properties vary among the different phage types. In standing bodies of water, this property is not important. Thus, phages remain the preferred tracers in lakes and seas. However, even in karsts with comparatively low surface contact possibilities, extensive losses can be expected when tracing with phages, as was seen in the tracing test in the Peloponnesus in 1984.

In contrast to the fluorescent dyes and some salt tracers, phages cannot be measured directly. Examination results can be obtained at the earliest 24 hours after the sample has been delivered to the examining laboratory.

2.9 GEOBOMBS

W.Käss

A special kind of drift tracer is the sound wave producing floating body, the 'geobomb' = 'Opasno eksplosiv'. It was developed in Yugoslavia to investigate wide-open karst cavities with a steady water flow (ARANDJELOVIC 1977).

The geobomb was first used in May 1970. It consists of a plastic sphere with a diameter of 10-15 cm. One hemisphere is filled with plastic explosives (up to 930 g) and the other with air. In the air hemisphere there is also a delayed time-fuse, up to seven hours, a battery, and the detonator (Fig. 114). The bomb is balanced so that it floats (MILANOVIC 1972).

Several bombs are used at once in the karst water flow, with graduated detonation times. The sound waves that result from the explosion are registered with a network

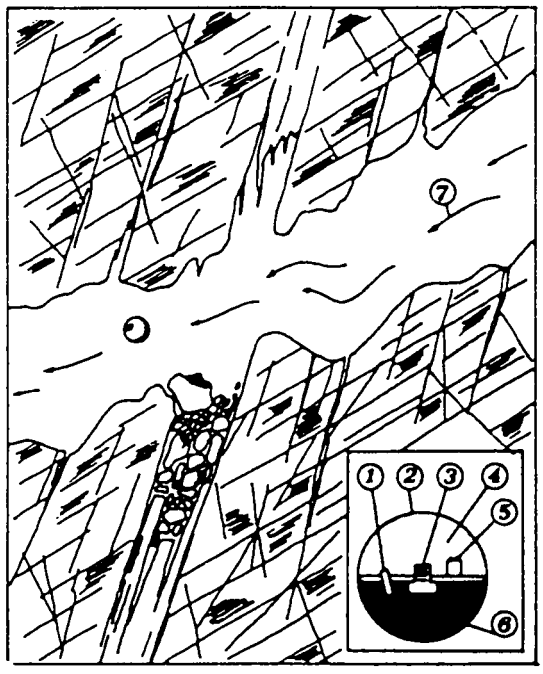

Figure 114. The geobomb (from MILANOVIC 1972). 1 = detonator cap, 2 = plastic sphere, 3 = time fuse, 4 = empty cavity, 5 = battery, 6 = explosives, 7 = flow paths in karst channels.

of geophones on the surface. Special calculation methods allow a three-dimensional determination of the explosion sites and thus the path of the karst channels.

Another method, which employs underground sound waves to follow karst channels, was often used by W.A. SCHNITZER (1967a, 1972) in the Franconian Alb (Southern Germany). This method does not belong per se to the drift tracers like the geobomb, but because of its similarity, the SCHNITZER method is included here also.

Already in 1912, TIMEUS suspected the possibility of investigating karst channels with sound waves and underwater microphones. He referred to a note in the magazine Nature (1908), in which an anonymous author reported about a Norwegian method, in which different types of schools of fish can be located by using a water proof tele-microphone underwater to detect the different sounds (Anonymous 1908).

SCHNITZER used 1-3 cartridges of Ammon-Gelite 1,2,3 to create sound waves in doline openings and recorded the underwater sound impulses with a portable recorder in the surrounding karst springs. An oscillograph was used to play back the impulses. He found that only those springs transmitted the sound waves, which were also reemergence sites for tracers injected in the same doline. It can be concluded then, that the pressure waves primarily propagate through the water-filled cavities. A prerequisite for such tests is to carefully dam up the doline, to assure that as much as possible of the pressure wave energy is transmitted into the karst cavities. Furthermore, the range of the underwater sound impulses is reached where the underground and surrounding noise drown out the impulses. According to the existing data, the range is ca. 6 km.

Unfortunately, these tests were not continued. It is certain that it would have been possible to easily carry out flow time measurements. Even with the usual provisions used in geophysics, underground and surrounding noise disturbances can be suppressed to a large extent.

2.10 OTHER DRIFT PARTICLES

W.Käss

Different kinds of drifting particles were the first substances to be used as tracers to investigate the underground connections of waterways. Initially, particles that could be had in large quantities were used. As described in Section 1.1, the first report of a tracing test with *chaff* came from the beginning of the Christian era (JOSEPHUS FLAVIUS). The results of this tracing test at the source of the Jordan are uncertain. Undoubtedly positive results with chaff were achieved by the priest M.J. MAYER in the Blautopf catchment in the Swabian Alb (MAYER 1681). In the Crailsheim Chronicle from LAUBER in the year 1736, it was reported that downstream of the city near the Helden mill, the Jagst loses its water, that it probably 'wanders to the Pühler river in the environment of Schwäbisch Hall (Hällisches Land). Chaff was also put inside it and all came again to daylight'. As a matter of fact, ZANDER (1973) was able to prove an underground connection between the river region of the Jagst and the Bühler in 1972. He dyed the Kreuzbach percolation a scant 1 km north of the Helden mill. The coloured water cut under the course of the Jagst and appeared a crow fly distance of 15.9 km away, in the karst springs of the Muschelkalk near Neubronn in the Bühler valley.

Great efforts were carried out in the Triestine Karst, to investigate the whereabouts of the Notranjska Reka. It was already suggested by PLINIUS, STRABO, and VERGIL, that the Timavo stems from the percolating water of the Reka. Several tests with *floating bodies*, which were put into the percolating Reka near San Cozian there failed. In these ancient manuscripts, what kind of floating body used, was not always recorded. In the sixteenth century, the Padre IMPERATI from the castle Duino tried using 'floating bodies' and *'exotic seeds'* (IMPERATI 1605). The chronicles of the engineer Pietro NOBILE hint at further such tests having been carried out. Between 1880 and 1882, the engineer GRABLOVIC conducted tests with 'gallegianti zavorrati,' i.e. with burdened down bodies as floating drift particles. In 1884, the 'società alpina delle Giulie' carried out a test with 3000 floating particles (TIMEUS 1910). Instead of chaff, *bits of straw* have also been injected (BOEGAN 1906). It was not until the turn of the year 1907/1908 that TIMEUS was able to prove the connection between the Reka and Timavo with lithium chloride (TIMEUS 1928).

In the following, drift particles which are used now and again are described. They are not listed in any order of importance. In fact, some particles are only listed to assure completeness, rather than due to their usefulness as a tracer. Some of the described drift particles are rather odd and something of a curiosity.

Sawdust, wood flour

BOEGAN mentioned in 1906, that sawdust had already been used to try and prove the connection between the percolating Reka and the mouth of the Timavo. TIMEUS (1926) spoke of hardwood sawdust in connection with this. MAURIN and ZÖTL came to the conclusion in 1959, that sawdust is an unsuitable tracer, after they carried out a tracing test in the Lur cave system with 15 kg of sawdust dyed blue and 10 kg of sawdust dyed red.

Wooden beads, wooden rods

After the failed tracing test from 1884 with 3000 wooden beads in the Reka percolation, KYRLE carried out drift tracing tests in February of 1927 into the Lurbach sinkhole with 1-1.5 cm in diameter softwood beads and with wooden rods, together approx. 1000 particles, also without success (KYRLE 1928).

Plastic rods

In 1963, DUNN described drift particles made of polypropylene. They were 2 mm thick and 25 mm long. Their use is very simple. They are poured into the sinkholes and at the reermergence sites they are caught with sieves and counted by hand.

Balls (SCHUDEL 1991)

Along with uranine, tennis and table tennis balls were used in Basel in a 1800 m long sewage canal between the Dreirosen bridge and the sewage treatment plant. The balls arrived faster than the uranine at the plant, since they float in the quicker flowing streamline.

Cork shavings, cork beads

KYRLE (1928) also used 5 kg of cork shavings in the Lurbach swallowhole in 1927. He could only follow them for 20 m, before they disappeared in the left swallowhole.

It is astonishing that in spite of these failures, that such light floating substances are considered at all.

Near Adelsberg, SCHMIDL (1854) threw 250 cork beads into the Poik, 'of which not a single one appeared in either of the arms in the cave of Planina. Neither did appear the ox bladder nor the cork stoppers, which were put onto quills. They must have been stopped by the rock walls which hang down like curtains under the water level inside the cave'.

Granulated plastics (MAURIN & ZÖTL 1959)
Granulated plastic, Type Vestyron N from the Chemical Company Hüls AG in Marl, Nordrhein-Westfalen/FRG, has been tried as a tracer in karst waters several times:

Feliferhof swallowhole southwest of Graz/Austria on 20 May 1958 with 10 kg granulated plastic together with *Lycopodium*-spores, diatomaceous earth, starch, and *S.marcescens*. The granulated plastic first reappeared after 33 hours in the Bründl spring, 800 m away, and after 42 hours as the peak reappearance together with spores and diatoms (Fig. 89).
Lurbach swallowhole north of Graz/Austria on 13 April 1959 with 25 kg of granulated plastic together with undyed *Lycopodium*-spores, diatomaceous earth, and blue dyed sawdust (Fig. 58). Between 15 and 17 April, the spores were detected in the Hammerbach, none of the other tracers however.
Dachstein massif-north rim. The same swallowhole that was successfully traced with blue dyed spores over a distance of 4500 m in 1957 (BAUER 1958), was used for an injection of granulated plastic and diatoms (Fig. 90); however, the already proven connection could not be verified.

The examination for the granulated plastic is done together with spores and diatoms in the samples from the plankton nets. Granulated plastic can only be used over short distances where positive results are expected.

ATKINSON et al. (1973) also traced with granulated plastic in an English karst region without success. They injected a swallowhole, which had a percolation flow of 49 l/s, with pyranine, lithium acetate, 1.5 kg green dyed spores, and 1.5 kg blue polyethylene granulated powder. In the karst spring located 1.1 km away, St.Dunstans Well, the pyranine and spores were detected, but the plastic and lithium not. The authors concluded that the reason for the negative yield for the plastic lay in the lower density of 0.96 as compared to water.

Diatoms (MAURIN & ZÖTL 1959)
Diatoms, like the granulated plastic, have been used with little success in drift tracing tests in the Styrian Karst:

Feliferhof swallowhole southwest of Graz/Austria (Fig. 89). On 20 May 1958 along with other drift tracers, 10 kg of diatomaceous earth was injected. The first detection and major breakthrough in the Bründl spring happened analogous to the granulated plastic after 33 and 42 hours.
Lurbach swallowhole north of Graz/Austria. The injection was completed just like first tracing test as a comparison with different drift materials to test their suitability as tracers in karsts. On 13 April 1959, 12 kg of diatomaceous earth was injected with other tracers. Whereas from 15-17 April, the undyed spores reappeared in the 3100 m away Hammerbach near Peggau, the diatoms were not detected.
Dachstein massif north rim. As described above, diatomaceous earth was also injected in the tracing test with the granulated plastic. Just as the granulated plastic was not detected, the diatoms

were also not detected in the major reappearance site 4.5 km away, although the spores had previously proven the flow path.

The examination for diatoms is done in the same way as for spores and granulated plastic, i.e. with plankton nets and with a stereo microscope. It can be concluded from these tests that diatoms can be used as a tracer at the most in short flow paths in karst.

Confetti

In 1903, MARBOUTIN (1904) conducted tracing tests in a tributary of the Loiret near Dhuy/Dpt. Loiret with 1 kg of red confetti together with starch, salt, and uranine (VAN DEN BROECK 1904). The confetti reached the first observation station, located at a flow distance of 650 m away, after 6¾ hours and then reached the second station at 1150 m after 9¾ hours. Compared to the salt and dye, this was a delay of 1¼ hours.

Starch

With more or less success, 5 kg of starch has also been used as a tracer. In the test by MARBOUTIN described above, the starch only reached the first station with a flow distance of 650 m; no starch was detected at the second station at 1150 m.

In the typhoid region in the Furler valley south of Lausen near Liestal, Canton Baselland/Switzerland, it was sought to verify the hydrological connection between the Furlerbach and the springs used for the Lausen water supply. After a salt tracing test had positive results, 50 pounds (25 kg) of flour were 'well stirred up' and injected in a swallowhole (Fig. 2). The Lausen springs, which had shown a 'very strong chlorine reaction', did not show the 'slightest trace of starch' (HÄGLER 1873).

MAYR (1954a) recommended using low-priced starch in water tracing tests with short flow paths. According to his study, the starch is easily detected with iodine solution in the filtered or centrifuged sample. Thus treated, the starch turns an intense blue colour. However, at longer flow distances, the heavier starch grains would settle.

In the same test site in the Offensee area, where MAYR conducted his first drift tracing test with *Lycopodium*-spores (Section 2.5.1), he tried to repeat the test (1954b) with potato starch. On 28 March 1954, he mixed '10 dkg' = 1 kg starch powder in a pot and injected the suspension between 10:45 and 10:50 in the swallowhole downstream of the small waterfall in the Gimbach. Already in 1950 it had been proven through salt tests and in 1953 through spore drift tests, that in dry periods, the completely percolated Gimbach water reappears in a spring group 180 m downstream on the left shore. He did not examine the samples taken there by treating with iodine solution, as he recommended, but rather under a polarization microscope at 50× magnification. Unfortunately, he did not report any particulars as to the volume of the centrifuged samples which were put on the slide glass:

Time	Starch grains	Time	Starch grains
10:30	0	11:30	207
11:00	0	11:45	293
11:15	4	12:00	115

Time	Starch grains	Time	Starch grains
12:15	97	13:00	20
12:30	33	13:15	7
12:45	28		

In the combined drift test in the Buchkogel region in May 1958, together with other drift tracers, 3 kg of untreated potato starch and 5 kg orange dyed and treated against swelling potato starch were injected in the Feliferhof swallowhole. Starch grains were not detected in any of the samples taken from the plankton nets placed in the Bründl spring (MAURIN & ZÖTL 1959).

Starch grains vary in size and form, according to their origin. Potato starch has grains with diameters up to 100 µm, rice starch however, only a few µm (WALTHER 1947). Starch that is treated against swelling could be used to determine the pore space of an aquifer. Starch can be detected by membrane filtration and dyeing with iodine-potassium iodide solution as well as under the polarization microscope.

Grass seeds

Drift particles such as grass seeds can travel through wide joints in rocks, as was observed by MATTHESS and SCHMITT (1967) in the Odenwald Bunter sandstone. The shoulder of a new road was sown with grass seeds in the fall. Following heavy rains, part of the grass seeds arrived via swallowholes in the roadside ditches in the underground and were found in the spring of 1969 in a spring 350 m away and ca. 80 m difference in altitude (Fig. 115). Furthermore, the same spring carried muddy water after heavy rains.

Tellurium Oxide (GROCHE 1964)

GROCHE describes an elegant procedure, to trace a water body at every point at any time. Electrically conductive tellurium metal beads with diameters of 2-5 mm are hung as anodes in the water. If a voltage between 12 and 20 V is applied, the tellurium oxidizes to tellurium oxide, which is given off to the water as black clouds. The intensity of the tellurium oxide release depends on the metal surface and the amperage, which should be between 10-100 mA. Due to the high density of 5.67, the tellurium oxide settles gradually. GROCHE used this procedure to investigate currents in sewage treatment plants.

Aluminium Powder (BÜHRER & AMBÜHL 1975)

The authors traced sewage water plumes in the bay of Hergiswil in the Vierwaldstätter Lake with aluminium powder and followed it with an ultrasound sonic depth finder.

Yeast

Synonyms: *Saccharomyces cerevisiae*, Faex medicinalis, brewer's yeast, baker's yeast.

The first indication that yeast could be used as a tracer came from MIQUEL (1901). He obtained good results in the Cretaceous karst in the Avre and Vanne regions (Picardie/Northern France). There, up to 40 kg of yeast from breweries were diluted

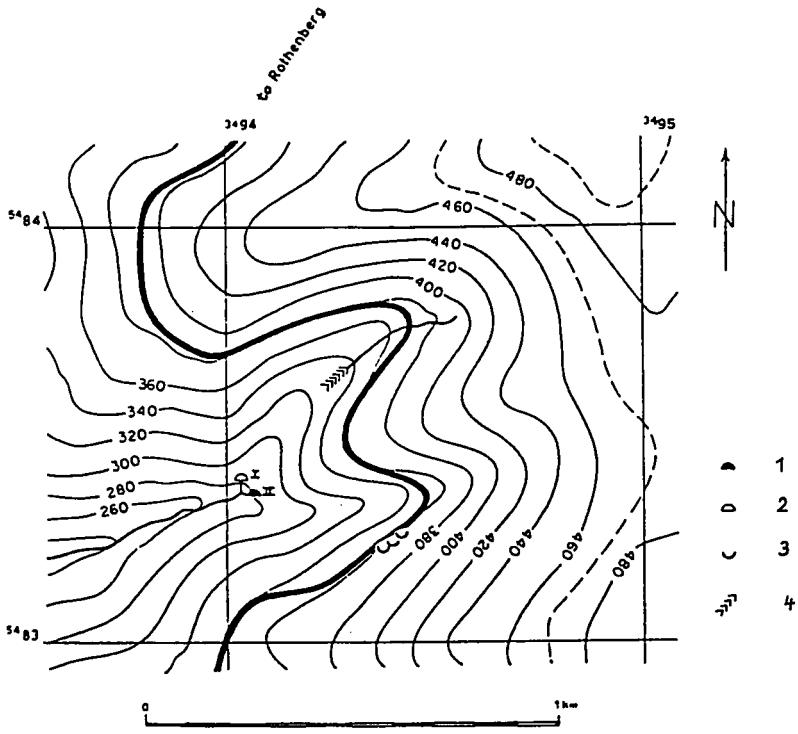

Figure 115. Tracing test in the Bunter sandstone. Since the percolation stretch of the stream below the road was dyed, only the spring I was involved. Grass seeds, which were sown above the road (at the numbers of contour line 380), reappeared after heavy rains in the spring II (from MATTHESS & SCHMITT 1967). 1= Spring, captured, 2 = spring, not captured, 3 = sink holes, 4 = percolation.

10 to 20 fold and injected in the underground. The yeast was detected in springs and wells over distances between 10 and 15 km. MIQUEL also observed that the yeast cells survived in water pipes for over two months and at distances of over 100 km. MIQUEL tested for yeast thus: The freshly taken water samples are poured into small flasks and an acidic peptone-sugar-bouillon (200 g saccharose + 1 g tartaric acid + some potassium bitartrate) added and kept at 25°C. If yeast is present, after 24 and 48 hours spots or colonies of *S.cerevisiae* will form on the flask bottom under heavy alcohol formation. If this procedure is followed, any lactic acid bacteria possibly present will not develop until later, they can however overgrow the whole bouillon.

DIENERT (1912) gives a more detailed description for using *S.cerevisiae* as a water tracer. He proposes stirring press-yeast into a 1% sugar solution and then fermenting for a ½ hour. He also reported that in comparison to uranine, approx. five times the amount of yeast is needed. The water samples taken should be kept and transported ice-cold. 100 ml bouillon is added to 100 ml sample water. The bouillon is made thus: 20 g peptone, 400 g sugar, 3 g tartaric acid are dissolved in 1 l water. A positive result is given if yeast cells collect on the bottom. The identification is completed either by distillation after LIEBIG for examining with alcohol or by yeast cell isolation. The second method is carried out by taking a sample of the bottom deposit with

a platinum loop and adding to 10 ml of a nutrient solution, made by dissolving 20 g peptone, 200 g sugar, 0.5 g tartaric acid, and 0.5 g potassium bitartrate in 1 l water. After 48 hours, the solution is decanted, the deposit washed twice and spread on a Petri dish covered with nutrient gel. If *S.cerevisiae* are present, a daily increasing sporulation occurs.

GÄRTNER (1915) suggests the following procedure for determining the fermentation efficiency of sugar: 100 ml of nutrient solution are added to a fermentation test tube containing 50 ml of sample water. One litre of the nutrient solution contains 40 g sugar, some tartaric acid, 5 g NaCl, 2 g K_2HPO_4 and 2 g $MgSO_4$. If yeast cells are present, CO_2 will form abundantly in the incubator.

The tests conducted by KISSKALT and KNORR (1930) in the Munich Municipal Waterworks tunnels in the glacial deposits were negative, although the potholes, through which the rainwater drained off and which were filled with 15 kg brewer's yeast, were only 43 m above the tunnels and 20 m to the side of them. Another test using *S.marcescens* was negative. However, other tracing tests using salt and uranine were positive. The potholes were therefore filled in and the inflowing water, essentially meltwater from the snow was channelled off with cement.

WOOD and EHRLICH (1978) found, that yeast, due to its ease in use and the negligible background, is an excellent tracer, compared to other microbiological bodies. Although they established in column tests that yeast had a delayed reappearance as compared to the sodium chloride solution, they were also able to quantitatively count the yeast that filtered through by using membrane filters. The membrane filters were placed on pads soaked with a yeast-malt-nutrient solution and incubated for 36 hours at 30°C.

The yeast colonies which form can be counted under low magnification (Fig. 86). It was determined in two field tests, each with an injection of 45 l of a water suspension containing 16 kg of yeast, and under a pump rate of 0.2 l/min, that large amounts of the yeast could flow up to 7.6 m through the gravel layers. Furthermore, the yeast arrived at the sampling site before the halogen ions chloride, bromide, and iodide, which had also been injected. WOOD and EHRLICH believe that the flow behaviour of yeast is comparable to bacteria and that when evaluating the permeability of certain undergrounds, yeast tracing tests are preferable to other tracing tests.

River water contains a substantial background of common yeast cells. Thus, WIMPENNY et al. (1972) suggested using other yeast cells. They used two pigment forming yeast types, that were isolated in 1967 from the Usk river (Wales/West England): *Hansenula* sp. *(cf. H.silvicola)* with pink and *Rhodotorula glutinis (cf. var.rubescens)* with red pigment formation. Before the tracing test was carried out in the Taff river (Wales), which is known for its pollution – the river flows through the Welsh coal mining district – background samples were taken which contained per ml only 0-50 whitish yeast colonies, however no pigment forming ones. Above Cardiff, a 2930 m long river section was injected with $1.4 \cdot 10^{13}$ pink yeast cells and 10^{13}-10^{14} red yeast cells, each in 3-l-suspension. At the sampling site, both yeast types showed good and similar breakthroughs:

First appearance after ca. 55 minutes,
maximum after ca. 68 minutes,
end of the breakthrough after ca. 85 minutes.

At both maxima, ca. 100 cells were present per ml. The breakthough was similar for the simultaneously injected bacterium *S.marcescens* (see Section 2.7). The samples were collected in 25-ml-sterile-bottles and examined thus:

Nutrient medium A:	Tryptone soy broth (Oxoid CM_{129})	30 g
	Oxoid Agar Nr.3 (L13)	20 g
	NaCl	10 g
	Water	500 ml
	Sterilized 20 min. at 1 bar	
Nutrient medium B:	Cane sugar	200 g
	Water	500 ml
	Sterilized 10 min. at 0.7 bar	

To be used, both solutions are mixed without letting gas bubbles form and brought with 20% sulphuric acid to a pH of 3.6. The surviving yeast cells can be, if necessary after appropriate dilution with sterile salt solution, grown in this nutrient solution and counted.

The preparation of the injection mass is completed using Tryptone-Soy-Nutrient solution with 1 volume-% glucose. The yeast count increases after 4 to 14 days in sterile river water as well as in sterile distilled water with 1% salt content.

The 2-3 µm large, oval or egg shaped yeast cells are only suitable under certain conditions as tracers. In karst channels, yeast cells can be used at the best as a secondary tracer. The tests from WOOD and EHRLICH in pore groundwater were carried out over comparatively short distances. WIMPENNY and his co-workers hold pigment forming yeast cells for one of the best available tracers for tracing polluted rivers. According to KESWICK et al. (1982a), the survival rate of yeast cells is dependent upon nutrient supply.

Preliminary samples are necessary in any case in tracing tests with yeast, to determine a possible natural background level. The samples collected should be transported as quickly as possible for the microbiological examination in the laboratory.

Marked eels

A remarkable test was carried out by SELLA (1929) in Triestine karst near the Reka percolation: A large number of eels were marked by cutting notches in their dorsal and tail fins, then they were released in the underground course of the Reka near San Cozian. Of the 494 marked eels, 29 of them were caught at the Timavo springs during the observation period of 38-367 days (WAGNER 1954, MOSETTI et al. 1963).

2.11 ENVIRONMENTAL ISOTOPES

H.Moser[1]

2.11.1 *Introduction*

Intentional water tracing tests in the hydrological system using those tracers listed in

[1] The author would like to thank W. DROST, Dr. K. FRÖLICH, Dr. W. GRAF, Dr. P. MALOSZEWSKI, W. STICHLER and Dr. S. WEISE for their critical review of this article and H. Rast for model calculations and preparation of the figures.

Sections 2.1-2.10 have the great advantage that they can be spatially, temporally, and proportionally (with respect to the quantity of tracer used) optimized with regard to the investigation goal. On the other hand, disadvantageous are the necessary temporal and spatial limits due to investigative techniques and groundwater protection: Observation periods lasting over several months are in general impracticable and a distribution of the tracer in large volumes of water (over 10^8 m^3) requires large injection amounts of the tracer. This is not only hard to manage, it is also often impossible to inject such a large quantity of tracer without disturbing the flow system and the ecology. Furthermore, intentional tracing tests generally only provide a 'momentary picture' of the hydrological system at the time of the test.

Compared to conventional tracers, natural tracers allow a much larger temporal and spatial scale. Thereby, knowledge of the temporal and spatial variability of the hydrological system under investigation can be won, which facilitates an optimal planning of intentional tracer tests.

As natural water tracers, the chemical characteristics of the water body (see Section 2.12) itself can be exploited. However, only in certain cases do the chemical components of the water act as conservative tracers; most of the time interaction occurs with e.g. the rocks in the aquifer. This provides information as to the origin and transport of the water, yet does not contribute to the knowledge of the hydraulic relationships.

Further natural tracers are the different isotopic compositions of the water molecule itself and those water constituents that have no or only very specific chemical interactions.

Table 20 lists these so-called environmental isotopes, as far as they are used today in hydrological investigations. In the group of isotope species of the water molecule, which do not chemically differ from isotopic 'normal' water ($^1H_2{}^{16}O$)[2], are the stable

Table 20. Environmental isotopes used as hydrological tracers.

Isotope	Main chemical compound in water	Half-life time (years)	Approximate isotope relationship in recharged groundwater	
^2H	$^2H^1HO$	Stable	$(9\text{-}17) \cdot 10^{-5}$	$^2H/^1H$
^{18}O	$H_2{}^{18}O$	Stable	$(188\text{-}202) \cdot 10^{-5}$	$^{18}O/^{16}O$
^3H	$^3H^1HO$	12.43	$10^{-16}\text{-}10^{-17}$	$^3H/H$ [1]
^3He	Dissolved noble gas	Stable	$1.4 \cdot 10^{-6}$	$^3He/^4He$
^4He	Dissolved noble gas	Stable		
^{39}Ar	Dissolved noble gas	269	10^{-15}	$^{39}Ar/Ar$
^{85}Kr	Dissolved noble gas	10.76	$6 \cdot 10^{-12}$	$^{85}Kr/Kr$ [3]
^{36}Cl	$^{36}Cl^-$	$3.01 \cdot 10^5$	$2 \cdot 10^{-12}$	$^{36}Cl/Cl$ [1]
^{13}C	$^{13}CO_2$, $H^{13}CO_3^-$	Stable	$1.1 \cdot 10^{-2}$	$^{13}C/^{12}C$
^{14}C	$^{14}CO_2$, $H^{14}CO_3^-$	5730	$1.2 \cdot 10^{-12}$	$^{14}C/^{12}C$ [1]
^{34}S	$^{34}SO_4^{2-}$	Stable	$4.2 \cdot 10^{-2}$	$^{34}S/^{32}S$
^{15}N	NO_3^-	Stable	$3.7 \cdot 10^{-3}$	$^{15}N/^{14}N$
^{234}U	U^{6+}	$2.47 \cdot 10^5$	$5 \cdot 10^{-3}$	$^{234}U/U$ [2]

[1] Anthropogenically influenced, varies temporally and spatially, [2] The ratio of the terrestrial isotopic activities of ^{234}U and ^{238}U is between 0.5 and 12. [3] Increasingly anthropogenically produced.

[2] Isotopes are characterized by their atomic number, placed at the left top of the element symbol.

isotopes deuterium (^{2}H) and oxygen-18 (^{18}O) and the radioactive tritium (^{3}H). Helium-3 (^{3}He), helium-4 (^{4}He), argon-39 (^{39}Ar), and krypton-85 (^{85}Kr) are present in groundwater as dissolved, chemically inert noble gases. Chlorine-36 (^{36}Cl) as a dissolved anion also reacts very little with the rocks (see Section 2.2). Only carbon-14 (^{14}C) and carbon-13 (^{13}C), which are present in the groundwater as dissolved CO_2 and bicarbonate-ion, are chemically seen problematic tracers (see Section 2.11.2.4). The isotopes sulphur-34 (^{34}S) and nitrogen-15 (^{15}N) have a special status, since they are essentially used to clarify the origin of these elements in water and therefore have only limited use as hydrological tracers (see Section 2.11.2.6). The relationship between the uranium isotopes uranium-234 and uranium-238 (^{234}U/^{238}U) in the groundwater can provide insight as to the hydrological development of the aquifer. This can be applied to determine hydrochronological classification of the groundwater system (OSMOND 1980, IVANOVICH & HARMON 1992), which is not covered here however.

The following contains a short review of the basics in hydrological environmental isotope applications, with special attention given to combining the use of environmental isotopes with tracing tests. For measurement techniques and methodical details, refer to summarizing publications from the more than thirty years of research in this field, e.g. MOSER & RAUERT 1980, GAT & GONFIANTINI 1981, IAEA 1983a, FRITZ & FONTES 1980,1986, FABER et al. 1985 as well as conference proceedings, especially those from the International Atomic Energy Agency, (IAEA, 1967, 1970, 1974, 1979, 1984, 1987, 1992a, 1993). The application and evaluation examples of measuring environmental isotope contents given in section five of this book were chosen so that the possibility of combining them with conventional tracing tests would be obvious.

2.11.2 *Detection, occurrence, and behaviour of environmental isotopes presently applied in hydrological investigations of the water cycle*

Table 20 clearly shows, that the listed isotopes occur in natural waters in very low concentrations or concentration ranges; the detection of the radioactive isotopes is only possible with the specialized 'Low-Level-Measuring-Technique', of the stable isotopes using mass-spectrometric precision isotope relationship measurements. The geostatistical validation of the results also requires a sample turnover as large as possible. These prerequisites can only be fulfilled by laboratories with appropriate personnel that specialize in such measurements. The cost of the analyses varies according to the required accuracy for each isotope. However, it is in the general order of the cost for the chemical analysis for the determination of the water contents.

The distribution of the different isotope species in water and its contents is determined by the different processes in the water cycle. Variations in the isotope content in water are the result of input from the atmosphere or the lithosphere, due to internal exchange processes, and transport phenomena as well as due to biological activity. For hydrological tracer applications, knowledge as exact as possible of the occurrence and behaviour of the environmental isotopes in the water cycle is a prerequisite. The state of the knowledge concerning each isotope varies greatly.

2.11.2.1 *Deuterium (^{2}H) and Oxygen-18 (^{18}O)*

In natural waters and in atmospheric water vapour, there are approximately 2000

$^1H_2{}^{18}O$-molecules and 320 $^2H^1H^{16}O$-molecules among 10^6 $^1H_2{}^{16}O$-molecules. The main reason for the given range in concentration listed in Table 20 for each isotope species of the water molecule is, that the water vapour pressure of the isotopically 'lighter' water (e.g. $^1H_2{}^{16}O$) is higher than for water with the 'heavy' isotopes ^2H and ^{18}O. As a result, at all phase transitions, e.g. evaporation, condensation, and also with solution and exchange processes, isotopic fractionation occurs, i.e. the isotope content changes.

Due to the temperature dependency of the vapour pressure, isotopic fractionation is also a function of the temperature. It can also be dependent upon the salinity of the water body due to the different bonds of the isotopic species of the water molecule in the ionic hydratation phase. Fractionation varies according to whether the phase system is in thermodynamic equilibrium or not. This is important especially for rapid evaporation processes.

The following effects in the water cycle are the essential results: a) During evaporation, there is a ^2H and ^{18}O enrichment of the water, during condensation, they are depleted in the water vapour. In contrast, during freezing, there is a heavy-isotope depletion in the liquid phase; b) Under otherwise identical conditions, isotopic fractionation increases with decreasing temperature; c) The ratio of the ^2H-content to the ^{18}O-content is influenced by thermodynamic processes during phase transition; in particular, with increasing evaporation rate, there is a stronger enrichment of ^{18}O in comparison with ^2H. Under certain circumstances, e.g. at high temperatures, this ratio can also shift due to specific isotope exchange, e.g. of ^{18}O with the rock of the aquifer.

These isotopic effects label precipitation in a spatially and temporally characteristic manner. However, this labelling is in its spatial and temporal distribution very complex (see e.g. YURTSEVER & GAT 1981, ROZANSKI et al. 1993): When rain falls out of a moist air mass, there is a steady depletion of the heavy isotopes ^2H and ^{18}O in the precipitation along the trajectories. This 'continental effect' is seasonally and locally dependent. For Europe and North Africa, SONNTAG et al. (1978) published values of ca. –2.5 δ^2H-‰ and –0.3 $\delta^{18}O$-‰[3], respectively, per 100 km trajectory distance from the coast, which however can only be used as rough approximations for regional investigations.

Another depletion of the ^2H- and ^{18}O-contents occurs with increasing amounts of precipitation ('amount effect') and when a moist air mass rises because of an orographic elevation ('altitude effect'). For the amount effect, changes in the ^{18}O-

---

[3] In isotope hydrolgy, instead of expensively determining the absolute isotope contents, generally the measure used for the ^2H- and ^{18}O-contents is the relative difference of the isotope ratio in the sample, R_{Sample}, as compared to the ratio of a standard, $R_{Standard}$, given as the socalled δ-value ($R = {}^2H/{}^1H$ and $^{18}O/^{16}O$, respectively):

$$\delta^2 H \text{ resp.} \delta^{18}O \overset{def}{=} \frac{R_{Sample} - R_{Standard}}{R_{Standard}} \cdot 1000‰,$$

whereby the isotope ratios R_{Sample} and $R_{Standard}$ must be measured under the same conditions. For δ^2H and $\delta^{18}O$, the internationally recognized standard, the socalled 'V-SMOW'-water is distributed by the International Atomic Energy Agency (IAEA), Vienna/Austria. The composition of the V-SMOW matches that of ocean water. Since precipitation usually has a lower ^2H- and ^{18}O-content than ocean water, δ^2H- and $\delta^{18}O$-values from precipitation, surface water, and groundwater are generally negative. Nowadays, routine measurements of water samples with standard commercial machines achieve an accuracy of 1 δ^2H-$^0/_{00}$ and 0.15 $\delta^{18}O$-$^0/_{00}$ (2σ-criterion). This corresponds to a difference in absolute isotope contents of ca. 0.3 ppm ^2H or ^{18}O, resp. Circa 5 ml of sample is needed to measure the ^{18}O-contents; to measure the ^2H-contents, only ca. 0.1 ml are needed.

contents from –1 to –1.5 ‰ per 100 mm monthly precipitation, for the altitude effect, changes from –0.1 to –0.5 ‰ per 100 m altitude increase have been measured, which however can also be only taken as approximations. With the altitude effect, in addition to the increased depletion of the heavy isotopes, the temperature dependency of the isotopic fractionation also plays a role. This also causes seasonal variations in the precipitation of the ^{2}H- and ^{18}O- contents (seasonal effect) (Fig. 116) and a depletion of these isotopes with increasing geographical latitude or decreasing mean yearly temperature, resp. (latitude effect).

For the mean, weighted with the precipitation amount, value of the $\delta^{18}O$-values of the monthly precipitation samples from the world-wide IAEA/WMO precipitation collection network (presently ca. 100 sampling stations, cf. e.g. IAEA 1981, 1983a, 1986, 1990, 1992b, 1994a) there is a dependency from station to station of the ^{18}O-contents upon the respective mean monthly temperature of ca. 0.58 $\delta^{18}O$-‰/K. The seasonal dependency of the ^{18}O-contents upon the temperature, at the same location, lie in the range from 0.17 to 0.66 $\delta^{18}O$-‰/K. For the station Vienna with a measurement time series from 1961-1990 this results in the relationship (0.65 ± 0.05) $\delta^{18}O$-‰/K with $r^2 = 0.36$. However with the same temperature, but different origins of the air masses, considerable differences in the $\delta^{2}H$- and $\delta^{18}O$-values can occur with each single precipitation event, which can lead to differences in the yearly mean of the δ-values. Within single precipitation events, the ^{2}H- and ^{18}O-contents can also vary considerably, due to the isotopic effects during the event.

The world-wide relationship between the $\delta^{2}H$- and $\delta^{18}O$-values has been determined for the long-term mean values, weighted with the precipitation amounts to

$$\delta^{2}H = (8.20 \pm 0.07)\delta^{18}O + (11.27 \pm 0.65)\ ‰\ (r^2 = 0.98,\ n = 205).$$

Regional deviations, especially near the intercept d expressed by the equation $\delta^{2}H = a\ \delta^{18}O + d$ have been observed. Variations in the slope, a, down to values < 8 are essentially caused by evaporation of the precipitation. However, the 'Deuterium excess' $d_D = \delta^{2}H - 8\ \delta^{18}O$, often taken as a measure of the deviation from the above mentioned world-wide $\delta^{2}H - \delta^{18}O$ relationship, cannot be generally used as a measure for this evaporation effect, since it is also determined by the humidity and temperature conditions in the oceanic sources of the precipitation.

2.11.2.2 *Tritium (^{3}H)*

The nuclear weapons tests carried out from 1952 to 1963 were connected with ^{3}H emissions into the atmosphere that were on a much larger scale than natural ^{3}H-contents produced by cosmic radiation with the nuclear reaction $^{14}N(n,^{3}H)^{12}C$. In the atmosphere, ^{3}H is primarily oxidized to water and enters the water cycle as precipitation. Figure 117 shows the temporal course of the monthly mean of the ^{3}H-contents from precipitation samples which are representative for Central Europe. The seasonal variations in the ^{3}H-concentrations with a maximum in early summer and a minimum in early winter are caused by the seasonally dependent exchange processes between the stratospheric ^{3}H-reservoir and the troposphere. It can also be seen from Figure 117 that the ^{3}H-contents in the precipitation has decreased strongly since the moratorium on above surface atom-bomb tests; only slight short-term increases caused by the Chinese and French atom-bomb tests since the second half of the six-

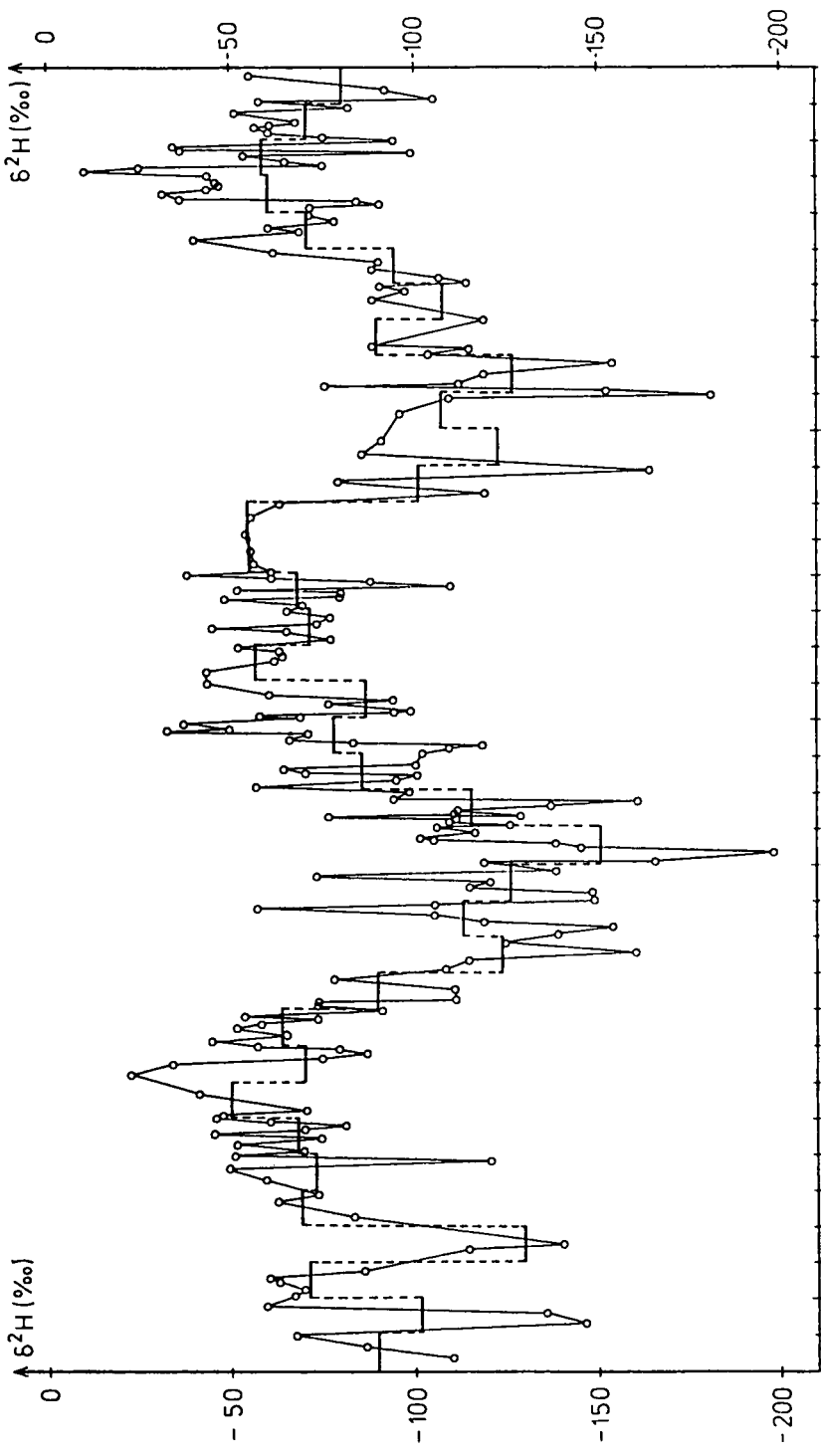

Figure 116. Seasonal variations in the ^2H-contents (δ^2H) in precipitation. The example shows the ^2H-contents from single precipitation events and their weighted mean monthly values in an alpine catchment area (Lainbach Valley, Upper Bavaria) during the years 1976-1978 (HERRMANN & STICHLER 1980).

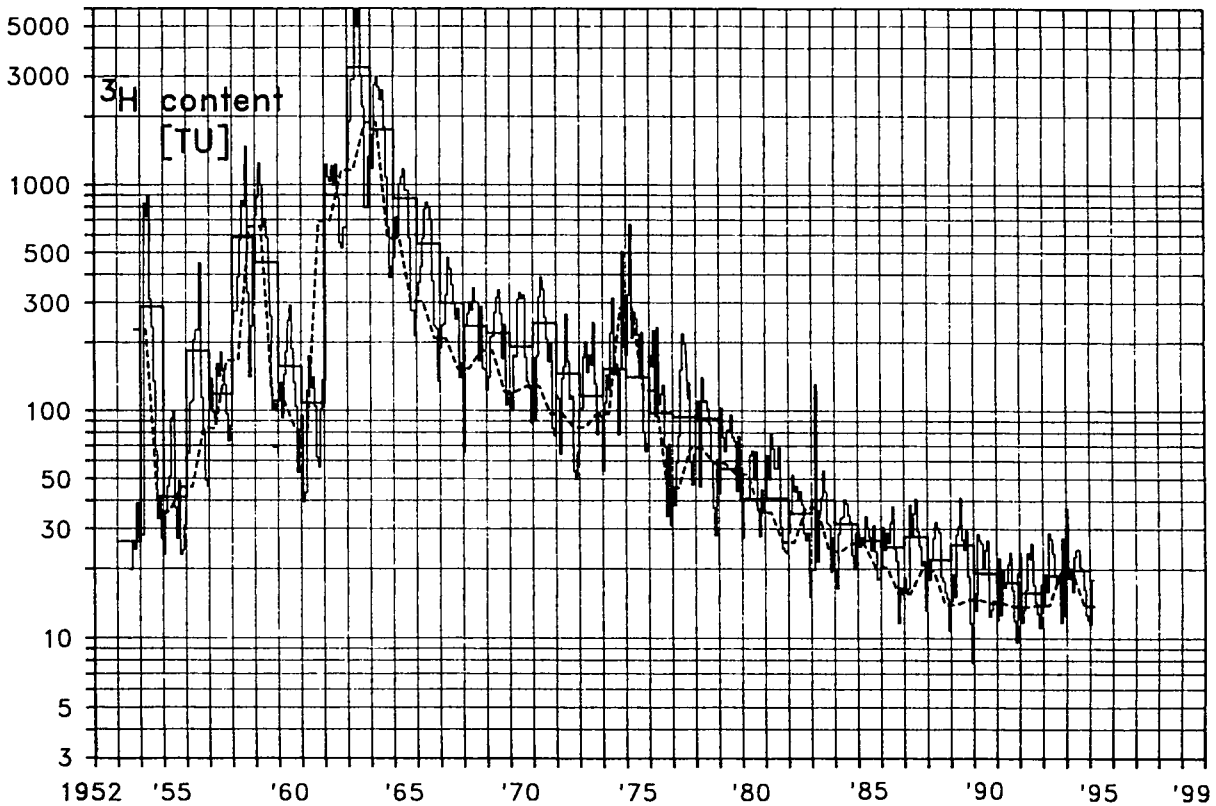

Figure 117. Temporal course of the ^{3}H-contents in precipitation: Precipitation samples from Ottawa/Canada (1953-1961), from Hohe Warte Vienna/Austria (1961-1970), from Hohenpeißenberg/Germany, Upper Bavaria (1970-1980) and from Neuherberg near Munich/Germany (1981-1995). Until 1970, the measured values were taken from publications of the IAEA (cf. e.g. IAEA 1981), after 1970 from the GSF-Institute for Hydrology (pers. comm.). The thin solid curve connects the ^{3}H-contents from the collected monthly samples weighted with the monthly precipitation amount. The bold solid step curve shows the yearly mean (total year input); the averages for October to March (winter input) are dotted.

ties have been observed. Due to the decreasing trend, the winter values from the last years are already sometimes close to the 'natural' ^{3}H-contents of under 10 TU[4].Other than the ^{3}H from the stratospheric reservoir, since ca. 1970 there have also been ^{3}H-emissions into the atmosphere from nuclear plants, which can create locally and temporally limited increases in the ^{3}H-concentrations in the precipitation.

The mean monthly values of the ^{3}H-contents in the precipitation are measured worldwide in the IAEA/WMO-collection network of precipitation (partially since 1953) mentioned above. This is necessary for two major reasons. Due to the fact that most of the ^{3}H-emission sites are in the northern hemisphere and due to local variations in the atmospheric water vapour, there are strong variations in the global distribution in the ^{3}H-contents. For example, the ^{3}H-contents in the middle latitudes are lower than the in higher latitudes. Moreover, knowledge of the temporal course of the yearly mean values of the ^{3}H-contents is an essential prerequisite for hydrological applications (cf. Section 2.11.3.2).

2.11.2.3 *Rare gas isotopes (^{3}He, ^{4}He, ^{39}Ar, ^{85}Kr)*

Rare gases, also called noble or inert gases, which are dissolved in water can generally be assumed to be good water tracers, since their concentration is not changed due to chemical interactions. However, changes in the tracer concentration in the hydrological system caused by physical effects such as gassing out and diffusion as well as by nuclear physical production can only be neglected, if the system is a closed system, i.e. if there are no drains or sources for the rare gas being investigated. Investigations regarding this are thus an imperative prerequisite for hydrological applications of rare gas isotopes.

Helium-4 and helium-3 (^{4}He, ^{3}He)

The ^{4}He sources are the helium in the mantle which has been present since the earth formed and the helium produced by nuclear decay of neutralized α-particles originating in the lithosphere. The helium that enters the atmosphere through diffusion has a fraction by volume of $5.22 \cdot 10^{-6}$.

^{3}He is a decay product of ^{3}H, which was formed in the lithosphere for example by the nuclear reaction ^{6}Li$(n,\alpha)^3$H and is also found in recently formed water as a result of the atmospheric nuclear reaction ^{14}N$(n,^3$H$)^{12}$C, from nuclear weapons tests and/or the emissions from nuclear plants (cf. Section 2.11.2.2). The isotope ratio ^{3}He/^{4}He in the lower atmosphere is $1.384 \cdot 10^{-6}$; in the helium from the upper mantle it is ca. 10^{-5}, whereas in the lithosphere, as a consequence of ^{4}He-production, it decreases to 10^{-7} to 10^{-9} [5].

A hydrological interpretation of helium-isotope contents in groundwater must consider their different origins (e.g. WEISE & MOSER 1987). Besides the ^{3}He which originates from the ^{3}H-content of the water, ^{3}He and ^{4}He can also enter the water cy-

---

[4] 1 TU (tritium unit) means a concentration of one ^{3}H-atom in 10^{18} H-atoms and corresponds to 0.118 Bq ^{3}H in 1 kg water. Nowadays, the detection limit for routine measurements in water samples without too much trouble is 0.3 TU (2σ-criterion). Some laboratories achieve 0.01 TU. The sample volume necessary for measuring is betwen 100-1000 ml H_2O.

[5] The measurement of ^{3}He/^{4}He-isotope ratios is very troublesome and therefore only carried out in a few laboratories. The detection limit is at ca. 10^{-9}. With a solute content of $4 \cdot 10^{-8}$ Ncm^3 ^{4}He/g H_2O in the normally used 40 ml-water samples, this corresponds to a detection of $1.6 \cdot 10^{-15}$ Ncm^3 ^{3}He (Ncm^3 = 1 cm^3 gas volume under standard conditions (1013 hPa and 0°C)). The ^{3}He-content, as a decay product of ^{3}H, is often given in TU = $2.49 \cdot 10^{-15}$ Ncm^3 ^{3}He/g H_2O.

cle from the atmosphere and the lithosphere. At that, the atmospheric helium can also be in concentrations over the solubility equilibrium (e.g. due to enclosed air bubbles). This He-excess must be determined by measuring the ^{20}Ne-contents, which is not affected by production in the lithosphere, and the He-content correspondingly corrected. With helium from the lithosphere, it must be differentiated whether it originated directly from the aquifer rock or originated in the groundwater from diffusion out of deeper layers in the earth's crust. Hereby, measurements of the ^{21}Ne-contents, which differs in its diffusive behaviour from He, can verify the ^{4}He-dating of old groundwaters (cf. Section 2.11.3.3) (WEISE et al. 1992). In any case, in a hydrological interpretation of He-isotope contents, sufficient hydrogeological, hydraulical and geochemical knowledge of the investigation area must be available.

Argon-39 (^{39}Ar)

In hydrology, ^{39}Ar is of interest especially due to its half-life time of 269 years, which enables the dating of groundwaters in the otherwise not accessible, but hydrologically very important range from 100 to 1000 years (cf. Section 2.11.3.1). It originates in the atmosphere through the impact of secondary neutrons from cosmic radiation according to the nuclear reaction ^{40}Ar(n,2n)^{39}Ar. An ^{39}Ar-content of 0.108 dpm ^{39}Ar/l Ar[6] develops in equilibrium between production and decay (^{39}Ar $\rightarrow$ ß$^-$ +^{39}K), which then enters the water cycle with the dissolved air in the rain.

The hydrological interpretation of the ^{39}Ar-content in groundwater is made difficult, similar as with ^{3}He, because ^{39}Ar is also produced underground by neutron-induced nuclear reactions in the aquifer rock. A high content of α-emitters (e.g. the uranium and thorium decay series) can so lead to ^{39}Ar-contents in the groundwater which are far above the atmospheric equilibrium value. Therefore, in evaluating ^{39}Ar-measurements, it is necessary to analyse the rock material in the aquifer for U-, Th-, K, and Ca-contents. Further indications concerning the underground isotope production are given by measuring the ^{37}Ar-content (half-life time: 35 days), whose underground production is correlated with ^{39}Ar (e.g. LOOSLI et al. 1989, 1992, FORSTER 1984, FORSTER et al. 1992).

Krypton-85 (^{85}Kr)

^{85}Kr is emitted from nuclear plants. The increase in these in the last decades has lead to a world-wide increase in the ^{85}Kr-contents in the atmosphere (Fig. 118), which, as with ^{39}Ar reflects the resp. equilibrium between production and decay (^{85}Kr $\rightarrow$ ß$^-$ + ^{85}Rb) and amounts to ca. 60 dpm ^{85}Kr/ml Kr[7] at this time. Due to the nearness to the surface of the emission sites and the quick mixing in the lower atmosphere, only relatively low seasonal variations and local differences in the atmospheric ^{85}Kr-contents have been observed (SALVAMOSER 1982, WEISS et al. 1992).

---

[6] dpm = disintegrations per minute. The detection of the low ^{39}Ar-contents in groundwater (cf. Table 20) requires large sample volumes (several m^3 water) and a complicated and painstaking preparation and measurement procedure. Up to now, this can be carried out only at two laboratories (Physics Institute of the Univ. Bern/Switzerland and GSF-Institute for Hydrology, Neuherberg/Germany). The detection limit is ca. 0.01 to 0.02 dpm ^{39}Ar/l Ar (LOOSLI 1983, FORSTER 1984).

[7] To measure the ^{85}Kr-contents in natural waters (cf. Table 20), a sample volume of several 100 l is necessary. A similar, yet somewhat less expensive preparation and measurement procedure due to the lower sample volume and the higher concentration, as with ^{39}Ar leads to a detection limit of several percent of the present specific ^{85}Kr-activity in the air. Worldwide, it is practised by only a few laboratories.

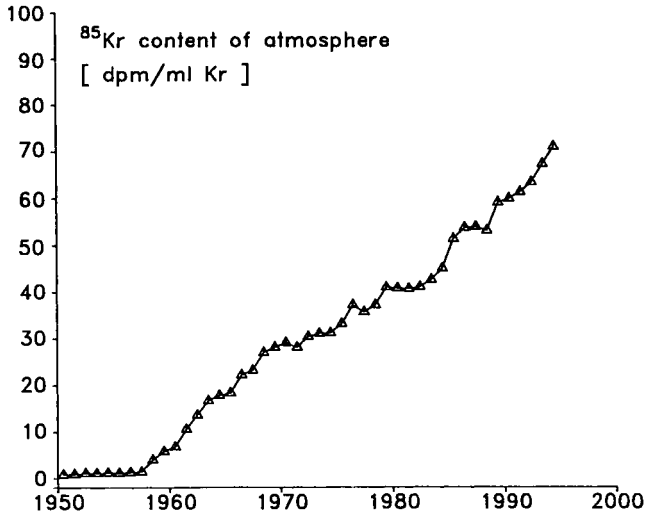

Figure 118. Temporal course of the ^{85}Kr-contents in the atmosphere. The measurements were carried out on samples from different sites between the latitudes of 40° to 60° N. dpm = decays per minute (values until 1989 from SALVAMOSER 1982, completed with values from WEISS (pers. comm.); after 1990, measurements from the GSF-Institute for Hydrology (pers. comm.)).

^{85}Kr enters the groundwater with the dissolved air in the rain and therefore marks the point in time of the groundwater recharge. The essentially monotonous temporal course of the ^{85}Kr-contents allows, in contrast to ^{3}H-contents (Fig. 117), a definite assignment of the model age (cf. Section 2.11.3) to the ^{85}Kr-content. In general, there is no disturbing underground production of ^{85}Kr to be expected.

2.11.2.4 *Carbon-13 and -14 (^{13}C, ^{14}C)*

The stable isotope ^{13}C occurs in natural carbon with a frequency of ca. 1%. The value listed in Table 20 shows natural variations of up to 30‰, which result from fractionation processes in the carbon cycle. Due to these processes, the carbon which originates from the assimilation cycle in the C_3-plants with a ^{13}C-content of $\delta^{13}C \approx -25‰$ is depleted compared to that in the C_4-plants with $\delta^{13}C \approx -12‰$[8]. The ^{13}C-content of the CO_2 in the air amounts to ca. -8‰, in marine limestone ca. 0‰. The ^{13}C-content therefore provides certain information concerning the origin of the carbon, e.g. in a water sample. This is also the essential hydrological application for measurements of the ^{13}C-contents, especially in the course of interpreting measurements of the ^{14}C-content (cf. below). ^{14}C is of interest in hydrology because of its half-life time of 5730 years. This enables the dating of groundwaters that range from a thousand to several ten thousand years in age, which cannot be dated with other methods. Similar to ^{3}H, ^{14}C originates in the atmosphere through the effect from secondary neutrons

[8] ^{13}C-contents are, as ^{2}H- and ^{18}O-contents, given in δ-values (cf. footnote [3]). The international standard used is a limestone, the Peedee Belemnite (PDB). In routine measurements of CO_2, which is usually in gas form, an accuracy of ca. 0.15 δ^{13}C-‰ (2σ-criterion) is achieved. This corresponds to an absolute contents of 1.5 ppm ^{13}C in carbon. The necessary sample amount is ca. 1 Ncm^3 CO_2.

from cosmic radiation upon nitrogen according to the nuclear reaction $^{14}N(n,p)^{14}C$. At equilibrium with the decay reaction ($^{14}C \rightarrow \beta^- + {}^{14}N$), this production leads to an isotope ratio of $1.2 \cdot 10^{-12}$ $^{14}C/C$. Modest variations in the production rate and thus in this isotope ratio, caused by e.g. solar activity, do not play an important role in hydrological applications.

In contrast, as with ^3H (cf. Section 2.11.2.2), the nuclear weapons tests lead to an increase in the ^{14}C-contents in atmospheric CO_2, which amounted to almost 200% modern[9] in 1964 and still causes a marked increase in ^{14}C-content of CO_2 in the air today.

The hydrological interpretation of the ^{14}C-contents in groundwater is often much more difficult than of the isotope species of water or the rare gases. Upon entering the hydrological system and in the system itself, ^{14}C is involved in a multiple of carbon reactions with the soil air, the water, and the rock matrix. On the one hand, these lead to different initial ^{14}C-contents in the recharged water, depending on the infiltration conditions and the geochemical environment. On the other hand, due to interaction with the rock matrix, changes in the ^{14}C-contents in the groundwater are also possible, which are not related to the dating based on the radioactive decay (cf. Section 2.11.3.1) and therefore are disturbances. Since ^{14}C is irreplaceable in long-term hydrological predications because its important dating range, many tests have been carried out recently to try and improve the interpretation of ^{14}C-contents in groundwater and its applications. Refer to the relevant literature (e.g. FONTES & GARNIER 1979, MOOK 1980, IAEA 1983a, PLUMMER et.al. 1991) for these tests.

As the quintessence from these works, it can be stated that for the hydrological interpretation of ^{14}C-contents, knowledge as accurate as possible of the geochemical environment as well as the hydrogeological and hydraulic situation in the investigation area must be presupposed and must be considered in the sampling program. The investigators should work closely with the ^{14}C-laboratory, if possible from the beginning. A ^{14}C-dating of the groundwater based only on the ^{14}C-contents is usually pointless.

2.11.2.5 *Chlorine-36 (^{36}Cl)*

Chloride, as the rare gases and the isotope species of the water molecule also, is a good water tracer; as an anion with a small radius it is only slightly adsorbed onto solid surfaces. Due to its long half-life time of $3 \cdot 10^5$ years, ^{36}Cl can be used to date groundwaters that are hundreds of thousands years old. This is a much longer period than possible with ^{14}C and is becoming more and more important in the exploitation of fossil groundwaters and in safety considerations concerned with the final disposal of radioactive material.

---

[9] '100% modern' are defined as the ^{14}C-content of wood, relative to the year 1950 (corrected with regards to the introduction of the ^{14}C occurring due to isotope fractionation and fossil fuel (industrial) CO_2 in the atmosphere). The realization of this recent standard is carried out with oxalic acid from the National Bureau of Standards; accordingly, 100 % modern corresponds to the 0.95 of the specific ^{14}C-activity of this oxalic acid. For hydrological applications, a detection limit of 1 % modern is generally sufficient. Conventional measurements are done with Low-Level-Activity-Measurements after extracting the carbon from water samples with volumes from 50-200 l (depending on the content of dissolved inorganic carbon). The necessary amount of carbon for this measurement of several grams can nowadays be reduced by using Acceleration-Mass-Spectroscopy (AMS). However, this procedure (cf. e.g. HENNING 1988) requires an expensive acceleration laboratory.

^{36}Cl originates in the atmosphere through different effects from cosmic radiation upon argon and enters the water cycle quickly in the form of rain and aerosols. The natural atmospheric ^{36}Cl-deposition is, dependant upon the latitude, between 5 and 30 ^{36}Cl-atoms/(m^2s). After 1952, as a result of the nuclear weapons test series, it increased strongly, up to 10^4 ^{36}Cl-atoms/(m^2s). After the moratorium on nuclear weapons tests from 1963, this increase has declined much more rapidly than with the 'bomb-^{3}H' (cf. Section 2.11.2.2).

^{36}Cl is also produced in the rocks of the near surface lithosphere through effects from cosmic radiation and its resulting products and thus depends on the altitude and the element composition of the rock. In deeper rocks, the production of ^{36}Cl is dependent upon the U/Th-content; here it is produced through activation of ^{35}Cl by fission neutrons during U/Th-decay.

Therefore, when used to date groundwater, the initial concentration in the newly recharged groundwater and the production rate in the aquifer must be known. Due to interference caused by evaporation and evapotranspiration during infiltration with the Cl-contents, it is expedient to use the ratio $^{36}Cl/Cl$ as a measure for the ^{36}Cl-content in the groundwater[10]. Values for the $^{36}Cl/Cl$ ratio in rain and fallout of between 20 and $640 \cdot 10^{-15}$ with increasing distance from the coast are listed for the USA (BENTLEY et al. 1986). This value range corresponds to the values for the $^{36}Cl/Cl$ ratio measured in groundwater in infiltration regions. The underground production of ^{36}Cl in deep aquifers must be taken into consideration in the case of low $^{36}Cl/Cl$-values with a correction factor. For this, one starts from the assumption for the values of the secular equilibrium for $^{36}Cl/Cl$ between production and decay, which is for granite ca. $30 \cdot 10^{-15}$, for sandstone ca. $5 \cdot 10^{-15}$, and for limestone ca. $10 \cdot 10^{-15}$ (cf. Section 2.11.3.1).

Overall, groundwater-model ages of several 10^6 years have been able to be dated with the present measurement technical requirements. Due to the usually hard to determine initial concentration as the sum of the input out of the atmosphere and the ^{36}Cl-production in the near surface lithosphere, there are still very large uncertainties with the ages determined. Additionally, with older waters there are also nonstationary mixing processes in the aquifer, which are especially effective and hard to model (cf. Section 2.11.3.3). In spite of all this, ^{36}Cl (along with ^{81}Kr, which however has not been used in hydrological applications yet) provides the only possibility for dating groundwaters that are older than 50,000 years.

2.11.2.6 *Sulphur-34 (^{34}S) and Nitrogen-15 (^{15}N)*

In addition to the isotopes handled in the preceding sections, which enable the dating of the groundwater either through the temporally variable input function or due to radioactive decay, ^{34}S and ^{15}N as hydrological tracers provide information as to the origin and geochemical evolution. Thus they supplement the applications using environmental chemical tracers (cf. Section 2.12). Additionally, ^{34}S and ^{15}N are gaining increasing importance in identifying environmentally dangerous sulphur and nitrogen releases into the biosphere.

---

[10] ^{36}Cl-contents are almost exclusively determined by Acceleration-Mass-Spectroscopy (AMS) measurements nowadays. The detection limit is ca. $5 \cdot 10^{-16}$ $^{36}Cl/Cl$ in a sample of 10 mg Cl^-.

Sulphur is normally present as sulphate in groundwater under non-reducing conditions. It originated mainly from evaporite rocks, can however have other sources (e.g. atmospheric fallout, oxidized sulfide). Dissolved sulphate in recent ocean water and thus also in oceanic rain has a $\delta^{34}S_{SO4}$-value of 20‰[11] and a $\delta^{18}O_{SO4}$-value of 9.6‰. Due to isotope fractionation, when sulphate precipitates as gypsum or anhydrite, ^{34}S and ^{18}O are enriched in the solid phase. Thus, these isotopes are depleted in the aqueous phase. As a result of the changing environmental conditions in the course of the earth's history and the corresponding different isotope fractionations, the evaporite sulphates can be differentiated in their ^{34}S- and ^{18}O-contents according to their geological age. Thus the geological formation, from which the groundwater originated, can be determined. Figure 119 shows, that the $\delta^{34}S_{SO4}$-values range from 10‰ (late Permian/early Triassic) to 35‰ (Cambrian).

If reducing conditions are present in the groundwater, considerable, especially with cases of bacterial reduction, isotope fractionations can occur. Since the biosynthetic products are strongly depleted in ^{34}S, a sulphate enriched in ^{34}S remains in the groundwater. The ^{18}O-content in SO_4^{2-} is also enriched, although to a lesser extent. If the groundwater flows from a reducing environment to an oxidizing zone, the sulphur is quickly oxidized to SO_4^{2-}, whereby this purely chemical process does not result in fractionation in the ^{34}S-content; with bacterial activity however, a small depletion in the ^{34}S-content can occur. The resulting ^{18}O-content in the SO_4^{2-} after oxidation depends on the origin of the oxygen (from the water or from dissolved O_2). In general, somewhat lower $\delta^{18}O_{SO4}$-values are found than with marine evaporites.

If the sulphur originated from atmospheric fallout, then the ^{34}S-content is determined by the fallout origin (e.g. from industrial plants), whereas the $^{18}O_{SO4}$-content can be used to draw conclusions about the redox conditions in the atmosphere. Typi-

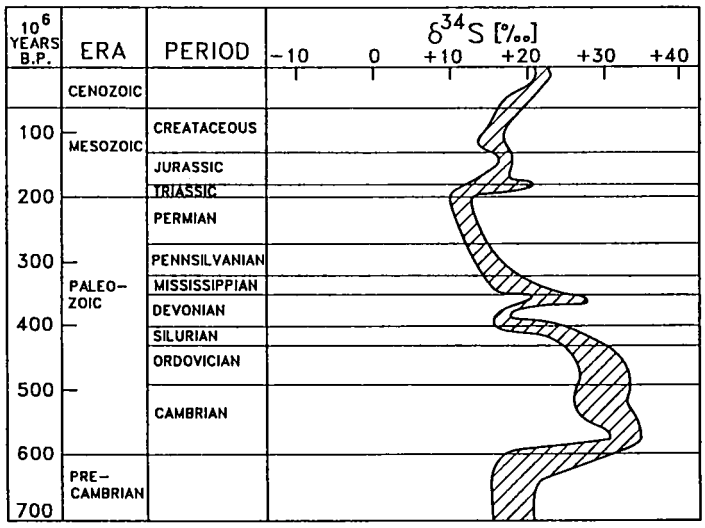

Figure 119. Sulphur-34-contents in evaporites from different geological ages (from KROUSE 1980).

[11] As with 2H- and 18O, δ-values are used as the measure for the 34S-contents (cf. footnote 3)), whereby the internationally recognised standard for 34S-contents is the Canyon-Diablo-Iron Meteorite (CD-Standard). Routine measurements of water samples achieve an accuracy for $\delta 34S_{SO4}$- and $\delta 18O_{SO4}$-values of ca. 0.25 ‰ (2σ-criterion); for this, ca. 2 mMol SO_4^{2-} are needed

cal values for industrial areas are (10 ± 5) $\delta^{34}S$-‰ and (3 ± 5) $\delta^{18}O_{SO4}$-‰ (e.g. NRIAGU et al. 1987).

Therefore, as with all other isotope investigations with sulphates, a combined determination of the $\delta^{34}S_{SO4}$- and the $\delta^{18}O_{SO4}$-values is always recommended. As a matter of fact, the knowledge of the hydrological sulphur cycle is still incomplete. Summarizing representations can be found in PEARSON & RIGHTMIRE (1980), NORDSTROM et al. (1985), KROUSE & GRINENKO (1991), and, with regards to thermal water, in TRUESDELL & HULSTON (1980).

Nitrogen usually enters the groundwater from the unsaturated zone as nitrate. To a large extent, its introduction into the soil is anthropogenic via mineral and organic nitrogen containing fertilizers, to some extent also through nitric acid rain. In many cases, only a combined measurement of the ^{15}N- and ^{18}O-contents in NO_3^- allows the differentiation of the origin of the nitrogen in the groundwater (SCHMIDT et al. 1989, AMBERGER & SCHMIDT 1987, VOERKELIUS 1990). Figure 120 shows, that technically produced, mostly from air-N_2, nitrate has $\delta^{15}N$-values[12] around 0‰ and $\delta^{18}O_{NO3}$-values around 20‰; the nitrate that is produced by nitrification of organic nitrogen (especially from NH_4^+), where at least two-thirds of the oxygen originated

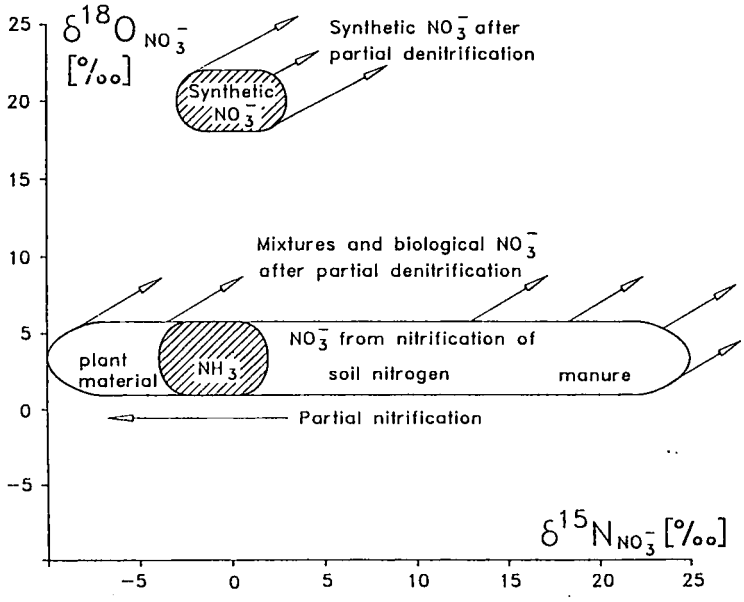

Figure 120. Nitrogen-15- and oxygen-18-contents in nitrates of different origin. Hatched areas are the ranges of synthetic NO_3^- and of NO_3^- from nitrification from synthetic NH_3. The arrows point in the direction of the secondary ^{15}N– and ^{18}O-enrichment in the remaining NO_3^- during the denitrification, resp. the ^{15}N-depletion during the nitrification (after AMBERGER & SCHMIDT 1987).

[12] ^{15}N-contents are given in δ-values, as are ^{2}H-, ^{18}O- and ^{34}S-contents (cf. footnote [3]). The standard is the ^{15}N-content in air-N_2. Routine measurements of water samples achieve an accuracy of $\delta^{15}N_{NO3}$- and $\delta^{18}O_{NO3}$-values of 0.6 ‰ and 1.0 ‰ (2σ criterion), resp., whereby samples of ca. 0.1 mMol NO_3^- are needed.

from soil water, indeed show, depending on the origin of the organic material, a wide range of $\delta^{15}N$-values, however, its $\delta^{18}O_{NO3}$-value is in a narrow band around 4‰. In many cases, nitrate in groundwater under unfertilized soil (e.g. in forests) has extremely high $\delta^{18}O_{NO3}$-values (up to 60‰), which indicate acid rain influence.

If there are reducing conditions in the groundwater, it is mostly due to bacterially caused denitrification, which leads to enrichments in the ^{15}N- and ^{18}O-contents in the remaining nitrate (cf. Fig. 120). Further isotope fractionations in the complex hydrological nitrogen cycle are described in length and summarized by HÜBNER (1986).

2.11.3 *Special evaluation methods for environmental isotope measurements*

2.11.3.1 *Radioactive decay*

Radioactive isotopes decay in the time t independently of external influences according to the decay law

$$n_t = n_0 \cdot e^{-\lambda t} \tag{2.12}$$

where n_t = number of radioactive atoms present after time t, n_0 = number of radioactive atoms present at time $t = 0$, λ = decay constant.

The decay constant is linked to the half-life time $T_{1/2}$ by the relationship

$$\lambda = \frac{\ln 2}{T_{1/2}} = \frac{0.693}{T_{1/2}} \tag{2.13}$$

and is characteristic for each radioactive isotope.

For the radioactive environmental isotopes listed in Section 2.11.2, the 'isotope content' is used as the unit for the number of radioactive atoms in the water (cf. e.g. Footnotes [4],[6],[7],[9], and [10]).

If the half-life time $T_{1/2}$ (cf. Table 20) is known, the time τ_a that has passed during radioactive decay, can be calculated from the ratio of the isotope contents at time t (n_t) and at time $t = 0$ (initial content n_0) using Equations 2.12 and 2.13:

$$\tau_a = \frac{T_{1/2}}{\ln 2} \ln \frac{n_0}{n_t} \tag{2.14}$$

The time τ_a is a measure for the 'groundwater age', if the radioactive decay occurred in a closed hydrological system, i.e. providing there is no inflow or outflow of the respective environmental isotope to or out of the system. Causes for this may be isotope production in the aquifer rock (e.g. with ^{39}Ar and ^{36}Cl, to a lesser degree also with ^{3}H and ^{14}C, cf. Section 2.11.2) and diffusion of gases out of the rock into the groundwater or out of the groundwater into the gas volume of the water unsaturated zone (e.g. with the ^{3}He produced from the ^{3}H-decay and with ^{39}Ar and ^{85}Kr). In these cases, the calculated groundwater age is falsified and can only be corrected in special cases, such as ^{36}Cl-dating of very old waters (BENTLEY et al. 1986).

Difficulties in applying Equation 2.14 also arise if the initial concentration, n_0, is not adequately known. In this respect, ^{14}C and ^{36}Cl are especially problematic (cf. Section 2.11.2). The curve PFM in Figure 122 comprehensively illustrates Equation 2.14 for ^{39}Ar, ^{14}C, and ^{36}Cl with the corresponding potential range for the ground-

water age determination, in case the conditions mentioned above are adequately fulfilled. However, the given ages can only be interpreted as real groundwater residence times if the hydraulic conditions are also considered (cf. Section 2.11.3.2).

2.11.3.2 *Input-output-models for determining groundwater residence times*

As opposed to groundwater tracing tests with intentionally injected tracers, that are momentarily or continuously injected at one or more distinct sites, the environmental isotopes enter the water cycle, and thus the groundwater, areawide. Furthermore, in many cases this is temporally and spatially dependent (cf. Section 2.11.2). For the evaluation of the environmental isotope content of a water sample, the knowledge of this 'input function' $C_{in}(t)$ in the investigation area is a prerequisite. To quantify the groundwater residence times or the age distribution of the groundwaters, hydraulic models are included, which calculate the 'output-functions' $C_{out}(t)$ from the input functions of the isotope contents. The output function should be a good approximation of the environmental isotope contents measured. The mean residence times can also be used to calculate hydraulic constants of the aquifer.

The most widely used models today are the dispersion model (DM) and the exponential model (EM) (SIEGENTHALER 1972a, ZUBER 1986).

With the dispersion model (DM), hydrodynamic dispersion is assumed along the groundwater flow path. The resulting distribution of the groundwater flow times between the recharge area and the groundwater sampling site is described by a dispersion function $f(\tau)$, which has as parameters the mean residence time t_m and the dispersion parameter D/vx. The output function $C_{out}(t)$ is then given by a convolution integral over the radioactive decay during the flow time corrected input function $C_{in}(t-\tau)\cdot e^{-\lambda\tau}$ with the dispersion function $f(\tau)$:

$$C_{out}(t) = \int_0^\infty C_{in}(t-\tau)\cdot e^{-\lambda\tau} f(\tau)d\tau. \tag{2.15}$$

With a tracer injection amount proportional to the discharge, as generally given with environmental isotopes, $f(\tau)$ results from the dispersion equation (MALOSZEWSKI & ZUBER 1982) to:

$$f(\tau) = \frac{1}{\tau}\left[4\pi P_D \frac{\tau}{\tau_m}\right]^{-1/2} \exp\left[-\left(\frac{\tau_m - \tau}{\tau_m}\right)^2\right]\cdot\frac{\tau_m}{4P_D\tau} \tag{2.16}$$

with $P_D = D/vx$ = dispersion parameter (D = dispersion coefficient, v = mean flow velocity (effective flow velocity), x = flow distance), τ_m = mean residence time at the sampling site.

Using a suitable fitting procedure, the relationship between the input ($C_{in}(t)$) and output ($C_{out}(t)$) functions given by Equations 2.15 and 2.16 can be used to approximate $C_{out}(t)$ onto the measured concentration-time-distribution and thus to determine the hydraulic parameters τ_m (mean residence time) and D/vx (dimensionless dispersion parameter).

A borderline case for the dispersion model with $D/vx = 0$ is the piston-flow model (PFM), with no mixing in the groundwater flow due to dispersion, diffusion, or ex-

change effects of any kind assumed. Here, the input concentration decreases only due to radioactive decay (if occurring):

$$C_{out}(t) = C_{in}(t - \tau_m) \cdot e^{-\lambda \tau_m} \tag{2.17}$$

With the exponential model (EM) it is assumed, that the groundwater sample contains precipitation from different time periods, whose amounts decrease exponentially with increasing residence time τ. The average of these residence times corresponds then to the mean residence time of the groundwater sample. In a stationary system with equal inflow and outflow, the model can be described by

$$f(\tau) = \frac{1}{\tau} e^{-\tau / \tau_m} \tag{2.18}$$

When applying the hydraulic model to the environmental isotope contents measured, it must be differentiated as to whether the input function, C_{in}, i.e. the initial contents, n_o, in the recharged groundwater (cf. Section 2.11.3.1) is constant in time (as with ^{14}C and ^{36}Cl (without the 'bomb-^{14}C and -^{36}Cl') as well as ^{39}Ar) or varies with time (as with ^{2}H, ^{3}H, ^{3}He (from ^{3}H), ^{18}O, bomb-^{14}C and ^{85}Kr). These models cannot be used for groundwater dating with isotopes, whose input function has no temporal dependency (^{13}C, ^{15}N, ^{34}S).

With a constant C_{in} in Equation 2.17, the mean residence time in the PFM becomes

$$\tau_m = \frac{1}{\lambda} \ln \frac{C_{in}}{C_{out}} \tag{2.19}$$

which corresponds to the simple age determination from the radioactive decay (Eq. 2.14).

In the EM, according to Equation 2.18, τ_m is

$$\tau_m = \frac{1}{\lambda} \left(\frac{C_{in}}{C_{out}} - 1 \right) \tag{2.20}$$

For the DM, a two-parameter model, τ_m can be determined with constant C_{in} only with the help of two environmental isotopes with different decay constants λ. With the limited choice of suitable isotopes, this is very hard to realize.

With a seasonally varying C_{in} (cf. e.g. Figs 116 and 117), the seasonal variations in the precipitation amounts and their percentage in the groundwater recharge must be considered. The isotope content in monthly cumulated samples $C_{pi}(t)$, monthly precipitation sums P_i, and monthly infiltration rates α_i yields an approximation of the annual mean to:

$$C_{in}(t) = \frac{\sum_i C_{Pi}(t) \alpha_i P_i}{\sum_i \alpha_i P_i} \tag{2.21}$$

Applying Equation 2.21 is problematic, mainly due to lacking knowledge of α_i. Therefore, whenever possible, $C_{in}(t)$ should be directly measured in the recharged groundwater.

In choosing the appropriate hydraulic model, the respective hydrogeological situation needs to be accounted for. Figure 121 shows schematic examples for the groundwater flow patterns with their respective recharge areas and sampling sites. The appropriate hydraulic models (DM, PFM, EM) fitted for the isotope contents in the groundwater samples are noted. Accordingly, a typical PFM situation is a homogeneous aquifer with a relatively small recharge area very far away from the sampling site (Case 1 in Fig. 121). The EM is appropriate for a sampling site in a homogeneous near-surface aquifer within a vast groundwater recharge area (Case 2 in Fig. 121). However, the residence time in the unsaturated zone should be small compared to the total mean residence time in the groundwater sample; if this is not the case, the seepage processes must be handled separately with the DM. In contrast, the DM is appropriate for sampling sites with no groundwater recharge in the immediate surroundings (Case 3 in Fig. 121).

It can also be seen from Figure 121, that certain dispersion parameters in the DM differ in the evaluation of the contents of the environmental isotopes that are introduced area-wide to the system and those which are intentionally, i.e. point-source or in-line injected tracers (cf. Section 4.2). In such cases, the 'dispersivity' D/v obtained has an apparent value on the order of the expansion of the groundwater recharge area, that has no direct relation to the dispersion process in the aquifer.

If the prerequisite for homogeneity in the aquifer in the investigation area is not fulfilled, the models used to evaluate the environmental isotope contents must be modified. This is usually done with multiple-box-models, where the hydraulic relationships in the different sections of the aquifer are simulated in the individual boxes. Examples for these models are given in ZUBER (1986) and MALOSZEWSKI et al. (1983). The important case of flow in fissured rocks with simultaneous matrix diffusion is handled in MALOSZEWSKI & ZUBER (1985, 1991), also with respect to the interpretation of the environmental isotope contents (especially ^{14}C). MALOSZEWSKI

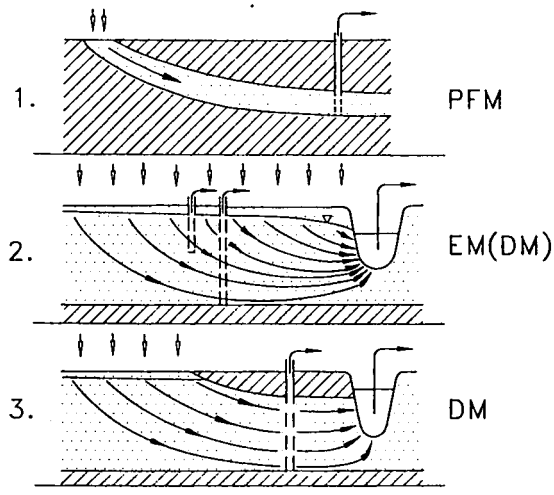

Figure 121. Schematic view of the application possibilities for the different hydraulic models, specifying the sampling site and groundwater recharge area (from MALOSZEWSKI & ZUBER 1982). DM = dispersion model, EM = exponential model, PFM = piston flow model.

(1994) shows that the residence times derived from the ^{14}C- and ^{3}H-ages of the mobile water without considering the retardation caused by matrix diffusion can lead to an overestimation of the mobile groundwater percentage. Knowledge of the corresponding retardation factors is therefore a prerequisite for determining the volume and the flow velocities of the mobile water in fissured aquifers.

Additionally, a comprehensive summary of the present applications using mathematical models with groundwater isotope content measurements is given in IAEA 1994b.

2.11.3.3 *Ranges and accuracy of groundwater dating with environmental isotopes*
For the environmental isotopes with constant input functions (^{14}C and ^{36}Cl (without 'bomb-^{14}C and -^{36}Cl'), and ^{39}Ar), the range for groundwater dating is essentially given by the decay constant λ or the half-life time $T_{1/2}$. This is clearly seen in the attached abscissas for ^{39}Ar, ^{14}C, and ^{36}Cl in Figure 122. For the environmental isotopes with time-dependent input functions (^{2}H, ^{3}H, ^{18}O, and ^{85}Kr), the dating range is determined first by their temporal course (Figs 116, 117, and 118). Aside from this, the accuracy of the groundwater dating with all the environmental isotopes depends upon the accuracy of the knowledge of the input function, upon the measuring accuracy, and upon the reality of the hydraulic model applied. The still, to some extent uncleared, problematics concerning the initial contents of ^{14}C, ^{36}Cl, and ^{39}Ar in groundwater, i.e. the input function, was handled in Section 2.11.2; this decisively limits the viability of groundwater dating with these isotopes.

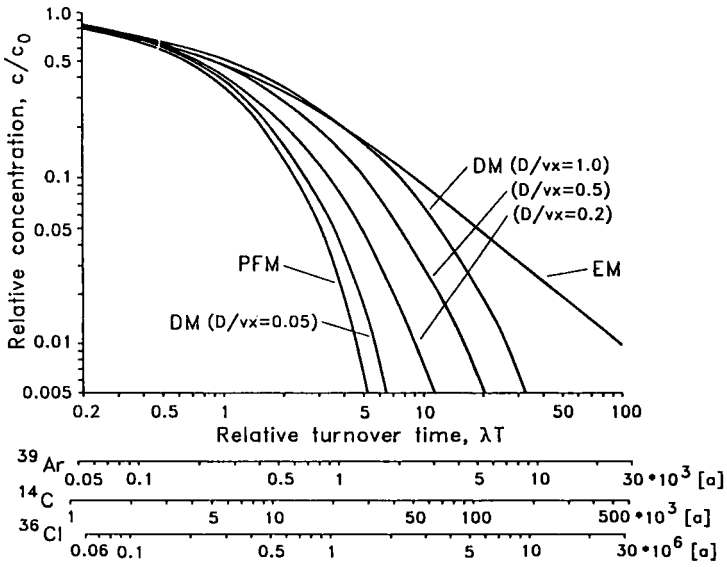

Figure 122. Relative isotope contents in dependency of the relative (mean) turnover time $\lambda\tau_m = (0.693/T_{½})\tau_m$ with constant input function C_{in} and for different hydraulic models. EM = exponential model, PFM = piston flow model, DM = dispersion model with dispersion parameter D/vx, λ = decay constant. In the attached abscissas, $\lambda\tau_m$ has been converted for ^{39}Ar ($T_{½}$ = 269 a), ^{14}C ($T_{½}$ = 5730 a) and ^{36}Cl ($T_{½}$ = 3·105a) (from MALOSZEWSKI & ZUBER 1982).

Groundwater dating with ^{2}H and ^{18}O is based on the semi-periodic seasonal variations in the isotope contents in precipitation (Fig. 116) and thus in recharged groundwater. As long as these variations are still detectable in the groundwater, i.e. in the output function, groundwater residence times can be determined with models. For example, the differences observed in Middle Europe between the ^{2}H- and ^{18}O-contents, resp. in summer and winter precipitation of ca. 100 $\delta^{2}H$-‰, resp. 15 $\delta^{18}O$-‰ can be used to calculate residence times ranging from months to several years.

Beside dating of young groundwaters, the ^{2}H- and ^{18}O-contents, due to their temperature dependency, can be indirectly used to determine a groundwater recharge in climates different from today's, e.g. past ice ages.

For groundwater dating with ^{3}H, the input function used is usually the course of the annual mean of the ^{3}H-content in the recharged groundwater. Hereby, the seasonal dependency described in Section 2.11.3.2 must be considered. In Figure 123, the output function in the groundwater, calculated with the models PFM and EM, are shown for the whole year input and for the winter input (October to March) of the precipitation (Fig. 117). The definite model dependency of the 'age' and the dating range is evident. Furthermore, the interpretation is also made more difficult since the model age for a large part of the ^{3}H-contents in the output function is ambiguous. (Similar problems occur when applying ^{14}C-peaks caused by the nuclear weapons test for groundwater dating.)

When using ^{85}Kr for groundwater dating, a definite output function results, that is for the most part independent of the seasonal groundwater recharge (Fig. 124), since

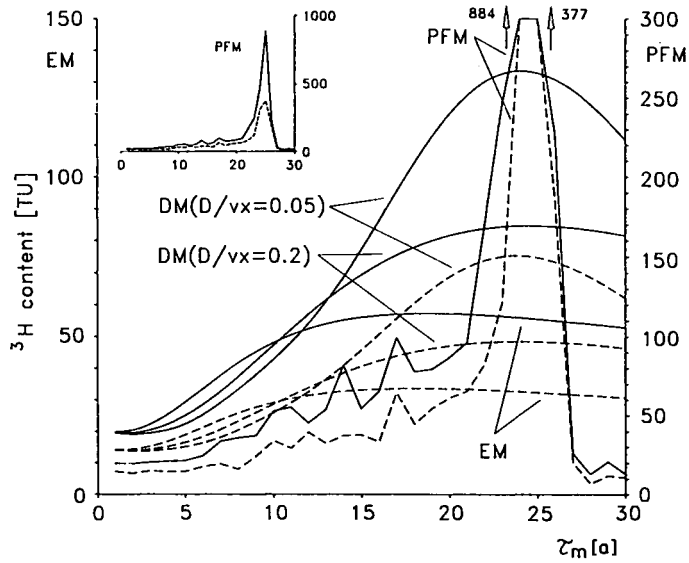

Figure 123. ^{3}H-contents in groundwater, calculated with the piston flow model (PFM), the exponential model (EM), and the dispersion model (DM) for different parameters *D/vx*, dependent upon the mean residence time τ_m; input function cf. Figure 117, samples taken in 1988. The solid curves correspond to groundwater recharge from a whole year, the dotted curves correspond to groundwater recharge from October to March (winter input).

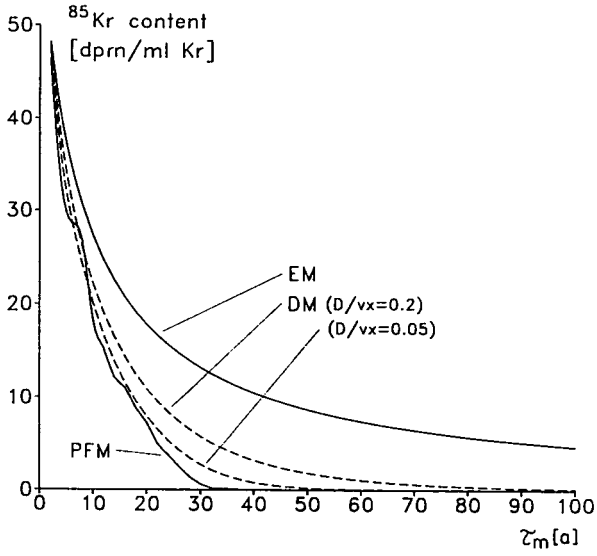

Figure 124. ^{85}Kr-contents in groundwater, calculated with the piston flow model (PFM), the exponential model (EM) and the dispersion model (DM) for different parameters *D/vx* dependent upon the mean residence time τ_m. Input function cf. Figure 118, samples taken 1988.

the input function (Fig. 118) grows for the most part monotonously and shows only small seasonal variations. Considerably disadvantageous however are the much more painstaking sampling, preparation, and measuring techniques needed for ^{85}Kr as-compared to ^{3}H. To a large extent, the range of the ^{85}Kr-dating is the same as ^{3}H and covers years to decades. This can be used for dating the young components of mixed waters, whose older components are ^{3}H- and ^{85}Kr-free (SALVAMOSER 1982). With this '^{3}H/^{85}Kr-method' it is decisive that the quotient of the ^{3}H- and ^{85}Kr-contents in the water sample yields an output function C_{out} independent of a mixing with older components. In Figure 125, the model dependency of this method can be seen and is substantial from τ_m = 10a on; at ^{3}H/^{85}Kr ratios above 15 TU/(dpm/mol Kr) however, it must be assumed that the hydraulic conditions for the EM are not given.

Groundwater dating with ^{3}H decay produced ^{3}He is based on the ^{3}H-input function (Fig. 117) with the mentioned uncertainties. In addition, other sources with ^{3}He-percentages in groundwater must also be assumed (cf. Section 2.11.2.3), which need to be cleared up with the help of the ^{3}He/^{4}He-ratio and the ^{20}Ne-content. The even stronger model dependency upon ^{3}H, displayed in Figure 126, together with the painstaking ^{3}He-detection analysis shows that the ^{3}He-method is hardly competitive with the ^{3}H-method. However, the combined measurements of ^{3}He and ^{3}H ('^{3}He/^{3}H-method'), much like with the ^{3}H/^{85}Kr-method, can yield age determinations for the young component of a two-component-groundwater (WEISS & JENKINS 1979, MALOSZEWSKI & ZUBER 1983, SCHLOSSER et al. 1988, SOLOMON et al. 1992, CARMI & GAT 1994). Figure 127 shows, that here, the dependency of the output function

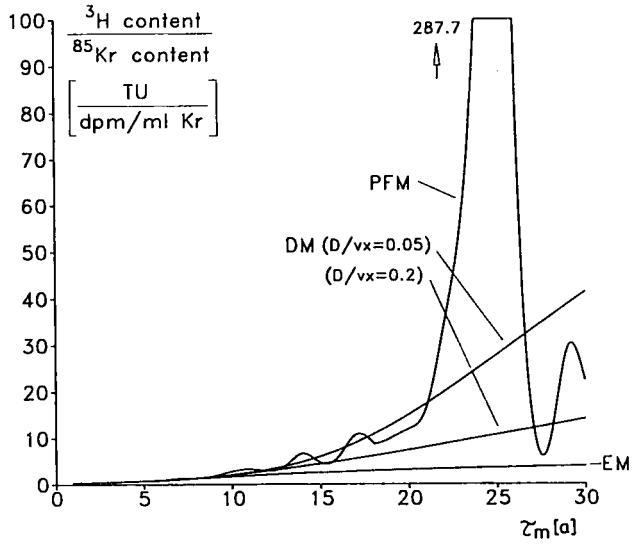

Figure 125. Quotients from ^{3}H- and ^{85}Kr-contents in groundwater, calculated with the piston flow model (PFM) and the exponential model (EM) in dependence of the mean residence time τ_m. Input functions cf. Figures 117 and 118, groundwater recharge during the whole year. Samples taken in 1988.

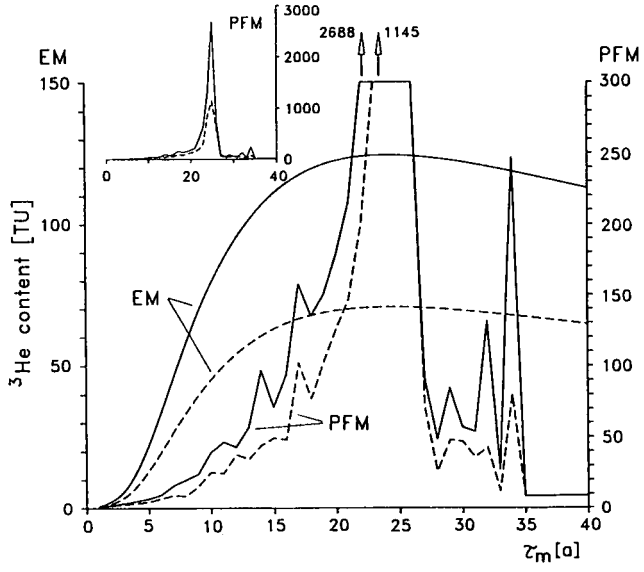

Figure 126. ^{3}He-contents in groundwater as decay product of ^{3}H, calculated with the piston flow model (PFM) and the exponential model (EM) in dependence of the mean residence time τ_m. The input function for ^{3}H corresponds approximately to the winter recharge from Figure 117 (October to March). Samples taken in 1988 (WEISE, pers. comm.).

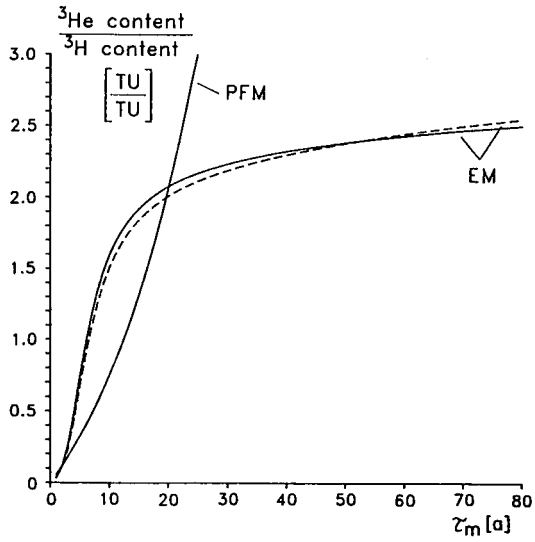

Figure 127. Quotients from ^{3}H-contents and ^{3}H-decay produced ^{3}He-contents in groundwater, calculated with the piston flow model (PFM) and the exponential model in dependency of the mean residence time τ_m. The input function for ^{3}H corresponds approximately to that in Figure 117, with a groundwater recharge from October to March, samples taken in 1988 (WEISE, pers. comm.).

upon the conditions of the groundwater recharge is much lower than with the ^{3}He- and the ^{3}H/^{85}Kr-method.

2.11.3.4 *Determining components in mixed waters*

Due to the largely ideal tracer properties of many environmental isotopes, they are also very suitable for determining components in mixed systems, e.g. in quantifying groundwater percentages of different origins. Usually, the simple mixing equation

$$c_m = \sum_i c_i a_i ; \sum_i a_i = 1 \tag{2.22}$$

is used, with c_m = isotope content of the mixed water, c_i = isotope content of the component i, a_i = discharge percentage of the component i.

Applying Equation 2.22 however, assumes that the isotope contents of c_i are so different, that the percentages a_i can be calculated accurately enough. This is the case with ^{2}H and ^{18}O, if the catchment areas of the discharge components have different altitudes or if one of the components is enriched in ^{2}H or ^{18}O due to evaporation processes in surface water. The same is true for differentiating in ^{3}H-, ^{14}C-, ^{39}Ar-, and ^{85}Kr-contents as a result of different groundwater ages and with ^{3}He-, ^{4}He-, ^{15}N-, and ^{14}S-contents due to originating from different geochemical and geological environments.

In the case of a two component mixed system, Equation 2.22 becomes:

$$c_m = a_1 c_1 + (1 - a_1) c_2 \tag{2.23}$$

The measuring points of the mixing system lie on a line with the end points c_1 and c_2 of the isotope contents ('mixing line'). With three component systems, the measurement of a second isotopic or chemical indicator, whose concentration is independent of the first, is necessary (e.g. ^3H with ^{18}O, Cl^- with ^2H, yet not with the closely correlated ^2H and ^{18}O).

The mean residence times calculated with environmental isotopes can also be directly used to determine the components in mixed systems. Thus, from the age determined by the $^3H/^{85}Kr$- or $^3He/^3H$-method of the young portion of a two-component-system (cf. Section 2.11.3.3) and the e.g. with ^{85}Kr determined model age of the mixed water, the volume percentage of both components can be estimated. With multiple component systems, Equation 2.22 must be fulfilled for the corresponding number of independent isotope contents or other tracers. Examples for this are given in the case studies in the Sections 4.4.3 and 5.5.1 as well as e.g. MOSER & RAUERT (1980) and in the investigations referred to in IAEA-publications.

2.11.3.5 *Further hydrological applications*

Other than age differentiation and the determination of mixing percentages in groundwater, measurements of environmental isotope contents can contribute to solving other hydrological questions. Differences in ^2H- and ^{18}O-contents due to the altitude effect, the continental effect, or evaporation, can indicate the catchment areas of the groundwater resources under investigation. In many cases, the ^2H- and ^{18}O-contents standardize groundwater resources, which differ in their genetics (e.g. climate, infiltration). This is especially true for thermal and mineral waters, for river bank filtration and sewage percentages. Variations in isotope content used for the age determination along the groundwater flow path can be evaluated for age differences; very low groundwater flow velocities can be determined with this. On the other hand, variations in the groundwater age at a certain site in the aquifer (e.g. in a well) can indicate changes in the aquifer and thus corresponding groundwater management consequences. For examples and further application possibilities refer to the literature cited in Section 2.11.1.

2.11.3.6 *Conclusions*

The preceding outlined possibilities for interpreting environmental isotope contents seem to advise carrying out hydrochemical analyses and also isotope measurements, *before* a tracing test is planned and conducted. The sampling must be adapted to the hydrogeological conditions. With a relatively quick groundwater flow, usually present in areas with planned tracing tests, the seasonal variations in the environmental isotope contents are an essential basis for the hydrological information. It is recommended to observe at least two annual cycles, whereby the sampling frequency must be adjusted to the temporal variability of the hydrological parameters. With rapid rises and falls in the groundwater level due to extreme precipitation events or groundwater withdrawals, this can lead to very short sampling intervals. However, repeated sampling should take place even with relatively stationary and slow groundwater movement. Observation periods of several years can also be achieved by adding data from earlier sampling series. The hydraulic models could thus be checked on a long-term basis by comparing the measured and calculated output functions.

In combination with tracing tests, usually ^{2}H-, ^{3}H-, and ^{18}O-content measurements are carried out, since these yield regional developments with groundwater residence times with a range between months and several years. However, since the natural groundwaters are often mixed waters with old components, for balance calculations, these components should be determined by measuring the ^{14}C-, ^{39}Ar-, and in some cases the ^{36}Cl-contents, i.e. the long-lived isotopes. A combination of measurements of as many as possible, independent isotopes in connection with hydrochemical parameters leads, under consideration of the hydrogeological and hydraulic conditions, to the best conception of the groundwater flow field.

2.12 ENVIRONMENTAL CHEMICALS

W.Käss

This chapter covers those substances that are chemicals in the liberal sense of the term and were inadvertently introduced into the system. Since they strongly differ from the natural constituents in water, they can be used as tracers. These substances enter the water system in two ways: creeping, i.e. long and continual release of the chemicals and spontaneous, i.e. short and limited release during accidents, although they cannot be always completely differentiated from each other.

2.12.1 *Creeping release*

At sites where there is a possibility for water-soluble substances to enter the environment over longer periods of time, an inadvertent water tracing occurs. If these substances, over more or less short flow paths, are not sorbed, exchanged, or decayed, they can even provide the basis for an evaluable water tracing test. Starting points for such tracing tests are e.g. purification plants, dumpsites, chemical stockpiles, and sewage farms among others.

Uranine

Many bathing products, cosmetics, and cleaning products contain uranine, some also pyranine (Table 21).

Uranine does not decay in sewage treatment plants, except for undergoing photolysis (KANOWSKI 1985). After passing through the plants, uranine enters the receiving streams or sewage farms almost undiminished.

Thus, the receiving groundwater is also injected with uranine along with the seepage water from the sewage farms. It was proven in the Freiburg sewage farm, that uranine does not undergo decay in seepage water, which is heavily polluted with organics and rich in microorganisms (Fig. 128). On 21 August 1983, the inflow to the sewage farm contained 2.6 µg/l uranine. In the central part of the sewage farm, the uranine content in the groundwater ranged between 0.2 and 0.3 µg/l. Some 1000 m downflow, where the groundwater already had drinking water quality again, 10 ng/l could still be well detected.

Akin to seepage water from municipal sewage water farms, groundwater downflow from dumpsite seepage water also receive uranine. It comes from not completely empty packages and containers of uranine containing cosmetics and cleaning

Table 21. Uranine contents in bathing products, cosmetics and cleaning products.

Product name/brand	mg/l or mg/kg	
Badedas 'Bubble bath'	2400	
Benny 'Vitalising bubble bath'	410	
Fa Bubble bath	500	
Trikana 'Dwarf-pine bath – '	55	
Silvodor 'Pine-needle bath'	638	
Dressin-International, Pine-needle bath tablets	1350	
Dressin-Kulmbach, Jeanette Pine-needle scented bath	100	(+150 mg/l pyranine)
Respond 'Green apple shampoo'	23	
Pat de Lux, Hegner 'Green apple shampoo'	5,5	(+pyranine)
General, ammonia cleaner	15.5	
Wundi, ammonia cleaner	2.5	
Palmolive – dish detergent	0	(+17 mg/l pyranine)
Asmara – dish detergent	0	(+ non fluoresc. green dye)

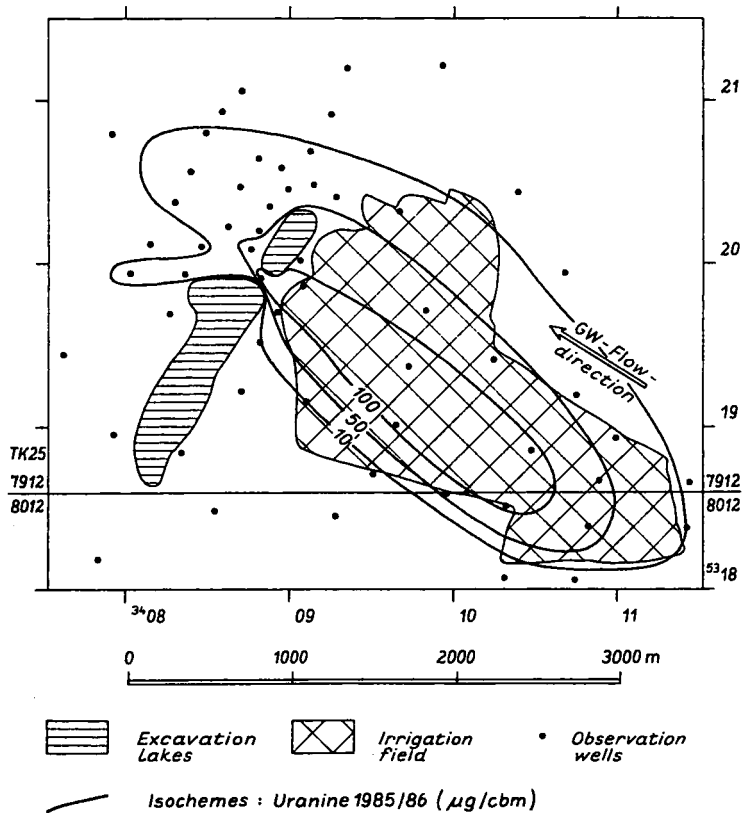

Figure 128. Uranine contents in pore groundwater under and downstream of the Freiburg sewage farm. Groundwater table depth in the southeast ca. 7 m, in the northwest ca. 1.5 m.

products. For example, 600 m away from the dumpsite Karlsruhe-West (Germany) in the Rhine valley-Pleistocene-groundwater, 0.16 µg/l uranine was detected.

Rivers from major urban regions can contain considerable uranine concentrations, which come from the sewage treatment plants (in µg/l):

Neckar near Heilbronn,	15 December 1980	0.200
Neckar near Heilbronn,	2 January 1992	0.045
Rhine, river-km 210, Breisach,	5 January 1992	0.025
Rhine, river-km 444, Worms,	21 January 1985	0.24 *
Main near Niederrad,	30 April 1982	0.015
Elbe near Hamburg-Wilhelmsburg,	16 May 1981	0.007

* Other fluorescences besides uranine are also present: Rhodamine B: 4.2 µg/l, and at 467 nm/484 nm with 1.5 µg/l uranine equivalents and at 520 nm/544 nm with 1.1 µg/l uranine equivalents. The latter are from industrial sewage treatment plants.

The uranine load in rivers varies strongly, temporally and spatially. Besides uranine, there are other fluorescing substances in the Rhine downstream of Ludwigshafen to the mouth of the river, which can hinder the uranine determination due to superimposition. Except for rhodamine B, these substances are unknown. However, they are also strongly sorbing. They can be removed by membrane filtration and are also retained by bank filtration.

Uranine remains undiminished after bank filtration. Along the lower and middle Neckar river, it was possible to calculate the percentage of bank filtered river water in several water catchments using the uranine concentration in tappings near the banks. It is recommended that other relevant bank filtrated parameters such as boric acid, surfactants, or isotopes also be included in the calculations to assure quality control (KUSSMAUL et al. 1977).

Boric acid

Similar to uranine, boric acid is also found in sewage and waste seepage water. It comes from laundry detergents that contain considerable amounts of perborates. Perborates release oxygen during the washing process and act therefore as a mild bleach. It leaves the treatment plants as boric acid, H_3BO_3 or HBO_2. In dumpsite seepage water the boric acid comes from the leftover deposits in the detergent packages and container. The analysis of such a seepage showed 82.4 mg/l HBO_2 (STARK 1987). Ground- and surface waters with catchments in agriculturally used areas can also have increased boric acid contents. Mineral fertilizers have namely boric compounds with contents up to 3% (as B_2O_3).

Figure 129 shows an example of the boric acid contents downstream of a gravel pit used as a waste landfill in the alpine foreland. The increased boric contents in the groundwater can be followed for almost 2 km.

No groundwaters are free from boric compounds; the background level is, excepting gypsum-containing underground, under 100 µg/l metaboric acid (HBO_2). Some background values are listed in Section 2.2.4. Data about the dynamics of the boric load in the Rhine can be found in HELLMANN & SCHUMACHER (1977). DIETZ (1975) views the boric content of a waterbody as an indicator for its pollution level. MULJADI and BLUME (1977) and BLUME et al. (1980) reported on the possible sorp-

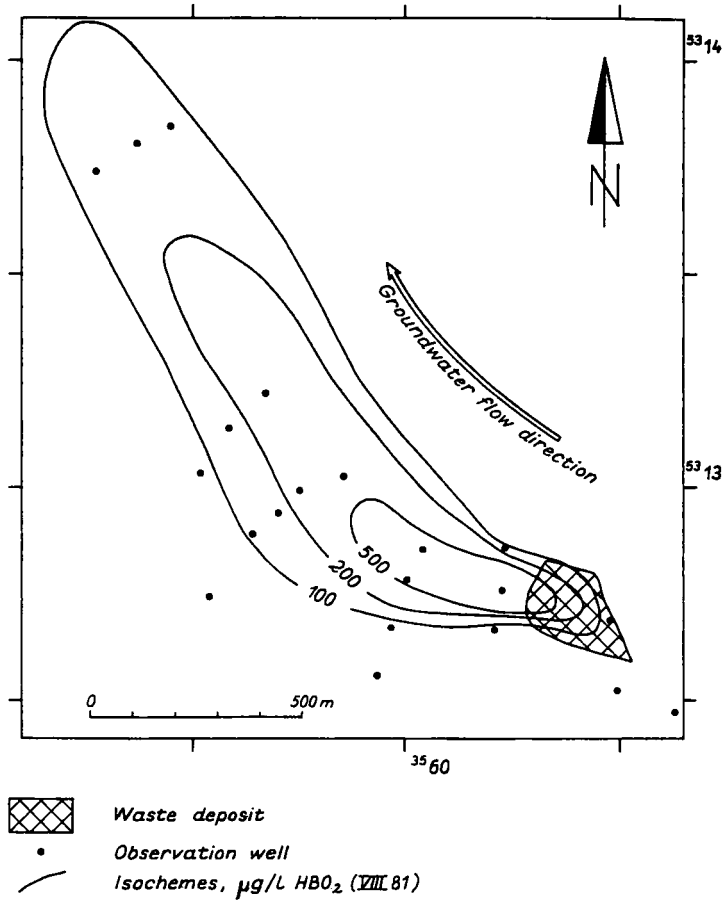

Figure 129. Borate contents downstream of a dumpsite in the alpine foreland. Aquifer: Würm glacial gravels.

tion of boric compounds in fine-grained aquifers. The authors found an adsorption maximum at pH 9.5.

Chloride

The literature contains much data about the impact of chloride upon water. Only the three major areas are handled here.

In the winter, road service scatter de-icing salt on the streets to ensure better driving conditions. These are composed mainly of sodium chloride. On highways, there is an average consumption of 20 t salt per km and winter. To a large extent, sodium undergoes ion exchange with hardeners in the unsaturated zone and in the aquifers. In some karstwater tappings in the eastern Swabian Alb, as a non-exchangeable ion, the chloride content has increased from ca. 8 mg/l in the beginning of the sixties to over 15 mg/l at the end of the seventies (SCHLOZ 1980).

Also well known is the oversalting of the groundwater due to overuse of wells in nearshore areas and on the East Friesian islands. Less known are cases when wells that are heavily pumped become oversalted due to the salt containing deeper water.

An example of this was described by HOPPE (1967) from the Bunter sandstone in the Southern Harz mountains (Germany). From 1960 on, the chloride content of a well in Bleicherode/Cty. Grafschaft Hohenstein increased approx. 30-40 mg/l to over 3000 mg/l, although the delivery was not increased. The chloride increase is due to an influx of water from the Zechstein formation, which underlies the Bunter sandstone.

In the potassium salt works on the upper Werra in Hessen and Thüringen (Germany), over 6 million tons of chloride, as a byproduct, accrue annually. The chloride containing wastewater is pressed, especially in the Thüringen region, in the sheet dolomite, which has almost reached its full capacity. As a result, groundwater discharge containing salt from the sheet dolomite flows into the Werra. The Werra and Fulda join and form the Weser at Hannoversch Münden and thus, bank-filtered water has increased chloride contents up to Bremen. Using several peak values from the salt load in the Weser, ORTLAM (1983) was able to trace these peaks in three wells above Bremen in 300-550 m distance. From the time-delay, he was able to calculate a mean residence time of 8.1 years.

ORTLAM (1983) calls all anthropogenic dissolved or emulsified substances in waterbodies (rivers, lakes, or seas), which infiltrate the groundwater with a specific flow velocity, 'Pollution Tracers'.

Two definite anthropogenically caused groundwater oversaltings emanate from the Upper Alsatian (France) potash mines. The first involves the subrosion of the spoil dumps and saturated sodium chloride solutions thus enter the underground. The salt-carrying groundwater flows north along with the Ill river and north of Colmar, after a flow path of over 40 km, still has a chloride content of 200 mg/l. The width of the salt-carrying groundwater flow is 10 km at Mülhausen and at Colmar still 5 km. South of Strassburg, this groundwater flow combines with the second case of groundwater oversalting, which results from discharging the waste brine into the Rhine river near Fessenheim. The salt-carrying groundwater accompanies the river on both banks as it flows north (Europarat 1975, 1982).

2.12.2 *Cases of accidents with groundwater damage*

Accidents with groundwater damage are temporally limited, usually only short-term environmental contaminations, which are caused by human and/or technical insufficiencies, as well as rare cases of force majeure. Such accidents, which inadvertently cause lasting groundwater contamination, are inadvertent water tracing tests. Sometimes these accidents reveal so far unknown or only supposed hydrological connections.

Case Pontarlier 1901

On Tuesday, 13 August 1901 at midday, the supervisor of the Loue spring (French Jura) power plant noticed a foreign odour, which became stronger towards three in the afternoon. At this time, André BERTHÉLOT, the son of the famed chemist Marcelin BERTHÉLOT, happened to be in Mouthier, 6 km downstream of the Loue spring. On the following day, he observed along the Loue river upstream of Mouthier an odour of absinthe, such 'as if one was sitting in a Caféhouse and had a glass in front of oneself.' The water that flowed from the Loue cave, tasted slightly like anise. Un-

der the waterfall on the Loue discharge, the water foamed with white flocs such as with soap foam (BERTHÉLOT 1902).

On the previous Sunday, 11 August 1901, a lightning bolt had caused a large-scale fire in the Pernod factory in Pontarlier at 12:30 in the afternoon and the absinthe container had burst. Thus, towards evening, large amounts of absinthe flowed into the nearby river Doubs. Downstream of Pontarlier, near the village Arçon, the Doubs enters into the calcareous region of the Upper Jura. Similar to the Upper Danube, the riverbed intermittently falls dry (CHAUVE et al. 1982, 1986). Whether and where the Doubs fell completely dry at the time of the fire was not recorded (FOURNIER 1901).

A. BERTHÉLOT filled two bottles with the foaming Loue water and sent them to his father. He was able to definitely detect anise oil in the distillate. Furthermore, he calculated from the alcohol content of the samples and using the delivery of the Loue of 15 m^3/s, that ca. 1 million litre absinthe had flown.

Through this notable accident, a connection between the Doubs-percolation sites and the Loue spring, the second strongest spring in France, was proven (Fig. 130). The connection had been long supposed; a salt tracing test in 1873 had brought no results (FOURNIER 1900). FOURNIER had then suggested repeating the test from 1873 with a 'powerful tracer'. Years after the fire from 1901, MARTEL, FOURNIER and MARÉCHAL carried out a dye tracing test on 31 August 1911, 2750 m downstream of the Doubs bridge in Arçon with 100 kg fluorescein (MARTEL 1913, 1921). The

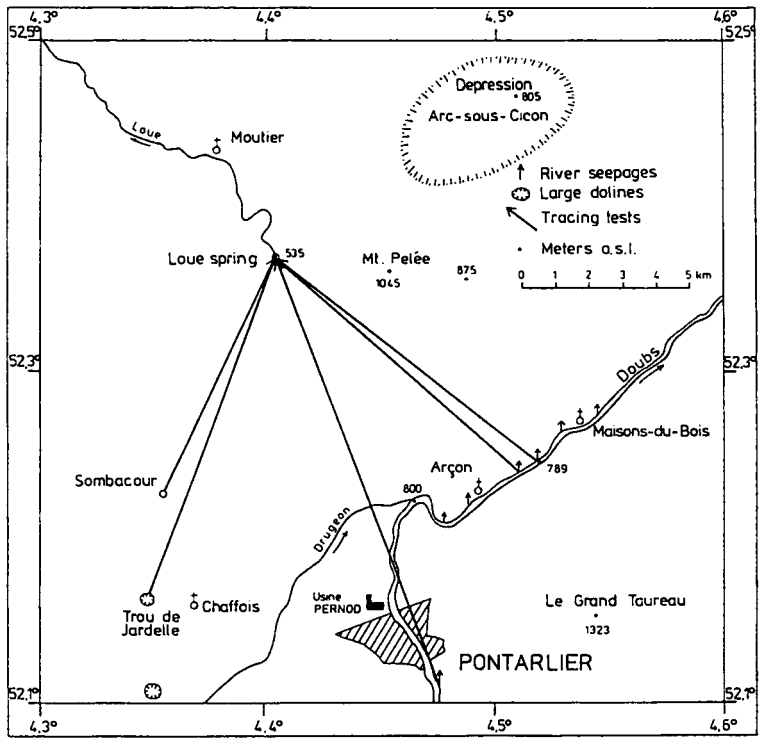

Figure 130. Catchment area of the Loue spring (French Jura). 'Usine PERNOD': Scene of the fire from 1901. Arrows indicate further tracing tests (after CHAUVE et al. 1986).

Loue spring carried coloured water 60 hours later and the Loue river was green for 3½ days over a distance of 60 km!

Case Karlsruhe

Numerous examples of groundwater contamination with highly volatile chlorinated hydrocarbons are known. These substances are liquid chemicals that are used for cleaning metal and in dry cleaners in numerous companies. Upon entering the underground, they do not interact with the aquifer nor with the water constituents. This is due to the unpolar structure as well as to the electrically uncharged nature of the organic molecule. A microbiological decay and a sorption onto organic material in the aquifer occur only on a minor level. Thus, these highly volatile chlorinated hydrocarbons could almost be labelled 'ideal tracers.' In the Rhine-Neckar-Region, contaminated groundwater flow stretches of 10 km in length have been proven. Groundwater with high-volatile chlorinated hydrocarbon contents over 25 µg/l is not suitable as drinking water, due to hygienic reasons.

Figure 131 displays one of many cases. In the contaminated area, the sum of the

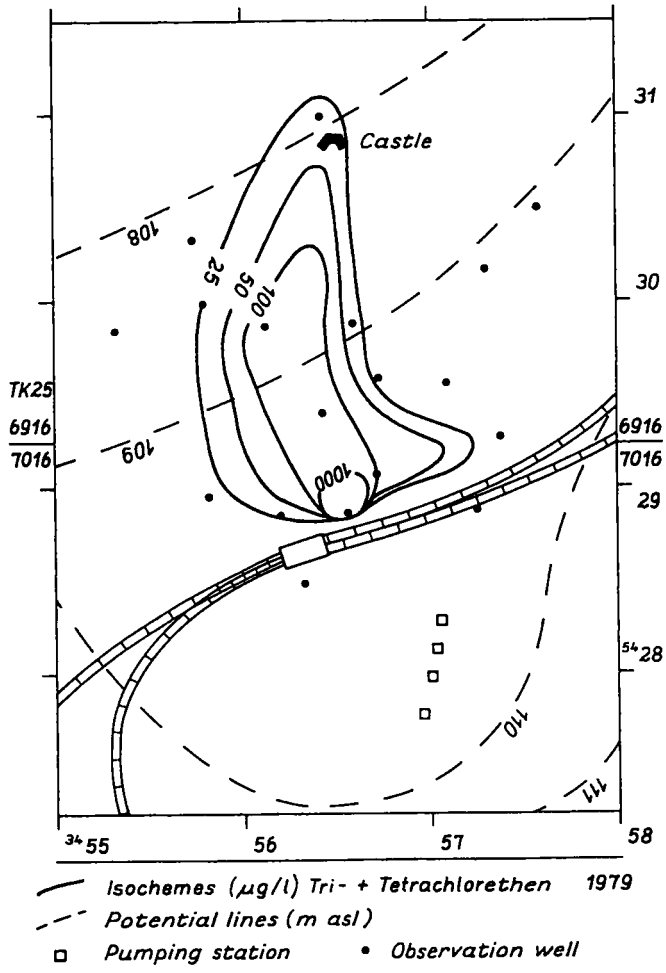

Figure 131. Contents of high-volatile chlorinated hydrocarbons in the pore-groundwater (Sum Tri + Per) (according to data from the Karlsruhe city works).

trichloroethylene and perchloroethylene amounts to over 1000 µg/l. Not until 2½ km farther downflow is the groundwater diluted strongly enough to be suitable as drinking water again (MELUF-BW 1983).

Other groundwater contaminations with tracing effects
In September 1954, on the Swabian Alb in the village of Temmenhausen, the streets were tarred with coal-tar. Rain washed the soluble phenol contents in the tar into the karstic groundwater, that was tapped 5 km away for the city of Ulm's water supply. Due to the chlorination in the drinking water treatment, chlorophenols were produced, which have an intense phenolic odour and taste (GROSCHOPF 1957). Almost simultaneously, SCHULZ (1957) reported a similar case near Kleinengstingen, where, at a distance of 4 km, the drinking water tappings of the city of Reutlingen in the upper Echaz valley were involved.

Other suddenly appearing disadvantageous impacts upon karst water tappings on the Swabian Alb are, among others, muddy water after heavy rains, percolation water used to fight fires, and discharging fruit juice wastewater into the underground (VILLINGER 1978).

QUINLAN and ROWE (1977) described an illegal discharge of ca. 340 t whey in a swallowhole. The water tapping in Smith Grove/Kentucky, 5 miles away became unusable as a result. In trying to hide smuggled whiskey, 2000 gallons were injected in a percolation site; the odour could be recognized in the karstwater near a school in Tennessee.

A list of such groundwater contamination cases with tracing effects could be continued with practically every pollutant.

2.13 ENVIRONMENTAL ORGANISMS
W. Käss

In the beginning of the sixties, DOMBROWSKI caused a considerable sensation in and out of expert circles with the discovery of viable bacteria in salt deposits (DOMBROWSKI 1965). This type of bacteria and Paleozoic pollen were detected by him in several mineral waters. As a result of finding Paleozoic pollen in the Bad Nauheim mineral water, DOMBROWSKI derived the origin of the Zechstein salt beds in Neuhof, 60 km to the east (DOMBROWSKI 1967). Later on, HÖLTING (1977) had doubts about the index fossil, e.g. the spore of *Lueckisporites virkkiae*. However, the connection between the Permian salt beds and Bad Nauheim is thereby not disproved.

During a pumping test in the Neckar flood plains downstream of Tübingen, it was possible to determine river bank water filtration percentages with microbiological tests (RITTER 1983). The pumping well at a distance of 130 m away from the heavily contaminated river first delivered 10 l/s with colony counts between 5 and 9 per ml; coliform bacteria were not detectable in 100 ml. At this time, the river had a colony count between 1600 and 3100 colonies per ml and between 74,000 and 92,000 coliform bacteria in 100 ml. Increasing the delivery of the well to 30 l/s, increased the colony count to 45/ml and the coliform count to 6/100 ml. RITTER concluded from these results, that at a pumping rate of 10 l/s, the well water contained no or very

well-filtered river water. With an increased pumping rate of 30 l/s, the filtration effect of the gravelly-sandy underground is not sufficient to maintain drinking water quality.

In the past, numerous groundwater contaminations due to sewage and waste water caused typhoid and cholera epidemics. Such epidemics happen nowadays, if only rarely. These cases can be considered spontaneous water tracing tests with pathogenic germs. For absolute proof and to provide more information, usually salt or dye tracing tests are conducted later at the supposed danger site. Some examples have already been covered:

> Case Lausen 1872 (Section 1.1 and 2.2.1, Fig. 2) (HÄGLER 1873),
> Case Pforzheim 1919 (Section 2.2.1) (DAUR & RÖHRER 1921),
> Case Hornisgrinde/Middle Black Forest 1935 (Section 2.2.1) (HORNUNG 1935).

The typhoid epidemics in 1893 and 1898 in Paderborn (Nordrhein-Westfalen/ Germany) were the reason that STILLE (1903) thoroughly investigated the catchment of the Pader springs. Essential parts of these investigations were the numerous dye tracing tests at stream percolation in the karst region east/southeast of Paderborn. STILLE was able to prove that the percolating stream water reappeared after only a short time in the Pader springs which were used as a drinking water source then. The residence times were between 19 and 89 hours, an insufficient time to assure that any bacteria present would die off.

2.14 PHYSICAL ENVIRONMENTAL EFFECTS

W. Käss

Of the physical environmental effects upon groundwater, the water temperature is the only effect that allows conclusions to be drawn about the origin of the water body.

River bank filtered water is substantially warmer in the summer months than the local groundwater. If the percentage of the bank filtered water is high, temperature measurements can be used to localize the influx from the surface water. Figure 132 shows the temperature relationship in a flood plain of the lower Neckar valley in the Odenwald. The flood plain on the left bank of the Neckar near Eberbach is bordered on the south by the Bunter sandstone of the 'Kleiner Odenwald'. From there, fissure groundwater with a temperature of ca. 11°C flows towards the flood plain. From the groundwater temperatures in the wells and in the groundwater monitoring wells, the main bank filtered water inflow can be determined.

BORIC (1988) conducted temperature measurements in two reservoirs of the largest depression without an outlet in Yugoslavia, the 'Livansko polje' (Herzegovina). The groundwater temperatures in 104 boreholes showed, that a permeation of the reservoir water occurred in certain spots. The temperature of the reservoir water fluctuates seasonally between 4 and 24°C, whereas the uninfluenced groundwater has fairly uniform temperatures of 8.5-9.5°C throughout the year.

ARMBRUSTER et al. (1988) also used temperature measurements to localize leaks in dams. They placed temperature sensors in the dam and registered the course of the temperature. They also used supplementary measurements of the self-potential of the

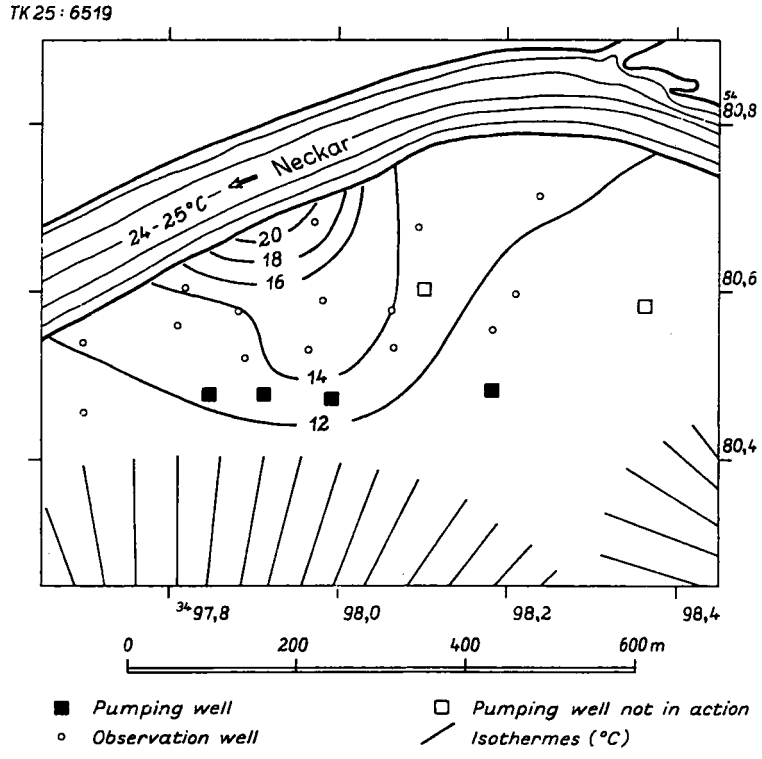

Figure 132. Isothermes in the pore-groundwater of the Neckar valley flood plains near Eberbach on the lower Neckar on August 10/11, 1976.

dam itself. The self-potential changes if the water flowing in the potential field changes its chemical makeup (salinity).

Temperature measurements in surface waters offer the possibility of localizing ascending water. KÜPPER (1954) carried out such measurements in streams of the Viennese Basin in November 1953. However, his measurement sites were too far apart, at 0.5-1 km, to localize ascending water.

Similar to the environmental isotopes, there is also an altitude effect with spring temperatures, which according to JÄCKLI & KLEIBER (1943) amounts to for the Gotthard region -0.3 to -0.4°C per 100°m altitude.

It is much more difficult to judge the origin of a spring from the temperature than from isotope measurements. Other than the seasonal fluctuations, there are also the factors exposition, uncontrollable inflows, heavy rains, the reappearance of percolated streams to consider.

In the Eastern Alps, STINI carried out many temperature measurements on springs and surface waters. In an example from the Kaprun valley (province of Salzburg/Austria), STINI (1948) was able to prove, based on temperature measurements alone, that a spring with an output of ca. 100 l/s had no connection to the 200 m away Kapruner Ache. Based on these observations, STINI holds the view that in such cases, temperature measurements can be a better choice than the more complicated dye and salt tracing tests.

If surface water with a much different temperature than the groundwater is pumped into wells, anomalies in the groundwater flow can be ascertained from the borehole temperature logs. KEYS and BROWN (1978) described three tests carried out in Texas/USA, which should be, if taken strictly, not really counted as physical environmental effects. In the tests, a spatial image of the permeability of the underground could be obtained. Good permeabilites displayed temperature changes quickly, lesser permeable layers not until later. Obviously, this is the only method with which, though restricted to small regions, up to ca. 100 m – differentiated permeablilities can be obtained.

Taylor & Francis
Taylor & Francis Group
http://taylorandfrancis.com

CHAPTER 3

Preparation and realization of tracing tests

W. Käss

Tracing tests must be thoroughly planned and prepared. The extent of the preparations depends upon the nature of the task. Smaller tests over short distances naturally need less preparation time, materials, and accessories than large combined tests. Unsatisfactory results are often obtained with badly prepared tests.

A tracing test usually starts with exploratory surveys in the investigation area. According to the nature of the tasks, the boundaries of the investigation area should be defined as well as the injection and observation sites chosen and the tracer(s) to be used. The exact course of the tracing test must be predefined so that no gaps in the observation net occur. An inspection of the investigation area is absolutely necessary and if necessary must be repeated.

KYRLE (1928) and MAURIN (1967) published detailed instructions on preparing and organizing large tracing tests. Even if these publications are mainly concerned with karst water tracing tests, to a large extent the instructions are valid for non-karst investigation areas.

3.1 PRELIMINARY SURVEYS AND PREPARATIONS

Before each tracing test is carried out, whether or not past tests were carried out must be known. Unfortunately, the documentation of the tests is not always as exemplary as in the German Federal States Bavaria or Baden-Württemberg (cf. Section 3.5). Often the data from past tests must be painstakingly collected from different documents, publications, or statements from the participants. In general, there are gaps in the data collected; a reason for the careful registration of each tracing test conducted, even if no results are obtained.

The results from earlier tests ease the estimation of the necessary injection amounts of the tracer(s) needed and the corresponding residence times and give indications for possible recovery sites. In special cases, a repeat test can be forgone.

Geological and hydrogeological maps provide knowledge about the underground, the latter also provides information about the quality and quantity of the groundwater regime under investigation. Groundwater contour maps show the given flow direction. With multiple groundwater occurrences, the contour maps generally only refer

to the top aquifer. There are only a few flow maps for standing bodies of water and are generally only applicable for a specific season.

Extensive tracing tests require ample preparation time. During this time, isotope-hydrological, water chemical (ZUPAN & KOLBEZEN 1976, MISEREZ 1976) and if necessary, microbiological (TRATNIK 1976) and virological (MOZETIC 1976) analyses and examinations should be conducted as early as possible. Regular discharge and precipitation measurements in relevant stations should be taken. Precipitation samples are to be included in the isotope measurements.

3.2 TEST PREPARATION

In order to optimally prepare tracing tests, its goals and purpose must be exactly outlined. In the preparation phase, the contracting authorities should be always available for further inquiries.

A cost estimate for the contracting authorities contains all costs for the necessary expenditures that are not carried out by the contracting authorities directly. The following costs are accrued in a tracing test:

- Tracer,
- Wear and tear on sampling containers,
- Expenditures for preliminary investigations,
- Possible costs for preliminary expert reports,
- Tracer analysis,
- A report of the investigation and results along with the necessary computer, secretarial, and graphic labour.

The tracing test's expenditures themselves are normally paid for or provided by the contracting authorities. However, the scientists in charge must also provide the necessary data for the following points:

- Fees for the authorization of the tracing test (Section 3.2.1),
- Expenditures for the sampling,
- Expenditures for storage and transport of the samples,
- Expenditures incured during priming of the injection site, injecting, and flushing of the tracer,
- Expenditures concerning the observation sites,
- Possible damage to crops and compensation thereof.

3.2.1 *Legal questions*

All tracing tests connote injecting a foreign substance into the water system, which requires an authorization according to the relevant water laws. Since the authorization procedure can be lengthy, care should be given to the tracer chosen as well as to the injection amount.

Each country has its own legalities as to the injection of foreign substances into water bodies. The proper authorities need to be opportunely informed about planned tracing tests and if required, the application supplied with the necessary reasons.

If radioactive substances are to be used, transport as well as handling authorizations must be acquired by the proper authorities. The applications must prove that the

concentration of the radioactive isotope at the recovery sites will be clearly under the maximum limits according to the radiation protection ordinances (BGBL 1976 and 1977a). It should also be mentioned here that such authorizations are hard to attain nowadays.

The results from the tracing tests are to be handled confidentially. Before they are published or made open to the public, the contracting authorities must give their consent. Since there is often a scientific interest connected with the publication of the results, this should be agreed upon beforehand. Normally, dissent only occurs with cases in connection with legal action.

3.2.2 *Choosing the injection site*

Often the success or failure of a tracing test depends upon the correct type and state of the injection site being chosen. The more careful and thorough the preliminary surveys and investigations carried out, the easier it is to choose the best arrangements for the test (MAURIN 1967). Multiple tracing tests are usually carried out in solid rock aquifers. The multiple injection of different tracers in different sites provides a more comprehensive hydrological picture of the aquifer. A prerequisite for this is a wide distribution of the injection sites in the investigation area. However, such multiple tests require that a painstaking and thorough decision be made in choosing the injection sites in accordance with the properties of the tracer and its analytical detection. An inspection of the site is indispensable in deciding whether or not the site is suitable. If necessary, required adjustments at the site can be made or arranged during the inspection of the site.

In karst regions, active swallowholes with continually water percolation are preferred injection sites. Cave water systems are also ideal injection sites, even though transporting the materials usually proves difficult. Less suitable injection sites are dolines without inflow or boreholes, even if they extend down into the karst water. In these cases, excavation or dredging down to the solid rock should take place.

Excavations are also conducted in nonkarstified underground.

3.2.3 *Choosing the observation sites*

The governing principle here is that it is better to have one too many observation sites as one too few. Tracing tests often proceed surprisingly (KLEINERT 1976). Due to karstification, bedding dip, or faults, the underground water divides rarely concur with those aboveground. Faults often seal off connections, instead of providing or continuing hydraulic connections.

Smaller water outlets, that certainly have only a limited catchment area can be neglected in most cases.

On the other hand, strong neighbouring springs cannot be viewed as common recovery sites. During a dye tracing test in 1965 in the Swabian Alb near Münsingen, the two karst springs Ursprung and Achursprung southeast of the injection site in the abandoned Schelkling Danube loop were observed. The first spring had a discharge of ca. 2 m^3/s (VILLINGER 1978), the latter circa half as much. The distance between the two was only 500 m. The distance between the injection site and the Ursprung was 12.0 km, and the Achursprung 12.3 km. The major portion of the dye was re-

covered in the Ursprung spring, that was slightly closer to the injection site; traces of the dye were also observed on the other side of the European water divide northwest of the injection site. Dye traces were never detected in the spring Achursprung! This test shows that groundwater tracing tests can always deliver surprises.

Even if the nature of the task only requires observing one point, neighbouring or intermediate sites should be observed and sampled also. In case the tracer is not detected in the observed site, the question as where the tracer went is still unanswered. However, if the tracer was detected elsewhere, the test results are more satisfactory than if never recovered. In such cases great uncertainties remain.

When water tappings are sampled, the raw water, i.e. the untreated groundwater, must be sampled. Often there are no raw water faucets in older water tappings. In such cases during the inspection of the site it should be stressed that one is indispensable. Taking samples of the *treated* water must be avoided. Water treatment plants with strongly oxidizing chemicals destroy or deplete not only some of the fluorescent dyes, including uranine, but also several other tracers. Activated carbon or sand filters are also unwanted impediments for many tracers.

If there are no suitable natural sampling sites in the observation area, digging a hole down to the aquifer or drilling a borehole can provide an adequate site. Another possibility can be sampling surface waters that could possibly be connected with the tracing area. However these samples are generally contaminated with organic and inorganic particles, which raise the detection limit for fluorescent dyes. Sample takers should be advised to take only clean samples if possible. The samples can also be filtered directly after being taken at times.

If light sensitive tracers such as eosin or uranine are used, the samples should be exposed to as little light during sampling as possible. This means that the sampling site should be as close as possible to the source (Fig. 30).

3.2.4 *Choosing the tracer*

In considering which type of tracer is to be used, several criteria must be considered. Since there is no one ideal tracer, let alone several ideal tracers available, the choice must be based on the thorough consideration of all limiting factors. With multiple tracing tests, the difficult planning can often only be carried out by experienced hydrogeological, hydrological, and analytical experts. The tracer's advantages and disadvantages, setting the order of importance of the observation sites, and difficulties or impediments during the injection of the tracer and sampling force compromises. Especially the mutual disturbances between fluorescent dyes during analysis must be considered. The success or failure of the tracing test depends upon the appropriate choice in the tracer. Finally the newest human-ecotoxicological valuations of the tracers are to be considered, too (UBA 1997).

3.2.4.1 *Sorptivity and ion exchange*

Tracers that tend towards sorption and ion exchange can only be rarely used in channels and aquifers that have large relative surfaces. As a rule, anionic substances do not tend towards sorption nor to ion exchange. Cations are all the more adsorbed, the higher the ionic charge and the smaller the ionic radius. Among the fluorescent dyes, uranine has the least sorptivity in neutral and alkaline media; it is the preferred tracer

in pore groundwater. Naphthionate, pyranine, eosin, and sulforhodamine B have low sorptivities, the other rhodamines and the optical brighteners are more strongly sorptive (Fig. 27).

All alkaline salts more or less strongly tend to ion exchange. Hereby, lithium undergoes the least, sodium stronger and potassium the strongest ion exchange. Borax is a salt, but does not undergo ion exchange. It is subject however to a sorption in the underground.

Radioactive and activated isotopes are transformed into strong complexes to suppress the sorption and ion exchange in the cases where they are not already anions. Only in the case of single-well measurements is a good sorption onto the borehole walls a wanted effect.

3.2.4.2 *Pore sizes*

The width of the pore spaces flown through is mainly for drift tracers a decisive criterion. The narrower the pores, the smaller the drift tracer is necessary. The smallest drift tracers are the phages. Phages, bacteria, and microspheres can be used in most porous aquifers and in fissured aquifers. Spores have proven themselves in karsts. There are no published reports of applications of spores in fissured aquifers.

3.2.4.3 *Water quality*

Before a tracing test is carried out, possible interactions between the water to be traced and the tracer need to be considered, as well as possible disturbances during analysis. Acidic water in moor areas or groundwater enriched with carbonic acid transform uranine into a strongly sorptive cation. This is not of such importance with the other fluorescent dyes. However, one should be well aware of the reactions of the dyes in the corresponding pH-ranges involved.

Humic acids fluoresce and increase the detection limit of the fluorescent dyes when present.

During salt tracing tests, the salt content of the water to be traced must be known beforehand. Possible variations in the salt content can also be the cause for a considerable increase in the detection limit in certain cases. Increases and variations in the chloride contents must be considered especially in surface waters, in river bank filtration water, in groundwater in industrial areas, and due to seepage of road salt.

Turbid samples are unwanted since, due to light scattering, the fluorimetrical detection limit is increased. Also, when examining for cations, bacteria, and phages there can be an increased sorption, with other chemical examination methods, e.g. colorimetry or titrimetry other disturbances can occur. Turbid water samples also strongly impair the counting of the drift tracers such as microspheres and spores.

3.2.4.4 *Light impact*

In glacial and groundwater tracing tests, the tracer's sensitivity to light is of no great importance. If surface waters are to be traced and quantitative results are wanted, substances which are stable in light must be used. If the light sensitive fluorescent dyes must be used, the tracing test must be conducted at night otherwise the results cannot be quantitatively evaluated. In many cases qualitative results are satisfactory.

The light has of course less impact, the lower the luminosity and shorter the exposure. In shallow channels with clear water, the influence due to light is the strongest.

In deep and turbid waters however, the short-wave radiation that destroys the dye cannot penetrate very deep.

Independent of the tracer's light sensitivity, the water samples should be protected from light and stored in the dark. Exposure to light influence not only destroys those substances sensitive to light, it also promotes the growth of algae in the sample containers.

3.2.4.5 *Water usage*

Whether the water resources under investigation are used or not is often the decisive criterion in the choice of the tracer.

Of course, tracing tests should impair the use of water captation facilities as little as possible.

There is a concentration difference between uranine's visibility limit and detection limit of 1000:1. Whenever possible, uranine's visibility limit should not be exceeded in tracing tests in water capatation facilities. If a water treatment with oxidizing chemicals is in use, even higher concentrations of uranine and eosin can be destroyed. In such cases there is no impairment of the water in use and therefore the water supply is not disturbed. If necessary, the dosage of the treatment chemicals can be increased for a short time.

A doctoral candidate had little success with several dye tracing tests in a Muschelkalk series in a karst region. After having dyed an active doline with a large amount of uranine, it reappeared in a water tapping which was set-up with a chlorine treatment, although the doline was nearer to the receiving stream. The uranine concentration was almost 10,000 µg/l and could only be partially removed by the chlorine treatment. Through mixing in the header tank, ca. 600 µg/l uranine entered the water supply and turned the water green in the village that was supplied with the water. Although the tap water in the village was green, one homemaker washed a load of laundry. The uranine caused spots on the laundry, most likely due to the softener used (KÖHLE 1980). Even rinsing with clear water did not remove the yellow spots. One of the spotted formerly white shirts was given to the author to see if he could remove the spots. Immersing the shirt twice in a diluted ammonia solution and allowing to work overnight, brought about the desired results.

This occurrence shows that the uranine, although indeed physiologically harmless, can lead to difficulties when misused. Consumers should be duly warned in such cases. Furthermore, other dyes can have consequences that are much worse than those described here.

As stated before, the dye concentrations that reappear in the observation sites are physiologically harmless. Nevertheless due to psychological reasons, care should be taken that the dye is unrecognizable when it reappears in water supply plants, springs, and receiving streams. Environmentalists, fishery owners or leasers, and particularly paper mill owners sound the alarm overly quickly, although there is no reason for it. Uranine is totally harmless for the production of paper. Firstly it is not sorptive, i.e. it does not stick to the paper fibers. Secondly, uranine would be fully destroyed in chlorine bleach used in the production. However, even though there are no damages to be expected, such occurrences should be avoided.

However, there are cases where visible dye effects are wanted by the contracting authorities as a public demonstration. Such cases can then be used to induce the mu-

nicipal councils to vote unanimously for a new clarification plant or a water treatment plant.

Salt tracing tests in groundwater are generally harmless for the water supply tappings. The dilutions are so high that at the reappearance sites no problems should be expected. However, with injections in surface waters, damages to the fish stock must be assumed. In the chronicles of salt tracing tests, there is a case in the Black Forest where after injecting 10 t rock salt in a stream with a discharge of 30-40 l/s, the trout stock did not survive over a distance of ca. 400 m. The fishery leaseholder proved damages due to a depletion of the fish stock over 4000 m to 75% and asked for compensation of DM 1,885.85 from the workers.

Radioactive substances that are to be injected in the catchment area of water tappings or in surface waters are not only rejected by the general public, but also by the authorities. In the meantime, sufficient other means for succeeding with such tracing tests in other ways are available.

Activated isotope elements are only used in small amounts. An impairment of the water supply is not to be expected.

Reservations are regularly brought against using phages and bacteria, although the type and concentration at the reappearance sites or in surface waters are harmless. Unfortunately, the tracing test workers do not receive sufficient support from the hygienists either and are limited in their ability.

Microspheres and spores are totally harmless even in large injection amounts. The first are artificially produced and do not interact with the environment. The latter are naturally produced and also totally harmless. The dyes that are attached to the surface of the spores adhere so tightly, that they would pose no problem even if they were not harmless.

Summarizing, only the fluorescent dyes cause mutual disturbances in the analytical determination during multiple tracing tests. The recommendation by SCHNITZER & WAGNER (1967) for using three different aromas is of no importance in practical use and can be neglected here. Without exception, the other tracers can be used without cross-influence.

3.2.4.6 *Analytical criteria*

To carry out the analyses needed for tracing tests, an analytical laboratory needs a modern spectro-fluorimeter or else the tracing tests cannot be optimally realized, since fluorescent dyes are the preferred tracers. The most important factor in multiple fluorescent dye tracing tests is their analytical separation, which as a rule must be carried out if more than one dye is involved.

If a tracing test is conducted with only one fluorescent dye or if the dyes used do not mutually disturb each other during the direct measurement, the determination is unproblematic. If the fluorescence spectra in the multiple dye tracing test are superimposed, the analytical effort needed to determine the individual dyes increases considerably.

Dyes disturb salt analyses only rarely, e.g. in the colorimetric boron determination in heavily dyed water samples. However, boron can easily be determined with ICP and here even higher dye concentrations do not cause problems. Dyes also do not impair the determination for alkali salts with flame photometry.

Phages, active and activated isotopes can only be determined in special laboratories. They are often not chosen as a tracer, because a possibility to determine them is not available. Colony counts for the bacterium *Serratia marcescens* can also be carried out in a normal laboratory, provided a closed-off room is available for it.

3.2.4.7 *Expenditure for the provision, transport, injection, sampling, and analysis*
Tracers are all the more costly, the more they cost to obtain and the higher their detection limit is. This means that an expensive tracer is equivalent to a reasonably priced tracer that has a higher detection limit. Uranine is reasonably priced and also detectable in low concentrations. If a large amount of tracer is needed, then there is a considerable expenditure for the transport, dissolution, and injection of the tracer necessary. Especially for hard to reach injection sites, e.g. in mountainous areas and in regions with little water the only tracers which can be considered are those tracers which can be detected in low concentrations and which require little water for dissolving or suspending and injecting. These are above all the fluorescent dyes, phages, bacteria, microspheres, and spores, as well as active and activated isotopes.

The portion of the expenditure for sampling is usually quite high for most tracing tests. This can be reduced with the help of automatic samplers and with accumulative samples, such as activated carbon and spore nets. However, accumulative samples only provide semi-quantitative results for certain time periods. Activated carbon can be used to enrich fluorescent dye samples and also active and activated analytical isotope samples. Spore nets are suitable for *Lycopodium*-spores and microspheres with a diameter over 25 μm.

Multiple tracing tests greatly reduce the sampling costs, since the tracers recovered can be detected in one sample. Only one sampling plan is needed for all of the tracers injected. The costs would be much higher if each tracing test were carried out individually.

Costs for the analyses are the lowest for direct measurements, that is when the samples are measured directly out of the bottle without further treatment. Such analyses are routinely carried out for one or more fluorescent dyes in the spectrofluorimeter or flame-photometrically in the AAS. Display, printout or storage of the data can be conducted without troublesome transformations directly as true concentrations. More painstaking are colorimetric and titrimetric or even more so gravimetric determination methods. Detection with HPLC can be automated, needs however comparatively longer test times.

Very painstaking are microbiological determinations for bacteria and phages; with these tracers also extensive preparations of the tracer-suspensions for the injection are required.

Enrichment procedures needed when the concentrations are near the detection limits for dyes, phages, and isotopes are also painstaking.

Sampling and analysis costs are also incurred in the registration of conductivity, radioactivity, or fluorescent dyes in situ. However, these measurements are not always as accurate as in the laboratory.

Activated isotopes are not only expensive to obtain, they are also expensive to determine. Their expenditure is so high that their use is more due to scientific interest.

3.2.4.8 *Injection site*

With surface water tracing tests, the type of substance injected generally does not play an important role. The injections are usually unproblematic to conduct. The injection site should be chosen so that at the first sampling site a thorough mixing has occurred over the entire river section.

When injecting tracer solutions through narrow tubes underground, only those substances should be used which need little water to dissolve or be flushed through.

During injections in the unsaturated zone, large amounts of suspensions or solutions are also hard to handle. Furthermore, adsorption of the tracer in the unsaturated zone must also be considered. Therefore, only those tracers should be used which do not undergo strong sorption.

3.2.4.9 *Sampling sites*

In choosing the tracer, the sampling possibilities must also be considered. In hard to reach mountainous areas for example, a dense sampling is usually not possible. Water soluble substances may then be not detectable or only observed undifferentiated. Therefore, in cases where an automatic sampling unit is not available, only those tracers should be chosen that can be sampled accumulatively. These are above all spores, which can be accumulated over long periods in spore nets. Similar long term sampling periods are achieved with activated carbon filters, which adsorb the dye tracers at the sampling site for definite time periods.

3.2.4.10 *Longterm behaviour of the tracers*

Some tracers undergo temporal degradation or decay. Therefore, in choosing the tracer the temporal course of the test must also be considered.

As living beings, bacteria that do not live in water undergo a natural reduction in viability. The bacteria type *Serratia marcescens* generally do not survive for longer than 10 days in groundwater. With phages, the decay rate is very different.

Active isotopes have very different half-life times. It must be assured that at the end of the tracing test their activities are still high enough to accurately measure so that calculated tracer concentrations are accurate enough.

3.2.5 *Deciding on the necessary tracer quantity*

A certain amount of experience is necessary to select the correct quantity of tracer, M. There are indeed several formulas for calculating the correct quantity in the literature, but they yield clues as to the quantity needed rather than exact values.

In 1912, DIENERT published detailed instructions for calculating the correct quantity of uranine. There were four formulas in his monography for different applications (cesspools, drains, dolines, and springs) which he simplified a year later.

Formula (DIENERT 1913): The following formula is listed on page 95 for undifferentiated undergrounds:

$$M = Q \cdot L \cdot k \text{ [kg]}$$

where Q = discharge or pumping rate of the spring or well [m^3/s], L = distance [km], k = coefficient for the tracer; k uranine = 0.25, k fuchsine = 5, k sodium chloride = 250.

For low permeable undergrounds with uranine as the tracer:

$$M = Q \cdot L \text{ [kg]}$$

ZÖTL (1974) noted that the formula is only valid for determining uranine with activated carbon and that spores require two to three times the quantity of uranine's. Aside from that, it should be mentioned here that fuchsine has strong sorptive properties and should not be used as a tracer.

Formula UNESCO 1 (1973-1983): The following formula is given for different aquifers:

$$M = L \cdot K \text{ [kg]}$$

where L = distance [km], K = coefficient for the aquifer; K sand groundwater = 0.2-1, K fissured groundwater = 0.2-2, K karst groundwater = 0.2-1, K cohesive aquifers = 0.5-2.

Since there are no further specifications to the formula, it can be assumed that the formula can be applied for uranine.

Formula UNESCO 2 (1973-1983) for porous and fissured groundwater:

$$M = K \{(Q \cdot L)/v\} + 0.02\ V \text{ [kg]}$$

where K = coefficient for the aquifer; K porous groundwater = 500, K fissured groundwater = 3000, Q = spring discharge [m^3/s], L = distance [km], v = estimated groundwater flow velocity [m/day], V = volume of the traced groundwater [1000 m^3].

It can also be assumed here that the formula is valid for uranine.

Formula TIMEUS (1926): Although it is not stated, the formula is obviously valid for karst water tracing tests and uranine:

– Over a few 100 m: 100 g,
– Over a few km : 1-2 kg, or
– 1-2 g per 100 m^3 water.

TIMEUS causually referred to an formula from C. THURMANN, without listing a source. This formula is the same as the following from MARTEL:

Formula MARTEL (1921) for uranine tracing tests in karst:

$$M = Q \cdot L \text{ [kg uranine]}$$

where Q = karst spring discharge [m^3/s], L = distance [km].

Formula USA for spore drift tracing tests in karst: In the USA the following rule of thumb circulates for calculating the spore quantity in karst regions:

$$M = 0.3\ Q \times 0.6\ L \text{ [kg spore]}$$

where Q = spring discharge [m^3/s], L = distance [m].

The following simple example shows that this rule of thumb can only be used under certain conditions: A karst spring with 1000 l/s discharge (e.g. Blautopf) should be marked from a doline 1.5 km away. Here only ca. 300 g spores would be needed, which would be totally unpracticable!

Formula SILINE-BEKTCHOURINE (1951): Actually this is not a formula, but rather an array of substance and underground specific parameters. The calculations can be realized thus:

$$M = L \cdot C \text{ [kg]}$$

where L = distance [km], C = factors for tracer and underground:

	Clay stone	Sandstone	Fissured rock	Karst
Uranine	0.5-2	0.2-1	0.2-2	0.2-1
Eosin	0.5-2	0.2-1	0.2-2	0.2-1
Erythrosine	1-4	1-3	1-4	1-4
Congo red	2-8	2-6	2-8	2-8
Methyl blue	2-8	2-6	2-8	2-8
Spirit blue	2-8	2-7	2-8	2-8
Ponceau red	1-4	1-3	1-4	1-4

The author most likely only had very short flow distances in mind, because he gave his data for distance of only 10 m. Here, the values have been adapted to better compare with the other formulas.

Excepting for the weakly fluorescing erythrosine, that has been used only in extremely special cases and then only with the express wish and permission of the health authorities, the other non-fluorescing dyes listed should be taken off the list. Their sorptivity is so strong, that they are adsorbed even in undergrounds with low surface contact, e.g. karst.

Formula LEIBUNDGUT (1974):

$$M = Q \cdot t \cdot C_{max} \cdot A \cdot S \times 0.0018 \text{ [kg]}$$

where Q = spring discharge or pump rate [m^3/s], t = assumed length of the dye passage [h]. For the estimation, PARRIAUX, among others, (1988) recommends: $t = 3\ L \cdot v$, whereby it is not noted which flow velocity is meant; possibly that at the peak concentration, C_{max} = assumed peak concentration [µg/l], A = adsorption coefficient, always larger than 1; it depends on the sorptive properties of the tracer and on the underground, S = certainty factor; it can be larger or smaller than 1 and is dependent on the test conditions and circumstances.

Although it is not expressly stated, the formula was most likely tailored for uranine usuage. It is assumed that the dye passage can be estimated for length and peak concentration. The anticipated breakthrough curve is replaced with an equilateral triangle. Due to problems with the formula in test areas where the samples are not taken from springs, but rather from e.g. piezometer tubes, LEIBUNDGUT and WERNLI adapted the formula in 1982 thus:

Formula LEIBUNDGUT & WERNLI (1982): This formula is basically for use in pore groundwater tracing tests and special attention is given to the sorptivity of tracers in the aquifer. It is based on the distribution of a dye cloud, that due to dispersion spreads to the sides, yet keeps its form for a certain flow path (Fig. 133).

$$M = tg\ \alpha/2\ h \cdot s\ (2s \cdot C_{max} + A_m\ (2s - s_1)) \text{ [kg]}$$

where α = entrance angle according to Figure 133, h = thickness of the aquifer traced [m], s_1 = fan length [m], s = distance between injection site and sampling site [km], C_{max} = peak dye concentration [µg/l], A_m = adsorbed dye quantity [mg/m^3].

For uranine set to 1.0, for other dyes >1, depending on their sorptivity.

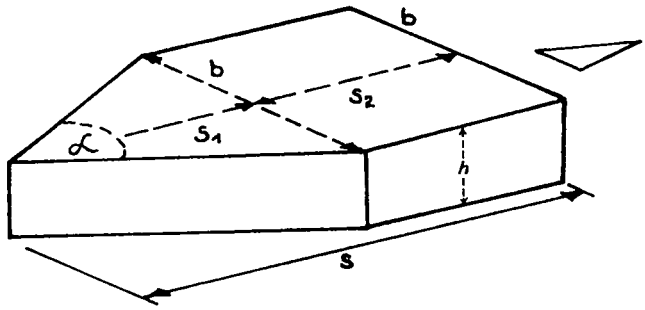

Figure 133. Assumed form of a traced aquifer. α = entrance angle, b = fan width, s_1 = fan length, s = distance injection site – sampling site, h = height of the aquifer traced.

Experience shows that the entrance angle, α, can be set to 30°, assuming a uniform injection over the entire thickness of the aquifer and that sufficient flushing of the tracer was carried out. Then the above formula becomes:

$$M = 0.268\, hs_1\, (2sC_{max} + A_m\, (2s + s_1))\ \text{[kg]}.$$

Formula ALEY & FLETCHER (1976): Valid for karst channels and fractured zones with uranine as the tracer.

$$M = 1.478\sqrt{LQ / v_a}\quad \text{[kg]}$$

where L = distance injection site – sampling site [km], Q = discharge or pumping rate at the sampling site [m³/h], v_a = estimated effective flow velocity [m/h].

That the formulas listed here can only be used as a basis for deciding the quantities needed can be clearly seen from two examples (PARRIAUX et al.1988):

1. Example: Pore-groundwater tracing test (Q = 20 l/s, v = 10 m/day, t = 3600 h, s = 0.5 km, s_1 = 100 m, V = 100, h = 10 m, C_{max} = 10 µg/l, $A = A_m$ = 1)

Formula	M [kg]
UNESCO 1 (clayey material)	0.25-1
UNESCO 2	3
BENDEL (sandy material)	0.0025
LEIBUNDGUT 1974	1.3
LEIBUNDGUT & WERNLI 1982	2.92

2. Example: Karst or fissured groundwater tracing test (Q = 100 l/s, v = 1000 m/day, t = 216 h, s = 3 km, s_1 = 100 m, h = 100 m, V = 300)

Formula	M [µg]
UNESCO 1	0.6-3
UNESCO 2	0.16.

Formula KINNUNEN (1978) for tracing tests in river water with phages:

$$M = Q \cdot t \cdot a \cdot 10^6 \text{ [phage count]}$$

where Q = discharge [m^3/s], t = estimated flow time [s], a = factor between 20 and 50 according to the phage properties and background.

With this abundance of recommendations for deciding the correct quantity of tracer, it is not always easy to select the correct formula without sufficient experience. Of course, even tracing experts with years of experience do not adhere to just one formula, but rather use their expertise to take into account all of the local and hydrometeorological conditions in a well known hydrological and geological test area to select the appropriate quantity or quantities of tracer. There are also outside factors that must be considered, such as when visible dye traces may not occur under any circumstances. On the other hand, the opposite can also be wanted, as when visible dye traces in the public water supply are needed to help pass a new water facility or to set the boundaries of a water protection area.

In spite of the considerable number of formulas for determining the appropriate quantity of tracer needed already listed, our own experience in deciding the appropriate amount should also be given here as a formula. It is stressed again that such rules of thumb only provide a basis for deciding the correct amount. It must also be conceded that even with years of experience, failures cannot be totally eliminated, i.e. tracing tests without a positive recovery.

The following empirical formula states that the quantity of tracer needed is mainly dependent upon the distance that will be covered. Furthermore, the properties and detection limits of the tracer used and the prevailing test conditions are also defining. The proposed formula is:

$$M = L \cdot k \cdot B \text{ [kg]}$$

where L = distance to the most important sampling site [km], k = coefficient for the tracer, if not uranine.

Eosin:	5.5
Amidorhodamine G:	2
Rhodamine B:	15
Sulforhodamine B:	4
Rhodamine WT (as 20% solution):	20
Pyranine:	5.5
Na-Naphthionate:	15
Tinopal:	3
NaCl:	20,000
KCl:	10,000
LiCl:	1,000
Spores:	1.5
Surfactants:	20
Phages (particle count):	10^{13}
Serratia marcescens (germs):	10^{13}
Microspheres:	10^{12}
Indium for activation analysis:	0.1

With these tracer relevant factors, the usual analysis methods, i.e. spectro-fluorimetrical dye determination, determination of alkalis with flamme-photometry and the other microbiological methods, etc. are assumed.

B = Factor for the prevailing test conditions.

The conditions taken into account here are those that are not considered in the distance nor included in the tracer-specific properties.

0.1-0.9:

– Surface or underground channels with rapid flow.

2-4:

– Light influence upon light sensitive tracer if injected in surface waters,
– Injection in surface waters with over 1000 m^3/s,
– River bank filtration with flow discharge up to 5 m^3/s,
– Pore groundwater investigations with k_f-values under 10^{-3},
– Solid rock investigations with an assumed scattering angle over 60°,
– Injection through the unsaturated zone between 1 and 30 m,
– Sample water with low tracer background levels,
– Turbid samples or samples with natural fluorescence.

5-10:

– Injection through the unsaturated zone over 30 m,
– Injection in the soil zone with cohesive underground,
– Groundwater tracing tests near a groundwater divide,
– Cases where special attention must be given to a secondary observation site instead of the anticipated main observation site.

3.2.6 *Test plan*

A listing of all necessary details is also a part of the preparation of the tracing test and should be arranged with and handed out to all participants to guarantee smooth operations. The test plan should contain the following:

– District and local designation,
– Exact description of the injection site,
– Home and work telephone numbers of the participants and their substitutes,
– Contracting authorities,
– Goal,
– Type and quantity of tracer,
– Injection time,
– Quantity of priming and flushing water needed,
– List of the sampling sites and times.

3.3 TRACING PROCEDURE

The following sections cover several aspects of the tracing procedure that need to be observed.

3.3.1 *Time of injection*

The begin of a tracing test should be set so that there is enough time for all preliminary preparations and so that all personnel and material are in place, allowing of course a safety margin. Normally, it should be at the start of the week, since at the

beginning of a tracing test the samples are taken closer together. Holidays and vacation periods should also be considered in planning the test. Factory hours in industrial areas should also be taken into account with smaller tracing tests (CLASSEN 1964).

In planning multiple tracing tests, it can be advantageous to plan delayed injections of the different tracers with respect to the sampling times and the possible overlapping of the tracer reappearance. The most effective tracer should be used for the longer flow distances and those which are less sensitive for the shorter distances.

Tracing tests are generally planned well in advance and have to take the weather that comes on the day of injection. Nevertheless, extreme hydrometeorological conditions such as long periods of dryness or continual heavy rains can be reasons to consider postponing the test.

3.3.2 *Tracer injection*

It is better to dissolve the fluorescent dyes in the laboratory. As an exception, uranine can be dissolved in the field, provided it is crystalline. Powdery dyes can be blown away by even light breezes, resulting in contamination and losses. Under no circumstances should people who are present at the tracer injection take samples.

A sufficient amount of water and containers for the tracer solution must be available at the injection site. Substances with a low solubility such as detergents or borax should be dissolved with electro-stirrers (cf. Fig. 68). Sometimes it helps to rock the filled tanks back and forth (DOSCH 1968). If the optical brighteners are not available as a liquid, as they usually are, they have a low solubility in the 10°C groundwater which is prevalent in the temperate zones and an even lower solubility in hard water. Adding 10 g of complexing agent per litre mixing water is recommended to increase the solubility. With the rhodamines, the addition of the solubilizer acetic acid or diethylene glycol is recommended for increasing the solubility.

Less problematic are the liquid tracers rhodamine WT or tinopal ABP, although harder to transport. However, they must be diluted at the injection site to prevent sinking caused by density differences. Sometimes, undiluted dye solutions can be injected directly into flowing rivers (Plate 2).

The injection procedure depends on the local conditions. Active dolines with a continuous water flow are ideal and the tracer solution can be injected without trouble. If the water flow is turbulent, even crystalline uranine can be poured in directly. The same is true for surface waters and rivers (Plate 1).

If the injection must take place through the unsaturated zone, priming and then afterwards flushing the tracer through the injection site is imperative. This is often wrongly thought of as unproblematic. An injection has only been competently carried out, if the priming and flushing were completed thus: although it seems rational that small amounts of tracers should be flushed with large amounts of water, both amounts should be approximately equal. First off, the seepage path underground must be primed and rinsed free. Not until it can be assumed that the priming water has reached the groundwater, should the injection take place and then started with the flushing process. The water flow must be uniform from start to finish, otherwise the individual water pulses could transport the tracer into nooks and niches where they could be bound.

Increasingly, tracing tests are conducted when planning new building sites in order to obtain information about the temporal and spatial discharge of possible immissions. In these cases, the tracer should not be provocatively injected deep underground. It can be assumed that during building, only part of the cohesive cover layers will be removed and that there will still be a sufficiently large part of the unsaturated zone with its cohesive material left to maintain a certain protective function. The following procedure has proven itself in such cases: A 1 × 1 × 1 m pit is dug and filled with 800 l water, i.e. up to 20 cm below the surface top edge. If less than half has seeped through in 24 hours, carrying out a tracing test would be senseless.

There are several different cases to be differentiated with tracing tests in wells or boreholes according to the type, diameter, and length of the open filter section.

The simplest case is when the top edge of the filter section is below the groundwater level. In this case, the tracer solution can be poured into the pipe. Only if the filter section is very long should suitable measures be taken to assure a uniform mixing in the pipe or in the well.

If a part of the filter section is in the unsaturated zone, simply pouring the tracer solution into the pipe would have dire consequences: like a sponge, the unsaturated zone would adsorb a considerable amount of the tracer solution and that part would then not be available for the actual tracing test (Fig. 134). The tracer solution has to be injected directly into the groundwater in these cases. Also priming or flushing with extraneous water through a hose would only produce an increase in the groundwater level which would then allow part of the tracer to enter the unsaturated zone, where it would stay after the injection was completed. An increase in the groundwater level can be avoided by withdrawing water near the bottom of the aquifer and then pumping it back in through a closed container with the tracer solution to be then injected under the groundwater level (Fig. 135). This is continued until only traces of the tracer solution can be detected in the pumped water. This can be visibly checked for dyes and by checking the electrolytical conductivity for salts.

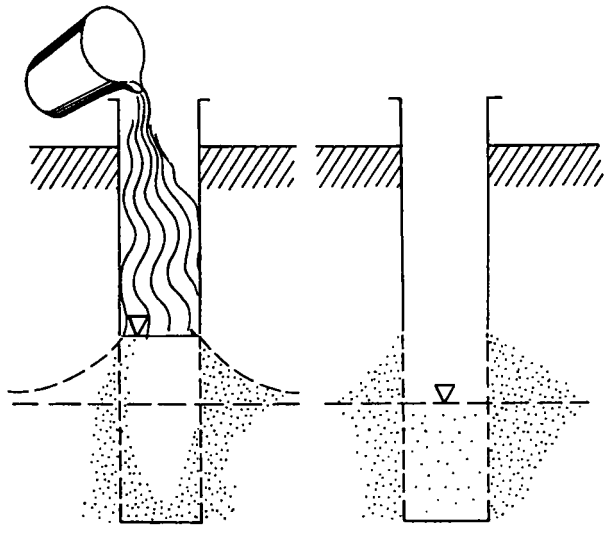

Figure 134. What happens when a tracer solution is poured into a borehole. Part of the solution is adsorbed in the unsaturated zone (left). After the injection is over, tracer remains in the unsaturated zone (dotted, right).

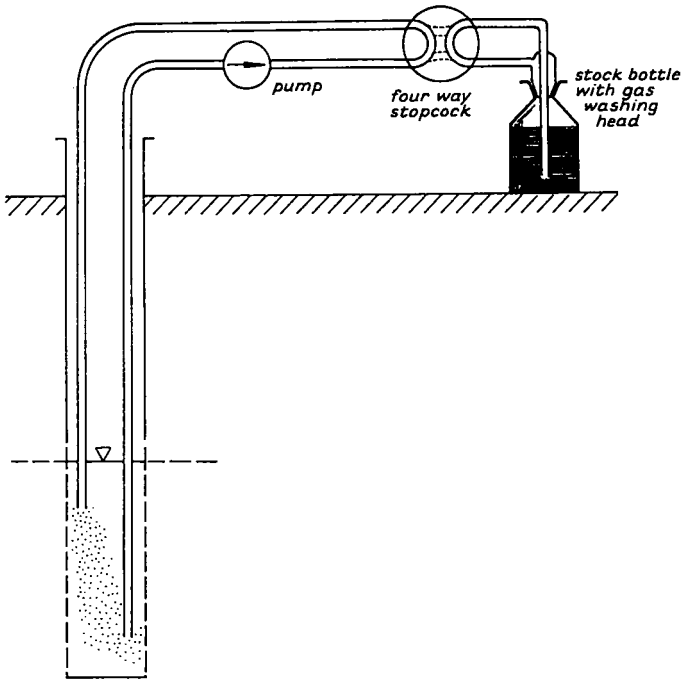

Figure 135. Injecting a tracer in a well through circulation pumping.

In cases with narrow monitoring wells or shallow aquifers, such a pumping procedure would take an excessive amount of time. Then the tracer can also be carefully injected in the groundwater column with a hose. The tracer is prevented from entering the unsaturated zone with a small amount of extraneous water above the water level (Fig. 136).

Injecting the tracer in flowing or standing water bodies is generally unproblematic. In some cases however, there are particularities that must be observed.

Again and again one hears the false assumption that a tracer injection over a certain time period in a channel with percolation possibilities is more effective than a temporal point source injection (LUKAS 1959a, CLASSEN 1964). The opposite is true (KÄSS 1970a). Namely, if percolation occurs, the percentage of the percolation in the channel flow and thus of the tracer is the same, independent of the time in which the percolation occurred. With a long continuous tracer injection, the concentration of the tracer at the observation site can be lowered to below the detection limit (Fig. 137). The recommendation from RICHTER (1944) that with 'fast flowing waters, the marking substance should be injected as drops over several hours' is incorrect.

With wide rivers, a simultaneous dyeing of the entire river cross-section is only possible with great effort. A successful distribution over the cross-section could be obtained close above or below an overfall weir.

The tracer injection in lakes is carried out according to the task at hand. The easiest case is when the plume of a river is to be followed in a lake. Then, the tracer just needs to be injected in the inflow. If a lake is to be uniformly marked with fluorescent dye, a motor boat towing the tracer in a linen sack can be used to distribute the tracer in zigzags over the surface.

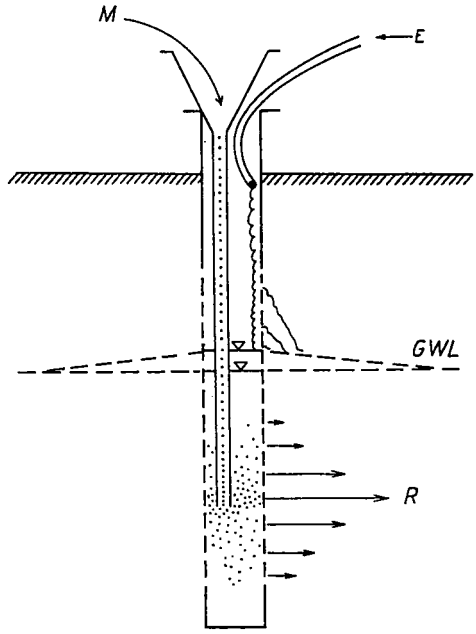

Figure 136. Injecting a tracer in a monitoring well. A low extraneous water inflow, *E*, prevents the tracer solution, *M*, from entering the unsaturated zone; *GWL* = groundwater level undisturbed and raised, *R* = flow direction of the marked groundwater.

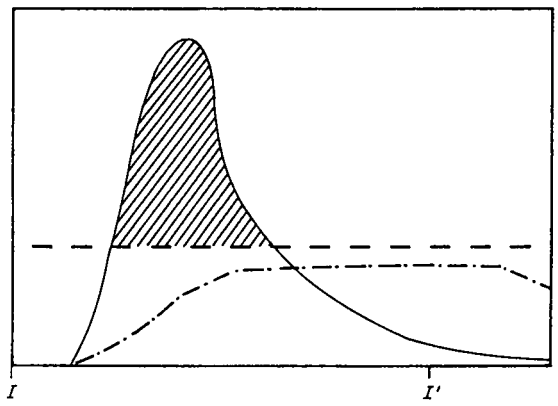

Figure 137. Breakthrough curves with a temporal point source injection (solid) and with a lengthy continuous injection I – I' (dash-dot). In the second case, the recovered concentration at the observation site is continually under the detection limit (dashed). In the first case (DIRAC pulse), the concentration is clearly over the detection limit (hatched area under curve).

If percolation sites are presumed in certain spots in a lake or river, linen sacks filled with the tracer substance and weights are sunk. The dye plume can be best followed at night with strong flood lights. Such measures were applied in 1957 in the southeast corner of Lake Formarin (Lechtaler Alps, Vorarlberg/Austria), to precisely locate the underwater swallow holes (ZÖTL 1958). Eleven kg of red spores in plastic containers were brought by professional divers to the swallow holes several metres underwater.

If strong turbulence prevails, e.g. in rapidly flowing surface water or in vacuum remediation wells, some tracers can develop strong foaming. Surfactants have this characteristic as also sulforhodamine B, which has even also caused systems breakdown.

3.3.3 *Sampling*

The people taking the water samples have a great responsibility. Incorrectly taken or treated samples are unusable and thus lost. Their absence often leaves important lacks in the observation period. Samples that are incorrectly labelled can be found and set back in their original place, but the work caused is unnecessary and often painstaking.

3.3.3.1 *Sample plan*

The sampling times and order for the individual sampling sites can be listed in the test plan. The basic rule still applies that it is better to have a sample too many than a sample too few, since especially groundwater tracing tests can have unexpected results (KLEINERT 1976). Normally, the samples are taken closer together at the beginning and then farther apart towards the end. With observation sites that are far apart, sampling plans can be set up with groups of sampling cycles, as in the following example from a karst tracing test:

Site No.	Distance to injection	Test day 1-2	3-4	5-7	8-14	15-21	22-49
1	600 m	2-hourly	4-hourly	4× daily	2× daily	daily	3× weekly
2	950 m	"	"	"	"	"	"
3	1.4 km	4-hourly	4× daily	2× daily	daily	daily	3× weekly
4	2.9 km	"	"	"	"	"	"
5	5 km	"	"	"	"	"	"
6	11 km	2× daily	2× daily	daily	daily	daily	3× weekly

The sampling must be carried out according to plan, even if the dye should visibly appear. However, the tracing test project head should be notified immediately, in case changes are to made.

3.3.3.2 *Sampling procedure*

Automatic sampling devices, some also battery operated, are available and the sampling plan can be programmed in the device. However, it is advisable to only set them up where outsiders cannot harm or tamper with them.

To assure that the samples taken are not contaminated from previous samples, the bottles must be adequately rinsed with the sample water before being filled. Care must also be taken to avoid contamination during filling if springs covered with algae or moss growth are sampled.

If several groundwater monitoring wells in porous aquifers are to be sampled in short intervals – and the groundwater level is less than 8 m – installing reasonably priced micro submersible motor pumps, socalled camping pumps, is recommended. These can be operated with 12 V DC (KÄSS 1989, Fig. 138).

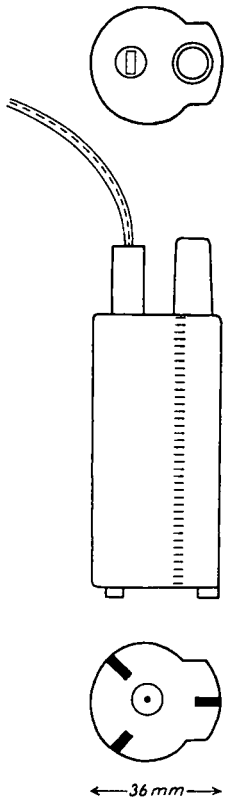

Figure 138. Micro-submersible motor pump 12 V DC. Top, side, and bottom view. Permanently installed cable connection and socket for tubes with 8 mm inner diameter.

After changing, the spore nets for *Lycopodium*-spores and activated carbon sacks for enriching the dye samples should be hung back in place the same way.

Samples for microbiological analyses must be taken under sterile conditions, which should not cause any problems sampling faucets from supply wells or springs. KÄSS et al. (1983) have described a procedure for sampling monitoring wells to a groundwater level of 3 m with a peristaltic pump, e.g. Masterflex-pump, and silicon tubing. Here, the sample water comes into contact only with the autoclavable silicon tubing (Fig. 101).

3.3.3.3 *Sample containers*

The type and size of sampling containers must be agreed upon with the laboratory conducting the analyses whereupon an ample sample container should be chosen. Even if the actual analysis only requires a fraction of the sample water, unforeseen events can make repeat measurements necessary or give reason for further analyses. Larger sample volumes are subject to less change during transport and storage than smaller ones.

For most investigations, rectangular brown glass bottles are the most suitable (Fig. 139). If 250 ml bottles are used, there is generally enough sample water for multiple tests. Besides fluorimetric analyses, there is enough sample water for titrimetric analyses, e.g. for chloride or for colorimetric analysis for boron. Such analyses can

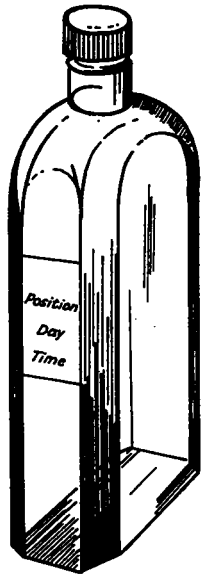

Figure 139. Shape of a space saving rectangular sample bottle, available from 50 ml contents.

be helpful in determining the right place for incorrectly labelled samples. Extra sample water is also advantageous when dealing with strongly varying tracer concentrations, since there is enough sample to rinse the flow-through cuvettes in the spectro-fluorimeter.

Modern spectro-fluorimeters have measuring programs, with which seveal wavelength pairs can be measured in a single sample one after the other. Repeated measurements with different settings are therefore not necessary. Thus, in certain circumstances, low sample volumes can be sufficient for multiple tests.

Plastic bottles are indeed unbreakable and frost-proof, but as brown bottles, they can generally only be ordered in extremely large quantities. Colourless bottles let in considerably more light than brown bottles and so contribute to dye decay, if the sample bottles are exposed to light. The microbiological activity is also furthered by light, and plastic is also a breeding ground for microorganisms. Furthermore, polyethylene bottles release substances that fluoresce near uranine's spectra (ZYGOWSKI 1985). Moreover, adsorption of sorptive fluorescent substances, ions, and particle tracers onto plastic can occur.

However, brown glass bottles can also release traces of lithium into the sample water. The darker the bottles and the longer the samples are in the bottles, the more lithium is released. The increase can be up to 3 µg/l Li, which causes problems in evaluating samples with low backgrounds.

It is important to be sure that the bottle tops do not have inserts. Screw tops with pads create a tight seal with the bottle. Both are reusable after washing and pose no tracer contamination threat.

The analysis for phages, bacteria, or radioactive substances often require large sample volumes. Such special containers are usually provided by the examining institute.

It is very important to make sure that the samples are correctly labelled. Sampling site, day, and time need to be clearly and legibly written with permanent ink. Magic markers, that contain fluorescent dyes (yellow, green, red) should not be used. The actual sampling time ±5 minutes should be recorded, not that noted in the sampling plan. In data processing, there is no 24:00 hours, but rather 0:00 hours of the next day. Gummed, not adhesive, labels should be used, since the latter are hard to remove and cause problems in dishwashers. However, gummed labels do not adhere well to plastic bottles.

The changing time for activated carbon sacks and spore nets, that have been hanging for a certain length of time, is to be recorded in the sample protocol. The number and/or name of the sampling site, the day and time, and the number of the replaced and the inserted samples are to be recorded. Remove the spore sample from the net with a wash bottle and fill into a 50-100 ml glass container. Thoroughly shake the activated carbon sacks free of water and pack into plastic bags. If the observation time is long, the originals of the changing protocols should sent to the laboratory or at the end of the observation period and copies should be kept by the sampler as a safety precaution.

3.3.3.4 *Sample transport and storage*

The sample should be stored and transported cool, yet frost-proof, and in the dark. Freezing the samples can lead to dye losses (HAIDER 1991). Stackable plastic boxes are available in different sizes for easy handling. A well-proven size is a 26 × 36 cm base and a 21 cm height, that holds 30 250-ml-rectangle-bottles. A full box of this size can still be easily carried by all. The walls of the boxes need to have air holes so that the water on the bottles can dry, or else mildew forms on the bottom of the box. If air holes are not available, they must be drilled through the sides, otherwise the mildew can even form on the bottle labels, making them illegible.

All samples, but especially those with perishable contents such as bacteria, phages, or radioactive substances, should be brought to the laboratory to be analysed as soon as possible. In rare cases, even uranine is subject to microbiological decay, which sets in ca. 10 days after sampling (SAYER 1988). Iodide can also be microbiologically decayed, even if it is radioactive (BEHRENS, pers. comm.).

3.4 SAMPLE ANALYSIS

When the samples arrive in the laboratory, they should be checked against the sample protocol and sorted chronologically. In doing so, possible mistakes can be discovered and perhaps corrected.

A better consistency in measuring the samples is achieved through series determination than with single determinations. On the other hand, waiting too long for a complete sample series causes delays in receiving the results, not to mention the possible changes in the sample contents due to long storage periods. An acceptable compromise needs to be found, especially since numerous samples from large tracing tests need corresponding storage room.

During series determinations, outliers can appear in the data; i.e. extremely high or low data points which do not fit in with the rest of the data. Generally, two sam-

ples were accidentally switched. If the other sample, often taken at the same time, is found, an internal switch can be done without having to inform the tracing test project head. Further water contents can be determined to provide certainty about the correct assignment of the samples.

The natural background must be determined for all tracers analysed. With physical measurement methods, this means that the apparatus' sensitivity must be high enough, to record a measurement signal, even if there is no tracer in the sample. It can also happen that the natural background is higher than normal. An example for the first case is the fluorimetrical uranine determination: Karst water from deep karsts are especially clear samples. However, the samples still produce a socalled background noise against a closed optical path of ca. 0.003 µg/l. For the second case, the flame-photometrical lithium determination can be mentioned, also with an example from deep karst. Such water samples have a low lithium content, yet still clearly over the detection limit of 1-2 µg/l. Only if the background noise and natural background of the water to be investigated have been determined, can the very first appearance of the tracer be exactly determined.

3.5 DOCUMENTATION OF TRACING TESTS

The test and sampling plans should be prepared so that electronic data processing can be conducted. A competent documentation, especially stored in a data bank, not only facilitates the evaluation of the tracing test, but is also an important source of information for further measures or tests (KÄSS 1982a,b, CRAMER 1982, BIDOVEC 1976).

File cards or data sheets should contain at least the following:

- Municipal and administrative district of the injection site,
- Number of the topographical map,
- Detailled designation of the investigation area,
- Name of the project head,
- Type and quantity of the tracer,
- Designation of the injection site with name, co-ordinates, altitude, geological formation,
- Start and finish times of the injection, priming and flushing water amounts or flow volume of a continual percolation,
- For each and every sampling site: Name, co-ordinates, altitude, geological formation and if appropriate discharge or pump rate. Furthermore a listing of the measured data for the tracer according to sampling time and concentration (with negative recovery, the start and finish of the observation period and the number of analysed samples is sufficient),
- Space for further plain text data about the weather conditions, special observations, literature, etc.

Such a data file can be sorted according to chronological or numerical order or other criteria. If however, the data are processed in a data bank, they can be called up and printed with simple or combined search options. Furthermore, electronic data processing enables the calculation of the effective flow velocity and recovery rate of the tracer. Moreover, programs that can plot the breakthrough curves – linear or time-logarithmic – can be installed (SCHWEIZER et al. 1985). Since the data that are

necessary for the documentation come from several different sources, an obligatory data ascertainment and data transmission noted in the test plan is advantageous.

As a matter of course, those connected with the tracing tests, such as the project head and analysts, sponsors as also active participants should be condignly mentioned in publications concerning the tracing test. Unfortunately this is often neglected.

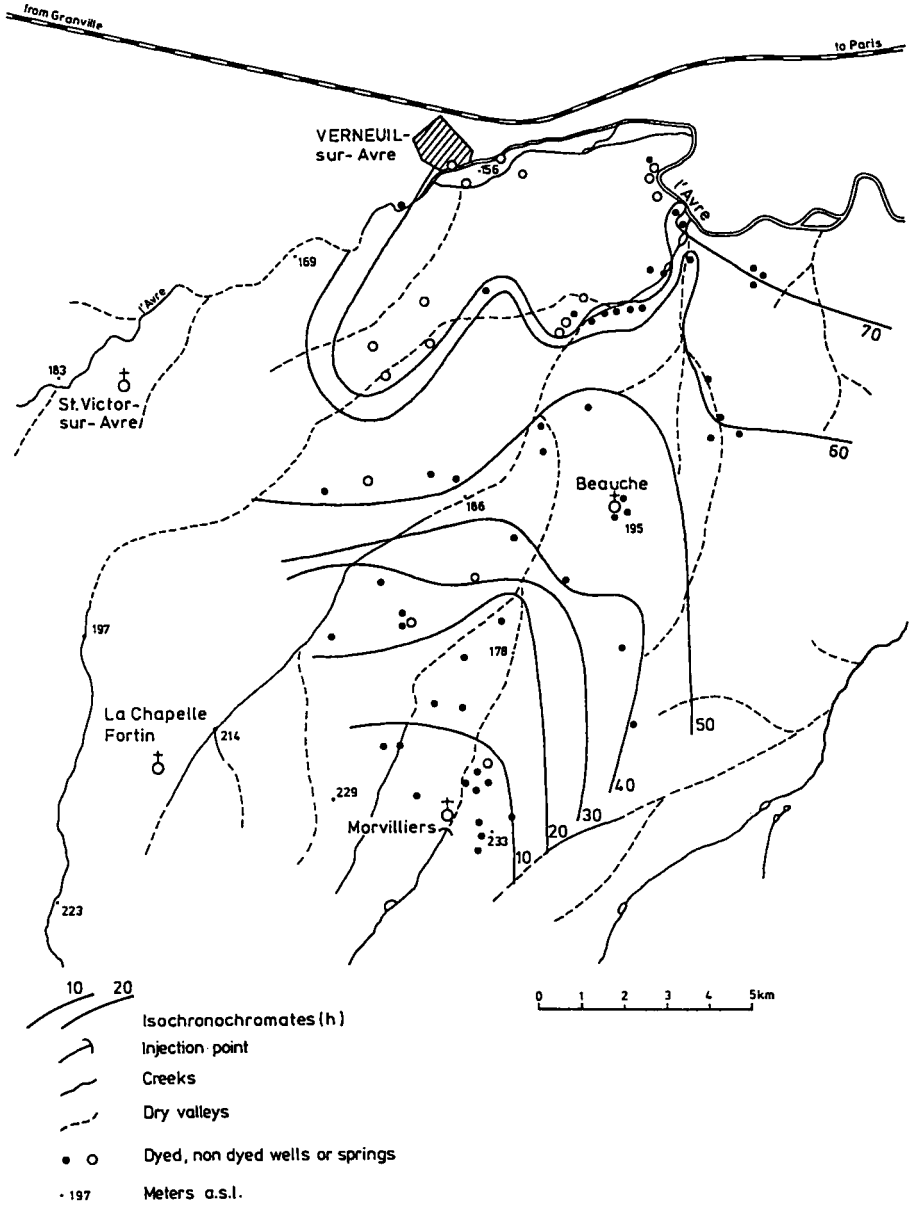

Figure 140. Cretaceous karst region south of Verneuil-sur-Avre (Dpt.Eure/France). Lines of equal residence times in a dye tracing test (after MARBOUTIN 1901a).

3.6 PRESENTATION OF THE RESULTS

The simplest way to present the results is in a list with the sampling site and corresponding finding listed. However, for a better and clearer understanding, breakthrough curves as time-concentration-plots are more appropriate. Here, summation curves $\Sigma c/c_{total}$ can also be plotted (Plate 4). Values can be taken from these curves for further evaluation (Chapter 4).

When using multiple tracers, 'normed curves' should be used in joint plots of the breakthrough curves. This allows a comparison of the concentrations independent of the injection quantity. Hereby, the dilution in reference to a certain water volume is given. Since in water analysis, the litre is the reference volume, it is the base here also:

$$V = \frac{c}{M}\, l^{-1}$$

where V = degree of dilution = normed concentration, c = concentration, M = injection quantity.

It is not only possible to give normed concentrations for dissolved substances, but also for particles and solutions. If a larger number of observation sites have a positive tracer recovery, the residence times can be spatially represented. $V = c \cdot 10^9/M\ (l^{-1})$ is a well-comparable dilution. With this, the usual units for concentration (µg/l) and injection quantity (kg) can be used in the above formula without difficulty: $V = c$ (µg/l)/M (kg). An example is given in Figure 18, middle.

Many years ago, MARBOUTIN (1901a,b) published another descriptive representation concerning residence times. He connected the lines of equal residence times for the first reappearance in a map, socalled isochronochromates (Fig. 140). However, a very large number of observation points are needed for such a representation. In spite of this, it is astonishing that no one has imitated this.

Taylor & Francis
Taylor & Francis Group
http://taylorandfrancis.com

CHAPTER 4

Evaluation and interpretation of tracing tests

H.D. Schulz

A fundamental problem in evaluating and interpreting tracing tests is that the large scale spatial patterns – the wanted results from the tests – are superimposed by numerous small scale flow patterns ranging down to those at the grain surface of unconsolidated rocks or in the finest fissures of solid rock. When evaluating and interpreting tracing tests, these important large scale patterns must be separated from the less interesting small scale ones. Beginning with the basic works from TAYLOR (1953), SCHEIDEGGER (1961), LENDA & ZUBER (1970), and especially BEAR (1972, 1979), a multitude of tracing test evaluation methods have been published. Particularly, KINZELBACH (1986) should be mentioned, who demonstrated modelling of the groundwater flow and solute transport in groundwater with the help of numerous examples from programs for personal computers.

In determining water protection areas in the drainage area of groundwater wells, GAILLARD (1976) demonstrated several different solutions for different boundary conditions. In doing so, field and lab experiments, model calculations, and also theoretical derivations based upon stochastics were compared. DREYBRODT (1988) published a detailed review of the physical processes during matter transport for different fissured and karst aquifers.

The following sections consider the theory of underground matter transport, especially with respect to hydrogeological significance.

However, the physical processes of solute transport underground only describe one side of the problem, since strictly speaking, they are only valid for those substances that do not react during transport with the rocks nor with other dissolved substances. Yet this simplifying boundary condition is not valid for most of the substances transported in groundwater. Instead reactions and interactions are the rule. Therefore, a further section covers the simultaneous processes involved during solute transport and reactions in the underground.

During the interpretation of a tracing test, it is only rarely possible to describe the spatial distribution of the tracer cloud in the underground for a specific point in time after the injection. To do this, a sufficiently large number of monitoring wells would have to be distributed uniformly over the entire flow field. This is usually not possible due to economical reasons and so the evaluation must be based on the breakthrough curves from tracer passage through the few monitoring wells that are avail-

able. The third section of this chapter deals exclusively with the evaluation of these breakthrough curves from tracing tests.

4.1 PHYSICAL FUNDAMENTALS OF SOLUTE TRANSPORT UNDERGROUND

H.D. Schulz

4.1.1 *Solute transport and dispersion*

Solute transport in groundwater corresponds to the flow direction and flow velocity (advection) of the groundwater. If a specific volume of water containing the injected tracer cloud was to move with the same velocity through the underground, after a specific time, the tracer cloud would be expected to appear in the same form and concentration distribution at the place determined by the flow direction and velocity. However, the effective flow velocity (v_a) determined with the DARCY equation with the gradient of the groundwater table (i), the permeability coefficient (k_f), and the effective porosity (n_e) of the rock is only a mean velocity.

$$v_a = \frac{k_f \cdot i}{n_e} \tag{4.1}$$

The individual parts of a volume of water that flow through the underground and the matter contained in it flow through very different paths. Therefore, they have very different individual velocities. Even in the pore channel or within the water flowing through a fissure, the flow velocities in the middle of the cavity are always higher than those near the rock (Fig. 141). On their way through nonhomogeneous geological material, parts of the water flow through the large open pores or fissures and attain high velocities, while other parts flow slowly through narrow pores or fissures. The length of the flow path covered can also be quite different (Fig. 141). All of these individual processes lead to the fact that the longer and farther a tracer cloud flows underground, the larger it will become and the concentrations in it will decrease. Since it is by chance whether the individual water or solute particle is transported quicker or slower than the mean flow velocity, a point source concentration input injected at a specific time will develop the form of a GAUSS-distribution. Whether a narrow and high or a broad and flat GAUSS-distribution is attained, depends upon how different the individual velocities, i.e. how nonhomogeneous the underground material is. This increasing further distribution of a specific amount of matter during transport is called hydrodynamic dispersion (Fig. 142).

The mathematical treatment of advection and dispersion depends very much upon the dimensionality of the flow field, thus before it is described the following must be considered:

Strictly speaking, a one-dimensional flow system would only be given within a pipe with a specific cross-section, where the individual concentrations could not leave the system through the pipe walls. The hydrodynamic dispersion would then map the different velocities flowing through the cross-section. If the same flow pattern and concentrations were outside the pipe as within and assuming the pipe walls

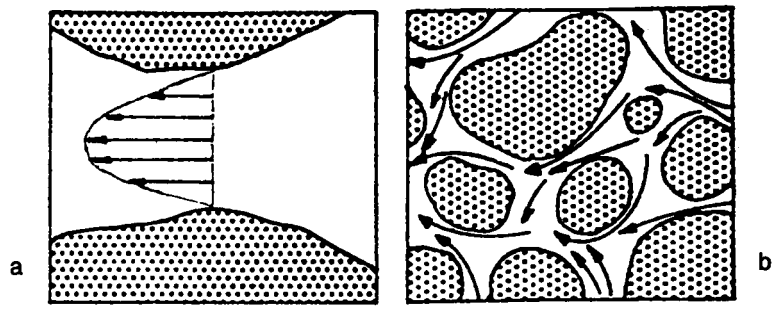

Figure 141. The mechanisms of hydrodynamic dispersion. Within a pore channel, the flow velocities in the middle are higher than near the grain surface (a). The individual flow paths around the different sized grains have different lengths (b) (from SCHRÖTER 1983).

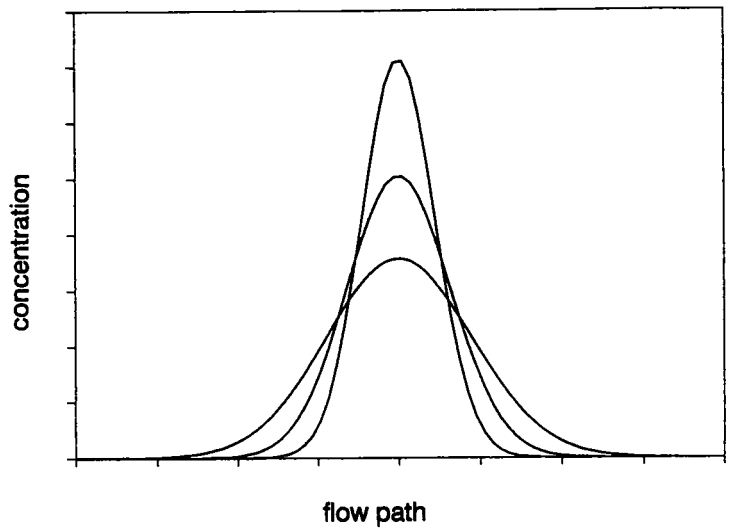

Figure 142. The impact of hydrodynamic dispersion. The three curves shown have the same effective flow velocity and time. They differ in the extent of the dispersion. With stronger effective dispersion, the concentration distribution is flatter and wider, with less intensive dispersion, the concentration distribution is steeper and narrower.

were not present, then a lateral matter exchange would occur. However, the same amount of particles would flow in and out of the initial flow field. Such a system can be considered one-dimensional. This means, that whenever the tracer injection is conducted over a large cross-sectional area, the central part of the flow field can be considered to be one-dimensional.

Strictly speaking, a two-dimensional flow system would only be given between two impermeable plates with a specific distance from each other. A concentration injected along the entire flow field between these two plates would spread out longitudinally (in the flow direction) due to hydrodynamic dispersion, but also transversally. A flow system in an aquifer, which is bordered at the top by the phreatic sur-

face or an impermeable layer and at the bottom by an impermeable bed, can be considered to be two-dimensional, if the injection and also the sampling cover the entire thickness of the aquifer. Over the third dimension, the groundwater thickness, is integrated, which however, is only valid if there are no essential flow velocity differences over the third dimension.

The general three-dimensional consideration of a flow system adds the vertical direction of the groundwater thickness to the longitudinal and transversal dimensions. This is always necessary, if the tracer cloud can spread out due to hydrodynamic dispersion in all three directions.

Caution must be taken before simplifying a three- or two-dimensional system to a one-dimensional system. Most natural flow fields are three-dimensional. Only if the stated prerequisites are sufficiently fulfilled, is a two-dimensional view valid and only in special cases is a one-dimensional view valid.

The combination of advection and dispersion is described by a partial differential equation:

$$\frac{dc}{dt} = D_l \cdot \frac{d^2c}{dx^2} + D_t \cdot \frac{d^2c}{dy^2} + D_v \cdot \frac{d^2c}{dz^2} - v_a \cdot \frac{dc}{dx} \tag{4.2}$$

Other than the three spatial co-ordinates x, y, and z, this equation also contains the time co-ordinate (t) and the concentration (c). The effective flow velocity of the groundwater (v_a), the dispersion-coefficients in longitudinal direction (D_l), transversal direction (D_t), and vertical direction (D_v) are needed as coefficients. The dispersion-coefficients, which will be covered in detail in the next section, describe the extent of the dispersion in the respective coordinate-directions, while the x-coordinate represents the direction of the flow.

This equation cannot be solved without predefining the flow field boundary conditions. However, for specific flow field configurations, there is a series of different analytical solutions for this equation used and several are presented here.

For the one-dimensional case, the terms for the transversal and vertical dispersion can be omitted in Equation (4.2). For a momentary, pulse-type tracer injection (DIRAC pulse), the maximal concentration of the tracer cloud is calculated as a function of the time since injection of the tracer ($C_{\max,t}$):

$$C_{\max,t} = \frac{m}{F \cdot n_e \cdot \sqrt{4 \cdot \pi \cdot D_l \cdot t}} \tag{4.3}$$

In this equation, the maximal concentration of the tracer cloud at time t since the injection of the tracer is directly proportional to the quantity of tracer injected (m) and inversely proportional to the flow area (F), the effective pore volume (n_e), and the root of the product of the longitudinal dispersion coefficient (D_l) and the time since the tracer was injected (t). At time t, this concentration is in the centre of the tracer cloud. The injection of the tracer was at $x = 0$. The concentration distribution along the one-dimensional flow path is calculated thus: the maximal concentration which represents the GAUSS-distribution is multiplied with an exponential function and gives the concentration at anywhere on the co-ordinate x at time t:

$$C_{x,t} = C_{\max,t} \cdot \exp\left(\frac{(x - v_a \cdot t)^2}{-4 \cdot D_l \cdot t}\right) \tag{4.4}$$

With two-dimensional flow, only the terms for vertical dispersion can be omitted in Equation (4.2). The maximal concentration of the two-dimensional tracer cloud is given as a function of time by the following equation:

$$C_{\max,t} = \frac{m}{M \cdot 4 \cdot \pi \cdot n_e \cdot t\sqrt{D_t \cdot D_t}} \tag{4.5}$$

In comparison to Equation (4.3), the transversal dispersion coefficient (D_t) is added and in place of the flow area (F), the thickness of the aquifer (M). The tracer injection site is defined with the co-ordinates $x = 0$ and $y = 0$. The concentration ($c_{x,y,t}$) anywhere in the two-dimensional flow field at time t is then given as in Equation (4.4) by multiplying the maximal concentration with an exponential function to represent the GAUSS-distribution:

$$C_{x,y,t} = C_{\max,t} \cdot \exp\left[-\frac{(x - v_a \cdot t)^2}{4 \cdot D_l \cdot t} - \frac{y^2}{4 \cdot D_t \cdot t}\right] \tag{4.6}$$

It is assumed in these equations that the tracer injection and the sampling of the water at the co-ordinates x and y is done over the entire thickness of the aquifer. Corresponding analytical solutions for three-dimensional flow and for radial flow conditions (drawdown of a well) are known.

Equations (4.3) to (4.6) are valid for momentary injections of highly concentrated tracer solutions in the smallest volume possible. With continuous, long-lasting point source tracer injections, limited tracer clouds do not occur. Instead, a concentration front occurs, which spreads with the flow velocity of the groundwater. The maximal concentration that so occurs is that of the tracer injection. The hydrodynamic dispersion has the effect that the initially steep concentration front becomes flatter with increasing flow time.

For the one-dimensional case, the concentration ($C_{x,t}$) at a distance (x) from the injection site and after time (t) since the begin of the continuous injection is calculated as:

$$C_{x,t} = \frac{c_0}{2} \cdot erfc\left(\frac{x - v_a \cdot t}{2 \cdot \sqrt{D_l \cdot t}}\right) \tag{4.7}$$

In this equation, (c_0) is the concentration of the tracer injection. All other constants and variables correspond to those in the Equations (4.3) to (4.6). Also in this equation is the error-function (erfc), which is related to the GAUSS-function. It can be approximated with the following relationship (KINZELBACH 1986):

$$\text{erfc}(a) = \exp(-a^2) \cdot (b_1 \cdot c + b_2 \cdot c^2 + b_3 \cdot c^3 + b_4 \cdot c^4 + b_5 \cdot c^5) \tag{4.8}$$

where $b_1 = 0.254829592$, $b_2 = -0.284496736$, $b_3 = 1.421413741$, $b_4 = -1.453152027$, and $b_5 = 1.061405429$, and $c = 1/(1 + 0.327591117 \cdot \text{abs}(a))$. For negative values of a, $\text{erfc}(a) = 2 - \text{erfc}(a)$.

Table 22 lists the approximated values for the function erfc(a) for different initial values of (a) from –2 to +2.

Figure 143 graphically displays the contents from Table 22. As the GAUSS-distribution had the form of a momentarily injected tracer cloud, the error-function maps the concentration front of the continuous tracer injection flattened by the hydrodynamic dispersion. Figure 144 displays five concentration fronts from different times since the begin of the continuous tracer injection at $x = 0$, calculated with

Table 22. Error-function erfc(a). The value combinations follow the approximation from Equation (4.8).

a	erfc(a)	a	erfc(a)	a	erfc(a)	a	erfc(a)
–2.000	1.995	–1.000	1.843	.000	1.000	1.000	.157
–1.950	1.994	– .950	1.821	.050	.944	1.050	.138
–1.900	1.933	– .900	1.797	.100	.888	1.100	.120
–1.850	1.991	– .850	1.771	.150	.832	1.150	.104
–1.800	1.989	– .800	1.742	.200	.777	1.200	.090
–1.750	1.987	– .750	1.711	.250	.724	1.250	.077
–1.700	1.984	– .700	1.678	.300	.671	1.300	.066
–1.650	1.980	– .650	1.642	.350	.621	1.350	.056
–1.600	1.976	– .600	1.604	.400	.572	1.400	.048
–1.550	1.972	– .550	1.563	.450	.525	1.450	.040
–1.500	1.966	– .500	1.520	.500	.479	1.500	.034
–1.450	1.960	– .450	1.475	.550	.437	1.550	.028
–1.400	1.952	– .400	1.428	.600	.396	1.600	.024
–1.350	1.944	– .350	1.379	.650	.358	1.650	.020
–1.300	1.934	– .300	1.329	.700	.322	1.700	.016
–1.250	1.923	– .250	1.276	.750	.289	1.750	.013
–1.200	1.910	– .200	1.223	.800	.258	1.800	.011
–1.150	1.896	– .150	1.168	.850	.229	1.850	.009
–1.100	1.880	– .100	1.112	.900	.203	1.900	.007
–1.050	1.862	– .050	1.056	.950	.179	1.950	.006

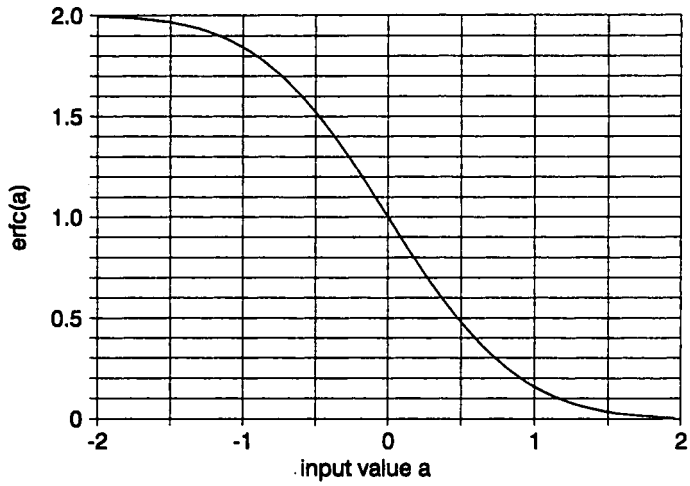

Figure 143. Error-function for the range of initial values from –2 to +2.

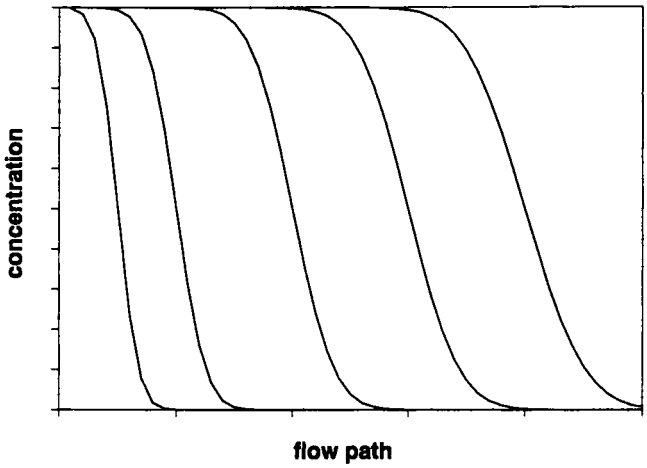

Figure 144. Concentration distribution at five different times after the begin of a continuous tracer injection at $x = 0$ of the transport path. The flow direction of the water is from left to right.

Equation (4.7). It can be clearly seen, that due to hydrodynamic dispersion, that the concentration front becomes flatter with increasing flow time. Corresponding analytical solutions for the two-dimensional case are known, are however much more complicated.

4.1.2 *The dispersion coefficient*

Equation (4.2) describes the extent of the dispersion in longitudinal, transversal and vertical directions with the respective dispersion coefficients. The longitudinal dispersion coefficients known from natural flow fields, vary over a range of several decimal powers. Also clear is the dependency upon the flow velocity. In Figure 145, SCHRÖTER (1983) matches known literature values for dispersion-coefficients against flow velocities. The dependency of the longitudinal dispersion coefficient upon the flow velocity is expressed by the following relationship by introducing the dispersivity or the dispersion length (α_l):

$$D_l = \alpha_l \cdot v_a \tag{4.9}$$

The dispersivity or dispersion length (α_l) represents the nonhomogeneity in the aquifer and is charactertistic for the rock type. Nevertheless, it is not a constant, for under natural conditions, an increase is always observed with an increase in the flow path (KLOTZ & SEILER 1980, BEHRENS & SEILER 1982). By combining different published tests, SCHRÖTER (1983) showed the dependency between flow path and dispersivity (Fig. 146). This dependency hides the fact that an increase in flow path includes an increase in nonhomogeneities in larger scales in the dispersion. From Figure 146, the dispersivity can be roughly approximated to a tenth of the flow path. With increasingly larger flow paths in natural aquifers, an increase in the different flow velocities due to different permeabilities factor into the dispersion. Such dispersion processes are frequently called macro-dispersion. Figure 146 clearly shows that the dispersivity

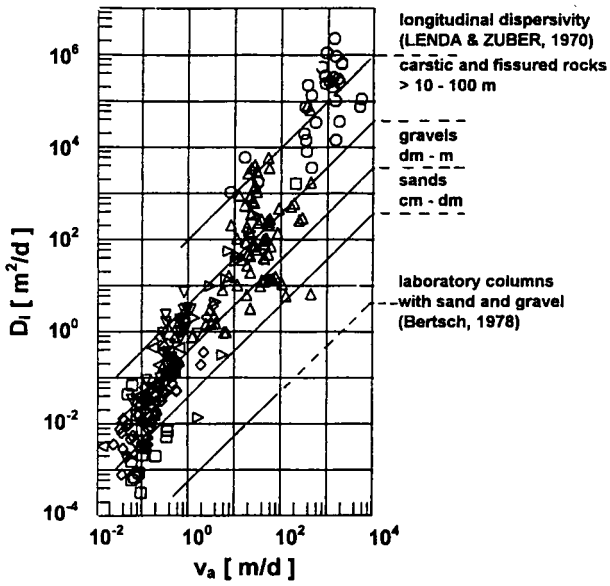

Figure 145. Correlation between the flow velocities and dispersion coefficients according to different rock types (changed after SCHRÖTER 1984).

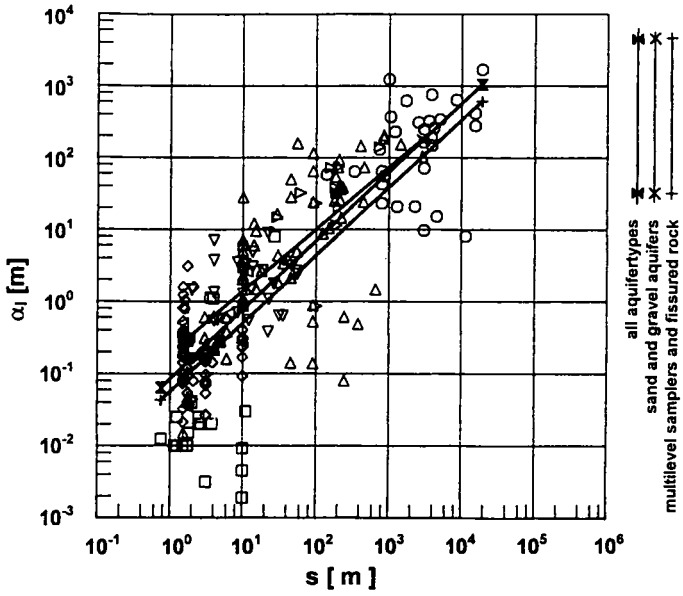

Figure 146. Correlation between the length of the flow path of a tracer cloud and the dispersivity (changed after SCHRÖTER 1984).

of fissured and karst aquifers is usually between 10 and 1000 m. In field tests, dispersivities of sands and gravels cover a range – depending on the flow path length – from 0.1 to 100 m. Usually, dispersivities in centimeter ranges are only found in laboratory tests. The dependency of the dispersivity upon aquifer parameters was investigated by KLOTZ (1973, 1982b).

The transversal and vertical dispersivity is usually much smaller than the longitudinal. In the literature, values between 1/400 and 1/2 of the longitudinal dispersivity are given (JOSSELIN DE JONG 1958, KLOTZ 1982c). Values between 1/5 and 1/10 of the longitudinal dispersivity are most frequent.

Also, the dispersion coefficient usually contains an imperceptible portion of the diffusion that is indistinguishable from the dispersion. The diffusion acts in the same direction as the dispersion and can be described with the same mathematical processes. However, the importance of the diffusion in practically all cases of groundwater flow is so low, that it disappears in the range of possible errors during the calculations of the dispersion. GASPAR and ONESCU (1972) found values for diffusion coefficients in groundwater between 1.2 and $2.3 \cdot 10^{-5}$ cm^2/s. Converted to the same units as in Figure 145, these are values between 1.0 and $2.0 \cdot 10^{-4}$ m/day. Such values would just appear as dispersion coefficients on the bottom scale of Figure 145, whereas the range for naturally occurring dispersion coefficients is several decimal powers higher.

4.1.3 *Spatial distribution of the tracer cloud*

The analytical solutions for the advection-dispersion-differential equation described above are used to calculate the spatial distribution of the concentration after the injection. Ideally, a one-dimensional flow field has the concentration distribution shown in Figure 147. This figure shows the concentration distribution for four points in time during transport after injection of the tracer. The injection site is displayed as the origin of the transport path axis. Theoretically, at the time of the injection, t_0, an infinitely large concentration was present in an infinitely small space. For the four sequential points in time displayed, the maximal concentration of the tracer cloud (Eq. 4.3), consistently decreases with increasing transport time and increasing transport path. At the same time the curve becomes wider, so that the area under the curve, which represents the total injection amount, stays the same. After a theoretically infinitely long transport time in an infinitely large flow field, the curve would

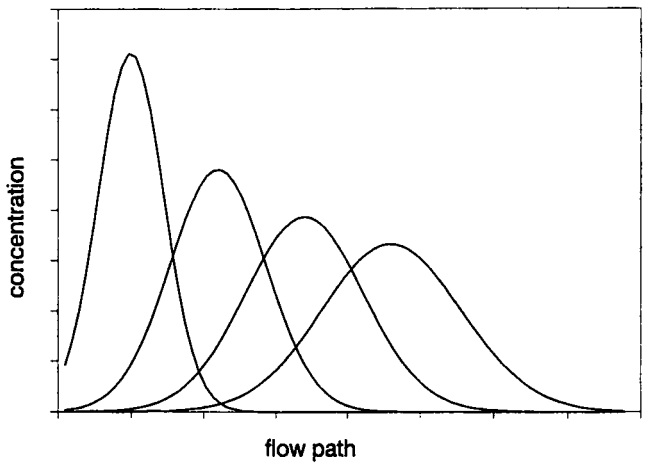

Figure 147. Concentration distribution at four different times after a momentary tracer injection at point zero of the transport path. Based on one-dimensional solute transport.

be infinitely wide and the maximal concentration equal to zero. Since infinitely long flow paths are not found in nature, this process ends, when the flow path of the respective groundwater ends in a spring or well. From the site of the maximal concentration in the flow field, i.e. its distance to the injection site and the known transport time, the mean effective flow velocity (v_a) of the groundwater can be calculated.

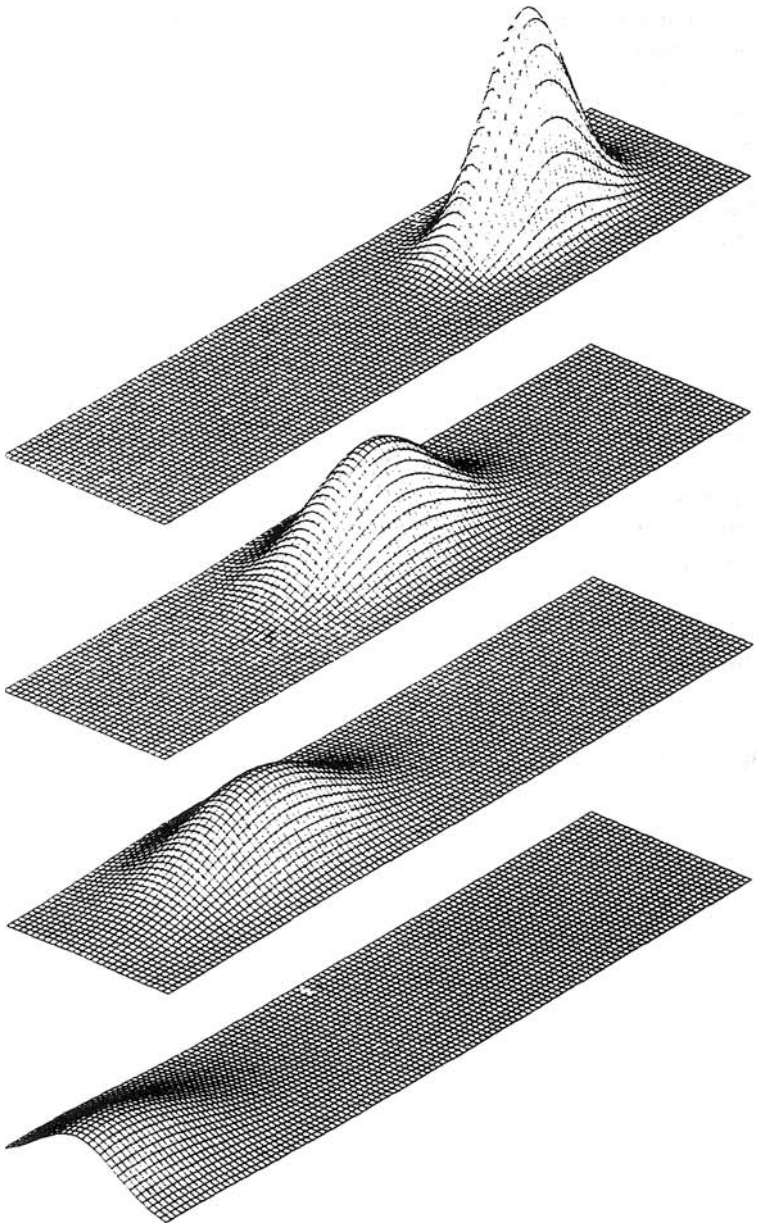

Figure 148. Concentration distribution at four different times after a momentary tracer injection. Based on two-dimensional solute transport.

In a two-dimensional flow field, the propagation of a tracer cloud is completely analogous to the one-dimensional flow case. In this case, the propagation perpendicular to the flow direction, in transversal direction, is added. Figure 148 shows the propagation of a tracer cloud in a two-dimensional flow field at four different times after the tracer injection. The increased spreading of the tracer cloud with the progression of the transport time and the simultaneous decrease in the maximal concentration is also obvious here (cf. Eq. 4.5).

With the tracer clouds from Figure 148, the ratio of the longitudinal dispersivity to the transversal dispersivity used was 5:1, as characteristic for very nonhomogeneous sand and gravel accretions. Figure 149 displays the spatial form of the two-dimensional tracer clouds in their dependency upon the ratio of the longitudinal dispersivity to the transversal dispersivity. The left tracer cloud (which corresponds to the second graph from the top in Fig. 148) a ratio for D_l/D_t was set to 5:1. The middle tracer cloud was based on a D_l/D_t ratio of 10:1 and the right one a ratio of 20:1. It is obvious that with decreasing transversal dispersivity, that the tracer cloud is stretched.

In each of the Figures 147 to 149, an ideal, propagation process that followed the Equations (4.3) to (4.6) was assumed. As a prerequisite, the distribution of the flow velocities in the underground must be uniformly random and thus can be appropriately described by the mean effective flow velocity (v_a). Unfortunately, this is rarely the case in natural, geological layers. If there are layers in a porous aquifer with very different permeabilities (e.g. interbedding of sands and gravels) or two or more fissure systems with clearly different fissure widths in a fissured aquifer, then the velocities in the underground are generally not normally distributed. In such cases, bimodal or polymodal distributions are observed, which can be then only appropriately described with several mean effective flow velocities with several respective normal distributions.

This has considerable impact upon solute transport and the propagation of the tracer clouds underground, since this means that the propagation of a cloud cannot be followed with only one mean effective flow velocity. In these cases, the concentration distribution in the underground must be taken as the addition of several, superimposed clouds that flow with different velocities through the aquifer. Figure 150

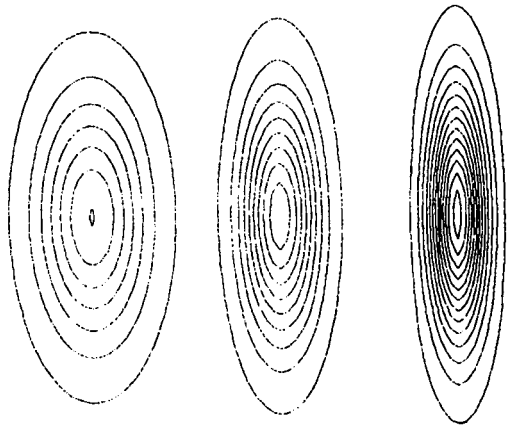

Figure 149. Different transversal dispersivities with two-dimensional solut transport. The left tracer cloud has a D_l/D_t ratio of 5:1. The middle tracer cloud a ratio of 10:1 and the right one a ratio of 20:1.

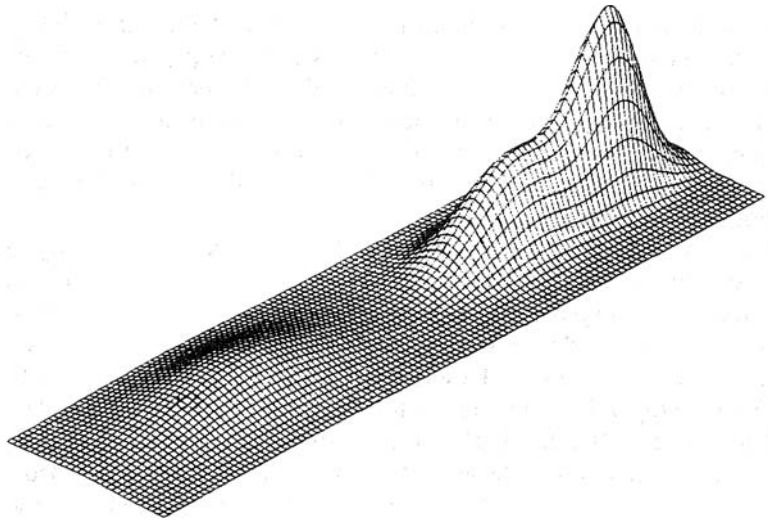

Figure 150. Superposition of tracer clouds with different flow velocities in a two-dimensional flow field with layers of different permeabilities in the aquifer.

shows the superposition of three clouds with different flow velocities in a two-dimensional flow field. The flow velocities of these three clouds have the ratios 1:2:5. Such flow velocity differences are not at all unusual for layered porous aquifers nor for fissured aquifer with different fissure systems. In the following section, this is demonstrated with real cases.

4.1.4 *Temporal distribution of tracer clouds*

In most practical cases, the documentation of a tracer cloud at a specific time in a flow field is very difficult to realize, since to do this a multitude of uniformly distributed monitoring wells are necessary. Therefore, special importance must be given to observing the tracer concentration passage in a monitoring well in the flow field. In many cases, the propagation of the tracers in the underground must be limited to evaluating one or several such breakthrough curves, although the mathematical evaluation of the temporal distribution is generally more complicated than the spatial distribution.

The breakthrough curve of an ideal tracer cloud, which follows the Equations (4.3) to (4.6) completely, and is symmetrical at each point in time, is always unsymmetric. Figure 151 shows the breakthrough curves for three tracer clouds with equal mean effective flow velocities, yet different dispersivities. These three curves were calculated with the Equations (4.3) and (4.4). The reason for the unsymmetrical form of the ideal breakthrough curve is that the increase in concentration in the monitoring well is caused by the inflowing tracer cloud which is still small and highly concentrated. However, the decrease in the concentration is caused by the overall further travelled cloud which has become increasingly larger and flatter. Figure 151 also clearly shows that the breakthrough curve is all the more unsymmetrical, the larger

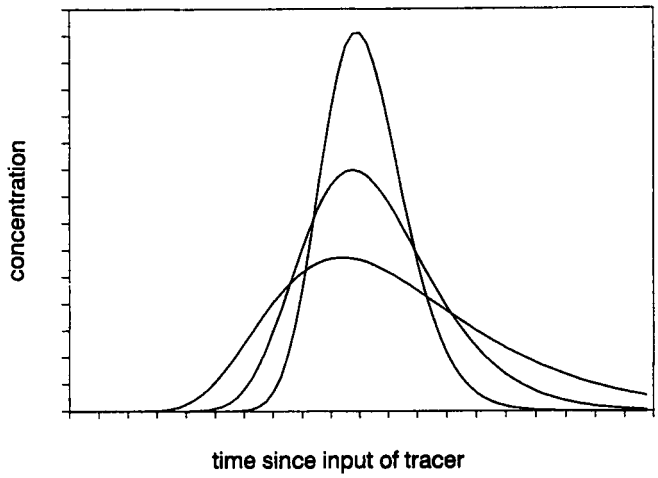

Figure 151. Breakthrough of three tracer clouds with equal effective flow velocities, but different dispersivities.

the dispersivity. It should be stressed here, that the point in time at which the peak concentration of the breakthrough curve is observed, is *not* the time which is used to calculate the mean effective flow velocity of the propagation process. This is clearly seen in Figure 151 also, since the peaks of the three breakthrough curves are not exactly one upon the other, although all three have the same effective flow velocity. There are several suitable procedures to determine the effective flow velocity from a breakthrough curve. These are covered in Section 4.3 in detail.

The superposition of tracer clouds with different flow velocities in the aquifer, which was spatially described in the preceding section, can also be found in most real breakthrough curves. A very impressive example for this was given by SCHRÖTER (1983) as the result of a tracing test in sandy material. The measured uranine breakthrough curve and its simulation are shown in Figure 152. Characteristic for this breakthrough curve is a very steep concentration rise and a too flat dropping off of the concentration, which does not fit in with the Equations (4.3) and (4.4). SCHRÖTER (1983) was able to explain this effect by simulating the superposition of three tracer clouds with different speeds. The flow velocities of these clouds are so similar, that secondary maxima cannot be observed in the breakthrough curve.

An example from the Merdingen test field near Freiburg/Germany (cf. Chapter 5, the test data were kindly supplied by W.KÄSS, Umkirch/Germany) clearly shows multiple peaks in the eosin and uranine breakthrough curves (Fig. 153). This can only be explained as the result of superposition of tracer clouds with different speeds in the underground. Accordingly, Figure 154 shows a reconstruction of the breakthrough curves in a simulation. To do this, three tracer clouds were assumed whose velocities were related with the ratio 1:2:5 (cf. Fig. 150). In the simulation, all three tracer clouds were assigned the same injection quantity corresponding to the percentage of the aquifer thickness. The simulation showed, that both slower clouds were overemphasized, so that it can be assumed that their thicknesses in the actual aquifer were somewhat lower than the faster tracer cloud. Furthermore, when comparing Figures 153 and 154, it is striking that in the real breakthrough curve, definitely measureable dye concentrations appeared for quite a long time after the three

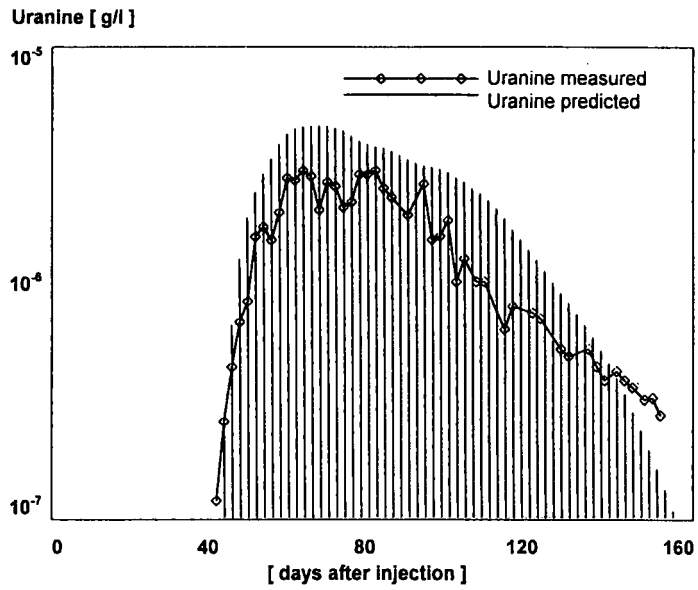

Figure 152. Uranine breakthrough curve as superposition of different flow velocities in an aquifer. The hatched area represents a model calculation, in which tracer clouds with different velocities were added together (from SCHRÖTER 1983).

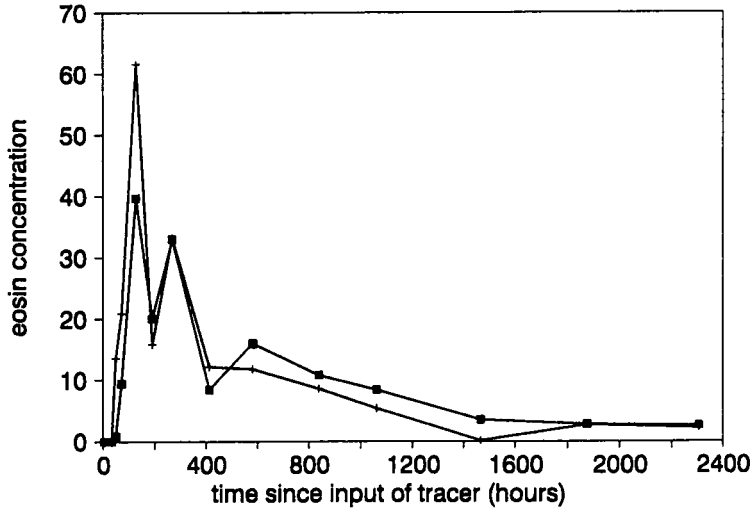

Figure 153. Breakthrough curves for the dye eosin in two neighbouring monitoring wells after a momentary tracer injection in the Merdingen test area near Freiburg/FRG. The different maxima of the breakthrough curves can only be explained as the superposition of different flow velocities in the aquifer. The test data were kindly supplied by W. KÄSS, Umkirch/FRG.

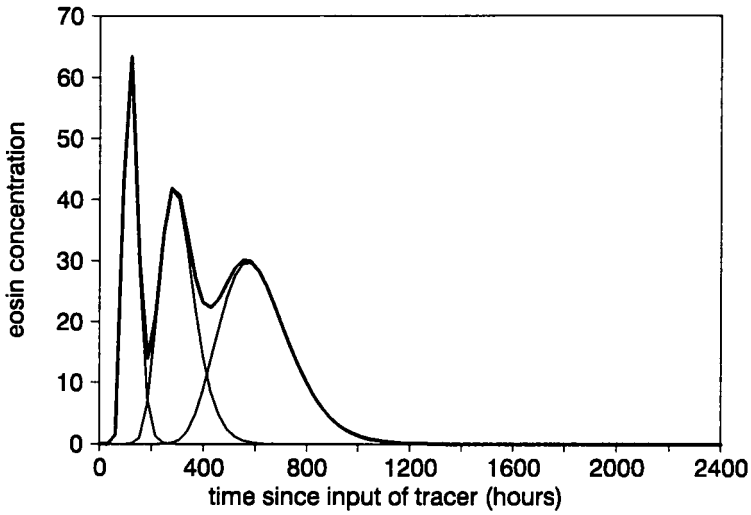

Figure 154. Simulation for the breakthrough curve with the symbol (+) from Figure 153. The top enveloping curve represents the addition of the concentrations of the tracer clouds with the different flow velocities.

maxima had passed through, which do not appear in the simulation. This can only be caused by further thin layers in the actual aquifer with even lower flow velocities, in addition to the three flow velocities assumed in the simulation.

4.1.5 *Computer models for solute transport simulation*

Nowadays, no one would think of computing the solute transport equations from the preceding Sections 4.1.1 to 4.1.4 by hand or with a pocket calculator, to fit the parameters to actual field experiments. Such evaluations are carried out with computers, whereby a personal computer is quite sufficient. By using a common spreadsheet-software (e.g. LOTUS), all the analytical solutions to the transport-dispersion-differential equations, that were given in the preceding sections, can be directly solved and graphically displayed, without the user having to know a program language. Even the multiple-layer-simulation from Figure 154 was carried out with spreadsheet-software exclusively.

The simulation of analytical solutions with spreadsheet-software has the advantage that after entering the parameters that control the transport (flow velocity, dispersivities), the results can be immediately seen on the monitor graphically and checked. In this way, the parameter can be quickly 'played with' until the result of the temporal or spatial concentration distribution matches the results of the actual tracing test.

In order to descriptively display two-dimensional tracer clouds, (cf. Figs 148-150), the use of personal computers and software for displaying areas (e.g. program system SURFER from the company Golden Software, Inc., Golden, Colorado/USA) is recommended. Such programs have as input data the x-coordinate, the y-

coordinate and a measured value. With these data, isolines maps or block diagrams can be made without having to have special programming knowledge.

Also for use with personal computers, KINZELBACH (1986) published numerous BASIC programs, with which practically all cases occurring in solute transport in the underground can be reconstructed. This book by KINZELBACH – which can also be ordered with a program-disk – is definitely recommended to everyone who is occupied with simulating solute transport in the underground on a personal computer and who wishes to understand what is happening.

For the simulation of one-dimensional solute transport through porous aquifers with layers of different permeabilities and with different dispersion and porosity properties, MALOSZEWSKI (1981) developed a FORTRAN computer program.

A larger, much more complicated computer-model for two-dimensional solute transport and dispersion in groundwater was published by KONIKOW & BREDEHOEFT (1984). This model, written in FORTRAN can be ordered from the authors as a disk for personal computer. The model allows the simulation of one-dimensional or two-dimensional problems, whereby advection, hydrodynamic dispersion, and mixing or dilution can be considered. In newer versions, simple solute reactions such as decay or retardation can also be considered. This program is especially suitable for simulation of continuous non-point source groundwater pollution.

4.2 SOLUTE TRANSPORT AND GEOCHEMICAL REACTIONS
H.D. Schulz

Strictly speaking, the mathematical solutions for solute transport in groundwater described in the previous sections are only valid for ideal or conservative tracers. These substances do not interact with the rock matrix nor with other dissolved substances during transport through the aquifer. Instead, they flow just as fast as the water through the rock matrix.

Only few substances behave conservatively during transport in groundwater. Therefore in many cases, geochemical reactions must be taken into consideration during simulation and evaluation of the solute transport processes. There are only a few geochemical reactions that are simple enough to be directly included in the analytical solutions of the transport-dispersion-differential equations (cf. Sections 4.2.1 and 4.2.2). Most reactions, especially those with more than one substance involved in the reaction, cannot be directly incorporated in the analytical solution of the transport-dispersion-differential equation (Sections 4.2.3 to 4.2.5).

4.2.1 *Distribution coefficient and retardation factor*

One of the simplest reactions between substances dissolved in groundwater and the rock matrix are the completely reversible sorption-desorption processes. Sorption is the immobilization of a substance dissolved in water onto the surface of grains or fissures in the aquifer. Desorption is the release of the substance back into solution. Since sorption-desorption reactions happen quickly, equilibrium between the concentration in solution and the amount in sorption develops very fast. The extent that a substance is inclined to go into sorption is described by the distribution coefficient (K_D-value).

$$K_D = \frac{c_{sorb}}{c_{dissolved}} \left[cm^3 / g\right] \tag{4.10}$$

The distribution coefficient states, that a portion of the tracer will always be unavailable for transport, since it is fixed to the rock. Thus, only that portion dissolved in the water can be transported. As soon as this dissolved portion has been transported away, a new portion of the originally sorbed dye tracer can be subjected to desorption, i.e. dissolves, so that it can be also transported. Not until this portion is also transported away, can further portions of the tracer be desorbed. Overall, this process leads to a slowing down of the transport, since large parts of the tracer are immobilized on the solid phase for part of the time. This process is expressed through the retardation factor (R_D), which is a direct function of the distribution coefficient.

$$R_D = 1 + \frac{\rho}{n_e} \cdot K_D \tag{4.11}$$

If all of the velocities and all of the dispersion coefficients in the analytical solutions to the Equations (4.3) to (4.6) are divided by this retardation factor, as a result, the sorption-desorption processes slow down the solute transport.

Table 23 lists (KLOTZ, 1982a) the retardation factors for different tracers determined in laboratory tests. For many organic substances, including most of the organic dyes, this is an acceptable procedure, as long as retardation coefficients larger than 2 to 3 are not obtained. The occurrence of higher retardation coefficients is an indication for irreversible sorption processes or other processes. However, for most substances dissolved in ionic form in groundwater, this simple view of the geochemical reactions is not sufficient. Usually much more complex reactions such as ion exchange reactions and/or dissolution/precipitation reactions are significant.

In spite of this, the described modelling for sorption-desorption reactions during solute transport in groundwater is carried out frequently – as described – using the distribution coefficients and retardation coefficients. However, the only reason for this is that this procedure is easy to compute. Realistically, this is not substantiated in groundwater, since most substances do not exist in real sorption-desorption-equilibrium. It has also been shown, that the distributions coefficients for different concentrations are not at all constant. Just retardation would have the effect that all substances would be indeed slowly, yet finally transported just as far as the flowing groundwater. If for example, one considers a natural ore deposit, there would have been enough time since its genesis for all of the metals to be transported quite far with the groundwater. However we only observe a limited concentration border around natural ore deposits in the groundwater. These deliberations clearly show that standard modelling with retardation coefficients is not suitable enough to simulate realistic long-term behaviour of solute transport.

4.2.2 *Decay reactions*

Decay is another simple substance reaction. The change in the concentration with time is described analogous to radioactive decay:

Table 23. Retardation factors R_D determined in column and modelling tests and distribution coefficients K_D cm³/g determined in batch tests of the investigated tracer for fluvioglacial gravels from the region near Murnau (from KLOTZ 1982a). N = Number of tests, γ = dry bulk density, n = porosity, R_{Db} = calculated R_D-value for the test parameter in the column (S) and the flow model (M).

	Tracer →		^{51}Cr-EDTA	$^{82}Br^-$	$^{131}I^-$	Na^+	Cl^-	F^-	NO_3^-	Uranine	Eosin	Pyranine
Quartz sand	Column tests γ = 1.7 g/cm³ n = 0.356	N R_D σR_D	4 1.01 0.03	2 0.98 0.02	3 1.00 0.01	5 1.01 0.04	4 0.98 0.03	1 1.09	3 1.00 0.01	4 0.99 0.03	3 1.02 0.01	1 1.08
	Batch tests	N K_d σK_d	3 0.381 0.080	3 0.052 0.027	1 0.13	1 0.00	3 0.00 0.00	1 0.00	1 0.17	4 0.060 0.020	1 0.016	1 8.5
	R_D after (4.11)	R_{Db}	2.8	1.2	1.6	1.0	1.0	1.0	1.8	1.3	1.1	42
Sloping gravel	Column tests γ = 2.2 g/cm³ n = 0.221	N R_D σR_D	4 1.15 0.14	2 0.97 0.01	3 0.95 0.03	5 1.30 0.13	4 1.00 0.12	1 1.84	3 1.00 0.00	4 1.22 0.18	3 1.55 0.02	1 1.12
	Batch tests	N K_d σK_d	3 0.061 0.007	6 0.045 0.033	4 2.79 0.52	4 0.010 0.000	3 0.349 0.062	3 0.320 0.177	4 0.027 0.054	7 0.060 0.058	4 0.034 0.025	3 0.040 0.087
	R_D after (4.11)	R_{Db}	1.6	1.4	29	1.1	4.5	4.2	1.3	1.6	1.3	1.4
Tertiary gravel-sand	Column tests γ = 2.3 g/cm³ n = 0.165	N R_D σR_D	4 1.11 0.09	2 0.96 0.00	3 1.00 0.03	5 2.17 0.36	4 0.98 0.08	1 1.80	3 0.98 0.02	4 0.99 0.01	3 1.12 0.01	1 1.04
	Batch tests	N K_d σK_d	3 1.00 0.02	5 0.116 0.124	4 0.013 0.005	2 0.862 0.432	3 0.057 0.050	2 0.086 0.000	4 0.054 0.077	7 0.055 0.025	4 0.074 0.023	3 0.391 0.227
	R_D after (4.11)	R_{Db}	15	2.6	1.2	13	1.8	1.2	1.8	1.8	2.0	6.5
Fluvioglacial gravel	Column tests γ = 2.1 g/cm³ n = 0.239	N R_D σR_D	4 1.24 0.06	2 0.97 0.02	3 1.03 0.01	5 1.47 0.11	4 0.96 0.04	1 2.54	3 1.03 0.01	4 1.18 0.10	3 1.69 0.02	1 1.18
	Modelling γ = 2.1 g/cm³ n = 0.22	N R_D ΔR_D		2 0.95 0.15						1 1.0 0.2	1 1.7 0.3	
	Batch tests	N K_d σK_d	3 0.370 0.015	6 0.034 0.031	4 0.208 0.026	7 0.264 0.095	3 0.121 0.142	3 0.882 0.198	4 0.260 0.065	7 0.108 0.099	4 1.13 9.19	3 0.005 9.030
	R_D after Equ.(4.11)	R_{Db} S) R_{Db} M)	4.3	1.3 1.3	2.8	3.3	2.1	8.8	3.3	1.9 2.0	10.9 11.8	1.7

$$c_t = c_0 \cdot e^{-\lambda t} \tag{4.12}$$

This means, that the concentration at time (c_t) is dependent upon the initial concentration and the time constant (α) of the decay. If this is applied to all concentrations in the analytical solutions of the Equations (4.3) to (4.6), the decay or degradation of a substance can be simulated. This is a common and suitable procedure for radioactive tracers with short half-life times. Also, the mostly microbiological decay of some organic substances, without considering metabolites, is frequently represented so. MATTHESS and PEKDEGER (1982) showed that the death rate of bacteria and viruses transported in groundwater can be adequately modelled with this procedure in many cases. This procedure has also been applied to filtration processes of substances transported as particulates in groundwater. However, usually it does not produce usable results.

4.2.3 *Cation exchange reactions, selectivities*

Frequently the substance amount is underestimated that is in equilibrium with the groundwater in the aquifer and sorbed onto the rock matrix. Even sands and gravels with relatively low exchange-capacities between 0.5 and 2 mmol(eq.)/100g generally have 20- to 50-fold of the groundwater-solution contents loosely fixed to the rock surface. Corresponding to the solution content of the main cations calcium, magnesium, sodium, and potassium, the exchange sites are occupied with different percentages of these ions.

The equilibrium between the resp. substance amount at the exchanger and the concentrations in solution can be expressed with the selectivity-coefficient. Equation (4.13) describes the selectivity of an exchanger for calcium, resp. magnesium, through the selectivity-coefficient $K_{Ca/Mg}$:

$$K_{Ca/Mg} = \frac{X_{Ca} \cdot a_{Mg}}{X_{Mg} \cdot a_{Ca}} \tag{4.13}$$

In this equation, X_{Ca} and X_{Mg} are the equivalent fractions of the sorbed ions as part of the total exchange-capacity. The activities of the ions magnesium and calcium are given by a_{Mg} and a_{Ca}. Analogously, the selectivity of the rock matrix for the relationship calcium to sodium or, resp. calcium to potassium can be described so:

$$K_{Ca/Na} = \frac{X_{Ca} \cdot a^2_{Na}}{X^2_{Na} \cdot a_{Ca}} \tag{4.14}$$

$$K_{Ca/K} = \frac{X_{Ca} \cdot a^2_{K}}{X^2_{K} \cdot a_{Ca}} \tag{4.15}$$

It must be observed that the equivalent fractions and the activities of the univalent ions sodium and potassium enter into the Equations (4.14) and (4.15) as a square resp., as compared to the bivalent calcium. Further selectivity-combinations of these cations, e.g. magnesium to sodium or sodium to potassium, are implicitly included in

the selectivity-coefficient Equations (4.13) to (4.15). These so described selectivity-coefficients are, in contrast to the distribution-coefficients (cf. Section 4.2.1) constant over wide concentration ranges and characterize the respective rocks with regards to the cation exchange-equilibrium. In an uninfluenced aquifer, the cations in solution and the corresponding substance amounts at the ion-exchanger are in equilibrium. The addition of a cation or a different ratio of cations into such an aquifer, e.g. during a salt tracing test, leads to a momentary and generally very sensitive disturbance of the equilibrium. Figure 155 displays the results of a KCl tracing test in a limy sand aquifer (Segeberger Forst, Schleswig-Holstein/FRG) as breakthrough curves for the main cations. Before the injection of the tracer KCl, the exchange sites of this aquifer were predominantely occupied with calcium, only ca. 10% of the exchange sites were allotted to the sorbed ions magnesium, sodium, and potassium. The momentary injection of KCl and therefore the concentration increase in the solution resulted in calcium being displaced at the exchanger through large fractions of the injected potassium. Thus, parallel to the potassium cloud, a calcium cloud and also, with lower concentration sodium and magnesium clouds passed through the aquifer. After the injection of the tracer, as the natural groundwater began to flow again, the ion-exchanger sites were predominantely occupied with potassium. Then, in accordance with the flow velocity, a slow reverse exchange and a return to the previous ratios settles in. As a result, in the breakthrough curves there is a relatively long increase in the potassium concentrations, after the maximal-concentration for potassium is reached. This is potassium, that was displaced at the exchanger by subsequently flowing calcium containing water. Correspondingly, after the passage of the calcium-

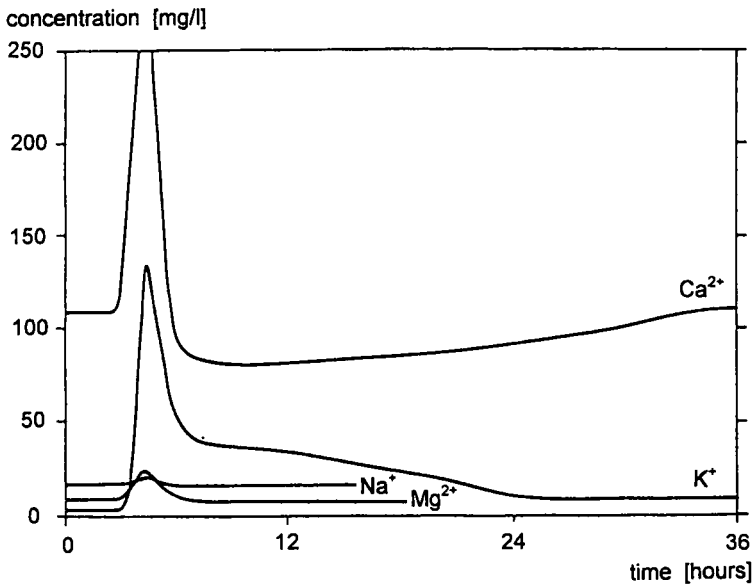

Figure 155. Tracing test with KCl in outwash material from the Segeberger Forst (Schleswig-Holstein/FRG). Due to the injection of potassium-ions in the aquifer, different concentrations of calcium, sodium, and magnesium were set free by cation exchange processes. These ions are then free to move through the aquifer as 'ghost clouds'.

maximum, the calcium concentration sinks below the initial value, since this calcium is now substituted for the displaced potassium at the exchanger. In accordance with the much lower equivalent fractions of magnesium and sodium at the ion exchanger, the corresponding ratios for these ions appear only weakly at the ion exchanger.

The extent of the reactions that are described in Figure 155, depends very much upon the resp. exchange capacity of the rock in contact with the flowing groundwater. In the described example, the aquifer was a middle to coarse sand with a low exchange capacity around 1 mmol(eq.)/100 g. As a result, the cation concentrations in porous aquifers are generally unsuitable for evaluating salt tracing tests with regards to the transport behaviour of the aquifer. Instead, one is limited to the corresponding breakthrough curves of the anionic chloride. The same is certainly true for fissure aquifers with very fine fissure systems.

Only with very large flow cross-sections in karst is the evaluation of the cation-concentrations along with the anion meaningful.

4.2.4 *Dissolution and precipitation reactions*

Whereas with the cation exchange reactions, the governing equilibrium conditions are well known and according to previous experience settle in quickly – usually within minutes, dissolution and precipitation reactions during solute transport in the underground are only insufficiently quantitatively known, excepting for a few subsystems. When calculating the saturation using the solubility product for a dissolving or precipitating mineral, the complex-concentrations of the concerned species must be taken into consideration and to calculate the necessary activities, the total concentration in solution. This can be done descriptively for specific groundwater analyses by applying geochemical modelling-programs of the WATEQ-family (e.g. WATEQ2 from BALL et al. 1979). During solute transport, there are additional difficulties, such as the fact that the dissolution and precipitation equilibriums do not settle in practically momentarily as e.g. the above mentioned cation exchange-equilibriums, but rather that the reaction kinetics must always be taken into consideration, if during a tracing test there is only limited contact time between the water with a specific concentration and the rock matrix.

During salt tracing tests, carbonate dissolution and precipitation processes are important in the carbonate equilibrium. If in a tracing test with KCl, as shown in Figure 155, the concentration of calcium in solution is changed considerably due to the injection of the potassium, the result will be an increase in the calcium concentration and supersaturation for carbonates, with which the water was in equilibrium before. Correspondingly, a decrease in the calcium concentration in solution – as also happened in the test – will cause an undersaturation of the water for corresponding carbonates. The publications from DREYBRODT (1988) and SCHULZ (1988) cover the kinetics of dissolution and precipitation of carbonates in groundwater in theory and laboratory tests in detail. It can be concluded, that normal groundwater, in contact with calcareous rock, needs hours to days for equilibrium to set in on the path from undersaturation, resp. supersaturation, until saturation through dissolution or precipitation. Therefore, in the example from Figure 155 with relatively fast flowing groundwater, dissolution and precipitation processes of carbonates do not become all too important. However, in slowly flowing groundwaters with longer contact times

between the water with a specific composition and the rock matrix, corresponding carbonate dissolution and precipitation processes must be taken into consideration, even if complete equilibrium is not always achieved.

Changes in the carbonate equilibrium always result in changes in the pH-value. Changes in pH-value and especially changes in the redox-potential (Eh-value) also govern dissolution and precipitation processes of many other minerals. For example, an increase in the pH-value and especially an increase in the redox-potential cause a decrease in the solubility of iron and manganese hydroxides. It is known that these hydroxides dissolve and precipitate within a relatively short time (from minutes to hours). If an oxygen containing, oxydizing tracer solution is injected into a reducing groundwater with usually high iron and manganese concentrations, there will most likely be precipitation of iron and manganese hydroxides, at least near the injection site.

Since the description of dissolution and precipitation reactions in tracing tests can only be considered with the simultaneous consideration of the respective solution in contact with the solid phase, the quantification of such processes cannot be practically carried out. Individual carbonate dissolution and precipitation examples will be covered in Section 4.2.5.

4.2.5 *Computer models for simulation of reactive solute transport*

The simple groundwater flow reactions described in Sections 4.2.1 and 4.2.2 can be simulated with the computer models from KINZELBACH (1986) or KONIKOW and BREDEHOEFT (1984) covered in Section 4.1.5. These reactions portray only one substance and its behaviour during transport as a function of time. When two or more substances are involved in more complex reactions in the underground, these models cannot be applied in most cases. The analytical solutions to the transport-dispersion-differential equations no longer work then, since the concentrations of the interacting substances are then no longer only a function of the transport time, but are also dependent upon each other at each point in time. The simulation of such multiple substance reactions during solute transport requires subdividing the continuous transport and reaction processes into discrete time steps and subdividing the continuum of the transport path into discrete cells or nodes. Generally, this is done by carrying out the transport and the hydrodynamic dispersion for all involved substances for a specific time step, without considering the reactions. Then, in all of the cells or nodes of the flow field under consideration, the simulation of the chemical reactions or resp. the adjustment of the equilibrium is carried out separately. Using the resulting changed concentrations, in the next time step the transport and the dispersion in each cell to the neighbouring cell is calculated and then again the chemical reactions and so on. This technique is called operator splitting.

Such a model was published first by SCHULZ & REARDON (1983). It considers a two-dimensional flow field with a flow parallel to one co-ordinate. The solutes that react during transport that are handled are the concentrations of sodium, potassium, calcium, magnesium, carbonate, and bicarbonate. The model takes two complexes as geochemical reactions into consideration:

1. The adjustment of the cation exchange equilibrium (cf. Section 4.2.3), and

2. The adjustment of the carbonate equilibrium through the dissolution and precipitation of calcite.

Figure 156 shows the simulation of a tracing test using this model. Hereby a solution was injected in the flowing groundwater which contained an increased concentration of potassium. All other parameters had the concentrations present in the flowing groundwater. Similar to the one-dimensional test in Figure 155, the injection of only a single substance had a strong impact on all of the other substances. In this case also, the injection of potassium ions into the groundwater flow releases preferably calcium ions into solution. As a result, in addition to the actual tracer cloud produced by the injected potassium, other 'ghost clouds' from other ions move through the aquifer, although they had not been injected. Behind the primary calcium ghost clouds, a secondary decrease in the calcium contents in the aquifer can be found here also. This is caused by the fact that the subsequent flow of calcium releases the originally sorbed potassium. The concentration changes in the calcium content also effect the carbonate balance. In areas with increased calcium concentrations, this causes carbonate precipitation, which is evident in the lower bicarbonate concentrations.

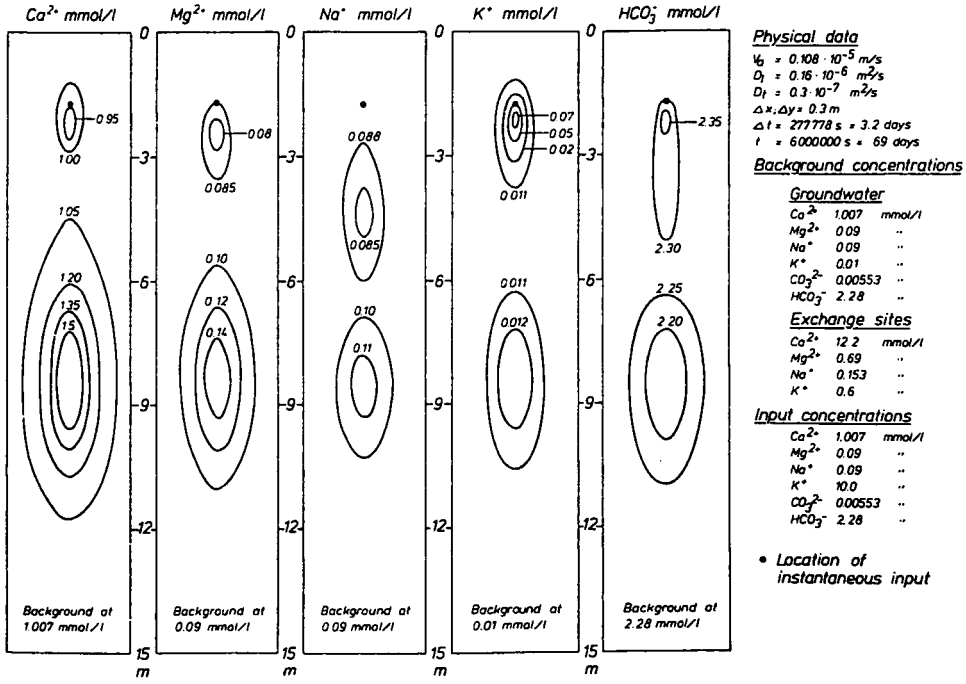

Figure 156. Two-dimensional modelling of a combination of solute transport, dispersion, cation exchange-reactions and adjustment of the carbonate equilibrium. As in the tracing test shown in Figure 155, only an injection of KCl at the presented injection site took place. The tracer clouds calculated with the model, as well as the 'ghost clouds' correspond exactly with those from the tracing test in Figure 155 (from SCHULZ & REARDON 1983).

The described example is suited for simulation of salt tracing tests in porous aquifers, as far as the main cations are concerned. The applied chemical reactions – cation exchange and carbonate equilibrium – are the complexes, which essentially govern the character of the groundwater. Frequently lithium is used in tracing tests, and it must also cause similar effects in the aquifer. Normally it does not play an important role in ion exchange, only because its concentration is much lower than the main cations. Thus in tracing tests with lithium, it is important to follow the concentration of the other main cations also, at the least the calcium content.

Today, transport models that consider even more complex reactions are still essentially hindered by three problem-areas:

– There are few tracing tests conducted where extensive analyses for numerous parameters are carried out,

– Many geochemical reaction paths, especially in the area of trace-concentrations, are still not sufficiently well-known. The reaction kinetics necessary for the simulation are not known,

– The combination of transport models and very complicated geochemical reactions for larger two-dimensional flow fields leads to unjustifiable computing time, even with state of the art computers.

The following describes basic approaches for combining dispersive solute transport with complicated geochemical reactions for one-dimensional transport. Figure 157 shows the basic structure of such a model. In this model, the impact of the hydrodynamic dispersion is simulated so: the content of each cell is transferred after the

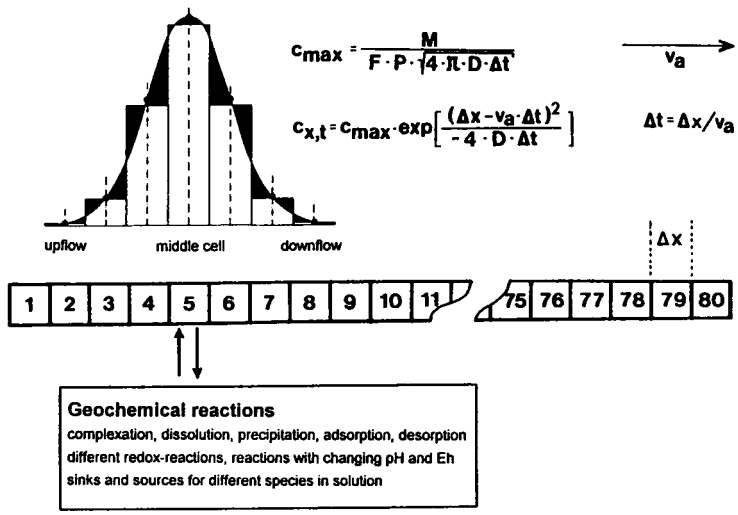

Figure 157. Basic schematics of a computer model to combine solute transport, dispersion, and geochemical reactions. The upper part of the figure depicts solute transport and dispersion along a one-dimensional row of discrete cells. In each time step, the solution content is transferred one position to the right with simultaneous dispersion into the other neighbouring cells. The bottom part of the figure lists examples of geochemical reactions for a cell, which the model calculations repeat in each time step for each cell.

time step not only to the following cell, but also to the cells before and behind it, in accordance to the given percentage depending upon the size of the dispersivity. The continuous GAUSSian curve of the dispersion is thus approximated in each time step by a step curve frequency distribution (Fig. 157, top part). Any geochemical reaction can be thus simulated in each time step and for each cell. The bottom part of Figure 157 depicts the basic schematics of incorporating geochemical reactions in a cell at a time step.

Incorporating mineral-precipitaions into a transport/reaction model results in a considerable increase in the computing time. For each cell considered and for each time step, the total species distribution – e.g. for iron – must be iteratively calculated again. To do this, the geochemical equilibria model WATEQ2 (BALL et al. 1979) was changed so that it could function as a subroutine in the model. When this model has calculated the species distribution and the saturation state for many minerals in each time step for all cells, then the concentrations, e.g. for iron in solution, are changed so that the solution is just saturated for iron hydroxide. The same can be carried out for other substances with regards to other mineral solid phases, accordingly. If an increased iron-concentration is continuously injected into cell 1 in each time step, the increased iron-concentration in the following cells will be decayed to iron hydroxide saturation depending on the transport, dispersion, and precipitation corresponding to the respective reaction kinetics. A stable concentration distribution is the result which is independent of the number of time steps taken in the model (Fig. 158). As in natural deposits, the increased iron injection has a border of increased

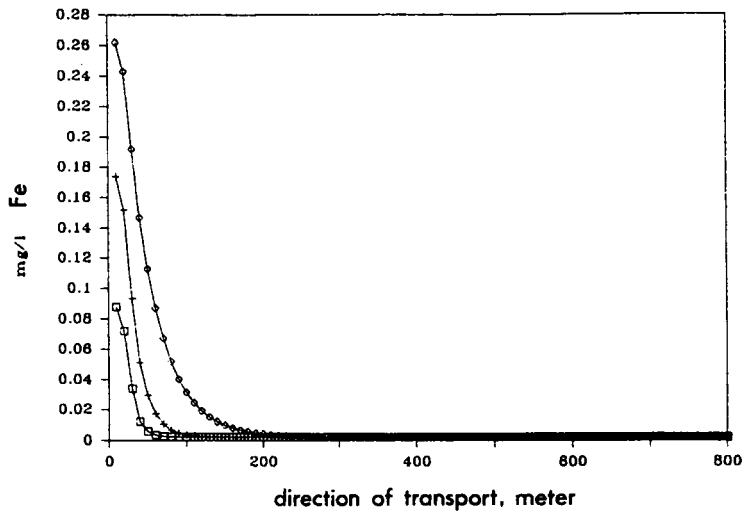

Figure 158. Results of a model calculation according to the principles shown in Figure 157. A continuous input of an increased iron-concentration occurs in cell 1 (0 on the transport axis) at each time step. In each time step, the solution content is transferred one position to the right with simultaneous dispersion into the other neighbouring cells. Due to precipitation processes depending upon the pH-value and the redox-potential of the groundwater, a stable concentration distribution develops due to the constant subsequent delivery of the iron with the groundwater flow. Each of the three curves shown is based on a different precipitation-kinetic.

concentrations in the groundwater, that stays constant in time and whose dimensions are controlled by the precipitation-kinetics. The three curves depicted in Figure 158 represent different precipitation-kinetics. Such model approaches can simulate any number of and any kind of complicated geochemical reactions – assuming that they are sufficiently well known so that they can be quantitatively described.

4.3 EVALUATION OF BREAKTHROUGH CURVES
H.D. Schulz

As mentioned before, tracing tests are generally evaluated due to practical reasons in most cases with the help of the temporal changes in the concentration at one site. The evaluation of such concentration-breakthrough curves provides the advection and dispersion characterizing parameters which govern the transport process. Although, especially the mean flow velocity (v_a) can be more directly derived from the spatial distribution of a tracer cloud at a specific point in time than from the breakthrough curve, the advection and dispersion parameters can be derived from breakthrough curves with sufficient accuracy.

4.3.1 *Determination of the effective flow velocity*

It is readily assumed, that the time passed since the injection of the tracer and the passage of the maximal-concentration at the sampling site together with the distance between the injection site and the sampling site are used to calculate the mean effective flow velocity (v_a). Especially in cases with steep and narrow breakthrough curves with a well-defined (through measurements) maximal-concentration, this assumption also provides a good approximation, even though it is not mathematically exact. The time which corresponds to the effective flow velocity (v_a), together with the known flow distance, occurs after the passage of the maximal-concentration and cannot be directly derived from the breakthrough curve. As stated above, for narrow and steep breakthrough curves, this time is only insignificantly larger than the time of the passage of the maximal-concentration and the difference can be practically neglected. However, with wide and flat breakthrough curves, this error can become quite considerable and cannot be neglected.

Most likely due to these uncertainties involved in determining the time which corresponds to the effective flow velocity from the breakthrough curves, there are different, differently well-defined flow velocities taken from the breakthrough curves used. The velocity that corresponds to the first appearance of the tracer is taken as the maximal flow velocity. The dominant velocity is defined as the time that corresponds to the passage time of the maximal-concentration at the sampling site. Furthermore, there is a mean flow velocity used, which corresponds to the time in the breakthrough curve, at which 50% of the recovered tracer amount has passed the sampling site. Figure 159 shows three theoretically calculated, differently steep breakthrough curves. For each curve, the times are marked from left to right that correspond to the following velocities: maximal effective flow velocity, dominant effective flow velocity, real effective flow velocity, and mean velocity. It can be

clearly seen that the last three are all the closer together, the steeper the breakthrough curve is and farther apart for wider and flatter breakthrough curves.

The maximal velocity is defined the worst, because it is directly connected together with the first appearance of the tracer in the sampling site and with the analytical detection limit of the tracer. With regards to the transport of pathogenic germs in groundwater, this may well be meaningful, for then the first appearance is already a deciding characteristic. However, for determining the parameters for advection and dispersion, the time corresponding to the first appearance of the tracer and the thus derived maximal velocity is not meaningful.

The time of the passage of the maximal-concentration and the thus derived dominant velocity does not exactly correspond, especially with wide and flat breakthrough curves, to the real effective flow velocity. It is however, just as good an approximation as the mean velocity. Usually, the time which corresponds exactly to the real effective flow velocity is in the middle between the time of the passage of the maximal-concentration and the time which corresponds to the mean velocity (Fig. 159). Especially with breakthrough curves, that are influenced by essential chemical reac-

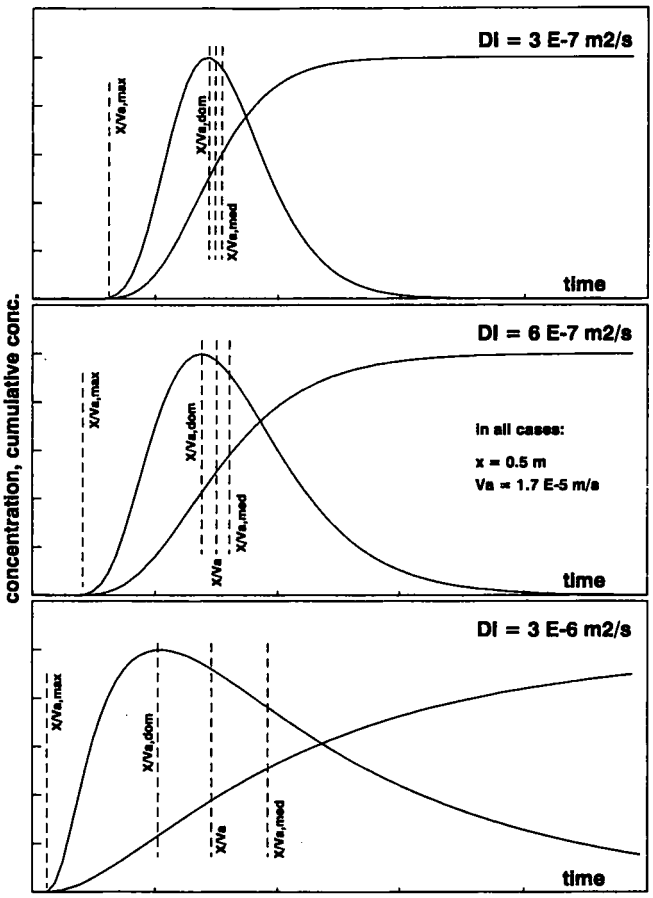

Figure 159. Breakthrough curves with different dispersion coefficients under otherwise identical boundary conditions. In the breakthrough curves the times that correspond to the following are marked: maximal effective flow velocity, dominant effective flow velocity, real effective flow velocity, and the mean velocity. The respective cast lines are also depicted.

tions (cf. Fig. 155) and with those from aquifers with layers with different velocities (Figs 150-154), after a comparatively steep rise in concentration only a very slow decrease in concentration follows the passage of the maximum. In some cases, the passage is characterized by a slightly increased concentration for a long time after the maximum. For such breakthrough curves, applying the mean velocity is totally unsuitable.

In most cases, the effective flow velocity is determined from the breakthrough curves thus: As a first approximation, the time of the passage of the maximal-concentration from the breakthrough curve is used to determine the dominant velocity. With this velocity and a first approximation of the dispersivity (cf. Section 4.3.2) as described in Section 4.1.5, a first simulation with a program for spreadsheet calculations (e.g. LOTUS) is carried out. Depending on the quality of the first approximations of the effective flow velocity and the dispersivity, a fairly good picture of the breakthrough curve is obtained. Through goal-oriented small changes in the input parameters by constantly checking the results on the monitor, a close fit is achieved and the final values for the parameters determined. Figure 160 proves that this method is quite effective. The spreadsheet calculation software LOTUS was used to calculate three different breakthrough curves. All of the input parameters are the same for the three curves, except for the effective flow velocity. The right and the left curve differ from the middle curve by a 20% higher, resp. 20% lower effective flow velocity. This clearly shows, that fitting the parameters to a measured curve can determine the effective flow velocity with a much lower deviation.

Another method for evaluating breakthrough curves was described by SAUTY (1977). This method, which allows the simultaneous determination of the effective flow velocity and the dispersivity by comparing the normalised breakthrough curve with a calculated type curve, is described in the next section.

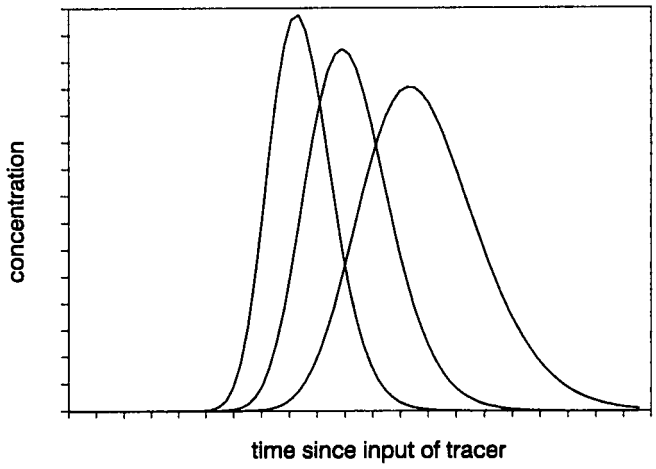

Figure 160. In the three breakthrough curves displayed, the left one has a 20% higher and the right one has a 20% lower effective flow velocity as compared to the middle curve, respectively.

4.3.2 *Determination of the dispersivities*

In principle, at least the longitudinal dispersion coefficient should be able to be determined in the fitting procedure described above using a spreadsheet calculation software program to fit the calculated curve to the measured breakthrough curve. However, the dispersion coefficient cannot be determined with enough certainty, as the effective flow velocity could be in the section covered before. For otherwise equal boundary conditions, Figure 161 shows three breakthrough curves calculated for three different dispersion coefficients, whereby the top and bottom curves each differ from the middle curve by 20% higher or lower, respectively. The figure clearly shows that striking differences can only be found in the peak area of the curve. However, just this area around the peaks is not always sufficiently well specified, in order to correctly determine a proper fitting. Therefore, larger errors are not avoidable if the dispersion coefficients are determined this way.

An interesting method for the simultaneous, fairly sure and mathematically exact determination for effective flow velocity and dispersion coefficients out of the breakthrough curve was published by SAUTY (1977). The essential point of this method is that concentration and time in the measured breakthrough curves are normalized and brought to cover with the respective type curves. The different dispersivities of the type curves and the measured curves are described by the PECLET-number:

$$\mathrm{Pe} = \frac{x}{\alpha_l} \tag{4.16}$$

The PECLET-number (Pe) is dimensionless, since the length of the flow path from the injection site to the sampling site (x) is divided by the length of the dispersivity (α_l). Type curves with both interdependent variables, type concentration (c_r) and the time of the type curve (t_r) are calculated for different PECLET-numbers (Pe) in one-dimensional transport with the following equation:

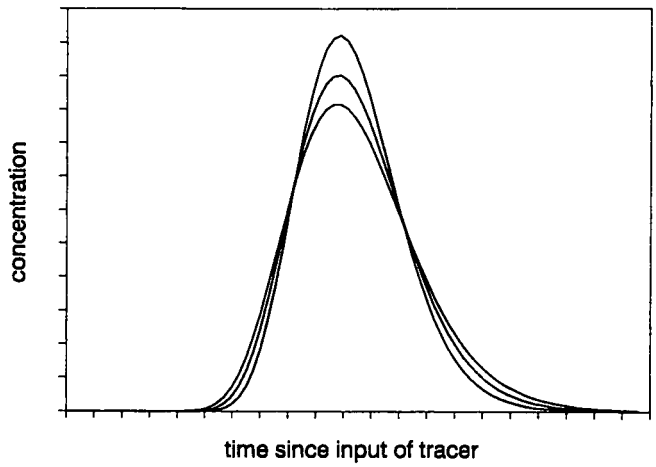

Figure 161. In the three breakthrough curves displayed, the top one has a 20% lower and the bottom one a 20% higher dispersivity as compared to the middle curve, respectively.

$$c_r = \frac{A}{\sqrt{t_r}} \cdot \exp\left[-\frac{\mathrm{Pe}}{4 \cdot t_r} \cdot (1 - t_r)^2\right] \tag{4.17}$$

Figure 162 shows the corresponding type curves for six different PECLET-numbers. The individual type curves are respectively normalized to the same maximal concentration of c_r over the variable A.

$$A = \frac{1}{c_{r,\max}} \tag{4.18}$$

The measured breakthrough curve under investigation is then graphed in the same logarithmic time scale as the type curve. In doing so, the measured concentrations are also normalized so that the maximal concentration becomes 1 and the minimal concentration becomes 0. Then, the normalized breakthrough curve can be brought to cover with one of the type curves. At times, it may be necessary to interpolate between two type curves with different PECLET-numbers. The proper fit produces the corresponding PECLET-number from the type curve, which fit the normalized breakthrough curve. Then the time of the maximal-concentration of the type curve ($t_{r,\max}$) is read from the logarithmic time axis and from the time axis of the normalized breakthrough curve, the time of the measured maximal-concentration ($t_{\max}$). The time, (t_k), that corresponds to the real effective flow velocity, is then given by the following equation:

$$\log t_k = \log t_{\max} - \log t_{r,\max} \tag{4.19}$$

The size of the time ($t_{r,\max}$) conceals the time, which causes (cf. Fig. 159) the time of

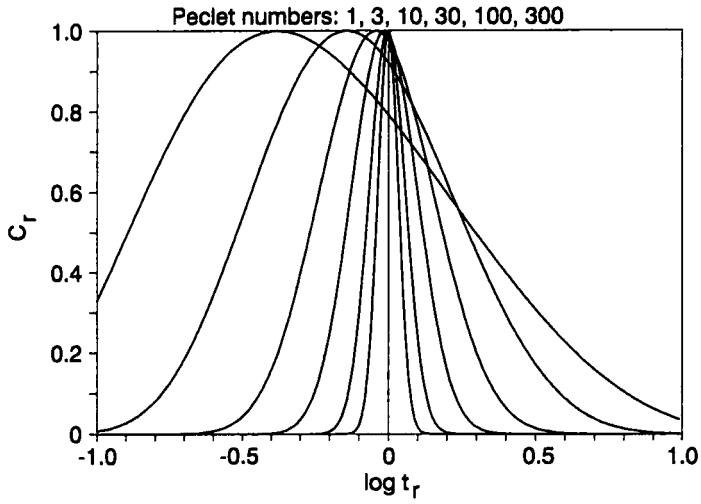

Figure 162. Using such type curves as shown and fitting onto a normalized measured breakthrough curve, the real effective flow velocity and the dispersion coefficient can be determined. The six type curves shown (from left to right) are based on the following PECLET-numbers: 1, 3, 10, 30, 100, 300.

the maximal-concentration in the breakthrough curve to occur *before* the time which corresponds to the real effective flow velocity. The so determined time (t_k) is used to determine the effective flow velocity.

$$v_a = \frac{X}{t_k} \tag{4.20}$$

The PECLET-number that from the type curve which fits the normalized breakthrough curve the best, is used to calculate the dispersion-coefficient.

$$D_l = \frac{v_a \cdot X}{Pe} \tag{4.21}$$

A corresponding evaluation with regards to the transversal dispersion coefficients was also published by SAUTY (1977).

This evaluation method for breakthrough curves can be quickly and easily carried out with spreadsheet calculation software programs. For example, Figure 162 was created using only the program system LOTUS.

4.3.3 *Recognition and rating of geochemical reactions*

Even if much is known about the possible and actual geochemical reactions which take place during solute transport in the underground (cf. Section 4.2), it is still difficult in most cases to quantify the geochemical reactions from measured breakthrough curves. If only one tracer was injected and if the samples were only examined for that tracer, irregularities in the breakthrough curve and deviations from the theory need not only be explained by geochemical reactions. In most cases, several other sources of influence are possible.

Sorption/desorption processes and the resulting retardation of the solute transport (cf. Section 4.2.1) only cause a slowing down of the solute transport. The breakthrough curve has otherwise the same characteristics. If however, an additional ideal (conservative) tracer was not used in the tracing test, the retardation will not be noticed and will incorrectly incorporated into the effective flow velocity determination during the evaluation of the breakthrough curve. Sorption/desorption processes during solute transport can only be determined by comparing several simultaneously injected tracers with another.

Frequently the determination of the retardation coefficients is attempted in laboratory tests with so-called batch tests. To do this, a specific amount of the aquifer material is mixed with water, in which a known amount of the tracer under investigation is dissolved. The mixture is shaken for a certain period of time and then analysed to determine how much tracer is still dissolved in the water and how much has been sorbed onto the aquifer material. This results in the distribution coefficient (cf. Eq. 4.10), from which then with Equation (4.11), the retardation coefficient can be calculated. As can be seen in Table 23, the retardation coefficients determined in this manner can deviate quite considerably from those determined in tracing tests. The reason for these deviations is most likely because the batch tests only provide an imperfect approximation of the processes in the aquifer. Even when carefully conducted, batch tests are only suitable for providing a general idea of the sorp-

tion/desorption behaviour of a tracer in an aquifer. Their only advantage is that they are easy to conduct.

Cation exchange reactions are also practically indeterminable from breakthrough curves, if only the injected cation was measured for the breakthrough curve. As the test from Figure 155 shows, there is practically no retardation for the maximal-concentration in the breakthrough curve for the injected cation potassium. With regards to the injected tracer potassium, the cation exchange reactions during the solute transport only caused a much too low maximal-concentration for potassium in the breakthrough curve and too large of a tail in the potassium concentration. Therefore, the cation exchange reactions can be quantified, if in addition to the injected cation, also all other cations involved in the exchange processes are measured in the sampling sites. This was documented for potassium as the tracer in the tracing test from Figure 155, is valid however also for lithium, which is frequently used as a tracer.

Decay reactions as well as dissolution and precipitation processes during solute transport are incorporated in the breakthrough curves basically only through the changes they cause in the concentrations, i.e., primarily in the recovery rates of the tracers. The recovery rate however, can be practically only checked in column tests in the laboratory. Especially in two-dimensional field tests, a recovery rate that is too low will most likely be attributed to an insufficient observation of the tracer cloud. As a consequence, decay reactions as well as dissolution and precipitation processes in tracing tests will only attract attention if they cause concentration changes that are much larger than those caused by the hydrodynamic dispersion.

4.3.4 *Case evaluations from tracing tests*

In addition to the tracing test described in Section 4.1.4 from the Merdingen test field near Freiburg/FRG, the evaluations from two other tracing tests in very different aquifer material are given here. In one case, the potassium breakthrough curve from the tracing test influenced strongly by cation exchange processes shown in Figure 155 is evaluated. The other case is the evaluation of a karst tracing test in the Lur cave system north of Graz/Austria. Here, although several tracers were injected, the evaluation is limited to the breakthrough curve from lithium. The tracing test data were kindly supplied by W. KÄSS, Umkirch/FRG.

In the tracing test in the Lurbach cave system, 100 kg of lithium chloride with 16.25 kg lithium as a concentrated solution were injected in the Lurbach swallowhole. Among other sampling sites, the spring source of the Hammerbach was sampled. The underground distance between the injection site and the spring source was ca. 3000 m. Figure 163 shows the breakthrough curve for lithium in the Hammerbach spring source. It is striking in this breakthrough curve, that the rise in concentration is very steep and that the fall in concentration after the passage of the maximum is also quite steep at first. However, after the concentration dropped to ca. 1/4 to 1/5 of the maximal-concentration, the lithium concentrations in the breakthrough curve continue to decrease only slowly. Concentrations clearly over the initial concentration were measured for a long time after the passage of the maximum.

Such a definite maximum peak in the breakthrough curve as shown in Figure 163 allows the direct determination of the effective flow velocity, because the difference between the dominant velocity and the actual effective flow velocity (cf. Section

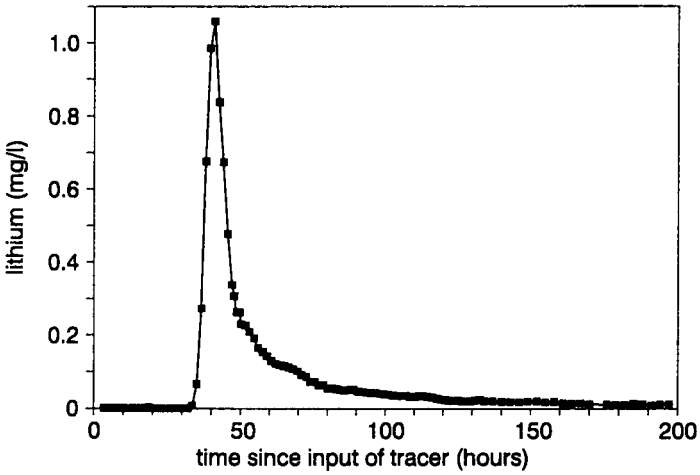

Figure 163. Tracing test in the Lur cave system north of Graz/Austria. The breakthrough curve for lithium is shown. The test data were kindly supplied by W. KÄSS, Umkirch/FRG.

4.3.1) is certainly negligible here and disappears in the inaccuracy from the determination of the maximum through sampling. With a flow distance of $x = 3000$ m and a transport time of 145,800 s, the effective flow velocity can be calculated to $2.0 \cdot 10^{-2}$ m/s. Comparing the normalized breakthrough curve with the type curves from Figure 162 results in a PECLET-number of 250 (the curve from this example is not shown, since this evaluation method is covered in the second example). Using the Equation (4.21) results in a dispersion coefficient of 0.25 m^2/s and with the Equation (4.9), a dispersivity α_l of 12 m. These determined values for the effective flow velocity and the dispersion coefficient fall in the range expected for fissured rock, given in Figure 145.

There are basically two different explanations for such a slow fall in concentration in the breakthrough curve shown in Figure 163. It would be possible that it is caused by similar geochemical processes such as those with potassium in Figure 155. However, since this effect was also observed in the breakthrough curves from other tracers in the tracing test (fluorescent microspheres), this is most likely not the case. Instead, this effect is probably caused by the fact that part of the tracers injected are caught up in slower flowing areas of the cave system and therefore reappear with a delay in the sampling site. This means, that as in the example from the tracing test in Merdingen (Fig. 153), the velocities in the flow system are not statistically distributed. This fact is actually trivial, since the opposite – a perfect statistical distribution of the velocities in the flow system – would be a rarity. Therefore, a similar simulation as for the tracing test from Merdingen shown in Figure 154 was chosen, in that two subordinate and much lower velocities were added to the dominant velocity evaluated. The result of the simulation is shown in Figure 164.

The tracing test shown in Figure 155 was conducted in the laboratory with outwash material from the Segeberger Forst (Schleswig-Holstein/FRG). This material is a mixture of middle to coarse sand and the flow distance was $x = 3.6$ m. Since the absolute concentrations caused by the cation exchange processes in the breakthrough curve could not be taken into account in the evaluation, the potassium concentration from Figure 155 is normalized in Figure 165, i.e. is displayed in the concentration

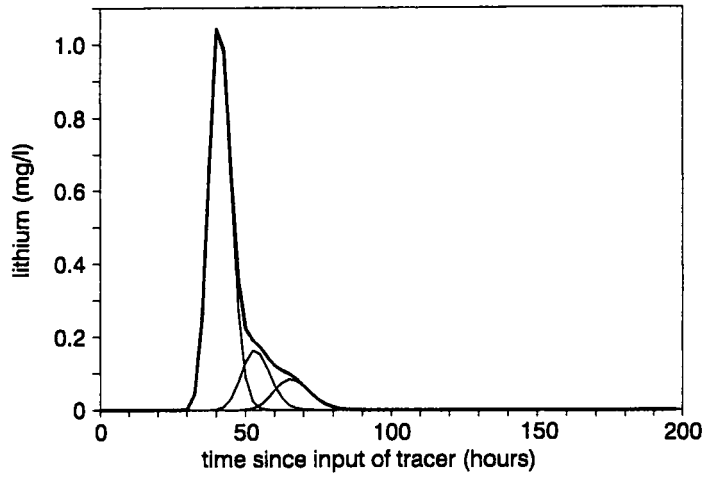

Figure 164. Simulation of the breakthrough curve from Figure 163. Similar to the test in Figure 154, there was a superposition of the prominent tracer cloud and two other tracer clouds with slower velocities.

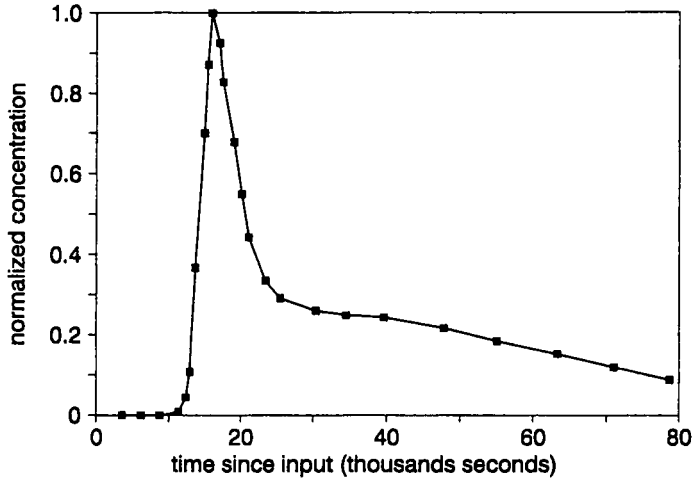

Figure 165. Potassium breakthrough curve from the tracing test shown in Figure 155. Since the absolute concentrations from this test were strongly influenced by cation exchange processes, the concentration was normalized to the range between zero and one.

range from zero to one. It can be clearly seen from Figure 165, that the rise in concentration up to the maximum and the decline in concentration down to about half of the maximum follows the course of a theoretical breakthrough curve. Thus, with regards to the flow velocity and dispersivity only this section of the curve is evaluated.

In Figure 166, this breakthrough curve is graphed against time so that it corresponds to the scale from the type curves in Figure 162. Comparing Figure 166 with

Figure 162, results in a time t_k of 16,600 s, for the resp. effective flow velocity. Together with the known flow distance x = 3.6 m, this gives an effective flow velocity of $v_a = 2.2 \cdot 10^{-4}$ m/s. The form of the normalized breakthrough curve in Figure 166 fits best to a type curve with a PECLET-number of 100 in Figure 162. Using this PECLET-number and the Equation (4.21), a dispersion coefficient $D_l = 7.8 \cdot 10^{-6}$ m²/s and a dispersivity of $\alpha_l = 3.6 \cdot 10^{-2} = 3.6$ cm can be calculated. If these values are used in the one-dimensional simulation according to the Equations (4.3) and (4.4) (Fig. 167), the result is a breakthrough curve whose first part corresponds perfectly to the breakthrough curve shown in Figure 165. Of course, the tail section of the breakthrough curve in Figure 165 which shows the cation exchange impact cannot be determined with the simulation.

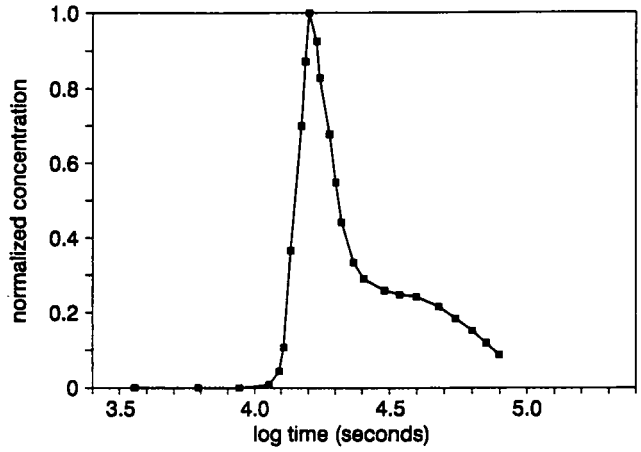

Figure 166. Potassium breakthrough curve shown in Figure 165 with the time axis displayed logarithmically for in order to fit the curve to a type curve from Figure 162.

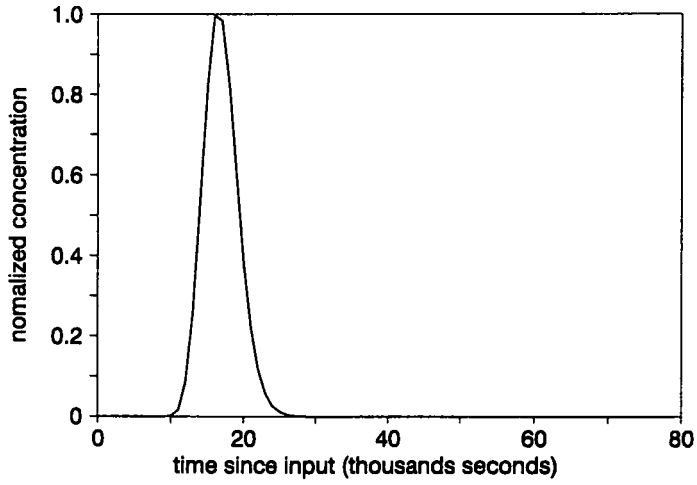

Figure 167. Simulation of the breakthrough curve from Figure 165. The first part of the breakthrough curve is correctly simulated, since the cation exchange processes have no impact upon this section. In the second part, the impact due to the cation exchange processes is missing.

Table 24. Overview of analytical solutions for the interpretation of tracer tests in porous aquifers.

Dimension	Initial-/Border-Conditions	Analytical Solution	Fit parameters	Application	References
1-D ①	$C_f(0,t)=\frac{M}{Q}\delta(t)$ $C_f(\infty,t)=0$ $C_f(x,0)=0$	$C_f(x,t)=\frac{M}{Q\cdot t_0\cdot\sqrt{4\pi P_D\left(\frac{t}{t_0}\right)^3}}\exp\left[-\frac{\left(1-\frac{t}{t_0}\right)^2}{4P_D\frac{t}{t_0}}\right]$	t_0 P_D	Field experiments with measured discharge Q	BEAR 1972 KREFT & ZUBER 1978
1-D normalised ②	$C_{fN}(0,t)=\frac{M}{Q}\delta(t)$ $C_{fN}(\infty,t)=0$ $C_{fN}(x,0)=0$	$C_{fN}(x,t)=\frac{C_f(x,t)}{C_N(x,t_N)}=\sqrt{\left(\frac{t_N}{t}\right)^3}\exp\left[\frac{1-\frac{t_N}{t}}{4t_N t_0}\left(P_D-\frac{t_N t}{P_D}\right)\right]$	t_0 P_D	Field experiments with unknown discharge Q	KREFT & ZUBER 1978
2-D ③	$C_{2D}(0,0,t)=\frac{M}{Q}\delta(t)$ $C_{2D}(\infty,\infty,t)=0$ $C_{2D}(x,y,0)=0$	$C_{2D}(x,y,t)=\frac{M}{nh}\frac{x}{4\pi v t^2\sqrt{D_L D_T}}\exp\left[\frac{-(x-vt)^2}{4D_L t}-\frac{y^2}{4D_T t}\right]$	t_0 D_L D_T	Field experiments	LENDA & ZUBER 1970 KINZELBACH 1986
2-D normalised ④	$C_{2N}(0,0,t)=\frac{M}{Q}\delta(t)$ $C_{2N}(\infty,\infty,t)=0$ $C_{2N}(x,y,0)=0$	$C_{2N}(x,y,t)=\frac{C_{2D}(x,y=0,t)}{C_N(x,y=0,t_N)}=\left(\frac{t_N}{t}\right)^2\exp\left[\frac{-(x-vt)^2}{4D_L t}+\frac{(x-vt_N)^2}{4D_L t_N}\right]$	t_0 D_L	Field experiments with observation point on the main stream line	ATH 1992
1-D ⑤	$C_p(0,t)=\frac{M}{Q}\delta(t)$ $C_p(\infty,t)=0$ $C_p(r,0)=0$	$C_p(r,t)=\frac{M}{Qt_r\sqrt{4\pi P_D\left(\frac{t}{t_R}\right)^3}}\exp\left[\frac{-\left(1-\frac{t}{t_R}\right)^2}{4P_D\frac{t}{t_R}}\right]$	t_R P_D	Pump-tracer-tests	

4.4 TRACI – AN EXAMPLE FOR MATHEMATICAL TRACING-INTERPRETATION-MODEL

A. Werner

The mathematical evaluation of breakthrough curves from a tracing test is possible using analytical and numerical procedures. Especially the simple explicit form of analytical solutions allows a quick determination of transport parameters. The following presents several solutions, that are suitable for evaluating tracing tests in different aquifer types. The methodology used in carrying out and evaluating tracing tests is then described. The analytical solution presented is available in the attached computer program 'TRACI 95'. Further information about the program can be obtained from the file 'Readme.TXT' on the disc.

4.4.1 *Analytical solutions*

The three-dimensional transport of an ideal tracer in groundwater with one flow direction parallel to the X-axis can be described with the advection-dispersion-Equation (4.22) (BEAR 1972):

$$\frac{\delta C}{\delta t} = D_x \frac{\delta^2 C}{\delta x^2} + D_y \frac{\delta^2 C}{\delta y^2} + D_z \frac{\delta^2 C}{\delta z^2} - v \frac{\delta C}{\delta x} \tag{4.22}$$

where C = concentration, D_x = longitudinal dispersion in x-direction, D_y, D_z = transversal and vertical dispersion, v = mean flow velocity, x, y, z = spatial coordinate variables, t = time variable.

Notation to Table 24.

C	(mg/m³)	tracer concentration in water
C_N	(mg/m³)	normalised concentration
M	(mg)	injected tracer mass
Q	(m³/s)	flow rate, discharge or pumping rate
t_0	(s)	mean transit time
x	(m)	direct distance between injection and observation point
v	(m/s)	mean flow velocity $v = \frac{x}{t_0}$
P_D	(-)	dispersion parameter $P_{D=} \frac{D_L}{v \cdot x}$
D_L	(m²/s)	longitudinal dispersion coefficient $D_L = \alpha_L \cdot v$
D_T	(m²/s)	transversal dispersion coefficient $D_T = \alpha_T \cdot v$
α_L	(m)	longitudinal dispersivity
α_T	(m)	transversal dispersivity
t	(s)	time variable
t_N	(t)	time after injection when the normalised concentration was observed
n	(-)	effective porosity
x,y	(m)	space variables
r	(m)	radius
t_R	(s)	mean transit time in the radial flow field $t_R = \frac{r}{v_r} = \frac{n\pi r^2 h}{Q}$
v_R	(m/s)	mean flow velocity in the radial flow field
h	(m)	thickness of the aquifer

Assuming simple flow relationships, homogeneity, and an isotropic aquifer, Equation (4.22) can be analytically solved for certain initial and border conditions (KINZELBACH 1986, 1992). For practicability – in order to reduce the unknown parameters – especially one-and two-dimensional solutions are suitable for evaluation. The following solutions presented are for evaluating tracing tests with ideal tracers with an instantaneous injection according to the DIRAC-function.

4.4.1.1 *Porous aquifers*

Table 24 lists an overview of the possible analytical solutions for describing the transport processes in a porous aquifer. However, the model functions presented are only a small selection taken from the numerous solutions available. There are other solutions available, especially for special cases and for tests with continuous injection of the tracer (KINZELBACH 1986, 1992, FETTER 1993, KREFT & ZUBER 1978, ATH 1992, HÖTZL & WERNER 1992).

The three-dimensional solution of the advection-dispersion-Equation (4.22) is possible, but not applicable for evaluating tracing tests due to the many unknown parameters. However, many field tests can be considered as one-dimensional (SAUTY 1980, KINZELBACH 1986), although the type of injection and sampling have an impact upon the analytical solution. An overview of the possible variations is given in KREFT & ZUBER (1978). For most field tests – injection in wells, sampling in springs and pumping wells – the solution 1 (Table 24) is suitable. With an unknown flow rate Q in the system under consideration, the normalized (at least over the maximal concentration) variation 2 can be applied.

Two-dimensional field tests (uniform distribution of the tracer over the total thickness) can be evaluated with solution 3. Indeed, even this solution requires the determination of three unknown parameters. For monitoring sites in the area of the main flow path, the normalized solution 4 can be applied.

For the evaluation of simple steady-state pump-tracer-tests in a radial-symmetric flow field, the variation 5 of solution 1 is applicable.

4.4.1.2 *Fissured aquifers*

The transport processes during flow in a fissured aquifer are described in detail in Section 5.3.3. The presented SFDM-solution (MALOSZEWSKI et al. 1985, 1990), which considers along with advection and dispersion also the matrix diffusion as a transport process, is especially suitable for evaluating tracing tests in fissured aquifers. In particular the limiting to only three fitting parameters allows a rapid evaluation.

4.4.1.3 *Karst aquifers*

The transport processes in a karst aquifer can be very different. For tracing tests in the conduit system of a karst aquifer, the analytical solution 1 (Table 24) can be applied in many cases. However, many karst breakthrough curves are characterized by tailing or peaks. Such breakthrough curves can be evaluated with the Multi-Dispersion-Model, MDM (MALOSZEWSKI et al. 1992, 1994). This model is an extension of the solution 1 (Table 24). The obtained breakthrough curve is taken to be a superposition of different flow paths (Fig. 168). In the evaluation, the parameters of the individual curves are determined step by step. The MDM has been

Multi-Dispersion-Model (MDM)
Interpretation of Breakthrough Curves in Karst Systems

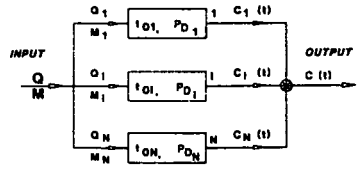

(from MALOSZEWSKI et al. 1992)

$$C_i(t) = \frac{M_i}{Q_i} \cdot \frac{1}{t_{0_i}\sqrt{4\pi P_{D_i}\left(\frac{t}{t_{0_i}}\right)^3}} \cdot \exp\left[-\frac{\left(1-\frac{t}{t_{0_i}}\right)^2}{4P_{D_i}\left(\frac{t}{t_{0_i}}\right)}\right]$$

$$C(t) = \sum_{i=1}^{N} C_i(t)$$

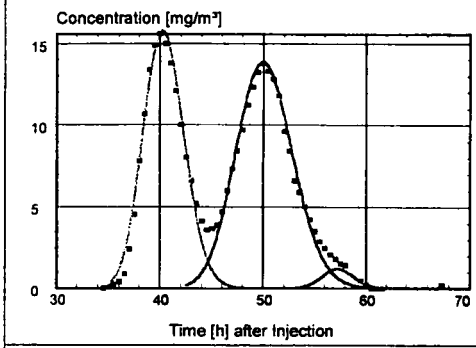

	Peak I	Peak II	Peak III
t_0 [h]	40	50	57
PD [-]	0.0012	0.0015	0.0004
α_L [m]	14	18	5

Figure 168. Principle of MDM.

successfully applied in karst regions many times (MALOSZEWSKI et al. 1992, 1994, WERNER et al. 1997a,b, WERNER & MALOSZEWSKI 1997).

4.4.2 *Conducting a tracing test for an evaluation with analytical solutions*

The planned mathematical evaluation of a tracing test must be taken into account in planning the tracing test. A suitable model for the evaluation of the test should be determined before the test begins, so that the required initial and border conditions can be kept during the test.

The following prerequisites must be fulfilled so that the test can be mathematically evaluated:

– Use of an ideal tracer,

– High temporal resolution of the breakthrough curve with samples taken close together,

– Exact observance of the initial and border conditions (DIRAC-pulse).

4.4.3 *Determination of the parameters*

In using an analytical solution to evaluate a tracing test, the unknown parameters (Table 24) can be determined for the advection and dispersion transport process.

The results of the mathematical evaluation must always be critically checked. It is especially important to verify the validity of the selected model. For example, an injection in the unsaturated zone of an aquifer can cause a long tailing of the breakthrough curve. This curve could be described with a fissured aquifer-model.

However, the actual transport processes would not have been taken into account with this model and thus the determined results would not be valid.

4.4.3.1 *Direct evaluation*

In a direct evaluation, the optimal best-fit of the solution function to the results from the tracing test is won by directly simulating the unknown parameters. These parameters are varied manually until the optimal best-fit is achieved. The direct fitting can be carried out using a spreadsheet program such as EXCEL, LOTUS, or QUATTRO PRO (Fig. 169). The procedure can be time-consuming and never allows an exact, but rather only an approached solution. This procedure is only practicable for analytical solutions with maximal two parameters.

4.4.3.2 *Inverse evaluation*

In an inverse evaluation, the results of the tracer experiment are iteratively fitted through a minimization procedure, e.g. TAYLOR method, gradient method, or MARQUART procedure, onto the analytical solution function (Fig. 170). A quality assessment method, e.g. least squares method, is used to check which distribution of the fitting parameters provides the best-fit. An advantage of the inverse method is the rapidness and exactness of the solution. In particular, with suitable optimization procedures, a best-fit for analytical solutions for three or more parameters can be

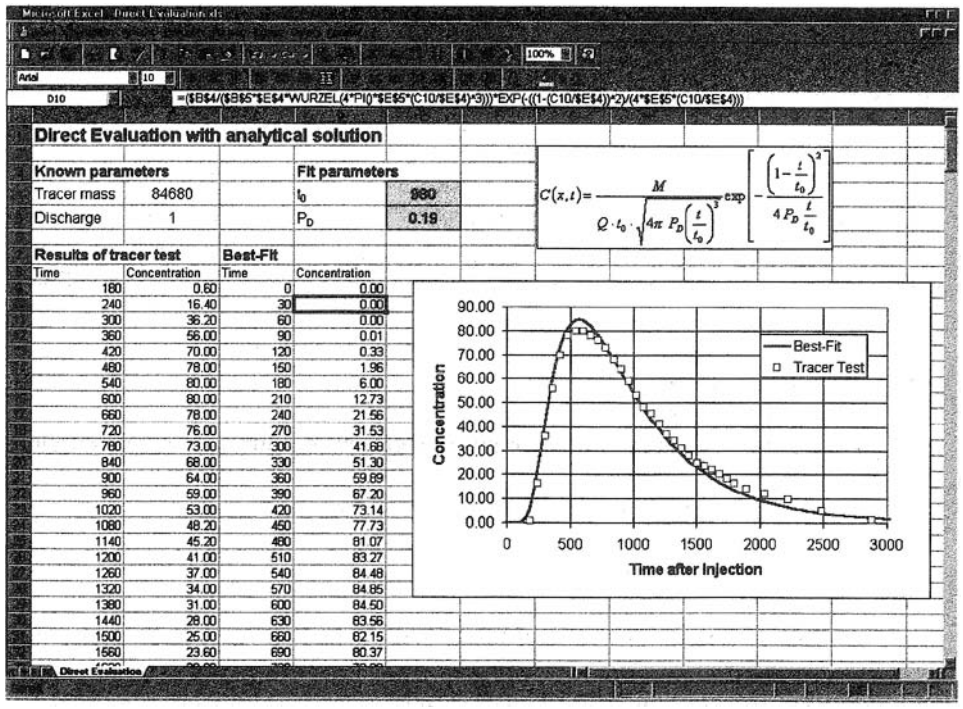

Figure 169. Direct evaluation of tracing tests with the means of a calculation program.

found. However, it must always be taken into account that in such cases there are also more than one possible solution. Thus, these can be dependent upon the initial values of the procedure. Especially with the models with three unknown parameters, the initial values should be in the vicinity of the expected solution (Fig. 171). To estimate the initial values, empirical methods (C_{max}-procedure, cast line) or the moment method are suitable.

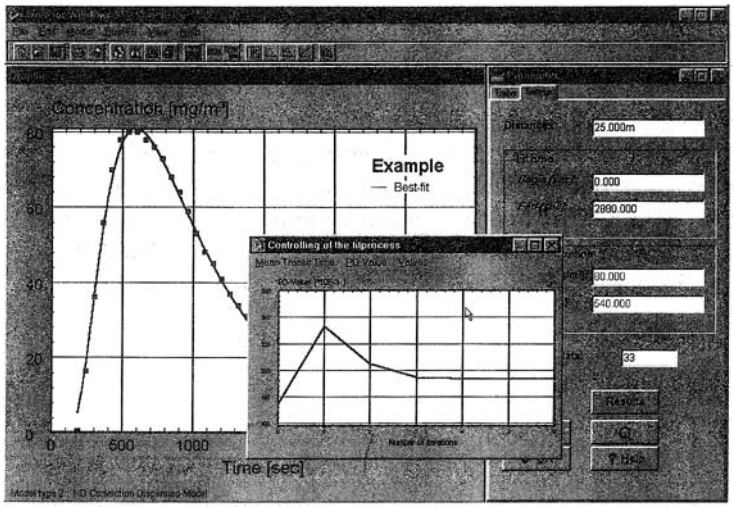

Figure 170. Inverse evaluation with an analytical solution function.

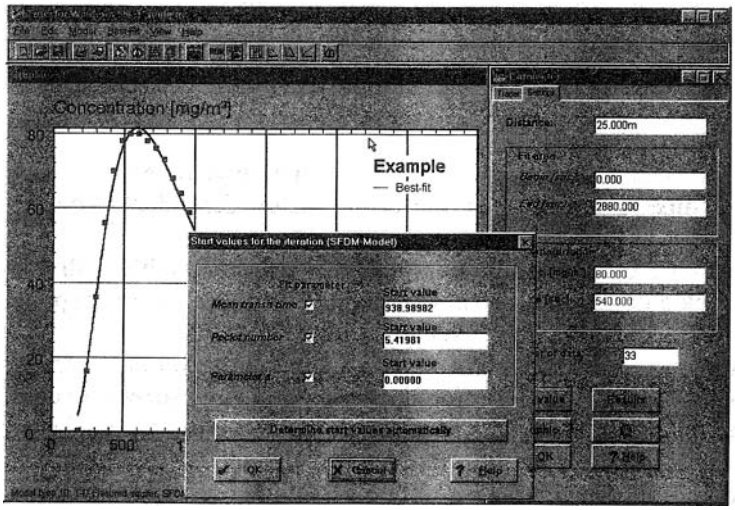

Figure 171. Inverse solution with three unknown parameters.

4.5 RADIOHYDROMETRICAL SINGLE-WELL-METHODS

*H. Moser**

4.5.1 *Introduction*

Since 1957, quantitative groundwater investigations have applied the single-well-method using radioactive nuclides (cf. Section 2.4) to determine groundwater flow (MOSER et al. 1957). The accuracy, the resolution capability, and the interpretation ability of this method have been greatly improved during the last decades. Now, this method can be rationally and economically utilized for prompt determination of local, spatial, and temporal parameters of the groundwater flow.

Radiohydrometrical single-well-methods require a monitoring well in the aquifer under investigation, that covers either the entire aquifer or at least the part under investigation. The well should be developed by a circular screen and gravel pack, so that the groundwater movement through the well is free of sand and suspended solids at low screen resistance. With respect to the aquifer, the gravel pack must have the correct grain size distribution and the filter screen slots must be smaller than the minimum grain size of the gravel pack (for more information, see e.g. DROST & MOSER 1980).

4.5.2 *Tracer dilution logging and tracer flowmeter*

Radiohydrometrical single-well-methods have been described many times in the literature (IAEA 1983a,b, DROST 1983, 1984, 1986, 1989). Therefore, the following handles only those procedures which are applied most frequently, tracer dilution logging and tracer flowmeter.

In tracer dilution logging, the water column in the dilution volume of the filter screen is labelled homogeneously with a tracer. Due to the stationary groundwater flow, in time t there is a horizontal tracer flow, which leads to a concentration decrease in the filter screen (Fig. 172). This yields the filtration velocity v_f:

$$v_f = \frac{\pi r}{2\alpha t} \ln \frac{C_0}{C} \tag{4.23}$$

where r = radius of the filter screen, C_0 = tracer concentration at time $t = 0$, C = tracer concentration at time t, α = α-value, correction factor, dependent upon the well construction.

In principle, all naturally occurring filtration velocities are measurable with this method. At very low velocities ($v_f < 1$ m/y), diffusion of the tracer can overlap the dilution to be measured due to convection, and thus forms a lower limit.

Vertical flow movements in the well screen make the interpretation of the tracer dilution with Equation (4.23) difficult. Therefore, tracer probes with packers are used to isolate the dilution volume in the well screen. Such a probe is shown in Figure 172. Before the tracer probes are put in, the entire water column in the well screen is marked and then the concentration decrease as a function of the depth and time

* The author would like to thank Dipl.-Phys W.DROST for his critical review of the manuscript.

logged. This method is still used today, when the vertical flow in the well screen is small enough to be neglected for use in the dilution method (IAEA 1983b).

The filtration velocity can also be indirectly measured with the vertical flow Q_v in the well screen, since its changes are essentially due to the exchange of water with the surrounding layers of the aquifer and thus dependent upon the hydraulic conductivity. The vertical flow velocity v_v is measured, where, besides the hydrometric propeller, for low values of v_v above all the tracer flowmeter has proven itself. It is shown in Figure 173. With Equation (4.24) and the measured values of v_v, the vertical flow can be calculated and from its variations, the inflow and outflow in the well screen be localized and quantified.

$$Q_v = v_v\, q \tag{4.24}$$

where q = cross-section of the well screen.

The radioactive isotopes bromine-82 (^{82}Br) and technetium-99m (^{99m}Tc) are preferably used as the tracers in dilution and flowmeter logging. These can be detected in situ in such low concentrations, that such additions cause practically no changes in the physical and chemical properties of the groundwater. The measurement activity necessary is below the limit set by the radiation protection

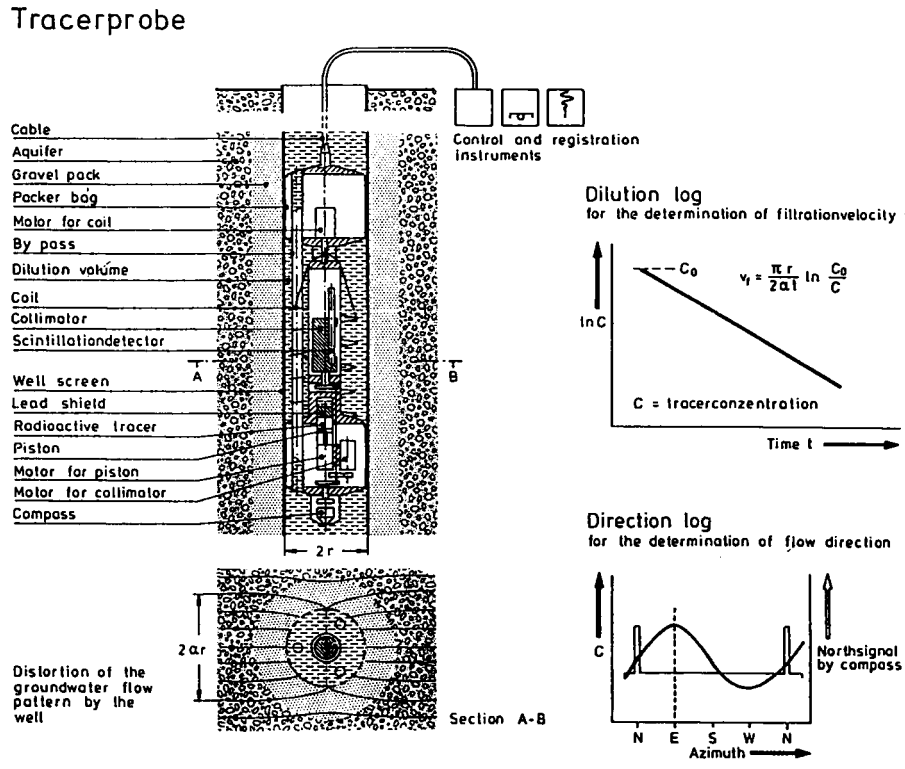

Figure 172. Tracer probe and principle for determining filtration velocity v_v and flow direction Ri of groundwater (DROST 1983). Height of the dilution volume: 50 cm.

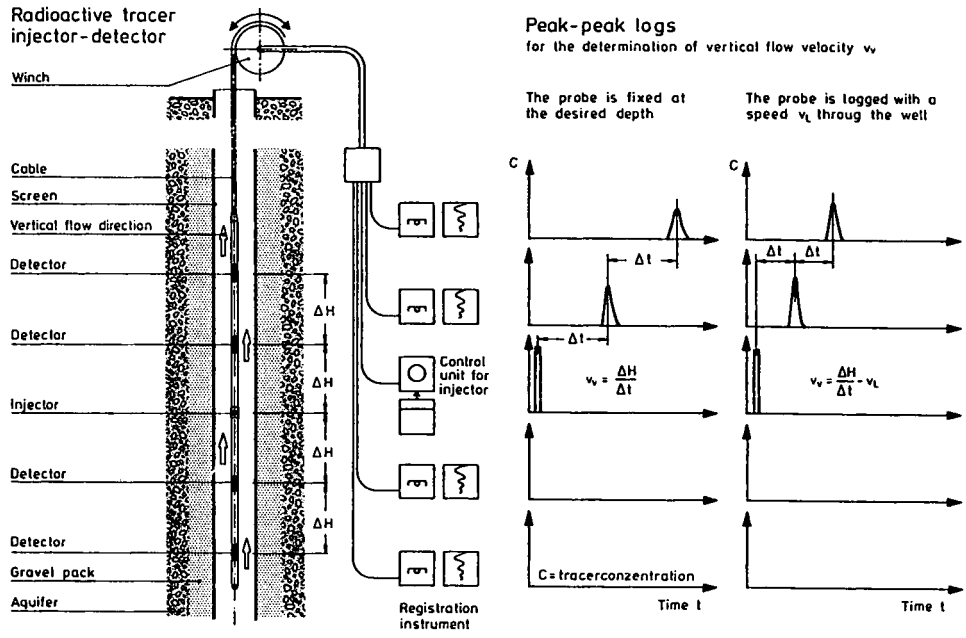

Figure 173. Tracer flowmeter and principle for determining the vertical groundwater velocity in the well screen of a groundwater monitoring well (DROST 1983).

ordinances and is, also considering the short half-life times (Br-82: 35h; Tc-99m: 6h, cf. Section 2.4) harmless to the public.

Using radioactive tracers in these methods allows the simultaneous determination of the groundwater flow direction, after the tracer cloud has flowed out into the aquifer. A suitable detector is used to record the azimuth of the tracer distribution, as shown in Figure 172. Direction logging can be used together with dilution logging or separately.

4.5.3 *Application areas*

The radiohydrometrical single-well-methods described in Section 4.5.2 have been used for around 20 years in quantitative groundwater investigations. Just in the GSF-Institute of Hydrology, Neuherberg near Munich/FRG, these methods have been used in more than 200 investigation areas. The applications were mostly in porous groundwater; however questions as to flow movements and the local flow direction in fissured groundwater could also be answered.

The manifold application areas are:

– In groundwater exploitation investigations (e.g. estimating the available water resources, determining the water protection zones, determining the impact of river bank filtration upon the groundwater),

– In measures concerned with groundwater pollution (e.g. determining the possible range of contaminants, measuring the disturbance of the natural hydraulic relationship due to e.g. waste seepage),

– In engineering (e.g. investigation of foundation conditions with underground engineering projects during the geotechnical exploration, building, and determining the variation in the groundwater regime due to the project).

Such examples can be found in Sections 5.5.1 and 5.9, and in the annual reports and publications of the GSF-Institute for Hydrology (IfH, 1989), as well as in MOSER & RAUERT (1980), DROST (1989), and IAEA (1983a,b, 1990).

Radiohydrometrical single-well-methods can only deliver the necessary values for a geostatistical evaluation of a larger area in aquifer, if there are enough groundwater monitoring wells that tap the aquifer and thus consider the variance of the filtration velocity and flow direction in the aquifer. These are mainly dependent upon the structural and textural properties of the sediments in the aquifer. Typical distributions of groundwater filtration velocities in unconfined, quasi-infinite aquifers with constant hydraulic boundaries are shown in the probability diagram in Figure 174. The v_f-values are distributed log-normally, so that the mean and the standard deviation $\sigma(v_f)$ can be read from the probability diagram in Figure 174. Generally, the variance of the filtration velocity correlates with the variance of the flow directions (DROST 1984): The more the v_f-values in an aquifer scatter, the larger the variation in the flow direction.

Most of the investigations were carried out in aquifers where pumping tests had also been conducted and the transmissivity determined. Therefore, a comparison could be set up between the values from the pumping tests for hydraulic

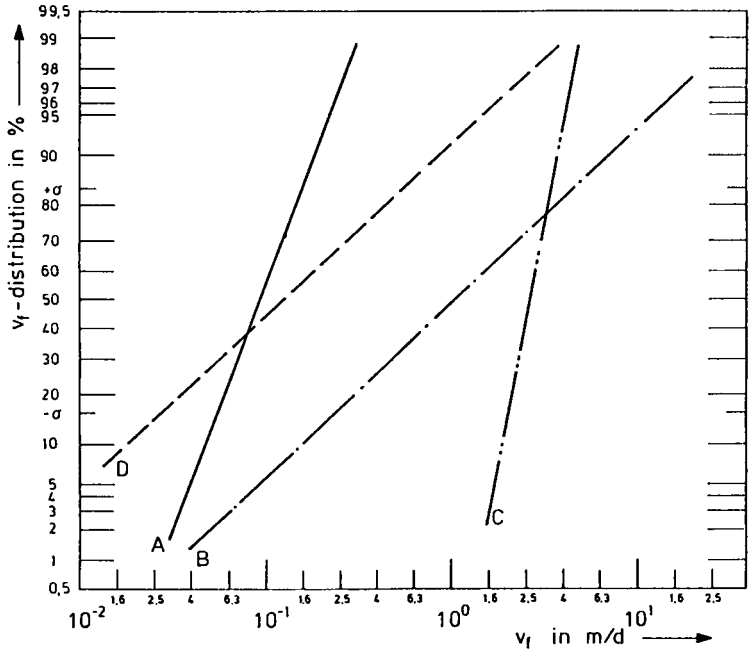

Figure 174. Frequency distribution of filtration velocities v_f in porous groundwater from different aquifers. A = aeolian sands, B = fluvioglacial gravels and sands, C = well sorted fluvioglacial gravels, D = glacio-fluvial sands (DROST 1986).

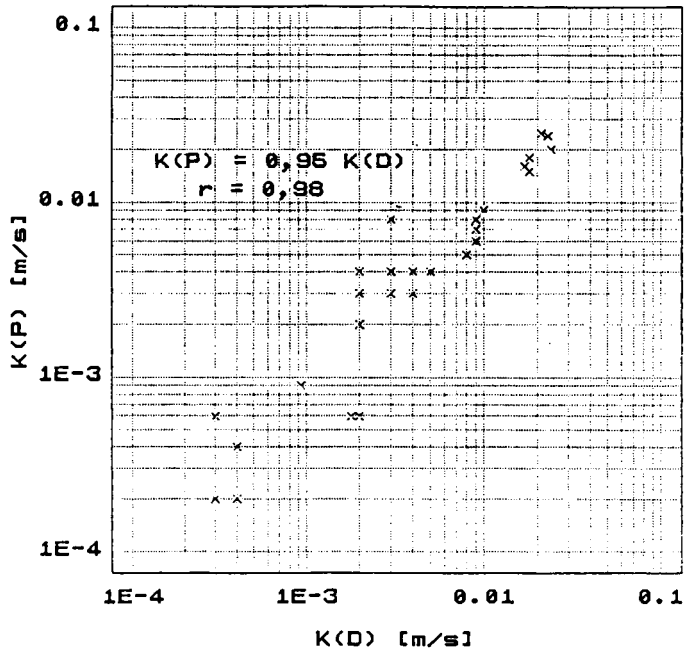

Figure 175. Hydraulic conductivities of different aquifers determined by single well dilution tests ($k(D)$) and by pumping tests ($k(P)$) (DROST 1984).

conductivity, $k(P)$, and those from the tracer dilution logging tests, $k(D)$, determined from the mean filtration velocities. Figure 175 shows that for the k-value range from 10^{-4} to 10^{-1} m/s, the independently determined hydraulic conductivity values agree very well. Thus, radiohydrometrical single-well-methods can be utilized as a reliable procedure for determining k-values.

The dispersivity as an essential parameter of an aquifer is generally determined through direct measurements of the spreading of conservative tracers or other water constituents. SEILER (1985) was able to show however, that the dispersivity values, usually determined over relatively short distances, increase with increasing flow path and that only after a very long flow path, that can only be measured in special cases, do the values join asymptotically in a plateau, the macro-dispersivity. To overcome these methodical difficulties, it was proposed (GELHAR 1986), that the macro-dispersivity of an aquifer be determined from the variance of the log-normally distributed k-values. DROST and HOEHN (1989) have tried to use this method in the Glatt valley (Canton Zürich, Switzerland) to calculate the macro-dispersivity for fore-alpine fluvioglacial sediments from the log-normal distribution of the filtration velocities. The results show that the values thus determined are indeed higher than the value determined with direct measurements of the tracer propagation over a short flow path. Therefore, the radiohydrometrical single-well method is proven to be a simple procedure for the determination of the dispersivity of an aquifer, provided there is a sufficient density of monitoring wells.

CHAPTER 5

Practical examples of applications and interpretations

W. Käss

The preceding chapters covered aspects pertaining to the materials, to the measurement-analytical, organisation, and interpretation techniques. This chapter describes case examples from the large range of practicable applications in hydrological tracing techniques. As was aforementioned, each hydrological situation requires an individual solution concept. Thus, the case examples described here can only be used as an aid for setting up each individual case concept.

5.1 UNSATURATED ZONE

Numerous chemical and microbiological reactions occur in the aqueous phase of the unsaturated zone. The intensity of these transformations increases with increasing residence time and increasing (micro-)biological activity.

KÄSS (1985) compiled a review with examples of the possibilities in seepage water tracing tests. Seepage water tracing tests using elements, whose active isotopes enter the environment through nuclear plants or nuclear weapon tests are of great interest. However, such investigations can only be rarely found in the literature (AURAND et al. 1972). Most of the publications handle the infiltration into and seepage through the unsaturated zone with the environmental isotope tritium (MATTHESS et al. 1976). Case applications using conservative tracers can be found in e.g. BOWMAN & RICE (1986) or HARVEY (1993).

5.1.1 *Hazardous waste site – Eckenweiherhof/Mühlacker*
H. Hötzl

Tracing problems at hazardous waste sites

Nowadays, waste disposal and the disposal of other non-recyclable materials are subject to strict regulations, that were set up to prevent the emission of contaminants into the area surrounding a waste site. To avoid soil and groundwater contamination due to the seepage of the leachate, different security measures as a multiple barrier system are implemented. This should assure that in case of failure in part of the system, the seal is still in function.

The components of such a protection system are a controllable leachate drainage, artificial base liners, and the natural geological barrier of the underground.

Due to misjudgement and partially to incorrect assumptions concerning the ambiguity of possible contamination propagation, some of the older waste sites have no or only insufficient security measures. Inevitably, many of these dumpsites have become contamination sites with polluted seepage water infiltrating the underground through individual leaks or through large scale leakage. If the underground has no retention capacity, the dumpsite seepage water can infiltrate the unsaturated zone, down even to the groundwater level, thus causing not only soil, but also groundwater contamination.

Applying tracing techniques can aid not only in checking for possible leaks in old and new waste sites, they can also supply information when investigating the propagation paths of known contaminations. Although dumpsite leachate is already labelled by a characteristic spectrum of constituents and thus acts as a tracer solution, the addition of a suitable tracer can simplify the investigation of the propagation considerably. This is especially true for leachates, whose problematic constituents or characteristic components are either present only in low concentrations or strongly sorptive, so that after only very short flow distances underground, they can no longer be detected. Furthermore, applying artificial tracers can be necessary in order to investigate special areas in a dumpsite, which is suspected of leaking.

Using tracers in leachates presumes a high chemical stability of the tracer. In solution with the aggressive or strongly acidic or alkaline seepage waters, reactions must not occur which would change the properties of the tracer or cause it to decay. Furthermore, the detection sensitivity can also be reduced due to superposition with other constituents. These prerequisites must be fulfilled when applying tracers with leachates.

A case of applying tracing tests in connection with leachate propagation is detailed in the example of the former hazardous waste dumpsite Eckenweiherhof near Mühlacker/Germany. During the pilot investigations conducted in the state of Baden-Württemberg for determining old contaminations, this site was chosen among others for the detail investigation (HÖTZL et al.1987). The deposits, mostly galvanic sludge enriched with heavy metals and organic solvents, were stored in four separate basins inside the weathered Gypsum Keuper (Fig. 176).

After the wastes were deposited, control examinations showed that pollutants had entered into the dumpsite surroundings. A survey of the extent of the pollution underground (Fig. 177) was completed by carrying out detailed investigations of the geological and hydrogeological relationships and the contamination of the soil air, leachate, and groundwater (CROCOLL 1990). Knowledge of the extent of the spatial and temporal course of the contaminated water propagation was necessary for pending remediation measures. It was obtained with additional tracing of the dumpsite seepage water in the individual deposit basins and tracing of possible hydraulic routings in the marly-clayey Keuper sediments. The groundwater table was ca. 30 m below the surface, whereby within the unsaturated zone individual impervious layers developed.

In preparation of these tracing experiments, extensive comparison investigations were carried out as to the suitability of the chosen fluorescent dyes in the seepage water from the dumpsite Eckenweiherhof (REICHERT & HÖTZL 1990). The waste site

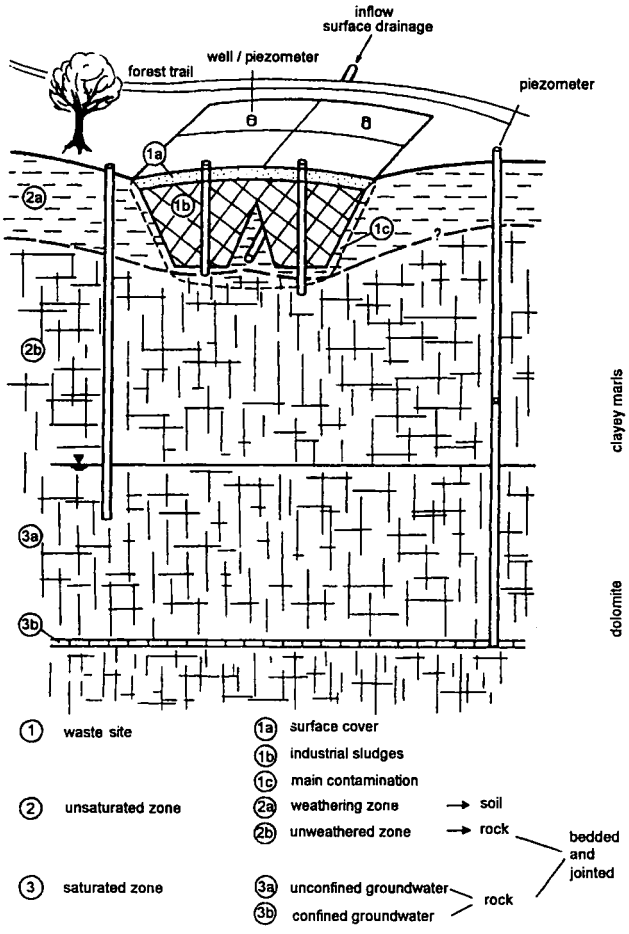

Figure 176. Spatial layout of the hazardous waste site Eckenweiherhof near Mühlacker, Baden-Württemberg/Germany, with a schematic-geological profile (HÖTZL et al. 1987).

seepage water is a two-phase mix from a brown oily liquid and a light yellow aqueous phase, which do not separate until the mix has stood for a long time. The main components are different hydrocarbon compounds, among them LNAPL and BTEX-components as well as concentrations of heavy metals.

Tracer suitability for the leachate and contaminated waters

When applying fluorescing tracers, the self-fluorescence of the seepage water is the deciding factor in choosing the correct tracer. Here, the seepage water had a pronounced fluorescence maximum in the UV-range and two clear weaker peaks at 524.5 nm and 552.5 nm excitation wavelengths (Fig. 178). Temporal variations as well as changes in the peaks were observed at different mixing ratios from the four separate areas.

To check the suitability of the fluorescent dyes, seven tracers (Table 25) were mixed with the seepage water and diluted to create calibration series (REICHERT & HÖTZL 1990). The decrease in detection sensitivity and the chemical stability were examined. All of the tested dye tracers suffered a clear reduction in the detection

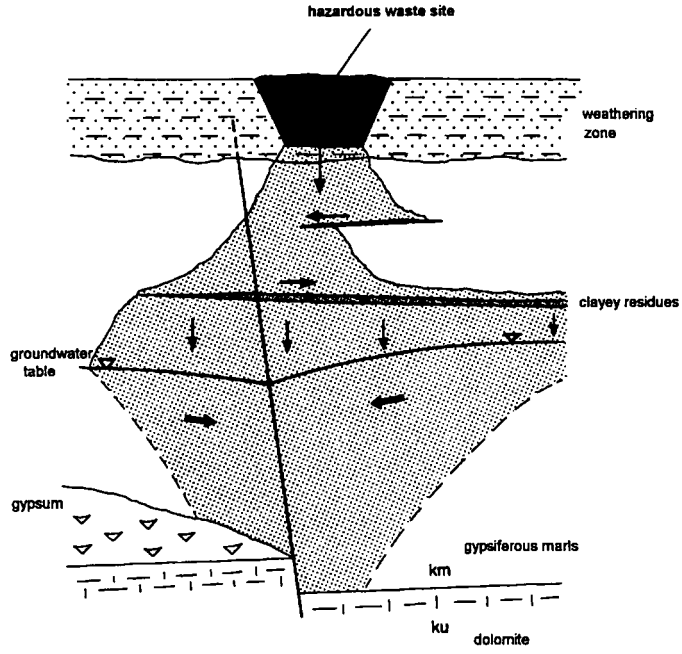

Figure 177. Propagation of the organic pollutants in the underground of the presently covered up hazardous waste site Eckenweiherhof (from CROCOLL 1990). The distribution of the contaminants is influenced by the different degrees of gypsum subrosion.

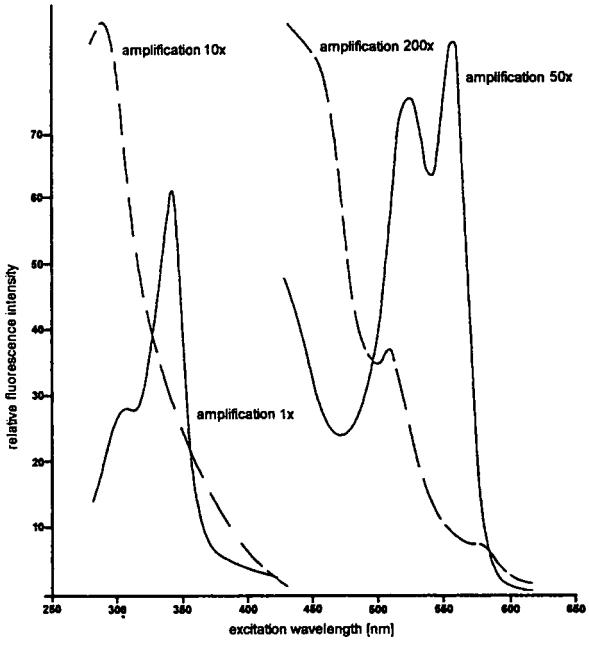

Figure 178. Fluorescence spectra of leachate from the hazardous waste site Eckenweiherhof. Dashed line: seepage water from basin 1, solid line: from basin 4. The spectra were run as a synchronscan procedure with a difference of excitation- and emission monochrometer of 95 nm (250 to 450 nm excitation) and 25 nm (450 to 650 nm excitation). The leachate from basin 4 clearly shows peaks (at 338.5, 524.5, and at 552.5 nm), which are partially in the same wavelength range as conventional tracers.

Table 25. Detection limits for fluorescence dyes in dilution series with tap water and leachate mixes from the hazardous waste site Eckenweiherhof.

Dye	Tap water µg/l	Dumpsite water µg /l
Naphthionate	0.080	80.0
Uranine	0.002	0.3
Eosin	0.025	4.0
Pyranine	0.050	4.0
Rhodamine B	0.008	2.0
Amidorhodamine G	0.007	0.9
Sulforhodamine B	0.009	8.0

sensitivity when mixed with the seepage water, mostly due to the high fluorescent background. Due to the increased fluorescent peaks of the contaminated water in parts of the spectrum, the tracers affected the most were naphthionate and at both longwave peaks, rhodamine B and sulforhodamine B. It was necessary to clean the mixed samples with the leachate water before the fluorescence was measured by filtering through a single use filter with a 0.45 µm pore size. This turned out to be disadvantageous, due to further reductions in the detection sensitivity of the individual tracers caused by adsorption that is dependent upon substance specific factors.

The chemical stability of the chosen fluorescent dyes in the leachate of the hazardous dumpsite Eckenweierhof were checked with storage tests. The dye-leachate-mixtures were fluorimetrically examined regularly over 40 days. The samples were filtered before measuring.

A direct influence of the leachate upon the chemical stability of the investigated fluorescent dyes could not be determined. However, the sorption of the dye tracer onto the oil phase of the contaminated water lead to a considerable decrease in the concentration during the observation period of the storage tests. The cationic rhodamine dyes also showed an increased tendency towards adsorption onto the oil phase. During a direct injection in the dumpsite area, an increased amount of the dye will become fixed, so that the rhodamine dyes are less suited for use in test areas with high leachate fractions. The anionic dyes uranine, pyranine, and eosin were only slightly retained in the oil phase. They are suitable for a direct injection into the dumpsite. With low shares of the leachate in the groundwater, for example in the area surrounding the dumpsite, it would be possible to use all of the investigated dyes.

To check the suitability of the chosen dyes in dependency upon the rock type, Keuper marls from different borehole depths were used. The high fraction of clay minerals in the weathered marls caused a very high adsorption capacity in the columns. An influence upon the migration behaviour of the tracers tested by the leachate was not observed. However, the tracers tested displayed very different fixation rates in the Keuper marls. The rhodamine dye group was highly adsorbed. Eosin and uranine were moderately sorptive. Sorption and exchange processes only slightly impaired the propagation behaviour of pyranine, naphthionate and lithium in the Keuper rocks.

Based on the laboratory tests, different tracers are suitable for determining the pollutant propagation in the underground of the hazardous waste site Eckenweiherhof/Mühlacker with combined tracing tests. In the actual dumpsite area, the fluores-

cent dyes uranine, pyranine, and eosin were recommended for injection in each of the four separate basins, since these anionic dyes are characterized by good chemical resistence with respect to the leachate and by low sorption tendencies in the Keuper rocks. The reduction of the detection sensitivity in the three fluorescent dyes caused by the fluorescence background in the leachate could be compensated with increased injection quantities. Lithium could be used as a further tracer, since the Keuper rocks only display a low sorption and exchange capacity for it. In the area surrounding the dumpsite with low leachate fractions, the additional use of naphthionate and amidorhodamine G was possible. It was not recommended to use the strongly sorptive tracers rhodamine B and sulforhodamine B.

Conducting the experiment and results

The combined tracing experiment in the area around the former hazardous waste site was carried out in April 1990 after a pumping test that had lasted several months. Based on the previous tracer comparison tests, in two of the individual basins, 10 kg of dissolved uranine was injected in the seepage water monitoring well P 1 and 10 kg of dissolved pyranine was injected in P 3 (Fig. 179). Each tracer was flushed with 200 l, a very small amount that was deliberately chosen. The natural leachate conditions should not be too strongly influenced by the tracing test and furthermore, since increased washing out of pollutants from the dumpsite should not occur.

For the parallel determination of the groundwater flow under the dumpsite, tracing tests were carried out in two groundwater monitoring wells in the direct surroundings of the dumpsite. At a depth of 38 m, 3 kg of eosin were injected in the monitoring well B 1 and 10 kg of lithium chloride in the monitoring well B 13 at a depth of 26 m.

All of the other available groundwater monitoring wells were monitored. The

Figure 179. Tracing test Eckenweiherhof 1990. Uranine injection in the leachate monitoring well P 1. The dissolved uranine was pumped into the monitoring well with a drill pump and PVC-hoses (Photo: HÖTZL 1990).

sampling was done with permanently installed submersible electromagnetic reciprocating pumps. Since a niveau orientated sampling over the whole borehole depth was not possible, a flowmeter was first used to determine the most pervious fissure zones and the pumps were then installed at these levels. Before each sample was taken, ca. 10 l of water was pumped to assure a sufficient rinsing of the pumps and hoses. A complete exchange of the water volume in the monitoring well was neither technically possible nor desired, due to possible disturbances in the natural flow conditions as a result of the low yield.

The fluorescent dyes were determined fluorimetrically with the synchronscan procedure (cf. Section 2.1.3.3) and lithium with atomic absorption spectroscopy. For quantitative evaluation, calibration curves were recorded from solutions of the original substance of the injected tracer with the leachate, with groundwater and a high leachate fraction, and with uncontaminated groundwater.

For slightly over a year, ca. 3500 samples, appropriately temporally staggered, were taken from 20 sampling sites and analysed. During the course of the tracing test, all of the injected tracers were recovered in different monitoring wells; however, the detected concentrations were generally very low. Compared to tracing tests in other fissured aquifers, classical breakthrough curves were not observed. The different tracers were sometimes only detected in single samples and longer tracer breakthrough curves were sometimes interrupted by negative samples (Fig. 180). A modelling evaluation of the recorded breakthrough curves, e.g. with the dispersion model, was not possible. As hydraulic characteristic values, only the maximal effective flow velocity, which is the quotient of the distance to the sampling site and the time of the first tracer detection could be determined from the detected tracers. With clear breakthrough curves, the dominant effective flow velocity (distance divided by the time up to the tracer maximum) could also be determined.

The determined characteristic values for uranine are summarized in Table 26. The flow velocities V_{max} and V_{dom}, calculated from the initial and maximal concentration, except for B 9, were determined as effective horizontal flow velocities. The spatial

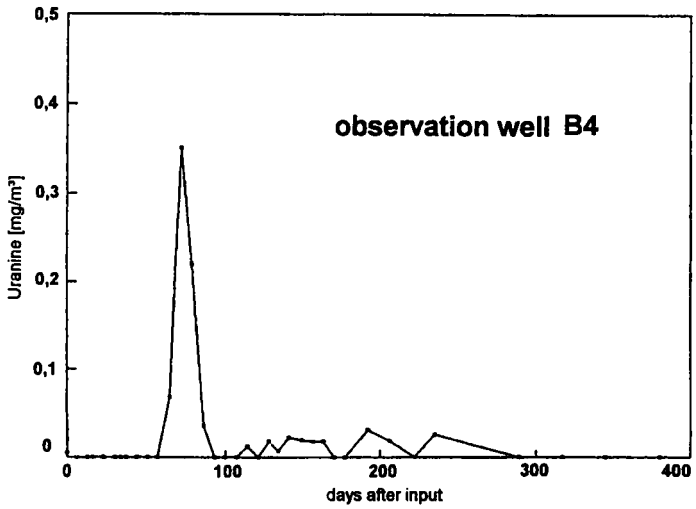

Figure 180. Tracing test hazardous waste site Eckenweiherhof 1990. Uranine breakthrough in the groundwater monitoring well B 4.

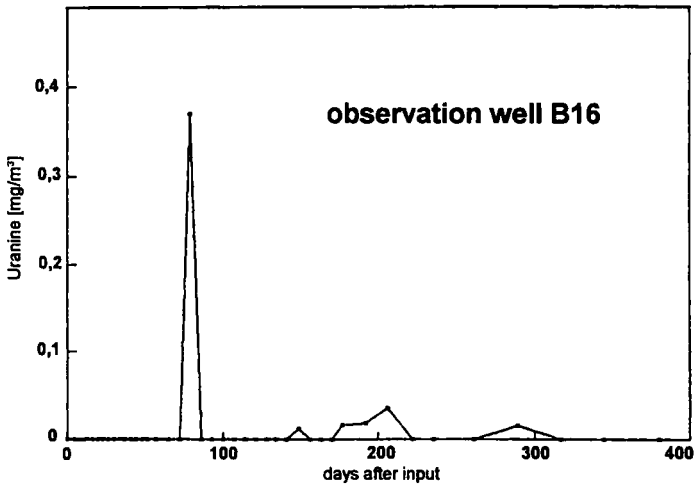

Figure 180. Continued. Tracing test hazardous waste site Eckenweiherhof 1990. Uranine breakthrough in the groundwater monitoring well B 16.

Table 26. Tracing test hazardous waste dumpsite Eckenweiherhof April 1990. Propagation characteristic values for the uranine injected in the basin 1 of the dumpsite. Uranine (leachate monitoring well P1).

Well	Distance	1st proof date	Initial concentr. (µg/l)	V_{max} (m/d)	Conc. maximum	C_{max} (µg/l)	V_{dom} (m/d)
B4	186 m	08.06.90	0.068	2.9	15.06.90	0.35	1.0
B5	241 m	28.09.90	0.028	1.5	25.11.90	0.13	1.0
B10	105 m	22.06.90	0.065	1.3	single value		
B10		13.10.90	0.030	0.6	single value		
B10		21.12.90	0.030	0.4	single value		
B12	203 m	22.06.90	0.130	> 2.6	single value		
B14b	75 m	15.06.90	0.360	1.0	15.06.90		
B15	82 m	10.08.90	0.075	0.6	single value		
B15		27.10.90	0.023	0.4	single value		
B16	133 m	22.06.90	0.370	1.7	single value		
B16		31.08.90	0.012	0.9	single value		
B16		28.09.90	0.016	0.8	27.10.90	0.035	0.6
B17	200 m	20.06.90	0.029	> 1.9	16.08.90	0.041	1.5
B9	35 m [1]	08.05.90	1.300	1.0 [2]	08.05.90		

[1] vertical seepage path; [2] seepage flow velocity.

propagation of the tracers is shown in Figure 181. Corresponding to the fissure pattern, a strong fanning out of the flow can be seen, whereby the SE-NW-direction parallel to the course of a fault here, is dominant. However, the flow is also influenced by cross-fissures. Whereas the tracer injection in the unsaturated zone (waste basin ca. 30 m above the groundwater table) displays a flow pattern on both sides of the fault, resp. a radial flow pattern, the injection in the saturated zone only shows one dominant flow direction.

Overall, a fairly quick seepage through the unsaturated zone (ca. 1 m/d) presumedly through a few, strongly pervious fissures is given. A portion of the contaminated water flows on impervious layers (Fig. 181) preferably towards the SW,

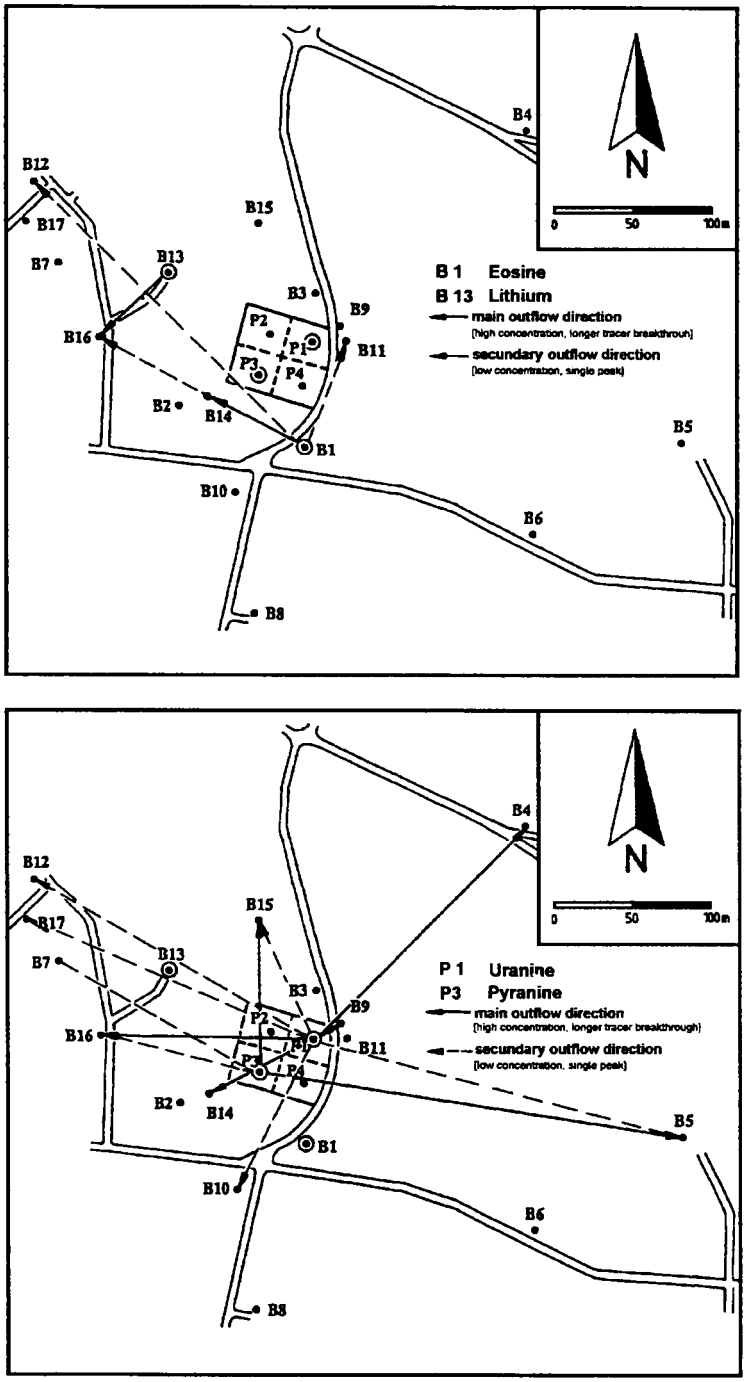

Figure 181. Tracing test hazardous waste site Eckenweiherhof 1990. Top: Tracer injection into the groundwater monitoring wells. Bottom: Tracer injection into the dumpsite basin. Established tracer flow directions (solid lines: main flow; dashed lines: secondary flow).

resp. N, before they seep deeper through fissures. The groundwater itself shows a preferred flow direction towards the NW, with a secondary flow component towards SW with velocities of 6 m/day. The simultaneously determined flow direction towards SE is mainly due to the propagation in the unsaturated zone and infers a groundwater crest nearby east of the dumpsite. These results from the tracing test provide important information for further planning of the groundwater remediation and criteria for estimating the damage potentials of the leachate propagation.

5.1.2 *Horizontal lysimeter – Egelsee*
W. Käss

From 1975 to 1982, during the course of the hydrogeological field mapping in Baden-Württemberg/Germany, extensive hydrogeological and hydrological investigations were conducted in the middle region of the Iller river (MELU/MWMV 1982). The investigation area 'Erolzheimer Feld' is located south of Ulm in the northern alpine foreland. In a part of the project, the evaporation and groundwater recharge rate were determined with two lysimeters. One of the lysimeters (Egelsee) was set up in a former Iller oxbow. A horizontal lysimeter was constructed in the terrace edge (Fig. 182 top). The lysimeter was divided into 4 consecutive chambers each with a length of 2.5 m. Each chamber had a separate discharge, so that a differentiated sampling for the determination of the seepage rates and chemical, bacteriological, and fluorimetrical investigations was possible.

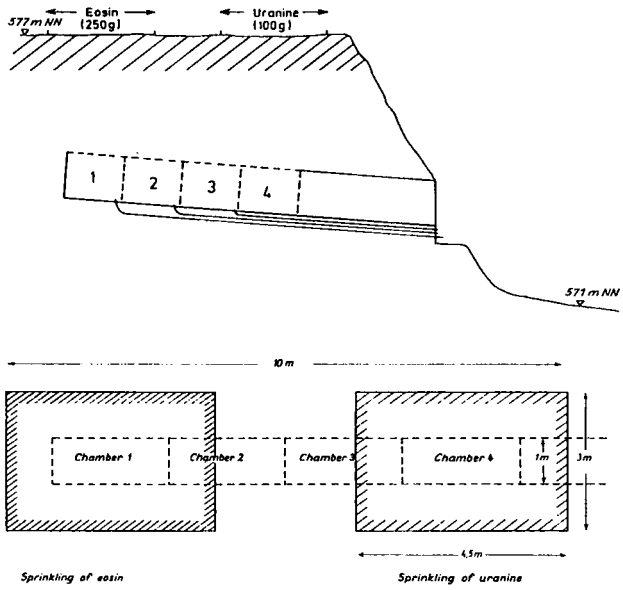

Figure 182. Horizontal lysimeter Egelsee. District Berkheim/Cty. Biberach (Southwestern Germany). Top: Section through the lysimeter set-up. Hatched area: Cover layers (sod, underneath 0.3 m loamy-gravelly filling, to 0.95 m para-brown earth), downwards transition to coarse gravels of the lower terrace. Middle: Top view with the areas sprayed with the dyes (each 3 × 4.5 m), left with eosin, right with uranine.

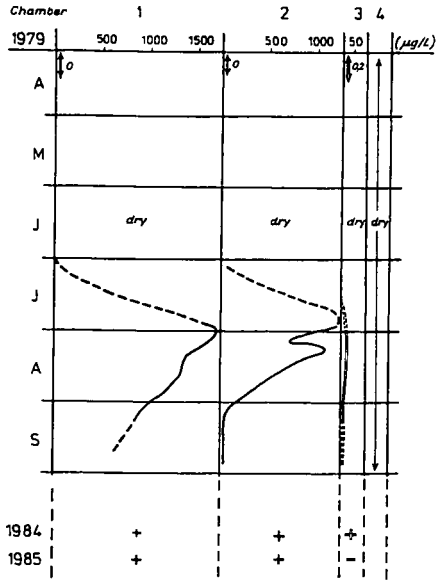

Figure 182. Continued. Bottom: Dye values in the lysimeter chambers 1-4. Eosin: solid curve, uranine: hollow double curve, dotted lines: presumed dye passage (after KÄSS 1985).

The mean annual precipitation for Egelsee is 910 mm. For 1979, with a precipitation of 940 mm, a seepage of 370 mm was determined, which corresponds to a groundwater recharge rate of ca. 12 l s^{-1} km^{-2}.

On 3 April 1979, the area shown in Figure 182 (middle) was sprayed with solutions of 250 g eosin and 100 g uranine. The middle of the area sprayed with eosin lay over the rearmost chamber 1, that from uranine over the foremost chamber 4. Shortly after the dye was sprayed, traces of uranine were detected in chamber 3 (Fig. 182 bottom). In the following dry-weather period, there was no seepage water flow recorded. Not until during the month of July were there strong pulses of eosin in the rearmost chambers 1 and 2. In chamber 2, only low concentrations of uranine were present at this time. Later, the seepage water samples were free of dye.

Surprisingly, in 1984 and 1985 after heavy rains, visible eosin and uranine reappearances were observed in the chambers 1 and 2, resp. 3, which however could not be quantitatively recorded. In chamber 3, such high dye concentrations as observed in chambers 1 and 2, farther downhill, were never observed. Chamber 4 never carried dye.

The following conclusions can be drawn from the results of the tests described above:

– The fluorescent dyes uranine and eosin are well-suited for use in seepage water tracing tests,

– The recovery of the dye depends on the water saturation in the unsaturated zone, which is dependent upon the precipitation,

– Lysimeters, that are installed too close to a bank, display a hindered seepage water flow due to partial drying up,

– To determine seepage water movements using tracers, very long observation periods are often necessary, which can last several years.

5.2 KARST GROUNDWATER

H. Hötzl

5.2.1 *Recommendations for conducting tracing tests*

5.2.1.1 *Tasks and applications*

The drainage of karstified catchment areas is unique, not only with respect to the extensive lack of surface flow systems, but also due to the characteristic underground flow behaviour. The enlarged underground flow paths in the usually fissured carbonate rocks, that were widened by solution processes, cause permeabilities that are hardly determined by hydraulic measures since they are strongly heterogeneous (FORD & WILLIAMS 1989, ZÖTL 1974). The irregular spatial course of the comparatively wide karst channels, well-known from numerous cave maps and their continuously cross-sectional variations (BÖGLI 1980) lead to a differentiated flow behaviour, as compared to porous and fissured aquifers.

Even over short distances, the karst water flow can show different effects. Beside laminar flow, especially in deep karst, in the wide channels there are also shifting turbulent flow conditions, whereby, depending on the cross-sectional variations, high pressure head flow or pressure free channel flow can alternate. As a result of the rather wide hydraulic paths, relatively high flow velocities occur, that lead to a low retention capacity and to a quick emptying of the karst reservoir.

Therefore, karst springs show large variations in their discharge. They react quickly to precipitation events and can quickly fall dry after longer periods with no rain. The high permeability in the unsaturated zone not only favours the infiltration of the precipitation, it also leads to the seeping of surface water. Due to the quickly developing retrogressive erosion in the karst underground, the drainage there orientates itself toward superordinalic hierarchic flow systems, especially to new ones with even higher relief energy. As a result, the subterranean water divide is shifted with respect to the topographic divide and thus creates divergent flow directions (SWEETING 1972, WHITE 1988).

These karst drainage features make it hard to describe and quantify the flow conditions with theoretical-hydraulic basic approaches and can also even make point source hydrogeological in situ tests impossible. Therefore, in order to consider the spatially nonhomogeneous and large temporal variations, special procedures are necessary to assimilate the temporal and spatial propagation of the karst groundwater. Tracing techniques are especially well-suited for this task.

Therefore, it is not surprising that the decisive impulses and research developments in hydrogeological tracing techniques were made in the karst research. As described in Section 1.1 which covered the historical development of these methods, the first professionally substantiated applications of tracing techniques were to solve actual problems and scientific investigations in karsts (HÄGLER 1873, KNOP 1878).

Today, these tasks are still the same as those one hundred years ago in the first tests. However, the application areas have been essentially broadened due to improved methods and the evaluation of the techniques. New solution methods and also more comprehensive answers to detailed hydrogeological questions were made possible. Specifically for karsts, in the beginning the question as to where the percolat-

ing water from rivers or sink holes would reappear was the most important. Even today, this question has the highest priority in less investigated regions. However, tracing tests are frequently applied to investigate environmental problems, such as sewage discharge or contamination accidents. The goals of these investigations are not only to determine the major re-emergence sites, but also the secondary re-emergence sites, in order to comprehend the overall contamination propagation.

Further major tracer application areas in karst regions are determining the boundaries of the catchment areas and the temporal evaluation of the discharge behaviour. Since the topographical and subterranean water divides frequently do not coincide in karsts, special investigation measures must be conducted. Due to the extensive non-homogeneity and anisotropy, theoretical hydraulic reasonings can generally not be applied. Tracing tests are frequently the only possibilities for determining the subterranean boundaries of large drainage systems or the catchment areas of springs and wells.

For the most part, conventional hydraulic procedures cannot be applied in karsts to determine the temporal discharge behaviour. However, important information and characteristic values can be obtained by analysing tracer breakthrough curves (SCHÄDEL & STOBER 1988). At the same time, combined tracing tests, with temporally parallel injections of the tracers in different injection sites allow the determination of the discharge conditions for large catchment areas under uniform hydrological conditions.

5.2.1.2 *Conducting tracing tests*

The general prerequisites and possibilities for conducting tracing tests were handled in Chapter 3. They are also applicable for experiments in karst regions. However, due to the special hydrogeological relationships in karsts, some of the boundary conditions need special consideration.

Even the preliminary investigations for the final planning stages of tracing tests in karsts require a high level of accuracy in the gathered information to be able to estimate the potential tracer propagation, in order to plan a sucessful test. Older, yet still effective, drainage channels or reactivated palaeokarsts can lead to discharge conditions, that are not directly recognizable from the present day hydrogeological topographical conditions. In order to assure, that all possible tracer re-emergence sites are included in the sampling, a negative sampling frame has to be established (MAURIN & ZÖTL 1959)

As a consequence of its wide waterpaths, karsts are also suitable for those tracer groups, that cannot be applied in other aquifers. This is especially true for drift tracers, as for spores (ZÖTL 1974) or microspheres (cf. Section 2.6). Reactive tracers, that undergo high losses in narrow porous aquifers due to adsorption, such as the fluorescent dye rhodamine B, can achieve very good results in karst aquifers (QUINLAN 1986). Thus, a very broad spectrum of tracers are applicable in karsts, which facilitates the parallel use of tracers in combined experiments.

Often, the tracer injection in karst regions is also facilitated by the presence of active swallow holes. They allow a direct injection of the tracer over the flowing water into the hydraulically connected karst water system (Fig. 183). When swallow holes are present, they should be preferred as the injection sites over other sites, since a hydraulically evaluable pulse (DIRAC) injection can thus be best achieved.

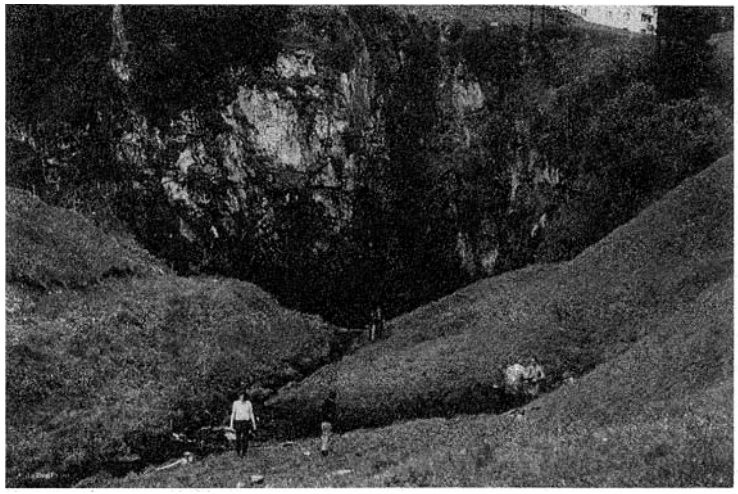

Figure 183. The active karst sink hole La Brevine, in the folder Jura mountains, west of Neuchâtel, Switzerland. The percolation of the stream Brion was used in 1979 for a tracing test (BAUER et al.1980). In the foreground to the right is a secondary sink hole. In the background, the main sink hole in the area of a 50 m wide doline (Photo: HÖTZL 1979).

On the other hand, wide karst areas without surface water sometimes present a difficult problem (Fig. 184). For the tracer injection, large amounts of water are required to prime and flush the injection sites, especially with relatively deep karst water table levels. Their transport and availability can be so difficult, that many a planned tracing test had to be shelved.

It is also possible to inject the tracer through the unsaturated zone from the surface without using sink holes, precondition is that water is available for a sufficient pre- and postflushing and that the karst channels are not clogged by residual sediments or fine outwash. Tracing tests could thus be successfully carried out in alpine karsts without overly large time delays in the recovery, even with a unsaturated zone that was several hundred metres thick (TOUSSAINT 1971). However, if the karst channels are filled with weathering residuals or eluvial loam, conducting a tracing test through the unsaturated zone must be critically considered. Even if there is a detectable reappearance of the tracer, it is usually extremely delayed (Fig. 185) and often no longer hydraulically evaluable. In general, only the flow direction can be thus proven.

Due to the different mechanisms of the tracer propagation in karsts, breakthrough curves with strong temporal variations are obtained. The tests must be correspondingly planned, especially the necessary observation periods. With effective flow velocities of up to several hundred metres per hours in areas with pronounced karst channels, the breakthrough curves often occur with quite short notice in the outflows of these systems. Frequently, the pronounced maximum occurs after only a few days and the passage of the tracer even with distances up to 10 km is completed within 4 to 8 weeks. Hereby, only the fast flowing karst water discharge component (conduit flow) is determined. In contrast, injections through the unsaturated zone and through the finely ramified, yet not directly connected to the karst channels, fissured network

Figure 184. A karstified alpine area without an outlet (Huttererböden, Warscheneck, Northern Calcareous Alps) with dolines and karst shafts. In order to conduct the tracing test, a helicopter was required to transport the necessary large quantities of water to prime and flush the injection site (Photo: HÖTZL 1978).

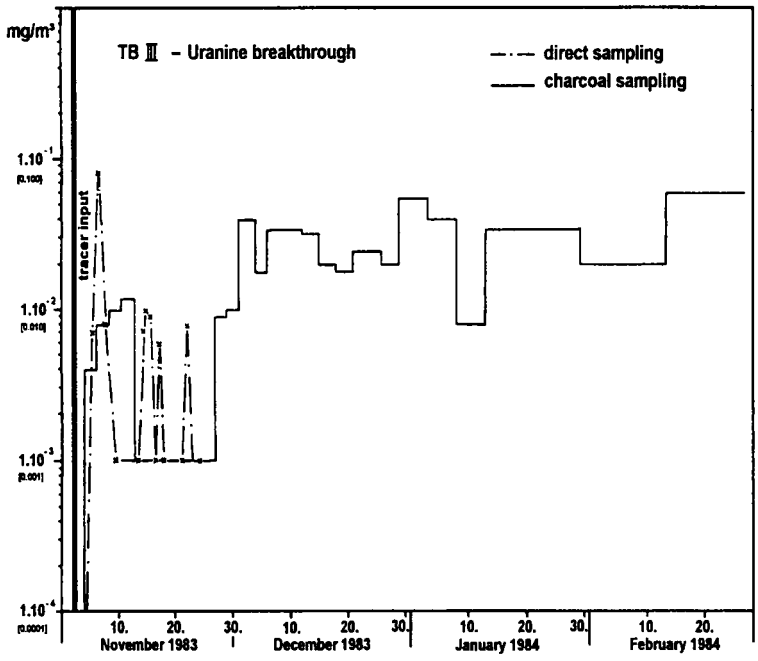

Figure 185. Delayed tracer recovery due to insufficient connection of the injection site (borehole or unsaturated zone) to the aquifer. Example from the tracing test Grenzach-Wyhlen 1983 (HÖTZL 1989). Due to the slow flushing of the tracer, the test acts like a permanent tracing.

of the saturated zone, e.g. in many boreholes, result in a strongly delayed and temporally long reaching recovery curve (diffuse flow). In all cases, conducting karst tracing tests requires very thorough planning and correspondingly detailed preliminary investigations.

5.2.2 *Drainage systems of alpine karsts*

5.2.2.1 *Geological boundary conditions*

Carbonate rocks are widespread in the young folded and overthrust mountains of our earth and in part, essentially involved in the development of the mountains (HERAK & STRINGFIELD 1972). Examples for this are the Alps, but also many of the Mediterranean mountain chains such as the Dinarids and the Hellenids. Independent of the climatic conditions, these rock series tend towards intensive karstification. As a result of the mechanical stress during genesis, they are generally intensively fissured and thus allow a quick advance of the aggressive water and deep-acting solution processes.

The deformation pattern which develops during orogenesis is determined by the lithological and facial character of the sediment series. Whereas thinly bedded carbonate rock series can undergo intensive folding and imbrication, massive carbonate rock series, e.g. thick reef limestones, react as very rigid and brittle plates. Through mechanical stress, they are frequently exposed to shear deformation, which leads to sets of steep diagonally orientated fissures. Later on, these determine the orientation of the karstification and the subterranean karst drainage.

With folded carbonate rocks, the bedding plane is an important factor in determining the character of the water paths. On the one hand, lithological differences, especially interbedding of marly or clayey series, promote increased water flow on the bedding planes. On the other hand during the folding process, concordant pressure solutions form, which facilitate a later karstification. Thus, trough structures inevitably represent preferred drainage paths, that are especially effective with an axial pitch of the folds. Other than the fold troughs, there are also cross-fissures, which are perpendicular to the fold axis and have an important function in draining the folded mountain chains also due to their extensional strain character.

The subterranean drainage of alpine karst regions is especially prejudiced by the geology and the deformation history of the affected area. Detailed geological structure investigations can deliver important preliminary indications, yet are generally insufficient to decisively determine the actual flow paths or catchment areas. Since hydraulic tests which could be used to clarify the situation generally cannot be applied in karstified alpine areas, tracing tests remain the only possible choice to determine the orientation and temporal course of the karst drainage.

With two examples from alpine areas, both major types, determined by the geological structure, of karst drainage are presented in the following. For the type plateau-like limestone massif, the drainage system of the Tennen Mountains of the Northern Calcareous Alps are presented. For the documentation of the drainage paths of a folded mountain chain, the karst region of the Upper Muota valley in Central Switzerland was chosen. Both regions belong to high alpine karst areas, that are bordered by deep valleys and thus characterized by extreme relief and slope conditions.

5.2.2.2 *Karst plateau of the Tennen Mountains*

In the central and eastern sections, the Northern Calcareous Alps consist of different, morphologically and hydrographically divided karst massifs. With a total area of ca. 280 km^2, the Tennen Mountains represent one of the smaller massifs. However, due to the limiting deep valley cuts – the Salzach valley in the west, the Lammer valley in the east and north, and the Fritzbach valley in the south – it takes a completely independent position (Fig. 186).

Today, due to recent, in part Pleistocene uplifts, the graduated plateau surface, which is essentially the rest of a Miocene aggradation surface (SEEFELDNER 1952), lies at ca.2000 m a.s.l. and is towered by single elevations of up to 2500 m. At its borders, the massif drops steeply, whereby the bordering valleys have elevations from 500 to 800 m a.s.l.

Geologically, the development was determined by the over 1000 m thick Upper Triassic Dachstein limestones (Fig. 187). In their massive to coarsely bedded development, they represent a platform sedimentation. The southern border of the Tennen Mountains with its massive reef limestones still defines today the original plattform border with the transition to the deeper ocean basin. To the north, the coarse Dachstein limestones connect as the rear reefs and lagoon basin. Whereas in the south, shallow bedding relationships are predominant, the whole stratigraphic sequence drops steeply to the north and is overlayed by tectonic upper nappes. The base of these limestone series consists of Middle Triassic Dolomites and Lower Triassic sandy-silty Werfen Formation. The latter also forms the hydrogeological base of the total sequence.

The Dachstein limestones of the Tennen Mountains are intensively karstified (TOUSSAINT 1971). The naked plateau surface is solely built up of a series of charac-

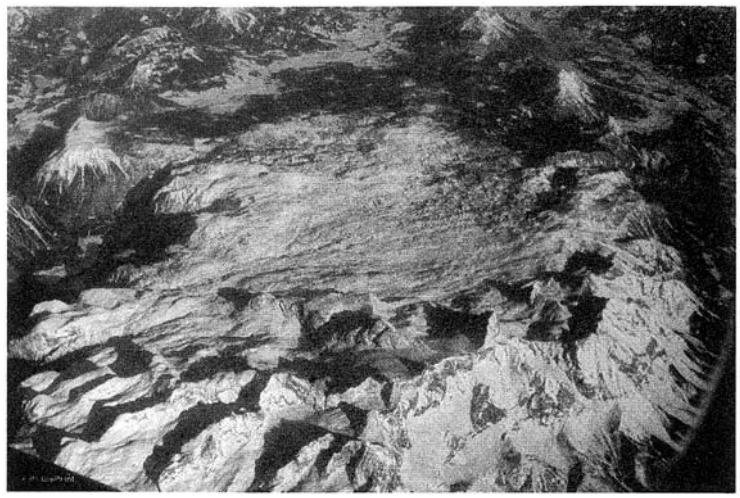

Figure 186. Aerial photograph of the Tennen Mountain, Northern Calcareous Alps, from SW to NE. In the front, the steep drop with the highest points (2200-2500 m a.s.l.); in the middle, the plateau (1800-2000 m a.s.l.), in the back the Lammer valley (Photo: HÖTZL 1982).

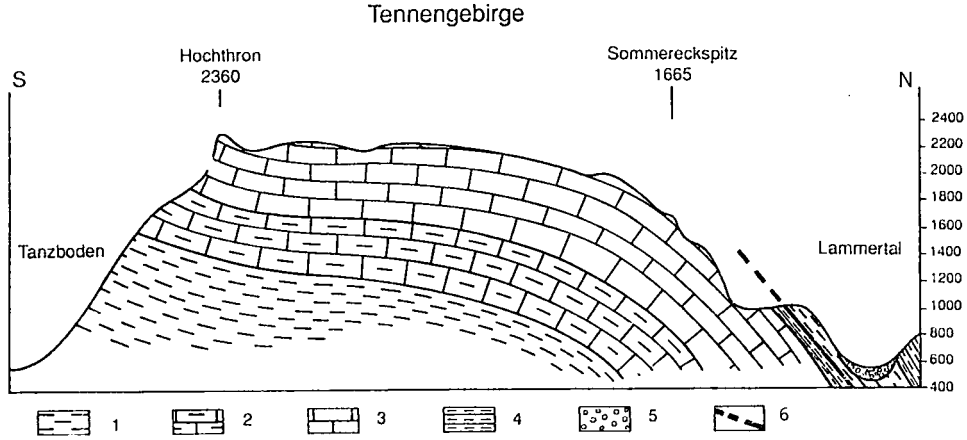

Figure 187. Geological cross-section through the Tennen Mountains. (1 = Werfen formation, 2 = Middle Triassic dolomites, 3 = Dachstein limestones, 4 = Strubberg formation, 5 = Quaternary gravels, 6 = overthrust border Tirolikum-Iuvavikum).

teristic karst forms, from simple solution karrens to pronounced karst lanes, from corrosively widened karst fissures to numerous karst shafts forming at the interfaces of the fissures and faults, as well as small solution dolines up to pronounced karst hollows (Fig. 188). The karstification continues downwards with the corresponding intensity. Pronounced cave systems which are bound to a certain level prove on the one hand the early and parallel to the upheaval of the mountains development of the karstification. On the other hand, this also documents the deep impact of the subterranean drainage.

This intensive karstification also corresponds to the karst hydrological situation: No surface run-off and in spite of the high annual precipitation amount of more than 2000 mm, the complete infiltration of the precipitation fraction (ca. 55%) that did not evaporate into the underground. The karst water re-emerges through many springs, that outcrop in the borders of the karst. Quantitatively, the main fraction of the subterranean discharge crops out in a few large karst springs on the northern border of the Tennen Mountains. The most important are the Salzachöfen springs on the Lueg Pass, the Schwarzenbach-Winnerfall springs near Oberscheffau, and the Tricklfall springs and Dachserfall springs near Abtenau.

The general discharge conditions from of the total karst massif can be explained through the hydrogeological and karsthydrological situatuion (Fig. 187). Caused by the at first flat, then steeper dipping of the karstified Dachstein limestone plate to the north with the deeper outcrop of the karst water table at ca. 600 m as compared to 1400 m in the south, the dominant drainage is to the north. The outcropping of the main springs is bound to the superposition of the impervious rock series of the upper nappe, so that the karst water spills over. In the northwest, where these sealing layers were removed by a glacial overdeepening (BRANDECKER & MAURIN 1982), part of the karst water crops directly out in the gravelly valley fill or crops out as a spring at the level of the receiving stream on the banks of the river Salzach.

Figure 188. High plateau of the Tennen Mountains (1800-2000 m a.s.l.). Naked alpine karst with characteristic small forms and extensive karst funnel (Uvala) in the middle of the photo (Photo: HÖTZL 1976).

To explain the flow relationships of the plateau of the Tennen Mountains to the springs and to determine the boundaries of the catchment area, in 1969 a combined tracing test was conducted (TOUSSAINT 1971). Based on experience and knowledge gained from the Dachstein karst massif further east (ZÖTL 1961) and the Toten Mountain (MAURIN & ZÖTL 1964), it was first assumed that a wide fanning out to radially divergent flow from the fairly uniform karst massif would occur. However, in view of the geological bedding conditions here as compared to the Dachstein, instead of a central axis, the culmination of the karst water table was expected further to the south. The injection sites were corresponding planned.

During this combined tracing test in 1969, three injection sites were chosen (TOUSSAINT 1971). In the central section, slightly to the south, 8 kg of uranine were injected in a doline type structure (S2) in the area of a larger karst depression. To prime and flush the injection, converging snow-melt water was used. Two further temporary sink holes (S1 and S3) in the eastern and western border area were injected parallel with differently dyed *Lycopodium*-spores (15, resp. 20 kg). The results shown in Figure 189 with the fan shaped division of the tracer flow to the north were in good agreement with the geological findings (bedding conditions and conjugated shear faulting). However, the expected radial flow as known from older investigations of karst massifs did not occur. Especially in the eastern and central injection sites with their presumed thick unsaturated zone, a radial fan-shaped flow had been expected, analogous to the tests in the neighbouring karst massif.

The flow velocities determined for the first appearance of the dye tracer were between 60 and 150 m/h and for the maximal concentrations between 35 and 60 m/h. For the central sink hole (S2), the distances to the major reappearance sites were around 7.5 km with altitude difference of ca. 1400 m, whereby several hundred metres of that is allotted to the unsaturated zone. The still relatively high effective flow

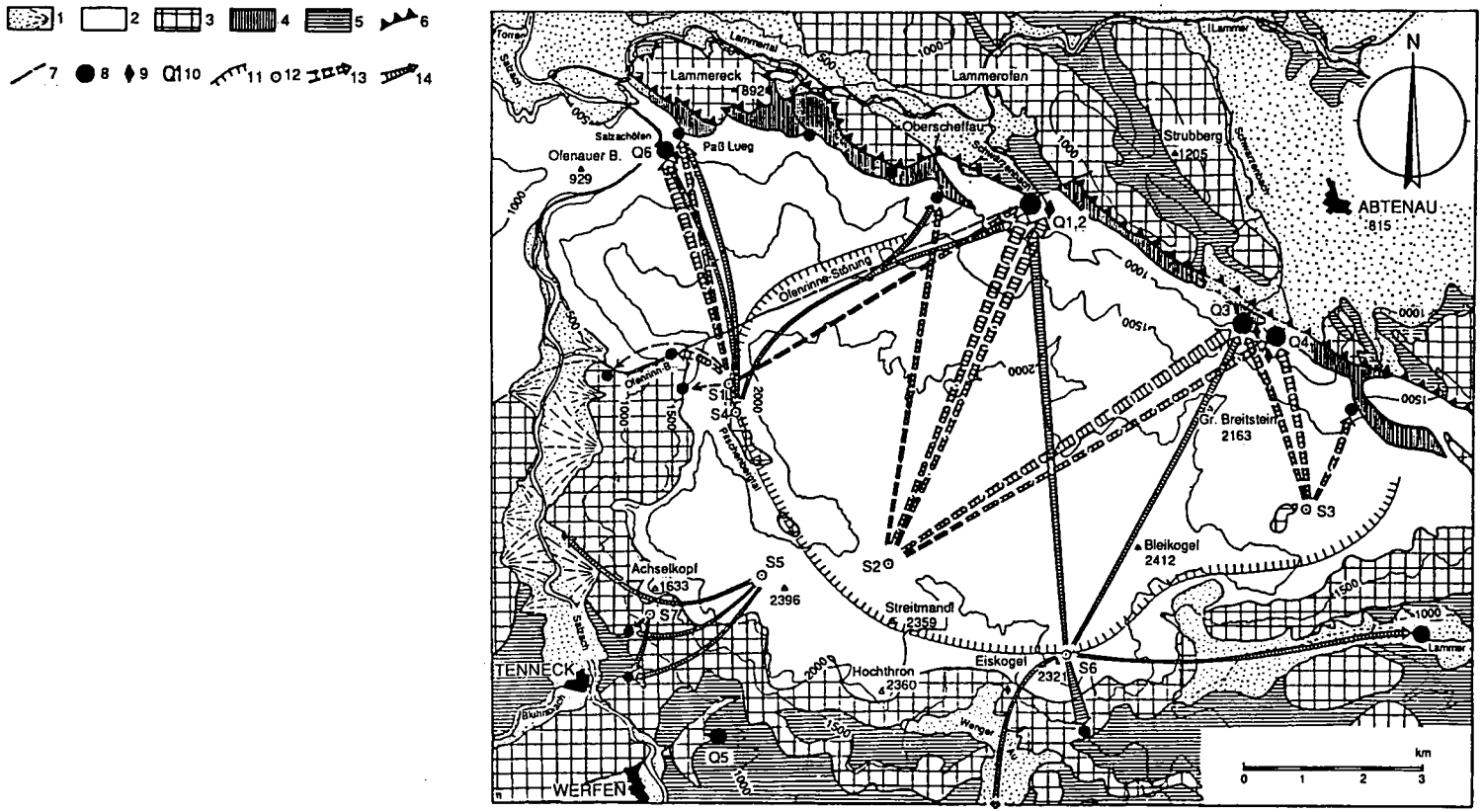

Figure 189. Karst hydrogeological map of the Tennen Mountains. Tracing tests in 1969 and 1977/78 with results (from BRANDECKER & MAURIN 1982). 1 = Quaternary, 2 = Dachstein limestone, 3 = different dolomites and limestones, 4 = Strubberg formation, impermeable, 5 = Werfen formation, impermeable, 6 = overthrust, 7 = faults, 8 = large karst springs, 9 = high water overfaults, 10 = spring numbers, 11 = subterranean borders of the catchment area of the karst springs in the north, 12 = tracer injection sites, 13 = tracing test 1969, 14 = tracing test 1977/78.

velocities and the quick reaction of the springs to precipitation events document the low storage capacity of this karst.

To further determine the flow conditions of the karst plateau, a second combined tracing test was conducted in 1977. The injections were carried out at the end of September at a generally low karst water level and a following dry weather period. The injection sites were chosen, so that they were south of the older sites, but still north of the plateau edge. Only fluorescent tracers were used in the second test. The injection site S4 (5 kg of rhodamine B), near the old injection site S1, was chosen to allow a direct comparison with the first test. The injection sites S5 (10 kg of tinopal CBS-X) and S6 (10 kg of uranine) were set at the southern edge of the plateau at an altitude of over 2100 m a.s.l. The injection site S7 (1 kg of amidorhodamine G), a sink hole on the southern edge of the mountain, was outside of the plateau areas and was used to determine the sewage water flow of a tourist center.

Together with the results (Fig. 189) from the first test, the results delivered a very good overview of the subterranean karst water flow from the high plateau. The bedding conditions with the dipping of the karstified Dachstein limestones to the north are obviously most significant. Favoured by the extreme slope relationships of the high alpine area, almost the whole plateau drains to the north. Only in the southwest, yet here also determined by the extreme slope situation, is there a larger independent catchment area.

The discharge orientation of the separate injection sites are determined by the joint pattern. The partially very pronounced karst lanes and karst crevices on the plateau follow this also. The fissure pattern, defined by diagonally orientated shear fissures causes a characteristic fan-shaped flow, that leads to considerable overlapping of the catchment areas of springs that are even far apart. The fan angle is generally smaller than 90°, corresponding to the position of the conjugated shear joints of this region. A larger fanning angle of 180° resulted from the injection in the sink hole S1 near a pronounced and morphologically effective fault zone. There, in the first injection at a high karst water level, a flow towards both directions was determined. During the low karst water level (injection site S4), the flow from this area only followed the main drainage direction towards the N, resp. NE.

Injection site S6 certainly represents an anomaly. On the southern plateau edge, it is already on the other side of the orographic water divide, the injected tracer was dispersed to the south, east, and north (fanning angle ca. 220°). It can be assumed that the injection was carried out directly in the crest area of the karst water culmination and thus this experiment is rather an exception.

Relative to the drainage of a high alpine karst plateau, these results clearly differ from earlier tests in neighbouring karst massifs. Based on the results of older numerous spore drift tracing tests in the neighbouring Dachstein plateau, as well as in the Toten Mountains farther east (BAUER et al. 1959, MAURIN & ZÖTL 1959, 1964, ZÖTL 1961), it had been assumed that radial flow would take place in the whole plateau surface and not just in the central part (Fig. 90). These investigation assumptions were based mostly on the older spore drift tracing tests, which were carried out on the one hand with undyed spores, on the other hand, at that time the technical possibilities for sampling and taking spore counts were not as refined as they are today in avoiding and prohibiting contamination.

Newer systematic investigations in the Dachstein massif (BAUER 1989, TRIMMEL 1993), carried out exclusively with fluorescent dyes, have not verified the drafted and assumed radial flow pattern to be characteristic for alpine karst massifs. Rather, the results show, comparable to those in the Tennen Mountains, a more or less uniform major flow direction, whereby in the individual injection sites, corresponding to the joint pattern, varying fanning widths are observed. This increasingly seems to be a major characteristic for the drainage of alpine karst massifs, as verified by further tests in other karsts, e.g. in the Hagen Mountains/Austria (BRANDECKER & MAURIN 1982) or in the Warscheneck in the Northern Calcareous Alps (KRAUTHAUSEN 1977).

5.2.2.3 *High alpine folded mountains – Muota Valley*

In the introductory section about the geological boundary conditions for alpine karst drainage, the importance of the structural orientation of the mountain chain and the belonging deformation pattern was pointed out. In addition to the massive limestone platforms, the following example from the folded mountains of the Upper Muota valley, should demonstrate the drainage system of a folded karst area. Again here, tracing tests are the key to explaining and understanding the subterranean connections.

The Upper Muota valley in Central Switzerland is built up of Jurassic and Cretaceous sediment series of the Helvetian nappes. In the sequence, limestones, such as the thick Quintner limestones or the Schrattenkalk, alternate with marly intercalations (Zementstein formation, Valangien marls or Drusberg formation), that together form a strong hydrogeological subdivision. The wavy folded sequence is repeated in the different thrust sheets and subordinate nappes, that belong to the Axen nappe (Fig. 190).

To determine the subterranean drainage here, tracing tests were also conducted (BÖGLI & HARUM 1981). The results are summarized in a hydrographic map (Fig. 191). The drainage system as well as the determined subterranean flow directions mirror the geological structures. These are first defined by the ENE-WSW progression of the folding axes as well as overthrust and overfault boundaries. This direction is followed above all by the different contributaries of the upper Muota, as well as different subterranean flow paths, determined through tracing tests. The second dominating element is the transverse jointing in the NNW-SSE direction. The Hüri valley follows this direction as well as smaller side valleys and gullies. Further-

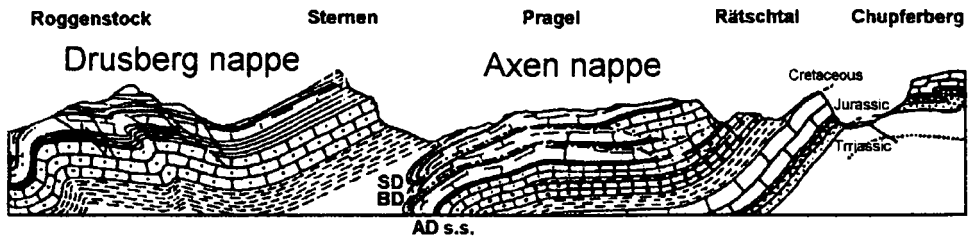

Figure 190. Geological north-south-profile through the Helvetian nappes in the Muota valley according to R. HANTKE (from BÖGLI & HARUM 1981). The combined tracing test in 1979 was conducted in the area of the folds and shingles of the Axen nappe.

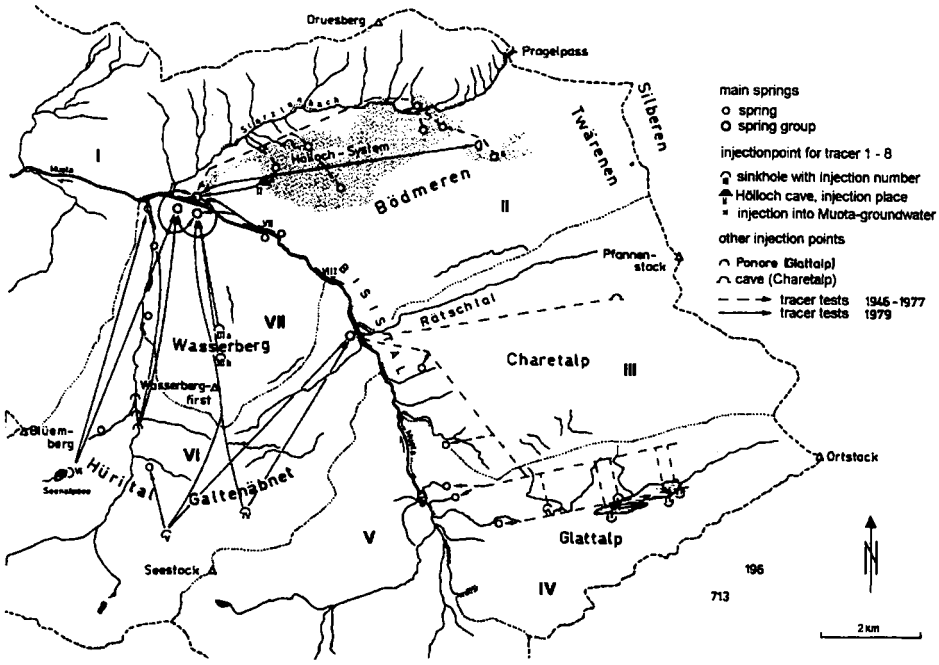

Figure 191. Hydrographic map of the Upper Muota valley (Bisistal) with the subterranean flow direction determined from the tracing tests (from BÖGLI & HARUM 1981).

more, the transverse jointing is definitive for the karst water discharge from the region of the Wasserberg and the Galtenäbnet. The Upper Muota valley (Bisistal) also essentially follows this structure direction. It owes its formation and especially its hydrographic importance to a transverse synclinal structure, which caused an axial depression in the dip of the fault. Thus, the folding axes dip from the west as from the east to the Bisistal and promote discharge to the receiving stream there.

Essential information about the complex flow relationship that resulted from the crossing of both main structural elements was obtained from a combined tracing test conducted in 1979 (BÖGLI & HARUM 1981). With the participation of the International Association of Tracer Hydrology (ATH), a total of 12 tracers were injected in 8 different sites, including fluorescent dyes, dyed *Lycopodium*-spores, and salts. Using Figure 192, the results from the southwestern section, the area of the Wasserberg and the Galtenäbnet will be handled here.

The tracer injections in the southern region in the Seenalpsee sinkhole (20 kg of uranine and 10 kg of red-dyed *Lycopodium*-spores) as well as in a sink hole in the region of the Riedboden (15 kg of amidorhodamine G) were carried out in the deep karst water storey of the Jurassic Quintner limestones. On the one hand, the subterranean flow here follows the axial dipping to the NE with dye reappearances in the springs in the Upper Muota valley. On the other hand, part of the flow from the Riedboden as well as the complete discharge from the Seenalpsee was totally collected by the transversal fissures and diverted to the north. The outflow of these waters took place in the Balm-Fugglen group of springs together with the tracer in-

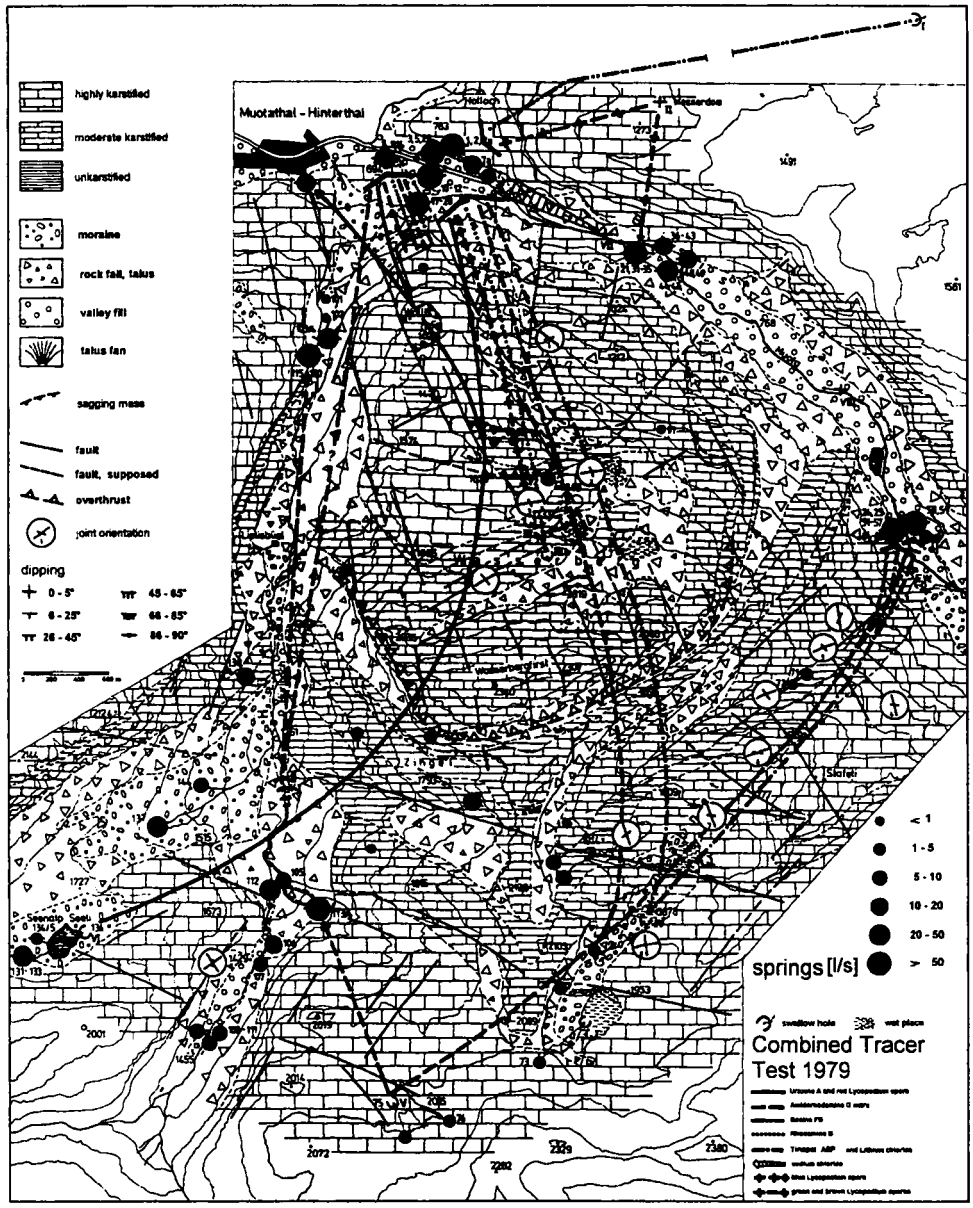

Figure 192. Hydrogeologic map of the Wasserberg, Muota valley, Switzerland, with the results from the tracing tests 1979 (from BÖGLI & HARUM 1981).

jected in the region of the Wasserberg crest in two sink holes from the Cretaceous Schrattenkalk (10 kg of rhodamine B and 15 kg of blue-dyed *Lycopodium*-spores). The outflow in the Balm-Fugglen springs is thus in the upper aquifer and therefore proves the water paths and hydraulic connections along the transversal fissures from the deep karst water storeys through a up to 400 m thick Lower Cretaceous marl sequence into the upper karst aquifer.

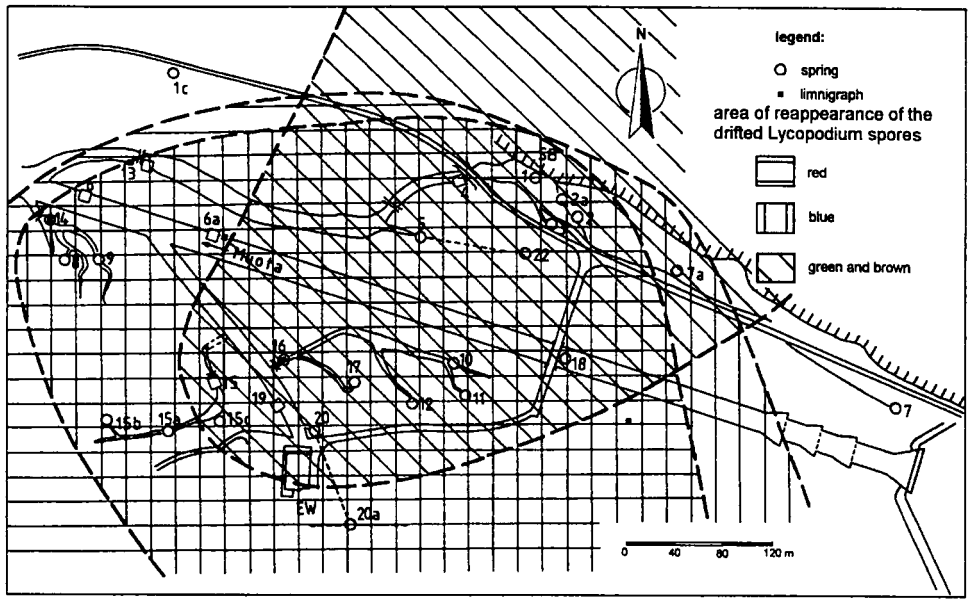

Figure 193. Overlapping of the re-emergence areas of the drifted spores in the spring region of Balm-Fugglen as an expression of the intensive mixing of the karst waters from the area to the north and south of the Muota (cf. Fig. 192). Combined tracing test Muota valley 1979 (BÖGLI & HARUM 1981).

The main drainage system of the adjoining karst region found on both sides of the upper Muota river is formed by the springs of the Balm-Fugglen spring group. They crop out on both valley flanks and from the valley floor above the Upper Muota valley. Whereas earlier the springs on each respective slope were attributed to the karst on each respective slope side and a part of the springs in the valley floor were considered as purely valley groundwater, the tracing test proved the complex connections of the mixing karst waters which were flowing to both sides. In Figure 193, the recovery of the spores from the different injection sites is used to show the overlapping of the inflow areas from the Hölloch-Bödmeren system in the north (green and brown *Lycopodium*-spores) as well as from the area Wasserberg-Galtenäbnet-Seealpsee in the south (red and blue *Lycopodium*-spores). In this glacial overdeepened valley section of Balm-Fugglen with the following valley floor sill, both differently structured drainage paths come together. The mixing processes are not just limited to the valley filling, but rather overlap, as observations in the Hölloch system have shown, under the valley filling into the neighbouring karst. Thus, the combined tracing test in the Hinter Muota valley impressively documents how tracer experiments can contribute to explaining and understanding karst hydrogeological connections.

5.2.3 *Defining the boundaries of catchment areas in the Swabian Alb*

5.2.3.1 *Hydrogeological characterization and problems*

The ridge of the Swabian Alb is formed by the cuesta step of the Upper Jurassic.

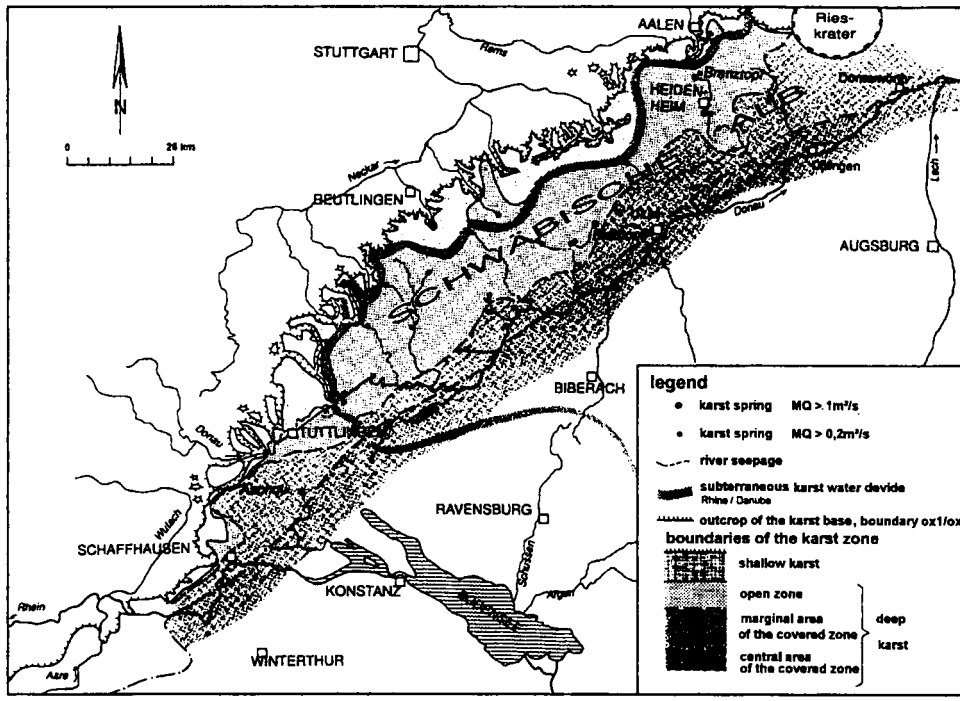

Figure 194. Overview of the Swabian Alb with karst zones (simplified from VILLINGER 1977).

This sediment formation consists of an up to over 400 metres thick limestone and marl sequence, that plunges to the SE to the Molasse basin (GEYER & GWINNER 1991). Following the strike of the rock series, the Swabian Alb stretches from the Hochrhein near Schaffhausen/Switzerland in a SW-NE-direction over to the region near Nördlingen, where its direct continuation is found in the adjoining Franconian Alb (Fig. 194). The steep cuesta scarp of the Alb benchland faces northeast, whereas the ca. 25 km wide cuesta back slope flatly dips towards the SE.

Morphologically, the ridge line near the Alb cuesta scarp forms the European continental water divide between the catchment areas of the Rhine and the Danube. The older Danubian system with its evened slope ratio has undergone a powerful constriction due to the Rhine and its contributaries, above all in the western part of the Alb, in the latest geological past (WAGNER 1961). In the area of the Middle and Eastern Alb, the Rhenish drainage system has only slowly extended itself from the Alb cuesta scarp towards the south. The major portion of the towards the SE dipping desk-like Alb surface drains as always to the Molasse basin (Fig. 195), where on its northern edge, the Danube, as an old drainage path, carries out the function of the receiving stream (HÖTZL 1973).

The total drainage of the Alb is characterized by more or less intensive karstification of the rock sequence of the Upper Jurassic. An active surface water network is missing to a large extent. The drainage occurs mainly underground, whereby the karst groundwater crops out in large springs above all on the southern edge of the Alb surface.

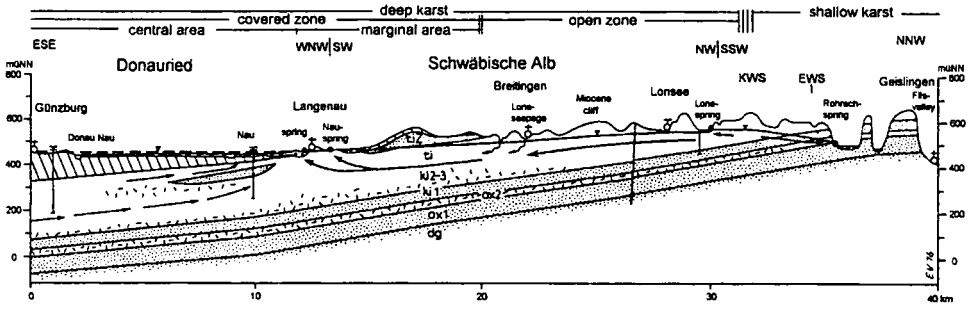

Figure 195. Generalized karst hydrogeological cross-section through the Swabian Alb (from VILLINGER 1977).

On the large-scale, the Upper Jurassic karst can be considered as a uniform aquifer (VILLINGER 1977). The lower confining bed is formed by the underlying Oxford marls, or first by the Dogger clays. The intercalated marls of the Kimmeridge and Tithons have multiple joints and are partially also karstified, so that they only lead locally to a subdivision of the karst into two groundwater storeys. As a further characteristic, depending on the position of the receiving stream relative to the lower confining bed, it can be differentiated between shallow and deep karst. Whereas the shallow karst is limited mainly to the northern Rhenish oriented edge, the major part of the Alb can be assigned to the deep karst.

This long and morphologically sparsely cross-divided karst area of the Swabian Alb presents great difficulties in trying to allocate the catchment areas as well in trying to determine the definitive subterranean water divides. As it is, the superior European continental water divide between the Rhenish and Danubian drainage systems can only be approximately defined. First of all, a position from the northern edge near the Alb cuesta scarp must be assumed for the topographical water divide on the tipped desk-like surface of the Alb as for the subterranean due to the overlap (cf. Figs 194 and 195).

Due to the intensified retrogressive erosion of the Rhenish oriented drainage, there is an increasing displacement of the subterranean divide towards the south. Its exact position can be only estimated from the assumed karst water culmination. An improvement of the positioning can be reached through tracing tests. This is especially true for the lateral delimitation of the catchment areas of springs, wells, and river systems. Since a multiple of these outlets pass under dry valleys and since only an insufficient network of groundwater monitoring wells are available, here tracing tests are also usually the only possibilities for solving the problems.

5.2.3.2 *Combination of separate tests for defining catchment area boundaries*

The application of tracing tests to determine subterranean water divides can be done by carrying out several separate tests in a staggered time frame or through a combined tracing test with parallel tracer injections. Both variations require comprehensive preliminary studies, so that the tracer can be injected as close as possible to the presumed water divide. An example of a combined tracing test conducted in the Upper Danube is handled in the next section that covers water management problems

and questions. The possibility of defining catchment area boundaries with a series of separate tracing tests is described here with an example from a test carried out in the Buchbrunnen (Egau valley) northeast of Ulm/Germany and the Blautopf, west of Ulm.

During the course of different karst hydrological investigations as well as special research tasks carried out in connection with the natural percolation of surface waters or artificial infiltration of sewage water, a series of tracing tests were conducted by the Geological Survey of Baden-Württemberg. The fluorescent dye tracers uranine and eosin were used mainly (SCHULZ 1957, KÄSS 1965, GROSCHOPF 1972, STRAYLE 1970, VILLINGER 1977). These tests verified the flow pattern towards the Molasse basin expected by the hydrogeological relationships. However, the deflection of the flow direction from the general direction of the slope towards several large karst springs indicates the lateral extent of the catchment area of these springs. For concrete tasks, the number of the tests in the region of the divides was increased and thus a sufficiently accurate delimitation of the involved catchment area was achieved.

A fine example is available in the documentation by SCHLOZ (1984) for the catchment area of the Egau river and the Buchbrunnen, in the Ostalb (Fig. 196). The Buchbrunnen spring is on the southern edge of the karstified Egau catchment areas and maintains a central drainage function. It is tapped for agricultural use and its mean discharge amounts to 0.9 m^3/s.

To define the boundaries of the Egau catchment area, 37 tracing tests from the years 1952 to 1982 were drawn on. Other than uranine as the most frequent tracer, eosin, tinopal CBS-X, and sodium, potassium, and lithium chloride were used. The longest distance from the injection site to the spring was more than 20 km. The effective flow velocities for the first reappearance were between 50 and 140 m/h. It is remarkable that none of the tracing tests with injection sites to the east of the Egau valley (Fig. 196) delivered definitely positive tracer proof. An allocation of separate temporally clearly delayed traces of tracers could not be done with certainty. It was a disadvantage that some of the earlier tests did not observe all possible karst water re-emergence sites due to correspondingly narrowly defined tasks. Independent of this, it cannot be excluded that parallel to the western part of the determined flow direction and drainage area of the Buchbrunnen spring, part of the karst water flows to the south and to the southeast in the area of the Donauried and there, due to a lack of suitable sampling sites or perhaps due to a too large of a delay, could not be detected.

A further impressive example (Fig. 197) of a delimitation of a catchment area supported by tracing tests concerns the Blautopf (VILLINGER 1977, 1978, 1987, VILLINGER & UFRECHT 1989). The Blautopf is the source of the river Blau, a contributary of the Danube, that flows into the Danube near Ulm. The mean discharge of the spring is 2.3 m^3/s. It is the second largest karst spring of the Swabian Alb and up to now its recorded maximal discharge of 25.7 m^3/s even beats the Aachtopf.

In the course of karst hydrological investigations and special practical tasks, different tracing tests have also been conducted in the region of the Blautopf (VILLINGER 1978). Up to 1986 there were a total of 9 tracer injections, with re-emergence in the Blautopf. 13 further tests in the adjoining areas lead to positive results in neighbouring karst springs. In the series of tracing tests, all set with different time spaces, the fluorescent dye uranine was used most often. However, eosin and

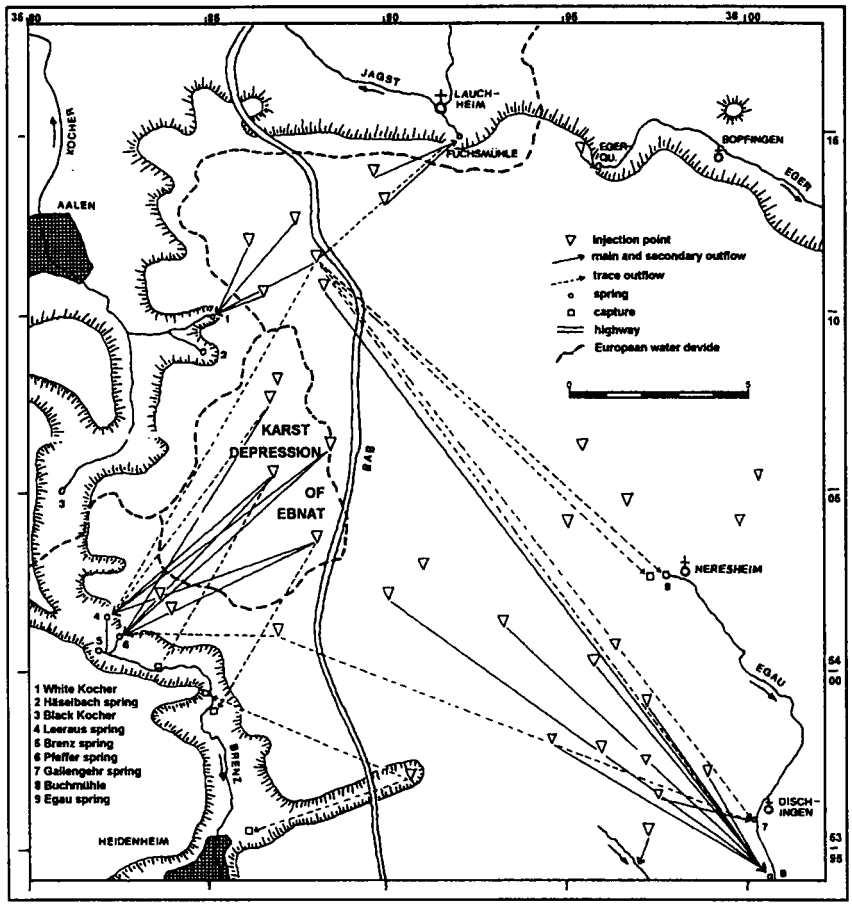

Figure 196. Delimitation of the subterranean catchment area of the Buchbrunnen (No.8), Egau Water Works Ostalb, against the Brenz region, based on the results from different tracing tests (after KÄSS 1991).

salts were also used. Overall, the tracers had fairly short passage times, which indicate an intensive karstification of the catchment area. For the first appearance, the effective flow velocities were on the average around 150 m/h, the mean velocity for the maximum of the tracer breakthrough was 95 m/h.

With the results from these tracing tests and knowledge of the hydrogeological conditions, a sufficiently accurate delimitation of the catchment areas also for water management questions is possible. For the Blautopf an allocated karst surface of ca. 160 km^2 was determined.

In the interpretation by VILLINGER (1977) the determined flow lines were also used to construct the potential contour lines of the karst water surface. With this and some groundwater monitoring wells, a presentation of the expected level of the karst water table was derived for the whole catchment area. Even if naturally in karsts, due to the irrregular and anisotropic assignment of the hydraulic water paths, the actual

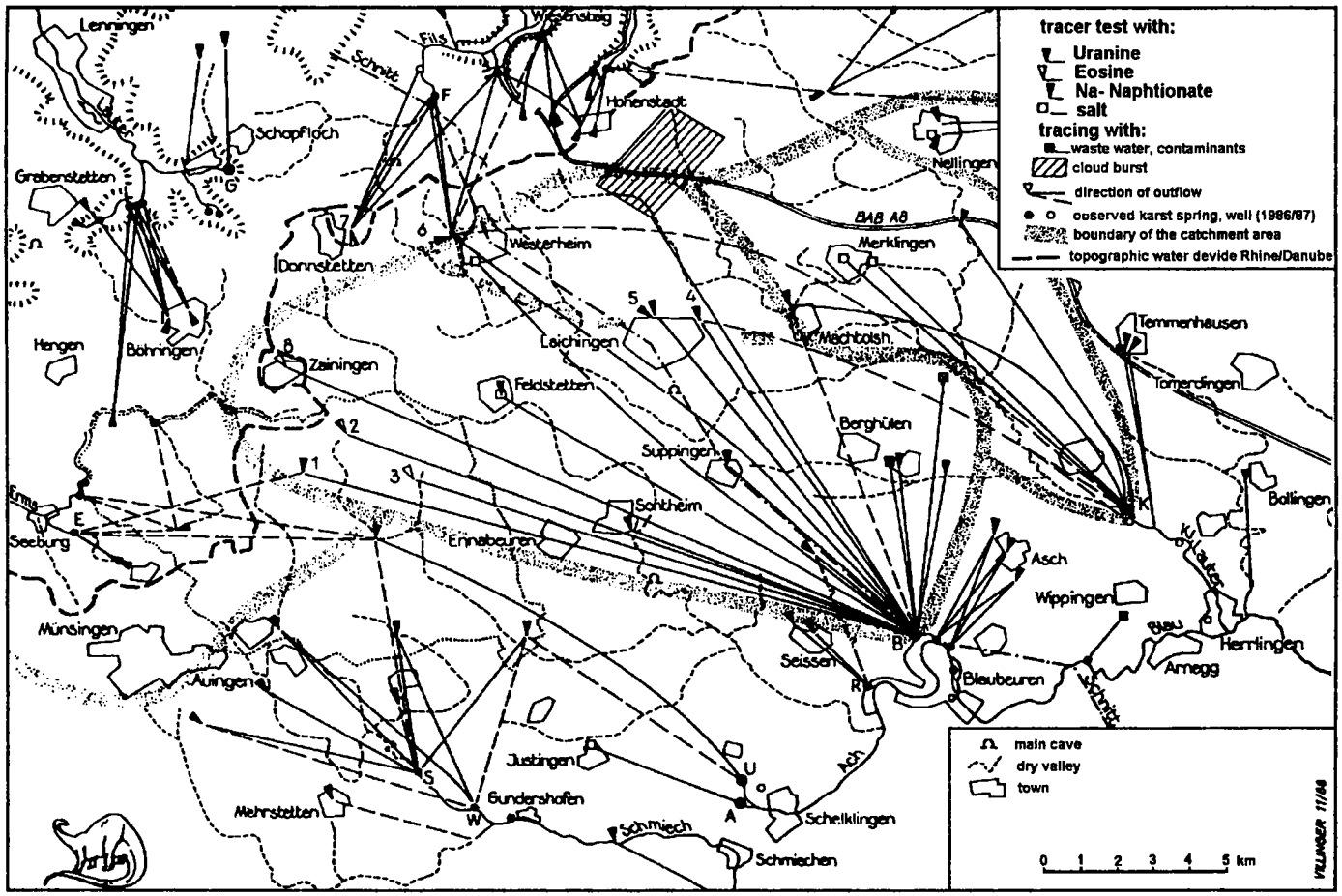

Figure 197. Delimitation of the subterranean catchment area of the Blautopf based on the results from tracing tests (from VILLINGER & UFRECHT 1989).

Table 27. Effective flow velocities of the subterranean karst drainage in the Swabian Alb (after VILLINGER 1977).

	SW-Alb (Danube-Aach) Deep karst	W-Alb Deep karst	Middle Alb Shallow karst	Middle Alb Deep karst	E-Alb Shallow karst	E-Alb Deep karst	W-Alb, Middle Alb and E-Alb deep karst
Arithm. mean of the max. effect. flow velocities v_{max} (m/h)	190	85	110	100	90	110	95
Largest single value of v_{max} (m/h)	400(968?)	280	240	525	125	900	900
Smallest single value of v_{max} (m/h)	25	4	15	3	55	2	2
Number of values n	19	77	70	83	4	28	187
Arithm. mean of the effect. flow velocities of the max. tracer concentr. v_t (m/h)	135	70	90	65	55	75	70
Number of values n_t	19	56	49	48	1	13	117

subterranean flow cannot be reproduced, such a map of contour lines represents an important help for the interpretation and evaluation of these charge conditions.

Overall, both examples from the Egau and the Blautopf show the applicability of using tracing tests that were conducted at different times and under different hydrological conditions for the delimitation of catchment areas. An exact determination of the water divide as a crest line is generally not possible with tracing test techniques. Moreover, this would also not do justice to the flat culminations of karst water surfaces and the flow behaviour of a karst. On the one hand, corresponding to the varying water levels, the displacement zones have different widths. On the other hand, as a result of the geometry of the karst paths in the border areas, there are branching flow directions and fan-shaped overlapping catchment areas.

In general, for the determination of such border zones, a manageable number of tracing tests provide sufficient accuracy, even with larger catchment areas. Furthermore, the results from a tracing test provide important information about the temporal flow behaviour in the catchment area itself and thus allow a comparative hydraulic evaluation of different karsts (Table 27).

5.2.4 *Water management aspects – Danube percolation*

5.2.4.1 *Tasks and goal of conducting the tracing test*

The western Swabian Alb is divided by the deep Danube valley into adjoining northern and southern karst plateaus. The Danube valley with its broad, wide valley meanders is a relict of the early Pliocene, when large parts of the Swiss alpine foreland drained through the Aare to the Danube (WAGNER 1961, HÖTZL 1973, 1992, VILLINGER 1986). Today, the upper Danube in the western Alb region has only a relatively small catchment area. The decimation of the old Danubian catchment area is the result of a large-scale rearrangement favouring the Rhenish drainage system.

Aided by the deep base level in the Upper Rhine region, the quick head erosion of the Rhine with its contributaries have enabled it to capture and divert more and more contributaries of the Danube.

This retrogressive erosion captured not only the topographic drainage network, but also the subterranean karst water flow of the western Swabian Alb. With the erosion of the adjoining Hegau basin to the south in the Middle Pleistocene and the corresponding cutting of the karstified Jurassic limestone sequence, the subterranean karst drainage became more and more oriented to this receiving stream level, that was compared to the Danube valley, ca. 125 m deeper (SCHREINER 1968, HÖTZL & HUBER 1972). This retrogressive to the north continuing subterranean karst drainage then eventually reached the Danube valley and produced more and more seepings in the river bed. Today, this intermittent complete drying up of the Danube between Immendingen and Möhringen (Figs 75, 198 and 199), and the Aach spring, which is fed to a large extent by the subterranean flow of the Danube belong to the most impressive karst phenomena of the western Alb. With an average discharge of ca. 8.5 m^3/s, the Aach spring (Fig. 200), which drains through Lake Constance to the Rhine, is the largest spring in Germany.

However, this impressive work of nature causes very definite water management problems. First off, especially in the dry summer months, the lack of water downstream of the stream-sinks and the not completely unavoidable sewage inflow create a decrease in the water quality. Furthermore, even farther downstream, below Ulm, withdrawal of Danube water for water supply, especially during the late summer low water flow, causes problems with the available amounts, which could be balanced by stopping the leaking of the upper Danube.

On the other hand, not only the Aach spring, but also the large groundwater reservoir in the Pleistocene gravels of the Hegau are obviously alimented to a large extent

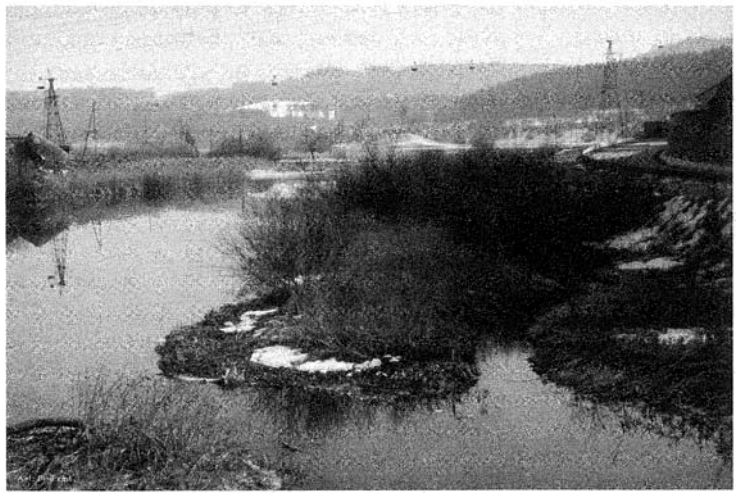

Figure 198. Danube sink above the Immendingen weir. Swallow holes on the right Danube banks with a thin rubble covering over the karstified, well-stratified Oxford limestones (Photo: HÖTZL 1976). Tracer injection site in 1969 tracing test.

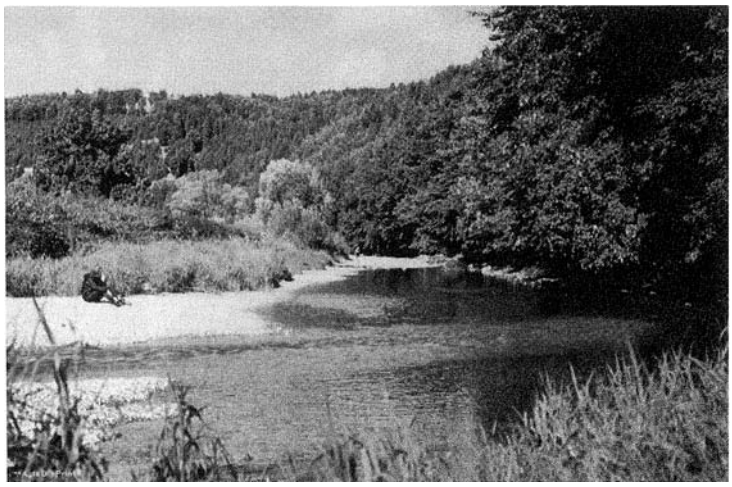

Figure 199. Danube sink in the Brühl bend between Immendingen and Möhringen. On the right bank in the Oxford limestone outcrop, corrosively widened joints and fissures are present. Tracer injection site in 1969 tracing test (Photo: HÖTZL 1969).

Figure 200. Aach spring in Hegau. With an average discharge of ca. 8.5 m^3/s, this is the largest spring in Germany. Major resurgence of the seeped Danube water. The water flows out of Tithonian limestones through vertical spring fissures (Photo: HÖTZL 1970).

from the out of the north flowing karst water. This creates a possible qualitative impact by nondegradeable or not well enough degradeable pollutants from the Danube. Also, there would again be problems with the amount of water, if the river loss were to be reduced through water management measures. Water management measures in parts of such complexly connected systems have an impact on the whole system. The

assessment of such measures requires detailed hydrogeological knowledge about the flow behaviour of the karst system.

Therefore, further considerations were made to determine how many more springs or groundwater reservoirs other than the Aach spring in the Hegau region were affected by the leaking of Danube water. The direct connection between the stream-sinks sites of the Danube in the Brühl bow near Immendingen and the Aach spring was already proven in the last century by KNOP (1878) and for the river losses near Fridingen by ENDRISS in 1908 (KÄSS 1965). Other karst springs were not observed in these tests.

Furthermore, by carrying out a karst water flow balance, the fraction of and the importance of the leaking Danube water for the groundwater in the Hegau could be estimated. This required an exact as possible delimitation of the Aach spring catchment area. At the same time, it should be checked to see how far a diversion of the Danube before the main water losses site near Immendingen – a diversion tunnel had already been built for this – to the farther downstream stream-sinks near Fridingen would shift the natural karst water flow from the western Hegau basin to the eastern part of the basin.

To answer these questions, a combined tracing test, with participation of the International Association of Tracer Hydrology (ATH), was conducted. At the same time, this test was used to compare different tracers in a parallel injection of the tracers. To plan the combined tracing test, a comprehensive preliminary investigation program corresponding to the complex set of problems and difficult evaluation of the karst hydrogeological boundary conditions was also carried out (BATSCHE et al. 1970, HÖTZL 1973).

5.2.4.2 *Preliminary investigations for planning the combined tracing test*

Planning a tracing test in karstified areas to determine subterranean flow relationships requires fairly detailed knowledge of the general geological, hydrogeological, and hydrological boundary conditions. Although quite a lot of information was available for this investigation area, due to the almost hundred year old conflict between the riparians and the water users concerning the pros and contras of water management measures, the information needed to be sorted and completed. Besides further explanation of the hydrogeological relationships, above all an interpretation of the spatial and temporal processes with the aid of the hydrochemical and isotope-hydrological data was wanted.

The general hydrogeological relationships are described with the help of the generalized cross-section in Figure 201. In the Upper Jurassic sequence, consisting of limestones and marls, a uniform karst aquifer can be assumed. Due to the different faults, but also due to the partial vertical penetration of the massive limestone facies, the intercalated marls have only local importance as impermeable beds. The drainage of the karst system follows the dip of the bedding planes to the southeast to a deeper receiving stream base level. The stream-sink of the Danube especially near Immendingen takes place in the deeper parts of the bedding sequence (Oxford limestones), whereas in the Hegau, the discharge discharges from the overlying series (Tithon). Through glacial erosion and accumulation in the Hegau basin, Quaternary gravels partially lie directly on the karstified limestones, so that it is possible for the karst water to enter the porous aquifer.

To determine the spatial connections in dependency upon the temporal hydrological variations, a comprehensive spring survey as well as a long-term investigation of the water through hydrochemical and isotope-hydrological parameters was conducted. The temporal variations (Fig. 202) provide important information as to the origin of the water. Pure karst water samples with long residence time show very little variations, whereas increased infiltration from the surface and increased fractions of the percolating surface waters produce larger variations in the respective parameters. The isotope data are extremely advantageous (Fig. 203), as they enable an esti-

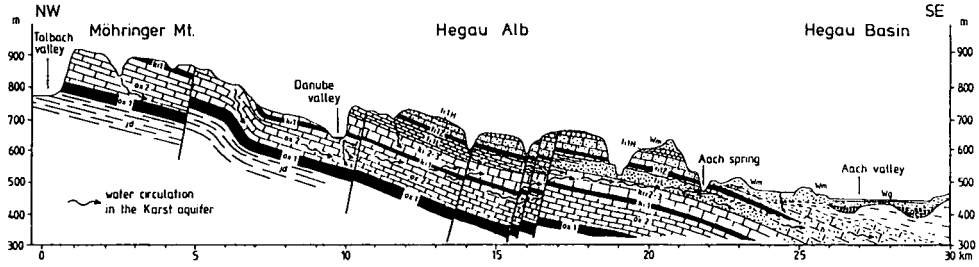

Figure 201. Geological cross-section of the western Swabian Alb. Limey and marly bedded sequences of the Upper Jura, overlayed in the south by Tertiary Molasse as well as Quaternary fluvioglacial sediments. The subterranean hydraulic connections between the Danube valley and the Aach spring are schematically suggested (extended profile according to SCHREINER in BATSCHE et al.1970).

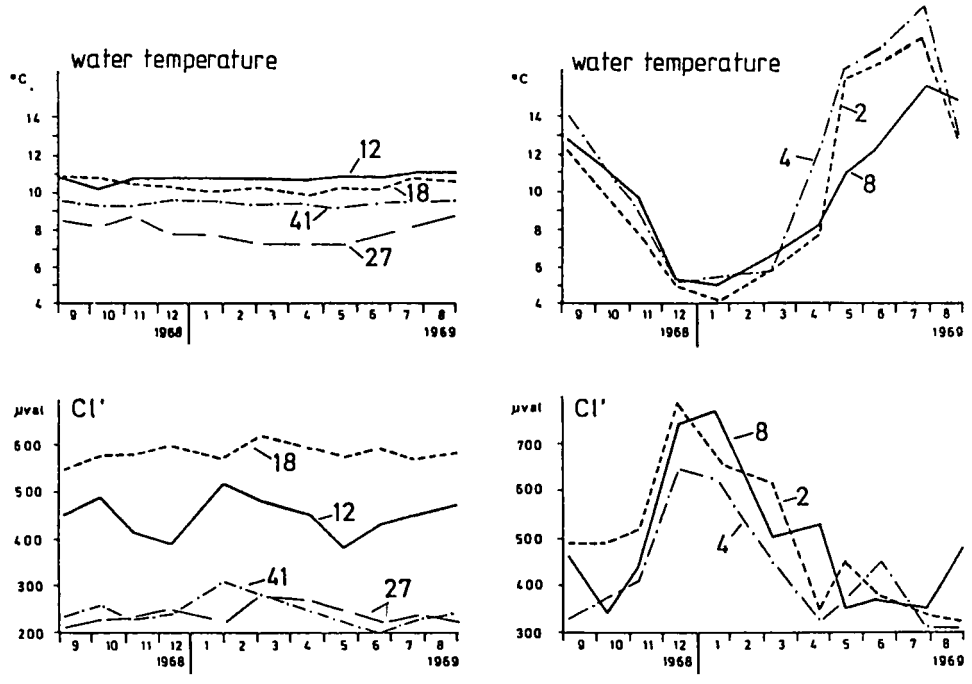

Figure 202. Annual variations of selected physical and chemical parameters in water samples from the Danube-Aach region.

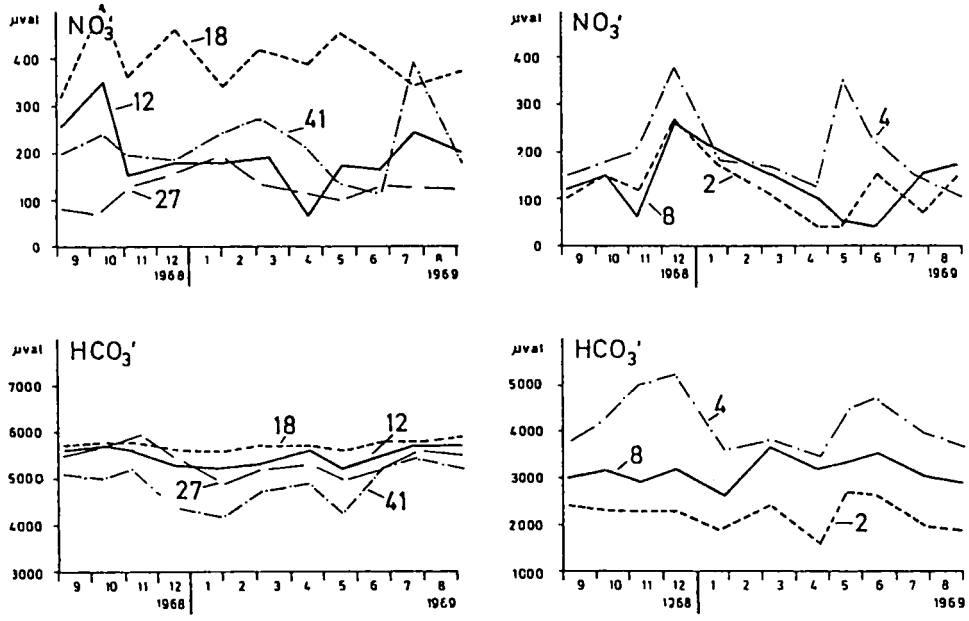

Figure 202. Continued. Left column: Wulfbach spring (41) shallow karst; Kressenloch spring (12) deep karst with Danube water; Bleiche-spring (18) covered karst; Dorstel valley (27) Juranagelfluh; right column: Aach spring (8); Danube water near Immendingen (2) and Fridingen (4) (according to HÖTZL in BATSCHE et al.1970).

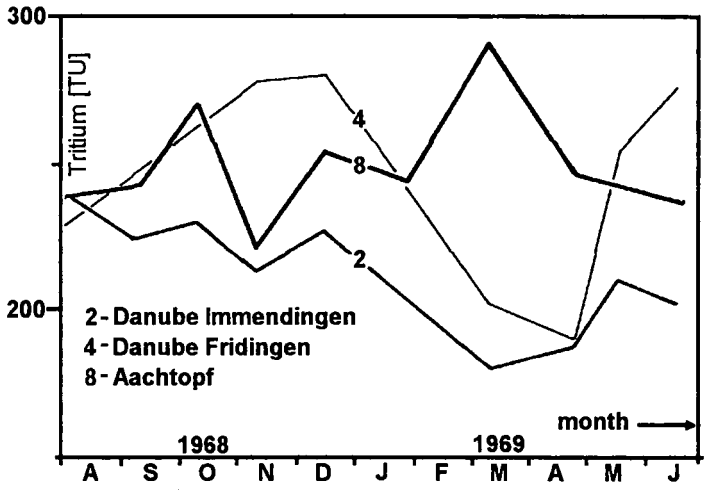

Figure 203. Annual variations in the tritium contents in water samples from the Danube near Immendingen (2) and near Fridingen (4) and from the Aach spring (8). A comparison of the curves shows the seasonally different mixing fraction of Danube water in the Aach spring (by GEYH & MAYRHOFER in BATSCHE et al.1970).

mation of even the temporally variable mixing ratios of the surface waters in the individual springs. Such constituents, as natural tracers, can deliver important preliminary information and facilitate the successful planning of a tracing test.

5.2.4.3 *Combined tracing test from 1969*

The injection sites were chosen according to two main goals: 1. Orientation of the underground discharge from the different stream-sinks at the Danube, and 2. Delimitation of the catchment areas of the Aach spring. Furthermore, various local goals were also of interest, such as sewage water inflow and the possible propagation of pollutants during accidents with hazardous materials. Considering the hydrogeological conditions, the following injection plan with nine injection sites (A to I cf. Fig. 75) was set-up (BATSCHE et al.1970).

A: Danube sink holes in the region of the Immendingen water (clarification of drainage flow),

B: Doline north of Stetten (delimitation of the catchment area in NW),

C: Borehole at the expressway bridge north of Engen (drainage flow in possible accidents with hazardous materials),

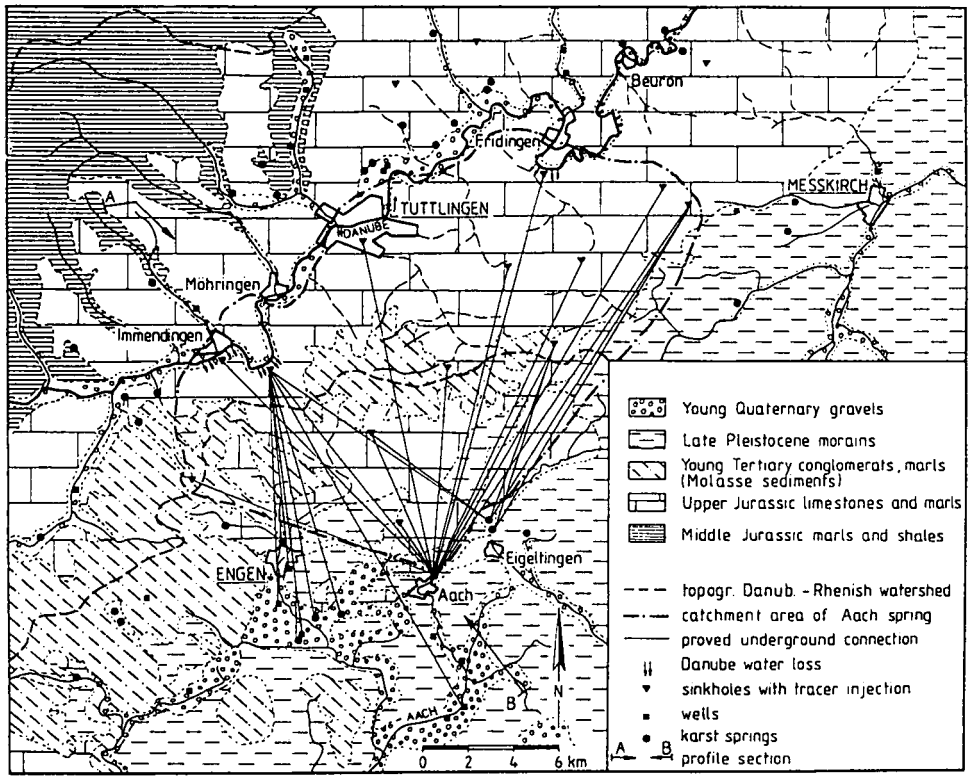

Figure 204. Results of the combined tracing test in the Danube-Aach region from August 1969 (by BATSCHE et al.1970). A-B: Cross-section of Figure 201.

D: Danube sink holes in the Fridingen river bend (clarification of the drainage flow, esp. secondary flow apart from the Aach spring),

E: Seepage shaft in the loam pit east of Liptingen (drainage relationships in the Alb plateau),

F: Quarry south of Buchheim (delimitation of the catchment area im NE),

G: Main stream-sink of the Danube at Brühl between Immendingen and Möhringen (clarification of the drainage flow, esp. secondary flow apart from the Aach spring),

H: Doline in southern city region of Tuttlingen (delimitation of the catchment area in N, clarification of the drainage flow from the rain canalisation),

I: Doline east of Neuhausen ob Egg (drainage relationships in the Alb plateau, drainage of treated sewage water).

The assignment of the tracers and the injection quantities can be taken from Table 28. The following tracers were used: fluorescent dyes, salts, dyed *Lycopodium*-spores, active and activable substance components, bacteria, foaming agents, and aromas. Since the tracers could not be directly compared due to different transport behaviour, the more sensitive tracers were assigned to the injection sites that were farthest away or according to priorities due to the flow conditions. The extremely detectable fluorescent dyes were injected in the far away border positions, drift tracers as comparisons in well-known flow paths, and less sensitive tracers were injected over short distances. At that time, new and unknown in the karst of the Swabian Alb, tracers were used parallel in the individual injection sites to have a comparison to known tracers. Among these were the bacterium *Serratia marcescens*, the activable tracer lanthan, and the aromas limonene and isobornylacetate.

To record the re-emergence of the tracers, 33 sampling sites were set-up. This en-

Table 28. Combined tracing test in the Danube-Aach-region from 1969. Overview of the tracers used and the results (by KÄSS in BATSCHE et al.1970). Injection site A-I see Figure 75.

Inject. site	Dist. to Aach spring (km)	Diff. in altitude/slope to Aach spr. in %	Tracer	Appearance in Aach spring after h effective flow velocity in m/h 1st app.	Max.	Highest concentration	Sec. appearance (see Fig. 75)
A	13.3	179/1.35	1000 kg KCl	34	54	0.44 mg/l	
				364	208	K^+	
			150 l limonene	31	36	ca. 0.13 mg/l	
				422	360		
B	11.4	290/2.54	8 kg amidorhodamine-G	111	129	2.1 µg/l	
				103	88		
C	6.45	63/0.97	250 kg NH_4Br	–	–	–	
D	18.3	142/0.78	4 Curie ^{51}Cr chelate	55	79		
			bound.	332	232	$6 \cdot 10^{-9}$ Ci/l	
			20 kg lanthan nitrate =	38	50	2.4 µg/l La	
			6.2 kg La, chelate bound	9,68?	350	12	
E	11.8	245/2.05	200 kg hard wetting	63	70	235 µg/l	
			agents + 200 kg soft wetting agents	190	170	11,12,13	

Table 28. Continued.

Inject. site	Dist. to Aach spring (km)	Diff. in altitude/slope to Aach spr. in %	Tracer	Appearance in Aach spring after h effective flow velocity in m/h 1st app.	Max.	Highest concentration	Sec. appearance (s. Fig. 75)
			75 kg iso-Bornylacetate	ca. 90 –	ca. 110 –		
F	19.8	310/1.56	50 kg uranine	1008 ca. 8	2600 20	0.009 µg/l	
G	11.7	178/1.56	*Serratia marcescens* ca. $3 \cdot 10^{13}$ 45 kg brown dyed *Lycopodium*- spores	39 304 27 450	47 252 46 255	4 germs in 0.5 ml 425 spore/ 6-h-sample	12,15,16, 18,24,60 10,24,25, 56
H	14.2	190/1.34	50 t thawing salt	64 222	71 212	0.70 meq/l	
I	15.4	260/1.69	28 kg green-dyed *Lycopodium*- spores	69 226	84 184	63 spores/ 6-h-sample	

abled an area of almost 500 km^2 to be supervised. This relatively low number of sampling sites was made possible by the intensive preliminary investigations. They allowed the removal of numerous small springs, that could be assigned to the non-karstifiable hydrogeological units of the karst covering (HÖTZL 1973).

The sampling rhythm was fitted to the expected tracer passage in accordance with the possible tracers and the expected effective flow velocities and the distance to the injection sites. In the Aach spring, samples were taken hourly to record the tracer breakthrough. Later, in the other springs also, the sampling rhythms were changed to several samples per day or even to taking only weekly samples. The recovery showed that a sufficiently accurate coverage of the tracer curves was achieved and could be quantitatively evaluated. The observation program was essentially carried out for three months. Selected sampling sites were observed throughout the winter on into the early spring of 1970, in order to record any potential re-increase in the tracer breakthrough curve due to the increased water flow.

The results of the combined tracing test are summarized in Table 28 and in Figure 204. For the first time, this experiment proved that the Danube water not only reappears in the Aach spring, but also in several other springs, above all in springs in the region near Engen. The alimenting of the porous aquifer in the western and central Hegau basin could also be proven and thus provided clarification of an important aspect for further water management measures.

The actual lateral fanning-out of the flow from separate sink holes is in part much larger than shown in the summarizing presentation in Figure 204.

This is above all caused by the high dilution of the tracers in the secondary re-emergence sites, so that detection was only possible with very sensitive tracers, such as drift particles. Less sensitive tracers, such as rock salt (injection site H), were to be sure registered in the main recovery site, the Aach spring, with a marked breakthrough curve. However, in the Kressenloch springs, slightly to the east, which had

positive results from the other tracers, there was no increase in the salt load, in spite of an injection quantity of 50 tons (!).

Another finding, liable to be misunderstood, is the seemingly crossed paths in the west. Whereas here the drift particles from the main percolation site at Brühl (injection site G) also reached the springs near Engen, the tracers injected at the western edge, sulforhodamine G (injection site B) and potassium salt (injection site A) could only be detected in the Aach spring. From the discolouration of the spore tracers due to sulforhodamine G deposits, it could be concluded that connections to the springs near Engen exist. In detail, a slight additional fan-shaped splitting of the main drainage flow can be assumed (Fig. 103).

With the flow direction determined by the tracing test (BATSCHE et al.1970), the catchment area of the Aach spring can be relatively accurately determined. It has an area of slightly more than 250 km^2. Based on this areal assigment for the precipitation region, it was possible to create a sufficiently accurate water balance. This shows that ca. 2.7 m^3/s of the mean discharge of the Aach spring of 8.5 m^3/s comes from its own catchment area (HÖTZL & HUBER 1972). Considering the water from the other sources (Danube leakage and temporary subterranean inflow from the karst region north of the Danube), this calculates for the total karst water drainage flow south of the Danube to a discharge of ca. 10 m^3/s. The surplus of ca. 1.5 m^3/s as compared to the mean discharge of the Aach spring is understood as spring discharge of the determined secondary re-emergence sites as well as direct discharge into the porous aquifer of the Hegau basin.

The combined tracing test from 1969 was started at the end of August during a low water flow with complete stream-sink of the Danube. Heavy rains only a few hours after the injection caused a flood discharge in the Danube, which also contributed to a considerable acceleration of the subterranean flow. The first appearance of the tracers in the Aach spring was observed after only 26 hours (= 450 m/h) as compared to older test results of 50 hours (= 233 m/h). The flood discharge through the relatively empty karst system lead conversely to a backflow of the infiltrating water from the plateau in the preferred karst conduits. As a result, there was a delay in the flow from the injection site I near Neuhausen ob Egg as compared to older tests, which lead to a decrease in the effective flow velocity for the first appearance from 320 m/h to 233 m/h (BATSCHE et al.1970). With reversed precipitation conditions, heavy rains in actual catchment area and constant flow in the Danube, on the contrary with high karst water levels, it can lead to backflow in the preferred karst conduits and thus the leaking capacity of the sink holes is decreased.

The combined tracing test at the upper Danube verified, that tracing tests in karst regions are an important support in water management planning. Well-directed interventions in the karst systems require funded knowledge of the usually complex flow relationships. Tracing tests can deliver the necessary information for these measures.

5.3 FISSURED AQUIFERS

5.3.1 *General remarks*

W. Käss

Up to now, there have been only a few systematic investigations in fissured aquifers.

Above all, this is due to the comparatively difficult test conditions. Not only are there difficulties with injecting the tracers into the aquifer, the observation possibilities are also difficult. Besides the complex flow paths in fissured rocks, some rock types especially sandstones, also have flow paths in the pore space. Tracing tests in fissured aquifers usually require much longer observation periods than tests in karsts or porous aquifers.

One of the goals of the International Association of Tracer Hydrology (ATH), is to improve upon this and thus, systematic investigations were set up in two investigation areas. One investigation area is in the Molasse sandstone near Luterbach, north of Bern (Switzerland), the other is in the granite of the southern Black Forest near Lindau (Southern Germany). Preliminary test results from the test area Luterbach show sawtooth-shaped, irregular tracer breakthrough curves, whereby many more years of observation will be necessary due to the thick overlying cover (WERNLI 1988). In the tracing tests in the second test area, an almost vertical lode has shown increased hydraulic conductivity as compared to the normal fissures in the granite (ACKERMANN et al. 1982a).

Another test area, in which ATH-members are also active, is in the Oberharz (Lower Saxony, NW-Germany). Due to its very complicated geological underground, which consists of clay slate, sandstones, and quartzites and due to the multiple forms of the tectonic elements, the preliminary investigations have required a very long time. The results published up to now contain theoretical modelling considerations and the results of the investigations about the natural isotopes, but not yet any results from the tracing tests (HERRMANN et al.1984, 1986).

Due to the high expenditure connected with tracing tests using artificial tracers in fissured aquifers, time series from environmental isotopes can be helpful. BALDERER (1982) regularly investigated the Funtenen spring in the Berner Oberland (Switzerland) for tritium, ^{18}O, and ^{85}Kr. With the investigation results, BALDERER was able to determine mean residence times as well as exchange processes with isotope. Similar investigations were conducted by SCHOTTERER and FELBER (1982) in the high alpine Grindelwald basin (Berner Oberland, Switzerland). Solely with isotope investigations from the most important water reservoir of the Grindelwald basin, was the latter author able to obtain valid information concerning residence times, storage capacities, and catchment areas.

Mining hydrogeology deals prepondently with fissured aquifers. Examples from tracing tests from magnesite mining (GOLDBRUNNER et al. 1982) and from the Mansfeld Kupferschiefer mines (LIEBISCH & REMUS 1966) are available. The investigation of the oil field water flow is also mainly carried out with tracing tests in fissured aquifers (Section 5.6.2).

The majority of the dams built are in rocks which have fissures. The actual bypass can only be determined with investigations with artificial or natural tracers (EGGER 1929, FRANK 1936, HEITFELD & TÄTZLER 1967 and Section 5.9.2).

An informative test was conducted by WEBSTER et al. (1970) during a pumping test in fractured crystalline rock in South Carolina (USA). The authors carried out a two-well tracer test with withdrawal from one well out of a fractured aquifer and reinjected the water after marking it with tritium into a well 540 metres away. Surprisingly, the breakthrough in the pumping well was very uniform, solely towards the

end of the two-year observation period were there any indications of a larger than the calculated dispersion.

During tracing injections in hillsides of the German Uplands, the tracer often does not reappear in the springs at the slope base. During several tests in the crystalline of the southern Black Forest, where small water-bearing gullies were injected before they percolated with uranine or lithium chloride, not a trace of either tracer was ever found in the lower-lying springs, in spite of a sufficient observation period (SCHNEIDER 1988). The same observation was made in the Bunter sandstone on the Kniebis west slope (Middle Black Forest, SW-Germany). Obviously during these negative tests, the injected tracer was able to find a path through slope disruption fissures down deeper depths, to reappear strongly diluted and delayed as well as spatially far apart at the base of the slope.

In fissured aquifer tracing tests, interactions with the rock surface must also be taken into account, just as in porous aquifers, if sorptive and exchange-capable tracers are injected.

5.3.2 *Deep-seated rock creeps and rock slides*
H. Hötzl

5.3.2.1 *Impact of the water*

Gravity induced mass displacements of rocks are always activated by changes in the existing equilibrium conditions. These are caused by additional external stress or reductions in the shear and frictional resistance. This leads to a disturbance in the existing force relationships in the scarps, slopes, and valley flanks (FECKER & REIK 1987, MÜLLER 1963a, PRINZ 1982).

In many cases these are long-term geological processes such as weathering and deep erosion, that gradually weaken the stability of slopes and scarps through disaggregation, oversteepening, and undercutting. Water is of multiple importance with respect to the changes which are effective here. On the one hand, it is the deciding impact factor for the named geological processes, on the other hand, it causes displacement of the force relationships in the ground and rock masses, that are not only responsible for the long-term destabilizing effects, but which can also even through short-term changes cause mass movement.

A rise in the mountain water table causes an increase in the load in the upper part of the slope. As a result, the fissure water pressure acts as normal stress upon the fissure walls and thus causes additional forces along possible slipping surfaces. At the same time, the water can cause a decrease in the friction angle and the shear resistance by changes in the mechanical rock properties. In the base of the slope, the rising water level causes an increase in the buoyancy, which contributes to a further displacement of the holding forces.

These effective mechanisms clearly show that a functioning drainage is of great importance for slopes which are just in equilibrium and especially for instable slopes and valley flanks. To safeguard destabilizied slopes and those affected or threatened by mass movement, an artificial lowering of the water table is often tried. To solve this geotechnical task, detailed hydrogeological mapping of the subterranean hydraulic routing is required.

The hydrogeological evaluation of a rock slide or of a deep seated rock creep is generally very difficult. The in-situ rock mass of the affected slope areas is considerably disturbed. Other than blocks, that might be only lightly rotated in the original rock mass, a complete small-sized disaggregation of the rocks can occur. A hydraulically uniform drainage is not given. All transitions of the water circulation can be observed, from preferred fissure flow, as often seen in the upper primary crack areas of the sagging mass, but also parallel to the different far reaching movement planes, to pore flow in the heavily loosened rock areas. Secondary cracks and slides cause interruptions in the drainage paths. Individual parts can then become completely hydraulically isolated and only connected with the rest of the system through springs, that percolate again after short surface flow in the movement plane.

To investigate such complex subterranean flow systems, steady state hydraulic measurement set-ups are only conditionally suitable. They usually deliver, even with high technical operating conditions, only partially usable data. Integrated complete considerations, even over differently structured partial areas, can be won with tracing tests, however. The deliberate and well-directed use of tracers allows, also in mass movements, an overview of the inflow and outflow conditions in their spatial and temporal distribution. The thusly derived knowledge about:

- the origin of the water in the sliding mass,
- depth of the water circulation,
- the connectivity of the fissure systems,
- the subterranean retention areas,
- the hydraulic connections between the separate partial areas

deliver, along with the water table measurement in the mountain, the prerequisites for well-directed geotechnical measures to safeguard and remediate rock slides and deep seated rock creeps.

The following uses two examples from alpine areas to explain the applications of tracing techniques in hydrogeological characterization of such sagging slopes. The glacial overdeepening of the alpine valleys since the melting of the ice masses after the last ice age has left many oversteepened valley flanks, that lead, partially on deep seated movement planes, to a lateral displacement of the valley base or cause instable rock sections to slide downhill.

5.3.2.2 *Sagging slope Gradenbach*

The deep seated rock creep Gradenbach is south of the main ridge of the Central Alps in Carinthia, Austria. The deeply cut Gradenbach valley empties south of Heiligenblut in the Möll valley. Shortly before it ends, the valley crosses a tectonically strongly stressed wedge zone (Matrei Zone), which consists of different phyllite series. On the southernly exposed valley flank, over a width of ca. 1000 m, a deep seated sagging slope has developed, which reaches on the steep, ca. 25°, inclined slope almost up to the ridge area of the Eggerwiesenkopf (2200 m a.s.l.) and thus has a vertical reach of ca. 1100 m (Figs 205 and 206).

During the flood water events from 1965/66, the Gradenbach eroded immense talus masses at the foot of the sagging slope, which lead to a complete overwash with debris and the destruction of an underlying settlement. To prohibit further such debris overwashes, powerful torrent regulation dams were built. However, these have been completely destroyed in the meantime by the pressure of the sagging slope. For

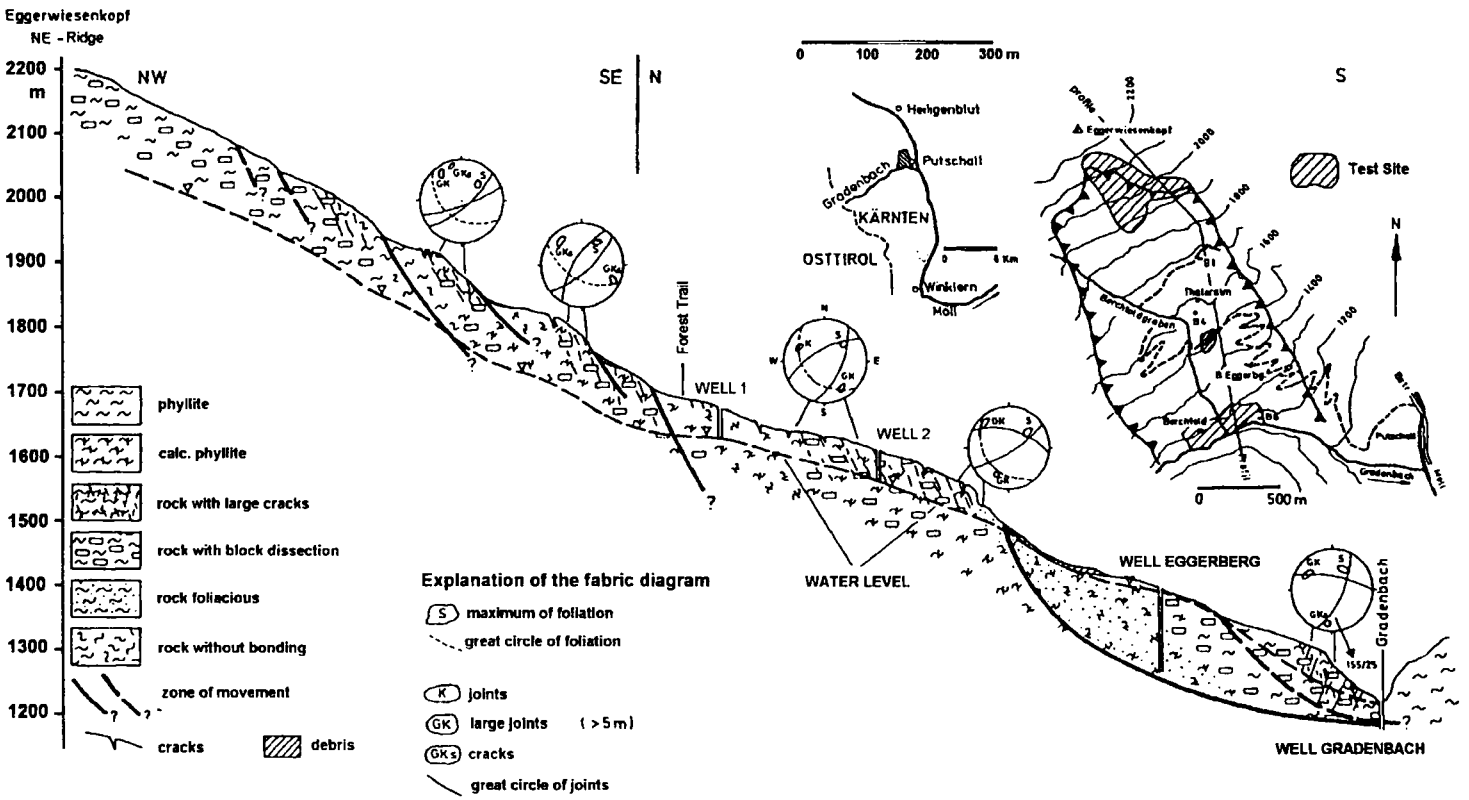

Figure 205. Sagging slope Gradenbach, NW-Carinthia, Austria. Site sketch and geotechnic profile (from MOSER & KIEFER 1988).

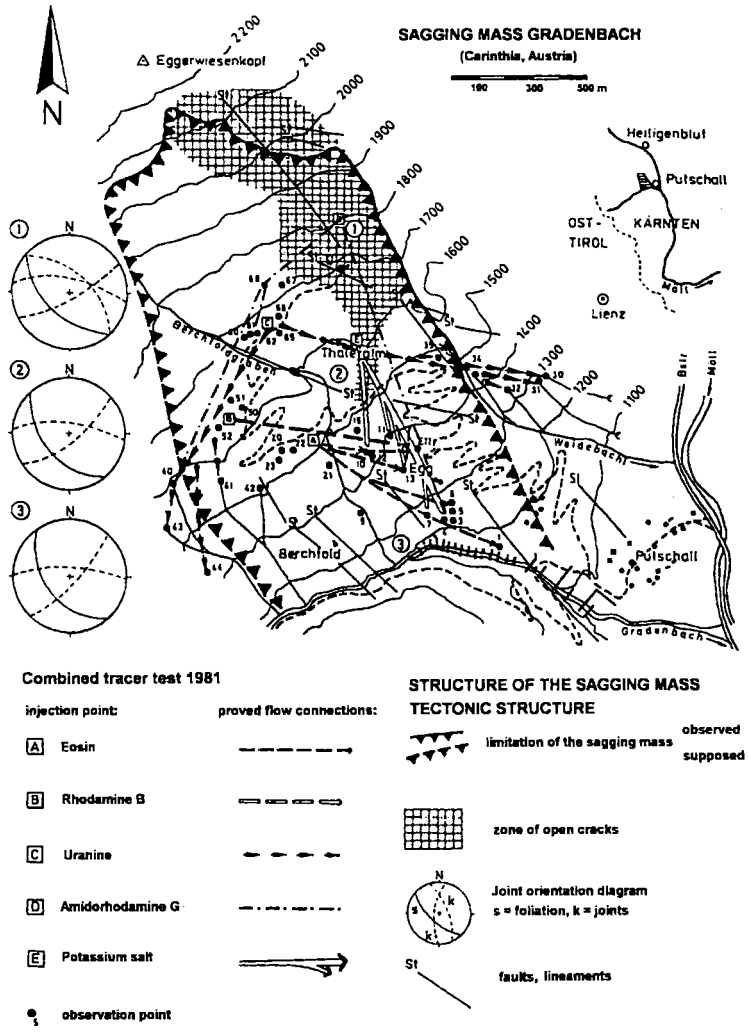

Figure 206. Border of the sagging slope mass Gradenbach with indications of the joint fabric as well as the results from the combined tracing test 1981 (from MOSER & KIEFER 1988).

the geotechnical determination of the deep seated rock creep, extensive investigations were set-up (KRONFELLER-KRAUS 1974, MOSER & GLUMAC 1983). They were partially supplemented by hydrogeological surveys (ZOJER & ZÖTL 1975), during which a tracing test was conducted. However, the tracing test was negative without any recovery of the injected tracer.

During the extended geotechnical, geodetic, and hydrogeological investigation program conducted by the University of Karlsruhe, Germany (MOSER & GLUMAC 1983, MOSER & KIEFER 1988) another tracing test was carried out in 1981, based on detailed hydrogeological surveying and hydrochemical investigations. The goal of this test was to obtain information about the residence time of the precipitation water and about the subterranean drainage paths in the sagging mass, in order to interpret the hydraulic efficacy of the individual planes of movement and the fissure systems caused by the disruption of the mountain slopes.

The combined test was carried out during snow melt with a rising water table at the end of May 1981. The following five tracers were injected (cf. Fig. 206):

Injection site A: Eosin	10 kg
Injection site B: Rhodamine B	10 kg
Injection site C: Uranine	10 kg
Injection site D: Amidorhodamine G	10 kg
Injection site E: Potassium chloride	400 kg

All of the water outcrops within the sagging slope and in the neighbouring slope areas were observed. Samples were taken for a period of 14 months and were taken as direct samples and as cumulative samples in activated carbon bags. The tracers were spectralfluorimetrically or spectralphotometrically detected.

The results are displayed as the spatial distribution in the water outcrops in Figure 206. Information pertaining to the temporal passage and the calculated effective flow velocities can be found in Table 29. In all, as often found in fissured aquifers, complete breakthrough curves were not obtained, so that no further parameter evaluations nor analytical model calculations were possible. The maximal concentration of the fluorescent dyes was at 1 µg/l, for potassium it was two- to three-fold the background level. The continuous recovery of uranine in the spring 40 was observed for three months (MOSER & KIEFER 1988).

Relative to the observed flow directions, an astounding parallelism with the observed joint fabric resulted, in spite of the mass movements. A WNW-ESE striking fault zone with an accompanying fissure set (uranine, eosin, and rhodamine flow) proved an especially effective deep flow path under parts of the sliding mass. In contrast, a fissure system (NE-SW), approximately parallel to the cleavage, showed clearly decreased hydraulic efficacy (uranine, amidorhodamine, and partially potassium), which was noticeable in the flow velocities above all. The third major flow direction (potassium, amidorhodamine, partially uranine) is apparently within the actual sliding mass. As a result of these tests, parts of the mass must be considered as hydraulical separate units. Favoured hydraulic routings can be seen especially in the

Table 29. Tracing test at the sagging mass of Gradenbach 1981. Maximal concentrations and the thus derived effective flow velocities of the tracer for the observed reappearances (MOSER & KIEFER 1988).

Observation site flow direction	Detected tracer	Day of max. concentr. (1981)	Distance to inject site (m)	Eff. flow velocity (m/day)
Q 40 SW	Uranine	17.09.	650	6
Q 35 ESE	Uranine	12.06.	600	46
Q 34 ESE	Uranine	20.08.	750	15
Q 4 ESE	Eosin	06.08.	600	9
Q 10 E	Eosin	10.09.	200	2
Q 13 ESE	Eosin	30.09.	350	3
Q 4 S	Potassium chloride	10.06.	750	68
Q 11 S	Potassium chloride	12.06.	350	27
Q 10 S	Potassium chloride	13.06.	400	29
Q 3 S	Potassium chloride	23.06.	750	31
Q 7 S	Potassium chloride	01.10.	700	6

eastern part, where calcareous phyllites outcrop. Mechanically, these rocks react more brittle. There are also some areas widened by carbonate-corrosion as far as to have produced pronounced karst phenomena.

Thus, the important fact pertaining to the whole sagging slope obtained, was that the infiltrating precipitation in the upper part is discharged over the major fissure systems out of the mobile area to the ESE, resp. the SW. This drainage is geomechanically especially important, because herewith at least under normal flow conditions, a further rise of the water pressure is stopped. However, with respect to the heavy rains that are frequent in this region, it should be tried to collect the surface flow before it seeps in the major fissure zones and to lead it out of the sagging mass.

The flow in the calcareous phyllites contained in the eastern part, seems to be a high risk factor. It intensifies the discharge of the groundwater into the critical lower part of the sagging mass. The high flow velocities prove, that it can come thereby to an accelerated rise of the water pressure in the lower parts of the slope. Due to secondary and successive fissures, in this extremely sensitive area partial movements are accelerated or renewed and lead downstream to devastating debris overwashes. The test results show that, along with the efforts made to divert the surface flow, an effective deep drainage to laterally divert the discharge from the partially karstified calcareous phyllites subterranean flow is urgently required.

5.3.2.3 *The sagging slope of the Reppwand*

This second example of a deep seated rock creep is also from Carinthia, near the Italian-Austrian border in the Carinthian Alps. The area investigated is ca. 1.75 km long and reaches from the initial part of the landslide Reppwand (ca. 1500 m a.s.l.) in the south to the stream Oselitzenbach (820 m a.s.l.) in the north (Figs 207 and 208). The active slip-off slope has already led to multiple disruptions in the highway which runs through this area, the Naßfeld-Bundesstraße. Geologically, the lower part of the slip-off slope consists of Carboniferous clay slates and of Upper Carboniferous to Permian sand- and limestone sequences (KAHLER & PREY 1963).

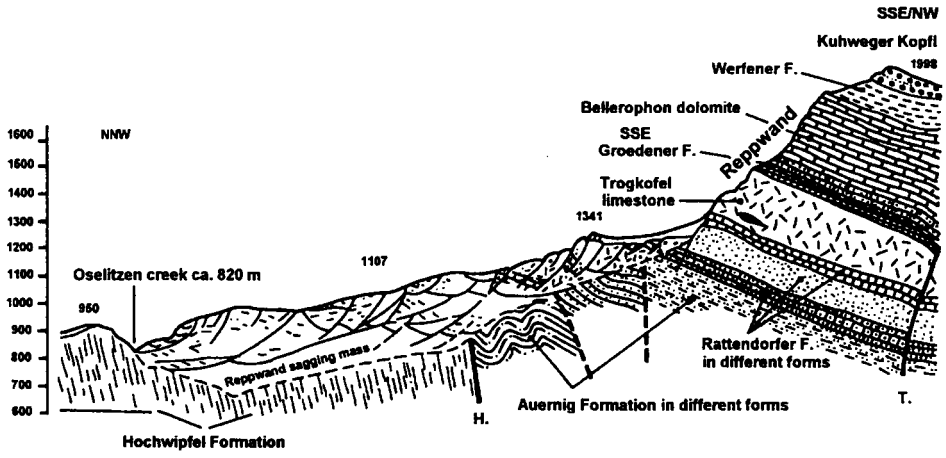

Figure 207. Sagging mass 'Reppwand', Karnian Alps, Carinthia, Austria. Geological longitudinal section after KAHLER & PREY 1963.

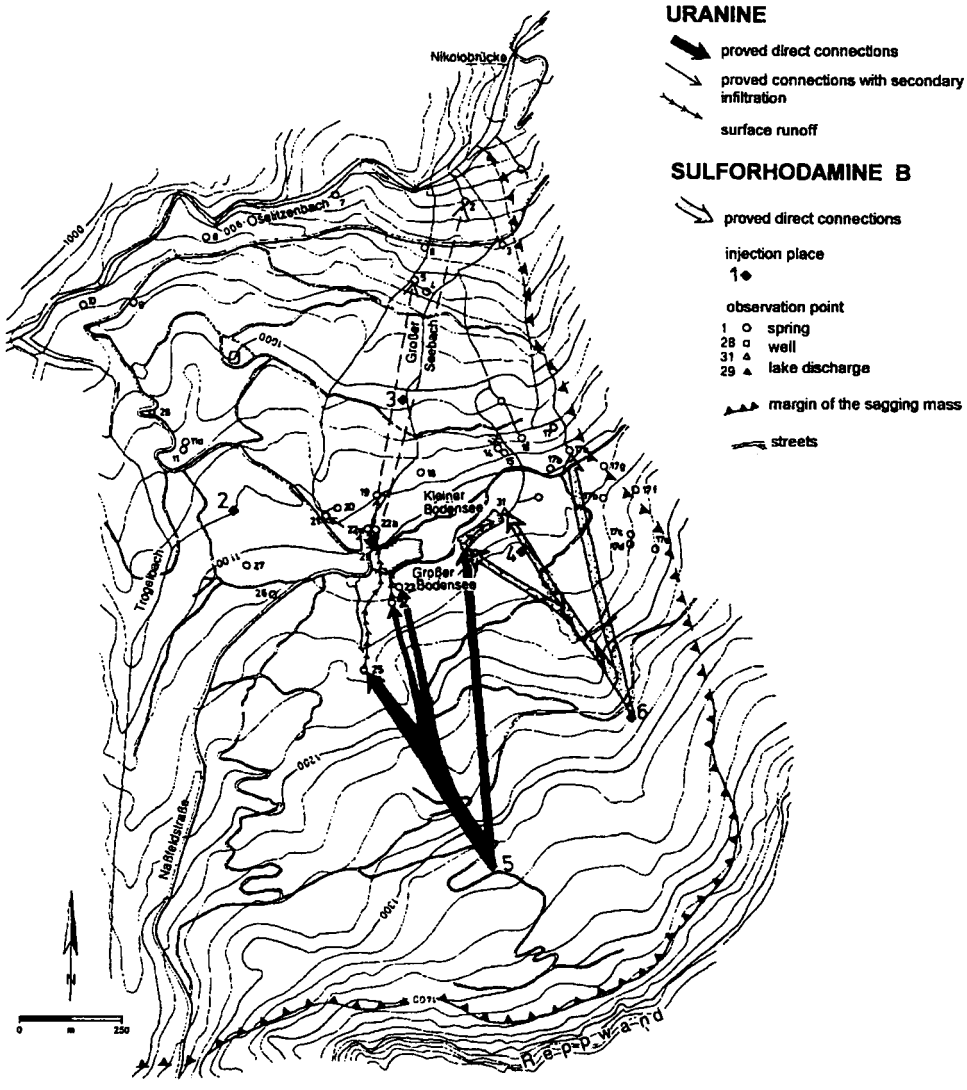

Figure 208. Results of the combined tracing test 'Reppwand' 1989 with the positive tracer detections from the injection sites 5 (uranine) and 6 (sulforhodamine B). The tracing injections in the injection sites 2, 3, and 4 were negative (HÖTZL et al.1992).

With comprehensive geotechnical investigations it was possible to determine the major zones of movement and to subdivide the sagging slope in areas of relative homogeneity, according to rock-mechanical criteria (MOSER & WINDISCHMANN 1989). Under the topridge of the landslide, there are large connected, but displaced rock masses. They link up to slide masses which are still bonded, which show flat outcropping slide surfaces with clear indications of creeping movement as well as newly developed initial cracks and behind elongated landslide trenches leading to an additional splitting of the rock masses. Downward the sagging slope, strongly disintegrated masses with coarse block debris are present, showing deepgoing lystric sur-

faces. The velocity of the sliding movements were determined by geodetic surveying to > 5 cm/d and < 20 cm/d (MOSER et al. 1988).

To clarify the hydrogeological relationships, a combined tracing test was carried out after a comprehensive hydrogeologic survey (HÖTZL & MOSER 1992). The goal of the test was to determine the preferred dewatering paths, resp. drains within the sagging mass, so that it could be determined as to how helpful the deviation of the discharge of individual springs in the middle level of the sagging mass (region Kleiner and Großer Bodensee) would be in reducing the slope movement. Special attention was given to the hydraulic efficacy of the individual sliding surfaces as well as of the new crack zones caused by the mountain splitting.

For the simultaneous determination of the subterranean flow in the sagging mass under uniform hydrological conditions, tracers were injected in six swallow holes. The position of the injection sites can be taken from Figure 208. The following tracer quantities were used:

- Swallow hole 1 (seeping of the Großer Seebach): pretest 0.5 kg of sulforhodamine B,
- Swallow hole 2 (loss of the creek water): 10 kg of rhodamine B,
- Swallow hole 3 (seeping pond): 10 kg of eosin,
- Swallow hole 4 (dry swallow hole in a landslide trench): 10 kg of pyranine,
- Swallow hole 5 (dry swallow hole in the displaced rock mass): 10 kg of uranine,
- Swallow hole 6 (dry swallow hole in the displaced rock mass): 4.5 kg of sulforhodamine B

The tracing test was started in May of 1989 with the injection of the tracer. With regard to the possible deep-reaching and there only very slow water circulation, a long-term observation plan until the summer of 1990 was set up. During the first eight weeks, direct samples were taken, afterwards activated charcoal adapters were used. The evaluation of the fluorescence spectra was done with the synchronscan procedure.

Here again the results are only summarized in the form of the spatial distribution of the tracer reappearance (Fig. 208) and selected parameters listed in Table 30 (HÖTZL & MOSER 1992).

Basically, it is difficult to obtain positive results from such a hydraulically unmanageable sagging mass. From the six tracer injections, only three tracers could be detected in the 15-month observation period. Of the remaining three negative tracings, only one was obviously in an only episodically active swallow hole, whereas the other two showed long-term active percolations.

On the whole, the results show a definite, for further geotechnical measures important, dichotomy of the sagging mass. In the upper half, relatively flat rock slides dominate and their movement planes outcrop in the middle section. Over the entire width of the sagging mass, this region is characterized by the outcropping of numerous springs. The observed breakthrough times of the tracers (Table 30) show relatively moderate effective flow velocities (0.2 to 5 m/h), yet these are considerable for fissured aquifers and indicate particular hydraulic routings. The differences with respect to the mean flow times and the storage capacity of the individual partial areas can be clearly seen in the long-term recovery (cf. Fig. 209). The recovery rates are

Table 30. Tracing test 'Sagging mass: Reppwand' 1989. Characteristic values of the breakthrough of sulforhodamine B (Q 17a, Q 30, A 31) and uranine (Q 25, Q 24, Q 23, Q 30) registered in direct water samples.

Sampling site	x_{ein} (m)	t_{max} (h)	v_{max} (m/h)	t_{dom} (h)	v_{dom} (m/h)	c_{max} (mg/m^3)	W (%)
Q 17a	651	410	1.59	1390	0.46	0.339	1.9
Q 30	568	2184	0.26	–	–	0.077	–
A 31	583	815	0.71	1222	0.47	0.262	0.6
Q 25	560	118	4.75	620	0.9	13.73	16.5
Q 24	674	141	4.75	620	1.08	0.940	0.9
Q 23	705	164	4.30	669	1.05	2.540	0.5
Q 30	780	720	1.08	1245	0.62	0.254	–

x_{ein} = distance to injection site 5, resp. 6, t_{max} = time of the first tracer detection, v_{max} = maximal effective flow velocity, t_{dom} = time of the concentration maximum, v_{dom} = dominant effective flow velocity, c_{max} = maximal tracer concentration, W = recovery (yield) rate.

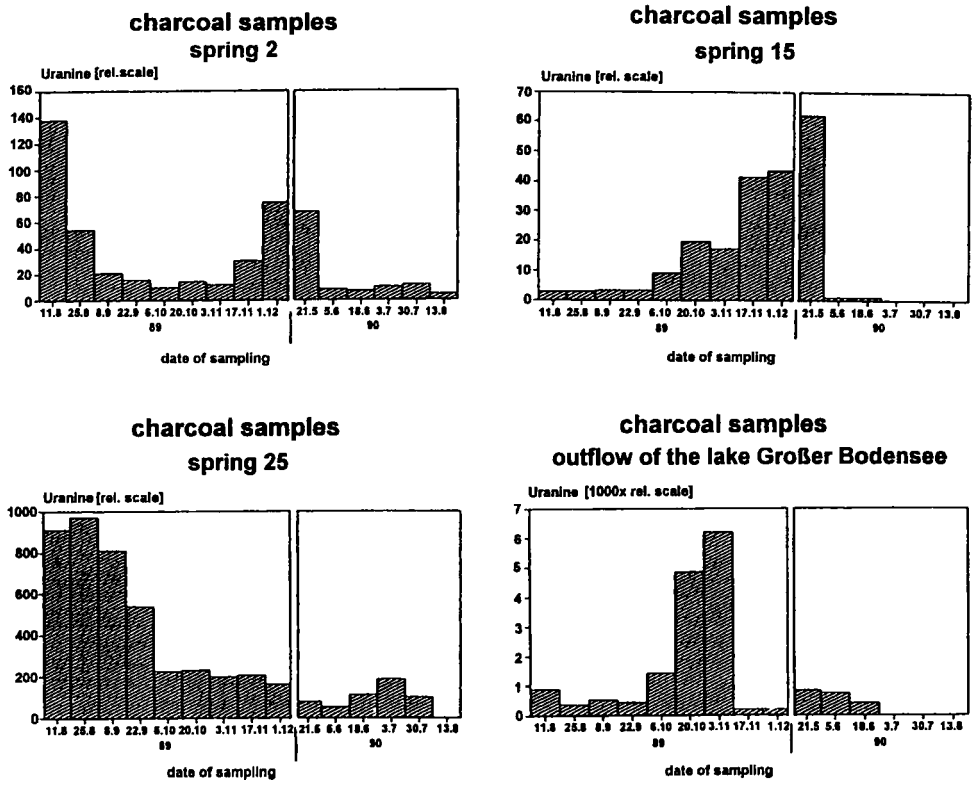

Figure 209. Tracing test 'Sagging mass: Reppwand' 1989. Long-term behaviour of the uranine recovery in selected springs according to the interpretation of activated charcoal adapters that had hung for 14 days (HÖTZL et al.1994).

accordingly low (< 20%). On the one hand, this is connected with the diffusion into the finely dissipated disaggregation fabric of the displaced rock mass, on the other hand, with a partial discharge into the lower part of the sagging slope.

In contrast to this, the drainage in the lower part of the sagging mass occurs mainly over newly developed, deep-reaching ellipsoide rotation planes. In the upper part of the landslide, these cause wide open cracks, that however obviously close up further down and cause the infiltrating water to backflow. The further flow occurs therefore only as a slow percolation flow through the highly mobile lower sagging mass with usually diffuse discharge directly in the receiving watercourse.

For the remediation, these results show the necessitiy of diverting the water that discharges in the middle areas away from the mobile area of the slope. The diversion of the streams, that are fed by these springs, with the corresponding stopping of the secondary infiltration can contribute to a settling of the movement of the especially active lower parts of the sagging mass.

In spite or even because of the partially negative results in comparison to the proven reappearance sites, the combined tracing test has delivered important information regarding the mechanisms and the mode of action of the subterranean drainage of the sagging slope. The results can be directly incorporated in the planning of geotechnical measures to stabilize the sliding masses.

5.3.3 *Tracer experiments in a highly permeable fault zone – Fractured rock test site Lindau*

Th. Himmelsbach

5.3.3.1 *Hydrogeology of the test site*

The fractured rock test site Lindau is located at the NE part of the Albtal granite pluton and is characterized by a widestanding orthogonal fracture system. Its surface is weathered to a fine grained granitic grus whose thickness is generally only a few metres. Therefore, the water cycle is expected to be restricted to the granitic grus unless the basement rock is transected by a fault zone. In the Black Forest, major Variscan faults became pathways for hydrothermal solutions with ensuing mineralization. The resulting ore bodies have been regarded in the past as impermeable, but investigations in connection with the planned dam site have shown that they are in fact highly permeable. The major hydrogeological unit at the test site is formed by such a fractured orebody whose permeability ($5 \cdot 10^{-6}$ m/s - $1 \cdot 10^{-4}$ m/s) is some orders of magnitude higher than the fissured granite ($5 \cdot 10^{-10}$ m/s - $1 \cdot 10^{-8}$ m/s) (HIMMELSBACH 1993). The orebody is nearly vertical and has a northerly strike (5/85 E) and a thickness between 0.3 and 3.0 m. The fracturing of the system is oriented more or less parallel to the orebody showing a steep eastbound dip. The fractures result from tectonic shear displacement (RENK 1981) and cut the general strike of the orebody obliquely. The permeability of the orebody results from fractures and from solution cavities of some of its constituents due to descending aqueous solutions. The mineralization of the fault zone began at its western margin and proceeded eastwards. During the early genetic phases, the orebody was affected by an increasing fracturing and the adjacent granite was hydrothermally altered leading to an asymmetric mineralization and nonhomogeneous fracture density.

The fractured orebody drains the adjacent rock leading to a lowering of hydraulic head which extends approximately 50 m on both sides. The groundwater affected by the drainage zone flows towards natural base levels where the orebody exfiltrates into intersecting rivulets. At the northern test site, the flow patterns are directed northward while at the southern part the dewatering of the orebody follows southbound patterns (Fig. 210). Cement injections separated the orebody hydraulically into two parts having no hydraulic exchange. At the southern part of the orebody hydraulic heads up to 60 m are measured at the well heads in the observation tunnel (Fig. 211) while the northern part of the orebody is characterized by hydraulic heads in the range of up to 25 m. The differences in hydraulic heads occur within a horizontal distance of less than 30 m (HIMMELSBACH & HÖTZL 1991).

The observation tunnel Lindau was excavated 90 m below the surface and the widestanding orthogonal jointing of the granite leads to a generally low percolation

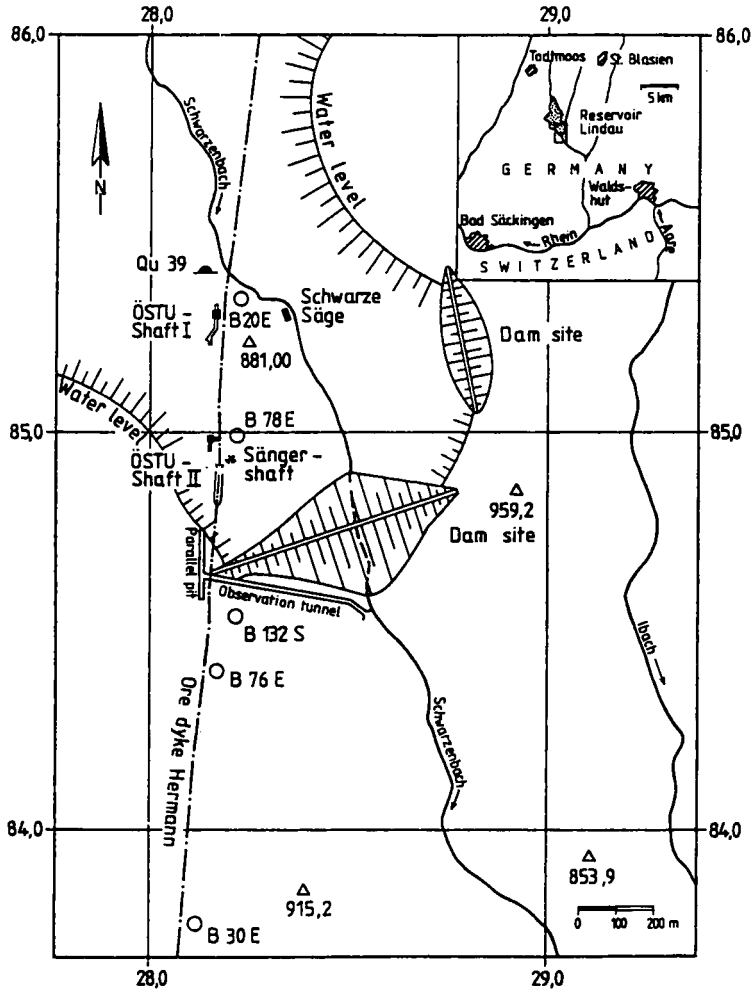

Figure 210. Map of the Lindau fractured rock test site. The general strike of the hydrothermal mineralized fault zone is shown as a dashed line.

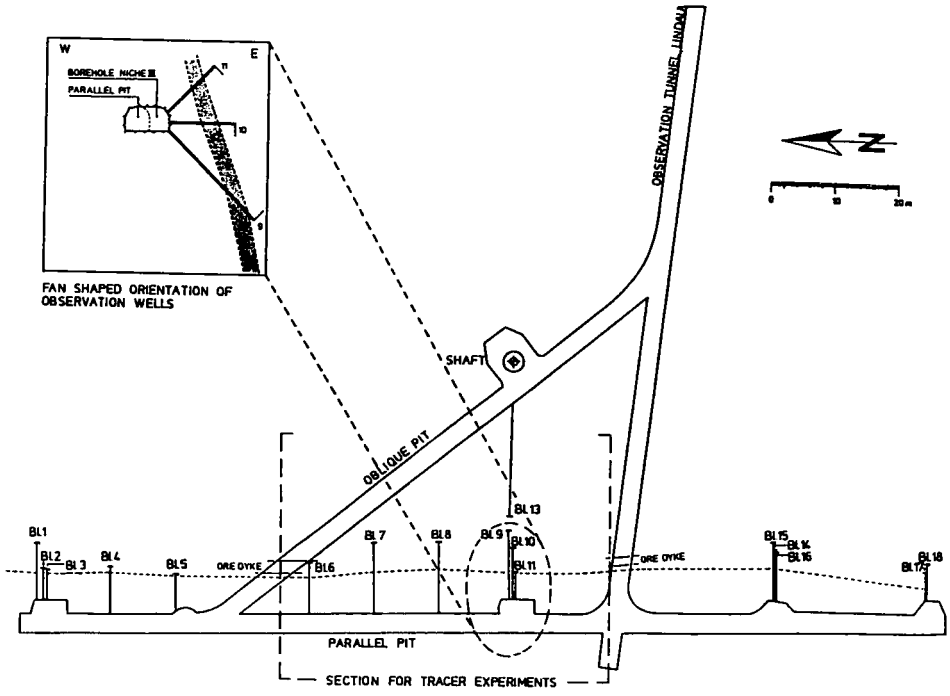

Figure 211. Map of the observation tunnel Lindau with the orebody section chosen for the forced gradient tracer experiments.

rate through the gallery back. Only in the direct vicinity of faults and fracture zones there is a noticeable percolation through the tunnel back. The observation tunnel has a length of 460 m and bifurcates near its end. Both tunnels penetrate the fault and fracture zone of the orebody. Each tunnel joins the so-called 'parallel pit', which was excavated a few meters aside the orebody (Fig. 211). The parallel pit is aligned parallel to the strike of the orebody and has a length of 150 m. Along the parallel pit seven borehole niches were excavated 10-12 m apart and 21 boreholes were drilled into the orebody. The boreholes were performed as vertically oriented fans, consisting of a horizontal borehole in the centre and two inclined boreholes 45° up- and downward (Fig. 211). They have a 2" diameter and they penetrate the fault and fracture zone completely. The well heads are shut by stainless steel valves and are equipped with pressure gauges.

The hydraulic boundary conditions at the northern part of the Lindau test site can be influenced artificially. Since the hydraulic gradient in the northern part of the orebody is relatively low, its direction can be reversed if a borehole in the northern part of the parallel pit is opened. Under such conditions, the distribution of hydraulic head within the northern part of the orebody changes within a few days, while the opened test well yields a constant discharge rate within less than two days. Hence, both groundwater flow directions, the normal as well as the reversed one, can be tested by tracer experiments at the northern test site.

5.3.3.2 *Tracer experiments*

In the course of the underground examinations, more than 200 boreholes were drilled into the fault zone and the granite. The dense network of boreholes offers nearly ideal conditions for conducting tracer experiments over varying distances and under different flow field conditions. This section summarizes in brief the results of four tracer experiments which were performed under different flow field conditions.

The large scale tracer experiments over distances of 49 m and 346 m were performed under natural flow field conditions. The small scale tracer experiments over a distance of 11.2 m were carried out under steady state flow field conditions in the observation tunnel Lindau where radial-convergent and dipole flow field geometries were applied. The breakthrough curves of the experiments were analysed with a convective-dispersive fracture flow model which allows matrix diffusion into the adjacent rock matrix. The solution of the inverse problem, e.g. fitting the analytical model to the experimental data, yielded hydraulic parameters such as fissure and matrix porosities and first estimates of the average fracture aperture. The results obtained concerning the matrix porosity were compared with results of independent core investigations in the laboratory (Table 31). Table 32 gives an overview depicting the number of tracer experiments, the flow field conditions, the distances, and the mass of fluorescent dye that was injected.

Table 31. Results of the mercury porosimetry of drill core samples from the central part of the parallel pit, test site Lindau (mercury porosimetry was performed at the Institute of Hydrogeology, Academy of Mining and Metallurgy, Cracow, Poland).

Sample	Core-length [m]	Porosity [%]	Description
9/1	8.40	2.2	Albtal granite
9/2	8.70	2.8	Albtal granite
9/3	9.50	2.6	Albtal granite, hydrothermally altered
9/4	10.40	3.6	Ore lode, fluorite, cavernouosity,
9/5	10.70	1.1	Ore lode, fluorite, strong cavernouosity, baryte, galena
9/6	11.30	1.2	Ore lode, fluorite, cavernouosity, rare galena
9/7	11.80	0.7	"
9/8	12.10	0.7	Albtal granite, hydrothermally altered, thin ore veins with diffuse mineralization
9/9	12.90	0.7	"
9/10	13.50	7.6	"
9/11	13.90	2.6	"
9/12	14.60	6.9	Altal granite, hydrothermally altered
10/1	2.50	2.6	Albtal granite
10/3	3.30	2.4	Albtal granite
10/5	4.20	1.0	Ore lode, dense fluorite, spare quartz
10/6	4.50	1.3	Ore lode, greenish fluorite
10/7	4.80	2.3	Ore lode, cavernous fluorite
10/8	5.20	2.1	Albtal granite, hydrothermally altered, ore veins
10/9	5.40	0.9	Albtal granite, hydrothermally altered, ore veins, feldspars altered
10/10	5.80	0.9	Ore lode, fluorite, cavernouosity, spare quartz
10/11	6.30	4.1	Albtal granite, intense hydrothermal alteration

Table 31. Continued.

Sample	Core-length [m]	Porosity [%]	Description
10/12	6.80	2.6	Albtal granite, intense hydrothermal alteration
10/13	7.40	3.0	Albtal granite, hydrothermally altered
11/1	1.60	1.6	Albtal granite
11/2	2.40	0.9	Albtal granite
11/3	2.70	1.9	Albtal granite, hydrothermally altered
11/4	3.20	1.0	Albtal granit, intense hydrothermal alteration
11/5	3.90	1.6	Ore lode, greenish cavernous fluorite, quartz
11/6	4.30	1.2	Ore lode, dense fluorite, quartz
11/7	4.70	1.2	Ore lode, fluorite, quartz
11/8	5.20	5.6	Albtal granite, hydrothermally altered, thin ore veins with diffuse mineralization
11/9	5.50	6.7	Ore lode, fluorite, quartz
11/10	6.20	4.6	Albtal granite, intense hydrothermal alteration
11/11	7.50	1.2	Albtal granite, hydrothermal alteration
11/12	7.90	1.7	Albtal granite

Table 32. Tracer experiments at the fractured rock test site Lindau.

Tracer experiment (tracer)	Injected mass [g]	Distance [m]	Natural flow field	Forced gradient experiments monopole	dipole
FLOW 1 (eosin)	2.000	346.4	X	–	–
FLOW 3 (pyranine)	500	49.0	X	–	–
BL8-BL10 (pyranine, D_2O)	2 (300)	11.2	–	X	–
BL8-BL10 (eosin)	2	11.2	–	–	X

Natural flow field

The large scale tracer experiment, *FLOW 1, B78E-B20E*, was interpreted as a natural gradient tracer test. The distance between the injection and the test well was 346 m (Table 32). The samples were taken at the artesian well B20 E that explores the orebody at a depth of 100 m below the surface (Fig. 212 top). The discharge rate was approximately 1.5 l/s. The wells were obviously located too far apart from each other to establish a radial convergent flow field for the pumping rate used, or the migration of the tracer followed different fracture sets intercepting each other. At the beginning of the experiment, the sampling was done twice a day, but was reduced later to one sample per day. Samples were taken for 2.5 years and more than 800 samples were analysed in the laboratory.

The tracer injection was performed using an inclined borehole at the test site surface. The wells at the test site surface have a length of more than 100 m and intersect the orebody at depths between 50 and 80 m (Fig. 212 bottom). The distances between the injection and the detection well were calculated considering the centre of piercement through the orebody as geometric information. A thin plastic hose was used to inject the tracer into the surface well. Its lower end was placed directly within the fractured part of the orebody. The injection was completed within less than 20 minutes, and 2 m^3 of groundwater were pumped into the injection well to flush

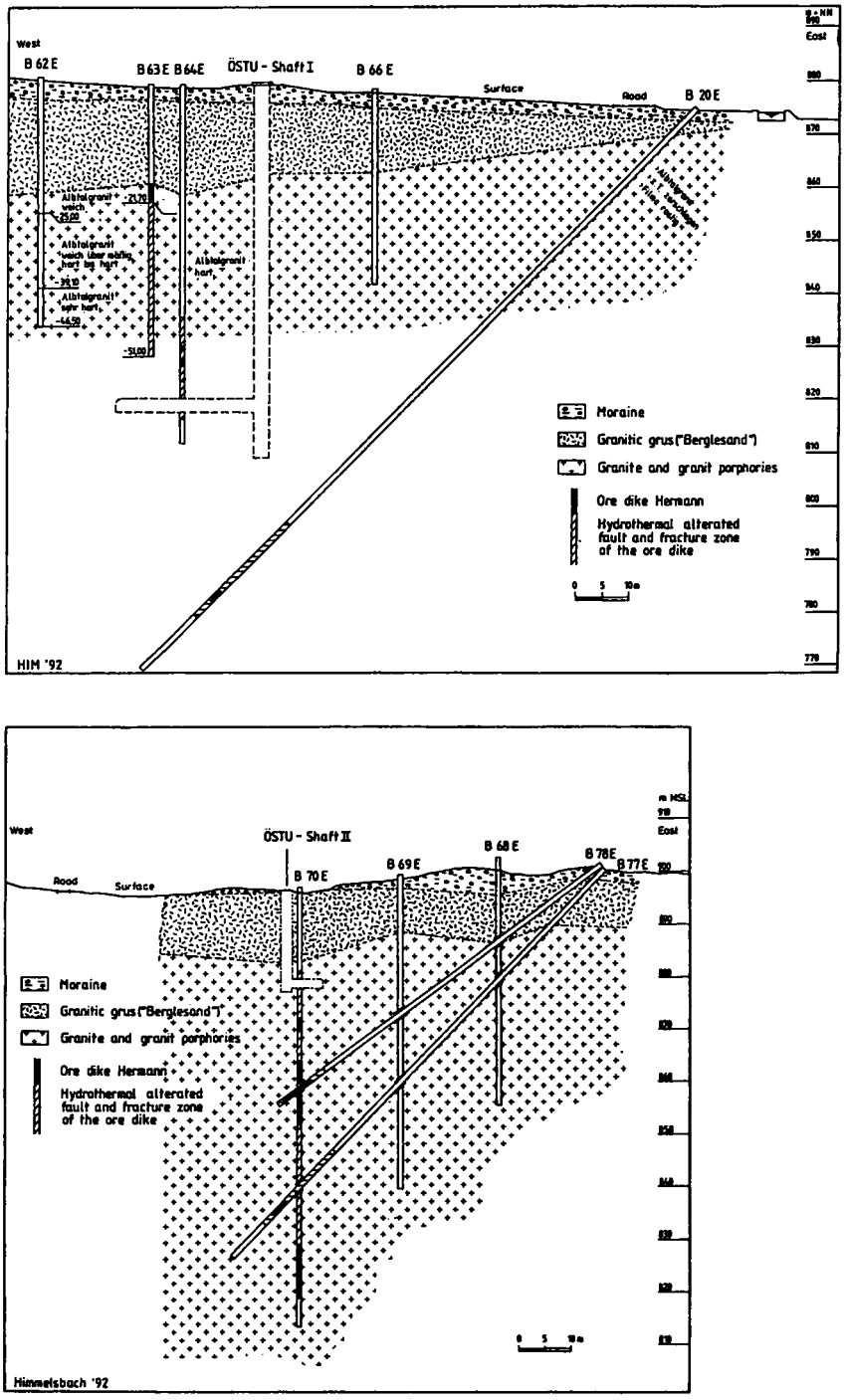

Figure 212. Cross section through the orebody 'Hermann'. Top: With the observation well B20E. Bottom: With the injection well B77E.

the tracer completely into the fault and fracture zone. The samples were taken with an automatic sampler to ensure a satisfactory resolution of the breakthrough curve.

Another tracer experiment under reversed flow field conditions (FLOW 3, BL12-BL2) used an experimental flow line in the tunnel (POHL 1994), which was located in the observation tunnel (Fig. 211). The horizontal wells in the tunnel are located at a depth of approximately 90 m and have a length of 10-70 m. They intersect the orebody either perpendicularly or at an oblique angle (Fig. 211). During this experiment the natural, northbound flow direction was reversed, because the detection well, BL2, in the northern part of the parallel pit was opened. The tracer was injected into the horizontal well BL12 in the tunnel. The distance between the wells was 49 metres (Table 32) and the orebody intersected by the injection well was separated by a packer to ensure an instantaneous and complete injection of the tracer into the fractured system. Due to the short distance the sampling was done in time intervals of 10 minutes. The discharge rate was measured using a large turbine flowmeter and after six weeks, when the tracer was injected, it amounted to 0.12 m^3/s showing no further decrease. The hydraulic head was measured at the test site surface and with pressure gauges at the well heads in the tunnel.

Forced gradient tracer tests

The forced gradient tracer test was performed at the subsurface in situ migration laboratory in the Lindau observation tunnel. The detection of hydraulic contacts between the different wells was done using pulse interference tests. The interference tests were performed by opening the shutin valve of one of the boreholes for a few seconds. The decrease and the subsequent recovery of the well head pressure were measured continuously by electronic pressure sensors at all test wells. During the tests different cross hole arrangements were used, so that different parts of the orebody were affected, to derive better spatial information about the hydraulic connec-

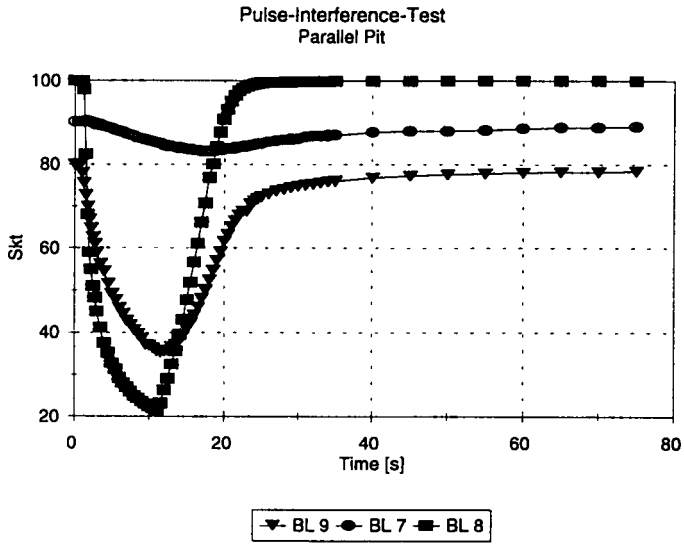

Figure 213. Example of a pulse interference test carried out at the central part of the parallel pit.

tions. An example of the results obtained is given in Figure 213. The pulse interference tests were interpreted qualitatively. If the phase shift between the hydraulic head measurements at the test well and the observation well became negligible, a direct hydraulic contact between the test wells was assumed. However, if a zone of decreased permeability was detected, the phase shift between the pressure signals became evident and it was assumed that the wells were not connected over the same fracture set.

The information about hydraulic contacts was an important precondition to predict the spatial length as well as the orientation of conductive sets of parallel fractures. The results confirmed the assumption, based on geological data, that the orebody at the central part of the parallel pit is hydraulically separated and forced gradient tracer experiments in this section would not affect others. Another important information was that the spatial extension of a discrete set of parallel fractures was within the experimental scale of approximately 15-20 m. Bearing in mind that flow processes in fractured rock are affected by nonhomogeneous fracture distribution, this information enables the tracer experiments to be carried out in a pseudo-homogeneous region of a discrete fracture set (HIMMELSBACH & HÖTZL 1991) connecting the four test wells BL8, BL9, BL10 and BL11 (Fig. 211, Table 33) directly.

The section of the orebody described above exists under stagnant water conditions (HIMMELSBACH 1993). This allowed the establishment of artificial flow fields of different geometry between the test wells. The forced gradient tracer experiments in the parallel pit were performed either under radial-convergent flow field conditions (e.g. monopole-tests) or under a dipole flow field of equal strength (e.g. dipole-tests). During the experiments, the hydraulic gradient within the test section was calculated from measurements of sensitive pressure sensors and the flow rate was controlled using small turbine flowmeters. While the dipole-tests required an injection-withdrawal well pair, the monopole-tests were performed using a single discharge well. In each test, the tracer was injected as a short pulse into the steady state flow field. For the dipole-experiments, approximately 1500 l of previously pumped water was stored in a pressure reservoir under nitrogen pressure to avoid any hydrochemical alteration of the oxygen unsaturated formation water. The reservoir prohibited a recirculation of tracer-contaminated formation water. The field fluorimeter in the flow line served to optimize the sampling intervals and the contaminated water was finally led out of the experimental site to avoid any contamination of the test area (Fig. 214).

Table 33. Transmissivities calculated from single well, hydraulic recharge tests at the test site Lindau.

Borehole	M [m]	T [m²/s]	Standard deviation σ
BL7	0.85	$1.3 \cdot 10^{-4}$	$2.7 \cdot 10^{-4}$
BL8	1.05	$6.5 \cdot 10^{-6}$	$3.3 \cdot 10^{-6}$
BL9	3.07	$2.5 \cdot 10^{-5}$	$3.5 \cdot 10^{-5}$
BL10	2.00	$4.7 \cdot 10^{-5}$	$3.3 \cdot 10^{-5}$
BL11	1.35	$5.4 \cdot 10^{-4}$	$2.1 \cdot 10^{-4}$

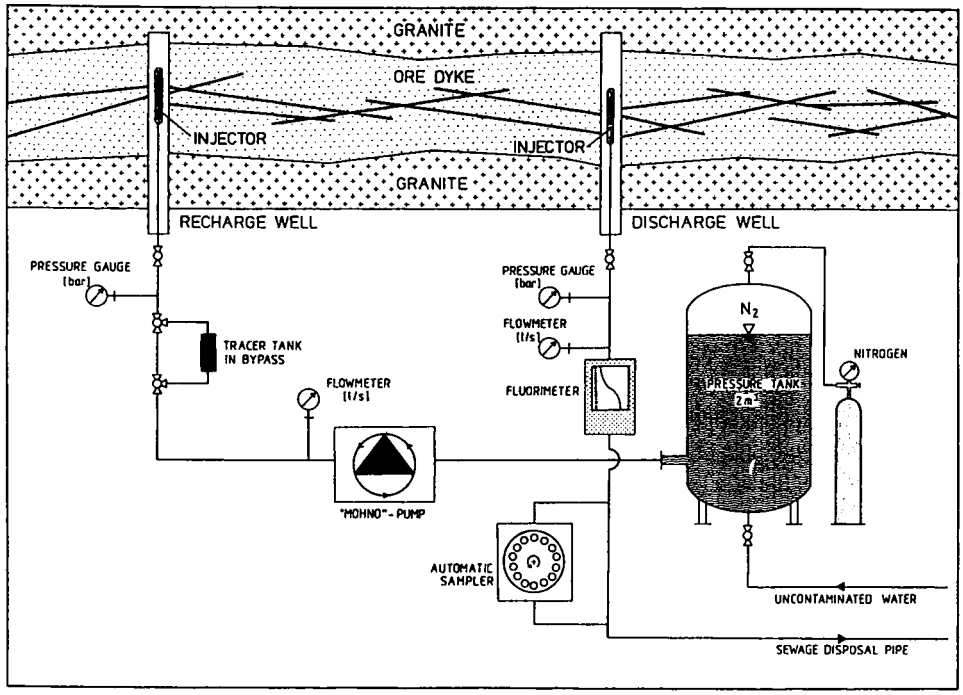

Figure 214. Schematic sketch depicting the experimental array required for the performance of forced gradient tracer tests in the observation tunnel Lindau.

5.3.3.3 *Transport model*

The general model

The tracer experiments were interpreted using the 1-D *S*ingle *F*issure *D*ispersion *M*odel (SFDM) developed by MALOSZEWSKI and ZUBER (1985, 1990). For short term tracer experiments the tracer propagation can be described analytically by the convective-dispersive flow through a single fissure, superimposed by diffusion processes into an adjacent infinitely extended matrix. The mean transit time of water has to be short enough (up to a few weeks) that the propagation of the diffusion front of adjacent fissures do not affect each other. This condition is usually satisfied for tracer tests performed in short time and over small space scales (MALOSZEWSKI 1992). With these assumptions the transport equations for a conservative tracer are as follows (SUDICKY & FRIND 1982):

$$\frac{\delta C_f}{\delta t} + v\frac{\delta C_f}{\delta x} - D\frac{\delta^2 C_f}{\delta x^2}\,\frac{n_p C_p}{b}\,\frac{\delta C_p}{\delta y} = 0 \quad y = b \tag{5.1}$$

$$\frac{\delta C_p}{\delta t} - D_p\frac{\delta^2 C_p}{\delta y^2} = 0 \tag{5.2}$$

where C_f and C_p are the concentration in the fissures and in the matrix, v is the mean flow velocity of water in the fissures, x is the spatial coordinate taken in direction of flow, y is the spatial coordinate perpendicular to the fissure orientation, D is the dispersion coefficient in the fissures, b is the half width of the fracture, t is the time variable, n_p is the matrix porosity, D_p is the molecular diffusion coefficient of the tracer in the porous matrix.

For a pulse injection, the initial and boundary conditions are as follows:

$$\begin{aligned} C_f(x, 0) &= 0 \\ C_f(0, t) &= M/Q\ \delta(t) \\ C_f(\infty, t) &= 0 \\ C_p(x, y, t) &= 0 \\ C_p(b, x, t) &= C_f(x, t) \\ C_p(\infty, x, t) &= 0 \end{aligned}$$

where M is the mass of injected tracer, Q is the volumetric flow rate, (t) is the DIRAC delta function.

The SFDM is obtained by solving the Equations (5.1) and (5.2) for an instantaneous injection of tracer with boundaries and initial conditions given above, and reads for a fixed distance (X) as follows (MALOSZEWSKI & ZUBER 1985):

$$C_f(t) = \frac{aM}{2\pi Q} \int_0^t \sqrt{\mathrm{Pe} t_0}\, ex\left[-\frac{\mathrm{Pe}(t_0 - u)^2}{4ut_0} - \frac{a^2 u^2}{t - u} \right] \cdot \frac{du}{\left[u(t-u)^3 \right]^{1/2}} \tag{5.3}$$

This model has three nondisposable fitting parameters:

$$t_0 = X/v \text{ or } V/Q \tag{5.4}$$

$$\mathrm{Pe} = vX/D \tag{5.5}$$

$$A = n_p (D_p)^{1/2} / (2b) \tag{5.6}$$

where X is the distance between the wells, V is the volume of mobile water in the system, Pe is the PECLET number, t_0 is the mean residence time of water, a is the parameter describing the matrix diffusion processes.

The solution (Eq. 5.3) for an instantaneous injection of tracer is called the Single Fissure Dispersion Model (SFDM). If the tracer test is performed under fixed hydraulic boundary conditions, which are generally fulfilled in the case of radial-convergent or divergent-convergent flow field geometries, the SFDM is especially suitable to include the concept of relative mass recovery (KLOTZ et al. 1988, MALOSZEWSKI & ZUBER 1990). The relative recovery is calculated from both, the experimental and theoretical tracer curve as a function of time. Comparing both improves the inverse fitting procedure, because it is very sensitive for diffusion processes affecting the tailing of the breakthrough curve. The relative recovery is defined as follows:

$$RR(t) = Q\int_0^t C_f(t)\delta t / M \tag{5.7}$$

The relative recovery can be calculated for monopole and dipole experiments, but not for tracer experiments under natural flow field conditions.

Adapting the model for natural flow field conditions

Under natural flow field conditions, the volumetric flow rate through a system of tortuous fissures is equal to:

$$Q = n_f v S$$

where S is the cross area perpendicular to the movement of water, and n_f is the fissure porosity.

For natural flow field conditions the fissure porosity is defined for a system of parallel fissures as follows:

$$n_f = 2b/L$$

where L is the average fissure spacing.

Under practical field conditions neither the cross-section area nor the fissure spacing can be determined with sufficient accuracy. To overcome this lack, the tracer curve has to be normalized to the maximum concentration C_{max} measured at the time $t = t_{max}$. The same procedure is done with the theoretical breakthrough curve $C_f(t)$ obtained with the SFDM.

If the distance X between the injection and the observation well is known, the fitting parameters t_0 and Pe (Eqs 5.4 and 5.5) can be used to evaluate the mean water velocity v and the longitudinal dispersivity α_l valid within the test section. However, one has to keep in mind that under natural flow field conditions, the tracer recovery in most cases will not exceed more than a few percent of the injected mass, because the withdrawal of water at the test well will not produce a radial convergent flow field between the test wells. The wells are either too remote from each other, or they do not intersect the same fracture sets. The latter reason is very likely, because discrete fractures are due to basic tectonic and rock mechanical reasons limited in their length. They are hydraulically connected to each other by oblique orientated fractures which do not connect the test wells directly. If the matrix porosity n_p and the effective diffusion parameter D_p of the tracer in the porous matrix is known from independent laboratory measurements, the average fracture aperture may be calculated according to NOVAKOWSKI et al. (1985) using POISEUILLE's Law as follows:

$$2b = \sqrt{\frac{12 v \tau_{f2} X^2}{g t_0 \Delta H_t}} \tag{5.8}$$

where $2b$ is the fracture aperture, t_0 is the mean residence time of water, g is the gravity acceleration, ΔH_t is the difference in piezometric head at the test wells, ν is the kinematic viscosity of water (10°C), τ_{f2} is the tortuosity factor of the fissures.

The calculation of the fissure aperture with Equation (5.8) depends on the movement of water and on directly measurable hydraulic parameters from the experiment.

It is based on the assumption that the hydraulic gradient between the test wells is linear. This is fulfilled due to the lack of a radial-convergent flow field.

Adapting the model to a radial-convergent flow field
If the tracer experiment is performed under radial-convergent flow field conditions (e.g. monopole-experiment), the flow rate through the fractured system, Q, is equal to the discharge rate at the withdrawal borehole. As long as the fault zone is under confined conditions, the volume of the depression cone is negligible. Then, the fissure porosity, n_f, can be calculated as follows (ZUBER 1974):

$$n_f = \frac{Qt_0}{\pi m X^2} \tag{5.9}$$

where m is the thickness of the tested ore dike section.

If the hydraulic conductivity, K, has been previously determined by a pumping test, the mean fissure aperture may be estimated. Under the assumption that the movement of water is restricted to a system of tortuous slits having the same aperture, the mean fissure aperture in the system can be obtained as follows (ZUBER 1974):

$$2b = 4.29 \cdot 10^{-6} \tau_f \sqrt{K/n_f} \tag{5.10}$$

where $2b$ is expressed in metres, K in metres per day, τ_f is the tortuosity factor of the fissures ($\cong$1.5).

Finally if the diffusion coefficient D_p of the tracer in the matrix is known, the matrix porosity, n_p, can be calculated from Equation (5.6). The use of Equation (5.10), however, requires that the hydraulic conductivity, K, of the test section can be determined with sufficient accuracy. Knowing very well that flow processes in the ore dike may be somewhat different to the previously assumed isotropic homogeneous conditions, the transit time of water particles in the cone of head depression can also be expressed using POISEUILLE's Law thus (NOVAKOWSKI et al. 1985, MALOSZEWSKI & ZUBER 1993):

$$t_0 = \ln\frac{X}{r_W} \frac{6\nu\tau_{f2} X^2}{g(2b)^2 \Delta H_t} \tag{5.11}$$

where r_w is the radius of the well.

The rearrangement of Equation (5.11) leads to an estimate of the fracture aperture, $2b$, which also depends on the movement of water and on hydraulic parameters directly measurable through the experiment. As it does not depend any longer on the hydraulic conductivity, whose determination may be surrounded by some uncertainties, the fracture aperture then has the form:

$$2b = \sqrt{\ln\frac{X}{r_W} \frac{6\nu\tau_{f2} X^2}{g t_0 \Delta H_t}}$$

Adapting the model to a dipole flow field
The flow field of a dipole experiment is symmetric and of equal strength if the injec-

tion rate ($Q+$) is equal to the withdrawal rate ($Q-$). If the aquifer is confined, infinitely extended, and is not affected by any natural hydraulic gradient, the symmetrical dipole flow field is not limited in its spatial extension. Therefore, the streamlines are arcs of circles with different radii, intersecting both the injection well and the withdrawal well. As the entire flux can be thought of as split to a finite number of narrow streamtubes having equal partial volumetric flow rates (Fig. 215), the transit time along these streamtubes is, due to symmetric reasons only a function of their length (GROVE & BEETEM 1971). Assuming there is no exchange of tracer between the different streamtubes, the SFDM model can be considered separately for each streamtube (HIMMELSBACH & MALOSZEWSKI 1992). As the dispersivity α_l is considered to be the same within the entire test section, the PECLET number of each stream tube, Pe_i, can also be calculated analytically by symmetric considerations. Consequently, the measured output concentration, $C_f(t)$, is then the superposition of all streamtubes entering the withdrawal well. The three fitting parameters of the transport model are the diffusion parameter, a, the mean transit time, t_{01} and the PECLET number, Pe_{01} of the direct stream tube connecting both wells rectilinearly:

$$t_{01} = \left(\pi n_f m X^2\right) / (3Q) \tag{5.12}$$

$$Pe_{01} = X / \alpha_l$$

The calibration of the model has to be done numerically for an assumed finite number of streamtubes. Only 35 streamtubes need to be considered for satisfactory results (HIMMELSBACH & MALOSZEWSKI 1992). Any higher discretization will only

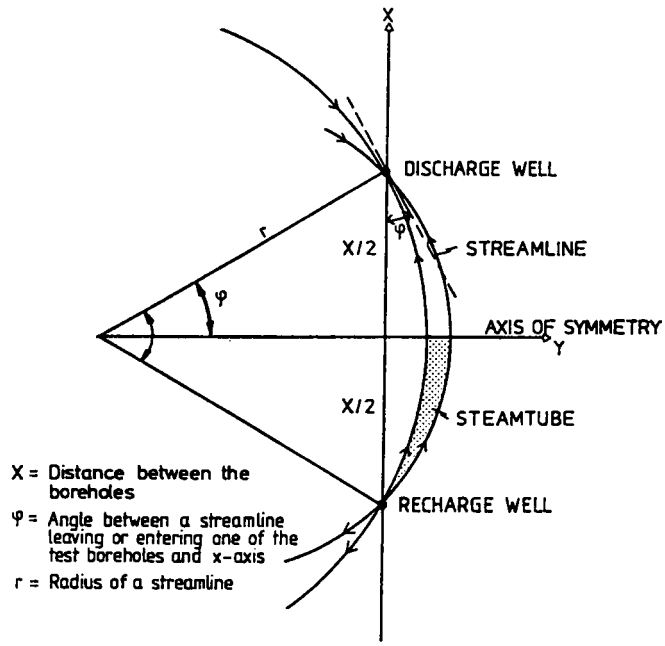

Figure 215. The streamtube approach chosen for the evaluation of dipole experiments of equal strength.

lead to a rapidly increasing CPU-time without enhancing the quality of results. After finding t_{01} one can derive the fissure porosity, n_f, valid for the direct streamline. The matrix porosity, n_p, may be calculated identically as for the monopole experiments (MALOSZEWSKI 1992). An estimation of the fissure porosity can be obtained by the rearrangement of Equation (5.12) and leads to the following expression:

$$n_f = 3Qt_0 / \pi m X^2$$

This equation is similar to Equation (5.9), but it considers a symmetrical dipole flow field of equal strength. For an injection-withdrawal array the mean fissure aperture, $2b$, can also be calculated using POISEUILLE's Law (NOVAKOWSKI et al. 1985, HIMMELSBACH & MALOSZEWSKI 1992). The estimation for the fracture aperture along the shortest flow path gets then the form:

$$2b = \sqrt{\ln\frac{X}{r_W}\frac{4\nu\tau_{f2}X^2}{gt_{01}\Delta H_t}}$$

5.3.3.4 *Results*

Natural flow conditions

In 1988, the tracer experiment *FLOW I, B78E-B20E* started over the largest distance (Table 34). The first traces of eosin were detected after 15 days and the peak concentration was reached after 41 days. The increase in concentration was at first smooth and continuous, but later showed sudden fluctuations. This may result from heavy precipitation leading to intense fluctuations of the groundwater level. As the precipitation during winter was fixed in a thick snow cap, the concentration development became smooth again. The second peak observed 100 days after the injection may be related to a sudden snowmelt event in March 1989, when adiabatic alpine winds caused a temperature increase on the order of up to 20°C. During these extreme hydrological conditions, the snow cap melted within less than one week causing again intense fluctuations of the groundwater level. After that event the measured concentration decreased slowly showing a pronounced tailing effect. Although the maximum concentration was reached rapidly, the tailing effect lead to tracer concentrations which can be detected even six years after the injection (Fig. 216).

The evaluation of groundwater level measurements yielded an average hydraulic gradient between the test wells B77E and B20E on the order of only 0.0044. The in-

Table 34. Flow parameter of the tracer tests

Parameter		Known				Assumed		
Experiment	Tracer	Q [m^3/s]	Dist. [m]	Inclin.	r_w [m]	τ_f^2 [/]	t_p [/]	D_m [m^2/s]
Flow 1 (B78E-B20E)	eosin	0.0015	346	1:52	0.0033	2.25	1.50	4.5E-10
Flow 3 (BL12-BL2)	pyranine	0.1200	49	1:50	0.0033	2.25	1.50	1.5E-09

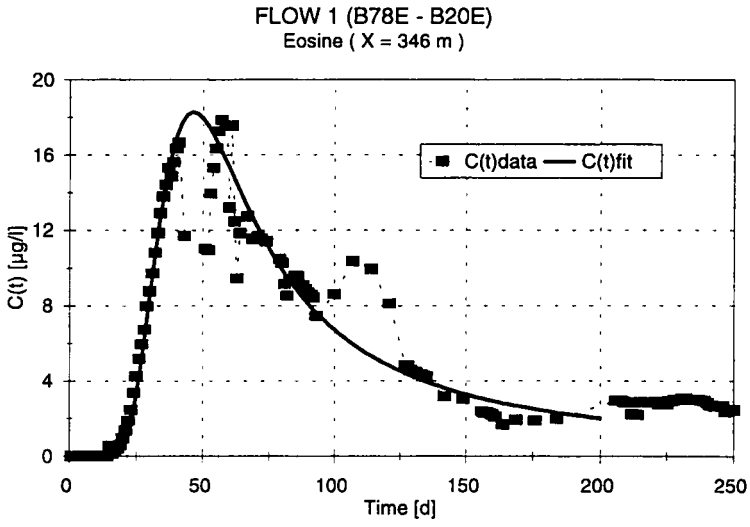

Figure 216. SFDM fitted to natural flow I. Best fit obtained with $t_0 = 432$ h, $a = 0.071$ h$^{-1/2}$, Pe = 100; experimental data shown as symbols, best fit depicted as solid curve.

Table 35. Fit parameter from natural gradient tracer tests.

Parameter Experiment	Tracer	Known i [/]	Fitted t_0 [h]	Pe [/]	a [h$^{-0,5}$]	Calculated α_l [m]	$2b$ [µm]	n_p [%]
Flow 1 (B78E-B20E)	Eosin	0.0044	432.0	100	0.071	3.46	434	3.0
Flow 3 (BL12-BL2)	Pyranine	0.0306	5.0	20	0.200	2.45	576	6.1

verse fitting procedure (Table 35) was obtained with the following parameters: $t_0 = 432$ h, Pe = 100, and $a = 0.071$ h$^{-½}$. Assuming a linear gradient between the wells, the average fracture aperture was calculated to be $2b = 434$ µm (Eq. 5.8). The matrix porosity (Eq. 5.6) was calculated as $n_p = 3.0$ % which corresponds quite well with the results obtained from the mercury porosimetry of cores from the central part of the parallel pit (Table 31). Since the cross section of the flow region cannot be determined with satisfactory accuracy any further interpretation, such as the determination of the fissure porosity n_f is questionable. It has to be pointed out that hydraulic parameters derived from tracer experiments under natural flow conditions represent only a certain part of the system, because the tracer migration followed preferential flow paths.

The second tracer experiment interpreted as a natural flow field experiment, *FLOW 3, BL12-BL2,* was performed by POHL (1994) in combination with an aquifer drainage test leading to a reversal of the flow direction (Fig. 217). The breakthrough curve showed no disturbances in the concentration history, because the time required

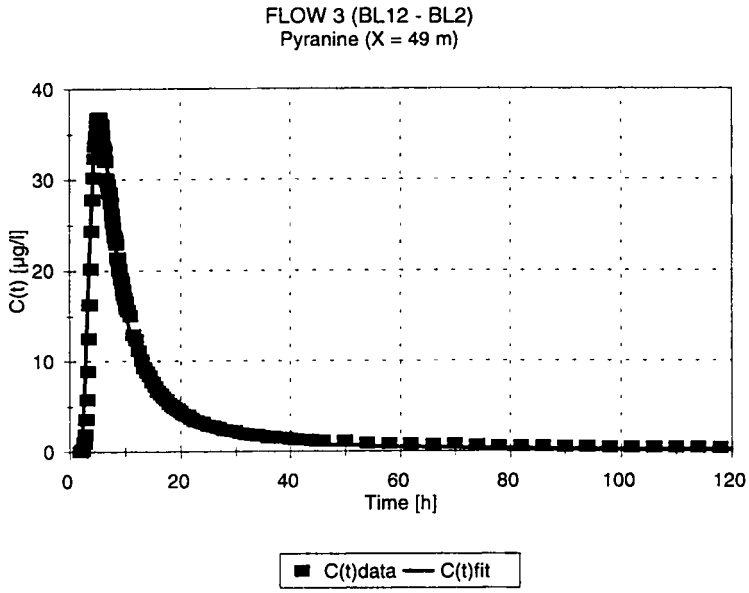

Figure 217. SFDM fitted to natural flow III. Best fit obtained with $t_0 = 5.0$ h, $a = 0.200$ h$^{-1/2}$, Pe = 20; experimental data shown as symbols, best fit depicted as solid curve.

for this experiment was much shorter. Additionally, the experiment was performed under hydrological conditions with only little precipitation. The inverse fitting procedure (Table 35) for this tracer experiment yielded the following parameters: $t_0 = 5.0$ h, Pe = 20 and $a = 0.200$ h$^{-1/2}$. Assuming again a linear gradient between the test wells, the average fracture aperture (Eq. 5.8) was calculated to be $2b = 576$ µm. The average matrix porosity (Eq. 5.6) was calculated to $n_p = 6.1$ %. The derived matrix porosity is within the bench marks of the results obtained from the mercury porosimetry (Table 31).

Forced gradient tracer tests

Monopole Test

The forced gradient tracer tests under convergent flow field conditions were performed in the tunnel over a horizontal distance of 11.2 m. The constant flow rate was 5.8 l/min (Table 36). The measured tracer concentrations are graphed as symbols, while the inverse fit is shown as a solid line. The tracer concentrations are normalized to the injected mass. The relative recovery, which was used to enhance the inverse fit, is shown as the ratio between injected mass and the integral over the breakthrough curve. The sought hydraulic parameters are summarized in Table 37.

The monopole tests were carried out twice between the wells BL8 and BL10 ($X = 11.2$ m). In the first experiment (*Monopole Test I*) pyranine was applied (Fig. 218), whereas in the second experiment (*Monopole Test VI*) pyranine and deuterium were injected simultaneously (Figs 219 and 220). For both experiments, which were performed with nearly equal pumping rates (Table 36), the inverse fit of

Table 36. Flow parameter from forced gradient tracer tests.

Parameter		Known				Assumed			
Experiment	Tracer	Q [m³/s]	X [m]	ΔH [m]	r_w [m]	M^* [m]	τ_f [/]	t_p [/]	D_m [m²/s]
Monopole I (BL8 – BL10)	Pyranine	0.98E-04	11.2	2.25	0.0033	1.53	1.50	1.50	1.5E-09
Monopole VI (BL8 – BL10)	Pyranine	0.96E-04	11.2	1.80	0.0033	1.53	1.50	1.50	1.5E-09
Monopole VI (BL8 – BL10)	D_2O	0.96E-04	11.2	1.80	0.0033	1.53	1.50	1.50	2.5E-09
Dipole I (BL8 – BL10)	Eosin	1.26E-04	11.2	20.83	0.0033	1.53	1.50	1.50	4.5E-10

Table 37. Fit parameter from forced gradient tracer tests.

Parameter		Known	Fitted			Calculated			
Experiment	Tracer	i [/]	t_0 or t_{01} [min]	Pe or Pe_1 [/]	a [min$^{-0,5}$]	α_1 [m]	$2b$ [mm]	n_p [%]	n_f [%]
Monopole I (BL8 – BL10)	Pyranine	0.201	120	37	0.0610	0.30	237	5.9	0.12
Monopole VI (BL8-BL10)	Pyranine	0.161	128	37	0.0500	0.30	256	5.3	0.12
Monopole VI (BL8-BL10)	D_2O	0.161	120	37	0.0650	0.30	265	5.4	0.11
Dipole I (BL8-BL10)	Eosin	1.860	42	67	0.0600	0.17	107	4.8	0.16

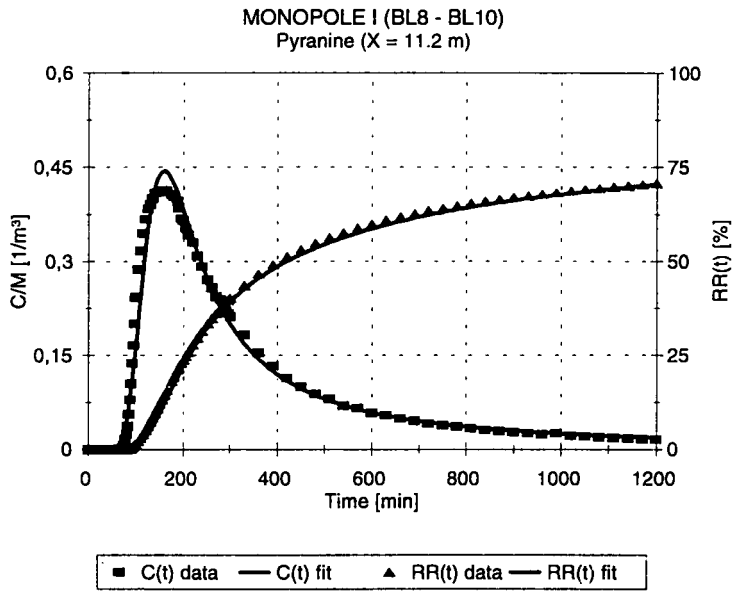

Figure 218. SFDM fitted to Monopole I. Best fit obtained with $t_0 = 120$ min, $a = 0.0610$ min$^{-1/2}$, Pe = 37; experimental data shown as symbols, best fit depicted as solid curve.

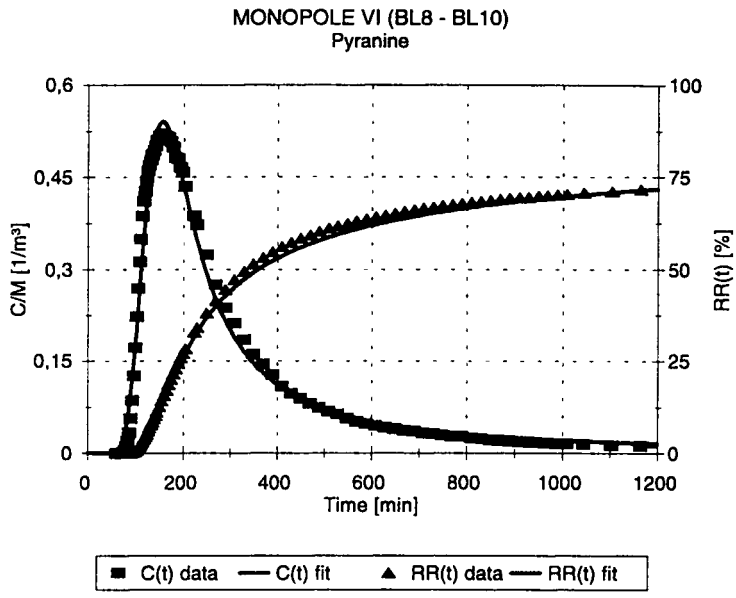

Figure 219. SFDM fitted to Monopole VI (pyranine). Best fit obtained with $t_0 = 128$ min, $a = 0.0500$ min$^{-1/2}$, Pe = 37; experimental data shown as symbols, best fit depicted as solid curve.

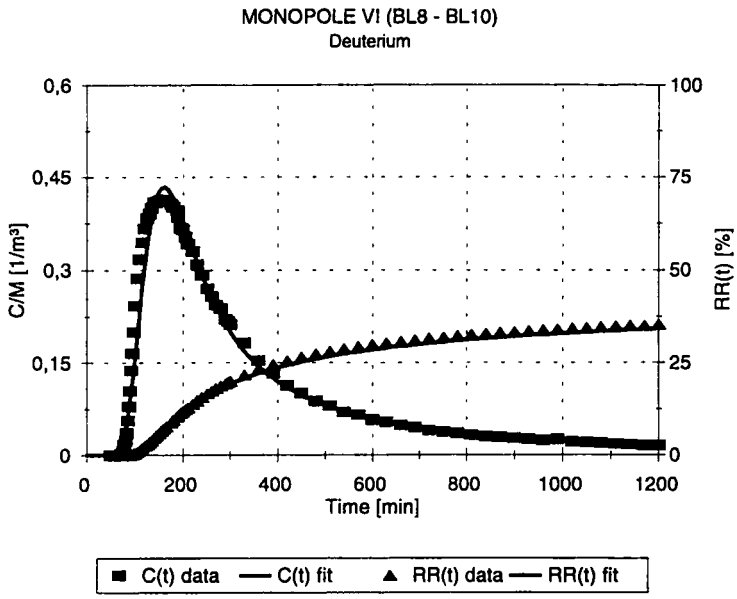

Figure 220. SFDM fitted to Monopole VI (D_2O). Best fit obtained with $t_0 = 120$ min, $a = 0.0650$ min$^{-1/2}$, Pe = 37; experimental data shown as symbols, best fit depicted as solid curve.

the concentration and the recovery curve was not possible without the additional assumption that a certain part of the tracer was lost. For the Monopole Test I it is assumed that 15 % and for Monopole Test VI it is assumed that 10 % of the injected tracer were lost during the injection. The fitting parameter obtained for the pyranine were nearly the same for both experiments ($t_0 = 120$ min and $t_0 = 128$ min, Pe = 37 and Pe = 37, $a = 0.061$ min$^{-½}$ and $a = 0.050$ min$^{-½}$ for Monopole Test I and VI respectively). The fissure porosity calculated for both experiments was the same and equal 0.12 %. Similarly, the mean fissure apertures calculated from both experiments were nearly identical with 237 µm and 256 µm. The matrix porosities calculated for $D_m = 1.5 \cdot 10^{-9}$ m^2/s and $\tau_p = 1.5$ were insignificantly different (5.9% and 5.3%, respectively).

The modelling of the deuterium was only possible under the assumption that more than one third of the deuterium was lost. Another problem that arose was the fact that the maximal measured concentration amounted to only ca. 200 mg/l, whereas the natural background concentration was ca. 150 mg/l. This low signal to background ratio probably caused a large part of the tracer curve to be undetectable. In other words, the mass of the injected deuterium was approximately 10 times too low. However, the fitting parameters obtained agree very well with those from the above cited experiments. The mean residence time of $t_0 = 120$ min, the Pe-number Pe = 37 and the diffusion parameter $a = 0.065$ min$^{-½}$ differ only slightly from the latter parameters. The derived value for the matrix porosity is with 5.4% neither in contradiction to the results obtained from the mercury porosimetry (Table 31) nor in contradiction with the results obtained from the pyranine-experiments.

On the other hand the diffusion parameter, $a = 0.065$ min$^{-½}$, found for the deuterium enabled to calculate the a priori unknown effective molecular diffusion coefficient for the pyranine. From Equation (5.6) it follows that the ratio of a^2 for both tracers pyranine and deuterium equals the ratio of their diffusion coefficients. By this way, the unknown diffusion coefficient for pyranine could be estimated from the known diffusion coefficient for deuterium, i.e. $D_m = 2.5 \cdot 10^{-9}$ m^2/s/$(1.6)^2 = 1.5 \cdot 10^{-9}$ m^2/s. The latter value was used to interpret all experiments where pyranine was applied (Table 35).

Dipole Test

The dipole experiment was performed with similar pumping rates and over the same distances, where the monopole tests were performed (Table 36). The *Dipole Experiment I* was performed along the flow path BL8-BL10 applying eosin. The best fit obtained for the tracer concentration as well as for the recovery curve are shown in Figure 221. For the Dipole Experiment I, the best fit parameters obtained were $t_{01} = 42$ min, $Pe_{01} = 67$ and $a = 0.060$ min$^{-½}$. The mean fissure porosity was calculated to 107 µm and is similar to those from the monopole experiments, although a factor of 1.5 must be considered. Assuming that the diffusion coefficient for eosin is equal to uranine's, the matrix porosity was calculated according Equation (5.6) to $n_p = 4.8$ %. The latter value agrees very well with the matrix porosity of the monopole experiment over the same distance, and is still within the bench marks of the mercury porosimetry (Table 31).

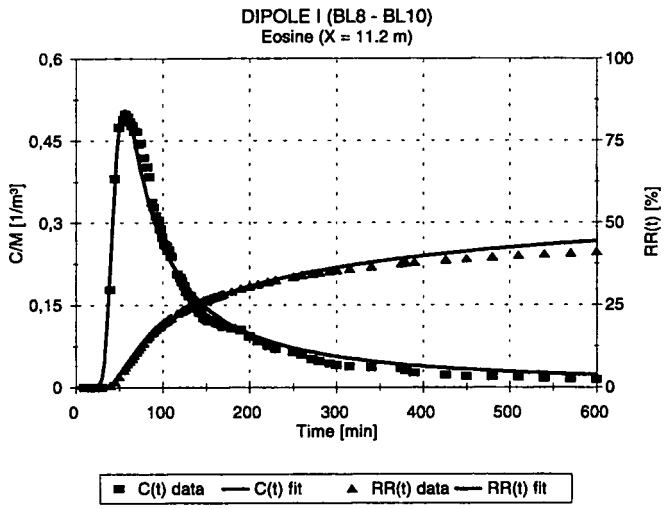

Figure 221. SFDM fitted to dipole I. Best fit obtained with $t_{01} = 42$ min, $a_{01} = 0.0600$ min$^{-1/2}$, $Pe_{01} = 67$; Experimental data shown as symbols, best fit depicted as solid curve.

5.3.3.5 *Dispersivities*

Since the tracer experiments were performed under different flow field conditions, the dispersivities derived cannot be interpreted in a simple dispersivity-distance approach. Only experiments performed under identical flow field conditions may be so compared.

The injected volumes of the tracer solution were always chosen so that the tracer was removed completely from the injection well. At the same time, the tracer cloud around the well was kept as small as possible in comparison with the inter-well distance. It is a very likely assumption that the injection of the tracer can be therefore considered as a piston-flow process, because the test wells were generally equipped with a thin inline injector. During all tracer experiments, the residence time of the tracer pulse in the injection flow line can be neglected, because it is very small compared with the mean residence within the tested formation. The latter fact is especially fulfilled during dipole tracer experiments, because the injection is performed directly into the flow line.

The dispersivities derived from the *Monopole Experiment I* and *VI* and from the *Dipole Experiment I* are generally low (Fig. 222), between 0.17 m and 0.30 m (Table 37). The experiments were performed between wells which are hydraulically connected over a discrete set of parallel fractures. This fact enabled the fitting of the breakthrough curve and the relative recovery rate. Hence, as long as the migration of the tracer follows a discrete fracture set connecting both wells directly, the dispersion will be small. If the tracer migration, however, follows several discrete fracture sets intercepting each other, the dispersivities will increase due to interstitial mixing between different fracture sets.

The tracer experiments which were performed under natural flow field conditions yielded much higher dispersivities (Fig. 222). The increase in dispersivity, however, is not only a result of the increased distance or a different fissure aperture distribu-

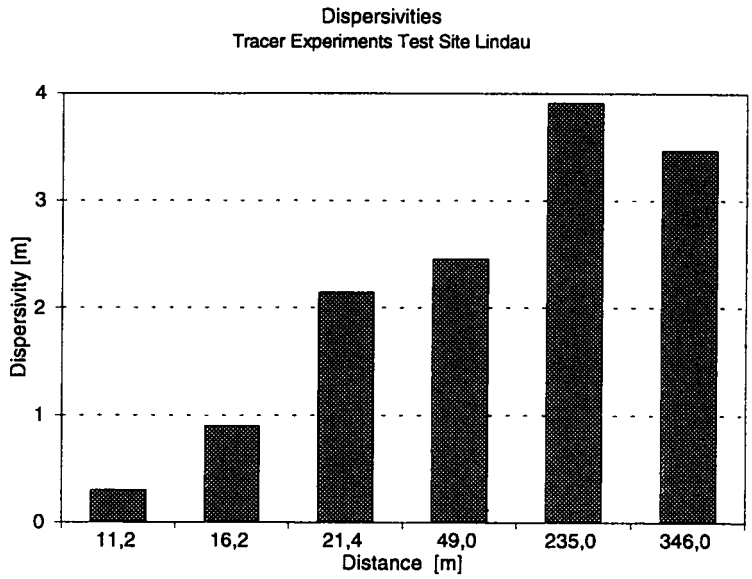

Figure 222. Dispersivities derived from the tracer tests at the Lindau fractured rock test site.

tion along the migration path. A more plausible explanation may be that the wells are not connected over the same set of fractures, because discrete fracture sets are, due to rock mechanical reasons, limited in their extension. Hence, the more fracture sets involved along the migration path, the higher the probability is that the migration of the tracer is not only affected by fracture aperture distribution and matrix diffusion, but also by interstitial mixing between different fracture sets and by slow flow into semi-stagnant pools of water (NERETNIEKS 1993). The increase in dispersion with increasing distance must therefore be controlled by a hydraulic 'coupling' of several discrete fracture sets along the migration path. At each interstitial intersection of such discrete fractures the dispersivity is therefore expected to increase. An indirect experimental evidence for this assumption might be that the recovery rates of natural flow tracer experiments did not exceed 0.3-0.5% of the injected mass.

The northern part of the orebody where the natural flow tracer experiments were performed is characterized by a higher permeability as the test section of the forced gradient tracer tests. The drilling records report large fractures extending over tens of metres. The modelling of the natural flow tracer tests for this test section generally yielded higher fissure apertures. The latter is in good correspondence with the drilling reports, because wide opened fractures have a higher lateral extension. Hence, the relatively low increase in dispersivity with increasing distance for tracer experiments performed in this section is not surprising.

5.3.3.6 *Conclusions*

The modelling of tracer experiments allows hydraulic parameters such as fissure aperture, matrix porosity, and in case of forced gradient tracer tests, fissure porosity to be derived. The modelling approach considers that the fissure porosity represents the total mobile water volume, while the matrix porosity (n_p) is assumed to represent the immobile water. The results of forced gradient tracer experiments performed in the

tunnel indicated that the fissure porosity (n_f) of the investigated fault zone is very small. The fissure porosities obtained were always in the range of 0.1-0.3% while the matrix porosities ranged between 3% and 7%. The latter represent 'dead end fissures' as well as solution cavities of some mineral constituents of the orebody. The results of the modelling agree very well with the results of the mercury porosimetry. The fissure apertures ($2b$) calculated were in the range of 100 to 300 µm for the low permeability section at the central part of the parallel pit. The modelling of natural flow tracer experiments is unsuitable to derive information about the fissure porosity. The fissure apertures of the high permeable northern part of the orebody were estimated to be in the range of 400 to 600 µm.

The results obtained are very consistent, although the tracer experiments were performed under different flow field conditions, flow field geometries, and over varying distances. The core analysis and the mercury porosimetry yielded valuable information about the spatial distribution of fractures and matrix porosity. The results indicate that convective dispersive fracture flow occurs only along a few discrete sets of fractures. The results of natural flow tracer experiments indicate that a non-negligible portion of the flow follows preferential flow paths which have only little exchange with the entire fracture system. In the far-field from the injection, the tracer migration is therefore controlled mainly by diffusion effects and by interstitial mixing. The ordinary dispersion model is unsuitable to describe the tracer transport in such a system.

5.4 POROUS GROUNDWATER

W. Käss

In Middle Europe, porous groundwater is not only by far the largest source for drinking water; porous groundwater is also better protected against contamination than fissured or karst groundwater and thus more valuable.

Of the many possibilities for applying tracing tests in porous aquifers to obtain data either about the aquifer or about the behaviour of the water constituents, only a few can be handled here.

A dye tracing test in porous groundwater during a pumping test is described in Section 5.9.3.

5.4.1 *Hydraulic – Merdingen*

In the Upper Rhine Valley (Southwest Germany), a test field was set up near the village of Merdingen. The goal of the tests is the comparative investigation of different hydrological tracers. Numerous pore groundwater tracing tests have been carried out here since 1979 (KÄSS 1988, 1990a, DE CARVALHO-DILL et al. 1992).

The test area lies in the Pleistocene gravel plain between the Tuniberg in the southeast and the volcanic mountain base Kaiserstuhl in the north (Fig. 223). The soil profile (Fig. 224) shows that under the strongly humic cover layers, a transition to limey gravelly-sandy deposits from the Würm Ice Age lower terrace gravels follows. The depth to the water table varies between 1.4 and 1.7 m, which is very advantageous for groundwater sampling with micro-submersible motor pumps (Fig.

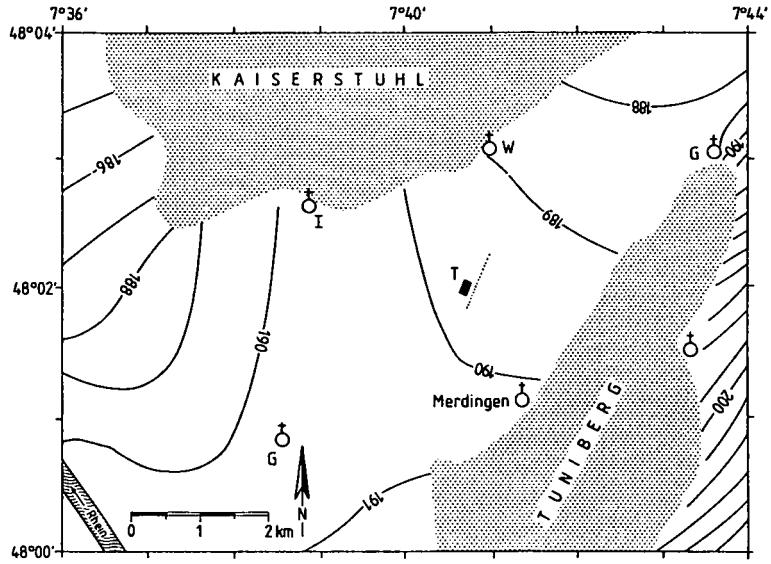

Figure 223. Location of the Merdingen test field. *T* = test field, solid lines: long-term groundwater contours, dotted line: geoelectric measurement profile.

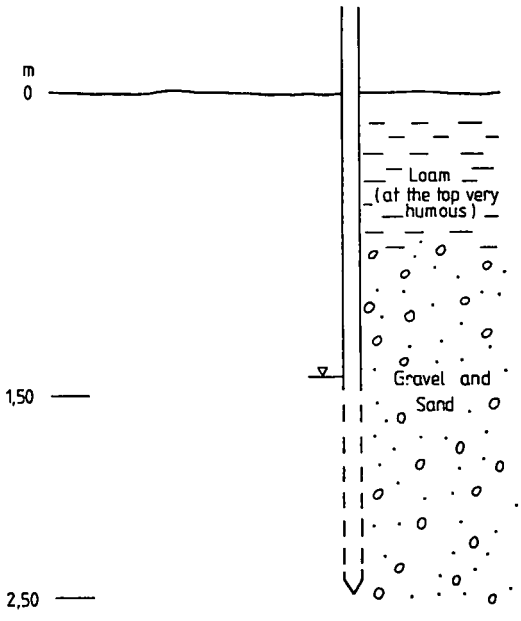

Figure 224. Soil profile, sampling pipe (filter section shown as dashed lines), and fluctuation zone of the water table in the Merdingen test field.

138). The upper section of the aquifer is fitted with a number of 38 mm (1½")-pipes, which have a filter section of 1-2 m under the surface. The characteristic hydrological values for the aquifer in this area are:

Annual mean precipitation	650 mm
Annual mean temperature	8.5°C

Gradient of the groundwater i	0.34‰ to the north-northeast
Average grain size diameter	14 mm
Effective porosity n_e	ca. 0.2

Using one of the numerous uranine tracing tests conducted in the test field Merdingen as an example, it is shown how the most important hydraulic parameters can be determined. It is stressed, that all of the tests were conducted under natural groundwater flow; no changes in the slope of the groundwater table occurred. Furthermore, the parameters that were determined in this way are only valid for this relatively small investigation area and only for the investigation period.

Figure 225 shows the area of the test field where on 6 Sept. 1984 two grams of uranine were injected within one minute into the groundwater through the monitoring pipe 200. Rows of narrowly spaced monitoring pipes at distances of 3, 6¼, 12½, and 25 m from the injection site allowed a complete coverage of the drifting dye cloud. It can be seen in Figure 225, that directly downflow of the injection site, the centre of the dye cloud did not flow exactly in the direction of the large-scale

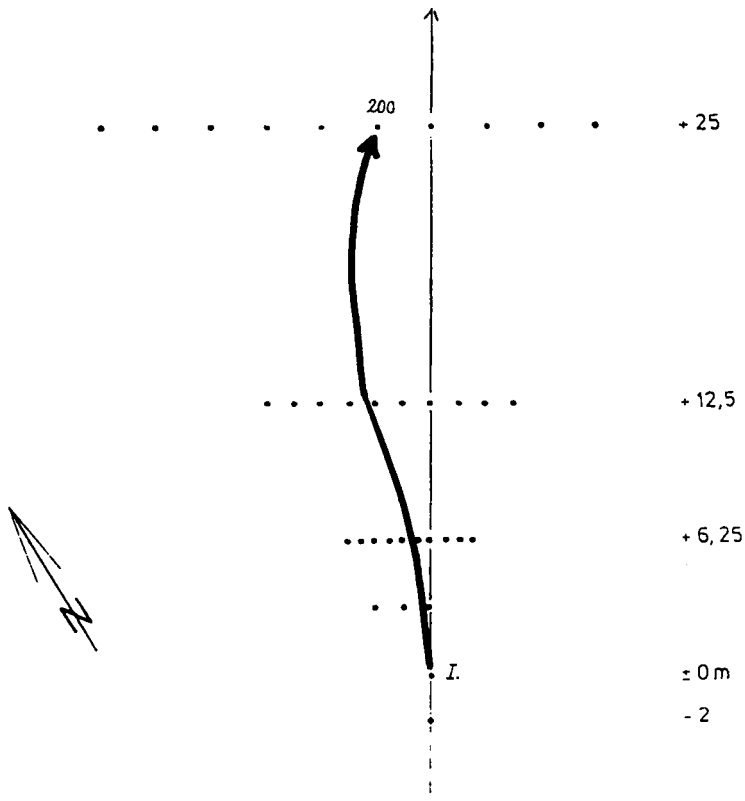

Figure 225. Partial test field 200 in the Merdingen test field. Path of the highest concentration of the dye cloud after the injection of 2 g uranine in the monitoring pipe I on 6 Sept. 1984 (bold arrow). Large-scale water table slope in the direction of the straight lines to the north-northeast. Dots: Sampling sites –2, 3, 6¼, 12½, and 25 m away from the injection site.

groundwater flow, but rather towards the left (west). An explanation for this diversion to the left could not be found through the water table measurements in the level-measured monitoring pipes, since the measurements in this area had differential amounts of only a few millimetres.

For the determination of the mean effective flow velocity (v_a), the monitoring pipe No. 200 from the 25 m profile row which had the strongest dye breakthrough was used. The dye breakthrough curve is displayed in Figure 226. Directly after the injection, the curve shows a steep increase with a maximum on the 5th day; a second, weaker dye maximum appeared between the 25th and 30th day of the test. This second maximum can be attributed to heavy rains on the 23rd day and the corresponding rise in the water table of 23 cm. For a better view of the graph, the breakthrough curve was stopped on the 50th day of the test. However in determining the cast line (dot-dashed line in Fig. 226), the concentration values through to the end of the detection on the 146th day of the test were taken into account.

The times, some are interpolated, in the breakthrough curve according to Figure 3 are:

t_0: time of injection: 6 Sept. 1984, 11:14 o'clock,
t_1: first appearance of the dye after 37 hours,
t_2: highest dye concentration (c_{max}) after 92 hours,
t_3: time of the concentration centre (c_m) after 13 days = 312 hours = $t_{0.5}$,
t_4: last detection after 146 days with 0.01 µg/l uranine.

From the mean residence time t_3 and the flow distance s (25 m), the mean *effective flow velocity* v_a can be calculated to 1.92 m/d = 0.08 m/h = $2.2 \cdot 10^{-5}$ m/s. Further-

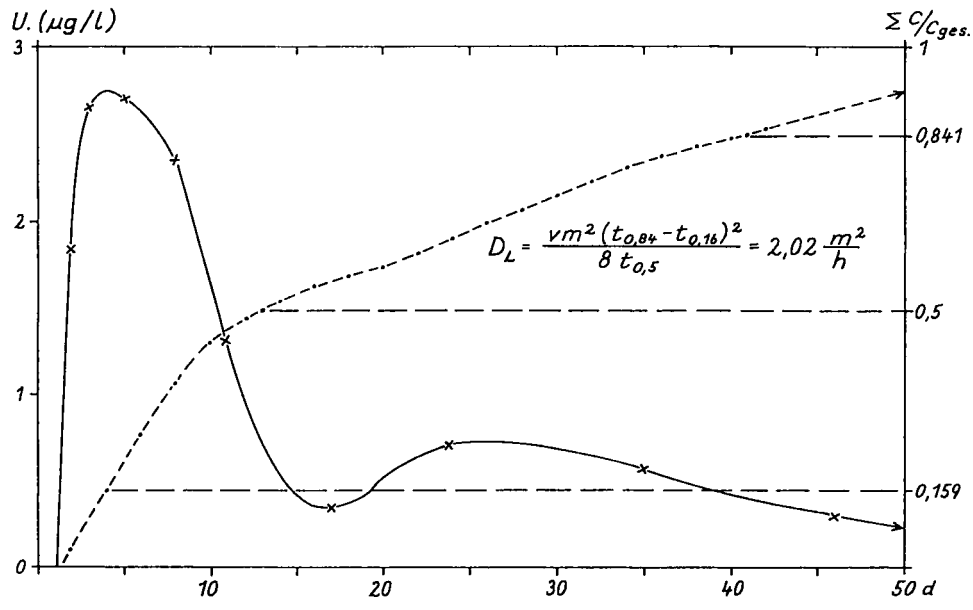

Figure 226. Dye breakthrough curve and cast line in the monitoring site 200 from the tracing test in the Merdingen test field 200 on 6 Sept. 1984 (Fig. 225). x = measured values of the breakthrough curve. Horizontal dashed lines for the determination of the longitudinal dispersion coefficients D_L.

more, using the law of DARCY, the hydraulic conductivity in the test path can be determined. The 'effective porosity n_e', determined from different accompanying tests to 0.2, is required for this. Also required is the slope $i = 0.00034$, valid for the test path as well as the large-scale dimensions.

The *hydraulic conductivity* k_f is

$$\frac{v_a \cdot n_e}{i} = 1.2 \cdot 10^{-2}\ \text{m/s}.$$

The *longitudinal dispersion coefficient* D_L is determined with the mean, the 16%, and the 84% residence times (t_0, $t_{0.16}$, $t_{0.84}$).

$$D_L = \frac{v_a^2 (t_{0.84} - t_{0.16})^2}{8\, t_{0.5}} = 2.02\ \text{m}^2/\text{h} = 5.6 \cdot 10^{-4}\ \text{m}^2/\text{s}.$$

The *dispersivity* α is: $D_L/v_a = 25.5$ m.

Similar to the longitudinal dispersion, the transversal dispersion D_T can be determined, if the dye cloud is completely recorded in a profile that is transversal to the flow direction. Figure 227 shows the integral over concentration and time in the 25 m profile from the tracing test in Figures 225 and 226. It can be seen that the monitoring pipe No. 200 with the highest dye concentration is not in the middle of the dye cloud (Fig. 227 top). To the right of pipe 209, there was a dye breakthrough in only two pipes; to the left, however, there were four. This is a considerable deviation from a GAUSS-distribution. Nevertheless, it was possible to determine a transversal dispersion by calculating the sum of the concentration-time-integrals (Fig. 227 bottom). The calculation corresponds to the longitudinal dispersion. A *transversal dispersion* $D_T = 0.5\ \sigma^2 \cdot (v_a/s)\ \text{m}^2/\text{s} = 0.0256\ \text{m}^2/\text{h} = 7.22 \cdot 10^{-6}\ \text{m}^2/\text{s}$ is obtained in this example.

The ratio of the longitudinal to the transversal dispersion is 77:1 (cf. Section 4.1.3).

This example clearly shows, that in nature, contrary to model deliberations, there are considerable deviations and differences in breakthrough curves and in the dispersive distribution of tracers.

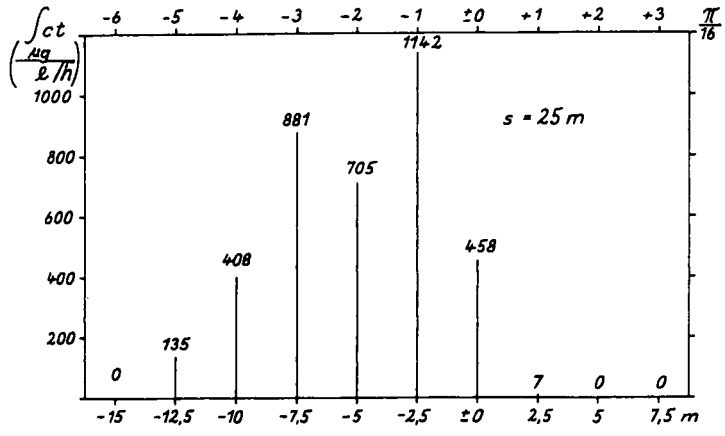

Figure 227. a) Integrals over concentration and time in the 10 monitoring pipes in the 25 m profile from Figure 225.

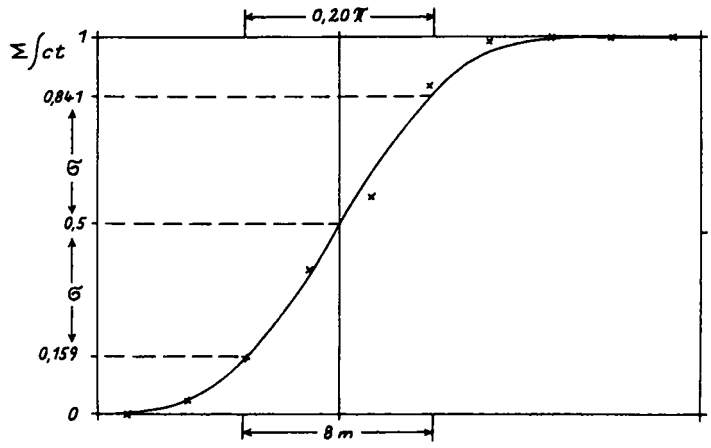

Figure 227. Continued. b) Cast line of the concentration-time-integrals to determine the transversal dispersion coefficient D_T.

5.4.2 *Solute transport – Savinja Valley*

Tracing tests can only solve individual problems concerning solute transport in groundwater. Yet, such results are also only valid for the respective hydrometeorological conditions and only for the investigation area. It must be carefully considered before the results can be used under different conditions, in other areas, and above all for other tracers. This section is *not* a description of a test, with an integrated transport model; rather with the help of a simple example it is shown how a specific solute transport problem can be handled.

In the Pleistocene aquifer of the Savinja Valley west of Celje (Slovenia), the problem to be solved was how far the potassium ion in the porous aquifer was retained. The test with potassium chloride was conducted in September 1973 with other tracers in two different depths. Details of this combined test have already been published (KÄSS 1976b), with maps and geological cross-sections.

Only the results from the potassium chloride will be discussed here. The potash-fertilizer used in the injection in the lower filter horizon also contained other constituents besides KCl, however, they did not interfere with the test. It was also not necessary to know the exact content of KCl.

The lower filter horizon was 7-8 m below the surface and 4-5 m below the water table. The location of the injection and sampling sites is shown in Figure 228.

Figure 229 shows the breakthrough curves for potassium and chloride in two sampling sites 5 and 25 m away from the injection site.

Here, the chloride ion is suitable as a non-reactive tracer, to determine the retention of the potassium ion. If there were no retention, both curves would be congruent. It can be clearly seen that with increasing distance away from the injection site, potassium, as compared to chloride, has a lower concentration. At a distance of 25 m, the maximal potassium increase is only 10% as compared to chloride. At greater distances, a potassium increase could not even be detected (cf. Sections 2.2.3 and 4.2.3).

The loss in potassium in the flow path is due to ion exchange at the grain surfaces. The exchange capacities, to a large extent saturated by the hardeners calcium and magnesium are displaced during a disturbance in the equilibrium – if other cations appear in increased concentration. Such a dissolution of the hardener ions causes a

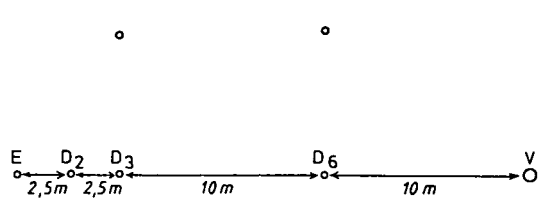

Figure 228. Location of the injection and sampling sites from the potassium chloride test in the Savinja Valley (Sept. 1973). Small circles: 50-mm-pipes, large circle: pumping test well 200 mm.

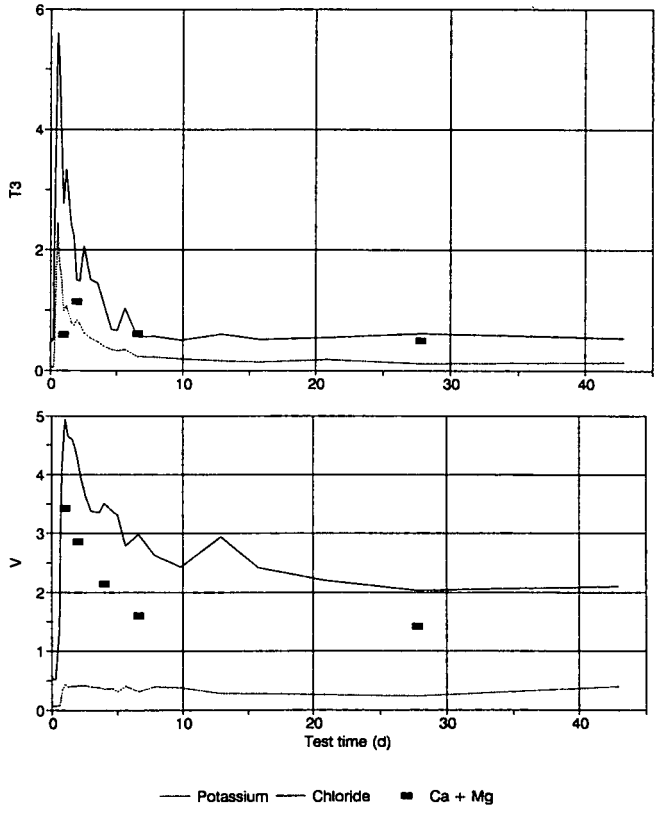

Figure 229. Breakthrough curves in 2 sampling sites, 5 and 25 m away from the injection site in Figure 228 (from top to bottom). Bold curve: Chloride, dashed curve: Potassium, ■ = hardener Ca^{2+}+Mg^{2+}; increases over the natural background. Y-axis: Concentration in meq/l.

hardening of the water. This was determined at several times and shown in Figure 229 by ■ symbols. This figure also shows that an increased hardening occurs, the more advanced the ion exchange is.

Further well documented examples can be found among others in JOB et al. (1969) and in KÄSS (1990a).

5.4.3 *Water protection area Merdingen*

Tracing tests are very useful in determining water protection areas, at times even indispensable. In Germany, the 50-day-line according to KNORR (1937) is the guideline used for determining the protection Zone II. The results from a research campaign group showed that individual germs can survive in groundwater longer than 50 days. However, within this time span, the bacteria population has decreased under the risk level (DVGW 1983, UBA 1985).

Several bacteria drift tests were carried out in the Merdingen test field for this research purpose (KÄSS et al. 1983), (Section 2.7.3.1). Further drift tests with bacteria and phages were conducted by OETZEL in Merdingen (OETZEL 1990, OETZEL et al. 1991, HÖTZL et al. 1991). In almost all of the bacteria and phage drift tests, uranine was also injected as a non-sorptive and non-degradeable tracer.

Figure 230 shows a typical breakthrough for bacteria, phages, and uranine in the monitoring site 245 in the field section 200 (Fig. 225), 12.5 m away from the injection site. The curves show that the bacteria and phages did not appear until shortly before the uranine maximum, but then in massive numbers. *Serratia marcescens* stayed in the monitoring site much longer than the phages. The last detection of the bacteria and the phages was very different, as was the longest flow path in the Merdingen investigation. Decisive for the last and farthest detection are along with the determination methods, the injected number of germs and phages. High injection numbers are required in pore-water drift tests. The tests in the Merdingen test field were carried out with two bacteria and two phage species (Table 38 and Fig. 231).

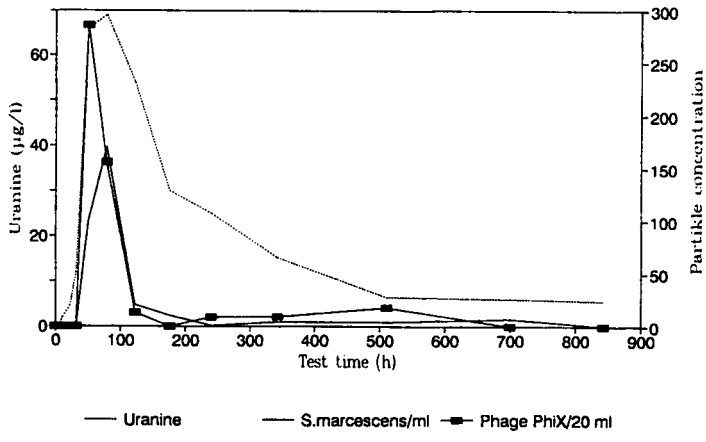

Figure 230. Breakthrough curves for uranine, *Serratia marcescens*, and bacteriophage ΦX174. In the injection site, 12.5 m away, the following were injected on 28 Aug. 1989: 52 g uranine, $2.66 \cdot 10^{11}$ *Serratia marcescens*-germs and $2.13 \cdot 19^{12}$ ΦX Coliphages.

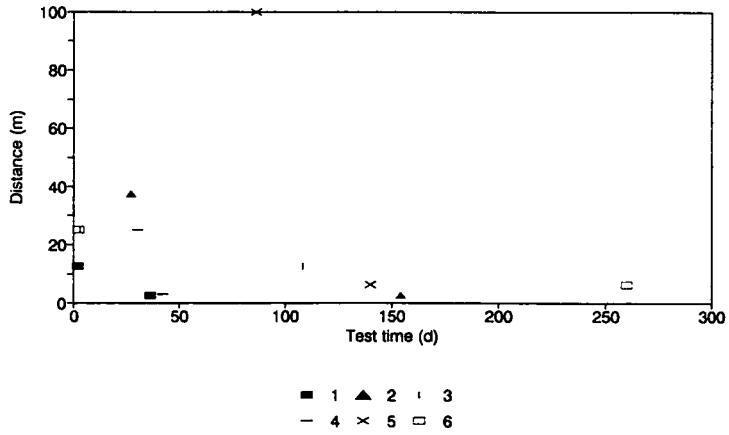

Figure 231. Last detection and the corresponding flow path with the bacteria and phage drift tests in the test field Merdingen. For each species there are two symbols; the left is for the farthest flow path and the right for the last detection. Symbol numbers according to Table 38.

Table 38. Microbiological drift test field Merdingen. Drift particle type and amount, farthest drift path, and last detection (Fig 231).

No. Fig. 231	Test day	Quantity and Species	Farthest drift path Dist. (m)	Test day	Concentration	Last detection Dist. (m)	Test day	Concentration
1	6 March 1982	$7 \cdot 10^7$ colonies *E.coli* ATCC 11229	12.5	(48h)	18/101 ml	2.5	36	5/100 ml
2	16 Aug 1987	$8 \cdot 10^{11}$ colonies *E.coli* ATCC 11229	37.5	27	>100/100 ml	2.5	154	1/100 ml
3	24 June 1983	$2 \cdot 10^{11}$ colonies *S.marcescens*	25	3	23 ml	12.5	108	1 ml
4	31 March 1989	$5 \cdot 10^9$ T_4 coliphages ATCC 13702	25	30	4/4.5 ml	3	42	1/4.5 ml
5	28 Aug 1989	$2 \cdot 13 \cdot 10^{12}$ ΦX174 coliphages	100	86	40/20 ml	6.25	140	5/20 ml
6	28 Aug 1989	$2 \cdot 66 \cdot 10^{11}$ colonies *S.marcescens*	25	(50h)	20 ml	6.25	260	1 ml

The table shows that in 4 of the 6 tests, detection of the bacteria and phages after more than 50 days as possible.

For a hygienic evaluation of tracing tests, it is necessary to conduct the tracing tests not only with conservative non-sorptive tracers, but also with microbiological drift particles. An evaluation and the determination of the protection zones with e.g. uranine as the only tracer does not provide sufficient indication of the range of drifting microbiological particles.

5.5 INVESTIGATIONS ON RIVER BANK INFILTRATION

5.5.1 *Drinking water protection*

H. Moser

In the last decades, tracing tests with dye tracers and increasingly isotope-hydrological methods have been used to quantitatively determine river bank filtration near drinking water supply facilities. Radiohydrometric single well methods for determining the DARCY-velocity and flow direction of the groundwater (cf. Section 4.5) and analyses of the environmental isotopes ^{2}H, ^{18}O, and ^{3}H (cf. Section 2.11) have proved important resources for observing the infiltration of surface water into the groundwater and for determining the river water fraction in the pumped well water.

The following uses an investigation from the Rhine left bank area near Düsseldorf (Nordrhein-Westfalen, Germany) to demonstrate this (DROST et al. 1982). The results from similar research campaigns have been published in e.g. DROST 1971, 1974, DROST & NEUMAIER 1974, DROST et al. 1977, STICHLER & TRIMBORN 1980, STICHLER 1981.

Figure 232 displays the investigation area, a peninsula formed by a Rhine meander between the river-km 740 and 749. The aquifer consists of ca. 5-20 m thick sand

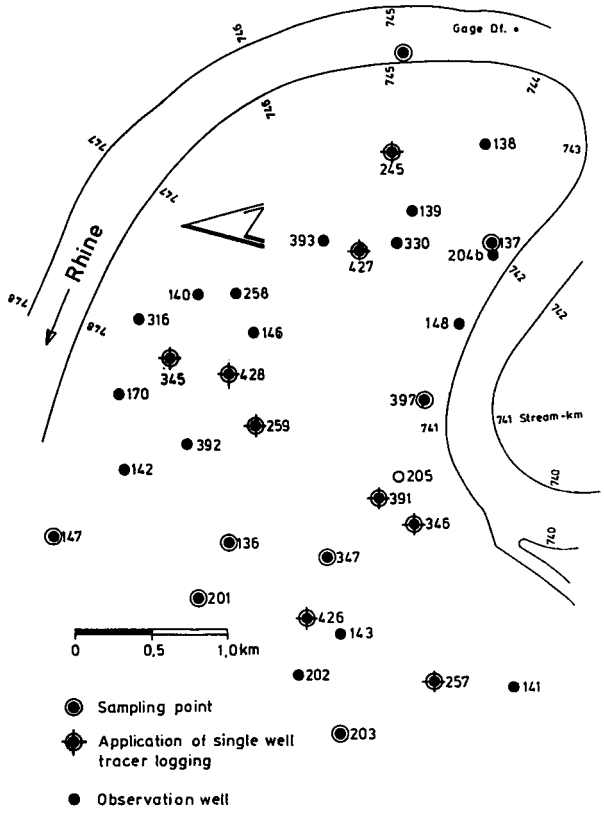

Figure 232. Left bank Rhine area near Düsseldorf: Map of the numbered groundwater monitoring sites.

and gravel deposits of the lower terrace. It is tapped by numerous monitoring wells, that were used from January until November 1981 for five measurement series, including single well measurements, and sampling for the analyses of the ^{18}O- and ^{3}H-contents. During this, the level of the Rhine varied up to 2 m.

The flow directions of the groundwater observed with the single well method are essentially in good agreement with the measured groundwater contours: The measurement series during a period of Rhine flood water, ca. 1 m over the groundwater level, a landwards directed groundwater flow developed, whose inflow came from the western valley border. Groundwater flows through the peninsula then from a south-north-direction with DARCY-velocities of 0.04 to 4.4 m/day. In contrast, in a measurement series during a period where the level of the Rhine was ca. 1 m under the groundwater table, the groundwater flowed to the peninsula from all sides. With a few exceptions, the DARCY-velocities measured here were 1.5 to 3 times lower than those stated above.

The analysis of the ^{18}O- and ^{3}H-contents resulted in the differentiation of two different groundwater types in the area of the peninsula (Fig. 233): In the eastern part the ^{18}O-contents range between –9.63 and –8.75‰, the ^{3}H-contents were between 95 and 119 TU, and in the western part higher ^{18}O-contents (–8.27 to –7.31‰) and lower ^{3}H-contents (46 to 95 TU) were measured. The zone with lower ^{3}H-contents also extends to the near-bank areas in the south-eastern part of the peninsula.

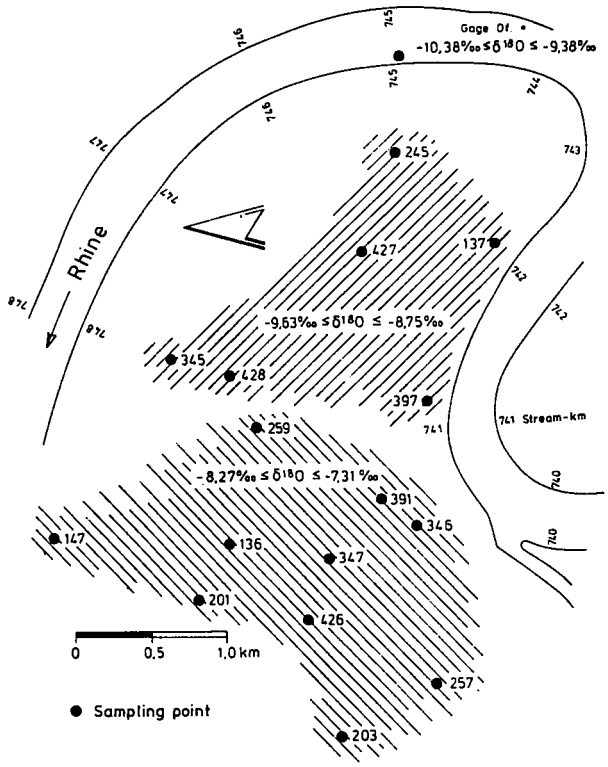

Figure 233. a) Left bank Rhine area near Düsseldorf. Spatial distribution of the ^{18}O-contents.

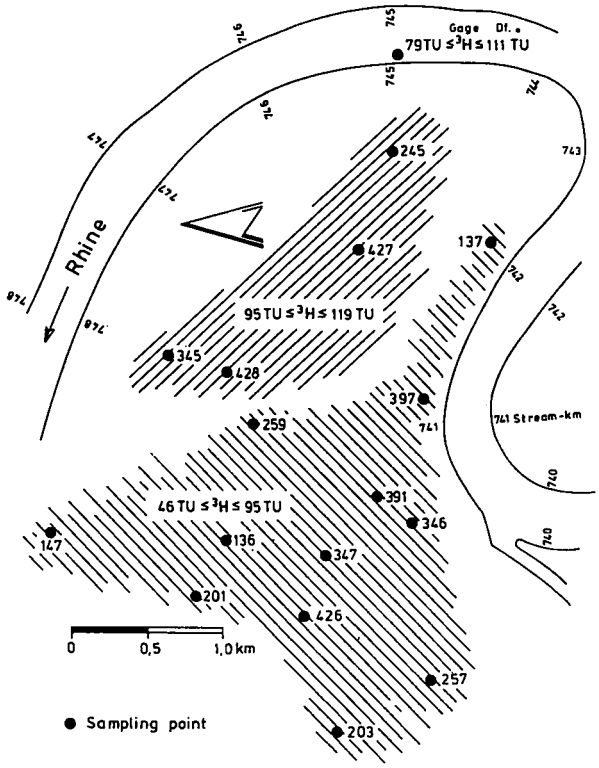

Figure 233. Continued. b) ^{3}H-contents in groundwater.

To identify the fraction of the river bank filtration water, the ^{18}O- and ^{3}H-contents in the Rhine were analysed. In summer, the ^{18}O-contents have their minimum (–10.32 ‰) and in winter their maximum (–9.38 ‰). The ^{3}H-contents display the known decrease during the course of the last few years (1980: ca. 120 TU, 1981: 92 ± 16 TU). By comparing these values with the isotope contents in the groundwater, it could be concluded that the groundwater in the eastern part is essentially formed through river bank filtration; based on the ^{18}O-contents, it can be assumed that in winter, there is a Rhine water input during flood periods. However, since the ^{3}H-contents of the Rhine in January 1981 was 79 ± 11 TU, the groundwater (95 to 119 TU) must originate from earlier years, and is thus older than the Rhine water now. Only in the monitoring sites 137 and 317 was current Rhine river bank filtration water detected during the winter sampling. In the western part of the peninsula, it can be concluded from the isotope contents that the groundwater originates from the regional precipitation with a partial input from the Rhine water. The groundwater from the monitoring site 257 is a typical groundwater, originating purely from precipitation, whereby here the ^{3}H-contents also show that it must be older than the current precipitation water.

During the whole investigation period, only isolated mixing processes in the monitoring sites 259 and 428 were observed between the groundwater areas shown in Figure 233. This can be explained by a groundwater flow out of the eastern area landward, caused by flooding in the Rhine. In general however, the impact of the

rising Rhine water level does not seem to cause large mass movements in the aquifer due to the steady state hydraulic pressure characteristics in the groundwater.

5.5.2 *Pollution propagation – Böckinger Wiesen, Heilbronn/Southwest Germany*
H. Hötzl

5.5.2.1 *Solute transport in groundwater*

The propagation of dissolved substances in groundwater is subject to different processes and was covered in detail in Chapter 4. For conservative matter, the hydrodynamic processes are the deciding factors. Advection, dispersion, and diffusion determine the migration of the matter. In the case of a homogeneous, isotropic medium, the propagation of such matter can be determined with the hydraulic laws if the aquifer parameters and flow conditions are known. In the case of undefined nonhomogeneous aquifers, the propagation behaviour deviates all the more from ideal conditions. Thus, the described behaviour of the transport processes according to the hydraulic laws becomes more and more incorrect.

Porous aquifers have approximate homogeneous conditions, at least with regards to the horizontal flow. However, anisotropic and usually very irregular fissure and karst aquifers do not. In such cases, the solute propagation can only be determined through experimental in-situ-tests. The numerous actual application examples described in the preceding sections showed that conducting tracing tests with conservative tracers can provide the basis for evaluating the propagation and transport behaviour even under heterogeneous aquifer conditions.

Many of the environmentally relevant pollutants are reactive substances and thus the propagation in groundwater is not only determined and influenced by hydrodynamic processes, but also through different physical, chemical, and biological processes. These are reversible as well as irreversible processes, that can lead to changes in the concentration. Examples of reversible reaction mechanisms are sorption and desorption reactions, precipitation and solution, and ion exchange. Irreversible processes are mainly microbial decay processes, as well as chemical and physical decay reactions (cf. Chapter 4). The effectivity of these processes is determined by the effective time of reaction.

An evaluation of the propagation processes of reactive solute components requires knowledge of the separate reactions and their intensities. For the mathematical description of such transport processes, the corresponding retardation factors, retention rates, and half-life times can be used. In detail, these matter-specific parameters are usually the result of the superposition of several physico-chemical and biological processes, that cause a change in the concentration of the dissolved organic and inorganic water constituents. Since the reaction kinetics are only known for a few substances, and since most of the mainly organic compounds cannot even be approximately quantified, corresponding investigations as to the propagation behaviour of these substances require, even in the case of comparatively homogeneous conditions for some porous aquifers, experimental in-situ-studies.

The experimental application of hazardous materials in aquifers is problematic and often prohibited by law. However, the transport behaviour of such materials is very important in determining their damage potential and for the remediation of

groundwater pollution cases. The application of unproblematic reference tracers with different reactivity can support the evaluation of these migration processes and provide help in the interpretation. A river bank infiltration is used here as an example to demonstrate possibilities in evaluating and interpreting the propagation of hazardous materials with tracing tests.

5.5.2.2 *Investigation area Böckinger Wiesen*

The test area Böckinger Wiesen in the Neckar flood plain near Heilbronn lies in one of the drinking water captation regions for the city of Heilbronn. In this ca. 2 km long section of the valley flood plain, there are a total of eight wells, that pump groundwater through river bank filtration.

The actual aquifer is built up of 3-5 m thick silty-sandy gravels, that are covered by the same thickness of alluvial loam sediments (Fig. 234). A mean hydraulic conductivity (k_f-value) of 0.01 m/s was determined through pumping tests (BRAND et al. 1990) for the gravel aquifer. However, due to the nonhomogeneous development of the aquifer, there are definite variations in the k_f-values, especially in the sand and silt lenticular deposits. The Pre-Quaternary underground consists of Lettenkeuper and Upper Muschelkalk. These sediments, together with individual permeable layers, build independent aquifers, from which only an unimportant amount of water rises into the higher gravel aquifer.

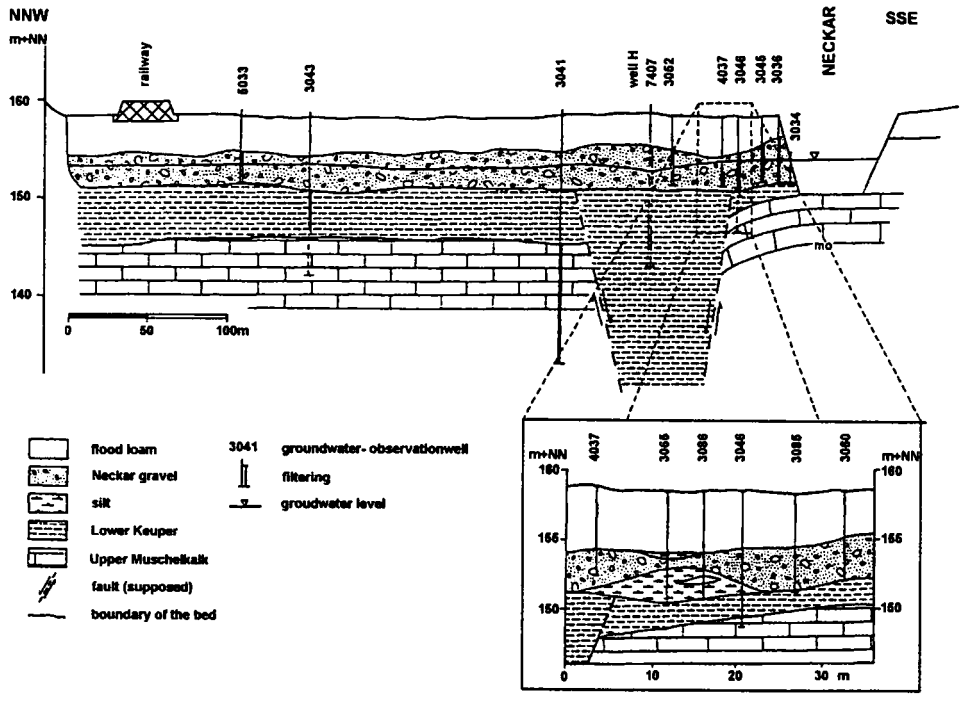

Figure 234. Geological cross-section through the investigation area Böckinger Wiesen, Heilbronn/Germany (from REICHERT 1991). The tracing tests were carried out in the aquifer of the Neckar gravels along the infiltration path from the Neckar river to the well H.

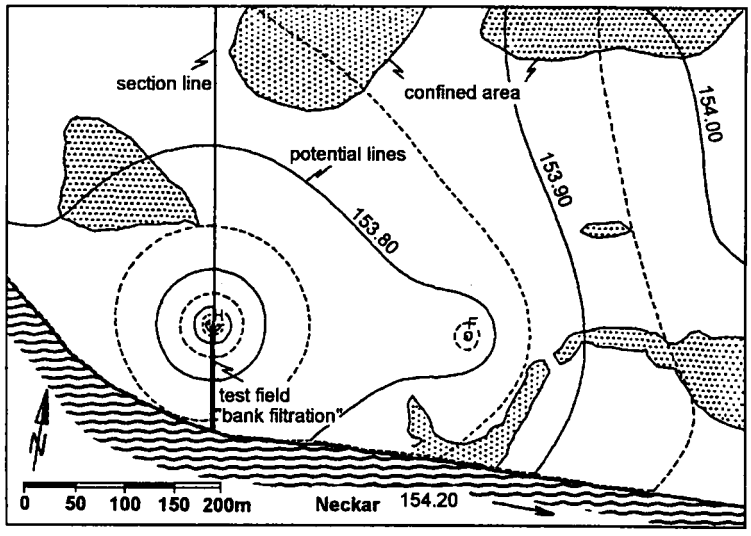

Figure 235. Potential distribution in the investigation area Böckinger Wiesen under defined infiltration conditions (= withdrawal from the wells H: 50 m^3/h, F: 25 m^3/h; after VOGT & HERRLING 1988).

The groundwater in the gravel aquifer is partially confined through the superimposed alluvial loam deposits. When not depressed, the depth to the groundwater table is 3-4 m (154-155 m a.s.l.). The bordering river, the Neckar, has a very constant water level of 154 m a.s.l. due to the dam up. During floods, the water level rises up to 2 m over the normal level. Before the groundwater was exploited in the Böckinger Wiesen, the Neckar was the natural receiving stream in this section of the gravel aquifer. Due to the drinking water captation and the corresponding pressure decrease, river bank filtration occurs increasingly (Fig. 235).

In a main focus investigation program funded by the German Research Association (Deutschen Forschungsgemeinschaft), interdisciplinary investigations were conducted from 1986 to 1991 in the test field Böckinger Wiesen as to the propagation behaviour of hazardous materials during river bank filtration (HÖTZL et al. 1989, BRAND et al. 1990, HÖTZL & REICHERT 1996). Besides hydraulic model calculations, hydrogeochemical, isotope-hydrological, and microbial investigations were a major part of the program. Their goal was to interpret the effective transport, retardation, elimination, and remobilization processes for individual organic and inorganic substance groups during the underground passage. To describe these processes, tracing tests were carried out in the test area with different reference tracers. They were used to describe the adjusting concentration distribution in the model of the hazardous material transport from the banks of the Neckar to the withdrawal well.

5.5.2.3 *In-situ-tests for hazardous material transport simulation*

A 100 m long test section from the Neckar to the main delivery well H (Figs 234 and 235) was selected for the comparative tracer tests (HÖTZL et al. 1989, REICHERT 1991). The investigation transsection was set up with groundwater-monitoring sites, some

with a 50 mm, some with a 100 mm finished diameter. Commercial micro-submersible motor pumps were installed in all of the monitoring sites (cf. Fig. 138). The samples were taken in the thin aquifer uniformly 1 m above the bottom of the aquifer.

For optimal planning of the tracing tests, along with the hydraulic model calculations extensive investigations were carried out to interpret the 'natural' tracers, that enter the groundwater through the Neckar. Suitable index substances to describe the convective transport are conservative materials with high permeation capabilities, such as the chloride ion (KLUDIG 1970), environmentally relevant trace substances, e.g. boric acid and uranine (cf. Section 2.12, KUSSMAUL et al. 1977), and various environmental isotopes (STICHLER et al. 1986). It was thus possible to determine the infiltration times in the investigation transsection. Particularly informative results concerning the aquifer parameters could be won from the ^{18}O-curves. A one-dimensional dispersion model as well as the least squares method for the best curve fit were used (MALOSZEWSKI 1985). The estimated flow velocities calculated from the dispersion model (Fig. 236) and those from the visual comparison of the concen-

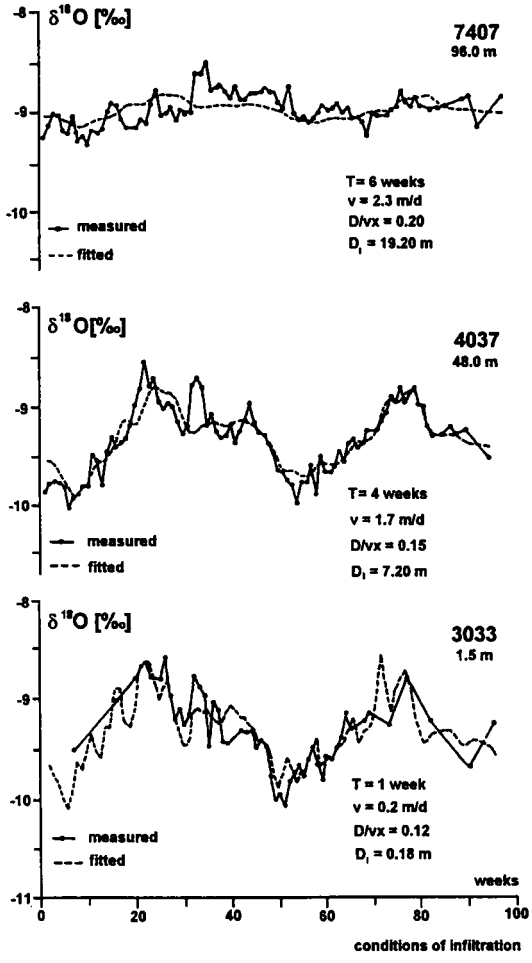

Figure 236. Evaluation of the oxygen-18 curves in the groundwater monitoring wells of the river bank filtration transsection Böckinger Wiesen (from HÖTZL et al. 1989). The distances from the monitoring sites to the Neckar were 1.5 m for site 3033, 48 m for site 4037, and 96 m for the well H (= 7407). The measured values were fitted with a theoretical curve according to the one-dimensional dispersion model and used to determine the listed aquifer parameters.

tration curves of specific index substances and the residence time were in good agreement (HÖTZL et al. 1989).

For the simulation of the propagation of the individual pollutants, suitable reference tracers were required, that approximately covered the spectrum of the corresponding pollutants in their different reactivities. This inevitably only leads to a comparison of an abstract cumulative value to describe the migration behaviour, e.g. the retardation factor and not to reproduce the complex matter-specific reaction kinetics. Comparison studies in column experiments were carried out by BRAND (1989) and REICHERT (1991) for the test area and then transformed by REICHERT into in-situ-tests. The following presents the results according to REICHERT (1991) and REICHERT & HÖTZL (1996) of a combined test.

As comparison tracers, pyranine, naphthionate, and lithium (as lithium chloride) were injected in a monitoring well on the bank. Uranine, as a control substance, was injected in a neighbouring monitoring site. To follow the spreading of the tracers through the ca. 100 m long transsection (total residence time derived from the natural tracers: 42 days), injection amounts for the fluorescent dyes between 0.5 and 2 kg and 12.5 kg of lithium chloride (corresponding to 2.05 kg Li) were selected. To check the propagation process, 28 monitoring wells were available. In accordance with the hydraulic situation (Fig. 235), the total recovery was completed in the pumping well H. With a constant withdrawal of 50 m^3/h over the entire observation period, it was possible to carry out a quantitative balance of the recovered tracer for the evaluation of the mobility of the tracer.

The results of the breakthrough curves in the well H are shown in Figure 237 as well as the theoretical breakthrough curves calculated with the dispersion model and the determined migration parameters. The mean flow time for the groundwater (t_3) from the injection site to the well used to calculate the retardation factor (R_D-value) was determined with the ideal tracer ^{18}O.

In varying degrees, the reaction mechanisms of the matrix flown through determines the transport of the four tracers. The form of the breakthrough and cumulative curves of pyranine correspond to a large extent to the ideal form of a non-reactive tracer. With 2.94 m/d, this results in the lowest dispersivity of 3.79 m. There was no delay relative to the ideal tracer ^{18}O, which results in a value of 1.0 for R_D. Although naphthionate and lithium were injected in the same site, the increased retardation with the increasing tailing effect mainly as a result of sorption processes can be clearly seen. For lithium, a systematic error lead to a recovery rate which was definitely too high. However, this does not change the validity of the course of the curves. Although the uranine results cannot be directly compared with the other three tracers, since it was injected in a different monitoring well, the curve definitely shows the effectiveness of the reaction mechanisms, that are above those of pyranine and naphthionate.

There are remarkable differences in the recovery rates. In the values relative to the injection amounts, pyranine shows the highest losses. Since irreversible fixing of over 95% of the injected pyranine mass onto the solid phase of the aquifer in comparative laboratory tests with the same rock material or from literature data (BEHRENS 1983, cf. also Chapter 2) are not derivable, biochemical decay processes could be the cause.

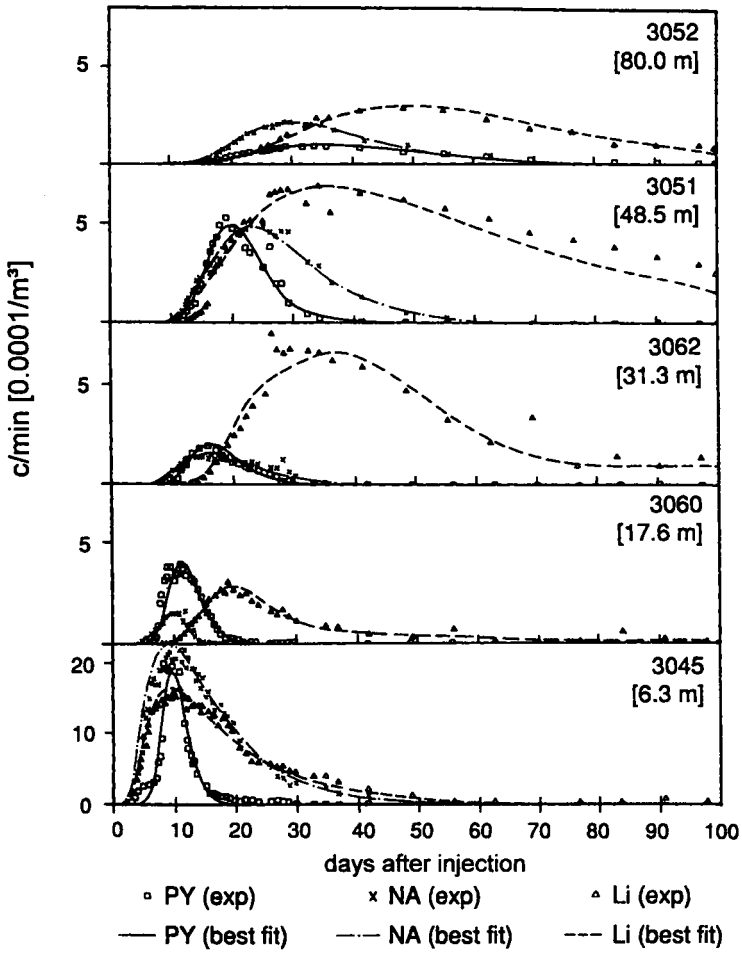

Figure 237. Combined tracing test Böckinger Wiesen 1988. Breakthrough curves for the tracers in monitoring wells located at varying distances away from the river bank. The fitting of the theoretical curves was done with the dispersion model. The ordinate shows the concentration relative to the amount of tracer (from REICHERT 1991).

The different transport behaviour of the tracers not only results in the deviating values in the well H, they also cause a different distribution pattern in the pollutant propagation in the test field. This is impressively documented in Figure 238, with the maximal concentration normalized to the injection amount (REICHERT 1991). In the first two rows of monitoring wells, pyranine, which has the lowest determined dispersivities, still shows a wide, yet compared to both other tracers, already reduced propagation. The main focus of the tracer cloud lies in the western part. In the third and fourth rows of monitoring wells, pyranine is only found in a narrow strip to the east. This corresponds to a flow through an aquifer to the west in an adjoining silt lens. From this winding course of the main flow, which was also evident in older tracing tests, it can be concluded that the pyranine flows through areas of preferential water paths in the sense of a macro-pore-flow.

In contrast, a clearly wider fanning out of the flow can be recognized in the case of naphthionate with its somewhat higher dispersivity. Comparatively high concentrations can be observed in the area of the silt lenses. These prove that the naphthion-

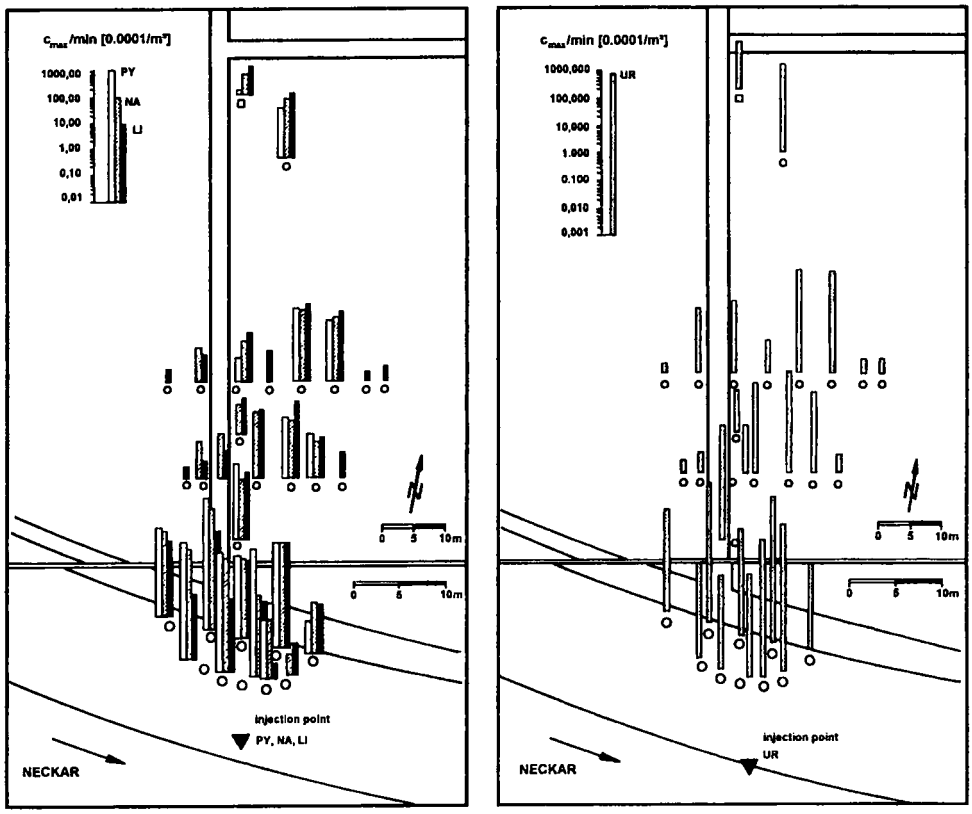

Figure 238. Combined tracing test Böckinger Wiesen 1988. Spatial distribution pattern (maximum concentration relative to injection amount) of the tracer propagation. Left: Injection well 3054 (pyranine, naphthionate, lithium), right: Injection well 3080 (uranine) (from REICHERT 1991).

ate also penetrates in the fine-pore area and can be further transported in these. The largest lateral propagation, at the same time however also the lowest maximal concentrations can be seen in the case of lithium, in accordance to its high dispersivity.

The variability of the maximal concentrations within the individual cross-sections is a definite expression of the heterogeneity of the gravel aquifer relative to the permeability and the sorptivity onto the solid phase. The varying, normalized maximal concentrations, relative to the injection amount of the individual tracers in a monitoring well are the result of the matter-specific reactivity. A seperate effect can be seen in the continuous overly proportional decrease in the maximal concentration in the case of pyranine. This is due to a selective elimination of the tracer, which in accordance to comparative laboratory studies and literature data (cf. above) can be perhaps explained by biochemical decay processes. It is noted that the clearly declining maximal concentrations at the end of the transsection in the well H are not due to sudden decay processes, but rather to the dilution effect of the unmarked groundwater, that flows in from all sides (Fig. 239).

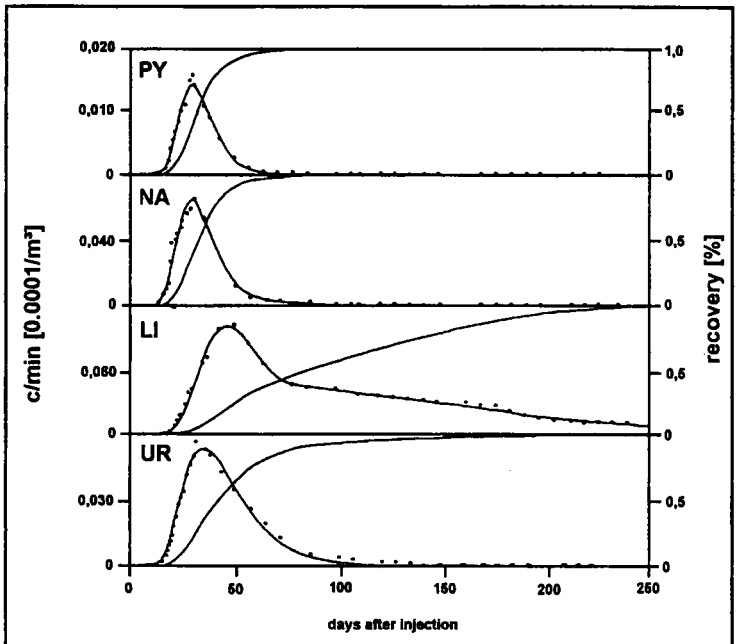

tracer	t_t [d]	v_t [m/d]	α_l [m]	R_d	W [kg]	W [%]
Pyranine	32,3	2,94	3,79	1,00	0,035	3,5
Naphtionate	33,5	2,82	4,74	1,04	0,367	18,5
Lithium	73,0	1,29	16,1	2,27		
Uranine	43,0	2,24	12,53	1,22	0,122	24,5

Figure 239. Combined tracing test Böckinger Wiesen 1988. Experimental (dotted) and theoretical (solid) breakthrough curves from different reactive tracers in the well H after flow through the ca. 100 m long river bank filtration route. Cumulative curve only for the experimental data; the migration parameters were determined with the dispersion model (from REICHERT 1991).

5.5.2.4 *Evaluation of the pollutant propagation using tracers*

The comparative tracer investigation in the river bank filtration transsection of the Böckinger Wiesen, described here with the three different reactive tracers, have shown that such tests can be useful in evaluating the transport behaviour of pollutants. Toxicologically harmless tracers, applied experimentally under in-situ-conditions, allow the simulation of the essential propagation processes. Of course, it is rare that an equivalent reference tracer, with the essential reaction processes, will be found for each specific pollutant, yet a comparison of the different reference tracers can be used to determine the decisive heterogeneities of the aquifer in matters of solute transport. Low reactive tracers are suitable for evaluating possible cases of fast pollutant transport along preferred flow paths.

In contrast, reactive tracers take part strongly in movements in the subordinate flow paths of the micropores. The increased dispersivities cause an increased fanning out of the pollutant propagation. In natural aquifers, even the smallest nonhomoge-

neities show deviating reaction mechanisms, which lead to changes in the concentration distribution. Using artifical tracers to determine concentration distribution patterns can provide important information for evaluating pollutant propagation. At the same time, these investigations can be used as examples in the interpretation of experiments conducted with different tracers for the fact that deviating results are not necessarily the expression of a changed hydrology, but rather often only a result of different, matter specific reactivity.

5.5.3 *Quantification in fissured rocks*
W.Käss

Many springs fed by fissured aquifers have fractions that originate from surface waters. This is almost standard in the springs at the base of the slopes in the side valleys of the Black Forest. Numerous dye and salt tracing tests have verified the infiltration of streams and their reappearance in springs further downhill in the Bunter Sandstone of the Black Forest and the Odenwald (Southwest Germany) (EISSELE 1963).

In the northern part of the district Hardt (Cty. Rottweil), the Kirnbach stream flows north to the city of the five valleys (Fünftälerstadt) Schramberg. The bacteriological analyses in a spring on the right slope caused objections. To check if the respective spring had surface water fractions from the Kirnbach, a dye tracing test was conducted on 30 November 1973. Two kg of dissolved uranine were injected in the Kirnbach above the spring (Fig. 240). Samples were taken from the spring at predetermined times and analysed for their dye content. The results of the the dye analysis is shown in Figure 241.

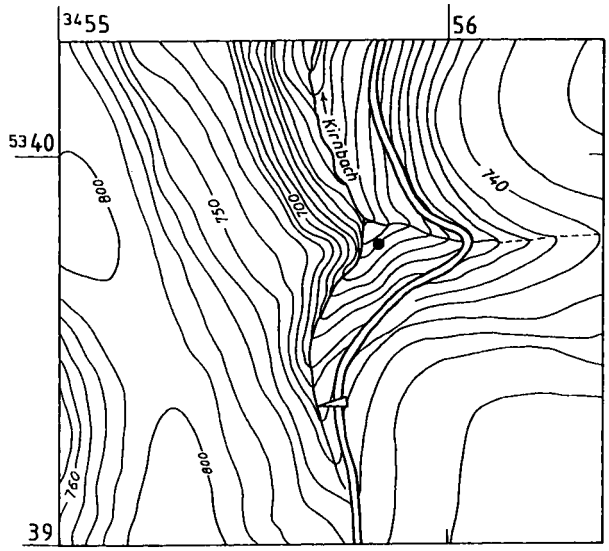

Figure 240. Map of the dye tracing test in the Kirnbach valley (Middle Black Forest /Southwestern Germany) with dye injection site (wedge) and observation site RAPP spring (solid circle) (according to documents from the Geological Survey of Baden-Württemberg).

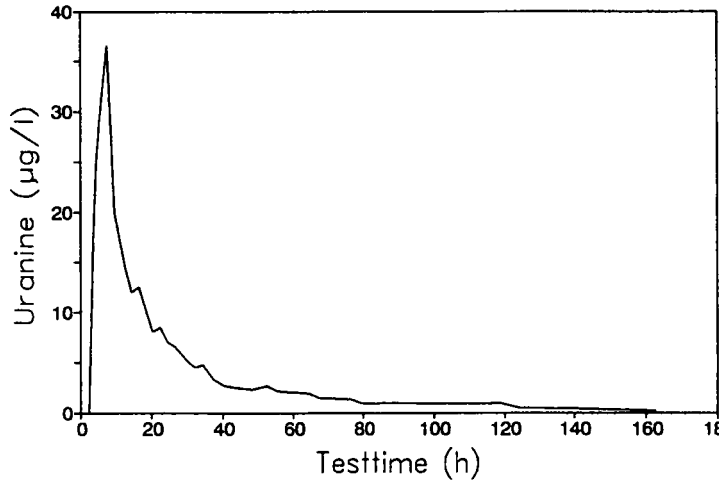

Figure 241. Dye breakthrough curve in the dye tracing test in the Kirnbach Valley.

An evaluation was possible based on the dye breakthrough curve, the discharge in the stream was 20 l/s, and the spring discharge was 2 l/s:

Test begin (t_0): 30 Nov. 1973, 1:30 p.m.
First dye detection (t_1): after ca. 3 hours
Dye maximum (t_2): after ca. 7.5 hours
Half-load (t_3): after 16½ hours
Last detection (t_4): after 162 hours

(hereafter only negligible dye traces were detected; the end of the detection was not observed).

Using the time-concentration-discharge integral, a uranine load in the spring of 4.0 g was determined. This is 0.2% of the injection, i.e. 0.2% of the stream (20 l/s) = 0.04 l/s feeds into the spring. With a spring discharge of 2 l/s this means that: 2% of the spring water originates from the Kirnbach with a mean residence time of less than one day. This residence time underground is decisively too short for sufficient clarification.

A similar calculation was carried out in a dye tracing test in the Aalbach Valley (Main-Tauber-County/Southwestern Germany). The underground there also consists of Bunter Sandstone. With a mean residence time of ca. 12 days, 0.92% stream water was determined in a pumped well (KÄSS 1970a).

5.6 DEEP WATERS

W. Käss

Deep waters are defined as groundwater that has a very low flow velocity due to the depth of its location. It is characterized by increased temperature, increased mineralization, and is tritium-free. Increases in the flow velocity are anthropogenic, caused by the exploitation of thermal water, oil, or other deposits. Tracing techniques can be applied to reconstruct the increase in the groundwater flow. Two examples are presented here where fluorescence dyes were successfully applied.

5.6.1 *Deep water circulation – Saulgau*

Numerous wells have been drilled in Upper Swabia since 1951 to exploit oil and natural gas deposits. It can be concluded from the results of the drill-hole surveying, that there are considerable amounts of thermal water resources in the area of the karstified and fissured Malm.

In 1977, the company Thermalwasser Saulgau GmbH & Co KG drilled the well, TB-1 Saulgau, and during the course of the federally funded 'Geothermal Demonstration Project Saulgau' also in 1981 the well GB-3 Saulgau. Both wells verified the assumption that large quantities of thermal water with an outflow temperature of 40°C could be exploited out of the Upper Malm. The yield of the well TB-1 is 30 l/s with a temperature of 42°C, the well GB-3 has a yield of 50 l/s with 40.5°C. TB-1 is used to operate a thermal bath and GB-3 produces heat. Both wells exploit the thermal water from the so-called Lochfels at a depth of ca. 650 m. They are 430 m apart (Fig. 242). To determine whether there was a mutual influence in using both wells, and to determine the impact in TB-1 of re-injecting warmed water into GB-3, two dye tracing tests were conducted (KÄSS 1987).

The first test started on 10 May 1982 with the injection of 2 kg of uranine in the well GB-3. During the main part of the test, 29 l/s were withdrawn from TB-1. Later on, water was also withdrawn from the injection well GB-3 and for a short time the delivery out of well TB-1 was stopped. Thus, after the 250th day of the test, the dye breakthrough curves (Figs 243 and 244) are not typical type curves. The first dye traces covered the distance between GB-3 and TB-1 in 22 days. On the 125th day of

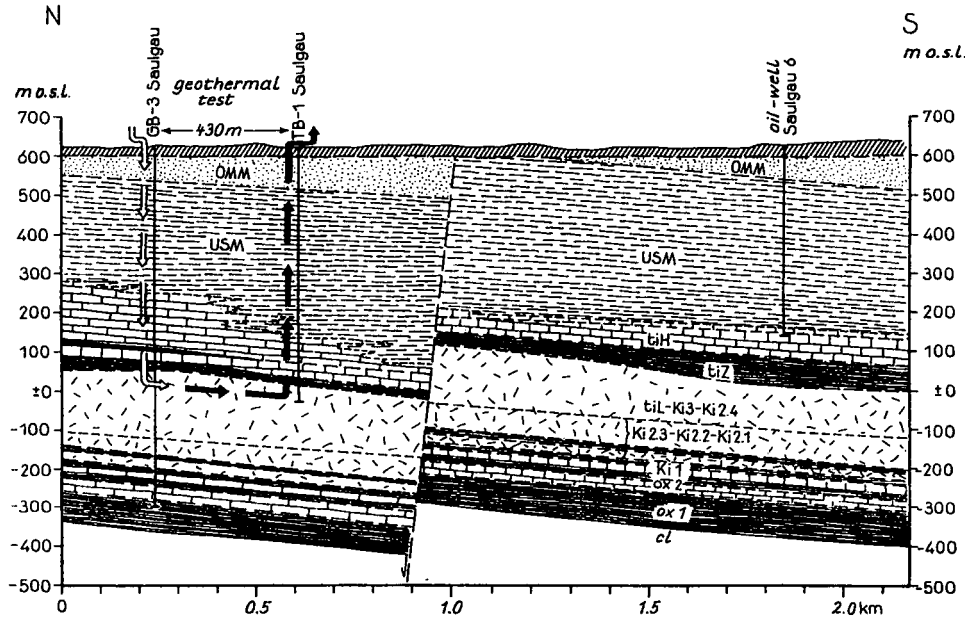

Figure 242. Geological cross-section for the tracing tests GB-3-TB-1 near Saulgau (according to documents from the Geological Survey of Baden-Württemberg/Germany).

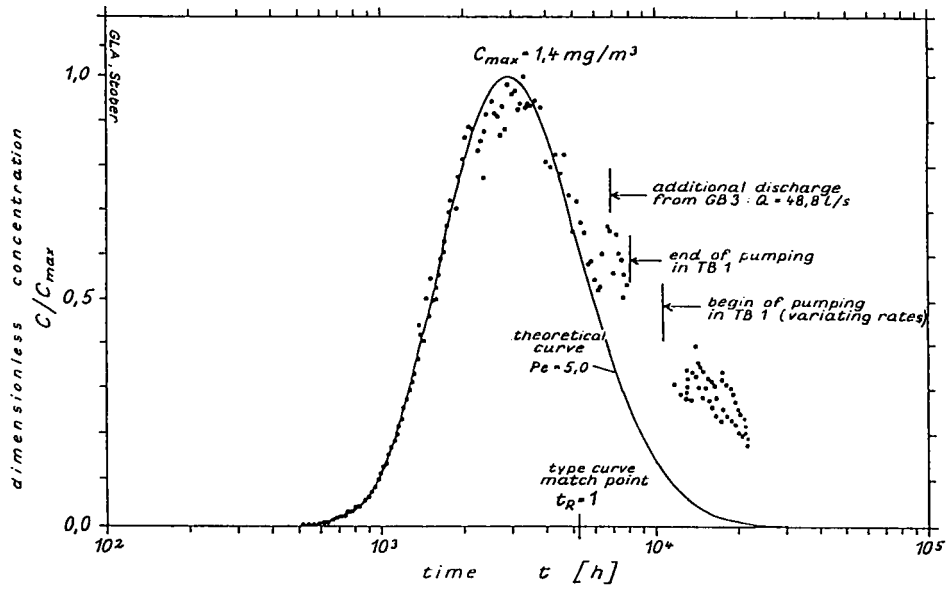

Figure 243. Dye breakthrough curve for the uranine tracing test in the Saulgau wells GB-3 and TB-1 on 10 May 1982. X-axis: logarithmic time scale, Y-axis: normalized dye concentration curve with C_{max} = 1.0 (from STOBER 1988).

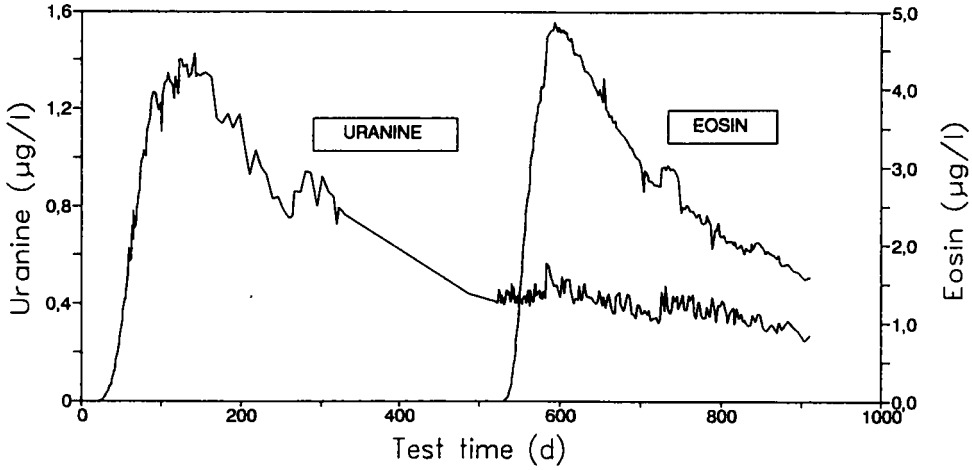

Figure 244. Dye breakthrough curve for uranine (left) and eosin (right) in the tracing tests between the Saulgau wells GB-3 and TB-1.

the test, the dye maximum of 1.4 µg/l was reached. The mean effective flow velocity v_a was circa 0.09 m/h = $2.4 \cdot 10^{-5}$ m/s; it could not be exactly determined since the hydraulic conditions changed during the falling off part of the dye breakthrough curve (cf. above). Nonetheless, the most important parameters could be determined (STOBER 1986, 1988):

Kinematic porosity = 27%,
DARCY-velocity = $1.14 \cdot 10^{-5}$ m/s,
longitudinal dispersion D_L= 84.5 m^2/d,
longitudinal dispersivity α_L = 85.8 m,
other determination methods could not be applied.

Under different conditions, a dye tracing test with eosin was started on 10 October 1983 with 5 kg of dye. From the beginning of this test, 21 l/s of water was withdrawn from the observation well TB-1. The same quantity of water was injected in well GB-3, Q = 21 l/s, composed of 50% thermal Malm water and 50% water from the tap. Due to the increased gradient, eosin's flow velocity was larger than uranine's. On 22 Oct. 1983, eosin first appeared in TB-1 and reached its maximum of 4.9 µg/l after 24 days on 23 Dec.1983.

The tests show that quantitative work can be completed with uranine and eosin even under high pressures and increased temperatures. The dyes are not known to decay. Further publications verify that even under much higher temperatures, the dye uranine is still stable (MCCABE 1991).

5.6.2 *Oil field waters – Steimbke*

Tracing techniques can provide answers to questions in mining hydrogeological areas.

In cases with water inflow in subsurface coal mining operations, the origin of the water inflow should be determined. In numerous cases, dye tracing tests have proven that surface water enters the mine diggings (SEMMLER 1937, 1953, KLIR 1967). When surface waters or wells run dry due to mining operations, it is termed mining subsidence. Dye tracing tests can also provide proof in such cases, as to whether there is a hydrological connection between the percolation site and the swamped water (SEMMLER 1958, SEMMLER & SCHMIDT 1958). Uranine can only be sucessfully applied during investigations of underground seepage water sites if the water to be traced is not acidic. This is very common in mine pits, where sulfidic ores are mined. However, uranine has been sucessfully applied in coal mines to prove hydrological connections between mining floors (SEMMLER 1953, CLASSEN 1964, 1967). Besides uranine, 2-naphthylamine-4,8-disulfonic acid = C-acid has also been used over smaller flow distances in the Mansfeld Kupferschiefer Mines (LIEBISCH & REMUS 1966). Water draining in soft coal mines not only changes the groundwater level, it can also change the flow direction in the immediate surroundings and farther away. To investigate such changes, MILDE (1962) used radioactive isotopes and uranine in the mining district Fürstenberg-Nord on the Oder/East Germany.

With water inflow into salt mines, the greatest danger is caused by flooding, if the inflow is due to surface water or near surface groundwater. Since such inflow usually consists of nearly saturated salt brines, salt tracing tests cannot be used to determine the origin of the inflow. In 1953, SEMMLER described a sucessful dyeing of salt brines with uranine in the Alsatian potash mine Staffelfelden. Uranine is also a suitable tracer if the salt brine contains other than sodium chloride also potassium and magnesium chloride: In the potash shaft Neuhof-Ellers (Hessen, Western Germany) a horizontal pilot hole was drilled over 100 m in a potash seam and a NaCl-$MgCl_2$-brine (pH = 7.2) was used as the drilling-cooling liquid. At two transverse faults 30

and 100 m away, the drilling liquid was able to return to the mine through a bore hole. In spite of the high salt concentration, it was possible to quantitatively determine the uranine without any problems.

In 1985, KOCKERT investigated the behaviour of different fluorescent and non-fluorescent dyes in salt brines with different compositions. Accordingly, NaCl-, KCl-, $MgCl_2$-, and $CaCl_2$-solutions have no impact upon the dyeing ability of uranine, eosin, rhodamine B, and auramine. Crystal violet has a more intensive blue, malachite green becomes darker and fuchsin B lighter. Congo red precipitates as a dark sediment.

Oil field waters are usually rich in sodium chloride; NaCl-concentrations can exceed 100 g/l. For an environmentally protective disposal of the brines and to help maintain the formation pressure, they can be reinjected into the watered border sections of the deposit. For the effectiveness of the salt water disposal, it is very important to determine whether underground connections are possible. Numerous methods of labelling the injection water have been tried and the use of radioactive isotopes has gained special importance (DOLL & SCHWEDE 1947, BIRD & DEMPSEY 1955, DOLAK 1966, 1968, 1969). Further tracers that have been more or less successfully used are borax (CARPENTER et al. 1952), surfactants (STURM & JOHNSON 1950), D-glucose (HECK 1954, DANIELS & MAYER 1957), and phenols (DOLAK 1966, 1969).

Compared to the other tracers mentioned, uranine has important advantages for use in tracing injection water: Uranine's detection is independent of the salt content in the injection water, it is unsoluble in the oil phase, and can be detected in very low concentrations.

The following describes an example of tracing with uranine in injection water in the oil field Steimbke-Alt, in Lower Saxony, Western Germany (KÄSS 1966b).

In the oil field Steimbke-Alt oil is exploited in several horizons (Fig. 245). The Wealden Sandstone has productive wells with different degrees of salt water ingress between 0.2 and 13 m^3/day and also wells that have gone fully to water. Three of these unproductive wells received circa 200 m^3/day of reinjection water. The northern reinjection well 174 was selected as the injection site for labelling the reinjection water with 2 kg of uranine on 25 Nov.1965. There were no problems with the injection of the dye solution to the reinjection water, since subpressure prevailed in the well. The reinjection water had a total salt content of 197 g/l and a pH-value of 7.06 close to the neutral point. The location of the wells can be seen in the subsurface contour map of the top of the Wealden Sandstone formation (Fig. 246). Uranine was detected only a few days after the injection in the neighbouring wells. The hatched area in Figure 246 shows the area around reinjection well 174, that had a maximum concentration of over 10 µg/l. The well 180, ca. 70 m downstructure from the reinjection well, was affected the most. The dye breakthrough curve is very irregular with several maxima. It can be concluded that the hydraulic routings are very ramified (Fig. 247). Also shown in Figure 246 are the probable flow directions (long arrows) of the trace detections of uranine. Soon after the tracer injection, the reinjection water carried traces of uranine of up to 40 µg/l due to the reinjection of the coloured aqueous phase from the oil production wells. Thus, the south-western wells 168, 165, 157, and 100 were probably influenced by the reinjection wells 133 and 134. Regular sampling was stopped on 25 Jan. 1966, the 61st day of the test. Taking into account the water discharge and the dye breakthrough curves, a total recovery of

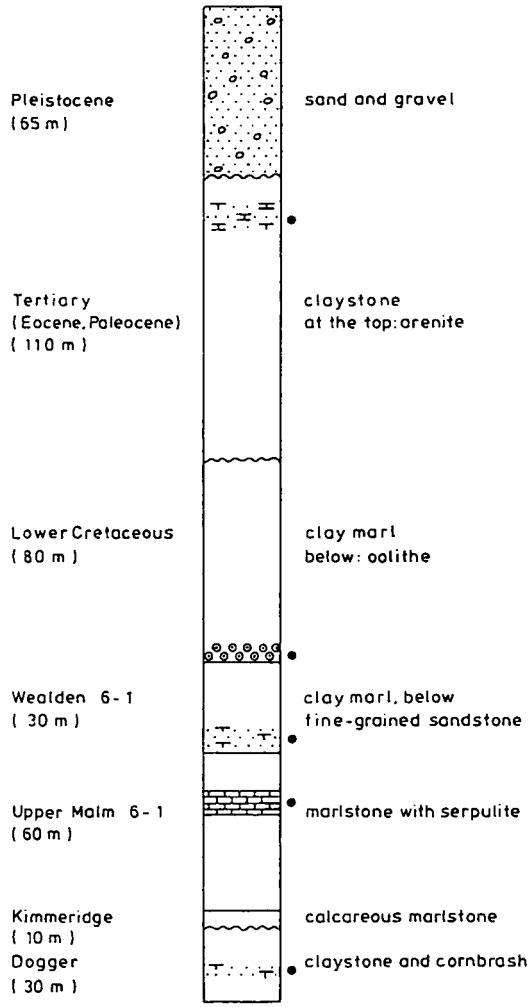

Figure 245. Geological columnar section of the oil field Steimbke-Alt, showing stratigraphy and layer thicknesses (left) and oil deposits (dots) and production horizons (right) (from KÄSS 1966b).

307 g uranine or 6.1% of the injection amount was calculated. The well 180 contained 151 g or 3%.

This test proves that uranine is probably the tracer best-suited for tests in determining reinjection short circuits. Other uranine tests in Lower Austrian oil fields are covered in DOLAK (1969). STURM and JOHNSON (1950) reported on tracing tests in reinjection water with uranine, NaCl, and surfactants in Pennsylvanian. WYSCHIGIN and TSCHEREPANOW (1962) described dye tracing tests using uranine in the oil-natural gas deposits of Kolinowsk in the Volga-Ural-area, where fissured dolomites of the Upper Permian are exploited. They found a two-dimensional irregular advancement of the dyed water.

Unfortunately, none of these publications list quantitative uranine analyses.

The author conducted a uranine tracing test in the oil productive Baustein layers of the alpine foreland in the oil field Mönchsrot (Cty. Biberach, Baden- Württemberg/Germany). There was a partial impact due to a uranine injection sev-

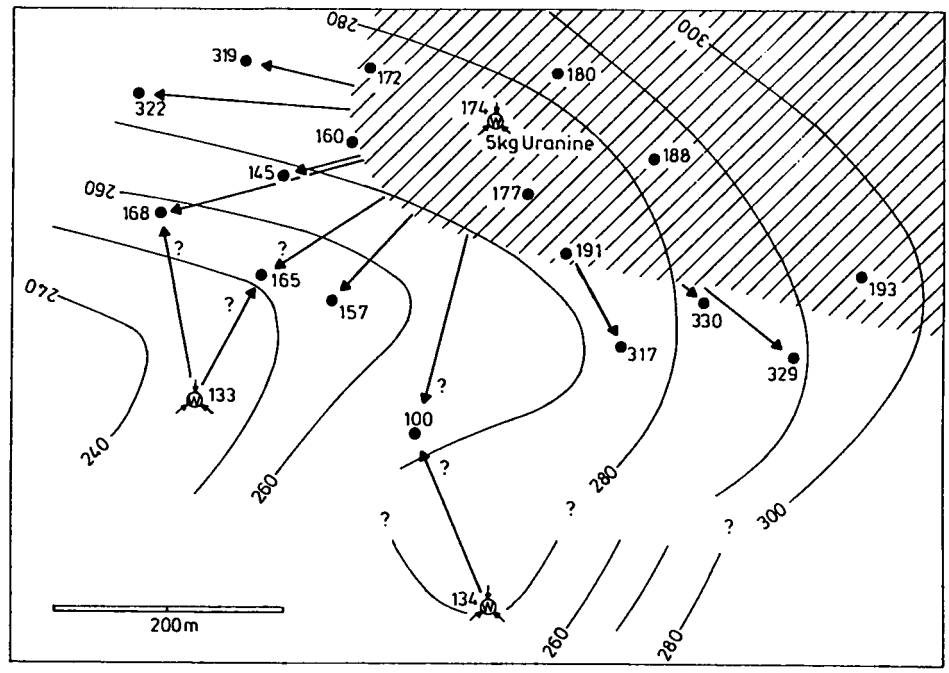

Figure 246. Subsurface contour map of the top of the productive Wealden Sandstone in m below sea level. Wells = dots with well number, the three reinjection wells are shown as 'W' with small arrows, hatched area in the north-east = massive dye appearance, long arrows = trace detections of uranine, ? = uncertain origin of uranine (from KÄSS 1966b).

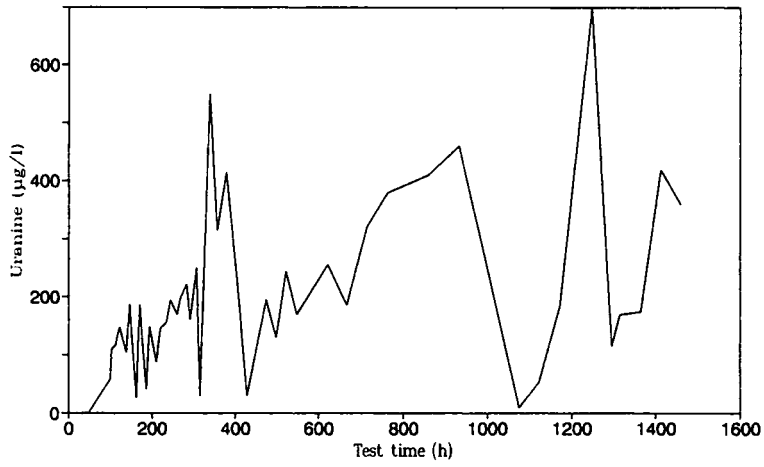

Figure 247. Dye breakthrough curve from the most affected well 180, circa 70 m north-east of the injection site, well 174.

eral years before. However, a cautious evaluation of the results showed that the reinjection water probably flows slowly in a broad front towards the production wells. A stronger fissuring of the Baustein layers would have resulted in a quicker reappearance of the dye.

5.7 GLACIERS

Ch. Leibundgut

Introduction

Natural and artificial tracers have manifold applications in hydroglaciology. The unique characteristics of glaciers as aquifers require special tracing methods. Hydrologically, glaciers show analogies to solid and unconsolidated rock aquifers. Depending on the development of the fissure or fracture system (intra- and subglacial), the compact ice corresponds approximately to a fissure or karst aquifer. However, the covering firn snow has porous aquifer properties.

In contrast to groundwater aquifers, water as snow, firn, or ice represents the actual aquifer. Due to solid-liquid phase transitions, storage and runoff alternate quickly in these special aquifers and the transitions are reversible. As a result of these highly dynamic components in the water cycle, investigations of the water flow in glaciers are very interesting, but also difficult.

Tracing tests can help in investigating glaciers as a little known hydrological system and are thus an important tool for developing flow behaviour models.

5.7.1 *Models in hydroglaciology*

In order to plan and interpret tracing tests, runoff models of the glaciers are usually required, but tracing tests can also deliver important basic information for new hypotheses as to how the hydroglaciological systems function. The water cycle of a glacierized catchment area can be understood as the total flow through a series of connected or parallel storage systems. This corresponds to a multiple component model with varying fractions of slow and fast components. Precipitation is the primary infiltration source, yet ablation is the deciding factor for the flow behaviour. The total flow consists of surface flow, intra- and subglacial flow, and groundwater flow. Due to practical and economical reasons, artificial tracers are best suited for use in investigating the fast flow storage systems and for the short-term runoff components. Among these are percolation through snow and firn layers, surface flow, and intra- and subglacial flow.

In the snow-firn layers, models used in porous unconsolidated rock aquifers can be used as first approximations (LANG et al. 1979, OERTER 1981). It is important to remember that the stratification during deposition causes large nonhomogeneity and anisotropy in the firn aquifer. During diagenesis, the hydraulic conductivity of the firn body decreases more and more and reaches in the glacier ice such low values that it can be taken as practically impervious. The intra- and subglacial water flow occurs in fissures and fractures, that were caused by pressure differences, and is analogous to the flow in fissure aquifers. Meltwater can widen these fissures to channels, whereby the flow collects in main subglacial drainage channels (RÖTHLISBERGER 1972). Therefore, analogies from karst hydrology are often applied for the intra- and subglacial runoff (LANG et al. 1979). The widening of these channels is undone when the water pressure in the ice channels falls under the ice pressure. The daily and seasonal variations in the runoff system are the result of the interplay of these processes (Fig. 248).

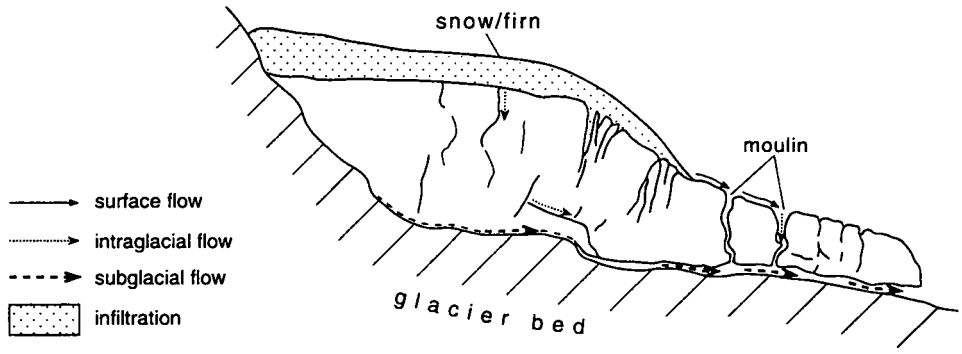

Figure 248. Schematic representation of a glacier aquifer. The flow behaviour is complex and shows analogies to karst aquifers, fissured aquifers, and porous aquifers.

5.7.2 *Tracer applications in hydroglaciology*

Applying natural and artificial tracers in hydroglaciology is generally a case of inverse system identification. A known initial value is transformed into a measurable end value through a system that is to be determined. Natural and artificial tracers allow an identification of either marked water bodies in cases with injection of artificial tracers or using tracers (isotopes, water constituents), which are naturally a part of the water body. This identification can be temporal (dating) or spatial (site of origin). The measured end value is the temporally variable runoff and the concentration of the applied tracer at the system exit. Analogous to spring catchment areas, glacier catchment areas usually have a collected runoff in the form of a glacial stream. The total runoff can be sampled at one site, near the glacier outlet. The hydrological information about the glacial catchment area is stored here naturally in the variations in the runoff amount, the mineralization, and the isotope concentrations, and also in the concentration of an injected tracer. If the information contained in the runoff can be sucessfully deciphered, important conclusions pertaining to the storage and runoff behaviour in the glacier can be made.

The characteristic scales of the problem under investigation are important criteria for the application areas of natural and artificial tracers. Natural tracers are suitable for investigating slow and large-scale effective processes. Thus, stratification and mass balance investigations are the domain for applying natural tracers. Ice flow can also be easily investigated with isotopes or natural drift tracers. The separation of the flow into its different components (hydrograph separation) can be carried out with natural tracers. Ice and snowmelt water can be separated with the environmental isotopes oxygen-18 and deuterium (BEHRENS et al. 1972, OERTER 1981). Pure meltwater differs from flow originating from groundwater by lower mineralization and can be separated with geogenic tracers such as Na^+, K^+, Ca^{2+}, Mg^{2+}, or electric conductivity (COLLINS 1977).

In contrast, artificial tracers are preferable for investigating fast flow components. These occur above all during the ablation periods. Tracing tests can prove hydrological connections and separate catchment areas or parts thereof. Furthermore, they allow the determination of aquifer parameters such as flow velocity and dispersion.

Tracing tests have been successfully used to investigate the development of the intra- and subglacial drainage systems (LANG et al. 1979, ASCHWANDEN & LEIBUNDGUT 1982, LEIBUNDGUT 1986, MOERI & LEIBUNDGUT 1986, SEABERG et al. 1988).

Since older tracing tests were usually not completely evaluated and only limited flow parameters determined, LEIBUNDGUT's (1986) use of the simple ratio of va_{max}/va_{med} provided a first insight of intraglacial flow systems. When complete tracing test data are available, corresponding evaluation procedures for determining flow and aquifer parameters can be laid down.

Up to now, the use of artificial tracers in glaciers was limited almost exclusively to alpine valley glaciers. In August 1988, a large tracer experiment was carried out for the first time in the western Greenland ice shield north-east of Jakobshavn (LEIBUNDGUT & GEES 1989). Its goal was to investigate the state of the drainage system to the ice border and to separate a subglacial catchment area. VATNE et al. (1995) reported a tracing test in an investigation of a polythermic glacier in Spitsbergen.

5.7.3 *Requirements of artificial tracers used in hydroglaciology*

The same criteria are valid for the suitability of artificial tracers in hydroglaciology as in other areas in hydrology. However, due to the special and extreme test conditions present, some of the criteria are weighted differently. Due to transport problems, only highly concentrated tracers can be used. Among these, the fluorescent tracers are best suited and have been used almost exclusively. Up to now, uranine and rhodamines, to a lesser extent also eosin and naphthionate have been used. Since backgrounds in glacial waters are normally very low, table salt, lithium- and strontium salts can also be considered for small scale tests.

Water solubility is an important criterion. On the one hand, the low water temperature lowers the solubility and on the other hand, the lowest possible weight of the dissolved tracer is needed for transport reasons. In order to avoid a contamination of the unprotected glacial aquifer with the dry tracer due to wind drift, the tracer should be dissolved in the specific rooms in the laboratory at home if possible or in the base camp below the glacier under investigation. Thus, the full physical solubility of the respective tracer can be exploited. The use of solubilizers is recommended.

In general, the injection should not be carried out with higher than 10% solutions. However, dilution of the highly concentrated solutions with meltwater is unproblematic. Under certain circumstances, the water needed for priming and flushing must be melted from snow and firn. When injecting highly concentrated tracer solutions in glaciers, there is always the danger of the solution precipitating at the low temperatures. Especially uranine reacts sensitively in this point. The possibility that the marked water can sink in stagnant water zones due to its higher density is low in well-developed drainage systems, but should still be considered.

Sorption of the tracer in glaciers is scarce due to the absence of adsorbing organic and clayey material (LEIBUNDGUT 1986). Also, chemical stability and pH-dependency of some of the fluorescent dyes are usually unproblematic. The light sensitivity of the fluorescent dyes is uncritical in investigating intra- and subglacial flow systems. However, it plays an important role in tracing snow and firn, especially in two-dimensional injection of the tracer.

The detection limit is low in tests in glaciers due to the pure glacial water. However, glacial water can contain large amounts of suspended solids. Through sedimentation of the suspended solids in the sample bottles and then decanting, this problem can be solved. With in-situ-measurements, the suspended solids content is a problem, however. It leads to an increase in the detection limit and to a higher error in varying suspended solids loads (varying measurement background). The temperature dependency of the tracers does not present a methodical problem. It is taken into account, that the fluorescence of the calibration solutions and the samples are measured at the same temperature in the laboratory and in the case of in-situ-measurements, a temperature correction is carried out in the software or afterwards (LEIBUNDGUT 1980).

In many cases in hydroglaciology, combined tracing tests must be conducted. Precisely because of the strong variations in the glacial runoff system, the same hydrological boundary conditions can only be achieved with the simultaneous injection of different tracers. In such cases, the tracer mixture must be separable.

5.7.4 *Conducting tracing tests*

Due to transport problems, the test materials must be limited to absolutely necessary items. Depending on the test goals, decisions concerning where, when, which, and how much tracer is to be injected and where and in which way the tracer passage is to be recorded must be predetermined.

In investigations of the firn layer or combined investigations of firn layer, intra- and subglacial system, tracers can be applied two-dimensionally, linearly, or as a point source injection directly onto the firn surface (BEHRENS et al. 1976). In investigations of the intra- and subglacial systems, naturally occurring moulins in the ablation area can be exploited for the injections. However, boreholes are being increasingly used to inject the tracer directly into the wanted site of the intra- or subglacial system. In the summer of 1991, the VAW-ETHZ (Versuchsanstalt für Wasserbau der Eidgenöss. Techn. Hochschule Zürich) at the Konkordiaplatz in the Aletsch glacier (Switzerland) drilled a 700 m deep borehole and injected 12 kg of eosin. In accumulation areas, it can be necessary to bridge the unsaturated firn zone with a borehole and to carry out the injection in a borehole (LANG et al. 1979).

The timing of the injection is very important when investigating water flow in glaciers due to the high temporal variability of the drainage system. Additional preliminary measurements of the meltwater levels or the water pressure in the drainage system can provide information as to the development of the drainage system (RÖTHLISBERGER 1972, IKEN & BINDSCHADLER 1986, OERTER 1981). In investigations of completely developed flow systems, the end of the ablation period with the maximal meltwater level is best suited. The goal of many glacial investigations is to obtain information about the development of the intra- and subglacial flow system. In such cases, the time-point of the injection depends on the goal of the investigation.

An approximate calculation of the required amount of tracer needed for the injection can be obtained based on the discharge Q at the glacial outlet (formula LEIBUNDGUT 1974 + Section 3.2.5).

In glaciers, the adsorption coefficient is low due to the absence of organic and cohesive, mineral material. The expected passage time, T, must be estimated from the

given flow path, the estimated flow velocity, and model assumptions. The wanted maximal concentration C_{max} can be estimated with 10 µg/l. For a generous estimation, the tracer amount can be approximated with the half of the area $Q \cdot T \cdot C_{max}$ using an approximated triangular passage. With injections in moulins, approximated 'piston flow', low dispersivity and thus low losses can be often assumed. However, losses due to freezing and unconnected cavities in the glacier can occur. These losses depend strongly upon the developmental stage of the flow system and its changes during the tracing test. When the meltwater abates, the channel system can reconvert due to the ice pressure and the tracer can freeze.

The sampling sites are determined by the goal of the test and the expected flow path. In glacial runoff tracing tests, spatial sampling is usually limited to the glacial outlet. At this site, all of the water usually exits. Sampling in the glacier itself can be completed with boreholes, whereby this type of sampling is usually not without problems (LEIBUNDGUT 1986). In cases where the firn body itself is to be investigated, special sampling arrangemnets must be set up. The registration of the tracer passage can be completed by taking individual samples and analysing later in the laboratory. Since this method has high personnel requirements due to the narrowly spaced sampling intervals needed with the hydrological conditions, the use of automatic samplers with independent power supplies is recommended. The sampler must also be heated to avoid freezing. Some samplers also allow a flow-controlled sampling, with shorter sampling intervals with increasing flow.

In-situ-measurements often fail in glacierized areas due to logistic problems (temperature, power supply, weight). However, in those cases where the logistic prerequisites are given, the varying suspended solids load still presents a problem with the calibration of the measurements.

When semi-quantitative or even qualitative detection of the tracer is sufficient, activated charcoal can be used. A disadvantage lies in the low evaluation possibilities, which do not correspond to the current evaluation possibilities for tracing tests. However, activated charcoal can provide important information and knowledge. For example, the winter runoff from the accumulation area of the Aletsch glacier could be proven thusly (LANG et al. 1979).

The correct determination of the sampling interval and how long samples are taken are important prerequisites for successful tracing tests. However especially with glacier investigations, it must be often decided between practicability and quality of the measurements. The sampling intervals are determined by the characteristic breakthrough times in the investigated areas on the one hand and the strongly weather-dependent flow dynamic of the glacier on the other hand. Due to the high variability of the glacial runoff, a high temporal resolution of the samples is necessary to determine the begin, rise, maximum, and secondary maxima of the tracer breakthrough curves. The sampling interval can have drastic effects upon the registration of the tracer breakthrough curve (Fig. 249). Often, an adequate determination of the curves is only possible with an automatic sampler.

5.7.5 *Case example: Findelen Glacier*

The catchment area of the Findelen glacier is in the Canton Wallis in the Swiss Alps and covers an area of over 24.5 km^2, of which 80% is glaciated. The altitude ranges

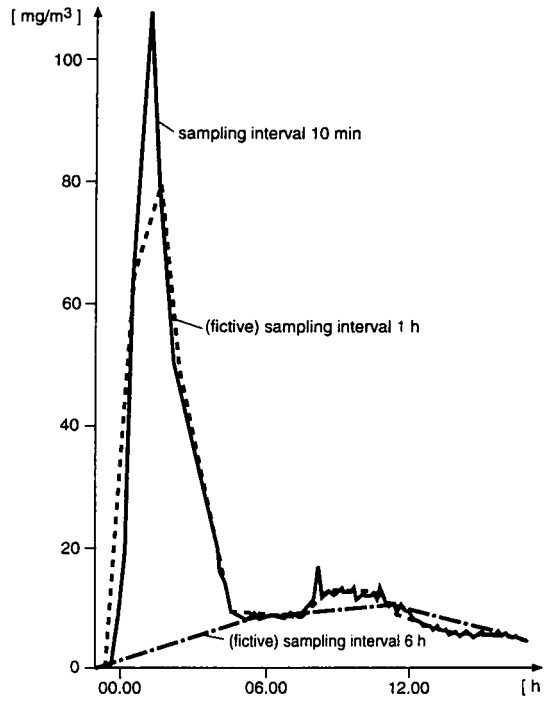

Figure 249. Effect of different sampling intervals on the tracer breakthrough curve.

from 2450 m up to 4190 m a.s.l. In the seventies and eighties, numerous glaciological studies have been carried out here. Their goals were to investigate the connection between the glacier movement on the one hand and the subglacial water pressure and the water flow and storage on the other hand. Specifically, numerous tracing tests were conducted to investigate the intra- and subglacial flow behaviour. The first test campaign was carried out at different times during the 1982 ablation phase, to determine the formation and backformation of the subglacial drainage system. The second was conducted during the accumulation phase in 1984, to complete the picture obtained of the seasonal development of the flow relationships (MOERI & LEIBUNDGUT 1986). Tracers were injected at different sites in boreholes or moulins, to determine the spatial heterogeneity of the drainage system.

In the first campaign in 1982, three combined tracing tests were carried out between June and the end of September, to characterize the drainage system at its initial, maximum, and final states. In doing so, two injections were carried out simultaneously at two different sites. The flow relationships in the glacial stream were used to determine suitable times for the injections. Furthermore, the times were bound to the weather conditions, since the tests were to be carried out under pure snow melt conditions. The first combined test was on 14 June 1982, after the meltwater had started at the beginning of June. The injections were carried out only in boreholes, whereas the later injections could be carried out in boreholes and moulins. As tracers, uranine and rhodamine B were used. In this test, 1 kg of dissolved rhodamine B was injected through a drilling hose in a borehole, that was 1712 m away from the sampling site. Water used to flush the tracer did not cause noted water level changes,

which indicates large water channels (fissures, fractures) nearby. The tracer breakthrough occurred relatively compactly within a few days with a median effective flow velocity of 0.15 m/s and a tracer return of 65% (Fig. 250).

Overall, the results from the first campaign during the ablation phase, showed that the timing of the tracer injection is decisive for the tracer return and the flow velocities. At the beginning of the ablation period the velocities were low, then rose, and then fell again at the end. The tracer return fluctuated between 15% and 93% and the median effective flow velocities reached values between 0.13 m/s and 0.69 m/s.

The different injection sites showed that depending on the distance to the main subglacial drainage channels, the tracer breakthrough can be compact, or also show definite secondary maxima and longer tracer detection tails. The present results indicate a delay in the runoff and water storage in the glacier depending on the weather and the daily course of the temperature. During the seasonal course, the subglacial drainage system widens at the beginning of the ablation phase and then narrows towards the end of the ablation phase again.

With the second test campaign in 1984 during the accumulation phase, rhodamine B was injected in a borehole and uranine injected in a then inactive moulin on 2 March. The lower part of the moulin was drilled in order to access the subglacial drainage system. The distance to the sampling site at the glacial outlet was 1495 m. The breakthrough curves from the accumulation phase differ greatly from those from the ablation period. The tracer reappeared with varying, decreasing concentrations over the total sampling time of six weeks (Fig. 251). The median effective flow velocities were a factor 100 lower than during the ablation phase and amounted to 0.16 cm/s (borehole) and 2.5 cm/s (moulin), the tracer return amounted to 15% (borehole) and 97% (moulin). The higher return and higher velocity from the test in the moulin show that the water also drains in winter in locally differing patterns in the subglacial system. Up to a certain degree, the main subglacial channels were still passable, although flow delays and water storage were considerably more significant than during the ablation phase. The occurrence of a second major peak after one month during the second test in the borehole shows that a strong temporary water storage occurred here.

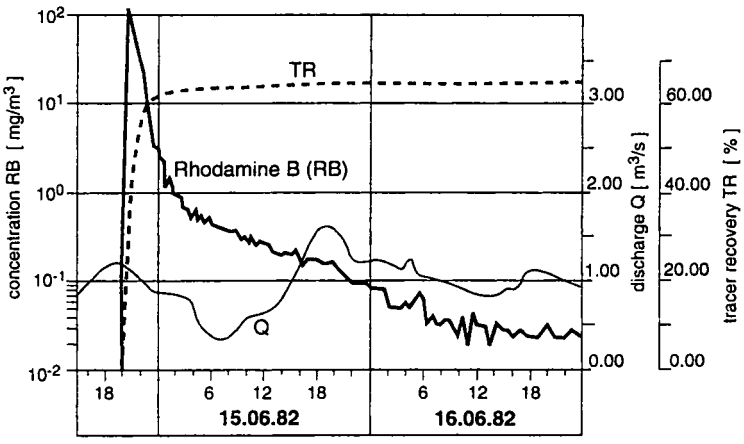

Figure 250. Tracer experiment Findelen Glacier with injection into a borehole under conditions of summer ablation.

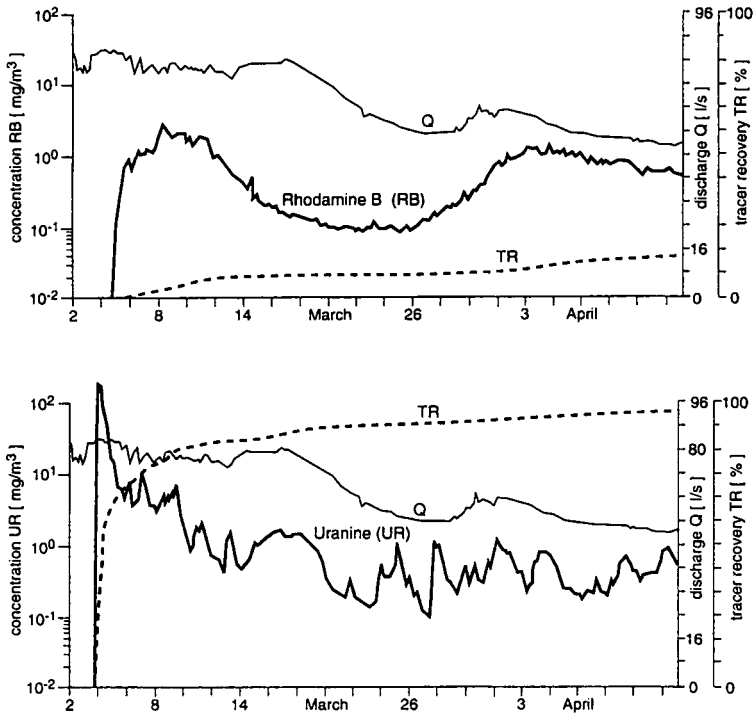

Figure 251. Tracer experiment Findelen Glacier with injection into a borehole (RB) and an inactive moulin (UR) under conditions of winter accumulation.

5.8 SURFACE WATER

Ch. Leibundgut

Artificial and natural tracers are used to obtain information concerning surface water, both standing and flowing water bodies. The information sought usually deals with water and matter transport processes in open water bodies (lakes and flowing water), but also with interactions with the bordering groundwater aquifers. With the help of natural tracers, long-term investigations of the entire water body are possible and thus also the determination of seasonally varying processes. Among the natural tracers, isotopes are frequently used for the investigations. For example, mixing and flow processes in lakes with different inflows from different catchment areas can be determined with the help of water isotopes (SIEGENTHALER 1982). A review of isotope methods in surface water can be found in MOSER & RAUERT (1980). NIR (1973) published detailed instructions for calculating flow rates, volume, evapotranspiration, and gas-exchange. Natural tracer applications will not be covered here further.

In contrast, artificial tracers are applied to investigate the momentary hydrological situation. Only water bodies up to a certain size can be traced and strictly speaking, the results are only valid for each respective hydrological situation. On the other hand, it is advantageous that artificial tracers can be specifically applied for each goal. The techniques are especially suitable for the simulation of point-source contaminations.

According to the literature, the first tracer experiments in surface water were conducted in oceanography. CARPENTER (1968) described a test in Baltimore Harbor with rhodamine B. The goal of the test was to investigate the exchange processes in the harbour, in order to determine the capacity of the harbour basin for industrial sewage. COSTIN (1963) reported about a similar test in the New York Bight. It can be concluded that such tests were often carried out by harbour and water management companies, without the results of these practically oriented tests ever being published. As early as 1964, JOSEPH et al. described a carefully conducted test series with rhodamine B in the North Sea. In 1966, ICHIYE et al. applied densiometry to register the spreading of a fluorescent tracer in the ocean. The distribution of sewage plumes in coastal water has been repeatedly followed with bacterial tracing tests. ROBSON (1956) and PIKE et al. (1969) also used the active isotope ^{32}P. To trace coastal water and also the open sea, perfluorochemicals can be applied. To do this, WANNINKHOFF et al. (1985) and WATSON et al. (1987) used sulfurhexafluoride, the latter also used perfluorohydrocarbons. Recently, ROLDAO et al. (1997) reported about large-scale tests with fluorescent tracers where they labelled industrial and domestic sewage, introduced in the sea by submarine outfalls, aiming to evaluate the effluent's dilution pattern in the sea water. This type of application in surface water will not be handled here further. The systematic investigation of lake currents with artificial tracers began in the seventies (LEIBUNDGUT & HIRSIG 1977). River investigations in the USA were also started at this time (HUBBARD et al. 1982), in Europe a decade later.

5.8.1 *Particularities of applying tracers in surface water*

There are considerable differences in the techniques used in surface water as compared with those in groundwater. These are due to the open accessibility of the water body to be traced and the high dynamics, to which they are subject. In contrast to tests in groundwater, where the sampling sites are set, a quickly spreading tracer plume in surface water can and must be followed. In addition, in standing bodies of water, a three-dimensional determination of the tracer cloud over time is required. As an exception, under one-dimensional conditions in flowing water (homogeneous mixing), stationary sampling can be used. In addition to technical problems with the tracers, there are also measurement-technical problems to be solved.

The high dynamics of the flow and transport processes in surface water basically require in situ measurements. However, only a few of the substances suitable as tracers can be measured in situ, among them, especially the fluorescent tracers. At the end of the seventies, HIRSIG et al. (1982) introduced the impulse-physics-technique, which was already known in oceanography, to limnology and further developed the measurement techniques. The VARIOSENS technique uses an underwater-filter-fluorimeter with an excitation light source, excitation filter, emission filter, and detector, that can be set up at the required depth under water. It is part of a measuring chain, in which the measurement signal, the depth signal (pressure probe), and the temperature measurement run through an analog-to-digital-converter to a laptop (Fig. 252). In addition, the position must be determined and stored digitally, in order to obtain the spatial co-ordinates for the profile sections. With the help of the measuring chain, a flexible measurement planning and storage of the data for later evaluations is

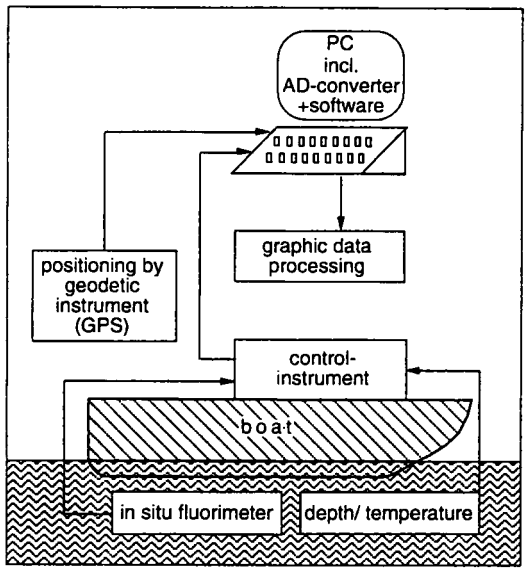

Figure 252. Schematic representation of the underwater fluorimeter measuring chain VARIOSENS.

possible (HIRSIG et al. 1982). This impulse technique is no longer state-of-the-art, but it is still applied successfully in surface water. Only one tracer at a time can be measured with a VARIOSENS-instrument set up with the corresponding excitation and emission filters.

New possibilities were opened with the use of optic fibre fluorimeter techniques (BARCZEWSKI 1990). With this technique, the excitation light is led through an optical system with an integrated excitation filter in an optic fibre channel, through which it reaches the probe. This can be brought to the required depth under water, by using the up to 300 m long optic fibre cable. There, the excitation light in the probe excites the fluorescent dye present. Part of the fluorescent light emitted is received by a parallel optic fibre receiver in the head of the probe. After its passage through another optic fibre channel, it is sent to a detector with an emission filter. Thus, using several channels and several excitations lamps, detectors, and filters, it is possible to simultaneously determine several fluorescent tracers. However, special measuring techniques for surface water determinations using optic fibres are not yet fully developed.

Further possibilities for determining tracers in surface water are e.g. taking the sample and then analysing later in the laboratory. However, due to the increased effort and time delay, this technique is only possible and sensible under special situations. An alternative is using flow-through measurements. For this, the water containing the tracer is pumped aboard the boat and measured with a flow-through cuvette in a fluorimeter. This procedure is often unsuitable because it is very painstaking and prone to interference. Calibration is also problematic due to the water constituents in surface water. Further details and information concerning this measuring technique can be found in LEIBUNDGUT & HIRSIG (1977).

Moreover, since surface water bodies are not covered, aerial photos can be used to evaluate the horizontal propagation of the tracer. Under good lighting, the detection

limit for fluorescent tracers in natural water is at 50-100 µg/l. Aerial photos can supplement measurement profiles, since they supply spatial information. The evaluation of the photos with the help of photo-densiometry through calibration of the colour values with measured concentrations allows the quantitative determination of the tracer concentrations at the surface.

The tracers used in surface water investigations must also meet special requirements. Due to the biological activity of surface water, the injected tracers are subject to higher biochemical decay as compared with groundwater. Since only degradable tracers should be applied due to environmental reasons, only short-term tests should be carried out with a maximum of several days.

Since fluorescent dyes are the most frequently applied artificial tracers, photochemical decay is very important. Eosin and uranine are very sensitive to light and thus are unsuitable for use in surface water. Tracing tests in the hypolimnion of lakes, tests at night, short-term tests with very short exposition times, and tests that do not require a quantitative detection are exceptions. The rhodamines are best suited for tracing tests in surface water. Due to their more or less strong tendency towards adsorption, they should be used preferably in water low in suspended solids. All other fluorescent tracers can be used due to filter-technical, physical, or chemical reasons only under special conditions. Naphthionate has been successfully used in groundwater, but cannot be used in surface water due to the high background (LEIBUNDGUT & WERNLI 1988).

Since aquatic life comes into contact with the tracers used, the ecotoxicological harmlessness is a further important requirement placed on the tracers used in surface water. Standardized ecotoxicity tests carried out on suitable aquatic lifeforms are used to evaluate the tracer suitability and to compare the tracers. These tests are carried out on algae, daphnia, and fish. During the tests, the species are exposed to a 'worst case scenario' with very high tracer concentrations of 100 mg/l over an exposition of 20 days. However, in field tests in surface water, the tracers are diluted much more quickly, so that high concentrations are only present for a short time. The tracers can be rated as harmless, if there are no provable effects in the test at the concentrations used during the tracing test. The mortality and the behaviour of the species are registered during the test.

LEIBUNDGUT and HADI (1997) collected the prevailing information in a literature study. Among the rhodamines, rhodamine B and sulforhodamine B should be avoided due to their increased ecotoxicity, relative to the other tracers. However, the other rhodamines, such as rhodamine WT and amidorhodamine G, as well as uranine and eosin are harmless. Due to their stability in light and their toxicological harmlessness, rhodamine WT and amidorhodamine G are best suited for tracing tests in surface water (UBA 1997).

5.8.2 *Lakes*

Fluorescent tracers are mainly used in tracing tests in lakes. Investigations with natural water isotopes can often supplement the use of artificial tracers, to obtain information about the mixing ratio, age, and residence times of the entire lake.

The selection of the tracer, the injection amount, the injection procedure, and the measurement process must all be co-ordinated with respect to the tracing test goal.

Additional relevant information should be gathered beforehand to ensure the correct classification and interpretation of the results. These are the inflow and outflow relationships, wind and weather relationships, as well as air temperature and irradiation conditions. The determination of the depth with a pressure probe and of the temperature-depth profiles at the tracer measurement profiles is indispensable. When necessary, the electrical conductivity and the oxygen distribution must also be determined. The measurement of these parameters is not problematic.

HIRSIG et al. (1982) differentiate between external and internal artificial tracer injections in lakes. With an external injection, the water that enters the lake as a natural or artificial inflow is traced, in order to observe its behaviour upon entering the lake and in the lake. In this case, a thorough mixing of the tracer solution must be guaranteed, i.e. a sufficiently long flow distance is necessary when using natural inflows. With an internal injection, the tracer is injected directly into the lake with a hose or a depth-injection device, which injects the tracer at a specific depth. It must be guaranteed that the denser tracer solution will not sink to the bottom of the lake, but rather stays in the wanted stratification depth. To ensure this, the tracer solution can be mixed with a low density liquid and injected horizontally through a hose with a fitted T-tubing-connector at the end (Fig. 253). Furthermore, a point-source or a continual injection can be carried out, depending on the goal. A point-source injection would simulate an accident, whereas a continual injection would simulate a sewage effluent.

If the VARIOSENS measuring chain is used, the VARIOSENS instrument must be towed at the wanted depth with a boat. Figure 254 shows a schematic view of the measurement principle. When the measurement instrument enters the tracer cloud, shown by a 'precipitous rise in the recorder trace', a buoy can be set out for better orientation of the cloud. The same can be done after leaving the cloud or at concentration changes within the tracer cloud. The depth of the measurement instrument, the position of the boat, and the fluorescence measurements are registered, to determine the size and position of the tracer cloud in the lake.

Problems with determining the positions of the boats during tracing tests in lakes are often underestimated. Since well-equipped research vessels are not always available, theodolites must be used to determine the position of the boat. Theodolites with a mapped location can be used, which have an overview of the lake surface. By determining the azimuth angle between the boat and a known fixed point and the verti-

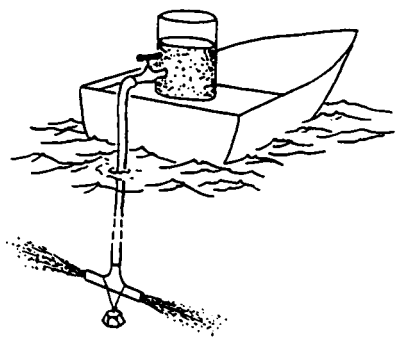

Figure 253. Injection of the tracer into the desired depth by means of a hose with a fitted T-tubing-connector at the end (after HIRSIG et al. 1982).

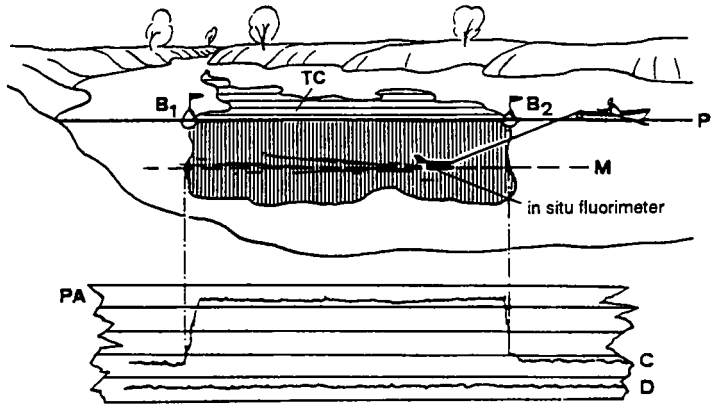

Figure 254. The principle of measurement of a tracer cloud within the body of lake water (after HIRSIG et al. 1982). TC = tracer cloud, P = profile line, M = measurement profile, B_1,B_2 = marker buoys, C = concentration of tracer, D = depth of measurement, PA = analogous record.

cal angle between the horizon and the boat, the position of the boat can be determined (LEIBUNDGUT et al. 1983). Determining the position with theodolites is indeed accurate, yet prone to errors, very painstaking, and cannot be transferred online to the data file. Moreover, distance and visibility impose limits upon this method. It cannot be used to determine the position at night or under foggy conditions. Thus, applying modern geodetic instruments, such as GPS, is recommended. However, the degree of accuracy can become problematic, since it depends on the price.

Artificial tracers can be used in lakes to solve various different limnological problems. Above all they are used to determine the current dynamics in lakes. The lateral currents can be inflow or wind induced. Especially currents caused by inflows are investigated preferably with tracing tests. Using the 'natural tracer' suspended solids, NYDEGGER (1967) elaborated the basics and was able to prove the impact of the CORIOLIS force in laboratory experiments with tracers in rotating lake models (NYDEGGER 1976). As a result, numerous tests have been conducted in primarily alpine and alpine foreland lakes with weak and strong currents (HIRSIG et al. 1982, HIRSIG 1983, PETERMANN et al. 1985, SALENCON & CALMELS 1995).

A classical example of a free from wind lake with weak currents is Lake Bled in Slovenia. In 1982, two tracing tests were carried out here, to determine the lake current patterns (LEIBUNDGUT et al. 1983). This example is especially interesting because the strongly eutrophic lake has an artificial sublacustric fresh water inflow and a deep water outlet for channeling off the oxygen-depleted deep water. A further goal was to investigate the internal lake remediation measures. The current relationships were investigated under two different fresh water inflow and deep water outflow conditions. The propagation of the tracer, which was injected externally through the fresh water inflow, was registered during measurement profiles with a VARIOSENS instrument. A detailed determination of the tracer propagation is displayed in Figure 255, which shows profile sections of the tracer concentration during different stages of the spreading of the tracer cloud after injection. The results of the investigation show that with higher inflow and outflow rates, the fresh water spreads through the

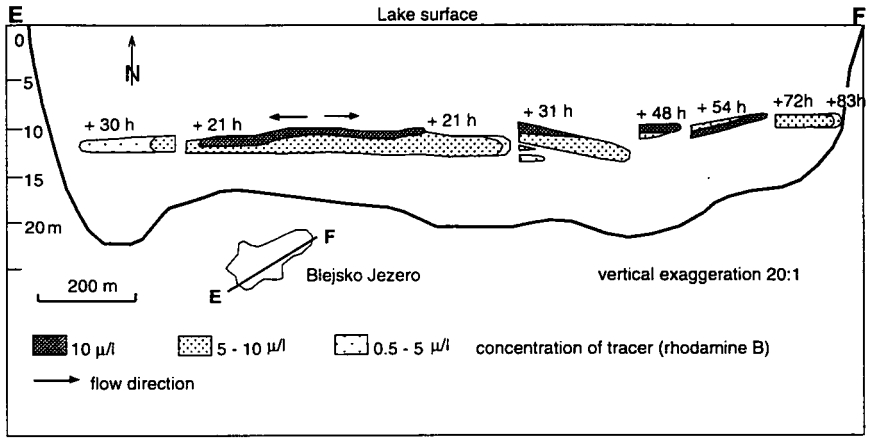

Figure 255. Rhodamine B tracer experiment in Lake Bled in Slovenia. Profiles during different stages of the spreading of the tracer cloud (+ 21 h = 21 hours after the tracer injection).

hypolimnion quicker and more broadly and reaches the deep water outflow faster (LEIBUNDGUT et al. 1983). Therefore, the mean turnover time of the hypolimnion is clearly reduced.

In the same lake, LEIBUNDGUT and ZUPAN (1992) were the first to try and determine mean residence times using an artificial tracer. Uranine was injected with the fresh water inflow into the hypolimnion. Using the lake volume and the artificial deep water outflow and the natural outflows during the stagnation phase, the uranine was balanced and thus a mean residence time calculated. The instability of the tracer in long-term tests was problematic.

Furthermore, artificial tracers can be applied to detect sublacustric inflows and outflows and to quantitatively determine them (ATTINGER & LEIBUNDGUT 1986, RIEG & LEIBUNDGUT 1992, LEIBUNDGUT 1995). Tracing techniques are especially suitable for determining water protection zone problems, such as hydrological connections between lakes, ponds, or pools and the bordering aquifers (LEIBUNDGUT & ADLER 1989).

Practical applications such as the spreading of sewage effluent in lakes or the impact of internal lake remediation measures such as deep water outlets are also preferably investigated with tracing tests. The use of artificial tracers allows the determination of convective, dispersive, and diffusive processes (WERTHEMANN 1980). In Lake Sempach, the impact of a lake ventilation was investigated with the help of tracer (HIRSIG & PETERMANN 1984).

Up to now, calibration and validation of mathematical current models based on experimental tracer results have been only rarely applied, seem however promising (LEIBUNDGUT et al. 1983, RAJAR & CETINA 1984).

5.8.2.1 *Case example: Optimization of a sewage effluent into Lake Murten*

Lake Murten is a well-mixed Swiss alpine foreland lake. The goal of the investigation was to follow the subaquatic stratification and propagation of a clarified sewage effluent into the lake, in order to determine the optimal effluent depth. The stratifica-

tion and propagation of the effluent are affected by physical environmental parameters such as the water temperature and the currents, which on the other hand are driven by wind and the water inflow (HIRSIG et al. 1982).

To accomplish this task, 6 kg of uranine were injected on 9 July 1980 over 3.5 hours through the existing sewage effluent at 8 m (external injection). The continuous injection ensured that possible short-term variable conditions upon entering the lake would be smoothed. During the following two days, the propagation of the tracer cloud in the lake was registered during 6 measuring boat rides with an underwater VARIOSENS fluorimeter.

As a result of the higher density due to the increased salt content of the sewage water and the heavy suspended solid load, the tracer solution sank at first and formed a ca. 1 m thick layer over the lake slope. At a depth of 10 to 12 m, the layer then stratified directly over the thermocline (Fig. 256). Additionally, the propagation of the tracer cloud was affected by the CORIOLIS force that caused a deflection to the right, a lake current induced by the La Broye, and a west wind induced current (Fig. 257). The current induced by the inflow was very strong during the test as a result of the high water level of the La Broye. Superimposed was the westward current caused by the wind, that was over the thermocline, where the stratification occurred. The superimposition of the currents is a plausible explanation of the observed spreading of the tracer cloud.

The maximal transport velocity was around 100-130 m/h. Based on the results of the tracing test, an optimal inflow depth of 9 m was recommended, since at this depth the La Broye induces a strong current over the thermocline. This ensures a dilution of the sewage and will thus prohibit an increased build-up of nutrients. Due to the superimposition of the currents caused by the inflow and the wind, part of the sewage water can rise to the surface of the opposite side of the lake (Fig. 258). However, by then, a sufficient dilution around the factor 1: 200-4000 has occurred, so that this is uncritical with respect to eutrophication.

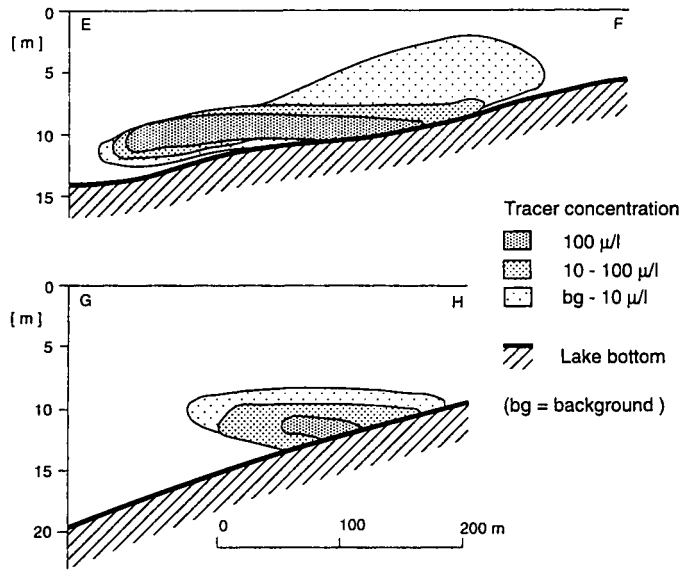

Figure 256. Vertical profiles E-F and G-H through the tracer cloud (for location see Fig. 257) (after HIRSIG et al. 1982).

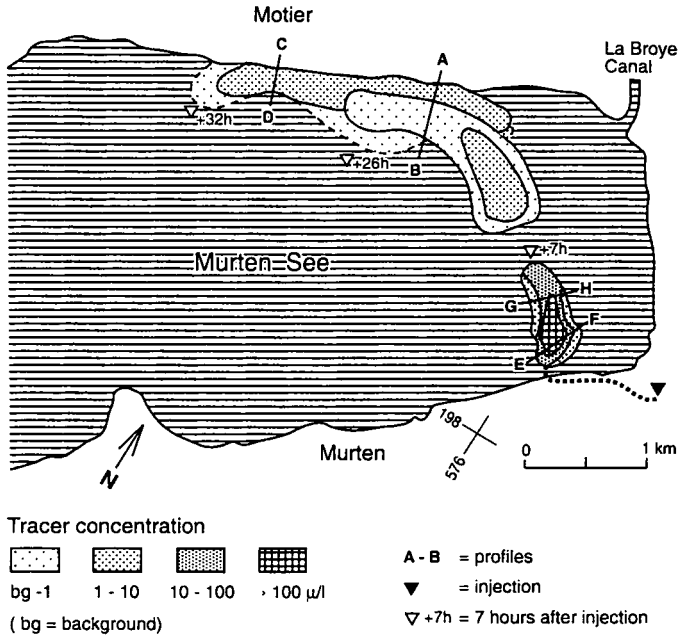

Figure 257. Discharge of treated effluent in the lake of Murten (July 1980). Situation and horizontal dispersion of the traced effluent (after Hirsig et al. 1982).

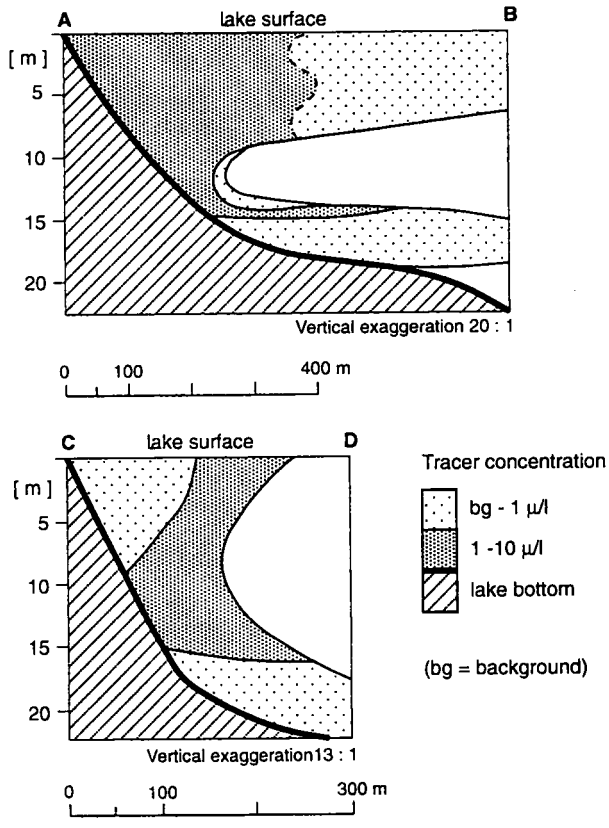

Figure 258. Vertical profiles A-B and C-D through the tracer cloud (for location see Fig. 257) (after HIRSIG et al. 1982).

5.8.3 *Flowing water*

The most important application of artificial tracers in flowing water is the investigation of flow and matter-transport processes. These results can be used in mathematical modeling, their calibration, and in simulations of pollutant propagation. The parameters determined with tracing tests, mean flow velocity and dispersion, describe pollutant propagation and dilution (HUBBARD et al. 1982, GRAF 1986, SPREAFICO 1991, LEIBUNDGUT et al. 1993).

Simple procedures allow the interpolation of the parameters onto unmeasured flow paths and other flow conditions (FRANÇOIS & CALMELS 1997). In an ideal case, the results of a tracing test to investigate matter-transport in flowing water lead to a mathematical modeling and a simulation of the pollutant propagation.

With the help of tracer calibrated matter propagation models, warning systems can be developed. During accidental pollutant inflow into the water, these systems can be used to predict the arrival time, the duration, and the concentrations of the pollutant plumes (VAN MAZIJK et al. 1992, IKSR/KHR 1993). For example, this tool can be used to disconnect river bank filtration systems from the public water supply in due time after an accident, in order to avoid direct public health hazards.

The application of tracers in flowing water can lead to the proof or exclusion of and to the quantification of flow connections with bordering groundwater aquifers. This is an important application with respect to the increasing importance of river bank filtration wells for drinking water.

Physical parameters of the water such as reaeration or irradiation can be determined with tracers. In the determination of the reaeration, which is a deciding factor for the recuperative power of flowing water, a gas tracer (e.g. ^{85}Kr) is injected into the water, which undergoes gas emission into the atmosphere. Since this gas emission process is determined by the same kinetics as reaeration, determining the tracer concentration after a flow distance can be used to calculate a value for the reaeration coefficient. The simultaneous concentration decrease of the gas tracers due to dispersion during the measurement procedure can be corrected by using a second conservative tracer (GÜNTHERT & BEHRENS 1982, KILKPATRICK et al. 1989).

Irradiation, important for photosynthesis and thus for primary production, can be integrally determined by injecting a light sensitive fluorescent tracer. It is also necessary in this case to correct the influence of the dispersion by using a second tracer that is not sensitive to light (BEHRENS & DEMUTH 1992).

With a tracing test, REBER and WEINGARTNER (1986) were able to investigate and quantify the phosphorus load from an upriver clarification plant in an old branch of the river Aare (Häftli).

Artificial tracers also allow the determination of the discharge of flowing water under strong turbulent conditions.

5.8.3.1 *Discharge measurement with the dilution method*

This method is based on determining the dilution of a known amount of tracer injected into the flowing water and has the advantage, that the discharge is determined integrally over the entire flow cross-section. Detailed instructions for determining discharge measurements are given in FISCHER (1982) and SPREAFICO (1994).

A prerequisite for carrying out such measurements is that the measurement of the

tracer occurs after a flow distance that guarantees a uniform mixing of the tracer over the entire cross-section. Formulas to estimate the minimum flow distances exist (KÄSS 1992), but they are not adequate since the channels are too heterogeneous. However, as a general rule, the following distances can be taken as the minimum flow distance: for turbulent small channels, 50 m; for larger streams, 200 m; and for rivers, several kilometres. With well-developed channels such as the Upper Rhine, the distance increases to several tens of kilometres. Experience is the best guarantee for correctly determining the flow distance needed.

If there are inflow sites between the injection and observation sites, the discharge is measured at the observation site. If water is withdrawn or there are percolation sites between the injection and observation sites, the discharge is only measured at the injection site.

The tracers usually used are sodium chloride and the light-stable, pH-independent, and non-sorptive fluorescent dyes rhodamine WT and amidorhodamine G. Due to environmental protection reasons, the often used chromates and active isotopes are no longer used in surface water. As a general rule, 10 kg of sodium chloride per m^3 discharge can be used to estimate the amount of tracer needed, depending on the background. For fluorescent tracers, this amount can be lowered corresponding to the detection limit by a factor of 10^{-4}. In discharge measurements, it must be differentiated between the 'instantaneous injection' and 'continuous injection' methods.

Instantaneous injection method (integration method)

The known amount of tracer is 'instantaneously' injected in the middle of the flowing water and after the necessary flow distance, the tracer breakthrough is determined (Fig. 259). To do this, either single samples are taken at short intervals or a continuous registration is recorded. The registration of sodium chloride can be carried out with a conductivity meter and the fluorescent dyes with an optic fibre fluorimeter or a field fluorimeter. In each case, a breakthrough curve of the tracer is obtained. With continuous registration, the discharge is determined with Equation (5.13) in which the injection amount is divided by the concentration-time-integral:

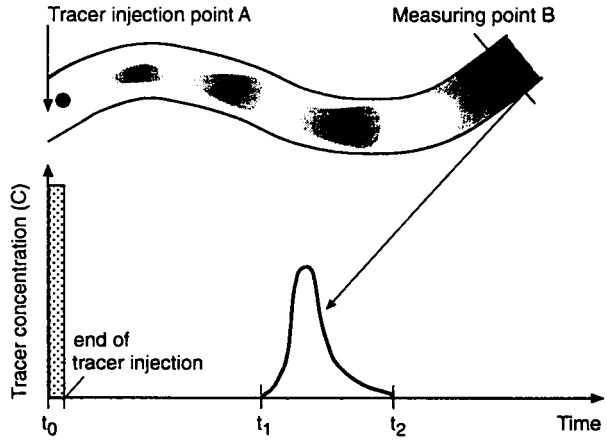

Figure 259. Schematic representation of a discharge measurement with instantaneous tracer injection (after MOSER & RAUERT 1980).

$$Q = \frac{M}{\int_0^\infty c_t \cdot \Delta t} \tag{5.13}$$

where Q = discharge in the flowing water, M = amount of injected tracer, c_t = tracer concentration at time t (the integral is the area under the breakthrough curve).

If single samples are taken, a temporally uniform sample interval is recommended. The calculation is carried out either in the discretizing form of Equation (5.13) or with uniform sample intervals according to Equation (5.14):

$$Q = \frac{M}{\sum_{i=1}^{n} c_{ti} \cdot \Delta t} \tag{5.14}$$

where c_{ti} = tracer concentration of the i^{th} sample interval, Δt = length of the constant time interval.

When single samples are taken, a mixed sample made from two samples with the same volume and time interval can be used. In this case the discharge is determined with Equation (5.15):

$$Q = \frac{M}{c_m \cdot (t_e - t_a)} = \frac{V_E \cdot c_E}{c_m \cdot (t_e - t_a)} \tag{5.15}$$

where c_m = tracer concentration of the mixed sample, t_a, t_e = time at the beginning and at the end of the tracer breakthrough, V_E = volume of the injection solution, c_E = concentration of the injection solution.

Sets for automatically measuring the discharge with instantaneous injection are available. They include a conductivity probe with a temperature sensor connected over an analog-digital-converter to a battery operated computer. It registers the passage of the instantaneously injected common table salt (NaCl) in the flowing water. The conductivity, corrected with the temperature sensor, is automatically registered and the background subtracted. The integrated plotter provides a measurement protocol, the breakthrough curve, and the calculated discharge. The results are ready in the field and the accuracy of the measurements can be checked. Under non-stationary discharge conditions, the instantaneous injection method results in the discharge at the time corresponding to the centre of the tracer breakthrough curve.

Continuous injection method

With this method, the tracer solution is injected over a sufficiently long time uniformly into the flowing water. The injection time span must be so calculated, that a sufficiently long plateau is reached in the concentration-time-curve at the observation site. The constant injection is either carried out with a MARIOTT bottle or with a constantly working pump (Fig. 260). The discharge is determined according to Equation (5.16):

$$Q = \frac{q \cdot c_E}{c_p} = \frac{M/t}{c_p} \tag{5.16}$$

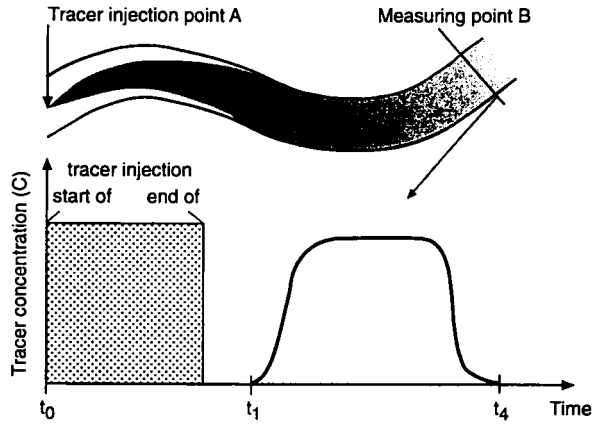

Figure 260. Schematic representation of a discharge measurement with continuous tracer injection (after MOSER & RAUERT 1980).

where q = volumetric flow of the injection, c_E = concentration of the injection solution, c_P = concentration of the plateau at the sampling site.

With the continuous injection method, the complete mixing can be checked by measuring the plateau value at different sites in the cross-section. In case the discharge relationships are unsteady, this method will not deliver a plateau value.

5.8.3.2 *Case example: Calibration of the Rhine alarm model*

After the contamination of the Rhine river caused by a fire in the Swiss chemical plant SANDOZ in 1986, a minister conference of the Rhine riparian countries decided to have an alarm model for the Rhine developed. It should be able to predict the arrival time and propagation of a pollutant plume in the Rhine. Between 1988 and 1992, numerous tracing tests were carried out in the Rhine, for use in the model development, calibration, and verification.

The model should be operationally applicable for real-time predictions and thus must be executable on a PC with current, generally available data. Therefore, a relatively simple one-dimensional dispersion model was selected (GRIFFIONEN 1989).

This model only considers the longitudinal dispersion and assumes a homogeneous distribution of the contaminant over the flow cross-section. Stationary discharge relationships are conditional and the decay can only be taken into consideration in a linear form. The results of the first tracing tests showed, that the model had to be enhanced with a stagnant water zone parameter, in order to satisfactorily simulate the tracer breakthrough. The matter transport in the water is retarded, due to the time spent by the contaminants in stagnant water zones in bank areas or on the river bottom. Thus the breakthrough curve has a larger loop.

Therefore, a proportionality constant α and a matter-transport, or respectively a stagnant water zone parameter β were added as calibration parameters (VAN MAZIJK 1996). Among others, the stagnant water zone parameter β takes into account the impact of the stagnant water zones upon the matter-transport velocity c of a tracer wave relative to the mean flow velocity v_m

$$c = \frac{v_m}{1+\beta} \tag{5.17}$$

The proportionality parameter α is defined by the longitudinal dispersion coefficient D_l

$$D_l = \alpha \cdot \frac{v_m^{\,2} \cdot B_S^{\,2}}{a \cdot v_S} \tag{5.18}$$

where B_S = width of the line of maximal flow velocity, v_S = shear stress velocity, a = mean water depth.

In order to consider the differences in the morphology of the Rhine, the river was subdivided into longitudinal sections. With the help of tracing tests, the matter-transport model parameters were to be determined for each section and the impact of the stagnant water zones upon the matter-transport was also to be investigated (VAN MAZIJK & VAN MIERLO 1992, VAN MAZIJK et al. 1992, VAN MAZIJK & WIESNER 1992, IKSR/KHR 1993).

The amount of tracer to be injected can be estimated with the help of a one-dimensional dispersion model, so that the tracer cloud passes the sampling sites with a sufficiently high concentration. During a test on 26 April 1988, 100 kg of rhodamine WT were injected downstream of Basel at Rhine-km 174.1 (cf. Plate 2). In order to achieve a lateral mixing of the tracer as fast as possible, it was injected upstream of the first power plant at the start of the Rhine lateral canal. The injection was completed in ca. 5 minutes as a point-source injection from a ferry in the middle of the canal. On the day of the injection, the Rhine had a discharge at station Pegel Rheinfelden of 1170 m^3/s. Automatic sampling devices were set up after the separate sections, to obtain complete tracer breakthrough curves. To ensure that the first appearance and maximal concentration of the tracer would be recorded during sampling, the devices were installed in the line of maximal flow velocity, downstream of the turbine outlets of the power plants, whenever possible. (Flow time differences in the cross-section). Through fitting of the matter propagation model for flowing water (Stoffausbreitungsmodell Fließgewässer, 'SAMF') with the measured tracer breakthrough curves, the parameters mean transport velocity and longitudinal dispersion coefficient were determined. SAMF is based on the analytical solution of the one-dimensional dispersion model.

The determined parameters were applied in the model calibration of the Rhine alarm model to obtain a first estimation of the needed parameters, which could then be exactly determined by fitting with the different breakthrough curves (LEIBUNDGUT et al. 1993).

To verify that the prerequisite of a homogeneous mixing of the contaminant over the river cross-section was fulfilled and to investigate the impact of the stagnant water zones and storage areas upon the distribution of the tracer, the one-dimensional data acquisition with the automatic sampling devices (APEG) was complemented with two-dimensional measurements (VARIOSENS-measuring chain). By taking profile measurements with an underwater fluorimeter from a research vessel, the longitudinal, lateral, and vertical matter propagation could be determined. The locations of the APEG's used to determine the longitudinal dispersion in the different sections are shown in Figure 261. Aerial photos of the tracer cloud complemented the investigations.

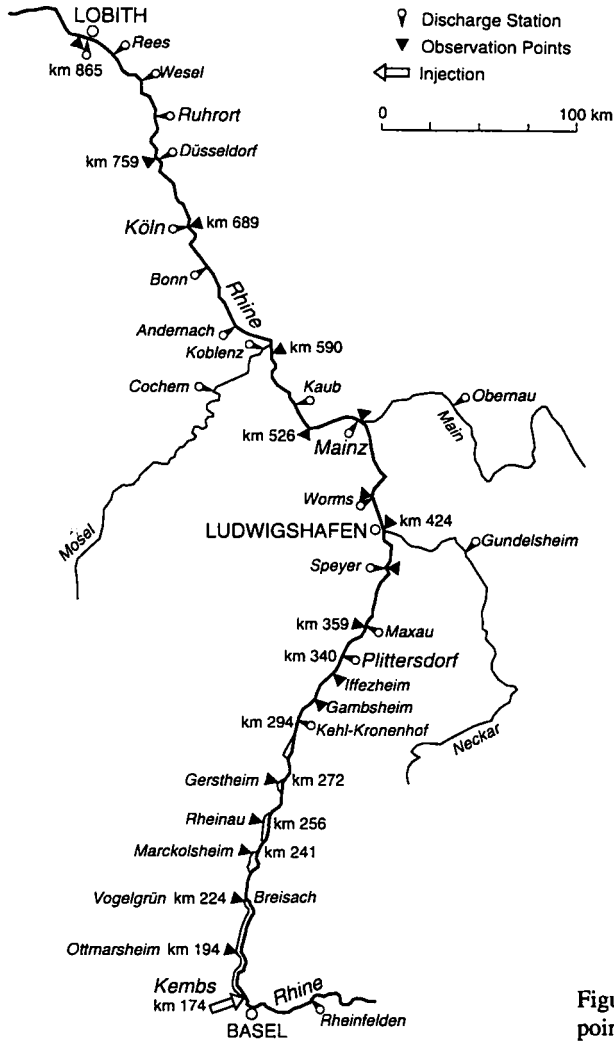

Figure 261. Injection and observation points in the river Rhine.

Figure 262 displays the measured concentration curves for the Upper Rhine sections. After a steep rise to the concentration maximum, they show, dependent upon the flow characteristics and the sampling site, a more or less slow decrease in concentration. Parameters such as the first appearance and maximal matter concentration can be taken from the breakthrough curves. The graphs illustrate the expected quick decrease of the maximal concentrations in the flow direction, which is attributed to the longitudinal dispersion. Figure 263 shows the tracer breakthrough curves modeled from the measured curves, which were used to calculate the transport parameters longitudinal dispersion and mean transport velocity. Table 39 lists the calculated mean transport velocities for each section and the longitudinal dispersion coefficients. All of the determined matter-transport parameters vary with the discharge of the Rhine and the determined parameters are only valid for the discharge of the Rhine during the tracing test. Furthermore, they are strongly dependent upon the de-

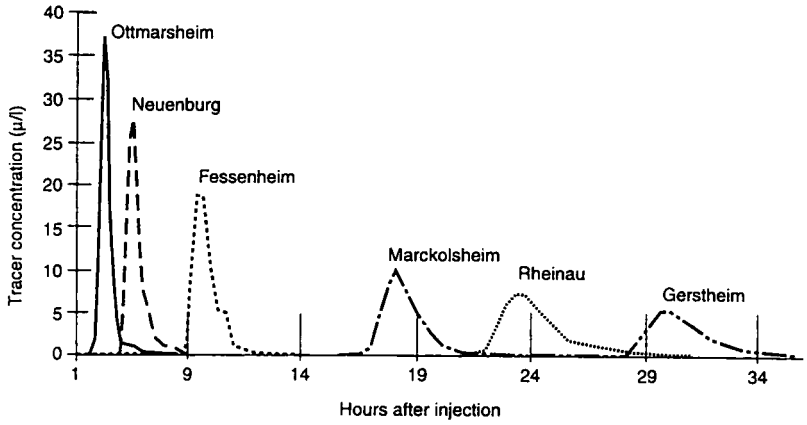

Figure 262. Tracer breakthrough curves for some observation points in the Upper Rhine.

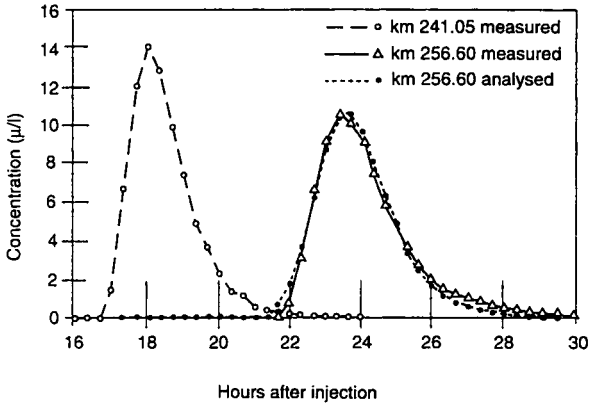

Figure 263. Input tracer curves (measured) and analysed transport parameters for Rhine section Marckolsheim-Rheinau. Longitudinal dispersion coefficient: 76 m^2/s, mean transport velocity: 0.8 m/s.

Table 39. Results of the tracing test in the Rhine river 1988.

Rhine section (KW: power station) (WSA: waterway service)	Rhine improvement	Rhine-km	Effective flow velocity (m/s)	Longitudinal dispersion coefficient (m^2/s)
Village-Neuf – KW Ottmarsheim	Bypass	174-194	1.09	20
KW Ottmarsheim – Neuenburg	Bypass	194-199	1.09	41
Neuenburg – KW Fessenheim	Bypass	199-211	1.08	42
KW Fessenheim – KW Marckolsheim	Transition	211-241	0.98	63
KW Marckolsheim – KW Rheinau	Meander	241-257	0.80	76
KW Rheinau – KW Garstheim	Meander	257-273	0.68	19
KW Garstheim – KW Strassburg	Meander	273-288	0.96	112
KW Strassburg – WSA Steiger Kehl	Transition	288-294	0.87	294
WSA Steiger Kehl – KW Gambsheim	Free flow	294-311	0.65	841
KW Gambsheim – Plittersdorf	Free flow	311-340	0.74	396

velopmental level of the Rhine in the different sections. As expected, the transport velocities in the Rhine lateral canal are higher than those in the meander solution and river improvement sections. The determined transport times in the section from Basel to Strassburg are especially interesting, since due to the complex course of the Rhine with river branches and numerous barrages, reliable transport forecasts with flow time models are difficult. This is especially true at discharge conditions, at which the power plants run the discharge controls at the so-called swelling action. If the relatively low values for the dispersion coefficients between Rheinau and Gerstheim are neglected, it can be ascertained that a low dispersion prevails in the Rhine lateral canals, that the meander solution sections have a middle dispersion, and that the Rhine improvement areas and the free flow sections have a high dispersion. These results are connected with the different velocity distributions in the various Rhine improvement types, which are decisively influenced by the respective wall roughness as well as the geometry of the cross- and longitudinal-sections.

Stagnant water zones can have a considerable influence upon matter propagation (Fig. 264). This is schematically displayed for a section with groynes in Figure 265.

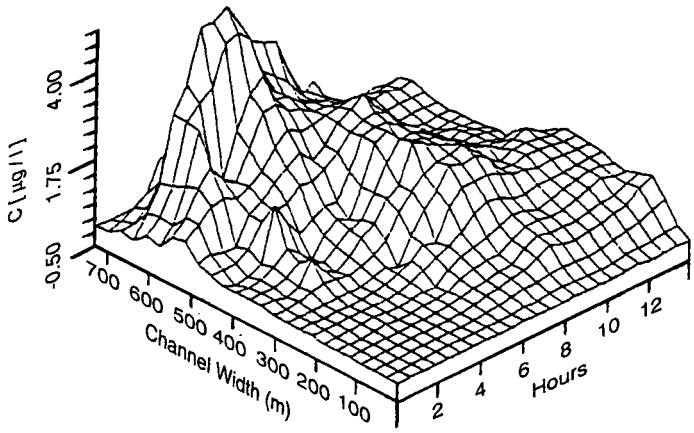

Figure 264. Tracer breakthrough in a river cross-section, influenced by stagnant water zones.

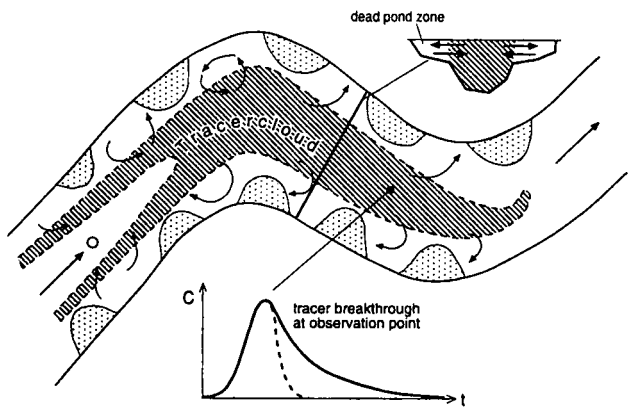

Figure 265. Schematic representation of the influence of stagnant water zones upon solute transport (tracer transport).

In the front section of the tracer cloud, the concentrations in the line of maximal velocity are larger than in the bank area, whereas after the concentration maximum passes, the relationships reverse (LEIBUNDGUT 1991).

Further tracing tests were carried out under other discharge conditions for the Rhine so that measured parameters were available for low, middle, and high water levels. Thus, the Rhine alarm model could be calibrated and verified. During the calibration at middle water levels, transport times with deviations from the model on the average of 2% were reproduced. Verification under other discharge conditions shows mean transport time differences of 5%, so that the model quality is satisfactory (VAN MAZIJK et al. 1992). Tracing tests represent an indispensable technique for investigating flow systems and for providing natural data for developing and calibrating matter-transport models for flowing water.

5.9 ENGINEERING

W. Käss

Hydrological tracing techniques can be helpful in many cases concerned with civil and mining engineering. This chapter handles examples from the following: hydraulic engineering, deep-well drilling techniques, a pumping test, and also remediation techniques.

5.9.1 *Leakage tests*

Leakage tests in science and technology deal with finding leaks in dams and embankments. It is important not only to determine if there are actual leaks in a dam, but also to recognize possible bypasses and to eliminate them.

There are numerous procedures to achieve this goal. The simplest method is to measure the groundwater levels in wells in and around the dam and then to determine possible underground flow paths from the groundwater contour maps. However, such maps reveal nothing about the velocity.

Another procedure was covered briefly in Section 2.14. Here temperature and self-potential measurements revealed leaks in the dams. Numerous leakage tests have been carried out since the fifties with active isotopes. SCHIECK (1958) investigated two dams in Thüringen/FRG with ^{131}iodine; MOSER and NEUMAIER (1958) also applied ^{131}iodine in the Lech Dam Roßhaupten near Füssen (Bavarian Swabia). Single well measurement methods applied in observation wells to determine vertical movements in the wells can reveal leaks in and around dams. DROST (1970) applied this method in the Upper Isar river on the Krün Dam and on the Sylvenstein Dam. Basic research was carried out by PLATA BEDMAR (1991).

Only a few publications describe leakage tests with dyes. During construction of the Dießbach-Reservoir (Steinernes Meer, Salzburg Alps/Austria), BRANDECKER et al. (1965) conducted successful dye and spore drift tracing tests. On the Bigge Valley Dam (Sauerland/Western Germany), leakage tests were carried out in the bedrock there that consists of sandy clay slates and Devonian greywackes (HEITFELD & TÄTZLER 1967). Both authors used uranine to label the seepage water.

Due to the limited possibilities for applying radioisotopes at this time, it seems advisable to describe an example using uranine to test for leaks.

To limit flood damage on the upper Nagold (Northern Black Forest/Southwestern Germany) near the township of Erzgrube of the town Seewald, a low weir upstream and a main reservoir dam were constructed. The bedrock is made up of Middle Bunter Sandstone, with fissures especially on the valley slopes. To decrease the possible water losses, that would be expected during the damming due to bypass and underflow, injection films were inserted. During construction and damming, dye tracing tests were conducted in the lake water in order to check various sealing measures.

In conclusion, the sixth dye tracing test was conducted on 18 September 1972 with 25 kg of uranine. The dye was partially injected by towing with a motor boat and partially by interspersing. The dye injection lasted just over two hours. Even several hours after the dye injection, the concentration distribution in the dammed water was irregular; from 1-1.4 µg/l.

Afterwards, a large number of samples were taken from observation sites and examined for uranine (Fig. 266):

Dam:	23 sites, with 9 positive dye detections,
Observation wells:	27 sites, with 12 positive dye detections,
Springs and drainages:	5 sites, with 4 positive dye detections.

Except for one exception, the positive dye detections were all on the right-hand side of the valley and in the right-hand valley floor. The dye concentrations in the observation wells and in the springs were always under 1 µg/l.

The dye breakthrough curve for observation site 44 is shown representatively in Figure 267. This site is ca. 500 m downhill of the dam crest.

Result: The dye tracing test at full capacity showed that leaks are present. Furthermore it showed that the permeabilities have strongly decreased as compared to those determined before the injection films were inserted (EISSELE & LINK 1981).

Summary

– Due to its negligible sorptivity, uranine is very suitable for investigations to determine leakage in and on dams.

– In dams that are turbid, and especially those that are also deep, the photolytic decay of uranine can be neglected in qualitative investigations.

– In quantitatively determining seepage water flow, it is almost impossible to achieve a uniform dye concentration distribution especially in large and deep reservoirs. Using a motor boat to tow water permeable sacks filled with the dye does not provide adequate uniformity in the dye distribution. In reservoirs with thermal stratification, only the epilimnion can be dyed anyway.

– Whereas injecting crystalline dye at presumed leakage points in the reservoirs provides high dye concentrations on the see bottom, this does not insure a dyeing of the actual water intake sites.

In contrast to the example from the Nagold Dam 'Erzgrube', the tracer can also be injected in observation wells in the dam. In leakage checks in river dams where the river water level is over the surrounding countryside, injecting the tracer in the river is not sensible. In such cases, the injection of uranine solutions in boreholes on top of the dam has proved useful.

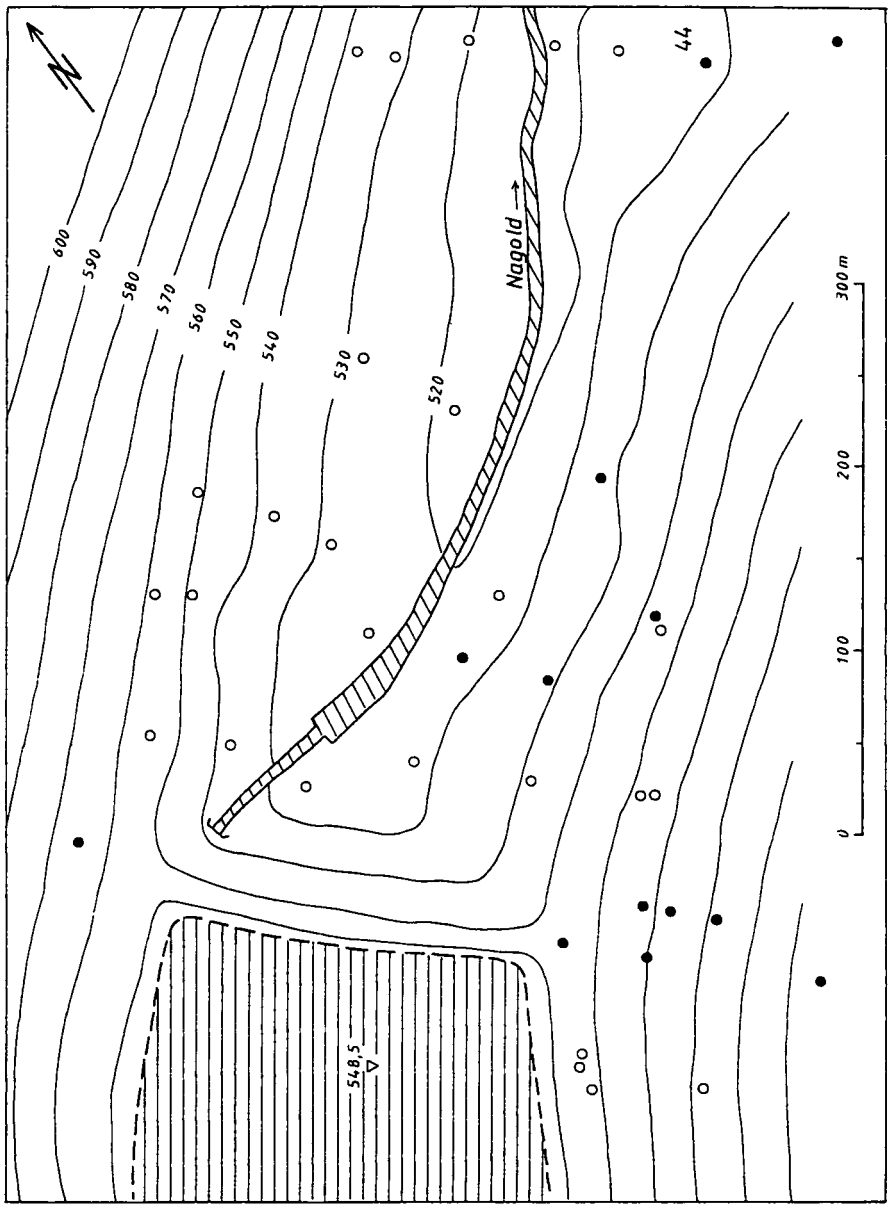

Figure 266. Map of the observation sites during the sixth dye tracing test in the Nagold-Dam 'Erzgrube'. Empty circles: no reappearance, solid circles: uranine detection. Contour lines at 10 m-distances. Observation site 44: Dye breakthrough curve Figure 267 (according to documents from the Geological Survey of Baden-Württemberg).

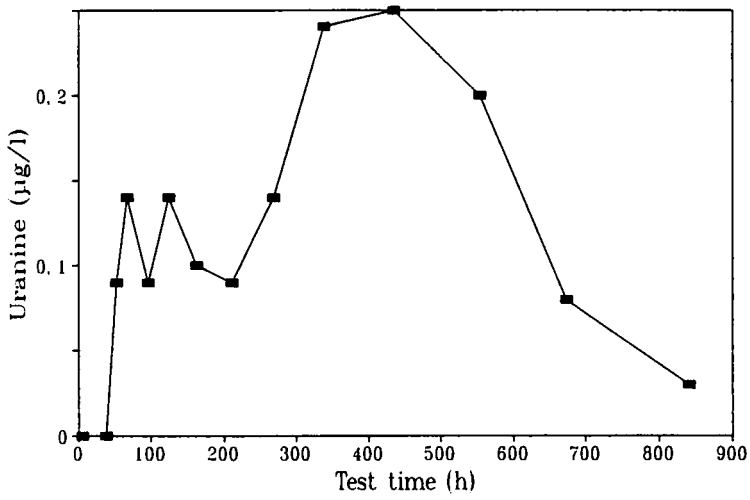

Figure 267. Dye breakthrough curve in observation site 44 (Fig. 266). The first dye detection occurred ca. 39 hours after the lake was injected.

5.9.2 *Deep well techniques*

In very deep boreholes, it is important to know how long the drilling mud requires for circulation. Of course this can be estimated with calculations. Exact values can be obtained with labelling the mud, since possible undercutting or mud losses cannot be determined with calculations. The engineer requires knowledge of the circulation time if the drilling mud is to be changed. The field geologist must be able to classify the drill cuttings that are taken from the shaking screen with the correct depth. This can only be accomplished if the ascent time is taken into account.

Conducting traces in drilling muds is difficult due to the clay minerals and the salt contents often present. If water is used as the mud, determining the circulation time is simplified. The Swiss National Association for Storage of Radioactive Waste (NAGRA) has developed a tracing method for checking borehole cleaning with m-trifluoromethyl benzoic acid (m-TFMB). However, the analysis using HPLC-analysis techniques is very demanding (Section 2.3.3) and time-consuming, so that the results needed for drill technical decisions usually arrive too late. NAGRA was able to obtain very good results in boreholes drilled with deionate, with m-TFMB as with uranine (NAGRA 1985).

Since in the field laboratories at the borehole sites press water from the drilling mud is regularly determined, uranine could also be used in clay or salt brine drilling mud to determine the circulation time. A semi-quantitative analysis for uranine in press water can be carried out with a quartz lamp, part of every field laboratory.

Radioactive tracing would be a very elegant tracing method with immediate results, if the handling of radioactive materials, especially in borehole sites, were not so regulated.

5.9.3 *Hydraulic tests*
I. Stober

Hydraulic tests, depending on how the test is carried out, its length, the type of withdrawal pumps, and the radius of the drawdown cone, can be applied to determine the development and characteristics of the well as well as those of the aquifer and the bordering rocks. A classic pumping test consists of an aquifer test and a well test, separated by the so-called recovery phase where the pumps are stopped (STRAYLE et al. 1994).

In connection with tracer tests, only the aquifer tests are of interest. In aquifer tests, a constant withdrawal rate is pumped out of a well over a long period of time and the resulting drawdown of the water level (pressure) in the well and in the surrounding monitoring wells is recorded. When the withdrawal is stopped, the rise of the water level is recorded as well. From the shape or form of the drawdown and recovery curves, conclusions concerning the well and the specific properties of the aquifer can be drawn.

Wellbore storage and skin factor are properties that specifically concern the well. The wellbore storage is only important at the beginning of the pumping phase, when the water pumped comes directly from the well. Drainage from the aquifer into the well starts after a delay. The wellbore storage is thus dependent upon the well radius and upon the transmissivity of the aquifer. The skin factor is a measure of the difference in permeability between the aquifer and the surroundings of the well. Skin effects can be caused during drilling, during the development of the well, or by other factors. In general, they are effective during the entire test (STOBER 1986).

In order to be able to draw conclusions concerning the aquifer properties from the drawdown and recovery curves, the evaluation of the pumping tests must be based upon a model using realistic hydraulic characteristics of the aquifer. There are numerous model approaches for porous and fissured aquifers (STOBER 1986). The following lists the most important ones:

- Homogeneous, isotropic aquifer,
- Aquifers with boundaries (rivers, lakes, confining valleys),
- Aquifers with vertical water inflow from low permeable layers (leaky aquifer) or with pore drainage,
- Aquifers, that have preferred flow and storage layers,
- Aquifers, that consist of a 'two-porosity medium' (e.g. fissured, permeable sandstone),
- Aquifers with a finite dimensioned fracture.

Selecting the correct evaluation procedure is oriented on the hydrogeological conditions. Furthermore, it is also dependent upon the form of the drawdown and recovery curves. The data from these curves must be exactly analysed with special techniques. Thus it is not possible to assign a certain aquifer model to a geological formation beforehand.

Depending on which aquifer model best fits the natural conditions, very different aquifer parameters can be determined when evaluating pumping tests. In the classic model of an homogeneous, isotropic aquifer only the transmissivity and the storage coefficient are determined. Within aquifers with vertical inflow, the leakage coefficient can also be determined. Aquifers, that have preferential flow and storage layers

or those that consist of a two-porosity medium, the properties of both systems can be determined. With pumping tests in aquifers with finite dimensioned fractures, survey data from the fractures, even as specific as their angle of inclination can be won.

The possibilities of gaining information about the hydraulics of an aquifer with pumping tests are undoubtedly immense. However, they cannot replace tracer tests. Only with the help of tracer tests can data about the spatial and temporal mixing and distribution of water constituents (dispersion, dispersivity) and the effective porosity of a confined aquifer be determined. In unconfined aquifers with free water tables, the storage coefficient determined by pumping tests corresponds roughly to the effective porosity. Moreover, with respect to accidents with hazardous materials and remediation cases, it is important and only possible with tracer tests, to obtain current data about the residence times of water constituents in the aquifer and their first appearance in the wells. Tracer tests that are carried out simultaneously with pumping tests are particularly informative, although this is seldom done.

The following compares the results from a pumping test with those from a simultaneous tracer test. The investigation area Kirchdorf-Unteropfingen lies in the Iller Valley. The Würm gravel valley filling is mainly composed of alpine Rhine glacial material, which consists of well rounded, stratified, fine to coarse gravels with intercalated sand fractions. This gravel fill makes up the aquifer, whose bottom confining bed is made up of fine sand and clayey marl layers of the Upper Fresh-Water Molasse (MELU/MWMV 1982). In the investigation area Kirchdorf-Unteropfingen, this underlying confining bed is fairly horizontal, so that the unconfined aquifer has almost a constant thickness (Fig. 100 top). The hydraulic investigations were based on the classic model of a homogeneous, isotropic aquifer.

The tracer test was carried out during a pumping test that lasted several months. A constant $Q = 0.38$ m^3/s was pumped from the Kirchdorf-Unteropfingen well. For the tracer test, 3 kg of uranine as a concentrated solution were injected in a groundwater monitoring site 585 m upflow. The injection well was filtered over the entire aquifer thickness. The test was carried out by the director of the Chemical Laboratory of the Geological Survey of Baden-Württemberg (W. KÄSS). During the tracer test, numerous water samples were taken. A detailed description and evaluation of the test can be taken from STOBER (1980). Plate 4 shows the determined uranine concentration in the Kirchdorf-Unteropfingen well as well as the cast line of the tracer breakthrough. The maximal concentration was 2.8 µg/l and was measured after ca.18 days in the well. The first traces of the tracer were observed after just under three days. Since the tracer test was carried out simultaneously with a pumping test, radial convergent flow conditions prevailed. The evaluation in Figure 268 is based on suitable type curves. The following aquifer parameters were determined:

From the pumping test:
- Transmissivity $T = 0.283$ m^2/s,
- Storage coefficient $S = 0.14$.

From the tracer test:
- Effective porosity $n_d = 0.08$,
- Effective flow velocity $u(r) = 0.52$ m/h,
- Dispersion $D_L(r) = 38$ m^2/h,
- Dispersivity $\alpha_L = 73$ m.

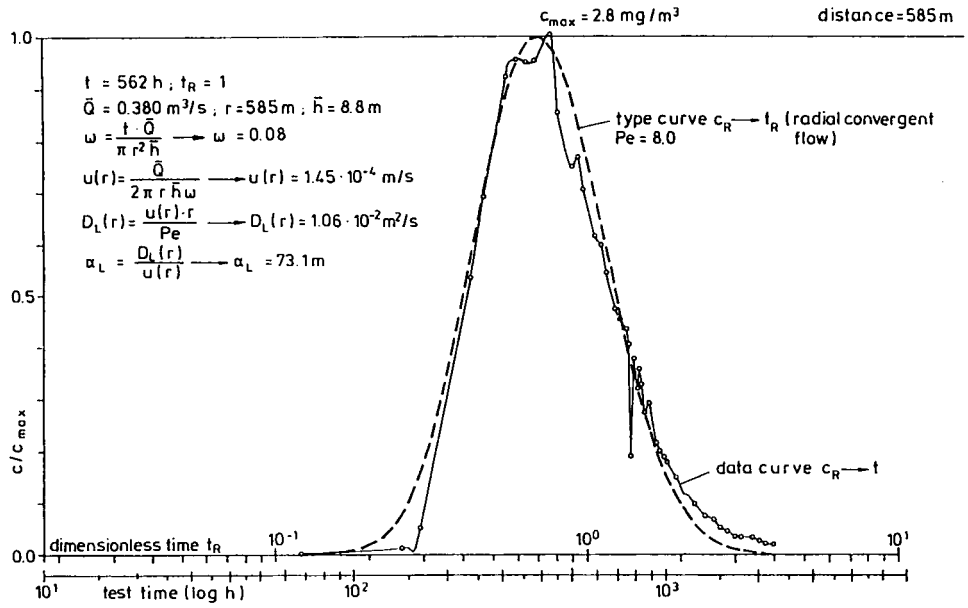

Figure 268. Dye breakthrough curve for the dye tracer test Kirchdorf/Iller-Unteropfingen on 19 Nov. 1979 with 3 kg of uranine. Logarithmic time scale in hours after injection. Type curve dashed. Equations for the parameter calculation (STOBER 1980).

The effective porosity gained from the tracer tests is slightly lower than the storage coefficient obtained from the pumping test. Theoretically, in unconfined aquifers, both values should be equal. There could be many reasons for this difference, e.g.:

– At the time of the dye injection, the injection site could have been outside of the cone of depression. The tracer cloud would then have spread out two-dimensionally in a linear flow field, before it would have reached the cone of depression. Later, most of the tracer cloud would have been affected by the radial convergent flow field, yet parts of it could have bypassed the well, as measurements in the downflow groundwater monitoring sites showed.

– The pumping test could have investigated different vertical and horizontal parts of the aquifer than the tracer test.

– The actual groundwater flow paths – as proven through numerous tracer tests – deviate, in part considerably, from the general flow direction given by the large-scale hydraulic gradient. The tracer propagation is determined by the naturally occurring heterogeneities present in almost all natural valley gravel deposits.

It is very important to ensure that constant flow conditions in the aquifer prevail during tracer tests. In Section 5.6.1 an example of a tracer test carried out between two thermal water wells describes this in detail.

5.9.4 *Partitioning tracing – The use of partitioning tracers to detect nonaqueous phase liquid contamination*

D. Hunkeler

Introduction

Contamination of aquifers with nonaqueous phase liquids (NAPLs) affects the quality of groundwater worldwide. The most common NAPLs found in aquifers are petroleum hydrocarbons which are lighter than water (lNAPLs) and chlorinated hydrocarbons which are denser than water (dNAPLs). Although NAPLs are immiscible with water, their solubilities are sufficiently high to result in concentrations of dissolved species that are orders of magnitude greater than drinking water standards (PANKOW & CHERRY 1996). Methods to detect and quantify NAPL contamination are required to assess the risk of NAPL contamination, to choose appropriate remediation measures and to verify the success of remediation measures. dNAPLs are particularly difficult to detect since they can move below the water table in aquifers and migrate along flow paths that are different from those of the groundwater (PANKOW & CHERRY 1996). lNAPLs are easier to detect because they float on the water table. NAPL contamination is usually detected and quantified by analysis of core samples. However, since core samples from bore holes only provide information at discrete points, it is often difficult to detect NAPL contamination using this technique. Furthermore, the volume of core samples is usually too small to obtain a representative average NAPL saturation (MAYER & MILLER 1992).

In the last several years, the use of partitioning tracers to detect and quantify NAPL contamination has found increasing interest (JIN et al. 1995, NELSON & BRUSSEAU 1996, WILSON & MACKAY 1995). Partitioning tracer methods to detect NAPLs consist of the simultaneous injection of one or several tracers that partition between the NAPL and the water or gas phase (denoted as partitioning tracers) and a conservative non-partitioning tracer. Based on the retardation of the partitioning tracers relative to the conservative tracer, the average NAPL saturation is estimated. The methods were originally developed to determine residual oil saturation in both water-saturated (SHEELY 1978, SHEELY & BALDWIN 1982, TANG 1992, TOMICH et al. 1973) and gas-saturated oil reservoirs (TANG & HARKER 1991a,b). Partitioning tracer methods have the advantage that they involve much larger volumes of aquifers than core samples. Furthermore, the same monitoring well can be used for repeated determinations of the NAPL saturation. The use of partitioning tracers to detect and quantify NAPL contamination in aquifers is a new technique which is still in development; however, several laboratory and field studies have yielded promising results.

5.9.4.1 *Single well partitioning tracing test*

Single well partitioning tracing tests (SHEELY 1978, SHEELY & BALDWIN 1982, TOMICH et al. 1973) have been widely used in petroleum engineering to estimate residual oil saturation before and after performing enhanced oil recovery operations. Single well tests consist of the injection of water containing an ester (e.g. ethyl acetate) followed by water without the ester. Pumping operations are then stopped for about two weeks to permit a portion of the ester to hydrolyze and form a short chain alcohol (e.g. ethanol). Finally, the water is extracted again and the breakthrough curves of the ester and the alcohol are measured. While the ester partitions between

the NAPL and water phase in the subsurface, the short chain alcohol is predominantly dissolved in the water phase. As a result, the alcohol travels with a higher velocity and arrives at the well earlier than the ester. The difference in arrival time allows the estimation of the residual oil saturation (SHEELY & BALDWIN 1982). Single well tracing tests can only be applied when the well is close to the location of the NAPL. Furthermore, single well tests are difficult to interpret if the groundwater migrates during the period without pumping. These disadvantages can be overcome by using interwell tracing tests (TANG 1992).

5.9.4.2 *Partitioning interwell tracing test*

Partitioning interwell tracing tests are used increasingly in petroleum engineering to determine residual oil saturations (ALLISON et al. 1991, TANG 1992). In the last several years, the method has been adapted to detect and quantify NAPL contamination in the water–saturated or unsaturated zone of aquifers by researchers of the University of Texas, USA (JIN et al. 1995, WHITLEY et al. 1995). The University of Texas and Intera, a private American company, jointly patented the new technology. The partitioning interwell tracing test consists of the simultaneous injection of one or several partitioning tracers and a conservative tracer at one or several injection wells and the subsequent detection of the tracers at one or several monitoring or extraction wells. During the test, water or air is continuously injected and extracted. Based on the retardation of the partitioning tracers relative to the conservative tracers (Fig. 269), the average NAPL saturation S (= Volume of NAPL/Volume of pore space) in the aquifer can be calculated. Mathematically, the retardation of the partitioning tracers can be described by the retardation factor R which is defined as the ratio of the mean travel time of partitioning tracer ($\bar{t}_{PT}$) to the mean travel time of the conservative tracer ($\bar{t}_{CT}$):

$$R = \frac{\bar{t}_{PT}}{\bar{t}_{CT}} = 1 + \frac{S}{1-S} \cdot K \tag{5.19}$$

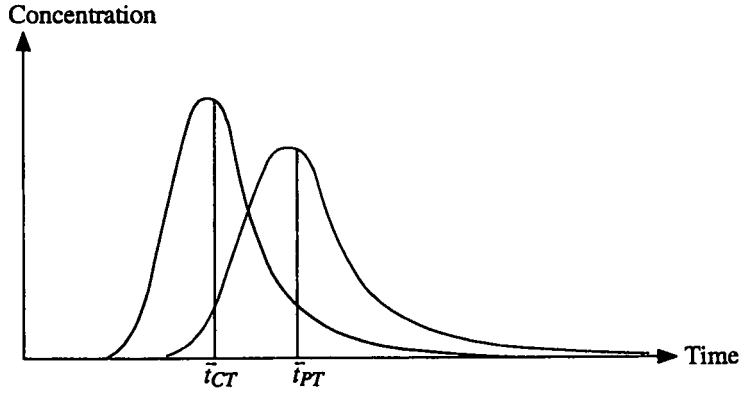

Figure 269. Schematic illustration of breakthrough curves of a conservative and a partitioning tracer. The methods to calculate the mean travel times of the tracers from the breakthrough curves are described in detail in other chapters. Based on the mean travel time of the partitioning tracer ($\bar{t}_{PT}$), the mean travel time of the conservative tracer ($\bar{t}_{CT}$) and the partition coefficient K, the average NAPL saturation S can be calculated using Equation (5.20).

where K = NAPL-water/gas partition coefficient (concentration of partitioning tracer in NAPL divided by concentration of partitioning tracer in water/gas phase at equilibrium).

Equation (5.19) can be derived from the advection–dispersion transport equation assuming that the distribution of the partitioning tracer between the NAPL and the water phase is always at equilibrium (NELSON & BRUSSEAU 1996). According to Equation (5.19), the retardation R of the partitioning relative to the conservative tracer increases with increasing NAPL saturation S. Rearrangement of Equation (5.19) yields Equation (5.20) which can be used to calculate the average NAPL saturation based on the mean travel time of the partitioning tracer, the mean travel time of the conservative tracer and the partition coefficient (JIN et al. 1995):

$$S = \frac{\bar{t}_{PT} - \bar{t}_{CT}}{(K-1)\cdot \bar{t}_{CT} + \bar{t}_{PT}} \tag{5.20}$$

In addition to the method presented above, inverse modeling methods are developed to analyse the breakthrough curves of the tracers and to calculate NAPL saturation. The inverse modeling methods have the potential to yield additional information about the spatial distribution of NAPL (JIN et al. 1995).

Ideally, partitioning tracers should be transported unretarded in the uncontaminated zone (no sorption to aquifer solids) and should partition between the NAPL present in the aquifer and the water or gas phase. Furthermore, they should be nontoxic, non-degradable, detectable at low concentrations, and their natural background concentration should be low. The partition coefficients of partitioning tracers that have been used so far are summarized in Table 40. As conservative tracers, tritiated water (JIN et al. 1995) and bromide (NELSON & BRUSSEAU 1996) have been used for studies in water-saturated sand columns or aquifer sections, and methane and argon (WHITLEY et al. 1995) for studies in unsaturated sand columns or aquifer sections. The partition coefficient K of the partitioning tracer should be large enough to ensure a good separation of the partitioning and the conservative tracers without unduly delaying the tracer recovery. If a partitioning tracer test is performed to detect NAPL contamination, a tracer with a large partition coefficient may be used. This allows observation of the retardation of the partitioning tracer and thus detection of NAPL even if the zone of contamination is small compared to the distance between injection and extraction well. If the location of the NAPL is known and a partitioning

Table 40. Properties of partitioning tracers used for partitioning tracer tests in the water-saturated and unsaturated zone of aquifers.

Partitioning tracer	NAPL/mobile phase	K	Temp.	
SF_6	Tetrachlorethylene/water	32 ± 1.33	22°C	WILSON & MACKAY 1995
	Dichlormethane/water	24 ± 1.27	22°C	WILSON & MACKAY 1995
	o-dichlorbenzene/water	45 ± 1.89	22°C	WILSON & MACKAY 1995
2,3-dimethyl-2-butanol (DMB)	Tetrachlorethylene/water	2.76	23°C	JIN et al. 1995
^{222}Rn	Diesel fuel/water	40 ± 2.3	12°C	HUNKELER et al. 1997a
C_4F_8	Trichlorethylene/air	4.8	20°C	WHITLEY et al. 1995
C_9F_{18}	Trichlorethylene/air			

tracer test is used to quantify NAPL saturation, a partitioning tracer with a smaller partition coefficient may be chosen to reduce the time of the experiment.

The partitioning and the conservative tracer are injected over hours to several days depending on the distance between injection and extraction well and the flow velocity of the groundwater. To obtain information about the vertical distribution of the NAPL contamination, the tracers may be injected and monitored at different depths using multilevel wells. The breakthrough curves of the tracers can be measured at monitoring wells between the injection and the extraction wells and/or at the extraction well. In the first case, the breakthrough curves of the tracers yield more local information on NAPL contamination upgradient of the monitoring well. In the second case, the NAPL saturation in the entire swept volume is detected (NELSON & BRUSSEAU 1996). Partitioning tracer tests reflect the average NAPL saturation along the flow paths of the groundwater and not necessarily the average saturation in a given volume of the aquifer. Variations of the hydraulic conductivity due to variations of the geological structure or due to the presence of NAPL may cause a bypassing of the NAPL contaminated zone and thus lead to an underestimation of the actual NAPL saturation. If the mass transfer of the partitioning tracer from the aqueous or gas phase to the NAPL phase is slow compared to the flow velocity of the water or gas, the partitioning of the tracer between the NAPL and the water or gas phase may not be in equilibrium. This also leads to an underestimation of the NAPL saturation.

The use of partitioning tracers to quantify NAPL saturation has been investigated in laboratory sand columns which were homogeneously contaminated with NAPL at residual saturation. In both water-saturated (JIN et al. 1995, WILSON & MACKAY 1995) and gas-saturated (WHITLEY et al. 1995) columns, a good agreement between the NAPL saturation that was calculated based on the partitioning tracing test and the added amount of NAPL in the column was found. Partitioning interwell tracing tests were applied to determine the nonaqueous phase saturation of chlorinated hydrocarbons in the water–saturated zone (NELSON & BRUSSEAU 1996) and unsaturated zone of aquifers. In a study by researchers of the University of Texas (USA), two tracers, one with a small partition coefficient (octofluorocyclobutane, C_4F_8) and one with a large partition coefficient (perfluoro-1,3,5-trimethylcyclohexane, C_9F_{18}) were injected and extracted at several depths in the unsaturated zone of a chemical waste landfill containing trichlorethylene. In the extraction well that withdrew air at depths between 20 and 24 m, similar breakthrough curves for C_4F_8 and C_9F_{18} were found, while in the extraction well reaching to shallow depths (3 to 11 m), C_9F_{18} was retarded relative to C_4F_8. This indicated that the TCE was mainly located in the shallow zone.

5.9.4.3 *The use of ^{222}Rn as a partitioning tracer*

The use of the naturally occurring ^{222}Rn as a partitioning tracer to detect and quantify NAPL saturation in the water-saturated zone of aquifers is based on differences between ^{222}Rn activities in the water phase in zones with and without NAPL. ^{222}Rn is produced by the α-particle decay of ^{226}Ra, an isotope of the natural radioactive decay series of ^{238}U. ^{222}Rn itself decays as α-particle decay with a half-life time of 3.8 days to a series of short-lived daughter products (^{218}Po, ^{214}Pb, ^{214}Bi, ^{214}Po). From minerals which contain ^{226}Ra, ^{222}Rn emanates to the surrounding gas or water phase

by alpha recoil and diffusion. Surface waters usually contain little^{222}Rn, since ^{222}Rn is released to the atmosphere. When surface water infiltrates into the subsurface, the ^{222}Rn activity in the infiltrated water increases until a steady state between emanation and radioactive decay is reached. Based on this increase of the ^{222}Rn activity, aquifer residence times of bank infiltration have been estimated (HOEHN & VON GUNTEN 1989). ^{222}Rn is a chemically inert noble gas, however it partitions into NAPL. When groundwater containing ^{222}Rn at emanation-decay steady state activity migrates into a NAPL contaminated zone of an aquifer, the ^{222}Rn activity in the water phase decreases due to the partitioning of ^{222}Rn between the NAPL and the water. If the ^{222}Rn emanation rate is constant in an aquifer, ^{222}Rn activities can be used to detect NAPL contamination. Furthermore, laboratory experiments indicated that the method can also be used to quantify NAPL saturation (HUNKELER et al. 1997a). The relationship between the water phase ^{222}Rn activities in the contaminated ($A_e^{S>0}$) and uncontaminated zone ($A_e^{S=0}$) at emanation decay steady state and the NAPL saturation (S) is given by the following equation (HUNKELER et al. 1997a):

$$\frac{A_e^{S=0}}{A_e^{S>0}} = 1 + S \cdot (K - 1) \tag{5.21}$$

According to Equation (5.21), the ^{222}Rn activity in the contaminated zone $A_e^{S>0}$ decreases with increasing NAPL saturation S. ^{222}Rn was used to estimate the remaining diesel fuel saturation in the water-saturated zone of an aquifer after treatment by in situ bioremediation (HUNKELER et al. 1997b). The ^{222}Rn activity was lower in water samples from monitoring wells within the contaminated zone than in water samples from monitoring wells upgradient of the contaminated zone (Fig. 270). In monitoring

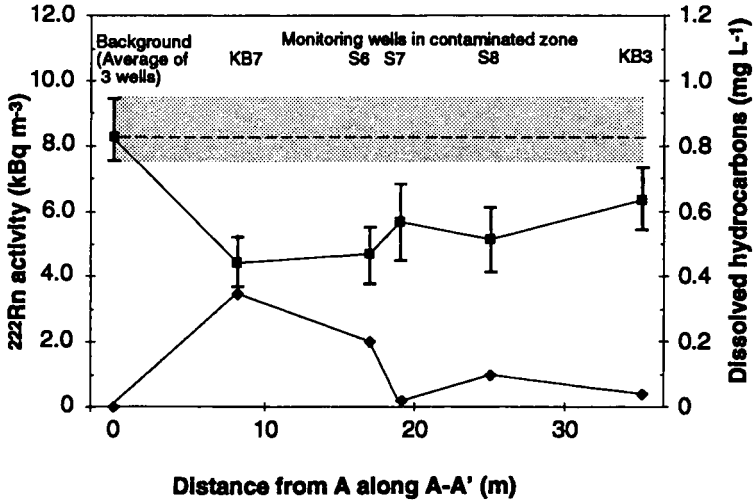

Figure 270. ^{222}Rn activities and dissolved hydrocarbon concentrations measured in monitoring wells upgradient and within the diesel fuel contaminated zone of an aquifer at Menziken, Switzerland. Hatched area: Range between highest and lowest ^{222}Rn activity measured in three monitoring wells upgradient of contaminated zone (from HUNKELER et al. 1997a).

wells with a reduced ^{222}Rn activity, dissolved hydrocarbons were detected. This confirms that the decrease of the ^{222}Rn activity was due to the presence of the diesel fuel.

Compared to artificially injected partitioning tracers, ^{222}Rn has the advantage that it is naturally present in most aquifers whereas adding an artificial tracer to a large groundwater volume requires an expensive groundwater injection scheme. Furthermore, ^{222}Rn activities have to be measured in principle only once while the use of artificial tracers requires many measurements to obtain complete breakthrough curves in order to quantify the NAPL saturation. However, in order to use ^{222}Rn as a partitioning tracer, it must be verified that the ^{222}Rn emanation rate is constant in the aquifer by measuring ^{222}Rn activities in the water phase at several locations in the uncontaminated zone. When using the ^{222}Rn method, the NAPL saturation close to the monitoring well is weighted more strongly than the NAPL saturation further away since distribution of ^{222}Rn between the NAPL and water phase reequilibrate in response to changing NAPL saturation. Furthermore, ^{222}Rn activities increase again once the groundwater has left the contaminated zone. Therefore, the monitoring wells that are used to determine ^{222}Rn activities should be located close to or within the NAPL contaminated zone.

References

ABBA, F., E. ORLANDI & A. RONDELLI 1899. Ueber die Filtrationskraft des Bodens und die Fortschwemmung von Bakterien durch das Grundwasser. *Z. Hygiene und Infectionskrankheiten* 31: 66-84. Leipzig: Veit & Comp.

ABIDI, S.L. 1982. Detection of diethylnitrosamine in nitrite-rich water following treatment with rhodamine flow tracers. *Water Res.* 16: 199-204. Great Britain.

ABU-ASHNOUR, J., D.M. JOY, H. LEE, H.R. WHITELEY & S. ZELIN 1993. Transport of microorganisms through soil. *Wat. Air. Soil Poll.* 75: 141-158.

ACKERMANN, G., A. BLINDE, E. FABIAN & H. HÖTZL 1982a. Anwendung der Markierungstechnik zur Untersuchung der Entwässerungsfunktion eines Erzgangs. *Beitr. Geol. Schweiz – Hydrol.* 28(II): 423-434. Bern: Kümmerly + Frey.

ACKERMANN, G., F.P. BUB & H. HÖTZL 1982. Erfahrungen mit der Dünnschichtchromatographie beim Nachweis von Fluoreszenztracern. *Beitr. Geol. Schweiz – Hydrol.* 28(I): 63-68. Bern: Kümmerly + Frey.

ACKERMANN, H.-W. & M.S. DUBOW 1987. *Virus of procaryotes*, vol.I: General properties of bacteriophages, 202 p.; vol. II: Natural groups of bacteriophages, 242 p. Boca Raton, Florida: CRC Press.

ADAMS, M.C., W.R. BENOIT, C. DOUGHTY, G.S. BODVARSSON & J. MOORE 1989. The Dixie Valley (Nevada) tracer test. *Trans. Geothermal Resources Council* 13: 215-220.

ADAMS, M.H. 1959. *Bacteriophages*. Interscience publishers, 592 p.. New York.

ADAMS, M.H. 1966. *Bacteriophages*. 2nd Ed., 592 p. New York: Intersciences Publishers Inc.

AKAMATSU, K. & M. MATUSO 1973. Safety of optical whitening agents. *Senryo To Yakuhin* 18(2): 2-11 (Jap.), (cit. after SMART & LAIDLAW 1977).

ALDRICH = Aldrich-Chemie GmbH & Co.KG 1986/7. Katalog Feinchemikalien, 1936 +632 p. Steinheim/Württ.

ALEXANDER, E., M. DAVIS & J. DALGLEISH 1988. Dye tracing through thick unsaturated zones. *Proc. 5.Int. Symp. Underground Water Tracing, Athens 1986*, pp 181-188. Athens: IGME.

ALEXANDER, I. & K.-D. SEILER 1983. Lebensdauer und Transport von Bakterien in typischen Grundwasserleitern – Münchner Schotterebene. *DVGW-Schriftenreihe Wasser* 35: 113-126. Eschborn.

ALEY, T. & M.W. FLETCHER 1976. The water tracers cookbook. *Missouri Spel. Soc. Bull.* 16(3), 32 p.

ALLISON, S.B., G.A. POPE & SEPEHRNOORI, K. 1991. Analysis of field tracers for reservoir description. *J. Pet. Sci. and Engineer.* 5: 173-186.

ALTHAUS, H. & K.D. JUNG 1983. Feldversuche im mittelsandigen Grundwasserleiter Haltern zur Feststellung der Lebensdauer und des Transportverhaltens von Bakterien und Viren in Grundwasserleitern, Bericht 1: 'Zwei Feldversuche mit *E.coli* und Beginn des noch laufenden dritten Feldversuches mit Coliphag F2'. 35 p. (Ms.). Gelsenkirchen.

ALTHAUS, H. & K.D. JUNG 1985. Feldversuche im mittelsandigen Grundwasserleiter Haltern zur Feststellung der Lebensdauer und des Transportverhaltens von Bakterien und Viren in Grundwasserleitern, Bericht 2: 'Dritter Feldversuch mit Coliphag F2'. 36 p. (Ms.). Gelsenkirchen.

ALTHAUS, H., K.D. JUNG, G. MATTHESS & A. PEKDEGER 1980. Literaturstudie 'Untersuchungen der Lebensdauer von Bakterien und Viren im Grundwasser im Hinblick auf die Ausweisung von Schutzgebieten für die Grundwasseranlagen'. Teil B: *Hygienische und hydrogeologische Grundlagen*, 190 p. (Ms.). Gelsenkirchen/Kiel.

ALTHAUS, H., M. BRICELJ, W. ENGEL, K.D. JUNG & G. KOSI 1986. 'Tracing with phages' in: karst hydrogeology of the Central and Eastern Peloponnesus (Greece). *Steir. Beitr. Hydrogeol.* 1985/86: 259-271. Graz.

ALTHAUS, H., W. ENGEL & K.D. JUNG 1985. Possible preservation of bacterial virus in water samples tested with coliphage F2. *Newsletter on Water Virology* 6: 15-16. London.

ALTHAUS, H., W. ENGEL & K.D. JUNG 1986. Tracing with coliphages f_2 and 'Kanatas G'. *Steir. Beitr. Hydrogeol.* 37/38: 263-269. Graz.

AMALRIC, P. (Ed) 1971. Fluorescein Angiography. *Proc. Int. Symp. Fluorescein Angiography, Albi 1969*. 124 Beiträge, 684 p. Basel-München-Paris-London-New York-Sydney: Karger.

AMBERGER, A. & H.L. SCHMIDT 1987. Natürliche Isotopengehalte von Nitrat als Indikatoren für dessen Herkunft. *Geochim. Cosmochim. Acta* 51: 2699-2705.

AMES, B.N., J. MCCANN & E. YAMASAKI 1975. Methods of detecting carcinogens and mutagens with the *Salmonella* (mammalian-microsane mutagenicity test). *Mutation Res.* 31: 347-364.

ANDRÉ, J.C. & I. MOLINARI 1976. Mises au point sur les différents facteurs physicochimiques influant sur la mesure de concentration de traceurs fluorescents et leurs conséquences pratique en hydrol. *J. Hydrol.* 30: 257-285. Amsterdam: Elsevier.

Anonymus 1908. La Pêche au téléphone. *La Nature, Supplément*, 1845, 3.Okt.1908: 137 p. Paris.

APEL, R. & J.-P. WROBEL 1975. Markierungsversuche im alpinen Karst des Krottenkopfgebietes und in der südlichen Fränkischen Alb. *Geologica Bavarica* 74: 209-216. München.

APHA-AWWA-WPCF 1976. *Standard methods for the examination of water and wastewater.* Prepared and published jointly by: American Public Health Association, American Water Works Association and Water Pollution Control Federation. Fourteenth Ed., pp 923-927.

ARAGNO, M. & I. MÜLLER 1982. Premières expériences de traçages des eaux souterraines dans le karst du jura neuchâtelois (Suisse) à l'aide de bactériophages. *Bull. Centre d'Hydrogéologie* 4: 59-81. Neuchâtel.

ARAGNO, M. & I. MÜLLER 1984. (Pers. Inf.).

ARANDJELOVIC, D. 1977. Determination of groundwaterflow in karst using 'geobomb'. *Mem. 12. Congr. Int. Ass. Hydrogeologists, Huntsville/Alab.*, pp 399-400. Huntsville.

ARBELOA, F.L., I. GONZALEZ P.R. OJEDA & I.L. ARBELOA 1982. Aggregate formation of rhodamine 6G in aqueous solution. *J. Chem. Soc., Faraday Trans.* 78(2): 989-994.

ARMBRUSTER, H., H. HÖTZL & G.-P. MERKLER 1988. Temperatures and salt-potentials as natural tracers of underground water flow. *Proc. 5th Int. Symp. Undergroundwater Tracing, Athen 1986*, pp 443-448. Athen: IGME.

ARMON, R. & V.J. CABELLI 1988. Phage f2 desorption from clay in estuarine water using nonionic detergents, beef extract and chaotropic agents. *Can. J. Microbiol.* 34: 1022-1024.

ARMON, R. & Y. KOTT 1993. A simple, rapid and sensitive presence/absence detection test for bacteriophage in drinking water. *J. Appl. Bacteriol.* 74: 490-496.

ASCHWANDEN H. & CH. LEIBUNDGUT 1982. Die Markierung der Wasser des Gornerseeausbruches mit drei Fluoreszenztracern. *Beitr. Geol. Schweiz – Hydrol.* 28(II): 535-549. Bern: Kümmerly + Frey.

ATH – Int. Association of Tracer Hydrology 1992. Transport phenomena in different aquifers (Investigations 1987-1992). *Steir. Beitr. Hydrogeol.* 43, 283 p. Graz/Austria.

ATKINSON, T.C., D.I. SMITH, J.J. LAVIS & R.J. WHITAKER 1973. Experiments in tracing underground waters in limestones. *J. Hydrol.* 19: 323-349. Amsterdam.

ATMAR, R.L., T.G. METCALF, F.H. NEILL & M.K. ESTES 1993. Detection of enteric viruses in Oysters by using the polymerase chain reaction. *Appl. Environ. Microbiol.* 59: 631-635.

ATTINGER, R. & CH. LEIBUNDGUT 1986. Hydrogeographical investigation in the coastal region between Argos and Astros (Peloponnesus). In Karst Hydrogeology of the Central and Eastern Peloponnesus (Greece). *Steir. Beitr. Hydrogeol.* 1985/86: 198-214. Graz.

AULENBACH, D.B., J.H. BULL & B.C. MIDDLESWORTH 1978. Use of tracers to confirm groundwater flow. *Ground Water* 16(3): 149-157.

AURAND, K. 1979. Written comm. to the Minist. für Landwirtschaft, Weinbau und Umweltschutz Rheinland-Pfalz vom 10. Mai 1979.

AURAND, K., G. MATTHESS & R. WOLTER 1972. Fallout-Strontium-90 als Markierungsstoff bei Grundwasseruntersuchungen. *Geol. Jb.* C2: 303-313. Hannover.

BØRSHEIM, K.Y. 1993. Native marine bacteriophages. *FEMS Microbiol. Ecology* 102: 141-159.

BAALSRUD, K. 1961. Distribution of bacteria in a stratified lake in SE-Norway. *Verh. int. Verein theoret. und angew. Limnologie* XIV: 1044-1048.

BABICH, H. & G. STOTZKY 1980. Reductions in inactivation rates of bacteriophages by clay minerals in lake water. *Water Res.* 14: 185-187.

BAEYER, A. 1871a. Über eine neue Klasse von Farbstoffen. *Ber. dt. chem. Ges. Berlin* 4: 555-558.

BAEYER, A. 1871b. Über die Phenolfarbstoffe. *Ber. dt. chem. Ges. Berlin* 4: 658-665.

BAGDASAR-JAN, G.A. & R.M. ABIJEWA 1970. Survival of entero- and adenoviruses in water. *GIGIENA i SANITARIA* 36: 10. Moscow (Russ.).

BALDERER, W. 1982. Die Bedeutung der $_{14}C$- und $_{13}C$-Bestimmungen an der Funtenenquelle hinsichtlich der Interpretation von Bestimmungen an Tiefenwässern. *Beitr. Geol. Schweiz – Hydrol.* 28(II): 367-379. Bern: Kümmerly + Frey.

BALES, R.C., L. SHIMIN, K.M. MAGUIRE, M.T. YAHYA & C.P. GERBA 1993. MS-2 and poliovirus transport in porous media: hydrophobic effects and chemical perturbations. *Water Resourc. Res.* 29: 957-963.

BALES, R.C., S.R. HINKLE, T.W. KROEGER, K. STOCKING & C.P. GERBA 1991. Bacteriophage adsorption during transport through porous media: chemical perturbation and reversibility. *Environ. Sci. Technol.* 25: 2088-2095.

BALL, J.W., E.A. JENNE & D.K. NORDSTROM 1979. Wateq2 – A computerized chemical model for trace and major element specication and mineral equilibria of natural waters. In E.A. JENNE (ed.), Chemical Modeling in Aqueous Systems. *Am. Chem. Soc. Symp.*, Ser. 93: 815-835. Washington D.C.

BANDT, H.J. 1957. Giftig oder ungiftig für Fische? *Dt. Fischereizeitung* 4(2): 170-171.

BARCZEWSKI, B. 1990. Optische Methoden zur in-situ Tracerkonzentrationsmessung in Strömungen. *Wasserwirtschaft* 80(11): 553-561.

BATSCHE, H., F. BAUER, H. BEHRENS, K. BUCHTELA, F. HRIBAR, W. KÄSS, G. KNUTSSON, J. MAIRHOFER, V. MAURIN, H. MOSER, F. NEUMAIER, L. OSTANEK, V. RAJNER, W. RAUERT, H. SAGL, W.A. SCHNITZER & J. ZÖTL 1967. Vergleichende Markierungsversuche im Mittelsteirischen Karst. *Steir. Beitr. Hydrogeol.* 1966/67: 331-404. Graz.

BATSCHE, H., F. BAUER, H. BEHRENS, K. BUCHTELA, H.J. DOMBROWSKI, R. GEISLER, M.A. GEYH, H. HÖTZL, F. HRIBAR, W. KÄSS, J. MAIRHOFER, V. MAURIN, H. MOSER, F. NEUMAIER, J. SCHMITZ, W.A. SCHNITZER, A. SCHREINER, H. VOGG & J. ZÖTL 1970. Kombinierte Karstwasseruntersuchungen im Gebiet der Donauversickerung (Baden-Württemberg) in den Jahren 1967-1969. *Steir. Beitr. Hydrogeol.* 1970: 4-165, 72 Fig., 15 Tab., 5 Plates. Graz.

BAUER, F. 1958. Quellwassergefährdung in Karstgebieten. Österr. *Wasserwirtsch.* 10: 100-103. Wien.

BAUER, F. 1967a. Erfahrungen beim Uraninnachweis mit Aktivkohle. *Steir. Beitr. Hydrogeol.* 1966/67: 169-178. Graz.

BAUER, F. 1967b. Die Durchführung und Auswertung von Sporentriftversuchen. *Steir. Beitr. Hydrogeol.* 1966/67: 249-266. Graz.

BAUER, F. 1969. Karsthydrologische Untersuchungen im Schneealpstollen in den steirisch-niederösterreichischen Kalkalpen. *Steir. Beitr. Hydrogeol.* 21: 193-214. Graz.

BAUER, F. 1972a. Untersuchungen über die Verwendbarkeit von zwei Fluoreszenzfarbstoffen im Rahmen eines Färbversuches. *Geol. Jb.* C2: 61-73. Hannover.

BAUER, F. 1972b. Weitere Erfahrungen beim Uraninnachweis mit Aktivkohle. *Geol. Jb.* C2: 19-27. Hannover.

BAUER, F. 1976. Untersuchungen über die Verwendbarkeit von Tinopal CBS-X als Tracer. Pap. 3rd *Int. Symp. Underground Water Tracing (3.SUWT) 1976*, pp 17-25. Ljubljana.

BAUER, F. 1989. *Die unterirdischen Abflußverhältnisse im Dachsteingebiet und ihre Bedeutung für den Karstwasserschutz*, 73 p., 8 Annex. (als Ms. gedruckt). Wien.

BAUER, F. & W. PERGELA 1980. Ergebnisse des Fluoreszenztracernachweises mittels Aktivkohle. *Steir. Beitr. Hydrogeol.* 32: 70-74. Graz.

BAUER, F., H. BEHRENS, F. BERNOT, B. BUKVIC, S. BUSER, M. DECHANT, F. DROBNE, R. GOSPODARIC, P. HABIC, H. HÖTZL, F. HRIBAR, W. KÄSS, M. KOLBEZEN, P. KRIVIC, F. LEWICKI, V. MAURIN, J.-J. MISEREZ, H. MOSER, M. MOZETIC, A. PICININ, M. PIRS, V. RAJNER, D. RANK, W. STICHLER, M. TRATNIK, R. VERBOVSEK, J.G. ZÖTL, MARTINA ZUPAN, M. ZUPAN & K. ZRIBIK 1976. Markierung unterirdischer Wässer – Untersuchungen in Slowenien 1972-1975. *Steir. Beitr. Hydrogeol.* 1976, 257 p. Graz.

BAUER, F., H. BEHRENS, W. DROST, W. KÄSS, CH. LEIBUNDGUT, H. MOSER, W. PERLEGA, V. RAJNER, D. RANK, W. STICHLER & H.R. WERNLI 1981. Tracerhydrologische Untersuchungen im Langetental (Schweiz). *Steir. Beitr. Hydrogeol.* 33: 5-123. Graz.

BAUER, F., J. ZÖTL & A. MAYR 1959. Neue karsthydrographische Forschungen und ihre Bedeutung für Wasserwirtschaft und Quellschutz – Ergebnisse des im Jahre 1958 vom Speläologischen Institut (Wien) im Dachsteingebiet durchgeführten Sporentriftversuches. *Wasser u. Abwasser* 3: 280-297. Wien.

BAUER, F., R. BENISCHKE, F.P. BUB, A. BURGER, H. DOMBROWSKI, R. GOSPODARIC, H. HÖTZL, F. HRIBAR, W. KÄSS, L. KIRALY, CH. LEIBUNDGUT, H.P. LEDITZKY, V. MAURIN, I. MÜLLER, H. PERLEGA, P. RAMSPACHER, U. SCHOTTERER, U. SIEGENTHALER, H. ZOJER, J. ZÖTL & MARTINA ZUPAN 1980. Karsthydrologische Untersuchungen mit natürlichen und künstlichen Tracern im Neuenburger Jura (Schweiz). *Steir. Beitr. Hydrogeol.* 32: 5-100. Graz.

BAUER, F., W. PERGELA & G. VÖLKL 1980. Markierungsversuch Peggau – 1979 (Tracing test with hostalux and uranine). 16 p. (Ms.). Wien.

BEAR, J. 1972. *Dynamics of Fluids in Porous Media*, 764 p. New York-London-Amsterdam: American Elsevier Publishing Comp.

BEAR, J. 1979. *Hydraulics of Groundwater*, 567 p. New York-London: McGraw-Hill Int. Book Comp.

BEDBUR, E. 1989. Laboruntersuchungen zum Einfluß sedimentologischer und hydraulischer Parameter auf die Filterwirkung gleichförmiger Sande. Berichte-Reports, Geol. Paläont. Inst. Univ. Kiel, 31: 77 p., 35 Fig., 23 Tab. Kiel.

Begriffsbestimmungen für Kurorte, Erholungsorte und Heilbrunnen vom 11.April 1987. Dt. Bäderverb. e.V. und Dt. Fremdenverkehrsverb. e.V. (ed.), 9. Ed., 59 p. Bonn.

BEHRENS, H. & G. TEICHMANN 1982. Neue Ergebnisse über den Lichteinfluß auf Fluoreszenztracer. Beitr. *Geologie Schweiz – Hydrol.* 28(I): 64-77. Bern: Kümmerly + Frey.

BEHRENS, H. & G. TEICHMANN 1989a. Lichtempfindlichkeit von Pyranin, Uranin und Eosin in Abhängigkeit vom pH-Wert. Jahresber. 1988, *Inst. Hydrol., GSF-HY* 38/88: 235-242. Neuherberg.

BEHRENS, H. & G. TEICHMANN 1989b. Untersuchungen zur Optimierung des sichtbaren Nachweises von Fluoreszenztracern in Mischungen durch gezielte pH-Einstellungen. *Jahresber. 1988, Inst. Hydrol., GSF-HY* 38/88: 176-188. Neuherberg.

BEHRENS, H. & K.-P. SEILER 1982. Beziehungen zwischen der Dispersivität und der Länge des Fließweges des Grundwassers nach Geländeversuchen in den fluvioglazialen Kiesen des oberen Loisachtales (Oberau) und von Dornach (Münchener Schotterebene). *GSF-Ber.* R 250: 323-330. München.

BEHRENS, H. & N. DEMUTH 1990. Lichtmessung in Gewässern über die Photolyse von Fluoreszenztracern. Jahresber. 1989, *Inst. Hydrol., GSF-HY* 1/90: 216-233. Neuherberg.

BEHRENS, H. & N. DEMUTH 1992. Measurement of light input into surface waters by photolysis of fluorescent dye tracers. In HÖTZL, H. & A.WERNER, Tracer Hydrology. *Proc. 6th Int. Symp. Water Tracing (SWT) of the ATH, 21.-26. Sept. 1992, Karlsruhe,* pp 49-56. Rotterdam: Balkema.

BEHRENS, H. 1967. Zur Anreicherung von radioaktiven Indikatoren. *Steir. Beitr. Hydrogeol.* 1966/67: 79-86. Graz.

BEHRENS, H. 1971. Untersuchungen zum quantitativen Nachweis von Fluoreszenzfarbstoffen bei ihrer Anwendung als hydrologische Markierungsstoffe. *Geologica Bavarica* 64: 120-131. München.

BEHRENS, H. 1973. Eine verbesserte Nachweismethode für Fluoreszenzindikatoren und ihre Anwendung zur Feststellung von Fließwegen im Grundwasser. *Z. Dt. Geol. Ges.* 124: 535-544. Hannover.

BEHRENS, H. 1980. Anwendungen von Isotopen im Oberflächenwasser – Offene Gerinne. In MOSER, H. & W. RAUERT, *Lehrbuch der Hydrogeologie, Bd. 8, Isotopenmethoden in der Hydrologie*, pp 78-95. Berlin-Stuttgart: Gebr.Borntraeger.

BEHRENS, H. 1982. Verfahren zum qualitativen und quantitativen Nachweis von nebeneinander vorliegenden Fluoreszenztracern. Beitr. *Geologie Schweiz – Hydrol.* 28(I): 39-50. Bern: Kümmerly + Frey.

BEHRENS, H. 1983. Comparison of radioactive and non-radioactive tracers. *IAEA-TECDOC* 291: 173-185. Vienna.

BEHRENS, H. 1985. Specification of radioiodine in aquatic and terrestrial systems under the influence of biogeochemical processes. In R.A.BULMAN & J.R.COOPER (eds), *Specification of Fission and Activation Products in the Environment.* London u.New York: Elsevier Applied Science Publishers.

BEHRENS, H. 1988a. Water tracer chemistry – A factor determining performance and analytics of tracers. *Proc. 5.Int. Symp. Underground Water Tracing, Athen 1986,* pp 121-133. Athen: IGME.

BEHRENS, H. 1988b. Quantitative Bestimmung von Uranin, Eosin und Pyranin in Gemischen mittels Fluoreszenzmessung bei definierten pH-Werten. *Steir. Beitr. Hydrogeol.* 39: 117-129. Graz.

BEHRENS, H. 1992. Results with Indium-114. *Steir. Beitr. Hydrogeol.* 43: 91-93. Graz.

BEHRENS, H., A. BÖGLI, H. HÖTZL, W. KÄSS, W. KRAUS, CH. LEIBUNDGUT, V. MAURIN, H. MOSER, V. RAJNER, D. RANK, W. STICHLER, H. ZOJER & J. ZÖTL 1981. Hydrogeologische Untersuchungen im Karst des hinteren Muotatales (Schweiz). *Steir. Beitr. Hydrogeol.* 33: 125-264. Graz.

BEHRENS, H., CH. LEIBUNDGUT, P. THEODORATOS & A. VITORIOU-GEORGOULI 1986. Tracing with fluorescent tracers. *Steir. Beitr. Hydrogeol.* 1985/86: 235-247. Graz.

BEHRENS, H., H. BERGMANN, H. MOSER, W. RAUERT, W. STICHLER, W. AMBACH, H. EISNER & H. PESSL 1971. Study of the discharge of alpine glaciers by means of environmental isotopes and dye tracers. *Z. Gletscherkde. und Glazialgeol.* 7(1/2): 79-102. Innsbruck: Wagner.

BEHRENS, H., H. MOSER & E. WILDNER 1977. Investigation of groundwater flow with the aid of Indium-EDTA-complex using neutron activation for the determination of the tracer. *J. Radioanal. Chem.* 38: 491-498.

BEHRENS, H., Martina ZUPAN & M. ZUPAN 1976. Methodik und Ergebnisse der Direktmessungen der Fluoreszenztracer. *Steir. Beitr. Hydrogeol.* 28: 125-149. Graz.

BEHRENS, H., R. BENISCHKE, M. BRICELJ, T. HARUM, W. KÄSS, G. KOSI, H.P. LEDITZKI, CH. LEIBUNDGUT, P. MALOCZEWSKI, V. MAURIN, V. RAJNER, D. RANK, B. REICHERT, H. STADLER, W. STICHLER, P. TRIMBORN, H. ZOJER & M. ZUPAN 1992. Investigations with natural and artificial tracers in the karst aquifer of the Lurbach System (Peggau-Tanneben-Semriach, Austria), 76 Fig., 30 Tab., *Steir. Beitr. Hydrogeol.* 43: 9-158. Graz.

BEN SHIAU, D.A. SABATINI & J.H. HARWELL 1992. Sorption of rhodamine WT as affected by molecular properties. In HÖTZL, H. & A. WERNER, Tracer Hydrology, *Proc. 6th Int. Symp. Water Tracing 21-26 Sept. 1992, Karlsruhe.* Rotterdam: Balkema.

BENDEL, L. 1948. *Ingenieurgeologie II*, 832 p. Vienna: Springer.

BENISCHKE, R. & H. SCHMERLAIB 1988. Pyranin: A fluorescent dye for tracer hydrology – Review of physico-chemical properties, the toxicity and applicability. *Proc. 5.Int. Symp. Underground Water Tracing (SUWT) Athens 1986*, pp 135-148. Athens: IGME.

BENOÎT-GUYOD, J.L., J. ROCHAT, J. ALARY, C. ANDRÉ & G. TAILLANDIER 1979 recd.1980. Correlations between physiochemical properties and eco toxicity of fluorescent xanthenic water tracers. *Toxicol. Eur. Res.* 2(5): 241-246. Paris.

BENTLEY, H.W., F.M. PHILLIPS & S.N. DAVIS 1986. Chlorine-36 in the terrestrial environment. In FRITZ, P. & J.CH. FONTES (eds), *Handbook of Environmental Geochemistry* 2: 427-480. Amsterdam-Oxford-New York: Elsevier.

BERGER, U. & K. HUMMEL 1964. *Einführung in die Mikrobiologie und Immunologie*, 98 p. München-Berlin: Urban & Schwarzenberg.

BERGH, Ø., K.Y. BØRSHEIM, G. BRATBAK & M. HELDAL 1989. High abundance of viruses found in aquatic environments. *Nature* 340: 467-468.

BERTARELLI, L.V. & E. BOEGAN 1926. *Duemila Grotte*, 494 p., Ed. Touring Club Italiano, Milano.

BERTARELLI, L.V. 1903. Untersuchungen und Beobachtungen über die Biologie und Pathogenität des *Bacillus prodigiosus*. *Zentralbl. Bakteriol., Parasitenkde. u. Infektionskrankheiten, I.Abt. Orig.* 34: 193-202 and 312-322. Jena: Gustav Fischer.

BERTHÉLOT, A. 1902. Sur les origines de la source de la Loue. *C.R.* 133: 394-397. Paris.

BERTSCH, K. 1942. Lehrbuch der Pollenanalyse. In *Handbücher der praktischen Vorgeschichtsforschung* 3, VIII + 195 p. Stuttgart: Enke.

BGBL 1961. Gesetz über Detergenzien in Wasch- und Reinigungsmitteln vom 5.September 1961. Bundesgesetzblatt I 72: 1653-1654 vom September 1961. Verordnung über die Abbaubarkeit von Detergenzien in Wasch- und Reinigungsmitteln vom 1.Dez.1962 trat am 1.Oktober 1964 in Kraft (Bundesgesetzblatt I, 49: 698-706 vom 12.Dez.1962) Bonn.

BGBL 1976. *Bundesgesetzblatt I, Gesetz zur Ordnung des Wasserhaushalts* (Wasserhaushaltsgesetz – WHG), 1976(128): 3017-3032. Bonn.

BGBL 1977a. *Bundesgesetzblatt I, Berichtigung der Strahlenschutzverordnung vom 21.Januar 1977*, 1977(6): 184-195. Bonn.

BGBL 1977b. *Bundesgesetzblatt I, Verordnung über kosmetische Mittel* (Kosmetik-Verordnung) vom 16.Dez.1977, 1977: 2589-2621, 21.Dez.1977. Bonn.

BGBL 1980. *Bundesgesetzblatt I* 42: 1071, Verordnung über gefährliche Arbeitsstoffe; Anhang II Nr.1; krebserzeugende Arbeitsstoffe, pp 257-263.

BGBL 1981. *Bundesgesetzblatt I*, Verordnung über die Zulassung von Zusatzstoffen für Lebensmittel vom 30.Dez.1981: 1981: 1633-1654. Bonn.

BGBL 1986a. *Bundesgesetzblatt I*, Verordnung über Trinkwasser und über Wasser für Lebensmittelbetriebe vom 26.Mai 1986, 1986(22): 760-773, 28.Mai 1986. Bonn.

BGBL 1986b. *Anlagenband zum Bundesgesetzblatt I*, (47) vom 5.Sept.1986: Anhänge I bis VI zur Gefahrstoffverordnung vom 26.August 1986, 247 p.,Bonn.

BIDOVEC, E. 1976. The register of discharges and the karst underground flow tracing. *Pap. 3rd Int. Symp. Underground Water Tracing* (3.SUWT), pp 27-34. Ljubljana.

BIRD, J.M. & J.G. DEMPSEY 1955. The use of radioactive-tracer surveys in water-injection wells. *Spec. Publ.* 8: 44-54. Kentucky Geol. Surv.

BITTON, G. & C.P. GERBA (eds) 1984. *Groundwater pollution microbiology*. New York: Wiley-Interscience Publication.

BITTON, G. & R. MITCHELL 1974. Effect of colloids on the survival of bacteriophages in seawater. *Water Research* 8: 227-229. Great Britain: Pergamon Press.

BITTON, G. 1975. Adsorption of viruses onto surfaces in soil and water. *Water Res.* 9: 473-484.

BITTON, G., S.R. FARRAH, R.M. RUSKIN, J. BUTNER & Y.J. CHOU 1983. Survival of pathogenic and indicator organisms in ground water. *Ground Water* 21: 405-410.

BIXBY, R.L. & D.J. O'BRIEN 1979. Influence of fulvic acid on bacteriophage adsorption and complexation in soil. *Appl. Environ. Microbiol.* 38: 840-845.

BLUME, H.-P., R. BORNKAMM, TH. KEMPF, S. MULJADI & F. RAGHI-ATRI 1980. Bor-Status Berliner Gewässer. *Arch. Hydrobiol.* 89(4): 426-439. Stuttgart.

BOEGAN, E. 1906. Le sorgenti d'Aurisina. 126 p., Società Alpina delle Giulie (ed.). Trieste.

BOEGAN, E. 1938. Il Timavo. *Mem. Istituto Italiano di Speleolog.* II: 251 p., 85 Plates. Trieste.

BÖGLI, A. & T. HARUM (eds) 1981. Hydrogeologische Untersuchungen im Karst des hinteren Muotatales (Schweiz). *Steir. Beitr. Hydrogeol.* 33: 125-264. Graz.

BÖGLI, A. 1980. *Karsthydrology and Physical Speleology.* Heidelberg-New York: Springer.

BOLTON, M. 1886. Ueber das Verhalten verschiedener Bacterienarten im Trinkwasser. *Z. Hygiene* I: 76-80, 105-114. Leipzig.

BORIC, M. 1988. The use of groundwater temperature monitoring of leakage from a surface storage in the Dinaric Karst. *Proc. 5.Int. Symp. Underground Water Tracing, Athens 1986*, pp 457-458. Athens: IGME.

BOWMAN, R.S. & R.C. RICE 1986. Transport of conservative tracers in the field under intermittend flood irrigation. *Water Resources Res.* 22(11): 1531-1536.

BRAND, K.H. 1989. Untersuchungen über die Festlegung und Remobilisierung der Schwermetalle Blei, Cadmium, Kupfer und Zink bei der Uferfiltration. *Schr. Angew. Geol. Karlsruhe* 6: 243 p. Karlsruhe.

BRAND, K.H., H. HÖTZL, W. KÄSS & B. REICHERT 1990. Migrationsverhalten ausgewählter Schadstoffe bei der Uferfiltration in einem natürlichen Testfeld am Neckar. *GWF, Wasser-Abwasser* 131: 311-317. München.

BRANDECKER, H. & V. MAURIN 1982. Die Trinkwasservorkommen im südlichen Salzburger Becken und seiner Umrahmung. *Österr. Wasserwirtsch.* 34: 105-122. Wien.

BRANDECKER, H., V. MAURIN & J. ZÖTL 1965. Hydrogeologische Untersuchungen und baugeologische Erfahrungen beim Bau des Dießbach-Speichers (Steinernes Meer). *Steir. Beitr. Hydrogeol.* 17: 67-106. Graz.

BRANNATH, A. 1991. Dokumentation und Bewertung von Grundwassersanierungen mittels UVB-Verfahren sowie Feldversuche an einem Standort im Lockergestein. *Diplomarb.* 2: 107 p., 24 Anl. Karlsruhe.

BRATBAK, G., M. HELDAL, S. NORLAND & T.F. THINGSTAD 1990. Viruses as partners in spring bloom microbial trophodynamics. *Appl. Environ. Microbiol.* 56: 1400-1405.

BRAUNER, F. & G. NIEBAUER 1955. Die Bestimmung der Durchströmungsgeschwindigkeit mittels Fluoreszein bei peripheren Durchblutungsstörungen. *Wiener med. Wochenschr.* 105: 338-341. Wien.

BREUNINGER, F.W. 1719. *Fons Danubii primus et naturalis oder die Urquelle des weltberühmten Donaustroms*, 388 p. Tübingen.

BRICELJ, M. & M. SISKO 1992. Inactivation of phage tracers by exposure to liquid-air interfaces. In HÖTZL & WERNER (eds), *Tracer Hydrology, Proc. 6th Int. Symp. Water Tracing 21-26 Sept. 1992, Karlsruhe*, pp 71-75. Rotterdam: Balkema.

BRICELJ, M. 1988. Pers. Comm.

BRICELJ, M., G. KOSI & D. VRHOUSEK 1986A. Tracing with Salmonella-phage P22H5. *Steir. Beitr. Hydrogeol.* 37/38: 269-271. Graz.

BRICELJ, M., H. HÖTZL, W. KÄSS, V. MAURIN, G. PROBST, B. REICHERT, F. REISS & MARTINA ZUPAN 1986b. Tracing with spores. *Steir. Beitr. Hydrogeol.* 1985/86: 252-258. Graz.

BROECK, E. VAN DEN 1904. L'étude des eaux courantes souterraines (eaux alimentaires en région calcaires) par l'emploi des matières colorantes (fluoresceïne). Discussion sur la vitesse de propagation des eaux souterraines et de la fluorescéine dans les canaux et fissures des terrains calcaires avec un exposé synthétique résument les points spécial édité par E.v.d.BROECK. Karte und Diagramme. *Bull. Soc. belge Géol., Paléontol., Hydrol.* XVII: 239-635. Brüssel.

BROWN, K.W., H.W. WOLF, K.C. DONNELLY & J.F. SLOWEY 1979. The movement of fecal coliforms and coliphages below septic lines. *J. Environmental Quality* 8: 121-125. Madison.

BRUSCATO, F.N. & J.R. MCHENRY 1970. Evaluation of selected cobalt-60 complexes as tracers of groundwater. *J. Hydrol.* 10: 406-417.

BUB, F.P. & H. HÖTZL 1980. Ergebnisse der dünnschichtchromatographischen Auswertung von Direktproben. *Steir. Beitr. Hydrogeol.* 32: 65-70. Graz.

BUB, F.P., H. HÖTZL & K. WISSER 1979. Dünnschicht-chromatographischer Nachweis von Fluoreszenztracern bei hydrogeologischen Markierungsversuchen. *Steir. Beitr. Hydrogeol.* 1979: 129-141. Graz.

BUCHTELA, K. & C. JOB 1970. Vergleichende Markierungsversuche mit Indium-ÄdtE und Kalisalz in einem Bergsturzgelände bei Bad Gastein. *Steir. Beitr. Hydrogeol.* 1970: 199-206. Graz.

BUCHTELA, K., J. MAIRHOFER, V. MAURIN, T. PAPADIMITROPOULOS & J. ZÖTL 1964. Vergleichende Untersuchungen an neueren Methoden zur Verfolgung unterirdischer *Wässer. Wasserwirtschaft* 54(9): 260-270. Stuttgart.

BUCHTELA, K., J. MAIRHOFER, V. MAURIN, T. PAPADIMITROPOULOS & J. ZÖTL 1968. Comparative investigations into recent methods of tracing subterranean water. *Nat. Speleol. Soc. Bull.* 30: 55-74.

BÜHRER, H. & H. AMBÜHL 1975. Die Einleitung von gereinigtem Abwasser in Seen. *Schweiz. Z. Hydrol.* 37(2): 347-369.

BURGE, W.D. & N.K. ENKIRI 1978. Virus adsorption by five soils. *J. Environmental Quality* 7: 73-76. Madison. (cit. after GERBA & GOYAL 1978) – Adsorption von Bakteriophagen).

CARLSON, G.F. Jr., F.E. WOODARD, D.F. WENTWORTH & O.J. SPROUL 1968. Virus inactivation on clay particles in natural waters. *J. Water Pollution Control Federation* 40(2): R89-R106.

CARMI, I. & J.R. GAT 1994. Estimating the turnover time of groundwater reservoirs by the helium-3/tritium method in the era of declining atmospheric tritium levels: Opportunities and limitations in the time bracket 1990-2000. *Isr. J. Earth Sci.* 43: 249-253.

CARPENTER, J.H. 1968. *Tracer for circulation and mixing in natural waters*. Palo Alto: Turner.

CARPENTER, P.G., T.D. MORGAN & E.D. PEARSON 1952. Use of boron components on water flood tracers. *Producers Monthly, Oct. 1952*, pp 12-19. Bradford, Pa.

CARVALHO-DILL, A. DE, K. GERLINGER, T. HAHN, W. KÄSS, P. MALOSZEWSKI, I. MÜLLER, S. OETZEL, D. RANK & A. WERNER 1992. Transport phenomena in different aquifers – Investigations of the Association of Tracer Hydrology (1987-1992) – Porous aquifer – Test site Merdingen/Germany. *Steir. Beitr. Hydrogeol.* 43: 251-280. Graz.

CHAI, W., A. DAI, G. YUAN, C. ZHAO & P. BIDAUX 1988. Studying the recharge boundary of a karst spring system by means of tracers. *Mem. IAH (Int. Ass. Hydrogeol.) 21. Congr. Oct.1988 in Guilin/China* XXI(2): 902-909. Beijing.

CHAUVE, P., G. CHARLES & A. LEONETTI 1982. A propos des pertes du Doubs. *Ann. Sci. de l'Université de Franche-Comté, Géol.* 4(4): 13-25. Besançon.

CHAUVE, P., PH. JACQUEMIN & J. MANIA 1986. Représentation des écoulements en milieu karstique de zone plissée: exemple des hauts bassins du Doubs et de la Loue. *Bull. Soc. Géol. France* (8), (II, 4): 645-652.

CLASSEN, H.J. 1964. Methodik und Beispiele von Färbversuchen. *Z. dt. geol. Ges.* 116: 231-236. Hannover.

CLASSEN, H.J. 1967. Der Einsatz von Färbeversuchen unter Verwendung von Uranin im Untertagebetrieb des Ruhrbergbaues und seine Handhabung. *Steir. Beitr. Hydrogeol.* 1966/67: 141-149. Graz.

COLLINS, D.N. 1977. Hydrology of an alpine glacier as indicated by the chemical composition of meltwater. *Z. Gletscherkde. und Glazialgeol.* 13(1/2): 219-238. Innsbruck.

COLLINS, D.N. 1982. Flow-routing of meltwater in an alpine glacier as indicated by dye tracer tests. *Beitr. Geologie Schweiz – Hydrol.* 28(II): 523-534. Bern: Kümmerly + Frey.

Colour Index 1971. Society of Dyers and Colourists (ed). 3rd Ed., 5 Bände, Bradford-Yorkshire. Supplement 1 (Vol. 1-4) 1974).

CORAPCIOGLU, M.Y. & J. SHIYAN 1993. Colloid-facilitated groundwater contaminant transport. *Water Resourc. Res.* 29: 2215-2226.

CORNAX, R., M.A. MORIÑIGO, I.G. PAEZ, M.A. MUÑOZ & J.J. BORREGO 1990. Application of direct plaque essay for detection and enumeration of bacteriphages of *Bacteriodes fragilis* from contaminated-water samples. *Appl. Environ. Microbiol.* 56: 3170-3173.

COSTIN, D. 1963. Dye diffusion experiments in the New York Bight. *Tech. Rep. Lamont, Geol. Obs.* No Cu-2-63 to AEC.

CRABTREE, H. 1970. Water tracing with optical brightening agents. *Univ. Leeds, Speleol. Ass. Rev.* 7: 26-28.

CRABTREE, H. 1971. Water tracing with optical brightening agents – Part II. *Univ. Leeds, Speleol. Ass. Rev.* 8: 29-31.

CRAMER, K. 1967. *Höhlen- und Karsterscheinungen.* Erläuterungen GK 25 Nr. 8432 (Oberammergau), pp 99-105. München.

CRAMER, K. 1982. Die Notwendigkeit der Dokumentation von Tracerversuchen. *Beitr. Geologie Schweiz – Hydrol.* 28(I): 135-142. Bern.

CROCOLL, R. 1990. Der hydrogeologische Standorttyp 'Gipskeuper' am Beispiel des 'naturdichten' Modellstandortes Mühlacker. *Z. dt. geol. Ges.* 141: 306-309. Hannover.

DANIELS, B. & P.C. MAYER 1957. Über die Verwendung von Dextrose als Indikator für Flutwasser. *Erdöl-Z.* 5: 126-128. Wien-Hamburg: Urban-Verlag GmbH.

D'ANS, J. & LAX, E. 1970. *Taschenbuch für Chemiker und Physiker*, 3rd Ed., Bd.III, 670 p. Berlin-Göttingen-Heidelberg: Springer.

DARLAND, G. & T.D. BROCK 1971. *Bacillus acidocaldarius* sp.nov., an acidophilic thermophilic spore-forming bacterium. *J. General Microbiol.* 67: 9-15. Great Britain.

DASCHNER, F.D. 1980. The epidemiology of *Serratia marcescens*. In v.GRÄVENITZ, A. & S.J. RUBIN (eds), *The Genus Serratia,* 187-196. Boca Raton/Florida: CRC Press Inc.

DAUBNER, I. 1972. *Mikrobiologie des Wassers*. München: Verlagsgesellschaft mbH.

DAUR, E. & F. RÖHRER 1921. Die Pforzheimer Typhusepidemie vom Jahre 1919, ihre Entstehung und die zur Vermeidung einer Wiederholung getroffenen Maßnahmen. *Gas- u. Wasserfach* 64(18): 277-302, 319-323. München.

DAVIS, J.T., E. FOLTZ & W.S. BLAKEMORE 1970. *Serratia marcescens,* a pathogen of increasing clinical importance. *J. Am. Med. Assoc.* 214 (12): 2190-2192. *Ref.: Naturwiss. Rdsch.* 24(10): 445 1971).

DAVIS, S.N., D.J. CAMPBELL, H.W. BENTLEY & T.J. FLYNN 1985. *Ground water tracers,* 200 p. Worthington, Ohio: Nat. Water Well Ass. (ed.).

DAVIS, S.N., G.M. THOMPSON, H.W. BENTLEY & G. STILES 1980. Ground-water tracers – a short review. *Ground Water* 18: 14-23.

DECHANT, M. & P. HACKER 1988. Neue Entwicklungen in der Methode des Sporennachweises. *Proc. 5th Int. Symp. Underground Water Tracing*, pp 149-155. Athen: IGME.

DECHANT, M. 1959. Das Anfärben von Lycopodiumsporen. In MAURIN, V. & J.ZÖTL (1959), Die Untersuchung der Zusammenhänge unterirdischer Wässer mit besonderer Berücksichtigung der Karstverhältnisse. *Steir. Beitr. Hydrogeol.* 1959: 145-149. Graz.

DECHANT, M. 1967. Die Färbung der Lycopodiumsporen. *Steir. Beitr. Hydrogeol.* 1966/67: 241-247. Graz.

DECHANT, M. 1976. Die Präparation von Lycopodiumsporen in Form einer Suspension. *Steir. Beitr. Hydrogeol.* 1976: 166-169. Graz.

DECHANT, M., V. MAURIN & J. ZÖTL 1958. Die Triftung gefärbter Sporen, eine neue Methode zur Untersuchung unterirdischer Karstgerinne. *Steir. Beitr. Hydrogeol., N.F.* 1958(1/2): 44-51. Graz.

DEMUTH, N. 1988. *Lichtmessung in Gewässern über die Photolyse von Fluoreszenzfarbstoffen.* Diplomarb., 115 p.(Ms.), 37 Tab., 53 Fig. Freiburg i.Br.

DERVEY, A. 1985. *Beitrag zum Sorptionsverhalten von Fluoreszenztracern.* Diplomarb., 80 p., (Ms.). Bern.

DEV = Deutsche Einheitsverfahren zur Wasser-, Abwasser- und Schlammuntersuchung, Teil A-S, Loseblattsammlung Weinheim, Verlag Chemie.

DFG 1971, 1977, 1984. Mitteilungen der Farbstoff-Kommission in der Deutschen Forschungsgemeinschaft, Kosmetische Färbemittel. Wiesbaden: Franz Steiner.

DIENERT, F. 1909a. Des matières fluorescentes contenues dans les eaux. *Bull. soc. chim. France* 5: 326-329. Paris.

DIENERT, F. 1909b. Des procédés employés pour mesurer la fluorescente des eaux. *Bull. soc. chim. France* 5: 330-332. Paris.

DIENERT, F. 1912. Eaux douces et eaux minérales – Collection de manuel pratique d'analyses chimiques, 363 p. Paris-Lüttich: Baudry et Cie.

DIENERT, F. 1913. Rémarques au sujet des expériences avec la fluorésceine. *C.R. Acad. Sci.* 157: 660-661. Paris.

DIETZ, F. 1975. Die Borkonzentration in Wässern als ein Indikator der Gewässerbelastung. *GWF, Wasser-Abwasser* 116(7): 301-308. München: Oldenbourg.

DIETZEL, K. 1978. Praktische Erfahrungen beim Bau und Betrieb von Wassermengenmeß-einrichtungen. Gezeigt am Beispiel der chemischen Industrie. *GWF, Wasser-Abwasser* 30: 149-183. Aachen: Ges. zur Förderung der Siedlungswasserwirtschaft an der RWTH e.V.

DIMITROULAS, C., T. PAPADIMITROULAS & N. PAPAKIS 1963. The loss of tracers in various geological formations. *Mem. Internat. Ass. Hydrogeol.* VI: 113-120. Belgrad.

DIMITROULAS, C., T. PAPADIMITROULAS & N. PAPAKIS 1964. Groundwater investigation by the use of neutron activation analysis. *Mem. Internat. Ass. Hydrogeol.* V: 83-103. Athens.

DIN = Deutsches Institut für Normung Berlin, DIN 38402-38414. Berlin: Beuth.

DIN 1988 1989. Deutsches Institut für Normung, DIN 1988: Technische Regeln für Trinkwasserinstallationen (TRW), Teil 1-8, 1.Ed., XII +500 p. Berlin-Köln: Beuth Verlag.

DODSON, W.H. 1968. *Serratia marcescens* Septicemia. *Arch. Intern. Med.* 121: 145-150. Chicago.

DOLAK, E.A. 1966. Sonderfälle der Markierungstechnik zur Klärung von Verwässerungsursachen ölführender Sande. *Erdöl-Erdgas-Z.* 82(9): 372-377. Wien-Hamburg: Urban-Verlag GmbH.

DOLAK, E.A. 1968. Radioactive tracers find new applications in oil production. *Oil and Gas Internat.* 8(10): 96-100.

DOLAK, E.A. 1969. Ergebnisse der Markierung von Tiefenwässern in Erdölfeldern. *Steir. Beitr. Hydrogeol.* 1969: 151-179. Graz.

DOLL, H.G. & H.F. SCHWEDE 1947. Radioactive markers in oil-field practice. *Technical Publ.* 2261, 10 p. New York: Am. Inst. Mining and Metallurgical Engineers, Class G: Petroleum Technology.

DOMBROWSKI, H. 1965. Das Alter des Lebens. *Bild der Wissenschaft* 8: 654-664. Stuttgart.

DOMBROWSKI, H. 1967. Durch fossile Pollen markierte Mineralwässer. *Steir. Beitr. Hydrogeol.* 1966/67: 267-274. Graz.

DOMBROWSKI, H. 1972. Zur Problematik der Markierung mit *Serratia marcescens*. *Geol. Jb.* C2: 247-250. Hannover.

DOMBROWSKI, H. 1977. *Serratia marcescens* Bizio 1823, Stamm 08/Novotny, als apathogene Species für den Einsatz bei Markierungsversuchen. *Pap. 3rd Int. Symp. Underground Water Tracing (3.SUWT)* 1: 73-75. Ljubljana-Bled, September 27 – October 1, 1976, Postojna.

DOMBROWSKI, H. 1978. Der Rückgang des Schwefelgehaltes in den Bad Nenndorfer Heilquellen und seine Ursache. *Fischer u. Teichwirt*, 7: Juli 1978.

DOSCH, F. 1956. Färbversuch Hochschneeberg 1955. *Gas/Wasser/Wärme* 10(1/2): 1-6 und 39-45. Wien.

DOSCH, F. 1968. Erfahrungen mit verschiedenen Methoden der Grundwassermarkierung. *Gas/Wasser/Wärme* 22: 1-8. Wien.

DRABAEK, I. 1982. Analysis and time stability of activable hydrospheric tracers. *J. Radioanalyt. Chem.* 75: 97-106.

DREW, D.P. 1968. A study of the limestone hydrology of St.Dunstan's Well and Ashwick drainage basins, Eastern Mendip. *Proc. Univ. Bristol, Speleol. Soc.* 11(B): 257-276.

DREYBRODT, W. 1988. Processes in karst systems: physics, chemistry and geology. *Springer Ser. Environments* 4: 288 p. Berlin-New York: Springer.

DREYER, J. 1987. *Anfärbung und Einsatz rotfluoreszierender Sporen als Grundwasser-markierungsmittel.* Diplomarb. Univ. Freiburg i.Br.(Ms.), 77 p. Freiburg i.Br.

DROST, W. & E. HOEHN 1989. Macrodispersivity in granular aquifers determined with single well techniques using ^{82}Br as a tracer. *Radiochim. Acta* 47: 13-20.

DROST, W. & F. NEUMAIER 1974. Application of single borehole methods in groundwater research. *Isotope Techniques in Groundwater Hydrology* II: 241-254. Vienna: IAEA.

DROST, W. & H. MOSER 1980. Einbohrlochmethoden. In H. MOSER & W. RAUERT, Isotopenmethoden in der Hydrologie. *Lehrbuch der Hydrogeologie*, Bd. 8: 224-252. Berlin-Stuttgart: Gebr. Borntraeger.

DROST, W. 1970. Groundwater measurements at the site of the Sylvensteindamm in the Bavarian Alps. *Isotope Hydrol.*, pp 421-437. Vienna: IAEA.

DROST, W. 1971. Grundwassermessungen mit radioaktiven Isotopen. *Geologica Bavarica* 64: 167-196. München.

DROST, W. 1974. Application of groundwater measurements by means of radioisotopes on groundwater exploration. *Water for the Human Environment* I: 357-369. Campagne: IWRA.

DROST, W. 1983. Single well techniques. Tracer Methods in Isotope Hydrology, *IAEA-TECDOC* 291: 7-16. Vienna: IAEA.

DROST, W. 1984. Einbohrlochmethoden zur Bestimmung der Filtergeschwindigkeit und der Fließrichtung des Grundwassers. *Wasser u. Boden* 36: 145-153.

DROST, W. 1986. Groundwater measurements by means of radioactive tracers. *Atomkernenergie Kerntechnik* 48: 81-86.

DROST, W. 1989. *Single-well and multi-well nuclear tracer techniques – A critical review.* Technical Documents in Hydrology, SC-89/WS-54, 10 + 96 p. Paris: UNESCO.

DROST, W., H. KUSSMAUL, H. MOSER, W. STICHLER & P. TRIMBORN 1977. Hydrologische und hydrochemische Untersuchungen zur Uferfiltration. Teil 2: Erfassung der Grundwasserströmung mit isotopenhydrologischen Methoden in einem Gebiet mit zwei Uferfiltrat fördernden Wasserwerken am Niederrhein. *GWF, Wasser-Abwasser* 118: 572-581. München: Oldenbourg.

DROST, W., W. RAUERT, W. STICHLER & G. LEHMANN 1982. Isotopenhydrologische Untersuchungen im linksrheinischen Teil von Düsseldorf. Beitr. über hydrologische Tracermethoden und ihre Anwendungen. *GSF-Ber.* R 290: 238-254. Neuherberg.

DRUCKREY, H. 1955. Schädliche und unschädliche Farbstoffe für Lebensmittel. *Z. Krebsforsch.* 60: 344-360.

DUNN, B. & D.E. VAUPEL 1965. Effects of sample and fluorometer-compartment temperatures on fluorometer readings. *Geol. Surv. Res., Prof. Pap.* 525-D: 225-227. Washington.

DUNN, J.A. 1963. New methods of water tracing. *J. Eldon Pothole Club* 5: 5 (cit. after DAVIS et al.1985).

DUNN, J.R. 1957. Streamtracing. *Bull. Mid.-Appalachian Region, Nat. Spel. Soc.* 2:7.

DURAND, J. et al. 1967. Étude de la flore bactérienne des poissons du Niger supérieur. *Cah. Ostrom, Sér. Hydrobiol.* 1: 133.

DÜRBAUM, H.-J. 1967. Zur Bestimmung der natürlichen Grundwasserströmung mit Tracern. *Atomkernenergie* 12(3/4): 130-132. München: Karl Thiemig KG.

DVGW 1983. Forum Mikroorganismen und Viren in Grundwasserleitern, München 1983. *DVGW-Schriftenreihe Wasser* 35: 169 p. Eschborn.

DVWK 1983. Uranin-Einsatz einschränken. *Wasser u. Boden* 35(1), DVWK-Nachr. p. 6. Hamburg-Berlin: Parey.

DZIKOWSKI, M., E. CARLIER, N. CRAMPON & G. de MARSILI 1993. Rélation entre responses impulsionelles et conditions hydrodynamiques dans le cadre de traçages artificiels des aquiferes karstiques: Applications sur colonne de laboratoire et sur un système karstique a double entrée dans le causses de Grammat (Lot, France). *IAHS-Publ.* 207: 391-404. Wallingford, UK.

EGGER, F. 1929. Arbeitserfahrungen beim Nachweis des Zusammenhanges von Wasservorkommen durch Fluoreszeineinfärbung. *Vom Wasser* 3: 22-33. Berlin.

EHMANN, W.D. & D. VANCE 1991. Radiochemistry and nuclear methods of analysis. In D.D. WINGFORDER (ed.), *Chemical analysis* 116, 531 p. New York-Chichester-Brisbane-Toronto-Singapore: J.Wiley & Sons.

EIELAND, E. 1966. Eine Untersuchung der Verunreinigung durch Abwasser bei den Seebadeorten Trondheims. Zbl. Bakteriol., Parasitenkde. *Infektionskrankheiten u. Hygiene, Erste Abt. Orig.* 199: 216-225. Stuttgart: Gustav Fischer.

EISENBRAND, J. 1953. Über die Fluoreszenz der Kondensationsprodukte einiger aromatischer Aldehyde mit Hippursäure (Azlacton). *Arch. Pharmazie*, 286(1) = *Ber. dt. pharmazeut. Ges.* 58(1): 441-447. Weinheim, Bergstr.: Verlag Chemie.

EISENBRAND, J. 1966. *Fluorimetrie,* 153 p., 81 Fig., 23 Tab. Stuttgart: Wiss. Verlagsges.

EISSELE, K. & G. LINK 1981. Gebirgsdurchlässigkeit im Nordschwarzwälder Buntsandstein und ihre Verminderung durch Injektionen, dargestellt am Beispiel der Nagoldtalsperre Erzgrube. *Jh. geol. Landesamt Baden-Württemberg* 22: 59-97. Freiburg i.Br.

EISSELE, K. 1961. Erfahrungen mit der Sporentriftmethode. *Jb. geol. Landesamt Baden-Württemberg* 5: 345-350. Freiburg i.Br.

EISSELE, K. 1963. Zur Deutung und Auswertung von Salzungsversuchen. *Gas- u. Wasserfach (Wasser-Abwasser 639)* 104(40): 1158-1160. München: Oldenbourg.

ELLIS, E.L. & M. DELBRUCK 1939. The growth of bacteriophages. *J. Gen. Physiol.* 22: 369-384.

ELLIS, W.R. 1967. A review of radioisotope methods of stream gauging. *J. Hydrol.* 5: 233-257.

ERDTMAN, G. 1954. *An introduction to pollen analysis,* 239 p. Woltham, Mass.: Chronica Bot. Co.

ERLICH, H.A (ed) 1989. *PCR Technology: Principles and applications for DNA amplification,* 246 p. New York: Stockton Press.

EUROPARAT 1975. Wissenschaftliche und technische Kommission – Arbeitsgruppe 'Rheingrundwasser', Karte der Salzhaltigkeit 1:200 000, Strassburg.

EUROPARAT 1982. Parlamentarische Versammlung – Arbeitsgruppe 'Rheingrundwasser', Karte der Chloridgehalte des Rheingrundwassers 1:500 000, Strassburg, 2.Ed.: 1983.

EVANS, G.V. 1983. Tracer techniques in hydrology. *Int. J. Appl. Radiat. Isot.* 34: 451-475.

EWG 1989. Verordnung (EWG-Nr.213/89) der Kommission vom 27.Januar 1989. Amtsblatt der Europäischen Gemeinschaften, L 25: 70 p., Brüssel.

FABER, E., H. FRIEDRICHSEN, M.A. GEYH, A. HÖHNDORF, H. MEYER, H. MOSER, P. TRIMBORN, H. NIELSEN W. STAHL, W. STICHLER, G.A. WAGNER & I. WENDT 1985. Isotopengeophysik. In BENDER, F. (ed.), *Angewandte Geowissenschaften, Bd. II: Methoden der Angewandten Geophysik und mathematische Verfahren in den Geowissenschaften,* pp 491-609. Stuttgart.

FABIOL, R. & H. POUZANCRE 1981. Evolution de la fluorescéine en milieu thermal jusqu'à 200°C. *Bull. BRGM* (2)III, 3 1980/81), 249 p. Orléans.

FAEGRI, I. & J. IVERSON 1964. *Textbook of pollen analysis.* Oxford: Blackwell.

FAY, S.R., R.C. SPONG, S.C. ALEXANDER & E.C. ALEXANDER 1995. Optical brighteners: Sorption behaviour, detection, septic system tracer applications. *Proc. IAH XXXVI Congress, Edmonton/CDN,* 8 p.

FECKER, E. & G.REIK 1987. *Baugeologie.* 418 p. Stuttgart: Enke.

FETTER, C.W. 1993. *Contaminant Hydrogeology,* 458 p. New York: Macmillan.

FEUERSTEIN, D.L. & R.F. SELLECK 1963. Fluorescent tracers for dispersion measurement. *Am. Soc. Civil Engineers Proc., J. Sanitary Engng. Div.* 89: 1-29.

FEULNER, A.J. & J.H. HUBBLE 1960. Occurence of strontium in the surface and groundwaters of Champaign County, Ohio. *Econ. Geol.*, 55: 176-186. New Haven, Conn.: The Economic Geology Publishing Comp.

FISCHER, M. 1982. Abflußmessungen mit Tracern nach dem Verdünnungsverfahren. *Beitr. Geol. Schweiz – Hydrol.* 28(II): 447-458. Bern: Kümmerly + Frey.

FISCHER, W.K. & P. GODE 1977. Die Prüfung von Chemikalien auf Toxizität gegenüber Kleinkrebsen (*Daphnia magna*). *Vom Wasser* 48: 247-254. Weinheim.

FISCHER, W.K. 1962. Nachweismethoden für Detergentien. *Münchener Beitr. z. Abwasser-, Fischerei- u. Flußbiol.* 9: 163-182. München.

FLETCHER, M.W. & R.L. MYERS 1974. Ground water tracing in karst terrain using bacteriophage T-4. *Abstr. Ann. Meet., Amer. Soc. Microbiol.* 74: 52.

FLORKOWSKI, T. 1991. Tritium in river flow-rate gauging – theory and experience. *IAEA-TECDOC* 601: 35-44. Vienna: IAEA.

FLORKOWSKI, T., T.G. DAVIS, B. WALLNDER & D.R.L. PRAK-HABAR 1969. The measurements of high discharge in turbulent rivers using tritium tracer. *J. Hydrol.* 8: 249-264.

FLURY, F. & H. FLÜHLER 1994. Brilliant Blue FCF as a dye tracer for solute transport studies – A toxicological overview. *J. Environ. Qual.* 23: 1108-1112.

FLURY, F. & H. FLÜHLER 1995. Tracer characteristics of brilliant blue FCF. *Soil Sci. Soc. Am.J.* 59: 22-27.

FLURY, F. 1984. Multitraçage sur le plateau de bure (Ajoie, Ju) à l'aide de bacteriophages et de traceurs fluorescents. *Bull. du Centre d'hydrogéologie* 5: 91-105. Bern-Frankfurt/M.-New York: Peter Lang.

FONTES, J.C. & J.M. GARNIER 1979. Determination of the initial ^{14}C activity of the total dissolved carbon: a review of the existing models and a new approach. *Water Resources Res.* 15: 399-413.

FORD, D. & P. WILLIAMS 1989. *Karstgeomorphology and Hydrology,* 601 p. London: Unwin Hyman.

FORSTER, A.E. 1922. Hydrographische Forschungen in Inner- und Unterkrain. *Mitt. Geogr. Ges. Wien* 65.

FORSTER, M. 1984. C-14 und Ar-39 in einem Grundwasserleiter des Saarlandes. Vergleich zweier Grundwasserdatierungsmethoden. Diss., Univ. München.

FORSTER, M., K. RAMM & P. MAIER 1992. Argon-39 dating of groundwater and its limiting conditions. In *Isotope Techniques in Water Resources Development 1991,* pp 203 214. Vienna: IAEA.

FÖRSTER, TH. 1951. *Fluoreszenz organischer Verbindungen,* 312 p., 81 Fig. Göttingen: Vandenhoek & Ruprecht.

FOURNEAUX, J.C. & J. ROCHAT 1982. Essais 'in situ' de quatre traceurs fluorescents. *Beitr. Geol. Schweiz – Hydrol.* 28(I): 91-100. Bern: Kümmerly + Frey.

FOURNIER, E. 1900. Recherches spéléologiques dans la Chaîne de Jura – 1.Partie: Grottes résurgences et gouffres. *Mém. Soc. Spel.* IV(24): 3-34. Paris.

FOURNIER, E. 1901. Les phénomènes de capture des cours d'eau superficiels par les cours souterrains, dans les régions calcaires. *C. R.* 133(2): 961-963. Paris.

FRANÇOIS, O. & P. CALMELS 1997. Field tracer tests for the simulation of pollutant dispersion in the Doller river. In KRANJC, A., Tracer Hydrology 97. *Proc. 7th Int. Symp. Water Tracing (SWT)of the ATH, 26-31 May 1997, Portoroz/Slovenia,* pp 121-125. Rotterdam: Balkema.

FRANK, M. 1936. Thermal- und Mineralwasserbohrungen im Gaistal und in Herrenalb und die Bohrungen im Eyachtal. *Württ. Jb. Statistik u. Landeskde.* 1934/35, pp 148-163. Stuttgart.

FRÄNKEL, C. & L. PIEFKE 1890. Versuche über die Leistungen der Sandfiltration. *Z. Hygiene* 8(1): 1-40. Leipzig: Veit u.Co.

FRASER, D.W. & E.A. JERREL 1953. The amino acid composition of T3 bacteriophage. *J. Biol. Chem.* 265: 291-295.

FRIEDLANDER, G., J. KENNEDY, E.S. MACIAS & J.M. MILLER 1981. *Nuclear- and Radiochemistry,* 3. Ed., 586 p. New York: Wiley & Sons, Inc.

FRISCHAUF, J. 1890. Zur Erforschung der unterirdischen Wasserläufe. *Mitt. dt. u. österr. Alpenverein* 10: 131-132.

FRITZ, P. & J.Ch. FONTES (eds) 1980. *Handbook of Environmental Isotope Geochemistry 1, The Terrestrial Environment, A,* 546 p. Amsterdam-Oxford-New York: Elsevier Publ.Co.

FRITZ, P. & J.Ch. FONTES (eds) 1986. *Environmental Isotope Geochemistry 2, The Terrestrial Environment, B,* 271 p. Amsterdam-Oxford-New York: Elsevier Publ.Co.

FRÜNGEL, F. & C. KOCH 1976. Practical experience with the variosens equipment in measuring chlorophyll concentrations and fluorescent tracer substances, like rhodamine, fluorescein, and some new substances. *EEE J. Oceanic Engng.* OE-1(1): 21-32, Inst. Electrical Electronics Eng., Inc., USA.

FRÜNGEL, F. & C. KOCH 1978. Zum Stand der Technik moderner in-situ-Fluorimeter. *Chemie-Techniker* 7: 217-219. Heidelberg: Hüthig.

GAILLARD, B. 1976. Méthode de traceurs pour la détermination des paramètres de transfert de substances en solution dans l'eau des aquifères. Diss. Univ. scientifique et médicale de Grenoble, Bd. I Textteil, pp 1-118, Bd. II Fig. 1-81.

GANDENBERGER, W. & E. OEHLER 1963. Verölung von Oberflächenwasser und seine Aufbereitung in Wasserwerken. *Schriftenreihe des dt. Arbeitskreises Wasserforsch. e.V. (DAW)* 1, 62 p. Berlin-Bielefeld-München.

GARDNER, G.D. & R.E. GRAY 1976. Tracing subsurface flow in karst regions using artificially colored spores. *Bull. Ass. Engr. Geologists* 13(3): 177-197.

GARDNER, R.P. & J.W. DUNN 1964. A single-sample radiotracer technique for determining stream flow rates. *Int. J. Appl. Radiat. Isot.* 16: 339-344.

GÄRTNER, A. 1902. Die Quellen in ihren Beziehungen zum Grundwasser und zum Thyphus. *Klinisches Jahrbuch* IX, 162 p. Jena: G.Fischer.

GÄRTNER, A. 1915. *Die Hygiene des Wassers*. Braunschweig: Vieweg.

GASCOYNE, M. 1974. Hydrogeological investigations in Northern Venezuela. *Trans. Brit. Cave Res. Ass.* 1(3): 169-179.

GASPAR, E. & M. ONCESCU 1972. *Developments in Hydrology 1; Radioactive Tracers in Hydrology,* 342 p. Amsterdam-London-New York: Elsevier. (Transl. from Rom. Original Edition 1967).

GASPAR, E. 1987. *Modern trends in tracer hydrology*. CRC Press, Inc. I, 145 p., II, 137 p. Boca Raton/Florida.

GAT, J.R. & R. GONFIANTINI (eds) 1981. Stable Isotope Hydrology, Deuterium and Oxygen-18 in the Water Cycle. *Techn. Rep. Ser.* No. 210, 337 p. Vienna: IAEA.

GEISLER, R. 1953. Mit Eosin gefärbte Futtertiere unschädlich. *Fischwirt* 3: 51-52, 123-124. Ed. Landwirtschaftskammer Kiel.

GEISTER-FRANZ, M. 1981. Written Comm. from 18 Nov.1981.

GELHAR, L.W. 1986. Stochastic subsurface hydrology from theory to applications. *Water Resources Res.* 22: 135-145.

GERBA, C.P. & G. BITTON 1984. Microbial pollutants, their survival and transport pattern to groundwater. In BITTON, G. & C.P. GERBA (eds), *Groundwater Pollution Microbiology*, pp 65-88. New York: John Wiley.

GERBA, C.P. & S.M. GOYAL 1982. Concentration of viruses from water by membrane filters. In GERBA, C.P. & S.M. GOYAL (eds), *Methods in environmental virology*, pp 59-116. New York: Marcel Dekker, Inc.

GERBA, CH.P. & S.M. GOYAL 1978. Adsorption of selected entero-viruses to soil. *State of Knowledge in Land Treatment of Wastewater* 2: 225-232. US-Government Printing Office, 1978 – 700-771/123.

GEYER, O.F. & M.P. GWINNER 1991. *Geologie von Baden-Württemberg,* 4.Ed., 482 p. Stuttgart: Schweizerbart.

GIBBS 1927. Phenol tests. *J. Biol. Chem.* 72: 649 Baltimore: Waverly Press. (cit. after HETTCHE 1941).

GILCREAS, F.W. & S.A. KELLY 1955. Relation of the coliform organism test to enteric virus pollution. *J. Am. Water Works Ass.* 47: 683. Dublin/Ohio.

GILATH, CH. 1983. Concentration dynamics in lakes and reservoirs studies using radioactive tracers. *IAEA-TECDOC* 291: 131-156. Vienna: IAEA.

GILLAND, O., L. HELGASON, P. LEISSNER & S. STATTIN 1965. Arm-retina fluorescein circulation time in carotic obstruction. *Acta Neurol. Scand.* 41(13/1): 319-333.

GLMZ 1980. Großpumpversuch im Erolzheimer Feld/Illertal vom 10.Oktober 1979 bis 6.März 1980, Teilbericht Grundwassermarkierungsversuche. Geol. Landesamt Baden-Württemberg, Landesanstalt für Umweltschutz Baden-Württemberg, Medizinisches Landesuntersuchungsamt Stuttgart und Zweckverband Landeswasserversorgung, 15 p.(Ms.), Oktober 1980.

GLOVER, R.R. 1972. Optical brighteners – a new water tracing regent. *Transactions Cave Research Group, Great Britain* 14(2): 84-88.

GLOXHUBER, CHR., G. HECHT & G. KIMMERLE 1962. Toxikologische Untersuchungen mit Aufhellern (Blankophor$_R$-Typen). *Arch. Toxikol.* 19: 302-312. Berlin-Göttingen-Heidelberg: Springer.

GOLDBRUNNER, J.E., P. RAMSPACHER, H. ZOJER, J.G. ZÖTL, H. MOSER, W. RAUERT & W. STICHLER 1982. Die Anwendung natürlicher und künstlicher Tracer in einem hochalpinen Magnesitbergbau. *Beitr. Geol. Schweiz – Hydrol.* 28(II): 407-422. Bern: Kümmerly + Frey.

GOYAL, S.M. & C.P. GERBA 1979. Comparative adsorption of human enterovirus, simian rotavirus, and selected bacteriophages to soils. *Appl. Environ. Microbiol.* 38: 241-247.

GRABOW, W.O.K. & P. COUBROUGH 1986. Practical direct plaque assay for coliphages in 100-ml samples of drinking water. *Appl. Environ. Microbiol.* 52: 430-433.

GRAF, J.B. 1986. Traveltime and longitudinal dispersion in Illinois streams. US Geol. Survey Water-Supply Paper 2269. Washington D.C.

GRANT, S.B., E.J. LIST & M.E. LINDSTROM 1993. Kinetic analysis of virus adsorption and inactivation in batch experiments. *Water Resourc. Res.* 29: 2067-2085.

GRÄVENITZ, A. VON 1980. Infection and colonization with *Serratia.* In *The Genus Serratia*, pp 167-186. Boca Raton/Florida: CRC Press Inc.

GRIFFIONEN, P.S. 1989. Alarmmodell für den Rhein. *Ber.* Nr. II-2 der KHR, Lelystad.

GROCHE, D. 1964. Die Messung von Fließvorgängen in ausgeführten Bauwerken der Abwasserreinigung. *Stuttg. Ber. Siedlungswasserwirtsch.* 13 (Diss.). München: Oldenbourg.

GROSCHOPF, P. 1957. Färbversuche auf der Ulmer Alb, ihre wissenschaftliche und praktische Bedeutung. *Mitt. Ver. Naturwiss. u. Mathematik in Ulm (Donau)* 25: 277-282. Ulm.

GROSCHOPF, P. 1972. Markierungsversuche und karsthydrographische Forschungen auf der östlichen Schwäbischen Alb. *Geol. Jb.* C2: 189-197. Hannover.

GROVE, D.B. & W.A. BEETEM 1971. Porosity and dispersion constant calculations for fractured carbonate aquifer using two well tracer method. *Water Resour. Res.* 7: 128-134.

GRÜTZNER, R. 1939. *Heterozyklische Verbindungen mit einem Ring-Sauerstoffatom,* Fortschr. Heilstoffchem., 2.Abt., III.Bd., pp 1-53. Berlin.

GUIZERIX, J., G. GRANDCLÉMENT, R. HOURS, H. ANDRÉ, R. WOLF & R. PEREZ 1963. Les mesures de débit effectuées en France à l'aide de traceurs radioactifs par la méthode d'integration. *Proc. Symp. on the Application of Radioisotopes in Hydrology, Held by the International Atomic Energy Agency in Tokyo, March 5-9, 1963*, pp 255-281. Vienna.

GÜNTHERT, W. & H. BEHRENS 1982. Messungen des physikalischen Sauerstoffeintrages in Fließgewässern mit Tracern – Verfahren und Anwendungsbeispiele. *Beitr. Geol. Schweiz – Hydrol.* 28(II): 471-482. Bern: Kümmerly + Frey.

HAAS, J.L. 1959. Evaluation of ground-water tracing methods used in speleology. *Bull. Nat. Spel. Soc.* 21: 67-76.

HACKER, P. 1988. Combined tracer experiments – An important tool for the determination of the sorption capability of a karst aquifer. *Proc. 21. IAH Congr. Guilin, 10.-15.Oct. 1988,* 21(2): 962-967. Beijing.

HACKER, P., H. ZOJER & J.G. ZÖTL 1983. Ergebnisse eines kombinierten Markierungsversuches im Basaltgebiet von Kibwezi (Kenya). *Steir. Beitr. Hydrogeol.* 34/35: 107-125. Graz.

HAGEDORN, C., D.T. HANSEN & G.H. SIMONSON 1978. Survival and movement of fecal indicator bacteria in soil under conditions of saturated flow. *J. Environmental Quality* 7: 55-59. (cit. after KESWICK et al.1982).

HÄGLER, A. 1873. Beiträge zur Entstehungsgeschichte des Typhus und zur Trinkwasserlehre. *Dt. Arch. Klin. Med.* 11: 237-267. Leipzig: F.W. Nagel. Ref.: Dt. Vierteljahresschr. öff. *Gesundheitspflege* 6: 154-157 (1874).

HAIDER, S. 1991. Durchflußmessung in Abwässerkanälen mittels Fluoreszeintracern. Diplomarb. (printed as Ms.), 265 p. Wien.

HAITINGER, H. 1959. *Fluoreszenzmikroskopie,* 2.Ed., 168 p. Leipzig.

HALEVY, E., A. NIR, Y. HARPAZ & S. MANDEL 1958. Use of radioisotopes in studies of groundwater flow: Part I. Laboratory and field experiments on the suitability of various tracers. *Proc. Sec. UN Int. Conf.on the Peaceful Uses of Atomic Energy* 20: 158-161.

HARDER, H. 1960/61. Einbau von Bor in detritische Mineralien. *Geochim. Cosmochim. Acta* 21: 284-294. Oxford.

HARVEY, J.W. 1993. Measurement of variation in soil solute tracer concentration across a range of effective pore sizes. *Water Resources Res.* 29(6): 1831-1837.

HARVEY, R.W., L.H. GEORGE, R.L. SMITH & D.R. LEBLANC 1989. Transport of microspheres and indigenious bacteria through a sandy aquifer: Results of natural- and forced-gradient tracer experiments. *Environ. Sci. Technol.* 23(1): 51-56.

HAVELAAR, A.H. 1986. F-specific RNA bacteriophages as model viruses in water treatment processes. Diss., 227 p. Utrecht.

HAVEMEISTER, G. & R. RIEMER 1983. Transport von Bakterien in verschiedenen porösen Medien. *DVGW-Schriftenreihe Wasser* 35: 101-111. Eschborn.

HAVEMEISTER, G., R. RIEMER & J. SCHRÖTER 1983. Lebensdauer und Transport von Bakterien in typischen Grundwasserleitern – Glazifluviale Sande im Segeberger Forst. *DVGW-Schriftenreihe Wasser* 35: 151-163. Eschborn.

HECK, E.T. 1954. Tracing fluids between wells. *Producers Monthly* 18: 31-33.

HEITFELD, K.H. & E. TÄTZLER 1967. Ergebnisse eines Färbversuches in tonig-sandigen Gesteinen an der Biggetalsperre (Sauerland). *Steir. Beitr. Hydrogeol.* 1966/67: 205-217. Graz.

HELLMANN, H. & M. SCHUMACHER 1977. Phosphate, Borate und Nitrate – Dynamik im Auftreten und Umsatz im Rheinstrom. *Tenside Detergents* 14(6): 321-325.

HENNIG, W. 1988. Beschleuniger-Massenspektroskopie- Isotopennachweis bei geringsten Konzentrationen. *Phys. Bl.* 44: 381-387.

HENRY, H.P. 1989. The use of the bacterial species *Escherichia coli* and *Bacillus globigii* as groundwater tracers. *Proc. Sligo Regional Technical College/Int. Ass. of Hydrogeologists (Irish Group) Seminar Sligo, 22nd September 1989*, pp 45-56. Sligo.

HERAK, M. & V.T. STRINGFIELD 1972. *Karst. Important karst regions of the Northern Hemisphere,* 551 p. Amsterdam: Elsevier.

HERRMANN, A. & W. STICHLER 1980. Groundwater-runoff relationships. *Catena* 7: 251-263.

HERRMANN, A., J. KOLL, CH. LEIBUNDGUT, P. MALOSZEWSKI, R. RAU, W. RAUERT & W. STICHLER 1986. Anwendung von Tracertechniken zur Erfassung des Wasserumsatzes in kleinen Einzugsgebieten – Stand und Fortgang der Arbeiten (Fortsetzung aus dem Juliheft 1984). *Dt. Gewässerkdl. Mitt.* 30(4): 85-93.

HERRMANN, A., P. MALOSZEWSKI, R. RAU, W. ROSENOW & W. STICHLER 1984. Anwendung von Tracertechniken zur Erfassung des Wasserumsatzes in kleinen Einzugsgebieten. Ein Forschungskonzept für die Oberharzer Untersuchungsgebiete. *Dt. Gewässerkdl. Mitt.* 28(3): 65-74.

HERZBERG, G. 1954. *Molecular spectra and molecular structure,* 402 p. Princeton-London-New York-Toronto: Van Norstrand.

HETTCHE, H.O. 1941. Ein neuer Indikator für Grundwasserströme. *Arch. Hygiene u. Bakteriol.* 125(1): 39-40. München-Berlin: Oldenbourg.

HEUMANN, K.G. & H. SEEWALD 1985. Gleichzeitige Bestimmung von Cl^-, Br^- und I^- in Wässern durch massenspektrometrische Isotopenverdünnungsanalyse. *Fresenius Z. anal. Chem.* 320: 493-497.

HILGERMANN, R. 1906. Über die Verwendung des *Bacillus prodigiosus* als Indikator bei Wasseruntersuchungen. *Arch. Hygiene* 59: 150-158. München-Berlin: Oldenbourg.

HIMMELSBACH, Th. & H. HÖTZL, 1991. Hydraulic investigations in high permeable fault and fracture zones of jointed granites. *Memoires of the 22nd Congress of IAH* XXVII: 216-224. Lausanne, Switzerland.

HIMMELSBACH, Th. & P. MALOSZEWSKI 1992. Tracer tests and hydraulic investigations in the observation tunnel Lindau. *Steir. Beitr. Hydrogeol.* 43: 197-223. Graz, Austria.

HIMMELSBACH, Th. 1993. Untersuchungen zum Wasser- und Stofftransportverhalten in Störungszonen im Grundgebirge (Albtalgranit, Südschwarzwald). Phd-Thesis Karlsruhe University, Schr. Angew. Geologie 23: 238 p. Karlsruhe, Germany.

HIRSIG, P. & J. PETERMANN 1984. Markierversuch im Sempachersee zur Ermittlung der Ausbreitungsvorgänge am Diffusor L2. Unveröffentl. Ber., 53 p. Kirchlindach.

HIRSIG, P. 1981. Markierung von gereinigtem Abwasser und dessen Verfolgung im See mittels fluoreszierender Tracer, am Beispiel der ARA der Region Murten. Publ. Gewässerkde./Geograph. Inst. Univers. Bern. *Gewässerkde.* 24. Bern.

HIRSIG, P. 1983. Wind- und zuflußbedingte Strömungen im Murtensee (Schweiz). Diss., Geograph. Inst. Univers. Bern.

HIRSIG, P., CH. LEIBUNDGUT & P. NYDEGGER 1982. The present situation regarding the use of fluorescent tracers in limnology. *Beitr. Geol. Schweiz – Hydrol.* 28(II): 495-510. Bern: Kümmerly + Frey.

HOEHN, E. & H.R. von GUNTEN 1989. Radon in groundwater: A tool to assess infiltration from surface waters to aquifers. *Water Resour. Res.* 25: 1795-1803.

HOFER, A. 1959. Das Mikroskopieren der Planktonnetzproben. *Steir. Beitr. Hydrogeol.* 1959: 140-145. Graz.

HOFMANN, K.A. & U.R. HOFMANN 1948. *Anorganische Chemie,* 12.Ed., 813 p. Braunschweig.

HÖLTING, B. & G. MATTHESS 1963. Ein Sporentriftversuch im Zechstein von Korbach/Hessen. Notizbl. hess. L. *Amt f. Bodenforsch.* 91: 237-255. Wiesbaden.

HÖLTING, B. 1977. Bemerkungen zur Herkunft der Salinarwässer am Taunusrand. *Geol. Jb. Hessen* 105: 211-221. Wiesbaden.

HOMMEL, G. 1987. *Handbuch der gefährlichen Güter (Merkblätter),* 5. Lief. Berlin-Heidelberg-New York: Springer.

HOPPE, W. 1967. Erhöhung des Chloridgehaltes und der Härte des Grundwassers durch Überbeanspruchung des Grundwasserleiters im Südharzkaligebiet. *Wiss. Z. der Hochschule für Architektur u. Bauwesen Weimar* 14(4): 393-396.

HORNUNG, H. 1935. Eine Trinkwasser-Typhusepidemie im Schwarzwald. *Arch. Hygiene* 113: 158-167.

HÖTZL, H. & A. WERNER 1992. In HÖTZL, H. & A. WERNER, Tracer Hydrology, *Proc. 6th Symp. on Water Tracing 21-26 Sept. 1992, Karlsruhe,* 464 p. Rotterdam: Balkema.

HÖTZL, H. & B. REICHERT (eds) 1996. *Deutsche Forschungsgemeinschaft. Schadstoffe im Grundwasser.* 4, 346 p. Weinheim: VCH Verlagsgesellschaft.

HÖTZL, H. & M. MOSER 1992. Applcation of tracer techniques for hydrogeologic studies of mass movements. In HÖTZL, H. & A. WERNER, Tracer Hydrology, *Proc. 6th Symp. on Water Tracing 21-26 Sept. 1992, Karlsruhe,* pp 357-363. Rotterdam: Balkema.

HÖTZL, H. & W. HUBER, 1972. Über die Hydrogeologie und wasserwirtschaftliche Nutzung der Aachquelle (Baden-Württemberg). *Geol. Jb.* C2: 359-382. Hannover.

HÖTZL, H. 1973. Die Hydrogeologie und Hydrochemie des Einzugsgebietes der obersten Donau. *Steir. Beitr. Hydrogeol.* 25: 5-102. Graz.

HÖTZL, H. 1989. Schadstoffausbreitung bei Überlagerung eines Karstaquifers mit einem Porengrundwasserleiter. *Oberrhein. geol. Abh.* 35: 17-35. Stuttgart.

HÖTZL, H. 1992. The lost Danube: Karst hydrogeology of the Western Swabian Alb, South Germany. *Int. Ass. Hydrogeologists, Int. Contrib. Hydrogeol.* 13: 179-196. Hannover: Heise.

HÖTZL, H., B. REICHERT, P. MALOSZEWSKI, H. MOSER & W. STICHLER 1989. Contaminant transport in bank filtration – Determining hydraulic parameters by means of artificial and natural labeling. In KOBUS, H.E. & W. KINZELBACH (eds), *Contaminant Transport in Groundwater,* pp 65-71. Rotterdam: Balkema.

HÖTZL, H., F. METZLER & P. ROTHENGATTER 1982. Die Kluftmarkierung – Eine Anwendung der Markierungstechnik zur Ermittlung von Durchlässigkeitseigenschaften klüftiger Gesteine. *Beitr. Geol. Schweiz – Hydrol.* 28(II): 381-393. Bern: Kümmerly + Frey.

HÖTZL, H., J. BRAUNS, K. CZURDA, H.J. SENG & W. MAZUR 1987. Vorstudie für ein Pilotprojekt zur Sanierung von Altlasten (Sondermülldeponie). *Schr. Angew. Geol. Karlsruhe* 2: 198 p. Karlsruhe.

HÖTZL, H., M. MOSER, B. REICHERT & K. RENTSCHLER 1994. Hydrogeologische Markierungsversuche in Massenbewegungen (Reppwandgleitung, Kärnten und Stubnerkogel, Salzburg). *Beitr. Hydrogeol.* 44: 69-92. Graz.

HÖTZL, H., W. KÄSS & B. REICHERT 1991. Application of microbial tracers in groundwater studies. *Wat. Sci. Tech. Great Britain* 24(2): 295-300. Oxford.

HOURS, R. 1955. Les traceurs radioactifs en hydrologie. *La Houille Blanche, No.Spec.*, pp 264-274.

HUBBARD, E.F., F.A. KILPATRICK, L.A. MARTENS & J.F. WILSON 1982. *Measurement of time of travel and dispersion in streams by dye tracing.* Techniques of Water-Resources Investigations of the US Geol. Survey, Book 3, Chapter A9, Washington D.C.

HUBER, L. 1989. Conclusions for an ecological evaluation of LAS. *Tenside, Surfactants, Detergents* 26(2): 71-74. München: Carl Hanser.

HUBER, L. 1989. Folgerungen für eine ökologische Beurteilung von LAS. *Tenside, Surfactants, Detergents* 26(2): 177-179. München: Carl Hanser.

HÜBNER, H. 1986. Isotope effects of nitrogen in the soil and biosphere. In FRITZ, P. & J.CH.FONTES (eds), *Handbook of Environmental Geochemistry* 2: 361-425. Amsterdam-Oxford-New York: Elsevier.

HULL, D.E. 1958. The total-count technique – A new principle in flow measurement. *Int. J. Appl. Radiat. Isotopes* 4: 1-15.

HUNKELER, D., E. HÖHN, P. HÖHENER & J. ZEYER 1997a. $_{222}$Rn as a partitioning tracer to detect diesel fuel contaminations: Laboratory studies and field observations. *Environ. Sci. Technol.*, in preparation.

HUNKELER, D., E. HÖHN, .P. HÖHENER & J. ZEYER 1997b. Can $_{222}$Rn be used as a partitioning tracer to detect mineral oil contaminations? – *Tracer Hydrology 97, Proceedings of the 7th International Symposium of Water Tracing, 26.-31. May 1997, Portoroz, Slovenia.* Rotterdam: Balkema.

HURST, C.J., C.P. GERBA & I. CECH 1980. Effects of environmental variables and soil characteristics on virus survival in soil. *Appl. Environ. Microbiol.* 40: 1067-1079.

IAEA 1963. *Radioisotopes in Hydrology,* 449 p. Vienna.

IAEA 1967. *Isotopes in Hydrology,* 740 p. Vienna.

IAEA 1970. *Isotopes in Hydrology* 1970, 918 p. Vienna.

IAEA 1974. *Nuclear Techniques in Groundwater Hydrology* I: 504 S, II: 499 p. Vienna.

IAEA 1979. *Isotope Hydrology* 1978, 984 p. Vienna.

IAEA 1981. Statistical Treatment of Environmental Isotope Data in Precipitations. *IAEA Techn. Rep. Ser.* 206: 255 p. Vienna.

IAEA 1983. *Guidebook on Nuclear Techniques in Hydrology,* 439 p. Vienna.

IAEA 1983a. Environmental Isotope Data No.7: World Survey of Isotope Concentration in Precipitation (1976-1979). *Techn. Rep. Ser.* 226: 241 p. Vienna.

IAEA 1983b. Tracer Methods in Isotope Hydrology. *IAEA-TECDOC* 291: 193 p. Vienna: IAEA.

IAEA 1984. *Isotope Hydrology* 1983, 873 p. Vienna.

IAEA 1986. Environmental Isotope Data No. 8: World Survey of Isotope Concentration in Precipitation (1980-1983). *IAEA Techn., Rep. Ser.* No. 264: 184 p. Vienna.

IAEA 1987. *Isotope Techniques in Water Resources Development,* 813 p. Vienna.

IAEA 1990. Environmental Isotope Data No. 9: World Survey of Isotope Concentration in Precipitation (1984-1987). *IAEA Techn. Rep. Ser.* 311, 188 p. Vienna.

IAEA 1991. Use of Artificial Tracers in Hydrology. *Proc. of an Advisory Group Meet., Vienna 19-22.März 1990, IAEA-TECDOC* 601: 230 p. Vienna.

IAEA 1992a. *Isotope techniques in water resources development* 1991, 787 p. Vienna.

IAEA 1992b. Statistical treatment of data on environmental isotopes in precipitation. *IAEA Techn. Rep. Ser.* 311, 781 p. Vienna.

IAEA 1992c. *Isotopes of noble gases as tracers in environmental studies,* 305 p. Vienna.

IAEA 1993. *Isotope techniques in the study of past and current environmental changes in the hydrosphere and the atmosphere,* 623 p. Vienna.

IAEA 1994a. Environmental isotope data No.10: World survey of isotope concentration in precipitation (1988-1991). *IAEA Techn. Rep. Ser.* 371, 214 p. Vienna.

IAEA 1994b. Mathematical Models and their Applications to Isotope Studies in Groundwater Hydrology – *IAEA-TECDOC-777, IAEA*, 283 p. Vienna.

ICARD, S. 1907. La mort apparente – Le certificat automatique des décès en l'absence du médecin. *La Nature* 35: 172-174. Paris: Masson et Co.

ICHIYE, P., H. TAKASHI & R. PLUTCHAK 1966. Photodensiometric measurements of dye concentration in the ocean. *Limnology and Oceanography* 11(2): 135-142.

IfH 1989. Jahresberichte 1963-1989 des Instituts für Hydrologie (bis 1987 Institut für Radiohydrometrie) der Ges. für Strahlen- und Umweltforschung mbH, Neuherberg.

IKEN, A. & R.A. BINDSCHÄDLER 1986. Combined measurements of subglacial water pressure and surface velocity of Findelengletscher, Switzerland: Conclusions about drainage systems and sliding mechanism. *J. Glaciology* 32(110): 101-119. Cambridge: International Glaciological Society.

IKSR/KHR Expertengruppe 1993. Alarmmodell Rhein. Ein Modell für die operationelle Vorhersage des Transportes von Schadstoffen im Rhein. Bericht Nr. I-12 der KHR, 122 p., Lelystad.

IMPERATI 1605. *Lettera del Padre Imperati ad Ulisse Aldovrandi di Bologna.* (cit. after TIMEUS, G. 1910a).

INMAN, E.I. Jr. & J.D. WINEFORDNER 1982. Constant energy synchronous fluorescence for analysis of polynuclear aromatic hydrocarbon mixtures. *Anal. Chem.* 54: 2018-2022.

Intern. Ass. Tracer Hydrology (eds) 1992. Transport phenomena in different aquifers – Investigations of the Association of Tracer Hydrology (1987-1992). *Steir. Beitr. Hydrogeol.* 43, 283 p. Graz.

IRSCH, W. 1980. Vom 'Blutstoff' zum Krankheitserreger – Ein Bakterium ändert sein Gesicht/Gezielte Bekämpfungsmethoden werden aktuell. *Bad. Neueste Nachr.* 22.3.1980.

IVANOVICH, M. & R.S. HARMON (eds) 1992. *Uranium series disequilibrium application to earth, marine and environmental sciences,* 907 p. Oxford: Clarendon Press.

IVANOVICH, M. & D.B. SMITH 1978. Determination of aquifer parameters by a two-well pulsed method using radioavtive tracers. *J. Hydrol.* 36: 35-45.

JÄCKLI, H. & K. KLEIBER 1943. Temperaturstudien an Gebirgsquellen. *Eclog. Geol. Helvetiae* 36(1): 7-14.

JAMES, J.M. & D.J. MARTIN 1980. Hydrological study in the Yu Atea catchment – The case of the disappearing of rhodamine; Problems encountered when using fluorescent water tracers in karst in Papua New Guinea. In JAMES, J.M.& H.J. DYSON (eds), *Caves and Karst in Muller Range,* pp 86-90.

JAWETZ, E., J.L. MELNICK & E.A. ADELBERG 1970. *Review of medical microbiology,* 9.Ed., 484 p. Los Altos.

JENNINGS, A.R. & M.C. SCHROEDER 1968. Laboratory evaluation of selected radioisotopes as ground-water tracers. *Water Resources Res.* 4: 829-838.

JENSEN, M. & K.K. KRISTENSEN 1989. Effects of rhodamine water tracer on *Escherichia coli* densities. *Water Res.* 23(2): 257-259. Great Britain.

JESTER, W.A., D.C. RAUPACH & F.G. HAASER 1977. A comparison of the bromide ion neutron activable tracer with tritiated water as groundwater tracers. In *Proc. 3rd Int. Conf.on Nuclear Methods in Environmental and Energy Research* (CONF-771072: J.R.VOGT, pp 253-264. University of Columbia, Missouri.

JIN, M., M. DELSHAD, V. DWARAKANATH, D.C. MCKINNEY, G.A. POPE, K. SEPEHRNOORI, C.E. TILBURG & R.E. JACKSON 1995. Partitioning tracer test for detection, estimation and remediation performance assessment of subsurface nonaqueous phase liquids. *Water Resour. Res.* 31: 1201-1211.

JOB, C. & J. ZÖTL 1969. Zur Frage der Herkunft des Gasteiner Thermalwassers. *Steir. Beitr. Hydrogeol.* 1969: 51-115. Graz.

JOB, C. 1972. Ionenumtausch bei Salzungsversuchen. *Geol. Jb.* C2: 103-110. Hannover.

JOB, C., G. MUTSCHLECHNER & J. ZÖTL 1969. Vergleichende Markierungsversuche an Hangwässern in einem Bergsturzgelände. *Steir. Beitr. Hydrogeol.* 1969: 181-191. Graz.

JOLY, J. 1922. On a new method of gauging the discharge of rivers. *Sci. Proc. Roy. Dublin Soc.* 16: 489-491.

JOSEPH, D., M. SENDNER & F. WEIDEMANN 1964. Untersuchung über die horizontale Diffusion in der Nordsee. *Dt. Hydrograph. Z.* 17(2): 245-253. Hamburg: Deutsches Hydrographisches Institut.

JOSSELIN DE JONG, G. DE 1958. Longitudinal and transverse diffusion in granular deposits. *Transactions, Am. Geophys. Union* 39(1): 67-74.

JUHNKE, I. & D. LÜDEMANN 1978. Ergebnis der Untersuchungen von 200 chemischen Verbindungen mit dem Goldorfentest. *Z. Wasser- u. Abwasserforsch.* 11: 161-164. München.

JUNG, K.D. & J. SCHRÖTER 1983. Lebensdauer und Transport von Bakterien in typischen Grundwasserleitern – Haltener Sande. *DVGW-Schriftenreihe Wasser* 35: 139-149. Eschborn.

JUNG, K.D. 1977. Briefl. Mitt. an das Medizinaluntersuchungsamt Koblenz vom 12.Dez.1977.

JUNG, K.D. 1986. *Newsletter on Water Virology* 8: 15-16. London: IAWPRC.

JUNGBAUER, H. (vol.I: General properties of bacteriophages, 202 p, 1983. Karsthydrologische Untersuchungen im Muschelkalk zwischen der Hohenloher Ebene und dem Taubergrund südlich von Bad Mergentheim, Nordwürttemberg. Diss., 184 p (Ms.), Stuttgart.

JÜTTE, A. & L. LEMKE 1968. Intravitalfärbung am Augenhintergrund mit Natrium-Fluoreszein. *Bücherei des Augenarztes, Klin. Mbl. Augenheilkde.* 49: 96-99 Stuttgart: Enke.

KAHLER, F. & S. PREY 1963. Erläuterungen zur geologischen Karte des Naßfeld-Gartnerkofel-Gebietes in den Karnischen Alpen. *Geol. Bundesanst.* 116 p. Wien.

KALTER, S.S., V.D. MORDANT & O.D. CHAPMAN 1946. Isolation of *Escherichia coli* phage by means of cationic detergents. *J. Bact.* 52: 237-240.

KANOWSKI, S. 1985. Schadstoffe in kommunalen Abwässern. *Wasserkalender 1986* 20: 74-93. Berlin.

KÄSS, W. & B. REICHERT 1988. Tracing of karst water with fluorescent spores. *Proc. 5.Int. Symp. Underground Water Tracing,* pp 157-165. Athen: IGME.

KÄSS, W. & G. STRAYLE 1990. UVB-Verfahren aus der Sicht des Anwenders – Ergebnisse von Markierversuchen. *Schriftenreihe Angew. Geol. Karlsruhe* 9: 291-304. Karlsruhe.

KÄSS, W. 1964. Die unmittelbare Bestimmung von Uranin-Spuren bei Färbversuchen. *Steir. Beitr. Hydrogeol., N.F.*, 15/16: 37-65. Graz.

KÄSS, W. 1965. Erfahrungen bei Färbversuchen mit Uranin. *Steir. Beitr. Hydrogeol., N.F.* 17: 21-65. Graz.

KÄSS, W. 1966a. Kalisalz als Markierungsstoff zur Verfolgung unterirdischer Gewässer. *Kali u. Steinsalz* 7: 223-228. Essen: Glückauf.

KÄSS, W. 1966b. Färbversuche bei Flutungsmaßnahmen in Erdölfeldern. *Erdöl u. Kohle, Erdgas, Petrochem.* 19: 882-887. Hamburg: Herrnhausen.

KÄSS, W. 1967a. Erfahrungen mit Uranin bei Färbversuchen. *Steir. Beitr. Hydrogeol.* 1966/67: 123-134. Graz.

KÄSS, W. 1967b. Salzungsversuche mit Kalisalz. *Steir. Beitr. Hydrogeol.* 1966/67: 275-279. Graz.

KÄSS, W. 1970a. Die Anwendbarkeit der hydrogeologischen Markierungsmittel zur Untersuchung der Beziehungen zwischen Grundwasser und oberirdischem Wasser – Allgemeine Gesichtspunkte. *Z. dt. geol. Ges., Sonderh. Hydrogeol. Hydrogeochem.*, pp 109-115, 2 Fig. Hannover.

KÄSS, W. 1970b. Der Salzungsversuch 1969 im Stadtgebiet von Tuttlingen und sein Ergebnis. *Tuttlinger Heimatblätter*, pp 3-15. Tuttlingen.

KÄSS, W. 1972. Grundwasser-Markierungsversuche im Pleistozän der Freiburger Bucht. *Geol. Jb.* C2: 119-151. Hannover.

KÄSS, W. 1976a. 100 Jahre Uranin!- *Pap. 3rd Int. Symp. Underground Water Tracing (3.SUWT)* 1: 113-122, Ljubljana-Bled, September 27-October 1, 1976, Postojna.

KÄSS, W. 1976b. Markierung von Porengrundwässern. *Steir. Beitr. Hydrogeol.* 1976: 219-233. Graz.

KÄSS, W. 1981a. Borax. Tracerhydrologische Untersuchungen im Langetental (Schweiz). *Steir. Beitr. Hydrogeol.* 1981: 66-68. Graz.

KÄSS, W. 1981b. Fluoreszierende Sporen. *Steir. Beitr. Hydrogeol.* 1981: 335-336. Graz.

KÄSS, W. 1982a. Ein Verfahren zur Datenerfassung für Grundwasser-Markierungsversuche. *Jh. geol. Landesamt Baden-Württemberg* 24: 71-90. Freiburg i.Br.

KÄSS, W. 1982b. Ein Verfahren zur Datenerfassung von Markierungsversuchen. *Beitr. Geol. Schweiz – Hydrol.* 28(II): 143-146. Bern: Kümmerly + Frey.

KÄSS, W. 1982c. Fluoreszierende Sporen als Markierungsmittel. *Beitr. Geol. Schweiz – Hydrol.* 29(I): 131-134. Bern: Kümmerly + Frey.

KÄSS, W. 1982d. Routinemäßige Bestimmung von zwei Fluoreszenzfarbstoffen nebeneinander. *Beitr. Geol. Schweiz – Hydrol.* 28(I): 51-62. Bern: Kümmerly + Frey.

KÄSS, W. 1985. Chemische Transportmechanismen in der Ungesättigten Zone – Untersuchung mit Markierungsmitteln. *Z. dt. geol. Ges.* 136: 481-496. Hannover.

KÄSS, W. 1987. Eignung und Einsatz nicht radioaktiver Markierungsstoffe im Bereich der Mineral- und Thermalwasserforschung. *Heilbad u. Kurort* 39(8): 211-212. Gütersloh: Flöttmann.

KÄSS, W. 1988. Markierung von Porengrundwasser. *Proc. 5th Int. Symp. Underground Water Tracing Athen 1986*, pp 191-201. Athen.

KÄSS, W. 1989. Grundwasser-Entnahmegeräte – Zusammenstellung von Geräten für die Grundwasserentnahme zum Zweck der qualitativen Untersuchung. *DVWK-Schr.* 84: 119-172. Hamburg-Berlin: Parey.

KÄSS, W. 1990a. Chemisorption als natürliche hydrologische Barriere. *Z. dt. geol. Ges.* 141: 225-331, 5 Fig. Hannover.

KÄSS, W. 1990b. Moderne Methoden der hydrologischen Markierungstechnik. *Wasserkalender 1991* 25: 24-49 Berlin-Bielefeld-München: E.Schmidt.

KÄSS, W. 1991. Entwicklung der karsthydrologischen Forschung in Deutschland KÄSS, W. – unter besonderer Berücksichtigung der Markierungstechnik. *Karst u. Höhle, Jb.* 1989/90(I): 131-149. München.

KÄSS, W. 1992. Geohydrologische Markierungstechnik. In G.MATTHESS (ed.), *Lehrbuch der Hydrogeologie* 9, 519 p., 234 fig., 30 tables, 4 plates. Berlin-Stuttgart: Gebrüder Borntraeger.

KÄSS, W., R. RITTER & C. SACRÉ 1983. Lebensdauer und Transport von Bakterien in typischen Grundwasserleitern – Oberrheinische Schotterebene. *DVGW-Schriftenreihe Wasser* 35: 127-138. Eschborn.

KAUFFMANN, H. 1917. Chromatophore mit auxochrom-ähnlicher Funktion. *Ber. dt. chem. Ges.* 50(I): 515-529. Berlin: Friedländer & Sohn.

KAUFMANN, W.J. & G.T. ORLOB 1956. Measuring groundwater movement with radioactive and chemical tracers. *J. Amer. Water Works Assoc.* 48: 559-572.

KEIL, K. 1959. *Ingenieurgeologie und Geotechnik*, 3. Ed., XL + 1456 p. Halle/Saale.

KEPLINGER, M.L., O.E. FANCHER, F.L. LYMAN & J.C. CALANDRA 1974. Toxicologic studies of four fluorescent whitening agents. *Toxicol. and Appl. Pharmacol.* 27: 494-506. New York-London: Academic Press.

KESWICK, B.H., C.P. GERBA, S.L. SECOR & T. CECH 1982b. Survival of enteric viruses and indicator bacteria in groundwater. *J. Env. Sci. Health* A17: 903-912.

KESWICK, B.H., DE-CHIN WANG & CH.P. GERBA 1982a. The use of microorganisms as groundwater tracers: a review. *Ground Water* 20(2): 142-149, 1290-1297.

KEYS, W.S. & R.F. BROWN 1978. The use of temperature logs to trace the movement of injected water. *Ground Water* 16(1): 32-48.

KILKPATRCK, F.A. & J. WILSON 1989. Determination of stream reaeration coefficients by the use of tracers. *Techniques of Water Resources Investigations of the United States Geological Survey, Applications of Hydraulics, Book 3.*

KILPATRICK, F.A. 1967. Dye-dilution discharge measurements made under total ice cover in Laramic River at Laramic, Wyoming. *US Geol. Surv. Pap. Resources Div. Bull.*, pp 41-47, July-Dec. 1967.

KIMERLE, R.A. 1989. Aquatic and terrestrial ecotoxicology of linear alkylbenzene sulfonate. *Tenside, Surfactants, Detergents* 26(2): 169-176. München: Carl Hanser.

KINNUNEN, K. & O. JOKINEN 1972. The use of bacteriophages in marking groundwater. *Vesitalous* 1/72: 16-17 (finnisch mit engl. Zusammenfassung).

KINNUNEN, K., S.NIEMELÄ & M.-L.PÖIKOLAINEN 1974. Use of bacteriophages as tracers of river water travel. *Vesitalous* 1/74: 25-30 (Finnish, Engl. summary).

KINNUNEN, K. 1974. *Bakterifaagen hyväksiäyttö merkkiaineena vesien kulkeutumistutkimuksissa,* 81 p., Lisentiaattityö-Helsingin Yliopiston Mikrobiologian Laitos (Finnish).

KINNUNEN, K. 1978. Tracing water movement by means of *Escherichia coli* bacteriophages. *Publ. Water Res. Inst., Nat. Board of Waters, Finnland* 25: 50 p. Helsinki.

KINZELBACH, W. 1986. Groundwater modelling – An introduction with sample programs in BASIC. *Devel. in Water Sci.* 25: 333 p., Amsterdam-Oxford-New York-Tokyo: Elsevier.

KINZELBACH, W. 1992. *Numerische Methoden zur Modellierung des Transports von Schadstoffen im Grundwasser,* 343 p. München: Oldenbourg.

KIRCHHEIMER, F. 1933. Die Erhaltung von Sporen und Pollenkörnern in den Kohlen sowie ihre Veränderungen durch die Aufbereitung. *Bot. Arch.* 35: 134-187. Leipzig: Akad. Verlagsges. m.b.H.

KISSKALT, K. & M. KNORR 1930. Die Gefährdung der Diluvialquellen und ihre Untersuchung mit Uranin und Kochsalz. *Arch. Hyg.* 103: 349-364.

KISSKALT, K. 1941. Quantitative Bestimmungen bei Untersuchungen über die Strömung des Grundwassers mittels Färbung und Salzung. *Arch. Hyg. u. Bakteriol.* 125: 29-38. München-Berlin: Oldenbourg.

KLATTE, O.J. 1962. Eine verbesserte Methode des Uraninnachweises im Grundwasser. *Arch. Hyg. Bakt.* 146: 98-107.

KLEINERT, K. 1976. Das Grundwasser im Kiesaquifer des Oberen Neckartals zwischen Tübingen und Rottenburg. Diss., 221 p., Anhang. Tübingen.

KLING, O. 1974. Spektralphotometrie. In *Handbuch der instrumentellen Meßtechnik,* pp 713-731. Essen: Vulkan.

KLIR, S. 1967. Feststellung der Grubenwasserbewegung durch Färbemethoden. *Steir. Beitr. Hydrogeol.* 1966/67: 135-139. Graz.

KLOTZ, D. & K.-P. SEILER 1980. Labor- und Geländeversuche zur Ausbreitung konservativer Tracer in fluvioglazialen Kiesen von Oberbayern. *GSF-Ber.* R 250: 74-89. München.

KLOTZ, D. 1973. Untersuchungen zur Dispersion in porösen Medien. *Z. dt. Geol. Ges.* 124: 523-533.

KLOTZ, D. 1982a. Verhalten hydrologischer Tracer in ausgewählten Sanden und Kiesen. *GSF-Ber.* R 290: 17-29. München.

KLOTZ, D. 1982b. Abhängigkeit der longitudinalen Dispersion von Parametern des Grundwassers und des Grundwasserleiters. *GSF-Ber.* R 290: 309-322. München.

KLOTZ, D. 1982c. Abhängigkeit der transversalen Dispersion von Parametern des Grundwassers und des Grundwasserleiters. *GSF-Ber.* R 290: 340-349. München.

KLOTZ, D. 1982d. Verhalten hydrologischer Tracer in ausgewählten fluvioglazialen Kiesen, Hangschutt-Kiesen und tertiären Kies-Sanden aus Bayern. *Beitr. Geol. Schweiz – Hydrol.* 28(II): 245-256. Bern: Kümmerly + Frey.

KLOTZ, D., P. MALOSZEWSKI & H. MOSER 1988. Mathematical modelling of radioactive tracer migration in water flowing through saturated porous media. *Radiocim. Acta* 44/45: 373-379.

KLUDIG, K.H. 1970. Ermittlung des Anteils von Uferfiltrat bei Mischungsgrundwasser. *GWF, Wasser-Abwasser* 111: 77-79. München.

KNOP, A. 1875 and 1878. Über die hydrographischen Beziehungen zwischen der Donau und der Aachquelle im badischen Oberlande. *N. Jb. Miner.* 1875: 942-958 und 1878: 350-363. Stuttgart.

KNOP, E. 1950/51. Messung der Durchlaufzeiten von Klärbecken mit Hilfe von radioaktiven Stoffen. *Wasserwirtschaft* 41(5): 117-121.

KNORR, M. & R.MUSELMANN 1940. Lotrechte Infiltration und Filtration in der Bedeutung für die Schutzzonenfrage. *Arch. Hyg. u. Bakteriol.* 123: 349-366. München-Berlin: Oldenbourg.

KNORR, M. 1935. Der Tyndalleffekt bei der Untersuchung von Quellen. *Arch. Hyg. u. Bakteriol.* 113: 274-278. München-Berlin: Oldenbourg.

KNORR, M. 1937. Die Schutzzonenfrage in der Trinkwasserhygiene. *GWF* 80: 330-334, 350-355, München.

KNORR, M. 1951. Zur hygienischen Beurteilung der Ergänzung und des Schutzes großer Grundwasservorkommen. *GWF, Das Gas- u. Wasserfach (Wasser)* 92: 104-110, 151-155. München: Oldenbourg.

KNUTSSON, G., K. LJUNGGREN & H.G. FORSBERG 1963. Field and laboratory tests of chromium-51-EDTA and tritium water as a double tracer for groundwater flow. In *Radioisotopes in Hydrology, Int. Atomic Energy Agency*, pp 347-363. Vienna.

KOCKERT, W. 1985. Zum Problem der Tracer in hochkonzentrierten natürlichen Salzlösungen. *Z. Angew. Geol.* 31(10): 257-259. Berlin.

KÖHLE, H. 1980. Hydrogeologische Untersuchungen im Einzugsgebiet der Stuttgart-Bad Cannstatter Mineralquellen. Diss., 326 + 120 p. (Ms.), Tübingen.

KONIKOW, L.F. & J.D. BREDEHOEFT 1984. Computer model of two-dimensional solute transport and dispersion in ground water. *In Techniques of Water-Resources Investigations of the United States Survey*, Chapter C2, 90 p. Washington D.C.: US Government Printing Office.

KORTÜM, G. 1955. *Kolorimetrie, Photometrie und Spektrometrie. Anleitungen für die chemische Laboratoriumspraxis*, Bd. II, 458 p. Berlin-Göttingen-Heidelberg: Springer.

KOSLOV, V.V. & A.M. SARZHEVSII 1975. Diffusion and solution of fluorescent molecules in aqueous solutions. *Zurnal prikladnoj spektroskopii* 22: 453-457. Minsk (Russ.).

KOTT, Y. 1966. Estimation of low numbers of *Escherichia coli* bacteriophages by use of the most probable number method. *Appl. Microbiol.* 14(2): 141-144. New York.

KÖVESDI, J. 1980. *Hydrologische Untersuchungen im untersten Langetental.* Diplomarb. Univ. Bern, 142 p.(Ms.). Bern.

KOYA, K.V. & M. CHAUDHURI 1977. Virus retention by soil. *Prog. Wat. Tech.* 9: 43-52.

KOZLOV, V.V. & A.M. SARZHEVSKII 1975. Diffusion and solvation of fluorescent molecules in aqueous solutions. *Zurnal Prikladnaj Spektroskopii* 22: 453-457. Minsk. (Russ.)

KRANJC, A. (ed.) 1997a. Tracer Hydrology 97. *Proc. Int. Symp. Water Tracing, Portoroz/Slovenia, 26-31 May 1997*, 450 p. Rotterdam: Balkema.

KRANJC, A. (ed.) 1997b. Karst hydrogeological investigations in South-Western Slovenia. *Acta Carsologica* XXVI/1, 388 p. Ljubljana.

KRAUTHAUSEN, B. 1977. *Karsthydrologische Untersuchungen im Warscheneck (Nördliche Kalkalpen).* Unveröff. Diplomarb., Univ. Karlsruhe.

KREFT, A. & A. ZUBER 1978. On the physical meaning of the dispersion equation and its solution for different initial and boundary conditions. *Chem. Eng. Sci.* 33: 1471-1480.

KRONFELLNER-KRAUS, G. 1974. Die Wildbacherosion im allgemeinen und der Talzuschub im besonderen. In *100 Jahre Forstliche Bundesversuchsanstalt.* Wien.

KROUSE, H.R. & V.A. GRINENKO (eds) 1991. *Stable isotopes: Natural and anthropogenic sulphur in the environment (SCOPE 43)*, 440 p. Chichester-NewYork-Brisbane-Toronto-Singapore.

KROUSE, H.R. 1980. Sulphur isotopes in our environment. In FRITZ, P. & J.CH. FONTES (eds), *Handbook of Environmental Geochemistry* 1: 435-471. Amsterdam-Oxford-New York: Elsevier.

KRUEGER, A.P. 1930. A method for the quantitative determination of bacteriophages. *J. Gen. Physiol.* 13: 557-563.

KRÜGER, F.K. 1876. Fluoreszein als Indikator beim Titrieren. *Ber. dt. chem. Ges. Berlin* 9: 1572.

KRULC, Z. 1967. Geophysikalische Untersuchungen unterirdischer Wasserwege im jugoslawischen Karst. *Steir. Beitr. Hydrogeol.* 1966/67: 111-120. Graz.

KRUSÉ, C.W., K. KAWATA, V. POLIVERI & K.E. LONGLEY 1973. Improvement in terminal desinfection of sewage effluents. *Water and Sewage Works* 120: 57-64.

KRUSE, W. 1919. Versuche mit absichtlich zugesetzten Bakterien. Kapitel 13 in: WEYL's *Handbuch der Hygiene, I.Bd.: Wasser und Boden*, 1.Abt.: Die hygienische Untersuchung und Beurteilung des Trinkwassers, pp 221-222, Leipzig: Johann Ambrosius Barth.

KÜPPER, H. 1954. Die Charakterisierung von Gewässern durch Temperaturmessungen. *Österr. Wasserwirtsch.* 6(4): 107-110. Wien.

KUSSMAUL, H., D. MÜHLHAUSEN & H. BEHRENS 1977. Hydrologische und hydrochemische Untersuchungen zur Uferfiltration, Teil 1: Chlorid, Borat und Uranin. *GWF, Wasser-Abwasser* 118: 521-524. München.

KYRLE, G. 1928. Kombinierte Chlorierung von Höhlengewässern. *Speläolog. Monogr.* XII, 94 p., 8 Plates. Wien.

LACEY, W.J. & DE LAGUNA 1956. Method of preparing radioactive cations for tracing ground water. *Science* 124: 402.

LAIDLAW, I.M.S. & P.L. SMART 1982. An evaluation of some orange fluorescent dyes. *Beitr. Geol. Schweiz – Hydrol.* 28(I): 113-117. Bern: Kümmerly + Frey.

LALLEMAND, A. & H. PALOC 1964a. Possibilités d'utilisation d'un nouveau colorant, le 'Pontacyl Brilliant Pink B', pour l'étude des circulations karstiques. *Spelunca Bull.* IV(4): 43-45.

LALLEMAND, A. & H. PALOC 1964b. Possibilités offertes par la méthode de détection au charbon actif pour les expériences de coloration a la fluorescéine. *Spelunca Mém.* 4: 25-40.

LALLEMAND, A. & H. PALOC 1967. L'intérêt de la 'méthode au charbon actif' dans des traçages à la fluorescéine en hydrogéologie – Quelques exemples. *Mem. Int. Ass. Hydrogeol.* VII: 220-226. Kongreß Hannover 1965, Hannover.

LANG, H., CH. LEIBUNDGUT & E. FESTEL 1979. Results from tracer experiments on the water flow through the Aletschgletscher. *Z. Gletscherkde. u. Glazialgeol.* 15(2): 209-218. Innsbruck.

LAUBER 1736. Crailsheimer Chronik (cit. after WAGNER, G. 1919): Die Landschaftsformen von Württembergisch Franken. *Erdgeschichtl. u. landeskundl. Abh. aus Schwaben u. Franken* 1: 96 p., Öhringen).

LEDERER, C.M. & V.S. SHIRLEY 1978. *Table of Isotopes,* Ed. VII, 1523 p. New York-Chichester-Brisbane-Toronto: J.Wiley & Sons.

LEFLER, E. & Y. KOTT 1975. Virus survival in water and waste water. *Israel J. Med. Sci.* 11(5): 511-512. Tel Aviv.

LEHMANN, K.B. 1899. Vier Gutachten über die Wasserversorgungsanlage Würzburg an der Mergentheimer Straße. *Verb. d. physik. Med. Ges. Würzburg* 33: 1-111. Würzburg.

LEIBUNDGUT, CH. & A. GEES 1989. Report on the tracer experiments on the Greenland iceshield. Unpublished.

LEIBUNDGUT, CH. & B. LÜTHI 1976. Bestimmung des Seihvermögens von Grundwasserleitern mittels Tracer. *Proc. 3rd Int. Symp. Undergroundwater Tracing (3.SUWT) Bled,* pp 141-148. Ljubljana.

LEIBUNDGUT, CH. & H.R. ATTINGER 1988. Grundzüge der Karsthydrologie des Alpsteins – Tracerhydrologische Untersuchungen im Hinblick auf Gewässerschutzmaßnahmen. Geogr. Inst. Univ. Bern, Abt. Physische Geogr. *Gewässerkde.; Publikation Gewässerkde.* 101, 137 p. (als Ms. gedruckt). Bern.

LEIBUNDGUT, CH. & H.R. WERNLI 1982. Zur Frage der Einspeisemengenberechnung für Fluoreszenztracer. *Beitr. Geol. Schweiz – Hydrol.* 28(I): 119-130. Bern: Kümmerly + Frey.

LEIBUNDGUT, CH. & H.R. WERNLI 1988. Naphthionate – Another fluorescent dye. *Proc. 5th Int. Symp. Underground Water Tracing (SUWT) Athen 1986,* pp 167-177. Athens: IGME.

LEIBUNDGUT, CH. & M. ZUPAN 1992. Determination of residence time in Lake Bled. In HÖTZL, H. & A. WERNER, Tracer Hydrology. *6th Int. Symp. Water Tracing (SWT) of the ATH, 21.-26. Sept. 1992, Karlsruhe,* pp 3-10. Rotterdam: Balkema.

LEIBUNDGUT, CH. & O. ADLER 1989. Einfluß der Wassernutzung auf Weiherbiotope – *Ber. Nr 1 Inst. Hydrol. Univers. Freiburg,* 63 p.

LEIBUNDGUT, CH. & P. HIRSIG 1977. Zur Anwendung fluoreszierender Tracer in der Limnologie. *Gas, Wasser, Abwasser* 12: 833-841. Zürich.

LEIBUNDGUT, CH. & S. HADI, 1997. A contribution to toxicity of fluorescent tracers. In KRANJC, A. (ed.), Tracer Hydrology 97. *Proc. 7th Int. Symp. Water Tracing (SWT) of the ATH, 26-31 May 1997, Portoroz/Slovenia,* pp 69-76. Rotterdam: Balkema.

LEIBUNDGUT, CH. 1974. Fluoreszierende Markierfarbstoffe in der Hydrologie. *Mitt. Naturforsch. Ges. Bern, N.F.* 31: 63-84. Bern.

LEIBUNDGUT, CH. 1980. Methodik der Tracerhydrologie – Beiträge zur Anwendung von künstlichen Tracern in der Hydrologie. *Ber. Geograph. Inst., Bern.*

LEIBUNDGUT, CH. 1981. Zum Adsorptionsverhalten von Fluoreszenztracern. *Festschrift Josef* G. ZÖTL, pp 111-129. Graz.

LEIBUNDGUT, CH. 1986. Zur Anwendung künstlicher Tracer in Gletschern. *Publikation Gewässerkde. Univers. Bern*, No. 85, 51 p. Bern.

LEIBUNDGUT, CH. 1991. Eichung und Verbesserung eines Alarmmodells für den Rhein. In Vorträge Wasserbau-Seminar Wintersemester 1990/91 'Schadstofftransport in Grund- und Oberflächengewässern' Sonderdruck # 81 des Instituts für Wasserbau und Wasserwirtschaft der Rheinisch-Westphälischen Technischen Hochschule Aachen, pp 29-46. Aachen.

LEIBUNDGUT, CH. 1995. Zur Hydrologie des Alpsteins. Hydrologische Untersuchungen im Karstgebiet des Alpsteins. *Innerrhoder Schriften*, Ed.:Kanton Appenzell, 125 p. Appenzell (CH).

LEIBUNDGUT, CH., TH. MOERI, H. PESCHEL. J. PETERMANN, M. STAMPFLI & R. WÄLTI 1983. Strömungsuntersuchungen mittels Tracerversuchen im Bledsee. *Geograph. Inst. Univers. Bern, Publ. Gewässerkde.* 39. Bern.

LEIBUNDGUT, CH., U. SPEIDEL & H. WIESNER 1993. Transport processes in rivers investigated by tracer experiments. In Tracers in Hydrology. *Proc. Yokohama Symp., July 1993. IAHS Publ.* 215: 211-217. Wallingford, UK: IAHS Press.

LENDA, A. & A. ZUBER 1970. Tracer dispersion in groundwater experiments. *Proc. Isotope Hydrol.*, pp 619-641. Vienna: IAEA.

LIEBISCH, K. & W. REMUS 1966. Hydrologische Ergebnisse mit Färbversuchen im Kupferschieferbergbau der Mansfelder Mulde. *Z. Angew. Geol.* 12(9): 486-489. Berlin.

LIEBMANN, H. 1960. *Handbuch der Frischwasser- und Abwasserbiologie,* Bd. II, 1149 p. München: Oldenbourg.

LIESER, K.H. 1991. *Einführung in die Kernchemie,* 3.Ed., 771 p. Weinheim-New York-Basel-Cambridge: Verlag Chemie.

LIEW, P.-L. & C.P. GERBA 1980. Thermostabilization of enteroviruses by estuarine sediments. *Appl. Environ. Microbiol.* 40: 305-308.

LIPSON, S.L. & G. STOTZKY 1983. Adsorption of reovirus to clay minerals: effects of cation-exchange capacity, cation saturation, and surface area. *Appl. Environ. Microbiol.* 46: 673-682.

LOGAN, K.B., G.E. REES & N.D. SEELEY 1980. Rapid concentration of bacteriophages from large volumes of freshwater: evaluation of positively charged microporous filters. *J. Virol. Methods* 1: 87-97.

LOMBARD, M. 1921. Procédé de recherche de la fluorescéine dans ses solutions très étendues. *Bull. Soc. Chim.* 29: 462-464. Paris.

LONGWELL, J. & W.D. MANIECE 1955. Determination of anionic detergents in sewage affluents and river waters. *Analyst* 80: 167.

LOOSLI, H.H. 1983. A dating method with ^{39}Ar. *Earth Planet. Sci. Lett.* 63: 51-62.

LOOSLI, H.H., B.E. LEHMANN & W. BALDERER 1989. Argon-39, argon-37 and krypton-85 isotopes in Stripa groundwaters. *Geochim. Cosmochim. Acta* 58: 8-22.

LOOSLI, H.H., B.E. LEHMANN, C. THALMANN, I.N. ANDREWS & T. FLORKOWSKI 1992. Argon-37 and argon-39: measured concentrations in groundwater compared with calculated concentrations in rock. In *Isotope Techniques in Water Resources Development 1991*, pp 189-201. Vienna: IAEA.

LTwS 1979. *Beurteilung und Behandlung von Mineralölschadensfällen im Hinblick auf den Grundwasserschutz*, Teil 3 Analytik, 45 p. Herausg. vom Umweltbundesamt, Berlin.

LTwS 1980. *Beirat 'Lagerung und Transport wassergefährdender Stoffe' beim Bundesminister des Innern.* Katalog wassergefährdender Stoffe, 24 + 13 p., Herausg. vom Umweltbundesamt, Berlin.

LUKAS, G. 1959a. Die Färbemethoden. In MAURIN, V. & J. ZÖTL (1959), Die Untersuchung der Zusammenhänge unterirdischer Wässer mit besonderer Berücksichtigung der Karstverhältnisse. *Steir. Beitr. Hydrogeol.* 1959: 94-107. Graz.

LUKAS, G. 1959b. Salzungsmethoden. In MAURIN, V. & J. ZÖTL (1959), Die Untersuchung der Zusammenhänge unterirdischer Wässer mit besonderer Berücksichtigung der Karstverhältnisse. *Steir. Beitr. Hydrogeol.* 1959: 107-121. Graz.

LUKAS, G. 1959c. Die Triftung von Bakterien. In MAURIN, V. & J. ZÖTL (1964), Karsthydrologische Untersuchungen im Toten Gebirge mit besonderer Berücksichtigung der versorgungswasserwirtschaftlichen Belange im Tauplitzgebiet. *Österr. Wasserwirtsch.* 16(5/6): 112-123. Wien.

LURIA, S.E., R.C. WILLIAMS & R.C. BACKUS 1951. Electron micrographic count of bacteriophage particles. *J. Bacteriol.* 61: 179-188.

LUTTY, G.A. 1978. The acute intravenous toxicity of biological stains, dyes and other fluorescent substances. *Toxikol. and Appl. Pharmacol.* 44: 225-249. New York-London: Academic Press.

LUTZ, T. & A. PARRIAUX 1988. The identification of uranine in natural water by High Performance Liquid Chromatography (HPLC). *Steir. Beitr. Hydrogeol.* 39: 141-147, Graz.

LUTZ, T., A. PARRIAUX & P. TISSIÈRES 1986. Traçage au gouffre du Chevrier (Préalpes Vaudoises) et méthode d'identification de l'uranine à faible concentration. *Bull. du Centre d'Hydrogéol.* 7: 139-168. Neuchâtel.

MÄGDEFESSEL, J. 1990. *Zum Fließverhalten von Tracern und Schadstoffen im Porengrundwasser.* Diplomarb., 109 p. Freiburg i.Br.

MAIRHOFER, J. 1967. Die Bestimmung der Fließrichtung in einem einzigen Bohrloch mittels radioaktiver Isotope. *Steir. Beitr. Hydrogeol.* 1966/67: 69-78. Graz.

MAISS, M. & I. LEVIN. 1994. Global increase of SF_6 observed in the atmosphere. *Geophys. Res. Letters* 21(7): 569-572.

MALCOLM, R.L., G.R. AIKEN, E.M. THURMANN & P.A. AVERI 1980. Hydrophylic organic solutes as tracers in groundwater recharges studies. *Contaminants and Sediments* 1: 71-87.

MALINA, J.F., K.R RANGANATHAN, B.P. SAGIK & B.E. MOORE 1975. Poliovirus inactivation by activated sludge. *J. of the Water Pollution Control Federation* 47(8): 2178-2183.

MALOSZEWSKI, P. & A. ZUBER 1982. Determining the turnover time of groundwater systems with the aid of environmental tracers. *J. Hydrol.* 57: 207-231.

MALOSZEWSKI, P. & A. ZUBER 1983. Theoretical possibilities of the $_3H$-$_3He$-method in investigations of groundwater systems. *Catena* 10: 189-198.

MALOSZEWSKI, P. & A. ZUBER 1985. On the theory of tracer experiments in fissured rocks with a porous matrix. *J. Hydrol.* 79: 333-358.

MALOSZEWSKI, P. & A. ZUBER 1991. Influence of matrix diffusion and exchange reactions on radiocarbon ages in fissured carbonate aquifers. *Water Resour. Res.* 27: 1937-1945.

MALOSZEWSKI, P. & A. ZUBER 1990. Mathematical modeling of tracer behavior in short-term experiments in fissured rocks. *Water Resour. Res.* 26: 1517-1528.

MALOSZEWSKI, P. & A. ZUBER 1993. Tracer experiments in fractured rock: matrix diffusion and the validity of models. *Water Resour.* Res. 29: 2723-2735.

MALOSZEWSKI, P. 1981. Computerprogramm für die Berechnung der Dispersion und der effektiven Porosität in geschichteten porösen Medien, 33 p, (Als Ms. gedruckt), GSF-Ber., R 269, München.

MALOSZEWSKI, P. 1985. Mathematical models and their applicability to the interpretation of the tracer experiments. *Geogr. Inst. Univ. Bern: Weiterbildungskurs in Tracerhydrology Okt.1985*, pp 19/0-19/30, unveröff. Kursunterlagen, Bern.

MALOSZEWSKI, P. 1992. Mathematical modelling of tracer transport in different aquifers: Results from ATH test fields. In HÖTZL, H. & A. WERNER (eds), Tracer Hydrology. *Proc. 6th Int. Symp. Water Tracing 21-26 Sept. 1992, Karlsruhe*, 25-30. Rotterdam: Balkema.

MALOSZEWSKI, P. 1994. Mathematical modelling of tracer experiments in fissured aquifers. *Freiburger Schriften zur Hydrologie* 2, 107 p. Freiburg i.Br.

MALOSZEWSKI, P., R. BENISCHKE, T. HARUM & H. ZOJER 1994. Estimation of solute transport parameters in heterogeneous groundwater systems of a karstic aquifer using artificial tracer experiments. *Water Down Under* '94, 2, Part A: 105-111. Adelaide/Australia.

MALOSZEWSKI, P., T. HARUM & R. BENISCHKE 1992. Mathematical modelling of tracer experiments in the karst of the Lurbach system. In BEHRENS et al., Investigations with natural and artificial tracers in the karst aquifer of the Lurbach system (Peggau-Tanneben-Semriach, Austria). *Steir. Beitr. Hydrogeol.* 43: 116-143. Graz.

MALOSZEWSKI, P., W. RAUERT, W. STICHLER & A. HERRMANN 1983. Application of flow models in an alpine catchment area using tritium and deuterium data. *J. Hydrol.* 66: 319-330.

MARBOUTIN, F. 1901a. Contribution à l'étude des eaux souterraines; Courbes isochronochromatiques. *C. R. Acad. Sci.* 132: 365-368. Paris.

MARBOUTIN, F. 1901b. Sur la Propagation des eaux souterraines. *Bull. Soc. belge Géol.* 15 (Mém.): 214-227. Brüssel.

MARBOUTIN, F. 1904. Fluoroscope ou Fluorescope – *Bull. Société belge de Géol., Paléont. et Hydrol.* XVII: 446-447. Brüssel.

MARICHAL, M. & R. BENOÎT 1961. Dosage de la Rhodamine B dans les eaux naturelles. *Chimie Analytique* (2): 70-72.

MARKING, L.L. 1969. Toxicity of Rhodamine B and fluorescein sodium to fish and their compatibility with Antimycin A. *Prog. Fish-Culturist* 31: 139-142, Washington, D.C.

MARTEL, E.-A. 1906. L'eaux – Étude hydrologique. *Traité d'Hygiène* 2: 87-200.

MARTEL, E.-A. 1913. Sur les expériences de fluorescéine à grandes distances. *C.R. Acad. Sci.* 157: 1102-1104. Paris.

MARTEL, E.-A. 1921. *Nouveau traité des eaux souterraines,* 838 p. Paris: Doin.

MARTI, F., G. DELLA VALLE, U. KRECH, R.A. GEES & E. BAUMGARTNER 1979. Markierversuch im Grundwasser mit Farbe, Bakterien und Viren. *Alimenta* 18: 135-145.

MARTIN, R. & A. THOMAS 1974. An example of the use of bacteriophage as a groundwater tracer. *J. Hydrol.* 23: 73-78. Amsterdam: North-Holland Publ. Comp.

MATHEY, B. 1971. La méthode au charbon actif dans les essais de coloration à la fluorescéine. *Extrait des Actes du 4e Congrès suisse de Spéléologie, Neuchâtel, septembre 1970,* pp 53-61. Neuchâtel.

MATHEZ, C. 1986. *Zum Abflußverhalten des Findelengletschers.* Diplomarb., Bern.

MATTHESS, G. & A. PEKDEGER 1982. Das Verhalten von pathogenen Bakterien und Viren im Grundwasser. *Mitt. Ing.- u. Hydrogeol.* 13: 111-130. Aachen.

MATTHESS, G. & O. SCHMIDT 1967. Ein Färbeversuch im Buntsandstein des Odenwaldes. *Steir. Beitr. Hydrogeol.* 1966/67(18/19): 227-230. Graz.

MATTHESS, G. 1980. Literaturstudie 'Untersuchungen der Lebensdauer von Bakterien und Viren im Grundwasser im Hinblick auf die Ausweisung von Schutzgebieten für die Grundwasseranlagen'. *Teil A: Hydrologische Untersuchungen,* 106 p. (Ms.). Kiel.

MATTHESS, G., H. MOSER, A. PEKDEGER, H. RAST, W. RAUERT & W. STICHLER 1976. Tritium as a tracer in hydrogeochemical studies of the unsaturated zone. *Pap. 3rd Int. Symp. Underground Water Tracing (SUWT),* pp 149-156. Ljubljana.

MATTSON, P. 1929. The laws of soil colloidal behavior I. *Soil Sci.* 27-29: 179-220.

MAURIN, V. & J.ZÖTL 1959. Die Untersuchung der Zusammenhänge unterirdischer Wässer unter besonderer Berücksichtigung der Karstverhältnisse. *Steir. Beitr. Hydrogeol.* 10/11: 184 p. Graz.

MAURIN, V. & J.ZÖTL 1964. Karsthydrologische Untersuchungen im Toten Gebirge. *Österr. Wasserwirtsch.* 16: 112-123. Wien.

MAURIN, V. 1967. Vorbereitung und Organisation größerer Markierungsversuche zur Verfolgung unterirdischer Wässer. *Steir. Beitr. Hydrogeol.* 1966/67: 311-320. Graz.

MAURIN, V., J. ZÖTL & A. HOFER 1959. Die Triftung von Lycopodiumsporen. *Steir. Beitr. Hydrogeol.* 1959: 125-149. Graz.

MAYER, A.S. & C.T. MILLER, 1992. The influence of porous medium characteristics and measurement scale on pore-scale distributions of residual nonaqueous-phase liquids. *J. Contam. Hydrol.* 11: 189-213.

MAYER, M.J. 1681. Vorstellung deß jüngst-erschienenen Cometen..beygefügt eine wahrhaffte Erzehlung und Beschreibung deß im Decembri 1680 entstandenen weit-beschreyten Erdbruchs bey Blaubeyren. Ulm (cit. after PFEIFFER, 1963).

MAYER, S.W. & E.R. TOMPKINS 1947. Ion exchange as a separation method: A theoretical analysis of the column separation process. *J. Am. Chem. Soc.* 69: 2866.

MAYR, A. 1953a. Blütenpollen und pflanzliche Sporen als Mittel zur Untersuchung von Quellen und Karstwässern. *Anzeiger d. österr. Akad. Wiss., Mathem.-naturwiss. Klasse* 90: 94-98, Wien: Springer.

MAYR, A. 1953b. Blütenpollen und Sporen als Mittel zum Nachweis von Gletscherwässern. *Z. Gletscherkde. u. Glaziol.* 2(2). Innsbruck.

MAYR, A. 1954a. Neue Wege zur Erforschung von Quellen und Karstwässeren. *Mitt. d. Höhlenkommission beim Bundesministerium für Land- u. Forstwirtsch.* 1953(1): 90-96. Wien.

MAYR, A. 1954b. Hydrogeologische Studien im Dachsteingebiet. Inaugural-Diss. an der Leopold-Franzens-Univ. Juni 1954, 97 p. (Ms.). Innsbruck.

MAZIJK, A. VAN, J.M.C. VAN MIERLO, H.WIESNER & CH.LEIBUNDGUT 1992b. Verifikation des Rheinalarmmodells anhand der Markierversuche 06/91 und 07/91. Ber. TU Delft, 50 p.

MAZIJK, A. VAN 1996. One-dimensional approach of transport phenomina of dissolved matter in rivers. *Landeshydrologie und -geologie*, 310 p. Bern.

MAZIJK, A. VAN, H. WIESNER & CH. LEIBUNDGUT 1992a. Das Alarmmodell für den Rhein – Theorie und Kalibrierung der Version 2.0. *Dt. Gewässerkundl. Mitt.* 36(2): 42-47. Koblenz.

MAZIJK, A. VAN. & J.M.C. VAN MIERLO 1992. Überprüfung der Kalibrierung des Rhein-alarmmodells Version 2.1 anhand des Markierversuches 04/89 Village Neuf. Ber. TU Delft, Niederlande.

MAZOR, E. 1976. The Ram Crater Lake, a note on the revival of a 2000-year-old groundwater tracing experiment. *Interpretation of Environmental Isotope and Hydromechanical Data in Groundwater Hydrology*, pp 171-181. Vienna: IAEA.

MCCABE, W.J. 1991. Artificial tracers in geothermical hydrology. In *Use of artificial tracers in hydrology. IAEA-TECDOC* 601: 165-178. Vienna.

MCDONALD, K., K. KASTEN, R. HERVEY, S. GREGG, C.A. ROBB & A.R. BORGMANN 1974. Acute and subacute toxicity evaluation of intravenous sodium fluorescein in mice, rats and dogs. *Toxicol. and Appl. Pharmacol.* 29: 97-98. New York-London: Academic Press.

MELU/MWMV 1982. Hydrologische Karte Baden-Württemberg Erolzheimer Feld (Illertal) mit 7 Karten 1:50 000 und 100 p. Erläuterungen. Herausg. vom Minist. für Ernährung, Landwirtsch. u. Umwelt und vom Minist. für Wirtsch., Mittelstand u. Verkehr Baden-Württemberg, Karlsruhe.

MELUF 1983. Leitfaden für die Beurteilung und Behandlung von Grundwasserverunreinigungen durch leichtflüchtige Chlorkohlenwasserstoffe. *Minist. für Ernährung, Landwirtsch., Umwelt u. Forsten, Wasserwirtschaftsverwaltung* 13: 104 p. Stuttgart.

MERCK, E. 1986. *Uranin AP zur Untersuchung von Wasserströmungen.* Druckschr. 99/17570/1/786, 8 p. Darmstadt.

MERKLI, B. 1974. Untersuchungen über Mechanismen und Kinetik der Elimination von Bakterien und Viren im Grundwasser. 89 p., Diss. ETH Zürich 1974.

METZ, H. 1973. Mikroorganismenmasse für Forschungszwecke. *Merck-Kontakte* 2: 22-26. Darmstadt.

MILANOVIC, P. 1972. The methods of exploration of karst underground water flow in Popovo polje, Yugoslavia. *Proc. 24th Int. Geol. Congr.*, Sect. 11, pp 80-88. Montreal, Canada.

MILANOVIC, P. 1976. The review of exploration of karst underground water flows in Eastern Hercegowina. *Pap. 3rd Int. Symp. Underground Water Tracing (3.SUWT)*, pp 157-167. Ljubljana.

MILDE, G. 1962. Die Anwendung von radioaktiven Isotopen bei montanhydrogeologischen Untersuchungen. *Isotopentechnik* 2: 325-335.

MILLS, R.F.N. 1955. Properties of a small bacteriophage and the action of some components on it. *J. Gen. Microbiol.* 12: 172-179.

MIQUEL, A.H. & R.D. BRAUN 1974. Fluorimetric analysis of nitrate in real samples. *J. Chem. Educ.* 51: 682-683. Tucson.

MIQUEL, P. 1901. Sur l'usage de la levure de bière pour déceler les communications des nappes d'eau entre elles. *C. R. Acad. Sci.*, pp 1515. Paris.

MISEREZ, J.-J. 1976. Ergänzende Bemerkungen zur Geochemie der Wässer des Karstsystems der Lubljanica. In Markierung unterirdischer Wässer – Untersuchungen in Slowenien 1972-1975, *Steir. Beitr. Hydrogeol.* 28: 78-88. Graz.

MITCHELL, R. 1971. Destruction of bacteria and viruses in seawater. *J. Sanit. Engng. Div. Amer. Soc. Civ. Engrs.* SA4: 425-432.

MOEBUS, K. & H. NATTKEMPER 1989. Bacteriophages sensitivity patterns among bacteria isolated from marine waters. *Helgoländer. Meeresunters.* 34: 375-385.

MOEBUS, K. 1992. Laboratory investigations on the survival of marine bacteriophages in raw and treated seawater. *Helgoländer. Meeresunters.* 46: 251-273.

MOERI, T. & CH. LEIBUNDGUT 1986. Winter dye tracer experiments on the Findelengletscher (Canton Wallis, Switzerland). *Z. Gletscherkde. u. Glazialgeol.* 22(1): 33-41. Innsbruck: Universitätsverlag Wagner.

MOESCHLIN, S. 1964. *Klinik und Therapie der Vergiftungen,* 4.Ed. Stuttgart: Thieme.

MOHR, K.F. 1855. *Lehrbuch der chemisch-analytischen Titriermethode.* Braunschweig.

MOHRING, E. & E. ALEXANDER 1988. Quantitative tracing of karst groundwater flow: Southeastern Minnesota, North Central USA. *Proc. 5th Int. Symp. Underground Water Tracing, Athen 1986,* pp 215-227. Athen.

MOLINARI, J. & J. ROCHAT 1978. Synthèse bibliographie sur la toxicité des substances fluorescentes utilisées en Hydrologie. *Int. J. Spéléol.* 10: 269-277.

MOOK, W.G. 1980. Carbon-14 in hydrogeological studies. In FRITZ, P. & J.CH. FONTES (eds), *Handbook of Environmental Geochemistry* 1: 49-74. Amsterdam-Oxford-New York: Elsevier.

MOORE, B.E., B.P. SAGIK & J.F. MALINA 1975. Viral association with suspended solids. *Water Research* 9: 197-203.

MOORE, R.S., D.H. TAYLOR, L.S. STURMAN, M.M. REDDY & G.W. FUHS 1981. Poliovirus adsorption by 34 minerals and soils. *Appl. Environ. Microbiol.* 42: 963-975.

MOORE, R.S., D.H. TAYLOR, M.M.M. REDDY & L.S. STURMAN 1982. Adsorption of reovirus by minerals and soils. *Appl. Environ. Microbiol.*, 44: 852-859.

MORFIS, A. & H. ZOJER (eds) 1986. Karst Hydrogeology of the Central and Eastern Peloponnesus (Greece). *Steir. Beitr. Hydrogeol.* 37/38: 301 p. Vienna-New York: Springer.

MOSER, H. & F. NEUMAIER 1957. Die Anwendung radioaktiver Isotopen in der Hydrologie. I: Ein Verfahren zur Ermittlung von Zu- und Abflüssen von Wasserläufen. *Atomkernenergie* 2: 1-3. München.

MOSER, H. & F. NEUMAIER 1958. Die Bestimmung der Sickerwasserströmung unter dem Staudamm Roßhaupten mittels radioaktiver Isotope. *Wasserwirtschaft* 48(I): 290-294. Stuttgart: Franckh.

MOSER, H. & H. SAGL 1967. Die Direktmessung hydrologischer Farbtracer im Gelände. *Steir. Beitr. Hydrogeol.* 1966/67: 179-183. Graz.

MOSER, H. & W. RAUERT 1980. Isotopenmethoden in der Hydrologie. *Lehrbuch der Hydrogeologie* 8, 400 p. Berlin-Stuttgart: Gebr. Borntraeger.

MOSER, H., F. NEUMAIER & W. RAUERT 1957. Die Anwendung radioaktiver Isotope in der Hydrologie. II: Ein Verfahren zur Ermittlung der Ergiebigkeit von Grundwasserströmungen. *Atomkernenergie* 2: 225-231.

MOSER, H., F. NEUMAIER & W. RAUERT 1962. Die Anwendung radioaktiver Isotope in der Hydrologie. V: Die Messung der Wasserführung in offenen Gerinnen mittels radioaktiver Indikatoren. *Atomkernenergie* 7: 321-324.

MOSER, M. & J. KIEFER 1988. Die hydrogeologischen Verhältnisse und ihre Beziehungen zur Kinematik im Bereich der Talzuschubmasse Gradenbach/Kärnten. *Steir. Beitr. Hydrogeol.* 39: 95-115. Graz.

MOSER, M. & S.GLUMAC 1983. Geotechnische Untersuchungen zum Massenkriechen im Fels am Beispiel des Talzuschubes Gradenbach, Kärnten. *Verh. Geol. Bundesanst. 1983* 3: 209-241. Wien.

MOSER, M. & TH. WINDISCHMANN 1989. Die Reppwandlgeitung/Kärnten – Geologische und geotechnische Betrachtungen. *Oberrhein. geol. Abh.* 35: 157-176. Stuttgart.

MOSER, M., J. ANGERER & S. SEITZ 1988. Geotechnische Untersuchungsergebnisse im Rahmen des Verbauungsprojektes Oselitzenbach, Kärnten. *Int. Symp. Interpraevent 1988 Graz, Tagungspubl.* 3: 77-102. Graz.

MOZETIC, M. 1976. Virologische Untersuchungen. In Markierung unterirdischer Wässer – Untersuchungen in Slowenien 1972-1975, *Steir. Beitr. Hydrogeol.* 28: 110-112. Graz.

MOZETTI, F., E. ERIKSSON, F. BIVODEC, K. HODOSCEK & L. OSTANEK 1963. Un nuovo contributio alla conoscenza dell' idrologia sotterranea del Timavo. *Tecnica Ital.* 4: 157-171. Triest.

MÜHLHAUSEN, D. 1990. Pers. Comm.

MULJADI, S. & H.-P. BLUME 1977. Borstatus subhydrischer Böden Berlins. *Mitt. Dt. Bodenkundl. Ges.* 25: 221-232.

MULL, D.S., T.D. LIEBERMANN, J.L. SMOOT & L.H. WOOSLEY Jr. 1988. *Application of dye-tracing techniques for determining solute-transport characteristics of ground water in karst terranes.* US Environmental Protection Agency 904/6-88-001, 103 p. Atlanta/Georgia.

MULLEN, B. & R. THORN 1988. Groundwater tracing and water quality analysis in the vicinity of a landfill in County Monaghan, Ireland. *Mem. IAH (Int. Ass. Hydrogeol.) 21. Congr. Oct.1988 in Guilin/China* XXI(2): 910-915. Beijing.

MÜLLER, F. 1891. Resultate der Färbung des Höhlenflusses Reka im Karste mit Fluoresceïn. *Mitt. dt. u. österr. Alpenver.* VII(17): 230-231. Wien.

MÜLLER, I. & W. KÄSS 1980. Einsatz und Durchgang von Kochsalz. In Karsthydrologische Untersuchungen mit natürlichen und künstlichen Tracern im Neuenburger Jura (Schweiz). *Steir. Beitr. Hydrogeol.* 32: 77-80. Graz.

MÜLLER, L. 1963. *Der Felsbau.* Bd.I, Theoretischer Teil, Felsbau über Tage, 1.Teil, 624 p. Stuttgart: Enke.

MÜLLER, R. 1950. *Medizinische Mikrobiologie.* 4.Ed., pp 195-196. München-Berlin: Urban und Schwarzenberg.

NAGRA = Nationale Gesellschaft für die Lagerung radioaktiver Abfälle 1985. Sondierungsbohrung Böttstein, Untersuchungsbericht. Techn.Rep. 85-01, Textbd. pp 156-158, Supplement B, Beil. 8.9 und 8.10 sowie Techn. Ber. 85-07, Supplement, Suppl. 3.1, Baden/Schweiz.

NASSER, A.M., A. ADIN & B. FATTAL 1993. Adsorption of poliovirus 1 and F+ bacteriophages onto sand. *Water Sci. Tech.* 27: 331-338.

NELSON, N.T. & M.L. BRUSSEAU 1996. Field study of the partitioning tracer method for detection of dense nonaqueous phase liquid in a tetrachlorethene-contaminated aquifer. *Environ. Sci. Technol.* 30: 2859-2863.

NERETNIEKS, I. 1993. Solute Transport in Fractured Rock – Applications to Radionuclide Waste Repositories. In BEAR, J., C.F. TSANG & G. de MARSILY (1993) (eds), *Flow and Contaminant Transport in Fractured Rock,* 560 p. San Diego, California: Academic Press.

NESTMANN, E.R., D.J. KOWBEL & J. ELLENTON 1980. Mutagenicity in *Salmonella* of fluorescent dye tablets used in water tracing. *Water Res.* 14(7): 901-902. London: Pergamon Press.

NIEMELÄ, S. & K. KINNUNEN 1968. An experiment with *Escherichia coli* T bacteriophage as tracer in river flow studies. *Geophysica* 10: 121-124. (cit. after KINNUNEN 1978).

NIEMI, M. 1976. Survival of *Escherichia coli*-phage T7 in different water types. *Water Res.* 10: 751-755.

NIR, A. 1973. Tracer relations in mixed lakes in non-steady state. *J. Hydrol.* 19: 33-41. Amsterdam: North-Holland Publ. Comp.

NOBLE, R.T. & J.A. FUHRMANN 1996. Virus decay and its causes in costal waters. *Mar. Ecol. Prog. Sci.*

NOONAN, J. & J.F. MCNABB 1979. Movement of bacteriophages in ground water in New Zealand. In *Ann. Meet. Amer. Soc. Microbiol.*, p. 221. (cit. after KESWICK et al. 1982).

NORDSTROM, D.K., J.N. ANDREWS, L. CARLSSON, J.-C. FONTES, P. FRITZ, H. MOSER & T. OLSSON 1985. Hydrogeological and hydrogeochemical investigations in boreholes – Final Rep. of the Phase I Geochemical Investigations of the Stripa Groundwaters. Stripa Project Techn. Rep. 85-06. Stockholm.

NOVAKOWSKI, K.S., G.V. EVANS, D.A. LEVER & K.G. RAVEN 1985. A field example of measuring hydrodynamic dispersion in a single fracture. *Water Resour. Res.* 21/8: 1165-1174.

NRIAGU, J.O., A.H. DOUGLAS & R.D. COKER 1987. Biogenic sulfur and the acidity of rainfall in remote areas of Canada. *Science* 237: 1189-1192.

NYDEGGER, P. 1967. Untersuchungen über Feinstofftransport in Flüssen und Seen, über Entstehung von Trübungshorizonten und zuflußbedingten Strömungen im Brienzersee und einigen Vergleichsseen. *Beitr. Geol. Schweiz-Hydrol.* 16: 53-69. Bern: Kümmerly + Frey.

NYDEGGER, P. 1976. Strömungen in Seen. Untersuchungen in situ und an nachgebildeten Modellseen. *Beitr. Geol. Schweiz-Kleinere Mitteilungen* 66: 141-177. Bern: Kümmerly+Frey.

OBST, U. & A. HOLZAPFEL-PSCHORN 1988. *Enzymatische Tests für die Wasseranalytik*, 86 p. München-Wien: Oldenbourg.

ODUM, H.T. 1951. In: BLACK, A.P. & E. BROWN, Chemical character of Florida waters. State of Florida. *Water Research Paper* 6: 20-21.

OERTER, H. 1981. Untersuchungen über den Abfluß aus dem Vernagtferner unter besonderer Berücksichtigung des Schmelzwasserabflusses im Vernagtferner. *GSF Ber.* 267, 133 p. München.

OETZEL, S. 1990. Transport- und Adsorptionsverhalten von *Serratia marcescens*, *ÒX174* und *T4* in einem Porengrundwasserleiter. Diplomarb. Univ. Tübingen, 118 p. (Ms.).

OETZEL, S., W. KÄSS, T. HAHN, B. REICHERT & K. BOTZENHART 1991. Field experiments with microbiological tracers in a pore aquifer. *Water Sci. Tech. Great Britain* 24(2): 305-308. Oxford.

OGUSEITAN, O.A., G.S. SAYLER & R.V. MILLER 1992. Application of DNA probes to analysis of bacteriophage distribution patterns in the environment. *Appl. Environ. Microbiol.* 58: 2046-2052.

OHLMÜLLER, W. & O. SPITTA 1921. Die Untersuchung und Beurteilung des Wassers und des Abwassers, 4.Ed. 10. *Die Benutzung farbstoffbildender Bakterien zur Filterprüfung und die damit zusammenhängenden Methoden*, pp 282-286. Berlin: Springer.

OHLMÜLLER, W. 1902. Gutachten, betreffend die Verunreinigung von Quellen im Innerstethale und der Innerste. *Arb. Kaiserl. Gesundheitsamt* 18: 169-193. Berlin.

OHLMÜLLER, W. 1904. Gutachten des Reichsgesundheitsamtes über die Einleitung des Mainzer Kanalwassers einschließlich der Fäkalien in den Rhein. *Arb. Kaiserl. Gesundheitsamt* 20: 258-337. Berlin.

ORMEROD, J.G. 1964. *Serratia indica* as a bacterial tracer for water movements. *J. appl. Bact.* 27(2): 342-349. London.

ORTLAM, D. 1983. Einsatz und Möglichkeiten von Pollution-Tracer-Verfahren am Beispiel der Weser. *N. Jb. Geol.-Paläont. Abh.* 165: 303-325. Stuttgart.

OSMOND, J.K. 1980. Uranium disequilibrium in hydrologic studies. In FRITZ, P. & J.CH. FONTES (eds), *Handbook of Environmental Isotope Geochemistry* 1: 259-282. Amsterdam-Oxford-New York: Elsevier.

OSTLE, A.G. & J.G. HOLT 1979. Elution and inactivation of ß on soil and cation exchange resin. *Appl. Environ. Microbiol.* 38: 59-65.

PANCIERA, M. 1967. The toxicity of rhodamine-B to eggs of *Crassostrea virginica. Nate: Shellfisheries Ass.Proc.* 58: 7-8.

PANKOW, J.F. & J.A. CHERRY. 1996. *Dense chlorinated solvents and other dNAPLs in groundwater.* Waterloo, Ontario, Canada: Waterloo Press.

PARKER, G.G. Jr. 1973. Tests of Rhodamine WT dye for toxicity to oysters and fish. *J. Res. US Geol. Surv.* 1(4): 499. Washington.

PARRIAUX, A., M. LISZKAY, I. MÜLLER & G. DELLA VALLE 1988. Leitfaden für den Gebrauch künstlicher Tracer in der Hydrogeologie. *Schweiz. Geol. Ges. (Schweizerische Gruppe der Hydrogeologen, Arbeitsgruppe 'Tracer')*, 49 p. Lausanne.

PASCAL, P. 1966. *Nouveau traité de chimique minérale.* II/1; Les éléments alkaline, lithium, sodium, 1048 p. Paris: Musson & Cie.

PÄSSLER, H. 1952. Die Angiographie zur Erkennung, Behandlung und Begutachtung peripherer Durchblutungsstörungen. Fortschr. auf dem Gebiete der Röntgenstrahlen, vereinigt mit Röntgenpraxis, VIII, Erg.-Bd. 67, 115 p. Stuttgart: Thieme.

PAYMENT, P., E. MORIN & M. TRUDEL 1988. Coliphages and enteric viruses in the particulate phase of river water. *Can. J. Microbiol.* 34: 907-910.

PEARSON, F.J. Jr. & C.T. RIGHTMIRE 1980. Sulphur and oxygen isotopes in aqueous sulphur componds. In FRITZ, P. & J.CH. FONTES (eds), *Handbook of Environmental Geochemistry* 1: 227-258. Amsterdam-Oxford-New York: Elsevier.

PERLEGA, W. 1976. Der Nachweis von Fluoreszenzfarbstoffen mittels Aktivkohle. *Pap. 3rd Int. Symp. Groundwater Tracing (3.SUWT)*, pp 195-201. Ljubljana.

PETERMANN, J., P. HIRSIG & T. DERVEY 1985. ARA-Pensier. Einleitung der geklärten Abwässer in den Schiffenensee. Schlußbericht. Naturaqua, Beratende Naturwissenschaftler, Bern.

PETERS, D. 1989. Der Einfluß hydraulischer und sedimentologischer Eigenschaften gleichförmiger Sande auf die Filtration ausgewählter Bakterienarten. Diss. der Univ. Kiel, Berichte – Reports, Geol.-Paläont. Inst. Univ. Kiel, 29: 109 p., 51 Fig., 17 Tab. Kiel.

PFEIFFER, D. 1963. Die geschichtliche Entwicklung der Anschauungen über das Karstgrundwasser. *Beih. geol. Jb.* 57, 111 p. Hannover.

PFUHL, E. 1896. Untersuchungen über die Verunreinigung der Grundwasserbrunnen von unten her. *Z. Hygiene u. Infectionskrankheiten* 21: 1-10. Leipzig: Veit & Comp.

PFUHL, E. 1897. Ueber die Verschleppung von Bakterien durch das Grundwasser. *Z. Hygiene u. Infectionskrankheiten* 25: 549-554. Leipzig: Veit & Comp.

PFUHL, E. 1899. Bemerkungen zu der Arbeit: 'Ueber die Filtrationskraft des Bodens und die Fortschwemmung von Bakterien durch das Grundwasser.' Versuche von ABBA, ORLANDI & RONDELLI. *Z. Hygiene u.Infectionskrankheiten* 31: 497-501, Leipzig, Veit & Comp.

PIKE, E.B., A.W.J. BUFTON & D.J. GOULD 1969. The use of *Serratia indica* and *Bacillus subtilis* var. *niger* spores for tracing sewage dispersion in the sea. *J. appl. Bact.* 32: 206-216. London.

PILGRIM, D.H. 1966. Radioactive tracing of storm runoff on a small catchment, 1.Experimental technique. *J. Hydrol.* 4: 289-305.

PILGRIM, D.H. 1978. Adsorption losses and performance of $_{51}$Cr-EDTA and $_{198}$Au in tracing of flood runoff. *J. Hydrol.* 36: 47-64.

PINNEKER, E.W. & G.B. PALSCHIN 1966. Report about the symposium for the pursuit underground waterways in Austria (Russ.). *Geology and Geophysics*, pp 137-139. Novosibirsk.

PLATA BEDMAR, A. 1991. Detection of leaks from reservoirs and lakes. *Use of Artificial Tracers in Hydrology. IAEA-TECDOC* 601: 71-129. Vienna.

PLATA BEDMAR, A., L. ARAGUAS, E. TORRES, E. OBANDO & G. JIMENEZ 1991. Hydraulic parameters of river Magdalena (Colombia) from large scale tracer experiments. *Int. Symp. on the Use of Isotope Techniques in Water Resources Development, 11.-15.März 1991* IAEA-8M-319/9. Vienna: IAEA.

PLUMMER, L.N., E.C. PRESTEMON & D.L. PARKHURST 1991. An interactive code (NETPATH) for modeling net geochemical reactions along a flow path. US Geological Survey, Water-Resources Investigations Report 91-4078, 227 p. Reston, Virginia.

POHL, A. 1994. Quantifizierung der hydraulischen Eigenschaften eines hochdurchlässigen Ganges im Grundgebirge mittels Lauf- und Tracerversuche (Albtalgranit, Südschwarz-wald). Unpub. Diploma-Thesis, University of Karlsruhe, 77 p. Germany.

POLLAK, A., J. PERKOVAC, F. HRIBAR & F. BIDOVEC 1967. Absorptive Ultramikro-Methode zur Bestimmung des Fluoreszeins im Wasser. *Steir. Beitr. Hydrogeol.* 1966/67: 159-168. Graz.

POLLARD, E. & M. REAUME 1951. Thermal inactivation of bacterial viruses. *Arch. Biochem. Biophys.* 32: 278-287.

POWELSON, D.K., J.R. SIMPSON & C.P. GERBA 1991. Effects of organic matter on virus transport in unsaturated flow. *Appl. Environ. Microbiol.* 57: 2192-2196.

PRIMROSE, S.B., D. SEELY & B. LOGAN 1982. Methods for the study of virus ecology. Experimental Microbial Ecology, edited by BURNS, G. & I. SLATER, *Blackwell Sci. Publ.*, 66-83, Oxford-London-Edinburgh-Boston-Melbourne. (cit. after Steir. Beitr. Hydrogeol., 1985/86. Vienna-New York: Springer).

PRINZ, E. 1923. *Handbuch der Hydrologie,* 2.Ed., 422 p. Berlin: Springer.

PRINZ, H. 1982. *Abriß der Ingenieurgeologie,* 419 p. Stuttgart: Enke.

PROCTER & GAMBLE 1965, 1970. (cit. after DFG 1984).

PSCHYREMBEL, W. 1964. *Klinisches Wörterbuch.* 154-184. Ed., 980 P. Berlin: W. de Gruyter u. Co.

PURDY, R.N., N.B. DANCER, M.J. DAY & D.J. STICKLER 1984. A novel technique for the enumeration of bacteriophage from water. *FEMS Microbiol. Letters* 21: 89-92.

PUTMAN, J.L., A.M. WILDBLOOD & J.E. ROBSON 1956. The use of radioactive and bacterial tracers to follow sewage pollution in the sea. *The Water & Sanitary Engineer* 6: 99-101. London: Dall, Reynolds & Co.

PYLE, B.H., L.W. SINTON, M.J. NONAAN & J.F. MCNABB 1979. The movement of micro-organisms in groundwater. The New Zealand Institution of Engineers – *Proc. of Techn. Groups* 5(3): 465-479 (Ms.). Wellington.

QUEDNAU, W. 1930. Die Unschädlichkeit des Farbstoffes Uranin-Kali für Fische und Fischnahrung und seine Bedeutung im landwirtschaftlichen Betrieb. *Mitt. dt. Fischereivereine für die Provinzen Brandenburg, Ostpreußen, Pommern, Oberschlesien u.für die Grenzmark Posen-Westpreußen*, 34: 72-74.

QUINLAN, J.F. & D.R. ROWE 1977. Hydrology and water quality in the Central Kentucky Karst, phase 1. Univ. of Kentucky Water Resources Research Institute, Res. Rep. 109, 93 p.

QUINLAN, J.F. & P.L. SMART 1976. Identification of dyes used in water-tracing: A suggestion to improve communication. *Pap. 3rd Int. Symp. Underground Water Tracing (3.SUWT)*, pp 263-267. Ljubljana.

QUINLAN, J.F. 1976. New fluorescent direct dye suitable for tracing groundwater and detection with cotton. *Pap. 3rd. Int. Symp. Underground Water Tracing (3.SUWT)*, pp 257-262. Ljubljana.

QUINLAN, J.F. 1986. Discussion of Ground Water Tracers. *Ground Water* 24(2): 253-259. Dublin-Ohio.

QUINLAN, J.F. 1989. *Ground-water monitoring in karst terranes: Recommended Protocols and implicit assumptions.* US Environmental Protection Agency 600/X-89/050, 79 p. (Ms.). Las Vegas/NV.

QUITZOW, W. 1915. Die Wasserfärbung mit Uranin O. *Das Wasser* 11: 75-76, 95-97. Leipzig.

RADLEY, J.A. 1946. Recent advances in fluorescent analysis. *Food Manifacture USA* 22: 149-151, 164. London: Morgan-Grampian, Process Press.

RAGAP-DEPRE, N.J. 1982. Water desinfection with the hydrogen peroxide-ascorbic acid-copper (II) system. *Appl. and Envir. Microbiol.* 44(3): 555-560.

RAHE, T.M., C. HAGEDORN, E.L. MCCOY & G.F. KLING 1978. Transport of antibiotic-resistant *Escherichia coli* through western Oregon hillslope soils under conditions of saturated flow. *J. Environ. Qual.* 7: 487-494.

RAJER, R. & M. CETINA 1984. Numerical and experimental simulation of two-dimensional turbulent flow. In BREBBIA, C.A., C. MAKSIMOVIC & M. RADOJKOVIC (eds), Hydrosoft/84. *Proceedings of the 1st International Conference on Hydraulic Engineering Software, Portorose, Yugoslavia, September 10-14, 1984.* Amsterdam: Elsevier.

RAMSPACHER, P. 1981. Markierungsversuche am inneren Abflußsystem des Pasterzengletschers (Großglocknergruppe). Festschr. Josef G.ZÖTL, pp 131-145, Graz.

RANK, D. 1991. Ground water tracing with tritium: Problems as exemplified by an 'unsuccessful' tracing experiment in 1964. *IAEA-TECDOC* 601: 157-163. Vienna: IAEA.

RAO, S.M. 1983. Use of radioactive tracers in studies on infiltration through unsaturated zone. *IAEA-TECDOC* 291: 47-66. Vienna: IAEA.

REBER, U. & R. WEINGARTNER 1986. Ökologische und tracerhydrologische Untersuchungen zum Einfluß der Kläranlage Orpund auf ein überdüngtes Naturschutzgebiet. *Gas-Wasser-Abwasser* 66(3): 146-149. Zürich.

REICHERT, B. & H. HÖTZL 1990. Application of artificial tracers in a hazardous waste site – Laboratory studies. *Int. Atomic Energy Agency, IAEA-TECDOC* 601: 201-212. Vienna.

REICHERT, B. 1991. Anwendung natürlicher u. künstlicher Tracer zur Abschätzung des Gefahrenpotentials bei der Wassergewinnung durch Uferfiltration. *Schr. Angew. Geol. Karlsruhe* 13: 226 p. Karlsruhe.

RENK, A. 1981. Zum Mineralinhalt des Hermannganges (Südschwarzwald). Internal report, Geologisches Landesamt Baden-Württemberg, 39 p. Freiburg, Germany.

RHYS WILLIAMS, A.T. 1980. *Fluorescence detection in liquid chromatography*, 86 p. Beaconsfield: PERKIN-ELMER.

RICHTER, G. 1944. Zur Kennzeichnung unterirdisch fließender Wässer – Untersuchungen an der Range und anderen Karstquellen bei Warstein (Westfalen). *Abh. Reichsamt für Bodenforsch., N.F.* 209: 299-336. Berlin.

RIEG, A. & CH. LEIBUNDGUT 1992. Gauging of high variable discharge using tracer dilution method. In HÖTZL, H. & A.WERNER, Tracer Hydrology. *Proc. 6th Int. Symp. Water Tracing (SWT) of the ATH, 21.-26. Sept. 1992, Karlsruhe*, pp 287-289. Rotterdam: Balkema.

RIEMER.R. 1983. Untersuchung zum Transportverhalten von Bakterien in sandigen und kiesigen Filtermedien. Diss. Univ. Kiel, 161 p.

RIPPON, J.E. 1963. The use of a coloured bacterium as an indicator of local water movement. *Chem. & Ind.*, 16.March 1963: 445.

RITTER, R. 1983. Hydrobakteriologische Untersuchungen bei Pumpversuchen zum Nachweis der Flußwasserinfiltration in den Grundwasserleiter. *Forum Städte-Hygiene* 34: 51-53.

ROBERTS, M.E. 1986. The use of fluorocarbon tracers to monitor the movement of water in unsaturated porous media: Column study and computer model. Diss. M.S., 166 p., 25/02, Univ. of Arizona (Tucson).

ROBSON, J.E. 1956. A bacterial method for tracing sewage pollution. *J. Appl. Bact.* 19(2): 243-246.

ROCHAT, J., J. ALARY, J. MOLINARI & R. CHARRIÈRE 1975. Séparations physicochimiques de colorants xantheniques utilisés comme traceurs en hydrologie. *J. Hydrol.* 26: 277-293. Amsterdam.

ROCHAT, J., P. DEMENGE & J.-C. RERAT 1978. Contribution à l'étude toxicologique d'un traceur fluorescent: la Rhodamine B. *Toxicol. europ. Res.* 1: 23-26. Paris.

RODIER, J. & M. MARICHAL 1961. Contribution à l'étude de la dilution des effluents radio-actifs dans le Rhône par le rejet expérimental de Rhodamine B. *La Houille blanche* 5: 636-641. Grenoble.

RÖGNER, K.J. 1979. Karsthydrologische Untersuchungen um die Zeitenwende bei Banyas (antikes Caesarea Philippi, Nordisrael). *Die Höhle, Z. Karst- u. Höhlenkde.* 30(3): 57-61. Wien.

ROLDÃO, J., J. PEGLY & L. LEAL 1997. 'In situ' determination of the dilution efficiency of submarine sewage outfall's with the help of fluorescent dye tracers. In KRANJC, A. (ed.), Tracer Hydrology 97. *Proc. 7.Int. Symp. Water Tracing (SWT) of the ATH, 26-31 May 1997, Portoroz/Slovenia*, pp 143-149. Rotterdam: Balkema.

ROSSI, P. 1994. Advances in biological tracer techniques for hydrology and hydrogeology using bacteriophages: optimization of the methods and investigation of the behaviour of the bacterial viruses in surface waters and in porous and fractured aquifers. Ph. D. thesis: 200 p. University of Neuchâtel.

ROSSI, P., A. DE CARVALHO-DILL, I. MÜLLER & M. ARAGNO 1994. Comparative tracing experiments in a porous aquifer using bacteriophages and fluorescent dye on a test field located at Wilerwald (Switzerland) and simultaneously surveyed in detail on a local scale by radio-magneto-tellury (12-240 kHz). *Environ. Geology* 23: 192-200. Berlin-Heidelberg: Springer Verlag.

ROSSI, P., N. DOERFLIGER, I. MÜLLER & M. ARAGNO 1996a. Traçage des eaux à l'aide de bactériophages. *GWA* 1/96: 41-49.

ROSSI, P., P.A. GRETILLAT, I. MÜLLER & M. ARAGNO 1996b. Use of a marine bacteriophage (virus of bacteria) as a river tracer. (submitted).

ROTH, L. & M. DAUNDERER 1990. *Giftliste*, 6.Ed., Loseblattsammlung, Landsberg/Lech (Ecomed).

RÖTHLISBERGER, H. 1972. Water pressure in intra- and subglacial channels. *J. Glaciology* 11(62): 177-203. Cambridge: International Glaciological Society.

ROZANSKI, K., L. ARAGUÁS & R. GONFIANTINI 1993. Isotopic patterns in modern global precipitation. In Climatic change in continental isotopic records. *Geophysical Monograph* 78, American Geophysical Union, pp 1-36. Washington D.C.

RUPP 1885. Die Verwendung von Uranin und Fluoreszein zum Färben von Wässern betreffend. *Ber. des Chem. Laboratoriums der Techn. Hochschule Karlsruhe vom 29.August 1885.* Badisches Generallandesarchiv Karlsruhe, 237/39752.

SABATINI, D.A. & T. AL AUSTIN 1991. Characteristics of rhodamine WT and fluorescein as adsorbing ground-water tracers. *Ground Water* 29(3): 341-349.

SACHS, F. & S. HILPERT 1906. Ueber Nitro-Stilbene.- Ber. dt. chem. Ges. 39(I): 899-906. Berlin: Friedländer & Sohn.

SALENCON, M.-J. & P. CALMELS 1995. Etude de la dynamique des masses d'eau du Lac de Pareloup par tracages. *Hydroecol. Appl.* 6(1-2): 19-58.

SALVAMOSER, J. 1982. $_{85}$Kr im Grundwasser – Meßmethodik, Modellüberlegungen und Anwendungen auf natürliche Grundwassersysteme. Diss. Univ. München.

SARGEANT, K. & R.G. YEO 1966. The production of a bacteriophage. *Biotechn. Bioenging.* XF8: 195-215.

SARGEANT, K., R.G. YEO, J.H. LETHBRIDGE & K.V. SHOOTER 1968. Production of bacteriophage T7. *Appl. Microbiol.* 16: 1483-1488.

SATTAR, S.A., E.J. SYNEK, J.E.N. WESTWOOD & P. NEALS 1972. Hazard inherent in microbial tracers; reduction of risk by the use of *Bacillus stearothermophilus* spores in aerobiology. *Appl. Microbiol.* 23(6): 1053-1059, Baltimore.

SAUTY, J.-P. 1977. Contribution à l'identification des paramètres de dispersion dans les aquifères par interprétation des expériences de traçage. *Bur. de Recherches Géol. et Minières; Dépt. Hydrogéol. 77SGN515HYD*, 157 p. (Ms.). Orléans.

SAUTY, J.-P. 1980. An analysis of hydrodispersive transfer in aquifers. *Water Resources Res.* 16: 145-158.

SAYER, C. 1988. Untersuchungen zum mikrobiologischen Abbau von Uranin. Diplomarb., Teil 2, 73 p., 23 Anl. (Ms.). Karlsruhe.

SAYER, C. 1990. *Mikrobiologischer Uraninabbau.* Abschlußber. für das Geologische Landesamt Baden-Württemberg, 93 p., 13 Fig., (Ms.). Freiburg i.Br.

SCANDURA, J.E. & M.D. SOBSEY 1981. Survival and fate of enteric viruses in on-site waste-water disposal systems in coastal plains soils. *Abstr. Ann. Meet. Amer. Soc. Microbiol.*, p. 175. (cit. after KESWICK et al.1982).

SCHABER, J. 1993. Markierungsversuche mit fluoreszierenden Mikropartikeln. Diplomarb. (Ms.), 107 p. Univ. Freiburg i.Br.

SCHÄDEL, K. & I. STOBER 1988. Dispersion als Hinweis auf den Karsttypus. *Dt. Gewässerkdl. Mitt.* 32(4): 107-110.

SCHÄPERCLAUS, W. 1954. *Fischkrankheiten,* 3.Ed., 708 p. Berlin.

SCHARDT, H. 1910. Färbungsversuche mit Fluoreszein an unterirdischen Wässern. *Ecl. geol. Helv.* 11(1): 271-275.

SCHAUB, S.A. & B.P. SAGIK 1975. Association of enteroviruses with natural and artificially introduced colloïdal solids in water and infectivity of solids-associated virions. *Appl. Microbiol.* 30: 212-222.

SCHAUB, S.A. & CH.A. SORBER 1977. Virus and bacteria removal from wastewater by rapid infiltration through soil. *Applied and Environmental Microbiol.* 33(3): 609-619.

SCHAUFELBERGER, P. 1929. Geologische und hydrologische Verhältnisse zwischen der Donauversickerung und der Aachquelle. Diss. Zürich, Mitt. bad. geol. Landesanstalt X(2): 1-77. Freiburg i.Br.: Herder.

SCHEIDEGGER, A.E. 1961. General theory of dispersion in porous media. *J. Geophys. Res.* 66(10): 3273-3278.

SCHIECK, K. 1958. Über den Einsatz radioaktiver Isotope bei der Untersuchung von Grundwasserströmen. *WWT-Wasserwirtschaft-Wassertechnik* 8: 365-368. Berlin.

SCHLEGEL, H.G. 1985. *Allgemeine Mikrobiologie,* 6.Ed., 571 p. Stuttgart: Thieme.

SCHLOSSER, P., M. STUTE, H. DÖRR, Ch. SONNTAG & K.O. MÜNNICH 1988. Tritium/^{3}He dating of shallow groundwater. *Earth Planet. Sci. Lett.* 89: 353-362.

SCHLOZ, W. 1980. Anmerkungen zur Hydrochemie des Karstgrundwassers der östlichen Schwäbischen Alb. *Laichinger Höhlenfreund* 15(1): 37-42. Laichingen.

SCHLOZ, W. 1984. Zur Geologie und Hydrogeologie der im Egauwasserwerk der Landeswasserversorgung genutzten Buchbrunnenquelle, Weißjura-Karst der östlichen Schwäbischen Alb. *Zweckverband Landeswasserversorgung, Schriftenreihe* 4: 20-34. Stuttgart.

SCHMÄHL, P. 1981. Briefl. Mitt. an das Geol. Landesamt Baden-Württemberg vom 22.Januar 1981.

SCHMEISER, K. 1963. *Radionuklide,* 2.Ed., 282 p. Berlin-Göttingen-Heidelberg: Springer.

SCHMID, G. & B. BARCZEWSKI 1995. Development and application of a fibre optic fluorimeter for *in situ* tracer concentration measurements in groundwater and soil. *IAHS-Publication No 229*: Tracer technologies for Hydrological Systems, pp 13-20.

SCHMIDL, A. 1854. *Die Grotten und Höhlen von Adelsberg, Lueg, Planina und Laas,* 316 p. Wien.

SCHMIDT, H.L., S. VOERKELIUS & A. AMBERGER 1989. Nitrogen and oxygen isotope abundances of nitrogen compounds as indicators for nitrification and denitrification. DFG-Abschlußbericht (in Vorber.).

SCHMITT, K., U. VEIEL & L. WEGNER 1969. Die Bestimmung des Durchflusses in Abwasserkanälen; Messungen mit radioaktiven und nicht-radioaktiven Indikatoren. *GWF, Wasser-Abwasser* 110: 652-656. München: Oldenbourg.

SCHMITZ, W. 1989. Art und Ausmaß des Schadensfalles Sandoz im Rhein. *Wasserkalender* 1989: 48-63. Berlin-Bielefeld-München.

SCHMOTZER, J.K., W.A. JESTER & R.P. PARIZEK 1973. Groundwater tracing with post sampling activation analysis. *J. Hydrol.* 20: 217-236.

SCHNEIDER, K. 1988. *Hydrogeologische und isotopenhydrologische Untersuchungen im Einzugsgebiet der Kleislewaldquellen (Südschwarzwald).* Diplomarb., 84 p., 37 Anl. Freiburg i.Br.

SCHNITZER, W.A. & W. WAGNER 1967. Markierungsversuche mit Geruchsstoffen in der Karsthydrologie. *Geol.-Bl. NO-Bayern* 17: 179-194. Erlangen.

SCHNITZER, W.A. & W. WAGNER - & – 1968. Welche Anforderungen müssen Geruchsstoffe für Karstwassermarkierungen erfüllen? – *Vom Wasser* 35: 227-236. Weinheim: Chemie Verlag.

SCHNITZER, W.A. 1965a. Die Markierung unterirdischer Wasserwege mit Hilfe von Alkylbenzolsulfonaten (Detergentien). *Geol.-Bl. NO-Bayern* 15(1): 50-56. Erlangen.

SCHNITZER, W.A. 1965b. Eine neue Methode zur Markierung von Karstwasserwegen. *Die Höhle* 16: 64-67. Wien.

SCHNITZER, W.A. 1967a. Schallimpulse und ihr Verlauf im Karst. *Geol.-Bl. NO-Bayern* 17(1): 13-20. Erlangen.

SCHNITZER, W.A. 1967b. Die Anwendung von Detergentien und verwandten Stoffen in der Hydrogeologie. *Steir. Beitr. Hydrogeol.* 1966/67: 231-234. Graz.

SCHNITZER, W.A. 1967c. Ergebnisse und Erfahrungen bei Markierungsversuchen im Karst der nördlichen Frankenalb. *Jh. Karst- u. Höhlenkde.* 7: 19-27. Erlangen.

SCHNITZER, W.A. 1967d. Die Anwendung von Alkylbenzolsulfonaten zur Markierung unterirdischer Wasserwege. *Mém. I.A.H.-Kongreß 1965* VII: 217-219, Hannover.

SCHNITZER, W.A. 1972. Neue Methoden zur Erforschung des Karstes. *Geol. Jb.* C2: 111-118. Hannover.

SCHÖLLER, F. 1983. Vorkommen von Bromid in Grundwässern. *Österr. Wasserwirtsch.* 35: 272-274. Wien-New York.

SCHOTTERER, U. & H.U. FELBER 1982. Tritium and oxygen-18 as natural tracers in the complex hydrology of the alpine basin of Grindelwald (Switzerland). *Beitr. Geol. Schweiz – Hydrol.* 28(II): 435-444. Bern: Kümmerly + Frey.

SCHREINER, A. 1968. Eiszeitliche Rinnen und Becken und deren Füllung im Hegau und westlichen Bodenseegebiet. *Jh. geol. Landesamt Baden-Württemberg* 10: 79-104. Freiburg i.Br.

SCHRÖTER, J. 1983. Der Einfluß von Textur- und Struktureigenschaften poröser Medien auf die Dispersivität. Diss. Univ. Kiel, 152 p.

SCHRÖTER, J. 1984. *Mikro- und Makrodispersivität poröser Grundwasserleiter.* Meyniana 36: 1-34. Kiel.

SCHRÖTER, J. 1987. In MATTHESS, G., M. ISENBECK & J. SCHRÖTER, *Reinigungswirkung des Untergrundes gegenüber Schadstoff-Gruppen in Trinkwasserschutzgebieten – Teil B: Felduntersuchungen*, 72 + 9 p. (Ms.) – Geol.-Paläontol. Inst. u. Mus. d. Christian-Albrecht-Univ. Kiel.

SCHÜBEL, F.W. 1936. Die hygienische Untersuchung und Beurteilung künstlicher Grundwasser-erweiterung. *Arch. Hyg. u. Bakt.* 116: 321-363.

SCHUBERT, R.H. & E. SCHÄFER 1971. Vergleichende Untersuchungen über die Eliminierung von Viren, Salmonellen und Aeromonaden im Vorfluter. *Gas- u. Wasserfach* 112(8): 401-403. München: Oldenbourg.

SCHUDEL, B. 1991. Einsatz tracerhydrologischer Methoden im Abwasser – Ermittlung von Fließzeiten und Verweilzeiten in Abwassernetzen und Abwasserreinigungsanlagen. *Gas-Wasser-Abwasser* 71: 441-448. Zürich.

SCHULZ, G. 1957. Färb- und Salzungsversuche an unterirdischen Wässern in Südwestdeutschland. *Jh. geol. Landesamt Baden-Württemberg* 2: 333-412. Freiburg i.Br.

SCHULZ, G. 1961. Erprobung verschiedener Markierungsstoffe für unterirdische Wässer bei Oberndorf am Neckar. *Jh. geol. Landesamt Baden-Württemberg* 5: 323-341. Freiburg i.Br.

SCHULZ, H.D. & E.J. REARDON 1983. A combined mixing cell/analytical model to describe two-dimensional reactive solute transport for undirectional groundwater flow. *Water Resources Res.* 19(2): 493-502.

SCHULZ, H.D. 1988. Labormessung der Sättigungslänge als Maß für die Lösungskinetik von Ionen im Grundwasser. *Geochim. Cosmochim. Acta* 52(11): 2651-2657. Pergamon Press.

SCHWEIZER, R., I. STOBER & G. STRAYLE 1985. Auswertungsmöglichkeiten und Ergebnisse von Tracerversuchen im Grundwasser. *Abh. geol. Landesamt Baden-Württemberg* 11: 93-139. Freiburg i Br.

SCOTT, C.H., V.W. NORMAN & F.K. FIELDS 1969. Reduction of fluorescence of two tracer dyes by contact with a fine sediment. *Geol. Surv. Prof. Pap.* 650-B: 164-168. Washington.

SEEFELDNER, E. 1952. Die Entwicklung der Salzburger Alpen im Jungtertiär. *Mitt. geogr. Ges. Wien* 94: 179-194. Wien.

SEELEY, N.D. & S.B. PRIMROSE 1980. The effect of temperature on the ecology of aquatic bacteriophages. *J. Gen. Virol.* 46: 87-95.

SEELEY, N.D. & S.B. PRIMROSE 1981. A review: the isolation of bacteriophages from the environment. *J. Appl. Bacteriol.* 53: 1-17.

SEELMANN-EGGEBERT, W., G. PFENNIG & H. MÜNZEL 1984. *Karlsruher Nuklidkarte.* München: Gersbach u. Sohn Verlag.

SEIDLITZ, H.K. & H. BEHRENS 1991. *Verbesserung der Nachweisempfindlichkeit von Fluoreszenztracern.* Jber. 1990 des Inst. f. Hydrol., pp 141-144. Neuherberg.

SEILER, K.P. 1985. Results of field experiments on hydrodynamic dispersion in quaternary gravels of Southern Germany. In *Scientific Basis for Water Resources Management (Proc. Symp. Jerusalem 1985)*, Wallingford, pp 153-169.

SELLA, M. 1929. Estese migrazioni dell'anguilla in aque sotterranee. *Le Grotte d'Italia* 3: 97-109, H. Juli-September 1929, Triest.

SEMMLER, W. & R. SCHMIDT 1958. Die Anwendung des Farbstoffes Uranin AP zur Nachweisung hydraulischer Zusammenhänge über und unter Tage. *Bergfreiheit* 23: 81-90. Essen.

SEMMLER, W. 1937. Untersuchungen, Wassermessungen und Färbungsversuche zur Ermittlung der Herkunft der Wasserzuflüsse im Felde der Grube Viktoria, Püttlingen-Saar. *Bergbau* 50(6): 87-93. Gelsenkirchen: Carl Bertenburg.

SEMMLER, W. 1953. Färbeversuche zur Ermittlung hydraulischer Zusammenhänge im Bergbau mit Uranin AP. *Glückauf* 89(9/10): 214-223. Essen.

SEMMLER, W. 1958. Eine Wasserentziehung als scheinbarer Bergschaden. *Techn. Mitt.* 51: 446-451.

SENFTEN, H. 1972. Borsäure in Trink- und Mineralwässern. Diss. Univ. Bern, 182 p.

SHEELY, C.Q. & D.E. BALDWIN 1982. Single-well tracer tests for evaluating chemical enhanced oil recovery processes. *J. Pet. Technol.* 34: 1887-1896.

SHEELY, C.Q. 1978. Description of field tests to determine residual oil saturation by single-well tracer method. *J. Pet. Technol.* pp. 194-202.

SHELANSKI, H.A. & M.V. SHELANSKI 1953. A new technique of human patch tests. *Proc. Sci. Sect. Toilet Goods Assoc.* 20: 46-49.

SEABERG, S.Z., J.Z. SEABERG, L.R. HOOKE & D.W.WIBERG 1988. Character of the englacial and subglacial drainage system in the lower part of the ablation area of Storglaciären, Sweden, as revealed by dye-trace studies. *J. Glaciology* 34(117): 217-227. Cambridge: International Glaciological Society.

SHOTTON, E. & A.S.F.A. HABEEB 1955. The stimulation of fluorescein in dilute solutions. *J. Pharmacy, Pharmacol.* 7: 456-462. London.

SIEGENTHALER, U. 1972. Bestimmung der Verweildauer von Grundwasser im Boden mit radioaktiven Umweltisotopen. *Gas-Wasser-Abwasser* 52: 283-290. Zürich.

SIEGENTHALER, U. 1982. Studium von Seedurchmischung und Fluß-Einschichtung im Bielersee mit Hilfe von $_{18}O/_{16}O$-Messungen. *Beitr. Geol. Schweiz – Hydrol.* 28(II): 511-521. Bern: Kümmerly + Frey.

SIHLER, H. 1929. Blautopf und Karsthydrographie. *Jh. Ver. vaterl. Naturkde. Württ.* 85: 210-241. Stuttgart.

SILINE-BEKTCHOURINE, A.I. 1951. Hydrogéologie spéciale. 1 vol., Moscow, Gossendarctvennoe izdatelctvo geologitcheshoi literatouri, 394 p. (cit. after SCHOELLER, H. 1959. Arid Zone Hydrology – *Arid Zone Research* 12: 125 p. Paris: UNESCO).

SINTON, L.W. 1979a. The use of bacteria as tracers of ground water movement. *Proc. Symp. Dept. of Agricult. Microbiol. Techn. Publ. No.2, Lincoln College, Canterbury, New Zealand*, pp 93-13. (cit. after KESWICK et al.1982).

SINTON, L.W. 1979b. Investigations into the use of the bacterial species *Bacillus stearothermophilus* and *Escherichia coli* (H_2S positive) as tracers of groundwater movement. *Water and Soil Techn. Publ. Ser.* (Ministry of Works and Development, Wellington, New Zealand). (cit. after PYLE, B.H. et al.1979).

SKILTON, H. & D. WHEELER 1988. Bacteriophage tracer experiments in groundwater. *J. Appl. Bacteriol.* 65: 387-395.

SMART, C.C. 1988. Artificial tracer techniques for the determination of the structure of conduit aquifers. *Ground Water* 26: 445-453.

SMART, P.L. & D.I. SMITH 1976. Water tracing in tropical regions, the use of fluorometric techniques in Jamaica. *J. Hydrol.* 30: 179-195. Amsterdam.

SMART, P.L. & I.M.S. LAIDLAW 1977. An evaluation of some fluorescent dyes for water tracing. *Water Resources Res.* 13(1): 15-33.

SMART, P.L. & M.C. BROWN 1975. The use of activated carbon for the detection of the tracer dye rhodamine WT. *Proc. 7th Int. Congr. Speleol., III, Sub-Sect. C6011*, pp 285-292. Olmolve.

SMART, P.L. 1976a. The use of optical brighteners for water tracing. *Trans. British Cave Res. Ass.* 3(2): 62-76.

SMART, P.L. 1976b. Use of optical brightener/Cellulose detector systems for water tracing. *Pap. 3rd Int. Symp. Underground Water Tracing (3.SUWT)*, pp 203-213. Ljubljana.

SMART, P.L. 1982. A review of the toxicity of 12 fluorescent dyes used for water tracing. *Beitr. Geol. Schweiz – Hydrol.* 28(I): 101-112. Bern: Kümmerly + Frey.

SMART, P.L. 1984. A review of the toxicity of twelve fluorescent dyes used for water tracing. *Nat. Speleol. Soc. Bull.* 46: 21-33.

SMITH, D.B. 1964. River-flow measurement using radioactive tracers. In V.K. COLLINGE & J.R. SIMPSON (eds), *Proc. Course on 'Dilution Techniques for Flow Measurement'*. Univ. Newcastle upon Tyne.

SMITH, E.M., C.P. GERBA & J.L. MELNICK 1978. Role of sediment in the persistence of enteroviruses in the estuarine environment. *Appl. Environ. Microbiol.* 35: 685-692.

SNYDER, F.H., D.L. OPDYKE & H.L. RUBENKOENIG 1963. Toxicologic studies on brighteners. *Toxicol. and Pharmacol.* 5: 176-183. New York-London: Academic Press.

SOLOMON, D.K., R.J. POREDA, S.L. SCHIFF & J.A. CHERRY 1992. Tritium and helium 3 as groundwater age tracers in the Bordon aquifer. *Water Resourc. Res.* 28: 741-755.

SONNTAG, CH., E. KLITZSCH, E.M. SHAZLY, CH. KALINKE & K.-O. MÜNNICH 1978. Paläoklimatische Information im Isotopengehalt ^{14}C-datierter Saharawässer: Kontinentaleffekt in D und $_{18}O$. *Geol. Rdsch.* 67: 413-424. Stuttgart.

SOWARDS, C.L. 1958. Sodium fluorescein and the toxicity of Pronoxfish. *Prog. Fish-Culturist* 20(1): 20. Washington/D.C.

SPEIDEL, U. Diplomarbeit

SPENCER, E.A. & J.S. TUDHOPE 1956. A literature survey of the salt-dilution method of flow measurement. *J. Inst. Water Engrs.* 12(2): 127-138.

SPREAFICO, M. 1991. Fließzeitbestimmung und Stofftransportuntersuchungen im Rhein. *Landeshydrologie und Geologie.* Mitt. Nr. 13. Bern.

SPREAFICO, M. 1994. Handbuch für Abflußmengenbestimmung mittels Verdünnungsverfahren mit Fluoreszenztracern. *Landeshydrologie und Geologie Bern*, Mitt. Nr. 20. Bern.

SPRING, W. 1905. Über die Grenze der Sichtbarkeit der Fluoreszenz und über die obere Grenze des absoluten Gewichts der Atome. *Chem. Zbl.* 1905 (II): 378. Berlin: Friedländer u. Sohn.

SPROUL, O.J. 1972. Virus inactivation by water treatment. *Amer. Water Work Ass.* 64(1): 31-35.

STAGG, C.H., C. WALLIS & C.H. WARD 1977. Inactivation of clay-associated bacteriophage MS-2 by chlorine. *Appl. Environ. Microbiol.* 33: 385-391.

STAMPFLI 1983. In WERNLI, H. & CH. LEIBUNDGUT, Fluoreszierende Markierstoffe, *Einführungskurs in die Tracerhydrologie, 17.-21.Oktober 1983*, Geogr. Inst. der Univ. Bern, Abt. Gewässerkde.

STARK, J. 1987. Hydrochemische Quell- und Grundwasseruntersuchungen auf Sickerwassereinflüsse der Hausmülldeponie 'Vulkan' bei Haslach i.K. Diplomarb., 137 + 47 p. (Ms.). Freiburg i.Br.

STEIN, M.R. & CH.W.PARKER 1971. Reactions following intravenous fluorescein. *Amer. J. Ophthal.* 72: 861-868. Chicago.

STERNAU, R., J.SCHWARZ, A.MERCADO, Y.HARPAZ, A.NIR & E.HALEVY 1967. *Proc. Int. Symp. Isotopes in Hydrology*, pp 489-505. Vienna: IAEA.

STICHLER, W. & P.TRIMBORN 1980. Hydrologische Untersuchungen im Bereich eines Baggersees mit $_2H$- und $_{18}O$-Analysen mit Einbohrlochmessungen. In *Traceruntersuchungen in Hydrogeologie und Hydrologie. GSF-Ber.* R 250: 29-38. Neuherberg.

STICHLER, W. 1981. Identifizierung von Grundwässern anhand ihres Gehalts an stabilen Isotopen. In *Festschrift Josef G.ZÖTL*, pp 147-157. Graz.

STICHLER, W., P.MALOSZEWSKI & H.MOSER 1986. Modelling of river water infiltration using oxygen-18 data. *J. Hydrol.* 83: 355-365. Amsterdam.

STILLE, H. 1903. Geologisch-hydrogeologische Verhältnisse im Ursprungsgebiet der Paderquellen zu Paderborn. Abh. der Königl. Preuß. Geol. Landesanstalt u. Bergakad., NF, 38, 129 p. Berlin. (Unveränderter Nachdruck in *Geol.Jb.* C14. Hannover 1976).

STINI, J. 1948. Die Wasserwärmemessung als Hilfsmittel bei der Bestimmung von Zusammenhängen zwischen Quellen und offenen Gerinnen. *Geol. u. Bauwesen* 16(3/4): 92-95. Wien: Springer.

STOBER, I. 1980. Bestimmung von Aquiferparametern aus Markierungsversuchen in Porengrundwasserleitern mit analytischen Lösungen. *Diplomarb.*, 90 p. Freiburg i.Br.

STOBER, I. 1986. Strömungsverhalten in Festgesteinsaquiferen mit Hilfe von Pump- und Injektionsversuchen. *Geol. Jb.* C42, 204 p. Hannover.

STOBER, I. 1988. Geohydraulische Ergebnisse. In Ergebnisse der Hydrogeothermiebestimmungen in Baden-Württemberg. *Jh. geol. Landesamt Baden-Württemberg* 30: 64-73. Freiburg i.Br.

STRAMER, L. & D.O. CLIVER 1981. Poliovirus removal from septic systems under conditions of soil saturation. *Abs. Annl. Microbiol.*, p. 178.

STRAYLE, G. 1970. Karsthydrologische Untersuchungen auf der Ebinger Alb (Schwäbischer Jura). *Jh. geol. Landesamt Baden-Württemberg* 12: 109-206. Freiburg i.Br.

STRAYLE, G., I. STOBER & W. SCHLOZ 1994. Ergiebigkeitsuntersuchungen in Festgesteinsaquiferen. *Geol. Landesamt Baden-Württemberg, Informationen 6/94*, 114 p. Freiburg i.Br.: Verlag GmbH Steinmann.

STURM, P.W. & W.E. JOHNSON 1950. Field experiments with chemical tracers in flood waters. *Producers Month.* 14: 11-17. Bradford/Pennsylvania.

SUDICKY, E.A. & E.O. FRIND 1982. Contaminant transport in fractured porous media: analytical solutions for a system of parallel fractures. *Water Resour. Res.* 18: 1634-1642.

SUTTLE, C.A., F. CHEN & A.M. CHAN 1992. Marine viruses: decay rates, diversity and ecological implications. In W. BROWN, *Int. Mar. Biotechnol. Conf. 'IMBC-91' Develop. Microbiol. Ser.*, pp 153-163.

SWEETING, M.M. 1972. *Karst landforms*, 362 p. London: Macmillan.

TANG, J.S. & B. HARKER 1991. Interwell tracer test to determine residual oil saturation in gas-saturated reservoir. Part I: Theory and Design; Part II: Field Applications. *J. Can. Pet. Technol.* 30: 34-42.

TANG, J.S. 1992. Interwell tracer tests to determine residual oil saturation to waterflood at Judy Creek BHL 'A' Pool. *J. Can. Pet. Technol.* 31: 61-71.

TARTERA, C. & J. JOFRE 1987. Bacteriophages active against *Bacteroides fragilis* in sewage polluted waters. *Appl. Environ. Microbiol.* 53: 1632-1637.

TAYLOR, G. 1953. Dispersion of soluble matter in solvent flowing slowly through a tube. *Proc. Roy. Soc. London, Ser. A* 219: 186-203.

TENHAEFF, G. & W. KÄSS 1987. Karsthydrologische Untersuchungen im Bereich der Bauschlotter Platte (Nordbaden). *Jh. geol. Landesamt Baden-Württemberg* 29: 209-254. Freiburg i.Br.

THATCHER, L.L. & D.A. RAMSEY 1977. Anion Complexes of gold as ground-water tracers by neutron activation analysis. In J.R.VOGT (ED.), *Proc. 3rd Int. Conf. on Nuclear Methods in Environmental and Energy Research (CONF-771072*, pp 265-275. Univ. of Columbia/Missouri.

THOMPSON, G.M., J.M. HAYES & S.N. DAVIS 1974. Fluorocarbon tracers in hydrology. *Geophysical Research Letters* 1: 177-180. (cit. after DAVIS, S.N. et al., Ground Water Tracers, Nat. Water Well Ass., Washington, Ohio, 1985).

TIETZE, E. & O. BAYER 1939. Die Sulfosäure des Pyrens und ihre Abkömmlinge. *Ann. Chemie* 540: 189-210.

TIMEUS, G. 1910. *Studi in relazione al provvedimento d'acqua per la città di Trieste. Dati idrologici, chimici e batteriologici*, 82 p. Comune di Trieste, Fisicato civico, Ufficio d'igiene, Triest.

TIMEUS, G. 1911. Sui mezzi d'indagine nell' idrologia sotterranea. Nuovi metodi. *Bull. Soc. adriatica di Sci. Nat.* XXV: 216-260. Trieste: Tip. Lloyd.

TIMEUS, G. 1912. Il litio e la radioattività quali mezzi d'indagine nell'idrologia sotterranea. L'origine del fiume Timova. *Bull. Soc. adriatica di Scienze Nat., Trieste, 1910 e Atti della Soc. ital. per il Progr. delle Scienze* V: 3-19. Roma.

TIMEUS, G. 1926. Le indagini sull'origini delle acque sotterranee. In BERTARELLI, I.V. & E. BOEGAN, *Duemila Grotte*, pp 153-166. Milano: Touring Club Italiano.

TIMEUS, G.1928. Nei misteri del mondo sotterrano – Resultati delle richerche idrologiche sui Timavo. *Alpi Giulie* XXIX/1: 1-40, 20 Fig., 1 Table, 1 map. Trieste.

TOMICH, J.F., R.L. DALTON, H.A. DEANS & L.K. SHALLENBERGER 1973. Single-well tracer method to measure residual oil saturation. *J. Pet. Technol.* pp. 211-218.

TORTORELLO, M.L., K.M. TROTTER, S.M. ANGELOS, R.A. LEDFORD & G.M. DUNNY 1991. Microtiter plate assay for the measurement of phage adsorption and infection in *lactococcus* and *Enterococcus. Analytical biochemistry* 109: 362-366.

TOUSSAINT, B. 1971. Hydrogeologie und Karstgenese des Tennengebirges (Salzburger Kalkalpen). *Steir. Beitr. Hydrogeol.* 23: 5-115. Graz.

TRATNIK, M. 1976. Bakteriologische Untersuchungen. In Markierung unterirdischer Wässer – Untersuchungen in Slowenien 1972-1975. *Steir. Beitr. Hydrogeol.* 28: 107-110. Graz.

TRAUB, W.H. 1975. Pers. Comm. from 7 Januar 1975. Erlangen.

TRESH, J.C. 1907. *The detection of pollution in underground waters.* J. Gas Lighting, Water Supply etc. Nr.2305, pp 164-166 vom 16.Juli 1907 (aufgegangen in: Gas World and Gas J., London).

TRILLAT, A. 1899a. Essai sur l'emploi des matières colorantes. *Ann. Inst. Pasteur* 13: 444-449, Paris.

TRILLAT, A. 1899b. Sur l'emploi des metières colorantes pour la recherche de l'origine des sources et les eaux d'infiltration. *C. R. Acad. Sci.* 128: 698-700. Paris.

TRIMMEL, H. 1993. Markierungsversuche und Karsthydrographie des Dachsteinstockes – Eine Würdigung der letzten Arbeiten von Dr. Fridtjof BAUER (†). *Wissenschaftl. Beih. z. Z. Die Höhle* 42: 33-44. Wien.

TRUESDELL, A.H. & J.R.HULSTON 1980. Isotopic evidence on environments of geothermal systems. In FRITZ, P. & J.CH.FONTES (eds): Handbook of Environmental Geochemistry, 1: 179-226, Amsterdam-Oxford-New York (Elsevier).

TURNER, T.D. 1958. Streamtracing. Bull. Mid.-Appalachian Region; Nat. Spel. Soc., 3: 6-7.

UBA 1985. Lebensdauer von Bakterien und Viren in Grundwasserleitern – Zusammengefaßter Abschlußber.; herausg. vom Umweltbundesamt, Materialien 2/85: 108 p. Berlin: E. Schmidt.

UBA 1988. Katalog wassergefährdender Stoffe. Bearbeitet vom Beirat 'Lagerung und Transport wassergefährdender Stoffe' beim Bundesminister des Innern; herausg. vom Umweltbundesamt, LTwS-Nr.12: 24 + 13 p. Berlin.

UBA 1997. Human- und ökotoxische Bewertung von Markierungsmitteln in Gewässern. *Grundwasser* 2(2): 61-64. Berlin-Heidelberg: Springer.

ULLMANN's Enzyklopädie der technischen Chemie 1978. 4.Ed., 16, 735 p. Weinheim: Verlag Chemie.

ULLMANN's Encyclopedia of Industrial Chemistry 1988. 5.Ed., A15: 630 p. Weinheim: Verlag Chemie.

UMEDA, M. 1956. Experimental study of xanthene dyes as carcinogenic agents. *Gann* 47: 51-78. Tokio.

UNESCO 1973 with Supplements 1975, 1977 and 1983. *Groundwater studies; an international guide for research and practice.* (cit. after PARRIAUX et al.1988).

UNKELBACH, U.M.E., H.D. BREDE, V. SCHÄFER, W.H. SIEDE, A. REGENITER, U.B. SEIFFERT, H.W. DOERR & H. RÜBSAMEN-WAIGMANN 1991. Eine Methode zur Überprüfung der Arbeitssicherheit im klinisch-chemischen Laboratorium. *GIT Labor-Medizin* 3/91: 79-85. Darmstadt.

VATNE, G., B. ETZELMÜLLER, J.L. SOLLID & R. STRAND ODEGARD 1995. Hydrology of a polythermal glacier, Erikbreen, Northern Spitsbergen. *Nordic Hydrology* 26: 169-190. Copenhagen: Munksgaard.

VAUGHN, J.M., E.F. LANDRY, L.J. BARANOWSKY, C.A. BECKWITH, M.C. DAHL & N.C.DELIHAS 1978. Survey of human virus occurance in wastewater-recharged groundwater on Long Island. *Appl. Envir. Microbiol.* 36: 47-51.

VILLINGER, E. & W. UFRECHT 1989. Ergebnisse neuer Markierungsversuche im Einzugsgebiet des Blautopfs (mittlere Schwäbische Alb). *Mitt. Verb. dt. Höhlen- u. Karstforsch.* 35(1/2): 25-38. München.

VILLINGER, E. 1977. Über Potentialverteilung und Strömungssysteme im Karstwasser der Schwäbischen Alb (Oberer Jura, SW-Deutschland). *Geol. Jb.* C18: 1-93. Hannover.

VILLINGER, E. 1978. Zur Karsthydrologie des Blautopfs und seines Einzugsgebietes (Schwäbische Alb). *Abh. geol. Landesamt Baden-Württemberg* 8: 59-127. Freiburg i.Br.

VILLINGER, E. 1986. Untersuchungen zur Flußgeschichte von Aare-Donau/Alpenrhein und zur Entwicklung des Malm-Karsts in Südwestdeutschland. *Jh. geol. Landesamt Baden-Württemberg* 28: 295-362. Freiburg i.Br.

VILLINGER, E. 1987. Die Blautopfhöhle bei Blaubeuren als Beispiel für die Entwicklung des Karstsystems im Schwäbischen Malm. *Geol. Jb.* C49: 71-103. Hannover.

VO-DINH, T. 1981. Synchronous excitation spectroscopy. In WEHRY, E.L., *Modern Fluorescence Spectroscopy* 4: 167-182. New York: Plenum Press.

VOERKELIUS, S. 1990. Isotopendiskriminierungen bei der Nitrifikation und Denitrifikation; Grundlagen und Anwendungen der Herkunfts-Zuordnung von Nitrat und Distickstoffmonoxid. Dissertation TU München.

VOGT, M. & B. HERRLING 1988. Application of transport modeling for verifying a flow model of an infiltration area. *Proc. Int. Symp. Interaction between groundwater and surface water, IAHR Conf.*, pp 339-346. Ystad, Sweden.

VÖLKL, G. 1981. Die Bedeutung von Markierungsversuchen für die Abgrenzung von Schutz- und Schongebieten. *Gas/Wasser/Wärme* 35(11): 365-369.

VÖLKL, G. 1988. Karsthydrologische Untersuchungen im Kaisergebirge. Markierversuch zur Feststellung der Quelleinzugsgebiete als Grundlage für Schutz- und Schongebietsverordnungen. 60 p. (printed as Ms.). Wien.

VORNATSCHER, J. 1962. Einige Bemerkungen zur Sporentrift. *Die Höhle* 13(4): 82-84. Wien.

VORTMANN, G. & G. TIMEUS 1910a. L'applicazione del cloruro di litio nelle indagini d'idrologia sotteranea – Le origini del Timavo. *Boll. Soc. Adriat. di Sci. Naturali* XXV: 233-237. Trieste.

VORTMANN, G. & G. TIMEUS 1910b. Indagini nella radioattività delle acque della Regione Giulia. *Boll. Soc.Adriat. di Sci. Naturali* XXV, P.II: 238-246. Trieste: Tip. Lloyd.

VORTMANN, G. & G. TIMEUS 1910c. L'applicazione di sostanze radioattive nelle ricerche d'idrologia sotterranea. *Boll. Soc. Adriat. di Sci. Naturali* XXV: 247-260. Trieste.

WAAGEN, L. 1926. Die Färbungs- und Salzungsversuche im Quellgebiet der Ersten Wiener Hochquellenleitung. *Verh. Geol. Bundesanst.* 1926: 195-198. Wien.

WAGNER, Gg. 1954. Der Karst als Musterbeispiel der Verkarstung. *Aus der Heimat* 62(9/10): 193-212. Öhringen: Rau.

WAGNER, Gg. 1961. Zur Flußgeschichte von oberer Donau und oberem Neckar. *Jber. u. Mitt. oberrh. geol. Ver., N.F.* 43: 93-98. Stuttgart.

WALTHER, H. 1947. Einführung in die Phytologie. Bd.I. Die Grundlagen des Pflanzenlebens, 2.Ed., 474 p. Stuttgart: Ulmer.

WAN, J., J.L. WILSON & T.L. KIEFT 1993. Influence of the gas-water interface on transport of microorganisms through unsaturated porous media. *Appl. Environ. Microbiol.* 60: 509-516.

WANG, D.-S. & C.P. GERBA 1980. Evaluation of F2 bacteriophage for tracing movement of viruses in groundwater. *EOS* 61(17): 233.

WANNINKHOF, R., J.R. LEDWELL & W.S. BROECKER 1985. Gas exchange – wind speed relation measured with sulfur hexafluoride on a lake. *Science* 227: 1224-1226.

WATSON, A.J., M.I. LIDDICOAT & J.R. LEDWELL 1987. Perfluorodecalin and sulphur hexafluoride as purposeful marine tracers: some deployment and analysis techniques. *Deep-Sea Res.* 34: 19-31. Oxford, Great Britain.

WEBB, J.M. & W.H. HANSEN 1961. Studies of the metabolism of Rhodamine B. *Toxicol. and Appl. Pharmacol.* 3: 86-95. New York-London: Academic Press.

WEBB, J.M., W.H. HANSEN, A. DESMOND & O.G. FITZHUGH 1961. Biochemical and toxicologic studies of Rhodamine B and 3, 6-Diaminofluoran. *Toxicol. and Appl. Pharmacol.* 3: 696-706. New York-London: Academic Press.

WEBER, B. 1941. Phenol als Zusatzstoff bei der Bestimmung von Grundwasserströmen. *Arch. Hyg. u. Bakteriol.* 125: 41-52. München-Berlin: Oldenbourg.

WEBSTER, D.S., J.F. PROCTOR & I.W. MARINE 1970. Two-well tracer test in fractured crystalline rock – General Ground-water Techniques. *US Geol. Surv. Water-Supply Pap.* 1544-I, 22 p.. Washington.

WEGENER, J.W., J.C. KLAMER, H. GOVERS & U.A.TH. BRINKMAN 1987. Determination of organic colorants in cosmetic products by high-performance liquid chromatography. *Chromatographia* 24: 865-875. Braunschweig: Friedr. Vieweg & Sohn Verlagsges. mbH.

WEIDENBACH, F. 1960. Trinkwasserversorgung aus Karstwasser in der östlichen Schwäbischen Alb. *Jhe. f. Karst- u. Höhlenforscher* 1: 169-192. Stuttgart.

WEISE, S.M., P. FABER & M. STUTE 1992. Neon-21 – a possible tool for dating very old groundwaters. In Isotope techniques in water resources development. *IAEA 1991*, pp 179-188. Vienna.

WEISE, S.M. & H. MOSER 1987. Groundwater dating with Helium isotopes. In *Isotope Techniques in Water Resources Development*, pp 105-126. Vienna.

WEISS, W., H. SARTORIUS & H. STOCKBURGER 1992. Global distribution of atmospheric $_{85}$Kr: A database for the verification of transport and mixing models. In Isotopes of noble gases as tracers in environmental studies. *IAEA*, pp 29-62. Vienna.

WEISS, W. & W.J. JENKINS 1979. Tritium-Helium-3 dating of natural waters. In *Isotope in der Natur, ZIF Mitt.* 29: 292-301. Leipzig.

WERNER, A. & P. MALOSZEWSKI 1997. Mathematical modeling with the multi-dispersion-model in karst hydrogeological investigations in South-Western Slovenia. *Acta Carsologica* XXVI/1: 321-328. Ljubljana/Slovenia.

WERNER, A., H. HÖTZL & W. KÄSS 1997b. The interpretation of a high water tracer test in the Danube-Aach-System (Western Swabian Alb, Germany). *Proc. 12th Int. Congr. Speleol., La Chaux-de-Fonds, 2, Actes. 6th Conference on Limestone Hydrology and FissuredMedia*, pp 187-190. Besançon.

WERNER, A., H. HÖTZL, W. KÄSS & P. MALOSZEWSKI 1997a. Interpretation of tracer experiments in the Danube-Aach-System with analytical models. *Proc. 5th Symp. on Karst Waters & Environmental Impacts 1995*, pp 153-160. Rotterdam: Balkema.

WERNLI, H.R. 1986. Naphthionat – ein neuer Fluoreszenztracer zur Wassermarkierung. *DGM* 30(1): 16-19. Koblenz.

WERNLI, H.R. 1988. Zur Anwendung von Tracermethoden in einem quartärbedeckten Molassegebiet. *Proc. 5th Int. Symp. Underground Water Tracing, Athen 1986*, pp 413-421. Athen.

WERTHEMANN, B. 1980. Experimente mit fluoreszierenden Tracern zur Erforschung der Diffusionsverhältnisse im Zürichsee. *Separatdruck Vierteljahrschrift der Naturforschenden Gesellschaft in Zürich* 125(3): 249-258.

WHISTON, W. 1957. *The life and works of FLAVIUS JOSEPHUS,* 1055 p. Philadelphia/Toronto: Winston.

WHITE, W.B. 1967. Modifications of fluorescein dye ground-water tracing techniques. *Steir. Beitr. Hydrogeol.* 1966/67: 151-158. Graz.

WHITE, W.B. 1988. Geomorphology and Hydrology of Karst Terrains. 464 p., Oxford (Univ. Press).

WHITLEY, G.A., G.A. POPE, D.C. MCKINNEY, B.A. ROUSE & P.E. MARINER 1995. Vadose zone nonaqueous-phase liquid characterization using partitioning gas tracers. In HINCHEE, R.E., G.S. DOUGLAS & S.K. ONG (eds), *Monitoring and verification of bioremediation*, pp 211-221. Columbus: Battelle Press.

WILKOWSKE, C.J., J.A. WASHINGTON II, W.J. MARTIN & R.E. RITTS, Jr. 1970. *Serratia marcescens* – biochemical characteristics, antibiotic susceptibility patterns, and clinical significance. *J. Amer. Med. Assoc.* 214(12): 2157-2162.

WILLHEIM, R. & A.C. IVY 1952. *Cancer Res.* 12: 308. (cit. n. DRUCKREY, 1955).

WILLIAMS, R.P., C.L. GOTT, S.M.H. QUADRI & R.H. SCOTT 1971. Influence of temperature of incubation and type of growth medium on pigmentation in *Serratia marcescens. J. Bacteriol.* 106(2): 438-443. Baltimore.

WILSON, J.F., jr. 1968. Fluorimetric procedures for dye tracing. *Techniques of Water-Resources Investigations US Geol. Surv.* 3: 31 p. Washington D.C.

WILSON, R.D. & D.M. MACKAY 1995. Direct detection of residual nonaqueous phase liquid in the saturated zone using SF6 as a partitioning tracer. *Environ. Sci. Technol.* 29: 1255-1258.

WIMPENNY, J.W.T., N. COTTON & M. STATHAM 1972. Microbes as tracers of water movement. *Water Res.* 6: 731-739. London: Pergamon Press.

WINKLER, U., K.B. HELLER & B. FOLLE 1978. Pleiotropic consequences of mutations towards antibiotic-hypersensitivity in *Serratia marcescens*. *Arch. Microbiol.* 116: 259-268. Springer.

WITTEKIND, D. 1979. Fluoreszenzmikroskope. In WITTE, S. & F. RUCH, *Moderne Untersuchungsmethoden in der Zytologie*, 2.Ed.: 36-69. Baden/Baden-Köln-New York: G.Witzstrock.

WITTWEN, R., H. WASER & B. MATHEY 1971. Essai de fixation de la Sulphorhodamine B et de la Sulphorhodamine G extra sur charbon actif. *Extrait des Actes du 4e Congr. suisse de Spéléol., Neuchâtel, septembre 1970*, pp 78-83.

WOMMACK, K.E., T.H. RUSSELL, M. KESSEL, E. RUSSEK-COHEN & R.R. COLWELL 1992. Distribution of viruses in the Chesapeake Bay. *Appl. Environ. Microbiol.* 58: 2965-2970.

WOOD, W.W. & G.G. EHRLICH 1978. Use of baker's yeast to trace microbial movement in ground water. *Ground Water* 16(6): 398-403.

WRIGHT, CH., S.D. KOMINOS & R.B. YEE 1976. Enterobacteriaceae and *Pseudomonas aeruginosa* recovered from vegetable salads. *Appl. Environmental Microbiol.* 31: 453-454. Washington/D.C.

WYSCHIGIN, G.W. & W.B. TSCHEREPANOW 1962. Erfahrungen mit barrierenartig-flächenmäßigem Fluten. *Z. Angew. Geol.* 8: 456-459. Berlin: Ref.

YATES, M.V., CH.P. GERBA & L.M. KELLY 1985. Virus persistance in groundwater. *Appl. Environmental Microbiol.* 49: 778-781. Washington.

YU, V.L. 1979. *Serratia marcescens* – Historical perspective and clinical review. *New Engl. J. Med.* 300: 887-893.

YURTSEVER, Y. & J.R. GAT 1981. Atmospheric Waters. In GAT, J.R. & R.GONFIANTINI (eds), Stable Isotope Hydrology, Deuterium and Oxygen-18 in the Water Cycle, IAEA Techn. Rep. Ser. 210: 103-142. Vienna.

ZANDER, J. 1973. Hydrogeologische Untersuchungen im Muschelkalk-Karst von Nord-Württemberg. Diss. Arb. Inst. Geol. Paläont. Univ. Stuttgart, N.F. 70: 87-182, Stuttgart.

ZANKER, V. & W. PETER 1958. Die prototropen Formen des Fluoreszeins. *Chem. Ber.* 91: 572-580.

ZETZSCHE, F. & O. KÄLIN 1931. Untersuchungen über die Membran der Sporen und Pollen, V, 4. Zur Autoxydation der Sporopollenine. *Helv. Chim. Acta* 14: 517-519. Basel.

ZHUJUN, Z. & W.R. SEITZ 1984. A fluorescence sensor for quantifying pH in the range from 6.5 to 8.5. *Anal. Chim. Acta* 160: 47-55.

ZOJER, H. & J. ZÖTL 1975. Hydrogeologische Untersuchungen im Bereich Großrutschung des Gradenbachtales bei Döllach/Kärnten. *Steir. Beitr. Hydrogeol.* 27: 65-84. Graz.

ZÖTL, J. 1957a. Neue Ergebnisse der Karsthydrologie. *Erdkunde* 11: 107-117. Bonn.

ZÖTL, J. 1957b. Der Einzugsbereich von Quellen im Karstgebirge. *Österr. Wasserwirtsch.* 9: 77-86, Wien.

ZÖTL, J. 1957c. Hydrologische Untersuchungen im östlichen Dachsteingebiet. *Beitr. z. alpinen Karstforsch.* 9: 187-205, Wien und Mitt. Naturwiss. Ver. Steiermark, 87.

ZÖTL, J. 1958. Beitrag zu den Problemen der Karsthydrographie mit besonderer Berücksichtigung der Frage des Erosionsniveaus. *Mitt. geogr. Ges. Wien* 100: 101-130. Wien.

ZÖTL, J. 1961. Die Hydrographie des nordalpinen Karstes. *Steir. Beitr. Hydrogeol.* 1960/61: 163 p. Graz.

ZÖTL, J. 1974. *Karsthydrogeologie*, 291 p. Wien-New York: Springer.

ZÖTL, J. 1989. Bibliography of the history of karst research. In *Hydrology of Limstone Terranes. Int. Contrib. Hydrogeol.* 10: 1-59. Hannover.

ZOTTER, H. 1963, 1965. Stream tracing techniques and results: Pocakontas and Greenbrier counties, West Virginia. *Nat. Spel. Soc. News* 21(1963): 136-142, 23(1965): 169-177.

ZUBER, A. 1974. Theoretical possibilities of the two-well pulse method. In *Isotope Techniques in Groundwater Hydrology* II: 277-294. Vienna: IAEA.

ZUBER, A. 1986. Mathematical models for the interpretation of environmental radioisotopes in groundwater systems. In FRITZ, P. & J.CH.FONTES (eds), *Handbook of Environmental Geochemistry* 2: 1-59. Amsterdam-Oxford-New York: Elsevier.

ZUPAN, M. & M. KOLBEZEN 1976. Hydrochemische Untersuchungen. In Markierung unterirdischer Wässer – Untersuchungen in Slowenien 1972-1975 *Steir. Beitr. Hydrogeol.*, 28: 63-78. Graz.

ZUPAN, M. 1982. Einfluß der Wasserverschmutzung an der Zerstörung der Fluoreszenztracer. *Beitr. Geol. Schweiz – Hydrol.* 28(I): 79-89. Bern: Kümmerly + Frey.

ZUPAN, M. 1989. Vplivi vodnega ekosittema fluorescencua barulva (The influence of water ecosystem to fluorescent dyes). *Acta Carsologica* XVIII: 297-309, (slowenisch mit engl.Kurzfassung). Ljubljana.

ZYGOWSKI, W. 1985. Beobachtungen zur Kontamination von Wasserproben aus hydrologischen Markierungsversuchen mit Fluoreszenztracern bei Probenahme und Lagerung. *bbr* 11: 419-424.

Taylor & Francis
Taylor & Francis Group
http://taylorandfrancis.com

Conversion Tables

Conversion factors.

Known	Desired	Factor
Li	LiCl	6.108
LiCl	Li	0.164
Na	NaCl	2.542
NaCl	Na	0.393
Cl	NaCl	1.648
NaCl	Cl	0.607
K	KCl	1.907
KCl	K	0.524
B	Borax	35.276
B	M-boric acid (HBO_2)	4.053
HBO_2	Borax	8.704
Tritium unit (TU)	Bequerel/l	0.118
Curie	Bequerel	$3.7 \cdot 10^{10}$
Millicurie (mCi)	Bequerel	$3.7 \cdot 10^{7}$

Relative molecular- and atomic masses.

Borax ($Na_2B_4O_7 \cdot 10H_2O$)	381.371
Bor (B)	10.811
Meta-boric acid, m-boric acid (HBO_2)	43.818
Li	6.941
LiCl	42.394
Na	22.990
NaCl	58.443
K	39.098
KCl	74.551
Cl	35.453

Taylor & Francis
Taylor & Francis Group
http://taylorandfrancis.com

Index of localities

AMERICA

Canada 187
  Chalk river test area/Ontario 216, 219
  Columbia glacier 49
  Ottawa 285
  Province Ontario 215
  Rosenmound Outwash 40
Jamaica 45, 49, 71
USA
  Baltimore Harbor 494
  Burkett Oil field143
  California 166
  Cape Cod 219
  Devens/MA 257
  Dixie valley 167
  Hawaii 235
  Kentucky 49
  New York Bight 494
  Oregon 241
  Pennsylvania 484
  Rockland lake 166
  Smith Grove/Kentucky 310
  South Carolina 427
  Tennessee 310
  Texas 313
Venezuela 54

ASIA

China
  Guilin 149, 150
Iraq
  Ninive 2
Israel
  Banyas 3
  Berekhat Ram 2
  Jordan source 2, 272
  Panium 2
  Phiale Lake, Phialo 2
Turkey
  Kolossä 2
  Lykos (Lykus) river 2
  Menderes valley 2

AUSTRALIA

New Zealand 238
Papua New Guinea 41

EUROPE

Austria
  alpine karst region 6
  Bad Gastein 140
  Bründl spring 191, 274
  Buchkogel region 155, 240, 276
  Buchkogel 8, 39, 193, 140
  Carinthia 429
  Carinthian Alps 433
  Dachstein karst 191
  Dachstein massif 52, 194, 274, 408
  Dachstein plateau 407
  Dachstein region 190, 193, 205
  Feliferhof swallowhole 274
  Gradenbach 429
  Graz 6, 7, 11
  Hagen mountains 408
  Hammerbach spring 128
  Kaprun valley 312
  Lake Formarin 332
  Leoganger Steinberge 52
  Lower Austrian oil field 484
  Lurbach cave system 8, 32, 35, 39, 46, 55, 56, 128, 204, 216, 220, 273, 372, 373
  Lurbach karst system 10
  Lurbach sinkhole 273, 274
  Neusiedler lake 182
  Northern Calcareous Alps 52, 401
  Offensee area 275
  Ramsau 205
  Reppwand 433
  Salzburg Alps 39, 510
  Semriach 8
  Styrian karst 132
  Tennen mountain 403
  Toten mountain 191, 407
  Vienna 10
  Viennese basin 312
  Warscheneck 401
  Weizer Bergland 214
  Zahmer Kaiser 52
Belgium
  Brussels 7
  La Rock 222
Croatia
  Istria 18
Denmark
  Jacobshavn 488

Finland 246, 263
Helsinki waterworks 264
Lake Saimaa 266
Vantaanjoki river 265
France 5
Alsatian potash mine 482
Arçon 308
Causse de Gramat 48
Clamouse 36
Dhuy/Dpt.Loiret 275
Doubs 308
French Jura 47, 48
Ill river 307
Loue spring 307
Marcoule 35
Mouthier 307
Picardie 276
Pontalier 14, 307
Rhône 35, 71
Strassburg 5, 225
Verneuil-sur-Avre 338
Germany
Aach spring 3, 5, 6, 8, 11, 13, 125, 240, 418, 426
Alpine foreland 126
Altmühl river 67
Bad Nauheim 310
Bad Nenndorf 239
Baden-Württemberg 7
Bamberg 246
Bavarian alpine foreland 237
Berlin 234
Bigge valley dam 510
Black Forest 10, 52, 71, 126, 428, 478
Blautopf spring 3, 32, 272, 414
Böckinger Wiesen 471
Bremen 307
Buchbrunnen 414
Danube percolation 5, 8, 11, 13, 23, 101, 213, 240, 417, 418
Danube river 4, 6, 23, 39, 56
Danube-Aach-area 153
Dinkelberg 52
Düsseldorf 467
East Friesian islands 306
Eberbach 311
Echaz valley 310
Erolzheimer Feld 396
Frauenbach sinkhole 216
Freiburg sewage farm 303
Freiburg/Br. 8, 36
Fuchtbach spring 108
Fürstenberg-Nord 482
Grenzach-Wyhlen 401
Haltern Sands 259
Heilbronn 471
Hohe Warte 285
Hohenpeißenberg 285
Iller valley 52, 226, 515
Immendingen 124
Karlsruhe 10, 309
Karlsruhe-West 305
Krottenkopf 39
Lainbach valley 284
Liptingen 156
Mangfall 164
Mansfeld Kupferschiefer mines 427, 482
Merdingen test field 10, 33, 36, 52, 54, 110, 135, 216, 219, 226, 353, 458, 465
Mönchsrot 484
Mühlacker 387
Munich Municipal waterworks 278
Munich 10, 126
Nagold dam 511
Neckar river 305, 310, 471
Neuhof-Ellers 482
Oberharz 46, 427
Oberndorf 133, 202, 240
Odenwald 276, 478
Paderborn 311
Pegnitz percolation 153, 161
Pforzheim 126, 236
Regnitz river 67
Rhine river 35, 41, 66, 305, 467, 505
Rhine valley 52
Rhine-Neckar-region 309
Riegel passage 8, 153
Roßhaupten 510
Rottenburg 127
Ruhr region 259
Saulgau 480
Schramberg 478
Schwäbisch Hall 272
Segeberger Forst 360, 373
Southern Harz 307
Southwestern Germany 108
Steimbke 483
Swabian Alb 3, 69, 195, 310, 317, 411
Swabian Jura 52
Sylvenstein dam 510
Thüringen 510
Tübingen 310
Tuttlingen 126
Upper Bavaria 64, 71
Upper Danube 3, 18, 124, 140, 198
Upper Rhine valley 5, 258, 458, 507
Warstein 240
Weißer Kocher 109
Werra 307
Weser 307
Württemberg 3
Great Britain
Blackwaters estuary 243
English karst 274
London 233
Lyme Bay 167
Mendip Hills 45, 54, 56
South Wales 55, 262
St.Dunstans Well 274
Taff river (Wales) 243, 278
Usk river (Wales) 278
Greece
Athens 9
Gulf of Argos 261
Marathon-dam 10
Peloponnesus 9, 32, 35, 46, 52, 106, 190, 261
Hercegovina
Livansko polje 311
Popovo polje 30
Ireland 242
Italy
Aurisina spring 6
Duino 132
Timavo spring 2, 3, 6, 18, 132, 186, 273, 279
Trebiciano 18
Trieste 6, 18
Triestine karst 186, 273, 279
Turin 6, 225
Middle Europe 298

Netherlands 268
North Sea 494
Norway 243
  Oslo fjord 244
  Trondheim fjord 244
Russia
  Volga-Ural-area 484
Slovenia 2, 9
  Bistra 9, 106
  Bled 8
  Celje 9, 141, 463
  Dinaric karst 52
  Idria 9
  Hubelj spring 137
  Karst 6
  Krain 6, 39, 35
  Lake Bled 10, 498
  Lake Cerknica 9
  Ljubljana springs 9
  Llubljana 8, 247
  Notranjska Reka 132, 273
  Planina basin 202
  Planina 9, 274
  Poik 274
  Portorosz 10
  Postojna 9
  Rak 9
  Reka percolation 3, 6, 18, 56, 186, 273
  San Cozian 2, 3, 18, 56, 186, 273, 279
  Savinja valley 9, 32, 141, 463
  Slovenian karst 78, 202
  Vertoce 146
  Vipava 9
  Vremski Britof 147
Switzerland
  Aare river 502
  Aletsch glacier 124, 489
  Areuse river 264
  Areuse spring 131
  Basel 41, 273, 506
  Baselland 4
  Bern 9
  Berner Oberland 427
  Findelen glacier 490
  Glatt valley 386
  Gorner glacier 54
  Gotthard region 312
  Grindelwald 427
  Hinter Muota valley 32, 35
  Hölloch cave 9, 214
  Jura mountains 400
  La Broye 500
  Lac des Tailleurs 131
  Lake Murten 499
  Lake Sempach 499
  Langenthal 32, 144
  Langeten valley 9, 143
  Lausen 3, 124
  Liestal 275
  Luterbach 427
  Muota valley 9, 39, 214, 402, 408
  Neuchâtel Jura 32, 35, 39, 54, 260
  Neuchâtel 9, 247
  Noiraigue-spring 54
  Northern Switzerland 238
  Orb spring 6
  Säntis-Altmann-Stocks 46
  Simplon 54
  St.Gallen 247
  Swiss Jurassic 3, 6, 77, 262
  Swiss Mittelland 46
  Swiss Molasse 9
  Val de Travers 131
  Vierwaldstätter lake 67, 276
  Wilerwald 34, 36, 259

WORLD

Gulf Stream 268
North Atlantic 166
Northern hemisphere 286
Oceans 166, 494

Taylor & Francis
Taylor & Francis Group
http://taylorandfrancis.com

Subject index

α-(alpha-)radiation 171
β-(beta-)radiation 171
γ-(gamma-)radiation 171
100% modern 289

ablation phase 492
absinthe 14, 307
absorption spectrum 19
acacia 212
accidents 14, 307, 517
accumulation phase 492
acid orange 11 32
acid rain 292
acid red 388 40
acid red 50 37
acid red 51 42
acid red 52 36
acid red 87 31
acid red 91 32
acid red 94 43
acid yellow 215:1 48
acid yellow 25 47
acid yellow 7 48
acid yellow 73 21
acidic reaction 60
acidorange 197
acridine orange 198
actinometer 67
activable isotopes 178
activated carbon 100
activation analysis 8
activation 178
adsorptions factor 63
aerial photos 495
Aeromonas hydrophila 243
AgCl 125
age determination 295
air 166
algae 120
alkali buffer 58
alkylbenzenesulfonates 151
alpine karst 201, 400
altitude effect 282, 302
aluminium powder 276
amidoflavine 48
amidorhodamine B 36
amidorhodamine G 8, 34, 37, 57, 63
amino G acid 46
Ammon-Gelite 1,2,3 272
ammonium bromide 8
ammonium sulfate 6
ammonium 148
amount effect 282
analysis 56
analytical criteria 321
analytical solutions 377
angio-fluoroscopy 31
angiography 121, 114
anhydrite 291
aniline red 5, 18, 23, 125
aniline violet 56
antibiotics 243
aquifer tests 514
argon-39 287
aromas 8, 10, 160
artificial tracers 11
assimilation 288
astra diamond green 56
atmosphere 286
atmospheric fallout 291
atom-bomb test 283
auramine 56
AVOGADRO's constant 170
Bacillus acidocaldarius 235
Bacillus globigii 242, 235
Bacillus pyocyaneus 235
Bacillus stearothermophilus 234
Bacillus violaceus 242
background fluorescence 71
background 17
bacteria drift test 229, 239
bacteria 223, 310
bacteriophages 11, 245
bacteriophage analysis 255
bacteriophages, detection 252
bacteriophages, enumeration 252
Bacterium violaceum 234
balls 273
bank filtration 14, 29, 302, 305, 310, 311, 471, 521
basalt conduits 201
basic blue 197
basic brown 197
basic green 197
basic orange 198
basic red 1 41
basic red 2 197
basic red 3 42
basic violet 10 32
basic violet 3 56, 197
batch test 371
bathing additives 30
bathing product 303
bengal rose 43
bentonite 29
benzenesulfonic acid 167

benzoic acid 167
bequerel 170, 569
bichromate 6
biosphere 290
Bismarck brown 197
Blankophor 50
borax 9, 143
borehole 513
boric acid 143, 305
boron analysis 145
brightening agents 50
brilliant acid yellow 8G 48
brilliant blue FCF 56
brilliant sulfoflavine 48
brilliantpink B 33
bromide 29, 150, 186
bromine-79 170
bromine-82 170, 180, 244, 383
bromodifluoromethane 166
brown glass bottle 335

C_3-plants 288
C_4-plants 288
calcofluor white ST 55
calibrating 89
Canyon-Diablo-Iron Meteorite 291
carbohydrates 165
carbon-13 288
carbon-14 288
carbonate equilibrium 362
carboxylated microspheres 220
CAS: 130-13-2 46
CAS: 17372-87-1 31
CAS: 2321-07-5 22
CAS: 2391-30-2 48
CAS: 27344-41-8 51
CAS: 3262-60-6 42
CAS: 3520-42-1 36
CAS: 37299-86-8 40
CAS: 3844-45-9 56
CAS: 518-47-8 21
CAS: 568-63-8 42
CAS: 5873-16-5 37
CAS: 632-69-9 43
CAS: 63358-69-6 43
CAS: 6359-85-9 47
CAS: 81-88-9 32
CAS: 86-65-7 46
CAS: 989-38-8 41
catchment area 14, 399
cation exchange 122, 127, 141, 359, 361, 372
cationic rhodamine 61
CD-standard 291
cesium 147
chaff 2, 3, 272
chelate complex 182
CHEZY's equation 264
chlorfluoroethane 166
chloride 3, 5, 125, 220, 306
chlorinated hydrocarbon 36, 309
chlorination 28
chlorine dioxide 28, 74
chlorine 74
chlorine-36 289
chlorophenol 310
chlorophyll bodies 212, 217, 218
chlorophyll 83
cholera epidemics 311
chromate 28
chromide-51 8
chromium-51 8, 9, 180
CI 18 835 47
CI 42 090 56
CI 42 510 56
CI 42 520 56
CI 42 535 31, 56
CI 42 685 56
CI 45 100 36
CI 45 160 41
CI 45 170 32
CI 45 210 42
CI 45 220 37
CI 45 350 21
CI 45 370 32
CI 45 380 31
CI 45 400 32
CI 45 430 42
CI 45 440 43
CI 56 205 48
CI 59 040 43
Citran 203
cleaning product 303
cleaning supplies 30
club moss spores 6, 187
coal mine 482
coal-tar 310
coastal water 243, 494
cobalt-58 180
cobalt-60 180
coincidence technique 174
coliphage F2 259
coliphage PhiX174 258
coliphages 9, 244
colourless dyes 50
column test 219, 242
combined tracing test 423
complex stability constant 183
Compton effect 172
computative dye separation 94
concentration maximum 12
concentration-time-curve 12
confetti 275
congo red 56, 197
continental effect 282, 302
continuous injection 504
cork beads 273
cork pieces 3
cork shaving 273
cosmetic dye 121
cosmetics 30, 303
cosmic radiation 290
cost estimate 316
cotton detector 50
cotton red 197
cotton swabs 49, 56
cotton wool 103
counting statistic 176
counting tubes 172
creeping release 303
crystal violet 128, 197
Curie 169
cytogenetical analysis 115

D & C green 8 43
daily death rate 226
dam leakage 15
damage 320
dam 510
daphnia test 120
DARCY equation 342
DARCY-velocity 467, 482
dating of groundwater 288
deaminoalkylation 34
decay constant 169, 293
decay law, decay rate 169, 293
decay reaction 357, 372
deep well 513
de-icing 306
denaturing road salt 31

denitrification 293
detection limit 13, 17, 19, 25, 30, 287, 332
detergents 138
deuterium excess 283
deuterium 280, 281
diatoms 274
dibrom fluorescein 32
dichromate 148
diethylfluorescein 43
dilution method 502
dimerisation 42
dimethylfluorescein 43
dipenten 160
diphenyl brilliant flavin 7GFF 49
dipole flow 448
dipole test 455
DIRAC pulse 332
direct evaluation 380
direct red 197
direct yellow 96 49
discharge measurement 182, 185, 502
discharge 14
dispersion coefficient 294, 347
dispersion equation 294
dispersion function 294
dispersion model 294
dispersion parameter 294
dispersion 342
dispersivity α 462
distribution coefficient 65
dNAPL 517
documentation 315, 337
dominating velocity 12
double-scanning-method 10
drift particles 272
drinking water protection 467
Duasyn-Säurerhodamin B 01 36
dumpsite 54, 305, 388
dye coupler 200
dye decay 106
dye separation 90
dyed spores 193
dyes 18
dysprosium 180, 184
EDTA 182
eels, marked 3, 279
effective porosity 342
electrolytic conductivity 128
electromagnetic reciprocating pump 229
electro-stirrer 153
ELISA technique 253
emanation 186, 520
ENDO-agar plate 234
enrichment method 99
environmental chemicals 303
environmental isotopes 279
environmental organisms 310
eosin blue 32
eosin bluish 21
eosin yellow 31
eosin yellowish 21
eosin 7, 8, 31, 57
error function 346
erythrosine 21, 42
Escherichia coli 234, 242
europium 180
evaporation 302
evaporite rock 291
evapotranspiration 493
EXCEL 380
exine 189
exotic seeds 18
exponential model 294, 295
extinction 81
extra 39
Extran 144

fallout 291
ferric hydroxide 69
fertilizer 292
fibre optic fluorimeter 83, 495
fifty-day flow time 224
filter fluorimeter 82
first detection 12, 13
fish 117
fissured aquifer 215, 236, 262, 378
fitting procedure 294
flame photometry 7
flavine 212
floating articles 18
flotation devices 6
flour 3
flowing water 502
fluocapteur 100
fluorescein derivatives 22
fluorescein 5, 21, 22
fluorescence analytical data 80
fluorescence decay 99
fluorescence microscope 197, *210*, 217
fluorescence quenching 73, 99
fluorescence spectrometry 82
fluorescence spectrum 19
fluorescent brightener 28, No.40 622 55
fluorescent brightener 351 51
fluorescent compounds 19
fluorescent micropheres 214
fluorescent microspheres, examining 217
fluorescing spores 9, 197
fluorescope 5, 6, 76
FluoSpheres 214
fluotransducer 100
foam forms 152
foaming 36
fontactoscope 186
food red 14 42
formacine unit 70
fossil fuel 289
fractures, nonhomogeneous 444
fractures, parallel 444
fractures, pseudo-homogeneous 444
fuchsine 6, 56

gamma radiation 243
gas-exchange 493
GAUSS-distribution 344
gentian violet 197
genus *Serratia* 224
geobombs 271
geochemical reaction 356, 371
geoelectric investigation 128
glacial traces 36, 41
glacial water 39, 46
glaciers 486
gold-198 180
gradient method 380

granite 10, 427
granulated plastics 274
grass seeds 276
gravel 64
groundwater age 293
groundwater dating 290, 297
groundwater recharge 288
groundwater residence time 294
groundwater-model age 290
gypsum 291

half load 13
half-life time 13, 169, 293
halogen hydrocarbons 11
Hauptrogenstein 3
hazardous waste 393
helium-3 286
helium-4 286
highest concentration 13
horizontal lysimeter 396
hospitalism 233
host fungus 224
Hostalux 50, 55
host-bacterium 253
HPLC 98
human organism 113
humic acid 69, 71
humic soil 62
hydraulic conductivity k_f 462
hydraulic tests 514
hydrocarbons 72
hydroglaciology 486
hygienist 12
hypolimnion 499

impurity 121
indigo 18, 37
indium 8, 9, 141, 168, 180
indium-EDTA-complex 183
industrial area 292
infiltration 388,397
infiltration gallery 225
injection site 317, 323
input 13
input-output-model 294
instantaneous injection 503
integration method 503
intraglacial flow 488
inverse evaluation 380
iodine 29, 151
iodine-131 6, 8, 180
ion exchange 60, 122, 128, 141, 318, 463
ion sensitive electrode 130
ionic potential 122
isoamylsalicylate 160
isobestic point 40, 82
isobornylacetate 8, 161
isochronochromates 76, 339
isomer 40
isopentylsalicylate 161
isosbestic point 82
isotopes, activable 167
isotopes, radioactive 167

janthine 234
jaune sulfacide 47

kaolinite 29, 62
karst channel 272
karst water 240, 260, 271, 315, 378
karst 6
KCl analysis 142
KCl 8, *138*
kinematic velocity 482
krypton-85 287

lake currents 494
lake tracings 266
lake 39, 496
lanaperl fast yellow 47
Lanaperl-Echtgelb 47
lanthanum 8, 184
last detection time 13
LC_{50} 117
leakage 388
leaks in dams 311
leaks 510
legal question 316
lethal concentration 117
Leukophor, leucophor 50, 54
LiCl 8
light green 197
light impact 319
limonene 8, 160
lipstick 31, 114
liquid-liquid-extraction 99, 104
liquid-solid-extraction 103
lissamine 48
lithium analysis 135
lithium chloride 6, 7, 273
lithium 131, 372, 335
lithium, toxicology 138
lNAPL 517
lode 427
longitudinal dispersion coefficient 462
longitudinal dispersion 506
LOTUS 355, 380
Lycopodium clavatum 187
Lycopodium selago 190
Lycopodium spores 8, 267
lysimeter 396

macro-dispersivity 386
magenta 56
mahonia 212
malachite green 56, 197
manganese salts 149
manganese 8
marine bacteriophages 269
marine phage H40/1 261
MARIOTT bottle 504
MARQUART procedure 380
mass displacement 428
mass-spectroscopy 290
maximal concentration 13
MBAS 158
mean residence time 295
mean velocity 342
measurement, radioactivity 172
meltwater 486, 487
membrane filter 70, 210
metabolites 121
methyl blue 56
methyl violet 31, 56, 197
mice 115
microbial tracer 244
microbiological decay 106, 110
microorganisms 120, 224
mineral oil 72
mineral water 302, 310
molybdate 150
moor water 71
moulin 492
mountain 402
MPM (most probable number) 254
m-TFMB 165

multi dispersion Model 378
multiple-box-model 296
Muschelkalk karst 53
mutagenity test 120
Mycoderma aceti 236

NaCl analysis 130
NaCl 123
NAGRA 166
naphthion acidic 46
NAPL 517
natural lithium contents 137
nickel salts 149
Nile blue 197
nitrate 74, 149
nitrification 292
nitrite 149
nitrogen-15 290, 292
nomogram 94
nonaqueous phase 517
non-fluorescing dyes 55
normalized breakthrough curve 38, 370
normed curve 339
nuclear plant 286
nuclear weapon test 283, 286, 289
nuclide chart, nuclide list 168

observation site 318
observation tunnel 438
ocean 494
oceanography 494
octofluorocyclobutane 520
oil field flood water 143
oil field water 483
ophthalmology 31, 114
optical brightener 49, 63
Orcoacid sulforhodamine B 36
orebody 437
oxidizing agents 27, 74
oxygen 281
ozone 74

parafuchsine 5, 197
pararosaniline 5, 18
Paris-violet 61
partitioning coefficient 519
partitioning tracer 517
PCR 253
PDB (Peedee Belemnite) 288
peat 62
PECLET-number 369, 373
Peedee Belemnite (PDB) 288
percolation 125, 128, 132, 308, 418
perfluor chemicals 166
perfluor hydrocarbon compounds 166
perfluoro-1,3,5-trimethyl-cyclohexane 520
perfluoro-3,4-dimethyl-cyclohexane 167
perfluorochemicals 494
perfluorodecalin 167
perfluoromethylcyclohexane 167
periglacial karst 41
peristaltic pump 229
permanganate 28, 30
permeability coefficient 342
pesticides 239
Pfu 247, 257
pH-adjustment 96
phage G 261
phage PhiX174 268
phage T52 267
phage T7 260, 262
phages *244*
phages, detection 252
phages, enumeration 252
phages, survival 249
pH-dependency 57
phenol 6, 164, 310
phorwite BBH 55
phosphorescence 19
phosphorus-32 243
photine CU 54, 58
photine 50, 63
photochemical decay 496
photo-conductor 83
photoluminescence 19
photolysis 66, 99
photolytical coefficient 66, 68
physical environmental effects 311
physico-chemistry 57
physiology 105
pigment red 81 41
piston-flow model 294
pitchblende 6, 185, 186
plants 120
plaque forming unit 247, 257
plastic bottle 335
plastic rods 273
POISEUILLE's law 447
polariser 77
polenta porporina 224
pollution tracers 307
polyacrolein microspheres 220
polystyrene 215
ponceau 197
ponds 499
Pontacyl Brilliant Pink B 36
pore groundwater 36, 237, 258, 378
porphyrines 212
potash fertilizer 139
potash mine 307
potassium chloride 8, *138*
potassium dichromate 148
potassium salt 128
potassium 7, 141, 373
potassium, physiology 142
potassium-40 168
precipitation, H-3-contents 285
prodigiosine 228
protection zone 14
prototropical states 25
Pseudomonas cepacia 242
Pseudomonas violacea 234
publication 338
pumping test 427, *514*, 515
pyranine 30, *43*, 45, 57, 60, 303
pyrazol brilliant flavin 7GF 49
pyrene 19
pyronin GY 199
pyronin 198

qualitative investigation 75
quantitative determination 79
quarry 55
quartz lamp 76
QUATTRO PRO 380

rabbits 115

radial-convergent flow 448
radiation properties 181
radiation safety 184
radioactive decay 168, 169, 293
radioactive isotopes 6, 167
radioactive tracers 6
radioactive waste 513
radioactivity 167
radionuclide 169
radium 170, 185
RAMAN-cuvette 87
RAMAN-line 86, 89
RAMAN-peak 50
rare gas isotopes *286*
rats 115
recovery rate 372
red ink 31
re-emergence 424
remediation techniques 510
residence time 223
retardation coefficient 371
retardation factor 37, 65, 356
retention 64
Rhine alarm model 505
rhodamine 3G 34, 42
rhodamine 6 GDN 41
rhodamine 6G 34, 41
rhodamine B 32, 42, 56, 57, 305
rhodamine FB 8
rhodamine WT 34, 40, 57, 62
river bank filtration 469, 472
river cross section 506
river discharge 15
river water 278
river 263
Rn-222 520
rosaceine 33
rosaniline 56
rose bengale 21, 43
ROSSI's method 255

S/N-ratio 89
Saccharomyces cerevisiae 276
safralinine 33
safranin 197
Salmonella phage P22H5 262
Salmonella thyphimurium 243
salmonella-microsomas 115
salt brine 482
salt deposit 310
salt mine 482
salt tracing test 130
salt 3, 5, 6, 7, 122
samarium 184
sample analysis 336
sample bottle, sample container 334, 335
sample plan 333
sampling procedure 333
sampling site 323
sampling 333
sand filter 234
sand 64
SANDOZ accident 122
Sarcina lutea 225
saturation factor 63
sawdust 3, 273
scintillation detector 173
sea water 243, 268
second maximum 13
semiconductor detector 174
Serratia indica 243, 244
Serratia marcescens 5, 8, 9, 224, 226, 237, 238, 240, 242, 243, 279, 465
Serratia marcescens, breeding 228
Serratia marcescens, examining for 231
Serratia marcescens, toxicology 232
sewage canal 273
sewage effluent 499
sewage farm 303
sewage percentage 302
sewage treatment plant 276
sewage water 75
sewage 29, 30, 71, 243, 267
sewer discharge traces 41
shale oil 5, 124, 164
Single Fissure Dispersion Model (SFDM) 444
single well method 382, 467
sink hole 400
skin factor 514
snow melt 432
sodium chloride 8, 123
sodium chloride, toxicology 131
sodium dichromate 148
sodium fluorescein 5, 21
sodium-24 180
sodium-naphthionate 46, 57
soil air 289
Solophenyl Flavin 7GFF 49
solute transport 342
solvent black 197, 209
solvent green 7 43
solvent red 197
sorption loss 65
sorption, sorptivity 60, 64, 318
sound waves 10, 272
specific decadic exstinction 26
spectrofluorimeter 80, 83
spectrophotometry 80
spore drift tracing test 201
spore dyeing 195, 198
spore sampling 203
spore-drift 187
spores 187
spores, blue 190, 193
spores, dyed 193
spores, examining 209
spores, red 190
spores, violet 193
sporopollenin 189
standardized breakthrough curve 53
starch 3, 275
STOKES rule 20
storage coefficient 514
storage test 226
stratosphere 286
straw 273
Streptoccocus faecalis 235, 242
strontium chloride 6
strontium 146
subglacial water 486
submersible pump 334
Sudanrot 197
sulfofluorescein 43
sulforhodamine B 34, 36, 38, 62, 333
sulfurhexafluoride 166, 494
sulphur-34 290
sunlight 66

surface water 35, 185, 243, 493
surfactant determination 157
surfactants 8, 10, 151, 333
SURFER 355
swallow hole 317, 399
synchronscan 37, 92
synchron-spectrum 90

tap water 225
TAYLOR method 380
technetium 180
technetium-99m 383
tellurium oxide 276
temperature coefficient 72
temperature dependency 72
temperature sensor 311
term schematics 19
test preparation 316
tetrapropylene benzene sulfonate 152
textile fibres 218
textile swabs 50
theatre blood 31
thermal water 302, 480, 516
thermocline 500
thin layer chromatography 97
thiocyanate 150
thiosulfate 149
thorium 168
three breakthrough curves 368
three-dimensional 494
time of injection 12, 328
tinopal 4BM 55
tinopal ABP liquid 53
tinopal CBS-X 51, 58, 198, 200
tinopal LPW 55
tinopal 9, 50
toxicity to humans 115
toxicological investigation 115, 121

toxicological property 115
toxicology 113
tracer amount, formula 327
tracer cloud 494
tracer dilution logging 382
tracer flowmeter 384
tracer injection 329
tracer quantity 323
tracer, choosing 318
TRACI 95 377
tracing procedure 328
tracing test, preparation 315
transmissivity 444, 514
transport simulation 355
transversal dispersion 462
tritium unit 286
tritium 8, 180, 283, 387
tropical karst 41, 201
trout 119, 130, 321
trypaflavine 72
turbidity 68, 83
turf 30
Turner field fluorimeter 82
two-porosity medium 515
two-well tracer test 427
Tyndall-effect 77
typ curve 370
typhoid epidemics 124, 236, 311
typhoid 3

ultracentrifuge 70
ultrasound 218
underwater-filter-fluorimeter 494
unsaturated zone 6, 41, 225, 240, 257, 330
uranine decay 109
uranine first used 5
uranine 6, 8, 21, 57, 59, 303, 320
uranium 168
uranyl glass 89
UVB 36
Uvitex 50
UV-lamp 75

VARIOSENS 83, 494, 497
vesuvin 197
Vibrionaceae 225
VIROSORB 247
viruses 245, 270
visibility limits 76
VLF 11
volume reduction 105
Vortex 229

warm-blooded animals 115
WATEQ 361
water organisms 119
water protection area 223
water quality 319
water usage 320
wetting agents 151
whey 310
whiskey 310
wild phage 260, 270
winter input 298
wood flour 273
wood 289
wooden balls 3
wooden beads 273
wooden rods 273

yeast 276

zinc salts 149

Taylor & Francis
Taylor & Francis Group
http://taylorandfrancis.com

Plate 1. Colour changing when dissolving uranine crystals. Red: concentrated solution; yellow; mixed colours; green: diluted, strongly fluorescent solution in the outer section of the dye cloud (Section 2.1.1.1).

Plate 2. Dyeing of the Rhine river with rhodamine WT near Basel, 11 Sept. 1990 (Section 2.1.1.6).

Plate 3. Microbiological decomposition of uranine. Uranine was added to water of the Fuchtbach spring to a cencentration of 612 µg/1. Observation time: 6 weeks. Left sample: untreated; right: sample was autoclaved after addition of uranine (Section 2.1.4.1).

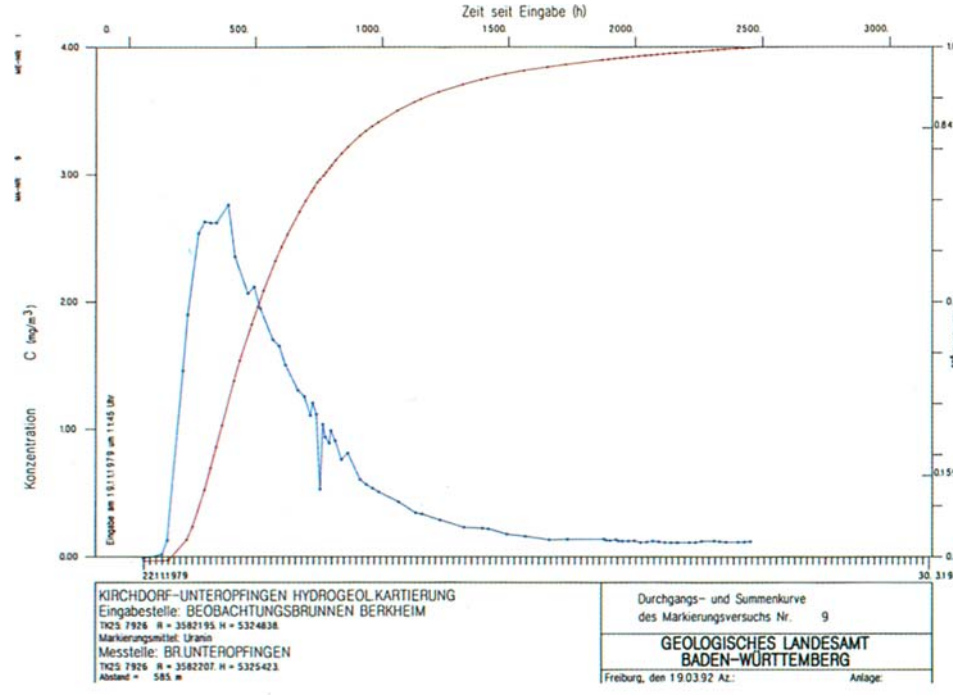

Plate 4. Breakthrough curve and castline with a pumping test (Section 5.9.3).

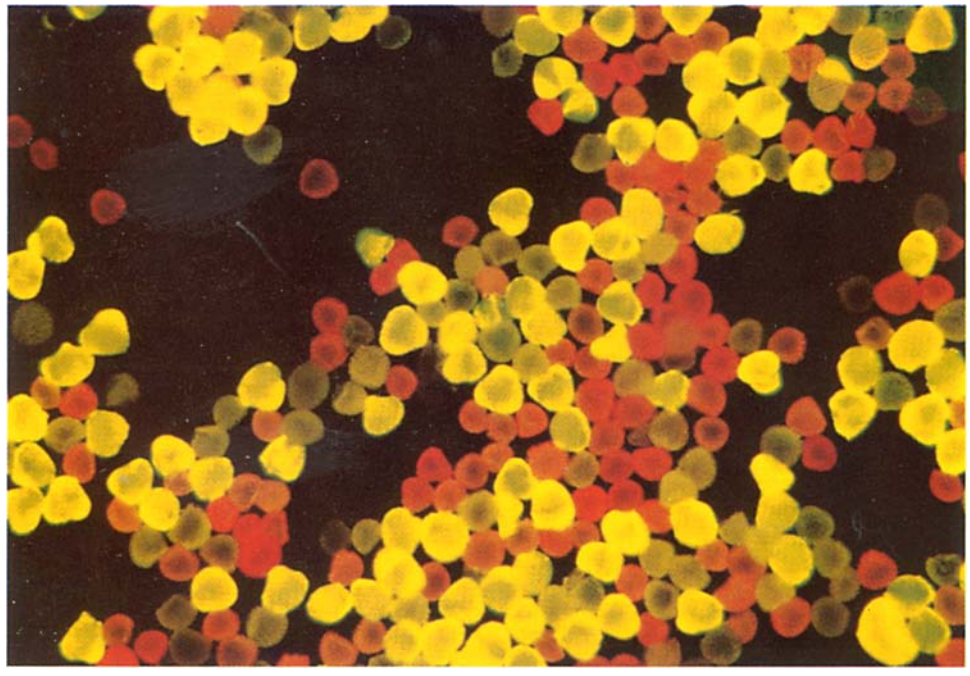

Plate 5. *Lycopodium* spores under the fluorescense microscope, dyed with different fluorescent dyes. Yellow: acridin orange; red: pyronin; weakly green: tinopal . (Enlargement ca. 150x, excitation 490 nm) (Section 2.5.3).

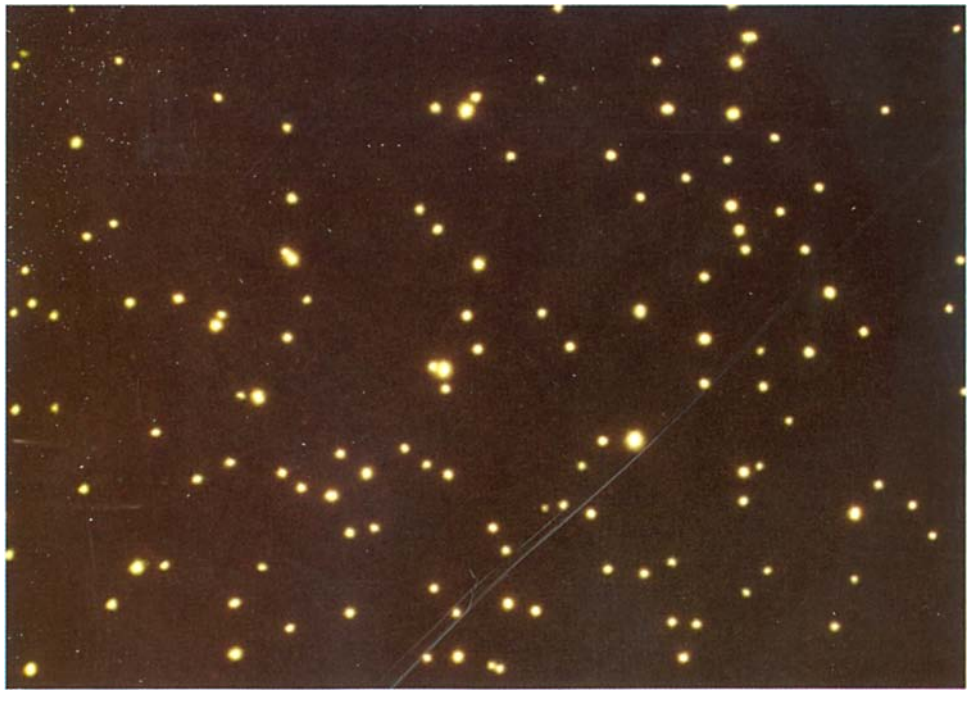

Plate 6. Fluorescent microspheres. (Enlargement ca. 800x) (Section 2.6).

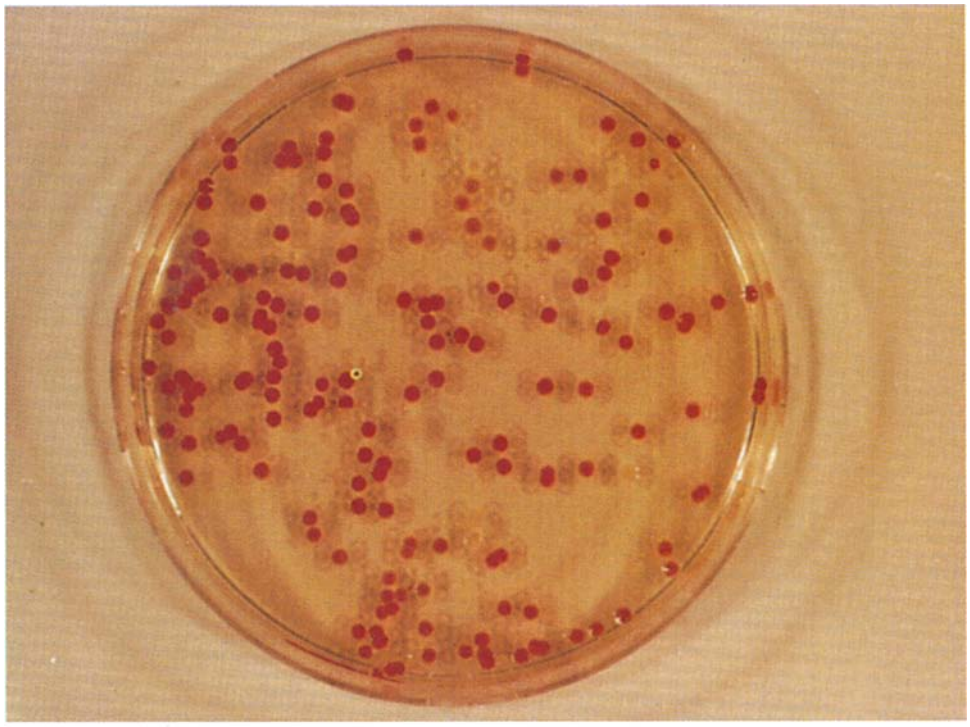

Plate 7. *Serratia marcescens*-colonies (Section 2.7.3.1).

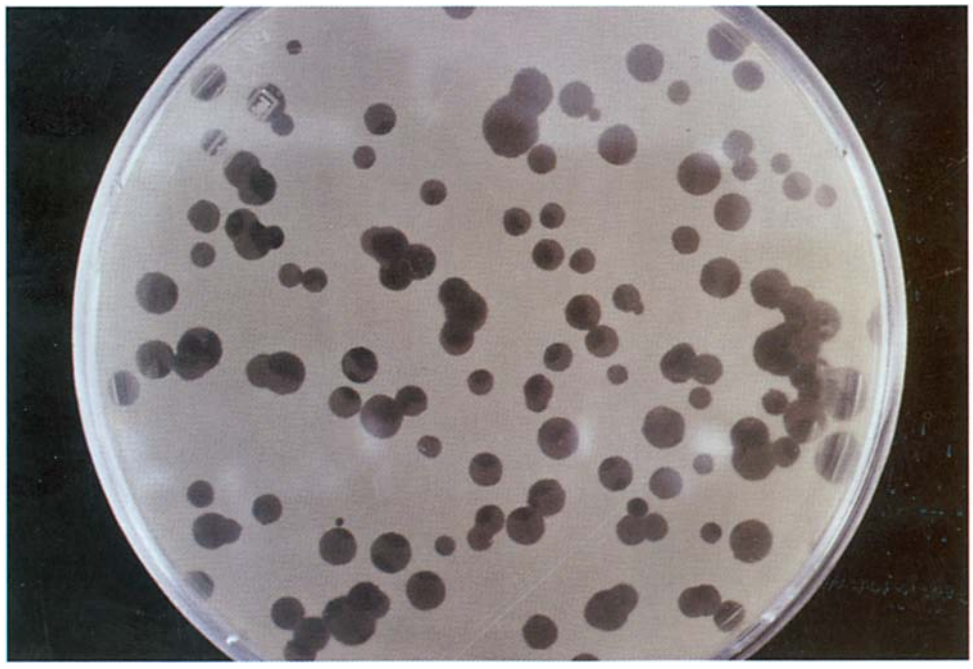

Plate 8. Bakteriophages ΦS1 as dark plaques in a pure culture of host bacteria of the species *Pseudomonas fluoreszens* ATCC 27663 (Section 2.8.6). (Photo: P.Rossi).